GAUGE FIELDS IN CONDENSED MATTER

Hagen Kleinert

Vol. I SUPERFLOW AND VORTEX LINES

Disorder Fields, Phase Transitions

Vol. II STRESSES AND DEFECTS

Differential Geometry, Crystal Melting

World Scientific

PART III

GAUGE FIELDS IN SOLIDS

Denique quae nobis durata ac spissa videntur haec magis hamatis inter sese esse necesset et quasi ramosis alte compacta teneri.

(Things which seem to us hard
Must needs be made of particles more hooked,
One to another, and be held in union,
Welded throughout by branch-like elements.)

Lucretius, *De Rerum Natura*, Rome, 57 B.C.

The description of superfluid ^{4}He in terms of a disorder field theory developed in Part II can serve as a prototype for the treatment of many other physical systems. For this to be true, these systems have to possess the following fundamental properties.

1. There exists an ordered ground state.
2. The important fundamental exitations are of two types, namely,
   a) soft long-wavelength exitations which only *slightly* disturb the order, and
   b) line-like disturbances which *drastically* disturb the order in their immediate neighbourhood.
3. There exists a phase transition where the line-like disturbances condense and completely destroy the order everywhere in the system.

In superfluid ^{4}He the long-wavelength exitations were the fluctuations of the phase angle, the line-like disturbances were the vortex lines, and the order which was destroyed in the phase transition was the superfluid order.

We shall now discuss the second important physical system of this type: the crystalline solid. In thermal equilibrium at low temperature, this consists of a regular array of atoms which form the ordered ground state. If the crystal is perturbed weakly, the atoms perform long-wavelength oscillations. These are observable in the form of sound waves. If the crystal is perturbed strongly, for example via local external forces, one obtains what is called a plastically deformed state. To a good approximation such a state can be described by means of line-like defects. The most important ones are of two types called dislocations and disclinations. These are the crystalline analogues of the vortex lines in superfluid ^{4}He. We shall develop a disorder field theory for these fundamental exitations in close analogy with the vortex lines in superfluid ^{4}He. The phase transition in which defect lines condense and destroy the crystalline order will be identified with the melting process. The melting process is a first order transition and thus of a nature different from the superfluid transition. Still, we shall see that a number of quasi-universal features of this process can be understood by means of this disorder field theory.

CHAPTER ONE

THE IDEAL CRYSTAL

1.1. DISPLACEMENT AND STRAIN

Consider an ideal simple crystal which consists of a periodic array of identical atoms situated on lattice points

$$\mathbf{x_n} = n_1\mathbf{a}_1 + n_2\mathbf{a}_2 + n_3\mathbf{a}_3, \tag{1.1}$$

where $\mathbf{a}_i$ are the fundamental lattice vectors and n_i are integers. The simplest example is that of a simple cubic (s.c.) lattice with atoms at

$$\mathbf{x}_n = a(n_1, n_2, n_3), \tag{1.2}$$

where a is the lattice spacing. Such a crystal is not very physical since, with the usual dominance of central forces, it is unstable against shear deformations. This is why there are only very few s.c. crystals in nature (e.g., solid polonium). For much of the development to come this aspect will, however, not be relevant. More stable configurations of identical atoms are the face-centered cubic (f.c.c.) crystal with

$$\mathbf{a}_1 = a(\tfrac{1}{2}, \tfrac{1}{2}, 0), \qquad \mathbf{a}_2 = a(0, \tfrac{1}{2}, \tfrac{1}{2}), \qquad \mathbf{a}_3 = a(\tfrac{1}{2}, 0, \tfrac{1}{2})$$

and the body-centered cubic (b.c.c.) crystal with

$$\mathbf{a}_1 = a(1, 0, 0), \qquad \mathbf{a}_2 = a(\tfrac{1}{2}, \tfrac{1}{2}, \tfrac{1}{2}), \qquad \mathbf{a}_3 = a(0, 0, 1).$$

If forces are applied, the crystal undergoes some distortion and the atomic positions change from $\mathbf{x_n}$ to, say,

$$\mathbf{x}'_{\mathbf{n}} = \mathbf{x_n} + \mathbf{u_n}. \tag{1.3}$$

There are a number of important phenomena which are smooth over many atomic distances. For these, it is sufficient to study the crystal in the continuum limit in which the lattice spacing a tends to zero. This has the advantage that the positional changes can be described by a *displacement field* $\mathbf{u}(\mathbf{x})$ which is defined on every space point,

$$\mathbf{x}' = \mathbf{x} + \mathbf{u}(\mathbf{x}). \tag{1.4}$$

After the distortion, the distance vector between two infinitesimally spaced neighboring material points at $\mathbf{x}$ and $\mathbf{y}$ is changed from $d\mathbf{x} = \mathbf{x} - \mathbf{y}$ to

$$dx'_i = dx_i + \partial_j u_i \, dx_j, \tag{1.5}$$

and its length from $d\ell = \sqrt{d\mathbf{x}^2}$ to

$$d\ell' = (d\ell^2 + 2u_{ij}\, dx_i\, dx_j)^{1/2}. \tag{1.6}$$

The symmetric matrix

$$u_{ij}(\mathbf{x}) \equiv \tfrac{1}{2}(\partial_i u_j + \partial_j u_i + \partial_i u_\ell \, \partial_j u_\ell) \tag{1.7}$$

is called the *strain* tensor. To linear approximation, this tensor is just

$$u_{ij}(\mathbf{x}) \sim \tfrac{1}{2}(\partial_i u_j + \partial_j u_i). \tag{1.8}$$

1.2. ELASTIC ENERGY

In elastic media with short-range forces between pointlike constituents, the *elastic energy* density can only depend on the differences $d\ell' - d\ell$ and thus only on the strain. To lowest approximation we may write

$$e(\mathbf{x}) = \tfrac{1}{2} c_{ijk\ell}\, u_{ij}(\mathbf{x})\, u_{k\ell}(\mathbf{x}). \tag{1.9}$$

There is no linear term since, in equilibrum, all $u_i(\mathbf{x})$ vanish by definition. With this energy, the thermal partition function of elastic fluctuations reads

$$Z = \int \mathscr{D} u_i(\mathbf{x}) \exp\left(-\frac{1}{T} \int d^3x\, e(\mathbf{x}) \right). \tag{1.10}$$

The elastic tensor $c_{ijk\ell}$ is symmetric under the exchanges $i \leftrightarrow j$, $k \leftrightarrow \ell$, $ij \leftrightarrow k\ell$. Thus it has 21 independent coefficients which may be displayed in the form of a symmetric 6×6 matrix

$$c_{ijk\ell} = \left(\begin{array}{ccc|ccc} c_{1111} & c_{1122} & c_{1133} & c_{1123} & c_{1131} & c_{1112} \\ & c_{2222} & c_{2233} & c_{2223} & c_{2231} & c_{2212} \\ & & c_{3333} & c_{3323} & c_{3331} & c_{3312} \\ \hline & & & c_{2323} & c_{2331} & c_{2312} \\ & & & & c_{3131} & c_{3112} \\ & & & & & c_{1212} \end{array} \right) \equiv c_{ab}.$$

where $a = 1, \ldots, 6$ denotes the i, j pairs 11, 22, 33, 23, 31, 12. Let us also introduce corresponding strain components as follows,

$$u_a = (u_{11}, u_{22}, u_{33}, 2u_{23}, 2u_{31}, 2u_{12}). \tag{1.11}$$

Then the energy (1.9) may be viewed as a quadratic form in a six-dimensional vector space

$$e = \tfrac{1}{2} c_{ab}\, u_a\, u_b. \tag{1.9'}$$

The elastic constants c_{ab} are not completely arbitrary. In order to guarantee *stability* under elastic fluctuations the energy has to be positive definite, $e > 0$, for all non-zero strains. This implies that all subdeterminants of the quadratic form are strictly positive, i.e.,

$$c_{11} > 0, \quad \begin{vmatrix} c_{11} & c_{12} \\ c_{21} & c_{22} \end{vmatrix} > 0, \quad \ldots \begin{vmatrix} c_{11} & \cdots & c_{16} \\ \vdots & & \vdots \\ c_{61} & \cdots & c_{66} \end{vmatrix} > 0. \tag{1.12}$$

Usually, only a few of the coefficients c_{ab} are really independent, due

to crystal symmetries. A single plane of reflection symmetry, for instance, removes 8 coefficients. If the xy plane is a plane of reflection symmetry, the matrix c has the form

$$c_{ab} = \left(\begin{array}{ccc|ccc} c_{11} & c_{12} & c_{13} & 0 & 0 & c_{16} \\ & c_{22} & c_{23} & 0 & 0 & c_{26} \\ & & c_{33} & 0 & 0 & c_{36} \\ \hline & & & c_{44} & c_{45} & 0 \\ & & & & c_{55} & 0 \\ & & & & & c_{66} \end{array}\right). \tag{1.13}$$

An additional symmetry about one orthogonal reflection plane leaves us with only

$$c_{ab} = \left(\begin{array}{ccc|ccc} c_{11} & c_{12} & c_{13} & & 0 & \\ & c_{22} & c_{23} & & & \\ & & c_{33} & & & \\ \hline & & & c_{44} & 0 & 0 \\ & 0 & & & c_{55} & 0 \\ & & & & & c_{66} \end{array}\right). \tag{1.14}$$

Exploiting such symmetry elements as well as the invariance under discrete rotations, the 32 crystallographic point groups give rise to 9 different classes of c matrices. These are listed in Appendix 1A. The number of independent elements c_{ab} is shown in Table 1.1 and Fig. 1.1.

We shall consider mostly crystals of cubic symmetry which have the smallest number of independent elastic constants, i.e., 3: c_{11}, c_{12}, c_{44},

$$c_{ab} = \left(\begin{array}{ccc|ccc} c_{11} & c_{12} & c_{12} & & 0 & \\ & c_{11} & c_{12} & & & \\ & & c_{11} & & & \\ \hline & & & c_{44} & 0 & 0 \\ & 0 & & & c_{44} & 0 \\ & & & & & c_{44} \end{array}\right). \tag{1.15}$$

For these crystals, the energy density reads

TABLE 1.1. The seven crystal systems with their 32 crystallographic point groups and numbers of quadratic and cubic elastic constants.

System		Hermann-Mauguin symbols	Schoenflies notation	u_{ij}^2 couplings	u_{ij}^3 couplings
Cubic	*a*	$23, \frac{2}{m}\bar{3}$	T, T_h	3	8
	b	$\bar{4}3m, 432, \frac{4}{m}\bar{3}\frac{2}{m}$	T_d, O, O_h		6
Tetragonal	*a*	$4, \bar{4}, \frac{4}{m}$	C_4, S_4, C_{4h}	7	16
	b	$4mm, \bar{4}2m, 422, \frac{4}{m}\frac{2}{m}\frac{2}{m}$	$C_{4v}, D_{2d}, D_4, D_{4h}$	6	12
Hexagonal	*a*	$6, \bar{6}, \frac{6}{m}$	C_6, C_{3h}, C_{6h}	5	12
	b	$6mm, \bar{6}m2, 622, \frac{6}{m}\frac{2}{m}\frac{2}{m}$	C_{6v}, D_{3h}, D_{6h}		10
Trigonal	*a*	$3, \bar{3}$	C_3, S_6	7	20
	b	$3m, 3\frac{2}{m}, 32$	C_{3v}, D_{3d}, D_3	6	14
Orthorhombic		$2mm, 222, \frac{2}{m}\frac{2}{m}\frac{2}{m}$	C_{2v}, D_2, D_{2h}	9	20
Monoclinic		$2, m, \frac{2}{m}$	C_2, C_{1h}, C_{2h}	13	32
Triclinic		$1, \bar{1}$	C_1, S_2	21	56

$$
\begin{aligned}
e(\mathbf{x}) &= \tfrac{1}{2}c_{11}(u_{11}^2 + u_{22}^2 + u_{33}^2) + c_{12}(u_{11}u_{22} + u_{11}u_{33} + u_{22}u_{33}) \\
&\quad + 2c_{44}(u_{23}^2 + u_{31}^2 + u_{12}^2) \\
&= c_{44}\sum_{i\neq j} u_{ij}^2 + \frac{c_{11} - c_{12}}{2}\sum_i u_{ii}^2 + \frac{c_{12}}{2}\left(\sum_i u_{ii}\right)^2 . \qquad (1.16)
\end{aligned}
$$

The stability condition (1.12) implies $c_{11} > 0$, $c_{11}^2 > c_{12}^2$, $(c_{11} - c_{12})^2 \times (c_{11} + 2c_{12}) > 0$, $c_{44} > 0$ and hence

$$
c_{11} > 0, \qquad c_{44} > 0, \qquad c_{11} > c_{12}, \qquad c_{11} + 2c_{12} > 0. \qquad (1.17)
$$

A further reduction occurs for isotropic systems. In general, one axis of

FIG. 1.1. The graphical representation of the symmetry elements in the given crystal systems with their 32 crystallographic point groups of Table 1.1. The notation is abbreviated. Boxes indicate centrosymmetric systems. The numbers on the lower right corners give the number of independent elastic constants in each case.

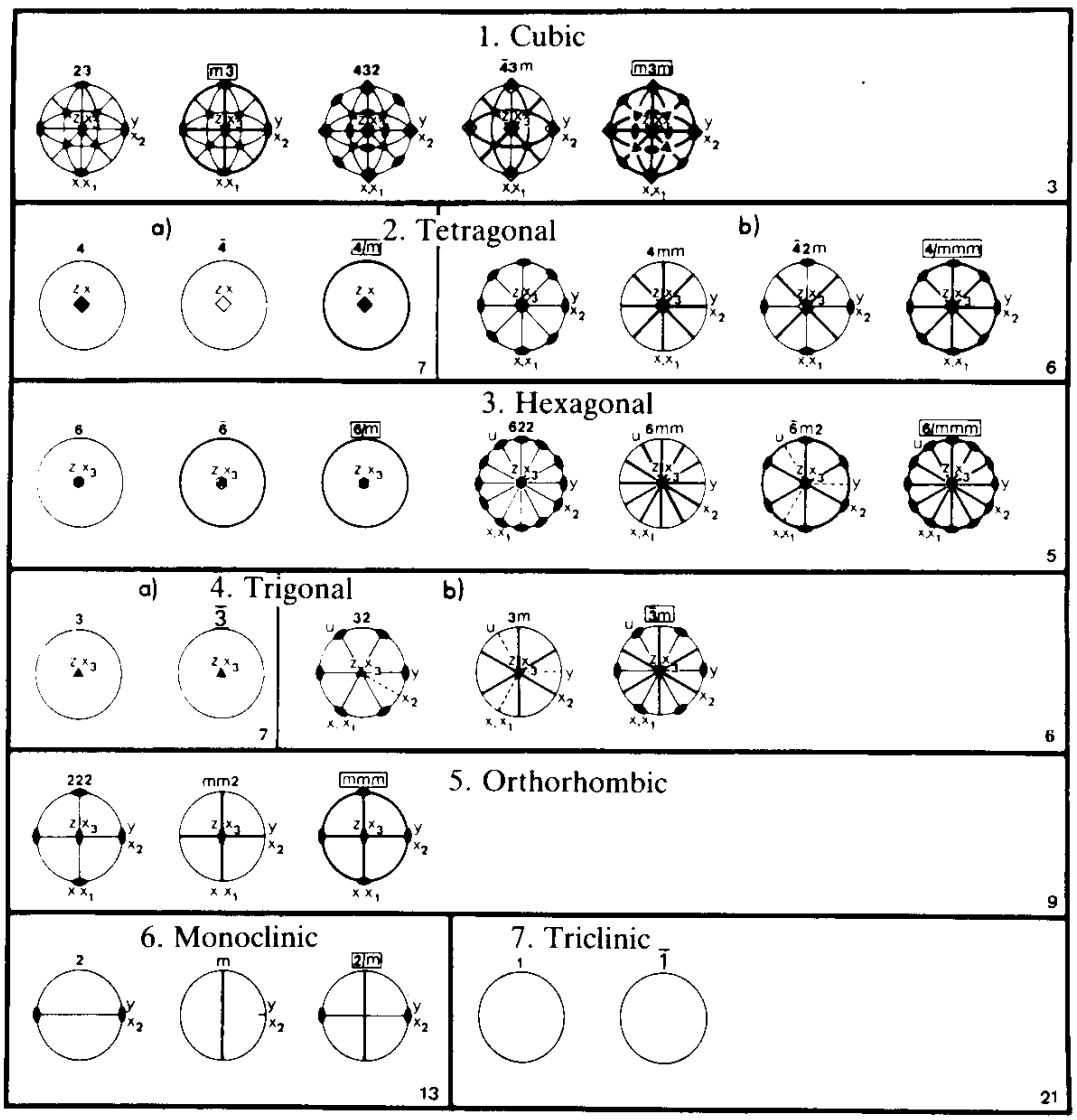

rotational symmetry reduces the 21 components to 5 independent ones. If this axis coincides with the z axis, the matrix c_{ab} becomes

$$c_{ab} = \left(\begin{array}{ccc|ccc} c_{11} & c_{12} & c_{13} & & & \\ & c_{11} & c_{13} & & 0 & \\ & & c_{33} & & & \\ \hline & & & c_{44} & 0 & 0 \\ & 0 & & & c_{44} & 0 \\ & & & & & \tfrac{1}{2}(c_{11}-c_{12}) \end{array}\right). \tag{1.18}$$

TABLE 1.2. Adiabatic elastic stiffness constants of cubic crystals at low temperature and at room temperature* Units are in 10^{12} dyne/cm^2. The last four columns show the thermal softening in % up to 300 K.

Crystal	T [K]	T_m [K]	Density [g/cm^3]	c_{11}	$c_{12} \equiv \lambda$	$c_{44} \equiv \mu$	$\xi \equiv \frac{c_{11}-c_{12}}{2c_{44}}$	$\frac{\lambda}{2\mu} = \frac{c_{12}}{2c_{44}}$	$\gamma = \left(\xi \frac{2\mu}{\lambda} + 3\right)$	$\Delta c_{11}/c_{11}^{\circ}$	$\Delta\lambda/\lambda^{\circ}$	$\Delta\mu/\mu^{\circ}$	$\Delta\xi/\xi^{\circ}$
W (f.c.c.)	0	2640.1	19.317	5.326	2.049	1.631	1.005	0.628	4.620	1.7	.20	1.47	1.29
	300		—	5.233	2.045	1.607	0.992	0.636	4.523				
Ta (b.c.c.)	0	3270	16.696	2.663	1.582	0.874	0.618	0.905	2.278	2	.51	3.42	−2.4
	300		—	2.609	1.574	0.818	0.633	0.962	2.316				
Cu (f.c.c.)	0	1357.6	9.018	1.762	1.249	0.818	0.314	0.763	1.070	4.4	2.8	7.82	.645
	300		—	1.684	1.214	0.754	0.312	0.805	1.057				
Ag (f.c.c.)	0	1235	10.635	1.315	0.973	0.511	0.335	0.952	1.122	5.7	3.7	9.8	1.8
	300		—	1.240	0.937	0.461	0.329	1.02	1.093				
Au (f.c.c.)	0	1337.5	19.488	2.016	1.697	0.454	0.351	1.8689	1.120	4.1	3.9	7.6	.9
	300		—	1.923	1.631	0.420	0.348	1.94	1.1064				
Al (f.c.c.)	0	933.5	2.733	1.143	0.619	0.316	0.829	0.979	3.189	6.6	1.9	10.8	1.5
	300		—	1.068	0.607	0.282	0.817	1.079	3.073				
K (b.c.c.)	4	336.3		0.0416	0.0341	0.0286	0.131	0.596	.422	23.8	7.9	34.3	−13.7
	295			0.0370	0.0314	0.0188	0.149	0.835	.473				
Pb (f.c.c)	0	600.6	11.599	0.555	0.454	0.194	0.260	1.170	.839	10.8	6.8	23.2	6.9
	300		—	0.495	0.423	0.149	0.242	1.42	.767				
Ni (f.c.c.)	0	1728.1	8.968	2.612	1.508	1.317	0.419	0.573	1.564	4	.53	6.2	2.6
	300		—	2.508	1.500	1.235	0.408	0.697	1.498				
Pd (f.c.c.)	0	1827.1	12.132	2.341	1.761	0.712	.407	1.247	1.356	3	0	−.7	12.5
	300		—	2.271	1.761	0.717	0.356	1.228	1.170				
V (f.c.c.)	0	2193.1	6.051	2.324	1.194	0.460	1.228	1.290	4.847	1.9	.58	7.4	−4.5
	300		—	2.280	1.187	0.426	1.283	1.393	5.030				

*References to the original papers are given in the article by C. Kittel in *Phonons*, ed. R.W.H. Stevenson (Oliver & Boyd, Edinburgh, 1966).

Symmetries about two orthogonal axes lead to complete isotropy, in which case we find the cubic shape but with the third constant, c_{44}, being related to c_{11}, c_{12} by

$$c_{44} = (c_{11} - c_{12})/2. \tag{1.19}$$

Then the energy can be expressed in terms of the two rotational invariants, u_{ij}^2 and u_{ii}, as

$$e(\mathbf{x}) = \mu u_{ij}^2 + \frac{\lambda}{2} u_{ii}^2, \tag{1.20}$$

where

$$\mu \equiv c_{44}, \qquad \lambda \equiv c_{12}, \tag{1.21a}$$

Here μ is called the *shear modulus* and λ the *Lamé constant*. For these, the stability conditions (1.17) read

$$\mu > 0, \qquad 2\mu + 3\lambda > 0. \tag{1.22}$$

In some materials, the deviation,

$$\xi \equiv \frac{c_{11} - c_{12}}{2c_{44}} > 0, \tag{1.21b}$$

from the isotropic value 1 can be considerable. A list of experimental data is given in Table 1.2. As an example, silver at 300 K has $c_{11} = 1.240$, $c_{12} = 0.937$, and $c_{44} = 0.511$ in units of 10^{12} dynes/cm^2 so that $\xi = 0.33$. Nevertheless we shall continue the discussion first for isotropic media, for simplicity, then generalize the theory to cubic systems, and give some remarks concerning the general case only from time to time.

In isotropic media it is convenient to stay with the notation (1.9) in which u_{ij} and $c_{ijk\ell}$ are tensors and have simple properties under rotations. In terms of the elastic constants μ, λ, we can write

$$c_{ijk\ell} = \mu(\delta_{ik}\delta_{j\ell} + \delta_{i\ell}\delta_{jk}) + \lambda\delta_{ij}\delta_{k\ell}. \tag{1.23}$$

As far as the total energy,

$$E = \int d^3x\, e(\mathbf{x}), \tag{1.24}$$

is concerned, we can perform partial intergrations and bring the energy density (1.20) to the equivalent form

$$e(\mathbf{x}) = \frac{\mu}{2}(\partial_i u_j)^2 + \frac{1}{2}(\lambda + \mu)(\partial_i u_i)^2. \tag{1.25}$$

The difference between (1.20) and (1.25) is a pure divergence, i.e., surface term in the energy E. It will be useful to separate the strain into rotational invariants consisting of the traceless part of u_{ij},

$$u_{ij}^{(2)} \equiv u_{ij} - \tfrac{1}{3}\delta_{ij} u_{kk} \tag{1.26}$$

of spin 2 and the trace itself,

$$u_{ij}^{(0)} \equiv \tfrac{1}{3}\delta_{ij} u_{kk} \tag{1.27}$$

of spin 0. The projection matrices into these channels are

$$P^{(2)}_{ijk\ell} = \tfrac{1}{2}(\delta_{ik}\delta_{j\ell} + \delta_{i\ell}\delta_{jk}) - \tfrac{1}{3}\delta_{ij}\delta_{k\ell}, \qquad P^{(0)}_{ijk\ell} = \tfrac{1}{3}\delta_{ij}\delta_{k\ell}. \tag{1.28}$$

They are orthonormal in the sense that

$$\begin{aligned} &(P^{(2)2})_{ijk\ell} \equiv P^{(2)}_{ijmn} P^{(2)}_{mnk\ell} = P^{(2)}_{ijk\ell}, \qquad (P^{(0)2})_{ijk\ell} \equiv P^{(0)}_{ijmn} P^{(0)}_{mnk\ell} = P^{(0)}_{ijk\ell}, \\ &(P^{(2)}P^{(0)})_{ijk\ell} \equiv P^{(2)}_{ijmn} P^{(0)}_{mnk\ell} = (P^{(0)}P^{(2)})_{ijk\ell} \equiv P^{(0)}_{ijmn} P^{(2)}_{mnk\ell} = 0, \end{aligned} \tag{1.29}$$

so that we can write in abbreviated form: $P^{(2)2} = P^{(2)}$, $P^{(0)2} = P^{(0)}$, $P^{(2)}P^{(0)} = P^{(0)}P^{(2)} = 0$, where multiplication amounts to contraction of adjacent index pairs. When added together, these projections span the space of symmetric tensors, resulting in the unit matrix in this space,

$$(P^{(2)} + P^{(0)})_{ijk\ell} = 1^s_{ijk\ell} \equiv \tfrac{1}{2}(\delta_{ik}\delta_{j\ell} + \delta_{i\ell}\delta_{jk}). \tag{1.30}$$

Therefore, the decomposition of u_{ij} can be written as

$$u_{ij} = 1^s_{ijk\ell} u_{k\ell} = (P^{(2)} + P^{(0)})_{ijk\ell} u_{k\ell} = u_{ij}^{(2)} + u_{ij}^{(0)}. \tag{1.31}$$

By using these matrices, the elastic tensor may be decomposed into spin-2 and spin-0 parts,

$$c_{ijk\ell} = c^{(2)}P^{(2)}_{ijk\ell} + c^{(0)}P^{(0)}_{ijk\ell}, \tag{1.32}$$

with

$$c^{(2)} = 2\mu, \qquad c^{(0)} = 3(\lambda + \tfrac{2}{3}\mu) \equiv 3\kappa \tag{1.33}$$

The spin-0 combination κ is called the *modulus of compression* for reasons to be seen shortly. On inserting the decomposition (1.32) into the energy (1.9) and using the projection property (1.29) we can write

$$e(\mathbf{x}) = \tfrac{1}{2}u(c^{(2)}P^{(2)} + c^{(0)}P^{(0)})u = \tfrac{1}{2}c^{(2)}u^{(2)2} + \tfrac{1}{2}c^{(0)}u^{(0)2} = \mu u^{(2)2} + \tfrac{3}{2}\kappa u^{(0)2}. \tag{1.34}$$

Here, we can verify once more the stability conditions (1.22) according to which μ and κ have to be positive.

1.3. STRESS

If a certain configuration u_{ij} is changed by a small increment δu_{ij}, the energy density changes by

$$\delta e = c_{ijk\ell}\, u_{k\ell}\, \delta u_{ij}. \tag{1.35}$$

The quantity

$$\sigma_{ij} \equiv \frac{\delta e}{\delta u_{ij}} = c_{ijk\ell}\, u_{k\ell} \tag{1.36}$$

is called *stress*. For isotropic media, we may insert (1.33) and obtain

$$\sigma_{ij} = c^{(2)}u^{(2)}_{ij} + c^{(0)}u^{(0)}_{ij} = 2\mu u^{(2)}_{ij} + 3\kappa u^{(0)}_{ij} = 2\mu u_{ij} + \lambda\delta_{ij}u_{kk}. \tag{1.37}$$

In the terms of strain, the energy change has the simple form

$$\delta e = \sigma_{ij}\,\delta u_{ij}. \tag{1.38}$$

The orthonormality properties of the projective matrices (1.29) make it easy to invert the stress strain relation (1.37) with the result

$$u_{ij} = (c^{-1})_{ijk\ell}\,\sigma_{k\ell} = \left(c^{(2)^{-1}}P^{(2)} + c^{(0)^{-1}}P^{(0)}\right)_{ijk\ell}\sigma_{k\ell} = c^{(2)^{-1}}\sigma_{ij}^{(2)} + c^{(0)^{-1}}\sigma_{ij}^{(0)}$$
$$= \frac{1}{2\mu}\left(\sigma_{ij} - \frac{1}{3}\delta_{ij}\sigma_{kk}\right) + \frac{1}{3\kappa}\frac{1}{3}\delta_{ij}\sigma_{kk} = \frac{1}{2\mu}\left(\sigma_{ij} - \frac{\lambda}{3\kappa}\delta_{ij}\sigma_{kk}\right). \tag{1.39}$$

The ratio $\lambda/3\kappa$ is usually expressed in terms of the *Poisson ratio*,

$$\nu \equiv \frac{\lambda}{2(\lambda + \mu)}, \tag{1.40}$$

as[a]

$$\frac{\lambda}{3\kappa} \equiv \frac{\nu}{1 + \nu}, \tag{1.41}$$

so that

$$u_{ij} = \frac{1}{2\mu}(\sigma_{ij} - \frac{\nu}{1 + \nu}\delta_{ij}\sigma_{kk}). \tag{1.42}$$

With this relation, the energy may be written in terms of stresses as follows:

$$e = \frac{1}{2}u(c^{(2)}P^{(2)} + c^{(0)}P^{(0)})u = \frac{1}{2}\sigma(c^{(2)^{-1}}P^{(2)} + c^{(0)^{-1}}P(0))\sigma$$
$$= \frac{1}{4\mu}\sigma^{(2)^2} + \frac{1}{6\kappa}\sigma^{(0)^2} = \frac{1}{4\mu}\left(\sigma_{ij} - \frac{1}{3}\delta_{ij}\sigma_{kk}\right)^2 + \frac{1}{18\kappa}\sigma_{kk}^2$$
$$= \frac{1}{4\mu}\left(\sigma_{ij}^2 - \frac{\nu}{1 + \nu}\sigma_{kk}^2\right). \tag{1.43}$$

The manipulations leading to this expression can be used to find another formulation of the thermal partition function of elastic fluctuations which involves both the strain and the stress tensor. Starting with (1.10) we write in the isotropic case

[a]Notice that in D dimensions $\lambda/\mu = 2\nu/(1 - (D - 1)\nu)$ and $D\kappa = 2\mu + D\lambda = 2\mu(1 + \nu)/(1 - (D - 1)\nu)) > 0$. Therefore, ν has to satisfy the stability condition $-1 < \nu < 1/(D - 1)$. In practice, ν is usually larger than zero. An exception for $D = 2$ is the triangle lattice of magnetic flux lines in a type-II superconductor (see Part II, Fig. 3.5). For $D = 3$, see Kittinger *et al.*, *Phys. Rev. Lett.* **47** (1981) 712. More relations between the different elastic constants are given in Table 1.3.

$$Z = \int \mathscr{D} u_i(\mathbf{x})\, e^{-(1/T)\int d^3x (1/2) u (c^{(2)} P^{(2)} + c^{(0)} P^{(0)}) u}$$

and introduce integrations over auxiliary variables σ_{ij},

$$\begin{aligned} Z &= \int \mathscr{D} u_i(\mathbf{x}) \int \frac{\mathscr{D}\, \sigma_{ij}(\mathbf{x})}{2\pi} \\ &\quad \times \exp\left(-\frac{1}{T} \int d^3x \left\{ \frac{1}{2} \sigma \left(\frac{1}{c^{(2)}} P^{(2)} + \frac{1}{c^{(0)}} P^{(0)} \right) \sigma + i \sigma_{ij} u_{ij} \right\} \right) \\ &= \int \mathscr{D} u_i(\mathbf{x}) \int \frac{\mathscr{D}\, \sigma_{ij}(\mathbf{x})}{2\pi} \\ &\quad \times \exp\left(-\frac{1}{T} \int d^3x \left\{ \frac{1}{4\mu} \left(\sigma_{ij}^2 - \frac{\nu}{1+\nu} \sigma_{\ell\ell}^2 \right) + \frac{i}{2} \sigma_{ij} (\partial_i u_j + \partial_j u_i) \right\} \right). \end{aligned} \tag{1.44}$$

In this formula we recognize the Hamiltonian form of the path integral of linear elasticity [recall Eq. (1.88), Part I) for the general field theoretic Hamiltonian path integral]. The field variables are now $u_i(\mathbf{x})$ and the stress fields σ_{ij} play the role of the canonical field momenta, so that (1.45) just fits into the general canonical form,

$$Z = \int \mathscr{D} u(\tau) \int \frac{\mathscr{D}\, \pi(\tau)}{2\pi} e^{-\int d\tau \{ i\pi \partial_\tau u + \pi^2/2 \}}.$$

The role of the "time" variable τ is now played by the space coordinates x_i.

In the Hamiltonian form, the path integral over $u_i(\mathbf{x})$ can be performed after rewriting $\int d^3x\, \sigma_{ij} (\partial_i u_j + \partial_j u_i)/2$ as $-\int d^3x\, \partial_i \sigma_{ij} u_j$. This leads to the divergenceless condition for the stress, $\partial_i \sigma_{ij} = 0$, in the absence of external forces, and the path integral (1.44) becomes

$$Z = \int \mathscr{D}\, \sigma_{ij}(\mathbf{x})\, \delta[\partial_i \sigma_{ij}] \exp\left(-\frac{1}{T} \int d^3x \frac{1}{4\mu} \left(\sigma_{ij}^2 - \frac{\nu}{1+\nu} \sigma_{\ell\ell}^2 \right) \right). \tag{1.45}$$

Let us now generalize these considerations to the anisotropic case. The stress-strain relation (1.36) reads, using the pair indices a, b,

$$\sigma_a = c_{ab} u_b .$$

Its inversion is, in general, quite difficult. For cubic crystals, however, one finds from (1.15),

$$c_{ab}^{-1} = \left(\begin{array}{ccc|ccc} (2\mu\xi)^{-1} & & & & & \\ & (2\mu\xi)^{-1} & & & 0 & \\ & & (2\mu\xi)^{-1} & & & \\ \hline & & & \mu^{-1} & & \\ & 0 & & & \mu^{-1} & \\ & & & & & \mu^{-1} \end{array}\right)_{ab} - \frac{\lambda}{6\mu\xi\kappa}\left(\begin{array}{ccc|ccc} 1 & 1 & 1 & & & \\ 1 & 1 & 1 & & 0 & \\ 1 & 1 & 1 & & & \\ \hline & & & & & \\ & 0 & & & 0 & \\ & & & & & \end{array}\right)_{ab} \tag{1.46}$$

where ξ is defined in (1.21b) and

$$\kappa \equiv \tfrac{2}{3}\mu\xi + \lambda.$$

Thus the energy can be expressed in terms of stresses as

$$e = \frac{1}{2}\sigma_a c_{ab}^{-1}\sigma_b$$

$$= \frac{1}{2\mu}(\sigma_{12}^2 + \sigma_{23}^2 + \sigma_{31}^2) + \frac{1}{4\mu\xi}(\sigma_{11}^2 + \sigma_{22}^2 + \sigma_{33}^2) - \frac{\lambda}{12\mu\xi\kappa}(\sigma_{11} + \sigma_{22} + \sigma_{33})^2. \tag{1.47}$$

Introducing the parameter

$$\gamma \equiv 3\xi\kappa/\lambda = 3\xi\left(\frac{2}{3}\xi\frac{c_{44}}{c_{12}} + 1\right), \tag{1.48}$$

this can be rewritten, in close analogy with (1.43), as

$$e = \frac{1}{4\mu}\left(\sum_{i\neq j}\sigma_{ij}^2 - \frac{1}{\xi}\sum_i \sigma_{ii}^2 - \frac{1}{\gamma}\left(\sum_i \sigma_{ii}\right)^2\right) \tag{1.49}$$

and the Hamiltonian version of the elastic partition function now reads

$$Z = \int \mathscr{D} u_i(\mathbf{x}) \int \frac{\mathscr{D} \sigma_{ij}(\mathbf{x})}{2\pi} \exp\left\{ -\frac{1}{T} \int d^3x \frac{1}{4\mu} \left(\sum_{i \neq j} \sigma_{ij}^2 + \frac{1}{\xi} \sum_i \sigma_{ii}^2 - \frac{1}{\gamma} \left(\sum_i \sigma_{ii} \right)^2 \right) \right.$$
$$\left. + i \int d^3x \, \sigma_{ij} (\partial_i u_j + \partial_j u_i)/2 \right\}. \tag{1.50}$$

In isotropic systems, $\xi = 1$, $\gamma = (1 + \nu)/\nu$ and Z reduces to (1.46). Notice that in terms of μ, λ, κ, the positivity conditions (1.17) are

$$\mu > 0, \qquad \xi > 0, \qquad 2\mu\xi + \lambda > 0, \qquad \kappa > 0. \tag{1.51}$$

The parameter γ can, in principle, be negative. In practice, however, $\gamma \gtrsim 1$ (just as $\nu \gtrsim 0$ in most isotropic materials).

1.4. EXTERNAL BODY FORCES

The linear elastic behavior of a solid under the influence of an external force density $f_i(\mathbf{x})$ can be studied by adding to the energy a source term for the external work acting on each volume element,

$$e_{\text{source}}(\mathbf{x}) = -u_j(\mathbf{x}) f_j(\mathbf{x}). \tag{1.52}$$

The equilibrium distortion can now be obtained by minimizing the total energy

$$F_{\text{tot}} = \int d^3x \, (e(\mathbf{x}) + e_{\text{source}}(\mathbf{x})) \tag{1.53}$$

with respect to variations in $\delta u_j(\mathbf{x})$. This gives

$$\int d^3x \, (\partial_i (\delta u_j) \sigma_{ij} - \delta u_j f_j) = 0.$$

A partial integration leads to

$$-\int d^3x \, \delta u_j (\partial_i \sigma_{ij} + f_j) + \int d^3x \, \partial_i (\delta u_j \sigma_{ij}).$$

The last term becomes, by Gauss' theorem, a surface integral

$$\int_S dS_j \, \delta u_i \, \sigma_{ij}.$$

If the force is applied to a finite region of the solid, δu_i vanishes at infinity and we can discard the surface integral. Taking $\delta u_i(\mathbf{x})$ to vanish everywhere except for a sharp δ-function singularity at an arbitrary but fixed place $\mathbf{x}$ we find the *Euler-Lagrange equation* for linear elasticity,

$$-\partial_i \sigma_{ij}(\mathbf{x}) = f_j(\mathbf{x}). \tag{1.54}$$

This formula gives a physical meaning to the strain components. Integrating over a small volume element, say of the form of a cube with faces along the $\hat{\mathbf{x}}$, $\hat{\mathbf{y}}$, $\hat{\mathbf{z}}$ directions, we obtain

$$-\int d^3x \, \partial_i \sigma_{ij} = -\int dS_i \, \sigma_{ij} = \int d^3x f_j. \tag{1.55}$$

Thus σ_{i1}, σ_{i2}, σ_{i3} are three components of the force per unit area acting on the surface element dS_i. With this physical meaning, the stress-strain relation (1.36) becomes the physical law discovered in a simplified form by Robert Hooke in 1678 in his work *De Potentia Restitutiva* ("*ut tensio sic vis*").

The two elastic constants μ and λ can be measured in a simple experiment. Suspending a weight F on a cylindrical wire of radius R and area $A = \pi R^2$ leads to a stress $\sigma_{11} = F/A$ with all other components vanishing. From (1.42), this results in the strains

$$u_{11} = \frac{1}{2\mu} \frac{1}{1+\nu} \sigma_{11}, \qquad u_{22} = u_{33} = -\nu u_{11}. \tag{1.56}$$

The diagonal strains u_{ii} (no sum over i) are observable as relative changes in the longitudinal and transversal length scales

$$u_{11} = \Delta \ell / \ell, \qquad u_{22} = u_{33} = \Delta R / R. \tag{1.57}$$

From (1.56) we see that the Poisson ratio ν is the ratio between the two. Usually, elongations lead to transverse contractions and $\nu > 0$ (see footnote a). The constant [not to be confused with (1.24)]

$$E \equiv 2\mu(1+\nu) \tag{1.58}$$

in the relation between σ_{11} and u_{11} is called *Young's modulus* and is extracted from the experimental ratio

$$E = \frac{F}{A}\Big/\frac{\Delta\ell}{\ell}. \tag{1.59}$$

The shear modulus is experimentally accessible by taking a cube of size a and pushing the upper face with the force F per area $A = a^2$ into one transverse direction (say $+\hat{\mathbf{x}}$), the lower face with the same force into the opposite direction (say $-\hat{\mathbf{x}}$). As a consequence, the right angle in the xz plane distorts to $\pi/2 + \theta$. This may be identified with $\partial_3 u_1$ or $2u_{31}$ (since $\partial_1 u_3 = 0$), to linear approximation. The stress is then $\sigma_{31} = F/a^2$. From (1.39) we see that

$$2u_{31} = \frac{1}{\mu}\sigma_{31} \tag{1.60}$$

so that we can measure μ directly from

$$\mu = \frac{F}{a^2}\Big/\theta. \tag{1.61}$$

An alternative simple experiment subjects an elastic body to hydrostatic *pressure* p. Then the stress on every surface element points along the normal, i.e.,

$$\sigma_{11} = \sigma_{22} = \sigma_{33} = -p \tag{1.62}$$

or

$$p = -\tfrac{1}{3}\sigma_{kk}\,. \tag{1.63}$$

From (1.37) we see that[b]

$$p = -\tfrac{1}{3}(2\mu + 3\lambda)u_{ii} = -\kappa u_{kk} = -\kappa\,\partial_k u_k\,. \tag{1.64}$$

[b]In anisotropic cubic media the role of κ is played by $\kappa = \lambda + (2/3)\xi\mu = c_{12} + (2/3)\xi c_{44}$, since $\sigma_{11} = c_{11}u_{11} + c_{12}(u_{22} + u_{33}) = (c_{11} - c_{12})u_{11} + c_{12}u_{\ell\ell}$ and hence $\sigma_{\ell\ell} \equiv -3p = ((2/3)\xi c_{44} + c_{12})u_{\ell\ell}$

But $\partial_k u_k$ is readily identified with the relative volume change of the body since [recall (1.5)]

$$\frac{d^3x' - d^3x}{d^3x} = \frac{dx_1' dx_2' dx_3'}{dx_1 dx_2 dx_3} - 1 = \det\frac{\partial x_i'}{\partial x_j} - 1$$
$$= \det(\delta_{ij} + \partial_j u_j) - 1 = \partial_k u_k + O((\partial u)^2). \qquad (1.65)$$

Thus we see that κ is directly measurable from

$$p = -\kappa\frac{\Delta V}{V}, \qquad (1.66)$$

which explains the name modulus of compression for κ. In Table 1.3 we summarize the connection of κ with the different elastic constants.

TABLE 1.3. Relations between isotropic elastic constants ($\varepsilon \equiv \sqrt{E^2 + 2\lambda E + 9\lambda^2}$).

in terms of	λ	μ	E	ν	κ
λ, μ			$\frac{\mu(3\lambda + 2\mu)}{\lambda + \mu}$	$\frac{\lambda}{2(\lambda + \mu)}$	$\frac{3\lambda + 2\mu}{3}$
λ, E		$\frac{\varepsilon + (E - 3\lambda)}{4}$		$\frac{A^{+} - (E + \lambda)}{4\lambda}$	$\frac{\varepsilon + (3\lambda + E)}{6}$
λ, ν		$\frac{\lambda(1 - 2\nu)}{2\nu}$	$\frac{\lambda(1 + \nu)(1 - 2\nu)}{\nu}$		$\frac{\lambda(1 + \nu)}{3\nu}$
λ, κ		$\frac{3(\kappa - \lambda)}{2}$	$\frac{9\kappa(\kappa - \lambda)}{3\kappa - \lambda}$	$\frac{\lambda}{3\kappa - \lambda}$	
μ, E	$\frac{\mu(2\mu - E)}{E - 3\mu}$			$\frac{E - 2\mu}{2\mu}$	$\frac{\mu E}{3(3\mu - E)}$
μ, ν	$\frac{2\mu\nu}{1 - 2\nu}$		$2\mu(1 + \nu)$		$\frac{2\mu(1 + \nu)}{3(1 - 2\nu)}$
μ, κ	$\frac{3\kappa - 2\mu}{3}$		$\frac{9\kappa\mu}{3\kappa + \mu}$	$\frac{3\kappa - 2\mu}{2(3\kappa + \mu)}$	
E, ν	$\frac{\nu E}{(1 + \nu)(1 - 2\nu)}$	$\frac{E}{2(1 + \nu)}$			$\frac{E}{3(1 - 2\nu)}$
κ, E	$\frac{3\kappa(3\kappa - E)}{9\kappa - E}$	$\frac{3E\kappa}{9\kappa - E}$		$\frac{3\kappa - E}{6\kappa}$	
ν, κ	$\frac{3\kappa\nu}{1 + \nu}$	$\frac{3\kappa(1 - 2\nu)}{2(1 + \nu)}$	$3\kappa(1 - 2\nu)$		

1.5. ELASTIC GREEN FUNCTION

The Euler-Lagrange equation (1.54) can be used to calculate the distortion under an arbitrary external force field $f_i(\mathbf{x})$. Inserting the stress-strain relation (1.36), the displacements are seen to obey the second order differential equation

$$-c_{ijk\ell}\,\partial_j\,\partial_\ell\,u_k(\mathbf{x}) = f_i(\mathbf{x}). \tag{1.67}$$

For isotropic media we insert (1.23) and have the rotationally invariant equation,

$$[-\mu\,\partial^2\delta_{ij} - (\lambda+\mu)\,\partial_i\,\partial_j]u_j(\mathbf{x}) = f_i(\mathbf{x}). \tag{1.68}$$

This equation is easy to solve. First, we exploit translational invariance via the Fourier transformation

$$u_i(\mathbf{x}) = \int \frac{d^3q}{(2\pi)^3} e^{i\mathbf{q}\cdot\mathbf{x}} u_i(\mathbf{q}), \tag{1.69}$$

with

$$u_i(\mathbf{q}) \equiv \int d^3x\, e^{-i\mathbf{q}\cdot\mathbf{x}} u_i(\mathbf{x}) \tag{1.70}$$

and a similar relation between $f_i(\mathbf{x})$ and $f_i(\mathbf{q})$. Then (1.68) becomes a 3×3 matrix equation,

$$[\mu q^2\delta_{ij} + (\lambda+\mu)\,q_i q_j]u_j(\mathbf{q}) = f_i(\mathbf{q}). \tag{1.71}$$

The matrix can be inverted easily by introducing spin projection matrices, one with transversal and one with longitudinal character,

$$P^T(\hat{\mathbf{q}})_{ij} = \delta_{ij} - \hat{q}_i\hat{q}_j, \tag{1.72}$$

$$P^l(\hat{\mathbf{q}})_{ij} = \hat{q}_i\hat{q}_j, \tag{1.73}$$

where

$$\hat{\mathbf{q}} = \mathbf{q}/|\mathbf{q}| \tag{1.74}$$

is the direction in which the $\mathbf{q}$ vector points. These matrices are orthonormal, just as $P^{(2)}$, $P^{(0)}$ were in (1.29), only that matrix multiplication now involves just one index. If we now write (1.71) in the form

$$\mathbf{q}^2(\mu P^T + (\lambda + 2\mu) P^L)_{ij} u_j(\mathbf{q}) = f_i(\mathbf{q}) \tag{1.75}$$

we can immediately invert this as

$$u_i(\mathbf{q}) = G_{ij}(\mathbf{q}) f_j(\mathbf{q}) \tag{1.76}$$

with

$$\begin{aligned} G(\mathbf{q})_{ij} &= \frac{1}{\mathbf{q}^2}\left(\frac{1}{\mu} P^T + \frac{1}{\lambda + 2\mu} P^L\right)_{ij} = \frac{1}{\mu \mathbf{q}^4}\left[\mathbf{q}^2 \delta_{ij} - \frac{\lambda + \mu}{\lambda + 2\mu} q_i q_j\right] \\ &= \frac{1}{\mu \mathbf{q}^4}\left[\mathbf{q}^2 \delta_{ij} - \frac{1}{2(1 - \nu)} q_i q_j\right]. \end{aligned} \tag{1.77}$$

Going back to $\mathbf{x}$ space, (1.76) becomes

$$u_i(\mathbf{x}) = \int dy\, G_{ij}(\mathbf{x} - \mathbf{x}') f_j(\mathbf{x}'), \tag{1.78}$$

where

$$G_{ij}(\mathbf{x} - \mathbf{x}') = \int \frac{d^3q}{(2\pi)^3} e^{i\mathbf{q}\cdot(\mathbf{x} - \mathbf{x}')} G_{ij}(\mathbf{q}) \tag{1.79}$$

is called the Green function of the source equation (1.68), since it satisfies the differential equation

$$-c_{ijk\ell}\, \partial_j \partial_\ell\, G_{kn}(\mathbf{x} - \mathbf{x}') = \delta_{in}\, \delta(\mathbf{x} - \mathbf{x}'). \tag{1.80}$$

The Fourier integral can easily be performed. First of all, we recall that

$$\begin{aligned} \int \frac{d^3q}{(2\pi)^3} \frac{1}{q^2} e^{i\mathbf{q}\cdot(\mathbf{x} - \mathbf{x}')} &= \frac{2\pi}{(2\pi)^3} \int_0^\infty dq \int_{-1}^1 d\cos\theta\, e^{iqR\cos\theta} \\ &= \frac{1}{2\pi^2 R} \int_0^\infty \frac{dq}{q} \sin qR = \frac{1}{4\pi R} \end{aligned} \tag{1.81}$$

is the standard Coulomb Green's function [see Eq. (3.30), Part I] where R denotes again the distance between $\mathbf{x}$ and $\mathbf{x}'$,

$$R \equiv |\mathbf{R}| \equiv |\mathbf{x} - \mathbf{x}'|. \tag{1.82}$$

In addition, we need

$$\int \frac{d^3q}{(2\pi)^3} \frac{q_i q_j}{q^4} e^{i\mathbf{q}\cdot(\mathbf{x}-\mathbf{x}')}. \tag{1.83}$$

This can formally be written as

$$-\partial_i \partial_i \int \frac{d^3q}{(2\pi)^3} \frac{1}{q^4} e^{i\mathbf{q}\cdot(\mathbf{x}-\mathbf{x}')} \tag{1.84}$$

and the integral is just

$$\int \frac{d^3q}{(2\pi)^3} \frac{1}{q^4} e^{i\mathbf{q}\cdot(\mathbf{x}-\mathbf{x}')} = \frac{1}{2\pi^2 R} \int_0^\infty \frac{dq}{q^3} \sin qR, \tag{1.85}$$

which unfortunately cannot be performed due to the divergence at the origin. In fact, this divergence is not really there since a physical crystal always has a finite size so that the momentum integration does not go all the way down to $q = 0$. The Green function should not, however, depend on the crystal size. Indeed, it does not. In order to see this we separate out the divergent part by performing a subtraction,

$$\int_0^\infty \frac{dq}{q^3} \sin qR = \int_0^\infty \frac{dq}{q^3} (\sin qR - qR) + \int_0^\infty \frac{dq}{q^2} R. \tag{1.86}$$

The first, finite, integral is related to $\int_0^\infty \frac{dq}{q} \sin qR = \pi/2$ appearing in the Coulomb Green function (1.81) by two differentiations with respect to R. It vanishes at $R = 0$ together with its first derivative (which is all contained in the second part). Thus we can integrate $(-\pi/2)$ twice in R and find for the entire expression (1.86)

$$\int_0^\infty \frac{dq}{q^3} (\sin qR - qR) = -\frac{\pi}{4} R^2. \tag{1.87}$$

which implies that

$$\int \frac{d^3q}{(2\pi)^3}\frac{1}{q^4}e^{i\mathbf{q}\cdot(\mathbf{x}-\mathbf{x}')} = -\frac{R}{8\pi} + \frac{1}{2\pi^2}\int_0^\infty \frac{dq}{q^2}. \tag{1.88}$$

Inserting this into (1.84) we see that the divergent part does indeed cancel out and we obtain

$$\int \frac{d^3q}{(2\pi)^3}\frac{q_iq_j}{q^4}e^{i\mathbf{q}\cdot(\mathbf{x}-\mathbf{x}')} = \frac{1}{8\pi}\partial_i\partial_j R. \tag{1.89}$$

Therefore, the elastic Green function is

$$G_{ij}(\mathbf{x}-\mathbf{x}') = \frac{1}{8\pi\mu}\left(\delta_{ij}\nabla^2 R - \frac{\lambda+\mu}{\lambda+2\mu}\partial_i\partial_j R\right), \tag{1.90}$$

where we may insert $\nabla^2 R = 2/R$, $\partial_i\partial_j R = \delta_{ij}/R - R_iR_j/R^3$, if we want to be more explicit.

The full anisotropic equation (1.67) can, in principle, be solved in the following way. Denote the 3×3 matrix multiplying $u_k(\mathbf{x})$ by

$$D_{ik}(-i\nabla) \equiv -c_{ijk\ell}\,\partial_j\partial_\ell. \tag{1.91}$$

In momentum space, the coefficients have the form

$$\begin{aligned}
D_{11} &= c_{11}q_1^2 + c_{66}q_2^2 + c_{55}q_3^2 + 2c_{16}q_1q_2 + 2c_{56}q_2q_3 + 2c_{15}q_3q_1,\\
D_{12} &= c_{16}q_1^2 + c_{26}q_2^2 + c_{45}q_3^2 + (c_{12}+c_{66})q_1q_2 + (c_{25}+c_{46})q_2q_3\\
&\quad + (c_{14}+c_{56})q_3q_1,\\
D_{13} &= c_{15}q_1^2 + c_{46}q_2^2 + c_{35}q_3^2 + (c_{14}+c_{56})q_1q_2 + (c_{36}+c_{45})q_2q_3\\
&\quad + (c_{13}+c_{55})q_3q_1,\\
D_{22} &= c_{66}q_1^2 + c_{22}q_2^2 + c_{44}q_3^2 + 2c_{26}q_1q_2 + 2c_{24}q_2q_3 + 2c_{46}q_3q_1,\\
D_{23} &= c_{56}q_1^2 + c_{24}q_2^2 + c_{34}q_3^2 + (c_{25}+c_{46})q_1q_2 + (c_{23}+c_{44})q_2q_3\\
&\quad + (c_{36}+c_{45})q_3q_1,\\
D_{33} &= c_{55}q_1^2 + c_{44}q_2^2 + c_{33}q_3^2 + 2c_{45}q_1q_2 + 2c_{34}q_2q_3 + 2c_{35}q_3q_1.
\end{aligned} \tag{1.92}$$

The inverse of $D_{ij}(\mathbf{q})$ is given by

$$D_{ij}^{-1}(\mathbf{q}) = M_{ij}(\mathbf{q})\frac{1}{|D(\mathbf{q})|}, \tag{1.93}$$

where $M_{ij}(\mathbf{q})$ are the cofactors of the 3×3 matrix associated with the elements D_{ij}, i.e.,

$$M_{ij}(\mathbf{q}) = \varepsilon_{jpq}\,\varepsilon_{imn} D_{pm}(\mathbf{q})\, D_{qn}(\mathbf{q}). \tag{1.94}$$

The determinant is a polynomial of sixth order in q. In the isotropic case

$$\begin{aligned} D(\mathbf{q}) &= \mu^2(\lambda + 2\mu)q^6, \\ M_{ij}(\mathbf{q}) &= \mu(\lambda + 2\mu)q^2[q^2\delta_{ij} - ((\lambda + \mu)/(\lambda + 2\mu))q_i q_j]. \end{aligned} \tag{1.95}$$

Consider now the vector

$$v_i(\mathbf{q}) \equiv \frac{1}{|D(\mathbf{q})|} f_i(\mathbf{q}).$$

From it, the displacements are found to be

$$u_i(\mathbf{q}) = M_{ij}(\mathbf{q})\, v_i(\mathbf{q}) = M_{ij}(\mathbf{q})\frac{1}{|D(\mathbf{q})|} f_i(\mathbf{q}), \tag{1.96}$$

so that $M_{ij}(\mathbf{q})/|D(\mathbf{q})|$ is the desired Green function in momentum space. For a general discussion see Every's paper quoted in the Notes and References. Due to the complexity of the expression (1.96) it is, in general, very difficult to go back to $\mathbf{x}$ space. One would have to calculate

$$G(\mathbf{x} - \mathbf{x}') = \int \frac{d^3q}{(2\pi)^3} e^{i\mathbf{q}\cdot(\mathbf{x} - \mathbf{x}')} \frac{1}{|D(\mathbf{q})|} \tag{1.97a}$$

and find $u_i(\mathbf{x})$ from

$$u_i(\mathbf{x}) = M_{ij}\left(\frac{1}{i}\nabla\right) \int d^3x'\, G(\mathbf{x} - \mathbf{x}') f_j(\mathbf{x}'). \tag{1.97b}$$

Only for cubic and hexagonal symmetry is the solution relatively simple. In the isotropic case,

$$G(\mathbf{x}-\mathbf{x}') = \frac{1}{\mu^2(\lambda+2\mu)}\int \frac{d^3q}{(2\pi)^3} e^{i\mathbf{q}\cdot(\mathbf{x}-\mathbf{x}')}\frac{1}{q^6}$$

$$= \frac{1}{\mu^2(\lambda+2\mu)}\frac{1}{96\pi}|\mathbf{x}-\mathbf{x}'|^3. \tag{1.98}$$

In the cubic case, the equations in momentum space,

$$D_{ik}\,u_k(\mathbf{q}) = f_i(\mathbf{q}), \tag{1.99}$$

take the form

$$D_{ik}\,u_k(\mathbf{q}) = (\mu+\lambda)q_i(\mathbf{q}\cdot\mathbf{u}) + (\mu\mathbf{q}^2 + \varepsilon q_i^2)u_i(\mathbf{q})$$

$$= f_i(\mathbf{q}), \quad \text{(no sum over } i\text{)}, \tag{1.100}$$

where we have introduced another anisotropy parameter

$$\varepsilon \equiv c_{11} - c_{12} - 2c_{44}, \tag{1.101}$$

which is related to the previous ξ via

$$\varepsilon = 2\mu(\xi - 1). \tag{1.102}$$

From (1.100) we see that

$$u_i(\mathbf{q}) = \frac{1}{\mu\mathbf{q}^2 + \varepsilon q_i^2}(f_i - (\mu+\lambda)q_i(\mathbf{q}\cdot\mathbf{u})). \tag{1.103}$$

On the other hand, dividing (1.100) by q_i and summing over i gives

$$(\mathbf{q}\cdot\mathbf{u}) = \frac{1}{3(\mu+\lambda)+\varepsilon}$$

$$\times\left[\sum_i \frac{f_i}{q_i} - \mu\mathbf{q}^2\sum_i \frac{1}{q_i}\frac{1}{\mu\mathbf{q}^2+\varepsilon q_i^2}(f_i - (\mu+\lambda)q_i(\mathbf{q}\cdot\mathbf{u}))\right].$$

From this we find

$$(\mathbf{q}\cdot\mathbf{u}) = \frac{1}{\left(3 + \dfrac{\varepsilon}{\mu+\lambda} - \mu\mathbf{q}^2\displaystyle\sum_j \frac{1}{\mu\mathbf{q}^2+\varepsilon q_j^2}\right)}\frac{\varepsilon}{\mu+\lambda}\sum_j \frac{f_j q_j}{\mu\mathbf{q}^2+\varepsilon q_j^2}.$$

Reinserting this into (1.103) yields

$$u_i(\mathbf{q}) = \left\{ a_i \delta_{ij} - \varepsilon q_i q_j a_i a_j \Big/ [3 + \varepsilon/(\mu + \lambda) - \mu \mathbf{q}^2 \sum_k a_k] \right\} f_j(\mathbf{q})$$

where

$$a_i \equiv 1/(\mu \mathbf{q}^2 + \varepsilon q_i^2). \tag{1.104}$$

The right-hand side displays the desired inverse matrix $G_{ij}(\mathbf{q}) = D^{-1}(\mathbf{q})_{ij}$. In the isotropic limit it reduces to (1.77). If the anistropy is small, one may use the approximate expression [compare (1.98)]

$$G(\mathbf{x} - \mathbf{x}') = \frac{(c_{11} c_{44}^2)^{-1}}{96\pi} |\mathbf{x} - \mathbf{x}'|^3. \tag{1.105}$$

Actually, the external force problem will not be of direct interest in our further discussion and was presented here mainly in order to give some insight into the structure of the differential equations associated with the stress problem. From now on, we shall only be concerned with the so-called internal stress problem in which there are no external body forces, i.e., $f_i(\mathbf{x}) = 0$. As a consequence, the stress tensor is always divergenceless,

$$\partial_i \sigma_{ij} = \partial_j \sigma_{ij} = 0. \tag{1.106}$$

1.6. TWO-DIMENSIONAL ELASTICITY

It will sometimes be useful to study the simplified situation of a two-dimensional crystal. In nature, such crystals do not really exist. It is nevertheless possible to prepare certain limiting systems which, to a certain approximation, behave like two-dimensional systems. Examples are monolayers of helium, xenon, argon, krypton, or methane on smooth graphite surfaces. We shall give more details about such systems later in Chapters 7 and 14.

In two dimensions, there are only three strain components u_{11}, u_{22}, u_{12} and six elastic constants c_{ab} with a, b running through, say, 1, 2, 4. For square lattices, there are again three independent c_{ab}'s (c_{11}, c_{12}, c_{44}) and the elastic energy density has the form [compare (1.16)]

$$e(\mathbf{x}) = \tfrac{1}{2}c_{11}(u_{11}^2 + u_{22}^2) + c_{12}u_{11}u_{22} + 2c_{44}u_{12}^2. \tag{1.107}$$

In the isotropic case this reduces to

$$e(\mathbf{x}) = \mu u_{ij}^2 + \frac{\lambda}{2}u_{ii}^2. \tag{1.108}$$

The stress tensor is given by

$$\sigma_{11} = c_{11}u_{11} + c_{12}u_{22}, \quad \sigma_{22} = c_{12}u_{11} + c_{22}u_{22}, \quad \sigma_{12} = 4c_{44}u_{12}, \tag{1.109}$$

so that

$$e(\mathbf{x}) = \frac{1}{4\mu}\left[2\sigma_{12}^2 + \frac{1}{\xi}(\sigma_{11}^2 + \sigma_{22}^2) - \frac{1}{\gamma}(\sigma_{11} + \sigma_{22})^2\right], \tag{1.110}$$

where $\gamma = \xi(2\xi(c_{44}/c_{12}) + 2)$ [in D dimensions, $\gamma = \xi(2\xi(c_{44}/c_{12}) + D) \equiv D\xi\kappa/\lambda$]. In the isotropic case [when $\xi = (c_{11} - c_{12})/2c_{44} = 1$, $c_{44} = \mu$, $c_{12} = \lambda$, $c_{11} = 2\mu + \lambda$]

$$\sigma_{ij} = 2\mu u_{ij} + \lambda\delta_{ij}u_{\ell\ell} \tag{1.111}$$

and

$$\sigma_{\ell\ell} = (2\mu + 2\lambda)u_{\ell\ell} \equiv 2\kappa u_{\ell\ell},$$

so that the modulus of compression is

$$\kappa = \mu + \lambda \tag{1.112}$$

[in D dimensions, $\kappa \equiv (2\mu + D\lambda)/D$]. The inverse relation of (1.111) is

$$u_{ij} = \frac{1}{2\mu}\left(\sigma_{ij} - \frac{\lambda}{4\mu\kappa}\delta_{ij}\sigma_{kk}\right), \tag{1.113}$$

and we find the Poisson ratio, as in (1.56), by setting only $\sigma_{11} \neq 0$ and calculating

$$u_{11} = \frac{1}{2\mu}\left(1 - \frac{\lambda}{2\kappa}\right)\sigma_{11}, \qquad u_{22} = -\frac{\lambda}{2\kappa}\sigma_{11}. \tag{1.114}$$

Hence

$$\nu = -\frac{u_{22}}{u_{11}} = \frac{\lambda}{2\kappa - \lambda} = \frac{\lambda}{2\mu + \lambda} \tag{1.115}$$

[in D dimensions $\nu = \lambda/(2\mu + (D-1)\lambda)$]. With this ν, $\lambda/2\kappa = \nu/(1+\nu)$ and the energy has the same stress form (1.43) as in three dimensions.

Since (1.68) is the same in all dimensions, the elastic Green's function in momentum space for isotropic materials is always

$$G_{ij}(\mathbf{q}) = \frac{1}{\mu \mathbf{q}^4}\left[\mathbf{q}^2\delta_{ij} - \frac{\lambda+\mu}{\lambda+2\mu}q_i q_j\right]. \tag{1.116}$$

Let us study this function in $\mathbf{x}$ space. First we form the Fourier transform of $1/\mathbf{q}^4$

$$v_4(\mathbf{x}) = \int \frac{d^2q}{(2\pi)^2} e^{i\mathbf{q}\cdot\mathbf{x}} \frac{1}{q^4}. \tag{1.117}$$

This integral is even more divergent than the three-dimensional case (1.88). Since the infinities are due to the small q region of $1/q^4$, we introduce a small regulator mass δ and express $v_4(\mathbf{x})$ in terms of the two-dimensional Yukawa potential [recall (6.105), (6.119) of Part I]

$$v_\delta(\mathbf{x}) = \int \frac{d^2q}{(2\pi)^2} e^{i\mathbf{q}\cdot\mathbf{x}} \frac{1}{q^2+\delta^2} = \frac{1}{2\pi} K_0(\delta|\mathbf{x}|), \tag{1.118}$$

namely,

$$v_4(\mathbf{x}) = \lim_{\delta\to 0}\left(-\frac{\partial}{\partial\delta^2} v_\delta(\mathbf{x})\right) = -\frac{|\mathbf{x}|}{2\delta}\frac{\partial}{\partial(\delta|\mathbf{x}|)} v_\delta(\mathbf{x}) = -\frac{|\mathbf{x}|}{2\delta}\frac{\partial}{\partial(\delta|\mathbf{x}|)}\frac{1}{2\pi} K_0|\delta|\mathbf{x}|). \tag{1.119}$$

For small $|\mathbf{x}|$, $K_0(\delta|\mathbf{x}|)$ can be expanded, using the well-known series

$$\begin{aligned} K_0(z) &= -\log\left(\frac{1}{2}z e^{\gamma}\right) I_0(z) + \frac{1}{4}z^2 + \dots \\ &\approx -\log\left(\frac{1}{2}z e^{\gamma}\right)\left(1 + \frac{z^2}{4}\right) + \frac{z^2}{4} + O(z^4 \log z). \end{aligned}$$

Hence

$$K_0'(z) = -\frac{1}{z} - \log\left(\frac{z}{2}e^{\gamma}\right)\frac{z}{2} + \frac{z}{4} + \dots \tag{1.120}$$

and

$$\begin{aligned} v_4(\mathbf{x}) &= -\frac{1}{2\pi}\frac{|\mathbf{x}|}{2\delta}\left[-\frac{1}{\delta|\mathbf{x}|} - \frac{\delta|\mathbf{x}|}{2}\left(\log|\mathbf{x}| + \log\left(\frac{\delta}{2}e^{\gamma}\right) - \frac{1}{2}\right)\right] \\ &= \frac{1}{4\pi\delta^2} + \frac{|\mathbf{x}|^2}{8\pi}\left(\log\left(\frac{\delta}{2}e^{\gamma}\right) - \frac{1}{2}\right) + \frac{|\mathbf{x}|^2}{8\pi}\log|\mathbf{x}| + \dots \end{aligned} \tag{1.121}$$

The first two terms diverge for $\delta \to 0$. For some purposes it will be useful to introduce the subtracted potential

$$v_4'(\mathbf{x}) = v_4(\mathbf{x}) - v_4(\mathbf{0}) = \frac{|\mathbf{x}|^2}{8\pi}\left(\log\left(\frac{\delta}{2}e^{\gamma}\right) - \frac{1}{2}\right) + \frac{|\mathbf{x}|^2}{8\pi}\log|\mathbf{x}|,$$

which has no quadratic divergence, and a further subtracted version

$$v_4''(\mathbf{x}) = v_4'(\mathbf{x}) - |\mathbf{x}|^2 v_4'(\mathbf{1}) = \frac{|\mathbf{x}|^2}{8\pi}\log(\mathbf{x}), \tag{1.122}$$

which is completely finite.

From (1.121) it is easy to derive the longitudinal Green function[c]

$$\begin{aligned} v_{ij}^L(\mathbf{x}) &= \lim_{\delta\to 0}\int \frac{d^2q}{(2\pi)^2}e^{i\mathbf{q}\cdot\mathbf{x}}\frac{q_iq_j}{(q^2+\delta^2)^2} = -\partial_i\partial_j v_4(\mathbf{x}) \\ &= \lim_{\delta\to 0}\left(-\frac{1}{4\pi}\delta_{ij}\log\left(\frac{\delta}{2}e^{\gamma}\right)\right) - \frac{1}{4\pi}\left(\delta_{ij}\log|\mathbf{x}| + \frac{x_ix_j}{|\mathbf{x}|^2}\right), \end{aligned} \tag{1.123}$$

as well as the transverse one

[c]Notice that

$$v_{ii}^L(\mathbf{x}) + \delta^2 v_4(\mathbf{x}) = -\frac{1}{2\pi}\left(\log\left(\frac{\delta}{2}e^{\gamma}\right) + \log|\mathbf{x}|\right) = \int\frac{d^2q}{2\pi}e^{i\mathbf{q}\cdot\mathbf{x}}\frac{1}{q^2+\delta^2} = v_2(\mathbf{x}) = \frac{1}{2\pi}K_0(\delta|\mathbf{x}|),$$

as it should. Also $v_{ii}^T(\mathbf{x}) = v_{ii}^L(\mathbf{x})$.

$$v_{ij}^T(\mathbf{x}) = \lim_{\delta\to 0}\int \frac{d^2q}{(2\pi)^2} e^{i\mathbf{q}\cdot\mathbf{x}} \frac{\delta_{ij}q^2 - q_iq_j}{(q^2+\delta^2)^2} = -(\delta_{ij}\nabla^2 - \partial_i\partial_j)v_4(\mathbf{x})$$
$$= -\frac{1}{4\pi}\left(\log\left(\frac{\delta}{2}e^{\gamma}\right)+1\right)\delta_{ij} - \frac{1}{4\pi}\left(\delta_{ij}\log|\mathbf{x}| - \frac{x_ix_j}{|\mathbf{x}|^2}\right). \quad (1.124)$$

Then the Green function is

$$G_{ij}(\mathbf{x}) = \frac{1}{\mu}v_{ij}^T(\mathbf{x}) + \frac{1}{\lambda+2\mu}v_{ij}^L(\mathbf{x})$$
$$= -\frac{1}{\mu}\frac{1}{4\pi}\left[\delta_{ij}\frac{\lambda+3\mu}{\lambda+2\mu}\left(\log\left(|\mathbf{x}|\frac{\delta}{2}e^{\gamma}\right)+\frac{1}{2}\right) - \frac{\lambda+\mu}{\lambda+2\mu}\left(\frac{1}{2}\delta_{ij} - \frac{x_ix_j}{\mathbf{x}^2}\right)\right]. \quad (1.125)$$

APPENDIX 1A. THE SYMMETRY CLASSES OF THE ELASTIC MATRIX

The 32 crystal classes associated with the different point groups are given in Table 1.2. For these, the matrices c_{ab} fall into the following 9 symmetry classes.

1. *Cubic, all five classes*:

$$c_{ab} = \left(\begin{array}{ccc|ccc} c_{11} & c_{12} & c_{12} & & & \\ & c_{11} & c_{12} & & 0 & \\ & & c_{11} & & & \\ \hline & & & c_{44} & & \\ & 0 & & & c_{44} & \\ & & & & & c_{44} \end{array}\right), \quad 3 \text{ constants.} \quad (1A.1)$$

2a. *Tetragonal* $\bar{4}$, 4, $\frac{4}{m}$:

$$c_{ab} = \left(\begin{array}{ccc|ccc} c_{11} & c_{12} & c_{13} & 0 & 0 & c_{16} \\ & c_{11} & c_{13} & 0 & 0 & -c_{16} \\ & & c_{33} & 0 & 0 & 0 \\ \hline & & & c_{44} & & \\ & 0 & & & c_{44} & \\ & & & & & c_{66} \end{array}\right), \quad 7 \text{ constants.} \quad (1A.2)$$

2b. *Tetragonal* $\bar{4}2m$, *4mm*, *422*, $\frac{4}{m}\frac{2}{m}\frac{2}{m}$:

$$c_{ab} = \left(\begin{array}{ccc|ccc} c_{11} & c_{12} & c_{13} & & & \\ & c_{11} & c_{13} & & 0 & \\ & & c_{33} & & & \\ \hline & & & c_{44} & & \\ & 0 & & & c_{44} & \\ & & & & & c_{66} \end{array}\right), \quad 6 \text{ constants.} \tag{1A.3}$$

3. *Hexagonal, all seven classes*:

$$c_{ab} = \left(\begin{array}{ccc|ccc} c_{11} & c_{12} & c_{13} & & & \\ & c_{11} & c_{13} & & 0 & \\ & & c_{33} & & & \\ \hline & & & c_{44} & & \\ & 0 & & & c_{44} & \\ & & & & & \tfrac{1}{2}(c_{11}-c_{12}) \end{array}\right), \quad 5 \text{ constants.} \tag{1A.4}$$

4a. *Trigonal*, $\bar{3}$, *3*:

$$c_{ab} = \left(\begin{array}{ccc|ccc} c_{11} & c_{12} & c_{13} & c_{14} & -c_{25} & 0 \\ & c_{11} & c_{13} & -c_{14} & c_{25} & 0 \\ & & c_{33} & 0 & 0 & 0 \\ \hline & & & c_{44} & 0 & c_{25} \\ & 0 & & & c_{44} & c_{14} \\ & & & & & \tfrac{1}{2}(c_{11}-c_{12}) \end{array}\right), \quad 7 \text{ constants.} \tag{1A.5}$$

4b. *Trigonal*, $3m\ell$, 32ℓ, $\bar{3}\frac{2}{m}\ell$:

$$c_{ab} = \left(\begin{array}{ccc|ccc} c_{11} & c_{12} & c_{13} & c_{14} & 0 & 0 \\ & c_{11} & c_{13} & -c_{14} & 0 & 0 \\ & & c_{33} & 0 & 0 & 0 \\ \hline & & & c_{44} & 0 & 0 \\ & 0 & & & c_{44} & c_{14} \\ & & & & & \tfrac{1}{2}(c_{11}-c_{12}) \end{array}\right), \quad 6 \text{ constants.} \tag{1A.6}$$

5. *Orthorombic, all three classes*:

$$c_{ab} = \left(\begin{array}{ccc|ccc} c_{11} & c_{12} & c_{13} & & & \\ & c_{22} & c_{23} & & 0 & \\ & & c_{33} & & & \\ \hline & & & c_{44} & 0 & 0 \\ & 0 & & & c_{55} & 0 \\ & & & & & c_{66} \end{array}\right), \quad 9 \text{ constants.} \tag{1A.7}$$

6. *Monoclinic, all three classes*:

$$c_{ab} = \left(\begin{array}{ccc|ccc} c_{11} & c_{12} & c_{13} & 0 & c_{15} & 0 \\ & c_{22} & c_{23} & 0 & c_{25} & 0 \\ & & c_{33} & 0 & c_{35} & 0 \\ \hline & & & c_{44} & 0 & c_{46} \\ & 0 & & & c_{55} & 0 \\ & & & & & c_{66} \end{array}\right), \quad 13 \text{ constants.} \tag{1A.8}$$

7. *Triclinic, both classes*:

All 21 elements of the matrix c_{ab} are independent. In a crystal lattice in which all atoms interact with central force only, and every atom is a center of symmetry, elastic constants satisfy Cauchy's relations $c_{ijkl} = c_{ikjl}$:

$$\begin{aligned} c_{23} &= c_{44}, & c_{31} &= c_{55}, & c_{12} &= c_{66}, \\ c_{14} &= c_{56}, & c_{25} &= c_{64}, & c_{36} &= c_{45}. \end{aligned}$$

They reduce the 21 independent constants to 15.

Just as in the isotropic case, the elastic constants can be measured by looking at the response to certain mechanical deformations. In the absence of symmetry, the crystal has to be subjected to a large number of different stresses in orders to measure all independent matrix elements c_{ab}. The most accurate information on the elastic constants comes from the measurements of sound velocities in different directions. The equation of motion of sound waves are obtained by equating $f_i(\mathbf{x})$ in (1.54) with the inertial force $-\rho\ddot{u}_i(\mathbf{x}, t)$ where ρ is the mass density. Then (1.91) becomes

$$-\rho\ddot{u}_i(\mathbf{x}, t) = D_{ij}\left(\frac{1}{i}\nabla\right)u_j(\mathbf{x}, t). \tag{1A.9}$$

With the ansatz $u_i(\mathbf{x}) \propto e^{i(\mathbf{q}\cdot\mathbf{x} - \omega t)}$, the sound velocity $v(\mathbf{q})$ is given by

$$\det(\rho\mathbf{q}^2v^2\delta_{ij} - D_{ij}(\mathbf{q})) = 0. \tag{1A.10}$$

For cubic symmetry and sound waves in the (1,0,0) direction this gives

$$\rho v_\ell^2 = c_{11}, \qquad \rho v_{t_{1,2}}^2 = c_{44}, \tag{1A.11}$$

for the one longitudinal and the two transverse polarizations. In the (1,1,0) direction,

$$\rho v_\ell^2 = \tfrac{1}{2}(c_{11} + c_{12} + 2c_{44}), \quad \rho v_{t_1}^2 = c_{44}, \quad \rho v_{t_2}^2 = \tfrac{1}{2}(c_{11} - c_{12}). \tag{1A.12}$$

In the (1,1,1) direction,

$$\rho v_\ell^2 = \tfrac{1}{3}(c_{11} + 2c_{12} + 4c_{44}), \qquad \rho v_{t_{1,2}}^2 = \tfrac{1}{3}(c_{11} - c_{12} + c_{44}). \tag{1A.13}$$

If only nearest and next nearest neighbours interact with harmonic springs of potential $(\alpha_1/2)x^2$, $(\alpha_2/2)x^2$, respectively, the elastic constants are

$$c_{44} = c_{12} = \frac{\alpha_2}{a}, \quad c_{11} = \frac{\alpha_1 + \alpha_2}{a}, \qquad \text{s.c.}, \tag{1A.14}$$

$$c_{44} = c_{12} = \frac{\alpha_1}{a}, \quad c_{11} - c_{12} - c_{44} = \frac{4\alpha_2}{a}, \qquad \text{f.c.c.}, \tag{1A.15}$$

$$c_{44} = c_{12} = \frac{2}{3}\frac{\alpha_1}{a}, \quad c_{11} - c_{12} = \frac{2\alpha_2}{a}, \qquad \text{b.c.c.}, \tag{1A.16}$$

NOTES AND REFERENCES

For an introduction into linear elasticity see any standard textbook on elasticity, for example,

L.D. Landau and E.M. Lifshitz, *Theory of Elasticity* (Pergamon Press, New York, 1970),
W. Voigt, *Lehrbuch der Kristallphysik* (Teubner, Leipzig, 1928), and also
A. Reuss, *Z. Angew. Math. Mech.* **9** (1929) 49,
J.P. Hirth and J. Lothe, *Theory of Dislocations* (McGraw-Hill, New York, 1968).

The anisotropic case is also treated in
W.P. Mason, *Piezoelectric Crystals and Their Application to Ultrasonics* (Van Nostrand, New York, 1950).
See also the discussion of
E. Kröner, in *The Physics of Defects*, eds. R. Balian *et al.* (North-Holland, Amsterdam, 1981) p. 264.
The elastic Green function for arbitrary symmetry classes was given by
A.G. Every, *Phys. Rev.* **B22** (1980) 1746.
For a derivation of Cauchy's relations see M. Born and K. Huang. *Dynamical Theory of Crystal Lattices (Clarendon, Oxford, 1954).*

CHAPTER TWO

LINE-LIKE DEFECTS IN CRYSTALS

2.1. GENERAL REMARKS

The question arises whether there can exist nontrivial distortions of a crystal if we remove all external body forces. At first sight, Eq. (1.54) is solved uniquely by $u_i(\mathbf{x}) \equiv 0$ and the discussion is apparently finished. This conclusion would be correct if we were to allow only for smooth field configurations. Such a requirement would be too restrictive, however, and could not account for many of the phenomena observed in actual crystals.

No crystal produced in the laboratory is perfect. It always contains a great number of defects. These may be chemical, electrical, or structural in character, i.e., there may be foreign atoms, excess or missing electrons, or the crystal symmetry may be destroyed locally.

In the present context we shall be interested only in the structural defects of the intrinsic type, i.e., with no foreign atoms involved. They may be classified according to their space dimensionality. The simplest type of defect is the point defect. It is characterized by the fact that within a certain finite neighbourhood only one cell shows a drastic deviation from the perfect crystal symmetry. The most frequent origin of such point defects is irradiation or an isotropic mechanical deformation under strong shear stresses. We have noted in the Introduction that there are two types of intrinsic point defects. Either an atom may be missing from its regular lattice site (vacancy) or there may be an excess atom (interstitial) (see

FIG. 2.1. Intrinsic point defects in a crystal. An atom may become interstitial, leaving behind a vacancy. It may perform random motion via interstitial places until it reaches another vacancy where it recombines. The exterior of the crystal may be seen as a reservoir of vacancies.

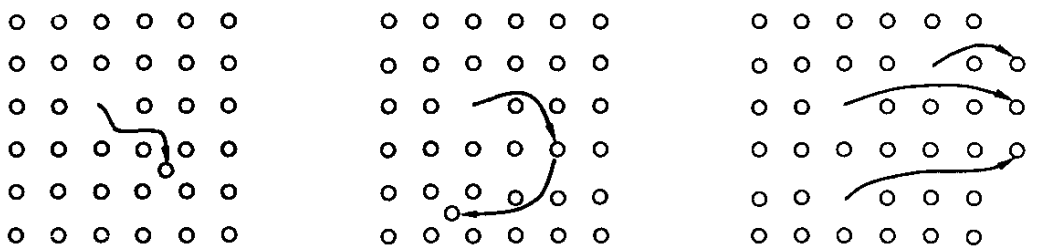

Fig. 2.1). Vacancies and interstitials are mobile defects. A vacancy can move if a neighboring atom moves into its place, leaving a vacancy at its own former position. An interstitial atom can move in two ways. It may hop directly from one interstitial site to another. This happens in strongly anisotropic materials such as graphite but also in some cubic materials like Si or Ge. Or it may move in a way more similar to the vacancies by replacing atoms, i.e., by pushing a regular atom out of its place into an interstitial position which, in turn, affects the same change on its neighbor, etc.

The thermal creation of point defects is suppressed by their large activation energies. For vacancies this is lower than for interstitials, with the following typical values:

$$\begin{aligned} &\text{Cu}: 0.8 - 1.0\,\text{eV},\\ &\text{Ag}: 0.6 - 0.9\,\text{eV},\\ &\text{Au}: 0.6 - 0.8\,\text{eV},\\ &\text{Li}\ : 0.55\,\text{eV},\\ &\text{Cs}\ : 0.26\,\text{eV}. \end{aligned}$$

The concentration $c = n/N$ of point defects per regular atoms is governed by Boltzmann's law $c = e^{-E/T}$. Since 1 eV corresponds to 11 600 K, there are about 1% vacancies at 1000 K.

For interstitial atoms, the formation energies lie in the range of $3 - 6$ eV which makes them even rarer. In practical terms this means that in thermal equilibrium a crystal contains at most some vacancies. If interstitial atoms are found they are usually remnants of irradiation or mechanical deformation which have not had time to return to an equilibrium position.

Point defects have the property that if a number of them move close together, the total energy becomes smaller than the sum of the individual energies. The reason for this is easily seen. If two vacancies in a simple

FIG. 2.2. Formation of a dislocation line (of the edge type) from a disc of missing atoms. The atoms above and below the missing ones have moved together and repaired the defect, except at the boundary.

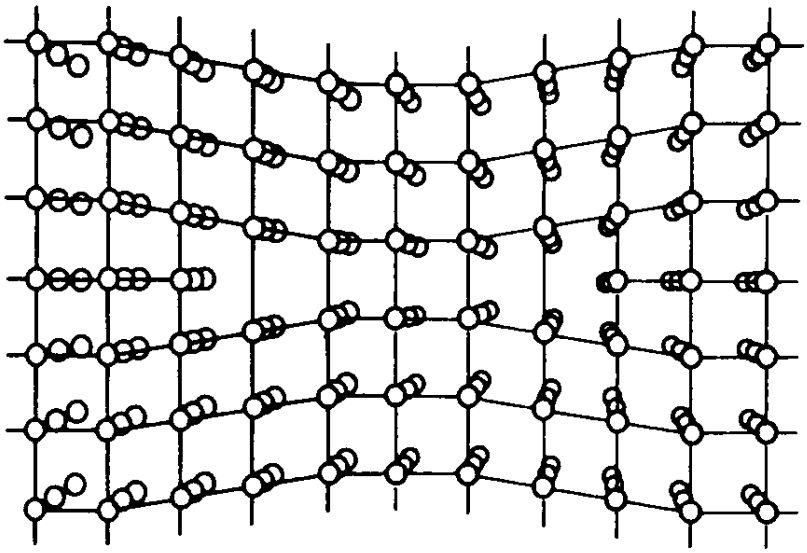

edge dislocation

cubic lattice come to lie side by side, there are only 10 broken valencies compared to 12 when they are separated. If a larger set of vacancies comes to lie side by side forming an entire disc of missing atoms, the crystal planes can move together and make the disc disappear (see Fig. 2.2). In this way, the crystal structure is repaired. Only close to the boundary line is such a repair impossible. The boundary line forms a line-like defect.

Certainly, line-like defects can arise also in the opposite process of clustering of interstitial atoms. If they accumulate side by side forming an interstitial disc, the crystal planes move apart and accommodate the additional atoms in a regular atomic array, again with the exception of the boundary line. Line-like defects of this type are called *dislocation lines*.

It is obvious that a dislocation line need not only consist of a single disc of missing or excessive atoms. There can be several discs stacked on top of each other. Their boundary forms a dislocation line of higher strength. The energy of such a higher dislocation line increases roughly with the square of the strength. Dislocations are created and set into motion if stresses exceed certain critical values. This is why they were first seen in plastic deformation experiments of the nineteenth century in the form of slip bands. The grounds for their theoretical understanding were laid much later by Frenkel who postulated the existence of crystalline defects in order to explain theoretically why materials yield to plastic shear about a thousand times more easily than one might expect on the basis of a naive estimate.

This estimate goes as follows. Suppose shear is applied to a crystal

FIG. 2.3. A naive argument concerning the maximal stress supported by a crystal under shear stress as indicated by the arrows. The two halves tend to slip against each other. Assuming a periodic behavior $\sigma = \sigma_{\max} \sin(2\pi x/a)$, this reduces to $\sigma \sim \sigma_{\max} 2\pi(x/a) \sim \mu(x/a)$. Hence $\sigma_{\max} = \mu/2\pi$. Experimentally, however, $\sigma_{\max} \sim 10^{-3}\mu$ to $10^{-4}\mu$.

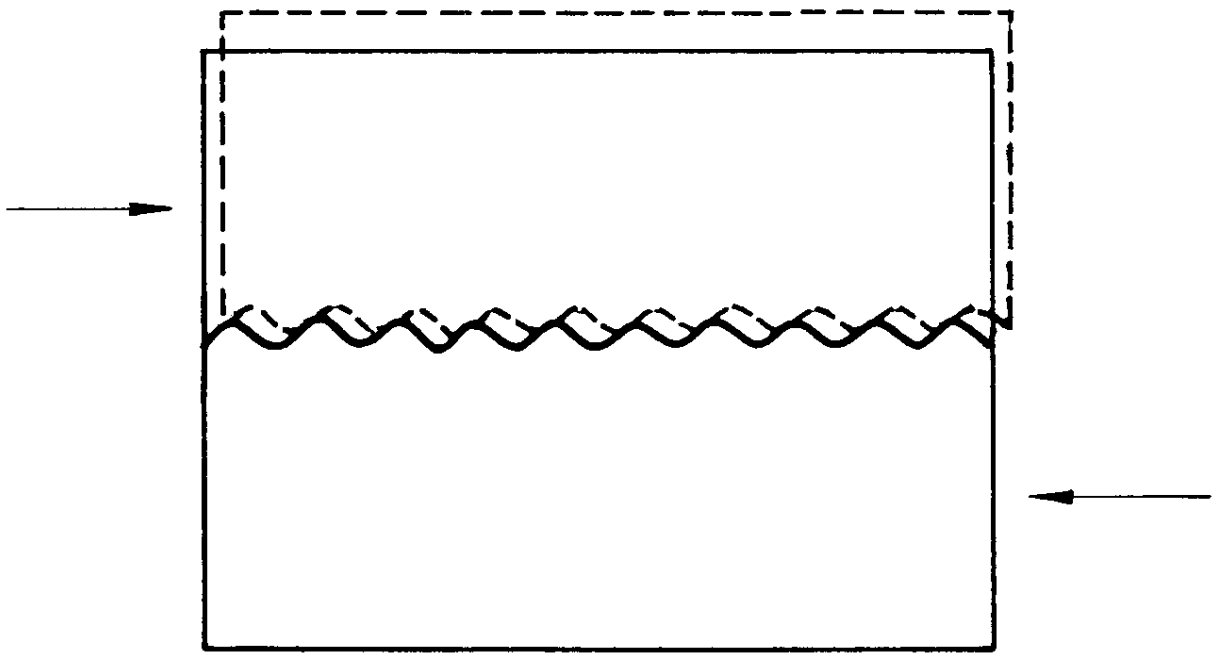

along the arrows in Fig. 2.3. We may imagine the material to consist of two continuous halves touching each other along a periodically undulated surface, to account for the crystal structure. The resistance to shear can then be parametrized by some periodic function in the displacement x of the top half against the bottom half since, if x is a multiple of the lattice spacing a, the pieces fit perfectly and there is no stress. If we choose to parametrize this periodic behaviour in a sinusoidal way, for simplicity, we may write roughly

$$\sigma \approx \sigma_{\max} \sin 2\pi x/a,$$

where $\sigma_{\max}$ is the maximal stress which the intertwined surfaces can support. For $x \ll a$,

$$\sigma \approx \sigma_{\max} 2\pi x/a.$$

But x/a corresponds to the strain of this deformation so that by Hooke's law the maximal stress is related to the shear modulus by

$$\sigma_{\max} = \mu/2\pi.$$

Experimentally, however, $\sigma_{\max}$ is much smaller, i.e.,

FIG. 2.4. A dislocation line permits the two crystal pieces to move across each other in the same way as a caterpillar moves through the ground. The bonds can flip direction successively which is a rather easy process.

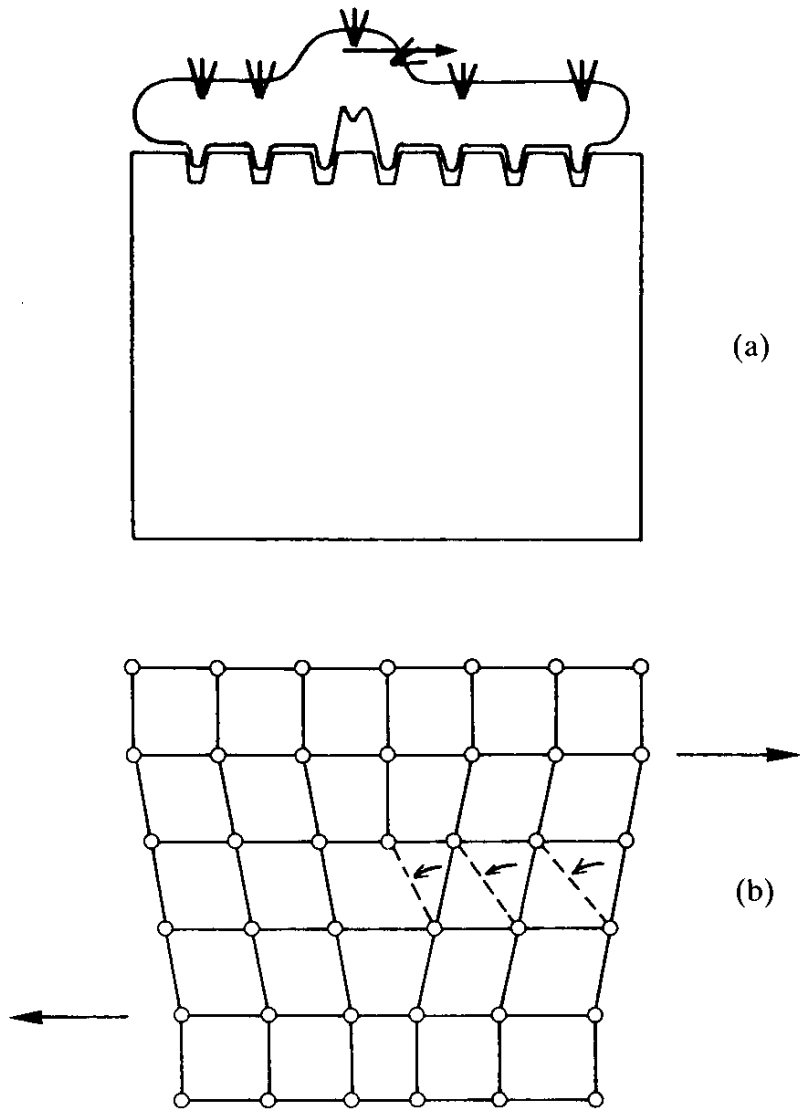

$$\sigma_{max} \sim 10^{-3} - 10^{-4}\mu.$$

Thus something in the argument must be wrong and Frenkel concluded that the plastic slip must proceed not by the two halves moving against each other as a whole but stepwise, by means of defects. In 1934, Orowan, Polanyi and Taylor recognized these defects as dislocation lines. The presence of a single moving edge dislocation allows for a plastic shear movement of the one crystal half against the other. The movement proceeds in the same way as that of a caterpiller. This is pictured in Fig. 2.4. One leg is always in the air breaking translational invariance and this is exchanged against the one in front of it, etc. In the crystal shown in the lower part of Fig 2.4, the single leg corresponds to the lattice plane of excess atoms. Under stress along the arrows, this moves to the right.

FIG. 2.5. Formation of a disclination from a stack of layers of missing atoms (cf. Fig. 2.2). Equivalently, one may cut out an entire section of the crystal. In a real crystal, the section has to conform with the symmetry angles. In the continuum approximation, the angle Ω is meant to be very small.

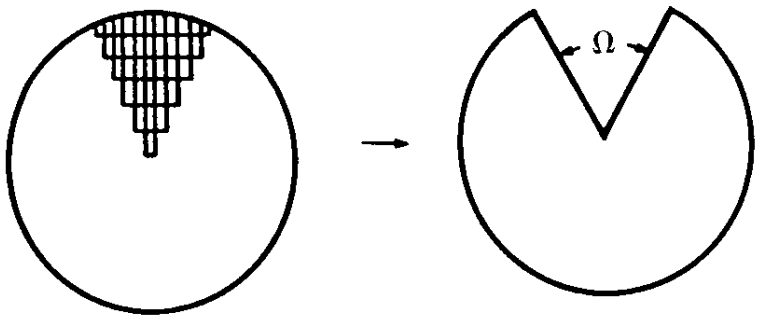

After a complete sweep across the crystal, the upper half is shifted against the lower by precisely one lattice spacing.

If many discs of missing or excess atoms come to lie close together there exists a further cooperative phenomenon. This is illustrated in Fig. 2.5. On the left-hand side, an infinite number of atomic half planes (discs of semi-infinite size) has been removed from an ideal crystal. If the half planes themselves form a regular crystalline array, they can fit smoothly into the original crystal. Only at the origin is there a breakdown of crystal symmetry. Everywhere else, the crystal is only slightly distorted. What has been formed is again a line-like defect called a *disclination.* Dislocations and disclinations will play a central role in our further discussion.

Before coming to this let us complete the dimensional classification of two-dimensional defects. They are of three types. There are *grain boundaries* where two regular lattice parts meet, with the lattice orientations being different on both sides of the interface (see Fig 2.6). They may be considered as arrays of dislocation lines in which half planes of point defects are stacked on top of each other with some spacing, having completely regular lattice planes between them. The second type of planar defects are *stacking faults*. They contain again completely regular crystal pieces on both sides of the plane, but instead of being oriented differently they are shifted one with respect to the other (see Fig 2.7). The third unavoidable type is the surface of the crystal.

From now on we shall focus attention upon the line-like defects.

2.2. DISLOCATION LINES AND BURGERS VECTOR

Let us first see how a dislocation line can be characterized mathematically. For this we look at Fig. 2.8 in which a closed circuit in the ideal

FIG. 2.6. A grain boundary where two crystal pieces meet with different orientations in such a way that not every atomic layer matches (here only every other one does).

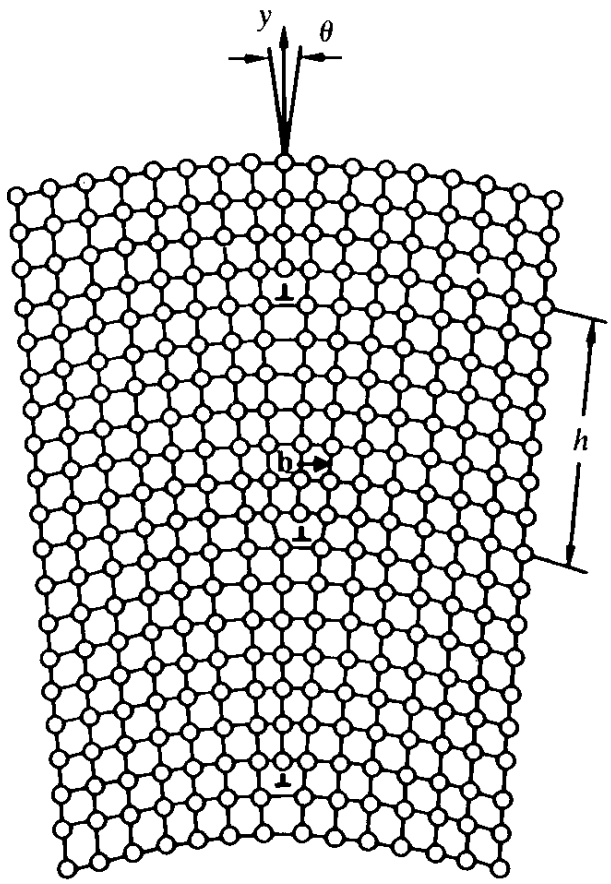

FIG. 2.7. Two typical stacking faults. The first is called growth-stacking fault or twin boundary, the second deformation-stacking fault.

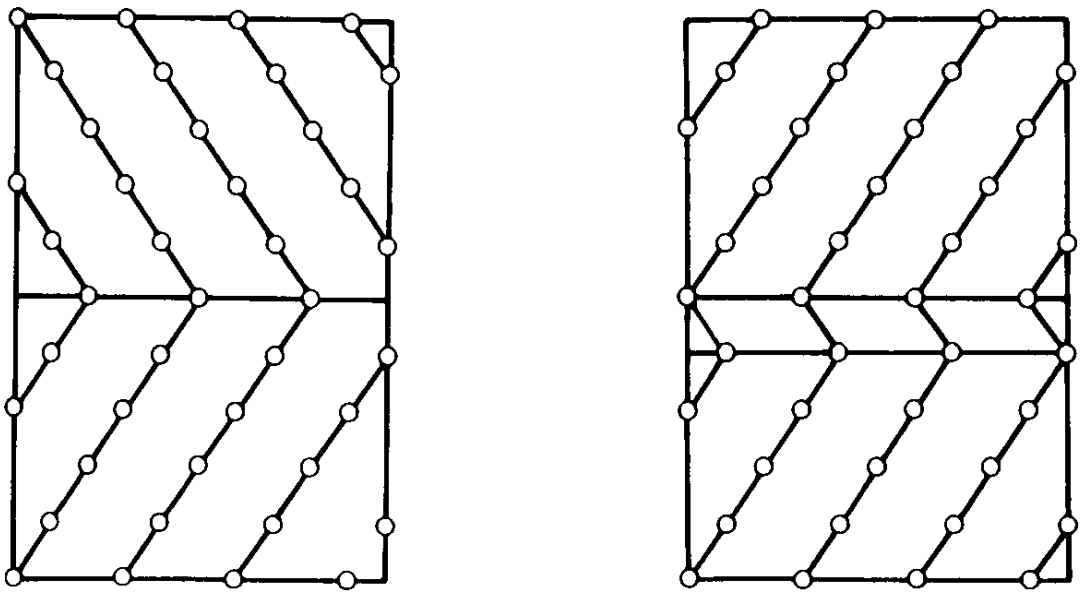

twin boundary stacking fault

FIG. 2.8. The definition of the Burgers vector **b**. In the presence of a dislocation line the image of a circuit which is closed in the ideal crystal fails to close in the defected crystal. The opposite is also true. The failure to close is measured by a lattice vector, called Burgers vector. The dislocation line in the figure is of the edge type and the Burgers vector points orthogonally to the line.

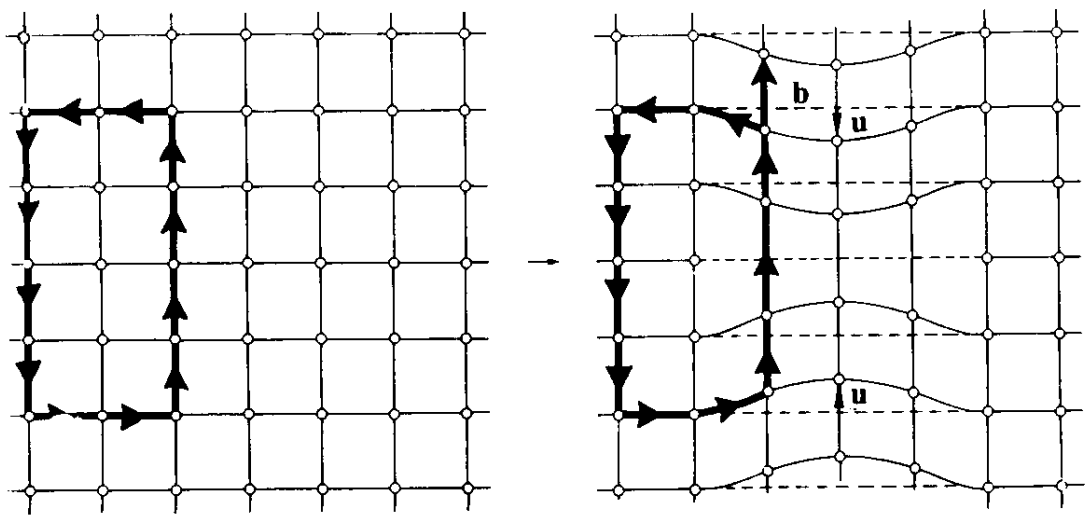

edge dislocation Burgers' vectors $\mathbf{b} = \Sigma\Delta\mathbf{u} \neq 0$

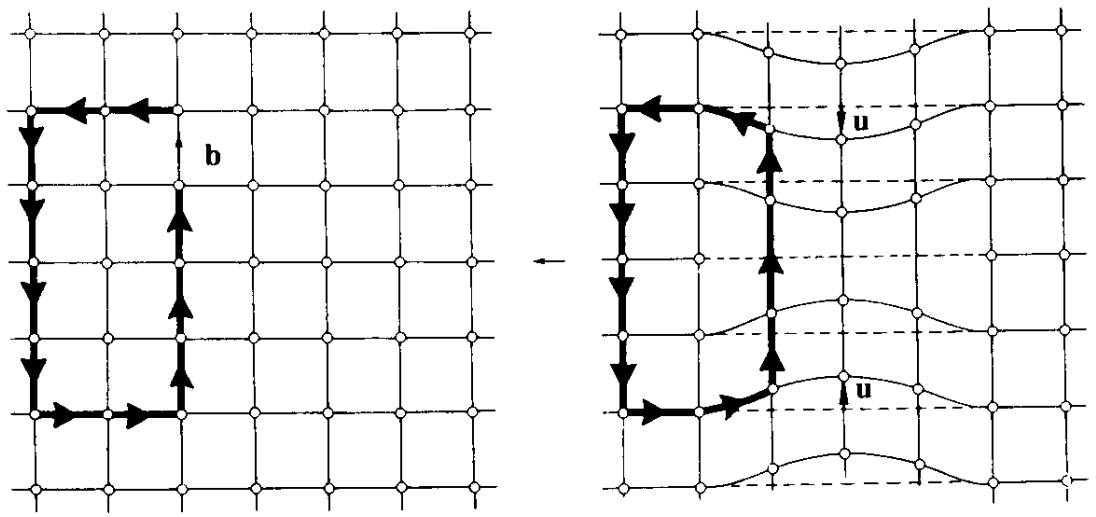

crystal is mapped into the disturbed crystal. The orientation is chosen arbitrarily to be anticlockwise. The prescription for the mapping is that for each step along a lattice direction, a corresponding step is made in the disturbed crystal. If the original lattice sites are denoted by $\mathbf{x}_n$, the image points are given by $\mathbf{x}_n + \mathbf{u}(\mathbf{x}_n)$, where $\mathbf{u}(\mathbf{x}_n)$ is the displacement amount field: At each step, the image point moves in a slightly different original point. After the original point has completed a closed circuit, call it B_0, the image point will not have arrived at the point of departure. The image of the closed contour B_0 is no longer closed. This failure to close is given precisely by a lattice vector $\mathbf{b}(\mathbf{x})$ called a *local Burgers vector*,

which points from the beginning to the end of the circuit.[a] Thus the dislocation line is characterized by the following equation,

$$\sum_{B_0} \Delta u_i(\mathbf{x}_n) = b_i, \tag{2.1a}$$

where $\Delta u_i(\mathbf{x}_n)$ are the increments of the displacement vector from step to step. Equivalently, we can consider a closed circuit in the disturbed crystal, call it B, and find that its counter image in the ideal crystal does not close by a vector $\mathbf{b}$ called the *true Burgers vector* which now points from the end to the beginning of the circuit.[a]

If we consider the same process in the continuum limit, we can write

$$\int_{B_0} du_i(x_a) = b_i, \qquad \int_B du_i(x'_a) = b_i. \tag{2.1b}$$

The closed circuit B is called *Burgers circuit*. The two Burgers vectors are the same if both circuits are so large that they lie deep in the ideal crystal. Otherwise they differ by an elastic distortion.

A few remarks are necessary concerning the convention employed in defining the Burgers vector. The singular line L is in principle without orientation. We may abitrarily assign a direction to it. The Burgers circuit is then taken to encircle this chosen direction in the right-handed way. If we choose the opposite direction, Burgers vector changes sign. However, the products $b_i\,dx_j$, where dx_j is the infinitesimal tangent vector to L, are invariant under this change. Notice that this is similar to the magnetic case discussed in Part II. There one defined the direction of the current by the flow of *positive* charge. The Burgers circuit gives $\oint du = I$. One could, however, also reverse this convention referring to the negative charge. Then $\oint du$ would give $-I$. Again, $I \cdot dx_i$ is an invariant. Only these products can appear in physical observables such as the Biot-Savart law.

The invariance of $b_i\,dx_j$ under reversal of the orientation has a simple physical meaning. In order to see this, consider once more the above dislocation line which was created by *removing* a layer of atoms. We can see in Fig. 2.8 that in this case $\mathbf{b} \times d\mathbf{x}$ points *inwards*, namely, towards

[a]Our sign convention is the opposite of Bilby *et al.* and the same as Read's (see Notes and References). Notice that in contrast to the local Burgers vector, the true Burgers vector is defined on a perfect lattice.

FIG. 2.9. A screw disclination which arises when tearing a crystal. The Burgers vector is parallel to the vertical line.

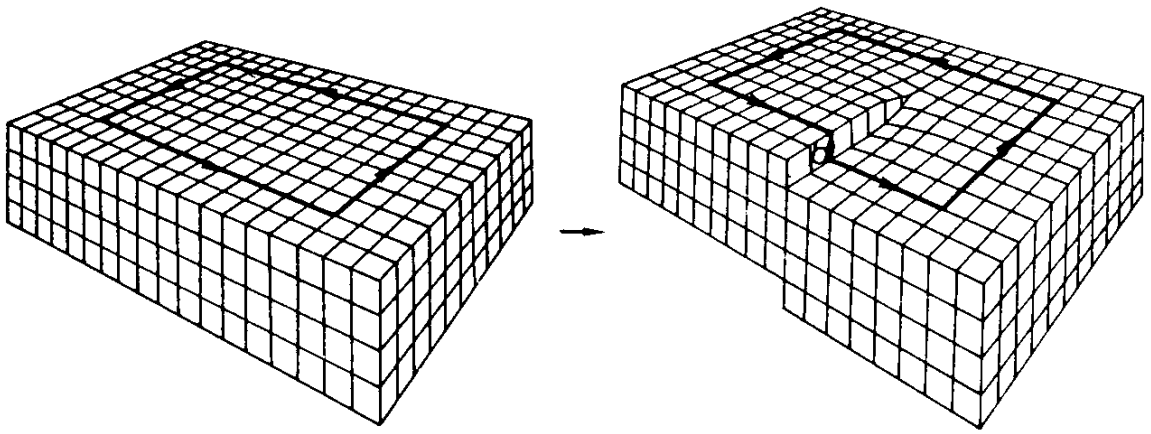

screw dislocation

the vacancies. Consider now the opposite case in which a layer of new atoms is inserted between the crystal planes, forcing the planes apart to relax the local stress. If we now calculate $\oint_B du_i(\mathbf{x}) = b_i$, we find that $\mathbf{b} \times d\mathbf{x}$ points *outwards*, i.e., away from the inserted atoms. This is again the direction in which there are fewer atoms. Both statements are independent of the choice of the orientation of the Burgers circuit. Since the second case has extra atoms inside the circle, where the previous one had vacancies, the two can be considered as antidefects of one another. If the boundary lines happen to fall on top of each other, they can annihilate each other and re-establish a perfect crystal. This can happen only piece-wise in which case the parts where the lines differ remain as dislocation lines. In both of the examples, the Burgers vectors are everywhere orthogonal to the dislocation line and one speaks of a pure *edge dislocation* (Fig. 2.2).

There is no difficulty in constructing another type of dislocation by cutting a crystal along a lattice half-plane up to some straight line L, and translating one of the lips against the other along the direction of L. In this way one arrives at the so-called *screw dislocation* shown in Fig. 2.9 in which the Burgers vector points parallel to the line L.

When drawing crystals out of a melt, it always contains a certain fraction of dislocations. Even in clean samples, at least one in 10^6 atoms is dislocated. Their boundaries run in all directions through space. We shall see very soon that their Burgers vector is a *topological invariant* for any closed dislocation loop. Therefore, the character "edge" versus "screw" of a dislocation line is not an invariant. It changes according to the direction of the line with respect to the invariant Burgers vector $\mathbf{b}_i$. It

is obvious from the Figs 2.2 to 2.9 that a dislocation line destroys the translational invariance of the crystal by multiples of the lattice vectors. If there are only a few lines this destruction is not very drastic. Locally, i.e., in any small subspecimen which does not lie too close to the dislocation line, the crystal can still be described by a periodic array of atoms whose order is disturbed only slightly by a smooth displacement field $u_i(\mathbf{x})$.

2.3. DISCLINATIONS AND THE FRANK VECTOR

Since the crystal is not only invariant under discrete translations but also under certain discrete rotations we expect the existence of another type of defect which is capable of destroying the global rotational order, while maintaining it locally. These are the disclination lines of which one example was given in Fig. 2.5. It arose as a superposition of stacks of layers of missing atoms. In the present context, it is useful to construct it by means of the following Gedanken experiment. Take a regular crystal in the form of cheese and remove a section subtending an angle Ω (see Fig. 2.10). The free surfaces can be forced together. For large Ω this requires considerable energy. Still, if the atomic layers on the free surfaces match together perfectly, the crystal can re-establish locally its periodic structure. This happens for all symmetries of the crystal. In a simple cubic crystal, Ω can be 90°, 180°, 270°. The 90° case is displayed in Fig. 2.11.

In Fig. 2.11 we can imagine also the opposite procedure going from the right in Fig. 2.10 to the left. We may cut the crystal, force the lips open by Ω and insert new undistorted crystalline matter to match the atoms in

FIG. 2.10. The Volterra cutting and welding process leading to a wedge disclination.

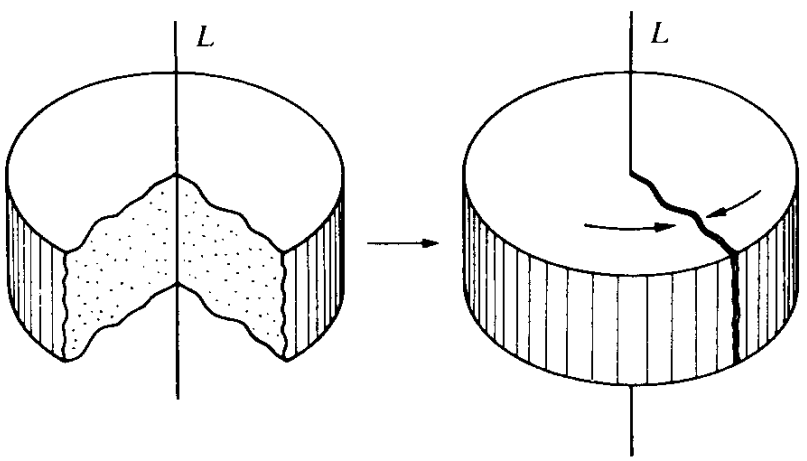

FIG. 2.11. The lattice structure at a wedge disclination in a simple cubic lattice. The Frank angle Ω is equal to the symmetry angles 90° or −90°. The crystal is locally perfect except close to the disclination line.

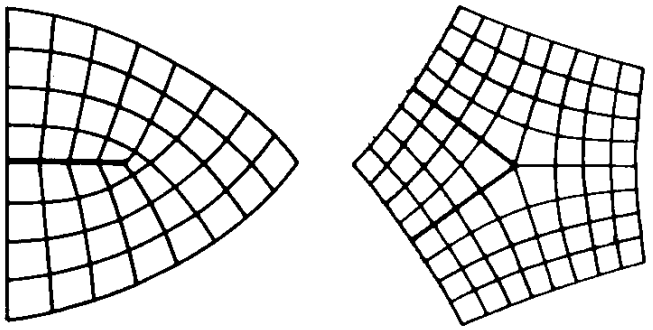

$\Omega = 90°$ $\Omega = -90°$

the free surfaces. These are the disclinations of negative angles. The case for $\Omega = -90°$ is shown in Fig. 2.11.

The local crystal structure is destroyed only along the singular line along the axis of the cheese. The rotation which has to be imposed upon the free surfaces in order to force them together may be represented by a rotation vector Ω which, in the present example, points parallel to L and to the cut. This is called a *wedge disclination*. It is not difficult to construct other rotational defects. The three possibilities are shown in Figs. 2.12. Each case is characterized by a vector. In the first case, Ω pointed parallel to the line L and the cut. Now, in the second case, it is orthogonal to the line L and Ω points parallel to the cut. This is a *splay disclination*. In the third case, Ω points orthogonal to the line and cut. This is a *twist disclination*.

The vector Ω is referred to as the *Frank vector* of the disclination. Just as in the construction of dislocations, the interface at which the material is joined together does not have any physical reality. For example, in Fig. 2.12a we could have cut out the piece along any other direction which is merely rotated with respect to the first around L by a discrete symmetry angle. Moreover, instead of a straight cut, we could have chosen an irregular piece as long as the faces fit together smoothly (recall Fig. 2.10). Only the singular line is a physical object.

The Gedanken experiments of cutting a crystal, removing or inserting slices or sections, and joining the free faces smoothly together were first performed by Volterra in 1907. For this reason one speaks of the creation of a defect line as a *Volterra process* and calls the cutting surfaces, where the free faces are joined together, *Volterra surfaces*.

FIG. 2.12.(a–c). Three different possibilities of constructing disclinations: (a) wedge, (b) splay, and (c) twist disclinations.

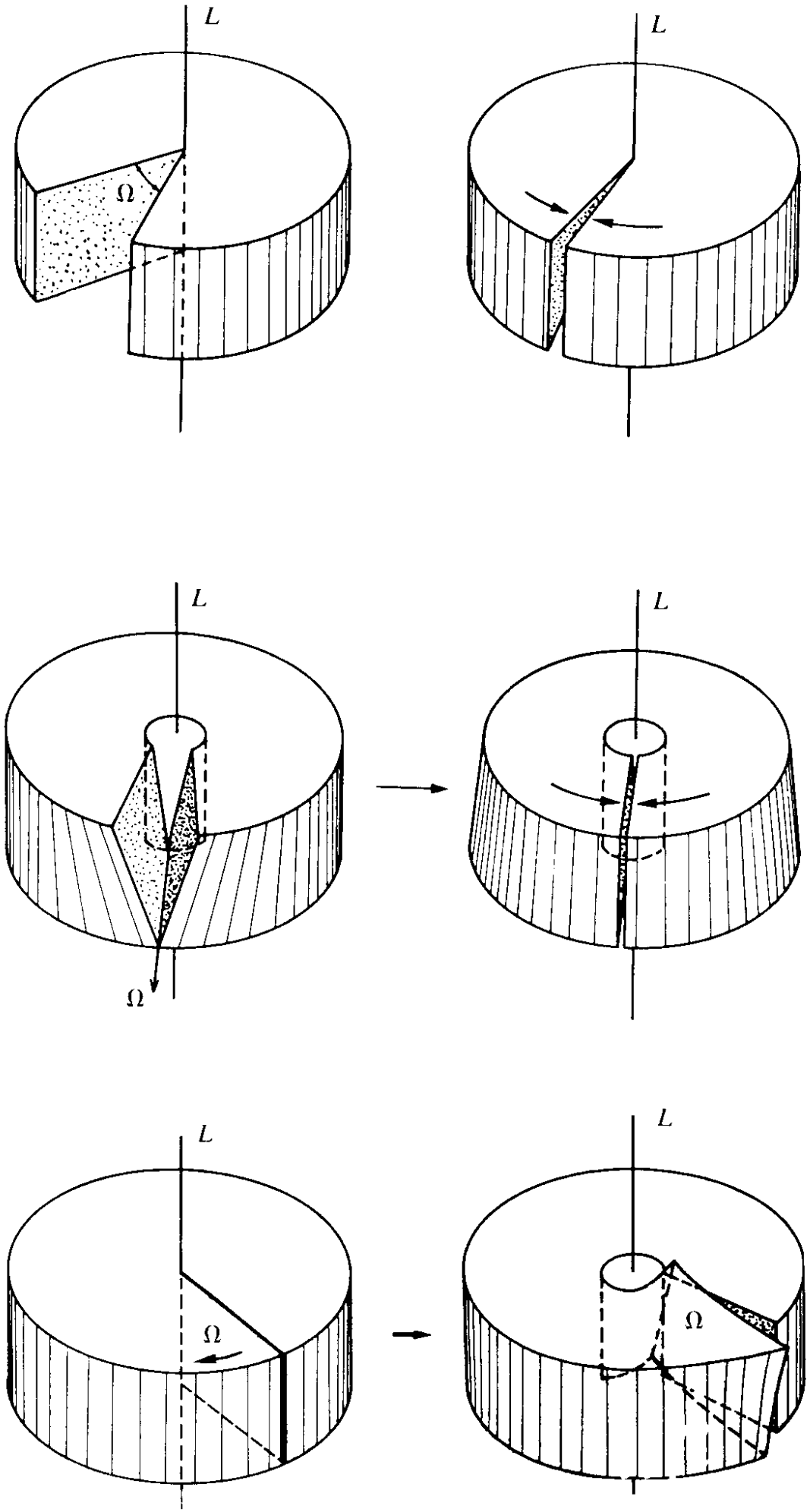

2.4. INTERDEPENDENCE OF DISLOCATIONS AND DISCLINATIONS

It must be pointed out that dislocation and disclination lines are not completely independent. We have seen before in Fig. 2.5 that a disclination line was created by removing stacks of atomic layers from a crystal. But each layer can be considered as a dislocation line running along the boundary. Thus a disclination line is apparently indistinguishable from a stack of dislocation lines, placed with equal spacing on top of each other.

Conversely, a dislocation line is very similar to a pair of disclination lines running in opposite directions close to each other. This is illustrated in Fig. 2.13. What we have here is a pair of opposite Volterra processes of disclination lines. We have cut out a section of angle Ω, but instead of removing it completely we have displaced it merely by one lattice spacing a. This is equivalent to generating a disclination of the Frank vector Ω and another one with the opposite Frank vector $-\Omega$ whose rotation axis is displaced by a. It is obvious from the figure that the result is a dislocation line with Burgers vector $\mathbf{b}$.

Because of this interdependence between dislocations and disclinations, the defect lines occurring in a real crystal will, in general, be of a mixed nature. It must be pointed out that disclinations were first observed and classified by F.C. Frank in 1958 in the context of liquid crystals. Liquid crystals are mesophases. They are liquids consisting of rod-like molecules. Thus, they cannot be described by a displacement field $u_i(\mathbf{x})$ alone but require an additional orientational field $n_i(\mathbf{x})$ for their description. This orientation is *independent* of the rotational field $\omega_i(\mathbf{x}) = \frac{1}{2}\varepsilon_{ijk}\partial_j u_k(\mathbf{x})$. The disclination lines defined by Frank are the rotational defect lines with respect to this *independent* orientational degree of freedom. Thus, they

FIG. 2.13. The generation of a dislocation line from a pair of disclination lines running in opposite directions at a fixed distance b. The Volterra process amounts to cutting out a section and reinserting it, but shifted by the amount $\mathbf{b}$.

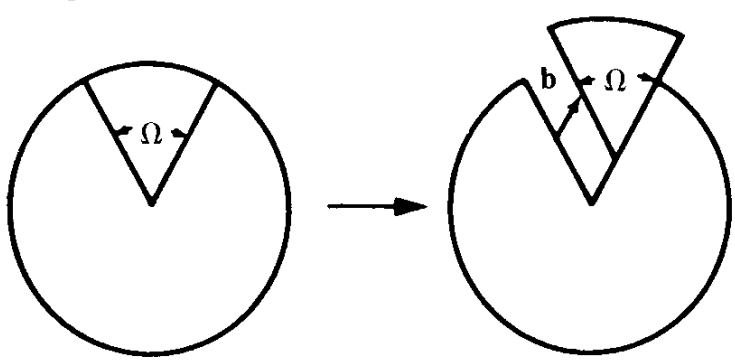

are *a priori* unrelated to the disclination lines in the rotation field $\omega_i(\mathbf{x}) = \frac{1}{2}\varepsilon_{ijk}\partial_j u_k(\mathbf{x})$. In fact, the liquid is filled with dislocations and ω-disclinations even if the orientation field $n_i(\mathbf{x})$ is completely ordered.

Friedel in his book on dislocations (see the references at the end) calls the n_i-disclinations, *rotation dislocations*. But later the name disclinations became customary (see Kléman's article cited in the Notes and References). In general, there is little danger of confusion, if one knows what system and phase one is talking about.

2.5. DEFECT LINES WITH INFINITESIMAL DISCONTINUITIES IN CONTINUOUS MEDIA

The question arises as to how one can properly describe the wide variety of line-like defects which can exist in a crystal. In general, this is a rather difficult task due to the many possible different crystal symmetries. For the sake of gathering some insight it is useful to restrict oneself to continuous isotropic media. Then defects may be created with arbitrarily small Burgers and Frank vectors. Such infinitesimal defects have the great advantage of being accessible to differential analysis. This is essential for a simple treatment of rotational defects. It permits a characterization of disclinations in a way which is very similar to that of dislocations via a Burgers circuit integral. Consider, for example, the wedge disclination along the line L (shown in Figs. 2.5, 2.10, 2.11 or 2.12a), and form an integral over a closed circuit B enclosing L.

Just as in the case of dislocations this measures the thickness of the material section removed in the Volterra process. Unlike the situation for dislocations, this thickness increases with distance from the line. If Ω is very small, the displacement field across the cut has a discontinuity which can be calculated from an *infinitesimal* rotation

$$\Delta u_i = (\boldsymbol{\Omega} \times \mathbf{x})_i, \tag{2.2}$$

where $\mathbf{x}$ is the vector pointing to the place where the integral starts and ends. In order to turn this statement into a circuit integral it is useful to remove the explicit dependence on $\mathbf{x}$ and consider not the displacement field $u_i(\mathbf{x})$ but the *local rotation field* accompanying the displacement instead. This is given by the antisymmetric tensor field

$$\omega_{ij}(\mathbf{x}) \equiv \tfrac{1}{2}(\partial_i u_j(\mathbf{x}) - \partial_j u_i(\mathbf{x})). \tag{2.3}$$

The rotational character of this tensor field is obvious by looking at the change of an infinitesimal distance vector under a distortion

$$dx_i' - dx_i = (\partial_j u_i)\,dx_j$$
$$= u_{ij}\,dx_j - \omega_{ij}\,dx_j. \tag{2.4}$$

The tensor field ω_{ij} is associated with a vector field ω_i as follows:

$$\omega_{ij}(\mathbf{x}) = \varepsilon_{ijk}\,\omega_k(\mathbf{x}) \tag{2.5}$$

i.e.,

$$\omega_i(\mathbf{x}) \equiv \tfrac{1}{2}\varepsilon_{ijk}\,\omega_{jk}(\mathbf{x}) = \tfrac{1}{2}(\nabla \times \mathbf{u})_i,$$

In terms of ω_i, the change of distance (2.4) takes the form

$$dx_i' - dx_i = u_{ij}(\mathbf{x})\,dx_j + (\boldsymbol{\omega}(\mathbf{x}) \times d\mathbf{x})_i, \tag{2.6}$$

with a transparent separation into a local change of shape and a local rotation. Now, when looking at the wedge disclination we see that due to (2.2), the field $\omega_i(\mathbf{x})$ has a constant discontinuity Ω across the cut. This can be formulated as a circuit integral

$$\Delta\omega_i = \oint_B d\omega_i = \Omega_i. \tag{2.7}$$

The value of this integral is the same for any choice of the circuit B as long as it encloses the disclination line L.

Notice the way in which this simple characterization depends essentially on the infinitesimal size of the defect. If Ω were finite, the differential expression (2.2) would not be a rotation and the discontinuity across the cut could not be given in the form (2.7) without specifying the circuit B. The difficulties for finite angles are a consequence of the non-Abelian nature of the rotation group. Only infinitesimal local rotations have additive rotation angles with only quadratic corrections, which can be neglected.

2.6. MULTIVALUEDNESS OF THE DISPLACEMENT FIELD

As soon as a crystal contains a few dislocations, it is realized that the definition of displacement field is intrinsically non-unique. The displace-

ment field is really *multivalued*. In a perfect crystal, in which the atoms deviate little from their equilibrium positions $\mathbf{x}$, it is natural to draw the displacement vector from the lattice places $\mathbf{x}$ to the nearest atom. In principle, however, the identity of the atoms makes such a specific assignment impossible. Due to thermal fluctuations, the atoms exchange positions from time to time by a process called *self-diffusion*. After a very long time, the displacement vector, even in a regular crystal, will run through the entire lattice. Thus, if we describe a regular crystal initially by very small displacement vectors $u_i(\mathbf{x})$, then, after a very long time, these will have changed to a permutation of lattice vectors, each of them occurring precisely once, plus some small fluctuations around them. Hence the displacement vectors are intrinsically multivalued, with $u_i(\mathbf{x})$ being indistinguishable from $u_i(\mathbf{x}) + aN_i(\mathbf{x})$, where $N_i(\mathbf{x})$ are integer numbers and a is the lattice spacing.

It is interesting to realize that this property puts the displacement fields on the same footing with the phase variable $\gamma(\mathbf{x})$ of superfluid ^{4}He. There the indistinguishability of $\gamma(\mathbf{x})$ and $\gamma(\mathbf{x}) + 2\pi N(\mathbf{x})$ had an entirely different reason. It followed directly from the fact that only the complex field $\psi(\mathbf{x}) = |\psi(\mathbf{x})| e^{i\gamma(\mathbf{x})}$, the wave function of the condensate, was physically observable.

Thus, in spite of the different physics described by the variables $\gamma(\mathbf{x})$, $u_i(\mathbf{x})$, they both share this characteristic multivaluedness. It is just as if the rescaled $u_i(\mathbf{x})$ variables, $\gamma_i(\mathbf{x}) = (2\pi/a)u_i(\mathbf{x})$ were phases of three complex fields,

$$\psi_i(\mathbf{x}) = |\psi_i(\mathbf{x})| e^{i\gamma_i(\mathbf{x})},$$

which describe the positions of the atoms.

In a regular crystal, this multivaluedness of $u_i(\mathbf{x})$ has no important physical consequences. The atoms are strongly localized and the exchange of positions occurs very rarely. The exchange is made irrelevant by the identity of the atoms and symmetry of the many-body wave function. This is why the natural assignment of $u_i(\mathbf{x})$ to the nearest equilibrium position $\mathbf{x}$ presents no problems. As soon as defects are present, however, the full ambiguity of the assignment comes up: When removing a layer of atoms, the result is a dislocation line along the boundary of the layer. Across the layer, the positions $u_i(\mathbf{x})$ jump by a lattice spacing. This means that the atoms on both sides are interpreted as having moved towards each other. Figure 2.14 shows that the same dislocation line could have been constructed by removing a completely different layer of atoms, say S', just as

FIG. 2.14. The figure shows that in the presence of a dislocation line, the displacement field is defined only modulo lattice vectors. This is due to the fact that the surface S on which the atoms have been removed is arbitrary as long as the boundary line stays fixed. Shifting S implies shifting of the reference positions, from which to count the displacements $u_i(\mathbf{x})$.

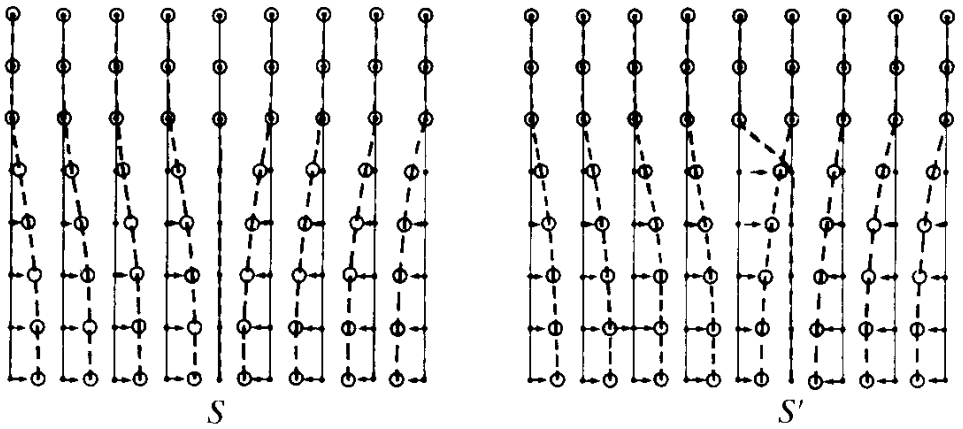

long as it has the same boundary line. The jump of the displacement field across the shifted layer S' corresponds to the neighbouring atoms of this layer having moved together and closed the gap. Physically, there is no difference. There is only a difference in the *descriptions* which amounts to a difference in the assignment of the equilibrium positions from where to count the displacement field $u_i(\mathbf{x})$. In contrast to regular crystals there now exists no natural choice of the nearest equilibrium point. It is this multivaluedness which will form the basis for the gauge field description of the solid.

2.7. SMOOTHNESS PROPERTIES OF THE DISPLACEMENT FIELD AND WEINGARTEN'S THEOREM

In order to be able to classify a general defect line we must first give a characterization of the smoothness properties of the displacement field away from the singularity. In physical terms, we have to make sure that the crystal matches properly together when cutting and rejoining the free faces.

In the scalar representation of magnetism and vortex lines described in Part II, Sections 1.5, 1.7, 1.8, this condition was given by the integrability condition [recall (1.79), Part II]

$$(\partial_i \partial_j - \partial_j \partial_i)\, \gamma(\mathbf{x}) = 0, \tag{2.8}$$

which really amounts to the Maxwell equation,

$$(\nabla \times \mathbf{H})_i = (\nabla \times \nabla\gamma)_i = \varepsilon_{ijk}\,\partial_j\,\partial_k\,\gamma = j_i\,, \tag{2.9}$$

with $j_i = 0$ away from the current loop. As long as the cutting faces are avoided, Eq. (2.8) was trivial since then the function $\gamma(\mathbf{x})$ was smooth. Close to the Volterra surface S at which the free faces join, however, there was danger. Due to the jump of $\gamma(\mathbf{x})$ across S, the gradient $\partial_i\,\gamma$ had a δ-function singularity on S. Nevertheless, the gradient was supposed to be the same on both sides of S and it was this condition from which we derived that fact that the jump $\Delta\gamma(\mathbf{x})$ across the sheet had to be a constant which, in turn implied, via Stokes' theorem, that $\gamma(\mathbf{x})$ satisfied the integrability condition (2.8) over the whole space including the surface S, except for the singular current line.

Let us now study the corresponding situation for the displacement field $u_i(\mathbf{x})$. Away from the cutting surface S, $u_i(\mathbf{x})$ is perfectly smooth and trivially satisfies the integrability condition

$$(\partial_i\,\partial_j - \partial_j\,\partial_i)\,u_k(\mathbf{x}) = 0. \tag{2.10}$$

Across the surface, $u_i(\mathbf{x})$ is discontinuous. However, the open faces of the crystalline material fit properly to each other. This implies that the strain as well as its first derivatives should have the same values on both sides of the cutting surface S:

$$\Delta u_{ij} = 0, \tag{2.11a}$$

$$\Delta\partial_k\,u_{ij} = 0. \tag{2.11b}$$

This severely restricts the discontinuities of $u_i(\mathbf{x})$ across S. In order to see this let $\mathbf{x}(1)$, $\mathbf{x}(2)$ be two different crystal points slightly above and below S and C^+, C^- be two curves connecting the two points. (See Fig. 2.15.) We can then calculate the difference of the discontinuities as follows:

$$\begin{aligned}\Delta u_i(1) - \Delta u_i(2) &= [u_i(1^-) - u_i(1^+)] - [u_i(2^-) - u_i(2^+)] \\ &= \int_{C^+}^{2^+} dx_j\,\partial_j u_i - \int_{C^-}^{2^-} dx_j\,\partial_j u_i\,.\end{aligned} \tag{2.12}$$

Using the local rotation field $\omega_{ij}(\mathbf{x})$ we can rewrite this as

FIG. 2.15. This figure defines the geometry used in the derviation of Weingarten's theorem [Eqs. (2.12)–(2.21)].

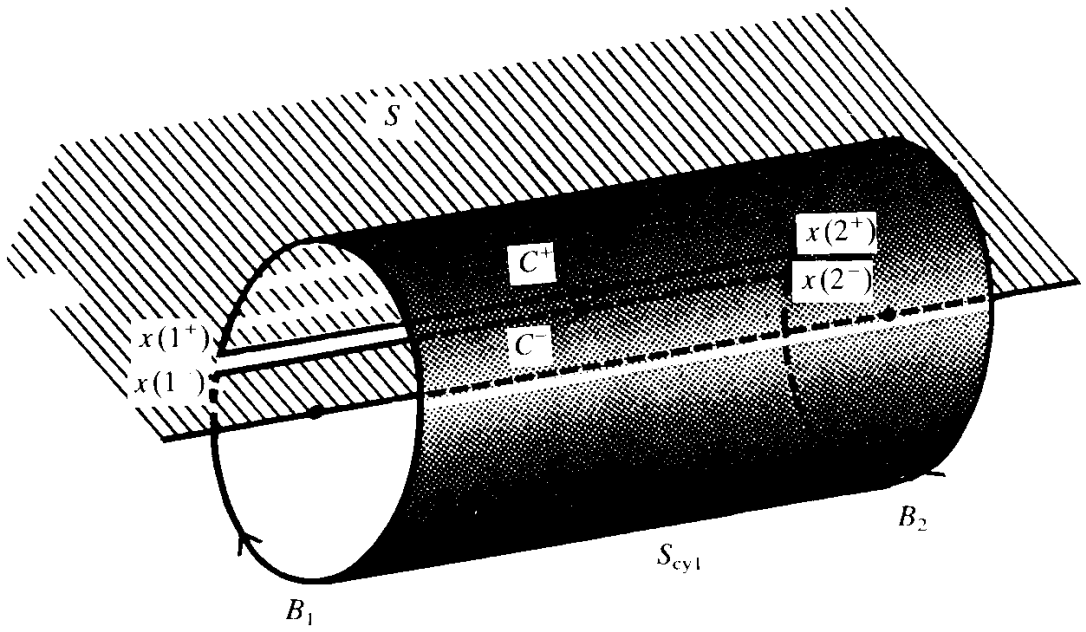

$$\Delta u_i(1) - \Delta u_i(2) = \int_{C^+}^{2^+} dx_j(u_{ij} - \omega_{ij}) - \int_{C^-}^{2^-} dx_j(u_{ij} - \omega_{ij}). \tag{2.13}$$

The ω_{ij} pieces may be integrated by parts:

$$\begin{aligned}
&-(x_j - x_j(1^+))\omega_{ij}\Big|_{1^+}^{2^+} + \int_{1^+}^{2^+} dx_k(x_j - x_j(1^+))\partial_k\omega_{ij} \\
&+(x_j - x_j(1^-))\omega_{ij}\Big|_{1^-}^{2^-} - \int_{1^-}^{2^-} dx_k(x_j - x_j(1^-))\partial_k\omega_{ij} \\
&= \left[-(x_j(2^+) - x_j(1^+))\omega_{ij}(2^+) + \int_{1^+}^{2^+} dx_k(x_j - x_j(1^+))\partial_k\omega_{ij}\right] - [+ \to -].
\end{aligned} \tag{2.14}$$

Since

$$x_j(1^+) = x_j(1^-), \qquad x_j(2^+) = x_j(2^-),$$

we arrive at the relation

$$\begin{aligned}
\Delta u_i(1) - \Delta u_i(2) &= -(x_j(1) - x_j(2))(\omega_{ij}(2^-) - \omega_{ij}(2^+)) \\
&+ \oint_{C^-} dx_k\{u_{ik} + (x_j - x_j(1))\partial_k\omega_{ij}\},
\end{aligned} \tag{2.15}$$

where C^{+-} is the closed contour consisting of C^+ followed by $-C^-$. Since C^+ and $-C^-$ are running back and forth on top of each other, the closed contour integral can be rewritten as a single integral along $-C^-$ with u_{ik} and $\partial_k \omega_{ij}$ replaced by their discontinuities across the sheet S. Moreover, the discontinuity of $\partial_k \omega_{ij}$ can be decomposed in the following manner:

$$\begin{aligned}\Delta(\partial_k \omega_{ij}) &= \tfrac{1}{2}\partial_k(\partial_i u_j - \partial_j u_i)(\mathbf{x}^-) - (\mathbf{x}^- \to \mathbf{x}^+) \\ &= \partial_i u_{kj}(\mathbf{x}^-) - \partial_j u_{ki}(\mathbf{x}^-) + \tfrac{1}{2}(\partial_k \partial_i - \partial_i \partial_k) u_j(\mathbf{x}^-) \\ &\quad - \tfrac{1}{2}(\partial_k \partial_j - \partial_j \partial_k) u_i(\mathbf{x}^-) + \tfrac{1}{2}(\partial_j \partial_i - \partial_i \partial_j) u_k(\mathbf{x}^-) - (\mathbf{x}^- \to \mathbf{x}^+).\end{aligned} \tag{2.16}$$

Since above and below the sheet, the displacement field is smooth, the two derivatives in front of $\mathbf{u}(x^{\pm})$ commute. Hence the integral in (2.15) becomes

$$-\int_C dx_k \{\Delta u_{ik} + (x_j - x_j)(1)\Delta(\partial_i u_{kj} - \partial_j u_{ki})\}. \tag{2.17}$$

This expression vanishes due to the physical requirement (2.11). As a result we find that the discontinuities between two arbitrary points 1 and 2 on the sheet have the simple relation

$$\Delta u_i(2) = \Delta u_i(1) - \Omega_{ij}(x_j(2) - x_j(1)), \tag{2.18}$$

where Ω_{ij} is a fixed infinitesimal rotation matrix given by

$$\Omega_{ij} = \Delta\omega_{ij}(2) = \omega_{ij}(2^-) - \omega_{ij}(2^+). \tag{2.19}$$

We now define the rotation vector

$$\Omega_k = \tfrac{1}{2}\varepsilon_{ijk}\Omega_{ij} \tag{2.20}$$

in terms of which (2.18) takes the form

$$\Delta\mathbf{u}(2) = \Delta\mathbf{u}(1) + \boldsymbol{\Omega} \times (\mathbf{x}(2) - \mathbf{x}(1)). \tag{2.21}$$

This forms the content of *Weingarten's theorem*: The discontinuity of the displacement field across the cutting surface can only be a constant vector plus a fixed rotation.

Notice that these are precisely the symmetry elements of a solid continuum. When looking back at the particular dislocation and disclination lines in Figs. 2.2 – 2.12 we see that all the discontinuities obey this theorem, as they should. The vector $\mathbf{\Omega}$ is the Frank vector of the disclination lines. For a pure disclination line, $\mathbf{\Omega} = \mathbf{0}$ and $\Delta\mathbf{u}(1) = \Delta\mathbf{u}(2) = \mathbf{b}$ is the Burgers vector.

2.8. INTEGRABILITY CONSIDERATIONS

For vortex lines, the smoothness of the superflow velocity $v_s(\mathbf{x})_i \sim \partial_i \gamma(\mathbf{x})$ implied that the jump of $\gamma(\mathbf{x})$ was a constant and this, in turn, led to the integrability condition

$$(\partial_i \partial_j - \partial_j \partial_i)\, \gamma(\mathbf{x}) = 0$$

away from any vortex line [recall Eq. (1.78), Part II]. Here we can derive something quite similar for the rotation field $\omega_{ij}(\mathbf{x})$. Taking Weingarten's theorem (2.18) and forming derivatives, we see that the jump of the $\omega_{ij}(\mathbf{x})$ field is necessarily a constant, namely Ω_{ij}. Hence $\omega_{k\ell}$ also satisfies the integrability condition

$$(\partial_i \partial_j - \partial_j \partial_i)\, \omega_{k\ell} = 0, \tag{2.22}$$

everywhere except on the defect line. The argument is the same as that for the vortex lines. We simply observe that the contour integral over a Burgers circuit

$$\Delta\omega_{ij} = \oint_B d\omega_{ij} = \oint_B dx_k\, \partial_k\, \omega_{ij} \tag{2.23}$$

can be cast, by Stokes' theorem, in the form

$$\Delta\omega_{ij} = \int_{S^B} dS_m\, \varepsilon_{mk\ell}\, \partial_k\, \partial_\ell\, \omega_{ij}, \tag{2.24}$$

where S^B is some surface enclosed by the Burgers circuit. Since the result is independent of the size, shape, and position of the Burgers circuit as long as it encloses the defect line L, this implies

$$\varepsilon_{mk\ell}\, \partial_k\, \partial_\ell\, \omega_{ij}(\mathbf{x}) = 0 \tag{2.25}$$

everywhere away from L, which is what we wanted to show.

In fact, the constancy of the jump in ω_{ij} could have been derived somewhat more directly, without going through (2.22) – (2.25), by taking again the curves C^+, C^- on Fig. 2.15 and calculating

$$\Delta\omega_{ij}(1) - \Delta\omega_{ij}(2) = \int_{1'}^{2'} dx_k\, \partial_k\, \omega_{ij} - \int_{1}^{2} dx_k\, \partial_k\, \omega_{ij} = -\int_{1}^{2} dx_k\, \Delta(\partial_k\, \omega_{ij}). \tag{2.26}$$
$$C^+ \qquad C^- \qquad C^-$$

From the assumption (2.11) together with (2.16) we see that $\omega_{ij}(\mathbf{x})$ does not jump across the Volterra surface S. But then (2.26) shows us that $\Delta\omega_{ij}$ is a constant.

Let us now consider the displacement field itself. As a result of Weingarten's theorem, the integral over the Burgers circuit B_2 in Fig. 2.15 gives

$$\Delta u_i(2) = \oint_{B_2} du_i = \Delta u(1) - \Omega_{ij}(x_j(2) - x_j(1)). \tag{2.27}$$

By treating the integral over B_2 in the same way as those over C^+, C^- in (2.13)–(2.15), we arrive at the equation

$$\Delta u_i(1) - \Omega_{ij}(x_j(2) - x_j(1)) = \oint_{B_2} dx_k \{u_{ik} + (x_j - x_j(2))\partial_k \omega_{ij}\}. \tag{2.28}$$

Here we observe that the factors of $x_j(2)$ can be dropped on both sides by (2.23) and $\Delta\omega_{ij} = \Omega_{ij}$. By Stokes' theorem, the remaining equation then becomes an equation for the surface integral over S^{B_2},

$$\begin{aligned}\Delta u_i(1) + \Omega_{ij} x_j(1) &= \int_{S^{B_2}} dS_\ell\, \varepsilon_{\ell mk}\, \partial_m \{u_{ik} + x_j\, \partial_k\, \omega_{ij}\} \\ &= \int_{S^{B_2}} dS_\ell\, \varepsilon_{\ell mk} \{(\partial_m u_{ik} + \partial_k\, \omega_{im}) + x_j\, \partial_m\, \partial_k\, \omega_{ij}\}. \end{aligned} \tag{2.29}$$

This must hold for any size, shape, and position of the circuit B_2 as long as it encircles the defect line L. For all these different configurations, the left-hand side of (2.29) is a constant. We can therefore conclude that

$$\int_{S'} dS_\ell \{\varepsilon_{\ell mk}[\partial_m u_{ik} + \partial_k\, \omega_{im}] + x_j\, \varepsilon_{\ell mk}\, \partial_m\, \partial_k\, \omega_{ij}\} = 0 \tag{2.30}$$

for any surfaces S' which does *not* enclose L. Moreover, from (2.22) we see that the last term cannot contribute. The first two terms, on the other hand, can be rewritten, using the same decomposition of $\partial_k \omega_{im}$ as in (2.16), in the form

$$-\int_{S'} dS_\ell \, \varepsilon_{\ell mk}(S_{kmi} - S_{mik} + S_{ikm}) = \int_{S'} dS_\ell \, \varepsilon_{\ell mk} S_{mki}, \tag{2.31}$$

where we have abbreviated

$$S_{kmi}(\mathbf{x}) \equiv \tfrac{1}{2}(\partial_k \partial_m - \partial_m \partial_k) u_i(\mathbf{x}). \tag{2.32}$$

Since this has to vanish for any S', we conclude that away from the defect line, the displacement field $u_i(\mathbf{x})$ also satisfies the integrability condition

$$(\partial_k \partial_m - \partial_m \partial_k) u_i(\mathbf{x}) = 0. \tag{2.33}$$

On the line L, the integrability conditions for u_i and ω_{ij} are, in general, both violated. Let us first consider ω_{ij}. In order to give the constant result $\Delta\omega_{ij}(\mathbf{x}) \equiv \Omega_{ij}$ in (2.24) the integrability condition must be violated by a singularity in the form of a δ-function along the line L,

$$\delta_\ell(L) \equiv \oint_L ds \frac{dx_\ell(s)}{ds} \delta^{(3)}(\mathbf{x} - \bar{\mathbf{x}}(s)) \tag{2.34}$$

[shorthand for $\delta_\ell(\mathbf{x}, L)$, Eq. (II.1.76)] namely,

$$\varepsilon_{\ell mk} \partial_m \partial_k \omega_{ij} = \Omega_{ij} \delta_\ell(L). \tag{2.35}$$

Then (2.25) gives $\Delta\omega_{ij} = \Omega_{ij}$ via the formula

$$\int_{S^B} dS_\ell \, \delta_\ell(L) = 1. \tag{2.36}$$

In order to see how the integrability condition is violated for $u_i(\mathbf{x})$, consider now the integral (2.29) and insert the result (2.31). This gives

$$\Delta u_i(1) + \Omega_{ij} x_j(1) = \int_{S^{B_2}} dS_\ell \, \varepsilon_{\ell mk}(S_{mki} + x_j \partial_m \partial_k \omega_{ij}). \tag{2.37}$$

The right hand side is a constant independent of the position of the surface S^{B_2}. This implies that the singularity along L is of the form

$$\varepsilon_{\ell mk}(\partial_m \partial_k u_i + x_j \partial_m \partial_k \omega_{ij}) = b_i \delta_\ell(L), \tag{2.38}$$

where we have introduced the quantity

$$b_i \equiv \Delta u_i(1) + \Omega_{ij} x_j(1). \tag{2.39}$$

Inserting (2.35) into (2.38) leads to the following violation of the integrability condition for $u_i(\mathbf{x})$ along L,

$$\varepsilon_{\ell mk} \partial_m \partial_k u_i = (b_i - \Omega_{ij} x_j) \delta_\ell(L). \tag{2.40}$$

2.9. DISLOCATION AND DISCLINATION DENSITIES

In the last section we saw that the most general defect line L is characterized by a violation of the integrability condition for displacement and rotation fields which had the form of a δ-function along the line L. In analogy with the current density of magnetism and the vortex density γ in Part II, (1.78)

$$j_i(\mathbf{x}) \equiv \varepsilon_{ijk} \partial_j \partial_k \gamma(\mathbf{x}) = I \delta_i(L), \tag{2.41}$$

we introduce *densities* for dislocations and disclinations, respectively, as follows:

$$\alpha_{ij}(\mathbf{x}) \equiv \varepsilon_{ik\ell} \partial_k \partial_\ell u_j(\mathbf{x}), \tag{2.42a}$$

$$\Theta_{ij}(\mathbf{x}) \equiv \varepsilon_{ik\ell} \partial_k \partial_\ell \omega_j(\mathbf{x}), \tag{2.42b}$$

where we have used the vector form of the rotation field $\omega_i = \frac{1}{2} \varepsilon_{ijk} \omega_{jk}$, in order to save one index. For the general defect line along L, these densities have the form

$$\alpha_{ij}(\mathbf{x}) = \delta_i(L)(b_j - \Omega_{jk} x_k), \tag{2.43a}$$

$$\Theta_{ij}(\mathbf{x}) = \delta_i(L) \Omega_j, \tag{2.43b}$$

where $\Omega_i = \frac{1}{2} \varepsilon_{ijk} \Omega_{jk}$ is the Frank vector.

In (2.43) the rotation by Ω is performed around the origin. Obviously, the position of the rotation axis can be changed to any other point $\mathbf{x}_0$ by a simple shift in the constant $b_j \to b_j' = b_j + (\Omega \times \mathbf{x}_0)_j$. Then $\alpha_{ij}(\mathbf{x}) = \delta_i(L)\{b_j' + (\Omega \times (\mathbf{x} - \mathbf{x}_0)_j\}$. Notice that due to the identity

$$\partial_i \delta_i(L) = 0 \tag{2.44}$$

for closed lines L, the disclination density satisfies the conservation law

$$\partial_i \Theta_{ij} = 0, \tag{2.45}$$

which implies that disclination lines are always closed. This is not true for media with a directional field, e.g., nematic liquid crystal. Such media are not considered here since they cannot be described by a displacement field alone. Differentiating (2.43a) we find the conservation law for disclination lines $\partial_i \alpha_{ij} = -\Omega_{ji}\, \delta_i(L)$ which, in turn, can be expressed in the form

$$\partial_i \alpha_{ij} = -\varepsilon_{jk\ell}\, \Theta_{k\ell}\,. \tag{2.46}$$

From the linearity of the relation (2.42) in u_j and ω_j it is obvious that these conservation laws remain true for any ensemble of infinitesimal defect lines.

The conservation law (2.46) may, in fact, be derived by purely differential techniques from the first smoothness assumption (2.11a). Using Stokes' theorem, Δu_{ij} can be expressed in the same way as $\Delta \omega_{ij}$ in (2.24), and by the same argument as the one used for ω_{ij} we conclude that the strain is an integrable function *in all space* and satisfies

$$(\partial_i \partial_k - \partial_k \partial_i)\, u_{\ell j}(\mathbf{x}) = 0. \tag{2.47}$$

If we then look at α_{ij} in the general definition (2.42a), rewrite it as

$$\begin{aligned} \alpha_{ij} &= \varepsilon_{ik\ell}\, \partial_k\, \partial_\ell\, u_j = \varepsilon_{ik\ell}\, \partial_k (u_{\ell j} + \omega_{\ell j}) \\ &= \varepsilon_{ik\ell}\, \partial_k\, u_{\ell j} + \delta_{ij}\, \partial_k\, \omega_k - \partial_j\, \omega_i\,, \end{aligned} \tag{2.48}$$

and apply the derivative ∂_i, this gives directly (2.46).

In a similar way, the conservation law (2.45) can be derived by combining both smoothness assumptions (2.11a) and (2.11b). The first can be stated, via Stokes' theorem, as an integrability condition for the derivative of strain, i.e.,

$$(\partial_\ell\, \partial_n - \partial_n\, \partial_\ell)\, \partial_k\, u_{ij}(\mathbf{x}) = 0. \tag{2.49}$$

Let us recall that from the first assumption (2.11a) we have concluded in (2.16) that $\partial_k\, \omega_{ij}(\mathbf{x})$ is also a completely smooth function across the surface S. Hence, $\partial_k\, \omega_{ij}$ must also satisfy the integrability condition

$$(\partial_\ell \partial_n - \partial_n \partial_\ell)\, \partial_k \omega_{ij}(\mathbf{x}) = 0.$$

Together with (2.49) this implies that $\partial_k \partial_i u_j(\mathbf{x})$ is integrable:

$$(\partial_\ell \partial_n - \partial_n \partial_\ell)\, \partial_k \partial_i u_j(\mathbf{x}) = 0. \tag{2.50}$$

If we write down this relation three times, each time with ℓ, n, k exchanged cyclically, we find

$$\partial_\ell R_{nkij} + \partial_n R_{k\ell ij} + \partial_k R_{\ell nij} = 0,$$

where R_{nkij} is an abbreviation for the expression,

$$R_{nkij} = (\partial_n \partial_k - \partial_k \partial_n)\, \partial_i u_j(\mathbf{x}). \tag{2.51}$$

Contracting k with i and ℓ with j gives us

$$\partial_j R_{niij} + \partial_n R_{ijij} + \partial_i R_{jnij} = 0.$$

Now we observe that because of (2.47), R_{nkij} is anti-symmetric not only in n and k but also in i and j so that

$$2\partial_j R_{inji} - \partial_n R_{ijji} = 0.$$

This, however, is the same as

$$2\partial_j(\tfrac{1}{4}\varepsilon_{jpq}\,\varepsilon_{nk\ell}\,R_{pqk\ell}) = 0, \tag{2.52}$$

as can be verified using the identity

$$\begin{aligned}\varepsilon_{jpq}\,\varepsilon_{nk\ell} = {} & \delta_{jn}\,\delta_{pk}\,\delta_{q\ell} + \delta_{jk}\,\delta_{p\ell}\,\delta_{qn} + \delta_{j\ell}\,\delta_{pn}\,\delta_{qk} \\ & - \delta_{jn}\,\delta_{p\ell}\,\delta_{qk} - \delta_{jk}\,\delta_{pn}\,\delta_{q\ell} - \delta_{j\ell}\,\delta_{pk}\,\delta_{qn}.\end{aligned} \tag{2.53}$$

Recalling, now the definition (2.51) and $\omega_n = \frac{1}{2}\varepsilon_{nk\ell}\,\partial_k u_\ell$, Eq. (2.52) becomes

$$2\varepsilon_{ipq}\partial_i \partial_p \partial_q \omega_n = 0, \tag{2.54}$$

and this is precisely the conservation law for disclinations (2.45) $[\partial_i \Theta_{ik} = 0]$ which we wanted to prove.

FIG. 2.16. Illustration of Volterra process in which an entire volume piece is moved with the vector b_i.

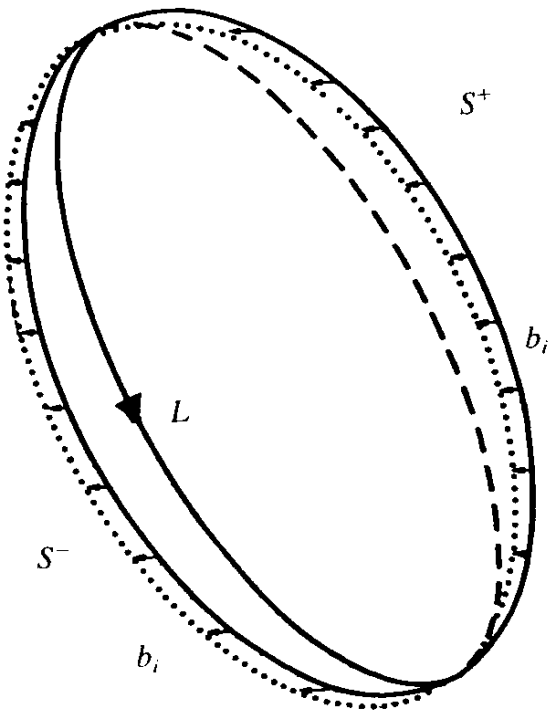

2.10. MNEMONIC PROCEDURE FOR CONSTRUCTING DEFECT DENSITIES

There exists a simple mnemonic procedure for constructing the defect densities and their conservation laws. This we now explain.

Suppose we perform the Volterra cutting procedure on a *closed surface* S, dividing it mentally in two parts, joined along some line L (see Fig. 2.16). On one part of S, say S^+, we remove material of thickness b_i and on the other we add the same material. This corresponds to a simple translational movement of crystalline material by b_i, i.e., to a displacement field

$$u_\ell(\mathbf{x}) = -\delta(V)\, b_\ell, \tag{2.55}$$

where the δ-function on a volume V was defined in Eq. (8.21), Part II. By this transformation the elastic properties of the material are unchanged.

Consider now the distortion field $\partial_j u_i(\mathbf{x})$. Under (2.55), it changes by

$$\partial_k u_\ell(\mathbf{x}) \to \partial_k u_\ell(\mathbf{x}) - \partial_k \delta(V)\, b_\ell. \tag{2.56}$$

The derivative of the δ-function is singular only on the surface of the volume V. In fact, in (8.20), Part II, we already derived the formula $-\partial_k \delta(V) = \delta_k(S)$ so that (2.56) reads

$$\partial_k u_\ell(\mathbf{x}) \to \partial_k u_\ell(\mathbf{x}) + \delta_k(S)\, b_\ell . \tag{2.57}$$

From this trivial transformation we can now construct a proper dislocation line by assuming S to be no longer a closed surface but an open one, i.e., we may restrict S to the shell S^+ with a boundary L. Then we can form the dislocation density

$$\alpha_{i\ell}(\mathbf{x}) = \varepsilon_{ijk}\, \partial_j \partial_k u_\ell(\mathbf{x}) = \varepsilon_{ijk}\, \partial_j \delta_k(S)\, b_\ell . \tag{2.58}$$

The superscript + was dropped. Using Stokes' theorem on the $\delta_k(S)$-function, as derived in (8.17), Part II, this becomes simply

$$\alpha_{i\ell}(\mathbf{x}) = \delta_i(L)\, b_\ell . \tag{2.59}$$

For a closed surface, this vanishes.

For a general defect line, the starting point is the trivial Volterra operation of *translating and rotating* a piece of crystalline volume. This corresponds to a displacement field

$$u_\ell(\mathbf{x}) = -\delta(V)(b_\ell + \varepsilon_{\ell qr}\Omega_q x_r). \tag{2.60}$$

If we now form the distortion, we find

$$\partial_k u_\ell(\mathbf{x}) = \delta_k(S)(b_\ell + \varepsilon_{\ell qr}\Omega_q x_r) - \delta(V)\, \varepsilon_{\ell qk}\Omega_q .$$

In this expression it is still impossible to assume S to be an open surface. If we, however, form the symmetric combination, the strain

$$u_{k\ell} = \tfrac{1}{2}(\partial_k u_\ell + \partial_\ell u_k) = \tfrac{1}{2}[\delta_k(S)(b_\ell + \varepsilon_{\ell qr}\Omega_q x_r) + (k\ell)], \tag{2.61}$$

is well defined for an open surface, in which case we shall refer to $u_{k\ell}$ as the *plastic strain* and denote it by $u^p_{k\ell}$. The field

$$\beta^p_{k\ell} \equiv \delta_k(S)(b_\ell + \varepsilon_{\ell qr}\Omega_q x_r) \tag{2.62}$$

plays the role of a dipole density of the defect line across the surface S. It is usually called a *plastic distortion*. It is a single valued field (i.e., derivatives in front of it commute). In terms of $\beta^p_{k\ell}$, the plastic strain is simply

$$u^p_{k\ell} = \tfrac{1}{2}(\beta^p_{k\ell} + \beta^p_{k\ell}), \tag{2.63}$$

The full displacement field (2.60) is not defined for an open surface due to the $\delta(V)$ term. It is multiple valued. The dislocation density, however, is single valued. Indeed, we can easily calculate

$$\begin{aligned}\alpha_{i\ell} &= \varepsilon_{ijk}\,\partial_j\,\partial_k u_\ell(\mathbf{x}) = \varepsilon_{ijk}\,\partial_j[\delta_k(S)(b_\ell + \varepsilon_{\ell qr}\Omega_q x_r) - \delta(V)\,\varepsilon_{\ell qk}\Omega_q] \\ &= \delta_i(L)(b_\ell + \varepsilon_{\ell qr}\Omega_q x_r),\end{aligned} \tag{2.64}$$

and see that this is the same as (2.43a).

Let us now turn to the disclination density $\Theta_{pj} = \varepsilon_{pmn}\,\partial_m\,\partial_n\,\omega_j$. From (2.60) we find the gradient of the rotation field

$$\begin{aligned}\partial_n\,\omega_j &= \tfrac{1}{2}\,\varepsilon_{jk\ell}\,\partial_n\,\partial_k\,u_\ell \\ &= \tfrac{1}{2}\,\varepsilon_{jk\ell}\,\partial_n[\delta_k(S)(b_\ell + \varepsilon_{\ell qr}\Omega_q x_r) - \delta(V)\,\varepsilon_{\ell qk}\Omega_q] \\ &= \tfrac{1}{2}\,\varepsilon_{jk\ell}\,\partial_n\,\beta^P_{k\ell} + \delta_n(S)\,\Omega_j.\end{aligned} \tag{2.65}$$

This is defined for an open surface S in which case it is called the *plastic bend-twist* and denoted by $\varkappa^p_{nj} \equiv \partial_n\,\omega^p_j$. It is useful to define the *plastic rotation*

$$\phi^p_{nj} \equiv \delta_n(S)\,\Omega_j, \tag{2.66}$$

which plays the role of a dipole density for disclinations. With this, the plastic gradient of ω_j is given by

$$\varkappa^p_{nj} = \partial_n\,\omega^p_j = \tfrac{1}{2}\,\varepsilon_{jk\ell}\,\partial_n\,\beta^p_{k\ell} + \phi^p_{nj}. \tag{2.67}$$

We can now easily calculate the disclination density:

$$\Theta_{pj} = \varepsilon_{pmn}\,\partial_m\,\partial_n\,\omega_j = \varepsilon_{pmn}\,\partial_m\,\varkappa^p_{nj} = \tfrac{1}{2}\,\varepsilon_{jk\ell}\,\varepsilon_{pmn}\,\partial_m\,\partial_n\,\beta^p_{k\ell} + \varepsilon_{pmn}\,\partial_m\,\phi^p_{nj}.$$

In front of $\beta^p_{k\ell}$, the derivatives commute [see (2.62)] so that the first term vanishes. Use of Stokes' theorem on the second term gives

$$\Theta_{pj} = \varepsilon_{pmn}\,\partial_m\,\phi^p_{nj} = \delta_p(L)\,\Omega_j, \tag{2.68}$$

in agreement with (2.44).

Notice that according to the second line of (2.64), the dislocation density can also be expressed in terms of $\beta^p_{k\ell}$ and $\phi^p_{\ell i}$ as

$$\alpha_{i\ell} = \varepsilon_{ijk}\partial_j\beta^p_{k\ell} + \delta_{i\ell}\phi^p_{pp} - \phi^p_{\ell i}. \tag{2.69}$$

In fact, this is a direct consequence of the decomposition (2.48), which can be written in terms of plastic strain and bend-twist as

$$\alpha_{ij} = \varepsilon_{ik\ell}\partial_k u^p_{\ell j} + \delta_{ij}\varkappa^p_{qq} - \varkappa^p_{ji} \tag{2.70}$$

Expressing $u^p_{\ell i}$ in terms of $\beta^p_{\ell i}$ and $\varkappa^p_{ij}$ in terms of ϕ^p_{ij} [see (2.63) and (2.67)] we find

$$\alpha_{ij} = \tfrac{1}{2}\varepsilon_{ik\ell}\partial_k\beta^p_{\ell j} + \delta_{ij}\phi^p_{qq} - \phi^p_{ji} + \tfrac{1}{2}(\varepsilon_{ik\ell}\partial_k\beta^p_{j\ell} + \delta_{ij}\varepsilon_{qk\ell}\partial_q\beta^p_{k\ell} - \varepsilon_{ik\ell}\partial_j\beta^p_{k\ell}).$$

But the quantity inside the parentheses is equal to $\frac{1}{2}\varepsilon_{ik\ell}\partial_k\beta^p_{\ell j}$, as can be seen from applying the identity

$$\delta_{ij}\varepsilon_{qk\ell} = \delta_{jq}\varepsilon_{ik\ell} + \delta_{jk}\varepsilon_{i\ell q} + \delta_{j\ell}\varepsilon_{iqk}$$

to $\partial_q\beta_{k\ell}$. Thus α_{ij} takes again the form (2.69).

2.11. BRANCHING DEFECT LINES

We recall that from the geometric point of view, the conservation laws state that disclination lines never end and dislocations end at most at a disclination line. Consider, for example, a configuration of three lines shown in Part II, Figs. 1.11, 1.12. Assign an orientation to each line and suppose that their disclination density is

$$\Theta_{ij}(\mathbf{x}) = \Omega_i\delta_j(L) + \Omega'_i\delta_j(L') + \Omega''_i\delta_j(L''), \tag{2.71}$$

with their dislocation density being

$$\begin{aligned}\alpha_{ij}(\mathbf{x}) = {} & \delta_i(L)\{b_j + [\Omega\times(\mathbf{x}-\mathbf{x}_0)]_j\} + \delta_i(L')\{b'_j + [\Omega'\times(\mathbf{x}-\mathbf{x}'_0)]_j\} \\ & + \delta_i(L')\{b''_j + [\Omega''\times(\mathbf{x}-\mathbf{x}''_0)]_j\}.\end{aligned} \tag{2.72}$$

The conservation law $\partial_i\Theta_{ij} = 0$ then implies that the Frank vectors satisfy the equivalent of Kirchhoff's law for currents

$$\Omega_i + \Omega_i'' = \Omega_i'. \tag{2.73}$$

This follows directly from the identity [see Eq. [II.1.83)] for open lines

$$\partial_i \delta_i(L) = \int ds \frac{d\bar{x}_i}{ds} \delta^{(3)}(\mathbf{x} - \bar{\mathbf{x}}(3)) = \delta^{(3)}(\mathbf{x} - \mathbf{x}_i) - \delta^{(3)}(\mathbf{x} - \mathbf{x}_f),$$

where $\mathbf{x}_i$ and $\mathbf{x}_f$ are the initial and final points of the curve L. The conservation law $\partial_i \alpha_{ij} = \varepsilon_{ik\ell} \Theta_{k\ell}$, on the other hand, gives

$$b_i - (\Omega \times (\mathbf{x} - \mathbf{x}_0))_i + b_i'' - (\Omega'' \times (\mathbf{x} - \mathbf{x}_0'')_i)_i = b_i' - (\Omega \times (\mathbf{x}' - \mathbf{x}_0'))_i. \tag{2.74}$$

If the same position is chosen for all rotation axes, the Burgers vectors b_i satisfy again a Kirchhoff-like law:

$$b_i + b_i'' = b_i'. \tag{2.75}$$

But Burgers vectors can be compensated for by different rotation axes, for example, L' and L'' could be pure disclination lines with different axes through $\mathbf{x}_0'$, $\mathbf{x}_0''$ and L' a pure dislocation line with $\mathbf{b}' = -\Omega' \times (\mathbf{x}_0' - \mathbf{x}_0'')$ which ends on L', L''. Equation (2.73) renders different choices equivalent.

2.12. DEFECT DENSITY AND INCOMPATIBILITY

As far as classical linear elasticity is concerned, the information contained in α_{ij} and Θ_{ij} can be combined into a single symmetric tensor, called the *defect density* $\eta_{ij}(\mathbf{x})$ [In higher gradient elasticity this is no longer true; see chapter 18.]. It is defined as the double curl of the strain tensor

$$\eta_{ij}(\mathbf{x}) \equiv \varepsilon_{ik\ell} \varepsilon_{jmn} \partial_k \partial_m u_{\ell n}(\mathbf{x}). \tag{2.76}$$

In order to see its relation with α_{ij} and Θ_{ij}, we take (2.42a) and contract the indices i and j, obtaining

$$\alpha_{ii} = 2\partial_i \omega_i. \tag{2.77}$$

Using this, (2.48) can be written in the form

$$\varepsilon_{ik\ell} \partial_k u_{\ell n} = \partial_n \omega_i - (-\alpha_{in} + \tfrac{1}{2} \delta_{in} \alpha_{kk}). \tag{2.78}$$

The expression in parentheses was first introduced by Nye and called *contortion*[b]

$$K_{ni} \equiv -\alpha_{in} + \tfrac{1}{2}\delta_{in}\alpha_{kk}\,. \tag{2.79a}$$

The inverse relation is

$$\alpha_{ij} = -K_{ji} + \delta_{ij}K_{kk}\,. \tag{2.79b}$$

Multiplying (2.78) by $\varepsilon_{jmn}\partial_m$, we find with (2.42b)

$$\begin{aligned}\eta_{ij} &= \varepsilon_{jmn}\varepsilon_{ik\ell}\partial_m\partial_k u_{\ell n} = \varepsilon_{jmn}\partial_m\partial_n\omega_i - \varepsilon_{jmn}\partial_m K_{ni} \\ &= \Theta_{ji} - \varepsilon_{jmn}\partial_m K_{ni}\,.\end{aligned} \tag{2.80a}$$

The final expression is not manifestly symmetric. Let us verify that it is, nevertheless. Contracting it with the antisymmetric tensor $\varepsilon_{\ell ij}$, we find $\varepsilon_{\ell ij}\Theta_{ij} + \partial_\ell K_{ii} - \partial_i K_{\ell i} = \varepsilon_{\ell ij}\Theta_{ij} + \partial_i\alpha_{i\ell}$. But this vanishes due to the conservation law (2.46) for the dislocation density. Thus η_{ij} is symmetric.

There is yet another version of the decomposition (2.80a) which is obtained after applying the identity $\varepsilon_{ijn}\delta_{mq} + \varepsilon_{jmn}\delta_{iq} + \varepsilon_{min}\delta_{jq} = \varepsilon_{ijm}\delta_{nq}$ to $\partial_m\alpha_{qn}$ giving $\varepsilon_{njm}\partial_m(\alpha_{in} - \tfrac{1}{2}\delta_{in}\alpha_{kk}) = -\tfrac{1}{2}\partial_m(\varepsilon_{mjn}\alpha_{in} + (ij) + \varepsilon_{ijn}\alpha_{mn})$. Hence

$$\eta_{ij} = \Theta_{ij} - \tfrac{1}{2}\partial_m(\varepsilon_{min}\alpha_{jn} + (ij) - \varepsilon_{ijn}\alpha_{mn})\,. \tag{2.80b}$$

This type of decomposition will be encountered in the context of general relativity later in Part IV.

The double curl operation is a useful generalization of the curl operation on vector fields to symmetric tensor fields. Recall that the vanishing of a curl everywhere in space implies that a vector field can be written as the gradient of a scalar potential which satisfies the integrability condition $(\partial_i\partial_j - \partial_j\partial_i)\,\gamma = 0$ everywhere in space:

$$\nabla \times \mathbf{H} = 0 \rightarrow H_i = \partial_i\gamma. \tag{2.81}$$

[b]In terms of the plastic quantities introduced in the last section the plastic part of K_{ij} reads

$$K^p_{ij} = -\varepsilon_{jk\ell}\partial_k\beta^p_{\ell i} + \tfrac{1}{2}\delta_{ij}\varepsilon_{nk\ell}\partial_k\beta^p_{\ell n} + \phi^p_{ij}.$$

The double curl operation implies a similar property for the symmetric tensor, as was shown a century ago by Riemann and by Christoffel. If the double curl of a symmetric tensor field vanishes everywhere in space, this field can be written as the strain of some displacement field $u_i(\mathbf{x})$ which is integrable in all space [i.e., it satisfies (2.33)]. We may state this conclusion briefly as follows:

$$\varepsilon_{ik\ell}\,\varepsilon_{jmn}\,\partial_k\,\partial_m u_{\ell n}(\mathbf{x}) = 0 \rightarrow u_{ij} = \tfrac{1}{2}(\partial_i u_j + \partial_j u_i). \tag{2.82}$$

If the double curl of $u_{\ell n}(\mathbf{x})$ is zero one says that $u_{\ell n}(\mathbf{x})$ is *compatible* with a displacement field and calls the double curl the *incompatibility*, i.e.,

$$(\text{inc } u)_{ij} \equiv \varepsilon_{ik\ell}\,\varepsilon_{jmn}\,\partial_k\,\partial_m u_{\ell n}. \tag{2.83}$$

The proof of statement (2.82) follows from (2.81) for a vector field: we simply observe that every vector field $V_k(\mathbf{x})$ vanishing at infinity and satisfying the integrability condition $(\partial_i\partial_j - \partial_j\partial_i)\,V_k(\mathbf{x}) = 0$ can be decomposed into transverse and longitudinal pieces, namely, a gradient whose curl vanishes and a curl whose gradient vanishes,

$$V_i = \partial_i\varphi + \varepsilon_{ijk}\,\partial_j A_k, \tag{2.84}$$

both fields φ and A_k being integrable. Explicitly these are given by

$$\varphi = \frac{1}{\partial^2}\,\partial_i V_i, \tag{2.85}$$

$$A_k = \frac{1}{-\partial^2}\,\varepsilon_{k\ell m}\,\partial_\ell V_m + \partial_k C, \tag{2.86}$$

where

$$(-\partial^2)^{-1} = 1/(4\pi|\mathbf{x} - \mathbf{x}'|) \tag{2.87}$$

is the Coulomb Green function. Notice that the field A_k is determined only up to an arbitrary pure gradient $\partial_k C$.

By repeated application of this formula, we find the decompositions of an arbitrary not necessarily symmetric tensor u_{il}:

$$u_{i\ell} = \partial_i\varphi'_\ell + \varepsilon_{ijk}\,\partial_j A'_{k\ell} = \partial_i\varphi'_\ell + \varepsilon_{ijk}\,\partial_j(\partial_\ell\varphi_k + \varepsilon_{\ell mn}\,\partial_m A_{kn}). \tag{2.88}$$

Setting

$$\varphi_i'' \equiv \varepsilon_{ijk}\,\partial_j \varphi_k, \tag{2.89}$$

this may be cast as

$$u_{i\ell} = \partial_i \varphi_\ell' + \partial_\ell \varphi_i'' + \varepsilon_{ijk}\,\varepsilon_{\ell mn}\,\partial_j \partial_m A_{kn}. \tag{2.90}$$

For the special case that $u_{i\ell}$ is symmetric we can symmetrize this result and decompose it as

$$u_{i\ell} = \partial_i u_j + \partial_j u_i + \varepsilon_{ijk}\,\varepsilon_{\ell mn}\,\partial_j \partial_m A_{kn}^S, \tag{2.91}$$

where

$$u_i = \tfrac{1}{2}(\varphi_i' + \varphi_i''), \tag{2.92}$$

and A_{kn}^S is the symmetric part of A_{kn}, both being integrable fields. The first term in (2.91) has zero incompatibility, the second has zero divergence when applied to either index.

In the general case, i.e., when there is no symmetry, we can use the formulas (2.85), (2.86) twice and determine the fields φ_ℓ', φ_i'', A_{kn} as follows:

$$\varphi_\ell' = \frac{1}{\partial^2}\,\partial_k u_{k\ell}, \tag{2.93}$$

$$A_{k\ell}' = -\frac{1}{\partial^2}\,\varepsilon_{kpq}\,\partial_p u_{q\ell} + \partial_k C_\ell, \tag{2.94}$$

$$\varphi_k = -\frac{1}{\partial^4}\,\varepsilon_{kpq}\,\partial_p \partial_\ell u_{q\ell} + \frac{1}{\partial^2}\,\partial_k \partial_\ell C_\ell, \tag{2.95}$$

$$A_{kn} = -\frac{1}{\partial^4}\,\varepsilon_{k\ell m}\,\varepsilon_{npq}\,\partial_\ell \partial_p u_{mq} + \partial_k\left(-\frac{1}{\partial^2}\,\varepsilon_{nj\ell}\,\partial_j C_\ell\right) + \partial_n D_k, \tag{2.96}$$

so that from (2.88)

$$\varphi_i'' = -\frac{1}{\partial^4}\,\partial_i \partial_p \partial_q u_{pq} + \frac{1}{\partial^2}\,\partial_\ell u_{i\ell}. \tag{2.97}$$

Reinserting this into decomposition (2.90) we find the identity

$$u_{i\ell} = \frac{1}{\partial^2}(\partial_i \partial_k u_{k\ell} + \partial_\ell \partial_k u_{ik}) - \frac{1}{\partial^4}\partial_i \partial_\ell (\partial_p \partial_q u_{pq})$$

$$+ \frac{1}{\partial^4}\varepsilon_{ijk}\,\varepsilon_{\ell mn}\partial_j \partial_m (\varepsilon_{kpr}\varepsilon_{nqs}\partial_p \partial_q u_{rs}), \tag{2.98}$$

which is valid for any tensor of rank two. This may be verified by working out the contractions of the ε tensors.[c]

While the statements (2.81) and (2.82) for vector and tensor fields are completely analogous to each other, it is important to realize that there exists an important difference between the two cases. For a vector field with no curl, the potential can be calculated uniquely (up to boundary conditions) from

$$\varphi = \frac{1}{\partial^2}\partial_i H_i. \tag{2.99}$$

This is no longer true, however, for the compatible tensor field $u_{i\ell}$. The point of departure is the fact that the functions φ'_ℓ and φ''_i in the decomposition (2.90) are not unique. They are determined only modulo a common arbitrary local rotation field $\omega_i(\mathbf{x})$. In order to see this we introduce the replacements

$$\partial_i \varphi'_\ell(\mathbf{x}) \to \partial_i \varphi'_\ell(\mathbf{x}) + \varepsilon_{i\ell q}\omega_q(\mathbf{x}), \tag{2.100}$$

$$\partial_\ell \varphi''_i(\mathbf{x}) \to \partial_\ell \varphi''_i(\mathbf{x}) + \varepsilon_{\ell i q}\omega_q(\mathbf{x}), \tag{2.101}$$

and see that (2.90) is still true. The field (2.92) is only *a particular example* of a displacement field which has the strain tensor equal to the given $u_{k\ell}$,

[c]Later, starting with Chapter 4, we shall introduce an efficient technique for handling such involved derivative expressions using helicity projections. For the reader who is already familiar with this technique let us mention that (2.98) can be derived from two identities:

$$\varepsilon_{jmj'}\varepsilon_{\ell n\ell'}p_m p_n = \mathbf{p}^2(P^{(2,2)} + P^{(2,-2)} - P^L + P^{(1,0)})_{j\ell,j'\ell'},$$

$$p_j p_{j'}\delta_{\ell\ell'} + p_\ell p_{\ell'}\delta_{jj'} - p_j p_\ell p_{j'} p_{\ell'} = \mathbf{p}^2(P^{(2,1)} + P^{(2,-1)} + P^{(1,1)} + P^{(1,-1)} + P^{L'})_{j\ell,j'\ell'}$$

The first will be derived in a footnote to Eq. (5.19). The second is a direct consequence of (4.127) and (5.14). If we square the first identity and add the second we obtain a decomposition of the identity which coincides with (2.98).

$$u^0_{k\ell} = \tfrac{1}{2}(\partial_k u^0_\ell + \partial_\ell u^0_k) = u_{k\ell}. \tag{2.102}$$

This displacement field may not, however, be the true displacement field $u_\ell(\mathbf{x})$ which is actually present in the crystal which also satisfies

$$\tfrac{1}{2}(\partial_k u_\ell + \partial_\ell u_k) = u_{k\ell}. \tag{2.103}$$

In order to find this true displacement field we would need additional information, namely, the rotation field

$$\omega_{k\ell} = \tfrac{1}{2}(\partial_k u_\ell - \partial_\ell u_k). \tag{2.104}$$

Only if we know both $u_{k\ell}(\mathbf{x})$ *and* $\omega_{k\ell}(\mathbf{x})$ can we calculate

$$\partial_k u_\ell(\mathbf{x}) = u_{k\ell}(\mathbf{x}) + \omega_{k\ell}(\mathbf{x}) \tag{2.105}$$

and solve this for $u_\ell(\mathbf{x})$.

In order to make use of this observation we have to be sure that $\omega_i = \frac{1}{2}\varepsilon_{ijk}\omega_{jk}$ can, in fact, be written as the curl of a displacement field $u_i(\mathbf{x})$. This is possible if

$$\partial_i \omega_i = \varepsilon_{ijk}\partial_i \partial_j u_k = 0, \tag{2.106}$$

which implies that [see (2.77)]

$$\alpha_{ii}(\mathbf{x}) = 0. \tag{2.107}$$

In later discussions we shall be confronted with the situation in which $u_{k\ell}$ and $\partial_i \omega_j$ are given. In order to obtain ω_i from the latter we would have to make sure that ω_i is an integrable field, which is assured by the constraint

$$\Theta_{ij} = \varepsilon_{ik\ell}\,\partial_k \partial_\ell\, \omega_j = 0. \tag{2.108}$$

Thus we can state the following important result: Given a crystal with a strain $u_{k\ell}(\mathbf{x})$ and a specific rotational distortion $\omega_{k\ell}(\mathbf{x})$. If we want to find from these field quantities a single valued displacement field $u_\ell(\mathbf{x})$, the crystal has to have a vanishing defect density $\eta_{ij}(\mathbf{x})$, a vanishing disclination density $\Theta_{ij}(\mathbf{x})$, and a vanishing $\alpha_{ii} = 0$, i.e.,

$$\eta_{ij}(\mathbf{x}) = 0, \qquad \Theta_{ij}(\mathbf{x}) = 0, \qquad \alpha_{ii}(\mathbf{x}) = 0. \tag{2.109}$$

The relation (2.80b) implies that for this to be true it is sufficient to have

$$\eta_{ij}(\mathbf{x}) = 0, \qquad \alpha_{ij}(\mathbf{x}) = 0, \tag{2.110a}$$

or

$$\Theta_{ij}(\mathbf{x}) = 0, \qquad \alpha_{ij}(\mathbf{x}) = 0. \tag{2.110b}$$

Notice that it is possible to introduce, into a given elastically distorted crystal, nonzero rotational and translational defects in such a way that Θ_{ij} and α_{ij} in (2.80b) cancel each other.[d] Then the elastic distortions do in fact remain unchanged. The local rotation field, however, can be changed drastically. In particular it may no longer be integrable.

2.13. DEFECTS IN TWO DIMENSIONS

At some places we shall consider defects in two-dimensional systems. It is useful to imagine such systems as lying in the XY plane of some three-dimensional space. Then dislocation lines degenerate into points and the dislocation density is a vector which coincides with the 3, i components of the three-dimensional density

$$\alpha_i(\mathbf{x}) \equiv \alpha_{3i}(\mathbf{x}) = \varepsilon_{pq}\partial_p\partial_q u_i = (\partial_1\partial_2 - \partial_2\partial_1)u_i, \tag{2.111}$$

where $\varepsilon_{pq} = \varepsilon_{pq3}$. The local rotation vector has only one component, i.e.,

$$\omega \equiv \omega_3 \equiv \tfrac{1}{2}\varepsilon_{pq}\omega_{pq} = \tfrac{1}{2}\varepsilon_{pq}\partial_p u_q = \tfrac{1}{2}(\partial_1 u_2 - \partial_2 u_1) \tag{2.112}$$

so that the disclination density becomes a scalar quantity

$$\Theta \equiv \Theta_{33} = \varepsilon_{pq}\partial_p\partial_q\omega = (\partial_1\partial_2 - \partial_2\partial_1)\omega. \tag{2.113}$$

By writing the dislocation density as

$$\alpha_i = \varepsilon_{k\ell}\partial_k(u_{\ell i} + \varepsilon_{\ell i}) \tag{2.114}$$

[d]For an accurate counting of the defect degrees of freedom see the discussion accompanying Eqs. (16.14)–(16.28).

and inserting $\omega_{\ell i} = \varepsilon_{\ell i}\omega$ we find the following two-dimensional version of (2.48),

$$\alpha_i = \varepsilon_{k\ell}\partial_k u_{\ell i} - \partial_i \omega. \tag{2.115}$$

As was true with Θ_{ij}, the defect density $\eta_{ij}(\mathbf{x})$ also has only a 33 component $\eta(\mathbf{x})$,

$$\eta(\mathbf{x}) \equiv \eta_{33}(\mathbf{x}) = \varepsilon_{k\ell}\varepsilon_{mn}\partial_k\partial_m u_{\ell n} \tag{2.116}$$

and applying $\varepsilon_{mn}\partial_n$ to (2.115) we find the two-dimensional analogue of (2.80b),

$$\eta(\mathbf{x}) = \Theta(\mathbf{x}) + \varepsilon_{mn}\partial_m \alpha_n(\mathbf{x}). \tag{2.117}$$

A contortion vector K_n may be introduced as $K_n = -\alpha_n$ but since there is only a sign difference with respect to α_n there is no real use this.

For completeness, let us also introduce the plastic distortions and rotations $\beta^p_{k\ell}$, $\phi^p_{k\ell}$ which were defined in three dimensions in Section 2.10. Here they follow from the trivial Volterra operation [compare (2.60)]

$$u_\ell(\mathbf{x}) = -\delta(V)(b_\ell - \Omega\varepsilon_{\ell r}x_r)$$

as

$$\beta^p_{k\ell} = \delta_k(S)(b_\ell - \Omega\varepsilon_{\ell r}x_r) - \delta(V)\,\Omega\varepsilon_{k\ell}, \qquad \phi^p_k = \delta_k(S)\,\Omega, \tag{2.118}$$

where S is now the *line* along which the Volterra cut has been performed. The δ-function $\delta_k(S)$ is defined to point along the normal of this line, i.e., it is given by

$$\delta_k(S) = \varepsilon_{k\ell}\int_S d\bar{x}_\ell\,\delta^{(2)}(\mathbf{x} - \bar{\mathbf{x}}). \tag{2.119}$$

It satisfies the two-dimensional version of Stokes' formula (II.8.17):

$$\varepsilon_{jk}\partial_j\delta_k(S) = \varepsilon_{jk}\varepsilon_{k\ell}\partial_j\int_S ds\frac{d\bar{x}_\ell}{ds}\delta^{(2)}(\mathbf{x} - \bar{\mathbf{x}}(s)) = -\int_S ds\frac{d\bar{x}_j}{ds}\partial_j\delta^{(2)}(\mathbf{x} - \bar{\mathbf{x}}(s))$$

$$= \int_S ds\frac{d}{ds}\delta^{(2)}(\mathbf{x} - \bar{\mathbf{x}}(s)) = \delta^{(2)}(\mathbf{x} - \bar{\mathbf{x}}_f) - \delta^{(2)}(\mathbf{x} - \bar{\mathbf{x}}_i), \tag{2.120}$$

FIG. 2.17. Illustration of $\delta_K(L)$ in two dimensions, defined in Eqs. (2.121), (2.122), which is singular only at the points where L pierces the x_1x_2 plane.

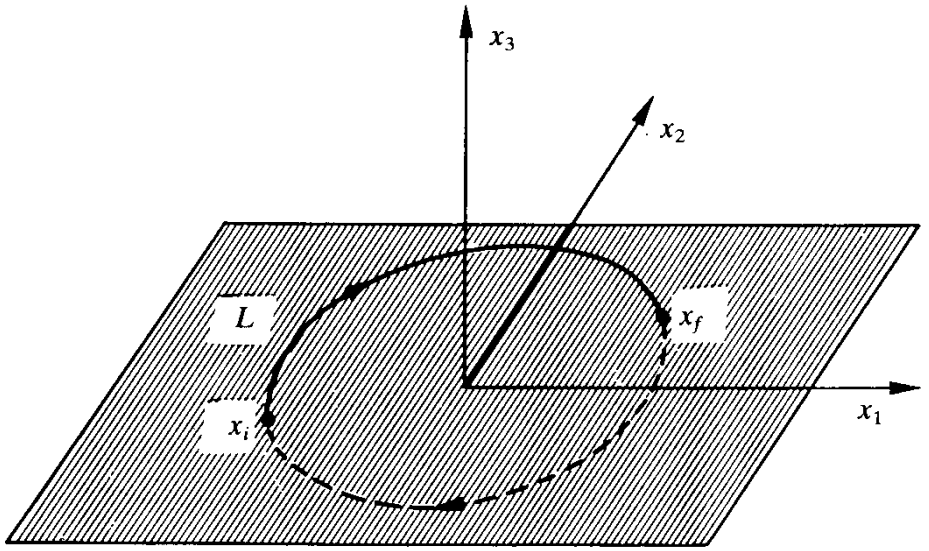

where $\mathbf{x}_i$ and $\mathbf{x}_f$ are the initial and final points of the line S. The right-hand side is the 2-dimensional version of $\delta_k(L)$. It can be thought of as being the third component of the three-dimensional δ-function for a closed line L,

$$\delta_k(L) = \oint_L dS \frac{d\bar{x}_k}{dS} \delta^{(3)}(\mathbf{x} - \bar{\mathbf{x}}(S)), \tag{2.121}$$

which picks up the two points where L pierces the xy-plane (see Fig. 2.17)

$$\begin{aligned} \delta_3(L)|_{x_3=0} &= \oint_L d\bar{x}_3 \, \delta(\mathbf{x}_3 - \bar{\mathbf{x}}_3) \, \delta^{(2)}(\mathbf{x}_\perp - \bar{\mathbf{x}}_\perp)|_{x_3=0} \\ &= \delta^{(2)}(\mathbf{x} - \bar{\mathbf{x}}_f) - \delta^{(2)}(\mathbf{x} - \mathbf{x}_i)|_{x_3=0} \end{aligned} \tag{2.122}$$

Using (2.118) and the notation (2.122), the dislocation and disclination densities read explicitly

$$\begin{aligned} \alpha_i &= \varepsilon_{k\ell} \, \partial_k \, \beta^p_{\ell i} - \phi^p_i = \delta_3(L)|_{x_3=0}(b_i - \Omega \, \varepsilon_{ir} x_r), \\ \Theta &= \varepsilon_{k\ell} \, \partial_k \, \phi^p_\ell = \delta_3(L)|_{x_3=0} \Omega. \end{aligned} \tag{2.123}$$

The first is the $i3$ component of the three-dimensional density $\alpha_{ij}(\mathbf{x})$, the second the 33 component of $\Theta_{ij}(\mathbf{x})$, both restricted to the 12 plane.

NOTES AND REFERENCES

The first observations and theoretical studies of dislocations are found in
O. Mügge, *Neues Jahrb. Min.* **13** (1883),
A. Ewing and W. Rosenhain, *Phil. Trans. Roy. Soc.* **A193** (1899) 353,
J. Frenkel, *Z. Phys.* **37** (1926) 572,
E. Orowan, *Z. Phys.* **89** (1934) 605, 634,
M. Polanyi, *Z. Phys.* **89** (1934) 660,
G.I. Taylor, *Proc. Roy. Soc.* **A145** (1934) 362,
J.M. Burgers, *Proc. Kon. Ned. Akad. Wetenschap.* **42** (1939) 293, 378,
F. Kroupa and P.B. Price, *Phil. Mag.* **6** (1961) 243,
W.T. Read, Jr., *Dislocations in Crystals* (McGraw-Hill, New York, 1953),
F.C. Frank and W.T. Read, Jr., *Phys. Rev.* **79** (1950) 722,
B.A. Bilby, R. Bullough, and E. Smith, *Proc. Roy. Soc.* **A231** (1955) 263.

Disclination lines were described by
F.C. Frank, *Disc. Farad. Soc.* **25** (1958) 1.
More details can be found in the books quoted below.

Weingarten's theorem is derived in
F.R.N. Nabarro, *Theory of Dislocations* (Clarendon Press, Oxford, 1967),
C. Truesdell and R. Toupin, in *Handbook of Physics*, Vol III(1), ed. S. Flügge (Springer, Berlin 1960).

The plastic strain described in Section 2.9 was used efficiently by
J.D. Eshelby, *Brit. J. Appl. Phys.* **17** (1966) 1131
to calculate elastic field configurations. The plastic distortions and rotations were introduced by
T. Mura, *Phil. Mag.* **8** (1963) 843, *Arch. Mech.* **24** (1972) 449, *Phys. Stat. Sol.* **10** (1965) 447, **11** (1965) 683.
See also his forthcoming book *Micromechanics of Defects in Solids* (Noordhoof, Amsterdam, 1987).
For an excellent review see
E. Kröner, in *The Physics of Defects*, eds. R. Balian *et al.* (North-Holland, Amsterdam, 1981) p. 264.
Further useful literature can be found in
J.P. Hirth and J. Lothe, *Theory of Dislocations* (McGraw Hill, New York, 1968),
J. Friedel, *Dislocations* (Pergamon Press, Oxford, 1964).
See also the 1980 lectures at Les Houches in *The Physics of Defects*, *op. cit.*,
M. Kléman, *The General Theory of Disclinations*, in *Dislocations in Solids*, ed. F.R.N. Nabarro (North-Holland, Amsterdam, 1980),
W. Bollmann, *Crystal Defects and Crystalline Interfaces* (Springer, Berlin, 1970),
B. Henderson, *Defects in Crystalline Solids* (Edward Arnold, London, 1972).

CHAPTER THREE

ENERGETICS OF DISLOCATION LINES

3.1. STRAIN AND STRESS AROUND DISLOCATION LINES

We are now in a position to study the elastic properties of a solid with defects. For a start, let us restrict ourselves to pure dislocation lines which are characterized by a constant discontinuity across some surface S with Burgers vectors $\mathbf{b}$:

$$\Delta u_i = \oint_B du_i = b_i. \tag{3.1}$$

This specification is sufficient to calculate a displacement field $u_i(\mathbf{x})$ over all space. Notice that the relation

$$u_i(\mathbf{x}) = \int d^3x' G_{ij}(\mathbf{x} - \mathbf{x}') f_j(\mathbf{x}') \tag{3.2}$$

with $f_j(\mathbf{x}') = 0$ cannot be used since it holds only for smooth field configuration $u_i(\mathbf{x})$.

The appropriate method to deal with singular surfaces is, however, well known in potential theory. There, one uses Green's theorem which is a simple consequence of Gauss' law for a vector field [recall Part II, Eq. (1.151)]. Here we have to generalize this to an arbitrary tensor field,

$$\int_V d^3x\, \partial_i T_{k_1 \ldots k_n} = \int_S dS_i T_{k_1 \ldots k_n}, \tag{3.3}$$

where S is the surface enclosing V with dS_i directed outward. Applying this to the tensors

$$T^1_k = u_i(\mathbf{x}')\, \partial'_k G_{mn}(\mathbf{x}' - \mathbf{x}), \qquad T^2_\ell = (\partial'_\ell u_i(\mathbf{x}'))\, G_{mn}(\mathbf{x}' - \mathbf{x}), \tag{3.4}$$

we have

$$\int_V d^3x'\, \partial_\ell (u_i(\mathbf{x}')\, \partial'_k G_{mn}(\mathbf{x}' - \mathbf{x})) = \int_S dS'_\ell u_i(\mathbf{x}')\, \partial'_k G_{mn}(\mathbf{x}' - \mathbf{x}),$$

$$\int_V d^3x'\, \partial_k (\partial'_\ell u_i(\mathbf{x}'))\, G_{mn}(\mathbf{x}' - \mathbf{x})) = \int_S dS'_k (\partial'_\ell u_i(\mathbf{x}'))\, G_{mn}(\mathbf{x}' - \mathbf{x}). \tag{3.5}$$

Subtracting these equations from each other, we obtain a generalized version of Green's theorem,

$$\int_V d^3x' [u_i(\mathbf{x}')\, \partial'_\ell \partial'_k G_{mn}(\mathbf{x}' - \mathbf{x}) - (\partial'_\ell \partial'_k u_i(\mathbf{x}'))\, G_{mn}(\mathbf{x}' - \mathbf{x})]$$

$$= \int_S dS'_\ell u_i(\mathbf{x}')\, \partial'_k G_{mn}(\mathbf{x}' - \mathbf{x}) - \int_S dS'_k (\partial'_\ell u_i(\mathbf{x}'))\, G_{mn}(\mathbf{x}' - \mathbf{x}). \tag{3.6}$$

Contracting this equation with the elasticity tensor $-c_{\ell ikm}$, the left-hand side becomes, by (1.68) and (1.80),

$$u_n(\mathbf{x}) - \int dx'\, G_{nm}(\mathbf{x} - \mathbf{x}') f_m(\mathbf{x}'). \tag{3.7}$$

The right-hand side becomes

$$-\int_S dS'_\ell c_{\ell ikm} u_i(\mathbf{x}')\, \partial'_k G_{mn}(\mathbf{x}' - \mathbf{x}) + \int_S dS'_k \sigma_{km}(\mathbf{x}')\, G_{mn}(\mathbf{x}' - \mathbf{x}) \tag{3.8}$$

so that we remain, in the absence of local body forces $f_m(\mathbf{x}')$, with

$$u_n(\mathbf{x}) = -\int_S dS'_\ell c_{\ell ikm} u_i(\mathbf{x}')\, \partial'_k G_{mn}(\mathbf{x}' - \mathbf{x}) + \int_S dS'_k\, \sigma_{km}(\mathbf{x}')\, G_{mn}(\mathbf{x}' - \mathbf{x}). \tag{3.9}$$

FIG. 3.1. The infinitesimally thin ellipsoid enclosing the Volterra cutting surface S of a dislocation line along L. The thickness is greatly exaggerated to allow for a better representation.

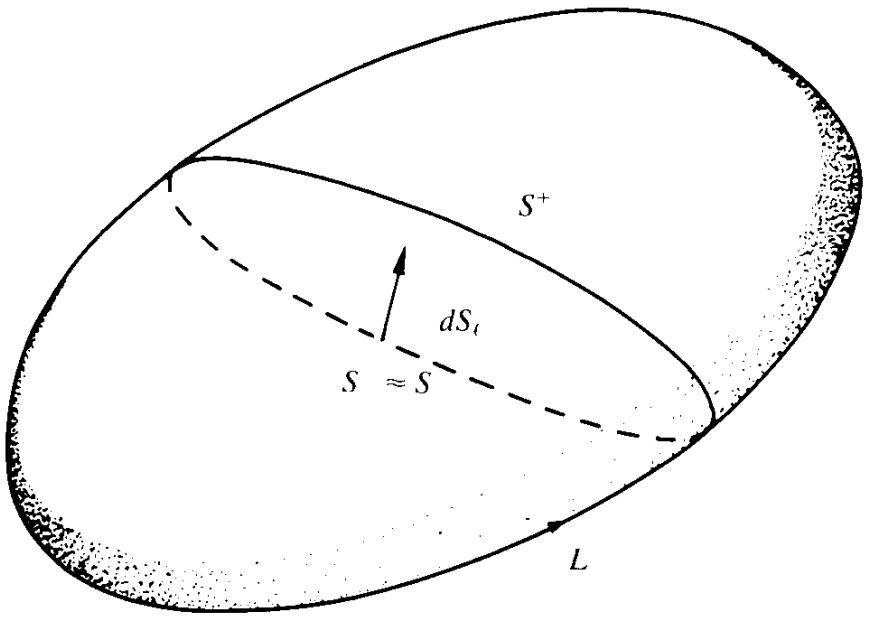

Consider now an infinite crystal with a single dislocation loop which is constructed by removing one or more layers of atoms from the lattice thus causing the discontinuity $\Delta u_i = \oint_B du_i = b_i$ (recall Fig. 2.2). The whole space outside the plane may be considered as V such that S becomes the surface of a very thin ellipsoid enclosing the surface of discontinuity (see Fig. 3.1). Let S^+ be the upper surface whose normal points downward and S^- the lower surface with the normal pointing upward. The integral (3.9) may then be transformed into a surface integral running only over $S^- \approx S$ if the integrands are replaced by their discontinuity across S. We may assume that $\mathbf{x}$ lies outside the surface S for otherwise we would be able to move S to another place. Since the stress as well as the Green function are the same on both sides of S, the second term in the integral disappears and we arrive at

$$u_n(\mathbf{x}) = -b_i \int_S dS_\ell \, c_{\ell ikm} \partial'_k G_{mn}(\mathbf{x}' - \mathbf{x}). \tag{3.10}$$

In the isotropic case, we may insert (1.23) and the explicit result (1.90) for G_{mn} and arrive at

$$u_n(\mathbf{x}) = -\frac{1}{8\pi\mu}\int_S dS'_\ell \left\{ \mu(b_n R_{,kk\ell} + b_m \delta_{\ell n} R_{,kkm}) + \lambda b_\ell R_{,kkn} \right.$$
$$\left. - \frac{\lambda+\mu}{\lambda+2\mu}[2\mu b_k R_{,n\ell k} + \lambda b_\ell R_{,kkn}] \right\}, \tag{3.11}$$

where we have introduced the notation

$$\partial_i R = R_{,i}, \qquad \partial_k \partial_n \partial_\ell R = R_{,\ell nk}, \qquad \ldots, \tag{3.12}$$

for brevity. This expression can be rearranged in the form

$$u_n(\mathbf{x}) = -\frac{1}{8\pi}\left\{ \int_S dS'_\ell\, b_n R_{,kk\ell} + \int_{S^-} [dS'_n b_\ell R_{,kk\ell} - dS'_\ell b_\ell R_{,kk\ell}] \right.$$
$$\left. + 2\frac{\lambda+\mu}{\lambda+2\mu}\int_S dS'_\ell\,(b_\ell R_{,kkn} - b_k R_{,n\ell k}) \right\}. \tag{3.13}$$

The integral still runs over the surface. The construction procedure à la Volterra however, has taught us that the position of this surface is irrelevant and only the boundary L can have a physical reality. Therefore, we may use Stokes' theorem to arrive at a contour integral over L. The most convenient form for the application needed here is

$$\oint dx'_k\, \varepsilon_{k\ell m} T_{n_1 n_2 \ldots} = \int dS'_i \varepsilon_{ijk} \varepsilon_{k\ell m} \partial'_j T_{n_1 n_2 \ldots}$$
$$= \int (dS'_\ell \partial'_m T_{n_1 n_2 \ldots} - dS'_m \partial'_\ell T_{n_1 n_2 \ldots}), \tag{3.14}$$

where ... denotes more possible tensor indices. In particular, we obtain the formulas

$$\oint_L dx'_i\, \varepsilon_{in\ell} b_\ell R_{,kk} = -\int_S (dS'_n b_\ell R_{,kk\ell} - dS'_\ell b_\ell R_{,kkn}),$$
$$\oint_L dx'_i \varepsilon_{i\ell k} b_\ell R_{,kn} = -\int_S (dS'_\ell b_\ell R_{,kkn} - dS'_k b_\ell R_{,\ell kn}), \tag{3.15}$$

where we have used the fact that $\partial_n R = -\partial'_n R$. With these formulas, we can bring (3.13) to the alternative form

$$u_n(\mathbf{x}) = -\frac{1}{8\pi}\int_S dS'_\ell\, b_n R_{,pp\ell} + \frac{1}{8\pi}\oint_S dx'_i\, \varepsilon_{in\ell} b_\ell R_{,kk}$$
$$+ \frac{1}{4\pi}\frac{\lambda+\mu}{\lambda+2\mu}\oint_L dx'_i\, \varepsilon_{i\ell k} b_\ell R_{,kn}$$
$$= \frac{b_n}{4\pi}\int_S dS'_\ell \frac{R_\ell}{R^3} - \frac{1}{4\pi}\int_L d\mathbf{x}' \times \frac{\mathbf{b}}{R} - \frac{1}{8\pi(1-\nu)}\partial_n \oint_L \mathbf{b}\cdot\frac{d\mathbf{x}'\times\mathbf{R}}{R}, \tag{3.16}$$

where $\mathbf{R}_i \equiv \mathbf{x}_i - \mathbf{x}'_i$ and where we have worked out the derivatives,

$$R_{,i} = R_i/R,\ R_{,ij} = \delta_{ij}/R - R_iR_j/R^3,\ R_{,pp} = 2/R,\ R_{,ppk} = -2R_k/R^3.$$

The first integral,

$$\frac{b_n}{4\pi}\int_S dS'_\ell\, R_\ell/R^3,$$

is recognized as the solid angle through which the positive side of S is seen from $\mathbf{x}$. It appeared in the vortex formula (1.157), Part I. Thus we have simply

$$\frac{b_n}{4\pi}\Omega.$$

This is the only term in (3.16) which keeps track of the surface of discontinuity S over which u_n jumps by b_n. If we change S_1 to S_2, the solid angle as defined by

$$\Omega(\mathbf{x}) = \int_{S_1} dS'_\ell \frac{R_\ell}{R^3}, \tag{3.17}$$

changes by

$$\Omega_2(\mathbf{x}) - \Omega_1(\mathbf{x}) = \int_{S_2 - S_1} dS'_\ell \frac{R_\ell}{R^3}.$$

In order to describe the same dislocation loop, S_1 and S_2 must have the

same boundary line so that $S_2 - S_1$ is a closed surface around some volume element V. Hence we can use Gauss' formula and write

$$\Omega_2(\mathbf{x}) - \Omega_1(\mathbf{x}) = \int_V d^3x'\, \partial'_\ell \frac{R_\ell}{R^2} = -\int_V d^3x'\, \partial_\ell \frac{R_\ell}{R^2} = \int_V d^3x'\, \partial_\ell^2 \frac{1}{R}$$

$$= 4\pi \int_V d^3x'\, \delta^{(3)}(\mathbf{x} - \mathbf{x}') = 4\pi\delta(V) = \begin{cases} 4\pi & x \in V, \\ 0 & x \notin V. \end{cases} \tag{3.18}$$

Thus the solid angle is unchanged for observation points $\mathbf{x}$ which lie outside the volume enclosed by the two surfaces S_2, S_1, while it changes by the discontinuity 4π if $\mathbf{x}$ lies inside.

The constancy of this change is what permits us to define strain and stress tensors which are independent of the surface S. Writing

$$\partial_i \Omega(\mathbf{x}) = \int dS'_\ell\, \partial_i \frac{R_\ell}{R} = -\int dS'_\ell\, \partial_i \partial_\ell \frac{1}{R}$$

$$= \partial_\ell \left(\int dS'_\ell\, \partial'_i \frac{1}{R} - \int dS'_i\, \partial'_\ell \frac{1}{R} \right) - \int dS_i \partial_\ell^2 \frac{1}{R}$$

$$= \varepsilon_{i\ell k} \partial_\ell \int_L dx'_k \frac{1}{R} + 4\pi \delta_i(S), \tag{3.19}$$

the first term is the same as the magnetic field of a unit current along the boundary line L of S. Only the second term depends on S. It corresponds to a magnetic field due to a layer of magnetic dipoles placed on S. The derivatives of the displacement field $\partial_i u_j(\mathbf{x})$ are smooth everywhere in space as long as $\mathbf{x}$ does not fall onto S. If $\mathbf{x}$ is to pass the surface S, we may simply shift S to another position S'. Then the derivatives can be continued smoothly through S. The whole procedure is recognized as the three-dimensional generalization of the continuation of an analytic function through a cut in the complex plane.

Since the dipole layer is an unphysical artefact of the Volterra construction, only the smooth part of the gradient of the displacement field

$$(\partial_i u_j)^{\text{smooth}}(\mathbf{x}) = (\partial_i u_j(\mathbf{x}) - \delta_i(S)\, b_j)$$

is a physical observable. This combination is invariant under changes of the surface S from S to S', under which

$$u_j(\mathbf{x}) \to u_j(\mathbf{x}) - \delta(V)\, b_j, \qquad \delta_i(S) \to \delta_i(S) - \partial_i \delta(V).$$

Looking back at (2.62) we recognize the piece

$$\beta_{ij}^{p}(\mathbf{x}) = \delta_i(S)\, b_j$$

as the *plastic distortion*. The distortion $\partial_i u_j(\mathbf{x})$ which still contains jumps in u_j is called the *total distortion* [sometimes written with a superscript T as in $(\partial_i u_j(\mathbf{x}))^T$].

Notice that while $\partial_i u_j(\mathbf{x})$ is not uniquely defined, depending on the position of the jumping surface S, the smooth part of the gradient $(\partial_i u_j)^{\text{smooth}}$ is unique. In fact, its symmetric composition

$$u_{ij}^{\text{smooth}} \equiv \tfrac{1}{2}((\partial_i u_j)^{\text{smooth}} + (ij)) = u_{ij} - \tfrac{1}{2}(\delta_i(S)\, b_j + (ij))$$

is an observable quantity, being proportional to the stresses of the system. The subtracted piece

$$u_{ij}^{p} \equiv \tfrac{1}{2}(\delta_i(S)\, b_j + (ij))$$

is recognized as the *plastic strain tensor* of a pure dislocation line [defined in (2.61)].

In the theory of linear elasticity of defects one often finds calculations of physical strains and stresses *without* this explicit subtraction. In that case, all formulas are understood as being evaluated *away* from the jumping surface S. For a while, we shall also adhere to this somewhat sloppy convention. Only later shall we be more careful and uncover the interesting gauge structures inherent in this subtraction procedure.

Forgetting the jumping surface S, we can find the strain tensor associated with a given dislocation line by using (3.16) and forming the derivative

$$u_{i,j} = \frac{1}{8\pi} \oint dx_k' \left[\varepsilon_{jk\ell} b_i R_{,pp\ell} - \varepsilon_{ik\ell} b_\ell R_{,ppj} - \frac{1}{1-\nu} \varepsilon_{kmn} b_n R_{,mij} \right], \quad (3.20)$$

after which the strain and stress can be expressed as follows:

$$u_{ij} = \frac{1}{8\pi} \oint dx_k' \left[\tfrac{1}{2}(\varepsilon_{jk\ell} b_i R_{,\ell} + \varepsilon_{ik\ell} b_j R_{,\ell} - \varepsilon_{ik\ell} b_\ell R_{,j} - \varepsilon_{jk\ell} b_\ell R_{,i})_{,pp} \right.$$

$$\left. - \frac{1}{1-\nu} \varepsilon_{kmn} b_n R_{,mij} \right],$$

$$\sigma_{ij} = -\frac{\mu}{4\pi} b_n \oint \Big[\tfrac{1}{2}(dx_i' \, \varepsilon_{jmn} + dx_j' \, \varepsilon_{imn}) R_{,mpp} + \frac{1}{1-\nu} dx_k' \, \varepsilon_{kmn} (R_{,mij} - \delta_{ij} R_{,mpp}) \Big]. \tag{3.21}$$

As a check in our calculation we may verify that the stress is divergenceless, $\partial_i \sigma_{ij} = 0$, as it should.

3.2. ELASTIC INTERACTION ENERGY BETWEEN TWO DISLOCATION LINES

Suppose a crystal contains two dislocation lines. Let us calculate their interaction energy. The stress field of the first line $\sigma_{ij}^{\mathrm{I}}(\mathbf{x})$ is given by (3.21). If a second line is introduced into the crystal, the atoms are displaced by an additional amount $u_i^{\mathrm{II}}(\mathbf{x})$ which can be calculated from (3.16). This is independent of the presence of the first dislocation line since, in the approximation of linear elasticity, all displacements are additive. Correspondingly, the change δE in elastic energy is simply obtained from the integral

$$\delta E = \int d^3x \, \sigma_{ij} \delta u_{ij} = \int d^3x \, \sigma_{ij} \partial_i \delta u_j$$

as

$$E^{\mathrm{I\,II}} = \int d^3x \, \sigma_{ij}^{\mathrm{I}} \partial_i u_j^{\mathrm{II}}. \tag{3.22}$$

This can be evaluated in complete analogy with the magnetic energy of the current loops or the stress energy of the vortex loops [see (2.137), Part II].

First we use $\partial_i \sigma_{ij} = 0$ to rewrite (3.22) in the form

$$E^{\mathrm{I\,II}} = \int d^3x \, \partial_i (\sigma_{ij}^{\mathrm{I}} u_j^{\mathrm{II}}). \tag{3.23}$$

Then we transform this into a surface integral,

$$E^{\mathrm{I\,II}} = \int_{S^\infty + S^- + S^+} dS_i^{\mathrm{II}} d\sigma_{ij}^{\mathrm{I}} u_j^{\mathrm{II}}, \tag{3.24}$$

where the part over the surface at infinity S^∞ vanishes and S^+, S^- form a thin ellipsoid enclosing S (see Fig. 3.1). For a dislocation line along L, u_i^{II} has the discontinuity $u_j^{\mathrm{II}}|_S - u_j^{\mathrm{II}}|_{S^+} = b_j$ across the thin ellipsoid $S^- + S^+$ enclosing it and the energy becomes

$$E^{\mathrm{I\,II}} = b_j \int_{S^-} dS_i^{\mathrm{II}} \sigma_{ij}^{\mathrm{I}}. \tag{3.25}$$

This differs from the magnetic formula in (1.146), Part II by the additional index j. It looks as though there were three "magnetic fields" σ_{i1}^{I}, σ_{i2}^{I}, σ_{i3}^{I}, each being divergenceless, $\partial_i \sigma_{i1}^{\mathrm{I}} = 0$, $\partial_i \sigma_{i2}^{\mathrm{I}} = 0$, $\partial_i \sigma_{i3}^{\mathrm{I}} = 0$, and associated with three "currents" b_1, b_2, b_3. Therefore, we can proceed as in the magnetic case and introduce three gauge fields A_{i1}^{I}, A_{i2}^{I}, A_{i3}^{I} in terms of which the stresses can be written as a curl,

$$\sigma_{ij}^{\mathrm{I}} = \varepsilon_{ik\ell}\, \partial_k A_{\ell j}^{\mathrm{I}}. \tag{3.26}$$

The properties of the gauge field $A_{\ell j}^{\mathrm{I}}$ will be discussed in detail in Section 4.1. Here will only make use of the fact that with (3.26) we can apply Stokes' theorem and bring the interaction energy into the local form

$$E^{\mathrm{I\,II}} = b_j^{\mathrm{II}} \oint_{L^{\mathrm{II}}} dx_\ell^{\mathrm{II}} A_{\ell j}^{\mathrm{I}}. \tag{3.27}$$

It is straightforward to find $A_{\ell j}^{\mathrm{I}}$. Using the stress formula (3.21), we can directly read off:

$$A_{\ell j}^{\mathrm{I}} = \frac{\mu}{8\pi} b_i^{\mathrm{I}} \oint_{L^{\mathrm{I}}} \varepsilon_{ikp}\, \varepsilon_{jmn} R_{,km} \left(\delta_{\ell p}\, dx_n^{\mathrm{I}} + \delta_{np}\, dx_\ell^{\mathrm{I}} + \frac{2\nu}{1-\nu} \delta_{\ell n}\, dx_p^{\mathrm{I}} \right). \tag{3.28}$$

Inserting this into (3.27) we obtain the analogue of Biot-Savart's law for dislocation loops, first found by Blin,

$$E^{\mathrm{I\,II}} = \frac{\mu}{8\pi} b_i^{\mathrm{I}} b_j^{\mathrm{II}} \oint_{L^{\mathrm{I}}} \oint_{L^{\mathrm{II}}} \varepsilon_{ik\ell}\, \varepsilon_{jmn} R_{,km} \left(dx_n^{\mathrm{I}} dx_\ell^{\mathrm{II}} + \delta_{\ell n}\, dx_p^{\mathrm{I}} dx_p^{\mathrm{II}} + \frac{2\nu}{1-\nu} dx_\ell^{\mathrm{I}} dx_n^{\mathrm{II}} \right)$$

$$= \frac{\mu}{4\pi} \oint_{L^{\mathrm{I}}} \oint_{L^{\mathrm{II}}} \left(\frac{\mathbf{b}^{\mathrm{I}} \cdot d\mathbf{x}^{\mathrm{I}} \mathbf{b}^{\mathrm{II}} \cdot d\mathbf{x}^{\mathrm{II}}}{R} - 2 \frac{\mathbf{b}^{\mathrm{I}} \times \mathbf{b}^{\mathrm{II}} \cdot d\mathbf{x}^{\mathrm{I}} \times d\mathbf{x}^{\mathrm{II}}}{R} \right.$$

$$\left. + \frac{1}{1-\nu} (\mathbf{b}^{\mathrm{I}} \times d\mathbf{x}^{\mathrm{I}})_i (\mathbf{b}^{\mathrm{II}} \times d\mathbf{x}^{\mathrm{II}})_j \partial_i \partial_j R \right). \tag{3.29}$$

Of course, this can be generalized to an arbitrary number of loops just as the magnetic formulas (1.162) to (1.163) of Part II. Also, the generalization to a continuous distribution is straightforward: all we have to do is replace

$$b_i^{\mathrm{I}} b_j^{\mathrm{II}} \oint_{L^{\mathrm{I}}} \oint_{L^{\mathrm{II}}} dx_\ell^{\mathrm{I}} dx_n^{\mathrm{II}} \tag{3.30}$$

by

$$\frac{1}{2} \int d^3x \, d^3x' \, \alpha_{\ell i}(\mathbf{x}) \, \alpha_{nj}(\mathbf{x}'), \tag{3.31}$$

where $\alpha_{\ell i}(\mathbf{x})$ is the dislocation (pseudo-current) density (2.59) [compare (1.164) of Part I].

NOTES AND REFERENCES

The contents of this chapter are standard and can be found in most books on this subject (see the references at the end of Chapter 2) and in the review article of
R. De Wit, *Solid St. Phys.* **10** (1960) 249.

CHAPTER FOUR

LOCAL FIELD DESCRIPTION OF INTERACTING DISLOCATIONS

4.1. ELASTIC PARTITION FUNCTION

In the case of superfluid ^{4}He we have seen that it was possible to describe the long-range interactions between vortex lines in terms of a *local* field theory. We simply had to express the bending energy in terms of a gauge field and couple this locally to the random chains of vortex lines. Their ensemble, in turn, followed a disorder field theory, thereby permitting a simple discussion of the superfluid phase transition.

In this section, we shall prepare the ground for a similar treatment of defect lines in crystals. As a first step we shall derive a partition function for the thermally fluctuating stress gauge field $A_{\ell j}(\mathbf{x})$ which was defined in Eq. (3.26). This yields the stress tensor via the curl operation applied to the first index:

$$\sigma_{ij} = \varepsilon_{ik\ell}\partial_k A_{\ell j}.$$

This decomposition is invariant under the local gauge transformations

$$A_{\ell j}(\mathbf{x}) \to A_{\ell j}(\mathbf{x}) + \partial_\ell \Lambda_j(\mathbf{x}). \tag{4.1}$$

The symmetry of σ_{ij} imposes the constraint [which is compatible with (4.1)]

$$\partial_i A_{\ell i}(\mathbf{x}) = \partial_\ell A_{jj}(\mathbf{x}). \tag{4.2}$$

This follows directly from the condition $\varepsilon_{nij}\sigma_{ij}(\mathbf{x}) = \partial_j A_{nj} - \partial_n A_{jj} = 0$.

As a consequence of (4.1) and (4.2), $A_{\ell j}$ has only three physical components, as was the case with the symmetric divergenceless stress tensor σ_{ij}. If we insert $\sigma_{ij} = \varepsilon_{ik\ell}\partial_k A_{\ell j}$ into the elastic energy in the form (1.43), we obtain a rather complicated looking expression,

$$E_{\rm el} = \frac{1}{4\pi}\int d^3x \Big[\partial_k A_{\ell i}\partial_k A_{\ell i} - \partial_\ell A_{\ell i}\partial_{\ell'} A_{\ell' i} - \frac{\nu}{1-\nu}(\partial_k A_{\ell i}\partial_k A_{\ell i} - \partial_k A_{ki}\partial_\ell A_{\ell i} + \partial_\ell A_{\ell i}\partial_j A_{ij} + \partial_i A_{\ell i}\partial_k A_{ki} - \partial_\ell A_{\ell i}\partial_\ell A_{\ell i} - \partial_i A_{\ell i}\partial_j A_{\ell j}) \Big]. \tag{4.3}$$

According to (3.27), the local interaction with a single dislocation line running along L was

$$E_{\rm int} = b_j \oint dx_\ell A_{\ell j}. \tag{4.4}$$

For a general distribution $\alpha_{\ell j}(\mathbf{x})$ of dislocations this becomes

$$E_{\rm int} = \int d^3x\, \alpha_{\ell j}(\mathbf{x})\, A_{\ell j}(\mathbf{x}). \tag{4.5}$$

Hence we expect the elastic partition function of the dislocation density $\alpha_{\ell j}(\mathbf{x})$ to be given, in analogy with the vortex lines in superfluid ^{4}He, by

$$Z = \int \mathscr{D}A_{\ell j}(\mathbf{x})\, \delta(\partial_j A_{\ell j} - \partial_\ell A_{jj})\Phi[A_{\ell j}] \exp\{(E_{\rm el} + iE_{\rm int})/T\}. \tag{4.6}$$

The δ-functional enforces the constraint (4.2). The factor $\Phi[A_{\ell j}]$ fixes the gauge in a convenient way which will be explained later. When integrating out the fluctuating gauge field, this partition function has to give

$$Z = \text{const.} \times \exp\left\{-\frac{1}{T}E_{\rm Blin}\right\}, \tag{4.7}$$

where $E_{\rm Blin}$ is Blin's energy formula (3.29)–(3.31). As was true for vortex

lines, a factor i in front of E_{int} is necessary in order to obtain the correct sign of this energy.

When looking at the complicated gauge field energy (4.3), the integration looks, at first sight, somewhat difficult; in particular, since we have to respect the constraint (4.2) and the gauge-fixing factor $\Phi[A_{ij}]$. The problem can be simplified considerably by transforming the field componentes $A_{ij}(\mathbf{x})$ to a more convenient basis in which the energy is diagonal.

As far as the spatial variables $\mathbf{x}$ are concerned, the energy diagonalizes by going to Fourier (= momentum) space and expanding

$$A_{ij}(\mathbf{x}) = \int \frac{d^3p}{(2\pi)^3} e^{i\mathbf{p}\cdot\mathbf{x}} A_{ij}(\mathbf{p}). \tag{4.8}$$

After this, the 3×3 index space can be diagonalized by finding another $\mathbf{p}$ dependent, basis known as the *helicity basis*. Since not every reader may be familiar with this concept, let us interrupt the discussion for a moment and give a brief, general description of the helicity decomposition of vector and tensor fields.

4.2. HELICITY DECOMPOSITION OF A VECTOR FIELD

Under a rotation of coordinates

$$x_i' = R_{ij} x_j, \tag{4.9}$$

a vector field $v_i(\mathbf{x})$ is defined by the transformation property [see (3.116), Part I]

$$v_i'(\mathbf{x}') = R_{ij} v_j(\mathbf{x}). \tag{4.10}$$

The rotation matrix can be expressed in terms of the rotation vector α whose direction points along the axis and whose length gives the angle of rotation, i.e.,

$$R_{ij} = (e^{i\alpha\cdot S})_{ij}, \tag{4.11}$$

where the matrices S_k form the adjoint (spin-one) representation of the Lie algebra of the rotation group,

$$(S_k)_{ij} = -i\varepsilon_{kij}. \tag{4.12}$$

For infinitesimal angles this gives the well-known formula [see (3.138), Part I]

$$\delta x_i = x_i' - x_i = \alpha_k \varepsilon_{kij} x_j = -(\boldsymbol{\alpha} \times \mathbf{x})_i. \tag{4.13}$$

Inserting this into (4.10), the *local change* of the vector $v_i(\mathbf{x})$ is, up to terms $O((\delta x)^2)$,

$$\begin{aligned}\delta v_i(\mathbf{x}) &\equiv v_i'(\mathbf{x}) - v_i(\mathbf{x}) \approx v_i'(\mathbf{x}') - v_i(\mathbf{x}') = v_i'(\mathbf{x}') - v_i(\mathbf{x}) + v_i(\mathbf{x}) - v_i(\mathbf{x}') \\ &= i\alpha_k (S_k)_{ij} v_j(\mathbf{x}) - \delta x_j \partial_j v_i(\mathbf{x}) = i\alpha_k (S_k)_{ij} v_j(\mathbf{x}) + \alpha_k \varepsilon_{k\ell j} x_\ell \partial_j v_i(\mathbf{x}) \\ &= i\alpha_k (S_k)_{ij} v_j(\mathbf{x}) + i\alpha_k L_k v_i(\mathbf{x}),\end{aligned} \tag{4.14}$$

where we have introduced in the second term the generator of orbital rotations,

$$L_k = -i\varepsilon_{kij} x_i \partial_j. \tag{4.15}$$

In momentum space, the transformation laws are found similarly,

$$p_i' = R_{ij} p_j, \tag{4.16}$$

$$v_i'(\mathbf{p}') = R_{ij} v_j(\mathbf{p}), \tag{4.17}$$

$$\begin{aligned}\delta v_i(\mathbf{p}) &\equiv v_i'(\mathbf{p}) - v_i(\mathbf{p}) = v_i'(\mathbf{p}') - v_i(\mathbf{p}') \\ &= i\alpha_k (S_k)_{ij} v_j(\mathbf{p}) + i\alpha_k L_k v_i(\mathbf{p}),\end{aligned} \tag{4.18}$$

with

$$L_k = -i\varepsilon_{kij} p_i \frac{\partial}{\partial p_j}. \tag{4.19}$$

The latter fields $v_i(\mathbf{p})$ have the advantage of diagonalizing the translation group generated by the differential operators

$$p_i = -i\partial_i. \tag{4.20}$$

These, together with (4.19), form the inhomogeneous rotation group (also called the Euclidean group $E(3)$) which is characterized by the commutation relations

$$[p_i, p_i] = 0, \tag{4.21}$$

$$[L_i, p_j] = i\varepsilon_{ijk} p_k, \tag{4.22}$$

$$[L_i, L_j] = i\varepsilon_{ijk} L_k. \tag{4.23}$$

The *helicity basis* is now introduced in the following two steps:

1. We choose an orthogonal set of three basis vectors $e_i^1(\hat{\mathbf{p}})$, $e_i^2(\hat{\mathbf{p}})$, $e_i^3(\hat{\mathbf{p}})$ in the subspace of a fixed momentum in such a way that $e_i^3(\hat{\mathbf{p}})$ *coincides with the unit vector along the momentum direction*,

$$\hat{\mathbf{p}} = \mathbf{p}/|\mathbf{p}|. \tag{4.24}$$

2. We form combinations of these, called the *spherical components*,

$$\mathbf{e}^{(+1)}(\hat{\mathbf{p}}) \equiv \frac{1}{\sqrt{2}}(\mathbf{e}^1 + i\mathbf{e}^2)(\hat{\mathbf{p}}) \equiv \mathbf{e}(\hat{\mathbf{p}}),$$

$$\mathbf{e}^{(-1)}(\hat{\mathbf{p}}) \equiv -\frac{1}{\sqrt{2}}(\mathbf{e}^1 - i\mathbf{e}^2)(\hat{\mathbf{p}}) \equiv -\mathbf{e}^*(\hat{\mathbf{p}}),$$

$$\mathbf{e}^{(0)}(\hat{\mathbf{p}}) \equiv \mathbf{e}^3(\hat{\mathbf{p}}) = \hat{\mathbf{p}}. \tag{4.25}$$

The vectors $e^{(h)}(\hat{\mathbf{p}})$ for $h = \pm 1, 0$ constitute the desired helicity basis.

They have the following properties. First they are an orthonormal set of vectors with respect to the complex scalar product,

$$e_i^{(h)*}(\hat{\mathbf{p}})\, e_i^{(h')}(\hat{\mathbf{p}}) = \delta^{hh'}. \tag{4.26}$$

Hence they also form a complete basis in three-dimensional space. This property can be expressed in terms of a completeness relation,

$$\sum_{h=0,\pm 1} e_i^{(h)}(\hat{\mathbf{p}})\, e_j^{(h)*}(\hat{\mathbf{p}}) = \delta_{ij}. \tag{4.27}$$

The different terms in this sum, i.e.,

$$P_{ij}^{(h)}(\hat{\mathbf{p}}) \equiv e_i^{(h)}(\hat{\mathbf{p}})\, e_j^{(h)*}(\hat{\mathbf{p}}), \tag{4.28}$$

for $h = \pm 1, 0$ have the products

$$P_{ij}^{(h)}(\hat{\mathbf{p}})\, P_{jk}^{(h)}(\hat{\mathbf{p}}) = P_{ik}^{(h)}(\hat{\mathbf{p}})\, \delta_{ik} \tag{4.29}$$

and are, therefore, projection matrices. With these, the completeness relation (4.27) reads

$$\sum_{h=0,\pm 1} P_{ij}^{(h)}(\hat{\mathbf{p}}) = \delta_{ij}. \tag{4.30}$$

This result makes it straightforward to expand an arbitrary vector function $v_i(\mathbf{p})$ in terms of the new basis: We only have to multiply $v_j(\mathbf{p})$ by (4.30) and obtain

$$v_i(\mathbf{p}) = \sum_{h=0,\pm 1} P_{ij}^{(h)}(\hat{\mathbf{p}}) v_j(\mathbf{p}) = \sum_{h=0,\pm 1} e_i^{(h)}(\hat{\mathbf{p}})\, e_j^{(h)*}(\hat{\mathbf{p}}) v_j(\mathbf{p}) = \sum_{h=0,\pm 1} e_i^{(h)}(\hat{\mathbf{p}}) v^{(h)}(\mathbf{p}). \tag{4.31}$$

The components $v^{(h)}(\mathbf{p})$ are called *helicity components* of the vector field $v_i(\mathbf{p})$.

Let us now come to the second characteristic property of the vectors $e_i^{(h)}(\hat{\mathbf{p}})$. Under rotations they transform as a vector field [recall (4.17)]. In order to see this we perform a rotation which changes p_i to $p_i' = R_{ij} p_j$. Then the vectors $e_i^{(h)}(\hat{\mathbf{p}})$ change according to

$$e_i^{(0)\prime}(\hat{\mathbf{p}}') = \hat{\mathbf{p}}_i' = R_{ij}\hat{\mathbf{p}}_j = R_{ij}\, e_i^{(0)}(\hat{\mathbf{p}}), \qquad e_i^{(\pm 1)\prime}(\hat{\mathbf{p}}') = R_{ij}\, e_j^{(\pm 1)}(\hat{\mathbf{p}}). \tag{4.32}$$

As a consequence, the components $v^{(h)}(\mathbf{p})$ have very simple transformation properties with respect to the basis $e_i^{(h)}(\hat{\mathbf{p}})$. While the old Cartesian components of $\mathbf{v}(\mathbf{p})$ were mixed with each other under rotations [see (4.17)], the new components $v^{(h)}(\mathbf{p})$ remain inert. They transform like a scalar field,

$$v^{(h)\prime}(\mathbf{p}') = v^{(h)}(\mathbf{p}). \tag{4.33}$$

Infinitesimally, this amounts to the transformation law

$$\delta v^{(h)}(\mathbf{p}) \equiv v^{(h)\prime}(\mathbf{p}) - v^{(h)}(\mathbf{p}) = i\alpha_k L_k v^{(h)}(\mathbf{p}), \tag{4.34}$$

where **L** is the differential operator (4.19).

The third property (which is actually not unrelated to the second) of the basis vectors $e_i^{(h)}(\hat{\mathbf{p}})$ is that they diagonalize the generator of spin rotations projected along the direction of momentum, i.e., the so-called *helicity matrix*

$$H(\hat{\mathbf{p}}) = \hat{p}_k S_k, \tag{4.35}$$

and h are its eigenvalues. This can be shown directly. Let us first take $\hat{\mathbf{p}}$ to point in the 3-direction so that H is the matrix

$$H(\hat{\mathbf{z}}) = S_3 = -i\begin{pmatrix} 0 & 1 & 0 \\ -1 & 0 & 0 \\ 0 & 0 & 0 \end{pmatrix}, \tag{4.36}$$

while $e_i^{(h)}(\hat{\mathbf{z}})$ are the vectors

$$e_i^{(0)}(\hat{\mathbf{z}}) = \begin{pmatrix} 0 \\ 0 \\ 1 \end{pmatrix}, \qquad e_i^{(\pm 1)}(\hat{\mathbf{z}}) = \pm\frac{1}{\sqrt{2}}\begin{pmatrix} 1 \\ \pm i \\ 0 \end{pmatrix}. \tag{4.37}$$

Then we find, trivially,

$$H_{ij}(\hat{\mathbf{z}})\, e_j^{(h)}(\hat{\mathbf{z}}) = h\, e_i^{(h)}(\hat{\mathbf{z}}). \tag{4.38}$$

For an arbitrary direction of $\mathbf{p}$ we may obtain the three vectors $e_i^{(h)}(\hat{\mathbf{p}})$ by (4.32)

$$e_i^{(h)}(\hat{\mathbf{p}}) = R_{ij}(\hat{\mathbf{p}})\, e_j^{(h)}(\hat{\mathbf{z}}), \tag{4.39}$$

where $R_{ij}(\hat{\mathbf{p}})$ is a rotation matrix which brings the z-axis in the direction $\hat{\mathbf{p}}$, i.e.,

$$\hat{p}_i = R_{ij}(\hat{\mathbf{p}})\, \hat{z}_j. \tag{4.40}$$

Applying (4.35) to (4.39) we can verify that $e_j^{(h)}(\hat{\mathbf{p}})$ is an eigenvector of $H(\hat{\mathbf{p}})$. First we note that

$$\begin{aligned} H_{ij}(\hat{\mathbf{p}})\, e_j^{(h)}(\hat{\mathbf{p}}) &= H_{ij}(\hat{\mathbf{p}})\, R_{jk}(\hat{\mathbf{p}})\, e_k^{(h)}(\hat{\mathbf{z}}) \\ &= R_{ij}(\hat{\mathbf{p}})\, R_{jk}^{-1}(\hat{\mathbf{p}})(\hat{p}_r S_r)_{k\ell} R_{\ell m}(\hat{\mathbf{p}})\, e_m^{(h)}(\hat{\mathbf{z}}). \end{aligned} \tag{4.41}$$

But the spin matrix S_r is a vector operator and satisfies

$$R_{jk}^{-1}(S_r)_{k\ell}R_{\ell n} = R_{rs}(S_s)_{jn} = (S_s)_{jn}(R^{-1})_{sr}, \tag{4.42}$$

so that

$$H_{ij}(\hat{\mathbf{p}})\,e_j^{(h)}(\hat{\mathbf{p}}) = R_{ij}(\hat{\mathbf{p}})(S_s)_{jm}(R(\hat{\mathbf{p}})_{sr}^{-1}\hat{p}_r)\,e_m^{(h)}(\hat{\mathbf{z}}).$$

By (4.40) this becomes

$$R_{ij}(\hat{\mathbf{p}})(S_s)_{jm}\hat{z}_s\,e_m^{(h)}(\hat{\mathbf{z}}) = R_{ij}(\hat{\mathbf{p}})\,H(\hat{\mathbf{z}})_{jm}\,e_m^{(h)}(\hat{\mathbf{z}}). \tag{4.43}$$

Then we may use (4.38) and (4.39) to obtain

$$H_{ij}(\hat{\mathbf{p}})\,e_j^{(h)}(\hat{\mathbf{p}}) = h\,R_{ij}(\hat{\mathbf{p}})\,e_m^{(h)}(\hat{\mathbf{z}}) = h\,e_m^{(h)}(\hat{\mathbf{p}}). \tag{4.44}$$

Thus $e_j^{(h)}(\hat{\mathbf{p}})$ are indeed eigenvectors of the helicity matrix $H_{ij}(\hat{\mathbf{p}})$, with eigenvalue h.

It turns out that what we have just shown could have been obtained more directly from the general relation

$$H'_{ij}(\hat{\mathbf{p}}') = R_{ik}R_{j\ell}H_{k\ell}(\hat{\mathbf{p}}) = (R\,H(\hat{\mathbf{p}})\,R^{-1})_{ij}, \tag{4.45}$$

where R is a matrix connecting $\hat{\mathbf{p}}'$ and $\hat{\mathbf{p}}$. Equation (4.44) is a consequence of the fact that the helicity operator is a rotational tensor field [compare (4.10)]. It is really for this reason that the helicity amplitudes defined in (4.31) do have the simple transformation law (4.33).

4.3. HELICITY DECOMPOSITION OF A TENSOR FIELD

The result obtained above can be generalized to tensor fields. In the present context, we shall be dealing only with tensors of second rank, say $t_{\ell i}(\mathbf{p})$. These transform as

$$t'_{\ell i}(\mathbf{p}') = R_{\ell m}R_{ij}t_{mj}(\mathbf{p}), \tag{4.46}$$

or infinitesimally,

$$\delta t_{\ell i}(\mathbf{p}) = -i\alpha_k(S_k)_{\ell m}t_{mi}(\mathbf{p}) - i\alpha_k(S_k)_{ij}t_{\ell j}(\mathbf{p}) - i\alpha_k L_k t_{\ell i}(\mathbf{p}). \tag{4.47}$$

It is easy to find the *helicity basis tensors* $e_{(i}^{(s,\,h)}(\hat{\mathbf{p}})$ which span the space of tensors and have the same transformation properties as these. They can be constructed from appropriate combinations of products of $e_i^{(h)}(\hat{\mathbf{p}})$, which diagonalize H. In the present case, the eigenvalue h of H is not sufficient to specify the basis tensors uniquely; an additional quantum number is needed. This is supplied by the total angular momentum s. It is well known that in order to span the whole 9-dimensional tensorial space, the products of vectors $e_i^{(h)}(\hat{\mathbf{p}})\, e_j^{(h)}(\hat{\mathbf{p}})$ have be coupled to form objects of total angular momenta $s = 0, 1, 2$, the dimensions of these spaces being 1, 3, and 5, respectively. The coupling can be found explicity by noting that H may be considered as the third component of the three generators of a helicity rotation (or little) group,

$$H(\hat{\mathbf{p}}) \equiv H_3(\hat{\mathbf{p}}) \equiv e_k^{(3)}(\hat{\mathbf{p}})\, S_k, \qquad H_{1,2}(\hat{\mathbf{p}}) \equiv e_k^{(1,\,2)}(\hat{\mathbf{p}})\, S_k. \tag{4.48}$$

By (4.35) and (4.40) we may write

$$H_i(\hat{\mathbf{p}}) = R_{ij}(\hat{\mathbf{p}})\, S_j. \tag{4.49}$$

These matrices satisfy the same commutation rules as the generators L_i [recall (4.23)], namely,

$$[H_i(\hat{\mathbf{p}}),\, H_j(\hat{\mathbf{p}})] = i\varepsilon_{ijk} H_k(\hat{\mathbf{p}}). \tag{4.50}$$

This follows directly from (4.23) and the invariance of the ε_{ijk} tensor under the rotation group,

$$\varepsilon_{ijk} = R_{ii'} R_{jj'} R_{kk'} \varepsilon_{i'j'k'}.$$

Therefore, we can define helicity raising and lowering operators

$$\begin{aligned} H_+(\hat{\mathbf{p}}) &\equiv (H_1 + iH_2)(\hat{\mathbf{p}}) = \sqrt{2}\, e_i^{(1)}(\hat{\mathbf{p}})\, S_i, \\ H_-(\hat{\mathbf{p}}) &= (H_1 - iH_2)(\hat{\mathbf{p}}) = -\sqrt{2}\, e_i^{(-1)}(\hat{\mathbf{p}})\, S_i, \end{aligned} \tag{4.51}$$

which commute according to the rules

$$[H_3,\, H_\pm] = \pm H_\pm, \qquad [H_+,\, H_-] = 2H_3. \tag{4.52}$$

Since $e_i^{(h)}(\hat{\mathbf{p}})$ are orthonormal, the total spin is measured by

$$\mathbf{H}(\hat{\mathbf{p}})^2 = \mathbf{S}^2. \tag{4.53}$$

The same algebraic relations remain valid if the spin-one matrices $(S_k)_{ij}$ are replaced by any higher dimensional representation. The possible eigenvalues of H^2 are $s(s+1)$ for $s = 0, 1, 2, \ldots$. Here we shall look at the tensor representation

$$(S_k)_{\ell i, mj} = \delta_{\ell m}(S_k)_{ij} + (S_k)_{\ell m}\delta_{ij}. \tag{4.54}$$

It is straightforward to construct linear combinations in the 3×3 dimensional product space of all $e_\ell^{(h)}(\hat{\mathbf{p}})\, e_i^{(h')}(\hat{\mathbf{p}})$ with $h, h' = 0, \pm 1$,

$$e_{\ell i}^{(s,\,h)}(\hat{\mathbf{p}}) = \sum_{h_1 + h_2 = h} C_{s,h}^{h_1 h_2}\, e_\ell^{(h_1)}(\hat{\mathbf{p}})\, e_i^{(h_2)}(\hat{\mathbf{p}}), \tag{4.55}$$

which diagonalize H and have total spins $s = 0, 1, 2$, i.e.,

$$\begin{aligned} H(\hat{\mathbf{p}})_{\ell i, mj}\, e_{mj}^{(s,\,h)}(\hat{\mathbf{p}}) &= h\, e_{\ell i}^{(s,\,h)}(\hat{\mathbf{p}}), \quad h = -s, \ldots, s, \\ H^2(\hat{\mathbf{p}})_{\ell i, mj}\, e_{mj}^{(s,\,h)}(\hat{\mathbf{p}}) &= s(s+1)\, e_{\ell i}^{(s,\,h)}(\hat{\mathbf{p}}), \quad s = 0, 1, 2, \ldots \end{aligned} \tag{4.56}$$

We simply use the well-known vector addition or *Clebsch-Gordan coefficients* $\langle s_1 h_1\, s_2 h_2 | sh \rangle$ and write

$$e_{\ell i}^{(s,\,h)}(\hat{\mathbf{p}}) = \sum_{h_1 + h_2 = h} \langle 1 h_1\, 1 h_2 | sh \rangle\, e_\ell^{(h_1)}(\hat{\mathbf{p}})\, e_i^{(h_2)}(\hat{\mathbf{p}}) = (-1)^h\, e_{\ell i}^{(s,\,-h)*}(\hat{\mathbf{p}}), \tag{4.57}$$

In particular

$$\begin{aligned} e_{\ell i}^{(2,\,2)} &= \langle 11\ 11 | 22 \rangle\, e_\ell^{(1)} e_i^{(1)} = e_\ell e_i = e_{\ell i}^{(2,\,-2)*}, \\ e_{\ell i}^{(2,\,1)} &= \langle 11\ 10 | 21 \rangle\, e_\ell^{(1)} e_i^{(0)} + \langle 10\ 11 | 21 \rangle\, e_\ell^{(0)} e_i^{(1)} \\ &= \frac{1}{\sqrt{2}}(e_\ell \hat{p}_i + \hat{p}_\ell e_i) = -e_{\ell i}^{(2,\,-1)*}, \\ e_{\ell i}^{(2,\,0)} &= \langle 11\ 1{-}1 | 20 \rangle\, e_\ell^{(1)} e_i^{(-1)} + \langle 1{-}1\ 11 | 20 \rangle\, e_\ell^{(-1)} e_i^{(1)} + \langle 10\ 10 | 20 \rangle\, e_\ell^{(0)} e_i^{(0)} \\ &= -\frac{1}{\sqrt{6}}(e_\ell e_i^* + e_\ell^* e_i) + \sqrt{\frac{2}{3}}\hat{p}_\ell \hat{p}_i = e_{\ell i}^{(2,\,0)*}. \end{aligned} \tag{4.58}$$

We now employ the completeness relation (4.27) of the three basic vectors $\mathbf{e}$, $\mathbf{e}^*$, $\hat{\mathbf{p}}$ in the form

$$e_\ell e_i^* + e_\ell^* e_i + \hat{p}_\ell \hat{p}_i = \delta_{\ell i}, \tag{4.59}$$

to rewrite the (2, 0) basis tensor as

$$e_{\ell i}^{(2,\,0)} = \sqrt{\frac{3}{2}}\left(\hat{p}_\ell \hat{p}_i - \frac{1}{3}\delta_{\ell i}\right). \tag{4.60}$$

For total spin one we obtain

$$\begin{aligned} e_{\ell i}^{(1,\,1)} &= \langle 11\ 10|11\rangle\, e_\ell^{(1)} e_i^{(0)} + \langle 10\ 11|11\rangle\, e_\ell^{(0)} e_i^{(1)} \\ &= \frac{1}{\sqrt{2}}(e_\ell \hat{p}_i - \hat{p}_\ell e_i) = -e_{\ell i}^{(1,\,-1)*}, \\ e_{\ell i}^{(1,\,0)} &= \langle 11\ 1{-}1|10\rangle\, e_\ell^{(1)} e_i^{(-1)} + \langle 1{-}1\ 11|10\rangle\, e_\ell^{(-1)} e_i^{(1)} + \langle 10\ 10|10\rangle\, e_\ell^{(0)} e_i^{(0)} \\ &= -\frac{1}{\sqrt{2}}(e_\ell e_i^* - e_\ell^* e_i) = e_{\ell i}^{(1,\,0)*}. \end{aligned} \tag{4.61}$$

These formulas can be rewritten, using

$$\begin{aligned} \frac{1}{\sqrt{2}}(e_\ell \hat{p}_i - p_\ell \hat{e}_i) &= \frac{1}{\sqrt{2}}\varepsilon_{\ell ik}\,\varepsilon_{\ell mn} e_m \hat{p}_n \\ &= \frac{1}{\sqrt{2}}\varepsilon_{\ell ik}\frac{1}{\sqrt{2}}(\mathbf{e}^{(1)} \times \hat{\mathbf{p}} + i\mathbf{e}^{(2)} \times \hat{\mathbf{p}})_k = \frac{i}{\sqrt{2}}\varepsilon_{\ell ik}\frac{1}{\sqrt{2}}(\mathbf{e}^{(1)} + i\mathbf{e}^{(2)})_k \\ &= \frac{i}{\sqrt{2}}\varepsilon_{\ell ik} e_k, \\ e_\ell e_i^* - e_\ell^* e_i &= \tfrac{1}{2}(e_\ell^{(1)} + ie_\ell^{(2)})(e_i^{(1)} - ie_i^{(2)}) - \text{c.c.} = -i(e_\ell^{(1)} e_i^{(2)} - e_\ell^{(2)} e_i^{(1)}) \\ &= -i\varepsilon_{\ell ik}\,\varepsilon_{k\ell' i'} e_{\ell'}^{(1)} e_{i'}^{(2)} = -i\varepsilon_{\ell ik}(\mathbf{e}^{(1)} \times \mathbf{e}^{(2)})_k = -i\varepsilon_{\ell ik}\hat{p}_k, \end{aligned}$$

as

$$e_{\ell i}^{(1,\,1)} = \frac{i}{\sqrt{2}}\varepsilon_{\ell ik} e_k = -e_{(\ell,\,i)}^{(1,\,-1)*} \qquad e_{\ell i}^{(1,\,0)} = \frac{i}{\sqrt{2}}\varepsilon_{\ell ik}\hat{p}_k. \tag{4.62}$$

Finally, the spin-zero tensor is

$$e_{\ell i}^{(0,\,0)} = \langle 11\ 1{-}1|00\rangle\, e_\ell^{(1)} e_i^{(-1)} + \langle 1{-}1\ 11|00\rangle\, e_\ell^{(-1)} e_i^{(1)} + \langle 10\ 10|00\rangle\, e_\ell^{(0)} e_i^{(0)}$$

$$= \frac{1}{\sqrt{3}}(e_\ell e_i^* + e_\ell^* e_i) + \frac{1}{\sqrt{3}}\hat{p}_\ell \hat{p}_i = \frac{1}{\sqrt{3}}\delta_{\ell i}. \tag{4.63}$$

The fact that

$$\mathbf{H}^2(\hat{\mathbf{p}})\, e^{(s,\,h)}(\hat{\mathbf{p}}) = s(s+1)\, e^{(s,\,h)}(\hat{\mathbf{p}}) \tag{4.64}$$

follows directly from the matrix elements

$$\begin{aligned} H_+(\hat{\mathbf{p}})\, e^{(s,\,h)}(\hat{\mathbf{p}}) &= \sqrt{(s-h)(s+h+1)}\, e^{(s,\,h+1)}(\hat{\mathbf{p}}), \\ H_-(\hat{\mathbf{p}})\, e^{(s,\,h)}(\hat{\mathbf{p}}) &= \sqrt{(s+h)(s-h+1)}\, e^{(s,\,h-1)}(\hat{\mathbf{p}}), \\ H_3(\hat{\mathbf{p}})\, e^{(s,\,h)}(\hat{\mathbf{p}}) &= h\, e^{(s,\,h)}(\hat{\mathbf{p}}), \end{aligned} \tag{4.65}$$

as can be verified by direct calculation:

$$\begin{aligned} \mathbf{H}^2 e^{(s,\,h)} &= [\tfrac{1}{2}(H_+H_- + H_-H_+) + H_3^2]\, e^{(s,\,h)} \\ &= [\tfrac{1}{2}((s+h)(s-h+1) + (s-h)(s+h+1)) + h^2]\, e^{(s,\,h)} \\ &= s(s+1)\, e^{(s,\,h)}. \end{aligned} \tag{4.66}$$

Because $e^{(s,\,h)}(\hat{\mathbf{p}})$ are all eigenvectors of the hermitian matrices $\mathbf{H}^2$ and H_3 with different eigenvalues, the eigenvectors are necessarily orthogonal. The Clebsch-Gordan coefficients automatically normalize their scalar products to

$$e_{\ell i}^{(s,\,h)*}(\hat{\mathbf{p}})\, e_{\ell i}^{(s',\,h')}(\hat{\mathbf{p}}) = \delta_{ss'}\delta_{hh'} \tag{4.67}$$

For this reason the matrices

$$P_{\ell i,\,mj}^{(s,\,h)}(\hat{\mathbf{p}}) = e_{\ell i}^{(s,\,h)}(\hat{\mathbf{p}})\, e_{\ell i}^{(s,\,h)*}(\hat{\mathbf{p}}) \tag{4.68}$$

satisfy

$$P_{\ell i,\,mj}^{(s,\,h)}(\hat{\mathbf{p}})\, P_{mj,\,nk}^{(s,\,h)}(\hat{\mathbf{p}}) = P_{\ell i,\,nk}^{(s,\,h)}(\hat{\mathbf{p}}) \tag{4.69}$$

and are projection operators into the s, h subspaces. The polari- tensors $e_{\ell i}^{(s,\,h)}(\hat{\mathbf{p}})$ are complete, a fact which may be expressed i projection matrices as

$$\sum_{s,h} P^{(s,h)}_{\ell i,mj} = \delta_{\ell m}\delta_{ij}. \tag{4.70}$$

One may verify this by inserting the explicit expressions, (4.68), (4.58)–(4.63), and using the completeness relation (4.27) for the basis vectors.

Therefore, given an arbitrary tensor field $A_{\ell i}(\mathbf{p})$, we can expand it as

$$A_{\ell i}(\mathbf{p}) = \sum_{s,h} P^{(s,h)}_{\ell i,mj}(\hat{\mathbf{p}})\, A_{mj}(\mathbf{p}) \tag{4.71}$$

$$= \sum_{s,h} e^{(s,h)}_{\ell i}(\hat{\mathbf{p}})\, A^{(s,h)}(\mathbf{p}), \tag{4.72}$$

the helicity amplitudes being

$$A^{(s,h)}(\mathbf{p}) \equiv e^{(s,h)*}_{\ell i}(\hat{\mathbf{p}})\, A_{\ell i}(\mathbf{p}). \tag{4.73}$$

4.4. HELICITY FORM OF THE MAGNETIC ENERGY

In order to illustrate the use of the helicity decompositions let us recall the familiar magnetic situation to which we apply this formalism. By Fourier transforming the fields, i.e.,

$$\mathbf{A}(\mathbf{x}) = \int \frac{d^3q}{(2\pi)^3} e^{i\mathbf{q}\cdot\mathbf{x}} \mathbf{A}(\mathbf{q}), \tag{4.74}$$

the magnetic field energy took the form [compare Part I, (3.10)]

$$E_{\text{mag}} = \frac{1}{2\mu}\int d^3x (\nabla \times \mathbf{A})^2 = \frac{1}{2\mu}\int \frac{d^3q}{(2\pi)^3} A_i(-\mathbf{q})(\mathbf{q}^2\delta_{ij} - q_i q_j) A(\mathbf{q}). \tag{4.75}$$

Using the completeness relation, the matrix $q^2\delta_{ij} - q_i q_j$ can now be expressed in terms of projection matrices (4.28) as

$$\mathbf{q}^2\delta_{ij} - q_i q_j = \mathbf{q}^2(\delta_{ij} - \hat{q}_i\hat{q}_j) = \mathbf{q}^2(e_i e_j^* + e_i^* e_j) = \mathbf{q}^2(P^{(1)}(\hat{\mathbf{p}}) + P^{(-1)}(\hat{\mathbf{p}})).$$

Therefore, E_{mag} diagonalizes as

$$E_{\text{mag}} = \frac{1}{2\mu}\int \frac{d^3q}{(2\pi)^3} \mathbf{q}^2 \mathbf{A}(-\mathbf{q})(P^{(1)}(\hat{\mathbf{q}}) + P^{(-1)}(\hat{\mathbf{q}}))\, \mathbf{A}(\mathbf{q})$$

$$= \frac{1}{2\mu} \int \frac{d^3q}{(2\pi)^3} \mathbf{q}^2 (|\mathbf{A}^{(1)}(\mathbf{q})|^2 + |A^{(-1)}(\mathbf{q})|^2). \tag{4.76}$$

Here we have used the fact that for a real field

$$\mathbf{A}(\mathbf{q}) = \int d^3x \, e^{-i\mathbf{q}\cdot\mathbf{x}} \mathbf{A}(\mathbf{x}) = \mathbf{A}(-\mathbf{q})^* \tag{4.77}$$

and thus

$$\mathbf{A}(-\mathbf{q})\, \mathbf{e}^{(h)}(\hat{\mathbf{q}})^* = \mathbf{A}^*(\mathbf{q})\, \mathbf{e}^{(h)}(\hat{\mathbf{q}})^* = (\mathbf{e}^{(h)}(\hat{\mathbf{q}})\, \mathbf{A}(\mathbf{q}))^* = \mathbf{A}^{(h)}(\mathbf{p})^*. \tag{4.78}$$

The gauge invariance of the magnetic energy manifests itself in the absence of the longitudinal helicity $A^{(0)}(\mathbf{q})$ in the expression for energy. That this has to happen follows immediately by considering the gauge transformation

$$A_i(\mathbf{x}) \to A_i(\mathbf{x}) + \partial_i \Lambda(\mathbf{x}), \tag{4.79}$$

which reads, in momentum space,

$$A_i(\mathbf{q}) \to A_i(\mathbf{q}) + iq_i \Lambda(\mathbf{q}). \tag{4.80}$$

On going to the helicity basis we see that while the $h = \pm 1$ components, whose spin is transverse to their momentum, remain unaffected, i.e.,

$$A^{(\pm 1)}(\mathbf{q}) \to A^{(\pm 1)}(\mathbf{q}), \tag{4.81}$$

the longitudinal component on the other hand, for which the spin is parallel to $\mathbf{q}$, changes by

$$A^{(0)}(\mathbf{q}) \to A^{(0)}(\mathbf{q}) + i|\mathbf{q}|\, \Lambda(\mathbf{q}). \tag{4.82}$$

Clearly, the energy can remain invariant under this gauge change only if the longitudinal component does not appear at all. This component is unphysical.

Consider now the interacting part of the energy

$$E_{\text{int}} = \int d^3x \, j_i(\mathbf{x})\, A_i(\mathbf{x}). \tag{4.83}$$

This is also diagonalized in the helicity basis. Let us Fourier transform and decompose the current in the same way as the field $A_i(\mathbf{x})$:

$$j_i(\mathbf{q}) = \sum_h e_i^{(h)}(\hat{\mathbf{q}})\, j^{(h)}(\mathbf{q}) = j_i(-\mathbf{q})^*, \tag{4.84}$$

with the helicity components

$$j^{(h)}(\mathbf{q}) \equiv e^{(h)*}(\hat{\mathbf{q}})\, j_i(\mathbf{q}). \tag{4.85}$$

The condition for zero divergence,

$$q_i j_i(\mathbf{q}) = 0, \tag{4.86}$$

eliminates the longitudinal $h = 0$ component so that

$$j_i(\mathbf{q}) = e^{(1)}(\hat{\mathbf{q}})\, j^{(1)}(\mathbf{q}) + e^{(-1)}(\hat{\mathbf{q}})\, j^{(-1)}(\mathbf{q}). \tag{4.87}$$

This decomposition shows that the current is purely transverse.

In the helicity decomposition therefore, the total magnetic field energy now has the simple diagonal form,

$$E = \int \frac{d^3q}{(2\pi)^3} \left\{ \frac{1}{2\mu} \mathbf{q}^2 (|A^{(1)}(\mathbf{q})|^2 + |A^{(-1)}(\mathbf{q})|^2) + j^{(1)*}(\mathbf{q}) A^{(1)}(\mathbf{q}) + j^{(-1)^*}(\mathbf{q}) A^{(-1)}(\mathbf{q}) \right\}. \tag{4.88}$$

The advantage of this form is obvious: The field equations are trivial, i.e.,

$$q^2 A^{(\pm 1)}(\mathbf{q}) = \mu j^{(+1)}(\mathbf{q}). \tag{4.89}$$

Only the two transverse components appear. The helicity formulation no longer requires invoking gauge invariance since it permits working only with physical field variables.

4.5. HELICITY FORM OF THE STRESS ENERGY

After this exercise we are ready to apply the same type of decomposition to the stress energy in (4.3). Let us first see how the constraints (4.2) manifest themselves in the helicity expansion,

$$A_{\ell i}(\mathbf{p}) = \sum_{s=0,1,2} e_{\ell i}^{(s,h)}(\hat{\mathbf{p}})\, A^{(s,h)}(\mathbf{p}). \tag{4.90}$$

Contracting $\hat{p}_i$ with the helicity basis gives

$$\hat{p}_i e_{\ell i}^{(2,\pm 2)} = 0, \tag{4.91}$$

$$\hat{p}_i e_{\ell i}^{(1,0)} = 0, \tag{4.92}$$

$$\hat{p}_i e_{\ell i}^{(2,0)} = \sqrt{\frac{2}{3}}\hat{p}_\ell, \tag{4.93}$$

$$\hat{p}_i e_{\ell i}^{(0,0)} = \frac{1}{\sqrt{3}}\hat{p}_\ell, \tag{4.94}$$

Furthermore,

$$p_i e_{\ell i}^{(2,1)} = \frac{1}{\sqrt{2}}|\mathbf{p}|\, e_\ell = p_i e_{\ell i}^{(1,1)}, \quad p_i e_{\ell i}^{(2,-1)} = -\frac{1}{\sqrt{2}}|\mathbf{p}|\, e_\ell^* = p_i e_{\ell i}^{(1,-1)}, \tag{4.95}$$

so that

$$p_i \frac{1}{\sqrt{2}}(e^{(2,\pm 1)} - e^{(1,\pm 1)})_{\ell i} = 0. \tag{4.96}$$

Also, since all $e_{\ell i}^{(s,h)}$, except $e_{\ell\ell}^{(0,0)} = \sqrt{3}$, are traceless we see that only the six components

$$e^{(2,\pm 2)}, \quad e^{(1,0)}, \quad \frac{1}{\sqrt{2}}(e^{(2,\pm 1)} - e^{(1,\pm 1)}), \quad \frac{1}{\sqrt{3}}(\sqrt{2}\, e^{(2,0)} + e^{(0,0)}),$$

satisfy the three constraints (4.2). The three orthogonal components $(1/\sqrt{2})\ (e^{(2,\pm 1)} + e^{(1,\pm 1)})$, $(1/\sqrt{3})(-e^{(2,0)} + \sqrt{2}\, e^{(0,0)})$ do not. In the following it will be useful to have an abbreviation for these combinations of polarization vectors; we shall call

$$e_{\ell i}^{++} \equiv \frac{1}{\sqrt{2}}(e^{(2,\pm 1)} + e^{(1,\pm 1)})_{\ell i} = \begin{cases} e_\ell \hat{p}_i, \\ -e_\ell^* \hat{p}_i, \end{cases}$$

$$e_{\ell i}^{-+} \equiv \frac{1}{\sqrt{2}}(e^{(2,\pm 1)} - e^{(1,\pm 1)})_{\ell i} = \begin{cases} \hat{p}_\ell e_i, \\ -\hat{p}_\ell e_i^*, \end{cases} \tag{4.97}$$

$$e^{L}_{\ell i} \equiv \frac{1}{\sqrt{3}}(-e^{(2,0)} + \sqrt{2}\, e^{(0,0)})_{\ell i} = \frac{1}{\sqrt{2}}(\delta_{\ell i} - \hat{p}_\ell \hat{p}_i),$$

$$e^{L}_{\ell i}{}' \equiv \frac{1}{\sqrt{3}}(\sqrt{2}\, e^{(2,0)} + e^{(0,0)})_{\ell i} = \hat{p}_\ell \hat{p}_i. \tag{4.98}$$

Then $A_{\ell i}$ can be expanded as follows

$$A_{\ell i}(\mathbf{p}) = e^{(2,2)}_{\ell i}(\hat{\mathbf{p}})\, A^{(2,2)}(\mathbf{p}) + e^{(2,-2)}_{\ell i}(\hat{\mathbf{p}})\, A^{(2,-2)}(\mathbf{p}) + e^{(1,0)}_{\ell i}(\hat{\mathbf{p}})\, A^{(1,0)}(\mathbf{p})$$
$$+ e^{-+}_{\ell i}(\hat{\mathbf{p}})\, A^{-+}(\mathbf{p}) + e^{--}_{\ell i}(\hat{\mathbf{p}})\, A^{--}(\mathbf{p}) + e^{L'}_{\ell i}(\hat{\mathbf{p}})\, A^{L'}(\mathbf{p}). \tag{4.99}$$

Let us now form the stresses

$$\sigma_{ij} = \varepsilon_{ik\ell}\, \partial_k A_{\ell j} = i|\mathbf{p}| \sum_{s,h} \varepsilon_{ik\ell}\, \hat{p}_k\, e^{(s,h)}_{\ell j}\, A^{(s,h)}(\mathbf{p}) \tag{4.100}$$

and expand them again in the helicity basis. For this, let us first consider

$$\varepsilon_{ik\ell}\, \hat{p}_k\, e^{(s,h)}_{\ell j}(\hat{\mathbf{p}}).$$

Using (4.58), (4.62), (4.97), (4.98) and the relations

$$i\mathbf{p} \times \mathbf{e} = \mathbf{e}, \qquad -i\mathbf{p} \times \mathbf{e}^* = \mathbf{e}^*, \tag{4.101}$$

we calculate directly:

$$i\, \varepsilon_{ik\ell}\, \hat{p}_k\, e^{(2,\pm 2)}_{\ell j} = \pm e^{(2,\pm 2)}_{ij}, \tag{4.102}$$

$$i\, \varepsilon_{ik\ell}\, \hat{p}_k\, e^{L}_{\ell j} = i\, \varepsilon_{ik\ell}\, \hat{p}_k \frac{1}{\sqrt{2}}(\delta_{\ell j} - \hat{p}_\ell \hat{p}_j) = -e^{(1,0)}_{ij}, \tag{4.103}$$

$$i\, \varepsilon_{ik\ell} \hat{p}_k\, e^{L'}_{\ell j} = i\, \varepsilon_{ik\ell}\, \hat{p}_k \hat{p}_\ell \hat{p}_j = 0, \tag{4.104}$$

$$i\, \varepsilon_{ik\ell}\, \hat{p}_k\, e^{++}_{\ell j} = i(\hat{\mathbf{p}} \times \mathbf{e})_i p_j = e_i p_j = e^{++}_{ij}, \tag{4.105}$$

$$i\, \varepsilon_{ik\ell}\, \hat{p}_k\, e^{+-}_{\ell j} = -i(\hat{\mathbf{p}} \times \mathbf{e}^*)_i p_j = e^*_i\, p_j = -e^{+-}_{ij}, \tag{4.106}$$

$$i\, \varepsilon_{ik\ell}\, \hat{p}_k\, e^{-+}_{\ell j} = i(\hat{\mathbf{p}} \times \hat{\mathbf{p}})_i e_j = 0, \tag{4.107}$$

$$i\, \varepsilon_{ik\ell}\, \hat{p}_k\, e^{--}_{\ell j} = -i(\hat{\mathbf{p}} \times \hat{\mathbf{p}})_i e^*_j = 0, \tag{4.108}$$

$$i\varepsilon_{ik\ell}\hat{p}_k e_{\ell j}^{(1,0)} = -\frac{i}{\sqrt{2}}[(\hat{\mathbf{p}}\times\mathbf{e})_i e_j^* - (\hat{\mathbf{p}}\times\mathbf{e}^*)_i e_j] = -\frac{1}{\sqrt{2}}(e_i e_j^* - e_i^* e_j)$$

$$= -\frac{1}{\sqrt{2}}(\delta_{ij} - \hat{p}_i\hat{p}_j) = -\frac{1}{\sqrt{3}}(-e^{(2,0)} + \sqrt{2}\,e^{(0,0)})_{ij}$$

$$\equiv -e_{ij}^L. \tag{4.109}$$

This leads to the formula

$$\sigma_{ij} = \varepsilon_{ik\ell}\partial_k A_{\ell j}$$
$$= |\mathbf{p}|\{e_{ij}^{(2,2)}A^{(2,2)} - e_{ij}^{(2,-2)}A^{(2,-2)} - e_{ij}^L A^{(1,0)} + e_{ij}^{++}A^{++} - e_{ij}^{+-}A^{+-}$$
$$- e_{ij}^{(1,0)}A^L\}. \tag{4.110}$$

Since the $A_{\ell i}$ have only the six nonzero components shown in (4.99), we obtain the decomposition

$$\sigma_{ij}(\mathbf{p}) = |\mathbf{p}|\{e_{ij}^{(2,2)}(\hat{\mathbf{p}})A^{(2,2)}(\mathbf{p}) - e_{ij}^{(2,-2)}(\hat{\mathbf{p}})A^{(2,-2)}(\mathbf{q}) - e_{ij}^L(\hat{\mathbf{p}})A^{(1,0)}(\mathbf{p})^L\}. \tag{4.111}$$

which displays the three physical components of the 3×3 matrix $A_{\ell i}$. They correspond to two transverse and one longitudinal phonon, respectively. Using the orthonormality of the polarization tensors we see that

$$|\sigma_{ij}(\mathbf{p})|^2 = \mathbf{p}^2\{|A^{(2,2)}(\mathbf{p})|^2 + |A^{(2,-2)}(\mathbf{p})|^2 + |A^{(1,0)}(\mathbf{p})|^2\},$$
$$|\sigma_{\ell\ell}(\mathbf{p})|^2 = 2\mathbf{p}^2|A^{(1,0)}(\mathbf{p})|^2. \tag{4.112}$$

Thus the stress energy [which we now can take directly from (1.43)] has the helicity form

$$E_{\mathrm{el}} = \int \frac{d^3p}{(2\pi)^3}\mathbf{p}^2\left(|A^{(2,2)}(\mathbf{p})|^2 + |A^{(2,-2)}(\mathbf{p})|^2 + \frac{1-\nu}{1+\nu}|A^{(1,0)}(\mathbf{p})|^2\right). \tag{4.113}$$

That only three of the six components of $A^{(s,h)}(\mathbf{q})$ in (4.99) survive is, of course, a direct manifestation of the gauge invariance of the decomposition (4.100) under local transformations,

$$A_{\ell j}(\mathbf{x}) \to A_{\ell j}(\mathbf{x}) + \partial_\ell \Lambda_j(\mathbf{x}). \tag{4.114}$$

In Fourier space, $\Lambda_j(\mathbf{p})$ may be expressed in terms of longitudinal and transverse parts, as defined in (4.31),

$$\partial_\ell \Lambda_j = i(p_\ell e_j \Lambda^{(1)} - p_\ell e_j^* \Lambda^{(-1)} + p_\ell \hat{p}_j \Lambda^{(0)},$$

where $\Lambda^{(\pm 1)}$, $\Lambda^{(0)}$ are arbitrary functions of momenta. In terms of helicity components (4.97), (4.98) this amounts to

$$\partial_\ell \Lambda_j = i|\mathbf{p}|(e_{\ell j}^{-+} \Lambda^{(1)} + e_{\ell j}^{--} \Lambda^{(-1)} + e_{\ell j}^{L'} \Lambda^{(0)}). \tag{4.115}$$

Thus gauge transformations modify precisely the last three components of the helicity expansion (4.99) and this is why they cannot occur in the gauge invariant energy (4.113).

In the helicity formalism the partition function (4.6) must contain only the three fluctuating physical gauge field components as integration variables,

$$Z = \int \mathscr{D} A^{(2,2)} \mathscr{D} A^{(2,-2)} \mathscr{D} A^{(1,0)} e^{-(1/T)(E_{\mathrm{el}} + iE_{\mathrm{int}})}. \tag{4.116}$$

The three physical components satisfy the specific gauge condition

$$\partial_\ell A_{\ell j} = 0, \tag{4.117}$$

as can be seen directly from (4.91), (4.92). The gauge-fixing factor in the formulation (4.6) is therefore

$$\Phi[A] = \prod_{\mathbf{x},j} \delta(\partial_\ell A_{\ell j}) = \delta(\partial_\ell A_{\ell j}). \tag{4.118}$$

Notice that this gauge together with the constraint implies the tracelessness of all $p \neq 0$ components of $A_{\ell j}(\mathbf{p})$, i.e.,

$$A_{\ell\ell}(\mathbf{p}) = 0, \quad \text{for all } p \neq 0. \tag{4.119}$$

It is useful to visualize the effect of the six δ-functionals in the integrand (4.6) for a particular Fourier component $A_{\ell j}(\mathbf{p})$. If the momentum $\mathbf{p}$ points in the z-direction, the constraint and gauge conditions read

$$p_3 A_{\ell 3}(\mathbf{p}) = \delta_{\ell 3} p_3 A_{pp}(\mathbf{p}), \tag{4.120}$$

and

$$p_3 A_{3j}(\mathbf{p}) = 0, \tag{4.121}$$

respectively. Inserting the second into the first we find

$$A_{\ell 3}(\mathbf{p}) = 0, \qquad A_{3j}(\mathbf{p}) = 0, \qquad A_{\ell\ell}(\mathbf{p}) = 0.$$

This leaves us with only three independent matrix elements A_{11}, A_{12}, A_{21}, as it should. Incidentally, it should be realized that in the helicity formalism we could have restricted the $A_{\ell j}$ fields to be traceless right from the beginning. The constraint would then have simplified to $\partial_i A_{\ell j}(\mathbf{x}) = 0$ and three components eliminated. Gauge invariance, on the other hand, would have been restricted to transverse functions Λ_j only, i.e.,

$$A_{\ell j} \to A_{\ell j} + \partial_\ell \Lambda_j,$$

with $\partial_i \Lambda_j = 0$. Correspondingly, the gauge condition $\partial_\ell A_{\ell j} = 0$ would no longer have implied three independent statements. In the example in which $\mathbf{p}$ and $\hat{\mathbf{z}}$ were parallel, this would have showed up with $A_3^3 = 0$ being automatically satisfied.

Let us now turn to the helicity-representation of the interaction in (4.6). Here we encounter a difference with respect to the magnetic case. The dislocation density $\alpha_{\ell i}(\mathbf{x})$ satisfies only the three divergenceless conditions

$$\partial_\ell \alpha_{\ell i}(\mathbf{x}) = 0 \quad (i = 1, 2, 3) \tag{4.122}$$

and nothing equivalent to the constraints (4.2) which would be cast as

$$\partial_i \alpha_{\ell i}(\mathbf{x}) = \partial_\ell \alpha_{ii}(\mathbf{x}). \tag{4.123}$$

Using the equations (4.91) to (4.96) and the fact that $e_{\ell j}^{(2,\,h)}$, $e_{\ell j}^{(0,\,0)}$ are symmetric in ℓ, j while $e_{\ell j}^{(1,\,h)}$ is antisymmetric, we see that the first condition is satisfied by the helicity components

$$e_{\ell i}^{(2,\,2)}, \quad e_{\ell i}^{(2,\,-2)}, \quad e_{\ell i}^{(1,\,0)}, \quad e_{\ell i}^{L} \equiv \frac{1}{\sqrt{2}}(-e^{(2,\,0)} + \sqrt{2}\, e^{(0,\,0)})_{\ell i},$$

$$e_{\ell i}^{++} = \frac{1}{\sqrt{2}}(e^{(2,\,1)} + e^{(1,\,1)})_{\ell i}, \quad e^{+-} = \frac{1}{\sqrt{2}}(e^{(2,\,1)} + e^{(1,\,1)})_{\ell i}.$$

The last three components would be eliminated by the condition (4.123) which, however, does not exist. Thus we have the peculiar feature that within linear elasticity, stress couples only to the first three of the six independent components of $\alpha^{(s,h)}$.

The field energy in the partition function (4.7) reads

$$-\frac{1}{T}(E_{\mathrm{el}} + iE_{\mathrm{int}})$$
$$= -\frac{1}{T}\int \frac{d^3p}{(2\pi)^3}\left\{\frac{\mathbf{p}^2}{4\mu}\left(|A^{(2,2)}(\mathbf{p})|^2 + |A^{(2,-2)}(\mathbf{p})|^2 + \frac{1-\nu}{1+\nu}|A^{(1,0)}(\mathbf{p})|^2\right)\right.$$
$$\left. + i(\alpha^{(2,2)}(\mathbf{p})^* A^{(2,2)}(\mathbf{p}) + \alpha^{(2,-2)}(\mathbf{p})^* A^{(2,-2)}(\mathbf{p}) + \alpha^{(1,0)}(\mathbf{p})^* A^{(1,0)}(\mathbf{p}))\right\}. \tag{4.124}$$

The three components $\alpha^{+\pm}$, α^L are absent. They carry no stress energy at the level of linear elasticity.

We can now integrate out the physical fields $A^{(2,2)}$, $A^{(2,-2)}$, $A^{(1,0)}$ in (4.116) and, after a quadratic completion, arrive at

$$Z = \text{const.} \times e^{-(\mu/T)\int (d^3p/(2\pi)^3)(1/\mathbf{p}^2)(|\alpha^{(2,2)}(\mathbf{p})|^2 + |\alpha^{(2,-2)}(\mathbf{p})|^2 + ((1+\nu)/(1-\nu))|\alpha^{(1,0)}(\mathbf{p})|^2)}. \tag{4.125}$$

The exponent must be the momentum space version of Blin's interaction energy for arbitrary dislocation densities which was derived before in the traditional way [see (3.29)–(3.31)]. In order to verify this not immediately obvious fact let us rewrite (4.125) in terms of the tensor of dislocation density $\alpha_{\ell j}(\mathbf{p})$ by using the projection matrices into the helicity states,

$$Z = \text{const.} \times e^{-(\mu/T)\int (d^3p/(2\pi)^3)(1/\mathbf{p}^2)\alpha^*_{\ell j}(\mathbf{p})(P^{(2,2)}_{\ell j,\ell' j'}(\hat{\mathbf{p}}) + P^{(2,-2)}_{\ell j,\ell' j'}(\hat{\mathbf{p}}) + ((1+\nu)/(1-\nu))P^{(1,0)}_{\ell j,\ell' j'}(\hat{\mathbf{p}}))\alpha_{\ell' j'}(\mathbf{p})}. \tag{4.126}$$

This can be brought into a somewhat more convenient form by observing that $(P^{(2,2)} + P^{(2,-2)} + P^{(1,0)})_{\ell j,\ell' j'}$ can also be written as $\delta_{jj'}\delta_{\ell\ell'}$ minus all orthogonal projections $P^{(2,1)}$, $P^{(2,-1)}$, $P^{(1,1)}$, $P^{(1,-1)}$, $P^{(2,0)}$, $P^{(0,0)}$. From (4.68), (4.58)–(4.63) we calculate

$$P^{(2,0)}_{\ell j,\ell' j'} = \tfrac{3}{2}\hat{p}_\ell \hat{p}_j \hat{p}_{\ell'} \hat{p}_{j'} - \tfrac{1}{2}(\hat{p}_\ell \hat{p}_j \delta_{\ell' j'} + \delta_{\ell j}\hat{p}_{\ell'}\hat{p}_{j'}) + \tfrac{1}{6}\delta_{\ell j}\delta_{\ell' j'},$$
$$(P^{(2,1)} + P^{(2,-1)})_{\ell j,\ell' j'} = \tfrac{1}{2}(e_\ell \hat{p}_j + \hat{p}_j e_\ell)(e^*_{\ell'}\hat{p}_{j'} + \hat{p}_{\ell'} e^*_{j'}) + \text{c.c.}$$

$$= \tfrac{1}{2}\{\hat{p}_\ell \hat{p}_{\ell'}(\delta_{ij'} - \hat{p}_j \hat{p}_{j'}) + \hat{p}_j \hat{p}_{j'}(\delta_{\ell\ell'} - \hat{p}_\ell \hat{p}_{\ell'})$$
$$+ \hat{p}_\ell \hat{p}_{j'}(\delta_{j\ell'} - \hat{p}_j \hat{p}_{\ell'}) + \hat{p}_j \hat{p}_{\ell'}(\delta_{\ell j'} - \hat{p}_\ell \hat{p}_{j'})\}$$
$$= \tfrac{1}{2}(\delta_{\ell\ell'} \hat{p}_j \hat{p}_{j'} + \delta_{jj'} \hat{p}_\ell \hat{p}_{\ell'} + \delta_{\ell j'} \hat{p}_j \hat{p}_{\ell'} + \delta_{j\ell'} \hat{p}_\ell \hat{p}_{j'})$$
$$- 2\hat{p}_\ell \hat{p}_j \hat{p}_{\ell'} \hat{p}_{j'},$$

$$(P^{(1,1)} + P^{(1,-1)})_{\ell j, \ell' j'} = \tfrac{1}{2}(e_\ell \hat{p}_j - \hat{p}_\ell e_j)(e_{\ell'} \hat{p}_{j'} - \hat{p}_{\ell'} e_{j'}) + \text{c.c.}$$
$$= \tfrac{1}{2}\{(\delta_{\ell\ell'} - \hat{p}_\ell \hat{p}_{\ell'}) \hat{p}_j \hat{p}_{j'} + (\delta_{jj'} - \hat{p}_j \hat{p}_{j'}) \hat{p}_\ell \hat{p}_{\ell'}$$
$$- (\delta_{\ell j'} - \hat{p}_\ell \hat{p}_{j'}) \hat{p}_j \hat{p}_{\ell'} - (\delta_{j\ell'} - \hat{p}_j p_{\ell'}) \hat{p}_\ell \hat{p}_{j'}\}$$
$$= \tfrac{1}{2}(\delta_{\ell\ell'} \hat{p}_j \hat{p}_{j'} + \delta_{jj'} \hat{p}_\ell \hat{p}_{\ell'} - \delta_{\ell j'} \hat{p}_j \hat{p}_{\ell'} - \delta_{j\ell'} \hat{p}_\ell \hat{p}_{j'}),$$

$$P^{(0,0)}_{\ell j, \ell' j'} = \tfrac{1}{3}\delta_{\ell j} \delta_{\ell' j'}. \tag{4.127}$$

By current conservation, $p_{\ell'} \alpha_{\ell' j'} = 0$, most terms in (4.126) cancel so that of these projection operators only the tensors

$$-\tfrac{1}{2} p_\ell p_j \delta_{\ell' j'} + \tfrac{1}{6}\delta_{\ell j}\delta_{\ell' j'}, \quad \tfrac{1}{2}(\delta_{\ell\ell'} p_j p_{j'} \pm \delta_{j\ell'} p_\ell p_{j'}), \quad \tfrac{1}{3}\delta_{\ell j}\delta_{\ell' j'}$$

survive in front of $\alpha_{\ell' j'}(\mathbf{p})$, respectively. This shows that

$$(P^{(2,2)} + P^{(2,-2)} + P^{(1,0)})_{\ell j, \ell' j'} \alpha_{\ell' j'}(\mathbf{p})$$
$$= [\delta_{\ell\ell'}(\delta_{jj'} - \hat{p}_j \hat{p}_{j'}) - \tfrac{1}{2}(\delta_{\ell j} - \hat{p}_\ell \hat{p}_j)\delta_{\ell' j'}]\alpha_{\ell' j'}(\mathbf{p}). \tag{4.128}$$

When multiplied from the left by $\alpha_{\ell j}(\mathbf{p})$ the last term vanishes (since also $\alpha_{\ell j} p_\ell = 0$) and (4.126) becomes

$$Z = \text{const.} \times e^{-(\mu/T)\int (d^3p/(2\pi)^3)(1/\mathbf{p}^2)\alpha(\mathbf{p})^*_{ij}[\delta_{\ell\ell'}(\delta_{jj'} - \hat{p}_j\hat{p}_{j'}) - (1/2)\delta_{ij}\delta_{\ell' j'} + 2\nu/(1-\nu) P^{(1,0)}_{ij,\ell' j'}]\alpha(\mathbf{p})_{\ell' j'}}. \tag{4.129}$$

A final simplification is based on the observation that the projection matrix $P^{(1,0)}$, whose explicit form is

$$P^{(1,0)}(\hat{\mathbf{p}})_{\ell j, \ell' j'} = \tfrac{1}{2}\varepsilon_{\ell j k}\, \varepsilon_{\ell' j' k'} \hat{p}_k \hat{p}_{k'},$$

[see (4.68), (4.62)] can be expanded as

$$P^{(1,0)}(\hat{p})_{\ell j, \ell' j'} = \tfrac{1}{2}(\delta_{\ell\ell'}\, \delta_{jj'} - \delta_{\ell j'}\, \delta_{\ell' j}) + \tfrac{1}{2}(-\delta_{\ell\ell'} \hat{p}_j \hat{p}_{j'} - \delta_{jj'} \hat{p}_\ell \hat{p}_{\ell'}$$
$$+ \delta_{\ell j'} \hat{p}_{\ell'} \hat{p}_j + \delta_{\ell' j} \hat{p}_\ell \hat{p}_{j'}). \tag{4.130}$$

Between conserved $\alpha_{\ell j}(\mathbf{p})$ matrices, only

$$\tfrac{1}{2}\delta_{\ell\ell'}(\delta_{jj'} - \hat{p}_j\hat{p}_{j'}) - \tfrac{1}{2}\delta_{\ell j'}\delta_{j\ell'}$$

survives and the exponent in (4.129) can be rewritten as

$$-\frac{\mu}{T}\int \frac{d^3p}{(2\pi)^3}\frac{1}{\mathbf{p}^2}\alpha^*_{ij}(\mathbf{p})\left(\delta_{\ell j'}\delta_{j\ell'} - \frac{1}{2}\delta_{\ell j}\delta_{\ell' j'} + \frac{2}{1-\nu}P^{(1,0)}_{\ell j,\ell' j'}\right)\alpha_{\ell' j'}(\mathbf{p}),$$

or

$$-\frac{\mu}{T}\int \frac{d^3p}{(2\pi)^3}\frac{1}{\mathbf{p}^2}\alpha^*_{\ell j}(\mathbf{p})\left[\frac{1}{2}\delta_{\ell j}\delta_{\ell' j'} - \varepsilon_{\ell\ell' k}\,\varepsilon_{jj' k} + \frac{2}{1-\nu}P^{(1,0)}_{\ell j,\ell' j'}\right]\alpha_{\ell' j'}(\mathbf{p}). \tag{4.131}$$

Going over to position space, this amounts to the partition function [recalling (1.81), (1.89)]

$$Z = \text{const.} \times \exp\left\{-\frac{\mu}{4\pi T}\int d^3x\, d^3x'\,\alpha_{\ell j}(\mathbf{x})\left[\frac{1}{2}\delta_{\ell j}\delta_{\ell' j'} - \varepsilon_{\ell\ell' k}\,\varepsilon_{jj' k}\frac{1}{R} + \frac{1}{1-\nu}\varepsilon_{\ell jk}\,\varepsilon_{\ell' j' k'}\,\partial_k\,\partial_{k'}R\right]\alpha_{\ell' j'}(\mathbf{x}')\right\}. \tag{4.132}$$

This exponent coincides with Blin's law (3.29)–(3.31) for arbitrary dislocation densities.

4.6. THE TWO-DIMENSIONAL CASE

Here the situation is much simpler. The conserved stress tensor can be expressed in terms of a field $A_j(\mathbf{x})$ as

$$\sigma_{ij} = \varepsilon_{jk}\,\partial_k A_j, \tag{4.133}$$

where ε_{ik} is the antisymmetric unit matrix, $\varepsilon_{11} = \varepsilon_{22} = 0$, $\varepsilon_{12} = -\varepsilon_{21} = 1$. Notice that A_j is no longer a proper gauge field. This is peculiar to two dimensions. When written out in component form, (4.133) reads

$$\sigma_{11} = \partial_2 A_1, \quad \sigma_{22} = -\partial_1 A_2, \quad \sigma_{12} = \partial_2 A_2, \quad \sigma_{21} = -\partial_1 A_1. \tag{4.134}$$

The symmetry is guaranteed by using a transverse A_j field.

$$\partial_1 A_1 + \partial_2 A_2 = 0. \tag{4.135}$$

In the isotropic case the stress energy becomes

$$E^{\mathrm{el}} = \int d^2x \frac{1}{4\mu}\left[(\varepsilon_{ik}\,\partial_k A_j)^2 - \frac{\nu}{1+\nu}(\varepsilon_{ik}\,\partial_k A_i)^2 \right]$$
$$= \int d^2x \frac{1}{4\mu}\left[(\partial_k A_i)^2 - \frac{\nu}{1+\nu}(\partial_1 A_2 - \partial_2 A_1)^2 \right]. \tag{4.136}$$

A partial integration in the mixed second term, together with (4.135), brings this to the form

$$E^{\mathrm{el}} = \frac{1}{4\mu(1+\nu)} \int d^2x (\partial_k A_j)^2. \tag{4.137}$$

apart from a surface term.

In two dimensions, for which defect lines degenerate into points, the density of a dislocation with Burgers vector $\mathbf{b}$ at the place x_0 is

$$\alpha_i(\mathbf{x}) \equiv \varepsilon_{k\ell}\,\partial_k\,\partial_\ell\, u_i(\mathbf{x}) = b_i\,\delta^2(\mathbf{x} - \mathbf{x}_0). \tag{4.138}$$

The interaction energy of a dislocation in the stress field of another is found, just as in (3.22), to be

$$E^{\mathrm{I,II}} = \int d^2x\, \sigma^{\mathrm{I}}_{ij}\,\partial_i u^{\mathrm{II}}_j = \int d^2x\, \varepsilon_{ik}\,\partial_k A_j(\mathbf{x})\,\partial_i u^{\mathrm{II}}_j = \int d^2x\, A_j(\mathbf{x})\,\varepsilon_{ik}\,\partial_i\,\partial_k\, u^{\mathrm{II}}_i$$
$$= \int d^2x\, A_j(\mathbf{x})\,\alpha_j(\mathbf{x}) = b_j A_j(\mathbf{x}_0). \tag{4.139}$$

The partition function of stress for a given set of dislocations is ($\beta \equiv 1/T$)

$$Z = \int \mathscr{D}A_j\,\delta(\partial_j A_j)\, e^{-\beta[1/(4\mu(1+\nu))]\int d^2x(\partial_i A_j)^2 + \beta i \int d^2x A_j(\mathbf{x})\alpha_j(\mathbf{x})}. \tag{4.140}$$

The A_j field can be integrated out with the result

$$Z = \text{const.} \times \det(\beta\partial^2)^{-1/2}\, e^{-\beta\mu(1+\nu)\int d^2x\, d^2x'\, \alpha_i(\mathbf{x}) v^T_{ij}(\mathbf{x}-\mathbf{x}')\alpha_j(\mathbf{x}')}, \tag{4.141}$$

where $v^T_{ij}(\mathbf{x} - \mathbf{x}')$ is the transverse Coulomb potential in two dimensions

calculated in (1.124). The exponent is the two-dimensional analogue of Blin's law.

The potential v_{ij}^T has an infinity. Let us isolate it and discuss it separately. It contributes an exponent

$$\beta\mu(1+\nu)\left(\int d^2x\,\alpha_i^T(\mathbf{x})\right)^2\frac{1}{4\pi}\left(\log\left(\frac{\delta}{2}e^{\gamma}\right)+\frac{1}{2}\right), \tag{4.142}$$

where δ is the small regulator mass. The superscript T of α^T records the fact that $v_{ij}^T(\mathbf{x})$ acts only on the transverse projection of $\alpha_i(\mathbf{x})$, $\alpha_i^T(\mathbf{x}) \equiv (\delta_{ij} - (\partial_i\partial_j/\partial^2))\,\alpha_j(\mathbf{x})$. In the limit $\delta \to 0$, this exponent diverges to $-\infty$ so that the dislocation can have a finite contribution only if

$$\int d^2x\,\alpha_i^T(\mathbf{x}) = 0. \tag{4.143}$$

We shall refer to this condition as *dislocation neutrality*. For such neutral systems, the infinity in (4.141) cancels and we can write

$$-\int d^2x\,d^2x'\,\alpha_i^T(\mathbf{x})\,v_{ij}^T(\mathbf{x}-\mathbf{x}')\,\alpha_j^T(\mathbf{x}) = -\int d^2x\,d^2x'\,\alpha_i^T(\mathbf{x})\,v'^T_{ij}(\mathbf{x}-\mathbf{x}')\,\alpha_j^T(\mathbf{x}'), \tag{4.144}$$

where

$$v'^T_{ij}(\mathbf{x}-\mathbf{x}') = -\frac{1}{4\pi}\left(\delta_{ij}\log|\mathbf{x}| - \frac{x_i x_j}{|\mathbf{x}|^2}\right) \tag{4.145}$$

is the subtracted transverse Coulomb potential.

The fact that the elastic energy couples only to the transverse part of the dislocation is the two-dimensional analogue of the coupling to only $\alpha^{(2,2)}$, $\alpha^{(2,-2)}$, $\alpha^{(1,0)}$. The energy is indifferent to modifications of the longitudinal part of α_i, $\alpha^L(\mathbf{x}) = (\partial_i\partial_j/\partial^2)\,\alpha_j(\mathbf{x})$, or in Fourier space to $\alpha^L(\mathbf{p}) = \hat{p}_i\hat{p}_j\alpha_j(\mathbf{p})$, just as it was previously indifferent to the components

$$\alpha^L = \frac{1}{\sqrt{3}}(-\alpha^{(2,0)} + \sqrt{2}\,\alpha^{(0,0)}), \quad \alpha^{++} = \frac{1}{\sqrt{2}}(\alpha^{(2,1)} + \alpha^{(1,1)}),$$

$$\alpha^{+-} = \frac{1}{\sqrt{2}}(\alpha^{(2,-1)} + \alpha^{(1,-1)})$$

[recall the discussion after (4.123)].

NOTES AND REFERENCES

See the end of the next chapter.

CHAPTER FIVE

STRESS ENERGY OF GENERAL DEFECT DISTRIBUTIONS

5.1. THE SYMMETRIC STRESS GAUGE FIELD

So far, the development has been very similar to that of vortex lines in superfluid ^{4}He. The forces between line elements are of the $1/R$ type and the only additional complication consists in the different possibilities of contracting the indices related to the Burgers vector. The situation changes drastically when it comes to including also the line-like defects of the rotational type, the disclinations. If they are present, the gauge field $A_{ij}(\mathbf{x})$ is no longer useful since it does not couple locally to disclinations. A further derivative is necessary to achieve this goal. We therefore introduce a gauge field $\chi_{\ell n}(\mathbf{x})$ which has the property that its *double curl* is equal to the stress tensor,

$$\sigma_{ij}(\mathbf{x}) = \varepsilon_{ik\ell}\,\varepsilon_{jmn}\,\partial_k\,\partial_m\,\chi_{\ell n}(\mathbf{x}). \tag{5.1}$$

This representation has the advantage of being automatically symmetric if $\chi_{\ell n}$ is. The local gauge transformations which leave σ_{ij} invariant are now

$$\chi_{\ell n}(\mathbf{x}) \to \chi_{\ell n}(\mathbf{x}) + \partial_\ell\,\xi_n(\mathbf{x}) + \partial_n\,\xi_\ell(\mathbf{x}). \tag{5.2}$$

This ensures that only three of the six components of $\chi_{ij}(\mathbf{x})$ are physical.

It is straightforward to derive the coupling of this gauge field to a general defect line. For this we consider again one line L^{I} in the stress field of another L^{II}, so that interaction energy is

$$E^{\mathrm{I,II}} = \int d^3x\, \sigma_{ij}^{\mathrm{I}} u_{ij}^{\mathrm{II}}. \tag{5.3}$$

Using the gauge field (5.1) this can be rewritten in the form

$$E^{\mathrm{I,II}} = \int d^3x\, (\varepsilon_{ik\ell}\, \varepsilon_{jmn}\, \partial_k\, \partial_m\, \chi_{\ell n}^{\mathrm{I}}) u_{ij}^{\mathrm{II}}. \tag{5.4}$$

A partial integration yields

$$E^{\mathrm{I,II}} = \int d^3x\, \chi_{\ell n}^{\mathrm{I}}\, \varepsilon_{\ell ki}\, \varepsilon_{nmj}\, \partial_k\, \partial_m\, u_{ij}^{\mathrm{II}}. \tag{5.5}$$

Hence we see that the symmetric gauge field $\chi_{\ell n}$ couples *locally* to the total defect density $\eta_{\ell n}$ which was introduced in (2.76),

$$E^{\mathrm{I,II}} = \int d^3x\, \chi_{\ell n}^{\mathrm{I}}(\mathbf{x})\, \eta_{\ell n}^{\mathrm{II}}(\mathbf{x}). \tag{5.6}$$

With the gauge field $\chi_{\ell n}$ it is now straightforward to derive a partition function for the stress fluctuations around an arbitrary defect configuration [the analogue of (4.116)]. For this it is again convenient to go to a helicity basis. Expanding the gauge field $\chi_{\ell n}(\mathbf{x})$ into its Fourier components [as in (4.72)], we use (4.71) to decompose

$$\chi_{\ell n}(\mathbf{p}) = \sum_{s,h} P_{\ell n,\ell' n'}^{(s,h)}(\hat{\mathbf{p}})\, \chi_{\ell' n'}(\mathbf{p}) = \sum_{s,h} e_{\ell n}^{(s,h)}(\hat{\mathbf{p}})\, \chi^{(s,h)}(\mathbf{p}), \tag{5.7}$$

with the helicity amplitudes

$$\chi^{(s,h)}(\mathbf{p}) \equiv e_{\ell n}^{(s,h)*}(\hat{\mathbf{p}})\, \chi_{\ell n}(\mathbf{p}). \tag{5.8}$$

By virtue of the symmetry of $\chi_{\ell n}(\mathbf{p})$, only the six components with spin $s = 0$ and 2 can be nonzero. Three of these are gauge modes. From (5.2), these have the general form

$$i(q_\ell \xi_n(\mathbf{p}) + p_n \xi_\ell(\mathbf{p})). \tag{5.9}$$

Decomposing $\xi_n(\mathbf{p})$ into longitudinal and transverse components,

$$\xi_n(\mathbf{p}) = \hat{p}_n \xi^{(0)} + e_n(\mathbf{p}) \xi^{(1)} + e_n^*(\mathbf{p}) \xi^{(-1)}; \tag{5.10}$$

we see that (5.9) can be written as [see (4.58)–(4.63)]

$$2i|\mathbf{q}|\left[\hat{p}_\ell \hat{p}_n \xi^{(0)}(\mathbf{p}) + \left(\frac{1}{\sqrt{2}}(e_\ell \hat{p}_n + \hat{p}_\ell e_n)\xi^{(1)}(\mathbf{p}) + \text{c.c.}\right)\right]$$
$$= 2i|\mathbf{q}|\left[\frac{1}{\sqrt{3}}(\sqrt{2}e^{(2,0)} + e^{(0,0)})\xi^{(0)} + (e^{(2,1)}\xi^{(1)} + \text{c.c.})\right]. \tag{5.11}$$

Hence the components (2, 1), (2, −1) and the linear combination $\chi^{L'} \equiv (1/\sqrt{3})(\sqrt{2}\chi^{(2,0)} + \chi^{(0,0)})$ are unphysical. Using the previously defined polarization tensor [see (4.98)]

$$e^{L'}_{\ell n}(\hat{\mathbf{p}}) \equiv \frac{1}{\sqrt{3}}(\sqrt{2}e^{(2,0)}_{\ell n}(\hat{\mathbf{p}}) + e^{(0,0)}_{\ell n}(\hat{\mathbf{p}}) = \hat{p}_\ell \hat{p}_n, \tag{5.12}$$

the unphysical components are spanned by $e^{(2,1)}$, $e^{(2,-1)}$, and $e^{L'}$. The physical components, on the other hand, are spanned by the orthogonal complements $e^{(2,2)}$, $e^{(2,-2)}$ and the previously defined

$$e^{L}_{\ell n}(\hat{\mathbf{p}}) = \frac{1}{\sqrt{3}}(-e^{(2,0)}_{\ell n}(\hat{\mathbf{p}}) + \sqrt{2}e^{(0,0)}_{\ell n}(\hat{\mathbf{p}})) = \frac{1}{\sqrt{2}}(\delta_{\ell n} - \hat{p}_\ell \hat{p}_n). \tag{5.13}$$

It is useful to introduce also projection matrices associated with the polarization tensors e^L and $e^{L'}$:

$$P^{L}_{\ell n \ell' n'}(\hat{\mathbf{p}}) = \varepsilon^{L}_{\ell n}(\hat{\mathbf{p}})\,\varepsilon^{L}_{\ell' n'}(\hat{\mathbf{p}}) = \tfrac{1}{2}(\delta_{\ell n} - \hat{p}_\ell \hat{p}_n)(\delta_{\ell' n'} - \hat{p}_{\ell'} \hat{p}_{n'}),$$
$$P^{L'}_{\ell n \ell' n'}(\hat{\mathbf{p}}) = \varepsilon^{L'}_{\ell n}(\hat{\mathbf{p}})\,\varepsilon^{L'}_{\ell' n'}(\hat{\mathbf{p}}) = \hat{p}_\ell \hat{p}_n \hat{p}_{\ell'} \hat{p}_{n'}. \tag{5.14}$$

In terms of these, the completeness relation reads

$$\left(\sum_{\substack{h=-2\\h\neq 0}}^{2} P^{(2,h)} + P^{L} + P^{L'}\right)_{\ell n,\,\ell' n'} = \frac{1}{2}(\delta_{\ell\ell'}\delta_{nn'} + \delta_{\ell n'}\delta_{n\ell'}). \tag{5.15}$$

The right-hand side is the unit matrix in the space of symmetric tensors. The physical components of $\chi_{\ell n}(\mathbf{p})$ are projected out via

$$\begin{aligned}\chi^{\text{phys}}_{\ell n}(\mathbf{p}) &= (P^{(2,2)} + P^{(2,-2)} + P^{L})_{\ell n,\,\ell' n'}\,\chi_{\ell' n'}(\mathbf{p}) \\ &= e^{(2,2)}_{\ell n}(\hat{\mathbf{p}})\,\chi^{(2,2)}(\mathbf{p}) + e^{(2,-2)}_{\ell n}(\hat{\mathbf{p}})\,\chi^{(2,-2)}(\mathbf{p}) + e^{L}_{\ell n}(\hat{\mathbf{p}})\,\chi^{L}(\mathbf{p}).\end{aligned} \tag{5.16}$$

They satisfy the obvious gauge condition

$$p_\ell\,\chi^{\text{phys}}_{\ell n}(\mathbf{p}) = 0. \tag{5.17}$$

These are three equations which suffice to eliminate the three unphysical components, since the corresponding polarization tensors would give

$$p_\ell\, e^{(2,1)}_{\ell n}(\hat{\mathbf{p}}) = \frac{1}{\sqrt{2}} e_n(\hat{\mathbf{p}}), \quad p_\ell\, e^{(2,-2)}_{\ell n}(\hat{\mathbf{p}}) = -\frac{1}{\sqrt{2}} e^{*}_n(\hat{\mathbf{p}}), \quad p_\ell\, e^{L}_{\ell n}(\hat{\mathbf{p}}) = \frac{1}{\sqrt{2}} p_n, \tag{5.18}$$

which are three nonzero independent vectors such that their sum vanishes only if the components do.

The stress tensor can be calculated from $\chi^{\text{phys}}_{\ell n}(\mathbf{p})$ by observing that the physical polarization tensors $e^{(2,\pm 2)}(\hat{\mathbf{p}})$, $e^{L}(\hat{\mathbf{p}})$ are invariant under the operation of the double curl, up to a factor $\mathbf{p}^2$, and a trivial sign change for the L component. For $e^{(2,\pm 2)}(\hat{\mathbf{p}})$, this follows directly from (4.102):

$$i\varepsilon_{ik\ell}\hat{p}_k\, i\varepsilon_{jmn}\hat{p}_m\, e^{(2,\pm 2)}_{\ell n}(\hat{\mathbf{p}}) = \pm\varepsilon_{jmn}\hat{p}_m\, e^{(2,\pm 2)}_{in}(\hat{\mathbf{p}}) = e^{(2,\pm 2)}_{ij}(\hat{\mathbf{p}}).$$

For $e^{L}(\hat{\mathbf{p}})$, we use (4.103) and calculate

$$i\varepsilon_{ik\ell}\hat{p}_k\, i\varepsilon_{jmn}\hat{p}_m\, e^{L}(\hat{\mathbf{p}})_{\ell n} = -i\varepsilon_{jmn}\hat{p}_m\, e^{(1,0)}_{in}(\hat{\mathbf{p}}).$$

The right-hand side becomes, with (4.109), $-(1/\sqrt{3})(-e^{(2,0)}(\hat{\mathbf{p}}) + \sqrt{2}\,e^{(0,0)}(\hat{\mathbf{p}})) = -e^{L}_{ij}(\hat{\mathbf{p}})$ and this proves our statement. Note that the unphysical components vanish under the same operation, as they should, due to the gauge invariance of the decomposition (5.1).

As a result, we can expand the stress tensor directly in the form[a]

$$\sigma_{ij}(\mathbf{p}) = \mathbf{p}^2(e_{ij}^{(2,2)}(\hat{\mathbf{p}})\,\chi^{(2,2)}(\mathbf{p}) + e^{(2,-2)}(\hat{\mathbf{p}})\,\chi^{(2,-2)}(\mathbf{p}) - e_{ij}^{L}(\hat{\mathbf{p}})\,\chi^{L}(\mathbf{p})) \tag{5.19}$$

and identify its helicity components as

$$\sigma^{(2,\pm 2)}(\mathbf{p}) = \mathbf{p}^2\chi^{(2,\pm 2)}(\mathbf{p}), \qquad \sigma^{L}(\mathbf{p}) = -\mathbf{p}^2\chi^{L}(\mathbf{p}). \tag{5.20}$$

Comparison with (4.111) shows that $\chi^{(s,h)}$ and the former gauge field $A^{(s,h)}$ are related by

$$A^{(2,+2)}(\mathbf{p}) = |\mathbf{p}|\,\chi^{(2,\pm 2)}(\mathbf{p}), \qquad A^{(1,0)}(\mathbf{p}) = -|\mathbf{p}|\,\chi^{L}(\mathbf{p}). \tag{5.21}$$

Inserting these into (4.113), the stress energy takes the helicity form

$$E = \frac{1}{4\mu}\int \frac{d^3p}{(2\pi)^3}\mathbf{p}^4\left(|\chi^{(2,2)}(\mathbf{p})|^2 + |\chi^{(2,-2)}(\mathbf{p})|^2 + \frac{1-\nu}{1+\nu}|\chi^{L}(\mathbf{p})|^2\right). \tag{5.22}$$

The linear coupling (5.6) with the defect density can be decomposed in a similar way. Since $\eta_{ij}(\mathbf{p})$ is symmetric and divergenceless, it has the same helicity decomposition as the stress tensor, namely,

$$\eta_{ij}(\mathbf{p}) = e_{ij}^{(2,2)}(\hat{\mathbf{p}})\,\eta^{(2,2)}(\mathbf{p}) + e_{ij}^{(2,-2)}(\hat{\mathbf{p}})\,\eta^{(2,-2)}(\mathbf{p}) + e^{L}(\hat{\mathbf{p}})\,\eta^{L}(\mathbf{p}) \tag{5.23}$$

and the general interaction energy now reads

$$\begin{aligned} E_{\text{int}} &= -\int \frac{d^3p}{(2\pi)^3}\eta_{ln}(\mathbf{p})^*\chi_{ln}(\mathbf{p}) \\ &= -\int \frac{d^3p}{(2\pi)^3}(\eta^{(2,2)}(\mathbf{p})^*\chi^{(2,2)}(\mathbf{p}) + \eta^{(2,-2)}(\mathbf{p})^*\chi^{(2,-2)}(\mathbf{p}) + \eta^{L}(\mathbf{p})^*\chi^{L}(\mathbf{p})). \end{aligned} \tag{5.24}$$

[a]More generally, we could have derived the following identity [using Eqs. (4.70), (4.68), (4.102)–(4.109)]:

$$\begin{aligned} &\varepsilon_{lml'}\varepsilon_{jnj'}\hat{p}_m\hat{p}_n \\ &\quad = \varepsilon_{lml''}\varepsilon_{jnj''}\hat{p}_m\hat{p}_n(P^{(2,2)} + P^{(2,-2)} + P^{(2,1)} + P^{(2,-1)} + P^{L} + P^{L'} \\ &\qquad + P^{(1,1)} + P^{(1,-1)} + P^{(1,0)})_{l''j'',l''j''} \\ &\quad = (P^{(2,2)} + P^{(2,-2)} - P^{L} + P^{(1,0)})_{lj,l'j'}. \end{aligned}$$

Applying this to $\chi_{l'j'}$ gives (5.19).

5.2. ELASTIC PARTITION FUNCTION FOR A FIXED GENERAL DEFECT DISTRIBUTION

After these preliminaries it is easy to write down the partition function for a fixed set of defects with all their stress fluctuations,

$$Z = \int \mathscr{D}\chi^{(2,2)}\, \mathscr{D}\chi^{(2,-2)}\, \mathscr{D}\chi^{L}\, e^{-(1/T)(E + iE_{\text{int}})}. \tag{5.25}$$

Since the physical components satisfy the gauge condition (5.17), the measure of integration can also be written as

$$\prod_{\mathbf{x},\ell \geq n} \left[\int \mathscr{D}\chi_{\ell n}(\mathbf{x}) \right] \prod_{\mathbf{x},n} \delta(\partial_\ell \chi_{\ell n}).$$

Integrating out the three physical gauge-field components gives

$$Z = \text{const.} \times e^{-(\mu/T)\int (d^3p/(2\pi)^3)(1/|\mathbf{p}|^4)(|\eta^{(2,2)}(\mathbf{p})|^2 + |\eta^{(2,-2)}(\mathbf{p})|^2 + ((1+\nu)/(1-\nu))|\eta^{L}(\mathbf{p})|^2)}. \tag{5.26}$$

This partition function is the proper generalization of formula (4.125). The exponent is the momentum-space version of the elastic energy for arbitrary defect distributions.

The expression can be simplified in a manner similar to (4.131). For this purpose we insert the projection matrices $(P^{(2,2)} + P^{(2,-2)} + (1+\nu)/(1-\nu)\,P^{L})_{\ell n,\,\ell' n'}$ and rewrite them as the symmetric traceless unit matrix in the subspace of symmetric tensors, $(1/2)(\delta_{\ell\ell'}\,\delta_{nn'} + \delta_{\ell n'}\,\delta_{n\ell'})$ minus the matrices

$$P^{(2,1)} + P^{(2,-1)} + P^{L'} - \frac{2\nu}{1-\nu} P^{L}. \tag{5.27}$$

These matrices are now contracted with the tensors $\eta_{\ell n}(\mathbf{p})^*$, $\eta_{\ell' n'}(\mathbf{p})$ which are divergenceless, i.e., they satisfy the conservation laws

$$p_\ell\, \eta_{\ell n}(\mathbf{p}) = 0, \qquad p_n\, \eta_{\ell n}(\mathbf{p}) = 0. \tag{5.28}$$

With the aid of the explicit polarization tensors (5.14) we see that $P^{L'}(\mathbf{p})$ gives no contribution while $P^{L}(\mathbf{p})$ can be replaced by $(1/2)\delta_{\ell n}\,\delta_{\ell' n'}$. Moreover, due to (4.58) and (4.59), the matrix $P^{(2,1)} + P^{(2,-1)}$ between the η tensors vanishes since it can be rewritten as

$$(P^{(2,1)}(\mathbf{p})+P^{(2,-1)}(\mathbf{p}))_{\ell n\ell' n'}=\tfrac{1}{2}(e_\ell\hat{p}_n+\hat{p}_\ell e_n)(e_{\ell'}p_{n'}+p_{\ell'}e_{n'})+\text{c.c.}$$
$$=\tfrac{1}{2}[(\delta_{\ell\ell'}-\hat{p}_\ell\hat{p}_{\ell'})\hat{p}_n\hat{p}_{n'}+(\delta_{nn'}-\hat{p}_n\hat{p}_{n'})\hat{p}_\ell\hat{p}_{\ell'}$$
$$+(\delta_{\ell n'}-\hat{p}_\ell\hat{p}_{n'})\hat{p}_n\hat{p}_{\ell'}+(\delta_{n\ell'}-\hat{p}_n\hat{p}_{\ell'})\hat{p}_\ell\hat{p}_{n'}];\tag{5.29}$$

clearly there are always momenta that are contracted with the η tensors and give zero. Thus we arrive at the matrix form of the exponent,

$$-\frac{\mu}{T}\int\frac{d^3p}{(2\pi)^3}\frac{1}{|\mathbf{p}|^4}\eta^*_{\ell n}(\mathbf{p})\left[\frac{1}{2}(\delta_{\ell n}\delta_{\ell' n'}+\delta_{\ell n'}\delta_{n\ell'})+\frac{\nu}{1-\nu}\delta_{\ell n}\delta_{\ell' n'}\right]\eta_{\ell' n'}(\mathbf{p}).\tag{5.30}$$

In position space, this amounts to a partition function for stress fluctuations, i.e.,

$$Z=\text{const.}\times e^{-(\mu/T)\int d^3x\,d^3x'[\eta_{\ell n}(\mathbf{x})\eta_{\ell n}(\mathbf{x}')+(\nu/(1-\nu))\eta_{\ell\ell}(\mathbf{x})\eta_{nn}(\mathbf{x}')]v_4(\mathbf{x}-\mathbf{x}')},\tag{5.31}$$

where $v_4(\mathbf{x})$ denotes the potential

$$v_4(\mathbf{x})=\int\frac{d^3p}{(2\pi)^3}e^{i\mathbf{p}\cdot\mathbf{x}}\frac{1}{\mathbf{p}^4}.\tag{5.32}$$

In Eq. (1.88) we had calculated this potential and found that it consisted of two terms: a constant

$$c=\frac{1}{2\pi^2}\int_0^\infty\frac{dq}{q^2}>0,\tag{5.33}$$

which diverges due to the small q fluctuations (infrared catastrophe) and a subtracted potential

$$v_4'(\mathbf{x})=v_4(\mathbf{x})-v_4(\mathbf{0})=-R/8\pi.\tag{5.34}$$

Inserting this decomposition into (5.31), the subtracted potential leads to

$$Z=\text{const.}\times e^{(\mu/T)\int d^3x\,d^3x'[\eta_{\ell n}(\mathbf{x})\eta_{\ell n}(\mathbf{x}')+(\nu/(1-\nu))\eta_{\ell\ell}(\mathbf{x})\eta_{nn}(\mathbf{x}')]v_4'(\mathbf{x}-\mathbf{x}')}.\tag{5.35}$$

The infinite constant can be treated following (4.141). It gives the overall factor

$$e^{-(\mu/T)c\int d^3x\, d^3x' [\eta_{\ell n}(\mathbf{x})\eta_{\ell n}(\mathbf{x}') + (\nu/(1-\nu))\eta_{\ell\ell}(\mathbf{x})\eta_{mm}(\mathbf{x}')]}, \tag{5.36}$$

which may be rewritten as

$$e^{-(\mu/T)c\left|\int d^3x(\eta_{\ell n}(\mathbf{x}) + \alpha\delta_{\ell n}\eta_{ii}(\mathbf{x}))\right|^2}, \tag{5.37}$$

where

$$\alpha = \frac{1}{3}\left(\sqrt{\frac{1+2\nu}{1-\nu}} - 1\right). \tag{5.38}$$

Since c diverges against plus infinity, the factor vanishes unless

$$\int d^3x\,(\eta_{\ell n}(\mathbf{x}) + \alpha\,\delta_{\ell n}\,\eta_{ii}(\mathbf{x})) = 0 \tag{5.39}$$

for each ℓ, n. Separating $\eta_{\ell n}(\mathbf{x})$ into its traceless spin-two part $\eta^{(2)}_{\ell n}(\mathbf{x})$ and the spin-zero part $\eta_{ii}(\mathbf{x})$, this amounts to the two equations

$$\int d^3x\,\eta^{(2)}_{\ell n}(\mathbf{x}) = 0, \qquad \int d^3x\,\eta_{ii}(\mathbf{x}) = 0. \tag{5.40}$$

These state that only such defect contributions have a non-vanishing stress partition function whose integrated densities vanish. We shall call this property charge neutrality of defects or *defect neutrality*.

Let us decompose the defect tensor $\eta_{ij}(\mathbf{x})$ into dislocation and disclination densities according to (2.79b), (2.80a)

$$\eta_{ij}(\mathbf{x}) = \Theta_{ij}(\mathbf{x}) + \varepsilon_{imn}\partial_m(\alpha_{jn}(\mathbf{x}) - \tfrac{1}{2}\delta_{jn}\alpha_{kk}(\mathbf{x})). \tag{5.41}$$

The dislocations by themselves satisfy automatically charge neutrality (5.40)[b] due to the derivatives in front of α_{in}. When inserted into (5.35), these derivatives ensure that the potential between dislocations goes like $1/R$ as given in formula (3.29). Just as for dislocations, the force between disclination lines is repulsive for line elements and attractive for opposite line elements, but the potential is linear. This leads to a "permanent confinement" of opposite line elements. In a statistical ensemble they can

[b]Under the usual assumption that $\alpha_{\ell n}(\mathbf{x})$ vanishes at large $|\mathbf{x}|$.

never be found far from each other. This situation is analogous to the permanent confinement of quarks and antiquarks in elementary particle physics, which apparently cannot be isolated in the laboratory. Only their bound states, the strongly interacting particles (mesons and baryons) are observable.

For disclination lines we have seen in the general discussion of Section 2.4 that the bound states of lines of opposite sign are dislocation lines. The permanent confinement implies that a crystal in thermal equilibrum never contains free disclination line elements. Only their bound states, the dislocation lines can be found. External forces are necessary to generate disclination via plastic deformations. Nevertheless we shall see later that it is possible to produce disclinations by heating, but only at the expense of a *complete* destruction of the crystalline order in a melting process.

5.3. TWO-DIMENSIONAL DEFECTS

In two dimensions, the stress tensor can be written as

$$\sigma_{ij}(\mathbf{x}) = \varepsilon_{ik}\,\varepsilon_{jm}\,\partial_k\,\partial_m\chi(\mathbf{x}) \tag{5.42}$$

and χ has lost both indices (since it corresponds to restricting χ_{lm} to χ_{33} only). As was previously true for A_i, it is no longer a gauge field. Explicitly we have

$$\sigma_{11} = \partial_2^2\chi, \qquad \sigma_{22} = \partial_1^2\chi, \qquad \sigma_{12} = \sigma_{21} = -\partial_1\,\partial_2\,\chi. \tag{5.43}$$

The field A_i is related to χ via

$$A_i(\mathbf{x}) = \varepsilon_{ik}\,\partial_k\chi(\mathbf{x}). \tag{5.44}$$

It is explicitly transverse. The elastic energy reads [compare (4.137)]

$$E^{\mathrm{el}} = \frac{1}{4\mu(1+\nu)}\int d^2x\,(\partial^2\chi)^2. \tag{5.45}$$

The field χ now couples to a defect tensor η (corresponding to η_{33})

$$E^{\mathrm{int}} = i\int d^2x\,\chi(\mathbf{x})\,\eta(\mathbf{x}). \tag{5.46}$$

Hence we obtain for the elastic partition function [compare (4.140), (4.141)]

$$Z = \int \mathscr{D}\chi(\mathbf{x})\, e^{-[\beta/(4\mu(1+\nu))]\int d^2x(\partial^2\chi)^2 + \beta i\int d^2x\,\chi(\mathbf{x})\,\eta(\mathbf{x})} \tag{5.47}$$

$$= \text{const.} \times \det(\beta\partial^4)^{-1/2}\, e^{-\beta\mu(1+\nu)\int d^2x\, d^2x'\,\eta(\mathbf{x})\, v_4(\mathbf{x}-\mathbf{x}')\,\eta(\mathbf{x}')}. \tag{5.48}$$

The potential $v_4(\mathbf{x})$ was calculated in (1.121). Using a small cutoff mass δ, it contains an infinity $1/(4\pi\delta^2) \to \infty$. This shows that Z vanishes for any defect distribution which does not satisfy the condition

$$\int d^2x\,\eta(\mathbf{x}) = 0. \tag{5.49}$$

This implies two-dimensional *defect neutrality*.

Neutrality is not yet sufficient to guarantee a finite Z. There is another infinity in $v_4(\mathbf{x})$ which goes like $-|\mathbf{x}|^2 \log\delta$. This is eliminated as follows. We write the exponent as

$$\begin{aligned} &-\log\delta\left[\int d^2x\, d^2x'(\mathbf{x}-\mathbf{x}')^2\,\eta(\mathbf{x})\,\eta(\mathbf{x}')\right] \\ &= -\log\delta\left[2\int d^2x\,\mathbf{x}^2\,\eta(\mathbf{x})\int d^2x'\,\eta(\mathbf{x}') - 2\left(\int d^2x\,\mathbf{x}\,\eta(\mathbf{x})\right)^2\right] \\ &= 2\log\delta\left(\int d^2x\,\mathbf{x}\,\eta(\mathbf{x})\right)^2. \end{aligned} \tag{5.50}$$

From this we see that only such defect distributions can occur which also have a vanishing dipole moment,

$$\int d^2x\,\mathbf{x}\,\eta(\mathbf{x}) = 0. \tag{5.51}$$

This condition will be called *dipole neutrality*. Once $\eta(\mathbf{x})$ fulfills both conditions, the partition function can be written in the form (5.48) but with $v_4(\mathbf{x})$ replaced by the finite potential $v_4''(\mathbf{x}) = (|\mathbf{x}|^2/8\pi)\log|\mathbf{x}|$ of (1.122).

NOTES AND REFERENCES

Gauge fields for stresses were first introduced by
J.C. Maxwell, *Transact. R. Soc.* (Edinburgh) **26** (1870) 1,
G. Morera, *Atti. Acc. Naz. Linc. Rend. d. Fis. Mat. Nat.* V. Ser. **1/1** (1892) 141,
E. Beltrami, *ibid.* (1892) 142,
H. Schäfer, *Z. Angew. Math. Mech.* **33** (1953) 356,
E. Kröner, "Kontinuumstheorie der Versetzungen und Eigen spannungen," in *Ergebnisse der Angew. Mathematik*, Vol. 5, eds. L. Collatz and F. Lösch (Springer, Heidelberg, 1958).

The helicity representation was first used in
H. Kleinert, *Lett. Nuovo Cimento* **34** (1982) 294, *Phys. Lett.* **89A** (1982) 294,
to analyze stress configurations.

CHAPTER SIX

KINEMATIC PROPERTIES OF DISLOCATION LINES

So far we have studied only static defect lines. For a complete understanding of the plastic properties of materials caused by defect lines it is necessary to know also their kinematic properties. In this text we shall be mainly interested in equilibrium thermodynamics of defects and stresses, where these properties are, to a large extent, irrelevant. For completeness, however, it will be useful to recapitulate the way defects move in a crystal.

6.1. GLIDE

In Section 2.1 we already saw that a dislocation line of the edge type facilitates the movement of one crystal piece over another. The movement proceeds in a slip plane parallel to the Burgers vector and orthogonal to the line. Such a movement is called planar glide. If the stress is not applied uniformly over the surface of a crystal, dislocation lines take a piece-wise screw character (see Fig. 6.1) and the slip planes become cylindrical (see Fig. 6.2a). Just as in the planar slip, only switching of bond directions is required as long as the lines move so as to keep a constant projection along the **b** direction.

FIG. 6.1.a. If a slip starts with a pure edge dislocation line and the shear forces become inhomogeneously distributed along the y-axis, the edge line acquires the screw and mixed sections shown in Fig. 6.1b.

FIG. 6.1.b. The atoms above and below a mixed dislocation piece connecting edge and screw parts. This can move to the right via slight shifts in bond directions. The circles and dots are atoms above and below the slip plane, respectively.

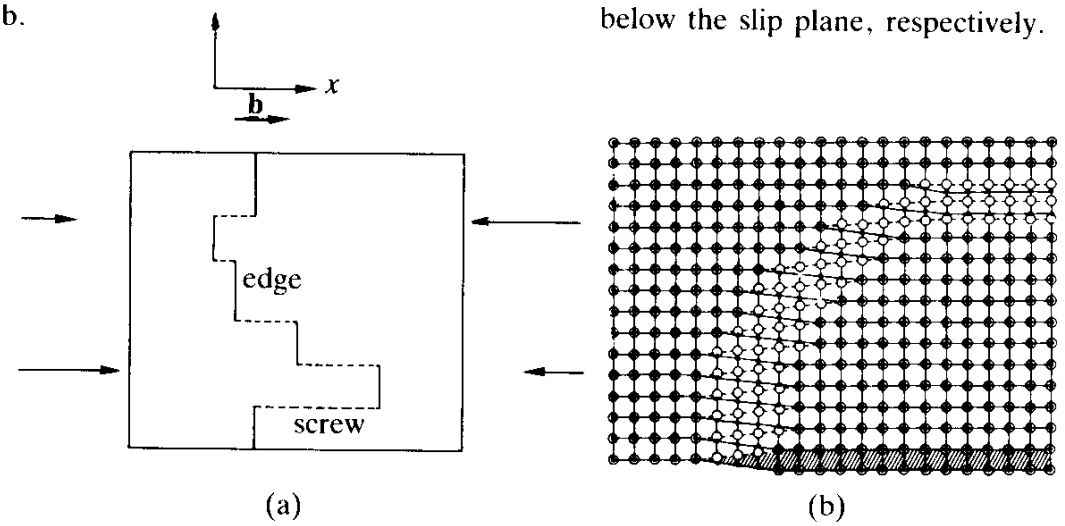

FIG. 6.2.a.b. The mixed edge-screw dislocation line in glide configurations on a cylindrical surface whose projection along **b** is the line shown to the left of the figure. This slip occurs if a force pushes to the right in the center and to the left outside the periphery. In Fig. 6.2b we also find a cross-slip away from the slip plane (see also Fig. 6.4).

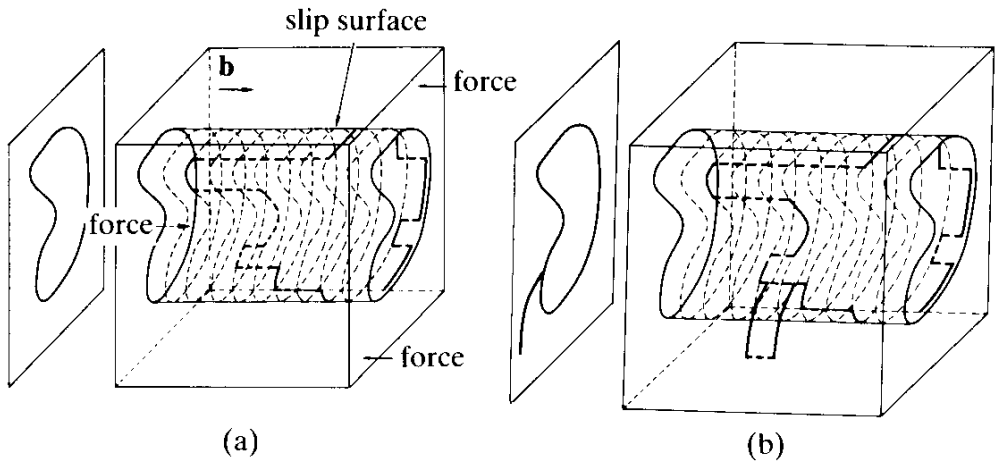

6.2. KINKS

It may be expected that the slip movement of a line is not a continuous one. Due to the periodic nature of the crystal, the positions where the dislocation line can lie most comfortably are determined by potential grooves which in a s.c. lattice would run parallel and orthogonal to **b** in the slip plane [see Fig. 6.3 for an illustration of the orthogonal grooves]. In such potentials a dislocation line may form kinks in which the line jumps across one potential barrier and proceeds in the next groove. Kinks are single line elements of screw character. A finite-line piece of screw character may be seen as a multi-kink jump in a pure edge dislocation.

FIG. 6.3. The kinks due to the undulation of the effective potential for a dislocation line which is caused by the periodicity of the lattice (Peierls potential). We have omitted the undulation orthogonal to **b** which is certainly also there.

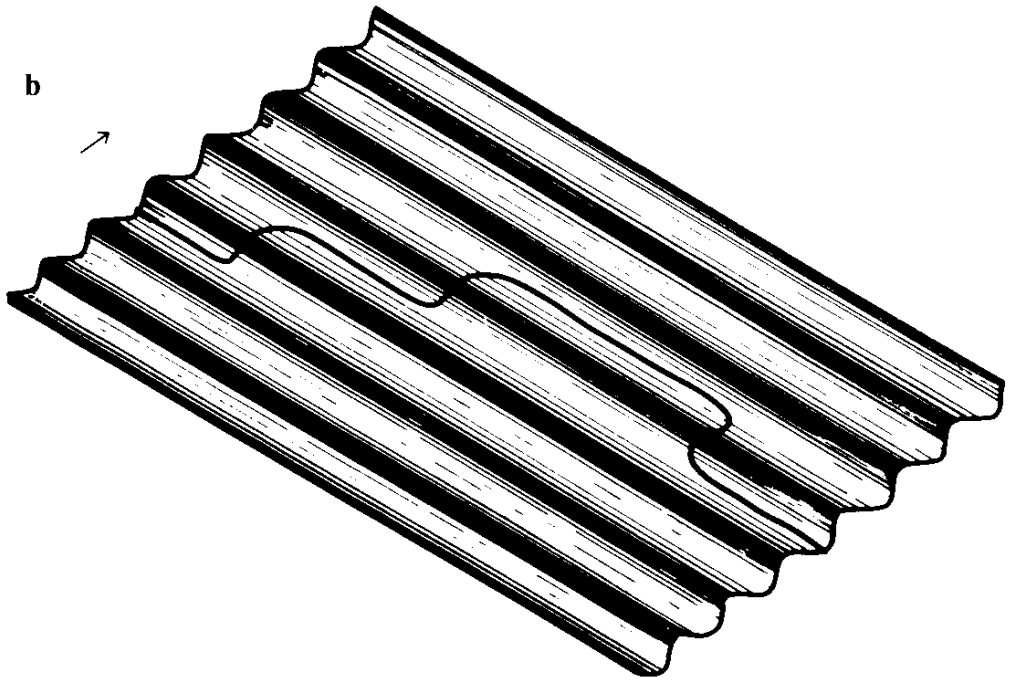

6.3. CLIMB

A movement of a line away from the slip surface is in general restricted. In order to understand this most simply, consider the possibility of a dislocation line moving orthogonal to $\mathbf{b} \times d\mathbf{x}$, a movement which is meaningful only to the non-screw piece of a dislocation line. Such a movement is called a *climb*. Looking at Fig. 2.2. we see that such a movement of the dislocation line to the right or left can only take place by extending the plane of excessive atoms. This, in turn, requires the presence and rearrangement of the interstitial atoms. We conclude that the climb must be a degree of freedom which hardly occurs in a plastic deformation. It can take place only on a long time scale which is needed by the interstitial atoms to diffuse to the climbing line.

6.4. GENERAL CONSERVATION MOTION

Closed dislocation loops have a slightly easier possibility of performing a climb without requiring extra interstitials. For they may use their own excess atoms and simply change their arrangement. Such a climb is called conservative. In general, any movement of defects which can take place

without the need of extra interstitial atoms is called *conservative*. It is characterized by the invariance of

$$\frac{1}{a^3}\int_S dS_i b_i, \tag{6.1}$$

since this obviously counts the number of excess atoms in the dislocation loop. The conservative movement may also be characterized by an integral along the dislocation line. Let $\delta\mathbf{x}(s)$ be the displacement of the line. The excessive atoms of a dislocation line lie in the direction $ds\dot{\mathbf{x}}(s) \times \mathbf{b}$ where $ds\dot{\mathbf{x}}(s)$ is the infinitesimal tangent vector. Thus a movement $\delta x(s)$ requires

$$\delta A = \frac{1}{a^3}\int ds(\dot{\mathbf{x}} \times \mathbf{b}) \cdot \delta\mathbf{x}(s) \tag{6.2}$$

additional atoms. In terms of this expression, we see that a glide always proceeds in such a way that for each line element it only *displaces* the same set of excessive atoms, i.e., $\delta\mathbf{x}(s)$ is orthogonal to the excessive layer:

$$(\dot{\mathbf{x}} \times \mathbf{b}) \cdot \delta\mathbf{x}(s) = 0. \tag{6.3}$$

Thus a glide is a conservative motion.

A climb is defined by (6.3) as being nonzero. One speaks of a conservative climb if it possesses at least a vanishing integral around the whole line

$$\frac{1}{a^3}\int_L ds(\dot{\mathbf{x}} \times \mathbf{b}) \cdot \delta\mathbf{x}(s) = 0. \tag{6.4}$$

Even though a conservative climb is much easier to generate than a non-conservative one since the diffusion of atoms along the dislocation line is easier than the diffusion in the bulk of the crystal, it nevertheless is extremely unfavorable when compared with the glide.

6.5. CROSS SLIP

At this place we may observe that there is another possible dislocation movement which is not a glide but also of the easy type by having $(\dot{\mathbf{x}} \times \mathbf{b}) \cdot \delta\mathbf{x} = 0$. It arises for screw dislocations for which $\dot{\mathbf{x}} \times \mathbf{b} = 0$.

FIG. 6.4. A cross slip. Two loops on different slip planes can fuse without need of extra intestitial atoms, or a screw piece of a dislocation may suddenly escape from the slip plane in such a way that its projection along **b** is a line (compare with the cross slip tongues forming in Fig. 6.5b).

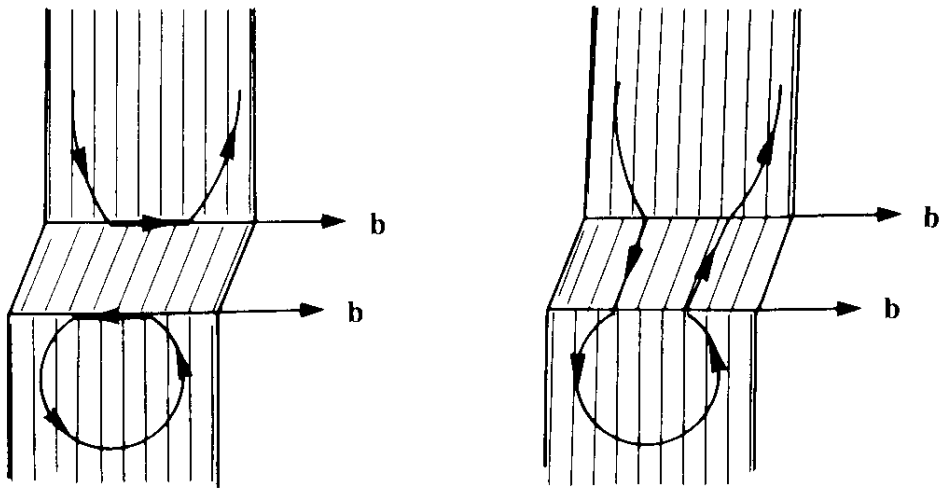

Therefore, a whole section of screw dislocations can move away from the slip plane without need of interstitial atoms. Such a movement is called cross slip and shown in Fig. 6.2b. It is characterized by its projection along **b** being a line. A cross slip may also form and connect two different dislocation loops on different slip planes as shown in Fig. 6.4.

6.6. DISLOCATION SOURCES

If a dislocation line has moved once through the crystal, the plastic displacement is equal to the Burgers vector **b** of the line. In order to arrive at macroscopic deformations, a great number of lines is necessary. It was pointed out by Kuhlmann-Wilsdorf and by Frank that in order to understand the large deformations observed in many materials, an efficient source must exist by which dislocation loops can be created under external stress. The basic mechanism by which this happens was discovered by Frank and Read and is nicely explained in the book by Read. A modification of his pictures is shown in Fig. 6.5a–d. By inspection we see that if the upper portion of the crystal is sheared against the lower, the section DC of the edge dislocation line starts circulating around the axis DE in the clockwise sense thereby expanding the slip plane once through the whole crystal. The result is a movement of the upper portion against the lower by **b**.

The importance of the mechanism lies in its periodicity: After one sweep, the line DC has returned to its initial position from where it can start the next sweep. In the illustration, the surface of the crystal seems to

FIG. 6.5. The periodic motion of a dislocation according to Frank and Read which cuts a crystal an arbitrary number of times and permits a plastic shift of the top half against the bottom half by any number of Burgers' vectors.

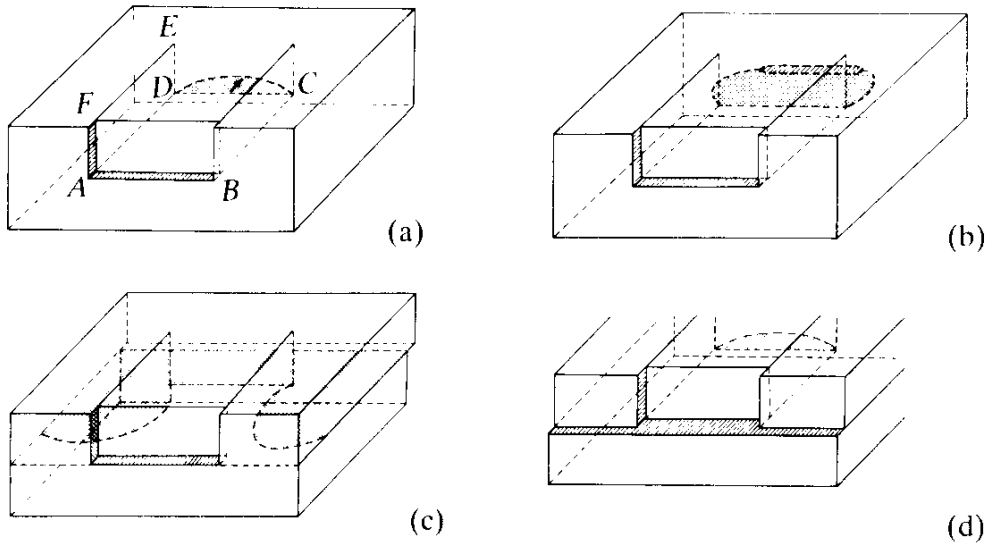

FIG. 6.6. The Frank-Read mechanism in Fig. 6.5a–d in a large crystal. It can produce dislocation loops which lie completely within the crystal. Only for small crystals, smaller than the typical loop size does it lead to a complete slip of the upper portion against the lower.

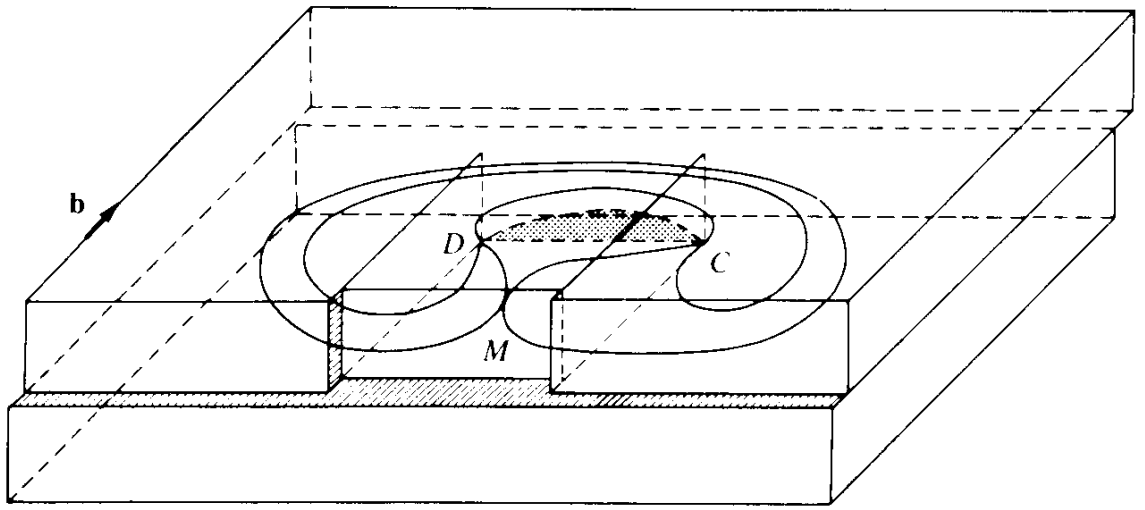

play an essential role. But this is not really true. A similar process can go on completely inside a crystal leading to the periodic formation of dislocation loops. In order to see this we may consider a symmetric initial configuration as shown in Fig. 6.6. By applying shear stress to the upper portion in the direction of **b** the line DC will bend and sweep out the same arc as those in Figs. 6.5a–b within the crystal. The return to the original position proceeds, however, in a different way. After a certain amount of sweeping, the curve collides at point M. There the section

DMC separates from the outside ring and re-establishes the initial line DC. The outside ring remains inside the crystal. This is obviously an easy movement since all that is necessary for a shift is a slight switching of bond directions as indicated by the dashed line.

Certainly, the dislocation lines in this plastic deformation process are not necessarily as smooth as shown. Even in a homogeneous stress field, the segments of the line have edge, screw, and predominantly mixed character.

It should be noted also that the lower part of the double cross slip in Fig. 6.4 can also act as a Frank-Read source.

6.7. INTERSECTING LINES AND JOGS

Another important aspect of dislocation movement is the possibility that lines can be driven to intersect and pass each other. This happens if external shear forces are large enough to overcome the elastic repulsion between the lines. The conservation of interstitial atoms does not permit the lines to have the same shape before and after intersections. A moment's thought shows us that, in general, each line acquires a jump orthogonal to its own slip surface whose size equals the component of the Burgers vector of the other line in this direction. An example is shown in Fig. 6.7 for two lines AB and XY which are straight before intersecting. Afterwards, the line XY is still straight since the Burgers vector $\mathbf{b}$ of AB lies in the slip plane of XY. The other line AB, however, acquires a vertical component PP'.

Such jumps orthogonal to the slip plane are called *jogs*. They are the counterparts of kinks, which are jumps within the slip plane. The main difference between the two consists in the fact that whereas a kink requires no migration of atoms, a jog does. In the example, the jog line contains an extra row of atoms below the line AP which is necessary for this partial climb of the line. These atoms have, of course, been left behind by the dislocation line XY. In order to see this we only have to keep in mind that the line XY before the intersection has a layer of excess atoms to the left while AB has such a layer extending downwards. After the intersection, the layer to the left of XY is reduced by one Burgers vector $\mathbf{b}$ so that it contains one row of atoms less. It is precisely these that have been left behind in the row to the right of the jog.

FIG. 6.7. Two lines before and after intersection. The line AB has a jog PP' as large as the Burgers vector of the line XY, which points orthogonal to the slip plane of AB. The other line XY remains straight since the Burgers vector of AB lies in the slip plane.

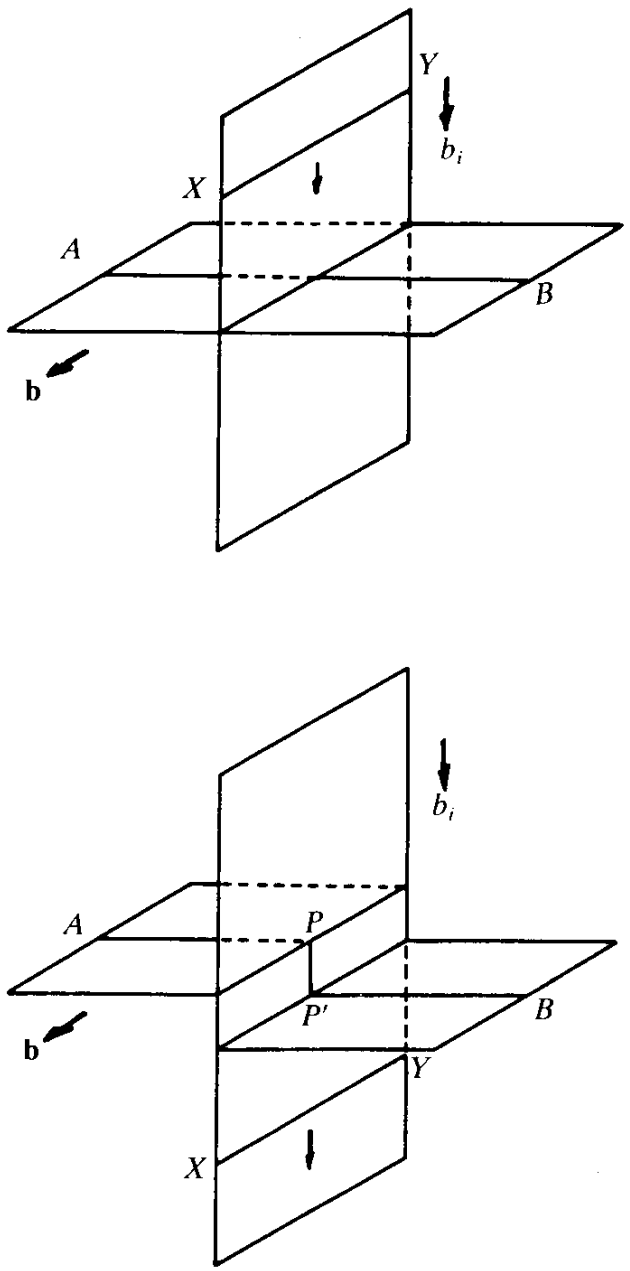

6.8. BASIC ENERGETIC CONSIDERATIONS OF BRANCHING OF DISLOCATION LINES

We saw in Section 2.11 that defect lines can branch off each other satisfying conservation laws like those for electric currents. If a pure dislocation line L_1 with Burgers vector splits $\mathbf{b}_1$ into two others L_2, L_3 with $\mathbf{b}_2$, $\mathbf{b}_3$, they obey the analogue of Kirchhoff's law:

$$\mathbf{b}_1 = \mathbf{b}_2 + \mathbf{b}_3. \tag{6.5}$$

Energetically, such branching configurations are usually unstable. Just as in the case of vortex lines, the elastic energy of a dislocation line increases roughly quadratically in **b**. Thus, if the square of one vector is larger than the sum of the others, say

$$\mathbf{b}_1^2 > \mathbf{b}_2^2 + \mathbf{b}_3^2, \tag{6.6}$$

the line L_1 will slice open in favor of two lines L_2 and L_3. This is analogous to the case with elementary particles where a decay process takes place with the conservation of the momentum vectors

$$\mathbf{p}_1 = \mathbf{p}_2 + \mathbf{p}_3 \tag{6.7}$$

as soon as the masses satisfy

$$m_1 > m_2 + m_3. \tag{6.8}$$

From this argument, it is obvious that among all admissible Burgers vectors only the shortest ones have the largest chance of being stable. Others may be stable because of elastic anisotropy or because their atomic configuration in the core has a low energy. In a simple cubic lattice, the Burgers vectors

$$\mathbf{b}_1 = (1, 0, 0)a, \qquad \mathbf{b}_2 = (0, 1, 0)a, \qquad \mathbf{b}_3 = (0, 0, 1)a, \tag{6.9}$$

and their mirror images are stable while all others decay into them. In a body-centered cubic lattice which is spanned by basic lattice vectors

$$\mathbf{a}_1 = (1, 0, 0)a, \qquad \mathbf{a}_2 = (0, 1, 0)a, \qquad \mathbf{a}_3 = (1/2)(1, 1, 1)a, \tag{6.10}$$

the shortest Burgers vectors which are of the form (6.10), as well as the next longer ones pointing to the six next nearest neighbors

$$\mathbf{b} = \tfrac{1}{2}(1, 1, 1)a, \tfrac{1}{2}(1, 1, -1)a, \ldots, \tfrac{1}{2}(-1, -1, -1)a \tag{6.11}$$

are stable. In a face-centered cubic lattice, the situation is similar. Here (6.9) and the twelve shortest Burgers vectors

$$\begin{aligned}\mathbf{b} = &\pm(1/2)(0,\ 1,\ 1)a,\ \pm(1/2)(0,\ 1,\ \pm 1)a\\ &\pm(1/2)(1,\ 0,\ 1)a,\ \pm(1/2)(1,\ 0,\ \pm 1)a\\ &\pm(1/2)(1,\ 1,\ 0)a,\ \pm(1/2)(1,\ \pm 1,\ 0)a.\end{aligned} \tag{6.12}$$

In the following it will be useful to think of all unstable dislocation lines as composite objects consisting of those stable lines into which they can decay. This is similar to the old fashioned theory of elementary particles in prequark days when all hadronic resonances were thought of as being composed of pions and nucleons. The smallest set of stable dislocation lines capable of building up all others will be referred to as *basic* or fundamental. Only these fundamental objects must be included explicitly in the field theory of defects to be developed later. The others can be viewed as consequences of the field interactions.

6.9. ANCHORED BRANCH POINTS

Branching dislocation lines have interesting properties as far as motion is concerned. In general, three slip planes intersect each other only in one point.[a] In this case the vertex cannot perform any conservative motion. One therefore speaks of anchoring a vertex. The Frank-Read source mechanism for dislocation loops can take place between any two such anchored vertices. In line configurations which are formed like the letter H and in which the four external lines do not lie in the slip plane of the cross connection, this can perform precisely the same periodic sweeps as discussed above, thereby producing sequences of loops.

NOTES AND REFERENCES

For more details see the books listed in Chapter 2 and the book by W.T. Read, Jr., *Dislocations in Crystals* (McGraw-Hill, New York, 1953).

[a]An important exception is that of

$$\mathbf{b}_1 = \frac{a}{2}(1,\ -1,\ 0),\quad \mathbf{b}_2 = \frac{a}{2}(1,\ 0,\ -1),\quad \mathbf{b}_3 = \frac{a}{2}(0,\ -1,\ 1)$$

with $\mathbf{b}_1 = \mathbf{b}_2 + \mathbf{b}_3$ and all three vectors lying in the plane orthogonal to the space diagonal $(1,\ 1,\ 1)$.

CHAPTER SEVEN

SOME GENERAL PROPERTIES OF THE MELTING PROCESS

So far we have studied specific defect configurations with their elastic long range stress interactions. These interactions were described by a gauge field coupled locally to the defect densities. In the previously investigated case of superfluid ^{4}He we saw that given a system of random lines with such a coupling, it is relatively easy to develop a disorder field theory for a grand canonical ensemble of such lines. This field theory permitted the study of phase transitions in which vortex lines condensed. In ^{4}He this transition carried the superfluid into the normal state.

In Chapters 4 and 5 we found gauge structures which are very similar to those in superfluid ^{4}He. Hence we might expect that a very similar disorder field theory can be set up for the defect lines in a perfect crystal. At a certain temperature, the entropy of the lines overcomes the energy and the lines become infinitely long and proliferate. Once the crystal is filled with long defect lines it loses its high degree of symmetry. The fluctuations of the defects carry the atoms of the crystal to arbitrary positions. The resulting disordered state may be expected to behave like a liquid[a]. Thus, once we succeed in finding a proper disorder field theory of defect lines, this should provide a possible theoretical basis for the study of the melting transition.

When attempting such an approach, however, one immediately realizes that there exists an important difference between the two phase tran-

[a]If the time scale of defect movements is sufficiently short. Otherwise the state will be glasslike.

sitions. The superfluid transition in ^{4}He is a second-order phase transition. Near the critical point, the physically relevant fluctuations are all of very long range. This makes the critical behavior, in particular the critical indices, *independent* of the properties of the system at short distances. For this reason a lattice model of the superfluid phase transition such as the classical XY model is able to reproduce the critical behavior with arbitrary accuracy, even though the phenomenon of superfluidity does certainly not take place on a lattice. The critical behavior does not depend on the particular choice of the lattice structure. This property of second-order phase transition is called *universality*. It has been one of the most important achievements in theoretical physics in the past decade to have recognized this property and developed methods to understand the different universality classes theoretically. Universality is the reason why the critical behavior of second order phase transitions can not only be described by various lattice models but also by a suitably chosen field theory. The field has only to be capable of representing properly those degrees of freedom of the system whose fluctuations acquire an infinite range at the critical point. For the superfluid transition, it had to be a complex field.

In contrast to this pleasant situation with the superfluid transition, the melting process which we would like to understand in this part of the text, is a first-order process. Just above the transition temperature, in the molten phase, all correlation lengths are finite. Thus the melting transition can certainly *not* be a universal phenomenon in the same sense as second order phase transitions are. Crystals with different lattice structures show different transitions. For these reasons, there cannot be a simple universal field theory from which to extract quatitative poperties of *all* melting transitions which are comparable to the critical indices in second order phase transitions. The results will depend on short range properties of the field theory which differ from crystal to crystal. This has to be kept in mind when we go about trying to construct a field theory of melting. The best we can hope to achieve is to exhibit a *universal mechanism* of the melting transition.

7.1. HISTORICAL NOTES

The process of melting was probably one of the very first phase transitions ever observed by man in prehistoric times. The ancient Greeks were certainly wondering about it. For its understanding they possessed, around 450 B.C., two important theoretical concepts.

1. Atomic build-up of matter, as advanced by Leucippus and Demo-

critus: In solids the atoms were supposed to be hooked together by branch-like elements. In liquids, they were imagined as smooth and rounded objects, comparable to poppy seeds.

2. Ceaseless motion of atoms: This concept was an extrapolation of the dance of dust particles as seen through a sunbeam. It can be considered as a predecessor of the Brownian motion, which was to be discovered in the 19th century.

Both concepts are beautifully recapitulated in the famous book on the history of science, *De Rerum Natura*, written in verse form in the year 57 B.C. by the Roman Lucretius (see the quotations in the beginning of Parts I, II, III, IV).

For a proper description of the transition between the solid and liquid phase the Greeks lacked, however, two important theoretical ingredients.

1. The connection between motion and heat.
2. The role of entropy, which gives a preference to states with many microscopic configurations over those with few.

The first of these two ingredients did not become available until 1762, when Joseph Black (1728–1795) discovered latent heat, a discovery which went hand in hand with the practical development of the steam engine by James Watt (1736–1819) in 1765. Many years later, in 1809, Humphry Davy (1778–1829) claimed to have demonstrated this connection even more directly: he showed that ice melts when two pieces are scraped against each other[b]. In 1850, Michael Faraday (1791–1867) observed that increased pressure lowers the melting temperature (a fact which in the opinion of many people forms the physical basis of the art of ice skating) and in 1860, R.W. Bunsen (1811–1899) determined the volume changes during the melting process. The second theoretical ingredient was discovered around 1850 by R. Clausius (1822–1888), W. Thomson (Lord Kelvin) (1824–1907), and W.M. Rankine (1820–1872) who formulated the second law of thermodynamics.

The statistical machanical basis embodying both ingredients was laid down in 1877 by L. Boltzmann (1814–1906), who showed that a macroscopic state of energy E occurs with a probability We^{-E/k_BT}, where W is the total number of microscopic possible configurations of this state. He also found that the experimental quantity S (entropy) was a measure for W, namely, $W = e^{S/k_B}$. Therefore, different configurations of energy E of a system occur with probability $e^{-F/k_BT} = e^{-(E-TS)/k_BT}$ and the quantity F was introduced as the *free energy* of a system.

Since then it has been clear, at least in principle, how the melting

[b]The experiment, however, seem to have been faulty. The friction between the pieces would have been too low to do the required work. There must have been a heat leak in his setup.

transition should be described theoretically. The practical calculation, however, remained very difficult due to the collective nature of the transition. While it is rather easy to describe a cold solid owing to its regular structure, the breakdown of crystalline order poses difficult theoretical problems, some of which are not yet understood even today.

Experimentally, the melting transition has been the subject of many detailed studies. Since there exists an excellent review by Borelius,[c] we shall not dwell into the many interesting aspects of the process but refer the reader to that article. We only display the specific heat and the thermal expansion coefficients for two typical simple crystals, Na and Pb (see Figs. 7.1, 7.2). We also show the important discontinuities, the jumps in volume, ΔV and entropy, $\Delta s \equiv \Delta S$ per atom, for a number of substances (see Table 7.1 and Fig. 7.3) which have to be reproduced by theory. Notice that the data lie approximately on a line which intersects the $\Delta s/k_B$ axis at about log 2.

7.2. THE LINDEMANN CRITERION

Within statistical mechanics, simple rough ideas about the temperature scale of the melting process can be formulated following Lindemann. In the ideal solid, each atom undergoes thermal vibrations about its equilibrium position. Its average displacement is controlled by the elastic energy. Neglecting the differences between the elastic constants we may estimate the energy by

$$E = \tfrac{1}{2}\mu \int d^3x\, (\partial_i u_j)^2 = \tfrac{1}{2}a^3\mu \sum_{\mathbf{x}} (\partial_i u_j)^2 = \tfrac{1}{2}a^3\mu \sum_{\mathbf{k}} k_i^2 u_j^2(\mathbf{k}), \qquad (7.1)$$

where a^3 is the volume per atom, $a^3 = V/N = v$. Thus, in Fourier space, the different modes decouple. According to the law of equipartition, each mode has the same average energy, i.e. (no sum over j),

$$a^3 \langle \mu \mathbf{k}^2 u_j^2(\mathbf{k}) \rangle = k_B T.$$

In x-space, this amounts to the correlation function

$$\langle u_i(\mathbf{x})\, u_j(\mathbf{x}') \rangle = \frac{k_B T}{\mu a^3} \frac{1}{N} \sum_{\mathbf{k}} e^{i\mathbf{k}\cdot(\mathbf{x}-\mathbf{x}')} \frac{\delta_{ij}}{\mathbf{k}^2} = \frac{k_B T}{\mu} \int \frac{d^3k}{(2\pi)^3} e^{i\mathbf{k}\cdot(\mathbf{x}-\mathbf{x}')} \frac{\delta_{ij}}{\mathbf{k}^2}. \qquad (7.2)$$

[c] See the Notes and References.

FIG. 7.1. The specific heat and the expansion coefficient of two typical Na (b.c.c.) through the melting transition (after Borelius, *op. cit.* in the Notes and References).

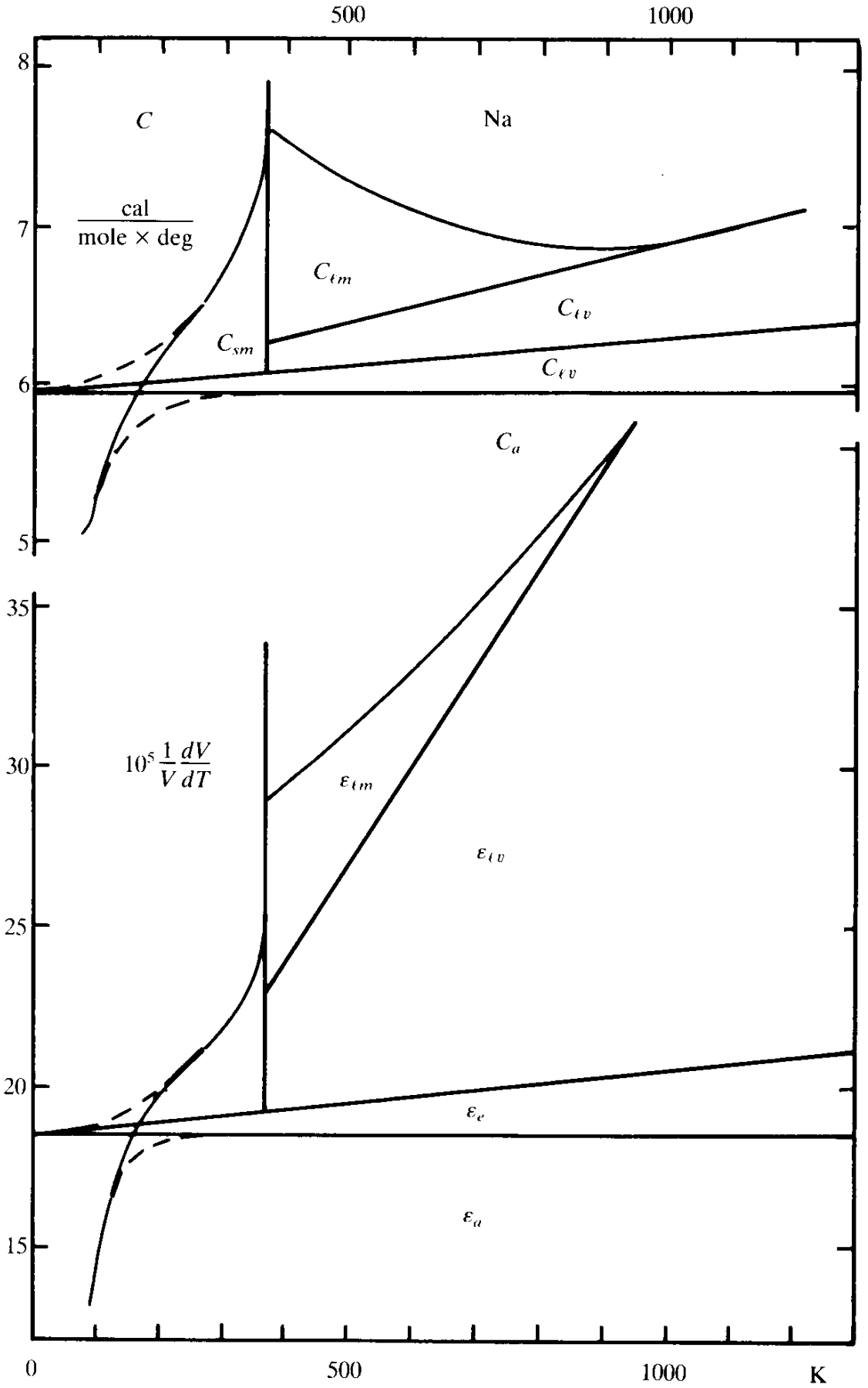

FIG. 7.2. The corresponding curves for Pb (f.c.c.).

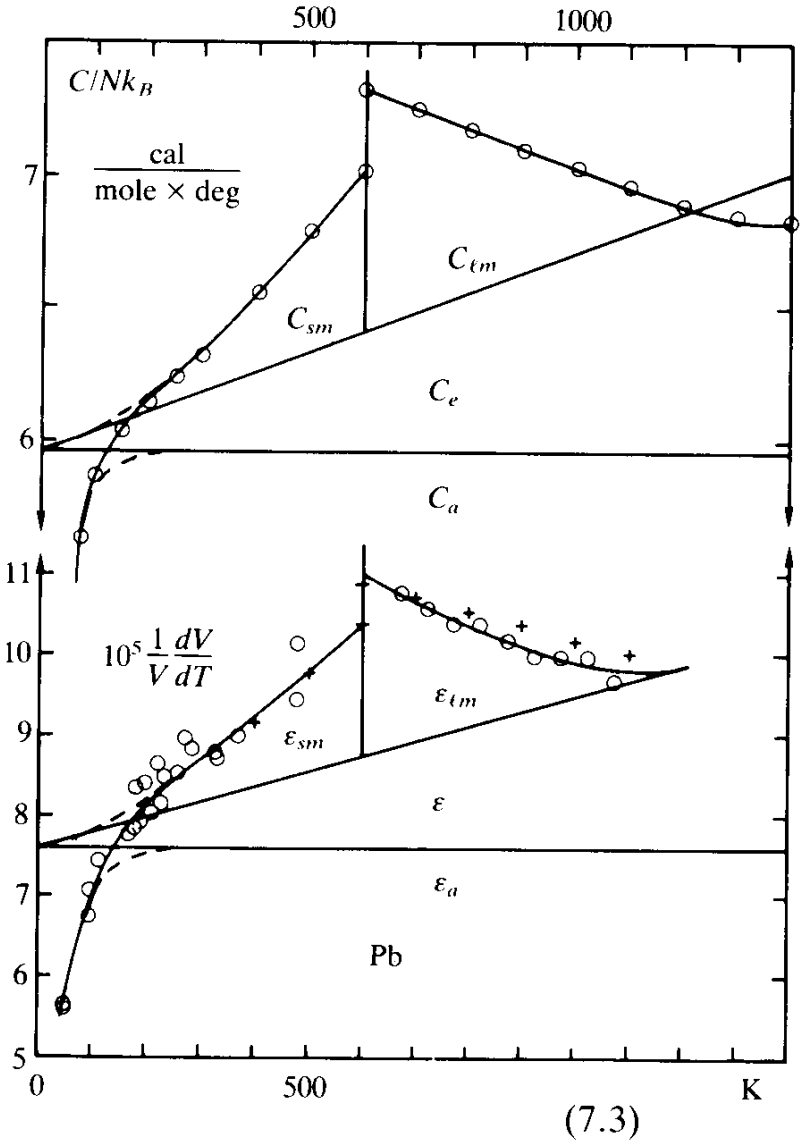

(7.3)

Thus the average size of the displacement is

$$\langle \mathbf{u}^2(\mathbf{x}) \rangle \sim 3\frac{k_B T}{\mu} \int \frac{d^3k}{(2\pi)^3} \frac{1}{\mathbf{k}^2}.$$

Since the momenta $\mathbf{k}$ all lie within the Brillouin zone of size $\approx \pi/a$, this gives, roughly [see also Eq. (7.166)]

$$\langle \mathbf{u}^2(\mathbf{x}) \rangle \sim \frac{3}{\pi}\sqrt{\frac{3}{4\pi}}\frac{k_B T}{\mu a} \sim \frac{k_B T}{2\mu a}. \tag{7.3}$$

Thus, for rising temperature, $\langle \mathbf{u}^2 \rangle$ increases linearly. It is obvious that this increase cannot go on indefinitely. As oscillating atoms begin to

FIG. 7.3. The entropy and volume jumps at the melting transition for various materials (after Lasocka and Tallon, *op. cit.* in the Notes and References). The two points for Ce (0.61, −1.1) and Pu (0.37, −2.4) are from Gschneider, *J. Less-Comm. Mat.* **43** (1975) 179, Table 2. I thank Prof. Lasocka for a communication of these points.

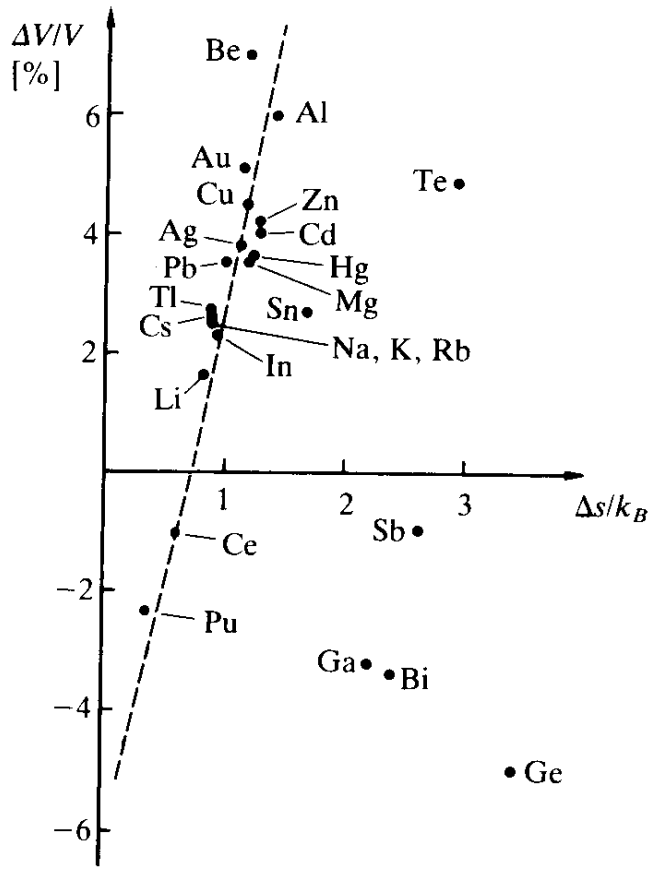

invade into the regime of the nearest neighbours the crystalline structure necessarily breaks down.

According to Lindemann, the melting temperature T_{melt} can therefore be characterized by a dimensionless number, the ratio of $\sqrt{\langle \mathbf{u}^2 \rangle}$ with the length scale a,

$$\frac{\sqrt{\langle \mathbf{u}^2 \rangle}}{a} \sim \sqrt{\frac{k_B T_{\text{melt}}}{\mu a^3}} = \sqrt{\frac{k_B T_{\text{melt}}}{\mu a^3}}. \tag{7.4}$$

The inverse of this ratio,

$$\bar{L} = \sqrt{\frac{\mu a^3}{k_B T_{\text{melt}}}} \tag{7.5a}$$

is tabulated in the literature as the so-called *Lindemann parameter.*

Actually, what is given in the tables is usually the following combination of material properties (see Table 7.2),

TABLE 7.1. Discontinuities in the melting transition, $\Delta s/k_B$ = entropy jump per atom, $(\Delta V/V)(\%)$ = relative volume change in percent (after A.R. Ubbelohde. *op. cit.* in the Notes and References).

b.b.c. metals	$2\Delta s/k_B$	$\frac{\Delta V}{V}(\%)$	f.c.c. metals	$2\Delta s/k_B$	$\frac{\Delta V}{V}(\%)$
Li	1.58	2.2	cAl	2.76	6.5
Na	1.67	2.5	Co	2.19	3.5
K	1.66	2.5	Ni	2.42	5.4
Rb	1.68	2.4	Cu	2.30	4.2
Cs	1.66	2.6	Pd	2.25	5.9
Tl	1.72	2.2	Ag	2.19	3.8
Ca	1.84	—	Pt	2.30	6.6
Sr	2.10	—	Au	2.24	5.2
Ba	1.85	—	Pb	1.91	3.6
Sc	1.86	—	Mn	2.31	1.7
Cr	1.62	—	Yb	1.51	—
Fe	1.82	3.5	Nb	2.34	—
			Mo	2.69	—
La	1.24	0.6	Sm	1.53	3.6
Ce	1.22	−1.1	Eu	2.02	4.8
Pr	1.36	0.02	Gd	1.52	2.0
Pu	0.74	−2.4	Tb	1.59	3.1
Nd	1.32	0.9	Dy	1.57	(4.5)
			Yb	1.67	5.1
h.c.p metals			W	2.31	—
			U	1.45	2.2
Mg	2.32	3.6			
Zn	2.53	4.3			
Cd	2.49	3.8			
Ho	(2.31)	(7.4)			
Er	2.65	(9.0)			
Tm	2.22	(6.9)			

$$L = \Theta_D V_{\text{mol}}^{1/3} (A/T_{\text{melt}})^{1/2}, \tag{7.5b}$$

where Θ_D is the Debye temperature, measured in K, V_{mol} the volume per mol in cm^3, A the atomic number, and T_{melt} the melting temperature in K. See, for example, the book by A.R. Ubbelohde (cited in the Notes and References). In order to find the relation between $\bar{L}$ and this L it is useful to recall a few basic properties of Debye's theory of specific heat.

7.3. REVIEW OF DEBYE'S THEORY OF SPECIFIC HEAT

The Debye temperature is experimentally accessible through measurements of the specific heat which for low temperature behaves as

TABLE 7.2. Lindemann parameters L and melting temperature T_m in K (from A.R. Ubbelohde, *op. cit.*).

f.c.c.	L	T_m/K	b.c.c.	L	T_m/K	hex.	L	T_m/K
Ag	148	1235.0	Ba	147	1983.1	Be	150	1558.1
Al	138	933.5	Cr	125	2133.1	Cd	168	594.2
Au	137	1337.5	Cs	118	301.7	Co	132	1767.1
Ca	124	1113.1	Fe	121	1813.1	Gd	129	1583.1
Cu	143	1357.6	K	122	336.3	Hf	143	2503.1
Ir	155	2720.1	Li	124	453.1	Ir	155	2720.1
Ni	143	1728.1	Mo	138	2893.1	Mg	134	923.1
Pb	149	600.6	Nb	104	2698.1	Re	134	3453.1
Pd	138	1827.1	Na	114	370.9	Ti	140	1943.1
Pt	151	2045.1	Rb	118	311.9	Tl	138	577.1
Rh	167	2236.1	Ta	110	3273.1	Zn	151	692.7
Sr	140	1043.1				Zr	133	2123.1
Th	159	1973.1				Se	91	493.1
V	123	2193.1				Te	178	723.1
W	135	2640.1						
Rhomb.	L	T_m/K	Orrhom.	L	T_m/K	Tetr.	L	T_m/K
Bi	201	472.4	Ga	261	302.9	In	142	429.7
Hg	171	234.2	V	192	2193.1	Sn	259	505.1
Sb	138	903.8						
As	170	886.1						

$$C_V = \frac{12\pi^4}{5} N k_B \left(\frac{T}{\Theta_D}\right)^3 . \tag{7.6}$$

The T^3 behaviour is a consequence of the quantum nature of the elastic lattice waves. In order to derive it we have to use the quantum partition function [recall (1.84), (1.86) in Part I]. The Euclidean action is

$$A_E = \int_0^{\hbar/k_B T} d\tau \int d^3x [-i\mathbf{p}(\mathbf{x}, \tau) \cdot \mathbf{u}(x, \tau) + E_{\text{kin}} + E], \tag{7.7}$$

E being the elastic energy [recall (1.20)],

$$E = \int d^3x \left(\mu u_{ij}^2 + \frac{\lambda}{2}\left(\sum_i u_{ii}\right)^2\right) = \frac{a^3}{2} \sum_{\mathbf{k}} (\mu \mathbf{k}^2 \delta_{ij} + (\mu + \lambda) k_i k_j) u_i^*(\mathbf{k}) u_j(\mathbf{k}) \tag{7.8}$$

and E_{kin} the kinetic energy

$$E_{\text{kin}} = a^3 \sum_{\mathbf{x}} \frac{\mathbf{p}^2(\mathbf{x}, \tau)}{2\rho}. \tag{7.9}$$

The parameter ρ denotes the mass density. The partition function of elastic waves, including quantum effects, reads

$$Z = \int \mathscr{D}^3 u(\mathbf{x}, \tau) \frac{\mathscr{D}^3 p(\mathbf{x}, \tau)}{2\pi} e^{-(1/\hbar) A_E}. \tag{7.10}$$

The measure of integration is well-defined only on a lattice. If a is the spacelike lattice distance and ε the timelike one, the action reads

$$A_E = a^3 \sum_{\mathbf{x}, \tau_n} \left\{ -i\mathbf{p}(\mathbf{x}, \tau_n) \cdot (\mathbf{u}(\mathbf{x}, \tau_n) - \mathbf{u}(\mathbf{x}, \tau_{n-1})) + \varepsilon \frac{\mathbf{p}(\mathbf{x}, \tau_n)^2}{2\rho} \right\}$$
$$+ a\varepsilon \sum_{\mathbf{x}, \tau_n} \mu \left[(u_{ij}(\mathbf{x}, \tau_n))^2 + \frac{\lambda}{2} \left(\sum_i u_{ii}(\mathbf{x} - \mathbf{i}, \tau_n) \right)^2 \right], \tag{7.11}$$

where $u_{ij}(\mathbf{x}, \tau)$ is a convenient lattice version of the strain tensor which we shall take in the form

$$u_{ij}(\mathbf{x}, \tau) = \tfrac{1}{2}(\nabla_i u_j(\mathbf{x}, \tau) + \nabla_j u_i(\mathbf{x}, \tau)). \tag{7.12}$$

We have shifted the argument of the λ term in (7.11) from $\mathbf{x}$ to $\mathbf{x} - \mathbf{i}$. This will be advantageous to us later when we come to calculating correlation functions of $u_i(\mathbf{x}, \tau)$ on the lattice. Integrating out the conjugate momentum variables $\mathbf{p}(\mathbf{x}, \tau_n)$ gives the lattice version of the elastic partition function,

$$Z = \prod_{\mathbf{x}, \tau_n, i} \left[\int \frac{du_i(\mathbf{x}, \tau_n)}{\sqrt{2\pi\varepsilon\hbar/a^3\rho}} \right] \exp\left[-\frac{1}{\hbar} a^3 \varepsilon \sum_{\mathbf{x}, \tau_n} \left\{ \frac{\rho}{2} \frac{1}{\varepsilon^2} (\nabla_\tau u_i(\mathbf{x}, \tau_n))^2 + \mu u_{ij}^2(\mathbf{x}, \tau_n) \right.\right.$$
$$\left.\left. + \frac{\lambda}{2} \left(\sum_i u_{ii}(\mathbf{x} - \mathbf{i}, \tau_n) \right)^2 \right\} \right]. \tag{7.13}$$

Recall that τ is an imaginary time. For real times, the $(\nabla_\tau u_i)^2$ term would have the opposite sign. Then, for $\varepsilon \to 0$, the extrema of the action would be given by

$$[\rho \partial_t^2 \delta_{ij} - \mu \bar{\nabla} \cdot \nabla \delta_{ij} - (\mu + \lambda) \nabla_i \bar{\nabla}_j] u_j(\mathbf{x}, t) = 0.$$

This is the first place where we see that it pays to have shifted the argument in the λ term. Had we not done so and used the naive form $(\Sigma_i u_{ii}(\mathbf{x}))^2$ instead, the equation would have read

$$(\rho\partial_t^2\delta_{ij} - \mu\bar{\nabla}\cdot\nabla\delta_{ij} - \mu\nabla_i\bar{\nabla}_j - \lambda\bar{\nabla}_i\nabla_j)u_j(\mathbf{x},\tau) = 0,$$

which contains three different matrices in ij – space. With the shift, there are only two matrices which can be diagonalized by the standard methods:

$$\left[\rho\partial_\tau^2 - \mu\nabla\cdot\bar{\nabla}\left(\delta_{ij} - \frac{\nabla_i\bar{\nabla}_j}{\bar{\nabla}\cdot\nabla}\right) - (2\mu+\lambda)\nabla\cdot\bar{\nabla}\frac{\nabla_i\bar{\nabla}_j}{\bar{\nabla}\cdot\nabla}\right]u_j(\mathbf{x},\tau) = 0,$$

where $\nabla_i\nabla_j/\bar{\nabla}\cdot\nabla$ and $\delta_{ij} - (\nabla_i\bar{\nabla}_j/\bar{\nabla}\cdot\nabla)$ are projection operators onto a lattice analogue of longitudinal and transverse sound waves. In Fourier space they satisfy the equations

$$(\rho\omega^2 - \mu\bar{\mathbf{K}}\cdot\mathbf{K})u_j^T(\mathbf{k},\omega) = 0, \quad (\rho\omega^2 - (2\mu+\lambda)\bar{\mathbf{K}}\cdot\mathbf{K})u_j^L(\mathbf{k},\omega) = 0, \tag{7.14}$$

with the two "transverse" and one "longitudinal" sound velocities

$$c_T = \sqrt{\frac{\mu}{\rho}}, \qquad c_L = \sqrt{\frac{2\mu+\lambda}{\rho}}. \tag{7.15}$$

The imaginary time variable is periodic in $\hbar/k_BT$ so that the Fourier decomposition reads

$$u_i(\mathbf{x},\tau) = \frac{1}{\sqrt{N}}\sum_{\mathbf{k},\omega_m} e^{i\mathbf{k}\cdot\mathbf{x} - i\omega_m\tau}u_i(\mathbf{k},\omega_m), \tag{7.16a}$$

where ω_m are the Matsubara frequencies

$$\omega_m = m\cdot 2\pi k_BT/\hbar, \quad m = 0, \pm1, \pm2, \ldots \tag{7.16b}$$

In terms of these variables, the action A_E reads

$$A_E = \frac{\rho}{2} a^3 \varepsilon \left\{ \sum_{\mathbf{k}, \omega_m} u_i^T(\mathbf{k}, \omega_m)^* \left(\frac{1}{\varepsilon^2} \bar{\Omega}_m \Omega_m + c_T^2 \frac{1}{a^2} \bar{\mathbf{K}} \cdot \mathbf{K} \right) u_i^T(\mathbf{k}, \omega_m) \right.$$
$$\left. + \sum_{\mathbf{k}, \omega_m} u_i^L(\mathbf{k}, \omega_m)^* \left(\frac{1}{\varepsilon^2} \bar{\Omega}_m \Omega_m + c_L^2 \frac{1}{a^2} \bar{\mathbf{K}} \cdot \mathbf{K} \right) u_i^L(\mathbf{k}, \omega_m) \right\}, \tag{7.17}$$

where Ω_m, $\bar{\Omega}_m$ are the analogues of $\mathbf{K}$ and $\bar{\mathbf{K}}$ for the timelike direction,

$$\bar{\Omega}_m \Omega_m \equiv 2[1 - \cos(\omega_m \varepsilon)] = 4 \sin^2 \left(\frac{\omega_m \varepsilon}{2} \right), \tag{7.18}$$

and u_i^T, u_i^L the lattice analogues of the transverse and longitudinal components, i.e.,

$$u_i^T(\mathbf{k}, \omega_m) \equiv (\delta_{ij} - K_i \bar{K}_j / \bar{\mathbf{K}} \cdot \mathbf{K}) u_j(\mathbf{k}, \omega_m),$$
$$u_i^L(\mathbf{k}, \omega_m) \equiv \frac{K_i \bar{K}_j}{\bar{\mathbf{K}} \cdot \mathbf{K}} u_j(\mathbf{k}, \omega_m). \tag{7.19}$$

Integrating out the u_i variables according to the rules of Chapter 1, Part I gives

$$Z = \prod_{\mathbf{k}} e^{-\sum_{\omega_m} [\log(\bar{\Omega}_m \Omega_m + c_T^2 (\varepsilon^2/a^2) \bar{\mathbf{K}} \cdot \mathbf{K}) + (1/2) \log(\bar{\Omega}_m \Omega_m + c_L^2 (\varepsilon^2/a^2) \bar{\mathbf{K}} \cdot \mathbf{K})]}. \tag{7.20}$$

The sum over Ω_m can now be performed using Eq. (6.248) of Part I. In the limit of zero timelike lattice spacing, the result is particularly simple and (6.250) of Part I leads to

$$Z = \prod_{\mathbf{k}} e^{-2((\hbar/k_B)(\omega_T(\mathbf{k})/2T) + \log(1 - e^{-\hbar \omega_T(\mathbf{k})/k_B T}))} e^{-((\hbar/k_B)(\omega_L(\mathbf{k})/2T) + \log(1 - e^{-\hbar \omega_L(\mathbf{k})/k_B T}))}, \tag{7.21}$$

where we have set

$$\omega_T \equiv c_T \sqrt{\bar{\mathbf{K}} \cdot \mathbf{K}/a^2}, \qquad \omega_L \equiv c_L \sqrt{\bar{\mathbf{K}} \cdot \mathbf{K}/a^2}. \tag{7.22}$$

The factor for each $\mathbf{k}$ represents the well-known partition function

$$Z_\omega = \frac{1}{2 \sinh \dfrac{\hbar \omega}{2 k_B T}} = \sum_{n=0}^{\infty} e^{-(n + 1/2)(\hbar \omega / k_B T)} \tag{7.23}$$

of a harmonic oscillator having frequencies ω_T, ω_L [see (6.251), Part I].

The internal energy is found by differentiating $\log Z$. This gives the standard "blackbody" radiation energy

$$U = \sum_{h=0,\pm 1} \sum_{\mathbf{k}} \hbar\omega_h(\mathbf{k}) \left(\frac{1}{2} + \frac{1}{e^{\hbar\omega_h(\mathbf{k})/k_B T} - 1} \right). \tag{7.24}$$

The sum over h covers the three polarization modes of the phonons. The momentum sum is usually evaluated in the approximation of an isotropic continuum for which [for the general case see Appendix 7B]

$$\omega_{L,T} \sim c_{L,T}|\mathbf{k}|, \tag{7.25}$$

so that one may change momentum integrals into frequency integrals, i.e.,

$$\sum_{\mathbf{k}} \to V \int \frac{d^3k}{(2\pi)^3} = V \int d\omega \frac{4\pi}{(2\pi)^3} \frac{\omega^2}{c_h^3} \equiv V \int d\omega\, g^{(h)}(\omega). \tag{7.26}$$

The functions $g^{(h)}(\omega)$ are called the *densities of states*. It is necessary to introduce a cutoff in the integration so that the total number of modes is equal to the number of atoms for each polarization. (Note that the proper lattice sum over $\mathbf{k}$ would have done so automatically, since $\Sigma_{\mathbf{k}} = N$.) This gives the conditions,

$$V \int_0^{\omega_D^{(h)}} d\omega\, g^{(h)}(\omega) = N, \quad h = 0, \pm 1, \tag{7.27}$$

where $\omega_D^{(h)}$ are called the *Debye frequencies*. Hence we have

$$g^{(h)}(\omega) = V \frac{4\pi}{(2\pi)^3} \frac{\omega^2}{c_h^3} = 3N \frac{\omega^2}{\omega_D^{(h)3}} \tag{7.28a}$$

$$\omega_D^{(h)} \equiv 2\pi \left(\frac{3}{4\pi V/N} \right)^{1/3} \cdot c_h = 2\pi c_h / r_0, \tag{7.28b}$$

where r_0 is the radius of the spherical volume associated with each particle.

A simpler but cruder approximation uses only a single density of states,

$$g(\omega) = \sum_{h=0,\pm 1} g^{(h)}(\omega),$$

which is given by

$$g(\omega) = 3 \times V \frac{4\pi}{(2\pi)^3} \frac{\omega^2}{\bar{c}^3}, \tag{7.29a}$$

where $\bar{c}$ is an average sound velocity

$$\bar{c} = \left[3 \Big/ \left(\frac{2}{c_T^3} + \frac{1}{c_L^3} \right) \right]^{1/3}. \tag{7.29b}$$

Then $g(\omega)$ can be parametrized as

$$g(\omega) = 3 \times 3N \frac{\omega^2}{\omega_D^3}, \tag{7.30a}$$

where

$$\omega_D = 2\pi \left(\frac{3}{4\pi V/N} \right)^{1/3} \bar{c} = 2\pi \bar{c}/r_0. \tag{7.30b}$$

The temperatures related to $\omega_D^{(h)}$, ω_D via $\hbar$ and the Boltzmann constant k_B are the Debye temperatures

$$\Theta_D^{(h)} = \hbar\, \omega_D^{(h)}/k_B, \qquad \Theta_D = \hbar\, \omega_D/k_B. \tag{7.31}$$

Using the averaged density of states $g(\omega)$, the internal energy (7.24) can be rewritten as the integral[d]

$$\begin{aligned} U &= 9Nk_B T \left(\frac{T}{\Theta_D} \right)^3 \int_0^{\Theta_D/T} d\xi \xi^3 \left[\frac{1}{2} + \frac{1}{e^\xi - 1} \right] \\ &= 9Nk_B \Theta_D \left[\frac{1}{8} + \left(\frac{T}{\Theta_D} \right)^3 \int_0^{\Theta_D/T} d\xi \xi^3 \frac{1}{e^\xi - 1} \right], \end{aligned} \tag{7.32}$$

and the specific heat at constant volume becomes

$$C = 9Nk_B \left(\frac{T}{\Theta_D} \right)^3 \int_0^{\Theta_D/T} e^\xi \frac{\xi^4 d\xi}{(e^\xi - 1)^2}. \tag{7.33}$$

[d]In D dimensions, $\bar{c} = [D/((D-1)/c_T^D + 1/c_L^D]^{1/D}$ and $r_0 = 2\pi\bar{c}/\omega_D = ((D/S_D)(V/N))^{1/3}$ where $S_D = 2\pi^{D/2}/\Gamma(D/2)$ is the surface of a D-dimensional sphere, so that $U \xrightarrow[T \to 0]{} N\omega_D{}^D T^{D+1} D\Gamma(D+1)\zeta(D+1) = VS_D(2\pi\bar{c})^{-D} T^{D+1}\Gamma(D+1)\zeta(D+1)$ per mode.

Using the well-known integral $\int_0^\infty d\xi \xi^D \frac{1}{e^\xi - 1} = \Gamma(D+1)\zeta(D+1)$ and $\zeta(4) = \pi^4/90$, the low temperature behaviour of U and C is seen to follow the well-known T^4 and T^3 laws, respectively

$$U \xrightarrow[T \ll \Theta_D]{} 9Nk_B\Theta_D\left(\frac{1}{8} + \frac{1}{15}\pi^4(T/\Theta_D)^4\right), \quad C \xrightarrow[T \ll \Theta_D]{} 9Nk_B\frac{4}{15}\pi^4(T/\Theta_D)^3. \tag{7.34a}$$

For high temperature, they tend to the classical limits

$$U \xrightarrow[T \gg \Theta_D]{} U^{\mathrm{cl}} = 3Nk_BT, \qquad C \xrightarrow[T \gg \Theta_D]{} C^{\mathrm{cl}} = 3Nk_B. \tag{7.34b}$$

This limit is in agreement with the *law of Dulong-Petit* according to which a classical harmonic system has a specific heat of $Nk_B/2$ for each degree of freedom, where kinetic and potential degrees are counted separately ($C = (3+3)Nk_B/2$). Using the Avogadro number of 6.022×10^{23} atoms per mole this amounts to a specific heat of

$$C = 5.96\frac{\mathrm{cal}}{\mathrm{K}} \times \text{number of moles.}$$

The ratio C/C^{cl} varies with temperature as a universal function of T/Θ_D which is plotted in Fig. 7.4.

In real materials, this universality is violated for increasing temperatures as a consequence of the anisotropy and anharmonicity of the crystal and the temperature dependence of the sound velocities which were neglected in the above derivation. It is customary to display the violations by fitting C to Debye's formula while allowing Θ_D to be a function of temperature, $\Theta_D(T)$. The deviations of $\Theta_D(T)/\Theta_D(0)$ from unity can be of the order of 10% (see Fig. 7.5).

After this interlude, it is now easy to find the relation between the parameter $\tilde{L}$ of (7.5a) and the Lindemann parameter L of (7.5b). We simply combine (7.30b), (7.29b) and find the Debye frequency

$$\omega_D = 2\pi\hbar\left(\frac{3\rho}{4\pi M}\right)^{1/3}\left(3\Big/\left(\frac{2}{c_T^3} + \frac{1}{c_L^3}\right)\right)^{1/3} = 2\pi\hbar\left(\frac{3\rho}{4\pi M}\right)^{1/3} c_T \frac{1}{(1 - \frac{1}{3}(1-r))^{1/3}}, \tag{7.35}$$

FIG. 7.4. The specific heat C_V (for constant volume) divided by the classical Dulong-Petit value $C_V^{\mathrm{cl}} = 3Nk_B$, for various materials with different Debye temperatures as compared to the universal Debye curve.

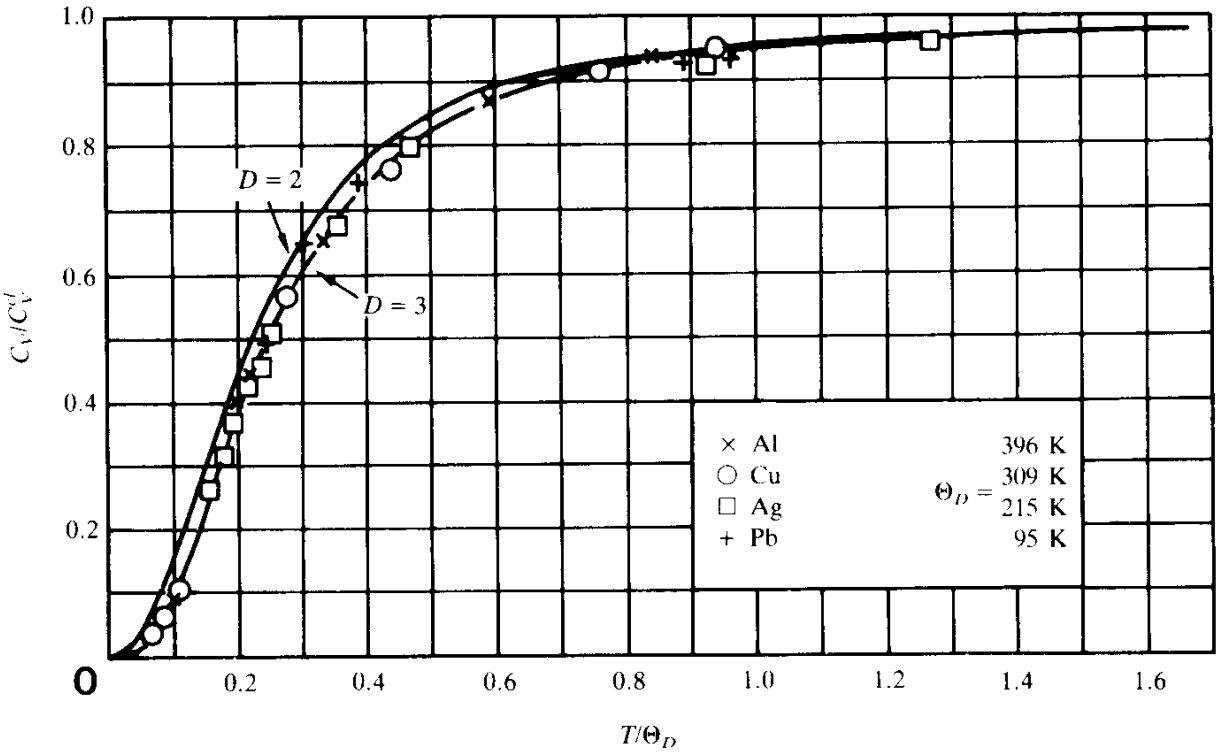

FIG. 7.5. The variation of the Debye temperature Θ_D with temperature necessary to achieve a perfect fit of the universal function (7.33) to the specific heat data of various materials.

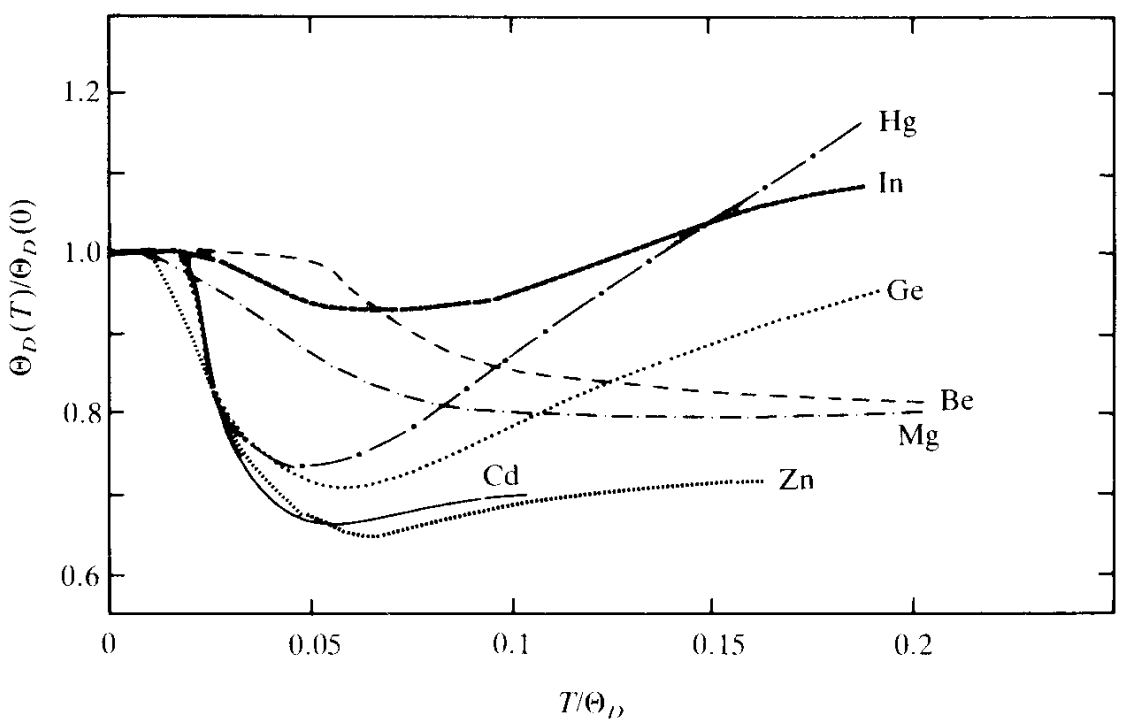

where M is the mass per unit cell and the ratio

$$r \equiv \frac{c_T^3}{c_L^3} \tag{7.36}$$

is a number which lies between 0 and 3/4. It is related to the Poisson ratio [see (1.40), $\nu \in (-1, 1/2)$] via

$$r = \frac{1/2 - \nu}{1 - \nu}, \qquad \nu = \frac{1/2 - r}{1 - r}. \tag{7.37}$$

Inserting (7.37) into (7.35) and (7.5b) we see that the Lindemann number is indeed proportional to $\sqrt{\mu a^3/T_{\text{melt}}}$. Before doing this however it is useful to rewrite (7.5b) in a slightly different form involving proper dimensional quantities:

$$L = \frac{\Theta_D}{\mathrm{K}}\left(\frac{A\,g}{\rho\,\mathrm{cm}^3}\right)^{1/3}\left(\frac{A}{T_{\text{melt}}/\mathrm{K}}\right)^{1/2}. \tag{7.38}$$

Using the fact that the mass per unit cell is $M = Am_p$ where $m_p = 1.6762 \times 10^{-24}\,\mathrm{gm}$ is the proton mass, this may then be reexpressed in the form

$$L = \left(\frac{m_p}{g}\right)^{-5/6} \frac{1}{\mathrm{cm}}\frac{1}{g^{1/2}}\frac{\hbar}{\sqrt{k_B \cdot \mathrm{K}}}\bar{L} = 5.84 \times \bar{L}, \tag{7.39}$$

where $\bar{L}$, which will be referred to as the modified Lindemann number, has the form

$$\bar{L} = \Theta_D k_B \left(\frac{1}{\hbar^2} a^2 M\right)^{1/2}\left(\frac{1}{k_B T_{\text{melt}}}\right)^{1/2} = (6\pi^2)^{1/3}\sqrt{\frac{\mu a^3}{k_B T_{\text{melt}}}}\,\frac{1}{\sqrt[3]{1 - \frac{1}{3}(1 - r)}}$$

$$= \bar{L}\,[6\pi^2/(1 - \tfrac{1}{3}(1 - r)]^{1/3} \tag{7.40}$$

Thus we arrive at the desired relation between $\bar{L}$ of (7.5a) and the Lindemann number L of (7.5b), (7.38):

$$L = 22.8(1 - \tfrac{1}{3}(1 - r))^{-1/3}\,\bar{L}. \tag{7.41}$$

Some experimental numbers for L are shown in Table 7.2 and we see that L ranges between 100 and 180 for materials of completely different hardness. As an example we may compare silver and beryllium which have

$$\rho = \begin{pmatrix} 10.4 \\ 1.87 \end{pmatrix} \frac{\text{g}}{\text{cm}^3}, \qquad \mu = \begin{pmatrix} 2.7 \\ 14.7 \end{pmatrix} \times 10^{11}\,\text{dyne cm}^{-2},$$

$$c_T = \begin{pmatrix} 1.61 \\ 8.88 \end{pmatrix} \times 10^5 \frac{\text{cm}}{\text{sec}}, \qquad c_L = \begin{pmatrix} 3.65 \\ 12.89 \end{pmatrix} \times 10^5 \frac{\text{cm}}{\text{sec}},$$

$$\nu = \begin{pmatrix} 0.38 \\ 0.05 \end{pmatrix}, \qquad T_{\text{melt}} = \begin{pmatrix} 1235 \\ 1558.1 \end{pmatrix} \text{K}. \tag{7.42}$$

In spite of the differences, their Lindemann numbers are almost the same: $L = \begin{pmatrix} 148 \\ 150 \end{pmatrix}$, $\bar{L} \sim \begin{pmatrix} 25 \\ 26 \end{pmatrix}$, $\bar{L} \sim \begin{pmatrix} 5.8 \\ 6.1 \end{pmatrix}$.

In general anisotropic media the Debye theory is quite complicated. Usually, however, the samples are polycrystalline, and sound propagates isotropically on the average. Then formula (7.15) can be applied again but with μ and κ in $\lambda = \kappa - \frac{2}{3}\mu$ replaced by the following averages of the elastic constants:

$$\bar{\mu} = \frac{1}{15}(c_{11} + c_{22} + c_{33} - c_{12} - c_{23} - c_{13}) + \frac{1}{5}(c_{44} + c_{55} + c_{66}),$$

$$\bar{\kappa} = \frac{1}{9}(c_{11} + c_{22} + c_{32}) + \frac{2}{9}(c_{12} + c_{23} + c_{13}). \tag{7.43}$$

This is derived in the classic book on elasticity by Voigt (referred to at the end of Chapter 1). For cubic materials one has simply

$$\bar{\mu} = \frac{1}{5}(c_{11} - c_{12} + 3c_{44}) = \frac{\mu}{5}(3 + 2\xi),$$

$$\bar{\kappa} = \frac{1}{3}(c_{11} + 2c_{12}) = c_{12} + \frac{1}{3}(c_{11} - c_{12}) = \lambda + \frac{2}{3}\mu\xi. \tag{7.44}$$

Let us translate the Lindemann number back to the physical quantity $\langle u_i^2 \rangle$ at the melting point. According to (7.41) we have $L \sim 150$, which corresponds to $\bar{L} \sim 25$, $\bar{L} \sim 6$ so that (7.3) leads to the estimate

$$\sqrt{\frac{\langle \mathbf{u}^2 \rangle}{3a^2}} \sim \frac{1}{\sqrt{6}} \frac{1}{\bar{L}} \sim 7\% \quad \text{(no sum in } i\text{)}. \tag{7.45}$$

This is an important observation: The melting process occurs when the displacements of the atoms are still very small compared to the distance between neighbors. For such small displacements the movement of the atoms can be considered nearly harmonic. The breakdown of crystalline order occurs all of a sudden, before the atoms invade deeply into the nonlinear regime of the interatomic potential. It is a strongly cooperative phenomenon. This fact will be essential when we comes to formulating our defect theory of melting in the next chapter.

7.4. QUANTUM CORRECTIONS TO THE LINDEMANN PARAMETER

If we include quantum effects, the atomic displacements are given by

$$\begin{aligned} \langle u_i(\mathbf{0})\, u_j(\mathbf{0}) \rangle &= \frac{k_B T}{\rho} \sum_n \int \frac{d^3k}{(2\pi)^3} \\ &\quad \times \left[\frac{1}{\omega_n^2 + \omega_T^2(\mathbf{k})} \left(\delta_{ij} - \frac{k_i k_j}{\mathbf{k}^2} \right) + \frac{1}{\omega_n^2 + \omega_L^2(\mathbf{k})} \frac{k_i k_j}{\mathbf{k}^2} \right] \\ &= \delta_{ij} \frac{k_B T}{3\rho} \sum_n \int \frac{d^3k}{(2\pi)^3} \left[\frac{2}{\omega_n^2 + \omega_T^2(\mathbf{k})} + \frac{1}{\omega_n^2 + \omega_L^2(\mathbf{k})} \right], \end{aligned} \tag{7.46}$$

where $\omega_n = 2\pi n k_B T/\hbar$ are the Matsubara frequencies. Summing these up according to formula (6.261) of Part I gives

$$\begin{aligned} \langle u_i(\mathbf{0})\, u_j(\mathbf{0}) \rangle = \frac{\delta_{ij}}{3\rho} \int \frac{d^3k}{(2\pi)^3} \Bigg[& \frac{2}{\omega_T^2(\mathbf{k})} \hbar \omega_T(\mathbf{k}) \left(\frac{1}{2} + \frac{1}{e^{\hbar \omega_T(\mathbf{k})/k_B T} - 1} \right) \\ & + \frac{1}{\omega_L^2(\mathbf{k})} \hbar \omega_L(\mathbf{k}) \left(\frac{1}{2} + \frac{1}{e^{\hbar \omega_L(\mathbf{k})/k_B T} - 1} \right) \Bigg]. \end{aligned} \tag{7.47}$$

This can be written as

$$\langle u_i(\mathbf{0})\, u_j(\mathbf{0}) \rangle = \delta_{ij} \frac{1}{3\rho} \int \frac{d^3k}{(2\pi)^3} \sum_h \frac{1}{\omega_h^2(\mathbf{k})} u_h(\mathbf{k}), \tag{7.48}$$

where h runs over the three polarizations and $u_h(\mathbf{k})$ is the average energy of a single harmonic mode of momentum $\mathbf{k}$.

In fact, this formula could have been written down directly. It is a consequence of the equipartition theorem. On the average, the energy for these modes is (no sum over i)

$$\overline{\frac{M}{2}|\dot{u}(\mathbf{k},\omega)|^2} = \frac{M}{2}\omega^2(\mathbf{k})\,\overline{|u_i(\mathbf{k},\omega)|^2} = \frac{1}{2}\bar{E}(\mathbf{k}) = \frac{1}{2}\hbar\,\omega(\mathbf{k})\left(\frac{1}{2}+\bar{n}(\mathbf{k})\right), \tag{7.49}$$

where $\bar{n}$ is the average number of quanta $1/(e^{\hbar\omega/k_BT}-1)$. At the level of the Debye theory we can replace $\sum_{\mathbf{k}} = V\int(d^3k/(2\pi)^3)$,

$$V\int_0^{\omega_D^{(h)}} d\omega\, g^{(h)}(\omega) = 3N\int_0^{\omega_D^{(h)}} d\omega\,\frac{\omega^2}{\omega_D^{(h)3}}$$

and find

$$\langle u_i(\mathbf{0})\,u_j(\mathbf{0})\rangle = \delta_{ij}\sum_h \frac{1}{M\omega_D^{(h)3}}\int_0^{\omega_D^{(h)}} d\omega\,\hbar\omega\left(\frac{1}{2}+\frac{1}{e^{\hbar\omega/k_BT}-1}\right), \tag{7.50}$$

where M is the mass of the atoms. Changing the variable of integration to ξ of (7.32) gives

$$\begin{aligned}\langle u_i(\mathbf{0})\,u_j(\mathbf{0})\rangle &= \delta_{ij}\sum_h \frac{\hbar}{M\omega_D^{(h)3}}\left(\frac{k_BT}{\hbar}\right)^2\int_0^{\Theta_D^{(h)}/T} d\xi\,\xi\left(\frac{1}{2}+\frac{1}{e^{\xi}-1}\right)\\ &= \delta_{ij}\sum_h \frac{\hbar^2}{4Mk_B\Theta_D^{(h)}}\left[1+4\left(\frac{T}{\Theta_D^{(h)}}\right)^2\int_0^{\Theta_D^{(h)}/T} d\xi\,\xi\frac{1}{e^{\xi}-1}\right].\end{aligned} \tag{7.51}$$

The ratio of $\sqrt{\frac{1}{3}\langle\sum_i u_i^2(\mathbf{0})\rangle}$ to the cell size $a=(V/N)^{1/3}=v^{1/3}$ is given by

$$\delta \equiv \frac{\sqrt{\frac{1}{3}\left\langle\sum_i u_i^2(\mathbf{0})\right\rangle}}{a} = \left[\frac{1}{4}\frac{\hbar^2}{Ma^2}\sum_h\frac{1}{k_B\Theta_D^{(h)}}\left[1+4\left(\frac{T}{\Theta_D^{(h)}}\right)^2\int_0^{\Theta_D^{(h)}/T} d\xi\,\xi\frac{1}{e^{\xi}-1}\right]\right]^{1/2}. \tag{7.52}$$

Using the modified Lindemann number $\bar{L}$ of (7.40), this ratio may be written as

$$\delta = \frac{1}{2}\frac{1}{\bar{L}}\sqrt{\frac{\Theta_D^2}{T_{\text{melt}}}\sum_h \frac{1}{\Theta_D^{(h)}} w(T/\Theta_D^{(h)})}, \tag{7.53}$$

where

$$w(\tau) = 1 + 4\tau^2 \int_0^{1/\tau} d\xi \xi \frac{1}{e^\xi - 1} = 1 + 4\frac{\pi^2}{6}\tau^2 + \ldots \tag{7.54}$$

This function is plotted in Fig. 7.6. For high temperatures, it grows linearly with τ, i.e.,

$$w(\tau) \underset{\tau \gg 1}{=} 4\tau + \frac{1}{9\tau} + \frac{1}{900\tau^3} \ldots$$

FIG. 7.6. The function which rules the temperature dependence of the mean square displacement $\langle \mathbf{u}^2 \rangle$ within the Debye approximation [see Eq. (7.53)]

$$\frac{1}{3}\frac{\langle \mathbf{u}^2 \rangle}{a^2} = \frac{1}{4\bar{L}^2}\frac{\Theta_D^2}{T_{\text{melt}}}\sum_h \frac{w(T/\Theta^{(h)})}{\Theta_D^{(h)}}.$$

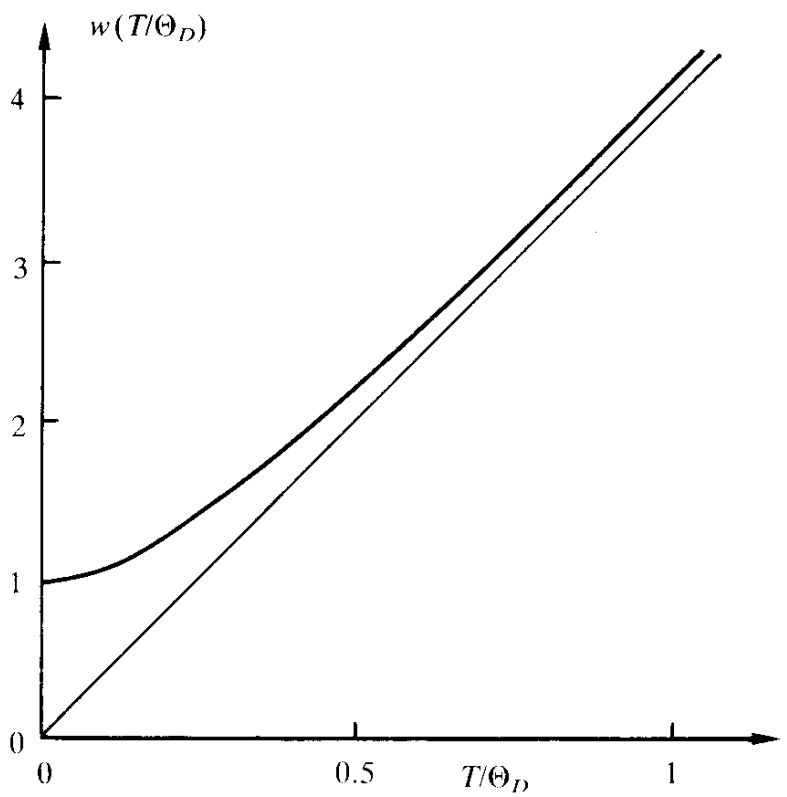

Thus, if the melting temperature lies far above the Debye temperature, which is usually the case (classical melting), then

$$\delta_{\rm cl} \sim \frac{\sqrt{3}}{\bar{L}} \left[\frac{T}{T_{\rm melt}} \left(\frac{1}{3} \sum_h \frac{\Theta_D^2}{\Theta_D^{(h)2}} \right) \right]^{1/2}, \tag{7.55}$$

which of the order of 7% at $T = T_{\rm melt}$ (for $\bar{L} \sim 25$).

In general, $\omega(T/\Theta_D)$ lies above T/Θ_D, due to quantum fluctuations. These are seen in pure form at zero temperature for which

$$\delta \underset{T=0}{=} \frac{1}{2} \frac{\sqrt{3}}{\bar{L}} \sqrt{\frac{\Theta_D}{T_{\rm melt}}} \sqrt{\frac{1}{3} \sum_h \frac{\Theta_D}{\Theta_D^{(h)}}}. \tag{7.56}$$

The classical value (7.55) can be checked by calculating [more accurately than in the estimate (7.3)] from (1.77)

$$\begin{aligned} \langle u_i(\mathbf{0}) u_j(\mathbf{0}) \rangle &= k_B T \int \frac{d^3k}{(2\pi)^3} \left[\frac{1}{\mu \mathbf{k}^2} \left(\delta_{ij} - \frac{k_i k_j}{\mathbf{k}^2} \right) + \frac{1}{\lambda + 2\mu} \frac{k_i k_j}{\mathbf{k}^4} \right] \\ &= \delta_{ij} \frac{k_B T}{3} \int \frac{d^3k}{(2\pi)^3} \left(\frac{2}{\mu \mathbf{k}^2} + \frac{1}{(\lambda + 2\mu)\mathbf{k}^2} \right). \end{aligned}$$

Using the frequency distribution $g^{(h)}(\omega)$ of (7.28a), this becomes

$$\begin{aligned} \langle u_i(\mathbf{0}) u_j(\mathbf{0}) \rangle &= \delta_{ij} \frac{k_B T}{V/N} \left[\sum_{h=\pm 1} \int_0^{\omega_D^{(h)}} d\omega \frac{\omega^2}{\omega_D^{(h)3}} \frac{c_T^2}{\mu \omega^2} + \int_0^{\omega_D^{(0)}} d\omega \frac{\omega^2}{\omega_D^{(0)3}} \frac{c_L^2}{(\lambda + 2\mu)\omega^2} \right] \\ &= \delta_{ij} \frac{k_B T}{M} \sum_h \int_0^{\omega_D^{(h)}} d\omega \frac{\omega^2}{\omega_D^{(h)3}} \frac{1}{\omega^2}. \end{aligned}$$

It follows that

$$\langle u_i(\mathbf{0}) u_j(\mathbf{0}) \rangle = \delta_{ij} \frac{k_B T}{M} \sum_h \frac{1}{\omega_D^{(h)2}}, \tag{7.57}$$

which implies

$$\delta_{\rm cl} = \sqrt{3} \frac{1}{\bar{L}} \left[\frac{T}{T_{\rm melt}} \frac{1}{3} \sum_h \frac{\Theta_D^2}{\Theta_D^{(h)2}} \right]^{1/2} \tag{7.58}$$

as in (7.55).

Some values for δ_{cl} at the melting point are given in Table 7.4. Actually, this table does not quite show the same δ as defined here but $\delta_{table} = \sqrt{\langle \frac{1}{3}\Sigma u_i^2 \rangle}/d$ where d is the nearest neighbour distance. In b.c.c. and f.c.c. lattices, d is given by $d=(a_0/2)\sqrt{3}=v^{1/3}(3^{1/2}/2^{2/3}) \sim v^{1/3}\times 1.09$, $d = a_0/\sqrt{2} = v^{1/3}(4^{1/3}/\sqrt{2}) \sim v^{1/3} \times 1.122$, respectively, where a_0 is the lattice spacing (so that $a^3 = v = a_0^3/2$)[e]. The second to last column is calculated from $\bar{L}$ of Eq. (7.40) and the purely classical approximation (7.58). The last column comes from a more elaborate numerical evaluation of (7.47) using a realistic $\omega_h(\mathbf{k})$. It does not assume crystal isotropy but respects the proper b.c.c. and f.c.c. symmetries (while restricting itself to central forces between the nearest and next neighbours, thus satisfying the Cauchy relations, i.e., $c_{12} = c_{44}$). We see that for each of the two groups of b.c.c. and f.c.c. crystals, the relative amplitude of the melting point is indeed quite universal, with $\delta_{table} = \sqrt{\langle \frac{1}{3}\Sigma_i u_i^2 \rangle}/d$ ranging from 0.11–0.46 for b.c.c. and 0.065–0.077 for f.c.c. symmetries. The strongest quantum effect in the table occurs for Li for which the result of a purely classical calculation would be 0.067 rather than 0.116.

Accepting the universality of the Lindemann number also for the quantum regime we are led to conclude from (7.56) that a crystal at zero temperature whose Lindemann number $\bar{L}$ when evaluated with T_{melt} replace by $\Theta_D/4$ [i.e., the number $2(v^{2/3}M/\hbar^2)^{1/2}(k_B\Theta_D)^{1/2}$] becomes smaller than 25 will melt. This is the case for ^{3}He and ^{4}He, which are solid only for pressures of more than 30 bar. There the sound velocities are of the order of[f]

$$c \sim 300 \frac{\text{m}}{\text{sec}} \sim 23\,\text{K}\text{Å}\frac{k_B}{\hbar}.$$

At a molar volume of $vN_{Avogadro} \approx 21\,\text{cm}^3$ ($v \approx 3.27\,\text{Å}$) this implies

$$\Theta_D \sim \frac{\hbar}{k_B}\sqrt{6\pi}c/v^{1/3} \sim 30.5\,\text{K} \tag{7.59}$$

so that the Lindemann number $\bar{L}$, for $T_{melt} \to \Theta_D/4$, becomes

$$\bar{L}|_{T_{melt}\to\Theta_D/4} = 2\sqrt{v^{2/3}Mk_B\Theta_D/\hbar^2} \approx 10. \tag{7.60}$$

[e]See the Appendix.

[f]More accurately, $c_{11}/\rho = 400\,\text{m/sec}$, $c_{44}/\rho = 337\,\text{m/sec}$, $c_{12}/\rho = 362\,\text{m/sec}$ (see the Notes and References for sources).

TABLE 7.3. Various material parameters associated with nonlinear elasticity (after A. Eucken, *Lehrbuch der Physikalischen Chemie* (Akad. Verlagsges., Leipzig, 1944) p. 675.

	coeff. of vol. expansion $\alpha \cdot 10^6$ [K^{-1}]	Grüneisen constant $\gamma = \frac{\alpha V \kappa}{C_V}$	compressibility k^{-1} [10^{12} $dyne^{-1}$ cm^2]	spec. heat per mole $c\ N_{Avog}$ [erg/(K · mole)]	molar volume $a^3 N_{Avog}$ [cm^3/mole]
Na	216	1.25	15.8	26.0	23.7
K	250	1.34	33	25.8	45.5
Cu	49.2	1.96	0.75	23.7	7.1
Ag	57	2.40	1.01	24.2	10.3
Al	67.8	2.17	1.37	22.8	10.0
C	2.9	1.10	0.16	5.66	3.42
Fe	33.6	1.60	0.6	24.8	8.1
Pt	26.7	2.54	0.38	24.5	9.2
NaCl	121	1.61	4.2	48.3	27.1
KCl	114	1.54	5.6	49.7	37.5
KBr	126	1.68	6.7	48.4	43.3
KJ	128	2.12	8.6	48.7	53.2

TABLE 7.4. The relative displacements $\delta = \sqrt{\frac{1}{3}\frac{\Sigma\langle u_i\rangle^2}{d^2}}$ calculated in two different ways (after Shaptro, cited in the Notes and References).

b.c.c.	L	T_m/Θ_D	δ_{melt} from L (classical)	δ_{melt} from latt. dyn. w. qu. corr.
Li	124	1.08	0.067	0.116
Na	114	2.47	0.073	0.111
K	122	3.36	0.068	0.112
Rb	118	5.20	0.070	0.115
Cs	118	6.70	0.070	0.111

b.c.c.	L	T_m/Θ_D	δ_{melt} from L (classical)	δ_{melt} from latt. dyn. w. qu. corr.
Al	138	2.42	0.072	0.072
Cu	143	4.38	0.058	0.068
Ag	148	5.61	0.056	0.071
Au	137	7.43	0.060	0.073
Pb	149	7.07	0.056	0.065
Ni	143	3.93	0.058	0.077

FIG. 7.7. The temperature dependence of the specific heats of molten metals at fixed volume (after Grimwall, *op. cit.* in the Notes and References).

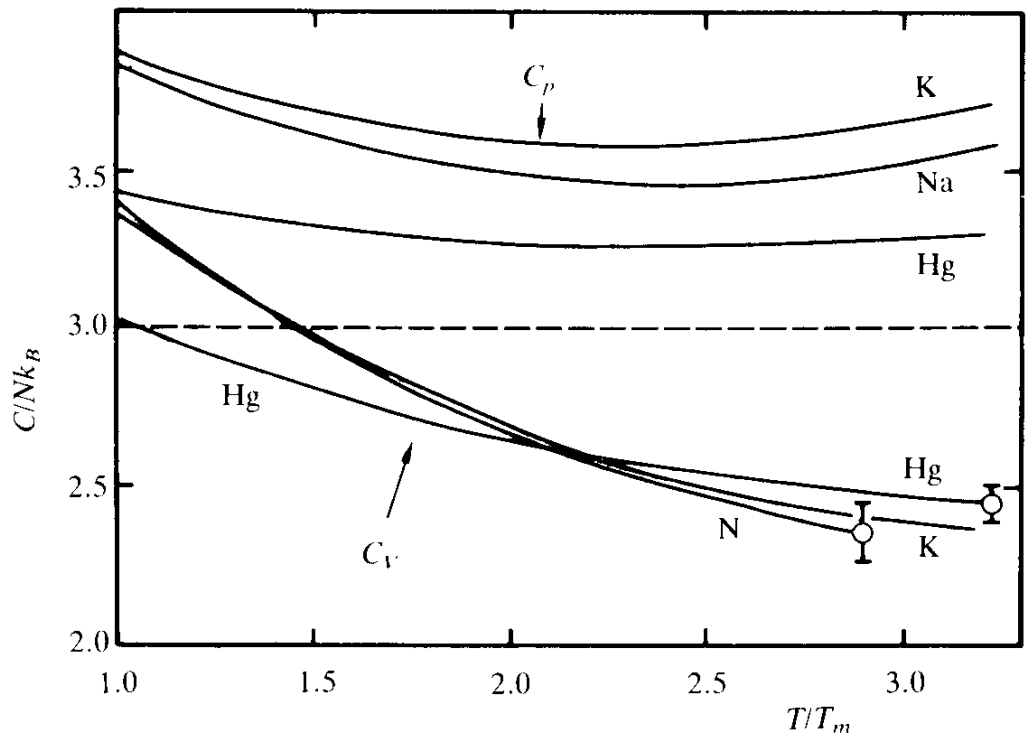

This is indeed smaller than the average number $\bar{L} \sim 25$ so that the zero-point fluctuations in solid ^{4}He exceed the Lindemann size. This is why the crystal exhibits melting into a quantum liquid at zero temperature, if pressure decreases below 30 bar.

Notice that the Lindemann criterium can be verified directly, at least in principle, by looking at the decrease of the Bragg intensities with temperature. The scattering cross section for X rays[g] is governed by the dynamic structure factor $S(\mathbf{q}, \omega)$ where

$$S(\mathbf{q}, \omega) = \int_{-\infty}^{\infty} \frac{dt}{2\pi} e^{i\omega t} \sum_n e^{-i\mathbf{q}\cdot\mathbf{x}_n} \left\langle e^{iq_i u_i(\mathbf{x}_n, t)} e^{-iq_i u_i(\mathbf{0}, 0)} \right\rangle. \tag{7.61}$$

In the harmonic approximation, this can be calculated, giving

$$S(\mathbf{q}, \omega) = e^{-2W} \int_{-\infty}^{\infty} \frac{dt}{2\pi} e^{i\omega t} \sum_n e^{-i\mathbf{q}\cdot\mathbf{x}_n} e^{\langle q_i u_i(\mathbf{x}_n, t) q_j u_j(\mathbf{0}, 0)\rangle}, \tag{7.62}$$

[g]The differential cross section per solid angle $d\Omega$ and energy interval dE is

$$\frac{d\sigma}{d\Omega\, dE} = N \frac{\sigma}{4\pi} \frac{p'}{p} \frac{1}{\hbar} S(\mathbf{q}, \omega),$$

where σ is the individual cross section for each atom in the lattice.

where

$$2W \equiv \langle (q_i u_i(\mathbf{0}, 0)^2 \rangle \tag{7.63}$$

is the so-called *Debye-Waller factor*. Expanding the last exponential in (7.62) into a power series, the sum over n can be analyzed according to a purely elastic contribution which carries a $\delta(\omega)$ function, due to energy conservation,

$$S_{\mathrm{el}}(\mathbf{q}, \omega) = e^{-2W} \delta(\omega) N \sum_{\mathbf{c}} \delta_{\mathbf{q},\mathbf{c}}, \tag{7.64}$$

where $\mathbf{c}$ are the reciprocal lattice vectors plus multi-phonon contributions. The elastic contribution gives the sharp peak seen in Bragg scattering. Its intensity has a temperature dependence, e^{-2W}. For isotropic systems

$$2W = \mathbf{q}^2 \frac{\langle \mathbf{u}^2 \rangle}{3}. \tag{7.65a}$$

If θ is the Bragg angle, then $\mathbf{q}^2 = 4 \sin^2 \theta \, (4\pi^2/\lambda^2)$, where λ is the wavelength of the light and

$$\begin{aligned} 2W &= \sin^2 \theta \, \frac{4\pi^2}{\lambda^2} \frac{\hbar^2}{M} \sum_h \frac{1}{k_B \Theta_D^{(h)}} W(T/\Theta_D^{(h)}) \\ &= \sin^2 \theta \, \frac{4\pi^2}{\lambda^2} a^2 \, 4\delta^2. \end{aligned} \tag{7.65b}$$

Thus, in Bragg scattering, one can directly observe the temperature behaviour of δ^2 (7.53). If the Lindemann criterion is right, all crystals melt when the Debye-Waller factor has reached the same size $e^{-2W_{\mathrm{melt}}}$ which depends only on the crystal structure.

7.5. CLASSICAL MELTING

When comparing the melting temperature T_{melt} with the Debye temperature Θ_D we realize that for most materials T_{melt} lies far above Θ_D (see Table 7.4). There are only a very few exceptions to this, one being

the quantum crystal of solid ^{4}He. Thus, in general, the melting process takes place in a region where all Debye expressions have approached their classical limit. In particular, the internal energy has approached the linear behavior (7.34b) and the specific heat, a constant (Dulong-Petit law). From (7.21) we see that for high temperatures, the partition function is dominated by the classical expression

$$Z_{\mathrm{cl}} = \prod_{\mathbf{k}} e^{-2\log(\hbar\omega_T(\mathbf{k})/k_BT) - \log(\hbar\omega_L(\mathbf{k})/k_BT)} \tag{7.66}$$

This, in turn, arises from the full partition function (7.20) if one uses only *one* infinitesimal τ interval in which the only Matsubara frequency is $\Omega_m = 0$.

In the path integral (7.13), we arrive at the same limit by noticing that for high temperatures, the τ interval is so small that $u(\mathbf{x}, \tau)$ has "no time" to vary and the time-dependent fluctuations are completely frozen out. One may therefore forget the infinitesimal time slicing and keep only the initial and final times $\tau_0 = 0$, $\tau_1 = \hbar/k_BT$, setting $\varepsilon = \hbar/k_BT$. Since $u(\mathbf{x}, \tau)$ is periodic in this interval, $u(\mathbf{x}, \tau_0) = u(\mathbf{x}, \tau_1)$, the kinetic term in the exponent of (7.13) disappears and the partition function reduces to the classical limit,

$$Z \to Z_{\mathrm{cl}} = \left(\sqrt{\frac{k_BTa^5\rho}{2\pi\hbar^2}}\right)^{3N} \prod_{\mathbf{x},i}\left[\int_{-\infty}^{\infty} \frac{du_i(\mathbf{x})}{a}\right] e^{-(1/k_BT)E_{\mathrm{cl}}[u_{ij}]}, \tag{7.67}$$

where

$$E_{\mathrm{cl}}[u_{ij}] = a^3 \sum_{\mathbf{x}} \left[\mu u_{ij}^2 + \frac{\lambda}{2}\left(\sum_i u_{ii}\right)^2\right] \tag{7.68}$$

is the static elastic energy and u_{ij} are the lattice versions of the strain tensor, $u_{ij} = (\nabla_i u_j + \nabla_j u_i)/2a$. The prefactor

$$Z_{\mathrm{kin,cl}} = \left(\sqrt{\frac{k_BTa^5\rho}{2\pi\hbar^2}}\right)^{3N} \tag{7.69}$$

leads to a specific heat per atom of $(3/2)k_B$. It collects the three kinetic degrees of freedom of the harmonic oscillations. The second factor

$$Z_{\text{pot,cl}} = \prod_{\mathbf{x},i} \left[\int \frac{du_i(\mathbf{x})}{a} \right] e^{-(1/k_B T) E_{\text{cl}}[u_{ij}]} \tag{7.70}$$

accounts for the three potential degrees of freedom. Integrating out the $u_i(\mathbf{x})$ fields we obtain

$$Z_{\text{pot,cl}} = \prod_{\mathbf{k}} (\sqrt{2\pi k_B T})^3 \frac{1}{(\sqrt{a^3 \mu \bar{\mathbf{K}} \cdot \mathbf{K}})^2} \frac{1}{\sqrt{a^3 (2\mu + \lambda) \bar{\mathbf{K}} \cdot \mathbf{K}}} \tag{7.71}$$

Combining this with (7.69) we obtain again

$$Z_{\text{cl}} = Z_{\text{kin,cl}} Z_{\text{pot,cl}} = \prod_{\mathbf{k}} \left(\frac{k_B T}{\hbar \omega_T} \right)^2 \left(\frac{k_B T}{\hbar \omega_L} \right) \tag{7.72}$$

in agreement with the classical result (7.66).

7.6. LATTICE EXPANSION UP TO THE MELTING TRANSITION

Since the interatomic forces are anharmonic, the crystalline phonons are not independent of each other but are subject to interactions. This gives rise to some changes in the results derived up till now. Fortunately, apart from a few quantum crystals, melting occurs at very small displacements. Therefore, the anharmonic effects are quite small. They can be taken into account by a simple lattice expansion and renormalization of the elastic constant (softening). In order to see how this happens let us consider the elastic energy of the crystal up to the cubic terms in the strain tensor. In the isotropic case this may be parametrized as[h]

[h]Some authors (see the references at the end) employ the invariants

$$I_1 = \tfrac{1}{2} \varepsilon_{ijk} \varepsilon_{ijl} u_{kl} = u_{ll}, \quad I_2 = \tfrac{1}{2} \varepsilon_{ijk} \varepsilon_{ilm} u_{jl} u_{km} = \tfrac{1}{2} (u_{ll}^2 - u_{ij}^2),$$
$$I_3 = \tfrac{1}{6} \varepsilon_{ijk} \varepsilon_{lmn} u_{il} u_{jm} u_{kn} = \tfrac{1}{6} (u_{ll}^3 - 3 u_{ll} u_{ij}^2 + 2 u_{ij} u_{jk} u_{ki})$$

and they expand

$$e_{\text{cl}} = (1 - I_1)[-2\mu I_2 + (\lambda + 2\mu)/2 I_1^2] + (\ell I_1^3 + m I_1 I_2 + n I_3)$$

so that

$$c_1 = (\ell - (\lambda + 2\mu)/2) + (m/2 + \mu)/2 + n/6, \quad c_2 = [(m/2 + \mu) + n]/2, \quad c_3 = n/2.$$

The factor $(1 - I_1)$ in e_{cl} comes from the expansion

$$\det(\delta_{ij} - 2u_{ij})^{1/2} = (1 - 2I_1 + 4I_2 - 8I_3)^{1/2} = 1 - I_1 + \ldots$$

due to which the quadratic energy density, which is defined with respect to the invariant volume elements, receives a cubic correction when expressed in terms of the volume elements of the ideal reference lattice, which appears as $\int d^3x$ in the integral (7.73).

$$E_{\mathrm{el}} = \int d^3x\, e_{\mathrm{el}}$$
$$= \int d^3x \left(\mu_0 u_{ij}^2 + \frac{\lambda_0}{2} u_{\ell\ell}^2 \right) + \int d^3x (c_1 u_{\ell\ell}^3 + c_2 u_{\ell\ell} u_{ij}^2 + c_3 u_{ij} u_{jk} u_{ki}), \tag{7.73}$$

where μ_0, λ_0, c_1, c_2, c_3 will be called "bare elastic constants." The elastic partition function on the lattice is now [see (7.13)]

$$Z = \prod_{\mathbf{x},\tau_n,i} \left[\int \frac{du_i(\mathbf{x},\, \tau_n)}{\sqrt{2\pi\varepsilon\hbar/a^3\rho}} \right] \exp\left\{ -\frac{1}{\hbar} a^3 \varepsilon \sum_{\mathbf{x},\tau_n} \left[\frac{\rho}{\varepsilon} \frac{1}{\varepsilon^2} \quad (\nabla_\tau u_i(\mathbf{x},\, \tau_n))^2 + e_{\mathrm{el}} \right] \right\}, \tag{7.74}$$

with the classical limit [see (7.70)]

$$Z_{\mathrm{pot,cl}} = \prod_{\mathbf{x},i} \left[\int \frac{du_i(\mathbf{x})}{a} \right] e^{-E_{\mathrm{el}}/k_B T}, \tag{7.75}$$

apart from a prefactor $Z_{\mathrm{kin,cl}} = (\sqrt{k_B T a^5 \rho / 2\pi\hbar^2})^{3N}$ [see (7.72)].

In Chapter 5, Part I, we introduced the concept of an effective energy which allowed us to study a field theory in the presence of a non-zero field expectation value. Let us apply these methods to the present partition function. Since the cubic terms produce an asymmetry between positive and negative dilations, we expect the fluctuations to lead to a new minimum at a non-vanishing strain $\langle u_{ij} \rangle \equiv U_{ij}$. For symmetry reasons, only the diagonal elements can be non-zero and must be equal to each other. Hence, they are equal to 1/3 of the relative volume expansion:

$$\langle u_{ij} \rangle = U_{ij} \equiv \delta_{ij} \frac{1}{3} \Delta = \delta_{ij} \frac{1}{3} \frac{\Delta V}{V}. \tag{7.76}$$

According to the rules of Section 5.4, Part I, we can calculate the effective energy by inserting the field $u_{ij} = U_{ij} + \delta u_{ij} = \delta_{ij} \frac{1}{3} \Delta + \delta u_{ij}$ into the exponent, expanding it in powers of δu_{ij}, and summing over all one-particle irreducible vacuum graphs involving the propagator and the interactions of δu_{ij}. The resulting expression can then be minimized in Δ and yields the volume expansion due to fluctuations. The smallness of $|\delta u|$ ($\ll a$) permits us to consider only the one-loop correction which is quite

easy to calculate. With[1] $u_{ij} = \delta_{ij}(1/3)\Delta + \delta u_{ij}$, the elastic energy density becomes

$$\begin{aligned} e_{\rm el} &= e_0(\Delta) + \delta e_{\rm el} + \delta^2 e_{\rm el} \\ &= e_0(\Delta) + e_{\rm el}^{(1)}(\Delta)_{ij}\,\delta u_{ij} + \tfrac{1}{2} e_{\rm el}^{(2)}(\Delta)_{ijk\ell}\,\delta u_{ij}\,\delta u_{k\ell} + \ldots, \end{aligned} \tag{7.77}$$

where

$$e_0(\Delta) = \left[\frac{\mu_0}{3} + \frac{\lambda_0}{2} + \left(c_1 + \frac{c_2}{3} + \frac{c_3}{9}\right)\Delta\right]\Delta^2 = \left[\frac{1}{2}\kappa_0 + \left(c_1 + \frac{c_2}{3} + \frac{c_3}{9}\right)\Delta\right]\Delta^2 \tag{7.78}$$

is the elastic energy of the dilated solid and

$$\delta e_{\rm el} = \left[\kappa_0 + 3\left(c_1 + \frac{c_2}{3} + \frac{c_3}{9}\right)\Delta\right]\delta u_{\ell\ell} \tag{7.79}$$

describes the linear deviations while

$$\delta^2 e_{\rm el} = \mu_0\,\delta u_{ij}^2 + \frac{\lambda}{2}\,\delta u_{\ell\ell}^2 + (c_2 + c_3)\Delta\,\delta u_{ij}^2 + \left(3c_1 + \frac{2}{3}c_2\right)\Delta\,\delta u_{\ell\ell}^2 \tag{7.80}$$

the quadratic ones. These can be rewritten succinctly as

$$\delta^2 e_{\rm el} = \mu_0(\Delta)\,\delta u_{ij}^2 + \frac{\lambda_0(\Delta)}{2}\,\delta u_{\ell\ell}^2, \tag{7.81}$$

where μ, λ are the bare elastic constants in the dilated crystal:

$$\mu_0(\Delta) = \mu_0 + (c_2 + c_3)\Delta, \qquad \lambda_0(\Delta) = \lambda_0 + 2(3c_1 + \tfrac{2}{3}c_2)\Delta. \tag{7.82}$$

[1]Hence

$$\operatorname{tr} u = \Delta + \delta u_{\ell\ell}, \quad \operatorname{tr}(u^2) = \frac{\Delta^2}{3} + \frac{2}{3}\Delta\delta u_{\ell\ell} + (\delta u_{ij})^2,$$

$$\operatorname{tr}(u^3) = \frac{\Delta^3}{9} + \frac{\Delta^2}{3}\delta u_{\ell\ell} + \Delta\delta u_{ij}^2 + (\delta u)_{\ell\ell}^3,$$

$$\operatorname{tr}(u^4) = \frac{\Delta^4}{27} + \frac{4}{27}\Delta^3\delta u_{\ell\ell} + 2\frac{\Delta^2}{3}(\delta u_{ij})^2 + \frac{4}{3}\Delta(\delta u)_{\ell\ell}^3 + (\delta u)_{\ell\ell}^4.$$

The bare modulus of compression defined by

$$\frac{d^2 e_0(\Delta)}{d\Delta^2} = \kappa_0(\Delta) \tag{7.83}$$

consists of the usual combinations,

$$\kappa_0(\Delta) = \frac{2}{3}\mu_0(\Delta) + \lambda_0(\Delta) = \kappa_0 + 6\left(c_1 + \frac{c_2}{3} + \frac{c_3}{9}\right)\Delta. \tag{7.84}$$

The anharmonic constants c_1, c_2, c_3 depend on the volume expansion and are experimentally accessible via the dependence of the sound velocity upon changes of the volume. What one can easily measure are the so-called *Grüneisen constants*,

$$\begin{aligned}
\gamma_{0T} &= -\frac{1}{c_{0T}}\frac{\partial c_{0T}(\Delta)}{\partial\Delta}\bigg|_{\Delta=0} \equiv -\frac{1}{2}\frac{1}{\mu_0}\frac{\partial}{\partial\Delta}\mu_0(\Delta)\bigg|_{\Delta=0} = -\frac{1}{\mu_0}\frac{1}{2}(c_2 + c_3), \\
\gamma_{0L} &= -\frac{1}{c_{0L}}\frac{\partial c_{0L}(\Delta)}{\partial\Delta}\bigg|_{\Delta=0} = -\frac{1}{2}\frac{1}{(2\mu_0 + \lambda_0)}\frac{\partial}{\partial\Delta}(2\mu_0 + \lambda_0)(\Delta)\bigg|_{\Delta=0} \\
&= -\frac{1}{(2\mu_0 + \lambda_0)}\frac{1}{2}\left(6c_1 + \frac{10}{3}c_2 + 2c_3\right).
\end{aligned} \tag{7.85}$$

With (7.81), we can now easily calculate one-loop fluctuation corrected effective potential [see Section 5.3, Part I] of the crystal, associated with the classical partition $Z_{\text{pot.cl}}$, which is equal to the free energy density of the anharmonic crystal:

$$\begin{aligned}
v_{\text{pot.cl}}(\Delta) = \frac{1}{V}\Gamma_{\text{pot.cl}}[\Delta] = e_0(\Delta) + \frac{k_B T}{2}\int\frac{d^3k}{(2\pi)^3}\Big\{2\log[\mu_0(\Delta)\,\bar{\mathbf{K}}\cdot\mathbf{K}] \\
+ \log[(2\mu_0(\Delta) + \lambda_0(\Delta))\,\bar{\mathbf{K}}\cdot\mathbf{K}]\Big\} + \frac{3}{2}\log(2\pi T/a^5).
\end{aligned} \tag{7.86}$$

To lowest order in Δ, we can replace $\mu_0(\Delta)$, $2\mu_0(\Delta) + \lambda_0(\Delta)$ by the full fluctuation corrected values μ, $2\mu + \lambda$. Including the prefactors of Z_{cl} [recall (7.67)], this gives

$$v_{\rm cl}(\Delta) = \frac{1}{V}\Gamma_{\rm cl}[\Delta] = e_0(\Delta) + \frac{k_B T}{2}\int \frac{d^3k}{(2\pi)^3}\left[2\log\left(\frac{\hbar c_T K}{k_B T}\right) + \log\left(\frac{\hbar c_L K}{k_B T}\right)\right], \tag{7.87}$$

where $K \equiv \sqrt{\bar{\mathbf{K}}\cdot\mathbf{K}/a^2}$ is the lattice version of $|\mathbf{k}|$ and

$$c_T \equiv c_T(\Delta) = \frac{\mu}{\rho}, \qquad c_L \equiv c_L(\Delta) = \frac{2\mu + \lambda}{\rho} \tag{7.88}$$

are now the properly renormalized sound velocities of the softened crystal. Apart from $e_0(\Delta)$, this energy coincides with the expression for the classical partition function (7.71) except that now

$$\omega_T(\mathbf{k}) = c_T K, \qquad \omega_L(\mathbf{k}) = c_L K \tag{7.89}$$

are the volume dependent frequencies of the sound waves of wave vector $\mathbf{k}$ extrapolated linearly to zero temperature.

If we now minimize $v_{\rm cl}(\Delta)$ with respect to the volume dilations we find, using

$$\int \frac{d^3k}{(2\pi)^3} = \frac{1}{a^3}\int \frac{d^3k a^3}{(2\pi)^3} = \frac{1}{a^3}, \tag{7.90}$$

a^3 being the volume per unit cell,

$$\kappa_0(\Delta)\Delta - (2\gamma_{0T} + \gamma_{0L})\frac{k_B T}{a^3} = 0. \tag{7.91}$$

To lowest order in T (which is really the only reliable order at the one-loop level), this amounts to

$$\Delta = \frac{1}{a^3\kappa_0}(2\gamma_{0T} + \gamma_{0L})\, k_B T + O(T^2) \tag{7.92}$$

The factor in front of T is the *thermal expansion coefficient* and is commonly denoted by α, i.e.,

$$\alpha \equiv \frac{\partial\Delta}{\partial T} = \frac{1}{a^3\kappa_0}(2\gamma_{0T} + \gamma_{0L})\, k_B + O(T). \tag{7.93}$$

Given the linear expansion law (7.92) we find from (7.82) that the elastic constants soften linearly with temperature as follows[j]

$$\mu = \mu_0(1 - 2\gamma_{0T}\alpha T), \quad 2\mu + \lambda = (2\mu + \lambda)_0(1 - 2\gamma_{0L}\alpha T). \tag{7.94}$$

It is straightforward to include also the quantum effects. For this, all we have to do is replace the logarithms in (7.87) by

$$\frac{k_B T}{2}\int \frac{d^3k}{(2\pi)^3}\left[2\left(\frac{\hbar\omega_T(\mathbf{k})}{2k_B T} + \log(1 - e^{-\hbar\omega_T(\mathbf{k})/k_B T})\right)\right.$$
$$\left. + \left(\frac{\hbar\omega_L(\mathbf{k})}{2k_B T} + \log(1 - e^{-\hbar\omega_L(\mathbf{k})/k_B T})\right)\right] \tag{7.95}$$

[recall (7.21)]. If we now minimize $v(\Delta)$ with respect to Δ, we find

$$\kappa\Delta - \int \frac{d^3k}{(2\pi)^3}\left[2\gamma_{0T}\hbar\omega_T(\mathbf{k})\left(\frac{1}{2} + \frac{1}{e^{\hbar\omega_T(\mathbf{k})/k_B T} - 1}\right)\right.$$
$$\left. + \gamma_{0L}\hbar\omega_L(\mathbf{k})\left(\frac{1}{2} + \frac{1}{e^{\hbar\omega_L(\mathbf{k})/k_B T} - 1}\right)\right] = 0. \tag{7.96}$$

The integrals can be replaced by as the internal energy densities $u_{T,L}$ associated with the transverse and longitudinal modes [compare (7.24)]

$$u_{T,L} = \int \frac{d^3k}{(2\pi)^3}\hbar\omega_{T,L}(\mathbf{k})\left(\frac{1}{2} + \frac{1}{e^{\hbar\omega_{T,L}(\mathbf{k})/k_B T} - 1}\right) \tag{7.97}$$

and the thermal expansion is now given by

$$\kappa_0(\Delta)\,\Delta = (2\gamma_{0T}u_T + \gamma_{0L}u_L). \tag{7.98}$$

In isotropic systems it is easy to calculate this expression. Let us work with the separate Debye approximation for each polarization with the densities of states [recall (7.26)]

$$g^T(\omega) = V\frac{4\pi}{(2\pi)^3}\frac{\omega^2}{c_T^3}, \qquad g^L(\omega) = V\frac{4\pi}{(2\pi)^3}\frac{\omega^2}{c_L^3}, \tag{7.99}$$

[j]Here we have omitted T^2 terms which, at the one-loop level, are unreliable.

each having its own Debye frequencies

$$\omega_D^{T,L} = 2\pi\hbar\left(\frac{3}{4\pi V/N}\right)^{1/3} c_{T,L}. \tag{7.100}$$

The three modes have a internal energy density

$$u_{T,L} = \frac{3N}{V} k_B T \left(\frac{T}{\Theta_D^{T,L}}\right)^3 \int_0^{\Theta_D^{T,L}/T} d\xi \xi^3 \left[\frac{1}{2} + \frac{1}{e^\xi - 1}\right]. \tag{7.101}$$

At high temperatures these have the Dulong-Petit behavior

$$u_{T,L} \to \frac{N}{V} k_B T = \frac{1}{v} k_B T, \tag{7.102}$$

so that (7.96) reduces to the previous classical equation (7.91). At low temperatures, the internal energies are given by (7.34a) i.e.,

$$\begin{aligned} u_{T,L} &\sim \frac{3}{v} k_B \Theta_D^{T,L} \left[\frac{1}{8} + \frac{\pi^4}{15}\left(\frac{T}{\Theta_D^{T,L}}\right)^4 + \dots\right] \\ &= \frac{3}{8}\frac{\hbar c_{T,L} 2\pi}{v r_0} + \frac{\pi^2}{30}\frac{1}{\hbar^3 c_{T,L}^3}(k_B T)^4 + \dots \end{aligned} \tag{7.103}$$

Thus, the cubic terms give rise to a volume expansion at zero temperature due to quantum fluctuations,

$$\kappa_0 \Delta_0 = (2\gamma_{0T} c_T + \gamma_{0L} c_L)\frac{3}{8}\frac{\hbar 2\pi}{v r_0}. \tag{7.104}$$

Starting from this value, the thermal expansion sets in with an expansion coefficient

$$\alpha \equiv \frac{\partial \Delta}{\partial T} = \frac{4}{\kappa_0}\left(2\gamma_{0T}\frac{1}{c_T^3} + \gamma_{0L}\frac{1}{c_L^3}\right)\frac{\pi^2}{30}\frac{1}{\hbar^3}(k_B T)^3 k_B. \tag{7.105}$$

It is useful to introduce the quantity

$$\gamma_0 = \bar{c}^3\left(2\gamma_{0T}\frac{1}{c_T^2} + \gamma_{0L}\frac{1}{c_L^2}\right), \tag{7.106}$$

called the *overall Grüneisen constant*. It governs the change of the Debye temperature due to volume expansion,

$$\gamma_0 = -\frac{\partial \log \Theta_D}{\partial \log V} = -\frac{1}{\Theta_D}\frac{\partial}{\partial \Delta}\Theta_D\bigg|_{\Delta=0} = -\frac{1}{\bar{c}}\frac{\partial}{\partial \Delta}\bar{c}\bigg|_{\Delta=0}$$
$$= \frac{1}{3}\bar{c}^3\frac{\partial}{\partial \Delta}\bar{c}^{-3}\bigg|_{\Delta=0} = \frac{1}{3}\bar{c}^3\frac{\partial}{\partial \Delta}\left(\frac{2}{c_T^3}+\frac{1}{c_L^3}\right) = \bar{c}^3\left(\frac{2\gamma_{0T}}{c_T^3}+\frac{\gamma_{0L}}{c_L^3}\right). \tag{7.107}$$

This quantity can be extracted from purely thermodynamic measurements. In order to see this we observe that within the Debye approximation (7.99), the free energy with quantum effects (7.95) has the general form

$$F = E_0 + T\sum_h f(\Theta_D^{(h)}/T) = E_0 + F_1, \tag{7.108}$$

where E_0 is independent of temperature. The internal energy is given by

$$U = \frac{\partial}{\partial(1/T)}(F/T)\bigg|_V \equiv \sum_h U_h = \sum_h \Theta_D^{(h)} f'(\Theta_D^{(h)}/T). \tag{7.109}$$

From this one finds the pressure,

$$p \equiv -\frac{\partial F}{\partial V}\bigg|_T = -\frac{\partial E_0}{\partial V} - \sum_h \Theta_D^{(h)} f'(\Theta_D^{(h)}/T)\frac{1}{\Theta_D^{(h)}}\frac{\partial}{\partial V}\Theta_D^{(h)} \tag{7.110}$$

and further the thermal expansion coefficient

$$\alpha \doteq \frac{1}{V}\frac{\partial V}{\partial T}\bigg|_p = \frac{1}{V}\frac{\partial p/\partial T|_V}{\partial p/\partial_V|_T} = \frac{1}{\kappa}\frac{\partial p}{\partial T}\bigg|_V$$
$$= \frac{1}{\kappa}\frac{1}{V}\sum_h \Theta_D^{(h)}\frac{\partial}{\partial T}f'(\Theta_D^{(h)}/T)\left(-\frac{V}{\Theta_D^{(h)}}\frac{\partial}{\partial V}\Theta_D^{(h)}\right). \tag{7.111}$$

We may identify

$$c_{Vh} = \frac{1}{V}\frac{\partial}{\partial T}U_h = \frac{1}{V}\Theta_D^{(h)}\frac{\partial}{\partial T}f'(\Theta_D^{(h)}/T)$$

with the specific heats of the modes of polarization h whose sum is the total specific heat at constant volume,

$$c_V = \sum_h c_{Vh}. \tag{7.112}$$

The derivatives

$$\gamma_h \equiv -\frac{V}{\Theta_D^{(h)}} \frac{\partial}{\partial V} \Theta_D^{(h)} = -\frac{1}{c_h} \frac{\partial}{\partial \Delta} c_h, \tag{7.113}$$

where c_h are the sound velocities $c_{T,L}$, are recognized as the Grüneisen constants defined before. Moreover, we may introduce the overall Grüneisen constant γ at arbitrary temperature T,

$$\gamma = \frac{\sum_h \gamma_h c_{Vh}}{\sum_h c_{Vh}} \tag{7.114}$$

[which has the same low T limit as (7.106), by (7.34a)]. In this way, (7.111) becomes

$$\alpha = \frac{1}{\kappa} \gamma c_V; \tag{7.115}$$

hence γ can indeed be obtained from a compressional experiment for $\kappa = -V(\partial p/\partial V)|_T$ and the thermodynamic measurements of $\alpha = (1/V)(\partial V/\partial T)|_p$ and $c_V = (1/V)(\partial U/\partial T)|_V = (1/V)\,T(\partial S/\partial T)|_V$. Actually, the latter quantity is usually taken from

$$c_V = c_p - T\alpha^2\kappa = c_p + T\left.\frac{\partial V}{\partial T}\right|_p^2 \Big/ \left. V\frac{\partial V}{\partial p}\right|_T, \tag{7.116}$$

since the specific heat at constant pressure,

$$c_p \equiv \frac{1}{V} T \left.\frac{\partial S}{\partial T}\right|_p, \tag{7.117}$$

is easier to measure. The connection follows from the well-known Jacobi identity

$$c_p = \frac{T}{V}\frac{\partial S}{\partial T}\bigg|_V = \frac{T}{V}\frac{\partial(S, V)}{\partial(T, V)} = \frac{T}{V}\frac{\partial(S, V)}{\partial(T, p)}\frac{\partial(T, p)}{\partial(T, V)}$$
$$= \frac{T}{V}\frac{1}{\dfrac{\partial V}{\partial p}\bigg|_T}\left(\frac{\partial S}{\partial T}\bigg|_p \frac{\partial V}{\partial p}\bigg|_T - \frac{\partial S}{\partial p}\bigg|_T \frac{\partial V}{\partial T}\bigg|_p\right) = c_V - \frac{T}{V}\frac{\partial S}{\partial p}\bigg|_T \frac{\partial V}{\partial T}\bigg|_p \frac{1}{\dfrac{\partial V}{\partial p}\bigg|_T}, \quad (7.118)$$

in conjunction with the Maxwell relation

$$\frac{\partial S}{\partial p}\bigg|_T = -\frac{\partial}{\partial p}\frac{\partial}{\partial T}[F + pV](p, T) = -\frac{\partial}{\partial T}\frac{\partial}{\partial p}[F + pV](p, T) = -\frac{\partial V}{\partial T}\bigg|_p. \quad (7.119)$$

It should be noted that all these relations are special cases of the very general properties of a phonon gas of frequencies $\omega_h(\mathbf{k})$, which does not necessarily factorize as $c_T \cdot K$, $c_L \cdot K$ and which may have an arbitrary dependence on the temperature. In the general case, the free energy is given by

$$F = E_0 + F^{\text{1 loop}} = E_0 + \frac{1}{2}\sum_{h,\mathbf{k}}\left[\frac{\hbar\omega_h(\mathbf{k})}{2} + k_B T \log(1 - e^{-\hbar\omega_h(\mathbf{k})/k_B T})\right], \quad (7.120)$$

where $E_0 = Ve_0$ is independent of temperature [compare (7.87) and (7.108)]. The pressure of this gas is found from

$$p = -\frac{\partial F}{\partial V}\bigg|_T = -\frac{\partial E_0}{\partial V} + \sum_{h,\mathbf{k}} u_h(\mathbf{k})\left[-\frac{1}{\omega_h(\mathbf{k})}\frac{\partial}{\partial V}\omega_h(\mathbf{k})\right], \quad (7.121)$$

where we have introduced the internal energy for each momentum state,

$$u_h(\mathbf{k}) = \hbar\omega_h(\mathbf{k})\left[\frac{1}{2} + \frac{1}{e^{\hbar\omega_h(\mathbf{k})/k_B T} - 1}\right]. \quad (7.122)$$

The coefficient of thermal volume expansion at constant pressure is therefore given by

$$\alpha = \frac{1}{V}\frac{\partial V}{\partial T}\bigg|_p = \frac{1}{V}\frac{\partial p/\partial T|_V}{\partial p/\partial V|_T} = \frac{1}{\kappa}\frac{\partial p}{\partial T}\bigg|_V$$
$$= \frac{1}{\kappa V}\sum_{h,\mathbf{k}}\left[\frac{\partial}{\partial T}u_h(\mathbf{k})\right]\left[-\frac{V}{\omega_h(\mathbf{k})}\frac{\partial}{\partial V}\omega_h(\mathbf{k})\right]. \tag{7.123}$$

The derivatives

$$\gamma_h(\mathbf{k}) \equiv -\frac{V}{\omega_h(\mathbf{k})}\frac{\partial}{\partial V}\omega_h(\mathbf{k}) \tag{7.124}$$

may be defined as the Grüneisen parameter per state. For a linear sound spectrum,

$$\omega_h(\mathbf{k}) = c_h|\mathbf{k}|, \tag{7.125}$$

these certainly reduce to the constants (7.113) introduced before.

We may also introduce the temperature derivative of $u_h(\mathbf{k})$,

$$c_{Vh}(\mathbf{k}) = \frac{\partial}{\partial T}u_h(\mathbf{k}) = k_B\left(\frac{\hbar\omega_h(\mathbf{k})}{k_BT}\right)^2\frac{e^{\hbar\omega_h(\mathbf{k})/k_BT}}{(e^{\hbar\omega_h(\mathbf{k})/k_BT}-1)^2}, \tag{7.126}$$

as the specific heat at constant volume for each momentum state. Its integral and sum over h,

$$c_V = \sum_h\int\frac{d^3k}{(2\pi)^3}c_h(\mathbf{k}), \tag{7.127}$$

is the total specific heat at constant volume. Using these quantities, the thermal expansion coefficient can again be written as

$$\alpha = \frac{1}{\kappa}\gamma c_V, \tag{7.128}$$

where

$$\gamma = \frac{\sum_{h,\mathbf{k}}\gamma_h(\mathbf{k})\,c_{Vh}(\mathbf{k})}{\sum_{h,\mathbf{k}}c_{Vh}(\mathbf{k})} \tag{7.129}$$

is the overall Grüneisen constant for a general phonon spectrum. For the linear spectrum $\omega_{ll}(\mathbf{k}) = c_{ll}|\mathbf{k}|$ it reduces to the previous constant (7.114).

7.7. SOFTENING OF ELASTIC CONSTANTS

In Eq. (7.82) we observed that the cubic terms not only cause an expansion of the crystal but also a softening of the elastic constants. If we force the total volume to remain constant, by some external walls for example, this mechanism becomes inoperative. Still there is softening of the elastic constant due to higher anharmonic terms, with the quartic term predominanting. Such a situation had been encountered before in Sections 7.6 and 7.7 of Part II in the context of the XY model. There, we had the partition function

$$Z = \prod_{\mathbf{x}} \left[\int_{-\pi}^{\pi} \frac{d\gamma(\mathbf{x})}{2\pi} \right] e^{\beta \sum_{\mathbf{x},i} \cos \nabla_i \gamma(\mathbf{x})}. \tag{7.130}$$

Recall that we had two options for dealing with the low temperature regime. One was the perturbative approach in which we expanded $\cos \nabla_i \gamma$ in powers of the argument

$$\sum_{\mathbf{x},i} \cos \nabla_i \gamma = \sum_{\mathbf{x},i} \left[1 - \frac{1}{2}(\nabla_i \gamma)^2 + \frac{1}{4!}(\nabla_i \gamma)^4 - \dots \right], \tag{7.131}$$

used the second term $\Sigma_{\mathbf{x},i}(\nabla_i \gamma)^2/2$ as a free-field energy, and treated the remaining powers as interactions. The other was the Hartree-Fock approach in which we removed from the exponent an unknown quadratic piece,

$$\beta \sum_{\mathbf{x},i} \cos \nabla_i \gamma = \beta D - \frac{\beta^R}{2} \sum_{\mathbf{x},i} (\nabla_i \gamma)^2 + \sum_{\mathbf{x},i} \left[\beta(\cos \nabla_i \gamma - 1) + \frac{\beta^R}{2}(\nabla_i \gamma)^2 \right] \tag{7.132}$$

and treated the rest in such a way that an infinite set of diagrams was automatically included, namely, those diagrams which brought the interaction to normal form. The renormalization of β which achieved this was determined by a self-consistency equation,

$$\beta^R = \beta e^{-1/(2\beta^R D)}. \tag{7.133}$$

This determined the softening of the effective stiffness β^R as a function of β.

Let us now follow a similar approach for the softening of the elastic constants. For this we write the partition function of the crystalline N body system in the form[k]

$$Z = \prod_{\mathbf{x},i} \left[\int_{-\infty}^{\infty} \frac{du_i(\mathbf{x})}{a} \right] e^{-(\beta/2)\sum_{\mathbf{x}\neq\mathbf{y}} \Phi(\mathbf{x}+\mathbf{u}(\mathbf{x})-\mathbf{y}-\mathbf{u}(\mathbf{y}))}, \tag{7.134}$$

where $\Phi(\mathbf{x}-\mathbf{y})$ is the (symmetric) pair potential, $\mathbf{u}(\mathbf{x})$ the displacement field and the sum over $\mathbf{x}$ covers all lattice sites. The bare elastic constants are obtained by expanding $\Phi(\mathbf{x})$ around the lattice sites, i.e.,

$$\begin{aligned}
&\frac{1}{2}\sum_{\mathbf{x}\neq\mathbf{y}} \Phi(\mathbf{x}+\mathbf{u}(\mathbf{x})-\mathbf{y}-\mathbf{u}(\mathbf{y})) \\
&\quad = \frac{1}{2}\sum_{\mathbf{x}\neq\mathbf{y}} \Phi(\mathbf{x}-\mathbf{y}) + \frac{1}{2}\sum_{\mathbf{x}\neq\mathbf{y}} \partial_i\Phi(\mathbf{x}-\mathbf{y})(u_i(\mathbf{x})-u_i(\mathbf{y})) \\
&\qquad + \frac{1}{4}\sum_{\mathbf{x}\neq\mathbf{y}} \partial_i\partial_j\Phi(\mathbf{x}-\mathbf{y})(u_i(\mathbf{x})-u_i(\mathbf{y}))(u_j(\mathbf{x})-u_j(\mathbf{y})) + \ldots,
\end{aligned} \tag{7.135}$$

where

$$\sum_{\mathbf{x}\neq\mathbf{y}} \partial_i\Phi(\mathbf{x}-\mathbf{y}) = 0, \tag{7.136}$$

since $\mathbf{x}$, $\mathbf{y}$ are the equilibrium positions. Rewriting the quadratic piece as

$$2\cdot\frac{1}{4}\sum_{\mathbf{x}\neq\mathbf{y}} \partial_i\partial_j\Phi(\mathbf{x}-\mathbf{y})\, u_i(\mathbf{x})(u_j(\mathbf{x})-u_j(\mathbf{y}))$$

and transforming $\mathbf{u}(\mathbf{x})$ to Fourier space,

$$\mathbf{u}(\mathbf{x}) = \frac{1}{\sqrt{N}}\sum_{\mathbf{k}} e^{i\mathbf{k}\cdot\mathbf{x}}\mathbf{u}(\mathbf{k}),$$

we have

[k] We omit the factor $1/N!$ due to particle identity and the kinetic part, for brevity.

$$\frac{1}{2}V_{ij}(\mathbf{k})u_i(\mathbf{k})u_j(\mathbf{k}) \equiv \frac{1}{2}\sum_{\mathbf{x}\neq 0}\partial_i\partial_j\Phi(\mathbf{x})(1-e^{-i\mathbf{k}\cdot\mathbf{x}})u_i^*(\mathbf{k})u_j(\mathbf{k}). \quad (7.137)$$

We now decompose $u_i(\mathbf{k})$ into eigenstates of $V_{ij}(\mathbf{k})$,

$$u_i(\mathbf{k}) = \sum_{\lambda}\varepsilon_i^{(\lambda)}(\hat{\mathbf{k}})\,u^{(\lambda)}(\mathbf{k}) \quad (7.138)$$

we rewrite (7.137) in the form

$$\frac{1}{2}\frac{M}{\rho}\sum_{\mathbf{k},\lambda}c^{(\lambda)}(\mathbf{k})\,\mathbf{k}^2|u^{(\lambda)}(\mathbf{k})|^2, \quad (7.139)$$

where ρ is the mass density MN/V and

$$c^{(\lambda)}(\mathbf{k}) = \frac{1}{M}\frac{\rho}{\mathbf{k}^2}\sum_{\mathbf{x}\neq 0}\partial_i\partial_j\Phi(\mathbf{x})(1-e^{-i\mathbf{k}\cdot\mathbf{x}})\,\varepsilon_i^{(\lambda)*}(\hat{\mathbf{k}})\,\varepsilon_j^{(\lambda)}(\hat{\mathbf{k}}). \quad (7.140)$$

These are the elastic constants for the wave vectors $\mathbf{k}$ and with polarization λ. If kinetic terms are included[1], $(M/2)\Sigma_{\mathbf{x}}\dot{u}_i^2(\mathbf{x})$, these have the corresponding decomposition $(1/2)M\Sigma_{\mathbf{k}}|\dot{u}_i^{(\lambda)}(\mathbf{k})|^2$ so that the elastic constants determine the frequency in the usual way,

$$\omega^{(\lambda)2}(\mathbf{k}) = \frac{c^{(\lambda)}(\mathbf{k})}{\rho}\mathbf{k}^2, \quad (7.141)$$

$[c^{(\lambda)}(\mathbf{k})/\rho]^{1/2}$ being the sound velocities.

Let us now see how these results change due to thermal fluctuations. We could again proceed as in Section 7.6, 7.7, Part II, but find it more convenient to use the effective action formalism as in the last section. We introduce expectation values of the displacements,

$$U_i(\mathbf{x}) = \langle u_i\rangle$$

and write

$$Z = \prod_{\mathbf{x},i}\int_{-\infty}^{\infty}\left[\frac{du_i(\mathbf{x})}{a}\right]e^{-(\beta/2)\Sigma_{\mathbf{x}\neq\mathbf{y}}\Phi(\mathbf{x}+\mathbf{U}(\mathbf{x})+\mathbf{u}(\mathbf{k})-\mathbf{y}-\mathbf{U}(\mathbf{y})-\mathbf{u}(\mathbf{y}))}. \quad (7.142)$$

[1]We suppress the time variable in the arguments of $u_i(\mathbf{x})$, $u_i(\mathbf{k})$.

Then we expand the exponent in powers of $\mathbf{U}(\mathbf{x}) - \mathbf{U}(\mathbf{y})$ as follows:

$$-\frac{\beta}{2}\sum_{\mathbf{x}\neq\mathbf{y}}\Phi(\mathbf{x}+\mathbf{u}(\mathbf{x})-\mathbf{y}-\mathbf{u}(\mathbf{y}))-\frac{\beta}{2}\sum_{\mathbf{x}\neq\mathbf{y}}\partial_i\Phi(\mathbf{x}+\mathbf{u}(\mathbf{x})-\mathbf{y}-\mathbf{u}(\mathbf{y}))$$
$$\times(U_i(\mathbf{x})-U_i(\mathbf{y}))-\frac{\beta}{4}\sum_{\mathbf{x}\neq\mathbf{y}}\partial_i\partial_i\Phi(\mathbf{x}+\mathbf{u}(\mathbf{x})-\mathbf{y}-\mathbf{u}(\mathbf{k}))$$
$$\times(U_i(\mathbf{x})-U_i(\mathbf{y}))(U_j(\mathbf{x})-U_j(\mathbf{y}))+\ldots \tag{7.143}$$

We now identify the renormalized elastic constants,

$$c^{(\lambda)}(\mathbf{k})=\frac{1}{M}\frac{\rho}{\mathbf{k}^2}\sum_{\mathbf{x}\neq\mathbf{0}}\langle\partial_i\partial_j\Phi(\mathbf{x}+\mathbf{u}(\mathbf{x})-\mathbf{u}(\mathbf{0}))\rangle(1-e^{-i\mathbf{k}\cdot\mathbf{x}})\,\varepsilon_i^{(\lambda)}(\hat{\mathbf{k}})\,\varepsilon_j^{(\lambda)}(\hat{\mathbf{k}}). \tag{7.144}$$

The self-consistent approach is based on taking the thermal expectation value with the harmonic vibrations,

$$e^{-(\beta/2N)(M/\rho)\sum_{\mathbf{k},\lambda}c^{(\lambda)}(\mathbf{k})\mathbf{k}^2|u^{(\lambda)}(\mathbf{k})|^2}, \tag{7.145}$$

where $c^{(\lambda)}(\mathbf{k})$ are the *same* as those in (7.144). We decompose $\Phi(\mathbf{x})$ into a Fourier series

$$\Phi(\mathbf{x})=\frac{1}{N}\sum_{\mathbf{q}}e^{i\mathbf{q}\cdot\mathbf{x}}\Phi(\mathbf{q}), \tag{7.146}$$

rewrite (7.144) in the form

$$c^{(\lambda)}(\mathbf{k})=-\frac{1}{M}\frac{\rho}{\mathbf{k}^2}\frac{1}{N}\sum_{\mathbf{q},\mathbf{x}\neq\mathbf{0}}\Phi(\mathbf{q})\,e^{i\mathbf{q}\cdot\mathbf{x}}(1-e^{-i\mathbf{k}\cdot\mathbf{x}})\,q_i\,\varepsilon_i^{(\lambda)}(\mathbf{k})\,q_i\,\varepsilon_j^{(\lambda)}(\mathbf{k})\langle e^{iq_i(u_i(\mathbf{x})-u_i(\mathbf{0}))}\rangle, \tag{7.147a}$$

and evaluate the exponent in the usual way, for harmonic modes

$$\langle e^{iq_i(u_i(\mathbf{x})-u_i(\mathbf{0}))}\rangle=e^{q_iq_jD_{ij}(\mathbf{x})}, \tag{7.147b}$$

where $D_{ij}(\mathbf{x})$ is the subtracted correlation function

$$D_{ij}(\mathbf{x})=\langle u_i(\mathbf{x})\,u_j(\mathbf{0})\rangle-\langle u_i(\mathbf{0})\,u_j(\mathbf{0})\rangle. \tag{7.148}$$

Under the self-consistency assumption, the correlation function $\langle u_i(\mathbf{x})\, u_j(\mathbf{0})\rangle$ is determined by (7.145),

$$\langle u_i(\mathbf{x})\, u_j(\mathbf{0})\rangle = \frac{1}{\beta} N \frac{\rho}{M} \sum_{\mathbf{k}} \frac{1}{c^{(\lambda)}(\mathbf{k})\mathbf{k}^2} e^{i\mathbf{k}\cdot\mathbf{x}}\, \varepsilon_i^{(\lambda)}(\mathbf{k})\, \varepsilon_j^{(\lambda)*}(\mathbf{k}). \quad (7.149)$$

Thus (7.147) has to be solved together with

$$D_{ij}(\mathbf{x}) = \frac{1}{\beta} N \frac{\rho}{M} \sum_{\mathbf{k}} \frac{1}{c^{(\lambda)}(\mathbf{k})\mathbf{k}^2} (e^{i\mathbf{k}\cdot\mathbf{x}} - 1)\, \varepsilon_i^{(\lambda)}(\mathbf{k})\, \varepsilon_j^{(\lambda)*}(\mathbf{k}). \quad (7.150)$$

It is easy to include also quantum effects. All one has to do is replace, $\rho/c^{(\lambda)}(\mathbf{k})\mathbf{k}^2 \equiv 1/\omega^{(\lambda)}(\mathbf{k})^2$ by the Matsubara sum [recall (6.261), Part I]

$$\sum_n \frac{1}{\omega_n^2 + \omega^{(\lambda)}(\mathbf{k})^2} = \frac{\beta}{\omega^{(\lambda)}(\mathbf{k})} \coth \beta\omega^{(\lambda)}(\mathbf{k}). \quad (7.151)$$

For $\mathbf{x} = 0$, $D_{ij}(\mathbf{x})$ vanishes, by construction. For large $\mathbf{x}$ it approaches a constant rapidly, namely, the quantity

$$-\langle u_i(\mathbf{0})\, u_j(\mathbf{0})\rangle,$$

which is related to the well-known Waller factor [recall (7.63)] by

$$2W \equiv q_i q_j \langle u_i(\mathbf{0})\, u_j(\mathbf{0})\rangle. \quad (7.152)$$

In cubic materials, upon which we shall now focus attention, the Debye-Waller factor is

$$2W = \tfrac{1}{3} q^2 \langle \mathbf{u}^2 \rangle$$

and the limit becomes

$$q_i q_j D_{ij}(\mathbf{x}) \xrightarrow[\mathbf{x}\to\infty]{} 2W = \tfrac{1}{3}\mathbf{q}^2 \langle \mathbf{u}^2(\mathbf{0})\rangle. \quad (7.153)$$

The approach to this asymptotic value is exponential. In practice, this is fast enough to permit the approximation,

$$q_i q_j D_{ij}(\mathbf{x}) \underset{\mathbf{x}\neq\mathbf{0}}{\approx} 2W = \tfrac{1}{3}\mathbf{q}^2 \langle \mathbf{u}^2(\mathbf{0})\rangle.$$

We thus arrive at the self-consistency equation for the elastic constants

$$c^{(\lambda)}(\mathbf{k}) = -\frac{1}{M}\frac{\rho}{\mathbf{k}^2}\frac{1}{N}\sum_{\mathbf{q},\mathbf{x}\neq\mathbf{0}} \Phi(\mathbf{q})(e^{i\mathbf{q}\cdot\mathbf{x}} - e^{i(\mathbf{q}-\mathbf{k})\cdot\mathbf{x}})\, q_i \varepsilon_i^{(\lambda)*}(\mathbf{k})\, q_j \varepsilon_j^{(\lambda)}(\mathbf{k})\, e^{-(\mathbf{q}^2/3)\langle \mathbf{u}^2(\mathbf{0})\rangle}, \tag{7.154}$$

where $\langle \mathbf{u}^2(\mathbf{0})\rangle$ depends again on $c^{(\lambda)}(\mathbf{k})$ via (7.149) since

$$\langle \mathbf{u}^2(\mathbf{0})\rangle = \frac{1}{\beta} N \frac{\rho}{M} 3 \sum_{\mathbf{k}} \frac{1}{c^{(\lambda)}(\mathbf{k})\,\mathbf{k}^2}. \tag{7.155}$$

We can go back to $\mathbf{x}$ space by performing the sum over $\mathbf{q}$. The extra factor $e^{-(\mathbf{q}^2/3)\langle \mathbf{u}^2(\mathbf{0})\rangle}$ amounts to replacing the pair potential $\Phi(\mathbf{x})$ by the renormalized one

$$\Phi^R(\mathbf{x}) = \frac{1}{\left(\sqrt{2\pi \dfrac{3}{2\langle \mathbf{u}^2(\mathbf{0})\rangle}}\right)^3} \int d^3x'\, e^{-((\mathbf{x}-\mathbf{x}')^2/2)/(3/2\langle \mathbf{u}^2(\mathbf{0})\rangle)} \Phi(\mathbf{x}'). \tag{7.156}$$

This has a simple physical interpretation: the renormalized potential is obtained from the original one by smearing the $\mathbf{x}$ variable out over a radius proportional to the mean square displacement $\langle \mathbf{u}^2(\mathbf{0})\rangle$.

In isotropic systems there are only two different sound waves, a longitudinal wave with an elastic constant along $\mathbf{k}$

$$c_L(\mathbf{k}) = -\frac{1}{M}\frac{\rho}{\mathbf{k}^2}\frac{1}{N}\sum_{\mathbf{q},\mathbf{x}\neq\mathbf{0}} \Phi^R(\mathbf{q})(e^{i\mathbf{q}\cdot\mathbf{x}} - e^{i(\mathbf{q}-\mathbf{k})\cdot\mathbf{x}})\frac{(\mathbf{q}\cdot\mathbf{k})^2}{\mathbf{k}^2} \tag{7.157}$$

and two degenerate transverse ones with

$$c_T(\mathbf{k}) = -\frac{1}{M}\frac{\rho}{\mathbf{k}^2}\sum_{\mathbf{q},\mathbf{x}\neq\mathbf{0}} \Phi^R(\mathbf{q})(e^{i\mathbf{q}\cdot\mathbf{x}} - e^{i(\mathbf{q}-\mathbf{k})\cdot\mathbf{x}})\left(\frac{\mathbf{q}^2}{2} - \frac{(\mathbf{q}\cdot\mathbf{k})^2}{\mathbf{k}^2}\right), \tag{7.158}$$

where we have used the obvious notation

$$\Phi^R(\mathbf{q}) = \Phi(\mathbf{q})\, e^{-(\mathbf{q}^2/3)\langle \mathbf{u}^2(\mathbf{0})\rangle}. \tag{7.159}$$

Performing the sum over $\mathbf{x}$ squeezes $\mathbf{q}$ once to $\mathbf{c}$ and once $\mathbf{c}+\mathbf{k}$ where $\mathbf{c}$ is the reciprocal lattice vectors [recall Part I, (6.29)]

$$\sum_{\mathbf{x}} e^{i\mathbf{q}\cdot\mathbf{x}} = N \sum_{\mathbf{c}} \delta(\mathbf{q} - \mathbf{c}) \tag{7.160}$$

and we find

$$\omega_L^2(\mathbf{k}) = c_L(\mathbf{k})\frac{\mathbf{k}^2}{\rho}$$
$$= \frac{1}{M}\left(\mathbf{k}^2\Phi^R(\mathbf{k}) + \sum_{\mathbf{c}\neq\mathbf{0}}\left(\frac{((\mathbf{c}+\mathbf{k})\cdot\mathbf{k})^2}{\mathbf{k}^2}\Phi^R(\mathbf{c}+\mathbf{k}) - \frac{(\mathbf{c}\cdot\mathbf{k})^2}{\mathbf{k}^2}\Phi^R(\mathbf{c})\right)\right),$$

$$\omega_T^2(\mathbf{k}) = c_T(\mathbf{k})\frac{\mathbf{k}^2}{\rho} = \frac{1}{M}\sum_{\mathbf{c}\neq\mathbf{0}}\left(\mathbf{c}^2 - \frac{(\mathbf{c}\cdot\mathbf{k})^2}{\mathbf{k}^2}\right)(\Phi^R(\mathbf{c}+\mathbf{k}) - \Phi^R(\mathbf{c})). \tag{7.161}$$

The important observation at this point is that the transverse elastic constant does not contain $\mathbf{c} = \mathbf{0}$ in the sum. Thus it begins with the nearest neighbor in reciprocal space, say $\mathbf{c}_1$. For small $|\mathbf{k}| \ll |\mathbf{c}_1|$, the leading term is

$$\omega_T^2(\mathbf{k}) \sim \frac{1}{M}\sum_{\mathbf{c}_1}\left(\mathbf{c}_1^2 - \frac{(\mathbf{c}_1\cdot\mathbf{k})^2}{\mathbf{k}^2}\right)(\Phi^R(\mathbf{c}_1+\mathbf{k}) - \Phi^R(\mathbf{c}_1)). \tag{7.162}$$

The longitudinal term, on the other hand, has the leading term

$$\omega_L^2(\mathbf{k}) \sim \frac{1}{M}\mathbf{k}^2\Phi^R(\mathbf{k}). \tag{7.163}$$

In general, the potentials fall off rapidly in momentum space such that it is a reasonable first approximation to neglect the higher $\mathbf{c}$ vectors.

This observation allows for two immediate conclusions: Since $\langle \mathbf{u}^2(\mathbf{0})\rangle$ increases toward larger temperature, the transverse elastic constant shows a much stronger thermal softening than the longitudinal constant. The transverse softening, for small $\mathbf{k}$, is approximately [using (7.159)]

$$\frac{c_T(\mathbf{k})|_{T\neq 0}}{c_T(\mathbf{k})|_{T=0}} \approx e^{-(\mathbf{c}_1^2/3)\langle \mathbf{u}^2(\mathbf{0})\rangle}. \tag{7.164}$$

Here [see (7.50)]

$$\langle \mathbf{u}^2(0)\rangle = 3\sum_{h}\frac{1}{M\omega_D^{(h)3}}\int_0^{\omega_D^{(h)}} d\omega\,\hbar\omega\left(\frac{1}{2} + \frac{1}{e^{\hbar\omega/k_BT}-1}\right) \tag{7.165}$$

Let us estimate $\langle \mathbf{u}^2(\mathbf{0}) \rangle$ from the classical limit of formula (7.57),

i.e.,

$$\langle \mathbf{u}^2(\mathbf{0}) \rangle = 3 \frac{k_B T}{M} \sum_h \frac{1}{\omega_D^{(h)2}}. \tag{7.166}$$

Using Eq. (7.28), this can also be written as

$$\langle \mathbf{u}^2(\mathbf{0}) \rangle = 3 \frac{k_B T}{M} \frac{1}{(2\pi)^2} \left(\frac{4\pi V}{3N} \right)^{2/3} \sum_h \frac{1}{c_h^2} = 3 \frac{k_B T}{M} \frac{r_0^2}{(2\pi)^2} \sum_h \frac{1}{c_h^2}, \tag{7.167}$$

where r_0 is radius of the sphere available to each atom. Here c_h are the three sound velocities. The transverse elastic constants $c_T(\mathbf{k})$, on the left-hand side of (7.164) are themselves (for small $\mathbf{k}$) proportional to the square of the transverse sound velocities c_T. Using $|c_1| = 2\pi/r_0 \times 0.695$ (b.c.c.), $2\pi/r_0 \times 0.676$ (f.c.c.) [see Appendix 7.A] we thus arrive at the nonlinear equation for sound velocities

$$\frac{c_T^2(T)}{c_T^2} \approx e^{-0.68^2 (k_B T/M) \sum_h 1/c_h^2(T)}. \tag{7.168}$$

To lowest order in T

$$\frac{c_T^2(T)}{c_T^2} \approx 1 - 0.68^2 \frac{k_B T}{M} \sum_h \frac{1}{c_h^2}. \tag{7.169}$$

Before comparing this with experimental data, e.g., those in Fig. 7.8, we have to perform an isotropic average a la Voigt [see (7.44)] and allow for the additional linear softening law due to volume expansion (7.94).

As a very rough approximation let us ignore that and study (7.168) itself. We also neglect, on the right-hand side of (7.168) the difference between elastic constants. Then we find the self-consistency equation

$$\frac{c_T^2(T)}{c_T^2} \approx e^{-0.68^2 \cdot 3 (k_B T/M)(1/c_T^2(T))}. \tag{7.170}$$

Setting $r \equiv c_T^2(T)/c_T^2$ and $\tau \equiv 1.38 (k_B T/M c_T^2)$ we can rewrite this as

$$\tau = \frac{\tau}{r} e^{-\tau/r} \tag{7.171}$$

FIG. 7.8. Experimental softening of elastic constants in Ag (after Grimwall op. cit.).

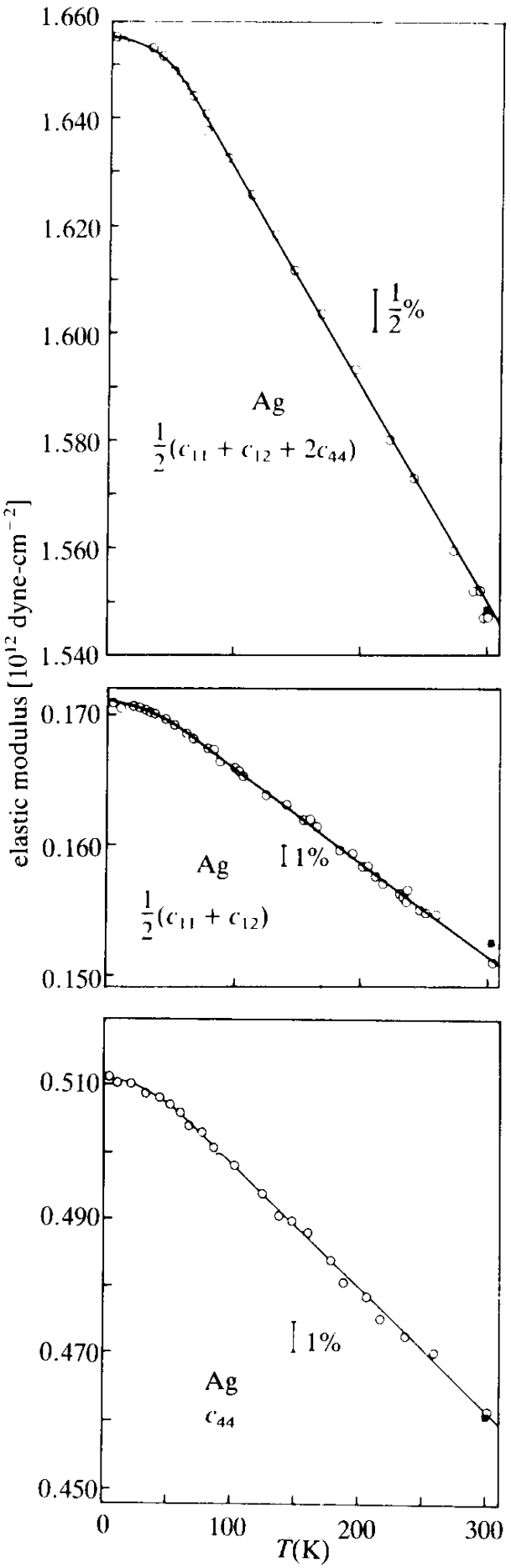

This has a solution only as long as τ is smaller than the maximum of the function on the right-hand side, which lies at $\tau/r = 1$ where $(\tau/r)e^{-\tau/r} = 1/e$ [compare (7.143) and Fig. 7.17 of Part II], i.e.,

$$\tau_{\max} = \frac{1}{e}. \tag{7.172}$$

At this point, the transverse elastic sound velocity constants have softened by a factor of $1/e$. The self-consistency approximation cannot be continued beyond this point. The maximal temperature is

$$T_{\max} = \frac{1}{k_B} M c_T^2 \frac{1}{1.38e}. \tag{7.173}$$

Let us translate the result to the mean square displacement. Using (7.167) we find

$$\delta_{\max} = \sqrt{\frac{1}{3}\frac{\langle \mathbf{u}^2(\mathbf{0})\rangle_{\max}}{a^2}} = \sqrt{\frac{k_B T_{\max}}{M}\sum_h \frac{1}{c_h^2}} \sim \sqrt{3}\sqrt{\frac{k_B T_{\max}}{M c_T^2}} \sim \sqrt{\frac{3}{1.38e}} \sim 0.89 \tag{7.174}$$

Since melting occurs at $\delta_{\text{melt}} \sim 0.07$ (from Table 7.4), in accordance with Lindemann's law, we conclude that the self-consistent approximation can well be used to describe softening of the elastic constants up to this point.

Notice that we can use the more precise determinations of δ at the melting point to calculate the softening of the elastic constants. For this we rewrite the exponential

$$e^{-(c_1^2/3)\langle \mathbf{u}^2(\mathbf{0})\rangle}$$

as follows

$$e^{-c_1^2 d^2 \langle \mathbf{u}^2(\mathbf{0})/3d^2\rangle} = e^{-c_1^2 d^2 \delta^2}, \tag{7.176}$$

where δ is the ratio of $\sqrt{\langle u_i^2\rangle/3}$ with respect to the nearest neighbour distance d. Then we use the fact that the classical regime δ^2 grows linearly with temperature,

$$\delta^2 \approx \delta_{\text{melt}}^2 \frac{T}{T_{\text{melt}}}, \tag{7.177}$$

and take δ^2_{melt} from Table 7.4. In b.c.c. and f.c.c. crystals, the smallest reciprocal lattice vectors are given by

$$|c_1| = \sqrt{\frac{3}{2}}\frac{2\pi}{d}, \tag{7.178}$$

where d is the nearest neighbour distance [see Appendix 7.A] so that (7.176)

$$e^{-59.2\,\delta^2_{\text{melt}}(T/T_{\text{melt}})}.$$

Inserting the classical numbers of Table 7.4 this gives us a softening ratio for the elastic constants,

$$\frac{c_T(T)}{c_T} \approx e^{-0.7(T/T_{\text{melt}})} \qquad \text{(b.c.c.)}, \tag{7.179}$$

$$\frac{c_T(T)}{c_T} \approx e^{-0.29(T/T_{\text{melt}})} \qquad \text{(f.c.c.)}. \tag{7.180}$$

For an order of magnitude comparison we take the experimental curves for the softening of the elastic constants of the f.c.c. crystal Ag as shown in Fig. 7.8. With $T_{\text{melt}} = 1235\,\text{K}$ we find the slope

$$\frac{c_T(T)}{c_T} \approx 1 - 0.3\frac{T}{T_{\text{melt}}}.$$

Despite the neglect of the contribution due to thermal expansion, (7.94), this agrees with (7.180). For the b.c.c. metal Ta we use the data of Table 1.2 and find with $T_{\text{melt}} = 3270\,\text{K}$

$$\frac{c_T(T)}{c_T} \approx 1 - 0.76\frac{T}{T_{\text{melt}}},$$

also in reasonable agreement with (7.179).

In the literature the breakdown of the self-consistent approximation has sometimes been associated with the melting transition[m]. From the

[m]See, for example, H. Fukuyama and P.M. Platzman, *Sol. St. Commun.* **15** (1974) 677, and *Phys. Rev.* **B10** (1974) 3150.

discussion of the XY model in Sections 7.6, 7.7, Part II however, we know that this breakdown bears no relation to the phase transition. The phase transition is *not* caused by perturbative effects, and cannot therefore be derived from a partial resummation of infinitely many diagrams. The XY model has taught us that the physical origin of the superfluid phase transition is the condensation of vortex lines. Only these lead to the destruction of the superfluid order.

We must therefore expect that a proper understanding of the melting transition will be possible only after an analogous treatment of line-like defects. This will be given in later chapters.

Let us end this chapter with a few comments on the two-dimensional situation.

7.8. TWO-DIMENSIONAL CRYSTALS

Just as was the case with superfluids, solids too can be studied experimentally in the reduced dimensionality $D = 2$, at least to a certain approximation. It is possible to prepare large monoatomic layers of atoms on grafoil (recall Section 11.1, Part II) and investigate their thermodynamic properties as well as their correlation functions (through X-ray scattering). The favourite systems are layers of rare gases like Helium, Xenon, Argon or Krypton.

Such layers are usually not completely uniform since the binding potential has the periodicity of the substrate and the diameter of the Xenon atoms is somewhat larger than the lattice spacing of graphite. Thus the atoms do not properly match with the optimal positions (see Fig. 7.9). Fortunately, however, the variations in the binding energy are quite small. For Xenon, for example it is ≈ 37K. Melting of Xenon occurs at $\approx 100 - 152$ K (for the phase diagram see Fig. 14.5). Hence the deviations from uniformity should be neglegible.

The Debye theory developed in the beginning of this chapter applies to such two-dimensional solids with only minor modifications. The Debye frequencies (7.28) are again equal to $2\pi c_h/r_0$, where c_h are the velocities of sound with polarization h and the radius r_0 associated with each particle is now equal to $(N/V)^{1/2}$, V being the two-dimensional volume, i.e., the area occupied by the atoms. Hence

$$\omega_D^{(h)} = 2\pi \left(\frac{1}{\hbar V/N} \right)^{1/2} \times c_h = 2\pi c_h/r_0 \tag{7.180}$$

FIG. 7.9. The geometry for the adsorption of Xenon on graphite. The Xe atoms are slightly larger than the lattice spacing so that the layer is not quite commensurate.

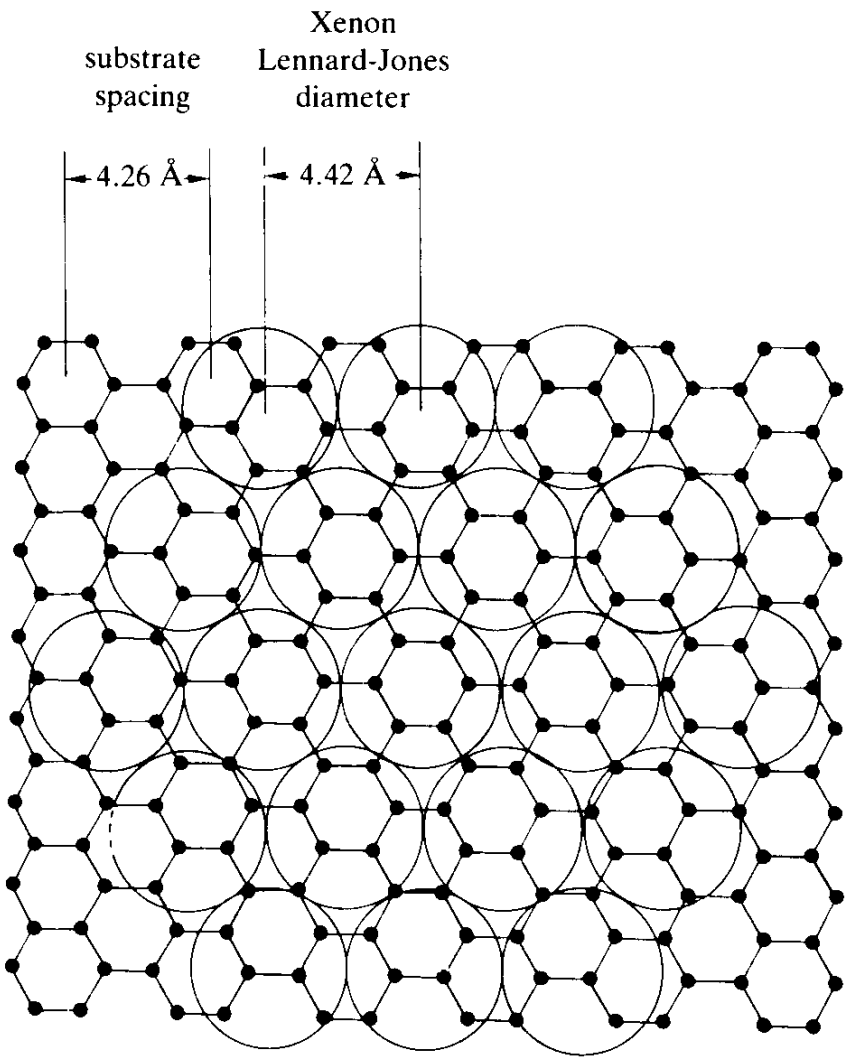

Xenon adsorbed on graphite (001) surface

There are only two polarizations $h = L,\ T$ whose density of states is $g^{(h)}(\omega) = V[1/2\pi](\omega/c_h^2)$. With the average sound velocity [recall (7.29b)]

$$\bar{c} = \left[2\Big/\left(\frac{1}{c_T^2} + \frac{1}{c_L^2}\right)\right]^{1/2}. \tag{7.181}$$

The single density of states is $g(\omega) = 2V(1/2\pi)(\omega/\bar{c}^2)$. The average Debye temperature is

$$\Theta_D = \hbar\omega_D/k_B, \quad \omega_D = 2\pi\bar{c}/r_0 \tag{7.182}$$

and the internal energy becomes

$$U = 4Nk_BT\left(\frac{T}{\Theta_D}\right)^2 \int_0^{\Theta_D/T} d\xi\xi^2\left[\frac{1}{2} + \frac{1}{e^\xi - 1}\right] \tag{7.183}$$

and the specific heat

$$C = 4Nk_B\left(\frac{T}{\Theta_D}\right)^2 \int_0^{\Theta_D/T} d\xi e^\xi \frac{\xi^3}{(e^\xi - 1)^2} d\xi. \tag{7.184}$$

For low temperatures, we use $\int_0^\infty d\xi\xi^2 \frac{1}{e^\xi - 1} = 2\zeta(3) = 2.404$ and find that U and C have the limiting behavior

$$U \xrightarrow[T \ll \Theta_D]{} 4Nk_B\Theta_D\left(\frac{1}{6} + 2.404\left(\frac{T}{\Theta_D}\right)^3\right), \qquad C \xrightarrow[T \ll \Theta_D]{} 4Nk_B 7.212\left(\frac{T}{\Theta_D}\right)^2. \tag{7.185}$$

The experimental T^2 behavior of C for monolarges of ^{3}He of various densities are shown in Fig. 7.10. The Debye temperature Θ_D extracted from data are plotted in Fig. 7.11 as a function of the molecular areas $a^2 = \pi r_0^2$. For large temperatures, U and C follow again the Dulong-Petit law,

$$U \xrightarrow[T \gg \Theta_D]{} U_{\text{cl}} = 2Nk_BT, \qquad C \xrightarrow[T \gg \Theta_D]{} U_{\text{cl}} = 2Nk_B. \tag{7.186}$$

Most of the other formulas can be transformed straightforwardly to two dimensions.

There are, however, a few pecularities due to the Landau-Peierls argument, mentioned before in the context of superfluidity in two-dimensional layers, i.e., based on the fact that $\int (d^2k/(2\pi)^2) e^{i\mathbf{k}\cdot(\mathbf{x}-\mathbf{x}')}(1/\mathbf{k}^2)$ is divergent. This fact has sometimes been used to argue that two-dimensional solids cannot exist, but this is not really true. What is true is that this divergence prevents two-dimensional crystals from having a proper long-range order with δ-function Bragg reflexes. The deviations are quantitatively not very significant. Theoretically, however, they are of great interest. This warrants a special discussion, which we now turn to.

In the continuum approximation, the linear elastic energy is

$$E_{\text{el}} = \int d^2x\left[\frac{\mu}{4}(\partial_i u_j + \partial_j u_i)^2 + \frac{\lambda}{2}(\partial_i u_i)^2\right] \tag{7.187}$$

FIG. 7.10. The specific heat data at low temperatures for high density ^{4}He on grafoil (from Hering and Vilches, 1973, see J.G. Dash op. cit. in the Notes and References). The densities in units of $n/\text{Å}^2$ are 0.078, 0.079, 0.080, 0.082, 0.087, 0.092, for increasing Θ_D.

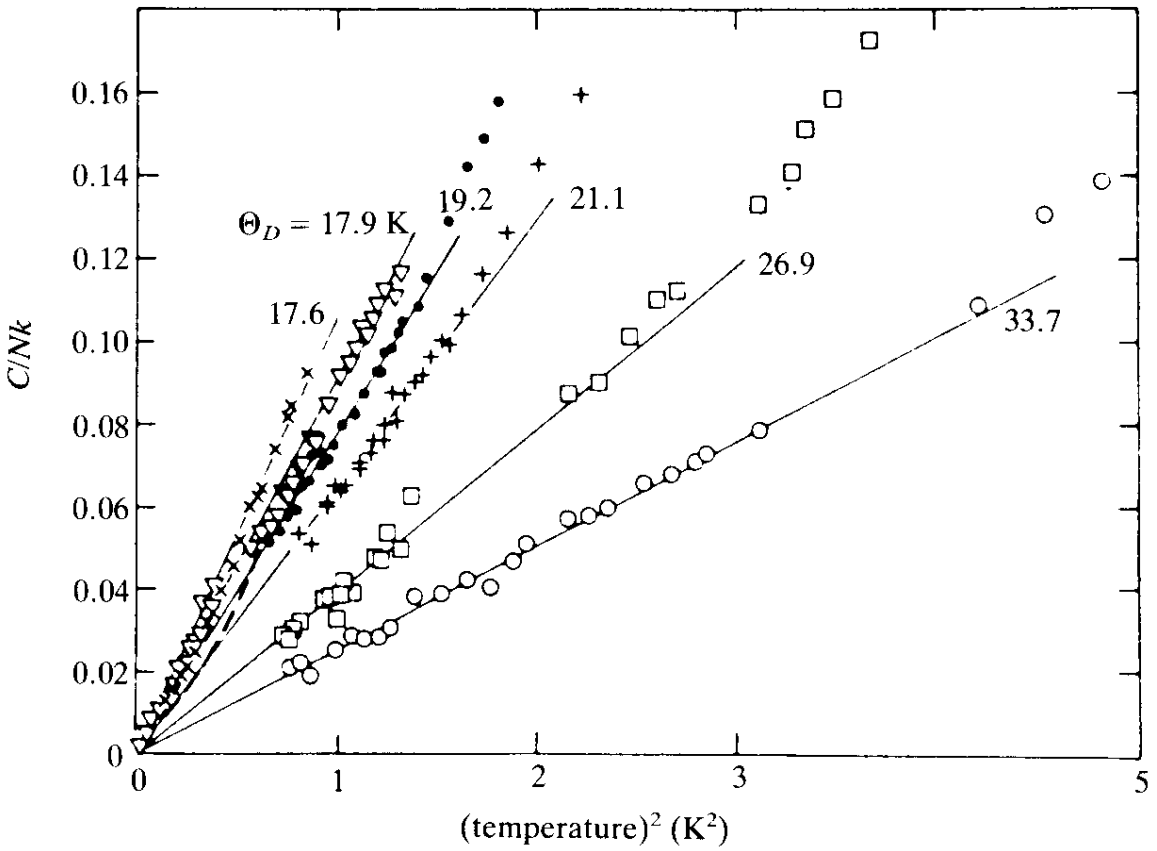

FIG. 7.11. The Debye temperature for layers of solid ^{4}He, as extracted from the low T behavior of the specific heat data, as a function of the molecular area $a^2 = \pi r_0^2$. For comparison, we show the data points of hcp ^{4}He on the same length scale a (after M. Bretz *et al.*, op. cit. in the Notes and References).

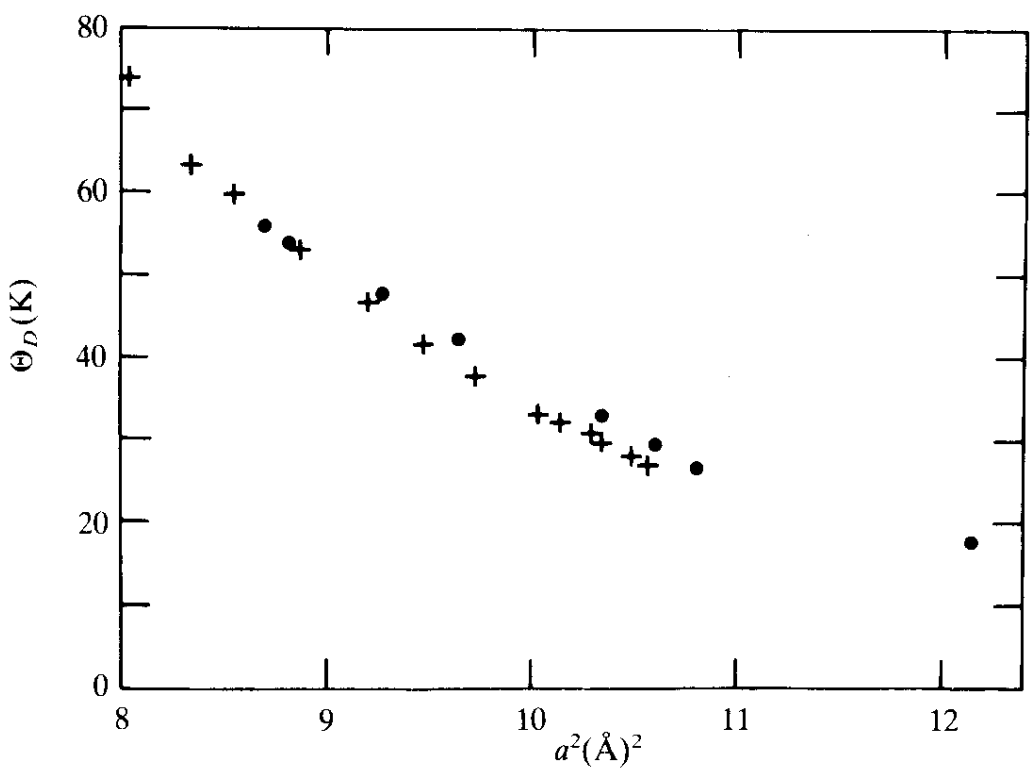

with a partition function[n]

$$Z = \prod_{\mathbf{x}} \left[\int \frac{du_i(\mathbf{x})}{a} \right] e^{-E_{\mathrm{el}}/T}. \tag{7.188}$$

This gives the correlation function

$$\langle u_i(\mathbf{x}) u_j(\mathbf{x}') \rangle = G_{ij}(\mathbf{x} - \mathbf{x}') = \int \frac{d^2k}{(2\pi)^2} e^{i\mathbf{k}\cdot(\mathbf{x}-\mathbf{x}')} \frac{1}{\mu k^4} \left(k^2 \delta_{ij} - \frac{\lambda + \mu}{\lambda + 2\mu} k_i k_j \right). \tag{7.189}$$

We can now convince ourselves that due to the logarithmic singularity of the Coulomb Green function $\int (d^2k/(2\pi)^2) e^{i\mathbf{k}\cdot(\mathbf{x}-\mathbf{x}')}(1/\mathbf{k}^2)$, the two-dimensional solid has indeed no proper long-range order, a fact which manifests itself in the absence of true δ-function Bragg peaks in scattering experiments. In order to see this we calculate the dimensionless structure factor[o]

$$S(\mathbf{q}) = \frac{1}{N} \int d^2x\, d^2x'\, e^{i\mathbf{q}\cdot(\mathbf{x}-\mathbf{x}')} \langle \rho(\mathbf{x}) \rho(\mathbf{x}') \rangle, \tag{7.190}$$

where $\rho(\mathbf{x})$ is the local particle density and N the total number. If the atoms are at their equilibrium positions [recall (1.1)], this is given by

$$\rho(\mathbf{x}) = \sum_n \delta^{(2)}(\mathbf{x} - \mathbf{x}_n). \tag{7.191}$$

Inserting this into (7.106) gives

$$S(\mathbf{q}) = \frac{1}{N} \sum_{\mathbf{n},\mathbf{n}'} e^{i\mathbf{q}\cdot(\mathbf{x}_{\mathbf{n}} - \mathbf{x}_{\mathbf{n}'})} = \sum_{\mathbf{n}} e^{i\mathbf{q}\cdot\mathbf{x}_{\mathbf{n}}} = \left(\frac{2\pi}{a} \right)^2 \sum_{\mathbf{c}} \delta^{(2)}(\mathbf{q} - \mathbf{c}) = N \sum_{\mathbf{c}} \delta_{\mathbf{q},\mathbf{c}}, \tag{7.192}$$

where $\mathbf{c}$ are the reciprocal lattice vectors $(2\pi/a)(c_1, c_2, \ldots)$ with c_i = integer. If the atoms are displaced by $u_i(\mathbf{x})$, one has instead

[n]We drop the trivial factor $(\sqrt{k_B T a^4 \rho / 2\pi\hbar^2})^{2N}$ [recall (7.67) in three dimensions].

[o]In terms of $S(\mathbf{q})$, the X-ray differential cross section is

$$\frac{d\sigma}{d\Omega} = \frac{a^2}{\hbar} N S(\mathbf{q}).$$

$$\rho(\mathbf{x}) = \sum_{\mathbf{n}} \delta^2(\mathbf{x} - \mathbf{x}_\mathbf{n} - u_i(\mathbf{x}_n)) \tag{7.193}$$

and finds

$$S(\mathbf{q}) = \frac{1}{N}\sum_{\mathbf{n},\mathbf{n}'} e^{i\mathbf{q}\cdot(\mathbf{x}_n - \mathbf{x}_{n'})} \left\langle e^{iq_i u_i(\mathbf{x}_n)} e^{-iq_i u_i(\mathbf{x}_{n'})} \right\rangle = \sum_{\mathbf{n}} e^{i\mathbf{q}\mathbf{x}_n} \left\langle e^{iq_i u_i(\mathbf{x}_n)} e^{-iq_i u_i(\mathbf{0})} \right\rangle. \tag{7.194}$$

As long as the displacement field is small and follows the laws of linear elasticity we can calculate directly [compare (11.92)–(11.96), Part II],

$$\begin{aligned} \left\langle e^{iq_i u_i(\mathbf{X})} e^{-iq_i u_i(\mathbf{0})} \right\rangle &= Z^{-1} \prod_{\mathbf{x}} \left[\int_{-\infty}^{\infty} \frac{du_i(\mathbf{x})}{a} \right] e^{-E_{\mathrm{el}}/T + iq_i \Sigma_\mathbf{x} u_i(\mathbf{x}) Q(\mathbf{x})} \\ &= Z^{-1} \prod_{\mathbf{x}} \left[\int_{-\infty}^{\infty} \frac{du_i(\mathbf{x})}{a} \right] e^{-(1/2T)\Sigma_\mathbf{x} u_i(\mathbf{x}) G_{ij}^{-1}(\mathbf{x}-\mathbf{x}') u_j(\mathbf{x}') + iq_i \Sigma_\mathbf{x} u_i(\mathbf{x}) Q(\mathbf{x})} \\ &= e^{-q_i q_j (T/2)\Sigma_{\mathbf{x},\mathbf{x}'} Q(\mathbf{x}) G_{ij}(\mathbf{x}-\mathbf{x}') Q(\mathbf{x}')} = e^{q_i q_j T G'_{ij}(\mathbf{X})}, \end{aligned} \tag{7.194'}$$

where we have used the abbreviations $Q(\mathbf{x}) = \delta_{\mathbf{x},\mathbf{X}} - \delta_{\mathbf{x},\mathbf{0}}$,

$$G'_{ij}(\mathbf{X}) \equiv G_{ij}(\mathbf{X}) - G_{ij}(\mathbf{0}). \tag{7.195}$$

In three dimensions, $G'_{ij}(\mathbf{X})$ would go to zero for large distances and $\left\langle e^{iq_i u_i(\mathbf{X})} e^{-iq_i u_i(\mathbf{0})} \right\rangle \to 1$. Inserting this into (7.194) we see that we obtain $S(\mathbf{q}) \propto \Sigma_\mathbf{c} \delta_{\mathbf{q},\mathbf{c}}$ so that thermal fluctuations *do not* destroy the δ-function peaks in the structure function.

In two dimensions, however, $G'_{ij}(\mathbf{X})$ diverges logarithmically and $\left\langle e^{iq_i u_i(\mathbf{X})} e^{-iq_i u_i(\mathbf{0})} \right\rangle$ falls off like a power of $|\mathbf{X}|$ instead of becoming constant. When inserting the power behaviour $|\mathbf{X}|^{-\eta(\mathbf{q})}$ into (7.194), the δ-functions widen into cusps around the reciprocal lattice vectors $\mathbf{c}$, with the behaviour

$$S(\mathbf{q}) \propto \sum_{\mathbf{c}} \frac{1}{|\mathbf{q} - \mathbf{c}|^{2-\eta(\mathbf{q})}}. \tag{7.196}$$

The precise value of $\eta(\mathbf{q})$ is found by extracting the long-range logarithmic term in (7.189). According to (1.125) this is given by

$$G_{ij}(\mathbf{x}) \underset{\delta \approx 0}{\approx} -\frac{1}{\mu}\frac{1}{4\pi}\delta_{ij}\frac{\lambda + 3\mu}{\lambda + 2\mu}\log\left(\frac{\delta}{2}|\mathbf{x}|\, e^{\gamma}\right), \tag{7.197}$$

so that the subtracted Green function has the finite limit

$$G'_{ij}(\mathbf{x}) = -\frac{1}{\mu}\frac{1}{4\pi}\delta_{ij}\frac{\lambda+3\mu}{\lambda+2\mu}\log|\mathbf{x}|, \tag{7.198}$$

giving[p]

$$\eta(\mathbf{q}) = q^2\frac{T}{4\pi}\frac{\lambda+3\mu}{\mu(\lambda+2\mu)}. \tag{7.199}$$

Since power behaviors like $|\mathbf{X}|^{-\eta}$ are typical for critical systems, the power η is called a *critical index*.

Experimentally, the power behaviour (7.196) is visible in the intensity profiles of X-rays scattered on adsorbed layers of atoms as illustrated in Fig. 7.12 with the data of Heiney et al. See the Notes and References.

The melting transition in two-dimensional systems was first observed in monolayers of ^{4}He by Bretz et al. (1973). The data show sharp peaks in the specific heat (see Fig. 7.13).

Certainly, it is possible to carry through all the discussions of the previous sections once more in two dimensions. For brevity, however, we shall not do this and embark directly in studying the role of defects in the melting transition. Later, after having improved our understanding of the three-dimensional transition we shall return and study also two-dimensional melting in more detail.

APPENDIX 7A. SOME LATTICE PROPERTIES

In a b.c.c. lattice, we use the basis

$$\mathbf{a}_1 = \frac{a_0}{2}(-\hat{\mathbf{x}}+\hat{\mathbf{y}}+\hat{\mathbf{z}}),\quad \mathbf{a}_2 = \frac{a_0}{2}(\hat{\mathbf{x}}-\hat{\mathbf{y}}+\hat{\mathbf{z}}),\quad \mathbf{a}_3 = \frac{a_0}{2}(\hat{\mathbf{x}}+\hat{\mathbf{y}}-\hat{\mathbf{z}}), \tag{7A.1}$$

and find the volume per cell

$$v = (\mathbf{a}_1\times\mathbf{a}_2)\cdot\mathbf{a}_3 = \frac{a_0^3}{2} \tag{7A.2}$$

[p]Notice that the combination of elastic constants in the same as in the Debye temperature

$$\Theta_D = \frac{2\pi\hbar}{k_B}\left(\frac{1}{\pi a^2}\right)^{1/2}\bar{c} = \frac{2\pi\hbar}{k_B}\sqrt{\frac{2}{\pi M}}\sqrt{\frac{\mu(\lambda+2\mu)}{\lambda+3\mu}}.$$

FIG. 7.12. Diffraction profiles illustrating the power-like peaks (solid lines) in the structure factor $S(\mathbf{Q})$ rather than the δ-like peaks in the Bragg reflexes of $3D$ solids (after Heiney et al., op. cit. in the Notes and References).

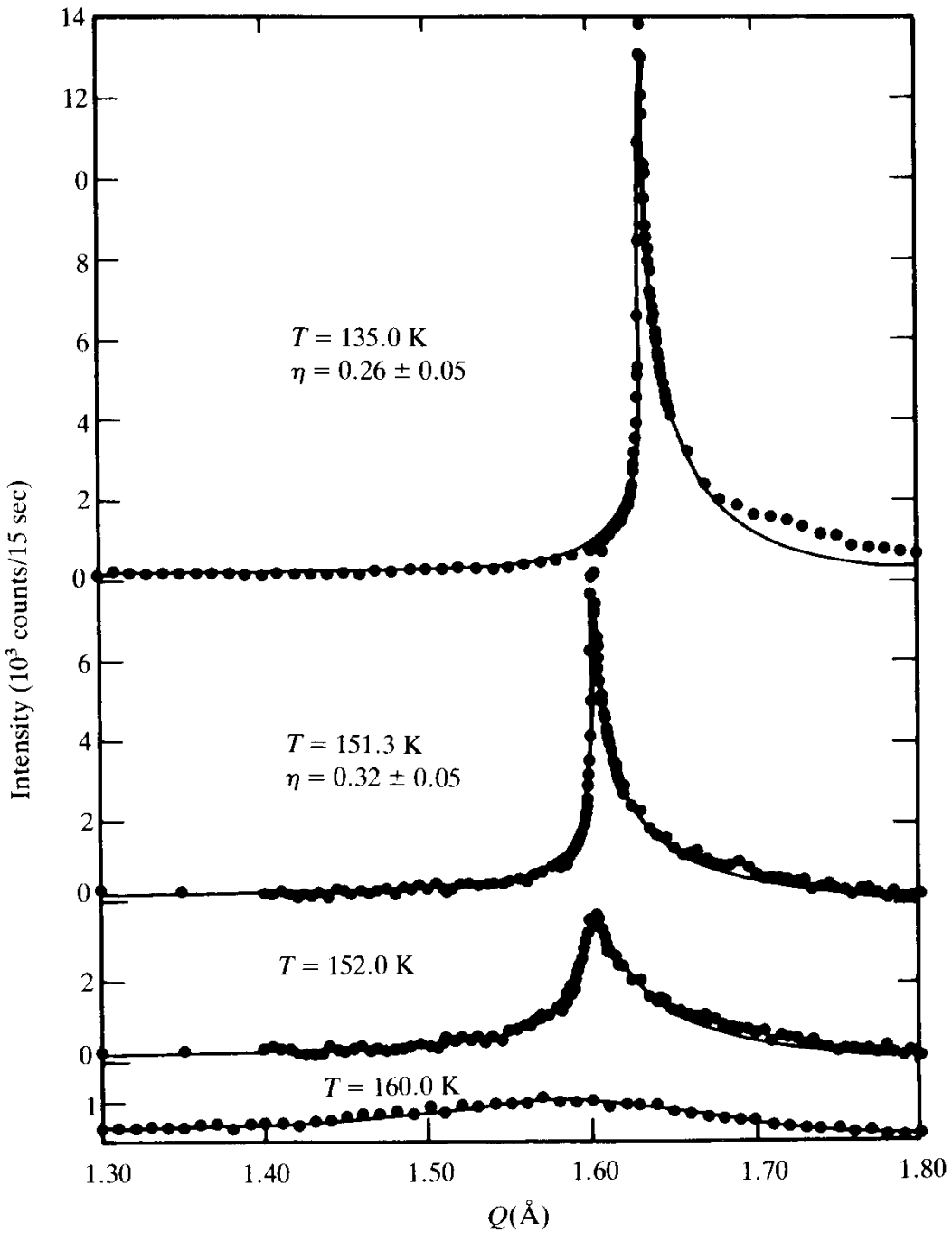

so that $a \equiv v^{1/3} = a_0/2^{1/3}$ and the nearest neighbour distance is $d = (a_0/2)\sqrt{3} = v^{1/2}(\sqrt{3}/2^{2/3}) \approx 1.0911\,a$. With $r_0 \equiv ((3/4\pi)\,v)^{1/3} = (3/4\pi)^{1/3}\,a$ we also have $d = 1.76\,r_0$.

In an f.c.c. lattice

$$\mathbf{a}_1 = \frac{a_0}{2}(\hat{\mathbf{y}} + \hat{\mathbf{z}}), \quad \mathbf{a}_2 = \frac{a_0}{2}(\hat{\mathbf{z}} + \hat{\mathbf{x}}), \quad \mathbf{a}_3 = \frac{a_0}{2}(\hat{\mathbf{x}} + \hat{\mathbf{y}}), \qquad (7A.3)$$

FIG. 7.13. The specific heat data of ^{4}He films on grafoil as found by Bretz et al. (1973) (op. cit. in the Notes and References).

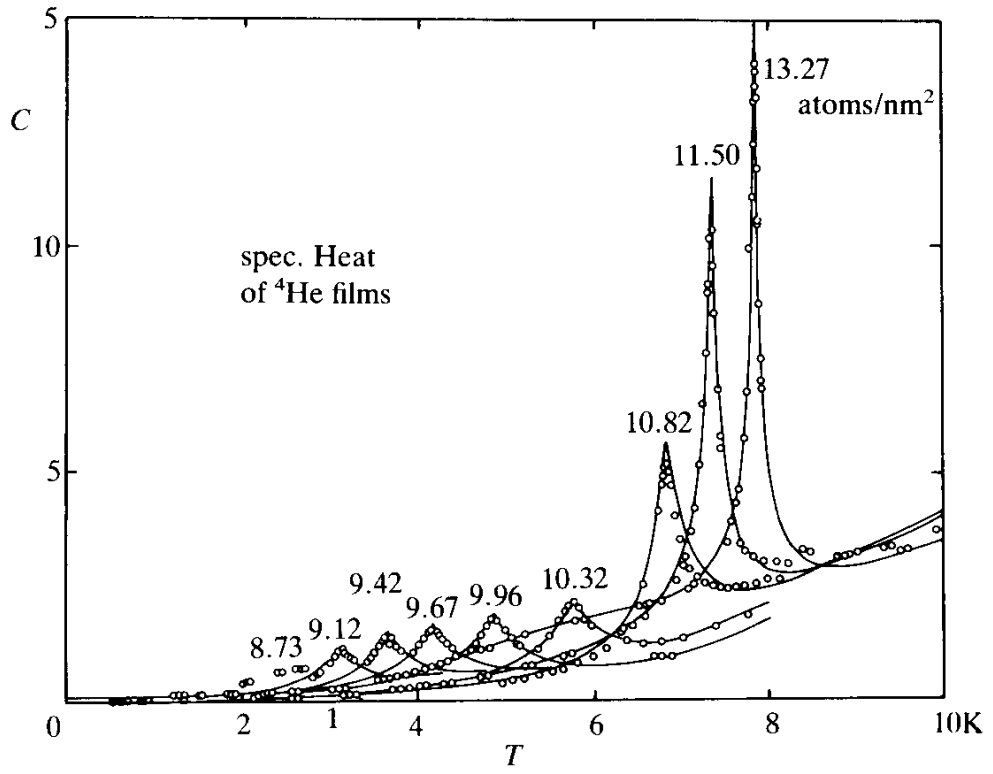

so that $v = a_0^3/4$ and $v^{1/3} = a = a_0/4^{1/3}$. The nearest neighbour distance is $d = a_0/\sqrt{2} = v^{1/3}(4^{1/3}/\sqrt{2}) \approx 1.1225\,a \sim 1.81\,r_0$. The reciprocal basis of an f.c.c. (b.c.c.) lattice is a b.c.c. (f.c.c.) lattice with $a_0^{\text{rec}} = 4\pi/a_0$ and a volume $(2\pi)^3/v = (2\pi/a)^3$ so that $a^{\text{rec}} = 2\pi/a$. Hence the smallest reciprocal lattice vectors of a b.c.c. lattice have a length $d_1^{\text{rec}} = (4^{1/3}/\sqrt{2})a^{\text{rec}} = (\sqrt{3/2})(2\pi/d) = 1.1225(2\pi/a)$ while those of an f.c.c. lattice have $d_1^{\text{rec}} = (\sqrt{3}/2^{2/3})a^{\text{rec}} = (\sqrt{3/2})(2\pi/d) = 1.0911(2\pi/a)$.

APPENDIX 7B. FREQUENCY DISTRIBUTIONS

For a general spectrum $\omega_h^2(\mathbf{k})$, the frequency distribution may be calculated as follows:

$$g^{(h)}(\omega) = \frac{2\omega}{V}\sum_{\mathbf{k}} \delta(\omega^2 - \omega_h^2(\mathbf{k})). \tag{7.B1}$$

By integrating this over ω it is obvious that it has the correct

normalization (7.27). We now observe that the right-hand side can be rewritten as

$$g^{(h)}(\omega) = \frac{N}{V}\frac{2\omega}{\pi}\operatorname{Im}\frac{1}{N}\sum_{\mathbf{k}}\frac{1}{-\omega^2 - i\varepsilon + \omega_h^2(\mathbf{k})}, \tag{7.B2}$$

where ε is an infinitesimal positive number. This implies that $g^{(h)}(\omega)$ can be obtained from the Green function $v_m^{(h)}(\mathbf{0})$ at the origin,

$$v_m^{(h)}(\mathbf{0}) \equiv \frac{1}{N}\sum_{\mathbf{k}}\frac{1}{m^2 + \omega_h^2(\mathbf{k})}, \tag{7.B3}$$

by an analytic continuation in the square mass m^2 to

$$m^2 = -\omega^2 - i\varepsilon \tag{7.B4}$$

and taking the imaginary part, i.e.,

$$g^{(h)}(\omega) = \frac{N}{V}\frac{2\omega}{\pi}\operatorname{Im} v_m^{(h)}(\mathbf{0})\Big|_{m^2 = -\omega^2 - i\varepsilon}. \tag{7.B5}$$

As an example, take the one-dimensional case where for lattice space $a = 1$ [see Part I, Eq. (6.184)],

$$v_m(\mathbf{0}) = [(m^2 + 2)^2 - 4]^{1/2}, \tag{7.B6}$$

so that

$$g(\omega) = \frac{N}{V}\frac{2}{\pi}\frac{1}{\sqrt{4 - \omega^2}}. \tag{7.B7}$$

On a square lattice we can use Eq. (6.134) of Part I,

$$v_m(\mathbf{0}) = \frac{1}{m^2 + 4}\frac{2}{\pi}K\left(\frac{1}{(1 + m^2/4)^2}\right), \tag{7.B8}$$

where $K(z)$ is the elliptic integral $\int_0^{\pi/2} d\theta(1 - z\sin^2\theta)^{-1/2}$, and find for a

mode with a lattice spectrum $\omega_n^2 = 2(1 - \cos k_1) + 2(1 - \cos k_2)$

$$g(\omega) = \frac{4\omega}{\pi^2\sqrt{4-\omega^2}} K\left(\frac{16}{\omega^2(4-\omega^2)}\right), \quad \omega^2(4-\omega^2) > 16,$$

$$= \frac{\omega}{\pi^2} K\left(\frac{\omega^2(4-\omega^2)}{16}\right), \qquad 0 < \omega^2(4-\omega^2) < 16, \quad \text{(7.B9)}$$

For a three dimensional simple cubic lattice we have to replace ω^2 by $\omega^2 - 2(1 - \cos k)$ and do one more integral over $\int_{-\pi/2}^{\pi/2} dk/2\pi$. Plots of these functions can be found in the book by Maradudin *et al.* [see Notes and References).

Similarly, we can use the Green functions of b.c.c., and f.c.c. lattices in Part I, Eqs. (6A.43), (6A.46) to calculate explicitly the associated frequency distributions.

NOTES AND REFERENCES

Experimental data on the melting transition are reviewed by
G. Borelius, *Solid State Physics* **15** (1963) 2.
The entropy and volume jumps upon melting are given by
M. Lasocka, *Phys. Lett.* **51A** (1975) 137 [his ΔS is given in units of cal/(K · mole), while we use $R = 8.314$, J/(K · mole) = 1.987 cal/(K · mole)].
See also
J.L. Tallon, *Phys. Lett.* **76A** (1980) 139.
The specific heat at constant volume is given in
G. Grimwall, *Physica Scripta* **11** (1975) 381
using data on the isothermal compressibility $\varkappa$ and on the thermal expansion α and the formula $c_p - c_v = \alpha^2 T/\varkappa$.

The Lindemann criterium was given in
E.A. Lindemann, *Z. Phys.* **11** (1910) 609.
He worked with polycrystals in the Einstein approximation to the specific heat. Further studies were made by
E. Grüneisen, *Ann. d. Phys.* **39** (1912) 257.
Lindemann's approach was improved, using experimental data at melting points by
J.J. Gilvarry, *Phys. Rev.* **102** (1956) 308, **103** (1956) 1700, **104** (1956) 909.

Lattice dynamics was used, taking numeric solutions of the secular equations at room temperature, by
A.K. Singh and P.K. Sharma, *Can. J. Phys.* **46** (1968) 1677.
A semi-analytic calculation, using the moment trace method of

E.W. Montroll, *J. Chem. Phys.* **10** (1942) 218, **11** (1943) 481, to calculate $g(\omega)$, was employed by
J.N. Shapiro, *Phys. Rev.* **B1** (1970) 3982.
Our values in columns 3 and 4 of Table 7.4 are from this reference.

Other early studies of the melting process are found in
W. Brauneck, *Z. Phys.* **38** (1926) 549 (instability of optical vibrations),
N.V. Raschevsky, *ibid* **40** (1927) 214 (instability of a particle under action of its neighbours),
K. Herzfeld and M. Goeppert-Mayer, *Phys. Rev.* **46** (1934) 995 (pressure minimum with respect to changes in volume),
M. Born, *J. Chem. Phys.* **7** (1939) 591 (collapse of shear stresses.
In this context, see also the more recent papers by
H. Fukuyama and P. Platzmann, *Sol. St. Commun.* **15** (1974) 677,
L. Boyer, *Phys. Rev. Lett.* **26** (1979) 584, **45** (1980) 1858,
J.E. Lennard-Jones and A.F. Devonshire, *Proc. Roy. Soc.* **A169** (1939) 317, **A170** (1939) 464 (here melting appears as an order-disorder transition, a crystal being an alloy of atoms and vacancies: the disadvantage is that the melt carries memory of crystalline positions),
J.A. Pople and F.E. Karasz, *J. Phys. Chem. Solids,* **18** (1961) 28, **20** (1961) 294 (like the previous one, but including two orientational degrees of freedom),
J.G. Kirkwood and E. Monroe, *J. Chem. Phys.* **9** (1941) 514 (disappearance of periodic Fourier components in density distribution),
K.K. Kobayashi, *Mol. Cryst. Liqu. Cryst.* **13** (1971) 137, *Phys. Lett.* **A31** (1970) 125, *J. Phys. Soc.* Japan **29** (1970) 101 (like the previous, but including orientational order),
G. Tamman, *Z, Phys. Chemie* **68** (1910) 205,
M. Volmer, O. Schmidt, *Z. Phys. Chemie* **35** (1937) 467,
I.N. Stranski, *Naturw.* **30** (1942) 425 (melting as a destruction of crystal starting from the surface).

Experimental data on the softening of the elastic constants can be found in many textbooks. The example in the text for Ag is taken from
J.R. Neighbors and G.A. Alers, *Phys. Rev.* **111** (1958) 767.
For Mo and W see D.I. Bolef, J. De Klerk, *J. Appl. Phys.* **33** (1962) 2311.
For Mo, W, Ta see F.A. Featherston, J.R. Neighbors, *Phys. Rev.* **130** (1963) 132.
For Al G.N. Kamm, G.A. Alen, *J. Appl. Phys.* **35** (1964) 327.
The specific heat of constant volume was given by
G. Grimwall, *Physica Scripta* **11** (1975) 381,
using data on isothermal compressibility $\varkappa = \kappa^{-1}$ and on thermal expansion α and the formula $c_p - c_V = \alpha^2 T/\varkappa$.
The Lindemann numbers are tabulated in
A.R. Ubbelohde, *The Molten State of Matter* (John Wiley and Sons, New York, 1978).
A.A. Maradudin, E.W. Montroll, G.H. Weiss, I.D. Ipatova, "Theory of Lattice Dynamic in the Harmonic Approximation", in *Solid State Physics* Suppl. 3, ed. H. Ehrenreich, F. Seitz and D. Turnbull (Academic, New York, 1971).

Nonlinear elasticity is discussed in
F.D. Murnaghan, *Am. J. Math.* **49** (1937) 235,
F. Birch, *Phys. Rev.* **71** (1947) 809.
The low temperature effect of the nonlinear terms can be found in
J.M. Ziman, *Electrons and Phonons* (Clarendon, Oxford, 1960),
M. Born and K. Huang, *Dynamical Theory* of *Crystal Lattices* (Clarendon, Oxford, 1954).
The softening of the elastic constants is further discussed in
H. Fukuyama, P.M. Platzmann, *Sol. St. Comm.* **15** (1974) 677 ($D = 3$),
P. Platzmann and H. Fukuyama, *Phys. Rev.* **B10** (1974) 3150.
See also

F.M. Peeters and P.M. Platzmann, *Phys. Rev. Lett.* **50** (1983) 2021.

The phase diagrams of solid and liquid ^{3}He and ^{4}He at low pressure and temperatures can be found in
C.M. Varma and N.R. Werthammer, in *The Physics of Liquid and Solid He Vol. II*, ed. K.H. Bennemann and J. B. Ketterson (John Wiley and Sons New York, 1978) p. 505.
The sound velocity in hcp and bcc solid ^{4}He can be taken from the review article by D.L. Price, *ibid*, Vol. II, p. 691 or p. 693.
The Debye theory of specific heat can be found in most textbooks on solid state physics; for example in
N.W. Ashcroft and N.D. Mermin, *Solid State Physics* (Holt, Rinehart and Winston, New York, 1978),
G. Busch and H. Schade, *Vorlesungen über Festkörperphysik* (Birkhäuser Verlag, Stuttgart, 1973).

For two-dimensional layers of ^{4}He on grafoil, the Debye temperatures were measured and the melting transition was first observed by
M. Bretz, J.G. Dash, D.C. Hichernell, E.O. McLean, O.E. Vilches, *Phys. Rev.* **A8** (1973) 1589, **A9** (1974) 2814.
See also
R.L. Elgin and D.L. Goodstein, *Phys. Rev.* **A9** (1974) 2657
For layers of ^{3}He see
S.V. Hering, O.E. Vilches, in *Monolayer and Submonolayer Helium Films*, ed. J.G. Daunt, E. Lerner (Plenum Press, New York, 1973) p. 1,
S.V. Hering, S.W. van Sciver, D.L. Goodstein, *J. Low Temp. Phys.* **25** (1976) 793,
J.G. Dash, *Films on Solid Surfaces* (Academic Press, New York, 1975)
Two-dimensional melting for layers of Xenon on grafoil was measured by
D.A. Heiney, R.J. Birgeneau, G.S. Brown, P.M. Hari, D.E. Moncton, and P.W. Stephens, *Phys. Rev. Lett.* **48** (1982) 106.
Argon and Krypton were studied by
J.P. McTague, J. Als-Nielsen, J. Bohr, and M. Nielsen, *Phys. Rev.* **B25** (1982) 7765,
R.J. Birgeneau, E.M. Hammons, P. Heiney, and P.W. Stephens, in *Ordering in Two Dimensions*, ed. S.K. Sinha (Elsevier, New York, 1980).
Other atoms (CD_4):
S.K. Sinha, P. Vora, P. Dutta, L. Pasell, *J. Phys.* **C15** (1975) L275.
Computer simulations were done by
S.W. Koch and F.F. Abraham, *Phys. Rev.* **B27** (1983) 2964,
S. Toxwaerd, *Phys. Rev. Lett.* **44** (1980) 1002,
R.K. Kalia and P. Vashinshta, *J. Phys.* **C14** (1981) L643.
For a popular review article see also
W.F. Brinkmann, D.S. Fisher, D.E. Moncton, *Science* **217** (1982) 693.
The Debye temperature (two-dimensional layers) can be found in
J.G. Dash and M. Schick, *The Physics of Liquid and Solid Helium, Vol. II*, eds K. Bennemann and J.B. Ketterson p. 550 (as a function of the density from 0.8 atoms to 1.2 atoms per 10 Å^2).
The melting transition was studied via computer simulations of the molecular dynamics in 2 dimensions by
R.M.J. Cotterill, L.B. Pedersen, *Solid State Commun.* **10** (1972) 439 (1972) (Lennard-Jones system),
F.F. Abraham, *Rep. Prog. Phys.* **45** (1982) 1113 and, in *Ordering in Two Dimensions*, ed. S.K. Sinha (North Holland, New York, 1980) p. 155 (Lennard-Jones system),
J. Tobochnik and G.V. Chester, *ibid.*, p. 339 (Lennard — Jones system),
J.P. Tague, D. Frenkel, M.P. Allen, *ibid*, p. 147 (r^{-6} potential)

S. Toxvaerd, *Phys. Rev. Lett.* **44** (1980) 1002,
and in three dimensions by
R.M.J. Cotterill, E.J. Jensen and W. Damgaard-Kistensen, *Phil. Mag.* **30** (1974) 245,
R.J.M. Cotterill, *Phys. Lett.* **44A** (1973) 127.
W.L. Slattery, G.D. Dolen, H.E. DeWitt, *Phys. Rev.* **A26** (1982) 2255 (Wigner lattice of electrons).
More details on 2*D* melting will be given in Chapter 14.

CHAPTER EIGHT

FIRST ATTEMPT AT A DISORDER FIELD THEORY OF DEFECT MELTING

The Lindemann criterion gave us some important information on the nature of the melting transition: the transition occurs at a temperature slightly below which the atoms still perform, to a very good approximation, harmonic fluctuations about their mean positions. The nonlinearities of the interatomic potential are not very important. They merely provide a shift in the mean position and a softening of the elastic constants. If these two effects are taken into account, the crystal, even right below the melting temperature, can be treated practically as an ideal crystal. Defects are quite rare, due to their high energy, and we can describe the interactions of defect lines by the methods developed in the previous chapters.

As we approach the melting temperature, the situation changes abruptly. All of a sudden, the crystalline order breaks down. In analogy with the superfluid phase transition we set for ourselves the goal of describing this breakdown by the condensation of defect lines. In the following chapters we shall try and follow the historical development which ultimately led to the lattice models to be described in Chapters 9–13. The disorder field theory which will arise in the course of the present chapter will not be used later on. The insights gained in this discussion will put us in a better position to appreciate the properties of these models.

The practically minded reader is therefore advised to skip this chapter and turn directly to Chapter 9.

8.1. DISORDER FIELDS OF DISLOCATION LINES

Let us begin by studying fluctuating ensembles of dislocation lines. We proceed in complete analogy with the vortex lines of Chapter 2, Part II.

The elastic energy of N lines $L^{(i)}$, $i = 1, \ldots, N$ with Burgers' vectors $b_\ell^{(i)}$ is given by (3.42):

$$E_{\text{Blin}} = \frac{\mu}{8\pi} \sum_{i,j} \oint_{L^{(i)}} \oint_{L^{(j)}} \times \left[(\mathbf{b}^{(i)} \cdot d\mathbf{x}^{(i)})(\mathbf{b}^{(j)} \cdot d\mathbf{x}^{(j)})/R - 2(\mathbf{b}^{(i)} \times \mathbf{b}^{(j)}) \cdot (d\mathbf{x}^{(i)} \times d\mathbf{x}^{(j)})/R + \frac{1}{1-\nu} (\mathbf{b}^{(i)} \times d\mathbf{x}^{(i)})_\ell (\mathbf{b}^{(j)} \times d\mathbf{x}^{(j)})_n \partial_\ell \partial_n R \right]. \tag{8.1}$$

This formula was based on the laws of linear elasticity which are valid for large distances between the lines.

In the near-zone around each line, nonlinear effects become important. Just as in the superfluid, these are difficult to calculate. We shall assume that they can be parametrized approximately by a core energy of the form

$$E_{\text{core}} = \sum_{i=1}^{N} \left(e_c \int_{L^{(i)}} ds^{(i)} + e_c' \int_{L^{(i)}} d\mathbf{x}^{(i)} \cdot \hat{\mathbf{b}}^{(i)} \right), \tag{8.2}$$

where $e_c^T \equiv e_c'$ is the energy per unit length of an edge dislocation (which has $d\mathbf{x} \perp \hat{\mathbf{b}}$) and $e_c^L \equiv e_c + e_c'$ that of a screw dislocation (which has $d\mathbf{x} \parallel \hat{\mathbf{b}}$, $\hat{\mathbf{b}} \equiv \mathbf{b}/|\mathbf{b}|$). The total partition function to be calculated is

$$Z = \sum_N \frac{1}{N!} \sum_{\{L\}} \exp\left\{ -\frac{1}{T} (E_{\text{Blin}} + E_{\text{core}}) \right\}. \tag{8.3}$$

As in Chapter 2, Part II, we shall proceed in two steps and suppose first that there is no elastic energy. We shall also assume, for a moment, that the parameters e^T and e^L are equal. Then it is straightforward to write down a disorder field theory for Z, in analogy with Eq. (2.3) of Part II:

$$Z = \int \mathscr{D}\varphi\, \mathscr{D}\varphi^{\dagger} \times \exp\left\{ -\int d^3x \left[\sum_b \left(\frac{1}{2} |\partial_\ell \varphi_b|^2 + \frac{m^2}{2} |\varphi_b|^2 \right) + \sum_{b,b'} \frac{g_{bb'}}{4} \; |\varphi_b|^2 |\varphi_{b'}|^2 \right] \right\}. \tag{8.4}$$

The mass is given by

$$m^2 = \left(\frac{\varepsilon_c^T}{T} - \log 2D \right) \frac{2D}{a^2}, \tag{8.5}$$

with $\varepsilon_c^T = e_c^T \cdot a$ being the energy per link. The sum over $b = 1, \ldots, n$ accounts for the fundamental Burgers vectors. We have initially assumed a quartic short range interaction which is purely phenomenological and whose precise form is unknown. It has to satisfy an important fundamental physical property: when dislocation lines interact with each other, the Burgers vectors are conserved just like electric charges (recall the discussion in Section 2.9 on branching defect lines). The corresponding property of the disorder field theory is that it is invariant under the *global* phase rotations,

$$\varphi_b(\mathbf{x}) \to e^{i\gamma_\ell b_\ell} \varphi_b(\mathbf{x}). \tag{8.6}$$

This is why we wrote the interaction immediately in the form $\Sigma_{b,b'} (g_{bb'}/4)|\varphi_b|^2 |\varphi_{b'}|^2$. The coupling matrix $g_{bb'}$ is further restricted by cubic symmetry. This permits only two independent matrix elements and we can parametrize the energy density as

$$e(\mathbf{x}) = \sum_b \left[\frac{1}{2} |\partial_\ell \varphi_b|^2 + \frac{m^2}{2} |\varphi_b|^2 \right] + \frac{g_1}{4} \left(\sum_{b=1}^{n} |\varphi_b|^2 \right)^2 + \frac{g_2}{4} \sum_{b=1}^{n} |\varphi_b|^4. \tag{8.7}$$

8.2. FLUCTUATION INDUCED FIRST-ORDER TRANSITION

Let us study the partition function associated with this energy. It is useful to view the complex field φ_b as a special case of a general $n \cdot q$ component field φ_i^α with $i = 1, \ldots n$, $\alpha = 1, \ldots, q$ and a field energy

$$e(\mathbf{x}) = \sum_{(i,\alpha)=1,1}^{(n,q)} \left[\frac{1}{2}(\partial_\ell \varphi_i^\alpha)^2 + \frac{m^2}{2}(\varphi_i^\alpha)^2\right] + \frac{g_1}{4}\left(\sum_{(i,\alpha)=1,1}^{(n,q)} (\varphi_i^\alpha)^2\right)^2 + \frac{g_2}{4}\sum_{i=1}^{n}\left(\sum_{\alpha=1}^{q}(\varphi_i^\alpha)^2\right)^2. \tag{8.8}$$

This is invariant under $O(q)$ rotations of the indices α and has a symmetry under the cubic point group in the indices i which count the different fundamental Burgers vectors.

Theories of this type have been discussed in the literature in great detail (see the Notes and References). They are used to illustrate the possibility that fluctuations may induce a full $O(n \cdot q)$ symmetry between all $n \cdot q$ components of φ_i^α. What is more important in the present context is that these field theories are also examples of a further type of fluctuation-induced first-order transition, similar to the one we had encountered previously in Section 3.11 in a superconductor for which the crucial fluctuation role was played by gauge fields. Let us recapitulate some of the well-known features of a field with energy (8.8) which could be relevant for our purposes. For simplicity, we shall first focus attention upon the simplest prototype of a field with arbitrary n and $q = 1$ at the mean-field level. Its energy is

$$e(\mathbf{x}) = \sum_{i=1}^{n}\left[\frac{1}{2}(\partial_\ell \varphi_i)^2 + \frac{m^2}{2}\varphi_i^2\right] + \frac{g_1}{4}\left(\sum_{i=1}^{n}\varphi_i^2\right)^2 + \frac{g_2}{4}\sum_{i=1}^{n}\varphi_i^4. \tag{8.9}$$

For $m^2 < 0$, the fields acquire non-zero expectation values. Their properties depend on the values of g_1, g_2. For $g_2 = 0$, $g_1 > 0$, the energy is invariant under n-dimensional rotations of the components $(\varphi_1, \ldots, \varphi_n)$, and the ground state is degenerate with respect to these rotations, with a field expectation value

$$\varphi = \sqrt{\sum_{i=1}^{n}\varphi_i^2} = \sqrt{-\frac{m^2}{g_1}}. \tag{8.10}$$

For $n = 2$, this ground state is the same as the ordered state in the $O(2)$ symmetric field theory of superfluid ^{4}He (or the XY model). If $g_2 < 0$, and $g_1 > -g_2$ the energy loses its isotropy and the ground state can no longer point along an arbitrary direction in the $O(n)$ field space but must select one of the three directions along the field axes, say,

$$\varphi_i = \varphi \delta_{i,1} = \sqrt{-\frac{m^2}{g_1 + g_2}}\,\delta_{i,1}. \tag{8.11}$$

If $g_2 > 0$, and $g_1 > -g_2/n$ the expectation value is diagonal in field space,

$$\varphi_i \equiv \frac{\varphi}{\sqrt{n}} = \frac{1}{\sqrt{n}} \sqrt{-\frac{m^2}{g_1 + g_2/n}}. \tag{8.12}$$

In the three cases, the ground state energy is given by the minima of the potentials which are

$$\begin{aligned} v_{g_2=0} &= \frac{m^2}{2}\varphi^2 + \frac{g_1}{4}\varphi^4 = -\frac{m^4}{4g_1}, \\ v_{g_2<0} &= \frac{m^2}{2}\varphi^2 + \frac{g_1 + g_2}{4}\varphi^4 = -\frac{m^4}{4(g_1 + g_2)}, \\ v_{g_2>0} &= \frac{m^2}{2}\varphi^2 + \frac{g_1 + g_2/n}{4}\varphi^4 = -\frac{m^4}{4(g_1 + g_2/n)}. \end{aligned} \tag{8.13}$$

These ground states exist only as long as g_1 and g_2 satisfy the conditions

$$g_1 + g_2 > 0, \qquad g_1 + g_2/n > 0. \tag{8.14}$$

These define what is called the *stability wedge* in the coupling constant plane (see Fig. 8.1). For each point within the wedge, there is a second order phase transition as m^2 passes through zero.[a]

We shall now convince ourselves that along the boundary of the stability wedge, and in some neighborhood thereof, fluctuations change the order of the transition from second to first. For this we calculate the one-loop effective potential. According to the rules spelled out in Part I, Section 5.3, this is given by [recall Eq. (I. 5.23)]

$$\begin{aligned} v(\Phi_i) = {} & \frac{m^2}{2}\sum_{i=1}^{n}\Phi_i^2 + \frac{g_1}{4}\left(\sum_{i=1}^{n}\Phi_i^2\right)^2 + \frac{g_2}{4}\sum_{i=1}^{n}\Phi_i^4 \\ & + \frac{1}{2}\int \frac{d^D p}{(2\pi)^D}\,\mathrm{tr}\log\left[(p^2 + m^2)\,\delta_{ij} + \frac{\partial^2 e}{\partial\Phi_i \partial\Phi_j}\right], \end{aligned} \tag{8.15}$$

[a]Notice that if we were to keep $g_1 > 0$ fixed and let g_2 pass through zero, the order parameter of the system would develop a discontinuity.

FIG. 8.1. The stability wedge in the coupling constant plane and the phases associated with the different regimes at the mean-field level. The axes $g_2 = 0$ and $g_1 = 0$ correspond to an $O(n)$ symmetric and a product of n Ising models, respectively and display the corresponding critical behavior.

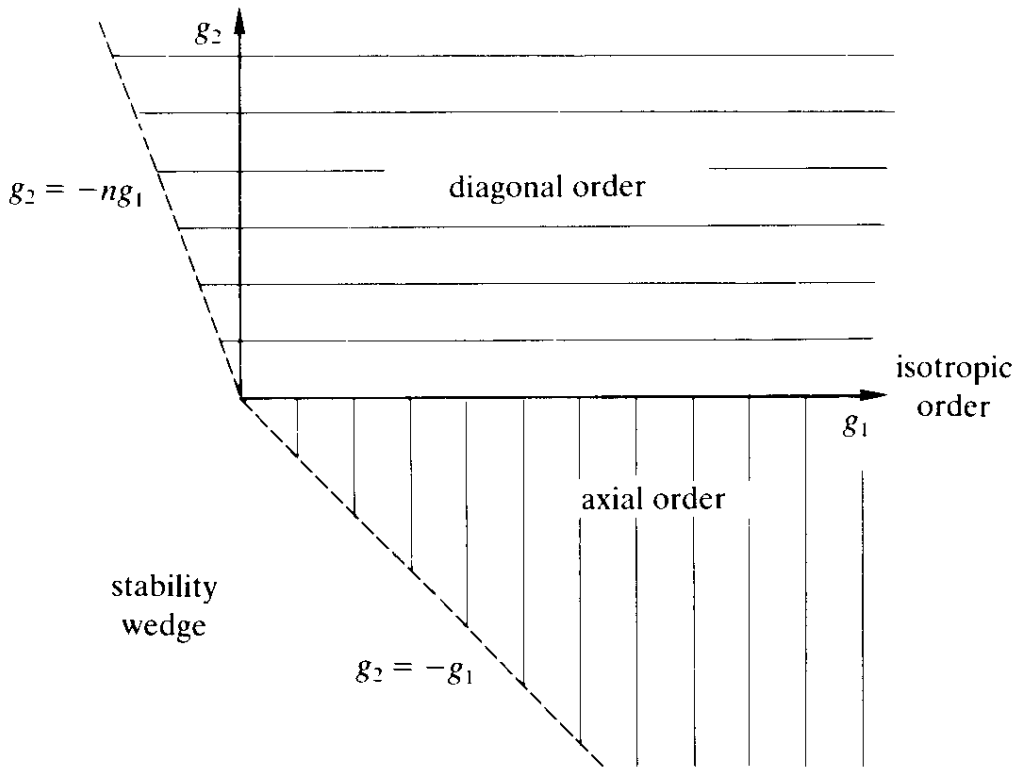

where Φ_i is the ground state expectation of the field φ_i [i.e., $\Phi_i \equiv \langle \varphi_i \rangle$]. In order to calculate the trace of the logarithm, all we have to do is to find the n eigenvalues M_i^2 of the "mass" matrix,

$$M_{ij}^2 = \frac{\partial^2 e}{\partial \Phi_i \partial \Phi_j} \tag{8.16}$$

and we can write directly

$$v(\Phi_i) = \frac{m^2}{2} \sum_{i=1}^{n} \Phi_i^2 + \frac{g_1}{4} \left(\sum_{i=1}^{n} \Phi_i^2 \right)^2 + \frac{g_2}{4} \sum_{i=1}^{n} \Phi_i^4 + \frac{1}{2} \sum_{i=1}^{n} \int \frac{d^D p}{(2\pi)^D} \log(p^2 + m^2 + M_i^2). \tag{8.17}$$

Explicitly, we have

$$M_{ij}^2 = g_1 \left(2\Phi_i \Phi_j + \delta_{ij} \sum_k \Phi_k^2 \right) + 3g_2 \delta_{ij} \Phi_i^2. \tag{8.18}$$

The eigenvalues depend on the state under consideration. Consider first the case $g_2 < 0$ with the "axial" ground state

$$\Phi_i = \Phi \delta_{i,1}. \tag{8.19}$$

Then

$$M_{ij}^2 = [g_1(2\delta_{i1}\delta_{j1} + \delta_{ij}) + 3g_2\delta_{i1}\delta_{j1}]\Phi^2. \tag{8.20}$$

This matrix has one eigenvalue, namely $3(g_1 + g_2)\Phi^2$ and $n-1$ degenerate eigenvalues $g_1\Phi^2$. Hence the effective potential reads

$$v(\Phi) = \frac{m^2}{2}\Phi^2 + \frac{g_1 + g_2}{4}\Phi^4 + \frac{1}{2}\int \frac{d^D p}{(2\pi)^D}[\log(p^2 + m^2 + 3(g_1 + g_2)\Phi^2) + (n-1)\log(p^2 + m^2 + g_1\Phi^2)]. \tag{8.21}$$

In the "diagonal" state

$$\Phi_i \equiv \frac{\Phi}{\sqrt{n}}, \tag{8.22}$$

the matrix M_{ij}^2 reads

$$M_{ij}^2 = \left[g_1\left(\frac{2}{n} + \delta_{ij}\right) + 3\frac{g_2}{n}\delta_{ij}\right]\Phi^2. \tag{8.23}$$

This has one longitudinal eigenvalue $3(g_1 + g_2/n)$ [asociated with the direction $(1, 1, \ldots, 1)$], and $n-1$ transverse ones $g_1 + 3g_2/n$ [associated with the directions $(1, -1, 0, \ldots, 0)$, $(1, 0, -1, 0, \ldots, 0)$, $\ldots$]. Thus the effective potential reads

$$v(\Phi) = \frac{m^2}{2}\Phi^2 + \frac{g_1 + g_2/n}{4}\Phi^4 + \frac{1}{2}\int \frac{d^D p}{(2\pi)^D}[\log(m^2 + 3(g_1 + g_2/n)\Phi^2) + (n-1)\log(m^2 + (g_1 + 3g_2/n)\Phi^2)]. \tag{8.24}$$

It is now easy to verify that close to the boundary of the stability wedge, the fluctuations indeed change the second-order of the phase transition into a first-order. Along the boundaries $g_1 + g_2 = 0$ and $g_1 + g_2/n = 0$, the potentials (8.21), (8.24) reduce (up to a trivial constant shift) to

$$v(\Phi) = \frac{m^2}{2}\Phi^2 + \frac{n-1}{2}\int \frac{d^D p}{(2\pi)^D} \log(p^2 + m^2 + g_1\Phi^2), \tag{8.25}$$

$$v(\Phi) = \frac{m^2}{2}\Phi^2 + \frac{n-1}{2}\int \frac{d^D p}{(2\pi)^D} \log\left(p^2 + m^2 + \frac{2g_2}{n}\Phi^2\right), \tag{8.26}$$

respectively, where in either expression g_1 and g_2 are positive quantities. The momentum space integrals in three dimensions were calculated before in Part I [Eq. (3.106)]. If Λ denotes the spherical cut-off in momentum space, we obtain

$$v(\Phi) = \frac{m^2}{2}\Phi^2 + \frac{n-1}{2}\frac{1}{6\pi^2} \times \left\{\left(\Lambda^3 \log\Lambda^2 - \frac{2}{3}\Lambda^3 + 3\Lambda m^2\right) + 3\Lambda(m^2 + g_1\Phi^2) - \pi(m^2 + g_1\Phi^2)^{3/2}\right\}, \tag{8.27}$$

with g_1 replaced by $2g_2/n$ in the second case, (8.26). This shows that, apart from a trivial additive shift of the potential, the fluctuations change the mass to the renormalized value $m_R^2 = m^2[1 + (n-1)(g_1/6\pi^2)3\Lambda]$ and produce an additional term $-((n-1)/2)(1/6\pi)(m^2 + g_1\Phi^2)^{3/2}$. This latter term destabilizes the potential. Hence the potential remains truly stable only *inside* the stability wedge.

Consider the immediate neighborhood of the lower boundary and set $g_1 + g_2 = \varepsilon$. Then the potential (8.21) becomes

$$\begin{aligned} v(\Phi) = {} & \frac{m^2}{2}\Phi^2 + \frac{\varepsilon}{4}\Phi^4 + \frac{n}{2}\frac{1}{6\pi^2}\left[\Lambda^3 \log\Lambda^2 - \frac{2}{3}\Lambda^3 + 3\Lambda m^2\right] \\ & + \frac{1}{2}\frac{1}{6\pi^2}3\Lambda[(m^2 + 3\varepsilon\Phi^2) + (n-1)(m^2 + g_1\Phi^2)] \\ & - \frac{1}{2}\frac{1}{6\pi}[(m^2 + 3\varepsilon\Phi^2)^{3/2} + (n-1)(m^2 + g_1\Phi^2)^{3/2}]. \end{aligned} \tag{8.28}$$

In order to proceed it is useful to include into the potential a further infinite number of loop diagrams which are trivial to do, namely, those which change the value of m^2 inside the terms $(m^2 + 3\varepsilon\Phi^2)^{3/2}$,

$(m^2 + g_1\Phi^2)^{3/2}$ to the renormalization value m_R^2. This is achieved by rewriting the original field energy (8.9) as

$$e(\mathbf{x}) = \sum_{i=1}^{n}\left[\frac{1}{2}(\partial_i\varphi_i)^2 + \frac{m_R^2}{2}\varphi_i^2\right] + \frac{g_1}{4}\left(\sum_{i=1}^{n}\varphi_i^2\right)^2 + \frac{g_2}{4}\sum_{i=1}^{n}\varphi_i^4 + \frac{m^2 - m_R^2}{2}\sum_{i=1}^{n}\varphi_i^2 \tag{8.29}$$

and considering the term $\frac{1}{2}(m^2 - m_R^2)\Sigma_i\varphi_i^2$ as a mass perturbation. Thus we calculate the effective potential only for the first three terms and find the expression (8.25), but with m^2 replaced by m_R^2. Then we add the mean field part of the mass perturbation $\frac{1}{2}(m^2 - m_R^2)\Phi^2$ which removes the terms $\frac{1}{2}(n-1)(1/6\pi^2)3\Lambda(3\varepsilon\Phi^2 + (n-1)g_1\Phi^2)$. Thus, up to a trivial constant shift, we can write the potential as

$$v(\Phi) = \frac{m_R^2}{2}\Phi^2 + \frac{\varepsilon}{4}\Phi^4 - \frac{1}{2}\frac{1}{6\pi}[(m_R^2 + 3\varepsilon\Phi^2)^{3/2} + (n-1)(m_R^2 + g_1\Phi^2)^{3/2} - nm_R^3]. \tag{8.30}$$

We have normalized $v(\Phi)$ so that it vanishes at zero field, $\Phi = 0$.

We are now ready to see the first-order of the transition. We set $m_R^2 = 0$ and observe that the potential

$$v(\Phi)_{m_R^2=0} = \frac{\varepsilon}{4}\Phi^4 - \frac{1}{2}\frac{1}{6\pi}[(3\varepsilon\Phi^2)^{3/2} + (n-1)(g_1\Phi^2)^{3/2}] \tag{8.31}$$

has a minimum away from the field origin at

$$\Phi_{\min} = \frac{1}{4\pi\varepsilon}[(3\varepsilon)^{3/2} + (n-1)g_1^{3/2}] \equiv \frac{a}{\varepsilon}, \tag{8.32}$$

where v is *negative*:

$$v(\Phi_{\min}) = -\frac{1}{12\varepsilon^3}a^4. \tag{8.33}$$

Since the field origin is locally stable down to $m_R^2 = 0$, we conclude that there must be some positive value of m_R^2 for which it is energetically

favorable for Φ to jump in a first-order transition from $\Phi = 0$ to a non-zero value close to (8.33).

Let us now see whether this conclusion is really trustworthy. For this we have to make sure that the higher loop corrections remain small compared with the mean-field and one-loop terms, which are of order g_1^6/ε^3. Otherwise they will completely change the result. We verify this assertion by observing that for finite g_1, the mass terms of the Φ fluctuations at the new minimum are very large, namely, of the order $3\varepsilon\Phi^2 \sim g_1^3/\varepsilon$ and $g_1\Phi^2 \sim g_1^4/\varepsilon^2$. This turns out to ensure the convergence of the loop expansion. For example, a two loop diagram like ⌀⌀ is at least small of the order $g_1(\varepsilon/g_1^3)^2 \sim \varepsilon^2/g_1^5$. A similar discussion holds for the other boundary $g_1 + g_2/n$ of the stability wedge.

Note that for the argument to go through, it is essential to have *two* coupling constants. For a simple $(\varepsilon/4)\varphi^4$ theory, there is only the first term in (8.32) so that $\Phi_{\min}$ is small, of the order $\varepsilon^{1/2}$ and so is the only mass term $3\varepsilon\Phi^2$ which is of the order ε^2. The latter causes the two-loop diagrams ⌀⌀ to be of order $\varepsilon(1/\varepsilon^4)$ and convergence is not ensured.

Let us now generalize this result to the case of a $n \cdot q$ component field φ_i^α with the energy (8.8). The energy is minimal for

$$\Phi_i^\alpha = \Phi\,\delta_{i1}\,\delta^{\alpha 1}, \tag{8.34}$$

or

$$\Phi_i^\alpha = \frac{\Phi}{\sqrt{n}}\,\delta^{\alpha 1} \tag{8.35}$$

and the potential reads again

$$v(\Phi) = \frac{m^2}{2}\Phi^2 + \frac{g_1 + g_2}{4}\Phi^4, \tag{8.36}$$

$$v(\Phi) = \frac{m^2}{2}\Phi^2 + \frac{g_1 + g_2/n}{4}\Phi^4, \tag{8.37}$$

respectively, just as before [recall Eqs. (8.13)]. Owing to invariance under $O(q)$ rotations of the indices α, any orthogonal linear combination of Φ_i^α can serve the same purpose.

The stability wedge is again given by $g_1 + g_2 > 0$ and $g_1 + g_2/n > 0$, respectively and the different phases have the same diagram as in Fig. 8.1.

The mass matrix (8.18) becomes

$$(M^2)_{ij}^{\alpha\beta} = g_1\left(2\Phi_i^\alpha\Phi_j^\beta + \delta_{ij}\delta^{\alpha\beta}\sum_{i,\alpha}(\Phi_i^\alpha)^2\right) + g_2\,\delta_{ij}\left(\delta^{\alpha\beta}\sum_\gamma(\Phi_i^\gamma)^2 + 2\Phi_i^\alpha\Phi_j^\beta\right). \tag{8.38}$$

In the axial ground state (8.34), it takes the specific form

$$(M^2)_{ij}^{\alpha\beta} = g_1(2\delta_{i1}\delta_{j1}\delta^{\alpha 1}\delta^{\beta 1} + \delta_{ij}\delta^{\alpha\beta}) + g_2\,\delta_{i1}\delta_{j1}(\delta^{\alpha\beta} + 2\delta^{\alpha 1}\delta^{\beta 1}). \tag{8.39}$$

This has one eigenvalue $3(g_1 + g_2)$ (associated with the eigenvector $\delta_{i1}\delta^{\alpha 1}$), $q-1$ eigenvalues $g_1 + g_2$ (associated with $\delta_{i1}\delta^{\alpha 2}$, $\delta_{i1}\delta^{\alpha 3}$, ...), and $(n-1)q$ eigenvalues g_1 (associated with $\delta_{i2}\delta^{\alpha\beta}$, $\delta_{i3}\delta^{\alpha\beta}$, ... for $\beta = 1, \ldots, q$). Hence the effective potential in the lower part of the stability wedge reads

$$\begin{aligned} v(\Phi) = \frac{m^2}{2}\Phi^2 + \frac{g_1+g_2}{4}\Phi^4 + \frac{1}{2}\int\frac{d^Dp}{(2\pi)^D}[&\log(p^2 + m^2 + 3(g_1+g_2)\Phi^2) \\ &+ (q-1)\log(p^2 + m^2 + (g_1+g_2)\Phi^2) \\ &+ (n-1)q\log(p^2 + m^2 + g_1\Phi^2)]. \end{aligned} \tag{8.40}$$

At the mean-field minimum, the total mass term in the second logarithm vanishes as a manifestation of the Nambu-Goldstone theorem applied to the $O(q)$ symmetry.

In the upper part of the stability wedge the mass matrix reads

$$(M^2)_{ij}^{\alpha\beta} = g_1\left(\frac{2}{n}\delta^{\alpha 1}\delta^{\beta 1} + \delta_{ij}\delta^{\alpha\beta}\right) + \frac{g_2}{n}\delta_{ij}(\delta^{\alpha\beta} + 2\delta^{\alpha 1}\delta^{\beta 1}). \tag{8.41}$$

This has a longitudinal eigenvalue $3(g_1 + g_2/n)$ [associated with the eigenvector $(1, 1, 1, \ldots)\delta^{\alpha 1}$], $n-1$ eigenvalues $g_1 + 3g_2/n$ [associated with $(1, -1, 0, 0, \ldots)\delta^{\alpha 1}$, $(1, 0, -1, 0, \ldots)\delta^{\alpha 1}$, ...] and $n(q-1)$ eigenvalues $g_1 + g_2/n$ [associated with $\delta_{ij}\delta^{\alpha 2}$, $\delta_{ij}\delta^{\alpha 3}$, ... for $j = 1, \ldots, n$].

At the mean field minimum, the total mass terms of the last modes vanish. The first-order transitions near the boundaries of the stability wedge follow in the same way as before.

It is possible to show, via renormalization group arguments in $4-\varepsilon$ dimensions, that in fact a first-order transition takes place for the entire section $g_2 < 0$, $g_1 > 0$ and $g_1 < 0$, $g_2 > 0$. For details we refer the reader to the works quoted in the Notes and References.

What does the above result imply about the forces between dislocation lines? Rewriting the interaction energy in (8.7) in the form

$$\frac{g_1+g_2}{4}\sum_{b=1}^{n}|\varphi_b|^4+\frac{g_1}{4}\sum_{b,b'=1}^{n}|\varphi_b|^2|\varphi_{b'}|^2, \tag{8.42}$$

we separate the self-energies of the lines from interaction energies between lines of different Burgers vectors. Hence the result implies that, for a small but positive self-energy and arbitrary positive interaction energy, the transition is of first order. This is in contrast with the disorder field theory of vortex lines in ^{4}He where positive self-energies always imply a continuous phase transition.

The other first-order transition occurs for negative g_1, i.e., at a slightly attractive interaction energy and a positive self-energy, g_1+g_2 in which g_2 is close to $-ng_1$, such that $g_1+g_2\sim-(n-1)g_1>0$. In the first case, only dislocation lines of one sort condense, owing to the fact that the ground state expectation has the form $\Phi_i=\Phi\delta_{i1}\delta^{\alpha 1}$. In the second case, there is an equal density of *all* dislocation lines $i=1,\ \ldots,\ n$, since $\Phi_i^\alpha=(\Phi/\sqrt{n})\delta^{\alpha 1}$ for all i.

If we want to interprete the phase transition of the above disorder field theory as a melting process, we have to assume the second situation to hold. Dislocation lines are the defects of translational order. The condensation of the lines φ_b destroys the lattice periodicity along the direction b. In a liquid, there is no translational order. Hence all φ_b fields have to condense.

In some crystals there exists an even more drastic difference between the disorder field theories of dislocation lines and those of vortex lines. Take for example, a hexagonal crystal. The basis vectors are

$$\mathbf{a}^{(1)}=a_0(1,\,0,\,0),\quad \mathbf{a}^{(2)}=a_0\left(\frac{1}{2},\,\frac{\sqrt{3}}{2},\,0\right),\quad \mathbf{a}^{(3)}=a_0(0,\,0,\,1), \tag{8.43}$$

so that there are four fundamental Burgers vectors

$$\mathbf{b}^{(1)}=a_0(1,\,0,\,0),\quad \mathbf{b}^{(2)}=a_0\left(-\frac{1}{2},\,-\frac{\sqrt{3}}{2},\,0\right),$$

$$\mathbf{b}^{(3)}=a_0\left(-\frac{1}{2},\,\frac{\sqrt{3}}{2},\,0\right),\quad \mathbf{b}^{(4)}=a_0(0,\,0,\,1). \tag{8.44}$$

The first three are of equal length and add up to zero. Since their energies are equal, each of them may be described by its own disorder field φ_b. In this case, the invariance (8.6) permits a cubic interaction of the form

$$\frac{g_3}{3}(\varphi_{b_1}\varphi_{b_2}\varphi_{b_3} + \text{c.c.}). \tag{8.45}$$

This interaction will *always* cause a first-order transition in which the three types of dislocation lines all condense at the same time. However, in most atomic lattices, which are of the b.c.c. or f.c.c. types, this mechanism is absent and the disorder theory is of the type (8.4) with the leading interactions being quartic in the fields.

Apart from these special features, the field energy of dislocation lines is structurally similar to that of vortex lines. In particular, the disordered phase of the field theory contains long-range Nambu-Goldstone modes associated with the fluctuations of the phase angles $\gamma^{(b)} = \gamma_\ell b_\ell$ of the disorder field φ_b. The gradients of the angles $\gamma^{(b)}(\mathbf{x})$ are proportional to the current densities of the three fundamental dislocation lines. If we rewrite the disorder fields in polar coordinates, i.e.,

$$\varphi_b(\mathbf{x}) = \rho^{(b)}(\mathbf{x})\, e^{i\gamma^{(b)}(\mathbf{x})}, \tag{8.46}$$

these currents are

$$j_{b\ell}(\mathbf{x}) = \frac{1}{2i}\varphi_b^\dagger \overleftrightarrow{\partial}_\ell \varphi_b(\mathbf{x}) = \rho^{(b)}(\mathbf{x})^2 \partial_\ell \gamma^{(b)}(\mathbf{x}). \tag{8.47}$$

The incorporation of the second piece of the core energy $e_c^{\mathrm{L}} - e_c^{\mathrm{T}}$, which we had omitted for a moment, represents no major difficulty. It merely requires a few more steps. First we observe that the coupling of the Burgers vector in (8.2) to the integral over the orbit $\int dx^{(b)}$ is of the same form as that for the magnetic potential in (2.6), Part I. Hence the e_c' term in (8.2) is equivalent to the minimal replacement

$$\partial_\ell \to \partial_\ell - \frac{i}{T} e_c' \hat{b}_\ell \tag{8.48}$$

in the gradient term of the disorder field theory. This leads to two additional terms in the exponent of (8.4)

$$-\sum_b \int d^3x \left(\frac{e_c'}{T} \frac{1}{2i} \varphi_b^\dagger \overleftrightarrow{\partial}_\ell \varphi_b \hat{b}_\ell + \frac{e_c'^2}{2T^2} |\varphi_b|^2 \right). \tag{8.49}$$

The second term represents an additional contribution to the mass of the φ_b field which is changed to

$$m'^2 = \left(\frac{e_c a}{T} + \frac{e_c'^2}{T^2} \frac{a^2}{2D} - \log 2D \right) \frac{2D}{a^2}. \tag{8.50}$$

In the mean-field approximation, this disorder field theory has a second order phase transition at

$$T_c = \frac{e_c'^2 a}{e_c D} \left(\sqrt{1 + \frac{2e_c'^2}{e_c^2 D} \log 2D} - 1 \right)^{-1}. \tag{8.51}$$

At this temperature, dislocation lines proliferate. The thermodynamic functions $-\beta f$ (free energy), u (internal energy), and s (entropy) have the same temperature dependence as that calculated for vortex lines.

While the resulting disorder theory of dislocation lines has many of the pleasant properties which are necessary to describe the melting process, the first-order transition discussed above cannot yet be identified with this process. First of all, in b.c.c. and f.c.c. lattices, when there is no cubic term (8.45), the existence and strength of the first-order transition would depend on a special combination of the coupling constants g_1, g_2. It would then be difficult to understand why *all* materials melt with similar transition entropies, lying between 1.5 and $2.5 k_B$ per atom (see Table 7.1).

A further problem is the following: Dislocations are defect lines only of the discrete translational symmetry of the crystal. When they condense, only this symmetry can be destroyed. We are faced with the problem of explaining how the ground state characterized by $|\varphi_b| \neq 0$ should also have lost the directional memory of the crystal. This second observation is crucial and provides the key for a proper treatment of the melting transition to be developed later. For the moment, however, let us ignore all these problems and proceed in complete analogy with the development in Part II for the superfluid, namely, with introducing the long-range elastic stress forces between dislocation lines into the disorder field theory. Although the resulting field theory will not yet be the correct one, it will provide some interesting insights into the physical properties of the

melting transition. In particular we shall run into several discrepancies between theory and experiment which can be resolved only by the final correct theory (see Chapters 18, 19).

8.3. INCLUSION OF STRESS AND THE MEISSNER EFFECT

The inclusion of stress forces is quite straightforward knowing the gauge-field representation (4.7) of Blin's law,

$$e^{-(1/T)E_{\text{Blin}}} = \int \mathscr{D}A_{\ell j}(\mathbf{x})\,\delta(\partial_j A_{\ell j} - \partial_\ell A_{jj})\,\Phi[A_{\ell j}] \sum_{\{L\}} e^{-(1/T)(E_{\text{el}} + i\Sigma_i b_j^{(i)} \oint_{L^{(i)}} dx_\ell^{(i)} A_{\ell i})}, \tag{8.52}$$

where the contour integrals run over all dislocation lines $L^{(i)}$. For an ensemble of lines with Burgers vector $\mathbf{b}$, the elastic energy is obtained by replacing the derivatives of the associated disorder fields $\varphi_b^{(i)}$ by the covariant derivative

$$\partial_\ell \varphi_b(\mathbf{x}) \to D_\ell \varphi_b(\mathbf{x}) = \left(\partial_\ell - \frac{i}{T} b_j A_{\ell j}\right) \varphi_b(\mathbf{x}). \tag{8.53}$$

In a simple cubic lattice, the fundamental Burgers vectors $b_j^{(i)}$ coincide with the unit vectors (1, 0, 0), (0, 1, 0), (0, 0, 1), apart from the scale factor a, and the covariant derivatives read

$$D_\ell \varphi_i(\mathbf{x}) = \left(\partial_\ell - i\frac{a}{T} A_{\ell i}\right) \varphi_i \qquad \text{(no sum over } i\text{)}, \tag{8.54}$$

where $i = 1, 2, 3$ labels the three spatial directions.

Let us turn our attention upon this case, for simplicity. We arrive at the following partition function for fluctuating dislocation lines under stress,

$$Z = \int \mathscr{D}A_{\ell j}(\mathbf{x})\,\delta(\partial_j A_{\ell j} - \partial_\ell A_{jj})\,\Phi[\mathbf{A}]\, e^{-(1/T)\int d^3x (1/4\mu)(\sigma_{ij}^2 - (\nu/(1+\nu))\sigma_{ii}^2)}$$

$$\times \int \mathscr{D}\varphi_i\, \mathscr{D}\varphi_i^\dagger\, e^{-\int d^3x \Sigma_j \{(1/2)(D_\ell \varphi_j)^2 + (m^2/2)|\varphi_j|^2 + \Sigma_{j'}(g_{jj'}/4)|\varphi_j|^2 |\varphi_{j'}|^2\}}. \tag{8.55}$$

As in the case of the vortex lines with superflow, the gauge field extends the global invariance (8.6), which guarantees the conservation of Burgers "charges," to local gauge invariance, i.e.,

$$\varphi_j(\mathbf{x}) \to e^{i(a/T)\Lambda_j(\mathbf{x})}\varphi_j(\mathbf{x}), \qquad A_{\ell j}(\mathbf{x}) \to A_{\ell j}(\mathbf{x}) + \partial_\ell \Lambda_j(\mathbf{x}). \tag{8.56}$$

Extremizing the energy with respect to variations $\delta\varphi_i(\mathbf{x})$ on φ_i we obtain the field equations for the dislocation fields,

$$\left[-\left(\partial_\ell - i\frac{a}{T} A_{\ell j} \right)^2 + m^2 + \sum_j g_{jj'} |\varphi_{j'}|^2 \right] \varphi_j(\mathbf{x}) = 0. \tag{8.57}$$

The derivation of the field equation for the gauge field is a little more subtle due to the constraints $\delta(\partial_j A_{\ell j} - \partial_\ell A_{jj})$. If we ignore these and vary the exponent formally we find

$$-\frac{1}{T}\frac{1}{2\mu}\left(\varepsilon_{\ell mn}\partial_m \varepsilon_{npq}\partial_p A_{qj} - \frac{\nu}{1+\nu}\varepsilon_{jk\ell}\partial_k \varepsilon_{mpq}\partial_p A_{qm} \right) = \alpha_{\ell j}(\mathbf{x}), \tag{8.58}$$

where

$$\alpha_{\ell j}(\mathbf{x}) \equiv \frac{a}{T}\frac{1}{2i}\varphi_j^\dagger \overleftrightarrow{\partial}_\ell \varphi_j - \frac{a^2}{T^2}|\varphi_j|^2 A_{\ell j} \tag{8.59}$$

is the dislocation current density. Equations (8.57) – (8.59) are a direct analogues of Eqs. (3.27), (3.28), (3.29) in Part II. Due to our neglect of the constraint, however, Eq. (8.58) is not true since in the derivation we are allowed to vary only the physical components of $A_{\ell j}$. This implies that only those parts of the dislocation current appear on the right-hand side which contain the helicity components (2, 2), (2–2), (1, 0) [recall (4.124)]. Notice that this situation is different from what happens to the equation of motion if the constraint is merely a gauge-fixing condition. In that case one obtains the same result as one would if there were no gauge fixing due to the fact that the current satisfies the conservation law

$$\partial_\ell \alpha_{\ell j}(\mathbf{x}) = 0. \tag{8.60}$$

This ensures that the three gauge-like components $(1/\sqrt{2})(\alpha^{(2,1)} + \alpha^{(1,1)})$ $(1/\sqrt{2})(\alpha^{(2,-1)} + \alpha^{(1,-1)})$, $(1/\sqrt{3})(\sqrt{2}\alpha^{(2,0)} + \alpha^{(0,0)})$ are absent [recall

(4.117)]. The same is true on the left-hand side of (8.58) which vanishes trivially when contracting with ∂_ℓ. This is why neglecting the gauge-fixing factor $\Phi[A_{\ell i}]$ in doing the field variations does no harm. For the constraint $\delta(\partial_j A_{\ell j} - \partial_\ell A_{jj})$, however, the situation is entirely different, due to the absence of an analogous property in the dislocation density $\alpha_{\ell j}(\mathbf{x})$ [recall our remarks regarding (4.123)]. Therefore, the right-hand side of (8.58) has to be replaced by the projection

$$\tilde{\alpha}_{\ell j}(\mathbf{x}) \equiv (P^{(2,2)} + P^{(2,-2)} + P^{(1,0)})_{\ell j,\ell' j'}\, \alpha_{\ell' j'}(\mathbf{x}),$$

which was calculated in (4.128) to be

$$\tilde{\alpha}_{\ell j}(\mathbf{x}) = \left(\delta_{jj'} - \frac{\partial_j \partial_{j'}}{\partial^2}\right)\alpha_{\ell j'}(\mathbf{x}) - \frac{1}{2}\left(\delta_{\ell j} - \frac{\partial_\ell \partial_j}{\partial^2}\right)\alpha_{ii}(\mathbf{x}). \tag{8.61}$$

The projected $\tilde{\alpha}_{\ell j}$ satisfy the constraints

$$\partial_j \tilde{\alpha}_{\ell j}(\mathbf{x}) = \partial_\ell\, \tilde{\alpha}_{nn}(\mathbf{x}), \tag{8.62}$$

which make it consistent with the left hand-side of Eq. (8.58). In fact, both sides of Eq. (8.62) vanish by themselves as a consequence of the simultaneous validity of the conservation law $\partial_\ell\, \tilde{\alpha}_{\ell j} = 0$ [recall Eq. (4.122)].

In order to extract some physical consequences from Eqs. (8.57) and (8.58), we now recall that the analogous equations [(3.27). (3.28) of Part II] were solved most conveniently by writing the fields $\varphi(\mathbf{x})$ in the polar form,

$$\varphi(\mathbf{x}) = \rho(\mathbf{x})\, e^{i\gamma(\mathbf{x})}, \tag{8.63}$$

with $\gamma(\mathbf{x}) \equiv q\Lambda(\mathbf{x})$, and observing that the phase could be removed by a gauge transformation:

$$A_\ell(\mathbf{x}) \to A_\ell(\mathbf{x}) + \partial_\ell \Lambda(\mathbf{x}). \tag{8.64}$$

We can do the same thing here by writing

$$\varphi_j(\mathbf{x}) = \rho^{(j)}(\mathbf{x})\, e^{i(a/T)\Lambda_j(\mathbf{x})}, \tag{8.65}$$

while changing the field $A_{\ell j}$ to $A_{\ell j} + \partial_\ell \Lambda_j$. This then results in the equations

$$\left(-\partial_\ell^2 + \frac{a^2}{T^2}\sum_\ell A_{\ell j}^2 + m^2 + \sum_{j'} g_{jj'}\rho^{(j')2}\right)\rho^{(j)}(\mathbf{x}) = 0 \quad \text{(no sum in } j\text{)}, \tag{8.66}$$

$$-\frac{1}{T}\frac{1}{2\mu}\left(\varepsilon_{\ell mn}\partial_m \varepsilon_{npq}\partial_p A_{qj} - \frac{\nu}{1+\nu}\varepsilon_{jk\ell}\partial_k \varepsilon_{mpq}\partial_p A_{qm}\right) = \tilde{\alpha}_{\ell j}(\mathbf{x}), \tag{8.67}$$

with

$$\tilde{\alpha}_{\ell j}(\mathbf{x}) = -\frac{a^2}{T^2}\sum_{\ell' j'}(P^{(2,\,2)} + P^{(2,\,-2)} + P^{(1,\,0)})_{\ell j,\,\ell' j'}\rho^{(j')2}A_{\ell' j'}. \tag{8.68}$$

Are these equations in accordance with physical observations? In the disordered state where all $\rho^{(j)} \equiv \rho \neq 0$, the current $\tilde{\alpha}_{ij}(\mathbf{x})$, in momentum space, is given by

$$\tilde{\alpha}_{\ell j} = -\frac{a^2}{2T^2}\rho^2(P^{(2,\,2)} + P^{(2,\,-2)} + P^{(1,\,0)})_{\ell j,\,\ell' j'}A_{\ell' j'}.$$

The left-hand side of (8.67), on the other hand, has the momentum-space helicity form [recall (4.113)]

$$\frac{1}{T}\frac{1}{2\mu}\mathbf{p}^2\left(P^{(2,\,2)} + P^{(2,\,-2)} + \frac{1-\nu}{1+\nu}P^{(1,\,0)}\right)_{\ell j,\,\ell' j'}A_{\ell' j'}. \tag{8.69}$$

Thus we find the free field equations

$$\frac{1}{2}\left(\frac{1}{\mu}\mathbf{p}^2 + \frac{a^2\rho^2}{T}\right)A^{(2,\,\pm 2)}(\mathbf{p}) = 0, \qquad \frac{1}{2}\left(\frac{1}{\mu}\mathbf{p}^2\frac{1-\nu}{1+\nu} + \frac{a^2\rho^2}{T}\right)A^{(1,\,0)}(\mathbf{p}) = 0. \tag{8.70}$$

This shows that there exists a dislocation version of the Meissner effect. In the phase transition to the disordered state, the gauge field of stress acquires a finite penetration depth. Thus stress cannot invade into a state filled with dislocations. If the disordered state is interpretated as a molten crystal, this result is only partially consistent with experiment. It is true, and well-known, that the molten state cannot support any *shear* stress.

The compressional sound waves, however, do survive the melting process and can traverse a boundary between the crystalline and the molten phase.

At first sight it appears as though one could remedy the disagreement by a slight modification of the theory. For this we note that before introducing the stress gauge field, the system had *three* long-range Nambu-Goldstone bosons associated with the flow of dislocation lines. After the minimal coupling, $\partial_\ell \to D_\ell = \partial_\ell - i(1/T)b_j A_{\ell j}$, these were turned into pure gauge degrees of freedom and could be absorbed into a redefinition of the $A_{\ell j}$. This suggests a simple way of retaining a long-range mode associated with sound waves: We remove the trace of the field from the outset and postulate that the gauge field satisfies the constraint

$$A_{\ell\ell}(\mathbf{x}) = 0. \tag{8.71}$$

Then the theory is no longer invariant under local gauge changes of all three phases of the dislocation fields

$$A_{\ell j}(\mathbf{x}) \to A_{\ell j}(\mathbf{x}) + \partial_\ell \Lambda_j(\mathbf{x}); \tag{8.72}$$

the $\Lambda_j(\mathbf{x})$ have to satisfy the transversality condition

$$\partial_j \Lambda_j(\mathbf{x}) = 0. \tag{8.73}$$

With these $\Lambda_j(\mathbf{x})$, the longitudinal combination of the phase fluctuations can no longer be removed from the field equation (8.57) and it survives as a long-range mode. This could, in principle, be associated with sound waves.

Actually, this procedure is less ad hoc than it might, at first, seem. We should remember that $A_{\ell j}(\mathbf{x})$ is not really the *fundamental* gauge field of stress. It is merely a *convenient* gauge field when restricting attention to dislocation lines only. A crystal can also have disclination lines and these cannot be coupled locally using the $A_{\ell j}(\mathbf{x})$. For a unified stress gauge theory of both types of defects it is therefore necessary to introduce the gauge field $\chi_{\ell n}(\mathbf{x})$ defined by [recall (5.1)]

$$\sigma_{ij}(\mathbf{x}) = \varepsilon_{ik\ell}\, \varepsilon_{jmn}\, \partial_k\, \partial_m \chi_{\ell n}(\mathbf{x}). \tag{8.74}$$

Hence the $A_{\ell j}(\mathbf{x})$ is really only an abbreviation for the object

$$A_{\ell j}(\mathbf{x}) \equiv \varepsilon_{jmn}\partial_m \chi_{\ell n}. \tag{8.75}$$

The proper gauge invariance of the stress coupled to all defects is

$$\chi_{\ell n}(\mathbf{x}) \to \chi_{\ell n}(\mathbf{x}) + \partial_\ell \xi_n(\mathbf{x}) + \partial_n \xi_\ell(\mathbf{x}). \tag{8.76}$$

Under this transformation, the field $A_{\ell j}(\mathbf{x})$ transforms as

$$A_{\ell j}(\mathbf{x}) \to A_{\ell j}(\mathbf{x}) + \partial_\ell \Lambda_j(\mathbf{x}), \tag{8.77}$$

where

$$\Lambda_j(\mathbf{x}) \equiv \varepsilon_{jmn}\partial_m \xi_n(\mathbf{x}). \tag{8.78}$$

This change is indeed purely transverse and $A_{\ell j}(\mathbf{x}) = \varepsilon_{jmn}\partial_m \chi_{\ell n}(\mathbf{x})$ is capable of absorbing only the transverse part of the Nambu-Goldstone modes of the three dislocation fields. Thus the longitudinal combination of the phases of the disorder field $\partial_j \Lambda_j$ does retain its long-range disorder and we may be led to conclude that $A_{\ell j}$ could describe, in principle, the sound waves in the molten phase.

We shall see later that this mathematical possibility does not correspond to physical reality. In fact, the phenomenological description of dislocation lines given in this section is quite unsatisfactory. It is unpleasant to be faced with a missing constraint $\partial_j \alpha_{\ell j}(\mathbf{x}) = \partial_\ell \alpha_{ii}(\mathbf{x})$ in the dislocation current to balance Eq. (8.58). A proper gauge theory of disorder should not contain any components of $\alpha_{\ell j}(\mathbf{x})$ which are not coupled elastically. The proper fundamental source of the gauge field $\chi_{\ell n}(\mathbf{x})$ is really the total defect tensor $\eta_{\ell n}(\mathbf{x})$. It is a symmetric conserved matrix field which carries only *three* independent components rather than the six in $\alpha_{\ell j}(\mathbf{x})$. It will be necessary to develop a disorder field theory for the statistical ensemble of precisely all independent configurations of the defect tensors. This will be done later after we have deepended our understanding of the problem via certain model studies.

What we shall find is that within a *time independent* theory of defects, all three physical components of the stress-gauge field $\chi_{\ell n}(\mathbf{x})$ are indeed Meissner screened so that, at the equilibrium level, the disordered phase of a defect system will not be capable of transmitting sound waves. In fact, this phase will not be a liquid but rather an ideal gas. Only if dynamical effects, i.e., those of defect *motion*, are included can this aspect of the melting transition be properly described. Among the

dynamical effects there is one which is of special physical importance, namely, that a defect line, on a short time scale of sound vibrations, can never climb but only glide. It is this property which ultimately leads to the survival of the longitudinal sound wave in the liquid state.

It turns out that there is a very simple counting argument which shows that at the level of classical equilibrum statistical mechanics of stresses and defects it is impossible to account for the different behaviours of the longitudinal and transverse sound waves during the melting transition: As we shall see in detail later, in two dimensions the gauge field of stress has only a single component [corresponding to $\chi_{33}(\mathbf{x})$]. This is obviously *incapable* of distinguishing the two polarizations of sound waves. Consequently, it cannot describe at the same time the Meissner screening of the transverse wave and the survival of the longitudinal wave when entering the liquid phase. The gauge description of time dependent stresses, on the other hand, does contain an extra vector field and the above difficulty is circumvented.

8.4. OTHER POSSIBLE MECHANISMS TO MAKE A TRANSITION FIRST ORDER

The subtleties discussed above in obtaining a first-order phase transition in the theory suggest the search for more effective mechanisms for the entropy jumps observed in the melting process. Some insight comes from stress fluctuations via the Coleman-Weinberg mechanism. We had seen in Section 3.4, Part II, in the discussion on the ordinary Ginzburg-Landau theory, that gauge fluctuations can raise the tricritical point of an ordinary $g|\psi|^4$ theory from $g = 0$ to a g of the order of e^2, where e is the charge coupling of the gauge field. The condition $g \lesssim e^2$ means that the Ginzburg-Landau theory corresponds roughly to a type-I superconductor. By analogy, we can expect the stress-gauge field to extend the first-order regime in the stability wedge of the dislocation field theory to larger couplings. It is therefore useful to introduce the concept of type-I and type-II dislocation theories depending on the ratio between the penetration depth λ of the stress field into the disordered state and the range of the size fluctuations ξ_{size} of the disorder field.

Thus we introduce a parameter κ,

$$\kappa = \frac{1}{\sqrt{2}} \frac{\lambda}{\xi_{\text{size}}}. \tag{8.79}$$

Let us estimate its size in terms of the coupling constants. From (8.70) we read off the length scales of stress in the disordered state,

$$\frac{1}{\lambda^2} = \mu a^2 \rho^2 / T. \tag{8.80}$$

According to (8.42), (8.11), (8.12), the size of the disorder parameter is

$$\rho^2 = -m^2/\bar{g} \equiv -\frac{m_0^2}{\bar{g}}\left(\frac{\beta}{\beta_c} - 1\right), \qquad \beta < \beta_c, \tag{8.81}$$

where $\bar{g}$ is equal to $g_1 + g_2$ or $ng_1 + g_2$, depending on the phase of the system. Hence[b]

$$\frac{1}{\lambda^2} = -\frac{\mu a^2}{T}\frac{m_0^2}{\bar{g}}\left(\frac{\beta}{\beta_c} - 1\right). \tag{8.82}$$

The size fluctuations of the disorder field, on the other hand, have the following two length scales.

(i) In the phase for which $g_2 > 0$, $g_1 > -g_2/n$, the ground state $\Phi_i^\alpha = (\Phi/\sqrt{n})(1, 1, \ldots)\delta^{\alpha 1}$ has

$$\begin{aligned}
\frac{1}{\xi_1^2} &= m^2 + 3\left(g_1 + \frac{g_2}{n}\right)\Phi^2 \qquad \text{(one mode)}, \\
&= -2m^2, \\
\frac{1}{\xi_2^2} &= m^2 + \left(g_1 + \frac{3g_2}{n}\right)\Phi^2 \qquad (n-1 \text{ modes}) \\
&= -2m^2\left(1 - \frac{g_1}{g_1 + g_2/n}\right).
\end{aligned} \tag{8.83}$$

(ii) In the phase for which $g_2 < 0$, $g_1 > -g_2$, the ground state $\Phi_i^\alpha = \Phi(1, 0, 0, \ldots)\delta^{\alpha 1}$ has

[b]This has the proper dimension since $\mu a^3/T$ is dimensionless [see (10.4)] and m_0^2, g have dimensions $1/\ell^2$, $1/\ell$, respectively (ℓ = length).

$$\frac{1}{\xi_1^2} = m^2 + 3(g_1 + g_2)\Phi^2 = -2m^2 \qquad \text{[one mode]},$$

$$\frac{1}{\xi_2^2} = m^2 + g_1\Phi^2 = \frac{g_2}{g_1 + g_2}m^2 \qquad [(n-1)\cdot q \text{ modes}]. \tag{8.84}$$

Hence we can introduce *two* κ parameters, each of them having the form

$$\kappa_{1,2} = \frac{1}{\sqrt{2}}\frac{\lambda}{\xi_{1,2}} = \sqrt{\frac{\bar{g}_{1,2}a}{\mu a^3/T}}\,, \tag{8.85}$$

$\bar{g}_{1,2}$ being appropriate combinations of the coupling constants. What do we know about the size of these parameters? The couplings $\bar{g}$ parametrize the self-energy and the short range steric repulsion between the dislocation lines; $\bar{g}a$ is a dimensionless constant. The dimensionless expression in the denominator, $\mu a^3/T$, compares the elastic energy per unit cell with the thermal energy. Its size is roughly known since the Lindemann number $L \approx 22.8\sqrt{\mu a^3/T}$ [recall Eq. (7.41)] is a number between 100 and 200 at the melting temperature of most materials. Much less is known about the steric interaction between the lines which is hard to measure precisely. A deep type-I dislocation field theory with the ground state $\Phi_i^\alpha = (\Phi/\sqrt{n})(1, 1, 1, \ldots)\delta^{\alpha 1}$ would imply an extremely weak self-energy compared with the elastic energy $\mu a^3/T$. It is not easy to see how this can come about. The steric repulsion is caused by nonlinear parts of the reduced elastic energy $\mu a^3/T$. Its order of magnitude seems to be tied to the elastic constant μ as well. Thus we expect κ to be rather of the order of unity and the Coleman-Weinberg mechanism seems to become a delicate quantitative matter. If this mechanism were really important in crystal melting, the question would now arise why it was not active before in the disorder theory of the superfluid phase transition. Both disorder theories look very similar, apart from the fact that there are three times as many dislocation lines as vortex lines. As in the case of crystals, the steric repulsion of vortex lines in superfluid ^{4}He is generated by the nonlinear parts of superflow and there we do know that it is strong enough to maintain the phase transition at second order. It is hard to believe that the rather universal entropy jumps observed in a process such as crystal melting should be the result of some special choices of the coupling constants. We are therefore led to conclude that the dislocation field theory constructed up to now misses out on a more essential aspect

of the melting transition which makes it completely different from the superfluid transition.

Indeed, let us remember that a little earlier, in Section 8.1, we obtained a first indication in this direction. There we observed that dislocation lines are merely the defects of translational crystal symmetry so that the phase transition discussed so far can only lead to a state in which this symmetry is violated. Atoms can move freely along the three crystal directions $\hat{\mathbf{x}}$, $\hat{\mathbf{y}}$ and $\hat{\mathbf{z}}$ but this does not imply that they can also move through space isotropically, as they do in a proper liquid. For this, also the other symmetry group of crystals, namely, that of discrete rotations, has to be destroyed. Now we do know that the crystal possesses a natural set of defects which are capable of destroying this symmetry: the disclination lines. A superfluid has no such second set of defect lines. This must then be the crucial difference between the two systems. At this point we are sure that a proper understanding of the melting transition must acount for the possibility of forming disclination lines.

8.5. DISORDER FIELDS FOR DISCLINATION LINES

It is instructive to see qualitatively that the possibility of forming disclination lines can, in principle, drive the transition to first-order via an avalanche mechanism triggered by the Meissner effect. The forces between arbitrary defects were derived in Chapter 5. The defect tensor $\eta_{ij}(\mathbf{x})$ can be decomposed into disclination and dislocation parts $\Theta_{ij}(\mathbf{x})$ and $\alpha_{\ell i}(\mathbf{x})$ [see (2.60), (2.61)]:

$$\begin{aligned}\eta_{ij}(\mathbf{x}) &= \Theta_{ij}(\mathbf{x}) + \tfrac{1}{2}\varepsilon_{imn}\partial_m(\alpha_{jn}(\mathbf{x}) - \tfrac{1}{2}\delta_{jn}\alpha_{\ell\ell}(\mathbf{x})) \\ &= \Theta_{ij}(\mathbf{x}) - \tfrac{1}{2}\partial_m(\varepsilon_{mi\ell}\alpha_{j\ell}(\mathbf{x}) + (ij) - \varepsilon_{ij\ell}\alpha_{m\ell}(\mathbf{x})).\end{aligned} \tag{8.86}$$

A disclination line along L may be introduced via a δ-function distribution [recall (2.44)],

$$\Theta_{ij}(\mathbf{x}) = \delta_i(L)\,\Omega_j, \tag{8.87}$$

where Ω_i is the Frank vector of the line. The gauge tensor $\chi_{\ell n}(\mathbf{x})$ field couples locally to $\eta_{ij}(\mathbf{x})$ [see (5.6)] and thus to $\Theta_{ij}(\mathbf{x})$. For the disclination line (8.87) this gives an interaction energy

$$E_{\text{int}} = \Omega_j \oint_{\text{L}} dx_i \chi_{ij}(\mathbf{x}). \tag{8.88}$$

This coupling is completely analogous to that for dislocation lines [see (8.52)]. It is therefore straightforward to set up a disorder field theory for a grand canonical ensemble of disclination lines. This has the same structure as that for dislocation lines.

Let Δ_i be the complex disorder fields associated with the fundamental disclinations whose Frank vector Ω_i is equal to $\Omega \mathbf{e}_i$ where $\mathbf{e}_i$ are the basis vectors in space. Then in analogy with (8.54), the covariant derivative is

$$D_\ell^\Delta \Delta_j(\mathbf{x}) = \left(\partial_\ell - i\frac{\Omega}{T}\chi_{\ell j}\right)\Delta_j(\mathbf{x}) \qquad \text{(no sum over } j\text{)}, \tag{8.89}$$

and the partition function of disclinations has the form

$$Z = \int \mathscr{D}\Delta_j \, \mathscr{D}\Delta_j^\dagger \, e^{-\int d^3x \{(1/2)|D_\ell^\Delta \Delta_j|^2 + (m^2/2)\Delta|\Delta_j|^2 + (1/4)\sum_{j'} g_{jj'}^\Delta |\Delta_j|^2 |\Delta_{j'}|^2\}}. \tag{8.90}$$

Just as in the case of dislocations, $g_{jj'}^\Delta$ parametrizes the steric repulsion between disclination lines and the mass parameter is

$$m_\Delta^2 = \left(\frac{e_\Delta a}{T} + \frac{e_\Delta'^2 a^2}{T^2 2D} - \log 2D\right)\frac{2D}{a^2}, \tag{8.91}$$

where e_Δ, e_Δ' are the two core energies per unit length. The total partition function of dislocation and disclination lines is [recall (5.25)]

$$Z = \int \mathscr{D}\varphi_j \, \mathscr{D}\varphi_j^\dagger \, \mathscr{D}\Delta_j \, \mathscr{D}\Delta_j^\dagger \, \mathscr{D}\chi_{\ell n} \delta(\partial_\ell \chi_{\ell n}) e^{-E/T} \tag{8.92}$$

with an energy

$$\begin{aligned} E = {} & \frac{1}{4\mu}\int d^3x \chi_{\ell n}(\mathbf{x})\left(P^{(2,\,2)} + P^{(2,\,-2)} + \frac{1-\nu}{1+\nu}P^L\right)_{\ell n,\,\ell' n'} \nabla^4 \chi_{\ell' n'}(\mathbf{x}) \\ & + T\int d^3x \left\{\sum_j \left(\frac{1}{2}|D_\ell \varphi_j|^2 + \frac{m^2}{2}|\varphi_j|^2\right) + \sum_{j,j'}\frac{g_{jj'}}{4}|\varphi_j|^2|\varphi_{j'}|^2\right. \\ & + T\int d^3x \left\{\sum_j \left(\frac{1}{2}|D_\ell^\Delta \Delta_j|^2 + \frac{m_\Delta^2}{2}|\Delta_j|^2\right) + \sum_{j,j'}\frac{g_{jj'}^\Delta}{4}|\Delta_j|^2|\Delta_{j'}|^2 + E_{\text{int}}[\varphi_j,\,\Delta_j], \end{aligned} \tag{8.93}$$

where E_{int} collects the short-range steric interactions between the two types of lines. Notice that in terms of the field $\chi_{\ell n}(\mathbf{x})$, the covariant derivative of the dislocation field $\varphi_j(\mathbf{x})$ takes the form

$$D_\ell \varphi_j(\mathbf{x}) \equiv \left(\partial_\ell - i\frac{a}{T} \varepsilon_{jmn} \partial_m \chi_{\ell n} \right) \varphi_j(\mathbf{x}) \qquad \text{(no sum in } j\text{)}. \tag{8.94}$$

Within the present formulation, the size of the core energy of disclination lines as well as the interaction $E_{\text{int}}[\varphi_j, \Delta_j]$ are hard to assess. In comparison with dislocation lines, however, one thing is quite clear: Disclinations cause a *long-range* distortion of the crystalline order. Therefore, an individual line carries an *enormous* amount of elastic energy. This makes them impossible to be created thermally and m_Δ^2 is very large compared to m^2 of the dislocation lines.

At first sight, this property seems to preclude disclinations from playing any role in the thermodynamics of crystals and hence in the melting transition so that it appears as though disclinations cannot resolve the puzzle of the order of the melting transition. This conclusion would, however, be too hasty since it neglects the Meissner effect in the disorder fields. Let us see what this implies for the partition function (8.93). At low temperatures, both types of defects are certainly very rare so that both field expectations $\langle \varphi_j \rangle$ and $\langle \Delta_j \rangle$ vanish. The correlation function of the stress gauge field behaves, in momentum space, like

$$\langle \chi_{\ell n}(\mathbf{p}) \chi^\dagger_{\ell' n'}(\mathbf{p}) \rangle \propto \frac{1}{\mathbf{p}^4}. \tag{8.95}$$

In real space, this corresponds to a linear behaviour in R. Since disclinations couple locally to $\chi_{\ell n}(\mathbf{x})$, this is directly the R behavior of the elastic interaction energy between disclinations. The coupling to dislocations on the other hand, involves the derivatives $\varepsilon_{jmn} \partial_m \chi_{\ell n}(\mathbf{x})$ and the elastic interaction energy of dislocations is governed by

$$\langle \partial_m \chi_{\ell n}(\mathbf{p}) \partial_{m'} \chi_{\ell' n'}(\mathbf{p}) \rangle \propto \frac{p_m p_{m'}}{\mathbf{p}^2} \triangleq \partial_m \partial_{m'} R \sim \frac{\widehat{R}_m \widehat{R}_{m'}}{R} \tag{8.96}$$

resulting in the Biot-Savart like expression of Blin's law (3.42).

Consider now the case $m^2 < 0$: the dislocation lines are infinitely long, and the fields φ_j have finite expectation φ. Then the stress-gauge field possess an additional energy term in the energy (8.93):

$$-\frac{a^2}{2T^2}|\varphi|^2 \int d^3x \sum_{\ell,j} (\varepsilon_{jmn}\partial_m \chi_{\ell n})^2$$
$$= -\frac{a^2}{2T^2}|\varphi|^2 \int d^3x \sum_{\ell} (\partial_m \chi_{\ell n})^2 \tag{8.97}$$

This contains two derivatives leading to a momentum space propagation of the type

$$\langle \chi_{\ell n}(\mathbf{p}) \chi_{\ell' n'}(\mathbf{p}) \rangle \propto \frac{1}{\mathbf{p}^4 + \dfrac{\mu a^2 |\varphi|^2}{T^2}\mathbf{p}^2}. \tag{8.98}$$

The long-distance part of the forces between defects is given by the small-momentum part of the correlation function. This, in turn, is governed entirely by the new term (8.97), i.e.,

$$\langle \chi_{\ell n}(\mathbf{p}) \chi_{\ell' n'}(\mathbf{p}) \rangle \propto \frac{T^2}{\mu a^2 |\varphi|^2} \frac{1}{\mathbf{p}^2} \hat{=} \frac{T^2}{\mu a^2 |\varphi|^2} \frac{1}{R}. \tag{8.99}$$

Hence, as a consequence of the Meissner effect, the correlation function changes from a linear dependence on distance to a Coulomb-like behaviour. In other words, in the presence of a "condensate" of dislocations, disclinations behave in the same way as dislocations previously did in an ideal crystal. They acquire a Blin or Biot-Savart like interaction energy,

$$E_{\text{int}}^{\text{discl.}} \propto \frac{T^2}{\mu a^2 |\varphi|^2} \oint_{L^{\text{I}}} \oint_{L^{\text{II}}} d\mathbf{x}^{\text{I}} \cdot d\mathbf{x}^{\text{II}} \frac{1}{R}, \tag{8.100}$$

and the ensemble of disclination lines has an effective partition function of the form

$$Z^{\text{discl.}} \approx \sum_{\{L\}} e^{-(c/T|\varphi|^2)\Sigma_{i<j} \oint_{L(i)} \oint_{L(j)} dx^{(i)} dx^{(j)} 1/R} \tag{8.101}$$

with $c = T^2/\mu a^2$.

The crucial observation which leads to the possibility of a first-order transition in the melting process comes from the observation that the temperature in the Boltzmann factor of this expression is accompanied by the density of dislocation lines $\propto |\varphi|^2$. We know from the study of dislocations (or of vortex lines in superfluid ^{4}He) that a partition function of

FIG. 8.2. The mean-field free energy of the subsystem of disclination lines as a function of the disorder field of dislocation lines. Due to Meissner screening, increasing $|\varphi|$ has the same effect as raising the temperature, causing a second order transition within the subsystem.

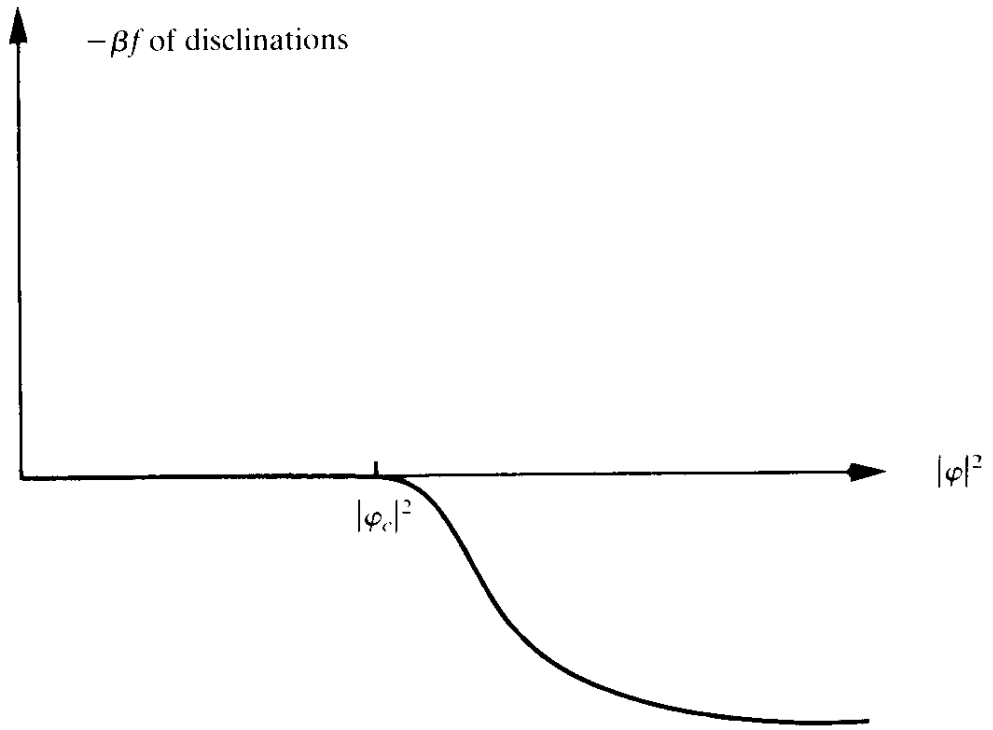

the type (8.101) has a second order transition where the lines $\{L\}$ condense. In $Z^{\text{discl.}}$, these are the disclination lines. Thus the free energy behaves just as in Eq. (3.127), Part II, i.e.,

$$-\beta f^{\text{discl.}} \approx -\beta_c f_0 \left(\frac{\beta}{\beta_c} - 1\right)^2. \tag{8.102}$$

Since the temperature is always accompanied by $|\varphi|^2$, the critical value of $\beta_c = 1/T_c$ must be explicitly proportional to $|\varphi|^2$, i.e.,

$$\tau \equiv \left(\frac{\beta}{\beta_c} - 1\right) \sim \left(\frac{\text{const}}{\beta_c |\varphi|^2} \frac{1}{T} - 1\right). \tag{8.103}$$

This shows that at a *fixed* temperature T, an increase in the density of dislocations $|\varphi|^2$ in the condensate has the same effect upon disclinations as heating. We can therefore identify a critical value $|\varphi_c|^2$ of $|\varphi|^2$ above which disclination lines would condense at a *fixed* temperature T. Thus, when viewed as a function of $|\varphi|^2$, the disclination lines undergo a second order phase transition. The behavior of the free energy as a function of $|\varphi|^2$ is shown in Fig. 8.2. [This follows directly from Eqs. (3.127) of Part II and (8.103)].

FIG. 8.3. The mean field behaviour of the disorder free energy of the dislocation lines alone as a function of the disorder field strength $|\varphi|$ above and below the transition. The transition is of second order.

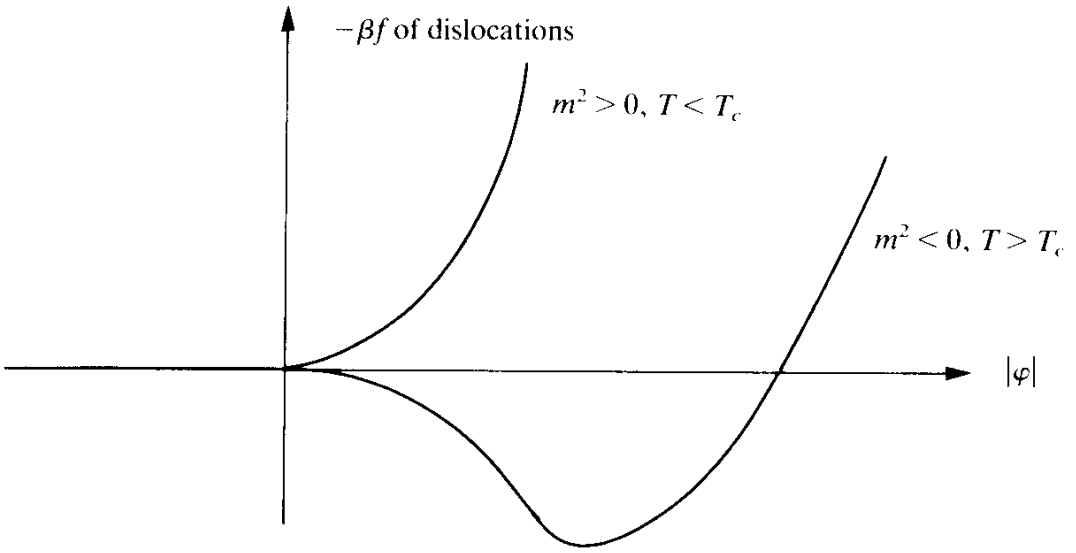

This behavior could indeed be the origin of the first order nature of the melting transition. Consider the effective potential of the dislocations alone. As a function of the common field expectation, it has the standard Landau shape shown in Fig. 8.3, with a second order transition of proliferations at some temperature T_c. Let us now add the free energy of disclinations of Fig. 8.2, also considered as a function of the dislocation density $|\varphi|^2$. This will cause a protrusion of the potential in Fig. 8.3 as indicated in Fig. 8.4. As the temperature is raised, the dislocation potential becomes flatter. At a temperature $T_m < T_c$, the combined curve touches the $|\varphi|$ axis at a point $|\varphi_m| \neq 0$ (see Fig. 8.4). At this temperature, the disorder parameter jumps from zero to $|\varphi_m|$. This implies a first order phase transition. Notice that this happens *before* (i.e., at *lower* temperature) the second-order condensation of dislocations would have taken place in the absence of disclinations.

In simple physical terms, the effect of disclinations can be described as follows: They represent a reservoir of entropy which in a crystal is unaccessible to thermal fluctuations, due to the high elastic energy. A virtual increase in dislocation density, however, can open up this reservoir. At a certain critical density the screening of the elastic forces is so strong that the elastic energy is weak enough to be outweighed by the entropy. This leads to the condensation of disclination lines. For a crystal whose temperature is sufficiently high, i.e., close to the temperature at which the dislocations themselves would proliferate, fluctuations can

FIG. 8.4. The combination of the two curves of Figs. 8.1. and 8.2. giving the effective potential of dislocations plus disclinations as a function of the dislocation density. The formation of a condensate of disclinations can cause a first order phase transition.

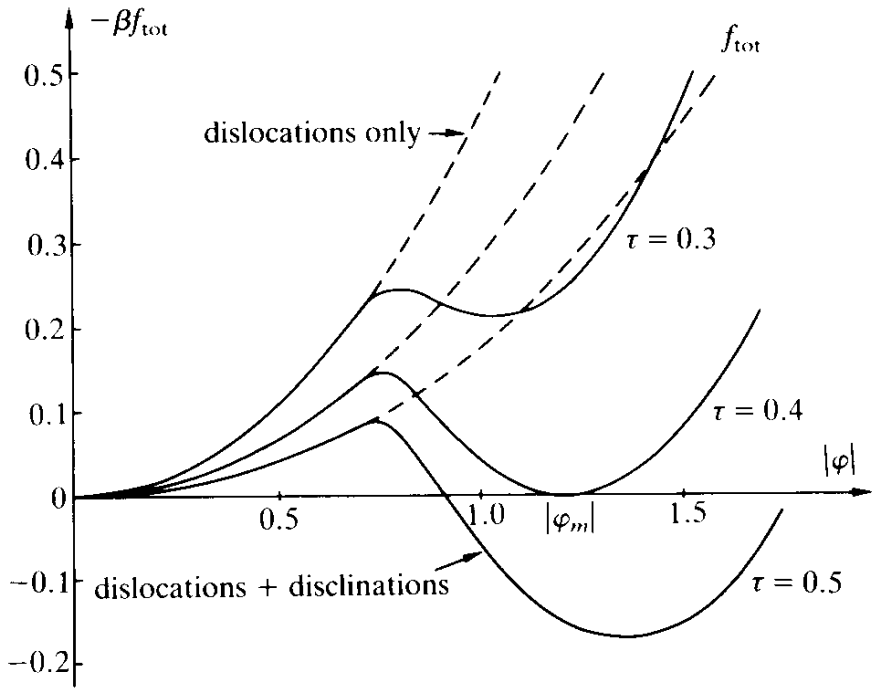

carry the dislocation field to such a critical density so that the condensation of disclinations takes place spontaneously. Then both types of defect lines condense jointly and can give rise to the first-order of the phase transition. Similar mechanisms have been observed in other physical systems in which the transition is governed by two types of coupled line ensembles (see Janke and Kleinert (1986), cited in the Notes and References). We therefore see that the condensation process involves defect lines related to both types of crystal symmetry. From this we may conclude that, in the disordered state, not only the translational order but also the rotational order are distroyed. Thus the disordered state has the chance of being a proper liquid and the transition can be identified with the melting process.

There are two objections to this description of the melting transition. First, the discussion is too qualitative. We have neither specified the sizes of the steric repulsions nor the core energies of the disclination lines. The equations had a mean-field character and fluctuations could, in principle, cause drastic changes in the conclusions. The second objection is of a more fundamental nature: The partition function (8.92) pretends that dislocations and disclinations are completely independent line-like defects. This is certainly not true as was discussed and illustrated in Section 2.4. An infinite number of dislocation lines with equal spacing

and equal Burgers vector can be piled up on top of the x-axis (say). If the spacing is equal to the lattice spacing, the result is a single disclination line along the x-axis. Thus in a consistent disorder field theory we should really use only *one* type of fundamental defect lines, for example, dislocations, and obtain the disclinations from superpositions of infinitely many dislocation fields. Such a description would not be unique since, conversely, dislocation lines can be viewed as bound states of neighbouring pairs of disclination and anti-disclination lines. Hence we could alternatively introduce fundamental disclination fields and generate dislocation fields from pairs of these. Technically, the latter approach would be easier to handle than the first since bound states of pairs are more tractable than infinite superpositions. One could proceed in analogy with the treatment of Cooper pairs of electrons in a superconductor.

Certainly, the interdependence between the two types of line-like defects does not completely invalidate the use of the partition function (8.92). Even if one of the fields is a bound state of the other it is often possible to introduce it explicitly in a phenomenological description. After all, the entire low energy treatment of nuclear physics is based on the concept of nucleon and meson fields even though these are really bound states of quarks and antiquarks. So, although the partition function (8.92) is fundamentally incorrect, this does not prevent it from having a certain phenomenological relevance. Still, the situation is far from being satisfactory and a more specific approach is desirable. Such a specific approach will be presented in the following chapters. We shall construct a lattice model of an ensemble of fundamental defects in which both dislocations as well as disclinations can appear on the same basis, generated by *one* type of fundamental defect variables. What we shall find is that the discussion just presented is much too simple-minded. It is true that the *possibility* of forming disclination lines is a crucial property of crystals which distinguishes their disorder theory from that of superfluids. However, this possibility does not have to be realized to its full extent. Instead of stacking up dislocations side by side, they may be spaced two lattice units apart thus forming only a partial disclination. The fact that the nearest neighbour stack has locally *no* energy concentrated on the Volterra sheet implies that the doubly spaced stack still has a rather moderate energy per unit area. Experimentally, such incompletely matched quasi Volterra surfaces are observable as a grain boundary (see Fig. 2.6). Grain boundaries combine a moderate energy with a tremendous entropy of random surfaces. This more subtle collective phenomenon is the proper basis of the first order nature of the melting

process. The crystal does *not* need to go all the way and form a condensate of independent disclination lines. The proliferation of "incomplete disclinations", i.e. of spaced stacks of dislocation lines which are grain boundaries, is sufficient to drive the transition to first-order and to destroy *both* the translational and the rotational symmetry.

Within the above formulated (not quite correct) pure dislocation description of the melting process, the possibility of forming disclination lines or grain boundaries may be viewed as the fundamental reason for a particularly weak steric repulsion between dislocation lines, which helps to drive the transition to first order. This is in contrast with the strong steric repulsion between vortex lines in superfluid ^{4}He. In both systems the short distance forces have their origin in the nonlinear regions of the elastic forces. But only in a crystal do these forces satisfy the extra constraint of allowing for a nearest neighbor stack up of dislocation lines without a build-up of stress across the Volterra sheet. This is what brings the steric repulsion down to such low values that the Ginzburg-Landau disorder theory lies deep within the type-I regime, where the Coleman-Weinberg or Halperin-Lubensky-Ma mechanisms can become active. The situation, however, is hard to formulate quantitatively. This is why we shall, from now on, have recourse to specific lattice models of defect melting, which are of the same simplicity as the XY model of superfluidity. Starting from such models if will be possible to find a field theory, in which all stack-up properties of defects are properly respected.

NOTES AND REFERENCES

The ideas that dislocations may drive the melting transition appeared in 1952 in a paper by
C. Mott, *Proc. Roy. Soc.* **A215** (1952) 1,
and in a lecture by
W. Shockley, in *L'Etat Solide* (Institut International de Physique Solvay, Brussels, 1952), p. 431.
Since then, many people have tried to formulate this idea quantitatively, notably
S. Mizushima, *J. Phys. Soc.* (Japan) **15** (1960) 70,
A. Ookawa, *J. Phys. Soc.* (Japan) **15** (1960) 2191,
M. Siol, *Z. Phys.* **164** (1961) 93,
D. Kuhlmann-Wilsdorf, *Phys. Rev.* **140A** (1965) 1595.

Dislocations have been observed in computer simulations of the 3-D melting transition via molecular dynamics by
R.M.J. Cotterill, *Phys. Rev. Lett* **42** (1979) 1541.
In two dimensions, progress in dislocation mediated melting was made (following the ideas of Kosterlitz and Thouless, who had given a successful description of a vortex mediated superfluid-normal transition in ^{4}He films) by
B.I. Halperin and D.R. Nelson, *Phys. Rev. Lett.* **41** (1978) 121,

D.R. Nelson, *Phys. Rev.* **B18** (1978) 2318,
D.R. Nelson and B.I. Halperin, *Phys. Rev.* **B19** (1979) 2457,
A.P. Young, *Phys. Rev.* **B19** (1979) 1855.
The first dynamical considerations are found in
A. Zippelius, B.I. Halperin and D.R. Nelson, *Phys. Rev.* **B22** (1980) 2514.

The importance of grain boundaries to the melting process was first pointed out in two dimensions by
S.T. Chiu, *Phys. Rev. Lett.* **48** (1982) 933
and confirmed via Monte Carlo simulations by
Y. Saito, *Phys. Rev. Lett.* **48** (1982) 1114, *Phys. Rev.* **B26** (1982) 6239.

The disorder field theory of dislocations was developed in
H. Kleinert, *Lett. Nuovo Cimento* **34** (1982) 464, *Phys. Lett.* **89A** (1982) 294, **91A** (1982) 295.

The induction of a first-order transition via fluctuations in an asymmetric $O(n \cdot q)\varphi^4$ theory is discussed in
A.Z. Patašhinskij and V.L. Pokrovskij, *Fluctuation Theory and Phase transitions* (Pergamm, Oxford, 1979),
D. Amit, *Field Theory, the Renormalization Group and Critical Phenomena* (World Scientific, Singapore, 1983).
The relevance of disclinations was discussed in
H. Kleinert, *Phys. Lett.* **95A** (1983) 493, **95A** (1983) 381

The generation of a first-order transition by a second type of lines in a system of non-self-backtracking vortex lines was observed in
W. Janke and H. Kleinert, *Phys. Rev. Lett.* **57** (1986) 279 and *Nucl. Phys.* **B270** [FS16] (1986) 399.

CHAPTER NINE

LATTICE MODEL OF DEFECT MELTING

9.1. SETTING UP THE MODEL

In Part II we studied superfluid ^{4}He and learned that lattice models allow for a simple way of incorporating vortex lines into a system carrying long-wavelength excitations. The steps were:

1. Rewrite the gradient energy of the long-wave-length excitations

$$E \propto \int d^3x \frac{1}{2}(\partial_i \gamma)^2 \tag{9.1}$$

in terms of lattice gradients,

$$E \propto a \sum_{\mathbf{x}} \frac{1}{2}(\nabla_i \gamma)^2, \tag{9.2}$$

where $\nabla_i \gamma(\mathbf{x}) = \gamma(\mathbf{x} + \mathbf{i}) - \gamma(\mathbf{x})$.

2. Set up the partition function for long-wavelength excitations on the lattice

$$Z = \prod_{\mathbf{x}} \left[\int_{-\infty}^{\infty} \frac{d\gamma(\mathbf{x})}{2\pi} \right] e^{-(\beta/2)\Sigma_{\mathbf{x}}(\nabla_i \gamma)^2}. \tag{9.3}$$

3. Account for the periodicity of the variable $\gamma(\mathbf{x})$ in 2π by going to a periodic Gaussian expression

$$Z = \sum_{\{n_i(\mathbf{x})\}} \prod_{\mathbf{x}} \left[\int_{-\infty}^{\infty} \frac{d\gamma(\mathbf{x})}{2\pi} \right] e^{-(\beta V/2)\Sigma_{\mathbf{x},i}(\nabla_i \gamma - 2\pi n_i)^2}. \tag{9.4}$$

The integer numbers $n_i(\mathbf{x})$ parametrize an ensemble of surfaces across which the phase variable can jump by multiples of 2π.

4. Observe that the partition function is degenerate with respect to vortex-gauge transformations consisting in deformations of the jumping surfaces

$$n_i(\mathbf{x}) \to n_i(\mathbf{x}) + \nabla_i N(\mathbf{x}) \tag{9.5}$$

with a simultaneous shift of the phase variable

$$\gamma(\mathbf{x}) \to \gamma(\mathbf{x}) + 2\pi N(\mathbf{x}). \tag{9.6}$$

5. Choose a gauge-fixing functional $\Phi[\mathbf{n}]$ in the sum. In the Villain model we took

$$\Phi[\mathbf{n}] = \delta_{n_3,0}, \tag{9.7}$$

which specifies the axial gauge $n_3(\mathbf{x}) = 0$.

The close analogy between superfluid ^{4}He and crystals in the description of both the long-wavelength excitations and the defect lines suggests that a similar procedure can be followed successfully for finding a lattice model of defect melting.

Let us do this step by step.

1. We take the gradient energy of linear elasticity on a simple cubic lattice,[a]

$$E = \mu \int d^3x \left[\sum_{i \neq j} u_{ij}^2 + \xi \sum_i u_{ii}^2 + \frac{\lambda}{2\mu} \left(\sum_i u_{ii} \right)^2 \right], \tag{9.8}$$

and replace the volume integral $\int d^3x$ by the lattice sum $a^3\Sigma$, the strain tensor $u_{ij} = \frac{1}{2}(\partial_i u_j + \partial_j u_i)$ by its lattice version [recall (7.12)]

[a]For the elastic constants see Eq. (1.49).

$$u_{ij}(\mathbf{x}) = \frac{1}{2a}(\nabla_i u_j(\mathbf{x}) + \nabla_j u_i(\mathbf{x})). \tag{9.9}$$

Introducing the same shift in the argument of the $u_{ii}(\mathbf{x})$ term which was found convenient in Eq. (7.11) this leads to an elastic energy on the lattice,

$$E = a\mu \sum_{\mathbf{x}} \left[\frac{1}{4} \sum_{i \neq j} (\nabla_i u_j + \nabla_j u_i)^2 + \xi \sum_i (\nabla_i u_i)^2 + \frac{\lambda}{2\mu} \left(\sum_i \nabla_i u_i(\mathbf{x} - \mathbf{i})^2 \right) \right]. \tag{9.10}$$

2. The partition function of classical elastic fluctuations is then given by

$$Z = \prod_{\mathbf{x},i} \left[\int_{-\infty}^{\infty} \frac{du_i(\mathbf{x})}{a} \right] e^{-(1/k_B T)E}. \tag{9.11}$$

We must remember that according to Eqs. (7.67)–(7.70) this is really only the potential part $Z_{\text{pot,cl}}$ of the full classical partition function which contains an extra factor $Z_{\text{kin,cl}} = (\sqrt{k_B T a^5 \rho / 2\pi\hbar^2})^{3N}$, due to the kinetic part of the classical fluctuations. Just as in the XY model we shall omit this factor, for brevity, it will be included only later when comparing our results with experimental data.

We are now ready to follow step 3. In the XY model, the phase variable was defined up to multiples of 2π. This was accounted for by going from the Gaussian energy to a periodic Gaussian form. In a crystal, there exists a completely analogous ambiguity in the definition of the displacement field $u_i(\mathbf{x})$. For very low temperature, this is not immediately obvious. The atomic positions deviate very little from those of an ideal crystal. It is therefore suggestive to use these small deviations for defining the displacement field $u_i(\mathbf{x})$. We have discussed before, in Section 2.3, that this definition can be consistent only for a limited duration of time. Due to fluctuations, thermal as well as quantum, the atoms are capable of exchanging positions with their neighbours and migrating, after a sufficiently long time, through the entire crystal. For this process of self-diffusion, which proceeds mainly via the support of vacancies, it is known from experiment that the diffusion constant carries, at higher temperatures, a Boltzmann factor with the vacancy energy [recall the values in Section 2.1]. The time scale factor is of the order of $\approx 0.2\,\text{cm}^2/\text{sec}$ for Na, Cu, Ag. We had pointed out before that self-diffusion makes it impossible to specify $u_i(\mathbf{x})$ uniquely since the assign-

ment of the original position of each atom to the nearest equilibrium position cannot be made after a long time. Thus, as a matter of principle, the displacement field is undetermined up to an arbitrary lattice vector. On a simple cubic lattice, it is impossible to say whether an atom is displaced by $u_i(\mathbf{x})$ or by

$$u_i(\mathbf{x}) + aN_i(\mathbf{x}). \tag{9.12}$$

Certainly, the field $N_i(\mathbf{x})$ has to obey many constraints which ensure that, after a reassignment of the starting position, no two atoms have come from the same place. These constraints will be ignored, for simplicity. We had also seen in Section 2.3 that the multivaledness of $u_i(\mathbf{x})$ is completely analogous to the multivaluedness of the phase variable $\gamma(\mathbf{x})$ in superfluid ^{4}He where $\gamma(\mathbf{x})$ and

$$\gamma(\mathbf{x}) + 2\pi N(\mathbf{x}) \tag{9.13}$$

were indistinguishable.

This analogy makes it straightforward to cast the elastic partition function into the appropriate periodic Gaussian form. Guided by (9.4) we introduce an extra sum over an integer-valued field $n_{ij}(\mathbf{x})$ and write ($k_B = 1$)

$$\begin{aligned} Z = \sum_{\{n_{ij}(\mathbf{x})\}} \prod_{\mathbf{x},i} \left[\int_{-\infty}^{\infty} \frac{du_i(\mathbf{x})}{a} \right] \\ \times \exp\left\{ -\frac{a\mu}{T} \sum_{\mathbf{x}} \left[\frac{1}{2} \sum_{i<j} (\nabla_i u_j(\mathbf{x}) + \nabla_j u_i(\mathbf{x}) - a(n_{ij} + n_{ji})(\mathbf{x}))^2 \right.\right. \\ \left.\left. + \xi \sum_i (\nabla_i u_i(\mathbf{x}) - a n_{ii}(\mathbf{x}))^2 + \frac{\lambda}{2\mu} \left(\sum_i (\nabla_i u_i(\mathbf{x} - \mathbf{i}) - a n_{ii}(\mathbf{x} - \mathbf{i})) \right)^2 \right] \right\}. \end{aligned} \tag{9.14}$$

The elastic constants μ, ξ, λ and the lattice spacing a may be considered as weakly temperature dependent quantities. They can either be calculated from the zero-temperature values, according to the methods outlined in Chapter 7 using the nonlinear terms of the elastic energy, or they may be taken directly from experiment. For the discussion to come we shall eliminate the temperature dependence of a by enclosing the system in a fixed volume V. The case $\xi = 1$ corresponds to an isotropic energy (9.8). The lattice version (9.14) is certainly not isotropic. Still we shall refer to this case (somewhat awkwardly) as isotropic, for convenience.

We now come to step 4 and observe that the partition function is invariant under the following integer-valued defect gauge transformations,

$$u_i(\mathbf{x}) \to u_i(\mathbf{x}) + aN_i(\mathbf{x}), \tag{9.15}$$

$$n_{ij}(\mathbf{x}) \to n_{ij}(\mathbf{x}) + \nabla_i N_j(\mathbf{x}). \tag{9.16}$$

The transformation on $u_i(\mathbf{x})$ expresses the intrinsic multivaluedness of the displacement variable; the transformation on $n_{ij}(\mathbf{x})$ accounts for the irrelevance of the jumping (Volterra) surfaces.

There is a further defect gauge invariance which did not exist in the Villain model. It is due to the fact that only the symmetric combination of $n_{ij}(\mathbf{x})$ and $n_{ji}(\mathbf{x})$ appears in the energy. The transformation law reads

$$u_i(\mathbf{x}) \to u_i(\mathbf{x}) + \varepsilon_{ikj} M_k(\mathbf{x}) x_j, \tag{9.17}$$

$$n_{ij}(\mathbf{x}) \to n_{ij}(\mathbf{x}) + \varepsilon_{ijk} M_k(\mathbf{x}), \tag{9.18}$$

where $M_k(\mathbf{x})$ is an arbitrary integer-valued field. This invariance is associated with the rotational symmetry of the crystal. Its implications will be studied later.

Step 5 consists in choosing a specific gauge in order to do away with a trivial infinite overall factor of the partition function, due to gauge degeneracy. The integer values of $n_{ij}(\mathbf{x})$ make the choice a non-trivial matter which will be dealt with in Section 10.1. Here we only state the result that we shall use a gauge in which $n_{ij}(\mathbf{x})$ is *quasi-symmetric* with the symmetrized combination $n^s_{ij} = \frac{1}{2}(n_{ij} + n_{ji})$ having three vanishing components

$$n^s_{22}(\mathbf{x}) = 0, \qquad n^s_{33}(\mathbf{x}) = 0, \qquad n^s_{13}(\mathbf{x}) = 0. \tag{9.19}$$

By *quasi-symmetric* we mean that if $n^s_{ij} = \frac{1}{2}(n_{ij} + n_{ji})$ is an integer, then n_{ij} is chosen to be properly symmetric, i.e., $n_{ij} = n_{ji}$. If, on the other hand, n^s_{ij} is half-integer, then $n_{ij} = n_{ji} \pm 1$ for $i \lesseqgtr j$.

The non-zero defect gauge fields are taken to satisfy the boundary conditions

$$\nabla_3 n^s_{11}(x_1, x_2, 0) = 0, \tag{9.20a}$$

$$n^s_{11}(x_1, x_2, 0) = 0, \tag{9.20b}$$

$$n^s_{12}(x_1, 0, x_3) = 0, \tag{9.20c}$$

and

$$n^s_{12}(0, x_2, 0) = 0, \tag{9.21a}$$

$$n^s_{23}(0, 0, x_3) = 0, \tag{9.21b}$$

$$n^s_{23}(0, x_2, 0) = 0, \tag{9.21c}$$

$$\nabla_1 n^s_{23}(0, x_2, 0) = 0. \tag{9.21d}$$

The product of Kronecker δ'_s which enforces these conditions will collectively be denoted by $\Phi[n^s_{ij}]$ and will constitute our gauge-fixing functional for the defect sum. We shall now proceed just as in the Villain model and first exhibit the defects implied by the sum over jump numbers $n^s_{ij}(\mathbf{x})$.

9.2. DEFECT REPRESENTATION OF LATTICE MODEL

Let us convince ourselves that the lattice partition function (9.14) does indeed describe what we want, namely a grand canonical ensemble of crystalline defects including their proper long-range interactions. For this we shall perform the same duality transformation as in the Villain form of the XY model. This goes as follows: First we introduce a set of canonically conjugate variables $\bar{\sigma}_{ij}$ and rewrite Z in the form

$$\begin{aligned} Z = &\left(\frac{1}{2^D \xi^D}\left(1 - D\frac{\xi}{\gamma}\right)\right)^{N/2} \prod_{\mathbf{x}, i \le j}\left[\int_{-\infty}^{\infty} \frac{d\bar{\sigma}_{ij}}{\sqrt{2\pi\beta}}\right] \sum_{\{n^s_{ij}(\mathbf{x})\}} \Phi[n^s_{ij}] \\ &\times \prod_{\mathbf{x}, i}\left[\int_{-\infty}^{\infty} \frac{du_i(\mathbf{x})}{a}\right] e^{-1/(2\beta)\sum_{\mathbf{x}}[\sum_{i<j}\bar{\sigma}^2_{ij}(\mathbf{x}) + 1/(2\xi)\sum_i \bar{\sigma}^2_{ii}(\mathbf{x}) - 1/(2\gamma)(\sum_i \bar{\sigma}_{ii}(\mathbf{x} - \mathbf{i}))^2]} \\ &\times e^{(2\pi/a)i(\sum_{\mathbf{x}, i<j}\bar{\sigma}_{ij}(\nabla_i u_j + \nabla_j u_i - 2an^s_{ij}) + \sum_{\mathbf{x}, i}\bar{\sigma}_{ii}(\nabla_i u_i - an^s_{ii}))}, \end{aligned} \tag{9.22a}$$

where

$$\beta \equiv \frac{a^3\mu}{T(2\pi)^2}, \tag{9.22b}$$

and the elastic constant γ is related to λ by [recall Eq. (1.48) and the statement after (1.110)]

$$\lambda = \frac{2\mu\xi^2}{\gamma - D\xi}. \tag{9.23}$$

For the variables $\bar{\sigma}_{ij}$ with $i \neq j$ this follows by direct quadratic completion. For $i = j$ we can rewrite the exponent of (9.22) in matrix form as

$$e^{-(1/2\beta)\sum_{i,j}\bar{\sigma}_{ii}(\mathbf{x}-\mathbf{i})M_{ij}\bar{\sigma}_{jj}(\mathbf{x}-\mathbf{j})} \tag{9.24}$$

with[b]

$$M_{ij} = \frac{1}{2\xi}\begin{pmatrix} 1-\frac{\xi}{\gamma} & -\frac{\xi}{\gamma} & -\frac{\xi}{\gamma} & & \\ -\frac{\xi}{\gamma} & 1-\frac{\xi}{\gamma} & -\frac{\xi}{\gamma} & & \\ -\frac{\xi}{\gamma} & -\frac{\xi}{\gamma} & 1-\frac{\xi}{\gamma} & & \\ & & & \ddots & \\ & & & & \ddots \end{pmatrix}. \tag{9.25}$$

This has a determinant,

$$\det M = \frac{1}{2^D\xi^D}\left(1 - D\frac{\xi}{\gamma}\right) = \frac{1}{2^D}\frac{2\mu}{\lambda}\frac{1}{\xi^{D-2}\gamma}, \tag{9.26}$$

with an inverse

$$M_{ij}^{-1} = \frac{2\xi}{\gamma - D\xi}\begin{pmatrix} \gamma-(D-1)\xi & \xi & \xi & & \\ \xi & \gamma-(D-1)\xi & \xi & & \\ \xi & \xi & \gamma-(D-1)\xi & & \\ & & & \ddots & \\ & & & & \ddots \end{pmatrix}$$

$$= 2\xi\delta_{ij} + \frac{\lambda}{\mu}, \tag{9.27}$$

so that a quadratic completion indeed reproduces (9.14).

[b]In the isotropic case where $1/\gamma = \nu/(1+\nu)$, this matrix is equal to

$$M_{ij} = \frac{1}{2(1+\nu)}(\delta_{ij}(1+\nu) - \nu)$$

with an inverse

$$M_{ij}^{-1} = 2\delta_{ij} + \frac{2\nu}{1+(1-D)\nu} = 2\delta_{ij} + \frac{\lambda}{\mu}.$$

Notice that the $\bar{\sigma}_{ij}^2$ part of the energy in (9.22) corresponds precisely to the stress energy of Chapter 1, Eq. (1.49). Indeed, the tensor $\bar{\sigma}_{ij}$ is the lattice version of $ia^3/(2\pi k_B T)$ times the physical stress tensor σ_{ij}.

We now integrate out the $u_i(\mathbf{x})$ variables in (9.22). Before doing this it is useful to complement the six components $\bar{\sigma}_{ij}$ with $i<j$ by three more elements $\sigma_{ij}=\sigma_{ji}$ for $i>j$ and form a symmetric matrix $\sigma_{ij}=\sigma_{ji}$ for $i,j=1,2,3$. Then the last exponential can be written as

$$e^{(2\pi/a)(i/2)\sum_{\mathbf{x},i,j}\bar{\sigma}_{ij}(\nabla_i u_j+\nabla_j u_i-2an_{ij}^s)}.$$

A partial integration brings it to the form

$$e^{-2\pi i\sum_{\mathbf{x},i}\bar{\nabla}_i\bar{\sigma}_{ij}u_j/a-2\pi i\sum_{\mathbf{x},i,j}\bar{\sigma}_{ij}n_{ij}^s}. \tag{9.28}$$

Now the integration over u_j/a leads to the δ-functions

$$\prod_{\mathbf{x},j}\delta(\bar{\nabla}_i\bar{\sigma}_{ij}). \tag{9.29}$$

These enforce the lattice version of the stress conservation law in the absence of external body forces.

Just as in the continuum formulation in Chapter 5 [see Eq. (5.1)], this conservation law is satisfied automatically by introducing a stress gauge field $\bar{\chi}_{\ell n}(\mathbf{x})$ and writing, in $D=3$ dimensions,

$$\bar{\sigma}_{ij}(\mathbf{x})=\varepsilon_{ik\ell}\,\varepsilon_{jmn}\bar{\nabla}_k\bar{\nabla}_m\bar{\chi}_{\ell n}(\mathbf{x}-\boldsymbol{\ell}-\mathbf{n}). \tag{9.30}$$

This decomposition [which is the stress version of the decomposition in Part II, Eq. (6.5)] is invariant under stress gauge transformations

$$\begin{aligned}\bar{\chi}_{\ell n}(\mathbf{x})&\to\bar{\chi}_{\ell n}(\mathbf{x})+\nabla_\ell\Lambda_n(\mathbf{x})+\nabla_n\Lambda_\ell(\mathbf{x})\\&=\bar{\chi}_{\ell n}(\mathbf{x})+\nabla_\ell\Lambda_n(\mathbf{x}+\boldsymbol{\ell})+\nabla_n\Lambda_\ell(\mathbf{x}+\mathbf{n}).\end{aligned} \tag{9.31}$$

Inserting (9.30) into (9.28), and performing two partial integrations, we find

$$e^{-2\pi i\sum_{\mathbf{x},\ell,n}\bar{\chi}_{\ell n}(\mathbf{x})\bar{\eta}_{\ell n}(\mathbf{x})}, \tag{9.32}$$

where the symmetric tensor $\bar{\eta}_{\ell n}(\mathbf{x})$ is defined by

$$\bar{\eta}_{\ell n}(\mathbf{x}) \equiv \varepsilon_{\ell k i}\varepsilon_{n m j}\nabla_k \nabla_m n^s_{ij}(\mathbf{x}+\boldsymbol{\ell}+\mathbf{n}). \tag{9.33}$$

The coupling of $\bar{\chi}_{\ell n}(\mathbf{x})$ to $\bar{\eta}_{\ell n}(\mathbf{x})$ is the same, up to a normalization factor, as the coupling of the stress gauge field $\chi_{\ell n}(\mathbf{x})$ to the defect tensor $\eta_{\ell n}(\mathbf{x})$ in the continuum formulation (5.6). Thus, $\bar{\eta}_{\ell n}(\mathbf{x})$ may be considered as the proper lattice version of the defect tensor $\eta_{\ell n}(\mathbf{x})$. Indeed, it satisfies the conservation law

$$\begin{aligned}\bar{\nabla}_\ell \bar{\eta}_{\ell n}(\mathbf{x}) &= \varepsilon_{\ell k i}\varepsilon_{n m j}\bar{\nabla}_\ell \nabla_k \nabla_m n^s_{ij}(\mathbf{x}+\boldsymbol{\ell}+\mathbf{n}) = 0 \\ &= \varepsilon_{\ell k i}\varepsilon_{n m j}\nabla_\ell \nabla_k \nabla_m n^s_{ij}(\mathbf{x}+\mathbf{n}) = 0.\end{aligned} \tag{9.34}$$

As a consequence, the coupling (9.32) is invariant under the stress gauge transformations (9.31)

$$\begin{aligned}\sum_{\mathbf{x},\ell,n} \bar{\chi}_{\ell n}(\mathbf{x})\,\bar{\eta}_{\ell n}(\mathbf{x}) &\to \sum_{\mathbf{x},\ell,n} [\bar{\chi}_{\ell n}(\mathbf{x})\,\bar{\eta}_{\ell n}(\mathbf{x}) + (\nabla_\ell \Lambda_n + \nabla_n \Lambda_\ell)\,\bar{\eta}_{\ell n}(\mathbf{x})] \\ = \sum_{\mathbf{x},\ell,n} \bar{\chi}_{\ell n}(\mathbf{x})\,\bar{\eta}_{\ell n}(\mathbf{x}) &- 2\sum_{\mathbf{x},\ell,n} \Lambda_n(\mathbf{x})\,\bar{\nabla}_\ell \bar{\eta}_{\ell n}(\mathbf{x}) = \sum_{\mathbf{x},\ell,n} \bar{\chi}_{\ell n}(\mathbf{x})\,\bar{\eta}_{\ell n}(\mathbf{x}).\end{aligned}$$

The decomposition (9.33) itself displays defect gauge invariance under (9.16), according to which

$$n^s_{ij}(\mathbf{x}) \to n^s_{ij}(\mathbf{x}) + \tfrac{1}{2}(\nabla_i N_j + \nabla_j N_i)(\mathbf{x}). \tag{9.35}$$

When expressing the partition function (9.22) in terms of the stress gauge field $\bar{\chi}_{\ell n}(\mathbf{x})$ we have to watch out to arrive at the correct measure of integration. The simplest gauge is the axial gauge where

$$\bar{\chi}_{3i}(\mathbf{x}) = 0. \tag{9.36}$$

Then the stress tensor has the following explicit decomposition,

$$\begin{aligned}\bar{\sigma}_{11}(\mathbf{x}) &= \bar{\nabla}_3^2 \bar{\chi}_{22}(x_1, x_2 - 2, x_3), \\ \bar{\sigma}_{22}(\mathbf{x}) &= \bar{\nabla}_3^2 \bar{\chi}_{11}(x_1 - 2, x_2, x_3), \\ \bar{\sigma}_{33}(\mathbf{x}) &= \bar{\nabla}_1^2 \bar{\chi}_{22}(x_1, x_2 - 2, x_3) + \bar{\nabla}_2^2 \bar{\chi}_{11}(x_1 - 2, x_2, x_3) \\ &\quad - 2\bar{\nabla}_1 \bar{\nabla}_2 \bar{\chi}_{12}(x_1 - 1, x_2 - 1, x_3),\end{aligned} \tag{9.37}$$

$$\bar{\sigma}_{12}(\mathbf{x}) = -\bar{\nabla}_3^2 \bar{X}_{12}(x_1 - 1, x_2 - 1, x_3),$$
$$\bar{\sigma}_{23}(\mathbf{x}) = \bar{\nabla}_3(\bar{\nabla}_1 \bar{X}_{12}(x_1 - 1, x_2 - 1, x_3) - \bar{\nabla}_2 \bar{X}_{11}(x_1 - 2, x_2, x_3)),$$
$$\bar{\sigma}_{13}(\mathbf{x}) = -\bar{\nabla}_3(\bar{\nabla}_1 \bar{X}_{22}(x_1, x_2 - 2, x_3) - \bar{\nabla}_2 \bar{X}_{12}(x - 1, x_2 - 1, x_3)). \tag{9.38}$$

We now see that the integrals over $\bar{\sigma}_{11}$, $\bar{\sigma}_{22}$ and $\bar{\sigma}_{12}$ can be exchanged freely with integrals over $\bar{X}_{22}$, $\bar{X}_{11}$, $\bar{X}_{12}$ since the only functional determinants which appear are products of $\det \nabla_3$, which are all unity. The integrations over $\bar{\sigma}_{13}$, $\bar{\sigma}_{23}$, $\bar{\sigma}_{33}$, on the other hand, are eliminated by the δ-functions (9.29),

$$\delta(\bar{\nabla}_1 \bar{\sigma}_{11} + \bar{\nabla}_2 \bar{\sigma}_{21} + \bar{\nabla}_3 \bar{\sigma}_{31})\, \delta(\bar{\nabla}_1 \bar{\sigma}_{12} + \bar{\nabla}_2 \bar{\sigma}_{22} + \bar{\nabla}_3 \bar{\sigma}_{32})$$
$$\times\, \delta(\bar{\nabla}_1 \bar{\sigma}_{13} + \bar{\nabla}_2 \bar{\sigma}_{23} + \bar{\nabla}_3 \bar{\sigma}_{33}), \tag{9.39}$$

where the functional determinants are again all trivial (due to $\det \bar{\nabla}_3 = 1$). Hence (9.22) can be written in $D = 3$ dimensions as

$$Z = \left[\frac{1}{8\xi^3}\left(1 - 3\frac{\xi}{\gamma}\right)\right]^{N/2} \frac{1}{(2\pi\beta)^{3N}} \prod_{\mathbf{x},i} \left[\int_{-\infty}^{\infty} d\bar{X}_{11}(\mathbf{x})\, d\bar{X}_{22}(\mathbf{x})\, d\bar{X}_{12}(\mathbf{x})\right]$$
$$\times \sum_{\{\bar{\eta}_{ij}(\mathbf{x})\}} \delta_{\bar{\nabla}_{ij}\bar{\eta}_{ij},0} \exp\left[-\frac{1}{2\beta}\sum_{\mathbf{x}}\left\{\sum_{i<j}\bar{\sigma}_{ij}^2 + \frac{1}{2\xi}\sum_i \bar{\sigma}_{ij}^2\right.\right.$$
$$\left.\left. - \frac{1}{2\gamma}\left(\sum_i \bar{\sigma}_{ii}(\mathbf{x} - \mathbf{i})\right)^2\right\} - 2\pi i \sum_{\mathbf{x},\ell,n} \bar{X}_{\ell n}(\mathbf{x})\, \bar{\eta}_{\ell n}(\mathbf{x})\right]. \tag{9.40}$$

Since the integrand is manifestly stress gauge invariant, it is possible to go from the gauge fixing $\bar{X}_{3i}(\mathbf{x}) = 0$ to any other gauge, for instance to the transverse gauge,

$$\bar{\nabla}_i \bar{X}_{ij}(\mathbf{x}) = 0. \tag{9.41}$$

The proper normalization is found by the methods developed in Part II, Chapter 3 and applied to lattice gauge theories in Part II, Chapter 6 [see Eq. (6.51)ff in Part II]. We take the integration measure in (9.40) and rewrite it as follows:

$$\prod_{\mathbf{x}} \int d\bar{X}_{11}(\mathbf{x})\, d\bar{X}_{22}(\mathbf{x})\, d\bar{X}_{12}(\mathbf{x}) = \prod_{\mathbf{x},i<j} \int d\bar{X}_{ij}(\mathbf{x})\, \Phi_a[\bar{X}_{ij}], \tag{9.42}$$

where $\Phi_a[\bar{\chi}_{ij}]$ is the axial gauge-fixing functional

$$\Phi_a[\bar{\chi}_{ij}] = \prod_{\mathbf{x},i} \delta(\bar{\chi}_{3i}) \tag{9.43}$$

and perform the integral over all gauge transformed versions of χ_{ij}, $\chi_{ij}^{\Lambda} \equiv \chi_{ij} + \nabla_i \Lambda_j + \nabla_i \Lambda_i$:

$$\prod_{\mathbf{x},i} \int d\Lambda_i(\mathbf{x})\, \delta(\chi_{3i} + \nabla_3 \Lambda_i + \nabla_i \Lambda_3). \tag{9.44}$$

The δ-functions involving Λ_1 and Λ_2 eliminate directly Λ_1, Λ_2 with only a trivial determinant $\det \nabla_3 = 1$. The third δ-function involving $\bar{\chi}_{33}$ leads to $\det(2\nabla_3)^{-1} = 2^{-N}$ so that the gauge integration of (9.43) gives

$$\prod_{\mathbf{x},i} \int d\Lambda_i(\mathbf{x}) \Phi_a[\bar{\chi}_{ij}^{\Lambda}] = 2^{-N}. \tag{9.45}$$

If we now pass over to the transverse gauge we can convince ourselves that the same normalization is achieved by the measure

$$\prod_{\mathbf{x},i<j} \int_{-\infty}^{\infty} d\bar{\chi}_{ij}(\mathbf{x})\, \Phi_t[\bar{\chi}_{ij}], \tag{9.46}$$

where $\Phi_t[\bar{\chi}_{ij}]$ is the transverse gauge-fixing functional [analogous to (6.56) of Part II]

$$\Phi_t[\bar{\chi}_{ij}] = \det(-\bar{\nabla} \cdot \nabla)^3 \prod_{\mathbf{x},j} \delta(\bar{\nabla}_{ij} \bar{\chi}_{ij}). \tag{9.47}$$

In order to see this we write down the integral over $\Phi_t[\bar{\chi}_{ij}^{\Lambda}]$ as follows:

$$\begin{aligned}
&\prod_{\mathbf{x},i} \int_{-\infty}^{\infty} d\Lambda_i(\mathbf{x})\, \Phi_t[\bar{\chi}_{ij} + \nabla_i \Lambda_j + \nabla_j \Lambda_i] \\
&\quad = \det(-\bar{\nabla}\cdot\nabla)^3 \prod_{\mathbf{x},i} \left[\int_{-\infty}^{\infty} d\Lambda_i(\mathbf{x}) \right] \prod_{\mathbf{x},j} \delta(\bar{\nabla}_i \bar{\chi}_{ij} + \bar{\nabla}_i \nabla_i \Lambda_j + \bar{\nabla}_i \nabla_j \Lambda_i) \\
&\quad = \det(-\bar{\nabla}\cdot\nabla)^3 \prod_{\mathbf{x},i} \left[\int_{-\infty}^{\infty} d\Lambda_i(\mathbf{x}) \right] \\
&\qquad \times \prod_{\mathbf{x},j} \delta\left(\bar{\nabla}_i \bar{\chi}_{ij} + \bar{\nabla}\cdot\nabla \left(\delta_{ij} - \frac{\nabla_j \bar{\nabla}_i}{\bar{\nabla}\cdot\nabla} \right) \Lambda_i + 2\bar{\nabla}\cdot\nabla \frac{\nabla_j \bar{\nabla}_i}{\bar{\nabla}\cdot\nabla} \Lambda_i \right).
\end{aligned} \tag{9.48}$$

In the δ-functions, the two transverse components of Λ_j [those which satisfy $\bar{\nabla}_j \Lambda_j = 0$] carry a factor $\bar{\nabla}\cdot\nabla$, the longitudinal component a factor $2\bar{\nabla}\cdot\nabla$. This leads to the functional determinants $\det(-\bar{\nabla}\cdot\nabla)^{-2}$ $\det(-2\bar{\nabla}\cdot\nabla)^{-1} = \det(-\bar{\nabla}\cdot\nabla)^{-3} 2^{-N}$ so that the integral (9.48) gives indeed 2^{-N} and $\Phi_t[\chi_{ij}]$ has the same normalization as $\Phi_a[\chi_{ij}]$.

Notice that it is possible to express $\bar{\eta}_{ij}$ in terms of the defect gauge fields n^s_{ij}, via the incompatibility relation (9.33), and perform the defect sum $\sum_{\{\bar{\eta}_{ij}\}} \delta_{\bar{\nabla}_i \eta_{ij}, 0}$ by summing over the defect gauge field n^s_{ij}. This sum requires, of course, its own gauge-fixing functional $\Phi_{\text{def}}[n^s_{ij}]$. It will be specified in detail in Chapter 11. The partition function (9.40) then involves a path integral over stress gauge fields and a sum over defect gauge fields, both with some gauge-fixing functional,

$$Z = \int \mathscr{D}\chi_{ij} \sum_{\{n^s_{ij}\}} \Phi_{\text{def}}[n^s_{ij}] \exp\{\text{as in (9.40)}\}. \tag{9.49}$$

In this form, the partition function describes a *double gauge theory of stresses and defects*. Let us perform the integral over the stress gauge field, first in the case of two dimensions. There, the decomposition (9.30) reduces to

$$\bar{\sigma}_{ij}(\mathbf{x}) = \varepsilon_{ik}\varepsilon_{j\ell}\bar{\nabla}_k \bar{\nabla}_\ell \bar{\chi}(\mathbf{x}). \tag{9.50a}$$

The components of $\bar{\sigma}_{ij}(\mathbf{x})$ are given by

$$\bar{\sigma}_{11}(\mathbf{x}) = \bar{\nabla}_2^2 \bar{\chi}(\mathbf{x}), \quad \bar{\sigma}_{22}(\mathbf{x}) = \bar{\nabla}_1^2 \bar{\chi}(\mathbf{x}), \quad \bar{\sigma}_{12}(\mathbf{x}) = -\bar{\nabla}_1 \bar{\nabla}_2 \bar{\chi}(\mathbf{x}). \tag{9.50b}$$

We can then easily change the measure of integration from

$$\prod_{\mathbf{x}, i \le j} \left[\int_{-\infty}^{\infty} \frac{d\bar{\sigma}_{ij}(\mathbf{x})}{\sqrt{2\pi\beta}} \right] \prod_j \left[\delta(\bar{\nabla}_i \bar{\sigma}_{ij})\right] \tag{9.51}$$

to

$$\frac{1}{(\sqrt{2\pi\beta})^3} \prod_{\mathbf{x}} \int_{-\infty}^{\infty} d\bar{\chi}(\mathbf{x}) \tag{9.52}$$

since the δ-functions are $\delta(\bar{\nabla}_1 \bar{\sigma}_{11} + \bar{\nabla}_2 \sigma_{21})\, \delta(\bar{\nabla}_1 \bar{\sigma}_{12} + \nabla_2 \bar{\sigma}_{22})$ and can be used to eliminate, for instance, $\bar{\sigma}_{12}(\mathbf{x})$, $\bar{\sigma}_{22}(\mathbf{x})$, with the trivial Jacobian $\det \bar{\nabla}_2^{-2} = 1$. After this $d\bar{\sigma}_{11}(\mathbf{x})$ can be turned into $d\bar{\chi}(\mathbf{x})$ with another trivial Jacobian $\det \bar{\nabla}_2^2 = 1$. Thus the partition function (9.22) becomes for $D = 2$

$$Z = \left[\frac{1}{4\xi^2}\left(1 - 2\frac{\xi}{\gamma}\right)\right]^{N/2} \frac{1}{(\sqrt{2\pi\beta})^{3N}} \prod_{\mathbf{x}} \left[\int_{-\infty}^{\infty} d\bar{\chi}(\mathbf{x})\right]$$

$$\times \sum_{\{\dot{n}_{ij}(\mathbf{x})\}} \Phi[n_{ij}]\, e^{-(1/2\beta)\Sigma_{\mathbf{x}}\{\bar{\sigma}_{12}^2(\mathbf{x}) + (1/2\xi)(\bar{\sigma}_{11}^2(\mathbf{x}) + \bar{\sigma}_{22}(\mathbf{x})^2) - (1/2\gamma)(\bar{\sigma}_{11}(\mathbf{x}-\mathbf{1}) + \bar{\sigma}_{22}(\mathbf{x}-\mathbf{2}))^2\}}$$

$$\times e^{2\pi i \Sigma_{\mathbf{x}} \bar{\eta}(\mathbf{x})\bar{\chi}(\mathbf{x})}, \tag{9.53}$$

where

$$\bar{\eta}(\mathbf{x}) = \varepsilon_{ki}\varepsilon_{\ell j}\nabla_k \nabla_\ell n_{ij}^s(\mathbf{x}) \tag{9.54}$$

is the two-dimensional defect density analogous to $\bar{\eta}_{ij}(\mathbf{x})$ of (9.33).

We now insert the decomposition (9.50) and see that the elastic energy becomes explicitly

$$-\frac{1}{2\beta}\sum_{\mathbf{x}} \bar{\chi}(\mathbf{x})\left\{\bar{\nabla}_1\nabla_1 \cdot \bar{\nabla}_2\nabla_2 + \frac{1}{2\xi}[(\bar{\nabla}_1\nabla_1)^2 + (\bar{\nabla}_2\nabla_2)^2] - \frac{1}{2\gamma}(\bar{\nabla}\cdot\nabla)^2\right\}\bar{\chi}(\mathbf{x}). \tag{9.55}$$

In the last term, a few manipulations were necessary to arrive at the form $(\bar{\nabla}\cdot\nabla)^2$. First we employed summation by parts

$$\sum_{\mathbf{x}} (\bar{\nabla}_2^2\bar{\chi}(\mathbf{x}-\mathbf{1}) + \bar{\nabla}_1^2\bar{\chi}(\mathbf{x}-\mathbf{2}))(\bar{\nabla}_2^2\bar{\chi}(\mathbf{x}-\mathbf{1}) + \bar{\nabla}_1^2\bar{\chi}(\mathbf{x}-\mathbf{2}))$$

$$= \sum_{\mathbf{x}} (\bar{\chi}(\mathbf{x}-\mathbf{1})\nabla_2^2\bar{\nabla}_2^2\bar{\chi}(\mathbf{x}-\mathbf{1}) + \bar{\chi}(\mathbf{x}-\mathbf{2})\nabla_1^2\bar{\nabla}_1^2\bar{\chi}(\mathbf{x}-\mathbf{2})$$

$$+ 2\bar{\chi}(\mathbf{x}-\mathbf{1})\nabla_2^2\bar{\nabla}_1^2\bar{\chi}(\mathbf{x}-\mathbf{2})). \tag{9.56}$$

Then we rewrote the last term as

$$2\sum_{\mathbf{x}} \nabla_1^2\bar{\chi}(\mathbf{x}-\mathbf{1})\nabla_2^2\bar{\chi}(\mathbf{x}-\mathbf{2}) = 2\sum_{\mathbf{x}} \bar{\nabla}_1\nabla_1\bar{\chi}(\mathbf{x})\bar{\nabla}_2\nabla_2\bar{\chi}(\mathbf{x})$$

$$= 2\sum_{\mathbf{x}} \bar{\chi}(\mathbf{x})\bar{\nabla}_1\nabla_1\bar{\nabla}_2\nabla_2\bar{\chi}(\mathbf{x}).$$

Using finally translational invariance we obtain, indeed, $\Sigma_{\mathbf{x}}\bar{\chi}(\mathbf{x})(\bar{\nabla}\cdot\nabla)^2\bar{\chi}(\mathbf{x})$.

Integrating out the $\bar{\chi}(\mathbf{x})$ field gives[c]

$$Z = \left(\sqrt{\frac{1-2\xi/\gamma}{2\xi(1-\xi/\gamma)}} \right)^N \frac{1}{\sqrt{2\pi\beta}^{2N}} \det\left[(\bar{\nabla}\cdot\nabla)^2 + 2\frac{(\xi-1)}{1-\xi/\gamma} \bar{\nabla}_1\nabla_1\bar{\nabla}_2\nabla_2 \right]^{-1/2}$$

$$\times \sum_{\{\bar{\eta}(\mathbf{x})\}} e^{-\beta 4\pi^2(\xi/(1-\xi/\gamma))\Sigma_{\mathbf{x},\mathbf{x}'}\bar{\eta}(\mathbf{x})G(\mathbf{x}-\mathbf{x}')\bar{\eta}(\mathbf{x}')}$$

$$= \frac{1}{(\sqrt{2\pi\beta})^{2N}} \det\left[\left(2\xi + \frac{\lambda}{\mu}\right)(\bar{\nabla}\cdot\nabla)^2 + 4(\xi-1)\left(\xi+\frac{\lambda}{\mu}\right)\bar{\nabla}_1\nabla_1\bar{\nabla}_2\nabla_2 \right]^{-1/2}$$

$$\times \sum_{\{\bar{\eta}(\mathbf{x})\}} e^{-\beta 4\pi^2\xi(1+\nu)\Sigma_{\mathbf{x},\mathbf{x}'}\bar{\eta}(\mathbf{x})G(\mathbf{x}-\mathbf{x}')\bar{\eta}(\mathbf{x}')} \tag{9.57}$$

where $G(\mathbf{x})$ is the lattice Green function[c]

$$G(\mathbf{x}) = \frac{1}{N}\sum_{\mathbf{k}} e^{i\mathbf{k}\cdot\mathbf{x}} \frac{1}{(\bar{\mathbf{K}}\cdot\mathbf{K})^2 + 2\dfrac{\xi-1}{1-\xi/\gamma}\bar{K}_1K_1\bar{K}_2K_2} = \int \frac{d^2k}{(2\pi)^2}$$

$$\times \frac{1}{(2-2\cos k_1 + 2 - 2\cos k_2)^2 + 2(\xi-1)(1+\nu)(2-2\cos k_1)(2-2\cos k_2)}. \tag{9.58}$$

where we have used the *anisotropic Poisson ratio*

$$\gamma = \frac{\lambda}{(D-1)\lambda + 2\xi\mu} = \frac{\xi}{\gamma - \xi}. \tag{9.59}$$

In the isotropic limit $\xi = 1$ the partition function becomes simply

$$Z = \frac{1}{(\sqrt{2\pi\beta/\mu})^{2N}} \frac{1}{(\sqrt{\mu(2\mu+\lambda)}^N} \frac{1}{\det(-\bar{\nabla}\cdot\nabla)}$$

$$\times \sum_{\{\bar{\eta}(\mathbf{x})\}} e^{-\beta 4\pi^2(1+\nu)\Sigma_{\mathbf{x},\mathbf{x}'}\bar{\eta}(\mathbf{x})G(\mathbf{x}-\mathbf{x}')\bar{\eta}(\mathbf{x}')}, \tag{9.60}$$

where now

[c]We have used the $D = 2$ identity

$$1 - \frac{\xi}{\gamma} = 1 - \frac{\xi\dfrac{\lambda}{\mu}}{2\xi\left(\dfrac{\lambda}{\mu}+\xi\right)} = \frac{2\xi + \dfrac{\lambda}{\mu}}{2\left(\xi + \dfrac{\lambda}{\mu}\right)}.$$

$$G(\mathbf{x}) = v_4(\mathbf{x}) = \frac{1}{N}\sum_{\mathbf{k}} e^{i\mathbf{k}\cdot\mathbf{x}} \frac{1}{(\bar{\mathbf{K}}\cdot\mathbf{K})^2}$$

$$= \int \frac{d^2k}{(2\pi)^2} e^{i\mathbf{k}\cdot\mathbf{x}} \frac{1}{(2-2\cos k_1 + 2 - 2\cos k_2)^2}. \tag{9.61}$$

Inserting $\beta = \mu a^2/(k_B T(2\pi)^2)$ and going to momentum variables, the prefactor becomes the two-dimensional version of the partition function (7.72),

$$Z_{\text{pot,cl}} = \prod_{\mathbf{k}} (\sqrt{2\pi k_B T})^2 \frac{1}{\sqrt{a^2\mu\bar{\mathbf{K}}\cdot\mathbf{K}}} \frac{1}{\sqrt{a^2(2\mu+\lambda)\bar{\mathbf{K}}\cdot\mathbf{K}}}. \tag{9.62}$$

Hence we expect the prefactor in the $\xi \neq 1$ partition function (9.57) to be the proper anisotropic version of this. Indeed, if we take the fluctuation energy of the elastic waves

$$e^{-\beta(\sum_{\mathbf{x},i} u_{ii}^2 + (\xi-1)\sum_{\mathbf{x},i} u_{ii}^2 + (\lambda/2\mu)\sum_{\mathbf{x}}(\sum_i u_{ii}(\mathbf{x}-\boldsymbol{\ell}))^2)} \tag{9.63}$$

and write it in momentum space as

$$e^{-(\beta/2)\sum_{\mathbf{k}} u_i(\mathbf{k})^*[K_i\bar{K}_i + \mathbf{K}\cdot\bar{\mathbf{K}}\delta_{ij} + 2(\xi-1)K_i\bar{K}_i\delta_{ij} + (\lambda/\mu)K_i\bar{K}_i]u_j(\mathbf{k})}. \tag{9.64}$$

Then the 2×2 determinant of the fluctuation matrix is

$$\det\begin{pmatrix} K\bar{K}_1 + \bar{\mathbf{K}}\cdot\mathbf{K} + 2(\xi-1)\bar{K}_1K_1 + \frac{\lambda}{\mu}\bar{K}_1K_1 & \left(1+\frac{\lambda}{\mu}\right)\bar{K}_1K_2 \\ \left(1+\frac{\lambda}{\mu}\right)K_2\bar{K}_1 & K_2\bar{K}_2 + \mathbf{K}\cdot\bar{\mathbf{K}} + 2(\xi-1)K_2\bar{K}_2 + \frac{\lambda}{\mu}K_2\bar{K}_2 \end{pmatrix}$$

$$= \bar{K}_1K_1\bar{K}_2K_2 + \left(2\xi+\frac{\lambda}{\mu}\right)^2\bar{K}_1K_1\bar{K}_2K_2 + \left(2\xi+\frac{\lambda}{\mu}\right)[(\bar{K}_1K_1)^2 + (\bar{K}_2K_2)^2]$$

$$- \left(1+\frac{\lambda}{\mu}\right)^2\bar{K}_1K_1\bar{K}_2K_2$$

$$= \left(2\xi+\frac{\lambda}{\mu}\right)(\bar{\mathbf{K}}\cdot\mathbf{K})^2 + 4(\xi-1)\left(\xi+\frac{\lambda}{\mu}\right)\bar{K}_1K_1\bar{K}_2K_2$$

$$= 2\xi(1-\nu)^{-1}[(\bar{\mathbf{K}}\cdot\mathbf{K})^2 + 2(\xi-1)(1+\nu)\bar{K}_1K_1\bar{K}_2K_2]. \tag{9.65}$$

Comparison with (9.57) confirms our expectation: the integral over the $u_i(\mathbf{k})$ fluctuations is indeed the same as the prefactor in (9.57).

Thus, due to the Gaussian form of the model, the partition function factorizes into a pure phonon part $Z_{\text{pot,cl}}$, the prefactor in (9.57), and a pure defect part,

$$Z_{\text{def}} = \sum_{\{\bar{\eta}(\mathbf{x})\}} e^{-\beta 4\pi^2 2\xi((\xi+\lambda/\mu)/(2\xi+\lambda/\mu))\Sigma_{\mathbf{x},\mathbf{x}'}\bar{\eta}(\mathbf{x})G(\mathbf{x}-\mathbf{x}')\bar{\eta}(\mathbf{x}')}, \tag{9.66}$$

which, in the isotropic case, is equal to

$$Z_{\text{def}} = \sum_{\{\bar{\eta}(\mathbf{x})\}} e^{-\beta 4\pi^2(1+\nu)\Sigma_{\mathbf{x}}\bar{\eta}(\mathbf{x})((-\nabla\cdot\nabla)^{-2}\bar{\eta})(\mathbf{x})}. \tag{9.67}$$

For the calculation of the Green function we may write it as

$$G(\mathbf{x}) = \int \frac{d^2k}{(2\pi)^2} e^{i\mathbf{k}\cdot\mathbf{x}} \frac{1}{(\bar{\mathbf{K}}\cdot\mathbf{K})^2 + \varepsilon \bar{K}_1 K_1 \bar{K}_2 K_2} \tag{9.68}$$

with the anisotropy parameter

$$\varepsilon = 4(\xi - 1)\frac{\xi + \lambda/\mu}{2\xi + \lambda/\mu} \tag{9.69}$$

and factorize

$$\frac{1}{(\bar{\mathbf{K}}\cdot\mathbf{K})^2 + \varepsilon \bar{K}_1 K_1 \bar{K}_2 K_2} = \frac{1}{\alpha \bar{K}_1 K_1 + \beta \bar{K}_2 K_2} \frac{1}{\beta \bar{K}_1 K_1 + \alpha \bar{K}_2 K_2}$$

with

$$\left\{\begin{matrix}\alpha^2 \\ \beta^2\end{matrix}\right\} = 1 + \frac{\varepsilon}{2} \pm \sqrt{\left(1 + \frac{\varepsilon}{2}\right)^2 - 1}.$$

Then we introduce a subtraction and define

$$G'(\mathbf{x}) = \int \frac{d^2k}{(2\pi)^2}(e^{i\mathbf{k}\cdot\mathbf{x}} - 1)\frac{1}{(\bar{\mathbf{K}}\cdot\mathbf{K})^2 + \varepsilon \bar{K}_1 K_1 \bar{K}_2 K_2}.$$

For large distances this diverges as

$$G'(\mathbf{x}) \to -\frac{\mathbf{x}^2}{4}\int \frac{d^2k}{(2\pi)^2}\frac{\bar{\mathbf{K}}\cdot\mathbf{K}}{(\bar{\mathbf{K}}\cdot\mathbf{K})^2+\varepsilon\bar{K}_1K_1\bar{K}_2K_2}$$

$$= -\frac{\mathbf{x}^2}{4}\frac{1}{\alpha+\beta}\int \frac{d^2k}{(2\pi)^2}\frac{(\alpha\bar{K}_1K_1+\beta\bar{K}_2K_2)+(\alpha\leftrightarrow\beta)}{(\alpha\bar{K}_1K_1+\beta\bar{K}_2K_2)\cdot(\alpha\leftrightarrow\beta)}$$

$$= -\frac{\mathbf{x}^2}{4}\frac{2}{\alpha+\beta}\int \frac{d^2k}{(2\pi)^2}\frac{1}{\alpha\bar{K}_1K_1+\beta\bar{K}_2K_2}.$$

Thus if we introduce the logarithmically divergent quantity

$$v_\varepsilon(0)=\int \frac{d^2k}{(2\pi)^2}\frac{\bar{\mathbf{K}}\cdot\mathbf{K}}{(\bar{\mathbf{K}}\cdot\mathbf{K})^2+\varepsilon\bar{K}_1K_1\bar{K}_2K_2}=\frac{2}{\alpha+\beta}\int\frac{d^2k}{(2\pi)^2}\frac{1}{\alpha\bar{K}_1K_1+\beta\bar{K}_2K_2},$$

we arrive at the finite twice subtracted anisotropic potential between disclinations,

$$G''(\mathbf{x}) = G'(\mathbf{x}) + \frac{\mathbf{x}^2}{4}v_\varepsilon(\mathbf{0})$$

$$= \int \frac{d^2k}{(2\pi)^2}\left(e^{i\mathbf{k}\cdot\mathbf{x}} - 1 + \frac{\mathbf{x}^2}{4}\mathbf{K}\cdot\bar{\mathbf{K}}\right)\frac{1}{(\bar{\mathbf{K}}\cdot\mathbf{K})^2+\varepsilon\bar{K}_1K_1\bar{K}_2K_2}$$

$$= \int \frac{d^2x}{(2\pi)^2}\left(\cos k_1x_1\cos k_2x_2 - 1 + \frac{\mathbf{x}^2}{4}\bar{\mathbf{K}}\cdot\mathbf{K}\right)\frac{1}{(\bar{\mathbf{K}}\cdot\mathbf{K})^2+\varepsilon\bar{K}_1K_1\bar{K}_2K_2}. \tag{9.70}$$

The Green function (9.68) itself is finite only after introducing a small regulator mass m. In the limit $m\to 0$, it contains the same two types of divergences as it would in the continuum since they are caused by the $\mathbf{k}\to 0$ limit of the integrand and for long distances all lattice gradients can be replaced by ordinary gradients. It is useful to remove these divergencies from $G(\mathbf{x})$ by defining $G''(\mathbf{x})$ as follows

$$G(\mathbf{x}) = G_{\text{div}}(\mathbf{x}) + G''(\mathbf{x}), \tag{9.71}$$

where, for $\varepsilon = 0$, the divergent part is given by

$$G_{\text{div}}(\mathbf{x}) \equiv \frac{1}{4\pi m^2} + \frac{1}{8\pi}|\mathbf{x}|^2\log m. \tag{9.72}$$

If we insert the above into (9.66) we see that there can be a finite limit only if

$$\sum_{\mathbf{x},\mathbf{x}'} \bar{\eta}(\mathbf{x})\,\bar{\eta}(\mathbf{x}') = \left(\sum_{\mathbf{x}} \bar{\eta}(\mathbf{x})\right)^2 = 0, \tag{9.73}$$

$$\sum_{\mathbf{x},\mathbf{x}'} |\mathbf{x}-\mathbf{x}'|^2\,\bar{\eta}(\mathbf{x})\,\bar{\eta}(\mathbf{x}') = 0. \tag{9.74}$$

The first condition enforces defect neutrality, i.e.,

$$\sum_{\mathbf{x}} \bar{\eta}(\mathbf{x}) = 0. \tag{9.75}$$

The second can be rewritten as

$$2\sum_{\mathbf{x}} \mathbf{x}^2\,\bar{\eta}(\mathbf{x}) \sum_{\mathbf{x}'} \bar{\eta}(\mathbf{x}') - 2\left(\sum_{\mathbf{x}} \mathbf{x}\,\bar{\eta}(\mathbf{x})\right)^2 = 0.$$

Using charge neutrality this reduces to

$$\sum_{\mathbf{x}} \mathbf{x}\,\bar{\eta}(\mathbf{x}) = 0, \tag{9.76}$$

i.e., in addition to charge neutrality there must also be dipole neutrality.

Notice that once the defects satisfy these two conditions, the Green's function $G''(\mathbf{x})$ can be exchanged by any other one which differs from it by an arbitrary constant plus a quadratic term

$$\Delta G(\mathbf{x}) = \text{const.} + c_{ij} x_i x_j. \tag{9.77}$$

Such an additional piece never contributes to the sum since

$$\frac{1}{2}\sum_{\mathbf{x},\mathbf{x}'} \bar{\eta}(\mathbf{x})\,\Delta G(\mathbf{x}-\mathbf{x}')\,\bar{\eta}(\mathbf{x}') = 0.$$

As a particular finite Green function we may therefore take the previously introduced subtracted expression (9.70) whose values will be given later in Table 11.2.

In three dimensions, the analogous derivation of the defect representation is much more tedious. One thing is immediately obvious: the partition function will certainly factorize in the same way as in two dimensions [see Eq. (9.57)],

$$Z = Z_{\text{pot,cl}}\, Z_{\text{def}}, \tag{9.78}$$

where the classical part can be obtained by simply integrating out the $u_i(\mathbf{k})$ fluctuations of the harmonic energy (9.11). Thus $Z_{\text{pot,cl}}$ will be the generalization of the isotropic expression (7.72),

$$Z_{\text{pot,cl}} = \prod_{\mathbf{k}} \left(\sqrt{2\pi k_B T^3} \frac{1}{(\sqrt{a^3 \mu \bar{\mathbf{K}} \cdot \mathbf{K}})^2} \frac{1}{\sqrt{a^3 (2\mu + \lambda) \bar{\mathbf{K}} \cdot \mathbf{K}}} \right) \tag{9.79}$$

to the anisotropic case. To be able to find this, all we have to do is replace the isotropic fluctuation determinant

$$\prod_{\mathbf{k}} \det \left(\mu (\bar{\mathbf{K}} \cdot \mathbf{K} \delta_{ij} + \bar{K}_i K_j) + \frac{\lambda}{\mu} \bar{K}_i K_j \right) = \prod_{\mathbf{k}} (\mu \bar{\mathbf{K}} \cdot \mathbf{K})^2 \prod_{\mathbf{k}} (2\mu + \lambda) \bar{\mathbf{K}} \cdot \mathbf{K} \tag{9.80}$$

by the full one. Writing (9.10) out in matrix from gives

$$E = a\mu \sum_{\mathbf{x}} \frac{1}{2} u_i(\mathbf{x}) \left(\bar{\nabla} \cdot \nabla \delta_{ij} + \nabla_i \bar{\nabla}_j + 2(\xi - 1) \nabla_i \bar{\nabla}_i \delta_{ij} + \frac{\lambda}{\mu} \nabla_i \bar{\nabla}_j \right) u_j(\mathbf{x}) \tag{9.81}$$

so that the full determinant becomes

$$\prod_{\mathbf{k}} \mu^3 \det \left(\mathbf{K} \cdot \bar{\mathbf{K}} \delta_{ij} + K_i \bar{K}_j + 2(\xi - 1) K_i \bar{K}_i \delta_{ij} + \frac{\lambda}{\mu} K_i \bar{K}_j \right). \tag{9.82}$$

This can easily be calculated after bringing it to the form

$$\prod_{\mathbf{k},i} \mu (\bar{\mathbf{K}} \cdot \mathbf{K} + 2(\xi - 1) \bar{K}_i K_i) \, e^{\sum_{\mathbf{k}} \operatorname{tr} \log [\delta_{ij} + (1 + \lambda/\mu) K_i \bar{K}_j / (\bar{\mathbf{K}} \cdot \mathbf{K} + 2(\xi - 1) \bar{K}_i K_i)]} \tag{9.83}$$

and expanding the logarithm in a power series,

$$-\sum \frac{1}{n} \left(-\left(1 + \frac{\lambda}{\mu} \right) \right)^n \operatorname{tr} M^n, \tag{9.84}$$

where M denotes the matrix

$$M_{ij} = \frac{K_i \bar{K}_j}{\bar{\mathbf{K}} \cdot \mathbf{K} + 2(\xi - 1) \bar{K}_i K_i}. \tag{9.85}$$

This is a projection matrix up to a factor

$$M_{ij}^2 = \left(\sum_\ell \frac{\bar{K}_\ell K_\ell}{\bar{\mathbf{K}} \cdot \mathbf{K} + 2(\xi - 1)\bar{K}_\ell K_\ell} \right) M_{ij} \equiv c M_{ij}, \tag{9.86}$$

where the factor c is just the trace of M, i.e.,

$$\operatorname{tr} M^n = \operatorname{tr}(c^{n-1} M) = c^n.$$

The sum (9.84) can now be performed with the result

$$\log\left[1 + \left(1 + \frac{\lambda}{\mu} c\right)\right].$$

Thus we obtain, for anisotropic materials in $D = 3$ dimensions,

$$Z_{\text{cl, pot}} = \left(\sqrt{\frac{2\pi k_B T}{\mu}} \right)^N \prod_{\mathbf{k},i} \frac{1}{\sqrt{\bar{\mathbf{K}} \cdot \mathbf{K} + 2(\xi - 1)\bar{K}_i K_i}} \times \prod_{\mathbf{k}} \frac{1}{\sqrt{1 + \left(1 + \frac{\lambda}{\mu}\right) \sum_\ell \frac{\bar{K}_\ell K_\ell}{\bar{\mathbf{K}} \cdot \mathbf{K} + 2(\xi - 1)\bar{K}_\ell K_\ell}}}. \tag{9.87}$$

Inserting $D = 2$, this formula is seen to reproduce correctly the two-dimensional prefactor in (9.57).

In order to calculate the infinite products in (9.57) (9.87) numerically we write them in two dimensions as

$$\exp\left\{ -\frac{1}{2}\log 2 - \frac{1}{2}\int \frac{d^2k}{(2\pi)^2} \log\left\{ \left[A_1 A_2 + \left(1 + \frac{\lambda}{\mu}\right)(\bar{K}_1 K_1 A_2 + \bar{K}_2 K_2 A_1) \right] \Big/ 2 \right\} \right\}, \tag{9.88a}$$

with

$$A_1 = (2\xi - 1)\bar{K}_1 K_1 + \bar{K}_2 K_2, \qquad A_2 = \bar{K}_1 K_1 + (2\xi - 1)\bar{K}_2 K_2$$

and in three dimensions as

$$\exp\left\{ -\frac{1}{2}\log 2 - \frac{1}{2}\int \frac{d^3k}{(2\pi)^3} \log\left\{ \left[A_1 A_2 A_3 + \left(1 + \frac{\lambda}{\mu}\right) \sum_{ijk \text{ cycl.}} \bar{K}_i K_j A_j A_k \right] \Big/ 2 \right\} \right\}, \tag{9.88b}$$

with

$$A_i = (2\xi - 1)\,\bar{K}_i K_i + \bar{K}_j K_j + \bar{K}_k K_k \quad (i,\ j,\ k = \text{cycl.}),$$

and approximate the momentum integral by a sum

$$\int \frac{d^D k}{(2\pi)^D} \approx \frac{1}{N^D} \sum_{\substack{k_i = \frac{2\pi}{N}(n_i - 0.5) \\ n_i = 1, 2, \ldots, N}} .$$

In three dimensions, the integral is so smooth that we obtain a reasonable accuracy for the rather small value $N = 3$. In two dimensions, the integral is not as well behaved at the origin in momentum space and we have to take at least $N = 10$ to obtain satisfactory accuracy (except for very small ξ for which N has to be taken much larger than that). In order to display the result we write the second exponential in (9.88a,b) as

$$e^{-(D/2)\ell} \tag{9.89}$$

and give ℓ as a function of ξ, for $\lambda = 0$ in Table 9.1. We also plot $\ell - \log(2D)$ for various ξ and λ in Fig. 9.1.

As a check of our accuracy we set $\xi = 1$, $\lambda = 0$ in which case we must recover the free field trace logs

TABLE 9.1. Logarithm of the fluctuation determinants in $D = 2$ and $D = 3$ dimensions for anisotropic lattice $\ell = \frac{1}{D}\int \frac{d^D k}{(2\pi)^D} \log\left[\left(\prod_{i=1}^{D} A_i\right)\left(1 + \left(1 + \frac{\lambda}{\mu}\right)\sum_{j=1}^{D} \frac{\bar{K}_j K_j}{A_j}\right)\Big/ 2\right]$, where $A_i = \bar{\mathbf{K}}\cdot\mathbf{K} + 2(\xi - 1)\bar{K}_i K_i$. For $\lambda = 1$, $\xi = 1$ this reduces to $\int (d^D k/(2\pi)^D) \log \bar{\mathbf{K}}\cdot\mathbf{K}$.

ξ	$\frac{\lambda}{\mu} = 0$	$\frac{\lambda}{\mu} = 1$	$\frac{\lambda}{\mu} = 2$	$\frac{\lambda}{\mu} = 3$	ξ	$\frac{\lambda}{\mu} = 0$	$\frac{\lambda}{\mu} = 1$	$\frac{\lambda}{\mu} = 2$	$\frac{\lambda}{\mu} = 3$
0.2	0.2060	0.6560	0.8844	1.0399	0.2	1.0352	1.2668	1.3998	1.4942
0.4	0.5980	0.9241	1.1187	1.2582	0.4	1.2708	1.4585	1.5774	1.6647
0.6	0.8411	1.1076	1.2803	1.4083	0.6	1.4351	1.5990	1.7083	1.7904
0.8	1.0214	1.2506	1.4071	1.5261	0.8	1.5649	1.7124	1.8143	1.8923
1.0	1.1662	1.3690	1.5128	1.6244	1.0	1.6734	1.8085	1.9044	1.9788
1.2	1.2880	1.4707	1.6042	1.7094	1.2	1.7672	1.8925	1.9833	2.0546
1.4	1.3934	1.5602	1.6850	1.7848	1.4	1.8503	1.9672	2.0536	2.1222
1.6	1.4866	1.6404	1.7577	1.8527	1.6	1.9249	2.0349	2.1174	2.1835

FIG. 9.1. The logarithm of the fluctuation determinants $\ell - \log(2D)$ as defined in (9.88), (9.89) [ℓ is the anisotropic version of $\int (d^D k/(2\pi)^D) \log(\bar{\mathbf{K}} \cdot \mathbf{K})$] as a function of $\xi = (c_{11} - c_{12})/2c_{44}$ for various values of $\lambda/\mu = c_{12}/c_{44}$.

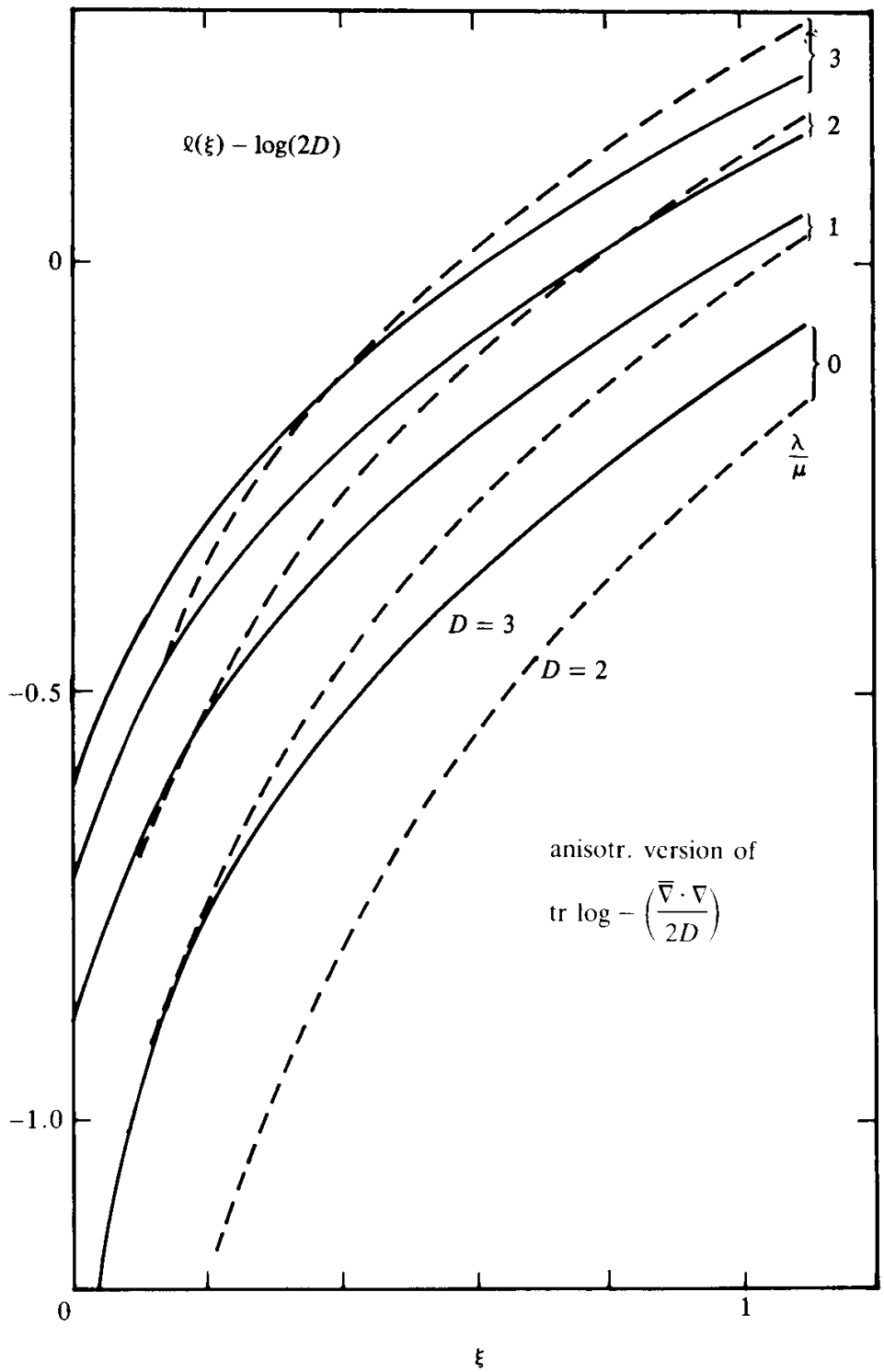

$$\ell = \int \frac{d^D k}{(2\pi)^D} \log(\bar{\mathbf{K}} \cdot \mathbf{K}) = \begin{cases} 1.1664 & D = 2, \\ 1.6734 & D = 3, \end{cases}$$

calculated in Part I, Chapter 6. Our approximate sums give, instead

1.1662 and 1.6734 and are in good agreement with these numbers.

Let us now come to the harder part, the calculation of the defect factor Z_{def} in (9.78). For this we take the gauge $\bar{\chi}_{3\ell} = 0$ and insert (9.37), (9.38) into the stress exponent (9.22) which takes the momentum-space form

$$-\frac{1}{2\beta}\sum_{\mathbf{x}}\left[(\bar{\sigma}_{12}^2+\bar{\sigma}_{23}^2+\bar{\sigma}_{31}^2)+\frac{1}{2\xi}(\bar{\sigma}_{11}^2+\bar{\sigma}_{22}^2+\bar{\sigma}_{33}^2)-\frac{1}{2\gamma}\left(\sum_{\ell}\bar{\sigma}_{\ell\ell}\right)^2\right]$$
$$=-\frac{1}{2\beta}\sum_{\mathbf{k}}\bar{\chi}_I^{\dagger}(\mathbf{k})\,M_{IJ}(\mathbf{k})\,\bar{\chi}_J(\mathbf{k})+2\pi i\sum_{k}\bar{\eta}_I^{\dagger}(\mathbf{k})\,\bar{\chi}_I(\mathbf{k}), \tag{9.90}$$

where $\bar{\chi}_I$ denotes the components

$$\bar{\chi}_{11}(\mathbf{x}-2\cdot\mathbf{1}-\mathbf{2}),\quad \bar{\chi}_{22}(\mathbf{x}-2\cdot\mathbf{2}-\mathbf{1}),\quad \bar{\chi}_{12}(\mathbf{x}-\mathbf{1}-\mathbf{2})$$

and η_I the components

$$\bar{\eta}_{11}(\mathbf{x}-2\cdot\mathbf{1}-\mathbf{2}),\quad \bar{\eta}_{22}(\mathbf{k}-2\cdot\mathbf{2}-\mathbf{1}),\quad 2\bar{\eta}_{12}(\mathbf{x}-\mathbf{1}-\mathbf{2}).$$

The matrix elements of M_{IJ} are

$$M_{11,11}=\bar{K}_2K_2\bar{K}_3K_3+\frac{1}{2\xi}[(\bar{K}_2K_2)^2+(\bar{K}_3K_3)^2]-\frac{1}{2\gamma}(\bar{K}_2K_2+\bar{K}_3K_3)^2,$$

$$M_{22,22}=\bar{K}_1K_1\bar{K}_3K_3+\frac{1}{2\xi}[(\bar{K}_1K_1)^2+(\bar{K}_3K_3)^2]-\frac{1}{2\gamma}(\bar{K}_1K_1+\bar{K}_3K_3)^2,$$

$$M_{12,12}=\bar{\mathbf{K}}\cdot\mathbf{K}\,\bar{K}_3K_3+2\left(\frac{1}{\xi}-\frac{1}{\gamma}\right)\bar{K}_1K_1\bar{K}_2K_2,$$

$$M_{11,22}=\frac{1}{2\xi}\bar{K}_1K_1\bar{K}_2K_2-\frac{1}{2\gamma}(\bar{K}_1K_1+\bar{K}_3K_3)(\bar{K}_2K_2+\bar{K}_3K_3),$$

$$M_{11,12}=-\bar{K}_1\bar{K}_2\left(\bar{K}_3K_3+\frac{1}{\xi}\bar{K}_2K_2-\frac{1}{\gamma}(\bar{K}_2K_2+\bar{K}_3K_3)\right),$$

$$M_{22,12}=-\bar{K}_1\bar{K}_2\left(\bar{K}_3K_3+\frac{1}{\xi}\bar{K}_1K_1-\frac{1}{\gamma}(\bar{K}_1K_1+\bar{K}_3K_3)\right). \tag{9.91}$$

This matrix can be made real by writing, in $M_{11,12}$, $M_{22,12}$,

$$\bar{K}_1 \bar{K}_2 = e^{-ik_1/2} e^{-ik_2/2} |K_1 K_2|$$

and absorbing the phase into the Fourier transform of $\bar{\chi}_{12}(\mathbf{k})$ i.e., by defining

$$\tilde{\chi}_{12}(\mathbf{k}) = e^{-ik_1/2} e^{-ik_2/2} \bar{\chi}_{12}(\mathbf{k}). \tag{9.92}$$

The remaining real matrix has the same form as its continuum limit, except that the k_i are replaced everywhere by $\tilde{K}_i = 2 \sin k_i/2$. If $\tilde{M}_{IJ}^{-1}(\mathbf{k})$ denotes the inverse matrix, we find

$$Z_{\text{def}} = \sum_{\{\bar{\eta}_{ij}(\mathbf{x})\}} \delta_{\bar{\nabla}_i \eta_{ij}, 0} \, e^{-(4\pi^2\beta/2)\Sigma_{\mathbf{k}} \bar{\eta}_I^*(\mathbf{k}) \tilde{M}_{IJ}^{-1}(\mathbf{k}) \bar{\eta}_J(\mathbf{k})}. \tag{9.93}$$

The wiggles on top of η_I record extra phases carried by $\bar{\eta}_{11}(\mathbf{k})$, $\bar{\eta}_{22}(\mathbf{k})$, $2\bar{\eta}_{12}(\mathbf{k})$, which arise from (9.92) together with the shifts in the arguments of $\chi_{\ell n}(\mathbf{x})$ to $\chi_{\ell n}(\mathbf{x} - \boldsymbol{\ell} - \mathbf{n})$,[d]

$$\begin{aligned}
\tilde{\eta}_{11}(\mathbf{k}) &\equiv e^{-2ik_1 - ik_2} \bar{\eta}_{11}(\mathbf{k}), \\
\tilde{\eta}_{22}(\mathbf{k}) &\equiv e^{-ik_1 - 2ik_2} \bar{\eta}_{22}(\mathbf{k}), \\
\tilde{\eta}_{12}(\mathbf{k}) &\equiv e^{-i(k_1/2 + k_2/2) - ik_1 - ik_2} \bar{\eta}_{12}(\mathbf{k}).
\end{aligned} \tag{9.94}$$

In order to simplify the expression (9.93) it should be realized that if we extend the defect matrix (9.94) to the full 3×3 form, defining also

$$\begin{aligned}
\tilde{\eta}_{13}(\mathbf{k}) &= e^{-i(k_1/2 + k_3/2) - ik_1 - ik_2} \bar{\eta}_{13}(\mathbf{k}), \\
\tilde{\eta}_{23}(\mathbf{k}) &= e^{-i(k_2/2 + k_3/2) - ik_1 - ik_2} \bar{\eta}_{23}(\mathbf{k}), \\
\tilde{\eta}_{33}(\mathbf{k}) &= e^{-i(k_1 + k_2 + k_3)} \bar{\eta}_{33}(\mathbf{k}),
\end{aligned} \tag{9.95}$$

then the new defect matrix satisfies the conservation law

$$\tilde{K}_i \tilde{\eta}_{ij} = 0. \tag{9.96}$$

[d]Recall that the defects were coupled as $\Sigma_{\mathbf{x}} \bar{\eta}_{\ell n}(\mathbf{x}) \bar{\chi}_{\ell n}(\mathbf{x}) \equiv \Sigma_{\mathbf{x}} \bar{\eta}_{\ell n}(\mathbf{x} - \boldsymbol{\ell} - \mathbf{n}) \bar{\chi}_{\ell n}(\mathbf{x} - \boldsymbol{\ell} - \mathbf{n})$ and it is $\bar{\chi}_{\ell n}(\mathbf{x} - \boldsymbol{\ell} - \mathbf{n})$ which appears in (9.90).

This is readily seen by writing these equations down explicitly, for example, for $j = 1$,

$$(e^{ik_1/2} - e^{-ik_1/2})\, e^{-2ik_1 - ik_2}\, \bar{\eta}_{11} + (e^{ik_2/2} - e^{-ik_2/2})\, e^{-i(k_1/2 + k_2/2) - ik_1 - ik_2}\, \bar{\eta}_{12}$$
$$+ (e^{ik_3/2} - e^{-ik_3/2})\, e^{-i(k_1/2 + k_3/2)}\, e^{-ik_1 - ik_2}\, \bar{\eta}_{31}$$
$$= e^{-(3/2)ik_1 - ik_2}[(1 - e^{-ik_1})\, \bar{\eta}_{11} + (1 - e^{-ik_2})\, \bar{\eta}_{21} + (1 - e^{-ik_3})\, \bar{\eta}_{31}], \tag{9.97}$$

and the bracket on the right-hand side vanishes due to

$$\bar{\nabla}_i\, \bar{\eta}_{ij} = 0. \tag{9.98}$$

This implies that the exponent in (9.93) has exactly the same matrix elements as the continuum expression for $\eta_{ij}(\mathbf{k})$, except that k_i is replaced everywhere by $\bar{K}_i$. We can therefore use a well-known result[e] for the defect energy in the continuum and obtain

$$Z_{\text{def}} = \sum_{\{\bar{\eta}_{ij}(\mathbf{x})\}} \delta_{\bar{\nabla}_i \eta_{ij},\, 0} \exp\left\{ -\left(\frac{4\pi^2\beta}{2}\right) \sum_{\mathbf{k}} \left[\sum_i |\bar{\eta}_{ii}|^2 (a\bar{\mathbf{K}}^2 + b\bar{K}_i^2) \right.\right.$$
$$+ 2|\bar{\eta}_{12}|^2 (d\bar{\mathbf{K}}^2 + e\bar{K}_3^2) + 2|\bar{\eta}_{23}|^2 (d\bar{\mathbf{K}}^2 + e\bar{K}_1^2) + 2|\bar{\eta}_{31}|^2 (d\bar{\mathbf{K}}^2 + e\bar{K}_2^2)$$
$$\left.\left. + \left| \sum_\ell \bar{\eta}_{\ell\ell} \right|^2 c\bar{\mathbf{K}}^2 \right] \frac{1}{\Delta} \right\}, \tag{9.99}$$

where Δ is the determinant of the matrix (9.82)

$$\Delta = (\bar{\mathbf{K}}^2 + 2(\xi - 1)\, \bar{K}_1^2)(\bar{\mathbf{K}}^2 + 2(\xi - 1)\, \bar{K}_2^2)(\bar{\mathbf{K}}^2 + 2(\xi - 1)\, \bar{K}_3^2)$$
$$\times \left[1 + \left(1 + \frac{\lambda}{\mu}\right) \sum_i \frac{\bar{K}_i^2}{\bar{\mathbf{K}}^2 + 2(\xi - 1)\, \bar{K}_1^2} \right]$$
$$= \left(2\xi + \frac{\lambda}{\mu}\right) \bar{\mathbf{K}}^6 + 4(\xi - 1)\left(\xi + \frac{\lambda}{\mu}\right)(\bar{K}_1^2 \bar{K}_2^2 + \bar{K}_2^2 \bar{K}_3^2 + \bar{K}_3^2 \bar{K}_1^2)\bar{\mathbf{K}}^2$$
$$+ 4(\xi - 1)^2 \left(2\xi + 1 + 3\frac{\lambda}{\mu}\right) \bar{K}_1^2 \bar{K}_2^2 \bar{K}_3^2, \tag{9.100}$$

and

[e]This result is due to E. Kröner, *Zeitschr. Phys.* **141** (1955) 386, who calculates

$$\chi_{11} = (\mu/\Delta)[a\mathbf{k}^2 + bk_1^2)\, \eta_{11} + \mathbf{k}^2 \eta_{\ell\ell}], \quad \chi_{12} = (\mu/\Delta)(d\mathbf{k}^2 + ek_3^2)\, \eta_{12}, \ \ldots$$

For a derivation of (9.98) from (9.93) see Appendix 9A.

$$a = 2\xi\left(2\xi + \frac{\lambda}{\mu}\right), \quad b = 4(\xi - 1)\left(2\xi^2 + (3\xi - 1)\frac{\lambda}{\mu}\right), \quad c = 2\xi\frac{\lambda}{\mu},$$
$$d = 2\left[2\xi^2 + (2\xi - 1)\frac{\lambda}{\mu}\right], \quad e = -4(\xi - 1)\left(\xi + \frac{\lambda}{\mu}\right). \tag{9.101}$$

For the individual $|\bar{\eta}_{\ell n}|^2$, the wiggles can be dropped, since they amount only to a phase. The only term for which the wiggles have a non-trivial effect is $|\Sigma_\ell\, \bar{\eta}_{\ell\ell}|^2$. Inserting the proper shift in the arguments, this reads in x-space

$$\sum_{\mathbf{x}} [\bar{\eta}_{11}(\mathbf{x} - 2\cdot\mathbf{1} - \mathbf{2}) + \bar{\eta}_{22}(\mathbf{x} - \mathbf{1} - 2\cdot\mathbf{2}) + \bar{\eta}_{33}(\mathbf{x} - \mathbf{1} - \mathbf{2} - \mathbf{3})]^2. \tag{9.102}$$

Shifting all the arguments by $\mathbf{1} + \mathbf{2}$, this becomes simply

$$\sum_{\mathbf{x}} \left(\sum_{\ell} \bar{\eta}_{\ell\ell}(\mathbf{x} - \boldsymbol{\ell})\right)^2, \tag{9.103}$$

in complete analogy with the shift of the argument in the stress energy $(\Sigma_i \sigma_{ii}(\mathbf{x} - \mathbf{i}))^2$ in (9.21). Thus we can render the defect partition function on a cubic lattice in the form

$$Z_{\text{def}} = \sum_{\{\bar{\eta}_{ij}(\mathbf{x})\}} \delta_{\bar{\nabla}_i \bar{\eta}_{ij}(\mathbf{x}),0} \exp\left\{-\frac{4\pi^2\beta}{2}\sum_{\mathbf{x},\mathbf{x}'}\left[\sum_i \bar{\eta}_{ii}(\mathbf{x})(aG + bG_i)(\mathbf{x} - \mathbf{x}')\,\eta_{ii}(\mathbf{x}')\right.\right.$$
$$+ 2\sum_{i,j,k\,=\,\text{cyclic}} \bar{\eta}_{ij}(\mathbf{x})(dG + eG_k)(\mathbf{x} - \mathbf{x}')\,\bar{\eta}_{ij}(\mathbf{x}')$$
$$\left.\left. + \sum_{\ell} \bar{\eta}_{\ell\ell}(\mathbf{x} - \boldsymbol{\ell})\, cG(\mathbf{x} - \mathbf{x}')\sum_{\ell'} \eta_{\ell'\ell'}(\mathbf{x}' - \boldsymbol{\ell}')\right]\right., \tag{9.104}$$

where G, G_i are the correlation functions

$$G(\mathbf{x} - \mathbf{x}') = \int \frac{d^3k}{(2\pi)^3} e^{ik(\mathbf{x} - \mathbf{x}')}\frac{\mathbf{K}\cdot\bar{\mathbf{K}}}{\Delta}, \qquad G_i(\mathbf{x} - \mathbf{x}') = \int \frac{d^3k}{(2\pi)^3} e^{ik(\mathbf{x} - \mathbf{x}')}\frac{K_i\bar{K}_i}{\Delta}, \tag{9.105}$$

with

$$\Delta = \left(2\xi + \frac{\lambda}{\mu}\right)(\bar{\mathbf{K}} \cdot \mathbf{K})^3 + 4(\xi - 1)\left(\xi + \frac{\lambda}{\mu}\right)(\bar{K}_1 K_1 \bar{K}_2 K_2 + 2 \text{ cyclic term})$$
$$+ 4(\xi - 1)^2\left(2\xi + 1 + 3\frac{\lambda}{\mu}\right) \bar{K}_1 K_1 \bar{K}_2 K_2 \bar{K}_3 K_3. \tag{9.106}$$

In the isotropic limit,

$$\Delta = \left(2 + \frac{\lambda}{\mu}\right)(\bar{\mathbf{K}} \cdot \mathbf{K})^3 \tag{9.107}$$

and

$$a = d = 2\left(2 + \frac{\lambda}{\mu}\right), \qquad c = 2\frac{\lambda}{\mu}, \qquad b = e = 0. \tag{9.108}$$

Writing

$$\frac{c}{2 + \dfrac{\lambda}{\mu}} = 2\frac{\nu}{1 - \nu},$$

the exponent in (9.104) reduces properly to

$$4\pi^2\beta \sum_{\mathbf{x}, \mathbf{x}'} \left(\bar{\eta}_{ij}(\mathbf{x})\, \eta_{ij}(\mathbf{x}') + \frac{\nu}{1 - \nu} \sum_{\ell} \bar{\eta}_{\ell\ell}(\mathbf{x} - \boldsymbol{\ell}) \sum_{\ell'} \bar{\eta}_{\ell'\ell'}(\mathbf{x}' - \boldsymbol{\ell}') \right) v_4(\mathbf{x} - \mathbf{x}') \tag{9.109}$$

with

$$v_4(\mathbf{x}) = \int \frac{d^3k}{(2\pi)^3} e^{i\mathbf{k}\cdot\mathbf{x}} \frac{1}{(\bar{\mathbf{K}} \cdot \mathbf{K})^2} \tag{9.110}$$

as it should.

The exponent contains the same infrared divergence already found in the continuum case. It can be finite only if the defect density satisfies [recall (5.40)]

$$\sum_{\mathbf{x}} \bar{\eta}_{\ell n}(\mathbf{x}) = 0. \tag{9.111}$$

For such neutral "defect gases" we can rewrite (9.109) in the form

$$-4\pi^2\beta \sum_{\mathbf{x},\mathbf{x}'} \left(\bar{\eta}_{ij}(\mathbf{x})\, \bar{\eta}_{ij}(\mathbf{x}') + \frac{\nu}{1-\nu} \sum_{\ell} \bar{\eta}_{\ell\ell}(\mathbf{x}-\ell) \sum_{\ell'} \bar{\eta}_{\ell'\ell'}(\mathbf{x}-\ell') \right) v_4'(\mathbf{x}-\mathbf{x}'), \tag{9.112}$$

where $v_4'(\mathbf{x})$ is the subtracted potential

$$v_4'(\mathbf{x}) = \int \frac{d^3k}{(2\pi)^3} \frac{1}{(\bar{\mathbf{K}}\cdot\mathbf{K})^2} (e^{i\mathbf{k}\cdot\mathbf{x}} - 1). \tag{9.113}$$

This potential may be calculated using the methods of Part I [Eq. (6.122)]. It is simply

$$\begin{aligned} v_4'(\mathbf{x}) &= -\frac{\partial}{\partial m^2} \int \frac{d^3k}{(2\pi)^3} \frac{1}{\bar{\mathbf{K}}\cdot\mathbf{K} + m^2} (e^{i\mathbf{k}\cdot\mathbf{x}} - 1) \Big|_{m=0} \\ &= \sum_{n=0}^{\infty} (n+1) \frac{H_n^{\mathbf{x}} - H_n}{(m^2 + 2D)^{n+2}} \Big|_{m=0} \end{aligned} \tag{9.114}$$

The nearest-neighbor value is found directly from [compare (6.127), Part I]

$$v_4'(\mathbf{1}) = -\frac{1}{2D} \int \frac{d^3k}{(2\pi)^2} \frac{-2\sum_{i=1}^{D} \cos k_i + 2D}{(2D - 2\Sigma \cos k_i)^2} = -\frac{1}{2D} v(\mathbf{0}) = -0.04212 \quad (D=3) \tag{9.115}$$

The other values are given in Table 9.3.

For large $|\mathbf{x}|$, $v_4'(\mathbf{x})$ tends to the continuum limit which was calculated in (1.88),

$$v_4'(\mathbf{x}) \to -|\mathbf{x}|/8\pi. \tag{9.114'}$$

It is gratifying to see that even at $|\mathbf{x}| = 1$, the asymptotic formula is correct up to 11%, $-|\mathbf{x}|/8\pi$ being equal to -0.03979.

The value $v_4'(\mathbf{1})$ can be used to express the sum in (9.110) in the form

$$\sum_{\mathbf{x}\neq\mathbf{x}'} \bar{\eta}_{\ell n}(\mathbf{x})\, v_4'(\mathbf{x}-\mathbf{x}')\, \bar{\eta}_{\ell n}(\mathbf{x}')$$

$$= v_4'(\mathbf{1}) \sum_{\mathbf{x}\neq\mathbf{x}'} \bar{\eta}_{\ell n}(\mathbf{x})\, \bar{\eta}_{\ell n}(\mathbf{x}') + \sum_{\mathbf{x}\neq\mathbf{x}'} \bar{\eta}_{\ell n}(\mathbf{x})(v_4'(\mathbf{x}-\mathbf{x}') - v'(\mathbf{1}))\, \bar{\eta}_{\ell n}(\mathbf{x}')). \tag{9.115'}$$

Due to the defect neutrality (9.109), the first term can also be rewritten as $-v_4'(\mathbf{1})\Sigma_{\mathbf{x}}\bar{\eta}_{\ell n}(\mathbf{x})^2$. This has the form of a core energy. The second sum begins now with the next nearest neighbors, a fact which will be denoted by a double prime. Hence we arrive at the following partition function

$$Z = Z_{\text{pot.cl}} \sum_{\{\eta_{ij}(\mathbf{x})\}} \delta_{\bar{\nabla}_i \bar{\eta}_{ij},0} \exp\left\{ 4\pi^2\beta\, v_4'(\mathbf{1}) \right.$$
$$\times \sum_{\mathbf{x}} \left[\eta_{\ell n}^2(\mathbf{x}) + \frac{\nu}{1-\nu}\left(\sum_{\ell} \eta_{\ell\ell}(\mathbf{x}-\boldsymbol{\ell}) \right)^2 \right] - 4\pi^2\beta \sum_{\mathbf{x}\neq\mathbf{x}}'' \left(\bar{\eta}_{ij}(\mathbf{x})\, \bar{\eta}_{ij}(\mathbf{x}') \right.$$
$$\left. \left. + \frac{\nu}{1-\nu} \sum_{\ell} \bar{\eta}_{\ell\ell}(\mathbf{x}-\boldsymbol{\ell}) \sum_{\ell'} \bar{\eta}_{\ell\ell}(\mathbf{x}'-\boldsymbol{\ell}) \right) v_4''(\mathbf{x}-\mathbf{x}') \right\}, \tag{9.116}$$

where

$$v_4''(\mathbf{x}) \equiv v_4'(\mathbf{x}) - v_4'(\mathbf{1}). \tag{9.117}$$

The sum over $\bar{\eta}_{ij}(\mathbf{x})$ represents a grand canonical ensemble of crystal defects.

Note that due to the conservation law $\bar{\nabla}_i \bar{\eta}_{ij}(\mathbf{x}) = 0$, all defect configurations restricted to a finite region in space automatically satisfy defect neutrality equation (9.111). But not only that! As we can see directly from the representation $\bar{\eta}_{ij}(\mathbf{x}) = \varepsilon_{ik\ell}\, \varepsilon_{jmn} \nabla_k \nabla_m\, n_{\ell n}(\mathbf{x}+\mathbf{i}+\mathbf{j})$, upon partial integration on the lattice, also the defect moments $\Sigma_{\mathbf{x}} x_k \bar{\eta}_{ij}(\mathbf{x})$ are neutral, as is true for two dimensions.

9.3. AN *XY* TYPE MODEL OF DEFECT MELTING

In Part II we saw that the properties of the phase transition of a model involving a periodic Gaussian are closely related to those in models of the *XY* type. In these, the periodicity of the fluctuating variable $\gamma(\mathbf{x})$ is accounted for by an energy of the cosine form in the lattice gradients. It is

quite straightforward to construct such an XY type model for the present case.

We proceed in two steps: First we take the displacement field $u_i(\mathbf{x})$ and split it into a variable $\hat{u}_i(\mathbf{x})$ which is restricted to run only over a unit cell, plus a lattice vector $aN_i(\mathbf{x})$ where $N_i(\mathbf{x})$ is an integer-valued field, i.e., we write

$$u_i(\mathbf{x}) = \hat{u}_i(\mathbf{x}) + aN_i(\mathbf{x}). \tag{9.118}$$

We then absorb the integer-valued field $N_i(\mathbf{x})$ into the gauge field by a defect gauge transformation

$$n_{ij}^s(\mathrm{x}) \to n_{ij}^s(\mathbf{x}) + \tfrac{1}{2}(\nabla_i N_j(\mathbf{x}) + \nabla_j N_i(\mathbf{x})). \tag{9.119}$$

The exponential in the partition function (9.14) is invariant under this change. The important consequence of this transformation is that with $N_i(\mathbf{x})$ running through *all* integers, the new jump numbers $n_{ij}^s(\mathbf{x}) + \frac{1}{2}(\nabla_i N_j + \nabla_j N_i)(\mathbf{x})$ no longer satisfy the gauge condition but become *unconstrained* variables. The diagonal elements $n_{ij}^s(\mathbf{x})$ cover all integers while the off diagonal elements take all integral *and* half-integral values precisely once. Hence we can rewrite the partition function as

$$Z = \sum_{\{n_{ij}^s\}} \prod_{\mathbf{x},\, i} \left[\int_{-a}^{a} \frac{d\hat{u}_i(\mathbf{x})}{a} \right] \exp\left\{ -\beta \frac{(2\pi)^2}{a^2} \left(\frac{1}{2} \sum_{\mathbf{x},\, i<j} (\nabla_i \hat{u}_j + \nabla_j \hat{u}_i - 2an_{ij}^s)^2 \right.\right.$$
$$\left.\left. + \xi \sum_{\mathbf{x},\, i} (\nabla_i \hat{u}_i - an_{ii}^s)^2 + \frac{\lambda}{2\mu} \sum_{\mathbf{x}} \left(\sum_i (\nabla_i \hat{u}_i - an_{ii}^s)(\mathbf{x} - \mathbf{i}) \right)^2 \right) \right\}. \tag{9.120}$$

This unrestricted sum puts us in the position to take the energy in the cosine form by using the Villain approximation

$$e^{\beta \cos \nabla u} \approx R_V(\beta) \sum_n e^{-(\beta_V/2)(\nabla u - 2\pi n)^2}, \tag{9.121}$$

where

$$R_V(\beta) = I_0^*(\beta)\sqrt{2\pi\beta_V}, \qquad \beta_V(\beta) = -1/(2\log(I_1(\beta)/I_0(\beta))). \tag{9.122}$$

In the present case, we want to use (9.121) in the opposite direction. Given β_V, we have to calculate β. Since we want to keep the notation β

for the periodic Gaussian model, it is useful to define the inverse transformation of (9.52) and write

$$\sum_n e^{-(\beta/2)(\nabla u - 2\pi n)^2} \approx R_{V^{-1}}(\beta)\, e^{\beta_{V^{-1}} \cos \nabla u}, \tag{9.123}$$

where $\beta_{V^{-1}}$ is the solution of

$$\beta = -1/(2 \log I_1(\beta_{V^{-1}})/I_0(\beta_{V^{-1}})) \tag{9.124}$$

and $R_{V^{-1}}(\beta)$ is the function

$$R_{V^{-1}}(\beta) = 1/(I_0(\beta_{V^{-1}})\sqrt{2\pi\beta}). \tag{9.125}$$

If $\lambda = 0$ we can apply this directly to (9.120) and find a cosine energy for each sum over n_{ij}^s, $i<j$ and n_{ii}^s:

$$Z \approx R_{V^{-1}}(\beta)^{DN} R_{V^{-1}}(2\xi\beta)^{DN} \sum_{\{n_{ij}^s\}} \prod_{\mathbf{x},i} \left[\int_{-a}^{a} \frac{d\hat{u}_i(\mathbf{x})}{a} \right]$$
$$\times e^{\beta_{V^{-1}} \Sigma_{\mathbf{x},i<j} \cos[(2\pi/a)(\nabla_i \hat{u}_j + \bar{\nabla}_j \hat{u}_i)] + (2\xi\beta)_{V^{-1}} \Sigma_{\mathbf{x},i} \cos[(2\pi/a)\nabla_i \hat{u}_i]}. \tag{9.126}$$

If $\lambda \neq 0$, the approximation is not immediately applicable since the diagonal numbers n_{ii}^s no longer appear in a single complete square. An obvious way out suggests itself via the introduction of an auxiliary integration. We can rewrite the $i = j$ pieces of the energy as

$$\exp\left\{ -\beta \frac{(2\pi)^2}{2} \left[\xi \sum_{\mathbf{x},i} (\nabla_i \hat{u}_i - a n_{ii}^s)^2 + \frac{\lambda}{2\mu} \sum_{\mathbf{x}} \left(\sum_i (\nabla_i \hat{u}_i - a n_{ii}^s)(\mathbf{x} - \mathbf{i}) \right)^2 \right] \right\}$$
$$= \prod_{\mathbf{x}} \left[\int_{-\infty}^{\infty} \frac{d\hat{u}(\mathbf{x})}{\sqrt{\pi/(\beta(2\pi)^2/a^2)}} \sqrt{D\xi - \gamma} \right] e^{-\beta[\xi \Sigma_{\mathbf{x},i} (\nabla_i \hat{u}_i - \hat{u}(\mathbf{x}+\mathbf{i}) - a n_{ii}^s)^2 - \gamma \Sigma_{\mathbf{x}} \hat{u}^2(\mathbf{x})]}. \tag{9.127}$$

Indeed, the exponent can be completed quadratically to give

$$-\beta \frac{(2\pi)^2}{a^2} \left[\xi \sum_{\mathbf{x},i} (\nabla_i \hat{u}_i - a n_{ii}^s)^2 + \frac{\xi^2}{\gamma - D\xi} \sum_{\mathbf{x}} \left(\sum_i (\nabla_i \hat{u}_i - a n_{ii}^s)(\mathbf{x} - \mathbf{i}) \right)^2 \right.$$
$$\left. + (D\xi - \gamma) \sum_{\mathbf{x}} \left(\hat{u}(\mathbf{x}) + \frac{\xi}{\gamma - D\xi} \sum_i (\nabla_i \hat{u}_i - a n_{ii}^s)(\mathbf{x} - \mathbf{i}) \right)^2 \right]. \tag{9.128}$$

Now if $D\xi - \gamma > 0$, the integration over $\hat{u}$ can be performed and produces the correct energy in (9.127) [recall that according to (9.23), $\xi^2/(\gamma - D\xi) = \lambda/2\mu$].

The application of the inverse Villain approximation to (9.127) is now straightforward. In this way we find

$$Z = R_{V^{-1}}(\beta)^{DN} R_{V^{-1}}(2\xi\beta)^{(1/2)D(D-1)N} \prod_{\mathbf{x},i} \left[\int_{-a}^{a} \frac{d\gamma_i(\mathbf{x})}{2\pi} \right]$$
$$\times \prod_{\mathbf{x}} \left[\int_{-\infty}^{\infty} \frac{d\delta(\mathbf{x})}{\sqrt{\pi/\beta}} \sqrt{D\xi - \gamma} \right] \exp\left\{ \beta_{V^{-1}} \sum_{\mathbf{x},i<j} \cos(\nabla_i \gamma_j + \nabla_j \gamma_i) \right.$$
$$\left. + (2\xi\beta)_{V^{-1}} \sum_{\mathbf{x},i} \cos(\nabla_i \gamma_j(\mathbf{x}) - \delta(\mathbf{x}+\mathbf{i})) - \beta\gamma \sum_{\mathbf{x}} \delta(\mathbf{x})^2 \right\}, \tag{9.129}$$

where we have rescaled the $\hat{u}_{ij}$, $\hat{u}$ variables and defined angle-like variables $\gamma_i \equiv (2\pi/a)\,\hat{u}_i$, $\delta = (2\pi/a)\,\hat{u}$.

The main problem with this derivation is that for most materials, $\gamma - D\xi$ is a positive quantity. This means that $D\xi - \gamma$ is negative and the integration over δ is impossible. At first sight it appears as though we could simply rotate the contour of integration to run along the imaginary axis. This, however, poses another problem, namely, that $\cos(\nabla_i \gamma_i - \delta)$ diverges.

It is still possible to find a cosine version of the melting model, for $\gamma - D\xi > 0$, albeit with a little more effort and at the expense of $D \cdot (D-1)/2$ auxiliary fields in D dimensions (γ_{12}, γ_{23}, γ_{13} in three dimensions, γ_{12} in two dimensions). For this purpose it is preferable to start out with the conjugate form (9.22) of the partition function,

$$Z = \frac{1}{(\sqrt{2})^{DN}} \left[\frac{1}{\xi^D} \left(1 - D\frac{\xi}{\gamma} \right) \right]^{N/2} \prod_{\mathbf{x},i\le j} \left[\int_{-\infty}^{\infty} \frac{d\bar{\sigma}_{ij}(\mathbf{x})}{\sqrt{2\pi\beta}} \right] \sum_{\{n_{ij}^s(\mathbf{x})\}} \Phi[n_{ij}^s]$$
$$\times \prod_{\mathbf{x},i} \left[\int_{-\infty}^{\infty} \frac{du_i(\mathbf{x})}{a} \right] e^{-(1/2\beta)\Sigma_{\mathbf{x}}[\Sigma_{i<j}\bar{\sigma}_{ij}^2 + (1/2\xi)\Sigma_i \bar{\sigma}_{ii}^2 - (1/2\gamma)(\Sigma_i \bar{\sigma}_{ii}(\mathbf{x}-\mathbf{i}))^2]}$$
$$\times e^{(\pi/a)i\Sigma_{\mathbf{x},i,j}\bar{\sigma}_{ij}(\nabla_i u_j + \nabla_j u_i - 2an_{ij}^s)}. \tag{9.130}$$

The troublesome feature is the negative sign of the $(\Sigma_i \bar{\sigma}_{ii}(\mathbf{x}-\mathbf{i}))^2$ term. We therefore reorganize the parts involving $\bar{\sigma}_{ii}$:

$$e^{-(1/2\beta)\Sigma_{\mathbf{x}}[(1/2\xi - D/2\gamma)\Sigma_i \bar{\sigma}_{ii}^2 - (1/2\gamma)\Sigma_{i<j}(\bar{\sigma}_{ii}(\mathbf{x}-\mathbf{i}) - \bar{\sigma}_{jj}(\mathbf{x}-\mathbf{j}))^2]}. \tag{9.131}$$

Using the identity $\gamma = D\xi\kappa'/\lambda = D\xi + 2\xi^2\mu/\lambda$ [see Eqs. (1.130), (9.23)] the coefficient before the first sum is $\mu/D\kappa' = \xi(\mu/\lambda)(1/\gamma)$. Hence both quadratic pieces appear with a positive energy and this is what we want. We then introduce $D(D-1)/2$ auxiliary angular variables γ_{ij} with $\gamma_{ij} = -\gamma_{ji}$ as well as three auxiliary fields with $\bar{\Delta}_{ij} = -\bar{\Delta}_{ji}$ and write the exponent (9.131) as

$$\prod_{\mathbf{x},i<j}\left[\int_{-\infty}^{\infty} d\bar{\Delta}_{ij}(\mathbf{x})\right]\prod_{\mathbf{x},i<j}\left[\int_{-\infty}^{\infty}\frac{d\gamma_{ij}(\mathbf{x})}{2\pi}\right] e^{-(1/2\beta)[(\xi\mu/\gamma\lambda)\Sigma_{\mathbf{x},i}\bar{\sigma}_{ii}^2 + (1/2\gamma)\Sigma_{\mathbf{x},i<j}\bar{\Delta}_{ij}^2)]}$$
$$\times e^{i\Sigma_{\mathbf{x},i<j}\bar{\Delta}_{ij}\gamma_{ij} - i\Sigma_{\mathbf{x},i,j}\bar{\sigma}_{ii}(\mathbf{x}-\mathbf{i})\gamma_{ij}(\mathbf{x})}. \tag{9.132}$$

The integrations over $\gamma_{ij}(\mathbf{x})$ ensure the identity

$$\bar{\Delta}_{ij}(\mathbf{x}) = \bar{\sigma}_{ii}(\mathbf{x}-\mathbf{i}) - \bar{\sigma}_{jj}(\mathbf{x}-\mathbf{j}), \tag{9.133}$$

so that (9.132) is the same as (9.131). We now split the integrals over γ_{ij} into sums over integers ℓ_{ij} times 2π plus integrals over the restricted interval $(-\pi, \pi]$ and obtain

$$Z = \frac{1}{(\sqrt{2})^{DN}}\left[\frac{1}{\xi^D}\left(1 - D\frac{\xi}{\gamma}\right)\right]^{N/2}\prod_{\mathbf{x},i\le j}\left[\int_{-\infty}^{\infty}\frac{d\bar{\sigma}_{ij}(\mathbf{x})}{\sqrt{2\pi\beta}}\right]\prod_{\mathbf{x},i<j}\left[\int_{-\infty}^{\infty} d\bar{\Delta}_{ij}(\mathbf{x})\right]$$
$$\times\sum_{\{n_{ij}^s(\mathbf{x})\}}\Phi[n_{ij}^s]\sum_{\{\ell_{ij}(\mathbf{x})\}}\prod_{\mathbf{x},i}\left[\int_{-\pi}^{\pi}\frac{d\gamma_i(\mathbf{x})}{2\pi}\right]\prod_{\mathbf{x},i<j}\left[\int_{-\pi}^{\pi}\frac{d\gamma_{ij}(\mathbf{x})}{2\pi}\right]\sum_{\{\ell_{ij}(\mathbf{x})\}}$$
$$\times e^{-(1/2\beta)[\Sigma_{\mathbf{x},i<j}\bar{\sigma}_{ij}^2 + (\xi\mu/\gamma\lambda)\Sigma_{\mathbf{x},i}\bar{\sigma}_{ii}^2 + (1/2\gamma)\Sigma_{\mathbf{x},i<j}\bar{\Delta}_{ij}^2]}$$
$$\times e^{i\Sigma_{\mathbf{x},i<j}\bar{\sigma}_{ij}(\nabla_i\gamma_j + \nabla_j\gamma_i - 4\pi n_{ij}^s) + i\Sigma_{\mathbf{x},i}\bar{\sigma}_{ii}(\nabla_i\gamma_i - \Sigma_j\gamma_{ij}(\mathbf{x}+\mathbf{i}) - 2\pi\Sigma_j\ell_{ij} - 2\pi n_{ii}^s) + \Sigma_{\mathbf{x},i<j}\bar{\Delta}_{ij}(\gamma_{ij} - 2\pi\ell_{ij})}. \tag{9.134}$$

Then, we integrate out the stress fields $\bar{\sigma}_{ij}$, $\bar{\Delta}_{ij}$ and arrive at

$$Z = \frac{1}{(\sqrt{2})^{DN}}\left[\frac{1}{\xi^D}\left(1 - D\frac{\xi}{\gamma}\right)\right]^{N/2}\frac{1}{(\sqrt{2\pi\beta})^{DN}}\left(\sqrt{2\pi\beta\frac{\gamma\lambda}{\xi\mu}}\right)^{DN}\sqrt{4\pi\beta\gamma}^{(1/2)D(D-1)N}$$
$$\times\sum_{\{n_{ij}^s(\mathbf{x})\}}\Phi[n_{ij}^s]\prod_{\mathbf{x},i}\left[\int_{-\pi}^{\pi}\frac{d\gamma_i(\mathbf{x})}{2\pi}\right]\prod_{\mathbf{x},i<j}\left[\int_{-\pi}^{\pi}\frac{d\gamma_{ij}(\mathbf{x})}{2\pi}\right]\exp\left\{-\beta\right.$$
$$\left[\sum_{\mathbf{x},i<j}(\nabla_i\gamma_j + \nabla_j\gamma_i - 2\pi n_{ij}^s)^2 + \frac{\gamma\lambda}{\xi\mu}\sum_{\mathbf{x},i}\left(\nabla_i\gamma_i - \sum_j\gamma_{ij}(\mathbf{x}+\mathbf{i}) - 2\pi\Sigma_j\ell_{ij} - 2\pi n_{ii}^s\right)\right.$$
$$\left.\left. + 2\gamma\sum_{\mathbf{x},i<j}(\gamma_{ij} - 2\pi\ell_{ij})^2\right]\right\}. \tag{9.135}$$

We may cross check this expression by going to low temperatures for which the jump numbers n_{ij}^s, ℓ_{ij} are frozen out and the last two terms in the exponent become

$$
\begin{aligned}
&-\frac{\beta}{2}\frac{\gamma\lambda}{\xi\mu}\sum_{\mathbf{x},i}\left(\nabla_i\gamma_i-\sum_j\gamma_{ij}(\mathbf{x}+\mathbf{i})\right)^2-\gamma\beta\sum_{\mathbf{x},i<j}\gamma_{ij}^2\\
&\quad=-\beta\frac{\gamma\lambda}{\xi\mu}\left[\frac{1}{2}\sum_{\mathbf{x},i}(\nabla_i\gamma_i)^2-\sum_{\mathbf{x},i<j}\gamma_{ij}(\mathbf{x}+\mathbf{i})(\nabla_i\gamma_i-\nabla_i\gamma_j)\right.\\
&\qquad\left.+\frac{1}{2}\sum_{\mathbf{x},i}\left(\sum_j\gamma_{ij}\right)^2+\xi\frac{\mu}{\lambda}\sum_{\mathbf{x},i<j}\gamma_{ij}^2\right].
\end{aligned}
\tag{9.136}
$$

We now write out the quadratic γ_{ij} terms explicitly,

$$
\frac{1}{2}\sum_i\left(\sum_j\gamma_{ij}\right)^2=\sum_{i<j}\gamma_{ij}^2+\sum_i\sum_{j\neq k}\gamma_{ij}\gamma_{ik}.
\tag{9.137}
$$

In the vector space of γ_{ij} with $i<j$, they take the quadratic form

$$
\gamma^{\mathrm{T}}M\gamma=\sum_{i<j}\sum_{k<\ell}\gamma_{ij}M_{ij,k\ell}\gamma_{k\ell},
\tag{9.138}
$$

where in two dimensions

$$
\gamma^{\mathrm{T}}M\gamma=\left(1+\xi\frac{\mu}{\lambda}\right)\gamma_{12}^2
\tag{9.139}
$$

and in three dimensions

$$
\begin{aligned}
\gamma^{\mathrm{T}}M\gamma&=\left(1+\xi\frac{\mu}{\lambda}\right)(\gamma_{12}^2+\gamma_{23}^2+\gamma_{13}^2)+(\gamma_{12}\gamma_{13}-\gamma_{12}\gamma_{23}+\gamma_{13}\gamma_{23})\\
&=\xi\frac{\mu}{\lambda}(\gamma_{12},\gamma_{23},\gamma_{13})\begin{pmatrix}1+\dfrac{\lambda}{\mu\xi} & -\dfrac{\lambda}{2\mu\xi} & \dfrac{\lambda}{2\mu\xi}\\ -\dfrac{\lambda}{2\mu\xi} & 1+\dfrac{\lambda}{\mu\xi} & \dfrac{\lambda}{2\mu\xi}\\ \dfrac{\lambda}{2\mu\xi} & \dfrac{\lambda}{2\mu\xi} & 1+\dfrac{\lambda}{\mu\xi}\end{pmatrix}\begin{pmatrix}\gamma_{12}\\ \gamma_{23}\\ \gamma_{13}\end{pmatrix}.
\end{aligned}
$$

The matrix M has determinant

$$\left.\begin{aligned} \det M &= \left(1+\xi\frac{\mu}{\lambda}\right) = \frac{\gamma}{2\xi} \\ \det M &= \frac{\mu}{\lambda}\left(\frac{3}{2}+\xi\frac{\mu}{\lambda}\right)^2 \xi = \frac{\mu}{\lambda}\frac{\gamma^2}{4\xi} \end{aligned}\right\} \text{ for } \begin{cases} D=2, \\ D=3, \end{cases} \tag{9.140}$$

and inverse

$$M^{-1} = \frac{\lambda}{\lambda+\xi\mu} = \frac{2\xi}{\gamma} \quad (D=2)$$

$$M^{-1} = \frac{2\lambda}{3\lambda+2\xi\mu}\begin{pmatrix} 1+\frac{\lambda}{2\mu\xi} & \frac{\lambda}{2\mu\xi} & -\frac{\lambda}{2\mu\xi} \\ \frac{\lambda}{2\mu\xi} & 1+\frac{\lambda}{2\mu\xi} & -\frac{\lambda}{2\mu\xi} \\ -\frac{\lambda}{2\mu\xi} & -\frac{\lambda}{2\mu\xi} & 1+\frac{\lambda}{2\mu\xi} \end{pmatrix} \tag{9.141}$$

$$= \frac{2\xi}{\gamma}\begin{pmatrix} 1+\frac{\lambda}{2\mu\xi} & \frac{\lambda}{2\mu\xi} & -\frac{\lambda}{2\mu\xi} \\ \frac{\lambda}{2\mu\xi} & 1+\frac{\lambda}{2\mu\xi} & -\frac{\lambda}{2\mu\xi} \\ -\frac{\lambda}{2\mu\xi} & -\frac{\lambda}{2\mu\xi} & 1+\frac{\lambda}{2\mu\xi} \end{pmatrix} \quad (D=3).$$

We can now complete the square and integrate out the γ'_{ij}s with the result

$$\frac{1}{\left(\sqrt{1+\frac{\beta\gamma\lambda}{\xi\mu}}\right)^{D(D-1)N/2}} \frac{1}{(\det M)^{1/2}}$$

$$\times e^{-\beta(\gamma\lambda/\xi\mu)\{(1/2)\Sigma_{x,i}(\nabla_i\gamma_i)^2 - (1/4)\Sigma_{i<j,k<l}(\nabla_i\gamma_i(\mathbf{x}-\mathbf{i})-\nabla_j\gamma_j(\mathbf{x}-\mathbf{j}))M^{-1}_{ij,kl}(\nabla_k\gamma_k(\mathbf{x}-\mathbf{k})-\nabla_l\gamma_l(\mathbf{x}-\boldsymbol{\ell}))\}}. \tag{9.142}$$

Inserting (9.140) we obtain in two dimensions

$$e^{-\beta(\gamma\lambda/\xi\mu)(1/2)\Sigma_{\mathbf{x},i}(\nabla_i\gamma_i)^2 + \beta(\lambda/2\mu)\Sigma_{\mathbf{x}}(\nabla_1\gamma_1-\nabla_2\gamma_2)^2}$$

$$= e^{-\beta(\gamma\lambda/\xi\mu)(1/2)\Sigma_{\mathbf{x},i}(\nabla_i\gamma_i)^2 + \beta(\lambda/2\mu)\Sigma_{\mathbf{x}}[2((\nabla_1\gamma_1)^2+(\nabla_2\gamma_2)^2)-(\nabla_1\gamma_1+\nabla_2\gamma_2)^2]} \tag{9.143}$$

and in three dimensions

$$\exp\Bigg\{-\beta\frac{\gamma\lambda}{\xi\mu}\frac{1}{2}\sum_{\mathbf{x},i}(\nabla_i\gamma_i)^2$$
$$+\beta\frac{\lambda}{2\mu}\sum_{\mathbf{x}}\Bigg[\left(1+\frac{\lambda}{2\mu\xi}\right)((\nabla_1\gamma_1(\mathbf{x}-\mathbf{1})-\nabla_2\gamma_2(\mathbf{x}-\mathbf{2}))+(23)+(31))$$
$$+\frac{\lambda}{\mu\xi}\sum_{\mathbf{x}}[(\nabla_1\gamma_1(\mathbf{x}-\mathbf{1})-\nabla_2\gamma_2(\mathbf{x}-\mathbf{2}))(\nabla_2\gamma_2(\mathbf{x}-\mathbf{2})-\nabla_3\gamma_3(\mathbf{x}-\mathbf{3}))$$
$$-(\nabla_1\gamma_1(\mathbf{x}-\mathbf{1})-\nabla_2\gamma_2(\mathbf{x}-\mathbf{2}))(\nabla_1\gamma_1(\mathbf{x}-\mathbf{1})-\nabla_3\gamma_3(\mathbf{x}-\mathbf{3}))$$
$$-(\nabla_2\gamma_2(\mathbf{x}-\mathbf{2})-\nabla_3\gamma_3(\mathbf{x}-\mathbf{3}))(\nabla_1\gamma_1(\mathbf{x}-\mathbf{1})-\nabla_3\gamma_3(\mathbf{x}-\mathbf{3}))]\Bigg\}$$
$$=\exp\Bigg\{-\beta\frac{\gamma\lambda}{\xi\mu}\frac{1}{2}\sum_{\mathbf{x},i}(\nabla_i\gamma_i)^2$$
$$+\beta\frac{\lambda}{2\mu}\sum_{\mathbf{x}}\Bigg[\left(1+\frac{\lambda}{2\mu\xi}\right)\left(3\sum_i(\nabla_i\gamma_i)^2-\left(\sum_i\nabla_i\gamma_i(\mathbf{x}-\mathbf{i})\right)^2\right.$$
$$\left.-\frac{\lambda}{2\mu\xi}\left(3\sum_i(\nabla_i\gamma_i)^2-\left(\sum_i\nabla_i\gamma_i(\mathbf{x}-\mathbf{i})\right)^2\right]\Bigg\}$$
$$=\exp\left\{-\beta\frac{\gamma\lambda}{\xi\mu}\frac{1}{2}\sum_{\mathbf{x},i}(\nabla_i\gamma_i)^2+\beta\frac{\lambda}{2\mu}\sum_{\mathbf{x}}\left(3\sum_i(\nabla_i\gamma_i)^2-\left(\sum_i\nabla_i\gamma_i(\mathbf{x}-\mathbf{i})\right)^2\right\}.\right. \tag{9.144}$$

In D dimensions, the exponential obviously becomes

$$e^{-\beta(\gamma\lambda/\xi\mu)(1/2)\Sigma_{\mathbf{x},i}(\nabla_i\gamma_i)^2+\beta(\lambda/2\mu)\Sigma_{\mathbf{x}}[D\Sigma_i(\nabla_i\gamma_i)^2-(\Sigma_i\nabla_i\gamma_i(\mathbf{x}-\mathbf{i}))^2]}. \tag{9.145}$$

Using $\gamma\lambda/\xi = D\lambda + 2\xi\mu$ and adding the first term in (9.135) (for $\overset{s}{n}_{ij}=0$) this gives the correct elastic energy

$$\frac{1}{2}\sum_{\mathbf{x},i<j}(\nabla_i\gamma_j+\nabla_j\gamma_i)^2+2\xi\sum_{\mathbf{x},i}(\nabla_i\gamma_i)^2+\frac{\lambda}{2\mu}\sum_{\mathbf{x}}\left(\sum_i\nabla_i\gamma_i(\mathbf{x}-\mathbf{i})\right)^2. \tag{9.146}$$

Also the pre-factors cancel properly by rewriting $[(1/\xi^D)(1-D\xi/\gamma)]^{N/2}$ as $[2(\mu/\lambda)(1/\xi^{D-2})(1/\gamma)]^{N/2}$.

It is now straightforward to take the partition function (9.135) to a cosine form using the inverse Villain approximation (9.123) so that

$$
\begin{aligned}
Z \approx Z_{V^{-1}} = & \left[2\frac{\mu}{\lambda}\frac{1}{\xi^{D-2}}\frac{1}{\gamma}\right]^{N/2}\sqrt{\frac{\gamma\lambda}{2\xi\mu}}^{DN} \\
& \times R_{V^{-1}}(\beta)^{(D(D-1)/2)N} R_{V^{-1}}\left(\beta\frac{\gamma\lambda}{\xi\mu}\right)^{DN} R_{V^{-1}}(2\beta\gamma)^{(D(D-1)/2)N} \\
& \times \prod_{\mathbf{x},i}\left(\int_{-\pi}^{\pi}\frac{d\gamma_i(\mathbf{x})}{2\pi}\right)\prod_{\mathbf{x},i<j}\left(\int_{-\pi}^{\pi}\frac{d\gamma_{ij}(\mathbf{x})}{2\pi}\sqrt{4\pi\beta\gamma}\right) \\
& \times \exp\left\{\beta_{V^{-1}}\sum_{\mathbf{x},i<j}\cos(\nabla_i\gamma_i+\nabla_j\gamma_i)+\left(\beta\frac{\gamma\lambda}{\xi\mu}\right)_{V^{-1}}\right. \\
& \left.\times\sum_{\mathbf{x},i}\cos\left(\nabla_i\gamma_i-\sum_j\gamma_{ij}(\mathbf{x}+\mathbf{i})\right)+(2\beta\gamma)_{V^{-1}}\sum_{\mathbf{x},i<j}\cos\gamma_{ij}\right\}.
\end{aligned}
\tag{9.147}
$$

The relationship with the original partition function (9.120) is best exhibited by expanding the exponentials into Bessel functions using the formula (4.15), Part II. Then

$$
\begin{aligned}
Z_{V^{-1}} = & \left[2\frac{\mu}{\lambda}\frac{1}{\xi^{D-2}}\frac{1}{\gamma}\right]^{N/2}\left(\sqrt{\frac{\gamma\lambda}{2\xi\mu}}\right)^{DN}(\sqrt{4\pi\beta\gamma})^{D(D-1)N/2} \\
& \times R_{V^{-1}}(\beta)^{(D(D-1)/2)N} R_{V^{-1}}\left(\beta\frac{\gamma\lambda}{\xi\mu}\right)^{DN} R_{V^{-1}}(2\beta\gamma)^{(D(D-1)/2)N} \\
& \times \prod_{\mathbf{x},i}\left[\int_{-\pi}^{\pi}\frac{d\gamma_i(\mathbf{x})}{2\pi}\right]\prod_{\mathbf{x},i<j}\left[\int_{-\pi}^{\pi}\frac{d\gamma_{ij}(\mathbf{x})}{2\pi}\right]\sum_{\substack{\{\bar\sigma_{ij}(\mathbf{x}),\,\bar\Delta_{ij}(\mathbf{x})\}\\ i<j \quad i<j}}\prod_{\mathbf{x},i<j} I_{\bar\sigma_{ij}}(\beta_{V^{-1}}) \\
& \times \prod_{\mathbf{x},i} I_{\bar\sigma_{ii}}\left(\left(\frac{\beta\gamma\lambda}{\xi\mu}\right)_{V^{-1}}\right)\prod_{\mathbf{x},i<j} I_{\bar\Delta_{ij}}((2\beta\gamma)_{V^{-1}}) \\
& \times e^{(i/2)\Sigma_{\mathbf{x},i,j}\bar\sigma_{ij}(\nabla_i\gamma_i+\nabla_j\gamma_i)+i\Sigma_{\mathbf{x},i<j}\bar\sigma_{ij}(\mathbf{x})\gamma_{ij}(\mathbf{x}+\mathbf{i})-i\Sigma_{\mathbf{x},i<j}\bar\Delta_{ij}(\mathbf{x})\gamma_{ij}(\mathbf{x})}.
\end{aligned}
\tag{9.148}
$$

Integrating out the angular variables gives the conservation law $\bar\nabla_i\bar\sigma_{ij}=0$ and the identity $\bar\Delta_{ij}=\bar\sigma_{ii}(\mathbf{x}-\mathbf{i})-\bar\sigma_{ij}(\mathbf{x}-\mathbf{i})$ and $Z_{V^{-1}}$ becomes the sum

$$
\begin{aligned}
Z_{V^{-1}} \propto & \sum_{\{\bar\sigma_{ij}(\mathbf{x})\}}\delta_{\bar\nabla_i\sigma_{ij},0}\prod_{\mathbf{x},i\le j} I_{\bar\sigma_{ij}}(\beta_{V^{-1}})\prod_{\mathbf{x},i} I_{\bar\sigma_{ii}}\left(\left(\frac{\beta\gamma\lambda}{\xi\mu}\right)_{V^{-1}}\right) \\
& \times\prod_{\mathbf{x},i<j} I_{\bar\sigma_{ii}(\mathbf{x}-\mathbf{i})-\bar\sigma_{jj}(\mathbf{x}-\mathbf{j})}((2\beta\gamma)_{V^{-1}})
\end{aligned}
\tag{9.149}
$$

apart from the above normalization factor.

In the limit of low temperatures, we can use the approximation $I_{\bar{\sigma}}(\beta)/I_0(\beta) \sim e^{-\bar{\sigma}^2/2\beta}$ and see that (9.149) reduces correctly to (9.130), rewritten with the use of (9.131) [to get the same expression we have to sum in (9.130) over all n_{ij}^s, which makes $\bar{\sigma}_{ij}$ integer, and integrate out the $u_i(\mathbf{x})$ variables, which enforces the conservation law $\bar{\nabla}_i \bar{\sigma}_{ij} = 0$].

APPENDIX 9A. DERIVATION OF DEFECT ENERGY (9.109) FROM STRESS ENERGY (9.90)

First we observe that, after the phase changes (9.92)–(9.95), the determinant of the matrix $M_{I,J}$ in (9.91) is (writing k_i instead of $\bar{K}_i$, for brevity)

$$|M| = \Delta k_3^6/[4\xi^2(2\xi + 3\lambda/\mu)], \tag{9.A1}$$

where Δ is the fluctuation determinant of the displacement field, (9.100). Inverting the matrix M and removing a common factor,

$$M^{-1} = \frac{1}{k_3^4}\frac{1}{\Delta} M'^{-1}, \tag{9.A2}$$

we find for the matrix M'^{-1}:

$$\begin{aligned} M'^{-1}_{11\,11} &= 4\left(2\xi + \frac{\lambda}{\mu}\right) k_1^2 k_2^2 k_3^2 \\ &\quad + 4\xi\left(\xi + \frac{\lambda}{\mu}\right)(k_3^6 + k_2^2 k_3^4 + k_1^2 k_3^4 + k_1^4 k_3^2 + k_1^4 k_2^2 + k_1^6) \\ &\quad + 8\xi^2\left(\xi + \frac{3}{2}\frac{\lambda}{\mu}\right) k_1^2 k_3^2 (k_3^2 + k_1^2), \\ M'^{-1}_{22\,22} &= 4\left(2\xi + \frac{\lambda}{\mu}\right) k_1^2 k_2^2 k_3^2 \\ &\quad + 4\xi\left(\xi + \frac{\lambda}{\mu}\right)(k_3^6 + k_2^2 k_3^4 + k_2^4 k_3^2 + k_1^2 k_3^4 + k_1^2 k_2^4 + k_2^6) \end{aligned}$$

$$+ 8\xi^2\left(\xi + \frac{3\lambda}{2\mu}\right) k_2^2 k_3^2 (k_3^2 + k_2^2),$$

$$M'^{-1}_{12}{}_{12} = 2\xi k_3^2(k_3^4 + k_2^4 + k_1^4) + 4\xi\left(\xi + \frac{\lambda}{\mu}\right)(k_2^2 k_3^4 + k_1^2 k_3^4 + k_1^2 k_2^4 + k_1^4 k_2^2)$$

$$+ 8\xi^2\left(\xi + \frac{3}{2}\frac{\lambda}{\mu}\right) k_1^2 k_2^2 k_3^2$$

$$+ \frac{\lambda}{\mu} k_3^2(k_3^4 - 2k_2^2 k_3^2 + k_2^4 - 2k_1^2 k_3^2 + 2k_1^2 k_2^2 + k_1^4),$$

$$M'^{-1}_{11}{}_{22} = 4\xi^2 k_1^2 k_2^2(-k_3^2 + k_2^2 + k_1^2) + 8\left[\xi^2\left(\xi + \frac{3\lambda}{2\mu}\right) + \frac{\lambda}{2\mu}\right] k_1^2 k_2^2 k_3^2$$

$$+ 2\frac{\lambda}{\mu}\xi(k_3^6 + 2k_2^2 k_3^4 + k_2^4 k_3^2 + 2k_1^2 k_3^4 + 2k_1^2 k_2^4 + k_1^4 k_3^2 + 2k_1^4 k_2^2),$$

$$M'^{-1}_{11}{}_{12} = 4\xi k_1 k_2^3 k_3^2 + 4\xi^2 k_1 k_2(k_3^4 + k_1^2 k_2^2 + k_1^4) + 8\xi^2\left(\xi + \frac{3\lambda}{2\mu}\right) k_1^3 k_2 k_3^2$$

$$+ 2\frac{\lambda}{\mu} k_1 k_2 k_3^2(-k_3^2 + k_2^2 + k_1^2)$$

$$+ 2\frac{\lambda}{\mu}\xi k_1 k_2(3k_3^4 + k_2^2 k_3^2 - 3k_1^2 k_3^2 + 2k_1^2 k_2^2 + 2k_1^4),$$

$$M'^{-1}_{22}{}_{12} = 4\xi k_1^3 k_2 k_3^2 + 4\xi^2 k_1 k_2(k_3^4 + k_2^4 + k_1^2 k_2^2) + 8\xi^2\left(\xi + \frac{3\lambda}{2\mu}\right) k_1 k_2^3 k_3^2$$

$$+ 2\frac{\lambda}{\mu} k_1 k_2 k_3^2(-k_3^2 + k_2^2 + k_1^2)$$

$$+ 2\frac{\lambda}{\mu}\xi k_1 k_2(3k_3^4 + k_1^2 k_3^2 - 3k_2^2 k_3^2 + 2 + 2k_2^4 k_1^2 k_2^2), \tag{9.A3}$$

The defect energy is then given by $4\pi^2\beta$ times the quadratic form

$$E = \frac{1}{2\Delta}\sum_{\mathbf{k}} \frac{1}{k_3^4}\eta_I^* M'^{-1}_{IJ}\eta_J, \tag{9.A4}$$

where $\eta_1 = \eta_{11}$, $\eta_2 = \eta_{22}$, $\eta_3 = 2\eta_{12}$.

The expression

$$2\pi i \frac{1}{k_3^4} M'^{-1}_{IJ} \eta_J \tag{9.A5}$$

gives, of course, the three non-zero components $\chi_I = (\chi_{11}, \chi_{22}, \chi_{12})$ of the stress gauge field in momentum space. The energy takes a more symmetric form if we use the defect conservation law (9.96),

$$\begin{aligned}
\eta_{12} &= -(\eta_{11}k_1^2 + \eta_{22}k_2^2 - \eta_{33}k_3^2)/2k_1k_2, \\
\eta_{23} &= -(\eta_{11}k_1^2 - \eta_{22}k_2^2 - \eta_{33}k_3^2)/2k_2k_3, \\
\eta_{13} &= -(\eta_{11}k_1^2 - \eta_{22}k_2^2 + \eta_{33}k_3^2)/2k_1k_3,
\end{aligned} \tag{9.A6}$$

to express η_{12} in terms of the diagonal componenets η_{11}, η_{22}, η_{33}. It then acquires manifest cubic symmetry

$$E = \frac{1}{2\Delta} \sum_{\mathbf{k}; i,j} \eta_{ii}^* A_{ij}^{(1)} \eta_{jj}, \tag{9.A7}$$

where

$$\begin{aligned}
A_{11}^{(1)} = \Bigg\{ & 2\xi k_1^2(k_3^4 + k_2^4 + k_1^4) + 4\xi\left(\xi + \frac{\lambda}{\mu}\right)(k_2^2k_3^4 + k_2^4k_3^2 + k_1^4k_3^2 + k_1^4k_2^2) \\
& + 8\xi^3 k_1^2k_2^2k_3^2 + (\lambda/\mu)k_1^2(k_3^4 + 2k_2^2k_3^2 + k_2^4 - 2k_1^2k_3^2 - 2k_1^2k_2^2 + k_1^4) \\
& + 12(\lambda/\mu)\xi(\xi - \tfrac{2}{3})k_1^2k_2^2k_3^2 \Bigg\} \Big/ (k_2^2k_3^2), \\
A_{11}^{(1)} = -\Bigg\{ & \left(2\xi + \frac{\lambda}{\mu}\right)(-k_3^4 + k_2^4 + k_1^4) + 4\left(\xi^2 + \frac{\lambda}{\mu}\xi - \frac{\lambda}{2\mu}\right)k_1^2k_2^2 \Bigg\} \Big/ k_3^2 \\
& + 2(\lambda/\mu)\xi(k_3^2 + k_2^2 + k_1^2).
\end{aligned} \tag{9.A8}$$

The other matrix elements follow from cubic symmetry. Alternatively, we may express all defect configurations in terms of the three off-diagonal components $\eta_k \equiv \eta_{ij}$ (i, j, k cyclic),

$$\eta_{11} = -(\eta_{12}k_2 + \eta_{13}k_3)/k_1, \quad \eta_{22} = -(\eta_{12}k_1 + \eta_{23}k_3)/k_2,$$

$$\eta_{33} = -(\eta_{13}k_1 + \eta_{23}k_2)/k_3. \tag{9.A9}$$

Then the energy reads

$$E = \frac{1}{2\Delta}\sum_{\mathbf{k},i,j} \eta_i^* A_{ij}^{(2)} \eta_j, \tag{9.A10}$$

with the matrix elements

$$A_{11}^{(2)} = \left\{4\xi\left(\xi + \frac{\lambda}{\mu}\right)(k_3^6 + k_2^6 + k_1^2k_3^4 + k_1^2k_2^4)\right\}\Big/(k_2^2k_3^2)$$

$$+ 8\left(\xi + \frac{\lambda}{2\mu}\right)k_1^2 + 8\xi^2\left(\xi + \frac{3}{2}\frac{\lambda}{\mu} + \frac{1}{2}\right)(k_3^2 + k_2^2),$$

$$A_{12}^{(2)} = 2(\lambda/\mu)\xi(k_3^6 + 2k_2^2k_3^4 + k_2^4k_3^2 + 2k_1^2k_3^4 + 2k_1^2k_2^4 + k_1^4k_3^2 + 2k_1^4k_2^2)/(k_1k_2k_3^2)$$

$$+ 4\xi^2k_1k_2(k_2^2 + k_1^2)/k_3^2 + 8\left(\xi^3 - \frac{1}{2}\xi^2 + \frac{3}{2}\frac{\lambda}{\mu}\xi^2 - \frac{\lambda}{\mu}\xi + \frac{\lambda}{2\mu}\right)k_1k_2. \tag{9.A11}$$

It is now easy to verify that (9.A3) and Kröner's expression (9.99) are identical. We merely have to express η_{13}, η_{23}, η_{13} in terms of η_{11}, η_{22}, η_{33} via (9.A6) and recover (9.A7). Alternatively, of course, we can insert (9.A9) into (9.A3) and recover (9.A10).

With the existence of powerful algebraic computer-software there is no problem, in principle, to calculate the defect energy in the continuum limit for any for the 9 classes of elastic matrices $c_{ijk\ell}$ specified in Appendix 1A. The expressions are much lengthier than those for the cubic case, so we refrain from writing them down.

Let us only mention that, in general, the 3×3 matrix M in the continuum form of the stress energy [defined as similar to (9.90)]

$$e = \frac{1}{2}\sigma_{ij}c_{ijk\ell}^{-1}\sigma_{k\ell} = \frac{1}{2}\chi_I M_{IJ}\chi_J, \tag{9.A12}$$

and the 3×3 matrix of the strain energy D_{ij}, Eq. (1.92),

$$e = \frac{1}{2}u_i D_{ij} u_j, \tag{9.A13}$$

have determinants related by

$$|M| = |D|(k_3^6/|c|), \tag{9.A14}$$

where $|c|$ is the determinant of the 6×6 matrix c. Thus the elastic Green function G_{ij} and the defect energy can be derived from the same fundamental scalar Green function $G = 1/|D|$. The first gets multiplied by the cofactors $(|D|D^{-1})$ (denoted by M_{ij} in Eq. (1.94), but not to be confused with the matrix M_{IJ} under consideration here) the second by

$$\frac{|c|}{k_3^6}(|M|M^{-1}), \tag{9.A15}$$

where $|M|M^{-1}$ is the cofactor of the matrix M_{IJ}.

NOTES AND REFERENCES

The lattice models described in this chapter were proposed in
H. Kleinert, *Phys. Lett.* **91A** (1982) 295,
see also
H. Kleinert, *Lett. Nuovo Cimento* **37** (1983) 295, *Phys. Lett.* **97A** (1983) 51, *ibid* **96A** (1983) 302.

CHAPTER TEN

DEFECT GAUGE FIELDS

In the last chapter we focused attention mostly upon the gauge structure of stresses, since it leads to a simple defect representation of the melting model. Initially, however, when constructing the model for linear elasticity plus jump numbers n_{ij}, it was the defect gauge fields which played a primary role. The partition function (9.14) was invariant under the defect gauge transformations (9.15)–(9.18) and required a gauge-fixing functional Φ which removed the gauge degeneracy. We stated that it was always possible to choose a gauge in which n_{ij} is quasi-symmetric and in which the symmetrized jump numbers $n^s_{ij} = (n_{ij} + n_{ji})/2$ have three components n^s_{22}, n^s_{33}, n^s_{13} vanishing identically with the non-zero components satisfying the boundary conditions (9.20), (9.21). With $\Phi[n^s_{ij}]$ denoting the Kronecker δ enforcing these conditions, the partition function reads [note the differences with (9.14)]

$$Z = \sum_{\{n^s_{ij}\}} \Phi[n^s_{ij}] \prod_{\mathbf{x},\, i} \left[\int_{-\infty}^{\infty} \frac{du_i(\mathbf{x})}{a} \right]$$
$$\times \exp\left\{ -\beta \left(\frac{2\pi}{a} \right)^2 \left[\frac{1}{2} \sum_{\mathbf{x},\, i<j} (\nabla_i u_j + \nabla_j u_i - 2a n^s_{ij})^2 + \xi \sum_{\mathbf{x},\, i} (\nabla_i u_i - a n^s_{ii})^2 \right.\right.$$
$$\left.\left. + \frac{\lambda}{2\mu} \sum_{\mathbf{x}} \left(\sum_i (\nabla_i u_i - a n^s_{ii}) \right)^2 \right] \right\}. \tag{10.1}$$

It is worthwhile studying the defect gauge properties of this partition function in detail.

10.1. GAUGE FIXING

In this section we shall first convince ourselves that our gauge choice is always possible. Due to the integer values of the fields, this is a non-trivial matter.

The first part of the gauge choice, namely, the quasi-symmetric property is trivial since the transformation (9.18), $n_{ij} \to n_{ij} + \varepsilon_{ijk} M_k$, can be used to change n_{ij}, n_{ji} for $i \neq j$ by adding and subtracting the same integer number from n_{ij} and n_{ji}, respectively. If $n^s_{ij} = \frac{1}{2}(n_{ij} + n_{ji})$ is integer so is the difference $n^a_{ij} = \frac{1}{2}(n_{ij} - n_{ji})$, which can be reduced to zero. Otherwise n^a_{ij} is half-integer and we can make the transformation $n^a_{ij} \to n^a_{ij} + \varepsilon_{ijk} M_k$ and reduce n^a_{ij} to $\pm 1/2$ for $i \lessgtr j$. This defines what we have called the *quasi-symmetric gauge*. In it, the symmetrized jump numbers n^s_{ij} for $i \neq j$ and $i = j$ run precisely through all half-integer and integer values, respectively.

We now turn to the further defect gauge invariance (9.16)

$$n^s_{ij}(\mathbf{x}) \to n^s_{ij}(\mathbf{x}) + \tfrac{1}{2}(\nabla_i N_j(\mathbf{x}) + \nabla_j N_i(\mathbf{x})). \tag{10.1'}$$

This will be used to bring n^s_{ij} to the gauge

$$n^s_{22}(\mathbf{x}) = 0, \quad n^s_{33}(\mathbf{x}) = 0, \quad n^s_{13}(\mathbf{x}) = 0. \tag{10.2}$$

Suppose $n^s_{ij}(\mathbf{x})$ did not satisfy these conditions. Then we can always perform the transformation to a new set of jump numbers $n^{s0}_{ij}(\mathbf{x})$ via

$$n^s_{ij}(\mathbf{x}) = n^{s0}_{ij}(\mathbf{x}) + \tfrac{1}{2}(\nabla_i N_j(\mathbf{x}) + \nabla_j N_i(\mathbf{x})) \tag{10.3}$$

which do. The integer transformation functions $N_i(\mathbf{x})$ are determined uniquely when we specify the boundary conditions (9.20), (9.21) for $n^{s0}(\mathbf{x})$:

$$\nabla_3 n^{s0}_{11}(x_1, x_2, 0) = 0, \quad n^{s0}_{11}(x_1, x_2, 0) = 0, \quad n^{s0}_{12}(x_1, 0, x_3) = 0, \tag{10.4a,b,c}$$

$$n^{s0}_{12}(0, x_2, 0) = 0, \tag{10.5a}$$

$$n^{s0}_{23}(0, 0, x_3) = 0, \quad n^{s0}_{23}(0, x_2, 0) = 0, \quad \nabla_1 n^{s0}_{23}(0, x_2, 0) = 0. \tag{10.5b,c,d}$$

In two dimensions, the analogous conditions are

$$n_{22}^{s0}(\mathbf{x}) = 0, \qquad n_{12}^{s0}(\mathbf{x}) = 0. \tag{10.6a,b}$$

with the non-zero component satisfying

$$n_{11}^{s0}(x_1, 0) = 0, \qquad \nabla_2 n_{11}^{s0}(x_1, 0) = 0. \tag{10.7a,b}$$

We will first consider this simpler case of two dimensions. Since the remainder of this section deals exclusively with $n_{ij}^{s}(\mathbf{x})$, $n_{ij}^{s0}(\mathbf{x})$, we shall, from now on, omit the superscripts s. Inserting (10.6a,b) into (10.3), we find the difference equations

$$n_{22}(\mathbf{x}) = \nabla_2 N_2(\mathbf{x}), \qquad n_{12}(\mathbf{x}) = \tfrac{1}{2}(\nabla_1 N_2(\mathbf{x}) + \nabla_2 N_1(\mathbf{x})). \tag{10.8}$$

When solving these it is useful to introduce the inverse of the difference operators as the following specific sum, valid for $x_1 \geqslant 1$

$$\left(\frac{1}{\nabla_1} f\right)(\mathbf{x}) \equiv \sum_{x_1'=0}^{x_1-1} f(x_1', x_2, x_3), \tag{10.9}$$

with a similar expression for ∇_2^{-1}, ∇_3^{-1}. For $x_1 < 1$ this sum is defined via

$$\left(\frac{1}{\nabla_1} f\right)(\mathbf{x}) = \sum_{x_1'=-\infty}^{x_1-1} f(x_1', x_2, x_3) - \sum_{x_1'=-\infty}^{-1} f(x_1', x_2, x_3). \tag{10.10}$$

Thus the operation $((1/\nabla_1)f)(\mathbf{x})$ satisfies the boundary condition

$$\left(\frac{1}{\nabla_1} f\right)(0, x_2, x_3) = 0. \tag{10.11}$$

For brevity, we shall often omit the parenthesis and write $\nabla_1^{-1} f(0, x_2, x_3)$ with the tacit understanding that $x_1 = 0$ is taken after the operation ∇_1^{-1}.

Using this notation, we can write the most general solutions of (10.8) as

$$N_2(\mathbf{x}) = \frac{1}{\nabla_2} n_{22}(\mathbf{x}) + f_2(x_1) \tag{10.12}$$

and

$$N_1(\mathbf{x}) = \frac{1}{\nabla_2}(2n_{12} - \nabla_1 N_2) + f_1(x_1)$$

$$= 2\frac{1}{\nabla_2}n_{12} - \frac{\nabla_1}{\nabla_2^2}n_{22}(\mathbf{x}) - x_2\nabla_1 f_2(x_1) + f_1(x_1), \qquad (10.13)$$

where $f_1(x_1)$, $f_2(x_1)$ are two arbitrary integer-valued functions of x_1. Taking this N_1, we can now calculate the non-zero component

$$n_{11}(\mathbf{x}) = n_{11}^0(\mathbf{x}) + \nabla_1 N_1$$

$$= n_{11}^0(\mathbf{x}) + 2\frac{\nabla_1}{\nabla_2}n_{12} - \frac{\nabla_1^2}{\nabla_2^2}n_{22} - x_2\nabla_1^2 f_2(x_1) + \nabla_1 f_1(x_1). \qquad (10.14)$$

We now make use of the boundary condition (10.7a) and find [by (10.11)]

$$f_1(x_2) = \frac{1}{\nabla_1}n_{11}(x_1, 0) + c_1, \qquad (10.15)$$

where c_1 is an arbitrary integer number. If we, on the other hand, differentiate (10.14) with respect to x_2 and set $x_2 = 0$ afterwards we find

$$\nabla_2 n_{11}(x_1, 0) = \nabla_2 n_{11}^0(x_1, 0) + 2\nabla_1 n_{12}(x_1, 0) - \nabla_1^2 f_2(x_1). \qquad (10.16)$$

Now we invoke the second boundary condition (10.5b) and determine f_2:

$$f_2(x_1) = -\frac{1}{\nabla_1^2}(\nabla_2 n_{11} - 2\nabla_1 n_{12})(x_1, 0) + c_2 + r_2 x_1, \qquad (10.17)$$

where c_2, r_2 are integers. In this way we arrive at the two integer functions

$$N_1(\mathbf{x}) = 2\frac{1}{\nabla_2}n_{12}(\mathbf{x}) - \frac{\nabla_1}{\nabla_2^2}n_{22}(\mathbf{x}) + x_2\frac{1}{\nabla_1}(\nabla_2 n_{11} - 2\nabla_1 n_{12})(x_1, 0)$$

$$+ \frac{1}{\nabla_1}n_{11}(\mathbf{x}) + c_1 - rx_2,$$

$$N_2(\mathbf{x}) = \frac{1}{\nabla_2}n_{22}(\mathbf{x}) - \frac{1}{\nabla_1^2}(\nabla_2 n_{11} - 2\nabla_1 n_{12})(x_1, 0) + c_2 + rx_1. \qquad (10.18)$$

The constants c_1, c_2 and r cannot be determined further in principle, since they do not change n_{ij} at all under the transformation (10.3).

Notice that these constants have a simple physical meaning. The constants c_1 and c_2 amount to an integer-valued translation, $u_i(\mathbf{x}) \to u_i(\mathbf{x}) + c_i$ while the constant r is the integer-valued version of an infinitesimal rotation of the entire crystal $u_i(\mathbf{x}) \to u_i(\mathbf{x}) + r\varepsilon_{ij}x_j$.

Let us now generalize this procedure to three dimensions. Here the conditions (10.2) amount to the following difference equations:

$$n_{22}(\mathbf{x}) = \nabla_2 N_2(\mathbf{x}), \quad n_{33}(\mathbf{x}) = \nabla_3 N_3(\mathbf{x}), \quad n_{13}(\mathbf{x}) = \tfrac{1}{2}(\nabla_1 N_3 + \nabla_3 N_1)(\mathbf{x}). \tag{10.19}$$

They are solved by

$$\begin{aligned} N_3(\mathbf{x}) &= \frac{1}{\nabla_3} n_{33}(\mathbf{x}) + f_3(x_1, x_3), \quad N_2(\mathbf{x}) = \frac{1}{\nabla_2} n_{22}(\mathbf{x}) + f_2(x_1, x_3), \\ N_1(\mathbf{x}) &= 2\frac{1}{\nabla_3} n_{13}(\mathbf{x}) - \frac{\nabla_1}{\nabla_3} N_3(\mathbf{x}) + f_1(x_1, x_2) \\ &= 2\frac{1}{\nabla_3} n_{13}(\mathbf{x}) - \frac{\nabla_1}{\nabla_3^2} n_{33}(\mathbf{x}) - x_3 \nabla_1 f_3(x_1, x_2) + f_1(x_1, x_2), \end{aligned} \tag{10.20}$$

where f_1, f_2 and f_3 are arbitrary integer functions of their arguments. For the discussion to come it will be useful to denote the determined parts of N_i by $\widehat{N}_i$ and write

$$\begin{aligned} N_{2,3}(\mathbf{x}) &\equiv \widehat{N}_{2,3}(\mathbf{x}) + f_{2,3}(x_1, x_{3,2}), \\ N_1(\mathbf{x}) &\equiv \widehat{N}_1(\mathbf{x}) - x_3 \nabla_1 f_3(x_1, x_3) + f_1(x_1, x_2). \end{aligned} \tag{10.21}$$

The initial conditions (10.4a–c) lead to the following difference equations for f_1:

$$\nabla_3 n_{11}(x_1, x_2, 0) = \nabla_1 \nabla_3 \widehat{N}_1(x_1, x_2, 0) - \nabla_1^2 f_3(x_1, x_2), \tag{10.22a}$$

$$n_{11}(x_1, x_2, 0) = \nabla_1 \widehat{N}_1(x_1, x_2, 0) + \nabla_1 f_1(x_1, x_2), \tag{10.22b}$$

$$n_{12}(x_1, 0, x_3) = \tfrac{1}{2}(\nabla_1 \widehat{N}_2 + \nabla_2 \widehat{N}_1)(x_1, 0, x_3) + \tfrac{1}{2}\nabla_1 f_2(x_1, x_3) + \tfrac{1}{2}\nabla_2 f_1(x_1, 0). \tag{10.22c}$$

The first and second can be solved by

$$f_3(x_1, x_2) = -\frac{\nabla_3}{\nabla_1^2} n_{11}(x_1, x_2, 0) + \frac{\nabla_3}{\nabla_1} \hat{N}_1(x_1, x_2, 0) + c_3(x_2) + d_3(x_2) x_1, \tag{10.23a}$$

$$f_1(x_1, x_2) = \frac{1}{\nabla_1} n_{11}(x_1, x_2, 0) - \hat{N}_1(x_1, x_2, 0) + c_1(x_2) \equiv \hat{f}_1(x_1, x_2) + c_1(x_2). \tag{10.23b}$$

With these we find from (10.22c),

$$\begin{aligned} f_2(x_1, x_3) = \frac{1}{\nabla_1} [2n_{12}(x_1, 0, x_3) - \nabla_2 \hat{N}_1(x_1, 0, x_3)] \\ - \hat{N}_2(x_1, 0, x_3) - \frac{\nabla_2}{\nabla_1} \hat{f}_1(x_1, x_2) - c_1'(0) x_1 + c_2(x_3) \\ \equiv f_2(x_1, x_3) - c_1'(0) x_1 + c_2(x_3), \end{aligned} \tag{10.23c}$$

where we have denoted the simple lattice derivative by a prime, for brevity.

In order to determine the functions $c_1(x_2)$, $c_2(x_3)$, $c_3(x_2)$ and $d_3(x_2)$ we now turn to the initial conditions (10.5) which read

$$n_{12}(0, x_2, 0) = \tfrac{1}{2}(\nabla_1 \hat{N}_2 + \nabla_2 \hat{N}_1) + \tfrac{1}{2}(\nabla_1 \hat{f}_2 + \nabla_2 \hat{f}_1) - \tfrac{1}{2} c_1'(0) + \tfrac{1}{2} c_1'(x_2), \tag{10.24a}$$

$$n_{23}(0, 0, x_3) = \tfrac{1}{2}(\nabla_2 \hat{N}_3 + \nabla_2 \hat{N}_2) + \tfrac{1}{2}(\nabla_2 \hat{f}_3 + \nabla_3 \hat{f}_2) + \tfrac{1}{2} c_3'(0) + \tfrac{1}{2} c_2'(x_3), \tag{10.24b}$$

$$n_{23}(0, x_2, 0) = \tfrac{1}{2}(\nabla_2 \hat{N}_3 + \nabla_3 \hat{N}_2) + \tfrac{1}{2}(\nabla_2 \hat{f}_3 + \nabla_3 \hat{f}_2) + \tfrac{1}{2} c_3'(x_2) + \tfrac{1}{2} c_2'(0), \tag{10.24c}$$

$$\nabla_1 n_{23}(0, x_2, 0) = \tfrac{1}{2}(\nabla_1 \nabla_2 \hat{N}_3 + \nabla_1 \nabla_3 \hat{N}_2) + \tfrac{1}{2}(\nabla_1 \nabla_2 \hat{f}_3 + \nabla_1 \nabla_3 \hat{f}_2) + \tfrac{1}{2} d_3'(x_2). \tag{10.24d}$$

From the first equation we find

$$c_1(x_2) = 2\frac{1}{\nabla_2} n_{12}(0, x_2, 0) - \frac{\nabla_1}{\nabla_2}\hat{N}_2(0, x_2, 0) - \hat{N}_1(0, x_2, 0)$$
$$- x_2\nabla_1\hat{f}_1(0, 0) - \hat{f}_1(0, x_2) + c_1'(0)x_2 + g_1$$
$$= \hat{c}_1(x_2) + c_1'(0)x_2 + g_1, \tag{10.25}$$

where $c_1'(0) \equiv -r_3$ and g_1 remain arbitrary integer constants of integration. The second equation gives

$$c_2(x_3) = 2\frac{1}{\nabla_3} n_{23}(0, 0, x_3) - \frac{\nabla_2}{\nabla_3}\hat{N}_3(0, 0, x_3) - \hat{N}_2(0, 0, x_3)$$
$$- x_3\nabla_2\hat{f}_3(0, 0) - \hat{f}_2(0, x_3) - c_3'(0)x_3 + g_2$$
$$\equiv \hat{c}_2(x_3) - c_3'(0)x_3 + g_2, \tag{10.26a}$$

with $c_3'(0) \equiv r_1$, g_2 being arbitrary integers.

The third equation leads to

$$c_3(x_2) = 2\frac{1}{\nabla_2} n_{23}(0, x_2, 0) - \hat{N}_3(0, x_2, 0) - \frac{\nabla_3}{\nabla_2}\hat{N}_2(0, x_2, 0)$$
$$- \hat{f}_3(0, x_2) - x_2\nabla_3\hat{f}_2(0, 0) - c_2'(0)x_2 + g_3.$$

Inserting (10.26a) evaluated at $x_3 = 0$, the second line becomes

$$-\hat{c}_2'(0)x_2 + c_3'(0)x_2 + g_3,$$

and we may write

$$c_3(x_2) = \hat{c}_3(x_2) + c_3'(0)x_2 + g_3, \tag{10.26b}$$

where

$$\hat{c}_3(x_2) = 2\frac{1}{\nabla^2} n_{23}(0, x_2, 0) - \hat{N}_3(0, x_2, 0) - \frac{\nabla_3}{\nabla_2}\hat{N}_2(0, x_2, 0)$$
$$- \hat{f}_3(0, x_2) - x_2\nabla_3\hat{f}_3(0, 0) - \hat{c}_2'(0)x_2. \tag{10.27}$$

There is only one constant of integration, g_3.

Finally the fourth equation (10.5d) is solved by

$$d_3(x_2) = 2\frac{1}{\nabla_2} n_{23}(0, x_2, 0) - \nabla_1 \hat{N}_3(0, x_2, 0) - \frac{\nabla_1 \nabla_3}{\nabla_2} \hat{N}_2(0, x_2, 0)$$
$$- \nabla_1 \hat{f}_3(0, x_2) - x_2 \nabla_1 \nabla_3 \hat{f}_2(0, 0) - r_2$$
$$\equiv \hat{d}_3(x_2) - r_2, \tag{10.28}$$

where r_2 is a constant of integration.

In this way we have determined all $N_i(\mathbf{x})$ uniquely, up to the following arbitrary integers,

$$\Delta N_2 = r_3 x_1 - r_1 x_3 + g_2, \quad \Delta N_3 = r_1 x_2 - r_2 x_1 + g_3, \quad \Delta N_1 = r_2 x_3 - r_3 x_2 + g_1. \tag{10.29}$$

These are integer-valued versions of translations plus infinitesimal rotations of the crystal as a whole. It is not possible to fix them any further since they do not contribute to the defect gauge transformations (10.3).

10.2. PHYSICAL CONTENT OF INTEGER-VALUED DEFECT GAUGE INVARIANCE

Previously, in the XY model, we saw that defect gauge invariance had a simple physical interpretation. It implied that the partition function does not depend on the way in which the jumping surfaces of the vortex lines are chosen. The same situation holds in the present case of defect lines. In order to see this, let us recall once more the classical theory of plasticity, which is formulated in the continuum. In the limit of zero lattice spacing, the jump numbers n_{ij}^s go over into what is generally called the plastic part of the strain tensor u_{ij}^p (apart from an overall factor; see Section 2.9). The exponent in the partition function (10.1) becomes the lattice version of the elastic energy in the presence of plastic deformations

$$E_{\mathrm{el}} = \int d^D x \left[\mu (u_{ij} - u_{ij}^p)^2 + \frac{\lambda}{2} (u_{\ell\ell} - u_{\ell\ell}^p)^2 \right]. \tag{10.30}$$

Note that as long as we are not interested in the statistical mechanics of the defects ensemble, but only in the elastic properties of a fixed *given* plastic deformation, then these properties can all be extracted from the partition function:

$$Z = \int \mathscr{D} u_i(\mathbf{x})\, e^{-(1/T)\int d^D x[\mu(u_{ij} - u^p_{ij})^2 + (\lambda/2)(u_{\ell\ell} - u^p_{\ell\ell})^2]}. \tag{10.31}$$

Following the same procedure which lead us to (9.22) from (9.14) this can be brought into canonical form,

$$Z = \int \mathscr{D} u_i(\mathbf{x}) \int \mathscr{D} \sigma_{ij}(\mathbf{x})\, e^{-(1/T)\int d^D x\{(1/4\mu)(\sigma^2_{ij} - (\nu/(1+\nu))\sigma^2_{\ell\ell}) + i\sigma_{ij}(u_{ij} - u^p_{ij})}, \tag{10.32}$$

where σ_{ij} is the fluctuating stress field. The plastic strain acts as an external source to the stress field. Minimizing the exponent we find the Euler-Lagrange equations

$$\partial_i \sigma_{ij} = 0, \tag{10.33}$$

with

$$\sigma_{ij} = \frac{1}{i}\,[2\mu\,(u_{ij} - u^p_{ij}) + \lambda\delta_{ij}(u_{\ell\ell} - u^p_{\ell\ell})]. \tag{10.34}$$

Inserting the second into the first gives

$$-[\mu(\nabla^2 u_i + \partial_i \partial_\ell\, u_\ell) + \lambda \partial_i \partial_\ell\, u_\ell] = -(2\mu\, \partial_j u^p_{ij} + \lambda \partial_i u^p_{\ell\ell}). \tag{10.35}$$

Thus the plastic strains have the same effect upon $u_i(\mathbf{x})$ as a volume force

$$f^p_i(\mathbf{x}) = -(2\mu \partial_j u^p_{ij} + \lambda \partial_i u^p_{\ell\ell}). \tag{10.36}$$

Using the expression (1.90) for the Green function we can solve (10.35) and obtain

$$u_i(\mathbf{x}) = 2\mu \int d^D x' \left[\partial_k G_{ij}(\mathbf{x} - \mathbf{x}')\, u^p_{jk}(\mathbf{x}') + \frac{\nu}{1 - 2\nu}\, \partial_j G_{ij}(\mathbf{x} - \mathbf{x}')\, u^p_{\ell\ell}(\mathbf{x}')\right] \tag{10.37}$$

With the explicit expression, $G_{ij}(\mathbf{x} - \mathbf{x}') = (1/8\pi\mu)(\delta_{ij}\nabla^2 R - (1/2(1 - \nu))\partial_i \partial_j R)$, this becomes

$$u_i(\mathbf{x}) = \frac{1}{8\pi}\int d^D x' \times \left(2\nabla^2 \partial_j R u^p_{ij}(\mathbf{x}') - \frac{1}{1-\nu}\partial_i\partial_j\partial_k R u^p_{jk}(\mathbf{x}') + \frac{\nu}{1-\nu}\nabla^2\partial_i R u^p_{\ell\ell}(\mathbf{x}')\right). \tag{10.38}$$

If we wish to use this formula to calculate the displacement field of a defect line we must choose u^p_{ij} appropriately. From the discussion in Section 2.8 we know that u^p_{ij} describes the discontinuity across some cutting surface S whose boundary is the defect line. The multivalued gradient $\partial_i u_j$ has the property

$$\oint_B dx_i \partial_i u_j = b_j + \varepsilon_{jk\ell}\Omega_k x_\ell,$$

when encircling the boundary line of S. This corresponds to the non-integrable "plastic" part of u_j having the form [compare Eqs. (2.60)–(2.62)]

$$\partial_i u^p_j = \delta_i(S)(b_j + \varepsilon_{jk\ell}\Omega_k x_\ell). \tag{10.39}$$

For the strain tensor this amounts to

$$u^p_{ij} = \tfrac{1}{2}\delta_i(S)(b_j + \varepsilon_{jk\ell}\Omega_k x_\ell) + (ij).$$

Inserting this expression into (10.38) and restricting it to a pure dislocation line ($\Omega_k = 0$) we find Eq. (3.13) which was derived in Chapter 3 via Volterra's cutting procedure. Formula (3.13) was valid only for $\mathbf{x}$ values which did not lie on the cutting surface. It is possible to change the position of the surface as long as the boundary line is anchored on the same dislocation lines. If the surface S is changed to S', the difference of S and S' forms a closed surface. For a pure dislocation line the difference between the two plastic gradients is

$$\partial_i u^{p\prime}_j - \partial_i u^p_j = [\delta_i(S') - \delta_i(S)]b_j = \delta_i(S' - S)b_j.$$

But the δ_i function on the right-hand side can be rewritten as the gradient of the volume V enclosed by $S' - S$ so that

$$\partial_i u^{p\prime}_j - \partial_i u^p_j = -\partial_i \delta(V) b_j$$

[recall Eq. (8.20), Part II]. Thus we see that under changes of the cutting surface of a dislocation line the plastic gradients undergo a gauge transformation

$$\partial_i u_j^p \to \partial_i u_j^p - \partial_i \delta(V) b_j. \tag{10.40a}$$

Correspondingly, the plastic strains transform like

$$u_{ij}^{p'} \to u_{ij}^p - \tfrac{1}{2}(\partial_i \delta(V) b_j + \partial_j \delta(V) b_i).$$

The energy (10.30) is invariant under this transformation if we simultaneously change the displacement field $u_i(\mathbf{x})$ by the trivial Volterra operation

$$u_i(\mathbf{x}) \to u_i(\mathbf{x}) - \delta(V) b_i \tag{10.40b}$$

[recall Eq. (2.60)]. This was the way we demonstrated that in the continuum the defect gauge invariance is a manifestation of the irrelevance of the position of the Volterra surface. As long as the boundary line stays fixed, it does not matter where the cutting surface is placed.

Let us now come back and consider the discrete case of a cubic crystal. For this case the δ-function over a volume can be represented by an integer field $N(\mathbf{x})$. The trivial Volterra operation for a dislocation (10.40b) is given by

$$u_i(\mathbf{x}) \to u_i(\mathbf{x}) - N_\alpha(\mathbf{x}) b_i^{(\alpha)},$$

where $b_i^{(\alpha)}$ for $\alpha = 1, 2, 3$ denotes the three fundamental Burgers vectors (1, 0, 0), (0, 1, 0), or (0, 0, 1), respectively, i.e.,

$$b_i^{(\alpha)} = \delta_{\alpha i}.$$

The higher Burgers vectors with $2b_i^{(\alpha)}$, $3b_i^{(\alpha)}$ are obtained by choosing $N_\alpha(\mathbf{x}) = 2, 3, \ldots$ over the volume V in question. If the crystal contains dislocations of any strength and of both orientations for each fundamental Burgers vector, the Volterra operation becomes

$$u_i(\mathbf{x}) \to u_i(\mathbf{x}) - \sum_\alpha N_\alpha(\mathbf{x}) b_i^{(\alpha)}, \tag{10.41}$$

where $N_\alpha(\mathbf{x})$ can be any integer number 0, ± 1, ± 2, ...

We now take the energy (10.30) and rewrite it as a lattice sum,

$$E_{\mathrm{cl}} = a^3 \sum_{\mathbf{x}} \left\{ \frac{\mu}{4} \sum_{i,j} (\nabla_i u_j + \nabla_i u_i - 2u_{ij}^p)^2 + \frac{\lambda}{2} \left[\sum_{\ell} (\nabla_\ell u_\ell(\mathbf{x}-\boldsymbol{\ell}) - u_{\ell\ell}^p(\mathbf{x}-\boldsymbol{\ell})) \right]^2 \right\}. \tag{10.42}$$

This is invariant under (10.41) if the plastic quantities undergo simultaneously the following changes:

$$\begin{aligned} u_{ij}^p(\mathbf{x}) &\to u_{ij}^p(\mathbf{x}) - \frac{1}{2}\left(\sum_\alpha \nabla_i N_\alpha(\mathbf{x}) b_j^{(\alpha)} + (ij) \right) \\ &= u_{ij}^p(\mathbf{x}) + \frac{1}{2}\left(\sum_\alpha n_{i\alpha}(\mathbf{x}) b_j^{(\alpha)} + (ij) \right). \end{aligned} \tag{10.43}$$

The integer vector fields $n_{j\alpha}(\mathbf{x}) \equiv -\nabla_i N_\alpha(\mathbf{x})$ are, of course, the lattice versions of the $\delta_j(S)$-functions which are singular on the surfaces S_α of V_α.

The plastic field of a defect is obtained by allowing the surfaces to have a boundary in which case all the vectors $n_{\alpha j}(\mathbf{x})$ become independent [rather than being the three components of the gradient of the field $N^{(\alpha)}(\mathbf{x})$]. Therefore, the general dislocation configuration is represented by the integer plastic tensor

$$u_{ij}^p(\mathbf{x}) = \frac{1}{2} \sum_\alpha (n_{i\alpha} b_j^{(\alpha)} + (ij)). \tag{10.44}$$

Using the explicit form of the fundamental Burgers' vectors $b_i^{(\alpha)} = \delta_{\alpha i}$ we find that

$$u_{ij}^p(\mathbf{x}) = \tfrac{1}{2}(n_{ij}(\mathbf{x}) + n_{ji}(\mathbf{x})) \tag{10.45}$$

or, for the plastic part of the lattice gradient itself,

$$\nabla_i u_j^p(\mathbf{x}) = n_{ij}(\mathbf{x}). \tag{10.46}$$

These are precisely the jump numbers introduced previously.

Note that in the presence of defects the impossibility of assigning a unique rest position to the atoms, from where to measure the displace-

ment fields $u_i(\mathbf{x})$, becomes quite obvious: If we consider the specific edge defect shown in Fig. 2.10, we see that the two choices of a Volterra surface S and S' correspond to two natural assignments of original lattice positions where the displaced atom has come from. When shifting S to S', which means that the plastic strain tensor undergoes a defect gauge transformation of the type (10.43), this assignment shifts $u_i(\mathbf{x})$ by a lattice vector (1, 0, 0). As a consequence, the displacement field is transformed by an integer field

$$u_1(\mathbf{x}) \to u_1(\mathbf{x}) - N(\mathbf{x}).$$

This is precisely a trivial Volterra operation of the type (10.41) which accompanies a defect-gauge transformation (10.43), thereby keeping the elastic energy invariant.

The observable quantities in the presence of defects are not the strains themselves but only the differences of the total strain and the plastic strain, i.e., the proper *elastic strains*

$$u_{ij}^{\mathrm{el}} \equiv u_{ij} - u_{ij}^{p}.$$

These are defect gauge invariant quantities. The physically observable stress is proportional to this quantity, i.e.,

$$\sigma_{ij}^{\mathrm{phys}} = 2\mu(u_{ij} - u_{ij}^{p}) + \lambda\delta_{ij}(u_{\ell\ell} - u_{\ell\ell}^{p})$$

[compare (10.34)] and, as such, it is defect gauge invariant as well.

10.3. INTERACTION ENERGY BETWEEN DEFECT LINES FROM THE DEFECT GAUGE FIELD

In Part II, Chapter 8, we saw that the defect gauge field allows for an alternative simple derivation of the interaction energy between vortex lines. The same thing is true for crystalline defect lines. For simplicity, we shall consider only defects in the continuum limit and use as a starting point the partition function of elasticity in the presence of an arbitrary plastic deformation (10.31),

$$Z = \int \mathscr{D} u_i(\mathbf{x})\, e^{-(1/T)\int d^3x[\mu(u_{ij} - u^p_{ij})^2 + (\lambda/2)(u_{\ell\ell} - u^p_{\ell\ell})^2]}. \tag{10.47}$$

Working out the exponent gives

$$-\frac{1}{T}\int d^3x \left\{ \frac{\mu}{2} u_i(\mathbf{x})(-\mu\nabla^2\delta_{ij} - (\lambda + \mu)\,\partial_i\partial_j)\,u_j(\mathbf{x}) - 2\mu u_i(\mathbf{x})\,\partial_j u^p_{ij}(\mathbf{x}) \right.$$
$$\left. - \lambda u_i(\mathbf{x})\,\partial_i u^p_{\ell\ell}(\mathbf{x}) + \mu u^{p2}_{ij} + \frac{\lambda}{2} u^{p2}_{\ell\ell} \right\}. \tag{10.48}$$

Going to the defect gauge[a] $\partial_i u^p_{ij} = 0$, the first coupling to the plastic strain vanishes. After a quadratic completion, the Boltzmann factor for the defect-gauge field becomes

$$e^{-(1/T)\{\int d^3x(\mu u^{p2}_{ij} + (\lambda/2)u^{p2}_{\ell\ell}) - (\lambda^2/2)\int d^3x\, d^3x'\,\partial_i u^p_{\ell\ell}(\mathbf{x})\, G_{ii'}(\mathbf{x}-\mathbf{x}')\,\partial_{i'} u^p_{\ell'\ell'}(\mathbf{x}')\}}, \tag{10.49}$$

where

$$G_{ii'}(\mathbf{x} - \mathbf{x}') = \int \frac{d^3q}{(2\pi)^3} e^{i\mathbf{q}\cdot(\mathbf{x}-\mathbf{x}')} \left(\frac{1}{\mathbf{q}^4}\right) \left[\frac{1}{\mu}(\mathbf{q}^2\delta_{ij} - q_i q_j) + \frac{1}{\lambda + 2\mu} q_i q_j \right] \tag{10.50}$$

is the elastic Green function. This satisfies

$$\partial_i G_{ii'}(\mathbf{x} - \mathbf{x}') = \frac{1}{\lambda + 2\mu}\partial_{i'} v(\mathbf{x} - \mathbf{x}'), \tag{10.51}$$

where $v(\mathbf{x} - \mathbf{x}')$ is the Coulomb Green function $\int (d^3q/(2\pi)^3) e^{i\mathbf{q}\cdot(\mathbf{x}-\mathbf{x}')} (1/\mathbf{q}^2)$, so that

$$\partial_i \partial'_{i'} G_{ii'}(\mathbf{x} - \mathbf{x}') = -\partial_i \partial_{i'} G_{ii'}(\mathbf{x} - \mathbf{x}') = \frac{1}{\lambda + 2\mu} \tag{10.52}$$

and (10.49) simplifies to

[a]For integer-valued defect-gauge fields, this is an illegal gauge. Recall the discussion in the superfluid case (Section 8.4, Part II). For the derivation of the defect energy, however, this does not matter. The argument given there also holds here.

$$e^{-(1/T)\int d^3x(\mu u_{ij}^{p2} + (\lambda/2)u_{\ell\ell}^{p2} - (\lambda^2/2(\lambda+2\mu))u_{\ell\ell}^{p2})} = e^{-(\mu/T)\int dx(u_{ij}^{p2} + (\lambda/(\lambda+2\mu))u_{\ell\ell}^{p2})}. \tag{10.53}$$

Using the Poisson ratio $\nu = \lambda/(2\lambda + 2\mu)$ we can also write

$$\frac{\lambda}{\lambda + 2\mu} = \frac{\nu}{1 - \nu}. \tag{10.54}$$

It remains to express u_{ij}^{p2} and $u_{\ell\ell}^{p2}$ in terms of the defect tensor

$$\eta_{ij}(\mathbf{x}) = \varepsilon_{ik\ell}\,\varepsilon_{jmn}\,\partial_n\,\partial_m\,u_{\ell n}^{p}(\mathbf{x}). \tag{10.55}$$

With the identity (2.53) we get

$$\eta_{ij} = -\nabla^2 u_{ij}^{p} + (\nabla^2\delta_{ij} - \partial_i\partial_j)\,u_{\ell\ell}^{p} + (\partial_i\partial_k\,u_{kj}^{p} + (ij)) - \delta_{ij}\,\partial_k\,\partial_\ell\,u_{k\ell}^{p}, \tag{10.56}$$

$$\eta_{\ell\ell} = \nabla^2 u_{\ell\ell}^{p} - \partial_k\,\partial_\ell\,u_{k\ell}^{p}. \tag{10.57}$$

In the transverse gauge, $\partial_k\,u_{k\ell}^{p} = 0$, we have directly

$$\eta_{\ell\ell} = \nabla^2 u_{\ell\ell}^{p}, \tag{10.58}$$

so that

$$\int d^3x\,u_{\ell\ell}^{p2} = \int d^3x\,\eta_{\ell\ell}(\mathbf{x})\frac{1}{\nabla^4}\,\eta_{\ell\ell}(\mathbf{x}). \tag{10.59}$$

Furthermore, since

$$\eta_{ij} = -\nabla^2 u_{ij}^{p} + (\nabla^2\delta_{ij} - \partial_i\partial_j)\,u_{\ell\ell}^{p},$$

we see that

$$\int d^3x\,\eta_{ij}^2(\mathbf{x}) = \int d^3x(\nabla^2 u_{ij}^{p}\nabla^2 u_{ij}^{p} + 2\partial_i\partial_j u_{ij}^{p}\,\nabla^2 u_{\ell\ell}^{p})$$

and find, in the transverse gauge,

$$\int d^3x\,u_{ij}^{p2}(\mathbf{x}) = \int d^3x\,\eta_{ij}(\mathbf{x})\frac{1}{\nabla^4}\,\eta_{ij}(\mathbf{x}). \tag{10.60}$$

This brings the Boltzmann factor (10.53) to the correct form [recall (5.31), (9.109)]:

$$e^{-(\mu/T)\int d^3x[\eta_{ij}(\mathbf{x})(1/\nabla^4)\eta_{ij}(\mathbf{x})+(\nu/(1-\nu))\eta_{\ell\ell}(\mathbf{x})(1/\nabla^4)\eta_{\ell\ell}(\mathbf{x})]}. \tag{10.61}$$

It should be pointed out that the present type of derivation is the most convenient one when working with crystals of arbitrary symmetry. The partition function (10.47) is then

$$Z=\int \mathscr{D}u_i(\mathbf{x})\, e^{-(1/T)\int d^3x(1/2)c_{ijk\ell}(u_{ij}-u^p_{ij})(u_{k\ell}-u^p_{k\ell})} \tag{10.62}$$

and (10.48) becomes

$$-\frac{1}{T}\int d^3x\left\{-\frac{1}{2}u_i(\mathbf{x})(-c_{ijk\ell}\partial_j\partial_\ell)u_k(\mathbf{x})-u_i(\mathbf{x})\partial_j c_{ijk\ell}u^p_{k\ell}(\mathbf{x})+\frac{1}{2}u^p_{ij}(\mathbf{x})c_{ijk\ell}u^p_{k\ell}(\mathbf{x})\right\}. \tag{10.63}$$

A quadratic completion in $u_i(\mathbf{x})$ brings this to the form

$$-\frac{1}{T}\left\{\int d^3x\left[\frac{1}{2}u^p_{ij}c_{ijk\ell}u^p_{k\ell}\right.\right.$$
$$\left.\left.-\int d^3x\,d^3x'\,\frac{1}{2}u^p_{k\ell}(\mathbf{x})c_{k\ell ij}\partial_j\partial'_{j'}G_{ii'}(\mathbf{x}-\mathbf{x}')c_{i'j'k'\ell'}u^p_{k'\ell'}(\mathbf{x}')\right\}, \tag{10.64}$$

where $G_{ii'}(\mathbf{x}-\mathbf{x}')$ is the elastic Green function which solves the differential equation

$$-c_{ijk\ell}\,\partial_i\partial_\ell\,G_{kn}(\mathbf{x}-\mathbf{x}')=\delta_{in}\delta^{(3)}(\mathbf{x}-\mathbf{x}'). \tag{10.65}$$

If $D(\partial)$ is the determinant of the matrix $M_{ik}=-c_{ijk\ell}\,\partial_j\partial_\ell$ and $D_{kn}(\partial)$ are the cofactors, $G_{kn}(\mathbf{x}-\mathbf{x}')$ is given by

$$G_{kn}(\mathbf{x}-\mathbf{x}')=D_{kn}(\partial)D^{-1}(\partial). \tag{10.66}$$

From (10.64) and (10.66) and the general closed form expressions for G_{kn} given by Every (1980) (cited in Chapter 1) it is, at least in principle, straightforward to find the long-range forces between defects in any crystal.

10.4. THE DEFECT MODEL AS AN APPROXIMATION TO A FIRST-PRINCIPLE N-BODY PARTITION FUNCTION

Up to now, the construction of the defect model of melting was based completely upon analogy with the XY model of superfluidity. It is instructive to see under what approximations this model can be derived from the fundamental partition function of N atoms. Assuming only pair potentials for simplicity, this reads

$$Z_{\text{pot}} = \int \frac{dx_1 \ \ldots \ dx_N}{N!} e^{-(\beta/2)\Sigma_{i \neq j} \Phi(\mathbf{x}_i - \mathbf{x}_j)}. \tag{10.67}$$

In this formula, the positions of all N particles are counted from *one common* origin. In the crystalline state at low temperature, the partition function becomes

$$Z_{\text{pot}} \approx e^{-(\beta/2)\Sigma_{\mathbf{x} \neq \mathbf{y}} \Phi(\mathbf{x} - \mathbf{y})}, \tag{10.68}$$

where $\mathbf{x}$ and $\mathbf{y}$ are the lattice positions.

Upon heating the crystal, the atoms begin fluctuating around these lattice positions. As long as the temperature is low enough it is economical to describe the ensemble of positions not be using the common origin but by specifying the displacements of each atom from its zero temperature rest position, i.e.,

$$\mathbf{x}' = \mathbf{x} + \mathbf{u}(\mathbf{x}).$$

Then the partition function can be written as

$$Z_{\text{pot}} = \frac{1}{N!} \sum_{\mathbf{x}, i} \prod_{\mathbf{x}, i} \left[\int_{-\infty}^{\infty} du_i(\mathbf{x}) \right] e^{-(\beta/2)\Sigma_{\mathbf{x} \neq \mathbf{y}} \Phi(\mathbf{x} - \mathbf{y} + \mathbf{u}(\mathbf{x}) - \mathbf{u}(\mathbf{y}))}. \tag{10.69}$$

If, in this formula, the displacement field is chosen so as to correspond to a permutation of all atoms, then the integrand is invariant. The $N!$ possibilities of doing this are cancelled by the prefactor $1/N!$

For the purpose of introducing defects it is essential to realize that the choice of the ideal crystal positions $\mathbf{x}$ as reference positions was a matter of convenience. We could have, instead, used an arbitrary distorted crystal. Among all these possibilities, an important role is played by a reference crystal whose position vectors differ from those of an ideal

FIG. 10.1. (a) A possible alternative to an ideal crystal of reference positions for the displacement field. It differs from the ideal crystal by a shift of an entire section by a lattice vector. This is a trivial Volterra operation $\mathbf{x} \rightarrow \mathbf{x} + aN(\mathbf{x})$. (b) In constrast, this shows a reference frame with defects.

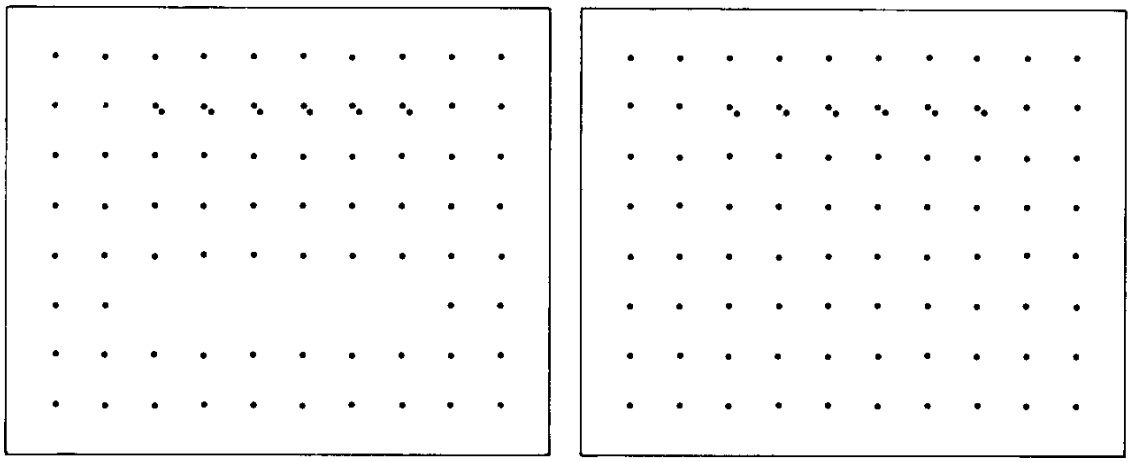

a b

crystal by special regular deformations. They consist in a shift of an entire section by a lattice vector. Such a shift may be written as

$$\mathbf{x} \rightarrow \mathbf{x} + a\mathbf{N}(\mathbf{x}). \tag{10.70}$$

An example is shown in Fig. 10.1, where a small cube has been displaced upwards by one lattice spacing. We recognize a trivial Volterra operation of the type (10.41). This operation has created a layer of missing atoms at the bottom and a double layer of atoms at the top. Obviously, we might just as well use these shifted positions to define the displacement field $u(\mathbf{x})$. For low temperature, the pair potential between the atoms will spread the double layers on top apart, due to the repulsive cores and remove the large distance across the empty layer on the bottom. The lowest energy state in the partition function will again be given by the equilibrium positions of a perfect crystal within the displacement field which is

$$u_i(\mathbf{x}) = -aN_i(\mathbf{x}). \tag{10.71}$$

There is no physical content in this change of the crystalline reference frame by a trivial Volterra operation.

The situation changes drastically if we permit, among the reference frames, crystals in which there are isolated layers of double or missing atoms without a near-lying counterpart. When turning on the pair

interaction, double layers will spread apart and gaps will be closed. But if the counterparts are absent or lie too far, it is impossible for the crystal to return to the perfect state. Thus the crystal will contain defects. If we are to include this possibility in the statistical mechanics of the system, we have to sum in the partition function (10.69), over all such crystalline reference frames which contain defects:

$$Z_{\text{pot}} = \frac{1}{N!} \sum_{\substack{\{\mathbf{x}\} \\ \text{with defects}}} \prod_{\mathbf{x},i} \left[\int_{-\infty}^{\infty} du_i(\mathbf{x}) \right] e^{-(\beta/2)\sum_{\mathbf{x}\neq\mathbf{y}} \Phi(\mathbf{x}-\mathbf{y}+\mathbf{u}(\mathbf{x})-\mathbf{u}(\mathbf{y}))}. \quad (10.72)$$

The characteristic feature of the "defect frames" is that the difference vectors $(x-y)_i$ can no longer be brought to an ideal crystal by simply adding two integer fields

$$a[N_i(\mathbf{x}) - N_i(\mathbf{y})].$$

In particular, for nearest neighbors, it is not sufficient to add

$$a[N_i(\mathbf{x}+\mathbf{j}) - N_i(\mathbf{x})] = a\nabla_j N_i(\mathbf{x}), \quad (10.73)$$

i.e., to add a lattice gradient of an integer field. Instead, the difference between points in the defect and in the ideal frame is given by

$$x_i - y_i|_{\text{def.}} = x_i - y_i|_{\text{ideal}} + a \sum_{\mathbf{x}}^{\mathbf{y}} n_{ji}(\mathbf{x}) \quad (10.74)$$

and the result depends on the path chosen for calculating the sum on the right-hand side. The numbers $n_{ji}(\mathbf{x})$ are, of course, the jump numbers introduced before into the model.

It is now straightforward to see to what approximation the model emerges from the full partition function (10.72). Consider first the ideal reference crystal. Assuming the displacement field to be small we can expand the energy as follows:

$$\frac{1}{2}\sum_{\mathbf{x}\neq\mathbf{y}} \Phi(\mathbf{x}-\mathbf{y}) + \frac{1}{2}\sum_{\mathbf{x}\neq\mathbf{y}} \partial_i\Phi(\mathbf{x}-\mathbf{y})(u_i(\mathbf{x}) - u_i(\mathbf{y}))$$

$$+ \frac{1}{4}\sum_{\mathbf{x}\neq\mathbf{y}} \partial_i\partial_j\Phi(\mathbf{x}-\mathbf{y})(u_i(\mathbf{x}) - u_i(\mathbf{y}))(u_j(\mathbf{x}) - u_j(\mathbf{y})) + \ldots \quad (10.75)$$

For a very smooth displacement field, the second and third terms are written as

$$\frac{1}{2}\sum_{\mathbf{x}\neq\mathbf{y}} \partial_i \Phi(\mathbf{x}-\mathbf{y})(x-y)_j \nabla_j u_i(\mathbf{y}) + \frac{1}{4}\sum_{\mathbf{x}\neq\mathbf{y}} \partial_i \partial_j \Phi(\mathbf{x}-\mathbf{y})(x-y)_k (x-y)_\ell \nabla_k u_i(\mathbf{y}) \nabla_\ell u_j(\mathbf{y}). \tag{10.76}$$

Since the reference crystal represents the equilibrium positions, the linear term must be absent,

$$\sum_{\mathbf{x}\neq\mathbf{0}} \partial_i \Phi(\mathbf{x}) x_j = 0. \tag{10.77}$$

Further, since a smooth uniform rotation $\nabla_k u_i = \frac{1}{2}\varepsilon_{ki\ell}\,\omega_\ell$ cannot change the energy, the constants

$$c_{ki\ell j} \equiv \frac{1}{2}\sum_{\mathbf{x}\neq\mathbf{0}} \partial_i \partial_j \Phi(\mathbf{x}) x_k x_\ell \tag{10.78}$$

must be symmetric in ki and ℓj and we can identify them with the usual elastic constants $c_{ki\ell j}$ introduced in Chapter 1.

For central forces,

$$\Phi(\mathbf{x}) = \psi(\mathbf{x}^2), \tag{10.79}$$

one has

$$\begin{aligned} \partial_i \Phi(\mathbf{x}) &= 2x_i \psi'(\mathbf{x}^2), \\ \partial_i \partial_j \Phi(\mathbf{x}) &= 2\delta_{ij}\psi'(\mathbf{x}^2) + 4x_i x_j \psi''(\mathbf{x}^2), \\ &\vdots \qquad\qquad \vdots \qquad\qquad \vdots \end{aligned} \tag{10.80}$$

and

$$c_{ki\ell j} = \sum_{\mathbf{x}\neq\mathbf{0}} [\delta_{ij}\psi'(\mathbf{x}^2) + 2x_i x_j \psi''(\mathbf{x}^2)] x_k x_\ell\,. \tag{10.81}$$

The equilibrium condition reads

$$\sum_{\mathbf{x}\neq\mathbf{0}} \partial_i \Phi(\mathbf{x}) x_j = 2 \sum_{\mathbf{x}\neq\mathbf{0}} \psi'(\mathbf{x}^2) x_i x_j = 0, \tag{10.82}$$

so that the first term in (10.81) vanishes and the symmetry is manifest,

$$c_{ki\ell j} = 2 \sum_{\mathbf{x}} \psi''(\mathbf{x}^2) x_i x_j x_k x_\ell . \tag{10.83}$$

For a defect frame, the lattice gradients $\nabla_k u_i(\mathbf{x})$ in the equilibrium positions are no longer zero. Instead, they prefer to be as close as possible to the jump numbers $n_{ki}(\mathbf{x})$. Only then will the equilibrium positions locally resemble that of a proper crystal. Thus an expansion of the energy has to be performed in powers of $(\nabla_k u_i - a n_{ki})$ rather than $\nabla_k u_i$. Far away from the defect line, the elastic energy will be practically the same as that for an ideal crystal. Obviously, the approximation of the Villain form of our model of defect melting, (10.1), consists in assuming that this approximation holds throughout the crystal.

NOTES

The integer valued defect-gauge fields were first discussed in the references quoted at the end of the previous chapter.

CHAPTER ELEVEN

THERMODYNAMICS OF THE MELTING MODEL

In the following two chapters we are going to analyze the thermal properties of the lattice model of defect melting in a way similar to that employed in the Villain model of the superfluid phase transition. For this we shall first expand the partition function Z of (9.40) into a high temperature series.

11.1. HIGH TEMPERATURE EXPANSION

We will proceed in two steps. First we sum over all defect tensors $\bar{\eta}_{ij}(\mathbf{x})$ which satisfy the defect conservation law

$$\bar{\nabla}_i \bar{\eta}_{ij}(\mathbf{x}) = 0. \tag{11.1}$$

We shall do so by letting $\bar{\eta}_{11}(\mathbf{x})$, $\bar{\eta}_{22}(\mathbf{x})$ run independently through all integers and $\bar{\eta}_{12}(\mathbf{x})$ through all half-integers while adjusting the remaining components in a unique way so as to satisfy (11.1). This is achieved by choosing

$$\bar{\eta}_{13} = \bar{\eta}_{31} = -\frac{1}{\bar{\nabla}_3}(\bar{\nabla}_1 \bar{\eta}_{11} + \bar{\nabla}_2 \bar{\eta}_{21}), \tag{11.2}$$

$$\bar{\eta}_{23} = \bar{\eta}_{32} = -\frac{1}{\bar{\nabla}_3}(\bar{\nabla}_1 \bar{\eta}_{12} + \bar{\nabla}_2 \bar{\eta}_{22}), \tag{11.3}$$

and

$$\bar{\eta}_{33} = -\frac{1}{\bar{\nabla}_3}(\bar{\nabla}_1 \bar{\eta}_{13} + \bar{\nabla}_2 \bar{\eta}_{23}) = \frac{1}{\bar{\nabla}_3^2}(\bar{\nabla}_1^2 \bar{\eta}_{11} + \bar{\nabla}_2^2 \bar{\eta}_{22} + 2\bar{\nabla}_1 \bar{\nabla}_2 \bar{\eta}_{12}). \tag{11.4}$$

It is understood that the boundaries in each equation are treated in the same way as previously in the equation

$$\ell_3 = -\frac{1}{\bar{\nabla}_3}(\bar{\nabla}_1 \ell_1 + \bar{\nabla}_2 \ell_2), \tag{11.5}$$

which was discussed in Part II [discussion following Eq. (6.40)].

Using the stress gauge $\bar{X}_{i3} = 0$, the defect coupling is

$$e^{2\pi i \Sigma_{\mathbf{x}}(\bar{X}_{11}\bar{\eta}_{11} + \bar{X}_{22}\bar{\eta}_{22} + 2\bar{X}_{12}\bar{\eta}_{12})}.$$

Therefore, the sum over the independent numbers $\bar{\eta}_{11}$, $\bar{\eta}_{22}$, $\bar{\eta}_{12}$ forces the gauge fields $\bar{X}_{11}(\mathbf{x})$, $\bar{X}_{22}(\mathbf{x})$, $\bar{X}_{12}(\mathbf{x})$ to become integer and the partition function turns into the sum

$$Z = \left[\frac{1}{(2\xi)^3}\left(1 - 3\frac{\xi}{\gamma}\right)\right]^{N/2} \frac{1}{(2\pi\beta)^{3N}}$$

$$\times \sum_{\{\bar{X}_{11},\, \bar{X}_{22},\, \bar{X}_{12}\}} e^{-(1/2\beta)\Sigma_{\mathbf{x}}\{\Sigma_{i<j}\bar{\sigma}_{ij}^2 + (1/2\xi)\Sigma_i \bar{\sigma}_{ii}^2 - (1/2\gamma)(\Sigma_i \bar{\sigma}_{ii}(\mathbf{x}-\boldsymbol{\ell}))^2\}}. \tag{11.6a}$$

This sum over all integer stress-gauge fields $\bar{X}_{11}(\mathbf{x})$, $\bar{X}_{22}(\mathbf{x})$, $\bar{X}_{12}(\mathbf{x})$ produces precisely all integer-stress fields $\bar{\sigma}_{ij}$ which satisfy the divergence condition $\bar{\nabla}_i \bar{\sigma}_{ij}(\mathbf{x}) = 0$. Thus we can rewrite the sum also as

$$\sum_{\{\bar{\chi}_{11},\bar{\chi}_{22},\bar{\chi}_{12}\}} = \sum_{\{\bar{\sigma}_{ij}\}} \delta_{\bar{\nabla}_i \bar{\sigma}_{ij},\,0}. \tag{11.6b}$$

In two dimensions, the summation over the defect tensors $\bar{\eta}_{ij}(\mathbf{x})$ reduces to the single sum over $\bar{\eta}(\mathbf{x})$ in (9.57) leading to the partition function

$$Z = \left[\frac{1}{(2\xi)^2}\left(1-2\frac{\xi}{\gamma}\right)\right]^{N/2} \frac{1}{(\sqrt{2\pi\beta})^{3N}} \times \sum_{\{\bar{\chi}(\mathbf{x})\}} \exp\left\{-\frac{1}{2\beta}\sum_{\mathbf{x}}\left[\bar{\sigma}_{12}^2+\frac{1}{2\xi}(\bar{\sigma}_{11}^2+\bar{\sigma}_{22}^2)-\frac{1}{2\gamma}(\bar{\sigma}_{11}(\mathbf{x}-\mathbf{1})+\bar{\sigma}_{22}(\mathbf{x}-\mathbf{2}))^2\right]\right\}, \tag{11.7a}$$

rather than (11.6). The sum over the integer stress-gauge field $\bar{\chi}(\mathbf{x})$ can again be replaced by a sum over conserved integer stress fields

$$\sum_{\{\bar{\chi}\}} = \sum_{\{\bar{\sigma}_{ij}\}} \delta_{\bar{\nabla}_i \bar{\sigma}_{ij},0}. \tag{11.7b}$$

The high-temperature expansion in now obtained by finding successively larger and larger $\bar{\sigma}_{ij}(\mathbf{x})$ configurations which satisfy $\bar{\nabla}_i \bar{\sigma}_{ij}(\mathbf{x}) = 0$.

The physical interpretation of this expansion is quite clear. In the hot crystal, β is so small that no $\bar{\sigma}_{ij}$ configurations can contribute. The crystal is completely stress free. For lower temperatures, clusters of atoms form by fluctuations which are locally capable of supporting stress. For decreasing temperature, these regions become larger. At the melting temperature, stress is allowed to spread over the entire crystal.

We shall study this process now in detail and consider first the case of two dimensions. At very high temperatures, where all $\bar{\sigma}_{ij}(\mathbf{x})$ configurations are frozen out, Z has the limit[a]

$$Z_0 = \left[\frac{1}{(2\xi)^2}\left(1-2\frac{\xi}{\gamma}\right)\right]^{N/2} \frac{1}{(\sqrt{2\pi\beta})^{3N}} = \left[(2\xi)\left(1+\frac{\lambda}{\xi\mu}\right)\right]^{-N/2} \frac{1}{(\sqrt{2\pi\beta})^{3N}}. \tag{11.8}$$

In order to find the stress configurations which form at lower temperatures we may resort to two graphical methods. The first proceeds in close

[a]Recall that $\lambda = 2\mu\xi^2/(\gamma - D\xi)$ so that $(1 - D\xi/\gamma) = \xi/[D\lambda/(2\mu) + \xi]$.

analogy with the superfluid case. We take advantage of the conditions $\bar{\nabla}_i \bar{\sigma}_{ij} = 0$ and represent the components

$$b_i^{(1)} \equiv \bar{\sigma}_{i1}, \qquad b_i^{(2)} \equiv \bar{\sigma}_{i2}, \tag{11.9}$$

as two sets of closed non-self-backtracking random loops. In order to guarantee the symmetry of the stress tensor they have to satisfy the condition

$$b_2^{(1)} = b_1^{(2)}. \tag{11.10}$$

If we draw $b_i^{(1)}$, $b_i^{(2)}$ as oriented solid and dotted lines, respectively, this amounts to the rule that whenever there is a solid line $\uparrow$ or $\downarrow$ it has to be joined by a dotted line $\cdots\!\rightarrow\!\cdots$ or $\cdots\!\leftarrow\!\cdots$, in the form

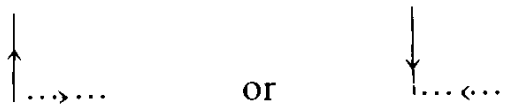

(11.11)

The lines $\rightarrow$, $\leftarrow$ and $\vdots$, $\vdots$, on the other hand, are unconstrained.

The smallest possible configuration which complies with these rules is

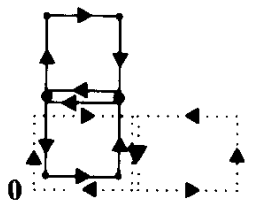

(11.12)

If the lower left corner is taken to be the origin, the corresponding $\bar{\sigma}_{ij}$ values are given by

$$\bar{\sigma}_{11}(\mathbf{0}) = 1, \quad \bar{\sigma}_{11}(\mathbf{2}) = -2, \quad \bar{\sigma}_{11}(2\cdot\mathbf{2}) = 1,$$
$$\bar{\sigma}_{22}(\mathbf{0}) = 1, \quad \bar{\sigma}_{22}(\mathbf{1}) = -2, \quad \bar{\sigma}_{22}(2\cdot\mathbf{1}) = 1,$$
$$\bar{\sigma}_{12}(\mathbf{0}) = -1, \quad \bar{\sigma}_{12}(\mathbf{1}) = 1, \quad \bar{\sigma}_{12}(\mathbf{2}) = 1, \quad \sigma_{12}(\mathbf{1}+\mathbf{2}) = -1. \tag{11.13}$$

Inserting this into (11.7), the Boltzmann factor becomes

$$e^{-(1/2\beta)[4+(1/2\xi)(1+4+1+1+4+1)-(1/2\gamma)20]} = e^{-(1/\beta)(2+3/\xi-5/\gamma)}. \tag{11.14}$$

The number associated with the third term $(\bar{\sigma}_{11}(\mathbf{x}-\mathbf{1})+\bar{\sigma}_{22}(\mathbf{x}-\mathbf{2}))^2/2\gamma$ is somewhat tedious to extract because of the shift in the arguments. But if we observe the identity

$$\sum_{\mathbf{x}} (\bar{\sigma}_{11}(\mathbf{x}-\mathbf{1})+\bar{\sigma}_{22}(\mathbf{x}-\mathbf{2}))^2 = \sum_{\mathbf{x}} (\nabla\cdot\bar{\nabla}\bar{\chi})^2 = \sum_{\mathbf{x}} (2\bar{\sigma}_{12}^2+\bar{\sigma}_{11}^2+\bar{\sigma}_{22}^2) \tag{11.15}$$

and compare the right-hand side with the first two terms in the exponent of (11.7) we see that there is a simple way of finding it: It has to be such that for $\xi = 1$, $\gamma = 1$ the exponent vanishes.

Graphically, the Boltzmann factor is found as follows: We simply count the numbers $n(\bullet\cdots\cdots) = n(\downarrow)$, $n(\bullet\!\!-\!\!-)$, $n(\vdots)$ of lines

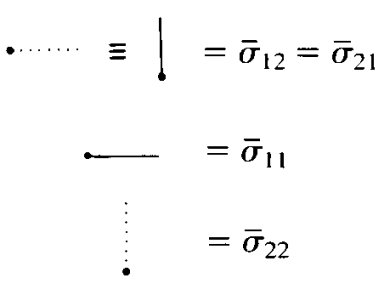

(11.16)

in a diagram. If i denotes their multiplicity, we form

$$A = \sum n(\bullet\cdots\cdots)\cdot i^2 = \sum n(\downarrow)\cdot i^2,$$

$$B = \sum n(\bullet\!\!-\!\!-)\cdot i^2 + \sum n(\vdots)\cdot i^2,$$

$$C = 2A + B, \tag{11.17}$$

and obtain the Boltzmann factor

$$e^{-(1/4\beta)(A+(B/2\xi)-(C/2\gamma))}. \tag{11.18}$$

In the above graph (11.12), for example, we have

$$n(\bullet\cdots\cdots) = n(\begin{smallmatrix}|\\\bullet\end{smallmatrix}) = 4\cdot 1, \quad n(\bullet\!\!-\!\!-) = 2\cdot 1 + 1\cdot 2, \quad n(\begin{smallmatrix}\vdots\\\bullet\end{smallmatrix}) = 2\cdot 1 + 1\cdot 2, \tag{11.19}$$

where the second factor in each product is the multiplicity i. Hence

$$A = 4\cdot 1, \quad B = 2\cdot 1 + 1\cdot 4 + 2\cdot 1 + 1\cdot 4 = 12, \quad C = 2A + B = 20, \tag{11.20}$$

and the Boltzmann factor is then

$$e^{-(1/\beta)(2 + 3/\xi - 5/\gamma)} \tag{11.21}$$

as in (11.14).

By superimposing two fundamental graphs side by side we obtain

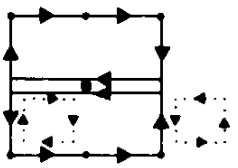

(11.22)

and count

$$n(\bullet\cdots\cdots) = n(\begin{smallmatrix}|\\\bullet\end{smallmatrix}) = 4\cdot 1, \quad n(\bullet\!\!-\!\!-) = 4\cdot 1 + 2\cdot 2, \quad n(\begin{smallmatrix}\vdots\\\bullet\end{smallmatrix}) = 4\cdot 1, \tag{11.23}$$

so that

$$A = 4\cdot 1, \quad B = 4\cdot 1 + 4\cdot 1 + 2\cdot 4 = 16, \quad C = 2A + B = 24, \tag{11.24}$$

and the Boltzmann factor becomes

$$e^{-(1/\beta)(2 + 4/\xi - 6/\gamma).} \tag{11.25}$$

Obviously, this graphical method quickly becomes very complicated. Fortunately it is possible to develop a more economical procedure based on the stress gauge field $\bar{\chi}(\mathbf{x})$. This has the advantage that for whatever choice of $\bar{\chi}(\mathbf{x})$, the stress tensor $\bar{\sigma}_{ij} = \varepsilon_{ik}\varepsilon_{j\ell}\bar{\nabla}_k\bar{\nabla}_\ell\bar{\chi}(\mathbf{x})$ is automatically traceless and symmetric. In fact, the complicated configuration (11.13) is the result of the simple choice

$$\bar{\chi}(\mathbf{x}) = \delta_{\mathbf{x},\mathbf{0}}. \tag{11.26}$$

This follows directly from the explicit equations

$$\bar{\sigma}_{11}(\mathbf{x}) = \bar{\nabla}_2^2\bar{\chi}(\mathbf{x}) = \bar{\chi}(\mathbf{x}) - 2\bar{\chi}(\mathbf{x}-\mathbf{2}) + \bar{\chi}(\mathbf{x}-2\cdot\mathbf{2}),$$

$$\bar{\sigma}_{22}(\mathbf{x}) = \bar{\nabla}_1^2\bar{\chi}(\mathbf{x}) = \bar{\chi}(\mathbf{x}) - 2\bar{\chi}(\mathbf{x}-\mathbf{1}) + \bar{\chi}(\mathbf{x}-2\cdot\mathbf{1}),$$

$$\bar{\sigma}_{12}(\mathbf{x}) = -\bar{\nabla}_1\bar{\nabla}_2\bar{\chi}(\mathbf{x}) = -\bar{\chi}(\mathbf{x}) + \bar{\chi}(\mathbf{x}-\mathbf{1}) + \bar{\chi}(\mathbf{x}-\mathbf{2}) - \bar{\chi}(\mathbf{x}-\mathbf{1}-\mathbf{2}).$$

The field configuration (11.26) can be represented graphically by a single point at the origin

The calculation of the stress energy is also straightforward. All we have to do is to use the explicit gradient form given in (9.55),

$$e^{-(1/2\beta)\Sigma_{\mathbf{x}}\bar{\chi}(\mathbf{x})\{\bar{\nabla}_1\nabla_1\bar{\nabla}_2\nabla_2 + (1/2\xi)[(\bar{\nabla}_1\nabla_1)^2 + (\bar{\nabla}_2\nabla_2)^2] - (1/2\gamma)(\bar{\nabla}\cdot\nabla)^2\}\bar{\chi}(\mathbf{x})}. \tag{11.27}$$

We rewrite it as

$$e^{-(1/4\beta)\Sigma_{\mathbf{x}}\bar{\chi}(\mathbf{x})\{(\bar{\nabla}\cdot\nabla)^2(1-(1/\gamma)) + [(\bar{\nabla}_1\nabla_1)^2 + (\bar{\nabla}_2\nabla_2)^2]((1/\xi)-1)\}\bar{\chi}(\mathbf{x})}. \tag{11.28}$$

The lattice Laplacian of $\bar{\chi}(\mathbf{x})$ is found directly from the following rule: Go around each lattice site and count the occupancies of all nearest neighbors. Then subtract four times the occupancy of the point itself, and square this number. For the operators $(\bar{\nabla}_1\nabla_1)^2$ and $(\bar{\nabla}_2\nabla_2)^2$ we follow the same procedure in the 1 or 2 directions only, subtracting only twice the occupancy of the point itself. For the diagram (11.27), we find the Laplacians

$(\bar{\nabla}\cdot\nabla)^2$ 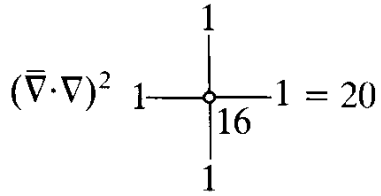

$= 20$

$(\bar{\nabla}_1\nabla_1)^2$ 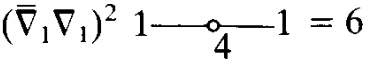

$= 6$

$$(\bar{\nabla}_2\nabla_2)^2 \quad \begin{matrix} & 1 & \\ & | & \\ & \circ 4 & \\ & | & \\ & 1 & \end{matrix} \quad = 6 \tag{11.29}$$

This gives a Boltzmann factor

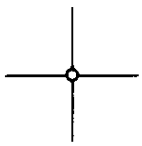

$$: \quad e^{-(1/\beta)\{5(1-(1/\gamma))+3((1/\xi)-1)\}} \tag{11.30}$$

in agreement with (11.14). The superposition (11.22) corresponds to the $\bar{X}$ graph

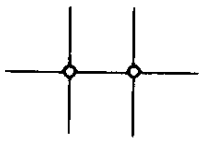

(11.31)

Its sum over Laplacians is easily found,

$$(\bar{\nabla}\cdot\nabla)^2 \quad \begin{matrix} & 1 & 1 & \\ 1 - & \circ & \circ & - 1 \\ & 9 & 9 & \\ & 1 & 1 & \end{matrix} \quad = 24,$$

$$(\nabla_1\bar{\nabla}_1)^2 \quad 1 - \circ - \circ - 1 \quad = 4,$$

$$(\nabla_2\bar{\nabla}_2)^2 \quad \begin{matrix} 1 & 1 \\ \circ 4 & \circ 4 \\ 1 & 1 \end{matrix} \quad = 12, \tag{11.32}$$

so that the Boltzmann factor is

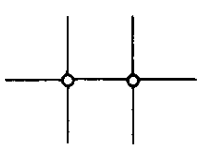

$$: \quad e^{-(1/\beta)\{6(1-(1/\gamma))+4((1/\xi)-1)\}} \tag{11.33}$$

The $\bar{X}$ graphs have the further advantage that it is easy to see how many of them go on the lattice. The graph (11.30) can obviously occur $2N$ times (N times for each sign of the "charge" of $\bar{X}$). The other graph (11.31) has, in addition, two directions so that it can occur $4N$ times.

Let us now organize the graphs according to the order they have in an isotropic $\gamma = \infty$ system. Then ⊣⊢ goes like $e^{-5/\beta}$ and will be said to be of order 5 while ⊣⊣ goes like $e^{-6/\beta}$ and is of order 6. A graph of the same order is seen to be

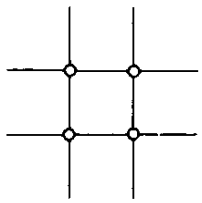

(11.34)

for which the lattice Laplacians have the values

$(\nabla\cdot\nabla)^2$ 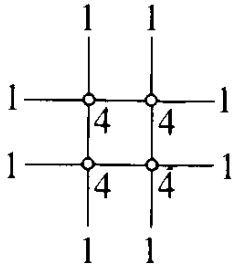 $= 24$

$(\bar{\nabla}_1\nabla_1)^2$ 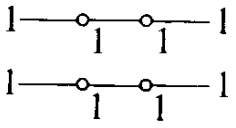 $= 8$

$(\bar{\nabla}_2\nabla_2)^2$ 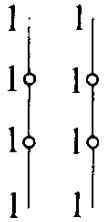 $= 8$

(11.35)

and the Boltzmann factor is

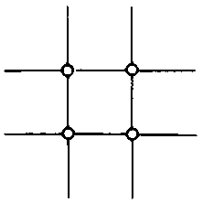 : $e^{-(1/\beta)\{6(1-(1/\gamma))+4((1/\xi)-1)\}}$. (11.36)

Since the number of graphs is again $2N$, the partition function up to order 6 is

$$Z = \left[\frac{1}{(2\xi)^2}\left(1 - 2\frac{\xi}{\gamma}\right)\right]^{N/2} \frac{1}{(\sqrt{2\pi\beta})^{3N}} \{1 + 2N e^{-(1/\beta)\{5(1-(1/\gamma))+3((1/\xi)-1)\}} + 6N e^{-(1/\beta)\{6(1-(1/\gamma))+4((1/\xi)-1)\}} + \ldots\}. \quad (11.37)$$

FIG. 11.1a–b. Graphical expansion of the $D = 2$ melting model (Villain type) according to integer stress gauge-field configurations. The lowest graphs of order 5 and 6 are given in the text [Eqs. (11.30), (11.33), (11.36)]. The first column counts the number of configurations on the lattice, the third and second to the last column the numbers # in the Boltzmann factors $e^{-(1/\beta)\#(1-(1/\gamma))}$, $e^{-(1/\beta)\#((1/\xi)-1)}$, respectively. The number in the third column is also the order of the graph.

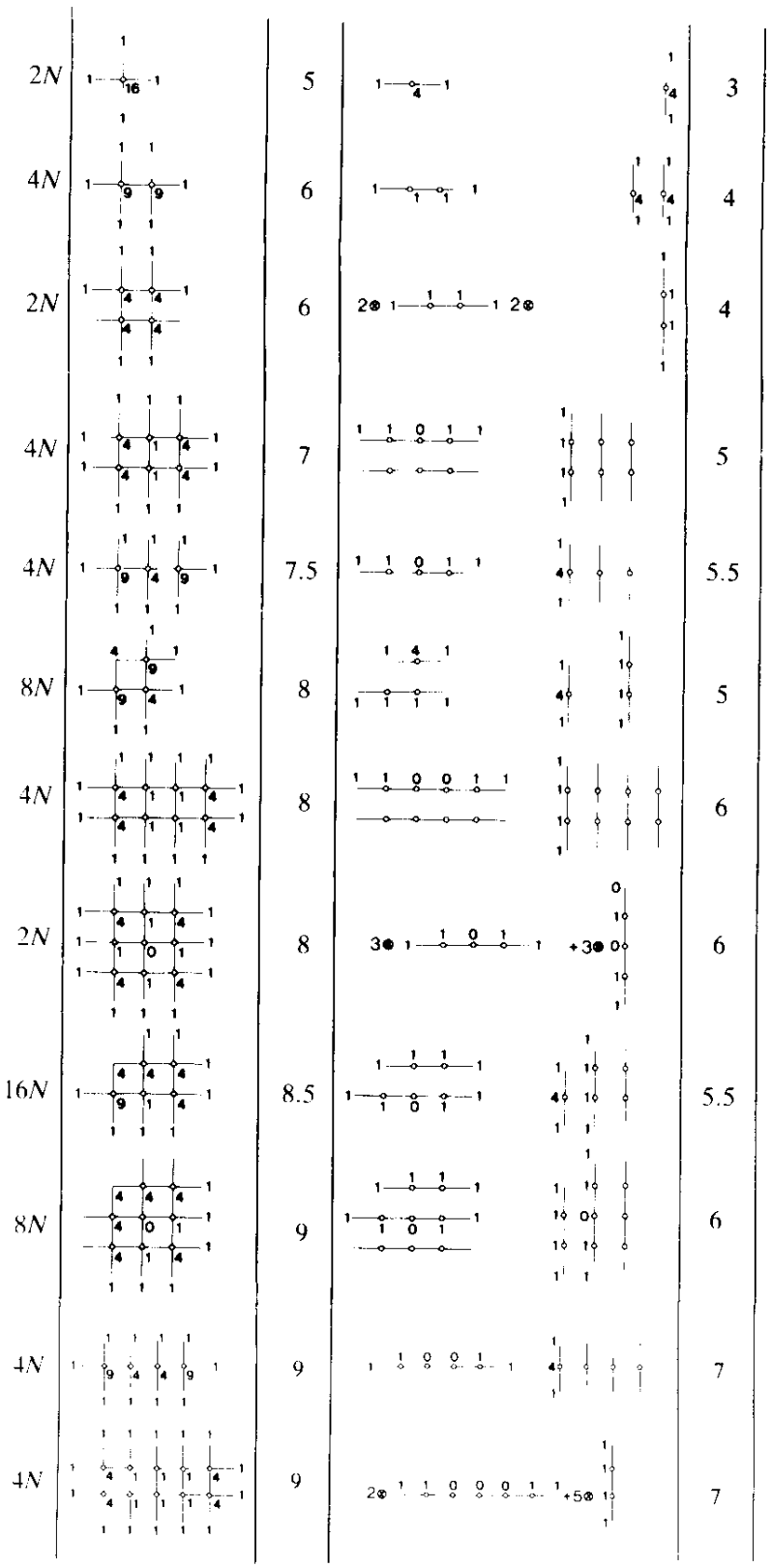

FIG. 11.1 (continued)

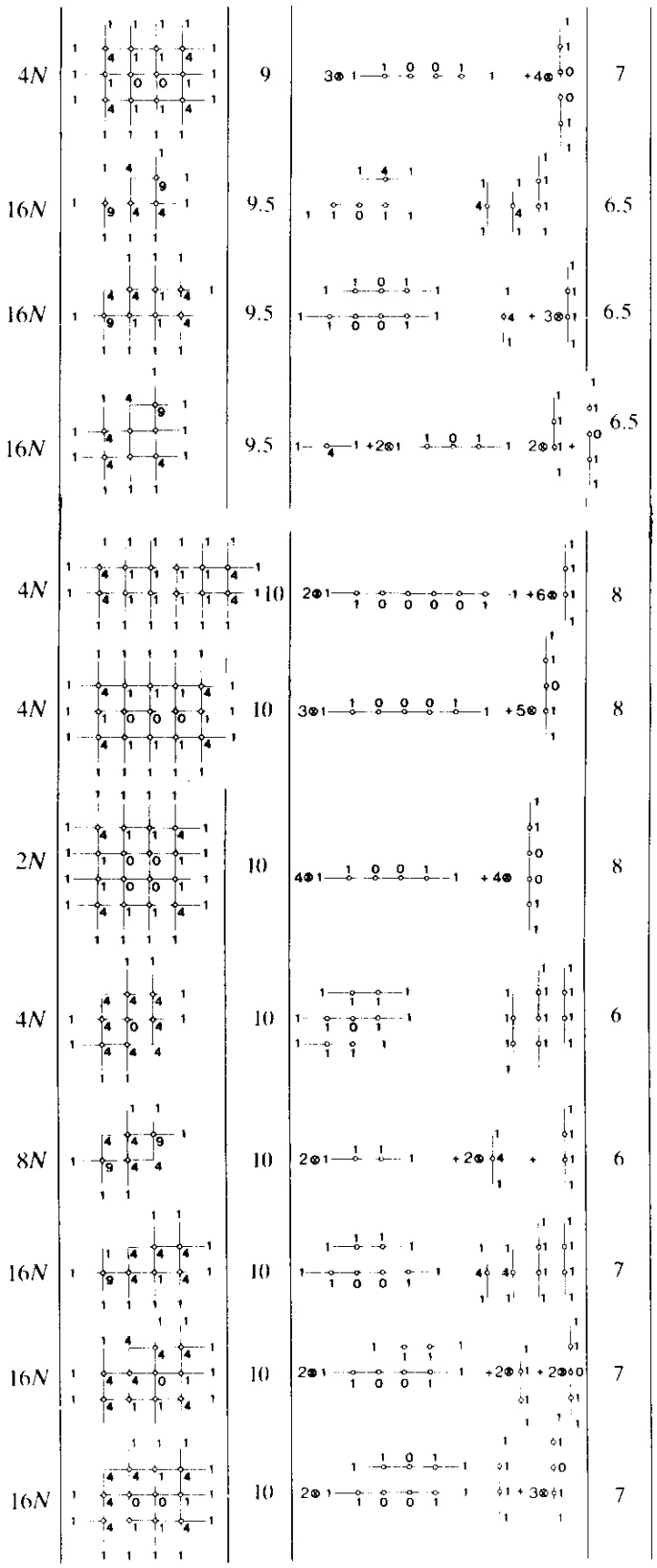

TABLE 11.1. Summary of Fig. 11.1a–c. exponents in the partition function $Z = 1 + N\Sigma\, e^{-(1/\beta)[n(1-(1/\gamma)+m((1/\xi)-1)]}$ and in the partition function $Z = 1 + N\Sigma\, I_1^{n_1}(\beta) I_1(2\beta\xi)^{m_1} I_2(2\beta\xi)^{m_2}$ which will be needed later in Section 13.4 [Eq. (13.85)].

#	Graph	n	m	n_1	m_1	m_2	t
$2N$		5	3	4	4	2	12
$4N$		6	4	4	8	2	16
$2N$		6	4	4	16	0	20
$4N$		7	5	4	20	0	24
$4N$		7.5	5.5	4	10	3	20
$8N$		8	5	6	12	2	22
$4N$		8	6	4	24	0	28
$2N$		8	6	4	24	0	28
$16N$		8.5	5.5	6	18	1	26
$8N$		9	6	6	24	0	30
$4N$		9	7	4	12	4	24
$4N$		9	7	4	28	0	32
$4N$		9	7	4	28	0	32
$16N$		9.5	6.5	6	14	3	26
$16N$		9.5	6.5	6	22	1	30
$16N$		9.5	6.5	6	22	1	30
$4N$		10	6	8	24	0	32
$8N$		10	6	8	16	2	28
$16N$		10	7	6	20	2	30
$16N$		10	7	6	28	0	34
$16N$		10	7	6	28	0	34
$4N$		10	8	4	32	0	36
$4N$		10	8	4	32	0	36
$2N$		10	8	4	32	0	36

The contribution of all diagrams up to order 10 are listed in Fig. 11.1a–c and summarized in Table 11.1.

If $e(n, m)$ stands for $\exp[-(1/\beta)\{n(1-(1/\gamma))+m((1/\xi)-1)\}]$ the free energy can be written as

$$\begin{aligned}-\beta f = \frac{1}{2}\log\left[\frac{1}{(2\xi)^2}\left(1-2\frac{\xi}{\gamma}\right)\right] - \frac{3}{2}\log(2\pi\beta) + 2e(5,3) + 6e(6,4) \\ + 4e(7,5) + 4e(7.5,5.5) + 8e(8,5) + 6e(8,6) \\ + 16e(8.5,5.5) + 8e(9,6) + 12e(9,7) + 48e(9.5,6.5) \\ + 12e(10,6) + 48e(10,7) + 10e(10,8) + \ldots \end{aligned} \tag{11.38}$$

To this order, there is also one disconnected graph in Z

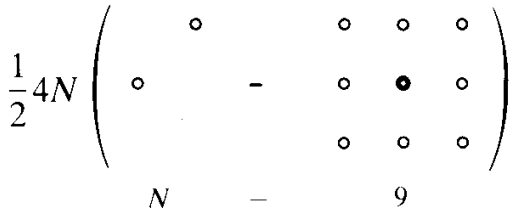

adding to $-\beta f$ a term

$$-\beta f^{\text{disc}} = -18e(10,6). \tag{11.39}$$

The free energy as a function of β is plotted for $\xi = 0.2, 0.4, \ldots, 1.2$ in Fig. 12.2.

Let us now turn to the case of three dimensions. The very high temperature limit of Z is given by [see (11.6)]

$$Z_0 = \left[\frac{1}{(2\xi)^3}\left(1-3\frac{\xi}{\gamma}\right)\right]^{N/2}\frac{1}{(2\pi\beta)^{3N}} = \left[(2\xi)^3\left(1+\frac{3\lambda}{2\xi\mu}\right)\right]^{-N/2}\frac{1}{(2\pi\beta)^{3N}} \tag{11.40}$$

with a free energy density

$$-\beta f_0 = -3\log(2\pi\beta) - \frac{1}{2}\log\left((2\xi)^3\left(1+\frac{3}{2\xi}\frac{\lambda}{\mu}\right)\right). \tag{11.41}$$

In order to construct the lowest stress diagrams in three dimensions, it is convenient to go into the stress gauge $\bar{\chi}_{3i}(\mathbf{x}) = 0$. Then the stresses $\bar{\sigma}_{ij} = \varepsilon_{ik\ell}\,\varepsilon_{jmn}\bar{\nabla}_k\bar{\nabla}_m\bar{\chi}_{\ell n}(\mathbf{x} - \boldsymbol{\ell} - \mathbf{n})$ are given by

$$\begin{aligned}
&\bar{\sigma}_{11}(\mathbf{x}) = \bar{\nabla}_3^2\chi_{22}(\mathbf{x}), \quad \bar{\sigma}_{22}(\mathbf{x}) = \nabla_3^2\chi_{11}(\mathbf{x}), \quad \bar{\sigma}_{12}(\mathbf{x}) = -\bar{\nabla}_3^2\chi_{12}(\mathbf{x}),\\
&\bar{\sigma}_{33}(\mathbf{x}) = \nabla_1^2\chi_{22}(\mathbf{x}) + \bar{\nabla}_2^2\chi_{11}(\mathbf{x}) - 2\bar{\nabla}_1\bar{\nabla}_2\chi_{12}(\mathbf{x}),\\
&\bar{\sigma}_{23}(\mathbf{x}) = \bar{\nabla}_3\nabla_1\chi_{12}(\mathbf{x}) - \bar{\nabla}_3\bar{\nabla}_2\chi_{11}(\mathbf{x}), \quad \bar{\sigma}_{13}(\mathbf{x}) = -\bar{\nabla}_3\bar{\nabla}_1\chi_{22}(\mathbf{x}) + \bar{\nabla}_3\bar{\nabla}_2\chi_{12}(\mathbf{x}),
\end{aligned} \tag{11.42}$$

where we have set $\chi_{\ell n}(\mathbf{x}) \equiv \bar{\chi}_{\ell n}(\mathbf{x} - \boldsymbol{\ell} - \mathbf{n})$, for brevity. The lowest contribution is obtained by choosing one element $\chi_{\ell n}$ to be non-zero. Taking, for example, $\chi_{22}(\mathbf{x}) = \delta_{\mathbf{x},\mathbf{0}}$ we find from

$$\begin{aligned}
&\bar{\sigma}_{11}(\mathbf{x}) = \chi_{22}(\mathbf{x}) - 2\chi_{22}(\mathbf{x} - \mathbf{3}) + \chi_{22}(\mathbf{x} - 2\cdot\mathbf{3}),\\
&\bar{\sigma}_{33}(\mathbf{x}) = \chi_{22}(\mathbf{x}) - 2\chi_{22}(\mathbf{x} - \mathbf{1}) + \chi_{22}(\mathbf{x} - 2\cdot\mathbf{1}),\\
&\bar{\sigma}_{13}(\mathbf{x}) = -\chi_{22}(\mathbf{x}) + \chi_{22}(\mathbf{x} - \mathbf{1}) + \chi_{22}(\mathbf{x} - \mathbf{3}) - \chi_{22}(\mathbf{x} - \mathbf{1} - \mathbf{3}),
\end{aligned} \tag{11.43}$$

the following non-vanishing elements

$$\begin{aligned}
&\bar{\sigma}_{11}(\mathbf{0}) = 1, \quad \bar{\sigma}_{11}(\mathbf{3}) = -2, \quad \bar{\sigma}_{11}(2\cdot\mathbf{3}) = 1,\\
&\bar{\sigma}_{33}(\mathbf{0}) = 1, \quad \bar{\sigma}_{33}(\mathbf{1}) = -2, \quad \bar{\sigma}_{33}(2\cdot\mathbf{1}) = 1,\\
&\bar{\sigma}_{13}(\mathbf{0}) = -1, \quad \bar{\sigma}_{13}(\mathbf{1}) = 1, \quad \bar{\sigma}_{13}(\mathbf{3}) = 1, \quad \bar{\sigma}_{13}(\mathbf{1} + \mathbf{3}) = -1.
\end{aligned} \tag{11.44}$$

This can be pictured by the same diagram (11.13) in the 13 plane as in the two-dimensional case.

Since this diagram can appear in each of the three lattice planes with two orientations, the partition function has the lowest defect contribution

$$\begin{aligned}
Z_1 &= Z_0 \cdot N \cdot 6e^{-(1/\beta)(2 + (3/\xi) - (5/\gamma))}\\
&= Z_0 \cdot N \cdot 6e^{-(1/\beta)(2 + (3/\xi) - (5/\xi)\nu/(1+\nu))}.
\end{aligned} \tag{11.45}$$

An independent low-order diagram is obtained by taking

$$\chi_{12}(\mathbf{x}) = \delta_{\mathbf{x},\mathbf{0}}. \tag{11.46}$$

Then the equations

$$\bar{\sigma}_{33}(\mathbf{x}) = -2\chi_{12}(\mathbf{x}) + 2\chi_{12}(\mathbf{x}-\mathbf{1}) + 2\chi_{12}(\mathbf{x}-\mathbf{2}) - 2\chi_{12}(\mathbf{x}-\mathbf{1}-\mathbf{2}),$$
$$\bar{\sigma}_{12}(\mathbf{x}) = -\chi_{12}(\mathbf{x}) + 2\chi_{12}(\mathbf{x}-\mathbf{3}) - \chi_{12}(\mathbf{x}-2\cdot\mathbf{3}),$$
$$\bar{\sigma}_{23}(\mathbf{x}) = \chi_{12}(\mathbf{x}) - \chi_{12}(\mathbf{x}-\mathbf{1}) - \chi_{12}(\mathbf{x}-\mathbf{3}) + \chi_{12}(\mathbf{x}-\mathbf{1}-\mathbf{3}),$$
$$\bar{\sigma}_{13}(\mathbf{x}) = \chi_{12}(\mathbf{x}) - \chi_{12}(\mathbf{x}-\mathbf{2}) - \chi_{12}(\mathbf{x}-\mathbf{3}) + \chi_{12}(\mathbf{x}-\mathbf{2}-\mathbf{3}), \qquad (11.47)$$

give the following non-zero elements

$$\bar{\sigma}_{33}(\mathbf{0}) = -2, \quad \bar{\sigma}_{33}(\mathbf{1}) = 2, \quad \bar{\sigma}_{33}(\mathbf{2}) = 2, \quad \bar{\sigma}_{33}(\mathbf{1}+\mathbf{2}) = -2,$$
$$\bar{\sigma}_{12}(\mathbf{0}) = -1, \quad \bar{\sigma}_{12}(\mathbf{3}) = 2, \quad \bar{\sigma}_{12}(2\cdot\mathbf{3}) = -1$$
$$\bar{\sigma}_{23}(\mathbf{0}) = 1, \quad \bar{\sigma}_{23}(\mathbf{1}) = -1, \quad \bar{\sigma}_{23}(\mathbf{3}) = -1, \quad \bar{\sigma}_{12}(\mathbf{1}+\mathbf{3}) = 1,$$
$$\bar{\sigma}_{13}(\mathbf{0}) = 1, \quad \bar{\sigma}_{13}(\mathbf{2}) = -1, \quad \bar{\sigma}_{13}(\mathbf{3}) = -1, \quad \bar{\sigma}_{13}(\mathbf{2}+\mathbf{3}) = 1. \qquad (11.48)$$

The energy $(1/2\beta)[\Sigma_{\mathbf{x},i<j}\bar{\sigma}_{ij}^2 + (1/2\xi)\Sigma_{\mathbf{x},i}\bar{\sigma}_{ij}^2 - (1/2\gamma)\Sigma_{\mathbf{x}}(\Sigma_{\ell}\bar{\sigma}_{\ell\ell}(\mathbf{x}-\boldsymbol{\ell}))^2]$ associated with these numbers is

$$\frac{1}{2\beta}\left(14 + \frac{1}{2\xi}16 - \frac{1}{2\gamma}16\right). \qquad (11.49)$$

This is much larger than (11.45) so that the contribution of this configuration is negligible compared with the previous one.

It is also possible to find in three dimensions a high temperature expansion based on the integer-valued stress gauge fields $\bar{\chi}_{11}(\mathbf{x})$, $\bar{\chi}_{22}(\mathbf{x})$, $\bar{\chi}_{12}(\mathbf{x})$. The counting becomes, however, much more difficult than in two dimensions since the existence of a gauge symmetry implies that large pile-ups of graphs are equivalent to a very simple graph in another gauge and can therefore have a very low energy. Fortunately, the higher graphs become rapidly unimportant which shows that fluctuations in the three dimensional defect system are very small. As a consequence we shall be able to reproduce the Monte Carlo data very well using only the lowest stress graph and may dispense with the difficult task of developing the high temperature series any further.

11.2. LOW TEMPERATURE EXPANSION

Let us now consider the opposite extreme of low temperatures. For $T \to 0$, The partition function has the classical limit [see (9.87)]

$$Z_{\text{pot, cl}} = \left(\sqrt{\frac{2\pi k_B T}{\mu a^3}}\right)^{DN} \prod_{\mathbf{k}, i} \frac{1}{\sqrt{\mathbf{K}\cdot\bar{\mathbf{K}} + 2(\xi - 1) K_i \bar{K}_i}}$$
$$\times \prod_{\mathbf{k}} \frac{1}{\sqrt{1 + \left(1 + \frac{\lambda}{\mu}\right) \sum_{\ell} \frac{K_\ell \bar{K}_\ell}{\mathbf{K}\cdot\bar{\mathbf{K}} + 2(\xi - 1) K_\ell \bar{K}_\ell}}}. \quad (11.50)$$

In the isotropic case, this can be calculated right away yielding

$$Z_{\text{pot, cl}} = \left(\sqrt{\frac{2\pi k_B T}{\mu a^2}}\right)^{DN} \frac{1}{(2 + \lambda/\mu)^{N/2}} e^{-(D/2)\int (d^D k/(2\pi)^D) \log \mathbf{K}\cdot\bar{\mathbf{K}}}$$
$$= \frac{1}{(\sqrt{2\pi\beta})^{DN}} \frac{1}{(2 + \lambda/\mu)^{N/2}} e^{-(D/2)\ell}, \quad (11.51)$$

with

$$\ell = \int \frac{d^D k}{(2\pi)^D} \log \mathbf{K}\cdot\bar{\mathbf{K}} \quad (11.52)$$

being known from (6.206a), Part I ($\ell = 1.16625$ for $D = 2$, $\ell = 1.67339$ for $D = 3$). This amounts to a free energy

$$-\beta f_0 = -\frac{D}{2}\log(2\pi\beta) - \frac{1}{2}\log\left(2 + \frac{\lambda}{\mu}\right) - \begin{cases} 1.16625 & \text{for } D = 2, \\ \frac{3}{5}1.67339 & \text{for } D = 3. \end{cases} \quad (11.53)$$

To this we have to add the contribution of the defect sum

$$Z_{\text{def}} = \sum_{\{\eta(\mathbf{x})\}} e^{-4\pi^2\beta(1+\nu)\sum_{\mathbf{x},\mathbf{x}'} \bar{\eta}(\mathbf{x}) v_4(\mathbf{x}-\mathbf{x}') \bar{\eta}(\mathbf{x}')} \quad (11.54)$$

in two dimensions and

$$Z_{\text{def}} = \sum_{\{\eta_{ij}(\mathbf{x})\}} \delta_{\bar{\nabla}_i \eta_{ij}(\mathbf{x}), 0} e^{-4\pi^2\beta\sum_{\mathbf{x},\mathbf{x}'} (\bar{\eta}_{ij}(\mathbf{x}) \bar{\eta}_{ij}(\mathbf{x}') + (\nu/(1-\nu)) \bar{\eta}_{kk}(\mathbf{x}) \bar{\eta}_{\ell\ell}(\mathbf{x}')) v_4(\mathbf{x}-\mathbf{x}')} \quad (11.55)$$

in three dimensions, where $v_4(\mathbf{x})$ is the lattice Green function (9.61):

$$v_4(\mathbf{x}) = \int \frac{d^D k}{(2\pi)^D} e^{i\mathbf{k}\cdot\mathbf{x}} \frac{1}{(\mathbf{K}\cdot\bar{\mathbf{K}})^2}. \tag{11.56}$$

Its values in two and three dimensions are given in Appendix 11A.

Let us calculate the first few terms in these sums.

In two dimensions, the lowest contribution which satisfies the defect and defect-moment neutrality [recall (9.75), (9.76)] is

$$\bar{\eta}(\mathbf{x}) = \delta_{\mathbf{x},\mathbf{0}} - \delta_{\mathbf{x},\mathbf{1}} - \delta_{\mathbf{x},\mathbf{2}} + \delta_{\mathbf{x},\mathbf{1}+\mathbf{2}}. \tag{11.57}$$

This is a quadrupole of neighboring disclinations which can be pictured as

$$\begin{matrix} - & + \\ + & - \end{matrix} \tag{11.58}$$

It has a stress energy

$$\begin{aligned} V\left(\begin{matrix} - & + \\ + & - \end{matrix}\right) &\equiv \frac{1}{2}\sum_{\mathbf{x},\mathbf{x}'} \bar{\eta}(\mathbf{x}) v_4(\mathbf{x}-\mathbf{x}')\,\bar{\eta}(\mathbf{x}') \\ &= \frac{1}{2}[4v_4(\mathbf{0}) - 2v_4(1,0) - 2v_4(0,1) + 2v_4(1,1) \\ &\qquad + 2v_4(1,1) - 2v_4(0,1) \\ &\qquad - 2v_4(1,0)]. \end{aligned} \tag{11.59}$$

The expression is made explicitly finite by performing the two subtractions explained in Appendix 11A giving

$$v_4''(\mathbf{x}) = v_4(\mathbf{x}) - v_4(\mathbf{0}) + \tfrac{1}{4}\mathbf{x}^2 v_2(\mathbf{0}), \tag{11.60}$$

where $v_2(\mathbf{x})$ is the lattice Coulomb potential $\int (d^2k/(2\pi)^2)\, e^{i\mathbf{k}\cdot\mathbf{x}}(1/\bar{\mathbf{K}}\cdot\mathbf{K})$. Then V has the same form as in (11.59), except that all the potentials $v_4(\mathbf{x})$ are replaced by the finite subtracted $v_4''(\mathbf{x})$. Notice that replacement is valid due to the properties of this $\Sigma_{\mathbf{x}}\,\bar{\eta}(\mathbf{x})$ and $\Sigma_{\mathbf{x}}\,\mathbf{x}\bar{\eta}(\mathbf{x})$. The subtracted potentials have $v_4''(\mathbf{0}) = 0$, $v_4''(1,0) = 0$, by construction, so that we arrive at

$$V\left(\begin{matrix} - & + \\ + & - \end{matrix}\right) = 2v_4''(1,1). \tag{11.61}$$

Using the numbers quoted in Table 11A.1 we find

$$V\left(\begin{matrix}-&+\\+&-\end{matrix}\right) = 2\frac{1}{8\pi} = 0.079577. \tag{11.62}$$

The next higher contribution is due to the configuration

$$\eta(\mathbf{x}) = \delta_{\mathbf{x},\mathbf{0}} - \delta_{\mathbf{x},\mathbf{2}} - \delta_{\mathbf{x},\mathbf{2}\cdot\mathbf{1}} + \delta_{\mathbf{x},\mathbf{2}\cdot\mathbf{1}+\mathbf{2}}, \tag{11.63}$$

corresponding to the diagram

$$\begin{matrix}-&:&+\\+&:&-\end{matrix} \tag{11.64}$$

It has a stress energy

$$\begin{aligned} V\left(\begin{matrix}-&:&+\\+&:&-\end{matrix}\right) &= \frac{1}{2}(4v_4(\mathbf{0}) - 2v_4(0,\,1) - 2v_4(2,\,0) + 2v_4(2,\,1) \\ &\qquad + 2v_4(2,\,1) - 2v_4(2,\,0) \\ &\qquad - 2v_4(0,\,1)) \\ &= 2v_4''(2,\,1) - 2v_4''(2,\,0) \\ &= 2\frac{3}{4\pi} - 2\left(\frac{1}{4} - \frac{1}{4\pi}\right) = \frac{2}{\pi} - \frac{1}{2} = 0.136619. \end{aligned} \tag{11.65}$$

The second next contribution comes from

$$\eta(\mathbf{x}) = \delta_{\mathbf{x},\mathbf{0}} - \delta_{\mathbf{x},-\mathbf{1}} + \delta_{\mathbf{x},\mathbf{2}} - \delta_{\mathbf{x},\mathbf{1}+\mathbf{2}}, \tag{11.66}$$

represented by

$$\begin{matrix}\cdot&+&-\\-&+&\cdot\end{matrix} \tag{11.67}$$

Its energy is

$$V\left(\begin{smallmatrix} \cdot & + & - \\ - & + & \cdot \end{smallmatrix}\right) = \frac{1}{2}(4v_4(\mathbf{0}) - 2v_4(1, 0) + 2v_4(0, 1) - 2v_4(1, 1) - 2v_4(1, 1) + 2v_4(2, 1) - 2v_4(1, 0))$$
$$= v_4''(2, 1) - 2v_4''(1, 1) = \frac{3}{4\pi} - \frac{2}{8\pi} = \frac{1}{2\pi} = 0.15915. \tag{11.68}$$

Notice that the similar configuration $\begin{smallmatrix} \cdot & - & + \\ - & + & \cdot \end{smallmatrix}$ is ruled out by moment neutrality $\Sigma_{\mathbf{x}} \mathbf{x}\bar{\eta}(\mathbf{x})$.

Counting the associated number of configurations gives a fourth contribution

$$- \oplus - \tag{11.69}$$

with a double charge in the middle. Its energy

$$\mathrm{V}(- \oplus -) = \tfrac{1}{2}(6v_4(\mathbf{0}) - 4v_4(1, 0) + 2v_4(2, 0) - 4v_4(1, 0))$$
$$= v_4''(2, 0),$$

can be expressed in terms of the other three,

$$\mathrm{V}(- \oplus -) = V\left(\begin{smallmatrix} - & + \\ + & - \end{smallmatrix}\right) - \frac{1}{2}V\left(\begin{smallmatrix} - & \cdot & + \\ + & \cdot & - \end{smallmatrix}\right) + V\left(\begin{smallmatrix} \cdot & + & - \\ - & + & \cdot \end{smallmatrix}\right) = -\frac{1}{4\pi} + \frac{1}{4} = 0.1704. \tag{11.70}$$

The defect partition function is

$$Z_{\mathrm{def}} = 1 + N(2e^{-8\pi^2\beta(1+v)(1/4\pi)} + 4e^{-8\pi^2\beta(1+v)((2/\pi)-(1/2))} + 8e^{-8\pi^2\beta(1+v)(1/2\pi)} + 4e^{-8\pi^2(1+v)((1/4)-(1/4\pi))} + \ldots), \tag{11.71}$$

which leads to a free energy due to defects,

$$-\beta f_{\text{def}} = 2e^{-\beta(1+\nu)\cdot 6.283} + 4e^{-\beta(1+\nu)\cdot 10.787} + 8e^{-\beta(1+\nu)\cdot 12.566} + 4e^{-\beta(1+\nu)\cdot 13.454} \tag{11.72}$$

This has to be added to (11.53) to arrive at the total free energy. In the anisotropic case, the expression (11.51) has to be replaced by

$$Z_{\text{pot,cl}} = \frac{1}{(\sqrt{2\pi\beta})^{DN}} \frac{1}{(\sqrt{2})^{N}} e^{-(D/2)\ell}, \tag{11.73}$$

where ℓ is the anisotropic generalization of the integral $\int (d^D k/(2\pi)^D) \log \bar{\mathbf{K}} \cdot \mathbf{K}$ which was introduced in (9.89). Its values are listed in Table 9.1 as a function of ξ and λ, and plotted in Fig. 9.1. The defect sum takes the form

$$Z_{\text{def}} = \sum_i e^{-8\pi^2\beta\xi(1+\nu)V(i)}, \tag{11.74}$$

where $V(i)$ are the anisotropic versions of the potentials of the lowest defect configurations (11.58), (11.64), (11.67), (11.69). Their values depend only on the combination of the elastic constants $\varepsilon = 2(\xi - 1)(1 + \nu) = 4(\xi - 1)((\xi + (\lambda/\mu))/(2\xi + \lambda/\mu)$. They are listed in Table 11.2, for $\varepsilon = -1.6, -1.2, \ldots, 1.3, 1.6$. From these we obtain the energy of the smallest defect configurations as shown in Table 11.3.

Let us now turn to three dimensions. In order to find the leading contribution to the defect sum (11.55), we shall construct elementary configurations of the conserved defect tensor $\bar{\eta}_{ij}(\mathbf{x})$. This can be done in analogy with the elementary stress configurations in the high temperature expansion. We express $\bar{\eta}_{ij}(\mathbf{x})$ in terms of the defect gauge field $n_{ij}(\mathbf{x})$, $\bar{\eta}_{ij}(\mathbf{x}) = \varepsilon_{ikl}\varepsilon_{jmn}\nabla_k\nabla_m n_{ln}(\mathbf{x} + \mathbf{i} + \mathbf{j})$, and choose a gauge (say) $n_{22} = 0$, $n_{33} = 0$, $n_{13} = 0$ so that we have explicitly

$$\begin{aligned}
\bar{\eta}_{11}(\mathbf{x}) &= -2\nabla_2\nabla_3 n_{23}(\mathbf{x} + 2\cdot\mathbf{1}),\\
\bar{\eta}_{22}(\mathbf{x}) &= \nabla_3^2 n_{11}(x + 2\cdot\mathbf{2}),\\
\bar{\eta}_{33}(\mathbf{x}) &= \nabla_2^2 n_{11}(x + 2\cdot\mathbf{3}) - 2\nabla_1\nabla_2 n_{12}(\mathbf{x} + 2\cdot\mathbf{3}),\\
\bar{\eta}_{12}(\mathbf{x}) &= -\nabla_3^2 n_{12}(\mathbf{x} + \mathbf{1} + \mathbf{2}) + \nabla_1\nabla_3 n_{23}(\mathbf{x} + \mathbf{1} + \mathbf{2}),\\
\bar{\eta}_{23}(\mathbf{x}) &= \nabla_1\nabla_3 n_{12}(\mathbf{x} + \mathbf{2} + \mathbf{3}) - \nabla_2\nabla_3 n_{11}(\mathbf{x} + \mathbf{2} + \mathbf{3}) - \nabla_1^2 n_{23}(\mathbf{x} + \mathbf{2} + \mathbf{3}),\\
\bar{\eta}_{13}(\mathbf{x}) &= \nabla_1\nabla_2 n_{23}(\mathbf{x} + \mathbf{1} + \mathbf{3}) + \nabla_2\nabla_3 n_{12}(\mathbf{x} + \mathbf{1} + \mathbf{3}).
\end{aligned} \tag{11.75}$$

TABLE 11.2. Numerical values of the anisotropic twice subtracted potential between two-dimensional disclinations on a square lattice

$$v_4''(\mathbf{x}) = \int \frac{d^2k}{(x)^2}\left(e^{i\mathbf{k}\cdot\mathbf{x}} - 1 + \frac{\mathbf{x}^2}{4}\overline{\mathbf{K}}\cdot\mathbf{K}\right)\frac{1}{(\overline{\mathbf{K}}\cdot\mathbf{K})^2 + \varepsilon\overline{K}_1 K_2 \overline{K}_2 K_2}$$

for various values of $\varepsilon = 2(\xi - 1)(1 + \nu) = -1.6, \ldots, 1.6$ (corresponding to the parameter of anisotropy $\xi = 0.2, 0.4, 0.6, 0.8, 1.0, 1.2, 1.4$ at $\lambda = 0$).

x_1	x_2	−1.6	−1.2	−0.8	−0.4	0.0	0.4	0.8	1.2	1.6
0	0	0.0000	0.0000	0.0000	0.0000	0.0000	0.0000	0.0000	0.0000	0.0000
0	1	0.0000	0.0000	0.0000	0.0000	0.0000	0.0000	0.0000	0.0000	0.0000
0	2	0.2258	0.2073	0.1926	0.1805	0.1704	0.1618	0.1544	0.1478	0.1421
0	3	0.7506	0.6895	0.6409	0.6010	0.5676	0.5394	0.5143	0.4927	0.4734
0	4	1.6133	1.4831	1.3793	1.2940	1.2225	1.1614	1.1084	1.0619	1.0207
0	5	2.8419	2.6140	2.4322	2.2827	2.1572	2.0499	1.9569	1.8752	1.8027
0	6	4.4589	4.1031	3.8180	3.5854	3.3891	3.2212	3.0755	2.9476	2.8341
1	1	0.0605	0.0534	0.0479	0.0434	0.0398	0.0367	0.0342	0.0319	0.0300
1	2	0.3266	0.2970	0.2737	0.2546	0.2387	0.2252	0.2136	0.2034	0.1945
1	3	0.8743	0.8007	0.7421	0.6940	0.6539	0.6196	0.5893	0.5635	0.5409
1	4	1.7522	1.6085	1.4940	1.4000	1.3211	1.2537	1.1954	1.1441	1.0987
1	5	2.9924	2.7503	2.5571	2.3987	2.2651	2.1512	2.0524	1.9656	1.8888
1	6	4.6188	4.2482	3.9522	3.7088	3.5044	3.3296	3.1779	3.0447	2.9265
2	2	0.6531	0.5941	0.5474	0.5093	0.4775	0.4504	0.4271	0.4069	0.3890
2	3	1.2537	1.1448	1.0583	0.9876	0.9284	0.8780	0.8345	0.7964	0.7628
2	4	2.1732	1.9904	1.8448	1.7254	1.6254	1.5400	1.4661	1.4014	1.3441
2	5	3.4467	3.1626	2.9360	2.7500	2.5939	2.4606	2.3451	2.2437	2.1539
2	6	5.1007	4.6858	4.3546	4.0825	3.8546	3.6586	3.4892	3.3405	3.2087
3	3	1.9148	1.7489	1.6171	1.5093	1.4192	1.3424	1.2760	1.2179	1.1666
3	4	2.8909	2.6447	2.4488	2.2883	2.1539	2.0394	1.9403	1.8535	1.7767
3	5	4.2139	3.8613	3.5803	3.3499	3.1566	2.9917	2.8489	2.7237	2.6129
3	6	5.9106	5.4231	5.0341	4.7149	4.4470	4.2181	4.0197	3.8457	3.6915
4	4	3.9277	3.5939	3.3283	3.1107	2.9285	2.7731	2.6387	2.5209	2.4167
4	5	5.3088	4.8620	4.5061	4.2144	3.9699	3.7612	3.5806	3.4224	3.2823
4	6	7.0588	6.4714	6.0031	5.6188	5.2965	5.0212	4.7828	4.5738	4.3886
5	5	6.7506	6.1836	5.7319	5.3615	5.0510	4.7861	4.5568	4.3558	4.1778
5	6	8.5597	7.8452	7.2756	6.8085	6.4167	6.0822	5.7926	5.5386	5.3137

The numbers n_{11} run through all integers and n_{12}, n_{13} through all half-integers.

The configuration with lowest energy is generated by

$$n_{12}(\mathbf{x}) = \tfrac{1}{2}\delta_{\mathbf{x},2\cdot\mathbf{3}+\mathbf{1}+\mathbf{2}}. \tag{11.76}$$

For it, the non-zero elements are

TABLE 11.3. Elastic energies of the lowest defect configurations on a square lattice.

ε	$\xi(\lambda = 0)$	$V\left(\begin{smallmatrix} \mp & \pm \\ \pm & \end{smallmatrix}\right)$	$V\left(\begin{smallmatrix} \mp & \pm \\ \pm & \end{smallmatrix}\right)$	$V\left(\begin{smallmatrix} \cdot & + & - \\ - & + & \cdot \end{smallmatrix}\right)$	$V(-\oplus-)$
−1.6	0.20	0.121098	0.201573	0.205469	0.225780
−1.2	0.40	0.106819	0.179546	0.190227	0.207273
−0.8	0.60	0.095735	0.162234	0.177941	0.192559
−0.4	0.80	0.086860	0.148223	0.167764	0.180512
0.0	1.00	0.079578	0.136623	0.159155	0.170422
0.4	1.20	0.073487	0.126841	0.151748	0.161815
0.8	1.40	0.068311	0.118468	0.145288	0.154365
1.2	1.60	0.063853	0.111210	0.139588	0.147835
1.6	1.80	0.059970	0.104853	0.134510	0.142054

$$\begin{aligned}
&\bar{\eta}_{33}(\mathbf{0}) = -1, \quad \bar{\eta}_{33}(\mathbf{1}) = 1, \quad \bar{\eta}_{33}(\mathbf{2}) = 1, \quad \bar{\eta}_{33}(\mathbf{1}+\mathbf{2}) = -1,\\
&\bar{\eta}_{12}(\mathbf{0}) = -\tfrac{1}{2}, \quad \bar{\eta}_{12}(\mathbf{3}) = 1, \quad \bar{\eta}_{12}(2\cdot\mathbf{3}) = -\tfrac{1}{2},\\
&\bar{\eta}_{23}(\mathbf{0}) = \tfrac{1}{2}, \quad \bar{\eta}_{23}(\mathbf{1}) = -\tfrac{1}{2}, \quad \bar{\eta}_{23}(\mathbf{3}) = -\tfrac{1}{2}, \quad \bar{\eta}_{23}(\mathbf{1}+\mathbf{3}) = \tfrac{1}{2},\\
&\bar{\eta}_{13}(\mathbf{0}) = \tfrac{1}{2}, \quad \bar{\eta}_{13}(\mathbf{2}) = -\tfrac{1}{2}, \quad \bar{\eta}_{13}(\mathbf{3}) = -\tfrac{1}{2}, \quad \bar{\eta}_{13}(\mathbf{2}+\mathbf{3}) = \tfrac{1}{2}. \qquad (11.77)
\end{aligned}$$

This corresponds to the stress configuration (11.48), except for a factor $\frac{1}{2}$ on each element.

The elastic energy associated with this defect is given by

$$\begin{aligned}
V_1 &= \frac{1}{2}\sum_{\mathbf{x},\mathbf{x}'} v_4(\mathbf{x}-\mathbf{x}')\Big\{2\bar{\eta}_{12}(\mathbf{x})\,\bar{\eta}_{12}(\mathbf{x}') + 2\bar{\eta}_{13}(\mathbf{x})\,\bar{\eta}_{13}(\mathbf{x}') + 2\bar{\eta}_{23}(\mathbf{x})\,\bar{\eta}_{23}(\mathbf{x}')\\
&\quad + \bar{\eta}_{33}(\mathbf{x})\,\bar{\eta}_{33}(\mathbf{x}') + \frac{\nu}{1-\nu}\eta_{33}(\mathbf{x})\,\eta_{33}(\mathbf{x}')\Big\}\\
&= \frac{1}{2}\Big\{2\cdot\frac{1}{4}[6v_4(\mathbf{0}) - 4v_4(1,0) + 2v_4(2,0)\\
&\qquad - 4v_4(1,0)]\\
&\quad + 2\cdot 2\cdot\frac{1}{4}[4v_4(\mathbf{0}) - 2v_4(1,0) - 2v_4(1,0) + 2v_4(1,1)\\
&\qquad + 2v_4(1,1) - 2v_4(1,0)\\
&\qquad -2v_4(1,0)]
\end{aligned}$$

$$+\frac{1}{1-\nu}[4v_4(\mathbf{0}) - 2v_4(1,0) - 2v_4(1,0) + 2v_4(1,1) + 2v_4(1,1) - 2v_4(1,0) - 2v_4(1,0)]\Big\}. \tag{11.78}$$

Performing the subtraction to $v_4'(\mathbf{x}) = v_4(\mathbf{x}) - v_4(\mathbf{0})$ and further to $v_4''(\mathbf{x}) = v_4'(\mathbf{x}) + (\mathbf{x}^2/6)v_2(\mathbf{0})$, and using the numbers quoted in Appendix 11A, we find

$$V_1 = \frac{1}{4}\Big(-24v_4'(1,0) + 8v_4'(1,1) + 2v_4'(2,0)\Big) + \frac{1}{1-\nu}\Big(-4v_4'(1,0) + 2v_4'(1,1)\Big)$$
$$= \frac{1}{4}(8v_4''(1,1) + 2v_4''(2,0)) + \frac{2}{1-\nu}v_4''(1,1) = \frac{1}{12} + \frac{2}{1-\nu}0.021. \tag{11.79}$$

Another fundamental $n_{ij}(\mathbf{x})$ configuration is

$$n_{11}(\mathbf{x}) = \delta_{\mathbf{x},2\cdot\mathbf{2}+2\cdot\mathbf{3}}. \tag{11.80}$$

For this we find the defect tensor

$$\bar{\eta}_{22}(\mathbf{0}) = 1, \quad \bar{\eta}_{22}(\mathbf{3}) = -2, \quad \eta_{22}(2\cdot\mathbf{3}) = 1,$$
$$\bar{\eta}_{33}(\mathbf{0}) = 1, \quad \bar{\eta}_{33}(\mathbf{2}) = -2, \quad \eta_{33}(2\cdot\mathbf{2}) = 1,$$
$$\bar{\eta}_{23}(\mathbf{0}) = -\tfrac{1}{2}, \quad \bar{\eta}_{23}(\mathbf{2}) = \tfrac{1}{2}, \quad \bar{\eta}_{23}(\mathbf{3}) = \tfrac{1}{2}, \quad \bar{\eta}_{23}(\mathbf{2}+\mathbf{3}) = -\tfrac{1}{2}. \tag{11.81}$$

This can be pictured by the same diagram (11.12) as the matrix elements (11.43) of $\bar{\sigma}_{ij}(\mathbf{x})$ except that the off-diagonal dual elements carry only half the weights. Its energy is considerably larger than (11.79):

$$V_2 = \frac{1}{2}\sum_{\mathbf{x},\mathbf{x}'} v_4(\mathbf{x}-\mathbf{x}')\Big\{2\bar{\eta}_{23}(\mathbf{x})\,\bar{\eta}_{23}(\mathbf{x}') + \bar{\eta}_{22}(\mathbf{x})\,\bar{\eta}_{22}(\mathbf{x}') + \bar{\eta}_{33}(\mathbf{x})\,\bar{\eta}_{33}(\mathbf{x}')$$
$$+ \frac{\nu}{1-\nu}(\eta_{22}+\eta_{33})(\mathbf{x})(\eta_{22}+\eta_{33})(\mathbf{x}')\Big\}$$

$$
\begin{aligned}
&= \frac{1}{2}\Bigg\{ 2\cdot\frac{1}{4}[4v_4(\mathbf{0}) - 2v_4(1,0) - 2v_4(0,1) + 2v_4(1,1) \\
&\qquad + 2v_4(1,1) - 2v_4(1,0) \\
&\qquad - 2v_4(1,0)] \\
&\quad + 2[6v_4(0) - 4v_4(1,0) + 2v_4(2,0) \\
&\qquad - 4v_4(1,0)] \\
&\quad + \frac{\nu}{1-\nu}[14v_4(0) - 4v_4(0,1) + 4v_4(0,2) - 4v_4(2,1) + 2v_4(2,2) \\
&\qquad - 8v_4(0,1) + 8v_4(1,1) - 4v_4(2,1) \\
&\qquad - 8v_4(1,0) + 4v_4(2,0) \\
&\qquad - 4v_4(1,0)]\Bigg\} \\
&= v_4''(1,1) + 2v_4''(2,0) \\
&\quad + \frac{\nu}{1-\nu}[4v_4'(1,1) + 4v_4''(2,0) - 4v_4''(2,1) + v_4''(2,2)] \\
&= 0.183 + \frac{\nu}{1-\nu}\times 0.176
\end{aligned}
\tag{11.82}
$$

and can therefore be neglected.

Note that due to the factor $\frac{1}{2}\times$ half-integer values of the off-diagonal $\bar{\eta}_{ij}(\mathbf{x})$ terms, the importance of the two lowest defect graphs is the reverse of the corresponding stress graphs in the high-temperature expansions. Taking only the lowest contributions, we arrive at a partition function

$$
Z_{\text{def}} = 1 + N6e^{-8\pi^2((1/12)+(2/(1-\nu))\cdot 0.021)} + \ldots, \tag{11.83}
$$

with a free energy

$$
-\beta f_{\text{def}} = 6e^{-8\pi^2\beta((1/12)+(2/(1-\nu))\cdot 021)} + \ldots \tag{11.84}
$$

APPENDIX 11A. CALCULATION OF THE GREEN FUNCTION $v_4 = 1/(\bar{\nabla}\cdot\nabla)^2$

For $D = 2$, two subtractions are required. We first define

$$
v_4'(\mathbf{x}) = v_4(\mathbf{x}) - v_4(\mathbf{0}) \tag{11A.1}
$$

so that the quadratic divergence is gone. Then we remove the remaining logarithmic divergence by forming

$$v_4''(\mathbf{x}) = v_4'(\mathbf{x}) + \frac{\mathbf{x}^2}{4} v_2(\mathbf{0}) = \int \frac{d^2k}{(2\pi)^2} \frac{1}{(\bar{\mathbf{K}}\cdot\mathbf{K})^2} \left(e^{i\mathbf{k}\cdot\mathbf{x}} - 1 + \frac{\mathbf{x}^2}{4} \bar{\mathbf{K}}\cdot\mathbf{K} \right), \quad (11A.2)$$

where

$$v_2(\mathbf{0}) = \int \frac{d^2k}{(2\pi)^2} \frac{1}{\bar{\mathbf{K}}\cdot\mathbf{K}} \quad (11A.3)$$

is the usual unsubtracted and thus divergent lattice Coulomb potential at the origin. This particular subtraction has the advantage that the potential $v_4''(\mathbf{x})$ satisfies the difference equation

$$-\bar{\nabla}\cdot\nabla v_4''(\mathbf{x}) = v_2(\mathbf{x}) - v_2(\mathbf{0}) = v_2'(\mathbf{x}). \quad (11A.4)$$

On a square lattice this implies

$$-4(v_4''(\mathbf{1}) - v_4''(\mathbf{0})) = v_2'(\mathbf{0}) = 0 \quad (11A.5)$$

so that

$$v_4''(\mathbf{1}) = 0. \quad (11A.6)$$

As explained in Chapter 6, Part I [after Eq. (6.192)], the difference equation permits us to calculate all values of $v_4''(\mathbf{x})$ knowing only those along a particular radial direction, for which we shall use the diagonal one $\mathbf{x} = (n, n)$, plus the values of $v_2'(\mathbf{x})$ from Table 6.6, Part I. Along the diagonal, the once subtracted potential can be written [using (I.6.190)] as

$$v_4'(n, n) = -\frac{\partial}{\partial m^2} v_m'(n, n) \Big|_{m=0}$$

$$= -\frac{\partial}{\partial m^2} \frac{1}{4} \int_0^\pi \frac{dp}{\pi} \int_0^\pi \frac{dq}{\pi} \frac{\cos(2np) - 1}{1 - \cos p \cos q + \dfrac{m^2}{4}} \Bigg|_{m=0}$$

$$= \frac{1}{16} \int_0^\pi \frac{dp}{\pi} \int_0^\pi \frac{dq}{\pi} \frac{\cos(2pn) - 1}{(1 - \cos p \cos q)^2}$$

$$= \lim_{\varepsilon \to 0} \frac{1}{16} \int_0^\pi \frac{dp}{\pi} (\cos(2pn) - 1) \frac{1}{\sin^2 p} \left[\frac{1}{\pi} \frac{\cos p \sin q}{1 - \cos p \cos q} \Big|_{q=\varepsilon}^{\pi} + \int_\varepsilon^\pi \frac{dq}{\pi} \frac{1}{1 - \cos p \cos q} \right]. \tag{11A.7}$$

The partial integration in q is necessary since the small q part of the integrand is quite singular in p and easy to miss. In fact for small ε we can write

$$\frac{\cos p \sin q}{1 - \cos p \cos q} \Big|_{q=\varepsilon}^{\pi} = \cos p \frac{2\varepsilon}{p^2 + \varepsilon^2} = \cos p \, 2\pi\delta(p), \tag{11A.8}$$

so that the partially integrated piece contributes to $v_4''(n, n)$ the quadratic term

$$\frac{n^2}{8\pi}.$$

The second piece can now be integrated in q with no subtlety [using (I.6.191)], and we find

$$v_4'(n, n) = \frac{n^2}{8\pi} + \frac{1}{16} \int_0^\pi \frac{dp}{\pi} (\cos(2pn) - 1) \frac{1}{\sin^3 p}.$$

The second subtraction $(\mathbf{x}^2/4) v_2(\mathbf{0})$ brings this to

$$v_4''(n, n) = \frac{n^2}{8\pi} + \frac{1}{16} \int_0^\pi \frac{dp}{\pi} (\cos(2pn) - 1 + 2n^2 \sin^2 p)/\sin^3 p. \tag{11A.9}$$

We now use the well-known formula

$$\cos(2pn) = 1 - \frac{(2n)^2}{2!} \sin^2 p + \frac{(2n)^2((2n)^2 - 2^2)}{4!} \sin^4 p - \frac{(2n)^2((2n)^2 - 2^2)((2n)^2 - 4^2)}{6!} \sin^6 p + \ldots + (-)^n \frac{(2n)^2((2n)^2 - 2^2) \cdots ((2n)^2 - (2n-2)^2)}{(2n)!} \sin^{2n} p \tag{11A.10}$$

and the integrals

$$\int_0^\pi \frac{dp}{\pi} \sin^{2\ell+1} p = \frac{(2\ell)!!}{(2\ell+1)!!} \frac{2}{\pi} \tag{11A.11}$$

to find

$$\begin{aligned} v_4''(n, n) = \frac{n^2}{8\pi} + \frac{1}{8\pi}\Bigg[& \frac{(2n)^2((2n)^2 - 2^2)}{4!} \cdot 1 - \frac{(2n)^2((2n)^2 - 4^2)}{6!} \frac{2}{3} \\ & + \frac{(2n)^2((2n)^2 - 4^2)((2n)^2 - 6^2)}{8!} \frac{8}{15} \\ & - \frac{(2n)^2((2n)^2 - 4^2)((2n)^2 - 6^2)((2n)^2 - 8^2)}{10!} \cdot \frac{16}{35} + \cdots \\ = \frac{1}{8\pi}\Bigg[& n^2 + \sum_{\ell=0}^{n-2} (-)^\ell \frac{(2n)^2((2n)^2-4^2)\cdots((2n)^2-(2\ell+2)^2)}{(2\ell+4)!} \frac{(2\ell)!!}{(2\ell+1)!!}\Bigg]. \end{aligned} \tag{11A.12}$$

The lowest values are

$$v_4''(1, 1) = \frac{1}{8\pi} = 0.039789,$$

$$v_4''(2, 2) = \frac{1}{8\pi}\left(4 + \frac{16(16-4)}{4!}\right) = \frac{3}{2\pi} = 0.477465,$$

$$v_4''(3, 3) = \frac{1}{8\pi}\left(9 + \frac{36(36-4)}{24} - \frac{36(36-4)(36-16)}{720}\frac{2}{3}\right) = \frac{107}{24\pi} = 1.41913,$$

$$v_4''(4, 4) = \frac{46}{5\pi}, \quad v_4''(5, 5) = \frac{4443}{280\pi}. \tag{11A.13}$$

The off-diagonal values can now be obtained from the difference equation (11A.4). For example

$$v_4''(0, 0) + v_4''(2, 0) + v_4''(1, 1) + v_4''(-1, 1) - 4v_4''(1, 0) = -v_2'(1, 0) = \tfrac{1}{4}. \tag{11A.14}$$

Hence

$$v_4''(2, 0) = \frac{1}{4} - \frac{1}{4\pi}. \tag{11A.15}$$

Another example is

$$v_4''(1, 0) + v_4''(2, 1) + v_4''(0, 1) + v_4''(2, -1) - 4v_4''(1, 1) = -v_2'(1, 1) = \frac{1}{\pi} \tag{11A.16}$$

and hence

$$v_4''(2, 1) = \frac{3}{4\pi}. \tag{11A.17}$$

The results are shown in Table 11A.1. Numerically, they can be fitted rather well by the asymptotic form

$$v_4''(\mathbf{x}) \approx \frac{1}{8\pi}\mathbf{x}^2 \log|\mathbf{x}| + A|\mathbf{x}|^2 + B\log|\mathbf{x}| + C, \tag{11A.18}$$

with

$$A = \frac{1}{8\pi}(\gamma - 1 + \log(2\sqrt{2})) \approx 0.02455, \quad \gamma = 0.577216649\ldots,$$

$$B = -\frac{1}{16\pi} \approx -0.01989,$$

$$C = \frac{1}{16\pi}\left(\frac{1}{6} - \gamma - \log(2\sqrt{2})\right) \approx -0.0289, \tag{11A.19}$$

with an error of only 0.5% for $n = 2$ (see Table 11A.2a). More compactly we may write

$$v_4''(\mathbf{x}) \approx \frac{1}{8\pi}|\mathbf{x}|^2 \log(|\mathbf{x}|2\sqrt{2}\, e^{\gamma - 1}) - \frac{1}{16\pi}\log(|\mathbf{x}|2\sqrt{2}\, e^{\gamma - 1/6}). \tag{11A.20}$$

TABLE 11A.1. Exact values of the defect potential on a square lattice:

$$v_4''(\mathbf{x}) = \int\int_{-\pi}^{\pi} \frac{d^2k}{(2\pi)^2}\left(e^{i\mathbf{k}\cdot\mathbf{x}} - 1 + \frac{\mathbf{x}^2}{4}\bar{\mathbf{K}}\cdot\mathbf{K}\right)\frac{1}{(\bar{\mathbf{K}}\cdot\mathbf{K})^2}.$$

x_2 / x_1	0	1	2	3	4	5
5						$\frac{4443}{280\pi}$ 5.0509
4					$\frac{46}{5\pi}$ 2.9285	$\frac{873}{70\pi}$ 3.9698
3				$\frac{107}{24\pi}$ 1.419	$\frac{203}{30\pi}$ 2.1539	$-1+\frac{1567}{120\pi}$ 3.1566
2			$\frac{3}{2\pi}$ 0.4775	$\frac{35}{12\pi}$ 0.9285	$\frac{3}{4}+\frac{11}{4\pi}$ 1.6254	$12-\frac{591}{20\pi}$ 2.5939
1		$\frac{1}{8\pi}$ 0.0398	$\frac{3}{4\pi}$ 0.2387	$-\frac{1}{2}+\frac{29}{8\pi}$ 0.06539	$-6+\frac{23}{\pi}$ 1.3211	$-\frac{99}{2}+\frac{1301}{8\pi}$ 2.2651
0	0	0	$\frac{1}{4}-\frac{1}{4\pi}$ 0.1704	$2-\frac{9}{2\pi}$ 0.5676	$13-\frac{37}{\pi}$ 1.2222	$82-\frac{1505}{6\pi}$ 2.1572

TABLE 11A.2a. Comparison of $v_4''(n, n)$ and the values from the asymptotic formula (11A.19).

n	$v_4''(n, n)$	Eq. (11A.20)	error
1	0.039789	0.04088	3%
2	0.477465	0.4777	0.05%
3	1.41913	1.4192	0.005%
4	2.92845	2.92849	0.001%
5	5.05089	5.05090	0.0002%
10	25.9092	25.9092	
20	125.931	125.931	

The calculation of this asymptotic form is somewhat tedious. Starting out with (11A.9), we rewrite the second term as follows:

$$
\begin{aligned}
&-\frac{1}{4\pi}\int_0^{\pi/2} dp\left(\frac{\sin^2 pn}{\sin^2 p}-n^2\right)\frac{1}{\sin p}\\
&\quad=-\frac{1}{4\pi}\int_0^{\pi/2} dp\left[\sin^2 pn\left(\frac{1}{p^2}+\frac{1}{\sin^2 p}-\frac{1}{p^2}\right)-n^2\right]\left(\frac{1}{p}+\frac{1}{\sin p}-\frac{1}{p}\right)\\
&\quad=-\frac{1}{4\pi}\int_0^{\pi/2} dp\left[\left(\frac{\sin^2 pn}{p^2}-n^2\right)\frac{1}{p}+\left(\frac{\sin^2 pn}{p^2}-n^2\right)\left(\frac{1}{\sin p}-\frac{1}{p}\right)\right.\\
&\qquad\left.+\sin^2 pn\left(\frac{1}{\sin^2 p}-\frac{1}{p^2}\right)\frac{1}{\sin p}\right]\\
&\quad=-\frac{1}{4\pi}\int_0^{\pi/2} dp\left\{\left(\frac{\sin^2 pn}{p^2}-n^2\right)\frac{1}{p}-n^2\left(\frac{1}{\sin p}-\frac{1}{p}\right)\right.\\
&\qquad\left.+\sin^2 pn\left[\frac{1}{\sin^3 p}-\frac{1}{p^3}\right]\right\}. \qquad \text{(11A.21)}
\end{aligned}
$$

In this way the integrand is separated into three pieces, no one piece having a singularity at $p=0$.

The first of these three pieces is now evaluated further as follows:

$$
\begin{aligned}
I_1&=\int_0^{\pi/2} dp\left(\frac{\sin^2 pn}{p^2}-n^2\right)\frac{1}{p}\\
&=-\frac{1}{2}\frac{\sin^2 pn}{p^2}\bigg|_0^{\pi/2}+n\int_0^{\pi/2} dp\left(\frac{\sin pn\cos pn}{p^2}-\frac{n}{p}\right)\\
&=-\frac{2}{\pi^2}\sin^2\frac{\pi}{2}n+\frac{n^2}{2}+n\left[-\frac{1}{2p}\sin(2pn)\bigg|_0^{\pi/2}+n\int_0^{\pi/2} dp\left(\frac{\cos(2pn)}{p}-\frac{1}{p}\right)\right]\\
&=-\frac{1}{\pi^2}(1-(-)^n)+\frac{3}{2}n^2+n^2\int_0^{\pi/2} dp\,\frac{\cos(2pn)-1}{p}. \qquad \text{(11A.22)}
\end{aligned}
$$

The last integral can be rescaled to $\int_0^{\pi n} dp(\cos p-1)/p$ so that I_1 can be expressed in terms of the well-known cosine integral

$$\mathrm{Ci}(z) = \gamma + \log z + \int_0^z dt \frac{\cos t - 1}{t} \tag{11A.23}$$

as

$$I_1 = -\frac{1}{\pi^2}(1 - (-)^n) + \frac{3}{2}n^2 + n^2(\mathrm{Ci}(n\pi) - \gamma - \log(\pi n)) \tag{11A.24}$$

Decomposing $\mathrm{Ci}(z)$ into auxiliary functions[b]

$$\mathrm{Ci}(z) = f(z)\sin z - g(z)\cos z \tag{11A.25}$$

with

$$f(z) = \int_0^\infty dt \frac{e^{-zt}}{t^2 + 1}, \qquad g(z) = \int_0^\infty dt \frac{te^{-zt}}{t^2 + 1}, \tag{11A.26}$$

we find the asymptotic behaviour

$$\mathrm{Ci}(\pi n) = -(-)^n \int_0^\infty dt\, e^{-\pi n t}(t - t^3 + \ldots) = -(-)^n\left(\frac{1}{(\pi n)^2} - \frac{3!}{(\pi n)^4} + \ldots\right) \tag{11A.27}$$

and

$$I_1 = n^2\left(\frac{3}{2} - \gamma - \log(\pi n)\right) - \frac{1}{\pi^2} + O\left(\frac{1}{n^2}\right). \tag{11A.28}$$

The second piece in (11A.21) gives directly

$$I_2 = -n^2 \int_0^{\pi/2} dp \left(\frac{1}{\sin p} - \frac{1}{p}\right) = -n^2\left\{\log\tan\frac{p}{2} - \log\frac{p}{2}\right\}_0^{\pi/2} = n^2 \log\frac{\pi}{4}. \tag{11A.29}$$

[b]See M. Abramowitz and I.A. Stegun, *Handbook of Mathematical Functions* (Dover, New York, 1965) formula 5.29.

The third piece, finally, can be evaluated exactly, after a power series expansion of the square brackets, using

$$\frac{1}{\sin p} = \frac{1}{p} + \frac{p}{6} + \frac{7}{360}p^3 + \frac{31}{15120}p^5 + O(p^7),$$

$$\frac{1}{\sin^\alpha p} = \frac{1}{p^\alpha} + \frac{\alpha}{6p^{\alpha-2}} + \left(\frac{\alpha}{180} + \frac{\alpha^2}{72}\right)\frac{1}{p^{\alpha-4}} + \ldots \qquad \text{(11A.30)}$$

Introducing the quantity

$$r_\alpha(p) \equiv \frac{1}{\sin^\alpha p} - \frac{1}{p^\alpha} - \frac{\alpha}{6p^{\alpha-2}} = \left(\frac{\alpha}{180} + \frac{\alpha^2}{72}\right)p + \ldots$$

we find

$$I_3 = -\frac{1}{2}\int_0^{\pi/2} dp \frac{\cos(2pn) - 1}{2p} - \frac{1}{2}\int_0^{\pi/2} dp\,(\cos(2pn) - 1)r_3(p)$$

$$\xrightarrow[n\to\infty]{} \frac{1}{4}(\gamma + \log(\pi n) - \mathrm{Ci}(\pi n)) + \frac{1}{2}\int_0^{\pi/2} dp\, r_3(p) + \ldots$$

$$= \frac{1}{4}(\gamma + \log(\pi n)) + \frac{R}{2} + O\left(\frac{1}{n^2}\right), \qquad \text{(11A.31)}$$

where the number R is found by integrating of $r_\alpha(p)$ and setting $\alpha \to 3$:

$$R = \frac{1}{2}\left[\frac{4}{\pi^2} - \frac{1}{6} - \log(\pi/4)\right] \approx 0.2401.$$

Collecting the three asymptotic forms of I_1, I_2 and I_3 into (11A.21) and adding $n^2/8\pi$ in (11A.9) we find, indeed, the asymptotic expression (11A.18) [recall that $n = |\mathbf{x}|/\sqrt{2}$ on the digonal]. Note that the term A could have been found right away from the identity $-\bar{\bar{\nabla}}\cdot\nabla v_4''(\mathbf{x}) = v_2'(\mathbf{x})$ and the asymptotic form of $v_2'(\mathbf{x})$ [see (6.196), Part I], which shows that $1 + 8\pi A = \log(2\sqrt{2}e^{\gamma})$.

For completeness, let us also calculate the corresponding twice subtracted potential for a triangular lattice:

$$v_4''(\mathbf{x}) = v_4'(\mathbf{x}) + \frac{\mathbf{x}^2}{4}v_2(\mathbf{0}) = \int \frac{d^2\mathrm{k}^{(i)}}{(2\pi)^2}\left(e^{i\mathbf{k}^{(i)}\cdot\mathbf{x}^{(i)}} - 1 + \frac{\mathbf{x}^2}{2}\bar{\mathbf{K}}\cdot\mathbf{K}\right)\frac{1}{(\bar{\mathbf{K}}\cdot\mathbf{K})^2}, \qquad \text{(11A.32)}$$

where [see Eqs. (6A.104), 16A.60) in Part I]

$$v_4'(\mathbf{x}) = \int \frac{d^2k^{(i)}}{(2\pi)^2}(e^{i\mathbf{k}^{(i)}\cdot\mathbf{x}^{(i)}} - 1)\frac{1}{(\bar{\mathbf{K}}\cdot\mathbf{K})^2}$$

and

$$\bar{\mathbf{K}}\cdot\mathbf{K} = 4 - \tfrac{1}{3}(\cos k^{(1)} + \cos k^{(2)} + \cos(k^{(1)} + k^{(2)})). \quad (11A.33)$$

Analytically, it is easy to find the asymptotic behavior along the line

$$(x^{(1)}, x^{(2)}) = (n, n), \quad (11A.34)$$

i.e., for the Cartesian coordinates

$$(x_1, x_2) = n(1, 0) + n\left(-\frac{1}{2}, \frac{\sqrt{3}}{2}\right) = n\left(\frac{1}{2}, \frac{\sqrt{3}}{2}\right), \quad (11A.35)$$

when $\mathbf{x} = n^2$.

The substitution (6A.61) in Part I leads, for the once subtracted potential, to the integral

$$v_4'(n, n) = \int_0^{2\pi}\frac{dp}{2\pi}\int_0^{\pi}\frac{dq}{\pi}\frac{\cos(2pn) - 1}{[4 - \frac{4}{3}(2\cos p\cos q + \cos(2p))]^2}. \quad (11A.36)$$

We now use the identity

$$\frac{1}{b}\frac{d}{dq}\left(\frac{\cos p\cos q}{a - b\cos p\cos q}\right) = \frac{b\sin^2 p + \dfrac{a^2}{b^2} - 1}{(a - b\cos p\cos q)^2} - \frac{a}{b}\frac{1}{a - b\cos p\cos q}, \quad (11A.37)$$

with $b = 8/3$, $a = 4 - (4/3)\cos(2p)$, to write $(\varepsilon \to 0)$

$$\int_0^{\pi}\frac{dq}{\pi}\frac{1}{[4 - \frac{4}{3}(2\cos p\cos q + \cos(2p))]^2}$$

$$= \frac{1}{8}\frac{1}{\sin^2 p(1+\frac{1}{3}\sin^2 p)}\left\{\frac{1}{\pi}\frac{\cos p \sin q}{4-\frac{4}{3}(2\cos p\cos q+\cos(2p))}\right|_{\varepsilon}^{\pi} + \int_{\varepsilon}^{\pi}\frac{dq}{\pi}\frac{1+\sin^2 p}{4-\frac{4}{3}(2\cos p\cos q+\cos(2p))}\Bigg\}. \tag{11A.38}$$

The partially integrated piece, i.e., the first term on the right-hand side, can again be written as a δ-function, just as in (11A.8),

$$\frac{\sqrt{3}}{8}\frac{\cos p}{p^2+\varepsilon^2/3}\frac{2\varepsilon}{\sqrt{3}} = \frac{\sqrt{3}}{8}\cos p\cdot 2\pi\delta(p). \tag{11A.39}$$

After doing the q integral we arrive at

$$v_4'(n,\, n) = \frac{\sqrt{3}}{4}\left[\frac{n^2}{8\pi}+\frac{1}{16}\int_0^{\pi}\frac{dp}{\pi}[\cos(2pn)-1] \times \frac{1}{\sin^3 p}\frac{1+\sin^2 p}{1+\frac{1}{3}\sin^2 p}\frac{1}{\sqrt{1+\frac{1}{3}\sin^2 p}}\right. . \tag{11A.40}$$

We are now ready to perform the second subtraction. Using Eq. (I.6A.62),

$$v_2(0,\, 0) = \frac{\sqrt{3}}{8}\int_0^{2\pi}\frac{dp}{2\pi}\frac{1}{|\sin p|}\frac{1}{\sqrt{1+\frac{1}{3}\sin^2 p}}, \tag{11A.41}$$

the addition of $(n^2/2)\,v_2(0,\, 0)$ gives

$$v_4''(n,n) = \frac{\sqrt{3}}{4}\left\{\frac{n^2}{8\pi}+\frac{1}{16}\int_0^{\pi}\frac{dp}{\pi}[\cos(2np)-1+2n^2\sin^2 p]\frac{1}{\sin^3 p}\frac{1}{(1+\frac{1}{3}\sin^2 p)^{1/2}} + \frac{1}{16}\int_0^{\pi}\frac{dp}{\pi}[\cos(2np)-1]\frac{1}{\sin p}\frac{2/3}{(1+\frac{1}{3}\sin^2 p)^{3/2}}\right\}. \tag{11A.42}$$

With the aid of the general integral formula

$$\int_0^\pi \frac{dp}{\pi} \frac{\sin^{2\mu-1}p}{(1+z\sin^2 p)^\rho} = \frac{1}{\pi} B(\mu, \tfrac{1}{2}) \frac{1}{(1+z)^\mu} F\left(\rho, \frac{1}{2}+\mu-\rho, \frac{1}{2}+\mu, \frac{z}{1+z}\right), \tag{11A.43}$$

where F is the hypergeometric function and

$$B(x, y) = \frac{\Gamma(x)\Gamma(y)}{\Gamma(x+y)};$$

we have for $\mu = 1$, $\rho = \dfrac{3}{2}$

$$\int_0^\pi \frac{dp}{\pi} \frac{\sin p}{(1+\frac{1}{3}\sin^2 p)^{3/2}} = \frac{1}{\pi}\frac{3}{2} \tag{11A.44}$$

and can rewrite (11A.42) as

$$v_4''(n, n) = \frac{\sqrt{3}}{4}\left\{\frac{1}{16}\int_0^\pi \frac{dp}{\pi}[\cos(2np) - 1 + 2n^2\sin^2 p]\frac{1}{\sin^3 p}\frac{1+\sin^2 p}{(1+\frac{1}{3}\sin^2 p)^{3/2}}\right\}. \tag{11A.45}$$

The expression in curly brackets can be treated in the same manner as that for the square lattice case, Eq. (11A.9), and we find, evaluating the integrals via (11A.43) and the hypergeometric functions as explained in Part I, Appendix 6A [in the context of $v_2'(x)$] the values shown in Table 11A.2 a [Kleinert (1988)]. In the limit of large n, we regroup the curly brackets as

$$-\frac{1}{4\pi}\int_0^{\pi/2} dp\left(\frac{\sin^2 pn}{\sin^2 p} - n^2\right)\frac{1}{\sin p}\frac{1+\sin^2 p}{(1+\frac{1}{3}\sin^2 p)^{3/2}} = -\frac{1}{4\pi}(I_1 + \tilde{I}_2 + \tilde{I}_3), \tag{11A.46}$$

with

$$\begin{aligned} I_1 &= \int_0^{\pi/2} dp\left(\frac{\sin^2 pn}{p^2} - n^2\right)\frac{1}{p}, \\ \tilde{I}_2 &= -n^2\int_0^{\pi/2} dp\left(\frac{1}{s\cdot\sin p} - \frac{1}{p}\right), \\ \tilde{I}_3 &= -\frac{1}{2}\int_0^{\pi/2} dp\,[\cos(2np) - 1] \end{aligned} \tag{11A.47}$$

where $\tilde{I}_2$, $\tilde{I}_3$ differ from the previous integrals defined in Eq. (11A.21) by the factor

$$\frac{1}{s} = \frac{1 + \sin^2 p}{(1 + \frac{1}{3}\sin^2 p)^{3/2}}. \tag{11A.48}$$

The limiting form of I_1 is known from (11A.28), i.e.,

$$I_1 \to n^2\left(\frac{3}{2} - \gamma - \log(\pi n)\right) - \frac{1}{\pi^2} + O\left(\frac{1}{n^2}\right). \tag{11A.49}$$

The integral $\tilde{I}_2$ is calculated by rewriting it as follows:

$$\begin{aligned}
&\int_0^{\pi/2} dp \left[\frac{1 + \sin^2 p}{(1 + \frac{1}{3}\sin^2 p)^{3/2}} \frac{1}{\sin p} - \frac{1}{p}\right] \\
&= \int_0^{\pi/2} dp \left[\frac{\sin^{-1} p}{(1 + \frac{1}{3}\sin^2 p)^{1/2}} - \frac{1}{p} + \frac{2}{3}\frac{\sin p}{(1 + \frac{1}{3}\sin^2 p)^{3/2}}\right] \\
&= \lim_{\mu \to 0} \int_0^{\pi/2} dp \left[\frac{\sin^{2\mu - 1} p}{(1 + \frac{1}{3}\sin^2 p)^{1/2}} - p^{2\mu - 1}\right] + \frac{2}{3}\int_0^{\pi/2} dp \frac{\sin^{2\mu - 1}}{(1 + \frac{1}{3}\sin^2 p)^{\mu + (1/2)}}.
\end{aligned} \tag{11A.50}$$

Using formula (11A.43), this may be cast as

$$\lim_{\mu \to 0}\left[\frac{1}{2}\frac{B(\mu, \frac{1}{2})}{(1 + \frac{1}{3})^{\mu}} - \frac{1}{2\mu}\left(\frac{\pi}{2}\right)^{2\mu}\right] + \frac{2}{3}\frac{1}{2}\frac{B(1, \frac{1}{2})}{(1 + \frac{1}{3})^1} = -\log\frac{\pi}{2\sqrt{3}} + \frac{1}{2}. \tag{11A.51}$$

Hence

$$\tilde{I}_2 \to -n^2\left(-\log\frac{\pi}{2\sqrt{3}} + \frac{1}{2}\right). \tag{11A.52}$$

In the last integral we observe that for small p, the expression within square brackets in (11A.47) has the expansion

$$\left[\frac{1}{s\sin^3 p} - \frac{1}{p^3}\right] = \frac{1}{p} - \frac{1}{15}p + \frac{68}{315}p^3 + \ldots \tag{11A.53}$$

We may therefore write

$$\bar{I}_3 = -\frac{1}{2}\int_0^{\pi/2} dp\,[\cos(2np) - 1]\left(\frac{1}{p} + \bar{r}_3\right), \tag{11A.54}$$

with $[s_0 \equiv \sqrt{1 + \frac{1}{3}\sin^2 p}]$

$$\bar{r}_\alpha = \frac{1}{\sin^\alpha p}\frac{1}{s_0^{4-\alpha}} + \frac{2}{3}\frac{1}{\sin^{\alpha-2} p}\frac{1}{s_0^{6-\alpha}} - \frac{1}{p^\alpha} - \frac{\alpha}{3p^{\alpha-2}}. \tag{11A.55}$$

Proceeding as in (11A.31) this gives the limit

$$\bar{I}_3 \to \frac{1}{2}(\gamma + \cos(\pi n)) + \frac{\bar{R}}{2}, \tag{11A.56}$$

where

$$\bar{R} = \int_0^{\pi/2} dp\,\bar{r}_3 = \frac{2}{\pi} + \log(2\sqrt{3}/\pi) - \frac{1}{6} \approx 0.1337, \tag{11A.57}$$

this number being obtained by integration of $\bar{r}_\alpha$ using (11A.43).

Collecting all terms we arrive at

$$\begin{aligned} v_4''(n, n) &= \frac{\sqrt{3}}{4}\left(-\frac{1}{4\pi}\right)\left\{n^2\left(\frac{3}{2} - \gamma - \log(\pi n)\right) - \frac{1}{\pi^2}\right. \\ &\quad \left. - n^2\left(-\log\frac{\pi}{2\sqrt{3}} + \frac{1}{2}\right) + \frac{1}{2}(\gamma + \log(\pi n)) + \frac{\bar{R}}{2} + \ldots\right\} \\ &= \frac{\sqrt{3}}{2}\left\{\frac{1}{8\pi}|\mathbf{x}|^2 \log|\mathbf{x}| + A|\mathbf{x}|^2 + B\log|\mathbf{x}| + C\right\} + \ldots, \end{aligned} \tag{11A.58}$$

with

$$\begin{aligned} A &= \frac{1}{8\pi}[\gamma - 1 + \log(2\sqrt{3})] \approx 0.0326135, \\ B &= -\frac{1}{16\pi} \approx -0.0198944, \\ C &= \frac{1}{2}\frac{1}{4\pi}\left[\frac{1}{\pi^2} - \frac{1}{2}(\gamma + \log\pi) - \frac{\bar{R}}{2}\right] \approx -0.0329. \end{aligned} \tag{11A.59}$$

We may therefore write more compactly

$$v_4''(\mathbf{x}) = \frac{\sqrt{3}}{2}\frac{1}{8\pi}\left[|\mathbf{x}|^2 \log(|\mathbf{x}|2\sqrt{3}e^{\gamma-1}) - \frac{1}{2}\log(|\mathbf{x}|2\sqrt{3}e^{\gamma-1/6})\right]. \tag{11A.60}$$

The $|\mathbf{x}|^2$ term could have been found directly from the asymptotic behavior (I.6A.70) of the Coulomb potential on the triangular lattice, using the identity

$$-\bar{\nabla}\cdot\nabla v_4''(\mathbf{x}) = v_2'(\mathbf{x}) \to -\frac{1}{2\pi}\log(|\mathbf{x}|2\sqrt{3}e^{\gamma}). \tag{11A.61}$$

In Table 11A.2b we have listed the values of $v_4''(\mathbf{x})$ obtained by numerically integrating the original formula (11A.32). Except for $(x^{(1)}, x^{(2)}) = (0, 0)$ and $(1, 0)$, where $v_4''(\mathbf{x})$ vanishes, it is possible to use the asymptotic formula (11A.58) with $|\mathbf{x}| = \sqrt{x^{(1)2} + x^{(2)2} - x^{(1)}x^{(2)}}$. The error is smaller than 3% at $(x, y) = (1, 1)$, smaller than 0.5% at $(x, y) = (2, 0)$, and decreases so rapidly for larger distances that all other values on Table 11A.2 can be taken directly from the asymptotic formula.

In three dimensions, only one subtraction is necessary to render $v_4(\mathbf{x})$ finite. We therefore calculate

$$\begin{aligned} v_4'(\mathbf{x}) &= \int \frac{d^3k}{(2\pi)^3}\frac{1}{(\bar{\mathbf{K}}\cdot\mathbf{K})^2}(e^{i\mathbf{k}\cdot\mathbf{x}} - 1) \\ &= \int_0^\infty ds\, e^{-6s} s(I_{x_1}(2s)I_{x_2}(2s)I_{x_3}(2s) - I_0^3(2s)). \end{aligned} \tag{11A.62}$$

A further subtraction of $-(\mathbf{x}^2/6)v_2(\mathbf{0})$ makes the integration even more regular but does not change the interaction energy (due to the moment neutrality of the defect tensor $\bar{\eta}_{ij}$):

$$\begin{aligned} v_4''(\mathbf{x}) \equiv v_4'(\mathbf{x}) + \frac{\mathbf{x}^2}{6}v_2(\mathbf{0}) &= \int \frac{d^3k}{(2\pi)^3}\frac{1}{(\bar{\mathbf{K}}\cdot\mathbf{K})^2}\left(e^{i\mathbf{k}\cdot\mathbf{x}} - 1 + \frac{\mathbf{x}^2}{6}\bar{\mathbf{K}}\cdot\mathbf{K}\right) \\ &= \int_0^\infty ds\, e^{-6s}\left[s(I_{x_1}(2s)I_{x_2}(2s)I_{x_3}(2s) - I_0^3(2s)) + \frac{\mathbf{x}^2}{6}I_0^3(2s)\right]. \end{aligned} \tag{11A.63}$$

In order to estimate the asymptotic behavior we rewrite the integral as

TABLE 11A.2b. Exact values of the twice subtracted Green function $v''_4(\mathbf{x})$ on a triangular lattice, Eq. (11A.32), at $\mathbf{x} = x^{(1)}(1, 0) + x^{(2)}(-1/2, \sqrt{3}/2)$.

(1) x	(2) $-x$	$v''_4(\mathbf{x})$	
0	2	$-9/8\sqrt{3}\pi + 3/8$	0.16825166
0	3	$-135/4\sqrt{3}\pi + 27/4$	0.54754992
0	4	$-1179/2\sqrt{3}\pi + 219/2$	1.16387204
0	5	$-37485/4\sqrt{3}\pi + 6897/4$	2.03636292
0	6	$-1156545/8\sqrt{3}\pi + 212571/8$	3.18011018
0	7	$-21924693/10\sqrt{3}\pi + 805857/2$	4.60752827
1	1	$9/16\sqrt{3}\pi$	0.10337416
1	2	$99/16\sqrt{3}\pi - 3/4$	0.38711584
1	3	$855/8\sqrt{3}\pi - 75/4$	0.89109189
1	4	$15057/8\sqrt{3}\pi - 1377/4$	1.63996576
1	5	$497727/16\sqrt{3}\pi - 22857/4$	2.65160690
1	6	$7882317/16\sqrt{3}\pi - 181065/2$	3.94010363
1	7	$151976727/20\sqrt{3}\pi - 2792961/2$	5.51711215
2	2	$-63/8\sqrt{3}\pi + 9/4$	0.80276164
2	3	$-2943/16\sqrt{3}\pi + 141/4$	1.44664709
2	4	$-34587/8\sqrt{3}\pi + 6375/8$	2.34114558
2	5	$-6360993/80\sqrt{3}\pi + 14616$	3.50314801
2	6	$-53935857/40\sqrt{3}\pi + 991233/4$	4.94613801
2	7	$-12213532197/560\sqrt{3}\pi + 8016291/2$	6.68132708
3	3	$10773/16\sqrt{3}\pi - 243/2$	2.23887896
3	4	$314793/40\sqrt{3}\pi - 1443$	3.28730813
3	5	$1721637/10\sqrt{3}\pi - 31635$	4.60751757
3	6	$352958985/112\sqrt{3}\pi - 579150$	6.21228942
3	7	$30357003429/560\sqrt{3}\pi - 39849237/4$	8.11239650
4	4	$-57249/2\sqrt{3}\pi + 5265$	4.49534433
4	5	$-85404951/280\sqrt{3}\pi + 56061$	5.97940668
4	6	$-1844444781/280\sqrt{3}\pi + 9684783/8$	7.75145807
4	7	$-6743261619/56\sqrt{3}\pi + 88518015/4$	9.82176526
5	5	$91744641/80\sqrt{3}\pi - 421497/2$	7.63159749
5	6	$6448242303/560\sqrt{3}\pi - 8464491/4$	9.57519348
5	7	$68991690141/280\sqrt{3}\pi - 181129059/4$	11.81990484
6	6	$-2468615697/56\sqrt{3}\pi + 32405265/4$	11.69376245
6	7	$-2628329362353/6160\sqrt{3}\pi + 313652421/4$	14.11630181
7	7	$185200539543/112\sqrt{3}\pi - 303888105$	16.71953008

$$v_4'(\mathbf{x}) = \int_{\mathbf{k}^2<\Lambda^2} \frac{d^3k}{(2\pi)^3} \frac{1}{(\mathbf{k}^2)^2} (e^{i\mathbf{k}\cdot\mathbf{x}} - 1)$$
$$- \left[\int_{-\pi}^{\pi} \frac{d^3k}{(2\pi)^3} - \int_{\mathbf{k}^2<\Lambda^2} \frac{d^3k}{(2\pi)^3} \right] \frac{1}{(\mathbf{k}^2)^2} (e^{i\mathbf{k}\cdot\mathbf{x}} - 1)$$
$$+ \int_{-\pi}^{\pi} \frac{d^3k}{(2\pi)^3} \left[\frac{1}{(\bar{\mathbf{K}}\cdot\mathbf{K})^2} - \frac{1}{(\mathbf{k}^2)^2} \right] (e^{i\mathbf{k}\cdot\mathbf{x}} - 1). \qquad (11A.64)$$

For $\Lambda \to \infty$, the first integral was calculated in (1.88) and gave

$$-\frac{|\mathbf{x}|}{8\pi}. \qquad (11A.65)$$

The second and third integrals are regular at the origin so that the limit $|\mathbf{x}| \to \infty$ gives the additional constant

$$c \equiv c_1 + c_2$$
$$= -\left[\int_{-\pi}^{\pi} \frac{d^3k}{(2\pi)^3} - \int_{-\infty}^{\infty} \frac{d^3k}{(2\pi)^3} \right] \frac{1}{(\mathbf{k}^2)^2} - \int_{-\pi}^{\pi} \frac{d^3k}{(2\pi)^3} \left[\frac{1}{(\bar{\mathbf{K}}\cdot\mathbf{K})^2} - \frac{1}{(\mathbf{k}^2)^2} \right]. \qquad (11A.66)$$

The first integral lies outside the cubic region $|k_i| < \pi$. We may approximate this region with a sphere whose volume is $(2\pi)^3$, i.e., of radius $k_0 = (6\pi^2)^{-1/3}$,

$$c_1 \approx \int_{|k|>k_0} \frac{d^3k}{(2\pi)^3} \frac{1}{(\mathbf{k}^2)^2} = \frac{4\pi}{(2\pi)^3} \int \frac{dk}{k^2} = \frac{1}{2\pi^2} \frac{1}{k_0} \approx 0.013. \qquad (11A.67)$$

More accurately, we may do the integral outside the sphere $|\mathbf{k}| = \pi$ exactly obtaining

$$c_1^{(1)} = \frac{1}{2\pi^3} \approx 0.0161,$$

and subtract the numerical integral over the volume between the sphere and the cube $|k_i| = \pi$, for which we find

$$c_1^{(2)} \approx 0.0027.$$

TABLE 11A.3. Numerical values of the twice subtracted potential between three-dimensional disclinations and comparison with the asymptotic form (11A.71).

x_1	x_2	x_3	$v_4'(\mathbf{x})$	$v_4''(\mathbf{x})_{as}$	x_1	x_2	x_3	$v_4'(\mathbf{x})$	$v_4''(\mathbf{x})_{as}$
0	0	0	0.000	−0.011	1	2	3	0.431	0.430
0	0	1	0.000	−0.009	1	2	4	0.692	0.691
0	0	2	0.082	0.078	1	2	5	1.035	1.035
0	0	3	0.251	0.249	1	3	3	0.616	0.616
0	0	4	0.505	0.504	1	3	4	0.882	0.881
0	0	5	0.844	0.843	1	3	5	1.228	1.228
0	1	1	0.021	0.017	1	4	4	1.151	1.150
0	1	2	0.113	0.111	1	4	5	1.500	1.500
0	1	3	0.286	0.284	1	5	5	1.853	1.853
0	1	4	0.542	0.541	2	2	2	0.357	0.357
0	1	5	0.882	0.881	2	2	3	0.542	0.541
0	2	2	0.215	0.213	2	2	4	0.805	0.805
0	2	3	0.394	0.393	2	2	5	1.151	1.150
0	2	4	0.654	0.653	2	3	3	0.729	0.729
0	2	5	0.997	0.996	2	3	4	0.996	0.996
0	3	3	0.579	0.578	2	3	5	1.344	1.344
0	3	4	0.843	0.843	2	4	4	1.267	1.267
0	3	5	1.189	1.189	2	4	5	1.618	1.618
0	4	4	1.112	1.112	2	5	5	1.971	1.971
0	4	5	1.461	1.461	3	3	3	0.920	0.920
0	5	5	1.814	1.814	3	3	4	1.189	1.190
1	1	1	0.049	0.046	3	3	5	1.539	1.539
1	1	2	0.146	0.144	3	4	4	1.461	1.461
1	1	3	0.322	0.320	3	4	5	1.814	1.814
1	1	4	0.579	0.578	3	5	5	2.168	2.169
1	1	5	0.920	0.920	4	4	4	1.735	1.735
1	2	2	0.250	0.249	4	4	5	2.089	2.090

It follows that

$$c_1 = c_1^{(1)} - c_1^{(2)} \approx 0.0134, \tag{11A.68}$$

close to (11A.66). For c_2, a numerical evaluation gives

$$c_2 \approx -0.0246. \tag{11A.69}$$

Hence we find

$$c = c_1 + c_2 \approx -0.011. \tag{11A.70}$$

The values of $v_4''(\mathbf{x})$ are found by numerical integration of (11A.62) and are shown in Table 11A.3. They are fitted optimally by the asymptotic formula

$$v_4''(\mathbf{x}) \to -\frac{|\mathbf{x}|}{8\pi} + \frac{\mathbf{x}^2}{6} v_2(\mathbf{0}) - 0.011, \tag{11A.71}$$

[with $v_2(\mathbf{0}) \approx 0.252731$] whose values are also listed in the same table.

NOTES AND REFERENCES

The lattice Green functions $-(\nabla \cdot \nabla)^{-1}$, $(\nabla \cdot \nabla)^{-2}$ on a triangular lattice and their asymptotic limits are calculated in
H. Kleinert, Berlin preprint (1988).
An asymptotic limit has also been given in
D. Nelson, *Phys. Rev.* **B26** (1982) 269.
but this is incorrect. The error has been repeated by
K. Strandburg *et al.* (see the papers quoted in the next chapter, and the discussion in Section 14.11).

CHAPTER TWELVE

THE MELTING TRANSITION IN THE DEFECT MODEL

Let us now study the properties of the defect model and see whether it properly describes the phase transition of melting. We shall first consider the leading approximations at high and low temperatures, thereby obtaining crude estimates for the location and type of the transition. Then we shall proceed and calculate the corrections due to stress and defect graphs (which, in three dimensions, will be found to produce amazingly small effects).

12.1. LOWEST ORDER RESULTS FOR $D = 2$

For two dimensions and isotropic materials, the free energy in the high-temperature limit is given by the first two terms in (11.38)

$$-\beta f^{T\to\infty} = -\frac{3}{2}\log(2\pi\beta) - \frac{1}{2}\log\left[4\left(1+\frac{\lambda}{\mu}\right)\right] = -\frac{3}{2}\log(2\pi\beta) - \frac{1}{2}\log\left[4\frac{1+\nu}{1-\nu}\right]. \tag{12.1}$$

The low temperature limit, on the other hand, is given by the pure phonon fluctuations (11.53) and reads

$$-\beta f^{T\to 0} = -\log(2\pi\beta) - \frac{1}{2}\log\left(2 + \frac{\lambda}{\mu}\right) - 1.16625$$

$$= -\log(2\pi\beta) - \frac{1}{2}\log\left(\frac{2}{1-\nu}\right) - 1.16625. \tag{12.2}$$

The two curves intersect at

$$\beta^0_{\text{melt}}(1+\nu) = \frac{1}{4\pi}e^{2.116625} = 0.820. \tag{12.3}$$

To lowest approximation, this determines the melting point. The Lindemann number associated with this point is [recall (7.5a), (9.22)]

$$\tilde{L} = \sqrt{\frac{\mu a^2}{k_B T_{\text{melt}}}} = 2\pi\sqrt{\frac{\mu a^3}{k_B T_{\text{melt}}(2\pi)^2}} = 2\pi\sqrt{\beta^0_{\text{melt}}} = 5.6893\frac{1}{\sqrt{1+\nu}}. \tag{12.4}$$

In the anisotropic case we have, to lowest order [see (11.38) and (11.73)]

$$-\beta f^{T\to\infty} = -\frac{3}{2}\log(2\pi\beta) - \frac{1}{2}\log\left(4\xi^2\left(1 + \frac{\lambda}{\xi\mu}\right)\right),$$

$$-\beta f^{T\to 0} = -\log(2\pi\beta) - \frac{1}{2}\log 2 - \ell.$$

The intersection gives

$$\beta^0_{\text{melt}}\,\xi = \frac{1}{4\pi\xi}\left(1 + \frac{\lambda}{\xi\mu}\right)e^{2\ell}.$$

Using Table 9.1 for the logarithm of the anisotropic fluctuation determinant ℓ we calculate melting points for $\lambda = 0$ listed in Table 12.1.

The internal energy and entropy and given by

$$u = -\frac{\partial}{\partial\beta}(-\beta f) = \begin{cases} \dfrac{3}{2\beta} \\ \dfrac{1}{\beta} \end{cases} \quad \text{for} \quad \begin{cases} T > T_{\text{melt}}, \\ T < T_{\text{melt}}, \end{cases} \tag{12.5}$$

$$s = \left(1 - \beta\frac{\partial}{\partial\beta}\right)(-\beta f) = -\beta f + \begin{cases} \frac{3}{2} & \text{for} \quad \begin{cases} T > T_{\text{melt}}, \\ T < T_{\text{melt}}, \end{cases} \\ 1 \end{cases} \tag{12.6}$$

in the hot phase and cold phase, respectively. This corresponds to a first order phase transition with a transition entropy per site of

$$\Delta s = \tfrac{1}{2}. \tag{12.7}$$

The specific heat of the model is given by

$$c_v = -\beta^2\frac{\partial}{\partial\beta}u = \begin{cases} \frac{3}{2} & \text{for} \quad \begin{cases} T > T_{\text{melt}}, \\ T < T_{\text{melt}}. \end{cases} \\ 1 \end{cases} \tag{12.8}$$

This is only the potential part. The kinetic part would add another $2 \cdot 1/2$.

Note that to this approximation, the internal energy, the entropy jump, and the specific heat are universal functions of β. They are independent of the elastic constants ξ and λ. As a consequence, the entropy jump Δs is also universal, to this approximation.

12.2. LOWEST ORDER RESULTS FOR $D = 3$

For three dimensions and isotropic materials, the high temperature limit is given by (11.41) for $\xi = 1$,

$$\begin{aligned} -\beta f^{T\to\infty} &= -3\log(2\pi\beta) - \frac{1}{2}\log\left(8\left(1 + \frac{3\lambda}{2\mu}\right)\right) \\ &= -3\log(2\pi\beta) - \frac{1}{2}\log\left(8\left(\frac{1+\nu}{1-2\nu}\right)\right). \end{aligned} \tag{12.9}$$

The low-temperature limit was calculated in (11.53) and found to be

$$\begin{aligned} -\beta f^{T\to 0} &= -\frac{3}{2}\log(2\pi\beta) - \frac{1}{2}\log\left(2 + \frac{\lambda}{\mu}\right) - \frac{3}{2}\cdot 1.67339 \\ &= -\frac{3}{2}\log(2\pi\beta) - \frac{1}{2}\log\left(2\frac{1-\nu}{1-2\nu}\right) - \frac{3}{2}\cdot 1.67339. \end{aligned} \tag{12.10}$$

These curves intersect at

$$\beta^0_{\text{melt}}\left(\frac{1+\nu}{1-\nu}\right)^{1/3} = \frac{1}{2\pi}\frac{1}{4^{1/3}}e^{1.67339} = 0.534, \tag{12.11}$$

which leads to a Lindemann number

$$\tilde{L} = 2\pi\sqrt{\beta^0_{\text{melt}}} = 4.593.$$

According to (7.41), this corresponds to

$$L \sim 105, \tag{12.12}$$

for $\nu \approx 0$, which lies at the lower end of the range of experimental numbers (100–200).

In the anisotropic case we have [see (11.41) and (11.73)]

$$-\beta f^{T\to\infty} = -3\log(2\pi\beta) - \frac{1}{2}\log\left(8\xi^3\left(1+\frac{3\lambda}{2\xi\mu}\right)\right),$$

$$-\beta f^{T\to 0} = -\frac{3}{2}\log(2\pi\beta) - \frac{1}{2}\log 2 - \frac{3}{2}\log\ell,$$

and find the zeroth-order melting point

$$\beta^0_{\text{melt}}\,\xi = \frac{1}{2\pi}\frac{1}{4^{1/3}}\frac{1}{\left(1+\frac{3\lambda}{2\xi\mu}\right)^{1/3}}e^{\ell}. \tag{12.13}$$

Using ℓ from Table 9.1 this gives the values listed for $\lambda = 0$ in Table 12.1.

The internal energy and entropy and obtained from

$$u = -\frac{\partial}{\partial\beta}(-\beta f) = \begin{cases} \dfrac{3}{\beta} \\ \dfrac{3}{2\beta} \end{cases} \text{ for } \begin{cases} T > T_{\text{melt}}, \\ T < T_{\text{melt}}, \end{cases} \tag{12.14}$$

$$s = \left(1-\beta\frac{\partial}{\partial\beta}\right)(-\beta f) = -\beta f + \begin{cases} 3 \\ \frac{3}{2} \end{cases} \text{ for } \begin{cases} T > T_{\text{melt}}, \\ T < T_{\text{melt}}. \end{cases} \tag{12.15}$$

This corresponds to a first-order phase transition with a transition entropy of

$$\Delta s = \tfrac{3}{2}. \tag{12.16}$$

Similarly the specific heat is

$$c = -\beta^2 \frac{\partial}{\partial \beta} u = \begin{cases} 3 & \text{for } \begin{cases} T > T_{\text{melt}}, \\ T < T_{\text{melt}}. \end{cases} \\ \frac{3}{2} \end{cases} \tag{12.17}$$

As in the two-dimensional case, the internal energy, specific heat and entropy jump are all independent of the elastic constants ξ and λ at this level of approximation.

The alert reader might rightfully object to the present approximation procedure. After all, by extrapolating high and low-temperature limits of the free energy into the opposite regimes where they do not apply and bringing them to intersection one will always find a first-order phase transition which, in general, lies at the wrong place. The pleasant property of our model, however, is that it is possible to calculate the corrections to this lowest approximation and show that they come out to be small for $D = 2$ and extremely small for $D = 3$, as we shall now see.

12.3. STRESS AND DEFECT CORRECTIONS IN ISOTROPIC MATERIALS

We will first restrict ourselves to the leading correction.

THE TWO-DIMENSIONAL CASE

In two dimensions at high temperatures, the additional energy for an isotropic crystal was given in (11.21) to be*

$$-\beta f_{\text{stress}} = 2e^{-(1/\beta)[5 - 5(\lambda/2\mu)(1/(1+\lambda/\mu))]} = 2e^{-(1/\beta)[5 - 5\nu/(1+\nu)]} \tag{12.18}$$

For low temperatures, the first defect corrections are, from (11.53),

$$-\beta f_{\text{def}} = 2e^{-2\pi\beta(1+\nu)}. \tag{12.19}$$

Near the melting point $\beta^{(0)}_{\text{melt}}$ of (12.3) (calculated to lowest order) both corrections are very small. Hence, we find the corrected melting

*Recall that in general $\frac{\lambda}{\mu} \frac{1}{D\lambda/\mu + 2\xi} = \xi/\gamma = \nu/(1+\nu)$.

temperature by using the values of (12.18) and (12.19) at $\beta^0_{\rm melt}$. For $\nu = 0$, they are

$$-\beta f_{\rm stress}|_{\beta^0_{\rm melt}} \approx 2e^{-(5/\beta^0_{\rm melt})} \sim 0.00449,$$
$$-\beta f_{\rm def}|_{\beta^0_{\rm melt}} \approx 2e^{-2\pi\beta^0_{\rm melt}} \sim 0.01158. \tag{12.20}$$

This leads to the corrected $\nu = 0$ equation

$$\tfrac{1}{2}\log(4\pi\beta) - 1.16625 - \beta f_{\rm def}|_{\beta^0_{\rm melt}} + \beta f_{\rm stress}|_{\beta^0_{\rm melt}} = 0, \tag{12.21}$$

or

$$\beta^1_{\rm melt} = \beta^0_{\rm melt}\, e^{-2(0.01158 - 0.00449)} = \beta^0_{\rm melt}(1 - 0.014) \approx 0.808.$$

This is to be compared with the value found by Monte Carlo simulations on a 60×60 lattice to be described further down (see Table 12.1):

$$\beta^{\rm MC}_{\rm melt} \approx 0.815.$$

Curiously, the zeroth order value (12.11) is better than the first corrected one. In fact we have to carry out the first four corrections in order to obtain a perfect agreement. The corrections to the anisotropic values can be found in the same way (see Table below).

TABLE 12.1. The intersection $\beta^{(n)}_m$ of high and low temperature expansions of the free energy for the $D = 2$ melting model (Villain type, $\lambda = 0$) including n corrections on both sides (see Fig. 12.1). The Monte Carlo data at the last column are from Janke and Kleinert (1985).

ξ	$\beta^0_m\xi$	$\beta^1_m\xi$	$\beta^4_m\xi$	$\beta^{\rm MC}_m$	β^0_m	β^1_m	β^4_m	Δs^0	Δs^1	$\Delta s^{\rm MC}$
0.2	0.601	0.602	0.608		3.004	3.008	3.039	0.5	0.358	
0.4	0.658	0.655	0.662		1.645	1.639	1.656	0.5	0.353	
0.6	0.713	0.707	0.715		1.189	1.179	1.191	0.5	0.347	
0.8	0.767	0.757	0.766		0.959	0.947	0.957	0.5	0.343	
1.0	0.820	0.806	0.814	0.818	0.820	0.806	0.814	0.5	0.339	0.28
1.2	0.871	0.853	0.862		0.726	0.711	0.718	0.5	0.335	
1.4	0.923	0.900	0.907		0.659	0.643	0.648	0.5	0.333	
1.6	0.973	0.946	0.952		0.608	0.591	0.595	0.5	0.330	

TABLE 12.2. Transition parameters of the $D = 3$ melting model (Villain type) as obtained from Figs. 12.6, for $\lambda = 0$ and various values of ξ, in comparison with Monte Carlo Data from Janke and Kleinert (1985).

ξ	$\beta^0\xi$	$\beta_m^0\xi$	β_m^0	β_m^1	β_m^{MC}	Δs^0	Δs^1	Δs^{MC}
0.2	0.283		1.42		1.400 ± 0.100	1.50		
0.4	0.360		0.900		0.8880 ± 0.015	1.50		
0.6	0.422		0.703		0.6875 ± 0.0025	1.50		
0.8	0.482		0.503		0.5875 ± 0.0025	1.50		
1.0	0.537	0.525	0.537	0.525	0.5175 ± 0.0025	1.50	1.33	1.2
1.2	0.590		0.492		0.4690 ± 0.0075	1.50		

THE THREE-DIMENSIONAL CASE

In three dimensions, the additional stress energy in isotropic systems with $\nu = 0$ is, according to (11.45),

$$-\beta f_{\text{stress}}|_{\beta_{\text{melt}}^0} = 6e^{-5/\beta_{\text{melt}}^0}. \tag{12.22}$$

The exponent has the same form as it had in two dimensions. The leading defect correction, on the other hand, becomes, due to (11.84),

$$-\beta f_{\text{def}}|_{\beta_{\text{melt}}^0} = 6e^{-\pi^2(2/3)\beta_{\text{melt}}^0(1 + 24\cdot 0.02106)}. \tag{12.23}$$

At the lowest order transition point, $\beta_{\text{melt}}^0 \sim 0.5344$ these have the values

$$-\beta f_{\text{stress}} \sim 0.0005, \qquad -\beta f_{\text{def}} \sim 0.0302, \tag{12.24}$$

leading to an extremely small correction

$$\begin{aligned}\beta_{\text{melt}}^1 &= \beta_{\text{melt}}^0 e^{-(2/3)(-\beta f_{\text{def}} + \beta f_{\text{stress}})} \\ &= \beta_{\text{melt}}^0 (1 - \tfrac{2}{3}0.0304) = 0.524.\end{aligned} \tag{12.25a}$$

This is in excellent agreement with the Monte Carlo value obtained on a 16^3 lattice as described below (see Table 12.2)

$$\beta_{\text{melt}}^{MC} \approx 0.5175 \pm 0.0025. \tag{12.25b}$$

The fluctuations are so small that the position of the strong first-order transition, shown by the model to lowest order, is modified only very slightly by higher corrections.

12.4. ANISOTROPIC CUBIC MATERIALS

For general cubic materials with $\lambda = 0$ the free energies with stress and defect corrections are plotted in Fig. 12.1 for $D = 3$ and in Fig. 12.2 for $D = 2$. In the first case we have not distinguished the zeroth and first orders on the high temperature side since the differences are too small to show up. On the low temperature side, they are visible and are given by the dotted curve for $\xi = 1$. We have not calculated the low temperature correction in the anisotropic case $\xi \neq 1$, due to the complexity of the anisotropic defect interactions. [See Eq. (9.104).] From these figures we extract the critical temperatures as listed in Tables 12.1, 12.2.

From the three-dimensional isotropic value of β_m ($\beta_m \approx 0.525$) we can calculate the Lindemann parameter of the model. Recalling relation (7.40) we find for isotropic systems

$$L \approx 22.8 \sqrt{\frac{\mu a^3}{k_B T_m}} \left[1 - \frac{1}{3}(1 - r)\right]^{-1/3} \approx 143 \sqrt{\beta_m} \left[1 - \frac{1}{3}(1 - r)\right]^{-1/3}, \tag{12.26}$$

where

$$r = \frac{c_T^3}{c_L^3} = \left(\frac{\mu}{2\mu + \lambda}\right)^{3/2}. \tag{12.27}$$

Since our model has $\lambda = 0$, L becomes

$$L \approx 155 \sqrt{\beta_m}. \tag{12.28}$$

With $\beta_m = 0.517$ we obtain

$$L \approx 112.3. \tag{12.29}$$

This is somewhat smaller than the Lindemann number of isotropic materials with small λ. A good candidate for comparison is W (for which $\xi = 1.005$, $\lambda/2\mu = 0.628$)(see Table 1.2) which has $L = 135$ (see Table 7.2). One source of discrepancy is obvious. The experimental Lindemann

FIG. 12.1. Free energy of the $D = 3$ melting model (Villain type) as a function of β for $\lambda = 0$ and various values of the anisotropy parameter $\xi = 0.2, 0.4, \ldots, 1.2$. The stress corrections at low β are too small to be visible on this graph. The lowest defect correction at high β is shown for the $\xi = 1$ curve ($-\cdot-\cdot-$). It is very small.

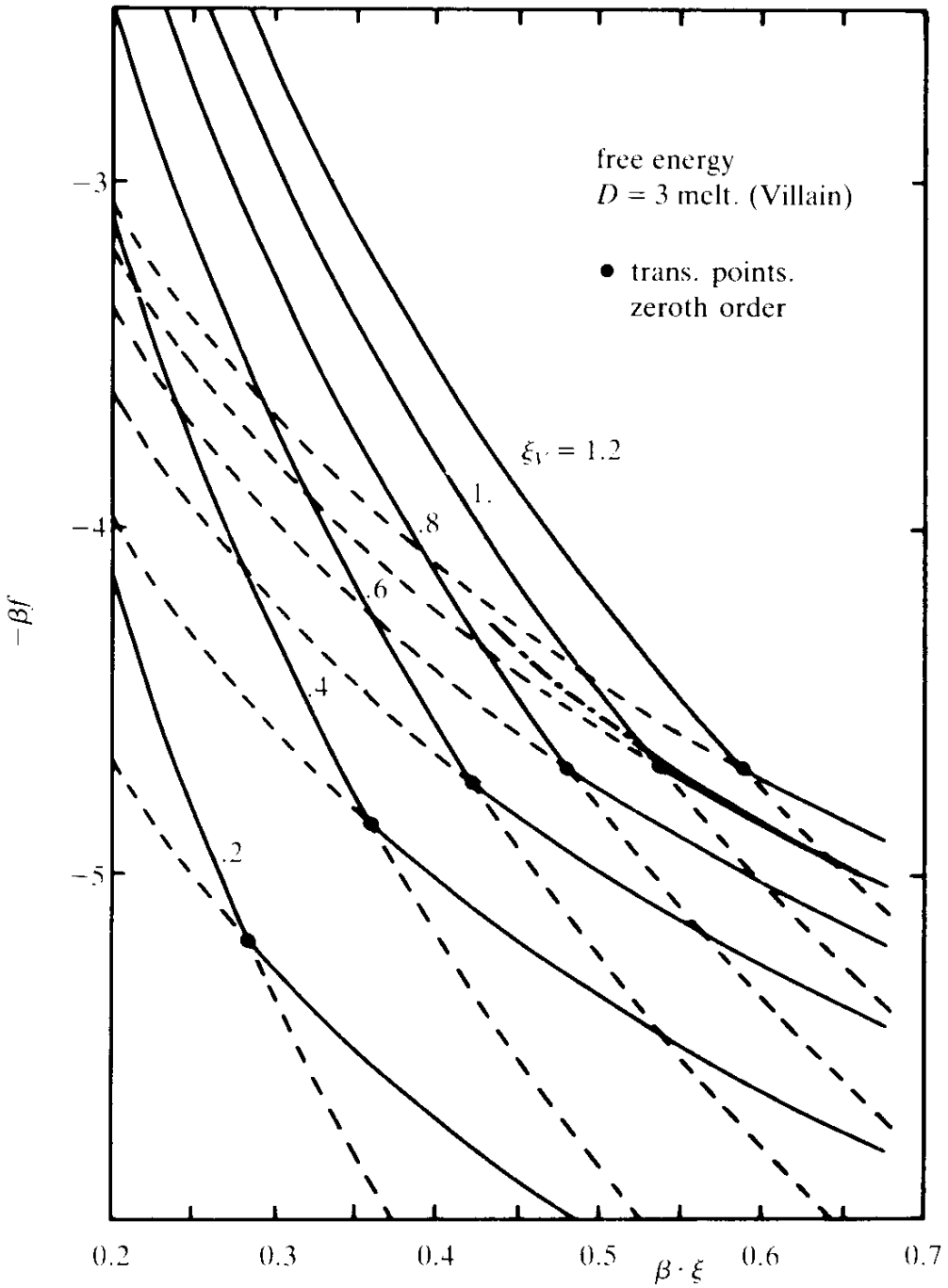

parameter is defined via the Debye temperature [see Eq. (7.38)] which is sensitive to the zero temperature elastic constants. The melting model, on the other hand, involves temperature dependent elastic constants. A look at Table 7.1 shows that the model's value of β_m has to be increased by roughly 15% before it can be inserted into formula (12.28). Still, this does not remove the discrepancy entirely and the model really melts at a fairly high temperature. In other words, when heating a crystal, the destruction

FIG. 12.2. The $D = 2$ energy density of the melting model as a function of β for $\lambda = 0$ and various values of $\xi(0.2, 0.4, \ldots, 1.2)$. The intercepts of the high and low temperature expansions give the transition temperatures in Table 12.1. On the high as well as the low temperature side, the lowest curves correspond to the lowest approximation without stress or defect graphs. The highest solid curves include the corrections (the dotted curves are the unphysical continuation of the corrected curves).

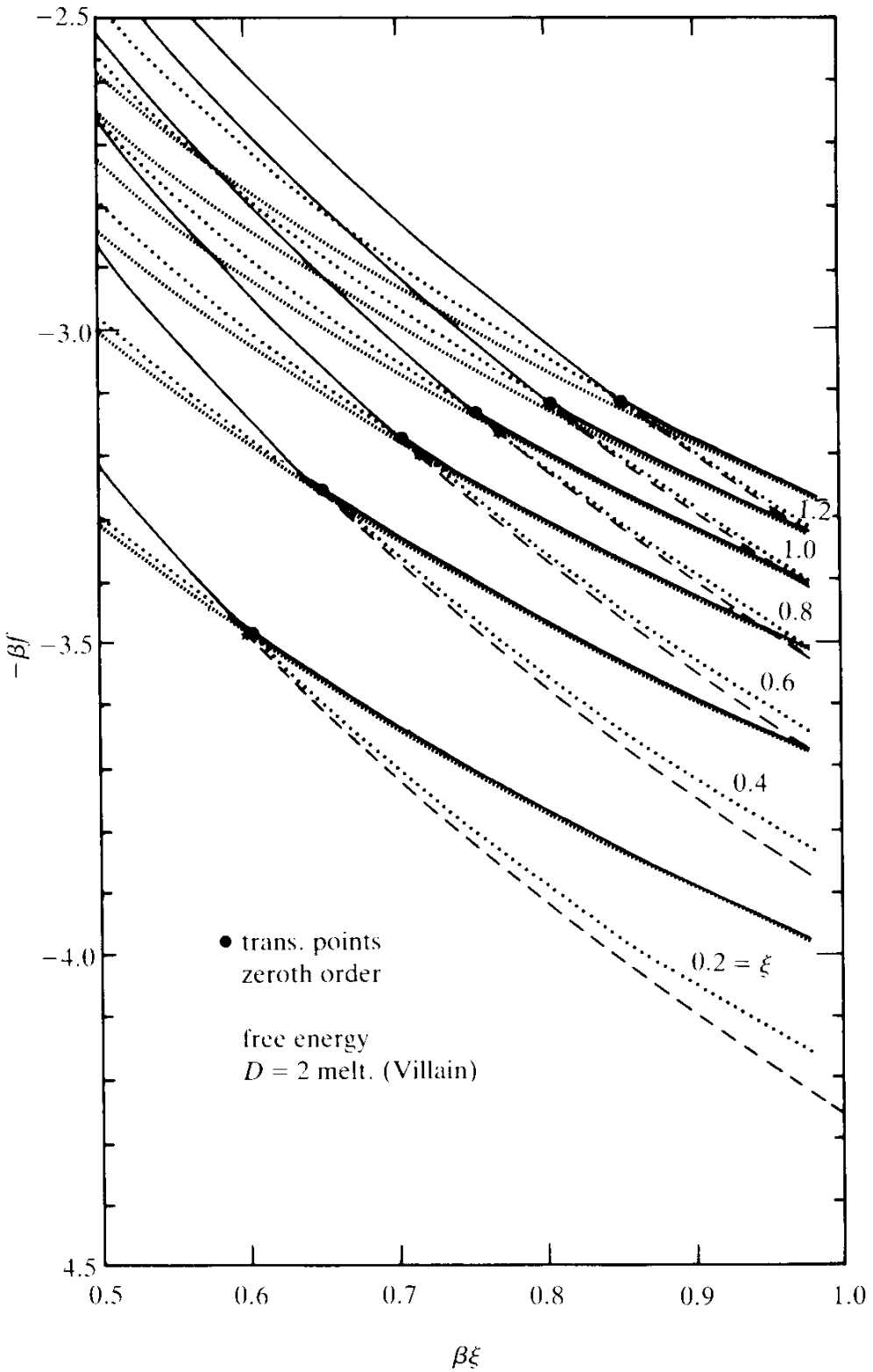

of crystalline order via defect formation sets in too late, in comparison with real crystals.

There can be different reasons for this. First, we have not taken the proper crystal structure into account. The metal W is really f.c.c., while the model is simple cubic. This could make a quantitative difference which must be studied in the future. Second, the model may contain too little information on point defects. The smallest defect loops may not be an adequate representation of these. The third reason, which we believe to be the most relevant one, will be understood only later, in Chapter 13. There we shall point out the main weakness of the model. We shall see that its disordered state is more disordered than that of a proper liquid. The reason is that the model has no input parameter for the hard cores of the atoms. In the disordered state these atoms are point-like objects which makes the liquid look more like a gas than a liquid (see Fig. 13.23). This causes a too large difference in the free energies between ordered and disordered phases leading to an intersection at a rather high temperature. Considerable work will be necessary to repair this inadequacy of the simple model.

Let us now turn to the internal energy. It is found by differentiation of $-\beta f$ with respect to $-\beta$. In the absence of stress and defect corrections, the internal energy was seen to be independent of T:

$$u = \begin{cases} \dfrac{3}{\beta} \\ \dfrac{3}{2\beta} \end{cases} \quad \text{for} \quad \begin{cases} T > T_{\text{melt}}, \\ T < T_{\text{melt}}, \end{cases} \quad D = 3, \tag{12.30}$$

$$u = \begin{cases} \dfrac{3}{2\beta} \\ \dfrac{1}{\beta} \end{cases} \quad \text{for} \quad \begin{cases} T > T_{\text{melt}}, \\ T < T_{\text{melt}}. \end{cases} \quad D = 2. \tag{12.31}$$

We add to these the stress and defect corrections. For $D = 3$ we shall do this only for $\xi = 1$, due to the complexity of the defect interaction potential in Eq. (9.104). The result is shown in Fig. 12.3. At the transition points, the entropy jumps are given in Table 12.2. For $\xi = 1$ we find $\Delta s \approx 1.49$ to lowest order and $\Delta s \approx 1.33$ after including the lowest stress and defect corrections. The Monte Carlo simulations to be described below give $\Delta s \approx 1.2$. This is in good agreement with the experimental number for W ($\Delta s_W \approx 1.5$ from Table 7.1). Actually, this comparison is not completely justified since this number for W was

FIG. 12.3. The internal energy of the $D = 3$ melting model (Villain type) at the same values of ξ as in Fig. 12.1. The curves now show the lowest stress corrections plus the lowest defect correction for $\xi = 1$ as in Fig. 12.1.

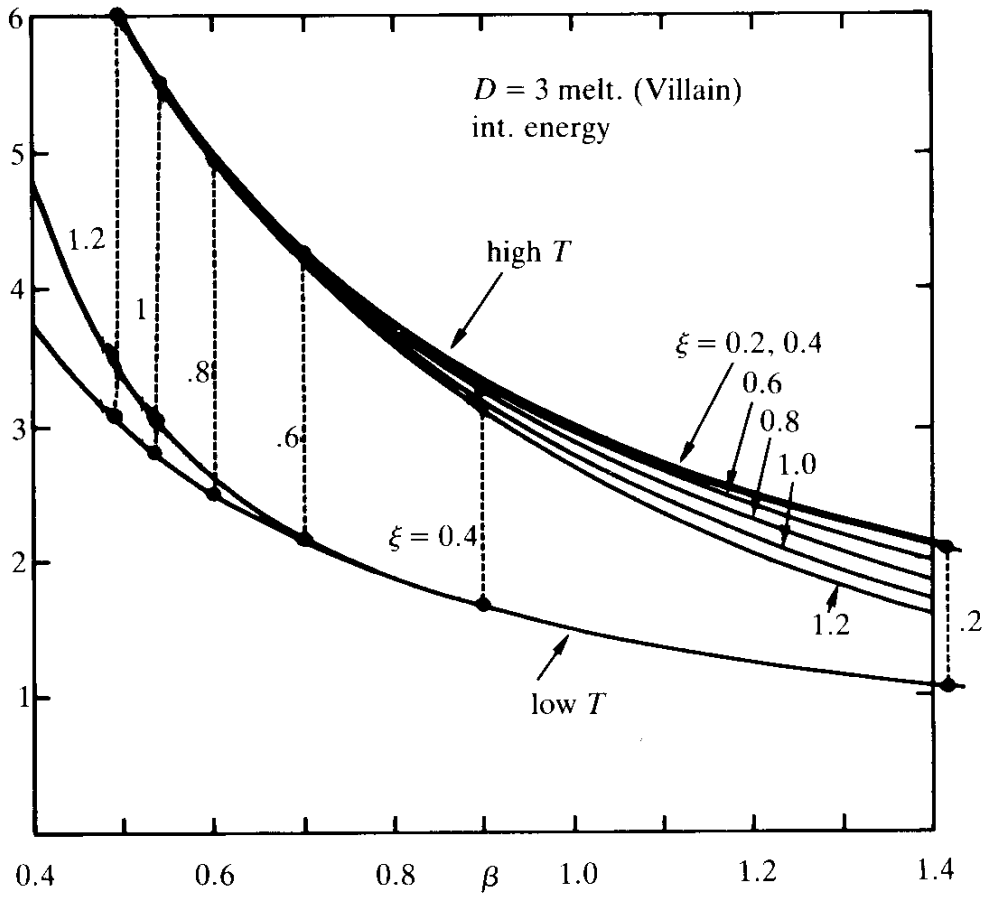

measured at constant pressure while our model's value is apparently observed at constant volume for which Δs should be much smaller. It is, however, not entirely clear what to take for the volume of the disordered state of the model, since this is defined not via the lattice sites $\mathbf{x}$ but via the displaced positions $\mathbf{x} + \mathbf{u}(\mathbf{x})$ and these are defined modulo defect gauge transformations. Quite possibly the correct size of Δs is partly a consequence of the too large disorder in the liquid state.

For the two dimensional model we can easily calculate all higher graphical corrections to the internal energy for various ξ and find the curves shown in Fig. 12.4. Using the transition values β_m obtained before from the free energies we find the transition entropies as listed in Table 12.2.

12.5. MONTE CARLO STUDY OF THE MELTING MODEL (VILLAIN TYPE)

In order to check the accuracy of our calculations we have performed Monte Carlo simulations of the model. Consider first the simpler case

FIG. 12.4. The internal energy of the $D = 2$ melting model (Villain type) at the same values of ξ as in Fig. 12.1. The jumps Δu at the transition points β_m give the transition entropies $\Delta s = \beta_m \Delta u$ listed also in Table 12.2.

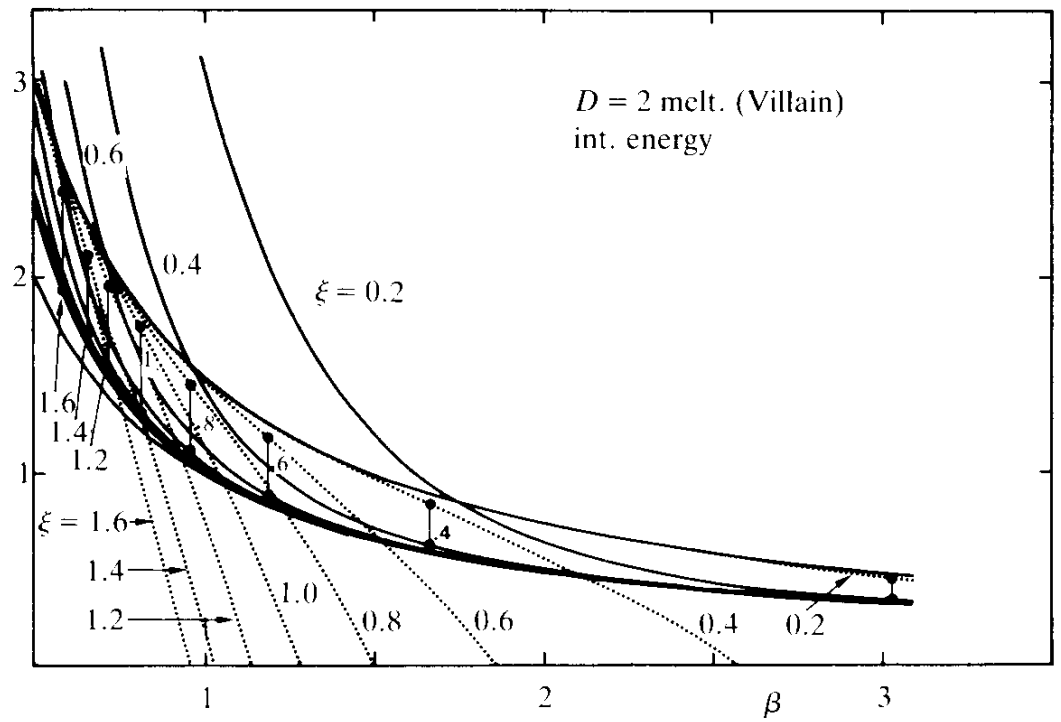

$D = 3$ for which we have used lattices of various sizes from 4^3 to 16^3 with periodic boundary conditions.

Equilibrium configurations were generated employing the standard heat-bath algorithm. In order to save computer time we have approximated the continuous $U(1)$ symmetry by its discrete $Z(N)$ subgroup and taken N to be once 16 and once 32. We have checked that the relevant transition region does not depend on this approximation. This is analogous to the situation in the XY model for which the additional transition caused by the discreteness of the $Z(N)$ variables (the so-called "freezing transition") increases with N as $\beta_m^2 N^2$ and thus lies at very high N. At each temperature, we have made 100 passes through the lattice to equilibriate the system and 250 more to measure the free energy and the specific heat. The resulting numbers for isotropic materials ($\xi = 1$) are listed in table 12.3 and the corresponding curves are shown in Figs. 12.5 and 12.6.[a] The inserts resolve the region near the transition point. We see that in three dimensions the fluctuations are quite unimportant and the approximate analytic calculations are very reasonable.

[a]For the sake of a better distinction with respect to the figures to be displayed in Chapter 13 for a cosine version of the melting model we have attached to labels β and ξ a subscript V. This is supposed to remind us of the Villain-like periodic Gaussian partition function (compare Chapter II).

TABLE 12.3. Internal energy and specific heat of the $D = 3$ melting model (Villain type) for $\lambda = 0$, $\xi = 1$ found in a Monte Carlo simulation on an $8 \times 8 \times 8$ simple cubic lattice. Each step in the thermal cycle involves 100 sweeps for equilibriation and 200 sweeps for measurement [Janke and Kleinert (1986)].

β	u (heat)	u (cool)	c (heat)	c (cool)
2.00	0.7432	0.7475	1.3997	1.1637
1.95	0.7704	0.7655	1.5124	1.4937
1.90	0.7834	0.7871	1.6110	1.6331
1.85	0.8112	0.8115	1.4039	1.2718
1.80	0.8291	0.8292	1.5330	1.5967
1.75	0.8542	0.8542	1.4153	1.2727
1.70	0.8781	0.8737	1.4693	1.2041
1.65	0.9083	0.9059	1.5342	1.2962
1.60	0.9359	0.9354	1.4787	1.6836
1.55	0.9615	0.9633	1.4964	1.6095
1.50	0.9995	0.9993	1.2907	1.2840
1.45	1.0328	1.0347	1.6478	1.8006
1.40	1.0709	1.0725	1.5141	1.5354
1.35	1.1129	1.1160	1.5709	1.5819
1.30	1.1517	1.1513	1.6278	1.6528
1.25	1.1971	1.2063	1.4825	1.7799
1.20	1.2453	1.2419	1.5432	1.4728
1.15	1.2949	1.3033	1.3540	1.3453
1.10	1.3716	1.3614	1.7440	1.8887
1.05	1.4293	1.4350	1.4587	1.3614
1.00	1.5049	1.4968	1.3345	1.5324
0.95	1.5790	1.5728	1.5331	1.4117
0.90	1.6675	1.6864	1.7417	1.6700
0.85	1.7626	1.7694	1.4675	1.4194
0.80	1.8860	1.8928	1.3710	2.0570
0.75	2.0228	2.0320	1.5393	1.4206
0.70	2.2213	2.2013	1.6052	1.8626
0.65	2.4059	2.9051	1.8863	73.3719
0.60	2.6731	4.7326	1.8815	3.3108
0.55	3.0771	5.2078	3.0595	3.8969
0.50	3.7711	5.8692	7.9192	3.2214
0.45	6.5738	6.5707	3.2643	3.1685
0.40	7.4347	7.4385	3.1995	3.5484
0.35	8.5480	8.5420	3.2445	3.0269
0.30	9.9615	9.9443	3.1429	2.9899
0.25	11.9727	12.0032	3.2393	2.8661
0.20	14.9715	15.0070	3.0202	2.8085
0.15	19.9825	19.3840	3.0044	2.9531
0.10	30.0042	29.9953	3.0089	2.9980
0.05	60.0058	59.9958	2.9989	2.9982

FIG. 12.5. Comparison of the $D = 3$ internal energy of the melting model (Villain type) of Fig. 12.3 for $\xi = 1$ with Monte Carlo data on a 8^3 and a 16^3 sc lattice. Notice that the 16^3 data show undercooling.

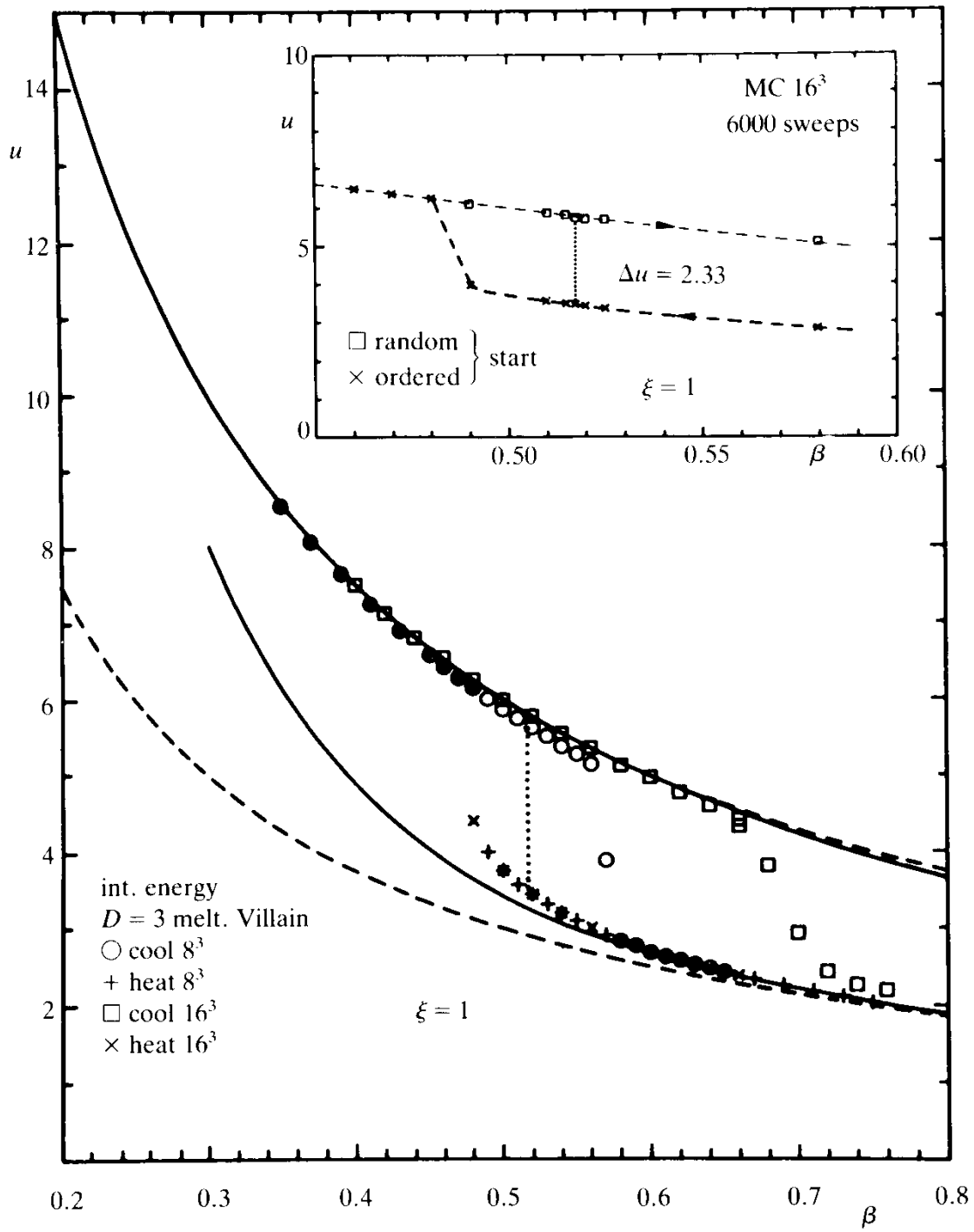

In order to find the melting temperature we have positioned the system into a mixed state [half liquid, half solid, where liquid means random $u_i(\mathbf{x}) \in (-\pi, \pi)$, and solid means $u_i(\mathbf{x}) \equiv 0$] and observed the development of the internal energy over many iterations. The system equilibriates very quickly and decides after less than 500 iterations into which state it belongs, even close to the point, for which melting occurs:

FIG. 12.6a. Comparison of the $D = 3$ specific heat of the melting model (Villain type) at $\xi = 1$, with Monte Carlo data. The insert resolves the jump in the specific heat at the melting point. This jump is very sensitive to ξ and changes sign at $\xi \approx 0.65$ (see Fig. 12.6b).

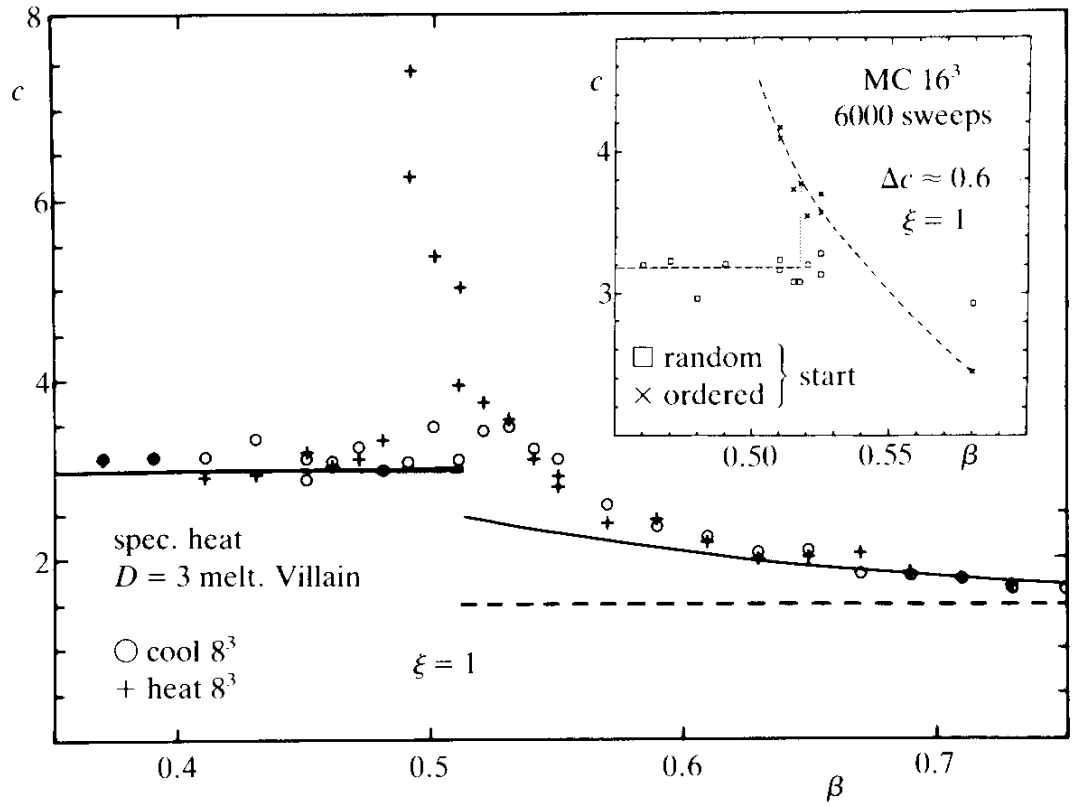

$$\beta_m \approx 0.5175 \qquad (D = 3,\ \xi = 1) \tag{12.32}$$

(see Fig. 12.6 for $\xi = 1$). This is in very good agreement with the analytic result obtained above.

The accuracy of this value was further tested by studying the stability of an initial solid or liquid state right at β_m. The internal energies are shown in Fig. 12.7. At $\beta_m = 0.5175$ they are completely stable and from their distance, shown in Fig. 12.8; we extract

$$\Delta u \approx 2.323, \quad \Delta s \approx 1.20 \quad (D = 3,\ \xi = 1). \tag{12.33}$$

We have repeated the same analysis for various values of ξ and found β_m and Δs as shown in Figs. 12.9 and 12.10, where they are also compared with the analytic results of Table 12.2. The values of β_m are seen to follow quite well a straight line given by

$$\beta_m \sim 0.5175\xi^{-0.57} \quad (D = 3). \tag{12.34}$$

For $\xi \to 0$, the transition temperature goes to zero. This has a simple

FIG. 12.6b. The ξ dependence of the difference between the specific heats of the solid and liquid phases. Most materials have $\xi \leqslant 0.6$ (see Table 7.1) so that Δc is positive, in agreement with experiment.

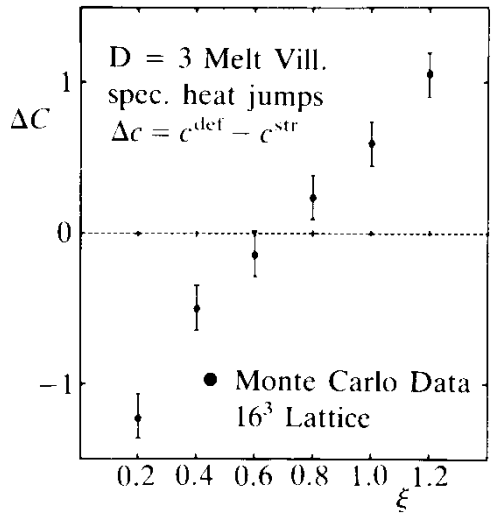

FIG. 12.7. Development of the internal energy of a mixed initial configuration (half solid, half liquid) over many Monte Carlo iterations for β near the transition value (isotropic crystal $\xi = 1$).

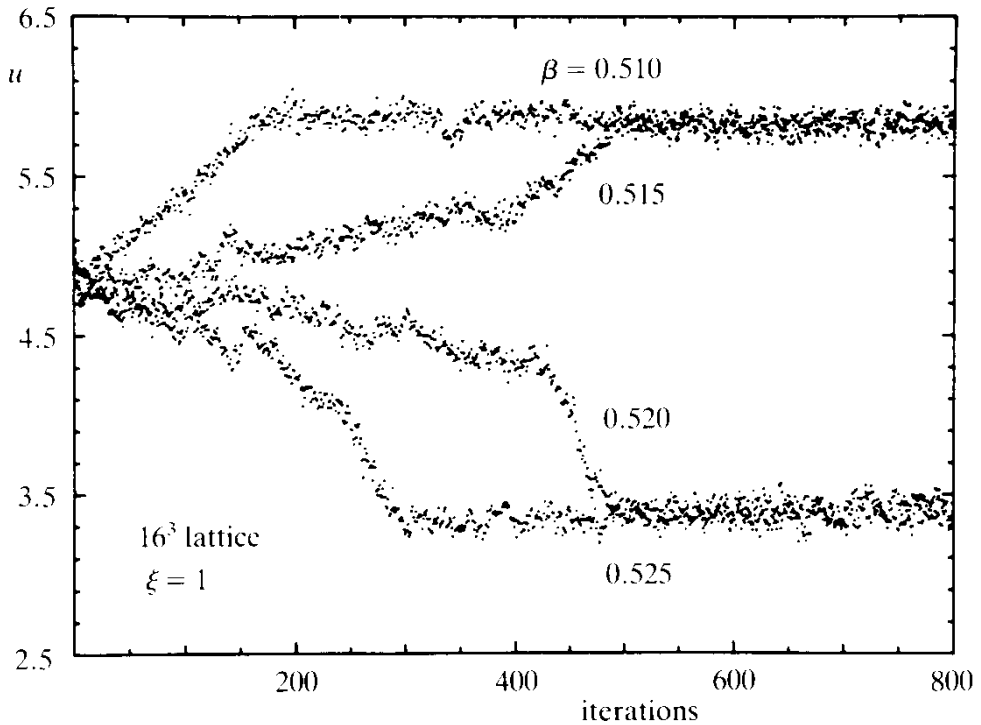

physical reason. We had seen in Section 1.2 [see the stability conditions in Eqs. (1.17) or (1.21b)] that at $\xi = 0$ a crystal becomes unstable with respect to shear stresses. Hence fluctuations diverge and destroy the crystalline order.

Since the transition entropy is rather large there is another way of estimating the transition point and the value of Δs. We may go to a

FIG. 12.8. Stability of solid and liquid phase at the transition point $\beta_m = 0.5175$ over many iterations. From the distance of the internal energies we extract $\Delta s \approx 1.2$.

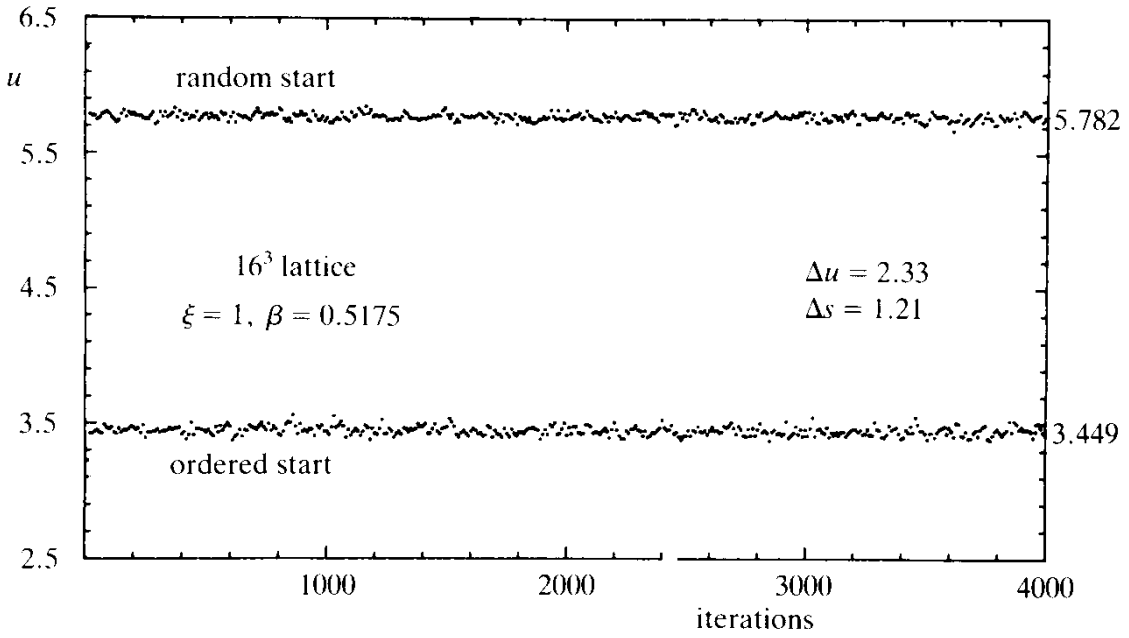

smaller lattice, say 4^3, and look again at the development of the internal energy over many iterations. At the transition point, the small system fluctuates back and forth between the two equilibrium states as shown in Fig. 12.11. If we plot a histogram for the distribution of the energies (also in Fig. 12.11) we find a pronounced double peak which shows that for $\beta < \beta_m$ the system rests predominantly in the liquid state, for $\beta > \beta_m$ in the solid state. At $\beta = \beta_m$ the two peaks are symmetric and their distance determines Δs. Notice that for a 4^3 lattice, the melting temperature is slightly lower than that for a 16^6 lattice ($\beta_m \approx 0.534$ versus $\beta_m \approx 0.5175$ at $\xi = 1$).

Let us now turn to the case of two dimensions. Here we use lattices of varying sizes, from 10^2 to 60^2, with periodic boundary conditions. Employing again the heat-bath algorithm and the $Z(16)$ approximation we find, after 50 sweeps for equilibriation and 100 sweeps for measurement, the internal energy and specific heat as shown in Table 12.4 and Figs. 12.12 and 12.13. We see that they compare rather well with the analytic results. It is also interesting to note that the peak in the specific heat has a shape quite similar to the experimental specific heat seen in the two-dimensional melting of adsorbed layers (see, for instance, Fig. 7.13).

It must be noted that the system has much stronger fluctuations than in three dimensions. This implies that much more care is needed when trying to find a precise values of β_m and Δs. In particular this is necessary since there are, in the literature, conflicting statements regarding the

FIG. 12.9. Dependence of β_m on ξ for the $D = 3$ melting model as found from the stability runs. The analytically obtained values of Table 12.1 are practically the same.

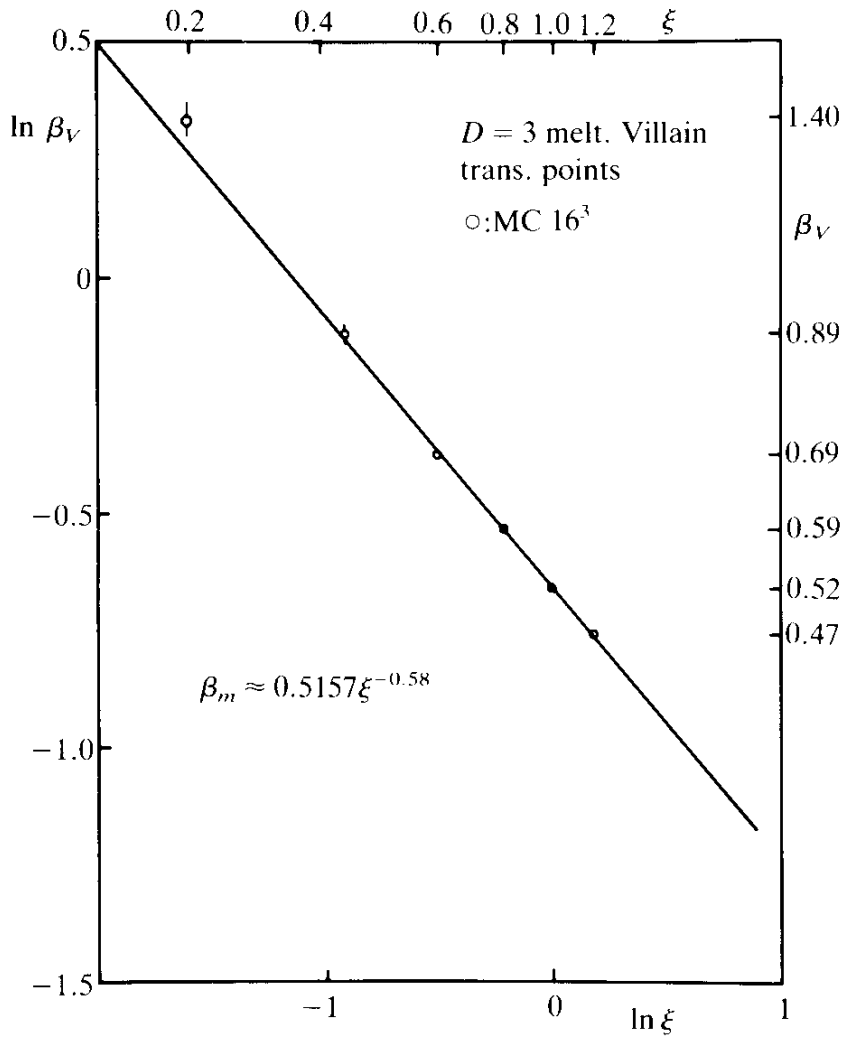

FIG. 12.10. Transition entropy Δs of the $D = 3$ melting model for various ξ from Monte Carlo simulations (compare with the $\xi = 1$ analytic result given in Table 12.3).

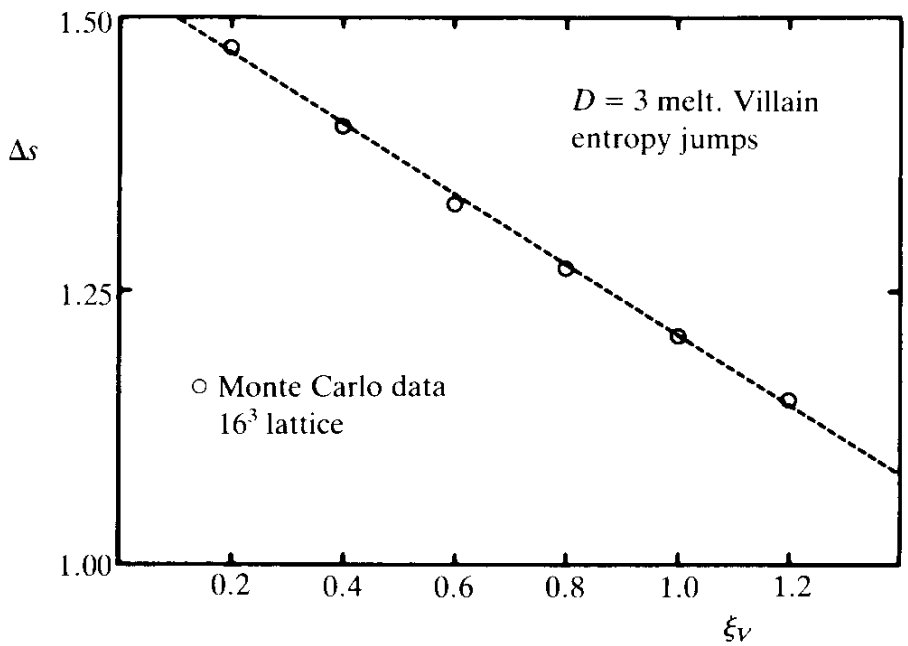

FIG. 12.11. Transition signal of the melting model on a smaller lattice (4^3). The internal energy jumps back and forth between the two phases. The histograms with a symmetric double peak indicate the first order transition.

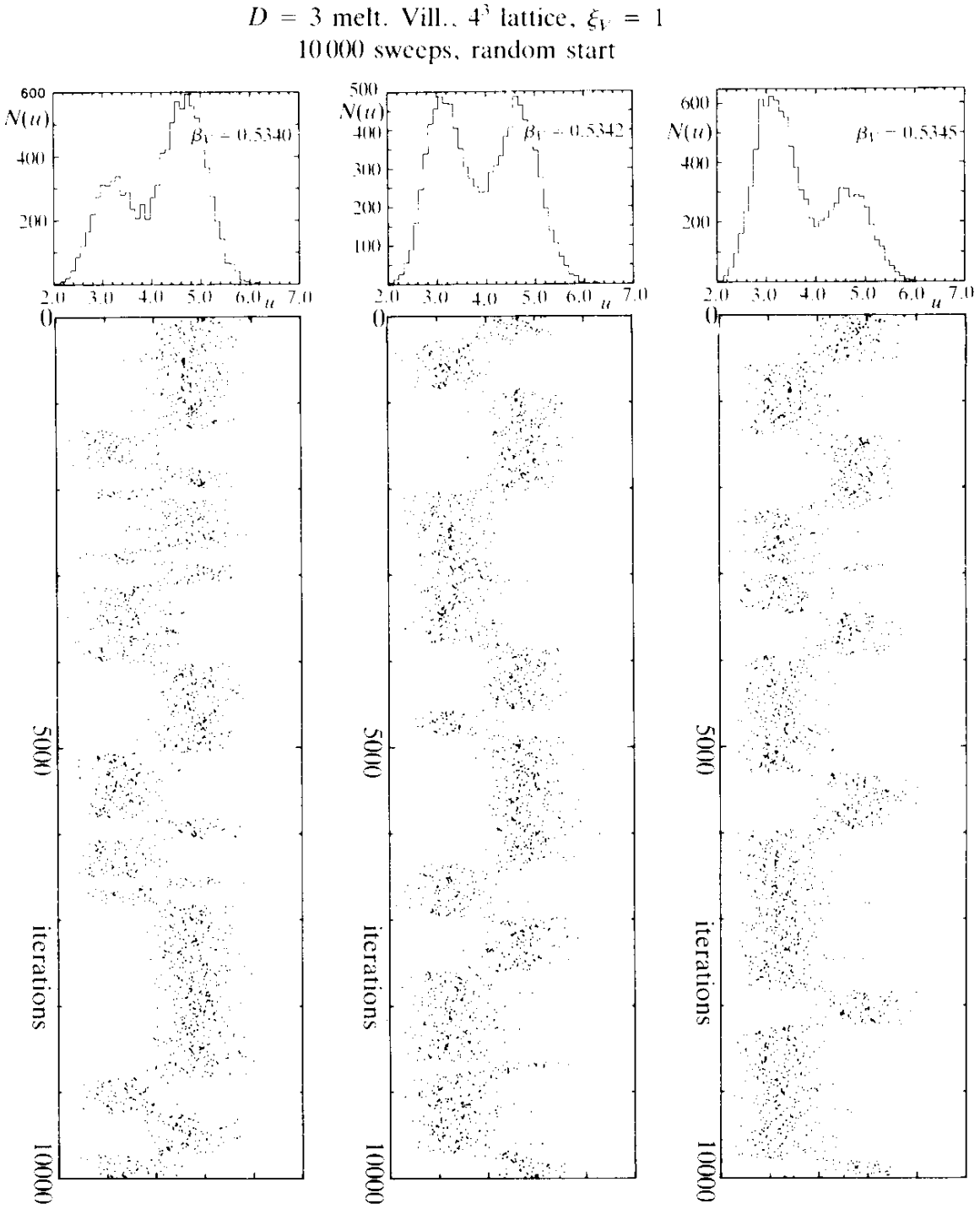

order of the two-dimensional melting transitions. These will be discussed in more detail below, particularly in Chapter 14.

In order to find β_m we proceed as in three dimensions and iterate the system many times starting once from a solid and once from a liquid state. The internal energies are shown in Fig. 12.14 and we extract

$$\beta_m \approx 0.815 \quad (D = 2,\ \xi = 1). \tag{12.35}$$

For this value of β_m, the two states are stable over as many as 15000 runs (see Fig. 12.14c). From the distance of the curves we deduce

$$\Delta u \approx 0, \quad \Delta s \approx 0.3. \tag{12.36}$$

Thus, with the definiteness which a Monte Carlo analysis statement can possibly have, our model undergoes a first order phase transition.

When repeating the same analysis for various values of ξ we find the ξ dependence of the transition point and of the entropy jump as shown in Fig. 12.16 and 12.17, respectively.

It should be mentioned, however, that some of the stability runs display a curious behavior, an example of which occurs in Fig. 12.14b. For some initial configurations, the energy of the solid phase jumps abruptly, after many iterations, towards the liquid phase, followed by further jumps later on. Also , the liquid state sometimes moves lower. This could be interpreted as a signal that the stability of the two phases, displayed in Fig. 12.14c, is only apparent and we just had not waited long enough for the system to equilibriate. The suddenness of the energy jumps, however, inclines us to believe that it may be some other phenomenon that could be taking place.

We therefore study the distributions of defects after such jumps. They are found by taking the configuration of displacements $u_i(\mathbf{x})$ and finding a set of integer numbers $n_{ii}(\mathbf{x})$ and half integers $n_{ij}(\mathbf{x})(i \neq j)$ so that

$$\sum_{\mathbf{x},i} (\nabla_i u_i(\mathbf{x}) - 2\pi n_{ii}(\mathbf{x}))^2, \tag{12.37}$$

$$\sum_{\mathbf{x},i<j} (\nabla_i u_j(\mathbf{x}) + \nabla_j u_i(\mathbf{x}) - 4\pi n_{ij}(\mathbf{x}))^2, \tag{12.38}$$

are minimal. From these numbers we obtain the defect distribution by forming the double curl

$$\eta_{ij}(\mathbf{x}) = \varepsilon_{ik\ell}\, \varepsilon_{jmn} \nabla_k \nabla_m n_{\ell n}(\mathbf{x} + \mathbf{i} + \mathbf{j}). \tag{12.39}$$

In two dimensions we are only dealing with the defect density $\eta(\mathbf{x}) \approx \eta_{33}(\mathbf{x})$, a few examples of which are shown in Fig. 12.17. The defect distributions show an interesting feature. As the free energy of the liquid moves down toward that of the solid, there are macroscopic sections of the crystal which are practically free of defects. Such sections

TABLE 12.4. Internal energy and specific heat of the $D = 2$ melting model (Villain type) for $\lambda = 0$, $\xi = 1$. The Monte Carlo simulations were performed on a 60×60 square lattice with 50 sweeps for equilibriation and 100 sweeps for measurement [Janke and Kleinert (1986)].

β	u (heat)	u (cool)	c (heat)	c (cool)
2.00	0.4990	0.7962	0.7548	0.9110
1.95	0.5112	0.6087	0.7579	0.7475
1.90	0.5252	0.6232	0.8927	1.2787
1.85	0.5376	0.6389	0.7967	1.1334
1.80	0.5559	0.6584	1.0974	0.8772
1.75	0.5721	0.6715	0.7393	0.9614
1.70	0.5891	0.6886	1.0022	0.9542
1.65	0.6035	0.7076	1.1414	1.0866
1.60	0.6256	0.7266	1.0722	0.7998
1.55	0.6413	0.7490	1.1222	1.0393
1.50	0.6642	0.7742	1.0356	1.1047
1.45	0.6906	0.7962	1.8727	0.7926
1.40	0.7164	0.8257	1.3910	0.9388
1.35	0.7392	0.8552	1.0191	0.8679
1.30	0.7672	0.8886	0.9279	1.0129
1.25	0.8074	0.9253	1.0081	0.9934
1.20	0.8374	0.9680	1.1057	1.1961
1.15	0.8767	1.0138	1.4215	0.9555
1.10	0.9179	1.0677	0.8685	1.2610
1.05	0.9685	1.1302	1.1580	1.1326
1.00	1.0317	1.2381	1.0001	2.3382
0.95	1.0879	1.3578	1.1523	1.3237
0.90	1.1621	1.4646	1.5221	1.2630
0.85	1.2631	1.6210	1.4976	1.8810
0.80	1.4009	1.7642	1.4947	1.5004
0.75	1.6045	1.9382	2.3084	1.3713
0.70	2.0387	2.1028	3.2047	2.2007
0.65	2.2845	2.2798	1.5969	1.8314
0.60	2.4807	2.4897	1.2777	1.1680
0.55	2.7191	2.7254	1.8126	1.2788
0.50	2.9906	3.0009	3.3905	1.1703
0.45	3.3134	3.3222	7.5173	1.2776
0.40	3.7461	3.7559	3.2282	1.5885
0.35	4.3012	4.2834	3.5455	1.2059
0.30	4.9946	4.9946	3.2809	1.2932
0.25	5.9950	6.0014	3.9873	1.7238
0.20	7.4901	7.5132	3.5328	1.4359
0.15	9.9912	9.9918	3.4499	1.4240
0.10	15.0034	15.0105	3.5394	1.5051
0.05	30.0000	30.0001	3.5001	1.5003

FIG. 12.12. Comparison of internal energy of the $D = 2$ melting model (Villain type) with Monte Carlo data.

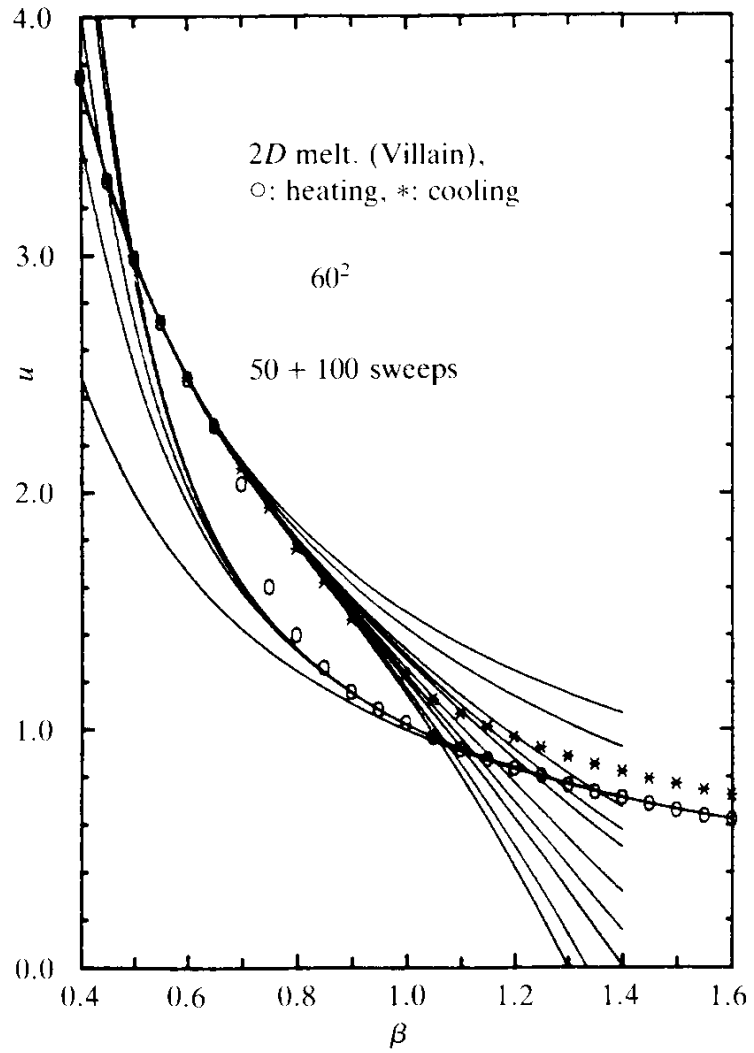

are chunks of solid. Thus it appears as though the approach of the two free energies is *not* a signal of an equilibriation of the system in a *pure* state near a contribution transition, but rather an indication that the system separates into a mixed state, with finite pieces of solid immersed in the liquid phase. As a matter of fact, in nature, precisely such a phenomenon happens if a crystal melts at fixed total volume. Due to the difference of the solid and liquid phases, the internal energy does not have a jump, as it does at fixed pressure, but moves continuously from one value to the other. This issue, (raised by Toxvaerd in 1980 and investigated further by Abraham in 1982, via molecular dynamics simulation) will be discussed in more detail later in Chapter 14 (see, in particular, Figs 14.11 and 14.12) which is dedicated entirely to the controversial results on the order of two-dimensional melting.

At this juncture let us only mention that our results are in disagreement with recent Monte Carlo investigations by Strandburg, Solla and Chester

FIG. 12.13. Comparison of specific heat of the $D = 2$ melting model (Villain type) with Monte Carlo data. The peak resembles the experimental peak in adsorbed solid ^{4}He films found by Bretz (cf. Bretz *et al.* 1973; see Fig. 7.13).

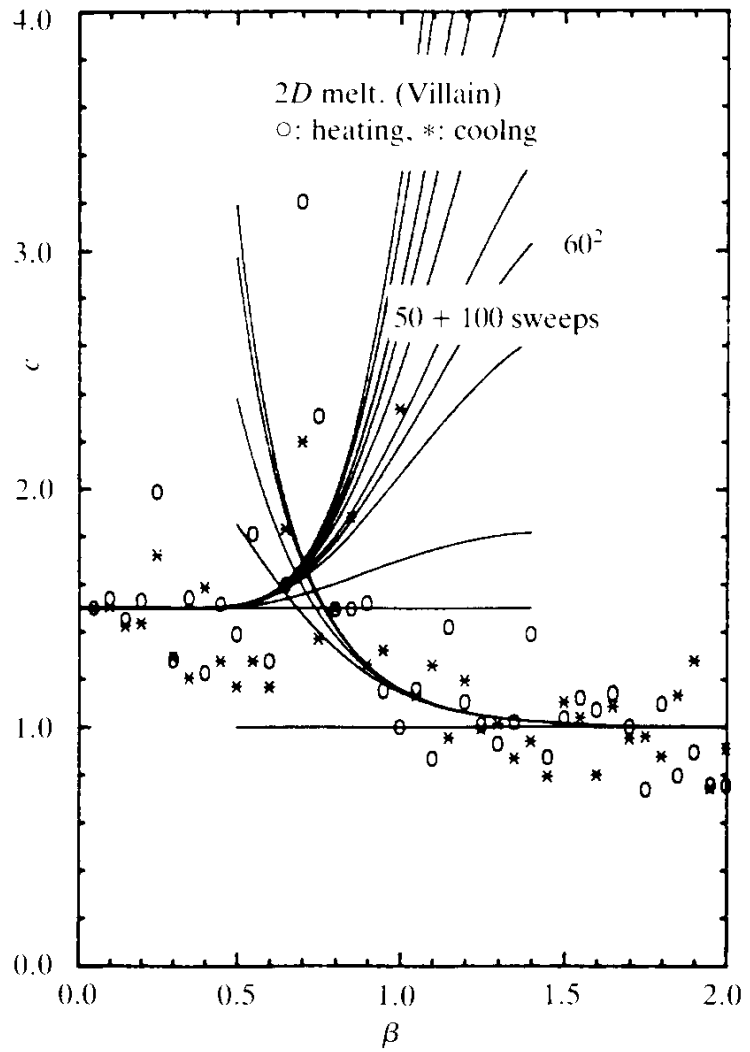

(1983) who claim to have seen two successive continuous transitions. Their evidence is not derived directly from our model but their study differs from ours in two respects.

(i) They use a triangular lattice rather than a square one.

(ii) They do not simulate our model but a dual form of it.

The first difference could, in principle, be important. But Bruce (1985) has redone the same work on a square lattice and found the same result (namely, two successive continuous transitions). If this were true, it could only be the use of the dual version of the model which causes difficulties in obtaining equilibrium in Monte Carlo simulations. Let us therefore describe that model briefly. It is given directly by the integer-stress gauge field form of the partition function. In two dimensions, this was written down in Eq. (9.53) and (9.55). After summing over all defect fields $\bar{\eta}(\mathbf{x})$ it reads

FIG. 12.14a,b,c. Stability of solid and liquid initial states for $D = 2$ near and at the melting point over many iterations.

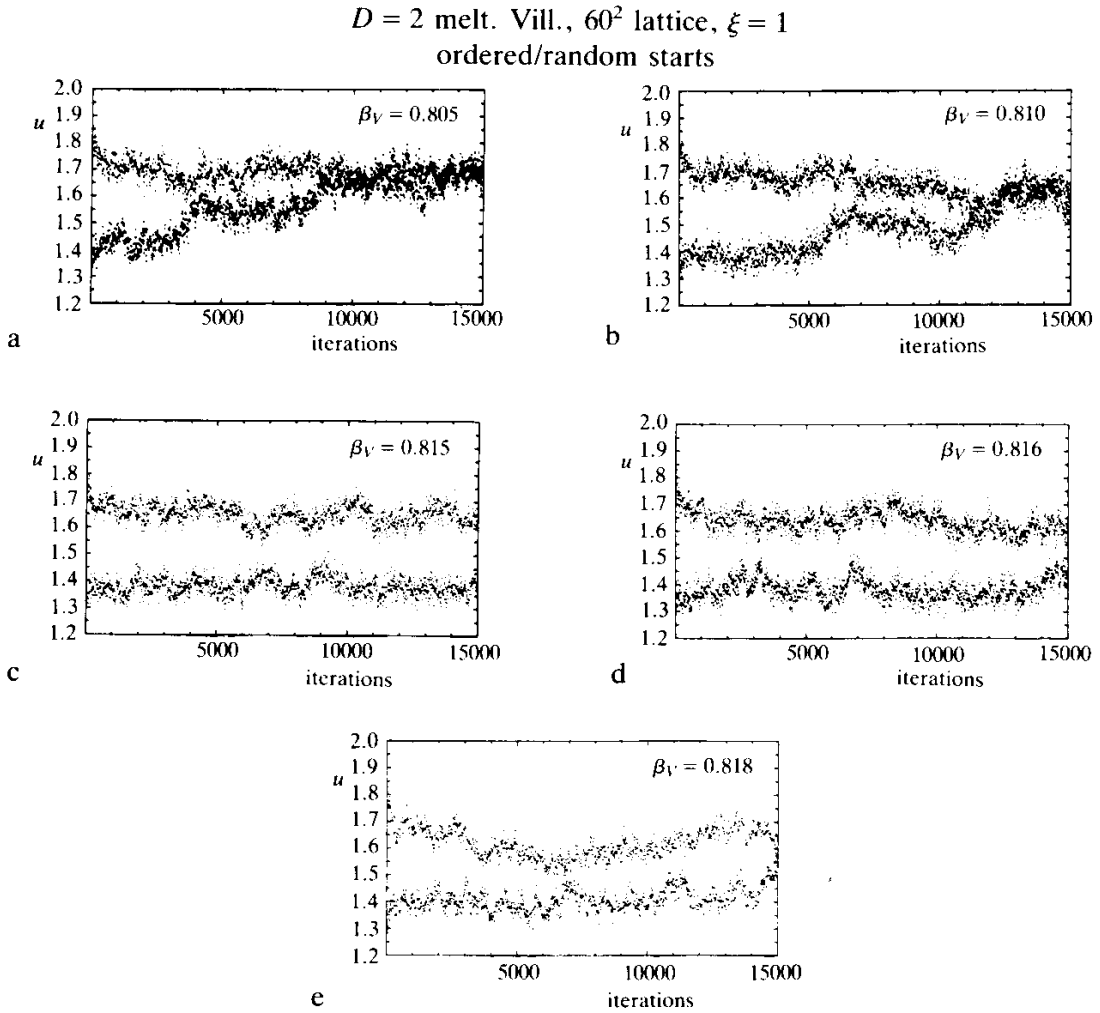

FIG. 12.15. The melting transition values β_m of the $D = 2$ melting model (Villain type) for various values of ξ. They follow only very roughly the empirical law $\beta_m \approx c\xi^{-\alpha}$ with α lying between 0.7 and 0.86.

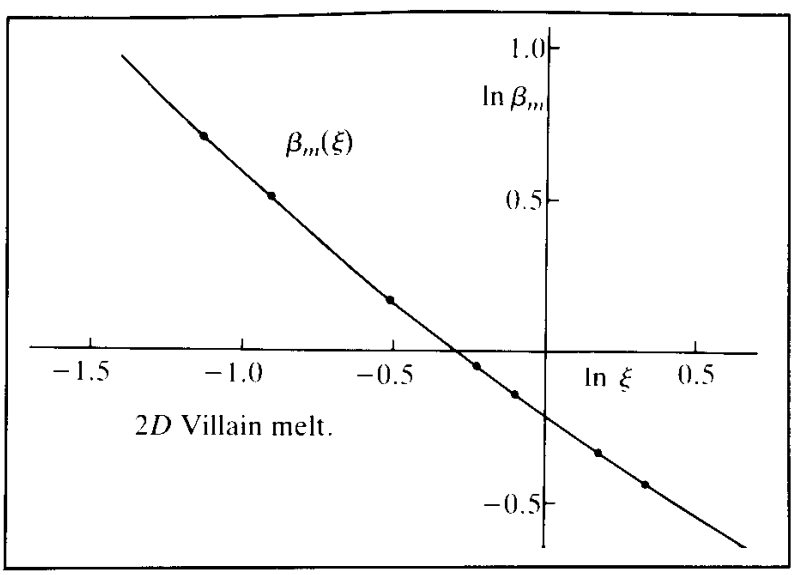

FIG. 12.16. Transition entropy Δs of the $D = 2$ melting model (Villain type) for various ξ.

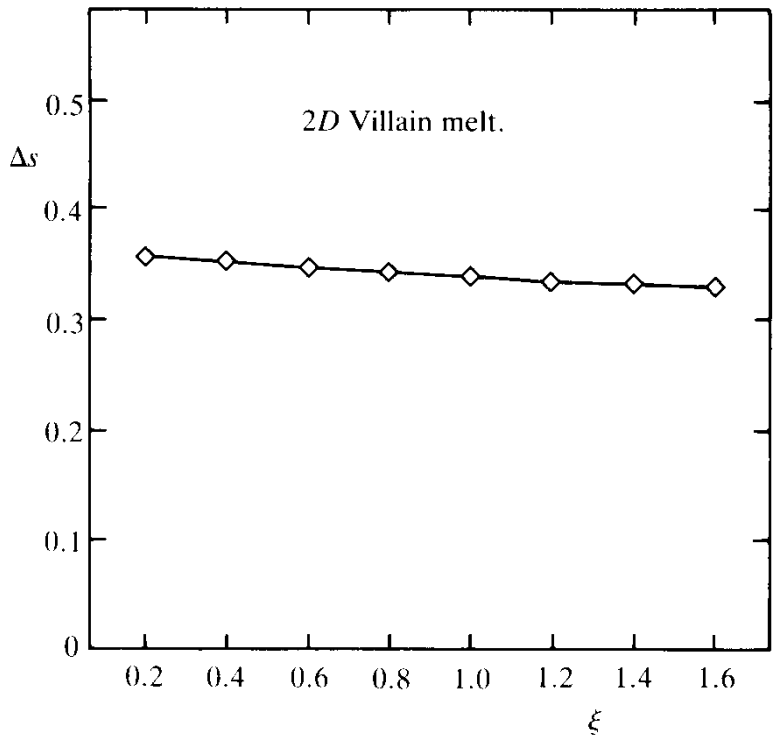

$$Z = \left[\frac{1}{(2\xi)^2}\left(1 - 2\frac{\xi}{\gamma}\right)\right]^{N/2} \frac{1}{(\sqrt{2\pi\beta})^{3N}} \sum_{\{\bar{\chi}(\mathbf{x})\}} \exp\left\{-\frac{1}{4\beta}\right.$$
$$\left. \times \sum_{\mathbf{x}} \bar{\chi}(\mathbf{x}) \left[(\bar{\nabla}\cdot\nabla)^2\left(-\frac{1}{\gamma}\right) + ((\bar{\nabla}_1\nabla_1)^2 + (\bar{\nabla}_2\nabla_2)^2)\left(\frac{1}{\xi} - 1\right)\right] \bar{\chi}(\mathbf{x})\right\}, \tag{12.40}$$

where the sum extends over all integers $\bar{\chi}(\mathbf{x})$. Dropping the prefactor, one remains with the sum

$$Z_{LR} = \sum_{\{\bar{\chi}(\mathbf{x})\}} e^{-(1/4\beta)\Sigma_{\mathbf{x}}\bar{\chi}(\mathbf{x})[(\bar{\nabla}\cdot\nabla)^2(1-(1/\gamma)) + ((\bar{\nabla}_1\nabla_1)^2 + (\bar{\nabla}_2\nabla_2)^2)((1/\xi)-1)]\bar{\chi}(\mathbf{x})}. \tag{12.41}$$

This partition function is reminiscent of the discrete Gaussian model which appeared before as the dual version of the ordinary Villain model:

$$Z_R = \sum_{\{\varphi(\mathbf{x})\}} e^{-(\beta_R/2)\Sigma_{\mathbf{x}}\varphi(\mathbf{x})(-\bar{\nabla}\cdot\nabla)\varphi(\mathbf{x})}. \tag{12.42}$$

We have seen that that model could be used to study the roughening

FIG. 12.17a,b. Defect pictures illustrating the equilibriation process for the run in Fig. 12.14c at $\beta = 0.81$ for ordered start (ord) and random start (ran), respectively. The numbers to the right of each picture tell the number (in thousands) of equilibriation sweeps [after Janke and Kleinert (1986)].

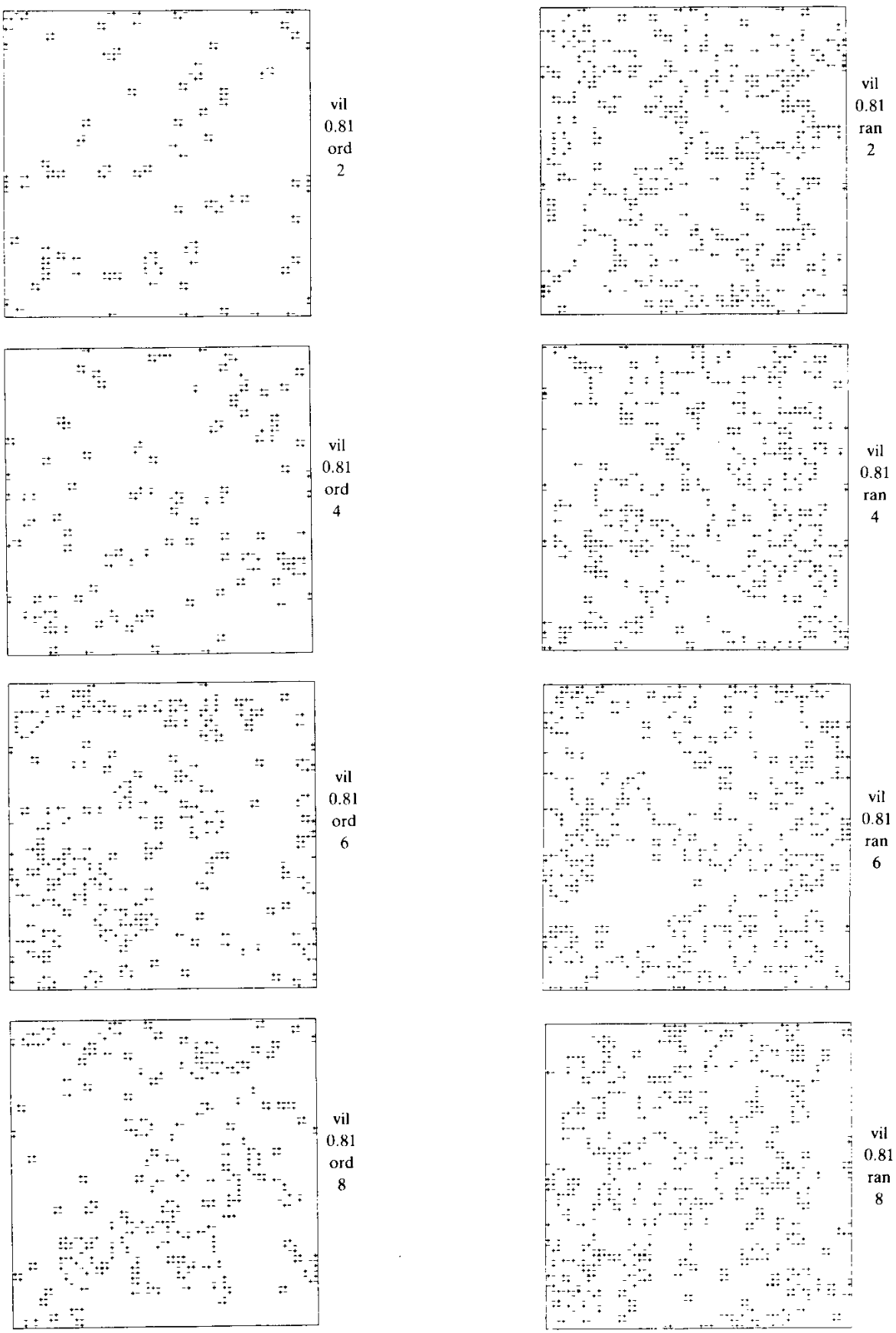

FIG. 12.17a,b. (continued)

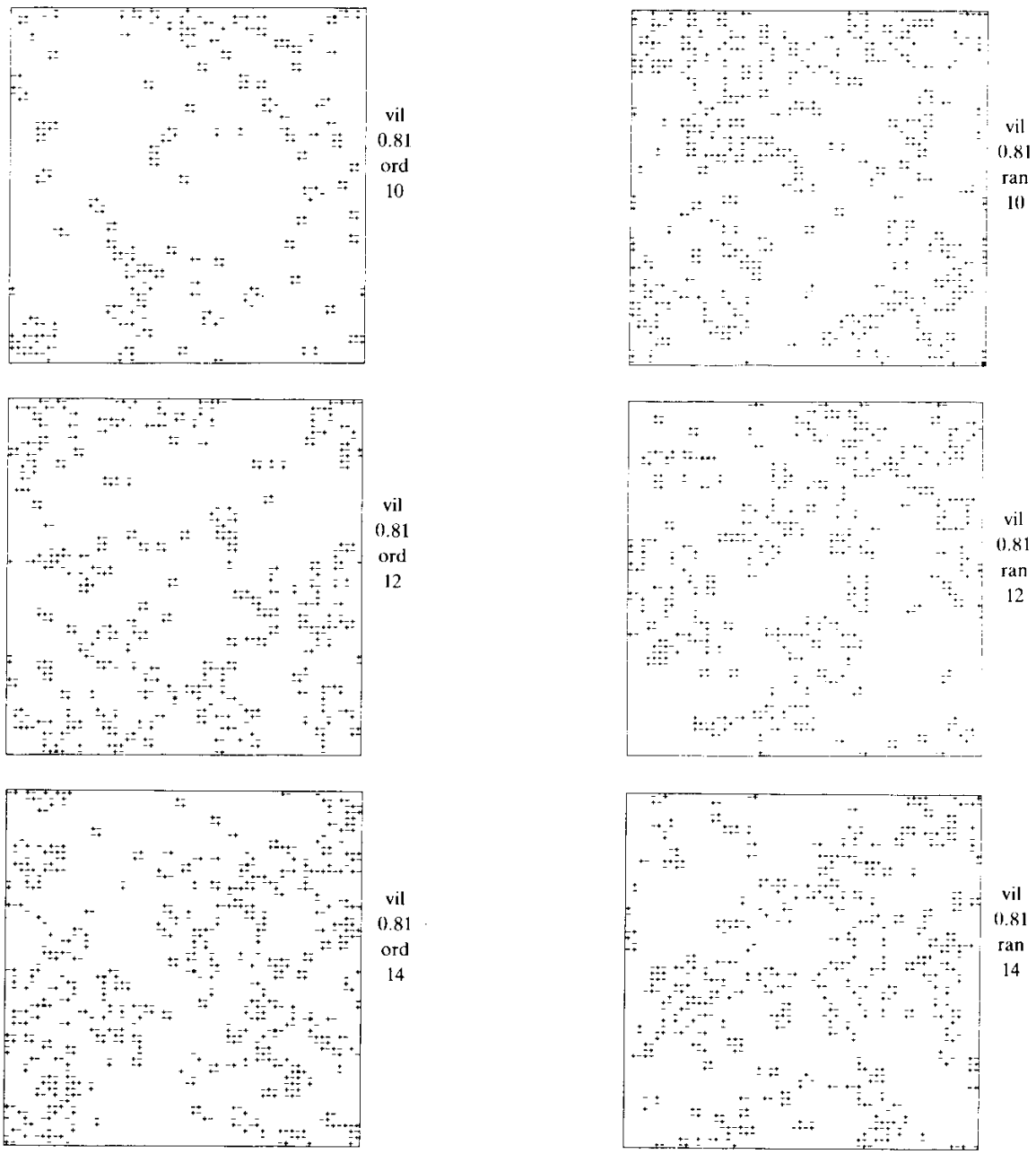

transition on crystal surfaces [recall Part II, Eqs. (11.254), (11.125)] with the identification $T_R = 1/\beta_R = \beta_V$.

The partition function (12.40) has a very similar appearance. In the isotropic case with $\xi = 1$ it differs by having an energy $(-\bar{\nabla}\cdot\nabla)^2$ term instead of $(-\bar{\nabla}\cdot\nabla)$. It has therefore been named the *Laplacian roughening model* by Nelson (1982). In this model, one usually defines the temperature T_{LR} such that $1/\beta$ in (12.41) is replaced by

$$\frac{2}{T_{LR}} = 2\beta_{LR}. \tag{12.43}$$

Taking the prefactor in (12.40) into account, the internal energy and

specific heat of the model (12.41) are related to those of the melting model (12.40) with $\xi = 1$ as follows:

$$u = \frac{3}{2\beta} - \frac{1}{2\beta^2} u_{LR}, \quad c = \frac{3}{2} - \frac{1}{\beta} u_{LR} + c_{LR}, \tag{12.44}$$

$$u_{LR} = \frac{3}{2\beta_{LR}} - \frac{1}{2\beta_{LR}^2} u, \quad c_{LR} = \frac{3}{2} - \frac{1}{\beta_{LR}} u + c. \tag{12.45}$$

The previously calculated high and low temperature expansions, which in the melting model had the general form

$$-\beta f = \text{constant} - \frac{3}{2}\log\beta + \sum e^{-(a/2\beta)}, \tag{12.46}$$

$$u = \frac{3}{2\beta} + \sum -\frac{a}{2\beta^2} e^{-(a/2\beta)}, \quad c = \frac{3}{2} + \sum \left(-\frac{a}{\beta} + \frac{a^2}{4\beta^2} \right) e^{-(a/2\beta)}, \tag{12.47}$$

for high temperatures and

$$-\beta f = \text{constant} - \log\beta + \sum e^{-\beta b}, \tag{12.48}$$

$$u = \frac{1}{\beta} + \sum b e^{-\beta b}, \quad c = 1 + \beta^2 \sum b^2 e^{-\beta b}, \tag{12.49}$$

for low temperatures, now read

$$-\beta f_{LR} = \sum e^{-\beta_{LR} a}, \tag{12.50}$$

$$u_{LR} = \sum a e^{-\beta_{LR} a}, \quad c_{LR} = \beta_{LR}^2 \sum a^2 e^{-\beta_{LR} a}, \tag{12.51}$$

and

$$-\beta f_{LR} = -\frac{1}{2}\log(2\pi\beta_{LR}) + \sum e^{-(1/2\beta_{LR})b}, \tag{12.52}$$

$$u_{LR} = \frac{1}{2\beta_{LR}} - \sum \frac{b}{2\beta_{LR}^2} e^{-(1/2\beta_{LR})b}, \quad c_{LR} = \frac{1}{2} + \sum \left(-\frac{b}{\beta_{LR}} + \frac{b^2}{4\beta_{LR}^2} \right) e^{-(1/2\beta_{LR})b}, \tag{12.53}$$

in the opposite temperature limits of the temperature T_{LR}.

FIG. 12.18. Internal energy of the Laplacian roughening model of melting and comparison with Monte Carlo data on a square lattice [taken from Janke and Kleinert (1986)].

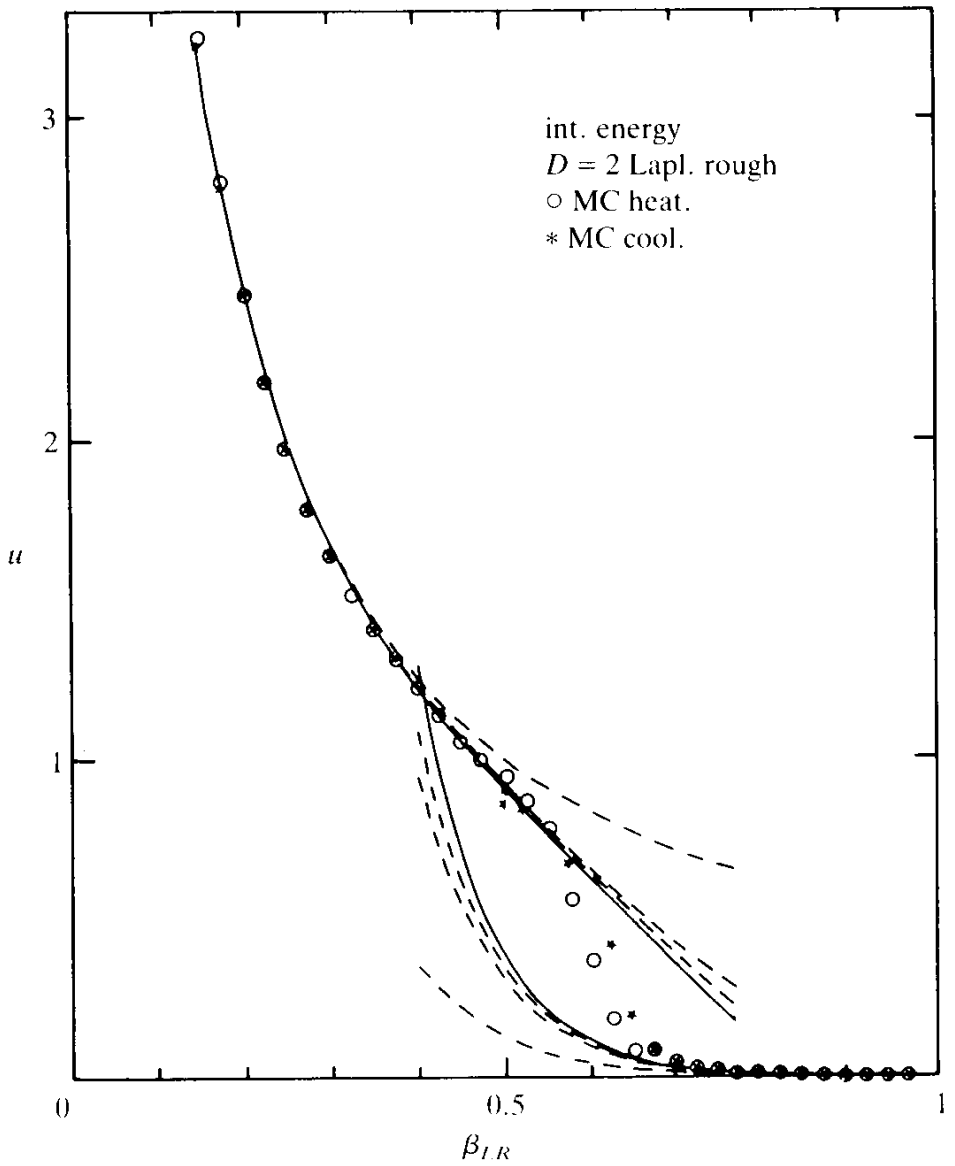

In Figs. 12.18 and 12.19 we have compared the calculated internal energy with the Monte Carlo data for $\xi = 1$. In the immediate neighborhood of the transition point the agreement is quite bad, demonstrating the importance of fluctuations. Since we have studied this model in the previous dual Villain form, there is no need to do this once more here. Let us simply mention that, for the simulation, it is useful to bring the energy to a more convenient form. First we rewrite

$$\sum_{\mathbf{x}} (\bar{\nabla}\cdot\nabla\bar{\chi}(\mathbf{x}))^2 = \sum_{\mathbf{x}} \left(\sum_{\pm\mathbf{i}} \left(\bar{\chi}(\mathbf{x}+\mathbf{i}) \right) - 4\bar{\chi}(\mathbf{x}) \right)^2$$

$$= \sum_{\mathbf{x}} \left\{ 20\bar{\chi}(\mathbf{x})^2 - 8\sum_{\pm\mathbf{i}} \bar{\chi}(\mathbf{x}+\mathbf{i})\bar{\chi}(\mathbf{x}) + \sum_{\substack{\pm\mathbf{i},\,\pm\mathbf{j} \\ \mathbf{i}\neq\mathbf{j}}} \bar{\chi}(\mathbf{x}+\mathbf{i}-\mathbf{j})\bar{\chi}(\mathbf{x}) \right\}. \tag{12.54}$$

FIG. 12.19. Specific heat of the Laplacian roughening model and comparison with Monte Carlo data on a square lattice.

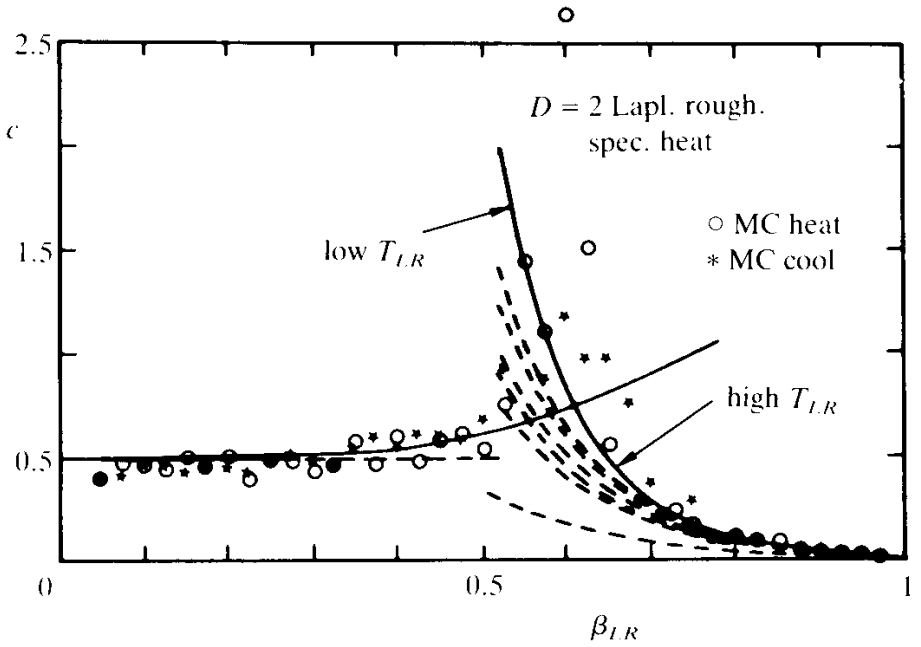

FIG. 12.20. The three types of vectors to the neighboring positions appearing in Eqs. (12.55)–(12.56) and (12.61)–(12.62), respectively.

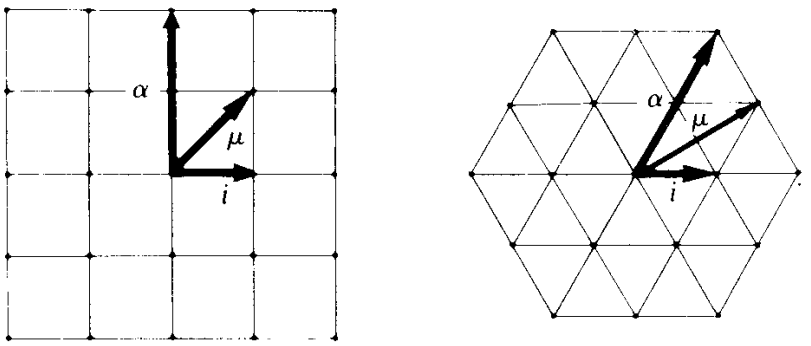

The vector sums over $\mathbf{i}$, $\mathbf{j}$ with $\mathbf{i} \neq \mathbf{j}$ covers twice the 4 next-nearest neighbours and once the 4 second-nearest neighbours. If the corresponding vectors are denoted by $\pm\boldsymbol{\mu}$, $\pm\boldsymbol{\alpha}$, respectively (see Fig. 12.20), we find

$$\sum_{\mathbf{x}} (\bar{\nabla}\cdot\nabla\bar{\chi}(\mathbf{x}))^2$$

$$= \sum_{\mathbf{x}} \left\{ 20\bar{\chi}(\mathbf{x})^2 - 8\sum_{\pm\mathbf{i}} \bar{\chi}(\mathbf{x}+\mathbf{i})\bar{\chi}(\mathbf{x}) + 2\sum_{\pm\boldsymbol{\mu}} \bar{\chi}(\mathbf{x}+\boldsymbol{\mu})\bar{\chi}(\mathbf{x}) + \sum_{\pm\boldsymbol{\alpha}} \bar{\chi}(\mathbf{x}+\boldsymbol{\alpha})\bar{\chi}(\mathbf{x}) \right\}$$

$$= \sum_{\mathbf{x}} \bar{\chi}(\mathbf{x}) \left(20\bar{\chi}(\mathbf{x}) - 8\sum_{\pm\mathbf{i}} \chi(\mathbf{x}+\mathbf{i}) + 2\sum_{\pm\boldsymbol{\mu}} \chi(\mathbf{x}+\boldsymbol{\mu}) + \sum_{\pm\boldsymbol{\alpha}} \chi(\mathbf{x}+\boldsymbol{\alpha}) \right), \tag{12.55}$$

which is the desired form. It can also be rewritten as

$$\sum_{\mathbf{x}} (\bar{\nabla}\cdot\nabla\bar{\chi}(\mathbf{x}))^2$$

$$= 4\sum_{\pm\mathbf{i}} (\bar{\chi}(\mathbf{x}+\mathbf{i})-\bar{\chi}(\mathbf{x}))^2 - \sum_{\pm\boldsymbol{\mu}} (\bar{\chi}(\mathbf{x}+\boldsymbol{\mu})-\bar{\chi}(\mathbf{x}))^2 - \frac{1}{2}\sum_{\pm\boldsymbol{\alpha}} (\bar{\chi}(\mathbf{x}+\boldsymbol{\alpha})-\bar{\chi}(\mathbf{x}))^2, \tag{12.56}$$

where the first term is the ordinary discrete roughening energy $8\Sigma_{\mathbf{x}}\bar{\chi}(\mathbf{x})(-\bar{\nabla}\cdot\nabla)\chi(\mathbf{x})$ and the others may be considered as next and second neighbor corrections. These are quite significant as can be seen by merely comparing the transition temperatures. If the other two terms were negligible, we should have $T_{LR}/8 = T_R$ where T_R is the roughening temperature. For β_{LR} we find from Fig. 12.19

$$\beta_{LR} \sim 0.602 \tag{12.57}$$

so that $T_{LR}/8 = 0.208$ which is much lower than $T_R = 0.605$.

The previous studies of this model by Nelson (1982) and by Strandburg *et al.* (1983) were performed on a triangular lattice for which the Laplacian reads

$$\bar{\nabla}\cdot\nabla\bar{\chi} \equiv \frac{2}{3}\sum_{\pm\mathbf{i}} (\chi(\mathbf{x}+\mathbf{i}) - \chi(\mathbf{x})) \tag{12.58}$$

and the vector $\mathbf{i}$ denotes the three oriented links

$$\mathbf{1} = (1, 0), \quad \mathbf{2} = \left(-\frac{1}{2}, +\frac{\sqrt{3}}{2}\right), \quad \mathbf{3} = \left(-\frac{1}{2}, -\frac{\sqrt{3}}{2}\right). \tag{12.59}$$

In momentum space, one has

$$\mathbf{K}\cdot\bar{\mathbf{K}} = \tfrac{2}{3}\{6 - 2[\cos(\mathbf{1}\cdot\mathbf{k}) + \cos(2\cdot\mathbf{k}) + \cos(\mathbf{3}\cdot\mathbf{k})]\}, \tag{12.60}$$

which for small $\mathbf{k}$ behaves correctly like $\mathbf{k}^2$.

The energy is the square of the expression (12.58). In analogy with (12.54), (12.55) it can be rewritten as follows:

FIG. 12.21. Monte Carlo data on the specific heat of the Laplacian roughening model on triangular lattices of various sizes $N = L^2$ whose finite-size scaling behavior $c = AN + B$ indicates a first order transition [(from W. Janke and D. Toussaint (1986)].

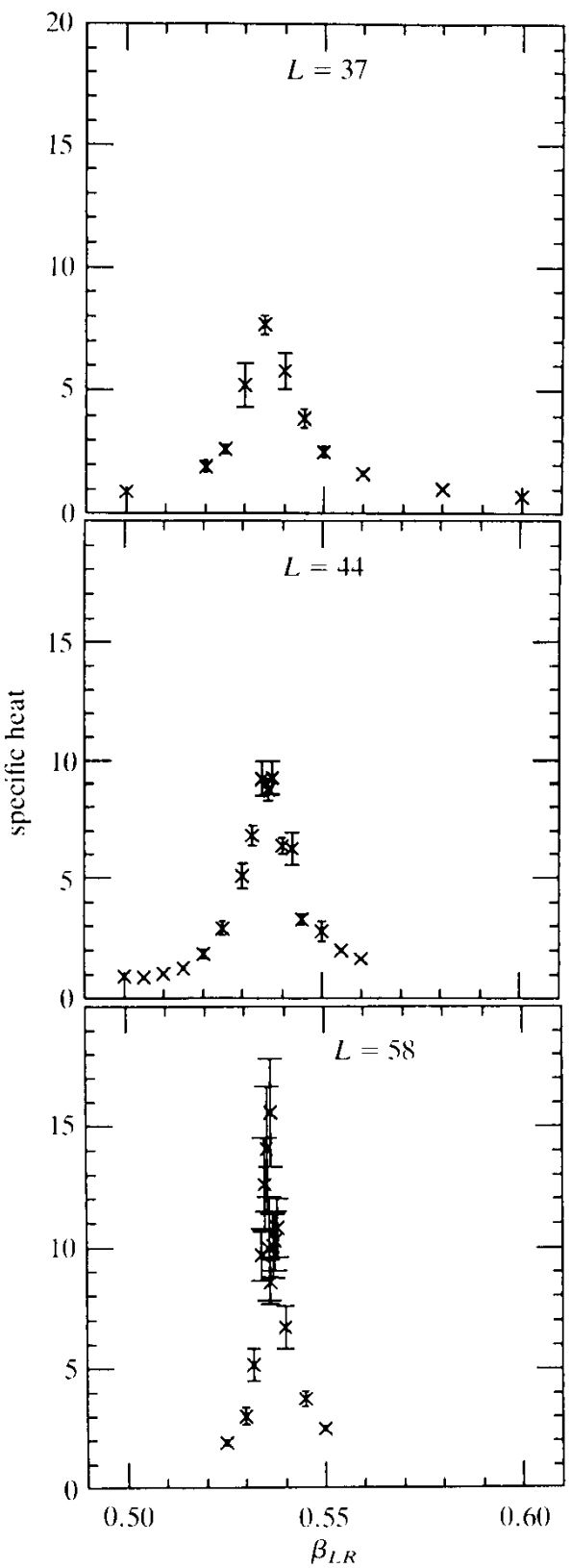

$$\sum_{\mathbf{x}} (\bar{\nabla}\cdot\nabla\bar{\chi}(\mathbf{x}))^2$$

$$= \frac{4}{9}\sum_{\mathbf{x}}\left\{42\bar{\chi}(\mathbf{x})^2 - 12\sum_{\pm\mathbf{i}}\bar{\chi}(\mathbf{x}+\mathbf{i})\bar{\chi}(\mathbf{x}) + \sum_{\substack{\pm\mathbf{i},\,\pm\mathbf{j}\\ \mathbf{i}\neq\mathbf{j}}}\bar{\chi}(\mathbf{x}+\mathbf{i}-\mathbf{j})\bar{\chi}(\mathbf{x})\right\}$$

$$= \frac{4}{9}\sum_{\mathbf{x}}\left\{42\bar{\chi}(\mathbf{x})^2 - 12\sum_{\pm\mathbf{i}}\bar{\chi}(\mathbf{x}+\mathbf{i})\bar{\chi}(\mathbf{x}) + 2\sum_{\pm\mathbf{i}}\chi(\mathbf{x}+\mathbf{i})\chi(\mathbf{x})\right.$$

$$\left. + 2\sum_{\pm\boldsymbol{\mu}}\bar{\chi}(\mathbf{x}+\boldsymbol{\mu})\chi(\mathbf{x}) + \sum_{\pm\boldsymbol{\alpha}}\bar{\chi}(\mathbf{x}+\boldsymbol{\alpha})\chi(\mathbf{x})\right\}$$

$$= \frac{4}{9}\sum_{\mathbf{x}}\bar{\chi}(\mathbf{x})\left\{42\bar{\chi}(\mathbf{x}) - 10\sum_{\pm\mathbf{i}}\bar{\chi}(\mathbf{x}+\mathbf{i}) + 2\sum_{\pm\boldsymbol{\mu}}\bar{\chi}(\mathbf{x}+\boldsymbol{\mu}) + \sum_{\pm\boldsymbol{\alpha}}\bar{\chi}(\mathbf{x}+\boldsymbol{\alpha})\right\}. \tag{12.61}$$

In this form the Monte Carlo runs are easiest to perform.

As with (12.56) there is yet another version

$$\sum_{\mathbf{x}} (\bar{\nabla}\cdot\nabla\bar{\chi}(\mathbf{x}))^2 = \frac{4}{9}\sum_{\mathbf{x}}\left\{5\sum_{\pm\mathbf{i}}(\bar{\chi}(\mathbf{x}+\mathbf{i}) - \bar{\chi}(\mathbf{x}))^2 - \sum_{\pm\boldsymbol{\mu}}(\bar{\chi}(\mathbf{x}+\boldsymbol{\mu}) - \bar{\chi}(\mathbf{x}))^2\right.$$

$$\left. - \frac{1}{2}\sum_{\pm\boldsymbol{\alpha}}(\bar{\chi}(\mathbf{x}+\boldsymbol{\alpha}) - \bar{\chi}(\mathbf{x}))^2\right\}, \tag{12.62}$$

in which the first term

$$\frac{10}{3}\sum_{\mathbf{x}}\bar{\chi}(\mathbf{x})(-\bar{\nabla}\cdot\nabla)\bar{\chi}(\mathbf{x}) \tag{12.63}$$

corresponds to the ordinary discrete Gaussion model and the other two terms represent next-nearest and second nearest neighbor corrections.

The simulation of this model by Strandburg *et al.* (1983) focused attention upon the long-range behavior of the correlation functions, as first suggested by Nelson (1982). From a change in this behavior they deduce two closely spaced continuous transitions at

$$T_{LR}^{(1)} = 1.825 \pm 0.025, \tag{12.64}$$

and at

$$T_{LR}^{(2)} = 1.925 \pm 0.025. \tag{12.65}$$

FIG. 12.22. The linear growth of the peak in the specific heat with size (= two-dimensional volume) characteristic of a finite-size δ-function and thus for a first-order transition [Janke and Kleinert (1988)].

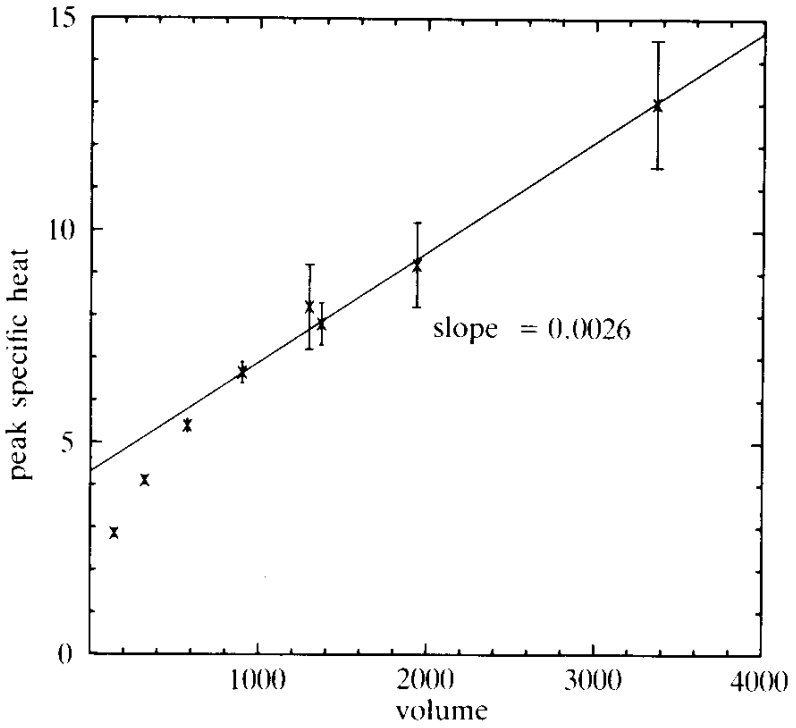

As far as the melting transition is concerned, this would mean that the crystalline order breaks down in two successive steps. In the first step, the translational order breaks down leading to a phase in which the atoms can move around freely but only along the six crystalline directions (hexatic phase). The second step destroys this remaining directional memory and leads to a completely disordered state.

On the basis of our own data we believe that these results are not trustworthy for three reasons.

(i) The Monte Carlo iterations of the model equilibriate very slowly since the interaction energy involves nearest and next-nearest neighbors.

(ii) The correlation function cannot distinguish whether the system is in a uniform phase during a continuous phase transition or in a mixed phase during a first-order phase transition.

(iii) The size of the lattice was not large enough to see the effect of a very weak first-order transition.

Our doubts were enhanced when reinvestigating the order of the transition on a square lattice [W. Janke and H. Kleinert (1986)], which gave only a single weak first order transition. This prompted a repetition of the simulation of the triangular model by W. Janke and D. Toussaint (1986) with much higher statistics than the one by Strandburg *et al* (1983). The

FIG. 12.23. Finite-size behaviour of peak positions in the specific heat of the Laplacian roughening model on an $L \times L$ triangular lattice. The intercept gives the transition point [Janke and Kleinert (1988)].

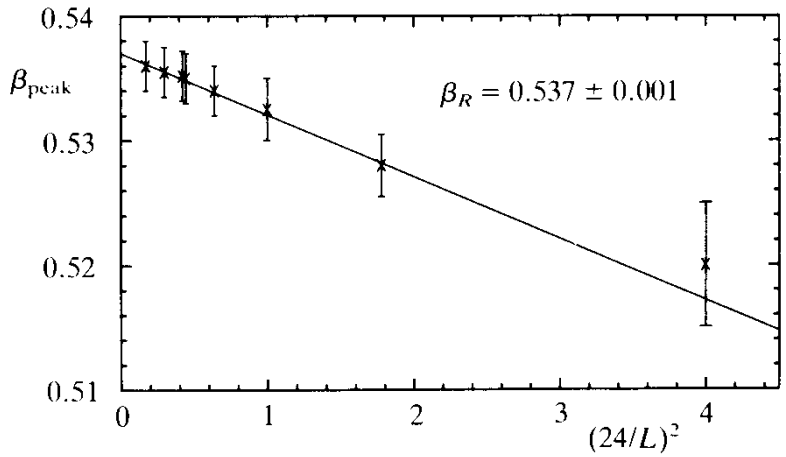

result suggests that the model on the triangular lattice has the same weak first order transition as on the square lattice.

A further simulation of the triangular model was performed recently by Strandburg (1986), ignoring any work that had appeared after Strandburg *et al.* (1983). The conclusion of a finite-size scaling analysis was, once more, that the model has two successive continuous transitions. By comparison with the work of Janke and Toussaint it appeared that Strandburg had not gone to large enough lattices to see the finite-size scaling associated with the first order transition of the model. This was confirmed in a high statistics study by Janke and Kleinert (1988) [see Fig. 12.22]. Figure 12.23 shows the finite size scaling of the transition point.

This transition will be discussed in more detail in Chapter 14.

NOTES AND REFERENCES

The transition entropy and their relation to the volume change is discussed in
M. Lasocka, *Phys. Lett.* **51A** (1975) 137.
See also
S.M. Stishov, I.N. Makarenko, V.A. Ivanov, and A.M. Nikolaenko, *Phys. Lett.* **45A** (1973) 18,
J.L. Tallon, *Phys. Lett.* **76A** (1980) 139,
K. Ohashi and Y.It. Ohashi, *Phys. Lett.* **86A** (1981) 179.
A general review of specific heats in solids is found in
G.G. Borelius, *Solid State Physics* **15** (1963) 2.

The thermal expansion was removed from c_P to get $c_V = c_P - \alpha^2 \kappa T$ [recall (7.96)] for a few materials by
G. Grimwall, *Phys. Scripta* **11** (1975) 381.
The Monte Carlo simulations were performed in three dimensions by

W. Janke and H. Kleinert, *Phys. Rev.* **B33** (1986) 6346 and also in two dimensions by
W. Janke and H . Kleinert, *Phys. Lett.* **114A** (1986) 255,
for square lattices and by
K.J. Strandburg, S.A. Solla and G.V. Chester, *Phys. Rev.* **B28** (1983) 2717,
W. Janke and D. Toussaint, *Phys. Lett.* **116A** (1986) 387,
K. Strandburg, *Phys. Rev. Lett.* **B34** (1986) 3536,
for triangular lattices.
After this text was written, D. Nelson drew my attention to a paper by D.A. Bruce, *Material Science Forum* **4** (1985) 51, who claims to have observed the same behavior on a square lattice as Stransburg *et al.* (1983) on a triangular one, in contradiction with Janke and Kleinert (1986), probably for the same reason discussed in the text. See also the theoretical paper by
D. Nelson, *Phys. Rev.* **B26** (1982) 269,
proposing the phenomena claimed to have been observed by Strandburg *et al.* (1983).
Recent work is contained in
W. Janke and H. Kleinert, *Phys. Lett.* **A** (1988), in press.

CHAPTER THIRTEEN

THE MELTING MODEL OF THE COSINE TYPE

For comparison we shall now investigate the melting transition in the cosine form of our model as defined in Eq. (9.147). For simplicity, let us omit the β dependent prefactors and consider the slightly modified partition function,

$$Z' = \prod_{\mathbf{x},i}\left[\int_{-\pi}^{\pi}\frac{d\gamma_i(\mathbf{x})}{2\pi}\right]\prod_{\mathbf{x},i<j}\left[\int_{-\pi}^{\pi}\frac{d\gamma_{ij}(\mathbf{x})}{2\pi}\sqrt{4\pi\beta\gamma}\right]$$
$$\times\exp\left\{\beta V^{-1}\sum_{\mathbf{x},i<j}\cos(\nabla_i\gamma_j+\nabla_j\gamma_i)\right.$$
$$\left.+\left(\beta\gamma\frac{\lambda}{\mu\xi}\right)V^{-1}\sum_{\mathbf{x},i}\cos\left(\nabla_i\gamma_i-\sum_j\gamma_{ij}(\mathbf{x}+\mathbf{i})\right)+(2\beta\gamma)V^{-1}\sum_{\mathbf{x},i<j}\cos\gamma_{ij}(\mathbf{x})\right\}. \tag{13.1}$$

In the last chapter we saw that the parameter λ produced little change in the transition temperature and entropy. We may therefore confine our attention to the case of $\lambda = 0$ for which $\gamma = D\xi + 2\mu\xi^2/\lambda \to \infty$ and the angular integrations over γ_{ij} are frozen out, leading to the partition function [compare (9.126)]

$$Z' \underset{\lambda \to 0}{=} \prod_{\mathbf{x},i} \left[\int_{-\pi}^{\pi} \frac{d\gamma_i(\mathbf{x})}{2\pi} \right] e^{\beta V^{-1} \Sigma_{\mathbf{x},i<j} \cos(\nabla_i \gamma_j + \nabla_j \gamma_i) + (2\beta\xi) V^{-1} \Sigma_{\mathbf{x},i} \cos(\nabla_i \gamma_i)}. \tag{13.2}$$

In order to simplify the notation we shall, from now on, omit the subscript V^{-1} and study the model as a function of β and ξ in its own right.

13.1. INEQUALITY FOR FREE ENERGY AND THE MEAN-FIELD APPROXIMATION

A study of this partition function within the mean-field aproximation becomes possible by observing that Z' can be expressed in terms of pure phase variables

$$U_i(\mathbf{x}) = e^{i\gamma_i(\mathbf{x})} \tag{13.3}$$

as follows:

$$Z' = \prod_{\mathbf{x},i} \left[\int_{-\pi}^{\pi} \frac{d\gamma_i(\mathbf{x})}{2\pi} \right] \exp \mathrm{Re} \left\{ \beta \sum_{\mathbf{x},i<j} U_i(\mathbf{x})\, U_j^{\dagger}(\mathbf{x}+\mathbf{i})\, U_i^{\dagger}(\mathbf{x}+\mathbf{j})\, U_j(\mathbf{x}) + 2\beta\xi \sum_{\mathbf{x},i} U_i^{\dagger}(\mathbf{x})\, U_i(\mathbf{x}+\mathbf{i}) \right\}. \tag{13.4}$$

The arrangement of the $U_i(\mathbf{x})$ variables in the first term can be pictured by a distortion graph around the site $\mathbf{x}$

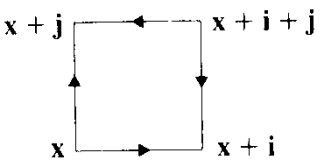

where each $U_i(\mathbf{x})$ is represented by a displacement arrow along the link $\mathbf{i}$ with $U_i^{\dagger}(\mathbf{x})$ pointing in the opposite direction.

Using the variational methods described in Part II, Section 5.1, we can now derive an upper bound for the free energy. For the trial partition function we choose the simplest product of independent one-link integrals,

$$Z_0 \equiv \prod_{\mathbf{x},i} \left[\int_{-\pi}^{\pi} \frac{d\gamma_i(\mathbf{x})}{2\pi} \right] e^{-\beta F_0[\gamma_i]} \equiv \prod_{\mathbf{x},i} \left[\int \frac{d\gamma_i(\mathbf{x})}{2\pi} \right] e^{\alpha \Sigma_{\mathbf{x},i} \mathrm{Re}\, U_i(\mathbf{x})} = \prod_{\mathbf{x}} I_0(\alpha)^D, \tag{13.5}$$

where α is the analogue to the magnetic field used in the ansatz (4.28) for the XY model. We now take the positive normalized measure

$$\prod_{\mathbf{x}} \int d\mu(\mathbf{x}) \equiv \frac{1}{Z_0} \prod_{\mathbf{x},i} \left[\int_{-\pi}^{\pi} \frac{d\gamma_i(\mathbf{x})}{2\pi} \right] e^{-\beta E_0[\gamma_i]} \tag{13.6}$$

and denote expectation values within this measure by $\langle\ \rangle_0$. Then we rewrite the partition function in the form

$$Z' = Z_0 \prod_{\mathbf{x}} \left[\int d\mu(\mathbf{x}) \right] e^{-\beta(E'[\gamma_i] - E_0[\gamma_i])}, \tag{13.7}$$

where

$$\beta E'[\gamma_i] = \beta \sum_{\mathbf{x},i<j} \cos(\nabla_i \gamma_j + \nabla_j \gamma_i) + 2\beta\xi \sum_{\mathbf{x},i} \cos \nabla_i \gamma_i. \tag{13.8}$$

Now we make use of Peierls' inequality, as in (II.5.12), and obtain the bound

$$-\beta F' \geq -\beta F_0 - \beta \langle E'[\gamma_i] - E_0[\gamma_i] \rangle_0. \tag{13.9}$$

The expectation value of E_0 is found in the same way as in (II.5.16): Since Z_0 is a product of independent integrals on link variables $U_i(\mathbf{x})$, the expectation values of all $U_i(\mathbf{x})$ is the same:

$$\begin{aligned} \langle U_i(\mathbf{x}) \rangle_0 &= \int d\mu(\mathbf{x})\, U_i(\mathbf{x}) = \frac{1}{Z_0} \int_{-\pi}^{\pi} \frac{d\gamma_i(\mathbf{x})}{2\pi} e^{\alpha \sum_{\mathbf{x},i} U_i(\mathbf{x})} U_i(\mathbf{x}) \\ &= \frac{1}{Z_0} \frac{\partial}{\partial \alpha} Z_0 = \frac{1}{I_0^D(\alpha)} \frac{d}{d\alpha} I_0^D(\alpha) = D \frac{I_1(\alpha)}{I_0(\alpha)}. \end{aligned} \tag{13.10}$$

Let us call this expectation value u

$$u \equiv \langle U_i(\mathbf{x}) \rangle_0 = D \frac{I_1(\alpha)}{I_0(\alpha)}. \tag{13.11}$$

Then we can calculate

$$\langle E_0[\gamma_i]\rangle_0 = \sum_{\mathbf{x},i} \alpha \langle U_i(\mathbf{x})\rangle_0 = ND\alpha u. \tag{13.12}$$

The expectation value of the full energy (13.8) is found as follows:

$$\begin{aligned}\beta\langle E'[\gamma_i]\rangle_0 = \prod_{\mathbf{x}}\left[\int d\mu(\mathbf{x})\right]\Bigg(&\beta\,\mathrm{Re}\sum_{\mathbf{x},i<j} U_i(\mathbf{x})\,U_j^\dagger(\mathbf{x}+\mathbf{i})\,U_i^\dagger(\mathbf{x}+\mathbf{j})\,U_j(\mathbf{x}) \\ &+ 2\beta\xi\,\mathrm{Re}\sum_{\mathbf{x},i} U_i^\dagger(\mathbf{x})\,U_i(\mathbf{x}+\mathbf{i})\Bigg) \\ &= N\left(\beta\frac{D(D-1)}{2}u^4 + 2\beta\xi D u^2\right).\end{aligned}$$

Inserting this, together with (13.12), into (13.9) we find the following bound for the energy density,

$$-\beta f' \geq \beta\frac{D(D-1)}{2}u^4 + 2\beta\xi D u^2 - D\alpha u + D\log I_0(\alpha). \tag{13.13}$$

This free energy has an important property: when changing β, one changes directly the *quartic* term u^4. This is in contrast with the XY model, where only the quadratic term has a β factor. As we can see immediately, it is this property which makes the melting transition first-order.

The value of u in the free energy is given by (13.11), but just as in the XY model, we can see that we might as well allow u to be an arbitrary variable and determine it by maximizing the right-hand side in α *and* u, independently. This gives the two equations

$$u = I_1(\alpha)/I_0(\alpha), \tag{13.14a}$$

$$2[\beta(D-1)u^3 + 2\beta\xi u] = \alpha. \tag{13.14b}$$

The β-dependent u^4 term in (13.13) appears here as a cubic u^3 term which leads naturally to a first-order transition. This goes as follows. In the limit $\alpha \to 0$, β approaches the value $\beta_d = 1/2\xi$ with $f' = 0$. This is the point at which the mean-field solution $u = 0$, $\alpha = 0$ destabilizes. As α increases, the free energy $-f'$ decreases first from zero to negative values, then, starting from, say, β_s it turns around and begins to grow monotonically [see Fig. 13.1]. In the region $\beta_s < \beta < \beta_d$, the free energy as a function of

FIG. 13.1. Signal for the first order transition at β_m. As α is increased from zero, the free energy moves along the arrow. The potentials are visualized on top of the figure.

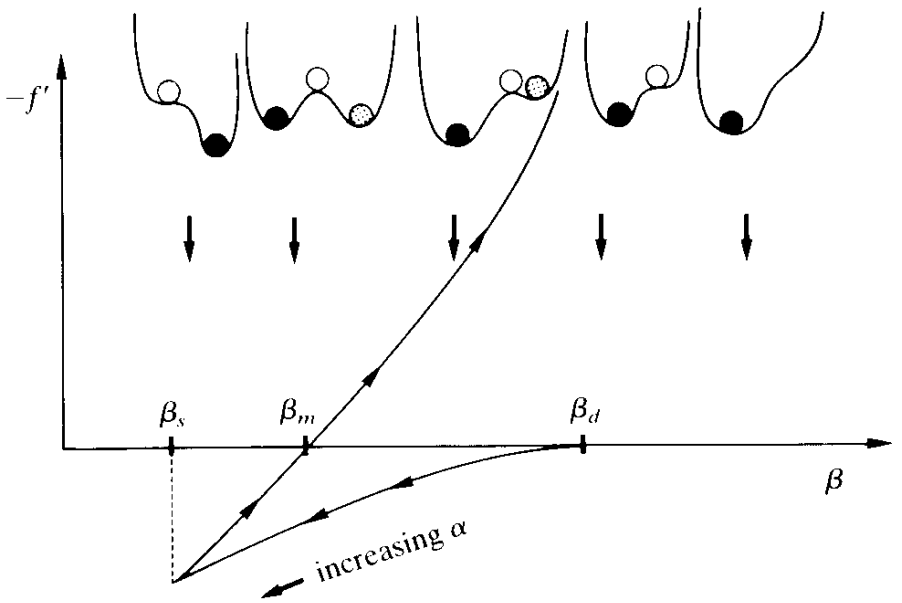

α and u has two minima (one at the field origin and one away from it), and one maximum (between the two minima). The phase transition occurs at a place β_m when the free energy at the second minimum passes through zero. There, the order parameters α and u jump from zero to a finite value. This is the signal for a first-order transition. In order to be specific, let us fix ξ to be 0.25, 0.5, 0.75, 1. Then we take α from zero to infinity, calculate $u(\alpha)$ from (13.14a) and $\beta(\alpha)$ from (13.14b). The resulting functions can then be inserted into (13.13) and we obtain the free energy $-f'$ as shown in Fig. 13.2 for $D = 3$. The transition points extracted from this are plotted in Fig. 13.3 as a function of ξ and tabulated in Table 13.1.

In $D = 2$ dimensions, the situation is somewhat different as shown in Figs. 13.4, 13.5 and listed in Table 13.2. Only for $\xi < 1$ is there a first order transition at the mean-field level. For $\xi \geq 1$ the transition is of second order. In fact, close to $\xi \approx 1$ the mean-field free energy has the Landau expansion

$$-\beta f'^{\mathrm{MF}} = \left(\beta\xi - \frac{1}{2}\right)\alpha^2 + \frac{1}{2^5}(1-\xi)\,\alpha^4 - \frac{5}{2^7 \cdot 3^2}\alpha^6 + \ldots, \quad (13.15)$$

which clearly shows that the point $\xi = 1$ is tricritical. We shall see later that fluctuation corrections change this result drastically with the consequence that melting in the two-dimensional cosine model is always a first order transition.

FIG. 13.2. The free energy of the cosine melting model as a function of $\beta\xi$ for various values of ξ in three dimensions. The intercepts between the high temperature expansion and the one-loop corrected mean field gives the transition points ($\beta_m = 1.69, 1.19, 0.95, 0.80, 0.71$ for $\xi = 0.25, 0.5, 0.75, 1.0, 1.25$). They are compared with Monte Carlo data in Table 13.1. The one-loop corrections can be taken in its limiting from (13.67) [i.e., involving only the pure phonon fluctuation determinant calculated in (9.87)]. The full one-loop correction shows practically no deviation from this down to the transition point. It merely changes the curves in the irrelevant neighborhood of the mean-field transition point (where the dashed curve intercepts the $\beta\xi$ axis) as indicated by the dotted curved bottom piece for $\xi = 1$.

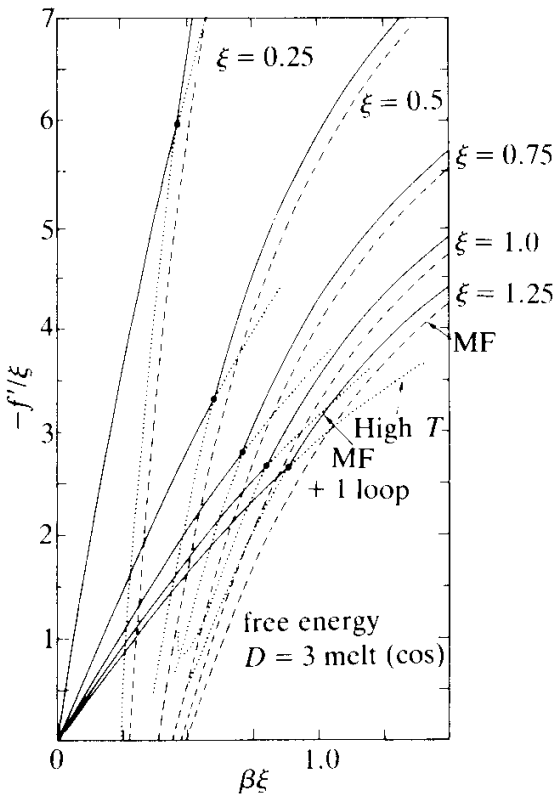

FIG. 13.3. The transition temperature of cosine melting model for $D = 3$, extracted from Fig. 13.2 (see Table 13.1) as compared to the Monte Carlo simulation of Jacobs and Kleinert (1983). They are fitted reasonably well by the formula $\beta_m \approx 0.77\xi^{-0.597}$.

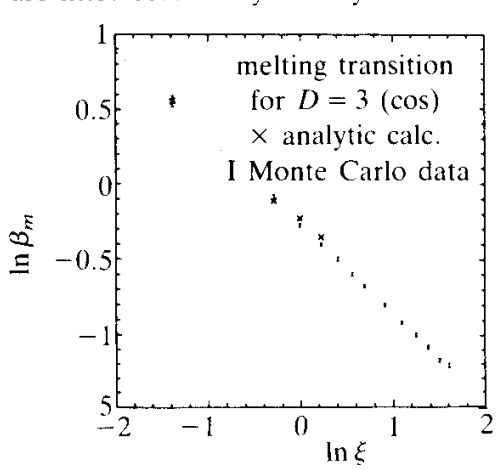

TABLE 13.1. Transition data of the $D = 3$ cosine melting model from various sources, in particular, the intersection of mean-field-plus-one-loop with the temperature curves (LT, HT). The sixth column shows the empirical best fit to the ξ dependence of β_m.

ξ	$\beta_{\text{dest}}^{\text{MF}}$	β_m^{HF}	$\beta_m^{\text{LT,HT}}$	β_m^{MC}	$0.77\xi^{-0.597}$	$\Delta s^{\text{LT,HT}}$	Δs^{MC}
0.25	2.00	1.09	1.69	1.73	1.76	1.68	1.64
0.50	1.00	0.77	1.19	1.17	1.16	1.77	1.58
0.75	0.67	0.59	0.95	0.91	0.91	1.65	1.45
1.00	0.50	0.47	0.80	0.786	0.77	1.45	1.33
1.25	0.40	0.40	0.71	0.67	0.67	1.20	1.20

FIG. 13.4. The free energy of cosine melting model in two dimensions, taken from Ami and Kleinert (quoted in the Notes and References). From the intercepts we extract the transition values $\beta_m = 4.46, 2.30, 1.71, 1.38, 1.18, 1.04$ for $\xi = 0.2, 0.4, 0.6, 0.8, 1.0, 1.2$ as compared to Monte Carlo data 2.35 ± 0.05, 1.36 ± 0.02, 1.15 ± 0.05 for $\xi = 0.4, 0.8, 1.0$ and obtained by Janke and Kleinert (see Fig. 13.5). The approximation has a second-order transition for $\xi = 1$.

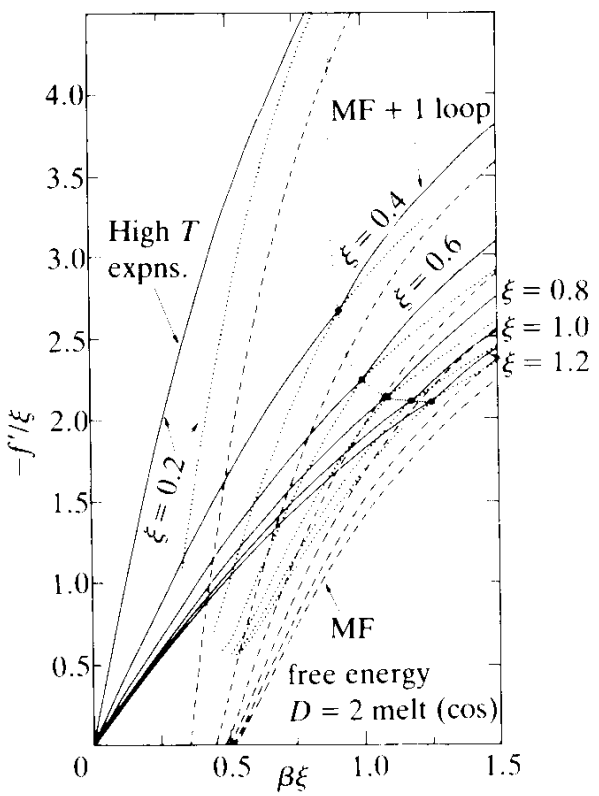

The internal energy per site is given by

$$u'^{\text{MF}} = -\frac{\partial}{\partial\beta}(-\beta f'^{\text{MF}}) = -D\left[\frac{D-1}{2}u^4 + 2\xi u^2\right] = \frac{1}{N}\langle E\rangle \tag{13.16}$$

and is shown in Fig. 13.6 for $D = 3$ and in Fig. 13.7 for $D = 2$ (more

FIG. 13.5. The transition temperatures of the cosine melting model for $D = 2$ (extracted from Fig. 13.4) as compared with the Monte Carlo data of Janke and Kleinert (1984). A reasonable fit is $\beta_m \approx 1.15\xi^{-0.78}$.

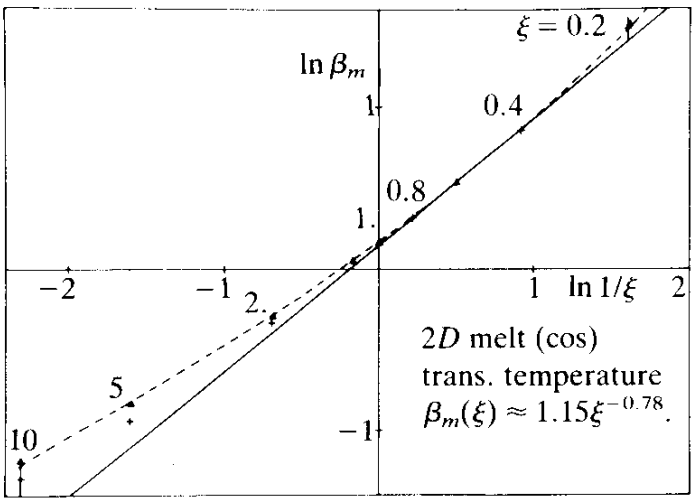

precisely, the figures give $u^{MF} = u'^{MF} + D[(D-1)/2 + 2\xi]$. Notice how in the latter case, the curves for $\xi = 1.0$ and 1.2 display the second order transition at the mean-field level.

The entropy per site is given in terms of the internal energy u'^{MF} and the free energy f'^{MF} by

$$s^{MF} = \beta u'^{MF} - \beta f'^{MF}. \tag{13.17}$$

Since f' is continuous, the transition entropy is determined by the jump in the internal energy u',

$$\Delta s = \beta \Delta u'. \tag{13.18}$$

Then if Δu^p denotes the jump in the powers p of the order parameter u,

$$\Delta s^{MF} = -\left[\beta \frac{D(D-1)}{2} \Delta u^4 + 2\beta\xi D \Delta u^2\right]. \tag{13.19}$$

Using the fact that $-\beta f'$ is zero just above and below the transition, one has

$$\beta \frac{D(D-1)}{2} \Delta u^4 + 2\beta\xi D \Delta u^2 = \Delta(D\alpha u - D \log I_0(\alpha)), \tag{13.20}$$

so that Δs can also be rewritten in the form

$$\Delta s^{\mathrm{MF}} = \Delta(D\alpha u - D \log I_0(\alpha)). \tag{13.21}$$

When comparing the curves with those of the Villain-type model calculated in the last chapter we have to keep in mind that the physical β and $2\beta\xi$ are actually $\beta_{V^{-1}}$ and $(2\beta\xi)_{V^{-1}}$ so that, in fact,

$$\Delta s^{\mathrm{MF}} = -\beta \frac{\partial}{\partial \beta}\left[\beta_{V^{-1}}(\beta) \frac{D(D-1)}{2} \Delta u^4 + (2\beta\xi)_{V^{-1}}(\beta) D\, \Delta u^2 \right]. \tag{13.22}$$

13.2. FLUCTUATIONS AROUND THE MEAN-FIELD SOLUTION

In the XY-model, we were able to derive corrections to the mean-field energy by rewriting the partition function as a theory involving two fluctuating complex fields. The new field energy had the property that the mean-field approximation gave exactly the expression which appeared in the bound for the free energy (13.14). The one-loop correction gave sufficient improvement, resulting in an adequate description of the overall behaviour of $-\beta f'$ in the cold phase up to the neighbourhood of the phase transition.

We shall now follow the same approach here. For this we first use the trivial identity (II.5.74) to liberate the phase variables $U_i(\mathbf{x})$ from the unit circle and rewrite $\mathring{Z}'$ as follows [compare (5.75), Part II]

$$\begin{aligned} Z' = \prod_{\mathbf{x},i} \left[\int_{-i\infty}^{i\infty} \frac{d\alpha_{i1}(\mathbf{x})}{2\pi i} \frac{d\alpha_{i2}(\mathbf{x})}{2\pi i} \right] \prod_{\mathbf{x},i} \left[\int_{-\infty}^{\infty} du_{i1}(\mathbf{x})\, du_{i2}(\mathbf{x}) \right] \\ \times \exp\left\{ \mathrm{Re}\left[\beta \sum_{\mathbf{x},i<j} u_i(\mathbf{x})\, u_j^{\dagger}(\mathbf{x}+\mathbf{i})\, u_i^{\dagger}(\mathbf{x}+\mathbf{j})\, u_j(\mathbf{x}) \right.\right. \\ \left. + 2\beta\xi \sum_{\mathbf{x},i} u_i^{\dagger}(\mathbf{x})\, u_i(\mathbf{x}+\mathbf{i}) \right] - \frac{1}{2} \sum_{\mathbf{x},i} (\alpha_i^{\dagger}(\mathbf{x})\, u_i(\mathbf{x}) + \mathrm{c.c.}) \\ \left. + \sum_{\mathbf{x},i} \log I_0(|\alpha_i(\mathbf{x})|) \right\}, \end{aligned} \tag{13.23}$$

where α_{i1}, u_{i1} and α_{i2}, u_{i2} are the real and imaginary parts of the complex fields α_i, u_i, respectively. Maximizing the exponent gives the equations

$$u = I_1(\alpha)/I_0(\alpha), \tag{13.24}$$

$$2[\beta(D-1)\, u^3 + 2\beta\xi u] = \alpha, \tag{13.25}$$

for each $i = 1, 2, 3$. These are precisely the equations (13.14a,b) and we see that the saddle-point approximation to (13.23) does indeed satisfy the bound (13.13).

Let us now calculate the one-loop corrections to the mean field solution (13.25). For this we rewrite α_i as $\alpha + \delta\alpha_i^\ell + i\delta\alpha_i^t$ and u_i as $u + \delta u_i^\ell + i\delta u_i^t$ and expand the exponent in (13.23) up to quadratic order in $\delta\alpha_i$, δu_i.[a] The linear terms vanish, since α and u lie at the maximum. The quadratic terms can be written in the form

$$-\beta\delta^2 E = -\frac{1}{2}\sum_{\mathbf{x},\mathbf{x}'} (\delta u_i^\ell,\ \delta\alpha_i^\ell)(\mathbf{x})\, M_{ij}^\ell(\mathbf{x},\ \mathbf{x}') \begin{pmatrix} \delta u_i^\ell(\mathbf{x}') \\ \delta\alpha_i^\ell(\mathbf{x}') \end{pmatrix} - \frac{1}{2}\sum_{\mathbf{x},\mathbf{x}'} (\delta u_i^t,\ \delta\alpha_i^t)(\mathbf{x})\, M_{ij}^t(\mathbf{x},\ \mathbf{x}') \begin{pmatrix} \delta u_i^t(\mathbf{x}') \\ \delta\alpha_i^t(\mathbf{x}') \end{pmatrix}. \tag{13.26}$$

The $\delta\alpha\,\delta u$ and $\delta\alpha\,\delta\alpha$ parts of the M matrix are the same as in the XY model, apart from an extra δ_{ij} factor and we can write

$$M^\ell(\mathbf{x},\ \mathbf{x}') = \begin{pmatrix} m_{ij}^\ell(\mathbf{x},\ \mathbf{x}') & -i\,\delta_{ij}\,\delta_{\mathbf{x},\mathbf{x}'} \\ -i\,\delta_{ij}\,\delta_{\mathbf{x},\mathbf{x}'} & \delta_{ij}\dfrac{d^2F}{d\alpha^2}\,\delta_{\mathbf{x},\mathbf{x}'} \end{pmatrix}, \tag{13.27}$$

$$M^t(\mathbf{x},\ \mathbf{x}') = \begin{pmatrix} m_{ij}^t(\mathbf{x},\ \mathbf{x}') & -i\,\delta_{ij}\,\delta_{\mathbf{x},\mathbf{x}'} \\ -i\,\delta_{ij}\,\delta_{\mathbf{x},\mathbf{x}'} & \delta_{ij}\dfrac{1}{\alpha}\dfrac{dF}{d\alpha}\,\delta_{\mathbf{x},\mathbf{x}'} \end{pmatrix}, \tag{13.28}$$

where

$$\frac{dF}{d\alpha} = \frac{1}{\alpha}\frac{I_1(\alpha)}{I_0(\alpha)} = \frac{u}{\alpha}, \quad \frac{d^2F}{d\alpha^2} = \left(\frac{I_1(\alpha)}{I_0(\alpha)}\right)' = \left(1 - \frac{u}{\alpha} - u^2\right), \tag{13.29}$$

and we have rotated the contour of integration in $\delta\alpha_i^t$ to run along the imaginary axis [just as in (II.5.83) and (II.5.84)].

The explicit calculation of the $m_{ij}^{\ell,t}$ matrices governing the δu_i fluctuations requires more work. Consider first the quartic pieces in u_i (of 13.23). They give

[a]The superscripts ℓ and t refer to "longitudinal" and "transverse" with respect to the ground state expectations α, u *in the complex plane* (not to be confused with the polarization directions in space, which are denoted by L and T).

$$\delta^2\left(\frac{1}{2}\sum_{\mathbf{x},\,i<j} u_i^\dagger(\mathbf{x})\,u_j(\mathbf{x}+\mathbf{i})\,u_i(\mathbf{x}+\mathbf{j})\,u_j^\dagger(\mathbf{x}) + \text{c.c.}\right)$$

$$= \frac{u^2}{2}\sum_{\mathbf{x},\,i<j} [\delta u_i^\dagger(\mathbf{x})\,\delta u_j(\mathbf{x}+\mathbf{i}) + \delta u_i^\dagger(\mathbf{x})\,\delta u_i(\mathbf{x}+\mathbf{j}) + \delta u_i^\dagger(\mathbf{x})\,\delta u_j^\dagger(\mathbf{x})$$

$$+ \delta u_j(\mathbf{x}+\mathbf{i})\,\delta u_i(\mathbf{x}+\mathbf{j}) + \delta u_j^\dagger(\mathbf{x})\,\delta u_j(\mathbf{x}+\mathbf{i}) + \delta u_j^\dagger(\mathbf{x})\,\delta u_i(\mathbf{x}+\mathbf{j}) + \text{c.c.}]$$

$$= \frac{u^2}{4}\sum_{\mathbf{x},\,i\neq j} [\delta u_i^\dagger(\mathbf{x})(1+\nabla_i)\,\delta u_j(\mathbf{x}) + \delta u_i^\dagger(\mathbf{x})(1+\nabla_j)\,\delta u_i(\mathbf{x}) + \delta u_i^\dagger(\mathbf{x})\,\delta u_j^\dagger(\mathbf{x})$$

$$+ (1+\nabla_j)\,\delta u_i(\mathbf{x})(1+\nabla_i)\,\delta u_j(\mathbf{x}) + \delta u_j^\dagger(\mathbf{x})(1+\nabla_i)\,\delta u_j(\mathbf{x})$$

$$+ \delta u_j^\dagger(\mathbf{x})(1+\nabla_j)\,\delta u_i(\mathbf{x}) + \text{c.c.}]$$

$$= \frac{u^2}{4}\sum_{\mathbf{x},\,i\neq j} [2\delta u_i^\dagger(\mathbf{x})(1+\nabla_i)\,\delta u_j(\mathbf{x}) + 2\delta u_i^\dagger(\mathbf{x})(1+\nabla_j)\,\delta u_i(\mathbf{x})$$

$$+ \delta u_i^\dagger(\mathbf{x})\,\delta u_j^\dagger(\mathbf{x}) + \delta u_i^\dagger(\mathbf{x})(1-\bar{\nabla}_j+\nabla_i-\nabla_i\bar{\nabla}_j)\,\delta u_j(\mathbf{x}) + \text{c.c.}]. \qquad (13.30)$$

The second term can be reorganized slightly as follows

$$\sum_{\mathbf{x},\,i\neq j} \delta u_i^\dagger(\mathbf{x})(1+\nabla_j)\,\delta u_i(\mathbf{x})$$

$$= 2\sum_{\mathbf{x},\,i} \delta u_i^\dagger(\mathbf{x})\,\delta u_i(\mathbf{x}) + \sum_{\substack{\mathbf{x},\,i \\ i,j,k=\text{cyclic}}} \delta u_i^\dagger(\nabla_j+\nabla_k)\,\delta u_i(\mathbf{x})$$

$$= 2\sum_{\mathbf{x},\,i} \delta u_i^\dagger(\mathbf{x})\,\delta u_i(\mathbf{x}) + \sum_{\mathbf{x},\,i} \delta u_i^\dagger(\mathbf{x})\sum_{\ell} \nabla_\ell\,\delta u_i(\mathbf{x}) - \sum_{\mathbf{x},\,i} \delta u_i^\dagger(\mathbf{x})\,\nabla_i\,\delta u_i(\mathbf{x})$$

$$= 2\sum_{\mathbf{x},\,i}\left[\delta u_i^\dagger(\mathbf{x})\left(1+\frac{\nabla_\ell\bar{\nabla}_\ell}{4}\right)\delta u_i(\mathbf{x}) - \delta u_i^\dagger(\mathbf{x})\,\nabla_i\,\delta u_i(\mathbf{x})\right]. \qquad (13.31)$$

From these expressions we can easily extract the matrices $m_{ij}^{\ell,t}(\mathbf{x},\mathbf{x}')$ in (13.28). For this, we replace the sum $\Sigma_{i\neq j}$ in (13.30) by $\Sigma_{i,j}(1-\delta_{ij})$, for example:

$$\sum_{\mathbf{x},\,i\neq j} \delta u_i^\dagger(\mathbf{x})(1+\nabla_i)\,\delta u_j(\mathbf{x}) = \sum_{\mathbf{x},\,i,\,j} \delta u_i^\dagger(\mathbf{x})(1-\delta_{ij})(1+\nabla_i)\,\delta u_j(\mathbf{x}).$$

Then the quartic piece gives the following contribution to $m_{ij}^{\ell,t}(\mathbf{x},\mathbf{x}')$:

$$m_{ij}^{\ell,t}(\mathbf{x},\mathbf{x}')|_{\text{quart}} = -\beta u^2\Bigg[2(1-\delta_{ij})(1+\nabla_i) + 4\delta_{ij}\left(1+\frac{\nabla_\ell\bar{\nabla}_\ell}{4}\right) - 2\delta_{ij}\nabla_i \pm (1-\delta_{ij}) \pm (1-\delta_{ij})(1+\nabla_i-\bar{\nabla}_j-\nabla_i\bar{\nabla}_j)\Bigg]\delta(\mathbf{x}-\mathbf{x}'), \tag{13.32}$$

where the upper sign holds for the longitudinal (real part), the lower for the transverse (imaginary) part of δu_i. In the last term we observe that

$$\delta_{ij}(1+\nabla_i+\bar{\nabla}_j-\nabla_i\bar{\nabla}_j) = \delta_{ij}(1+\nabla_i-\bar{\nabla}_i-\nabla_i\bar{\nabla}_i) = \delta_{ij} \tag{13.33}$$

so that the two δ_{ij} terms in the second row are, in fact, the same and cancel. Moreover if we use the fact that between real fields

$$-\sum_{i,j}\delta u_i(\mathbf{x})\,\bar{\nabla}_j\delta u_j(\mathbf{x}) = \sum_{i,j}\nabla_j\delta u_i(\mathbf{x})\,\delta u_j(\mathbf{x}) = \sum_{i,j}\delta u_j(\mathbf{x})\,\nabla_j\delta u_i(\mathbf{x}) = \sum_{i,j}\delta u_i(\mathbf{x})\,\nabla_i\delta u_j(\mathbf{x}), \tag{13.34}$$

then (13.32) reads

$$m_{ij}^{\ell,t}(\mathbf{x},\mathbf{x}')|_{\text{quart}} = -\beta u^2\{[2(1+\nabla_i) \pm 1 \pm (1+2\nabla_i) \mp \nabla_i\bar{\nabla}_j + \delta_{ij}[-2(1+\nabla_i)+4+\nabla_\ell\bar{\nabla}_\ell - 2\nabla_i \pm 2]\}\,\delta_{\mathbf{x},\mathbf{x}'}. \tag{13.35}$$

In momentum space we set $1+\nabla_i = e^{ik_i}$, $1-\bar{\nabla}_i = e^{-ik_i}$ and find

$$\begin{aligned} m_{ij}^{\ell,t}(\mathbf{k})|_{\text{quart}} &= -\beta u^2\left\{\pm(e^{ik_i}\pm 1)(e^{-ik_j}\pm 1) + 2\delta_{ij}\left(\sum_\ell \cos k_\ell - 2\cos k_i \mp 1\right)\right\} \\ &= \beta u^2\begin{cases} -(e^{ik_i}+1)(e^{-ik_j}+1) + \delta_{ij}(\mathbf{K}\cdot\bar{\mathbf{K}} - 2K_i\bar{K}_i - 2(D-3)), \\ K_i\bar{K}_j \qquad\qquad + \delta_{ij}(\mathbf{K}\cdot\bar{\mathbf{K}} - 2K_i\bar{K}_i - 2(D-1)), \end{cases} \end{aligned} \tag{13.36}$$

where we have used the fact that between real fields in $\mathbf{x}$ space only the real parts of the matrix elements contribute.

Consider now the piece quadratic in $u_i(\mathbf{x})$ of (13.23). Its fluctuation energy is

$$2\beta\xi\frac{1}{2}\sum_{\mathbf{x},i}(\delta u_i^{\dagger}(\mathbf{x})(1+\nabla_i)\,\delta u_i(\mathbf{x})+\text{c.c.}) \tag{13.37}$$

so that the matrices $m_{ij}^{\ell,t}(\mathbf{k})$ are extended by

$$m_{ij}^{\ell,t}(\mathbf{k})|_{\text{quadr}} = 4\beta\xi\cos k_i\,\delta_{ij} = 4\beta\xi(1-\tfrac{1}{2}K_i\bar{K}_i)\,\delta_{ij} \tag{13.38}$$

in both the longitudinal and the transverse parts.

Combining all terms, the fluctuation matrices M^{ℓ} and M^{t} read, in momentum space

$$M_{ij}^{\ell}(\mathbf{k}) = \begin{pmatrix} \beta u^2\left\{P^{t}(\mathbf{k})+\delta_{ij}\left[\mathbf{K}\cdot\bar{\mathbf{K}}+2\left(\frac{\xi}{u^2}-1\right)K_i\bar{K}_i-\left(4\frac{\xi}{u^2}+2(D-3)\right)\right]\right\} & -i\delta_{ij} \\ -i\delta_{ij} & \delta_{ij}\left(1-\frac{u}{\alpha}-u^2\right) \end{pmatrix}, \tag{13.39}$$

$$M_{ij}^{t}(\mathbf{k}) = \begin{pmatrix} \beta u^2\left\{P^{t}(\mathbf{k})+\delta_{ij}\left[\mathbf{K}\cdot\bar{\mathbf{K}}+2\left(\frac{\xi}{u^2}-1\right)K_i\bar{K}_i-\left(4\frac{\xi}{u^2}+2(D-3)\right)\right]\right\} & -i\delta_{ij} \\ -i\delta_{ij} & \delta_{ij}\frac{u}{\alpha} \end{pmatrix}, \tag{13.40}$$

where we have introduced the matrices

$$P_{ij}^{\ell} = (e^{ik_i}+1)(e^{-ik_j}+1), \quad P_{ij}^{t} = (e^{ik_i}-1)(e^{ik_j}-1) = K_i\bar{K}_j. \tag{13.41}$$

We now integrate out the $\delta\alpha^{\ell,t}$ fields. This leads to the following fluctuation matrices in $\delta u^{\ell,t}$ space alone:

$$D_{ij}^{\ell}(\mathbf{k}) = \beta u^2\left[-P_{ij}^{\ell}(\mathbf{k})+\mathbf{K}\cdot\bar{\mathbf{K}}\,\delta_{ij}+2\left(\frac{\xi}{u^2}-1\right)K_i\bar{K}_i\,\delta_{ij}-\left(4\frac{\xi}{u^2}+2(D-3)\right)\delta_{ij}\right] + \frac{1}{1-\frac{u}{\alpha}-u^2}\delta_{ij}, \tag{13.42}$$

$$D_{ij}^{t}(\mathbf{k}) = \beta u^2\left[K_i\bar{K}_j+\mathbf{K}\cdot\bar{\mathbf{K}}\,\delta_{ij}+2\left(\frac{\xi}{u^2}-1\right)K_i\bar{K}_i\delta_{ij}-\left(4\frac{\xi}{u^2}+2(D-1)\right)\delta_{ij}\right] + \frac{\alpha}{u}\delta_{ij}. \tag{13.43}$$

We now make use of the extremality condition (13.25) and see that the last two terms in (13.43) cancel. Thus the matrix $D^t_{ij}(\mathbf{k})$ describes massless fluctuations. This was to be expected on the basis of the Nambu-Goldstone theorem, since the imaginary parts of the fields δu^t point along the valley of symmetry in the energy of the disorder field theory (for phase rotations $u \to e^{i\theta}u$, $\alpha \to e^{i\theta}\alpha$). These massless fluctuations describe sound waves in a $T \neq 0$ crystal. In the limit of low temperature, they reduce to the sound waves of the initial elastic energy. Indeed, in this limit, $u \to 1$, $\delta u_i(\mathbf{x}) = iu\,\delta\gamma_i(\mathbf{x}) \to i\delta\gamma_i(\mathbf{x})$ and the fluctuations $\delta u^t_i(\mathbf{x})$ can be identified with $\delta\gamma_i(\mathbf{x})$. Thus the matrix $D^t(\mathbf{k})$ contributes a fluctuation energy

$$\frac{1}{2}\frac{\beta}{N}\sum_{\mathbf{k},i,j}\delta\gamma_i(\mathbf{k})[K_i\bar{K}_j + \mathbf{K}\cdot\bar{\mathbf{K}}\,\delta_{ij} + 2(\xi-1)\,K_i\bar{K}_i\delta_{ij}]\,\delta\gamma_j(\mathbf{k}).$$

This agrees with the fluctuation matrix for the elastic energy (9.10),

$$\frac{E_{\mathrm{el}}}{T} = \frac{\beta}{2}\sum_{\mathbf{x},i,j}\gamma_i(\mathbf{x})[-\nabla_i\bar{\nabla}_j - \nabla\cdot\bar{\nabla}\,\delta_{ij} + 2\nabla_i\bar{\nabla}_i\delta_{ij} - 2\xi\,\nabla_i\bar{\nabla}_i\delta_{ij}]\,\gamma_j(\mathbf{x}) \tag{13.44}$$

after over going to momentum space [see (9.64)].

For increasing temperatures, the matrix $D^t_{ij}(\mathbf{k})$ describes the softening of the elastic constants upon heating. As long as the temperature is still small, the extremality conditions (13.24) and (13.25) can be solved approximately as follows:

$$u \to 1 - \frac{1}{2\alpha} - \frac{1}{8\alpha^2} + O\left(\frac{1}{\alpha^3}\right), \qquad \alpha \to 2(\beta(D-1) + 2\beta\xi). \tag{13.45}$$

Thus u decreases linearly with temperature as

$$u \to 1 - \frac{1}{2\alpha} \to 1 - \frac{1}{4[\beta(D-1) + 2\beta\xi]}. \tag{13.46}$$

It remains to properly normalize the fluctuation energy. For $u \neq 1$ we have

$$\delta u^t_i(\mathbf{x}) = u\,\delta\gamma_i(\mathbf{x}), \tag{13.47}$$

which leads to the elastic energy

$$\frac{E_{\mathrm{el}}}{T} = \frac{1}{2}\frac{1}{N}\sum_{\mathbf{k},i,j} \delta\gamma_i(-\mathbf{k})[\beta u^4(K_i\bar{K}_j + \mathbf{K}\cdot\bar{\mathbf{K}}\,\delta_{ij} - 2K_i\bar{K}_i\delta_{ij}) + 2\beta\xi u^2 K_i\bar{K}_i\delta_{ij}]\delta\gamma_j(\mathbf{k}). \tag{13.48}$$

From this we extract the elastic constants at non-zero temperature,

$$\frac{\mu(T)}{\mu} = u^4, \qquad \frac{\xi(T)}{\xi} = u^2. \tag{13.49}$$

When comparing these results with the experimental softening of the elastic constants one must bear in mind the fact that β and $2\beta\xi$ do not reflect the proper temperatures but the inverse Villain transforms [recall (9.124), (9.125)]. These, in turn, were assumed to contain the softening effects of the cubic terms. Since we have given a detailed study of the temperature behaviour of the elastic constants at an earlier stage we shall refrain from repeating such an analysis within the present model.

The longitudinal modes described by the fluctuation matrix are all massive. The mass reflects the difficulty in creating defects. For low temperature, the mass diverges to infinity. This follows directly from the limit (13.45) according to which

$$\frac{1}{1 - \frac{u}{\alpha} - u^2} \to 2\alpha^2 + O(\alpha) \sim 8[\beta(D-1) + 2\beta\xi]^2, \tag{13.50}$$

which grows like β^2, whereas the gradient terms in grow more slowly, like β [see (13.42)].

13.3. ONE-LOOP CORRECTION TO THE MEAN-FIELD ENERGY

Having analyzed the fluctuation modes we can now turn to calculating their fluctuation determinants. From the integrals over $\delta\alpha_i$ which we performed to arrive at the pure δu_i fluctuation matrices (13.39) and (13.40), there is one trivial contribution to the free energy, which is

$$-\beta f_1^{1\text{ loop}} = -\frac{D}{2}\left[\log\left(1 - \frac{u}{\alpha} - u^2\right) + \log\frac{u}{\alpha}\right]. \tag{13.51}$$

After this, the integrals over $\delta u_i(\mathbf{x})$ produce the determinants $(\mathrm{Det}\, D^\ell)^{-1/2}(\mathrm{Det}\, D^t)^{-1/2}$ which give the remaining free energy at the one-loop level,

$$-\beta f_2^{1\text{ loop}} = -\frac{1}{2}\int \frac{d^D k}{(2\pi)^D}[\mathrm{tr}\log D^\ell(\mathbf{k}) + \mathrm{tr}\log D^t(\mathbf{k})]. \tag{13.52}$$

In order to treat the fluctuations of real and imaginary parts δu on the same footing it is useful to introduce the following abbreviations

$$\varepsilon^\ell = \beta u^2\left(1 - \frac{u}{\alpha} - u^2\right), \qquad \varepsilon^t = \beta u^2 \frac{u}{\alpha}, \tag{13.53}$$

and

$$N_i^{\ell,t} = 1 + \varepsilon^{\ell,t}\left[\mathbf{K}\cdot\bar{\mathbf{K}} + 2\left(\frac{\xi}{u^2} - 1\right)K_i\bar{K}_i - 4\frac{\xi}{u^2} - 2\begin{Bmatrix} D-3 \\ D-1 \end{Bmatrix}\right]. \tag{13.54}$$

Then we can rewrite (13.52) as

$$-\beta f_2^{1\text{ loop}} = \frac{D}{2}\left(\log\left(1 - \frac{u}{\alpha} - u^2\right) + \log\frac{u}{\alpha}\right) - \frac{1}{2}\int \frac{d^D k}{(2\pi)^D}[\mathrm{tr}\log(N_i^\ell\delta_{ij} - \varepsilon^\ell P_{ij}^\ell) + N\log(N_i^t\delta_{ij} + \varepsilon^t P_{ij}^t)]. \tag{13.55}$$

The first part cancels with (13.51) and the full one-loop correction energy becomes

$$-\beta f^{1\text{ loop}} = -\frac{1}{2}\int \frac{d^D k}{(2\pi)^D}\left[\sum_i \cos N_i^\ell + \sum_i N_i^t + \mathrm{tr}\log\left(\delta_{ij} - \varepsilon^\ell \frac{1}{N_i^\ell}P_{ij}^\ell\right) + \mathrm{tr}\log\left(\delta_{ij} + \varepsilon^t \frac{1}{N_i^t}P_{ij}^t\right)\right]. \tag{13.56}$$

In this form, the logarithms can be easily calculated by expanding them into a power series in $P_{ij}^{\ell,t}$:

$$-\sum_{n=1}^{\infty}\frac{1}{n}(\varepsilon^\ell)^n\,\mathrm{tr}\left(\frac{1}{N_i^\ell}P_{ij}^\ell\right)^n - \sum_{n=1}^{\infty}\frac{1}{n}(-\varepsilon^t)^n\,\mathrm{tr}\left(\frac{1}{N_i^t}P_{ij}^t\right)^n. \tag{13.57}$$

The traces can be calculated by observing that due to their factorized forms, the matrices

$$\hat{P}_{ij}^{\ell,t}(\mathbf{k}) = \frac{1}{N_i} P_{ij}^{\ell,t}(\mathbf{k}) \tag{13.58}$$

are essentially projection matrices,

$$(\hat{P}^{\ell}(\mathbf{k}))_{ij}^2 = \sum_n \frac{1}{N_i^{\ell}} P_{in}^{\ell}(\mathbf{k}) \frac{1}{N_n^{\ell}} P_{nj}^{\ell}(\mathbf{k})$$

$$= \sum_n \frac{1}{N_i^{\ell}} 4\cos\frac{k_i}{2}\cos\frac{k_n}{2} \frac{1}{N_n^{\ell}} 4\cos\frac{k_n}{2}\cos\frac{k_j}{2} = \left(\sum_n \frac{4\cos^2 k_n/2}{N_n^{\ell}}\right) \hat{P}_{ij}^{\ell}$$

and similarly

$$(\hat{P}^{t}(\mathbf{k}))_{ij}^2 = \left(\sum_n \frac{4\sin^2 k_n/2}{N_n^{t}}\right) \hat{P}_{ij}^{t}(\mathbf{k}). \tag{13.59}$$

Let us denote the sums on the right-hand side by $C^{\ell,t}(\mathbf{k})$, respectively, i.e.,

$$C^{\ell,t}(\mathbf{k}) = \sum_n \frac{4}{N_n^{\ell,t}} \begin{cases} \cos^2\dfrac{k_n}{2}, \\ \sin^2\dfrac{k_n}{2}. \end{cases} \tag{13.60}$$

Incidentially, these sums are the same as $\operatorname{tr}(\hat{P}_{ij}^{\ell,t}(\mathbf{k}))$. Using the relations

$$\begin{aligned} (\hat{P}^{\ell,t}(\mathbf{k}))_{ij}^n &= C^{\ell,t}(\mathbf{k})^{n-1}\, \hat{P}_{ij}^{\ell,t}(\mathbf{k}), \\ \operatorname{tr}(\hat{P}^{\ell,t}(\mathbf{k}))^n &= C^{\ell,t}(\mathbf{k})^{n-1} \operatorname{tr} \hat{P}^{\ell,t}(\mathbf{k}) = C^{\ell,t}(\mathbf{k})^n, \end{aligned} \tag{13.61}$$

we can rewrite (13.57) as

$$-\sum_{n=1}^{\infty} \frac{1}{n} (\varepsilon^{\ell} C^{\ell}(\mathbf{k}))^n - \sum_{n=1}^{\infty} \frac{1}{n} (-\varepsilon^{t} C^{t}(\mathbf{k}))^n, \tag{13.62}$$

which can now be summed up to

$$\log(1 - \varepsilon^{\ell} C^{\ell}(\mathbf{k})) + \log(1 + \varepsilon^{t} C^{t}(\mathbf{k})). \tag{13.63}$$

We thus arrive at the one-loop correction to the free energy,

$$-\beta f^{1\,\mathrm{loop}} = -\frac{1}{2}\int \frac{d^D k}{(2\pi)^D}\Bigg\{\sum_i (\log N_i^{\ell} + \log N_i^{t}) + \log(1 - \varepsilon^{\ell} C^{\ell}(\mathbf{k})) + \log(1 + \varepsilon^{\ell} C^{t}(\mathbf{k}))\Bigg\}. \tag{13.64}$$

This expression can be calculated numerically and the result is included in Figs. 13.2 and 13.4, where it is added to the mean-field energy (for details see the figure captions).

For very low temperatures, the real modes are very massive and can be neglected. Then only the sound waves contribute. Their contribution is found directly from (13.42), (13.48) by inserting the limits (13.45)

$$\mathrm{tr}\log(D_{ij}^{\ell}(\mathbf{k})) \to D\log\left[1 - \frac{u}{\alpha} - u^2\right]^{-1}, \tag{13.65}$$

$$\mathrm{tr}\log(D_{ij}^{t}(\mathbf{k})) \to \mathrm{tr}\log\beta\left(K_i\overline{K}_j + \mathbf{K}\cdot\overline{\mathbf{K}}\,\delta_{ij} + 2\left(\frac{\xi}{u^2} - 1\right)K_i\overline{K}_i\delta_{ij}\right). \tag{13.66}$$

The term (13.65) cancels with the corresponding term in (13.51). The other term in (13.51) has the limit

$$\frac{D}{2}\log\frac{\alpha}{u} \to \frac{D}{2}\log[2(\beta(D-1) + 2\beta\xi)]$$

and the full one-loop correction becomes, for very low temperatures,

$$-\beta f^{1\,\mathrm{loop}} \underset{\beta\to\infty}{\longrightarrow} \frac{D}{2}\log[2(\beta(D-1) + 2\beta\xi)] - \frac{1}{2}\int \frac{d^D k}{(2\pi)^D}\mathrm{tr}\log[\beta(K_i\overline{K}_j + \mathbf{K}\cdot\overline{\mathbf{K}}\,\delta_{ij} + 2(\xi - 1)K_i\overline{K}_i\delta_{ij})]. \tag{13.67}$$

This has to be added to the mean field energy

$$-\beta f'^{\mathrm{MF}} = \beta \frac{D(D-1)}{2} u^4 + 2\beta\xi D u^2 - D\alpha u + D \log I_0(\alpha). \tag{13.68}$$

Inserting the high β limits for u, α of Eq. (13.45) we find

$$\begin{aligned} -\beta f'^{\mathrm{MF}} \underset{\beta\to\infty}{\longrightarrow} & \beta \frac{D(D-1)}{2} + 2\beta\xi D - \frac{1}{2\alpha} 2D(\beta(D-1) + 2\beta\xi) \\ & - D\alpha\left(1 - \frac{1}{\alpha}\right) + D\alpha - \frac{D}{2}\log(2\pi\alpha) \\ \to & \beta D \frac{(D-1)}{2} + 2\beta\xi D - \frac{D}{2}\log(2\pi\alpha) \\ = & \beta D \frac{(D-1)}{2} + 2\beta\xi D - \frac{D}{2}\log(2\pi \cdot 2[\beta(D-1) + 2\beta\xi]) + O\left(\frac{1}{\beta}\right). \end{aligned} \tag{13.69}$$

Adding to this the one-loop correction (13.67) gives

$$\begin{aligned} -\beta f'^{\mathrm{MF+1\,loop}} \underset{\beta\to\infty}{\longrightarrow} & \beta \frac{D(D-1)}{2} + 2\beta\xi D - \frac{D}{2}\log(2\pi\beta) \\ & - \frac{1}{2}\int \frac{d^D k}{(2\pi)^D} \operatorname{tr} \log(K_i \bar{K}_j + \mathbf{K}\cdot\bar{\mathbf{K}}\,\delta_{ij} + 2(\xi - 1) K_i \bar{K}_i \delta_{ij}). \end{aligned} \tag{13.70}$$

This is just the pure phonon free energy of the partition function (13.2). The first term contains the trivial β dependence of the cosine energies for zero strain. The trace log is the sum of the purely quadratic fluctuations for small displacement fields, where the quadratic part of the cosine energy agrees with the energy of linear elasticity [see (13.44)].

After plotting the sum of the free energy (13.67) and (13.68) in Figs. 13.2 and 13.4, we find, in $D = 2$ and $D = 3$ dimensions, that up to the melting point (i.e., from large β down to β_m) it is practically the same as the complicated full one-loop curve based on a tedious numerical evaluation of (13.64) (see the $\xi = 1$ curve in Fig. 13.2). Taking the derivative with respect to β we obtain the internal energy $u'^{\mathrm{MF}} =$

FIG. 13.6. The internal energy of the $D = 3$ melting model as a function of $\beta\xi$ for different $\xi(= 0.25, 0.5, 0.75, 1.0, 1.25)$. The left-hand branches are the high temperature expansions, the right-hand branches, the mean-field expressions. The one-loop correction practically drops out when forming $-(\partial/\partial\beta)(-\beta f'^{\mathrm{MF}})$. The vertical lines indicate the jumps at the transition temperatures. From these we can calculate the transition entropies $\Delta s = \beta_m \Delta u$ and find the values listed in Table 13.1 and plotted in Fig. 13.14 where they are also compared with Monte Carlo data.

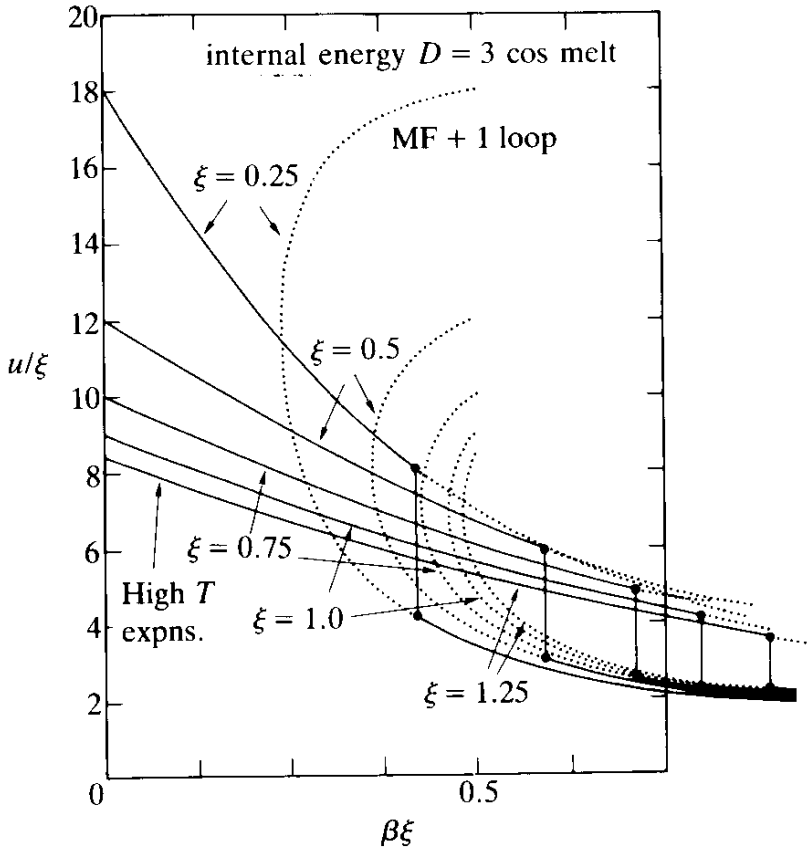

$-(\partial/\partial\beta)(-\beta f'^{\mathrm{MF}})$ as shown in Figs. 13.6, 13.7. Since the one-loop corrections are practically constant, for $\beta \gtrsim \beta_m$, they disappear from the derivative and the high β energies are given directly by the mean field approximation. The curves can be compared with Monte Carlo data and we see that they are in excellent agreement with each other (see, for example, Fig. 13.8 and 13.9).

13.4. HIGH TEMPERATURE EXPANSION OF THE COSINE MELTING MODEL

In order to determine the melting point of the model without recourse to Monte Carlo simulations we have to proceed as in the XY model, calculate the high-temperature expansion of the free energy and see where it intersects with the loop-corrected-mean-field curve. For this, the

FIG. 13.7. The internal energy of the cosine model in two dimensions (from Ami and Kleinert, quoted in the Notes and References). From these curves we read off the entropy jumps as shown in Table 13.2 and compared there with the Monte Carlo data.

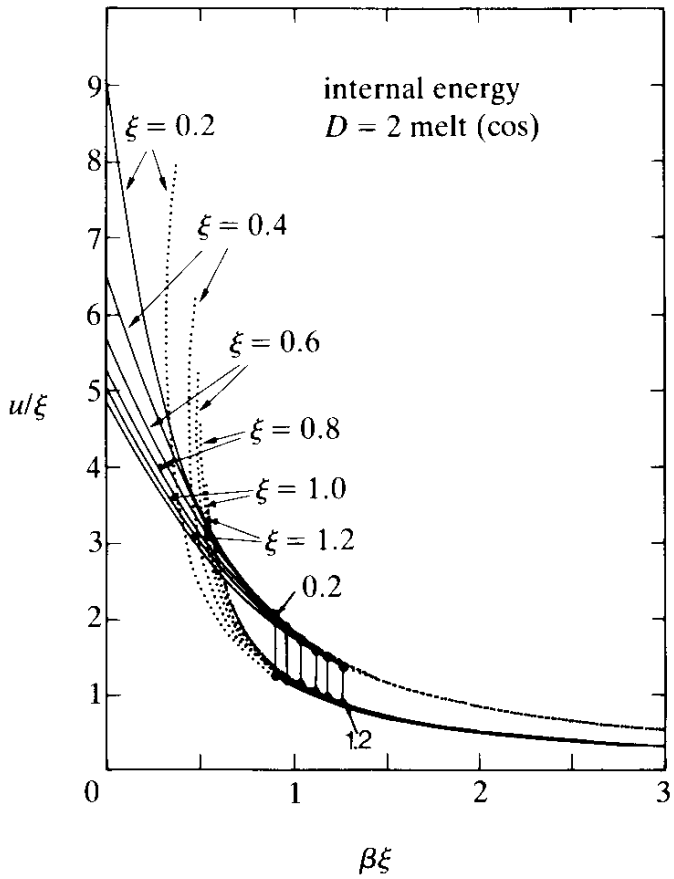

FIG. 13.8. Comparison of the calculated internal energy ($D = 3$) from Fig. 13.6 for $\xi = 1$ with data from Monte Carlo simulations on an 8^3 lattice (see Table 13.3).

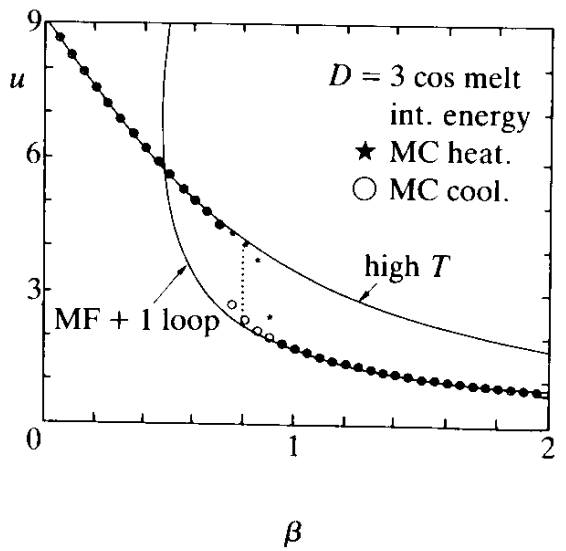

FIG. 13.9. Comparison of the calculated internal energy ($D = 2$) of Fig. 13.7 for $\xi = 1$ with data of the Monte Carlo simulation by Janke and Kleinert (1984).

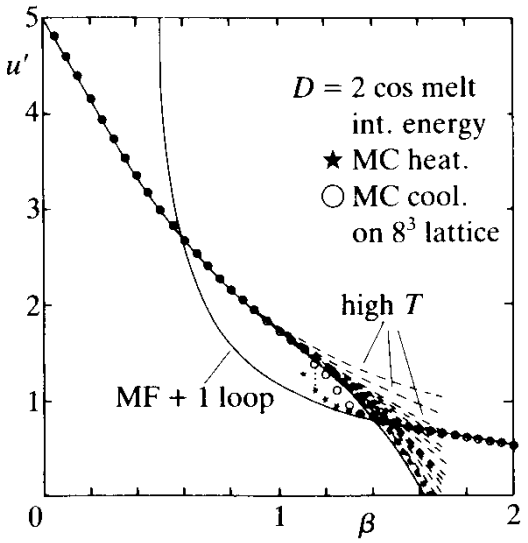

cosines are again expanded as in Part II [Eq. (4.15), and following] and the partition function (13.2) becomes

$$Z' = I_0(\beta)^{(1/2)D(D-1)N} I_0(2\beta\xi)^{DN} \sum_{\{\bar{\sigma}_{ij}(\mathbf{x}),\, i<j\}} \sum_{\{\bar{\sigma}_{ii}(\mathbf{x})\}} \prod_{\mathbf{x},\, i<j} \frac{I_{\bar{\sigma}_{ij}}(\beta)}{I_0(\beta)}$$

$$\times \prod_{\mathbf{x},\, i} \frac{I_{\bar{\sigma}_{ii}}(2\beta\xi)}{I_0(2\beta\xi)} \prod_{\mathbf{x},\, i} \left[\int_{-\pi}^{\pi} \frac{d\gamma_i(\mathbf{x})}{2\pi} \right] e^{i\Sigma_{\mathbf{x},\, i<j} \bar{\sigma}_{ij} (\nabla_i \gamma_j + \nabla_j \gamma_i) + i\Sigma_{\mathbf{x},\, i} \bar{\sigma}_{ii} \nabla_i \gamma_i}. \tag{13.71}$$

By rewriting the integrals over $\gamma_i(\mathbf{x})$ as

$$\prod_{\mathbf{x},\, i} \left[\int_{-\pi}^{\pi} \frac{d\gamma(\mathbf{x})}{2\pi} \right] e^{-i\Sigma_{\mathbf{x}} \bar{\nabla}_i \bar{\sigma}_{ij}(\mathbf{x})\, \gamma_j(\mathbf{x})}, \tag{13.72}$$

with $\bar{\sigma}_{ij} = \bar{\sigma}_{ji}$, we can evaluate them and find the stress conservation law

$$\bar{\nabla}_i \bar{\sigma}_{ij}(\mathbf{x}) = 0, \tag{13.73}$$

so that the high temperature series reads

$$Z' = I_0(\beta)^{(1/2)D(D-1)N} I_0(2\beta\xi)^{DN}$$

$$\times \sum_{\{\bar{\sigma}_{ij}(\mathbf{x}),\, i \geq j\}} \delta_{\bar{\nabla}_i \sigma_{ij},\, 0} \prod_{\mathbf{x},\, i<j} \frac{I_{\sigma_{ij}(\mathbf{x})}(\beta)}{I_0(\beta)} \prod_{\mathbf{x},\, i} \frac{I_{\sigma_{ii}(\mathbf{x})}(2\beta\xi)}{I_0(2\beta\xi)}, \tag{13.74}$$

We can now perform the same graphical expansion we employed previously in the Villain form, the only difference being that instead of

$$e^{-(1/2\beta)(\Sigma_{\mathbf{x},i<j}\bar{\sigma}_{ij}^2+(1/2\xi)\Sigma_{\mathbf{x},i}\bar{\sigma}_{ii}^2)}, \tag{13.75}$$

the weights of the graphs are now given by

$$\prod_{\mathbf{x},i<j}\frac{I_{\bar{\sigma}_{ij}}(\beta)}{I_0(\beta)}\prod_{\mathbf{x},i}\frac{I_{\bar{\sigma}_{ii}}(2\beta\xi)}{I_0(2\beta\xi)}. \tag{13.76}$$

These are the same for large β for which $I_b(a\beta)/I_0(a\beta)$ has the limit $e^{-(1/2a\beta)\bar{\sigma}^2}$.

We can now insert the lowest graph, discussed already in Chapter 2, and find in D dimensions

$$Z' = I_0(\beta)^{(1/2)D(D-1)N} I_0(2\beta\xi)^{DN} \times\left[1+ND(D-1)\left(\frac{I_1(\beta)}{I_0(\beta)}\right)^4\left(\frac{I_1(2\beta\xi)}{I_0(2\beta\xi)}\right)^4\left(\frac{I_2(2\beta\xi)}{I_0(2\beta\xi)}\right)^2+\ldots\right], \tag{13.77}$$

and hence

$$-\beta f' = \frac{D(D-1)}{2}\log I_0(\beta) + D\log I_0(2\beta\xi) + D(D-1)\left(\frac{I_1(\beta)}{I_0(\beta)}\right)^4\left(\frac{I_1(2\beta\xi)}{I_0(2\beta\xi)}\right)^4\left(\frac{I_2(2\beta\xi)}{I_0(2\beta\xi)}\right)^4+\ldots \tag{13.78}$$

In three dimensions, this term suffices to fit the precritical stress fluctuations on the high temperature side. In two dimensions, we have to carry the expansion to higher order. This is most conveniently done by taking recourse to the expansion in terms of integer-stress gauge field configurations whose diagrams were counted before in Fig. 11.1 in the context of the melting model of the Villain type. In order to use those results for the cosine model, we rewrite the product (13.76) in the form

$$\prod_{\mathbf{x}} I_{-\bar{\nabla}_1\bar{\nabla}_2\bar{\chi}(\mathbf{x})}(\beta)\prod_{\mathbf{x}} I_{\bar{\nabla}_1\bar{\nabla}_1\bar{\chi}(\mathbf{x})}(2\beta\xi)\prod_{\mathbf{x}} I_{\bar{\nabla}_2\bar{\nabla}_2\bar{\chi}(\mathbf{x})}(2\beta\xi). \tag{13.79}$$

Performing a trivial shift in $\mathbf{x}$, the second and third products become

$$\prod_{\mathbf{x}} I_{\bar{\nabla}_1\nabla_1\bar{\chi}(\mathbf{x})}(2\beta\xi) \prod_{\mathbf{x}} I_{\bar{\nabla}_2\nabla_2\bar{\chi}(\mathbf{x})}(2\beta\xi). \tag{13.80}$$

Thus, the Bessel functions $I_{\bar{\sigma}_{ii}}(2\beta\xi)$ which appear in the high-temperature series are determined by the values of the two-dimensional Laplacians $\bar{\nabla}_1\nabla_1$, $\bar{\nabla}_2\nabla_2$ for each graph. They can be extracted from Fig. 11.1 and are listed in Table 11.1 (actually, their squares since these were relevant for the Villain form of the energy). In the present case each number m_i on the graphs in the fourth and fifth columns of Fig. 11.1 amounts to a Bessel function $I_{\sqrt{m_i}}(2\beta\xi)$. For instance, the graphs and give $I_1(2\beta\xi)^4 I_2(2\beta\xi)^2$ and $I_1(2\beta\xi)^8 I_2(2\beta\xi)^2$ from 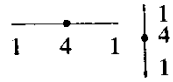 and 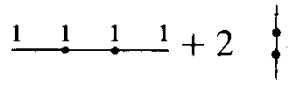 , respectively. The first Bessel function in (13.79) function in (13.79) occurs with the index

$$\bar{\nabla}_1\bar{\nabla}_2\bar{\chi}(\mathbf{x}) = \bar{\chi}(\mathbf{x}) - \bar{\chi}(\mathbf{x}-\mathbf{1}) - \bar{\chi}(\mathbf{x}-\mathbf{2}) + \bar{\chi}(\mathbf{x}-\mathbf{1}-\mathbf{2}). \tag{13.81}$$

We can obtain these numbers by placing an elementary square 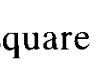 on top of each graph, site by site, and counting the occupied corners with alternating sign. Each number to gives a factor $I_k(\beta)$. For example, the graph

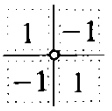 (13.82)

gives $I_1(\beta)^4$. So do the graphs

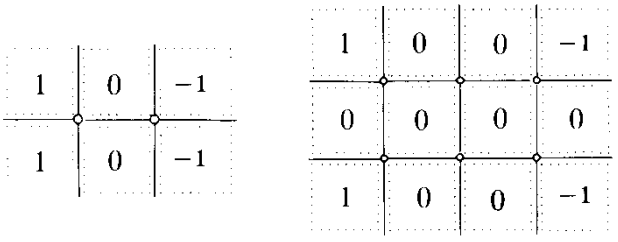 (13.83)

The indices of the Bessel function $I_{\bar{\sigma}_{12}}(\beta)$ are listed in column 7 of Fig. 11.1 (with 1^4 for $I_1(\beta)^4$, etc.). As long as there are no graphs with doubly occupied points, the index $\bar{\nabla}_1\bar{\nabla}_2\chi$ can only be zero or one and the power of $I_1(\beta)$ is directly equal to $2(n-m)$. If $e(n_1, m_1, m_2)$ denotes the free energy terms

$$e(n_1, m_1, m_2) \equiv \left(\frac{I_1(\beta)}{I_0(\beta)}\right)^{n_1} \left(\frac{I_1(2\beta\xi)}{I_0(2\beta\xi)}\right)^{m_1} \left(\frac{I_2(2\beta\xi)}{I_0(2\beta\xi)}\right)^{m_2}, \tag{13.84}$$

then the high temperature expansion in two dimensions reads

$$-\beta f = \log I_0(\beta) + 2\log I_0(2\beta\xi) + \underset{12}{2e(4,\ 4,\ 2)} + \underset{16}{4e(4,\ 8,\ 2)} + \underset{20}{2e(4,\ 16,\ 0)}$$
$$+ \underset{20}{4e(4,\ 10,\ 3)} + \underset{22}{8e(6,\ 12,\ 2)} + \underset{24}{4e(4,\ 24,\ 0)} + \underset{24}{4e(4,\ 12,\ 4)} + \ldots \tag{13.85}$$

The disconnected graph gives a further

$$-\beta f^{\text{disc}} = -\underset{24}{18e(8,\ 8,\ 4)}. \tag{13.86}$$

On the bottom of each term, we have listed the total power of $\beta(t = n_1 + m_1 + 2m_2)$ to which it reduces for small β. As a cross check, we let β grow very large in which case the product $\Pi_{\mathbf{x}} I_{\bar{\sigma}_{12}}(\beta)\, I_{\bar{\sigma}_{11}}(2\beta\xi)\, I_{\bar{\sigma}_{22}}(2\beta\xi)$ must tend to $\exp[-(1/\beta)\{n - m + m(1/\xi)\}]$, where n, m are the numbers in the expansion (11.38) in terms of

$$e(n,\ m) = \exp\left[-\frac{1}{\beta}\left\{n\left(1 - \frac{1}{\gamma}\right) + m\left(\frac{1}{\xi} - 1\right)\right\}\right].$$

$(1/4)m_1 + m_2$ and $(n_1/2) + (1/4)m_1 + m_2$ are equal to the numbers m and n in the expansion (11.38), respectively.

The internal energy associated with each term $e(n_1, m_1, m_2)$ is given by

$$-\frac{\partial}{\partial\beta} e(n_1,\ m_1,\ m_2)$$
$$= -n_1 \left(\frac{I_1(\beta)}{I_0(\beta)}\right)^{n_1 - 1} \left(\frac{I_1(2\beta\xi)}{I_0(2\beta\xi)}\right)^{m_1} \left(\frac{I_2(2\beta\xi)}{I_0(2\beta\xi)}\right)^{m_2} \left[1 - \frac{1}{\beta}\frac{I_1(\beta)}{I_0(\beta)} - \left(\frac{I_1(\beta)}{I_0(\beta)}\right)^2\right]$$
$$- m_1 \left(\frac{I_1(\beta)}{I_0(\beta)}\right)^{m} \left(\frac{I_1(2\beta\xi)}{I_0(2\beta\xi)}\right)^{m_1 - 1} \left(\frac{I_2(2\beta\xi)}{I_0(2\beta\xi)}\right)^{m_2} 2\xi \left[1 - \frac{1}{2\beta\xi}\frac{I_1(2\beta\xi)}{I_0(2\beta\xi)} - \left(\frac{I_1(2\beta\xi)}{I_0(2\beta\xi)}\right)\right]$$
$$- m_2 \left(\frac{I_1(\beta)}{I_0(\beta)}\right)^{n_1} \left(\frac{I_1(2\beta\xi)}{I_0(2\beta\xi)}\right)^{m_1} \left(\frac{I_2(2\beta\xi)}{I_0(2\beta\xi)}\right)^{m_2 - 1} 2\xi \left[\frac{I_1(2\beta\xi)}{I_0(2\beta\xi)} - \frac{1}{\xi\beta}\frac{I_2(2\beta\xi)}{I_0(2\beta\xi)}\right.$$
$$\left. - \frac{I_1(2\beta\xi)}{I_0(2\beta\xi)}\frac{I_2(2\beta\xi)}{I_0(2\beta\xi)}\right].$$

TABLE 13.2. Transition data for the $D = 2$ cosine melting model (with the same notation as in Table 13.1). The theoretical entropy jumps are now much less reliable than those for $D = 3$, due to larger fluctuations (after Ami and Kleinert, and Janke and Kleinert, quoted in the Notes and References).

ξ	$\beta_{\text{dest}}^{\text{MF}}$	β_m^{HF}	$\beta_m^{\text{LT,HT}}$	β_m^{MC}	$1.15\xi^{-0.78}$	$\Delta s^{\text{LT,HT}}$	Δs^{MC}
0.2	2.50	1.77	4.46	4.39 ± 0.15	4.04	0.71	0.48
0.4	1.25	1.12	2.30	2.35 ± 0.05	2.35	0.70	0.41
0.6	0.83	0.81	1.71		1.71	0.69	
0.8	0.62	0.62	1.38	1.36 ± 0.02	1.37	0.66	0.35
1.0	0.50	0.50	1.18	1.15 ± 0.05	1.15	0.62	0.30
1.2	0.42	0.42	1.04		1.00	0.60	0.20

If we denote this by $u(n_1, m_1, m_2)$ we can obviously write

$$
\begin{aligned}
&u(n_1, m_1, m_2) \\
&\quad = -n\left[e(n_1 - 1, m_1, m_2) - \frac{1}{\beta}e(n_1, m_1, m_2) - e(n_1 + 1, m_1, m_2)\right] \\
&\qquad - m_1\left[2\xi e(n_1, m_1 - 1, m_2) - \frac{1}{\beta}e(n_1, m_1, m_2) - 2\xi e(n_1, m_1 + 1, m_2)\right] \\
&\qquad - m_2\left[2\xi e(n_1, m_1 + 1, m_2 - 1) - \frac{2}{\xi}e(n_1, m_1, m_2) - 2\xi e(n_1, m_1 + 1, m_2)\right]
\end{aligned}
\tag{13.87}
$$

The free energies are plotted in Figs. 13.2, 13.4 for $D = 3$ and $D = 2$ and various values of the anisotropic parameter ξ. Their intercepts with the one-loop corrected mean field curves determine the melting points β_m as a function of ξ as shown in Tables 13.1 and 13.2 and in Figs. 13.3 and 13.5. The internal energies are shown in Figs. 13.6 and 13.7. The compare very well with Monte Carlo simulations as can be seen in Figs. 13.8, 13.9.

In order to find precise values of β_m (Monte Carlo) for the melting point we proceed as in Section 12.4 for the Villain version of the melting model. We place the system in a mixed initial state (half solid, half liquid) and iterate the internal energy many times. Above and below β_m, the system runs immediately into the solid or liquid phase. Melting occurs at the turnover point. Thus we see in Fig. 13.10 that in three dimensions we have, for $\xi = 1$,

FIG. 13.10. The development of the internal energy of a mixed initial state (half solid, half liquid) over many Monte Carlo iterations in the $D = 3$, isotropic ($\xi = 1$) model. This determines the transition value $\beta_m \approx 0.786$.

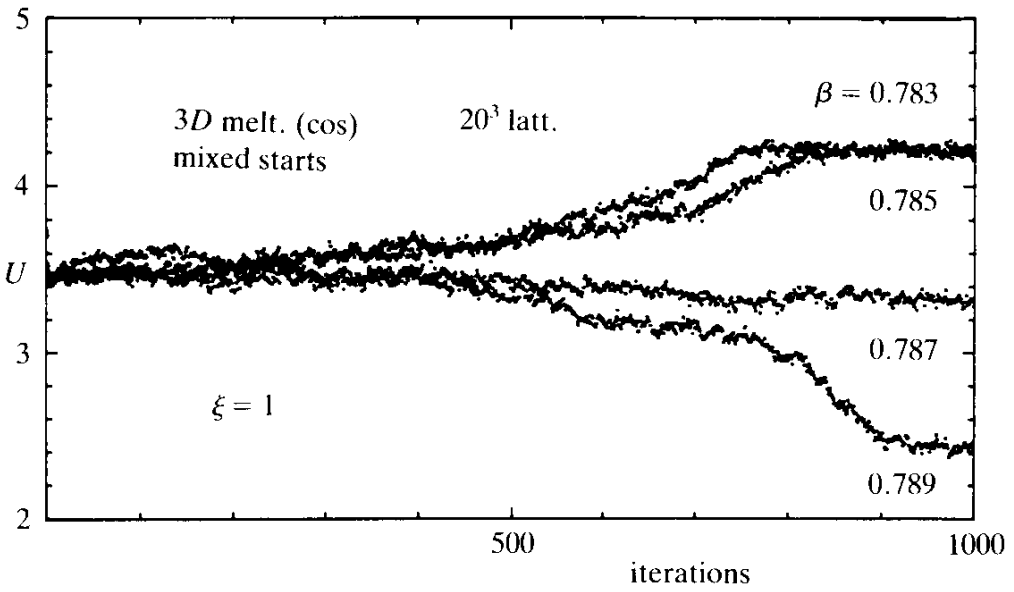

$$\beta_m \approx 0.786 \qquad (D = 3,\ \xi = 1). \tag{13.88}$$

The accuracy of this value is again tested by placing the system once in a solid and once in a liquid initial state and observing that after many iterations the energies are extremely stable. The resulting figure looks quite similar to that of the $D = 3$ Villain model (see Fig. 12.8) so we do not show it here. From the distance between the stable internal energies,

$$\Delta u \approx 1.69 \qquad (D = 3,\ \xi = 1), \tag{13.89}$$

we deduce the transition entropy

$$\Delta s = \beta_m \Delta u \approx 1.33 \qquad (D = 3,\ \xi = 1). \tag{13.90}$$

In two dimensions we go once more through the same procedure.

In Fig. 13.11 we exhibit the development of the mixed initial state for $\beta = 1.14,\ 1.15,\ 1.16,\ 1.17$ from which we extract

$$\beta_m \approx 1.155, \quad \Delta u = 0.34, \quad \Delta s = 0.39 \quad (D = 2,\ \xi = 1). \tag{13.91}$$

These values are confirmed by a stability test of the solid and the liquid

FIG. 13.11. Analogous plot to Fig. 13.6 for the $D = 2$, isotropic ($\xi = 1$) melting model giving $\beta_m \approx 1.155$.

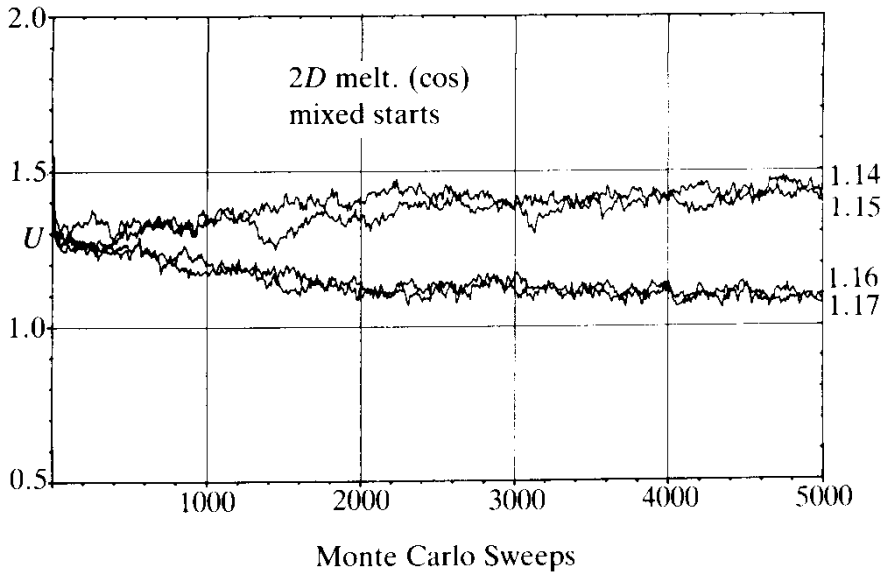

phase shown in Fig. 13.12 for various values of β in the neighborhood of β_m.

Similar runs are performed in $D = 3$ and $D = 2$ dimensions for different values of ξ. The results agree with the analytic calculations plotted in Figs. 13.3, 13.5 and tabulated in Tables 13.1, 13.2. The data fit very well with the following empirical formulas

$$\beta_m \approx 0.77\,\xi^{-0.597} \quad (D = 3), \tag{13.92}$$

$$\beta_m \approx 1.15\,\xi^{-0.78} \quad (D = 2). \tag{13.93}$$

For $\xi \to 0$, the melting temperatures approach zero since at $\xi = 0$ the crystal becomes unstable with respect to shear stresses [recall the stability conditions (1.17), (1.216)].

The good agreement between the analytic and Monte Carlo values shows that, for the free energy, the contribution of even the lowest non-trivial graph may be neglected up to the melting point and we might as well extract the intercept using only the first two Bessel function terms in (13.78). This corresponds to the physical fact that, as a liquid is cooled, the pre-transition fluctuations, which tend to form microcrystallites before the on-set of freezing, are extremely small.

Just as before in the melting model of the Villain type [recall Eq.

FIG. 13.12. Stability, in the $2D$ isotropic, melting model, of solid and liquid initial state over 4000 Monte Carlo iterations.

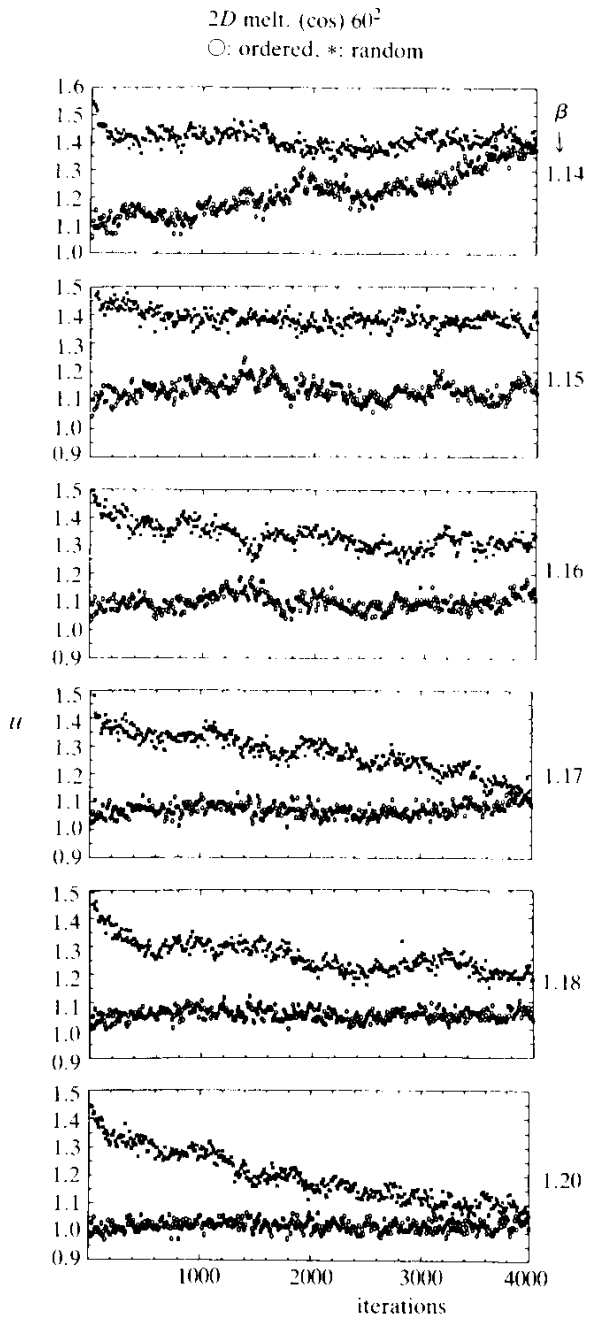

(12.26)] it is possible to compare the three-dimensional values of β_m with experimental numbers, provided we ignore the dependence of β_m on the elastic constant λ (which, as we recall, had been assumed to be zero throughout this discussion, for simplicity). An exploratory calculation for $\lambda/\mu \sim 0.5$ indicates a very weak λ dependence. We therefore decide to use $\beta_m = \mu a^3/T$ and calculate the Lindemann number associated with it

via (7.40). Since that formula was derived only for isotropic materials we employ the averaged elastic constants

$$\bar{\mu} = \frac{\mu}{5}(3 + 2\xi),$$

$$\bar{\lambda} = \lambda - \frac{2}{5}\mu(1 - \xi),$$

introduced by Voigt [see Eq. (7.44) and Voigt's book, quoted in Chapter 1, Part III] in order to describe sound propagation in polycrystalline samples. This gives the Lindemann numbers

$$L = 2\pi \cdot 22.76\left(\frac{3 + 2\xi}{5}\beta_m\right)^{1/2}\left(1 - \frac{1}{3}(1 - \bar{r})\right)^{-1/3}, \tag{13.94}$$

where

$$\bar{r} = \frac{\bar{c}_T^3}{c_L^3} = \left(\frac{\bar{\mu}}{2\bar{\mu} + \bar{\lambda}}\right)^{3/2} = \left(\frac{3 + 2\xi}{4 + 6\xi + 5\dfrac{\lambda}{\mu}}\right)^{3/2} \tag{13.95}$$

is the correction term in formula (7.40) involving the averaged longitudinal and transverse sound velocities, $\bar{c}_L = \sqrt{(2\bar{\mu} + \bar{\lambda})/\rho}$, $\bar{c}_T = \sqrt{\bar{\mu}/\rho}$. The result is shown as a function of ξ in Fig. 13.13. We may now use Table 7.1 and insert also the experimental values. They are seen to be in rather satisfactory agreement with our predictions.

Let us now turn to another important quantity of the melting process, the transition entropy. Using the theoretical transition values β_m of Tables 13.1, 13.2, we can extract from (13.6) and (13.7) the entropy jumps $\Delta s = \beta_m \Delta u$ for various ξ and find the values shown also in Tables 13.1 and 13.2.[b] For $D = 3$ they are plotted in Fig. 13.14 and are in good agreement with those obtained from Monte Carlo simulations as described above. For $D = 2$ the analytic Δs values are about twice as large as the Monte Carlo ones which are plotted in Fig. 13.15. The reason is

[b]In Figs. 13.8 and 13.9 we can verify once more the values Δs of Eqs. (13.90), (13.91).

FIG. 13.13. Comparison of the model's Lindemann numbers with experimental values from Table 7.1.

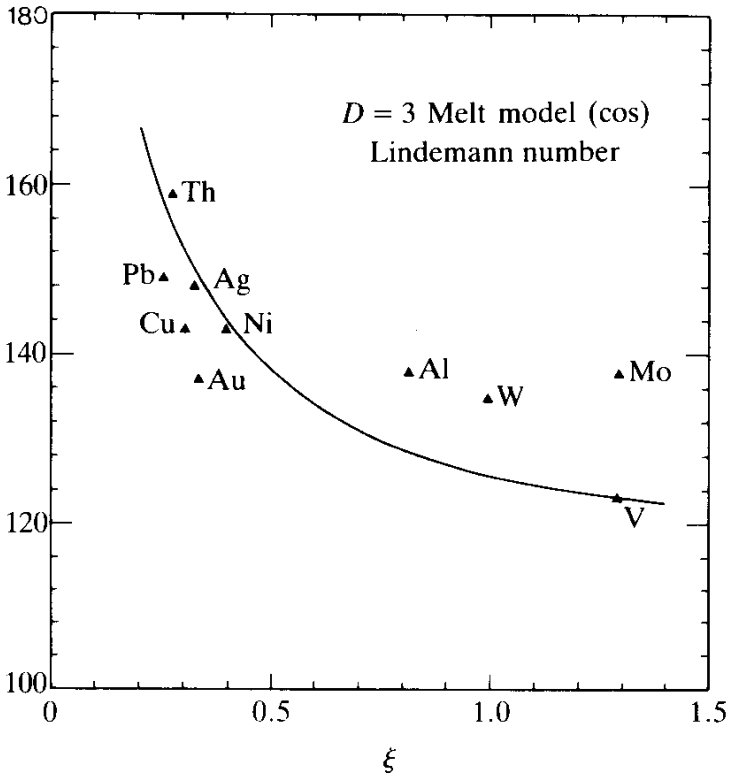

that fluctuations in two dimensions are much more important than those in three dimensions. Notice also that the fluctuation corrections produce an entropy jump even for $\xi > 1$ for which the mean-field approximation had a continuous transition [recall Eq. (13.15)].

Forming a further derivative with respect to β yields the specific heat $c = -\beta^2(\partial/\partial\beta)u'$. The analytic results are compared with the Monte Carlo data for $\xi = 1$ (listed in Table 13.1, 13.2) in Figs. 13.16 and 13.17. In Fig. 13.18 we have also compared the $D = 3$ data with the experimental data for lead (extracted from the curves in Fig. 7.2 after subtracting the electronic and vaporization parts).

It is instructive to study also the defect distribution in the model: for simplicity we take only the two-dimensional case. We proceed in the same way as in Section 12.4. The jump numbers $n_{ij}(\mathbf{x})$ are extracted according to Eqs. (12.37)–(12.39) after iterating an ordered or disordered initial state 4000 times (i.e., after arriving at the final states of the stability runs in Fig. 13.8). These are displayed in Figs. 13.19a–g. These lead to the defect densities $\eta(\mathbf{x})$ as shown in Fig. 13.20d,e. Notice that since the final state is a solid, there are very few defects. Nevertheless, the jump numbers obtained from ordered and disordered initial states differ vastly.

TABLE 13.3. Monte Carlo data for the $D = 3$ cosine melting model on an 8^3 lattice ($Z(16)$ approx.)($\xi = 1$, $\lambda = 0$). There were 100 + 200 sweeps for equilibriation and measurements, respectively. Note the "δ-function peak" in c(cool) at $\beta = 0.9$ as a signal for the first order of the transition (from Jacobs and Kleinert, 1983).

β	u(heat)	u(cool)	c(heat)	c(cool)	β	u(heat)	u(cool)	c(heat)	c(cool)
2.00	0.7863	0.7919	1.5786	2.0322	1.00	1.7319	1.7275	2.5359	2.3944
1.95	0.8182	0.8102	1.4309	1.7767	0.95	1.8467	1.8479	2.1596	2.2959
1.90	0.8336	0.8381	1.7355	1.5974	0.90	1.9890	2.4431	2.7781	133.3700
1.85	0.8602	0.8643	1.5558	1.5481	0.85	2.1433	3.6894	2.6490	7.4843
1.80	0.8883	0.8833	1.8540	1.3791	0.80	2.3722	4.0411	2.8292	3.0625
1.75	0.9122	0.9119	1.6688	1.7736	0.75	2.7337	4.2849	4.4629	3.3217
1.70	0.9378	0.9353	1.7834	1.6531	0.70	4.5123	4.5176	2.1423	2.5629
1.65	0.9767	0.9712	1.8210	1.7969	0.65	4.7621	4.7675	2.0221	2.0424
1.60	1.0084	1.0042	1.5658	1.8619	0.60	5.0536	5.0267	1.8545	1.4745
1.55	1.0364	1.0434	1.8064	1.9528	0.55	5.2905	5.2731	1.6750	1.5084
1.50	1.0785	1.0808	1.5886	1.5915	0.50	5.5890	5.5748	1.0598	1.5084
1.45	1.1220	1.1232	1.7185	1.6046	0.45	5.8698	5.8844	1.2755	1.1039
1.40	1.1693	1.1631	1.9998	2.0098	0.40	6.1815	6.1946	1.0187	1.0481
1.35	1.2089	1.2166	1.9086	1.9414	0.35	6.4857	6.5104	0.8585	0.7101
1.30	1.2682	1.2716	1.5930	1.9068	0.30	6.8264	5.8411	0.6789	0.6386
1.25	1.3289	1.3332	1.8468	1.8777	0.25	7.1722	7.1766	0.4327	0.3921
1.20	1.3922	1.3846	1.8658	2.0927	0.20	7.5137	7.5215	0.2682	0.2345
1.15	1.4449	1.4579	2.1894	2.1376	0.15	7.8793	7.8752	0.1633	0.1498
1.10	1.5491	1.5414	2.3550	2.0680	0.10	8.2505	8.2487	0.0746	0.0780
1.05	1.6367	1.6354	1.9019	1.7571	0.05	8.6318	8.6258	0.0168	0.0164

The difference consists, of course, mainly in a trivial defect-gauge transformation. The same analysis is performed for other values of β and the defects obtained are shown in the remaining Figs. 13.20. By comparison with the stability curves in Figs. 13.8 we can easily see the correspondence between the solid and liquid energies and the defect densities.

Finally, let us test the quality of the Villain approximation for the melting model. By taking the values β_m through the Villain transform, (9.124) and (9.125), i.e., by calculating[c]

$$\beta_V = -1/[2\log I_1(\beta)/I_0(\beta)],$$
$$2\beta_V \xi_V = -1/[2\log I_1(2\beta\xi)/I_0(2\beta\xi)], \tag{13.96}$$

[c]We have now attached the subscript V to the parameters of the Villain-type melting model.

FIG. 13.14. The entropy jumps of the $D = 3$ melting model extracted from the curves of Fig. 13.6 as compared with the Monte Carlo data of Jacobs and Kleinert (1984) (see also Table 13.1).

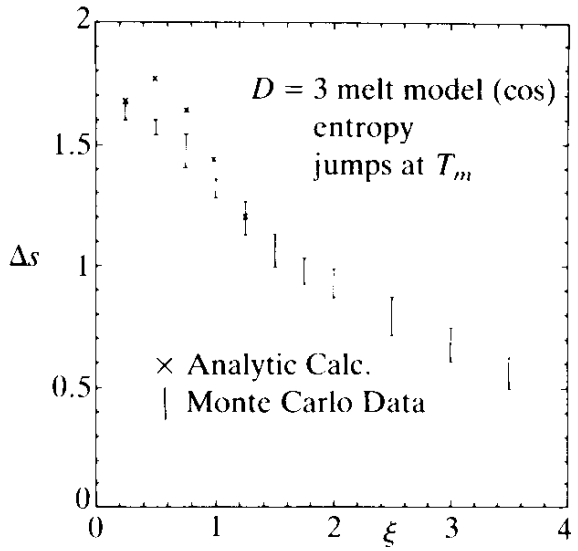

TABLE 13.4. Internal energy and specific heat of the cosine model of melting in $D = 2$ dimensions ($Z(16)$ approx.) with ($\xi = 1$, $\lambda = 0$). The lattice size is 32×32. There were 100 sweeps for equilibriation plus 200 for measurement (from Janke and Kleinert, 1984).

β	u(heat)	u(cool)	u(heat)	u(cool)	β	u(heat)	u(cool)	u(heat)	u(cool)
2.00	0.5365	0.5365	1.1841	1.1581	1.00	1.7080	1.7326	1.8140	1.3103
1.95	0.5506	0.5523	0.9798	1.1536	0.95	1.8130	1.8339	1.5476	1.8343
1.90	0.5692	0.5428	1.3140	1.2859	0.90	1.9367	1.9228	1.6133	1.5350
1.85	0.5911	0.5864	1.1905	1.1444	0.85	2.0400	2.0364	1.5579	1.3409
1.80	0.6063	0.6050	1.1676	1.2766	0.80	2.1452	2.1262	1.6984	1.6106
1.75	0.6247	0.6225	1.2698	1.2669	0.75	2.2603	2.2539	1.5546	1.6246
1.70	0.6459	0.6454	1.8193	1.4908	0.70	2.3952	2.3772	1.3375	1.0886
1.65	0.6654	0.6714	1.2197	1.3882	0.65	2.5136	2.5130	1.1330	0.9855
1.60	0.6910	0.6917	1.2903	1.1680	0.60	2.6496	2.6629	1.0812	1.4138
1.55	0.7199	0.7193	1.2425	1.3803	0.55	2.8198	2.7988	0.9650	0.9805
1.50	0.7452	0.7563	1.3487	1.3347	0.50	2.9684	2.9708	0.8242	0.7993
1.45	0.7842	0.7803	1.3297	1.3744	0.45	3.1495	3.1473	0.7896	0.8848
1.40	0.8222	0.8157	1.8275	1.4053	0.40	3.3174	3.3213	0.5834	0.4838
1.35	0.8507	0.8440	1.7549	1.4832	0.35	3.4998	3.5039	0.4233	0.5295
1.30	0.8993	0.9439	1.4988	1.8471	0.30	3.7091	3.6984	0.3697	0.4007
1.25	0.9450	1.0959	1.4825	1.7231	0.25	3.8976	3.9052	0.2538	0.2465
1.20	1.0135	1.2626	1.9586	2.6552	0.20	4.1194	4.1153	0.1509	0.1848
1.15	1.1100	1.3633	4.4383	6.2191	0.15	4.3298	4.3442	0.1052	0.1210
1.10	1.2796	1.5348	5.6822	3.2761	0.10	4.5493	4.5491	0.0444	0.0452
1.05	1.6329	1.6310	2.2055	1.9622	0.05	4.7709	4.7731	0.0119	0.0107

FIG. 13.15. The entropy jumps in two dimensions as a function of ξ as obtained from Monte Carlo simulations of Janke and Kleinert. The theoretical values in Table 13.2 are not in satisfactory agreement with these since in the mean-field-plus-one-loop calculation cannot do justice to the defect excitations of the model (cf. heading to Fig. 13.17).

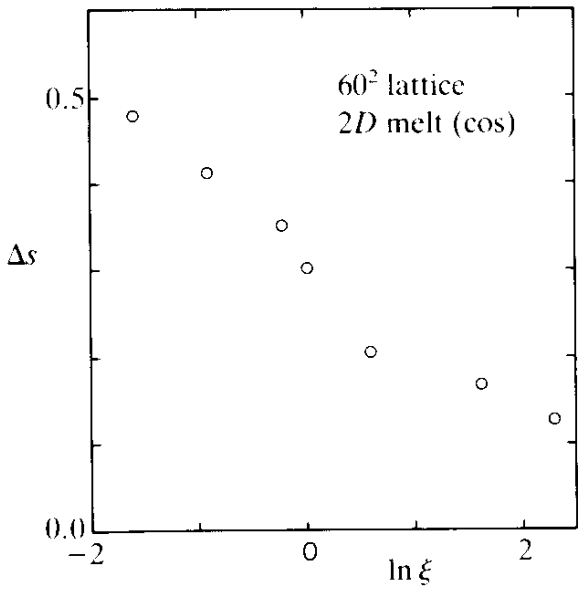

FIG. 13.16. Specific heat of the $D = 3$ cosine model for $\xi = 1$. Comparison between theoretical curves and Monte Carlo data (obtained by Jacobs and Kleinert).

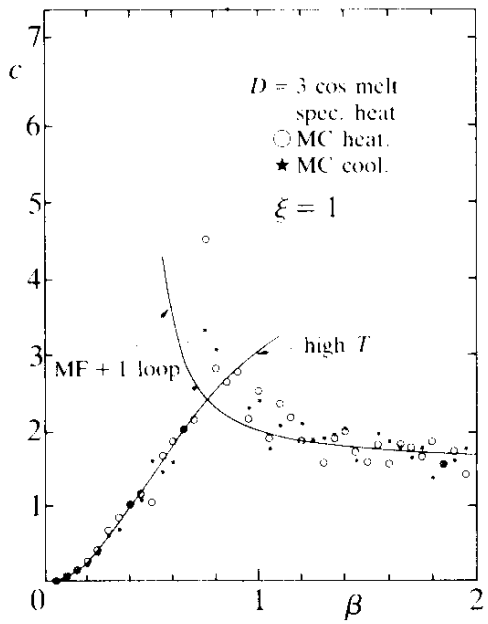

we find transition values for the Villain-type melting model which are in good agreement with those obtained in Chapter 12.

It must be noted, however, that this is somewhat of an accident. In fact, as far as the full high-temperature behavior of u and c is concerned, the Villain approximation is really much worse in this model than it is

FIG. 13.17. Specific heat of the $D = 2$ cosine model. Comparison of the Monte Carlo data with the mean-field-plus-one-loop correction (from Janke and Kleinert). We see the descrepancy due to the neglect of defects. This phenomenon was observed before and discussed in detail in the XY model of superfluidity, sec 7.19, Part I.

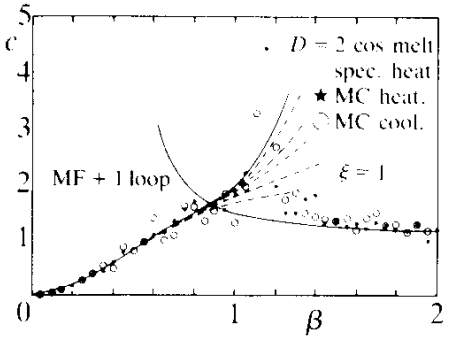

FIG. 13.18. Specific heat of the $D = 3$ model for $\xi = 0.25$. Comparison of Monte Carlo data with experimental data for lead as obtained from Fig. 7.2 with appropriate subtractions (after Jacobs and Kleinert).

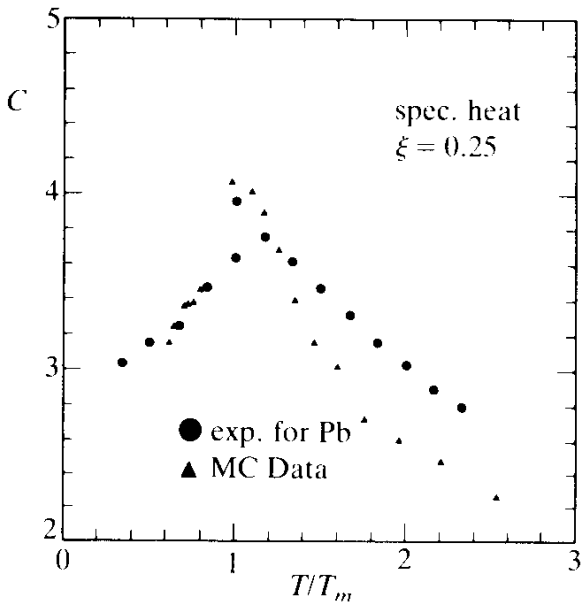

in the XY case. The reason is the following: We pointed out in Part II that the quality of the Villain approximation is *not* based on the equality of (13.75) and (13.76) for *large* β but rather on the approximate equality of the Bessel functions, for *small* β, i.e.,

$$I_{\bar{\sigma}}(\beta) \sim \frac{1}{\bar{\sigma}!}\left(\frac{\beta}{2}\right)^{\bar{\sigma}} \tag{13.97}$$

FIG. 13.19. The defect gauge fields $n_{11}(\mathbf{x})$, $n_{12}(\mathbf{x})$, $n_{22}(\mathbf{x})$ obtained from a Monte Carlo simulation of the $D = 2$ cosine melting model on a 60×60 sc lattice (Janke and Kleinert, 1984) taken after 4000 sweeps for equilibriation for the defect configuration at $\beta = 1.2$. Notice that with a random start, there are many $n_{ij}(\mathbf{x})$ excitations, most of them correspond to a pure defect gauge whose double curl vanishes. (Here o.s. and r.s. refer to ordered and random start; cf. Fig. 13.20.)

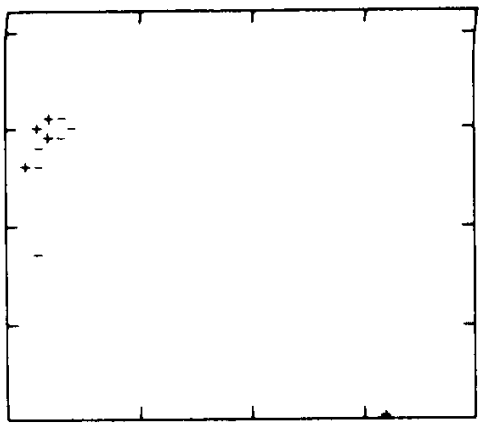

n_{11}, $\beta = 1.2$, o.s.

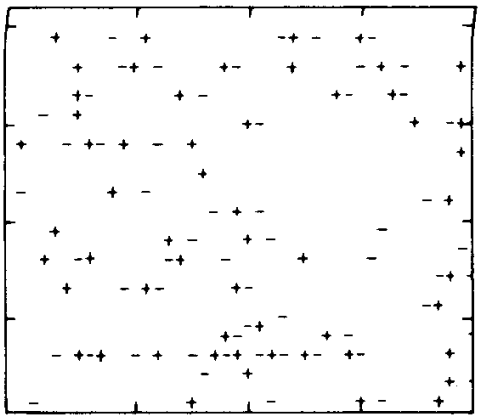

n_{11}, $\beta = 1.2$, r.s.

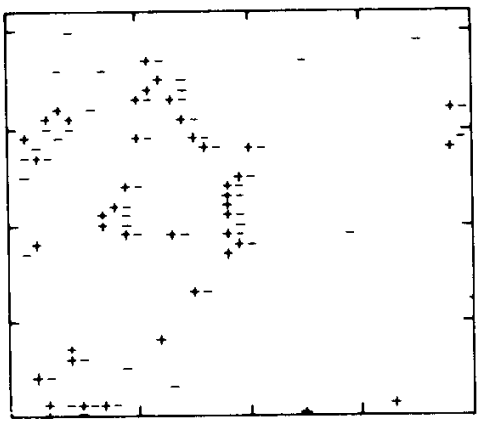

n_{12}, $\beta = 1.2$, o.s.

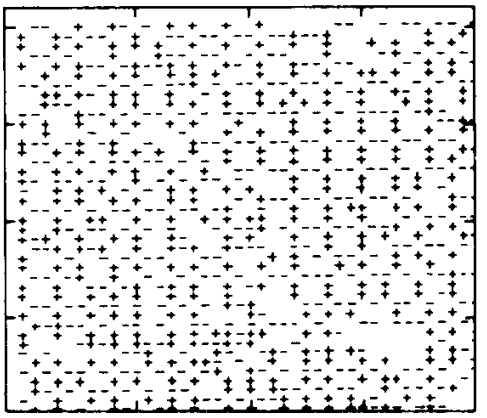

n_{12}, $\beta = 1.2$, r.s.

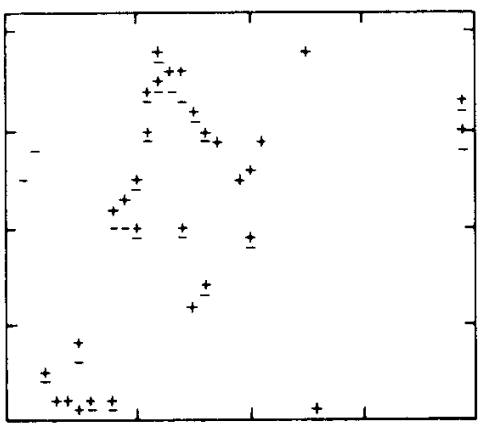

n_{22}, $\beta = 1.2$, o.s.

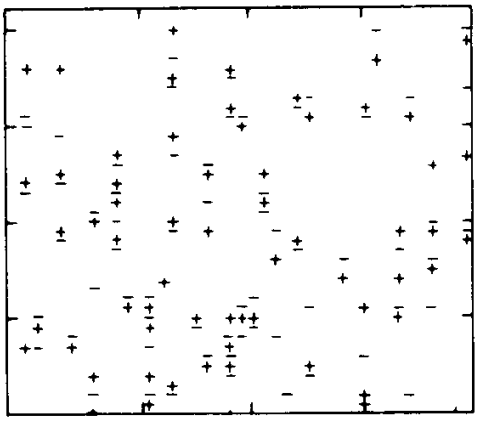

n_{22}, $\beta = 1.2$, r.s.

FIG. 13.20. Disclinations in the 2-dimensional cosine model of melting on a 60×60 sc lattice below and right above the melting transition $\beta_m \approx 0.135$. We see that in the molten state the disclinations of alternating sign are linked up into strings. Below the transition, there are mostly nearest neighbor and next-nearest neighbor quadruplets, i.e., short closed strings. As the melting temperature is passed the loops become large and break open. The pictures were taken after having performed 4000 sweeps for equilibriation, once with an ordered start (o.s.) and once with a random start (r.s.). The difference in the pictures is understood by looking at the development of the internal energy over the 4000 sweeps which are displayed in Fig. 13.12. For $\beta \leq 1.14$ the system always winds up in the liquid state, and for $\beta > 1.17$ in the crystalline state. This explains the similarity of the defect pictures for $\beta = 1.14, 1.18, 1.20$. For $\beta = 1.16$, on the other hand, the initial configuration remains practically frozen. The defect configurations are determined by finding for a fixed displacement field $u_i(\mathbf{x}) = (a/2\pi)\gamma_i(\mathbf{x})$ the defect gauge field $n_{ij}(\mathbf{x})$ by minimizing $\Sigma_{\mathbf{x},i,j}(\nabla_i\gamma_j + \nabla_j\gamma_i - 2\pi n_{ij}(\mathbf{x}))$ and $\Sigma_{\mathbf{x},i}(\nabla_i\gamma_i - 2\pi n_{ii}(\mathbf{x}))^2$. The resulting pictures of $n_{11}(\mathbf{x})$, $n_{12}(\mathbf{x})$, $n_{22}(\mathbf{x})$ are shown in Figs. 13.19 for $\beta = 1.2$. The defects are obtained by taking the double curl of these fields (from Janke and Kleinert, 1984). See also Fig. 12.17.

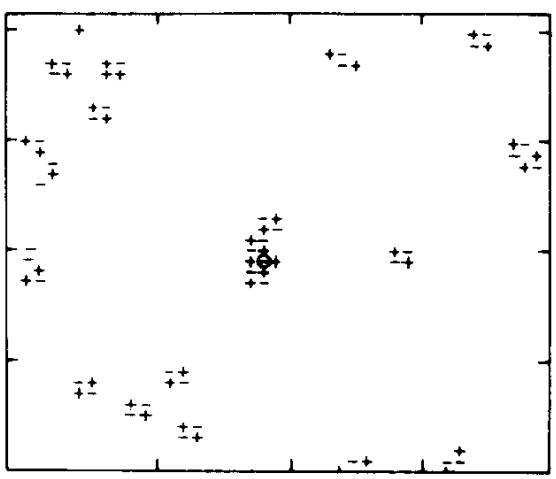

$\beta = 1.2$, o.s.

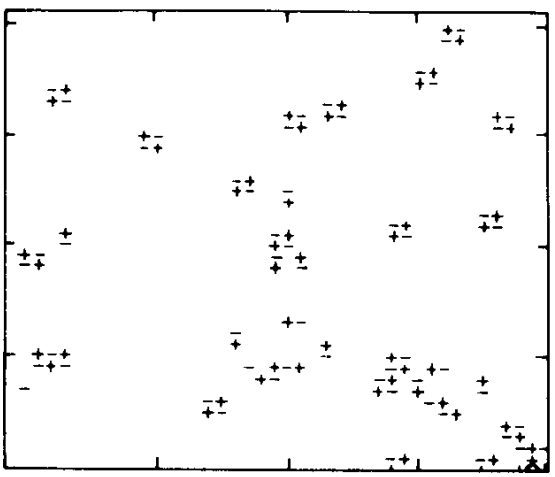

$\beta = 1.2$, r.s.

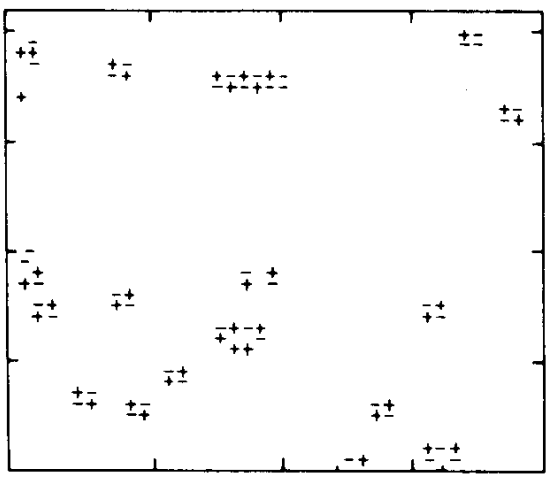

$\beta = 1.18$, o.s.

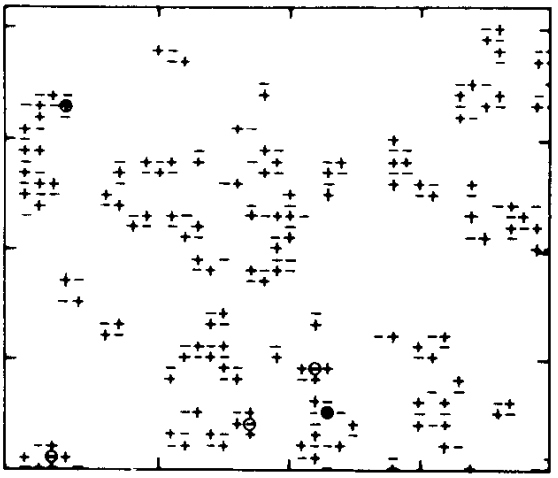

$\beta = 1.18$, r.s.

Fig. 13.20. (continued)

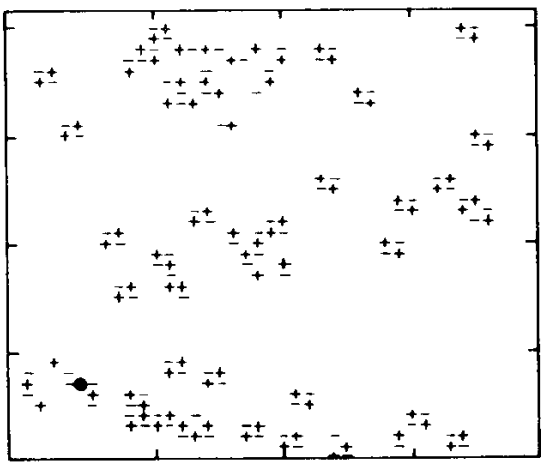

$\beta = 1.16$, o.s.

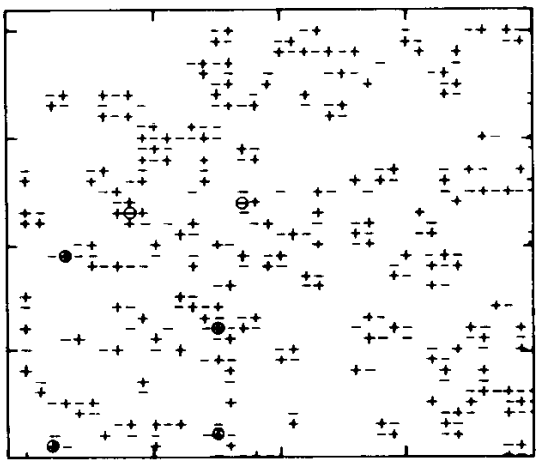

$\beta = 1.16$, r.s.

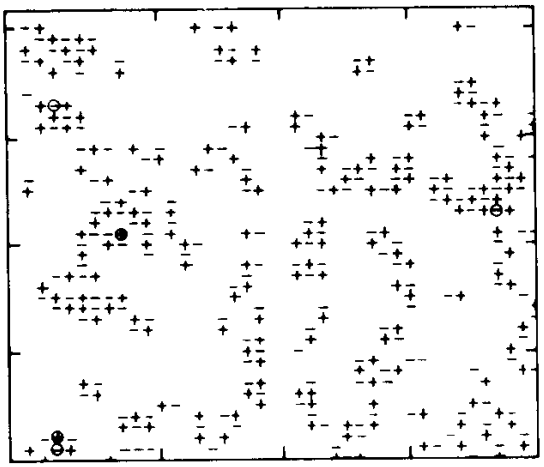

$\beta = 1.14$, o.s.

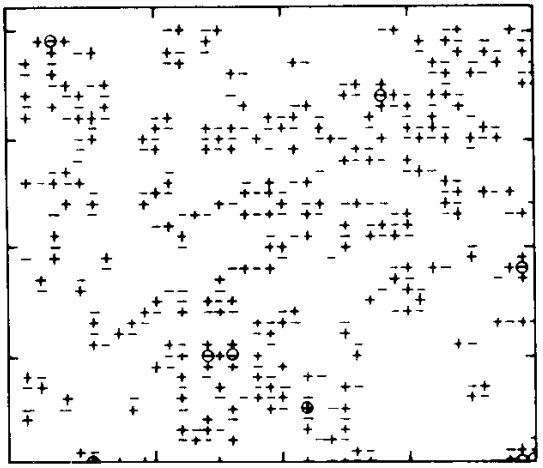

$\beta = 1.14$, r.s.

with the Gaussian approximation

$$e^{\log(\beta/2)\bar{\sigma}^2} \tag{13.98}$$

for $\bar{\sigma} = 0$ and $\bar{\sigma} = 1$. For $\bar{\sigma} \geq 2$ this is no longer a good approximation. In the case of vortex lines, this was not very serious since the phase transition was mainly caused by lines of unit strength as they were growing to infinite length. Here, however, even the *lowest* stress configuration contains $\bar{\sigma}_{ij}$ elements of strength *two* so that the approximation (13.97), (13.98) breaks down. For the determination of β_m from the free energy,

this breakdown was of little consequence since, as we observed above, even the lowest correction is quantitatively rather insignificant due to the smallness of pre-transitional fluctuations. But for the internal energy it becomes observable and for the specific heat quite important. A much more intimate relationship between the Villain type of melting model and cosine models is obtained by observing that all graphs included in the high-temperature expansion (13.85) involve the three Bessel functions

$$\frac{I_2(\beta_{V^{-1}})}{I_0(\beta_{V^{-1}})}, \qquad \frac{I_1((2\beta\xi)_{V^{-1}})}{I_0((2\beta\xi)_{V^{-1}})}, \qquad \frac{I_2((2\beta\xi)_{V^{-1}})}{I_0((2\beta\xi)_{V^{-1}})} \tag{13.99}$$

with the numbers n_1, m_1, m_2 in $e(n_1, m_1, m_2)$ giving their powers. In the model Villain-type melting, the corresponding terms are

$$e^{-(1/\beta)((n_1/2)+((m_1+m_2)/4)+((m_1+4m_2)/4)((1/\xi)-1))},$$

i.e., they are equal to the terms $e(n, m)$ of (11.38) with $n = n_1/2 + (m_1 + m_2)/4$, $m = (m_1 + 4m_2)/4$. From the discussion in Part II, Eq. (7.113) on the improvement of the Villain approximation to the XY model, we decided that for the melting models of the Villain and of the cosine type, a really close correspondence can be achieved only by the presence of a second $\cos(2\nabla_i u_i)$ term in the cosine energy. Thus we find the improved Villain approximation for $D = 2$,

$$\begin{aligned} Z &= \sum_{\{n_{ij}\}} \Phi[n_{ij}^s] \prod_{\mathbf{x},i} \left[\int_{-\pi}^{\pi} \frac{d\gamma_i(\mathbf{x})}{2\pi} \right] \\ &\quad \times \exp\left\{ -\beta \left[\sum_{\mathbf{x},i<j} (\nabla_i \gamma_j + \nabla_j \gamma_i - 4\pi n_{ij}^s)^2 + \xi \sum_{\mathbf{x},i} (\nabla_i \gamma_i - 2\pi n_{ii}^s)^2 \right] \right\} \\ &\approx R_{V^{-1}}(\beta) R_{V^{-1}}^{\delta}(2\beta\xi)^2 \prod_{\mathbf{x},i} \left[\int_{-\pi}^{\pi} \frac{d\gamma_i(\mathbf{x})}{2\pi} \right] \\ &\quad \times \exp\left\{ \beta_{V^{-1}} \sum_{\mathbf{x},i<j} \cos(\nabla_i \gamma_j + \nabla_j \gamma_i) + (2\beta\xi)_{V^{-1}} [\cos(\nabla_i \gamma_i) + \delta \cos(2\nabla_i \gamma_i)] \right\}, \end{aligned} \tag{13.100}$$

where

$$R_{V^{-1}}(\beta) = [I_0(\beta_{V^{-1}})\sqrt{2\pi\beta}]^{-1}, \qquad e^{-1/(2\beta)} = \frac{I_2(\beta_{V^{-1}})}{I_0(\beta_{V^{-1}})},$$

and

$$R_{V-1}(2\beta\xi) = [I_0^\delta((2\beta\xi)_{V-1})\sqrt{2\pi(2\beta\xi)}]^{-1},$$
$$e^{-1/(2(2\beta\xi))} = I_1^\delta((2\beta\xi)_{V-1})/I_0^\delta((2\beta\xi)_{V-1}),$$
$$e^{-4/(2(2\beta\xi))} = I_2^\delta((2\beta\xi)_{V-1})/I_0^\delta((2\beta\xi)_{V-1}). \tag{13.101}$$

With this identification we ensure that all terms in the high temperature series (13.85) become identically equal to the corresponding one in the Villain version (11.38).

In this form, the Villain approximation is very good throughout the entire high temperature region, including the transition point. For more details, see Janke and Kleinert (1986), quoted at the end of chapter 12.

13.5. PAIR CORRELATIONS IN THE DISORDERED PHASE

We have called the phase transition of the model "melting transition." Let us now investigate whether this terminology is really justified on physical grounds. For simplicity, we shall consider only the case of two dimensions. Since the defects comprise dislocations and disclinations we certainly expect the defect proliferation to destroy both translational and rotational order. This is necessary for the final state to become a liquid.

But there is more to a liquid than just complete disorder. A gas also has complete disorder. The difference between a liquid and a gas lies in the density correlation function, which is defined as follows:

$$D(\mathbf{x}, \mathbf{x}') \equiv D(\mathbf{x} - \mathbf{x}') \equiv \frac{1}{\rho_0^2}\langle \hat{\rho}(\mathbf{x})\,\hat{\rho}(\mathbf{x}')\rangle, \tag{13.102}$$

where

$$\hat{\rho}(\mathbf{x}) = \sum_{i=1}^{N} \delta(\mathbf{x} - \mathbf{x}_i) \tag{13.103}$$

is the density operator and ρ_0 is the average density $\langle\hat{\rho}(\mathbf{x})\rangle$. Separating out the disconnected part,

$$D(\mathbf{x}-\mathbf{x}') = \frac{1}{\rho_0^2}\langle\hat{\rho}(\mathbf{x})\,\hat{\rho}(\mathbf{x}')\rangle_c + \frac{1}{\rho_0^2}\langle\hat{\rho}(\mathbf{x})\rangle^2 = D_c(\mathbf{x}-\mathbf{x}') + 1 \qquad (13.104)$$

and using the fact that density correlations are of finite range (except at a critical point) the asymptotic behavior of $D(\mathbf{x}-\mathbf{x}')$ is

$$D(\mathbf{x}-\mathbf{x}') \xrightarrow[|\mathbf{x}-\mathbf{x}'|\to\infty]{} 1. \qquad (13.105)$$

Since $\delta(\mathbf{x}-\mathbf{x}_i)\,\delta(\mathbf{x}-\mathbf{x}_j) = \delta(\mathbf{x}-\mathbf{x}'-\mathbf{x}_i+\mathbf{x}_j)\,\delta(\mathbf{x}'-\mathbf{x}_j)$ the density correlation function can also be written as the expectation value

$$D(\mathbf{x}-\mathbf{x}') = \frac{1}{\rho_0^2}\sum_{i,j}\langle\delta(\mathbf{x}-\mathbf{x}'-\mathbf{x}_i+\mathbf{x}_j)\,\delta(\mathbf{x}'-\mathbf{x}_j)\rangle. \qquad (13.106)$$

Because of translational invariance, the sum over $\mathbf{x}_j$ is isotropic in $\mathbf{x}'$, on the average, and we can remove the second δ-function in favour of a factor ρ_0/N.[d] In this way, one arrives at another form,

$$D(\mathbf{x}-\mathbf{x}') = \frac{1}{\rho_0}\frac{1}{N}\sum_{i,j}\langle\delta(\mathbf{x}-\mathbf{x}'-\mathbf{x}_i+\mathbf{x}_j)\rangle. \qquad (13.107)$$

The average has to be taken, as usual, with the N-particle probability distribution

$$w(\mathbf{x}_1, \ldots, \mathbf{x}_N) = \frac{1}{Z_N}\,e^{-\beta(1/2)\sum_{i,j}\Phi(\mathbf{x}_i-\mathbf{x}_j)}, \qquad (13.108)$$

as

$$\langle O(\mathbf{x}_1, \ldots, \mathbf{x}_N)\rangle = \int\frac{d^D x_1 \ldots d^D x_N}{N!}\,O(\mathbf{x}_1, \ldots, \mathbf{x}_N)\,w(\mathbf{x}_1, \ldots, \mathbf{x}_N), \qquad (13.109)$$

where $\Phi(\mathbf{x}_i-\mathbf{x}_j)$ are the pair potentials between the atoms in the gas and Z_N is the classical partition function,

[d]This is due to the average $\delta(\mathbf{x}'-\mathbf{x}_j) \to \int(d^3x'/V)\,\delta(\mathbf{x}'-\mathbf{x}_j) = 1/V = \rho_0/N$.

$$Z_N = \int \frac{d^D x_1 \ \ldots \ d^D x_N}{N!} w(\mathbf{x}_1, \ \ldots, \ \mathbf{x}_N) \tag{13.110}$$

and the expression

$$\frac{d^D x_1 \ \ldots \ d^D x_N}{N!} w(\mathbf{x}_1, \ \ldots, \ \mathbf{x}_N)$$

is the probability of finding one particle in the volume element $d^D x_1$ another one in $d^D x_2$, etc.

In liquid state physics, it is customary to define the pair distribution function as

$$g(\mathbf{x} - \mathbf{x}') = \frac{1}{\rho_0^2} \int \frac{d^D x_3 \ \ldots \ d^D x_N}{(N-2)!} w(\mathbf{x}, \mathbf{x}', \mathbf{x}_3, \ \ldots, \mathbf{x}_N). \tag{13.111}$$

This is obviously the expectation value of the operator

$$\frac{1}{\rho_0^2} \sum_{i \neq j} \delta(\mathbf{x} - \mathbf{x}_i) \delta(\mathbf{x} - \mathbf{x}_j).$$

Hence the relation to the density correlation is the following

$$D(\mathbf{x} - \mathbf{x}') = \frac{1}{\rho_0} \delta(\mathbf{x} - \mathbf{x}') + g(\mathbf{x} - \mathbf{x}'). \tag{13.112}$$

From (13.110) we see that the normalization of $g(\mathbf{x} - \mathbf{x}')$ is

$$\rho_0^2 \int d^D x \, d^D x' \, g(\mathbf{x} - \mathbf{x}') = \rho_0^2 V \int d^3 x \, g(\mathbf{x}) = N^2 - N.$$

In a grand canonical ensemble, the right-hand side becomes

$$\langle N^2 \rangle - \langle N \rangle = k_B T \frac{\partial}{\partial \mu} \langle N \rangle |_{V,T}.$$

Using

$$\rho = \left. \frac{\partial P}{\partial \mu} \right|_{V,T} = \left. \frac{\partial P}{\partial \rho} \right|_{V,T} \left. \frac{\partial \rho}{\partial \mu} \right|_{V,T} = \frac{1}{V} \left. \frac{\partial P}{\partial \rho} \right|_{V,T} \left. \frac{\partial \langle N \rangle}{\partial \mu} \right|_{V,T},$$

we see that we can make the identification

$$\langle N^2\rangle - \langle N\rangle = k_B T\langle N\rangle \left.\frac{\partial\rho}{\partial P}\right|_{V,T}, \tag{13.113}$$

so that

$$\rho_0 V + \rho_0^2 V\int d^D x(g(\mathbf{x})-1) = \langle N^2\rangle - \langle N\rangle^2 = \langle N\rangle k_B T\left.\frac{\partial\rho}{\partial P}\right|_{V,T}$$

and we arrive at the so-called *compressibility sum rule*

$$1 + \rho_0\int d^D x(g(\mathbf{x})-1) = k_B T\varkappa/\rho_0, \tag{13.114}$$

where $\varkappa = (1/\rho)(\partial\rho/\partial P)|_{V,T}$ is the isothermal compressibility. In an ideal gas, $w(\mathbf{x}_1, \ldots, \mathbf{x}_N) = N!/V^N$ and

$$g(\mathbf{x}-\mathbf{x}') = 1 - \frac{1}{N} \xrightarrow[N\to\infty]{} 1. \tag{13.115}$$

The density correlation function is measurable quite directly in scattering experiments, typically with X-rays, electrons or neutrons, the first probing the electron distribution, the second the charge density, and the third the positions of the nuclei. Taking neutron scattering as an example, the atomic distances are usually larger than the scattering nuclei and the scattering cross section in the Born approximation is given by the well-known formula

$$\frac{d\sigma}{d\Omega} = \left(\frac{m_n}{2\pi\hbar^2}\right)^2\left|\int d^D x\, e^{i\mathbf{q}\cdot\mathbf{x}} V(\mathbf{x})\right|^2, \tag{13.116}$$

where Ω is the solid scattering angle, $\mathbf{q}$ the momentum transfer, and $V(\mathbf{x})$ is the scattering potential of the neutrons. For slow enough neutrons, for instance reactor neutrons with thermal energies and de Broglie wavelengths $\lambda \sim 1\text{Å}$, the nuclei may be approximated as point-like objects, whose effect upon the neutrons is described to a good approximation by a

simple phase shift a in the s wave. Such a phase shift is associated with a total cross section $4\pi a^2$ and can be thought of as coming from a potential

$$V(\mathbf{x}) = \frac{2\pi\hbar^2}{m_n} a \sum_i \delta(\mathbf{x} - \mathbf{x}_i) \tag{13.117}$$

i.e., using the particle density (13.103), as

$$V(\mathbf{x}) = \frac{2\pi\hbar^2}{m_n} a\, \hat{\rho}(\mathbf{x}). \tag{13.118}$$

In a thermal ensemble, the absolute square is replaced by the expectation

$$\left\langle \int d^D x\, e^{i\mathbf{q}\cdot\mathbf{x}} V(\mathbf{x}) \int d^D x'\, e^{-i\mathbf{q}\cdot\mathbf{x}'} V(\mathbf{x}') \right\rangle, \tag{13.119}$$

so that

$$\frac{d\sigma}{d\Omega} = a^2 \int d^D x\, d^D x'\, e^{i\mathbf{q}\cdot(\mathbf{x}-\mathbf{x}')} \langle \hat{\rho}(\mathbf{x})\, \hat{\rho}(\mathbf{x}') \rangle = a^2 N S(\mathbf{q}), \tag{13.120}$$

where N is the total number of atoms in the sample and

$$S(\mathbf{q}) = \rho_0 \int d^D x\, e^{i\mathbf{q}\cdot\mathbf{x}} D(\mathbf{x}) = \int d^D x\, e^{i\mathbf{q}\cdot\mathbf{x}} \frac{1}{N} \left\langle \sum_{i,j} \delta(\mathbf{x} - \mathbf{x}_i + \mathbf{x}_j) \right\rangle$$

$$= \frac{1}{N} \sum_{i,j} \langle e^{i\mathbf{q}\cdot(\mathbf{x}_j - \mathbf{x}_i)} \rangle \tag{13.121}$$

the Fourier transform of the density correlation function, i.e., the *structure factor* of the liquid. In terms of the pair correlation function $g(\mathbf{x})$, $S(\mathbf{q})$ is given by [see (13.112)]

$$S(\mathbf{q}) = 1 + \rho_0 \int d^D x\, e^{i\mathbf{q}\cdot\mathbf{x}} g(\mathbf{x}) \tag{13.122}$$

$$= 1 + \rho_0 \int d^D x\, e^{i\mathbf{q}\cdot\mathbf{x}} (g(\mathbf{x}) - 1) + \rho_0 (2\pi)^D \delta^D(\mathbf{q})$$

$$\equiv S_c(\mathbf{q}) + \rho_0 (2\pi)^D \delta^D(\mathbf{q}). \tag{13.123}$$

FIG. 13.21. Pair distribution of argon at 84.4K as obtained from neutron diffraction by Henshaw *et al.* (cited in the Notes and References). The curves of the atomic position for the $D = 2$ melting model are from Kahn (see Notes and References).

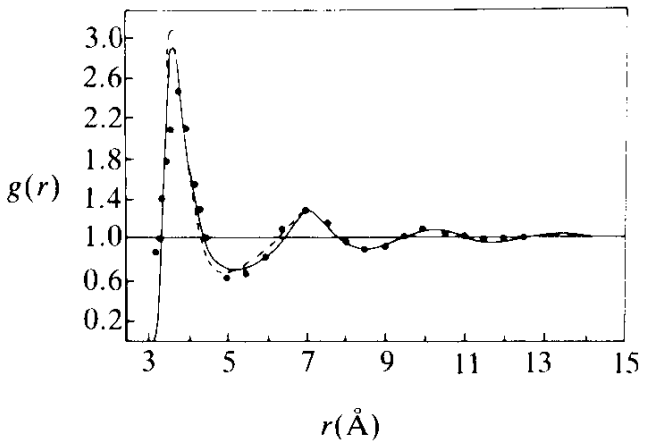

From (13.114), the value of $S_c(\mathbf{q})$ at $\mathbf{q} = 0$ is directly related to the isothermal compressionality:

$$S_c(\mathbf{q} = \mathbf{0}) = k_B T \frac{\partial \rho}{\partial P}\bigg|_{V,T}. \tag{13.124}$$

In an ideal gas, for which $g(\mathbf{x}) \sim 1$ we find

$$1 = k_B T \frac{\partial \rho}{\partial P}\bigg|_{V,T}, \tag{13.125}$$

in agreement with the equation of state $pV = Nk_B T$.

A typical pair distribution $g(\mathbf{x})$ is that of liquid argon at 84.4K shown in Fig. 13.21, as obtained from neutron diffraction data. The figure shows also two theoretical curves obtained by assuming Lennard-Jones potentials. If $r = |\mathbf{x}|$ is much smaller than the diameter of the atoms, the pair distribution vanishes. The "hole" at the origin leads to the peak in the Fourier transform $S_c(\mathbf{q})$ at $\mathbf{q} \sim 2\pi/d$ and $S_c(\mathbf{q})$ has the characteristic shape shown in Fig. 13.22 for another system, Rb, at 40K.

Let us now find the pair distribution function in the disordered phase of the melting model. For this we perform a Monte Carlo simulation of the cosine model and record the displacement variables $u_i(\mathbf{x})$. These can be used to find the atomic positions. Notice that the positions are not immediately given by

FIG. 13.22. Structure factor $S(Q)$ for a gas of hard spheres as calculated by Ashcroft and Lekner (cited in the Notes and References) and compared with experimental data on Rb at 40C.

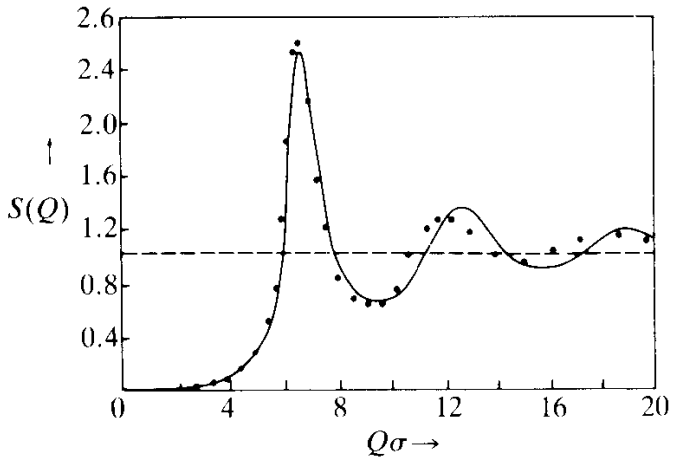

$$\mathbf{x}' = \mathbf{x} + \mathbf{u}(\mathbf{x}). \tag{13.126}$$

The reason is that the variables $u_i(\mathbf{x})$ in the cosine model run only from $-a$ to a so that the atoms can apparently never leave the unit cell. This would be unphysical. In order to permit an identification of $\mathbf{x} + \mathbf{u}(\mathbf{x})$ with particle positions we have to perform a defect-gauge transformation into a gauge in which the trivial fluctuations of the Volterra surface are absent. In order to understand this point more clearly, consider the Villain approximation to the cosine model (taking $\lambda = 0$, for simplicity):

$$Z = \sum_{\{n_{ij}(\mathbf{x})\}} \prod_{\mathbf{x},i} \left[\int_{-a}^{a} \frac{du_i(\mathbf{x})}{a} \right] \times \exp\left\{ -\beta \left(\frac{2\pi}{a} \right)^2 \sum_{\mathbf{x}} \left[\frac{1}{2} \sum_{i<j} (\nabla_i u_j + \nabla_j u_i - 2a n_{ij}^s)^2 + \xi \sum_i (\nabla_i u_i - a n_{ii}^s)^2 \right] \right\}. \tag{13.127}$$

In it the displacement fields $u_i(\mathbf{x})$ all remain within the unit cell and the jump numbers $n_{ij}^s(\mathbf{x})$ include all fluctuations of the Volterra surfaces. From our previous considerations in Chapter 10 we know that these fluctuations are unphysical. If we want to include only physical fluctuations, we have to remove the irrelevant parts by a defect-gauge transformation,

$$u_i(\mathbf{x}) \to u_i(\mathbf{x}) + a N_i(\mathbf{x}), \quad n_{ij}^s(\mathbf{x}) \to n_{ij}^s(\mathbf{x}) + \tfrac{1}{2}(\nabla_i N_j(\mathbf{x}) + \nabla_j N_i(\mathbf{x})), \tag{13.128}$$

FIG. 13.23. Atomic positions in the melting model before and after the transition. The molten state looks like a gas rather than a liquid due to the absence of a hard-core repulsion.

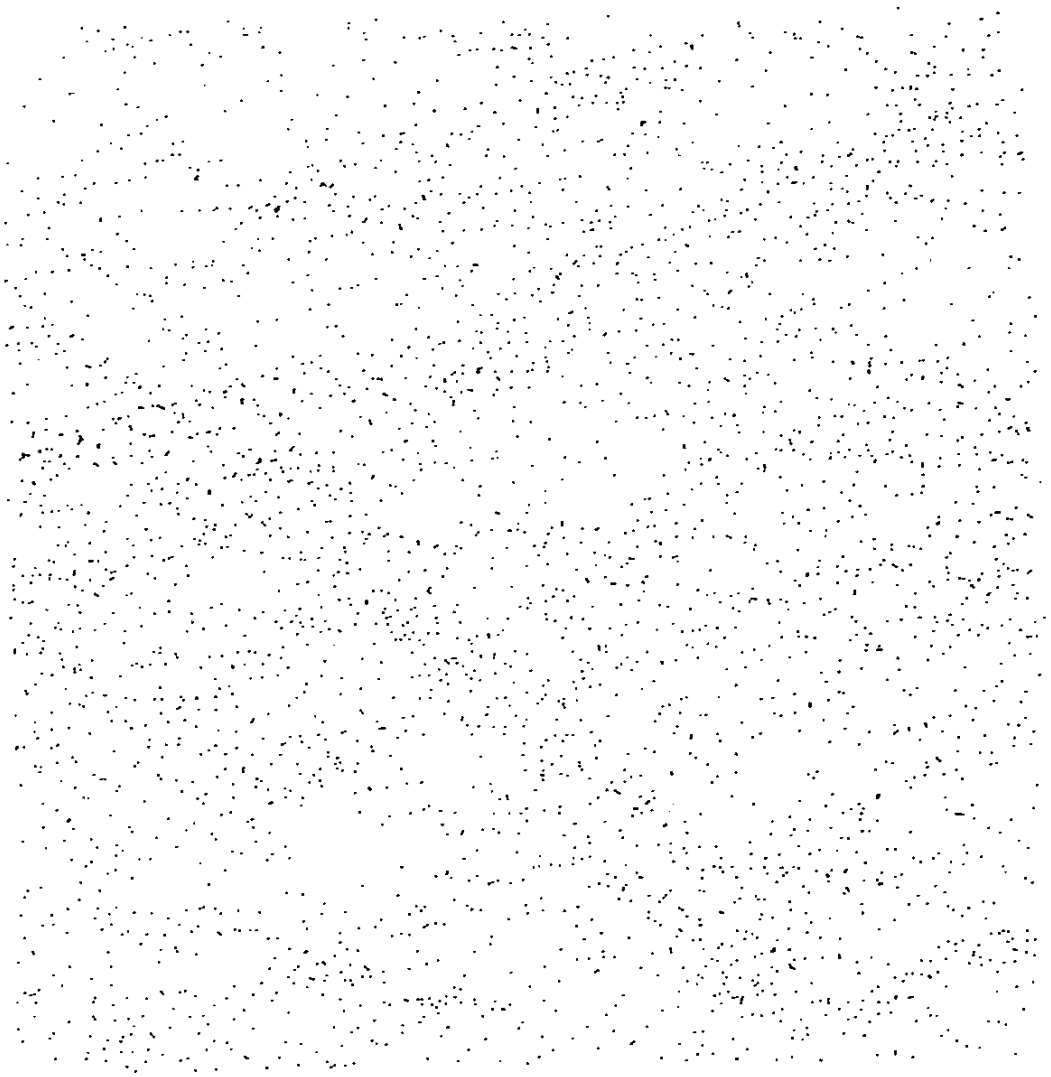

where we may choose the integer fields $N_i(\mathbf{x})$ such that n_{ij}^s satisfies the gauge conditions (10.4) and (10.5). Then the partition function reads

$$Z = \sum_{\{n_{ij}^s(\mathbf{x})\}} \Phi[n_{ij}^s] \prod_{\mathbf{x},i} \left[\int_{-\infty}^{\infty} \frac{du_i(\mathbf{x})}{a} \right] \times \exp\left\{ -\beta \left(\frac{2\pi}{a} \right)^a \sum_{\mathbf{x}} \left[\frac{1}{2} \sum_{i<j} (\nabla_i u_j + \nabla_j u_i - 2an_{ij}^s)^2 + \xi \sum_i (\nabla_i u_i - an_{ii}^s)^2 \right] \right\}, \tag{13.129}$$

$\Phi[n_{ij}^s]$ being the gauge-fixing functional enforcing the gauge (10.4), (10.5).

Now the different allowed configurations of the jump numbers n_{ij}^s correspond precisely to all physically different defect configurations. In addition, the displacement variables cover the entire crystal. Thus, in the fixed defect gauge, the variables

$$\mathbf{x}' = \mathbf{x} + \mathbf{u}(\mathbf{x})$$

can be identified with atomic positions. In Figs. 13.23 we have shown these positions above the melting transition. (Below the transition the positions show, of course perfect crystalline order with only small disturbances.) There is complete disorder with neither translational nor rotational memory. The pair distribution of this system is obviously not that of a real liquid but of an ideal gas. The reason for this is quite clear: the model contains no information on the hard cores of the atoms. It describes a crystal of *point-like* atoms. Consequently, the pair distribution function $g(\mathbf{x})$ does not vanish for $|\mathbf{x}|$ smaller than some atomic diameter and, in that respect, does not resemble that of a proper liquid. The model will need modifications in order to incorporate the finite atomic sizes into the system.

NOTES AND REFERENCES

The cosine model was proposed by
H. Kleinert, *Phys. Lett.* **91A** (1982) 295.
Its relation to lattice gauge theory was pointed out in
H. Kleinert, *Lett. Nuovo Cimento* **37** (1983) 295.

The methods developed in lattice gauge theories were used to calculate its thermodynamic properties in three dimensions by
S. Ami, T. Hofsäss and R. Horsley, *Phys. Lett.* **101A** (1984) 145
and in two dimensions by
S. Ami and H. Kleinert, *J. Phys.* (Paris) **45** (1984) 877.
Monte Carlo simulations were performed in three dimensions by
L. Jacobs and H. Kleinert, *J. Phys.* **A17** (1983) L361
and in two dimensions by
W. Janke and H. Kleinert, *Phys. Lett.* **105A** (1984) 134, *Phys. Lett.* **114A** (1986) 255
and by
H. Bohr and L. Kaznelson, *Phys. Lett.*

For a beautiful review on the liquid state see
J.A. Barker and D. Henderson, *Rev. Mod. Phys.* **48** (1976) 587.

The data for $g(r)$ of Argon are from
G.D. Henshaw, *Phys. Rev.* **105** (1957) 976,
A. Kahn, *Phys. Rev.* **134A** (1964) 367.
The Rubidium data and curves are taken from the paper of

N.W. Ashcroft and J. Lekner, *Phys. Rev.* **145** (1966) 83.
A calculation of the pair distribution in a hard sphere gas is found in
N.S. Ashcroft and J. Leckner, *Phys. Rev.* **145** (1966) 83,
using the solution of the (so-called PY) equations of
J.K. Percus and G.J. Yevick, *Phys. Rev.* **110** (1958) 1,
which were found by
E. Thiele, *J. Chem. Phys.* **39** (1963) 474,
M.S. Wertheim, *Phys. Rev. Lett.* **10** (1963) 321,
R.J. Baxter, *Phys. Rev.* **154** (1967) 170.
See also the monographs by
C.A. Croxton, *Liquid State Physics* (Cambridge Univ. Press, Cambridge, 1973),
P.A. Engelstaff, *An Introduction to the Liquid State* (Academic Press, London, 1967).

CHAPTER FOURTEEN

THE TWO-DIMENSIONAL KOSTERLITZ-THOULESS-HALPERIN-NELSON-YOUNG APPROACH TO DEFECT MELTING

Let us compare the properties of our defect models of melting with previous predictions on the behavior of two-dimensional defect melting as advanced by Kosterlitz, Thouless, Halperin, Nelson and Young (KTHNY).

14.1. DISSOCIATION OF DISLOCATION PAIRS

We begin with a slight modification of the partition function (9.53), namely (dropping now the bars on top of σ_{ij} and χ):

$$Z = \left[\frac{1}{4\xi^2}\left(1 - 2\frac{\xi}{\gamma}\right)\right]^{N/2} \frac{1}{(\sqrt{2\pi\beta})^{3N}} \prod_{\mathbf{x}} \left[\int_{-\infty}^{\infty} d\chi(\mathbf{x})\right] \sum_{\{n_{ij}(\mathbf{x})\}} \Phi[n_{ij}]$$
$$\times \exp\left\{-\frac{1}{2\beta}\sum_{\mathbf{x}}\left[\sigma_{12}^2 + \frac{1}{2\xi}(\sigma_{11}^2 + \sigma_{22}^2) - \frac{1}{2\gamma}(\sigma_{11} + \sigma_{22})^2\right]\right.$$
$$\left. + 2\pi i \sum_{\mathbf{x}} b_i(\mathbf{x})\, \varepsilon_{ik} \bar{\nabla}_k \chi(\mathbf{x})\right\}, \tag{14.1}$$

where the stress tensor is the double-curl of the stress "gauge field" $\chi(\mathbf{x})$,

$$\sigma_{ij}(\mathbf{x}) = \varepsilon_{ik}\, \varepsilon_{jm} \nabla_k \nabla_m \chi(\mathbf{x}) \tag{14.2}$$

and

$$b_i(\mathbf{x}) \equiv \alpha_i(\mathbf{x}) = \varepsilon_{\ell j} \nabla_\ell n_{ij} \tag{14.3}$$

is the two-dimensional lattice version of the dislocation density. Actually, KTHNY considered triangular lattices while our partition function was set up for cubic systems. In two dimensions the linear elastic energy of triangular lattices can be parametrized in the same way as in isotropic systems. We will, therefore, find it convenient to consider first isotropic square lattices and include the modifications due to the triangular structure at a later stage. In isotropic systems, where $\xi = 1$, the parameter γ is given in terms of the elastic Lamé constants μ and λ by

$$\frac{1}{\gamma} = \frac{\lambda/\mu}{2(\lambda/\mu + 1)} = \frac{\nu}{1+\nu}.$$

Hence $(1/4)(1 - 2/\gamma) = (1/4)1/(\lambda/\mu + 1) = (1/4)(1 - \nu)/(1 + \nu)$ and the partition function becomes

$$Z = \left[\frac{1}{4}\frac{1-\nu}{1+\nu}\right]^{N/2} \frac{1}{(\sqrt{2\pi\beta})^{3N}} \prod_{\mathbf{x}} \left[\int_{-\infty}^{\infty} d\chi(\mathbf{x})\right] \sum_{\{n_{ij}(\mathbf{x})\}} \Phi[n_{ij}]$$
$$\times \exp\left\{-\frac{1}{4\beta}\frac{1}{1+\nu}\sum_{\mathbf{x}} (\bar{\nabla}\cdot\nabla\chi)^2 + 2\pi i \sum_{\mathbf{x}} b_i(\mathbf{x})\, \varepsilon_{ik} \bar{\nabla}_k \chi\right\}. \tag{14.4}$$

The χ field can be integrated out giving

$$Z = \left[\frac{1}{2}(1-\nu)\right]^{N/2} \frac{1}{(\sqrt{2\pi\beta})^{2N}} \det{}^{-1}(-\bar{\nabla}\cdot\nabla) \sum_{\{n_{ij}(\mathbf{x})\}} \Phi[\eta_{ij}]$$
$$\times \exp\left\{-4\pi^2\beta(1+\nu)\sum_{\mathbf{x}} b_i(\mathbf{x})\left(\delta_{ij} - \frac{\nabla_i \bar{\nabla}_j}{\bar{\nabla}\cdot\nabla}\right)\frac{1}{-\bar{\nabla}\cdot\nabla} b_j(\mathbf{x})\right\}. \tag{14.5}$$

This is the same expression as (9.60) except that the defects are described in terms of the dislocation density $b_i(\mathbf{x})$ instead of the defect density $\eta(\mathbf{x})$. In the dislocation form, the defect representation is very similar to the vortex representation of the ordinary Villain model in two dimensions:

$$Z_V = \frac{1}{(\sqrt{2\pi\beta})^{2N}} \sum_{\{\ell(\mathbf{x})\}} \exp\left\{-4\pi^2\frac{\beta}{2}\sum_{\mathbf{x}} \ell(\mathbf{x})\frac{1}{-\bar{\nabla}\cdot\nabla}\ell(\mathbf{x})\right\}. \tag{14.6}$$

Indeed, the interaction energy between two dislocations has the form

$$v_{ij}^T(\mathbf{x}) = \left(\delta_{ij} - \frac{\nabla_i \bar{\nabla}_j}{\bar{\nabla}\cdot\nabla}\right)\frac{1}{-\bar{\nabla}\cdot\nabla} = (-\delta_{ij}\bar{\nabla}\cdot\nabla + \nabla_i\bar{\nabla}_j)\, v_4^\delta(\mathbf{x}), \tag{14.7}$$

where

$$v_4^\delta(\mathbf{x}) = \int \frac{d^2k}{(2\pi)^2} e^{i\mathbf{k}\cdot\mathbf{x}} \frac{1}{(\bar{\mathbf{K}}\cdot\mathbf{K} + \delta^2)^2} \tag{14.8}$$

is the potential $1/(\bar{\nabla}\cdot\nabla)^2$ with an infinitesimal regulator mass [recall Eq. (1.119)]. For large separations $|\mathbf{x}|$, the first term $-\delta_{ij}\bar{\nabla}\cdot\nabla\, v_4^\delta(\mathbf{x})$ gives rise to the same logarithmic potential as in the vortex case [see Eq. (1.123) and take the trace]:

$$\begin{aligned} -\delta_{ij}\bar{\nabla}\cdot\nabla\, v_4^\delta(\mathbf{x}) &= \delta_{ij}\bar{\nabla}\cdot\nabla(\partial/\partial\delta^2)v_\delta(\mathbf{x}) \\ &\xrightarrow[|\mathbf{x}|\to\infty]{} \delta_{ij}\left[-\frac{1}{2\pi}\log\left(|\mathbf{x}|\frac{1}{2}e^\gamma\right) - \frac{1}{2\pi}\left(\log\delta + \frac{1}{2}\right)\right]. \end{aligned} \tag{14.9a}$$

The second term contributes

$$\nabla_i\bar{\nabla}_j v_4^\delta(\mathbf{x}) \xrightarrow[|\mathbf{x}|\to\infty]{} \frac{1}{4\pi}\left[\delta_{ij}\log\left(|\mathbf{x}|\frac{1}{2}e^\gamma\right) + \frac{x_i x_j}{|\mathbf{x}|^2}\right] + \frac{1}{4\pi}\delta_{ij}\log\delta, \tag{14.9b}$$

so that both together give [see Eq. (1.124)]

$$v_{ij}^T(\mathbf{x}) \to -\frac{1}{4\pi}\left[\delta_{ij}\log|\mathbf{x}| - \frac{x_i x_j}{|\mathbf{x}|^2}\right] - \frac{1}{4\pi}\left[\log\left(\frac{\delta}{2}e^\gamma\right) + 1\right]\delta_{ij}. \tag{14.9c}$$

In the limit $\delta \to 0$, the second term enforces neutrality of the dislocation gas,

$$\sum_{\mathbf{x}} b_i(\mathbf{x}) = 0. \tag{14.10}$$

This is a manifestation of the dipole neutrality (9.76). For such neutral gases we can replace v_{ij}^T by the subtracted potential

$$v_{ij}'^T(\mathbf{x}) = v_{ij}^T(\mathbf{x}) - v_{ij}^T(\mathbf{0}) = -(\delta_{ij}\nabla\cdot\bar{\nabla} - \nabla_i\bar{\nabla}_j)v_4''(\mathbf{x}). \tag{14.11}$$

For long distances, the potential is dominated by the logarithmic part

$$-\frac{1}{4\pi}\delta_{ij}\log|\mathbf{x}| \tag{14.12}$$

just as in the ordinary XY model.

Since critical properties of a system are governed by its long-distance properties, Kosterlitz and Thouless concluded that there should be no difference between the phase transition of vortices in a thin film of superfluid ^{4}He and that of dislocations in a two-dimensional crystal. At low temperature, the crystal should contain only very few dislocations bound in pairs of opposite charge. As the temperature increases, the average separation increases. The long-range interaction energy of a pair of fundamental Burgers vectors with $b_i^2 = 1$ is

$$E_{\text{int}} \approx 4\pi^2\beta(1+\nu)2\frac{1}{4\pi}\log r,$$

where $r = |\mathbf{x}|$, is the separation of the pair. Using only this asymptotic formula the average of r^2 can easily be estimated as follows

$$\langle r^2\rangle \approx \frac{\int d^2x\, r^2 \exp\left\{-4\pi^2\beta(1+\nu)\frac{2}{4\pi}\log r\right\}}{\int d^2x \exp\left\{-4\pi^2\beta(1+\nu)\frac{2}{4\pi}\log r\right\}} = \frac{2-2\pi\beta(1+\nu)}{4-2\pi\beta(1+\nu)}. \tag{14.13}$$

For $\beta(1+\nu) \approx 2/\pi$ this expression has a pole of the form

$$\langle r^2\rangle \approx -\frac{2}{4-2\pi\beta(1+\nu)}. \tag{14.14}$$

Because of the frequent appearance of the combination $\beta(1+\nu)$ we shall, from now on, call this quantity $\tilde{\beta}$.

If renormalitation effects are taken into account, formula (14.14) implies that there should be a dislocation pair unbinding transition at a critical temperature at which

$$\tilde{\beta}_c^R \equiv \beta_c^R(1+\nu^R) = \beta_c^R\frac{\mu^R+\lambda^R}{\mu^R+\lambda^R/2} = \frac{2}{\pi} \approx 0.6366, \tag{14.15}$$

where ν^R, μ^R, λ^R are the renormalized elastic constants right at the transition point. Remembering that β was equal to $\mu a^3/(2\pi)^2 k_B T$ where a is the lattice spacing, this result can also be written more explicitly as

$$\frac{a^2\mu^R}{(2\pi)^2 k_B T_c}\frac{\mu^R+\lambda^R}{\mu^R+\lambda^R/2}=\frac{2}{\pi}\approx 0.6366. \tag{14.16}$$

In the literature on this subject one finds the results stated in terms of the stiffness parameter[a]

$$K\equiv\frac{a^2}{k_B T_c}2\mu\frac{\mu+\lambda}{\mu+\lambda/2}, \tag{14.17}$$

which is related to our $\tilde{\beta}$ by

$$K=8\pi^2\tilde{\beta}. \tag{14.18}$$

At the critical point, the renormalized K^R should have the value

$$K_c^R=16\pi\approx 50.265. \tag{14.19}$$

Equations (14.15), (14.16), or (14.19) are *universality* statements: A rare gas of dislocations undergoes a continuous phase transition whenever the combination of elastic constants on the left-hand side has softened to a point at which these equations are satisfied.

The relation (14.16) is, of course, the precise analogue of the universality condition for the critical superfluid density in films of ^{4}He,

$$\frac{\hbar^2\rho_s}{M^2}=\frac{2}{\pi}k_B T_c, \tag{14.20}$$

which was derived from the critical value [see Eq. (11.179)]

$$\beta_c^R=\frac{2}{\pi} \tag{14.21}$$

in the Villain model.

Notice that the critical index governing the width of the Bragg-like peaks (7.123) is *not* universal since it contains a combination of μ^R and λ^R, which is different from K^R.

[a]For triangular lattices, a^2 is the square of the lattice spacing a_0 and the cell volume is $v\equiv a^2=\sqrt{3}a_0^2/2$. See also footnote h below.

14.2. RENORMALIZATION GROUP EQUATIONS

A characteristic feature of the continuous pair unbinding mechanism is the unusual temperature behavior with which the coherence length ξ of the disordered phase goes to infinity when approaching the critical point. We have seen such a behavior in Part II, where the coherence length of the Villain model was found to have an essential singularity at $T = T_c$, of the form

$$\xi \approx \exp\{\text{const. } (T/T_c - 1)^{-1/2}\}, \tag{14.22}$$

rather than diverging with the usual critical power[b]

$$\xi \approx \left(\frac{T}{T_c} - 1\right)^{-\nu}. \tag{14.23}$$

A similar law can be derived for dislocations on a two-dimensional lattice. To do so we first find the general renormalization equation for the elastic constants which is analogous to Eq. (11.112) of Part II for the superfluid density in the Villain model. For this we define the renormalized elastic constants at a momentum $\mathbf{k}$ by the correlation functions of the stress tensor $\sigma_{ij} = \varepsilon_{ik}\varepsilon_{jl}\bar{\nabla}_k\bar{\nabla}_l\chi$:

$$\langle \sigma_{ij}^*(\mathbf{k})\,\sigma_{k\ell}(\mathbf{k})\rangle \equiv (\bar{\mathbf{K}}\cdot\mathbf{K})^{-2}\varepsilon_{im}\varepsilon_{jn}K_mK_n\varepsilon_{kr}\varepsilon_{\ell s}K_r\bar{K}_s[2\beta(1+\nu)]^R(\mathbf{k}). \tag{14.24}$$

In linear elasticity, $[\beta(1+\nu)]^R$ reduces to the $\mathbf{k}$ independent "bare" elastic constant. In the presence of defects, the correlations of $\sigma_{ij}(\mathbf{x})$ can be obtained from the partition function with external strain sources,

$$Z[u_{ij}^{\text{ext}}] \propto \prod_{\mathbf{x}}\left[\int \frac{d\chi(\mathbf{x})}{\sqrt{2\pi\beta}}\right]\delta_{\bar{\nabla}_i\sigma_{ij},0} \times \exp\left\{-\frac{1}{2\beta}\sum_{\mathbf{x},i,j}\sigma_{ij}c^{-1}_{ijk\ell}\sigma_{k\ell} + 2\pi i\sum_{\mathbf{x}}\sigma_{ij}n_{ij} + \sum_{\mathbf{x}}\sigma_{ij}u_{ij}^{\text{ext}}\right\}, \tag{14.25}$$

by forming the functional derivative

[b]We use the customary notation for this power ν even though this letter is already occupied by the Poisson number ν. The alert reader will, hopefully, not be confused.

$$\langle \sigma_{ij}(\mathbf{x})\, \sigma_{k\ell}(\mathbf{0}) \rangle = \frac{1}{Z} \frac{\delta^2 Z}{\delta u_{ij}^{\mathrm{ext}}(\mathbf{x})\, \delta u_{k\ell}^{\mathrm{ext}}(\mathbf{0})} \bigg|_{u_{ij}^{\mathrm{ext}} = 0}. \tag{14.26}$$

With σ_{ij} expressed in terms of the stress "gauge field" χ we can integrate out the χ field and find, for isotropic media [recall (17.34), Part II],

$$Z[u_{ij}^{\mathrm{ext}}] \propto \exp\left\{ -\frac{\beta}{2} 4\pi^2 2(1+\nu) \sum_{\mathbf{x}} \bar{\eta}(\mathbf{x}) \frac{1}{(\bar{\nabla}\cdot\nabla)^2} \bar{\eta}(\mathbf{x}) \right\}, \tag{14.27}$$

where $\bar{\eta}(\mathbf{x})$ is defined to be a modification of the defect density $\bar{\eta}(\mathbf{x})$ in which the plastic gauge field $2\pi n_{ij}$ appears together with the external source as follows

$$\bar{\eta}(\mathbf{x}) = \varepsilon_{ik}\, \varepsilon_{j\ell}\, \nabla_k \nabla_\ell \left(n_{ij}^s - \frac{i}{2\pi} u_{ij}^{\mathrm{ext}} \right). \tag{14.28}$$

Forming now, in (14.27), the derivatives with respect to u_{ij}^{ext} and setting $u_{ij}^{\mathrm{ext}} = 0$ we obtain

$$\begin{aligned} \langle \sigma_{ij}^*(\mathbf{k})\, \sigma_{k\ell}(\mathbf{k}) \rangle = {} & 2\beta(1+\nu) \frac{1}{(\bar{\mathbf{K}}\cdot\mathbf{K})^2} \varepsilon_{im}\, \varepsilon_{jn}\, K_m K_n\, \varepsilon_{kr}\, \varepsilon_{\ell s}\, \bar{K}_r \bar{K}_s \\ & \times \left(1 - 4\pi^2 \beta \frac{2(1+\nu)}{(\bar{\mathbf{K}}\cdot\mathbf{K})^2} \langle \bar{\eta}^*(\mathbf{k})\, \bar{\eta}(\mathbf{k}) \rangle \right). \end{aligned} \tag{14.29}$$

Contracting the indices ij with $k\ell$ gives

$$\langle \sigma_{ij}^*(\mathbf{k})\, \sigma_{ij}(\mathbf{k}) \rangle = 2\beta(1+\nu) \left(1 - 4\pi^2 \beta \frac{2(1+\nu)}{(\bar{\mathbf{K}}\cdot\mathbf{K})^2} \langle \bar{\eta}^*(\mathbf{k})\, \bar{\eta}(\mathbf{k}) \rangle \right). \tag{14.30}$$

The quantity on the left-hand side is, due to (14.24) equal to the renormalized value of $2\beta(1+\nu)$, so that we find the exact equation

$$2\tilde{\beta}^R(\mathbf{k}) = 2\tilde{\beta} \left(1 - 8\pi^2 \tilde{\beta} \frac{1}{(\bar{\mathbf{K}}\cdot\mathbf{K})^2} \langle \bar{\eta}^*(\mathbf{k})\, \bar{\eta}(\mathbf{k}) \rangle \right), \tag{14.31}$$

with $\tilde{\beta} \equiv \beta(1+\nu)$, as defined before. In a pure dislocation model, $\bar{\eta}(\mathbf{k})$ can be written as

$$\bar{\eta}(\mathbf{k}) = \varepsilon_{i\ell} K_\ell b_i(\mathbf{k}), \tag{14.32}$$

where $b_i(\mathbf{k})$ is the Fourier transformed dislocation distribution and the formula becomes

$$\tilde{\beta}^R(\mathbf{k}) = \tilde{\beta}\left(1 - 8\pi^2\tilde{\beta}\frac{1}{\bar{\mathbf{K}}\cdot\mathbf{K}}\left(\delta_{ij} - \frac{K_i\bar{K}_j}{\bar{\mathbf{K}}\cdot\mathbf{K}}\right)\langle b_i^*(\mathbf{k})\, b_j(\mathbf{k})\rangle\right). \tag{14.33}$$

Let us find the $\mathbf{x}$-space version of the limit $\mathbf{k}\to 0$ on the right-hand side:

$$\lim_{\mathbf{k}\to\mathbf{0}} \frac{1}{\bar{\mathbf{K}}\cdot\mathbf{K}}\left(\delta_{ij} - \frac{K_i\bar{K}_j}{\bar{\mathbf{K}}\cdot\mathbf{K}}\right)\langle b_i^*(\mathbf{k})\, b_j(\mathbf{k})\rangle. \tag{14.34}$$

As far as the first term is concerned, we may proceed as in Part II where we proved in equation (11.114) that due to charge neutrality, $\Sigma_{\mathbf{x}} b_i(\mathbf{x}) = 0$,

$$\lim_{\mathbf{k}\to\mathbf{0}} \frac{1}{\bar{\mathbf{K}}\cdot\mathbf{K}}\langle b_i^*(\mathbf{k})\, b_i(\mathbf{k})\rangle = \frac{1}{4}\sum_{\mathbf{x}} \mathbf{x}^2\langle b_i(\mathbf{x})\, b_i(\mathbf{0})\rangle. \tag{14.35}$$

Here we need a similar statement also for the second term, i.e.,

$$\lim_{\mathbf{k}\to\mathbf{0}} \frac{1}{(\bar{\mathbf{K}}\cdot\mathbf{K})^2} K_i\bar{K}_j\langle b_i^*(\mathbf{k})\, b_j(\mathbf{k})\rangle. \tag{14.36}$$

For this we consider a general tensor function

$$f_{ij}(\mathbf{k}) = \sum_{\mathbf{x}} e^{i\mathbf{k}\cdot\mathbf{x}} f_{ij}(\mathbf{x}), \tag{14.37}$$

which satisfies the charge neutrality condition $\Sigma_{\mathbf{x}} f_{ij}(\mathbf{x}) = 0$, so that $f_{ij}(\mathbf{k}=\mathbf{0}) = 0$. Invoking mirror reflection invariance, the lowest expansion terms of $f_{ij}(\mathbf{k})$ are

$$f_{ij}(\mathbf{k}) = \alpha k^2\delta_{ij} + \beta k_i k_j + O(\mathbf{k}^4). \tag{14.38}$$

On multiplying this by $(K_i \bar{K}_j)/(\bar{\mathbf{K}} \cdot \mathbf{K})^2$ and taking the limit $\mathbf{k} \to \mathbf{0}$ we find $\alpha + \beta$. If we, on the other hand, differentiate twice with respect to $\mathbf{k}$ we see that $-x_i x_j f_{ij}(\mathbf{x})$ and $-x^2 f_{ii}(\mathbf{x})$ have the Fourier transforms

$$\frac{\partial}{\partial k_i}\frac{\partial}{\partial k_j} f_{ij}(\mathbf{k}) = 4\alpha + 6\beta, \quad \frac{\partial}{\partial k_i^2} f_{jj}(\mathbf{k}) = 8\alpha + 4\beta. \tag{14.39}$$

Thus we may supplement the relation (14.35) by

$$\lim_{\mathbf{k}\to\mathbf{0}} \frac{1}{(\bar{\mathbf{K}} \cdot \mathbf{K})^2} K_i \bar{K}_j \langle b_i^*(\mathbf{k})\, b_j(\mathbf{k})\rangle = \frac{1}{8} \sum_{\mathbf{x}} \left(\frac{\mathbf{x}^2}{2} \delta_{ij} + x_i x_j \right) \langle b_i(\mathbf{x})\, b_j(\mathbf{0})\rangle. \tag{14.40}$$

Combining both limits gives

$$\lim_{\mathbf{k}\to\mathbf{0}} \frac{\delta_{ij} - K_i \bar{K}_j / \bar{\mathbf{K}} \cdot \mathbf{K}}{\bar{\mathbf{K}} \cdot \mathbf{K}} \langle b_i^*(\mathbf{k})\, b_j(\mathbf{k})\rangle = \frac{1}{16} \sum_{\mathbf{x}} (3\mathbf{x}^2 \delta_{ij} - 2x_i x_j) \langle b_i(\mathbf{x})\, b_j(\mathbf{0})\rangle, \tag{14.41}$$

so that the renomalization equation (14.31) becomes

$$\tilde{\beta}^R = \tilde{\beta} \left\{ 1 + \tilde{\beta} \frac{\pi^2}{2} \sum_{\mathbf{x}} (3\mathbf{x}^2 \delta_{ij} - 2x_i x_j) \langle b_i(\mathbf{x})\, b_j(\mathbf{0})\rangle \right\}, \tag{14.42}$$

where the expectation is to be formed within the partition function (14.5).

If the dislocation gas is very dilute, a fugacity expansion can be set up for evaluating the contributions of an increasing number of dislocations. The dominant contribution is a single pair of oppositely oriented fundamental Burgers vectors. Their interaction at a long range is given by a subtracted transverse potential (14.11), with the limit

$$v_{ij}'^T(\mathbf{x}) \xrightarrow[|\mathbf{x}|\to\infty]{} -\frac{1}{4\pi} \left(\delta_{ij} \log|\mathbf{x}| - \frac{x_i x_j}{\mathbf{x}^2} \right) - \frac{1}{4\pi} \delta_{ij} \log c, \tag{14.43}$$

c being a constant depending on the type of lattice. It can be determined most easily from the fact that the trace of $v_{ij}'^T(\mathbf{x})$ is equal to the lattice Coulomb potential $v_{ii}'^T(\mathbf{x}) = v'(\mathbf{x})$. Thus

$$v_{ii}'(\mathbf{x}) \xrightarrow[|\mathbf{x}|\to\infty]{} -\frac{1}{2\pi} \left(\log(|\mathbf{x}|c) - \frac{1}{2} \right) \tag{14.44}$$

has to coincide with the asymptotic behavior of the subtracted lattice Coulomb potential, which is known to be [see Part I, Eq. (6.196)]

$$v'(\mathbf{x}) \underset{|\mathbf{x}|\to\infty}{\longrightarrow} -\frac{1}{2\pi}\log(|\mathbf{x}|2\sqrt{2}e^{\gamma}) \tag{14.45}$$

on a square lattice. Hence we can identify

$$c_s = 2\sqrt{2}e^{\gamma+1/2} = 8.3057\ldots \tag{14.46}$$

On a triangular lattice, $v'(\mathbf{x})$, with the normalization $\bar{\nabla}\cdot\nabla v'(\mathbf{x}) = \delta_{\mathbf{x},\mathbf{i}}2/\sqrt{3}$, behaves like [see Appendix 6A, Part I, Eq. (6A.77)]

$$v'(\mathbf{x}) \underset{|\mathbf{x}|\to\infty}{\longrightarrow} -\frac{1}{2\pi}\log(|\mathbf{x}|2\sqrt{3}e^{\gamma}), \tag{14.47}$$

with $\mathbf{x}$ measured in units of the lattice spacing a_0, and

$$c_t = 2\sqrt{3}e^{\gamma+1/2} = 10.172. \tag{14.48}$$

In contrast to the vortices in the ordinary Villain XY model, the interaction energy of a pair of Burgers vectors $b_i(\mathbf{x})$ depends on the azimuthal angle θ of the distance vector between them [$\cos\theta \equiv (\mathbf{x}-\mathbf{x}')_1/|\mathbf{x}-\mathbf{x}'|$]. If the Burgers vectors point along the ± 1-direction, their energy is

$$E_{\text{int}} = b_i(\mathbf{x})\, v'^{T}_{ij}(\mathbf{x})\, b_j(0) = \frac{1}{4\pi}[\log(|\mathbf{x}|c) - \cos^2\theta] \tag{14.49}$$

Notice that due to the subtraction (14.11), there is no self-energy [$v'_{ij}(\mathbf{0}) = 0$]. Therefore, the expression

$$\sum_{b_i = \pm\hat{\mathbf{x}}} (3\delta_{ij}\mathbf{x}^2 - 2x_i x_j)\langle b_i(\mathbf{x}) b_j(\mathbf{0})\rangle \tag{14.50}$$

is equal to

$$-2(3 - 2\cos^2\theta)\mathbf{x}^2 \exp\left\{-4\pi^2 2\tilde{\beta}\frac{1}{4\pi}[\log(|\mathbf{x}|c) - \cos^2\theta]\right\}, \tag{14.51a}$$

which holds for square and triangular lattices. In both cases

$$\tilde{\beta} = \beta(1+\nu) = \frac{\mu a_0^2}{k_B T (2\pi)^2} \frac{2(\mu+\lambda)}{2\mu+\lambda} \equiv \frac{K}{8\pi^2}. \tag{14.52}$$

If the direction of the Burgers vectors is rotated by 90° we find once more the same expression with $\cos^2\theta$ replaced by $\sin^2\theta$,

$$-2(3-2\sin^2\theta)\mathbf{x}^2 \exp\left\{-4\pi^2 2\tilde{\beta}\frac{1}{4\pi}(\log(|\mathbf{x}|c) - \sin^2\theta)\right\}. \tag{14.51b}$$

We now perform the integration over the angles θ and use the formulas

$$\int_0^{2\pi} d\theta\, e^{4\pi^2 2\tilde{\beta}(1/4\pi)\cos^2\theta} = 2\pi e^{\pi\tilde{\beta}} I_0(\pi\tilde{\beta}), \tag{14.53a}$$

$$\int_0^{2\pi} d\theta \cos^2\theta\, e^{4\pi^2 2\tilde{\beta}(1/4\pi)\cos^2\theta} = 2\pi e^{\pi\tilde{\beta}} \frac{1}{2}[I_0(\pi\tilde{\beta}) + I_1(\pi\tilde{\beta})], \tag{14.53b}$$

where I_0 and I_1 are the associated Bessel functions. Then the two terms (14.51) together give

$$-8\pi e^{\pi\tilde{\beta}}[3I_0(\pi\tilde{\beta}) - (I_0(\pi\tilde{\beta}) + I_1(\pi\tilde{\beta}))] \tag{14.54}$$

and we obtain, from (14.42), the following renormalization equation for the elastic stiffness constant $\tilde{\beta} = \beta(1+\nu)$:

$$\tilde{\beta}^R = \tilde{\beta}\left[1 - 2\pi^2\tilde{\beta}\, z^2 [e^{\pi\tilde{\beta}}(I_0(\pi\tilde{\beta}) - (1/2)\, I_1(\pi\tilde{\beta}))] 2\pi \int_1^{\infty} \frac{dR}{R} R^{4-2\pi\tilde{\beta}}\right], \tag{14.55}$$

where

$$z = c^{-\pi\tilde{\beta}} \tag{14.56}$$

is the fugacity of a single dislocation.

This is to be compared with the equation in the ordinary Villain model

$$\beta^R = \beta\left(1 - 2\pi^2\beta z^2 2\pi \int_1^{\infty} \frac{dR}{R} R^{4-2\pi\beta}\right), \tag{14.57}$$

in which the fugacity was

$$z = (2\sqrt{2}\, e^{\gamma})^{-\pi\tilde{\beta}}. \tag{14.58}$$

Thus, apart from a multiplicity factor of 2 for the two directions of the Burgers vectors, the different fugacity

$$z = c^{-\pi\tilde{\beta}},$$

and the angular factor

$$e^{\pi\tilde{\beta}}[I_0(\pi\tilde{\beta}) - \tfrac{1}{2} I_1(\pi\tilde{\beta})],$$

the expression is the same.

For small fugacities and close to

$$\tilde{\beta}_c \sim \frac{2}{\pi} \tag{14.59}$$

we can therefore derive the renormalization group equations for $\tilde{\beta}$ and z as functions of the scale parameter $\ell = \log \lambda$ in the same way as in Sec. 11.6, Part II:

$$\frac{\partial \tilde{\beta}^{-1}}{\partial \ell} = 4\pi^2 z^2 2\pi e^{\pi\tilde{\beta}} \left[I_0(\pi\tilde{\beta}) - \frac{1}{2} I_1(\pi\tilde{\beta}) \right] \tag{14.60}$$

and

$$\frac{\partial z}{\partial \ell} = (2 - \pi\tilde{\beta})\, z. \tag{14.61}$$

14.3. TRIANGULAR LATTICE

Let us now see what modifications arise when working on a triangular lattice. Since in two dimensions the laws of linear elasticity for a hexagonal crystal are the same as those for an isotropic one, the long-range elastic forces between defects are unchanged. What is different for a triangular lattice is, first of all, the number of possible configurations of Burgers vectors. As on the square lattice, there can be two oppositely oriented vectors along the x-direction with the same interaction energy as in the isotropic lattice,

FIG. 14.1. Triplets of dislocations contributing to the renormalization equation (14.71).

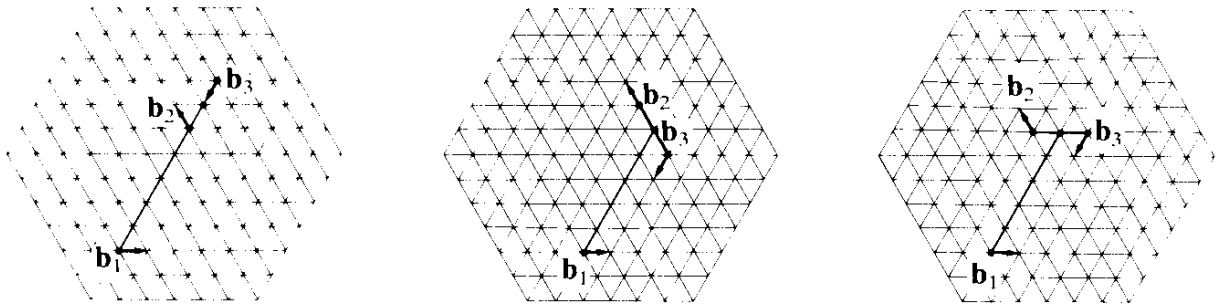

$$-4\pi^2 2\tilde{\beta}\frac{1}{4\pi}[\log(|\mathbf{x}|c) - \cos^2\theta].$$

Now instead of a contribution of the same type with $\cos^2\theta \to \sin^2\theta$, there are *two* more terms arising from the directions of one Burgers vector being rotated once by 60° and once more by 120°. Hence the expression (14.51a) plus (14.51b) is to be replaced by

$$\begin{aligned}
&-2(3-2\cos^2\theta)\exp\left\{-4\pi^2 2\tilde{\beta}\frac{1}{4\pi}[\log(|\mathbf{x}|c)-\cos^2\theta]\right\}\\
&-2\left(3-2\cos^2\left(\theta-\frac{2\pi}{3}\right)\right)\exp\left\{-4\pi^2 2\tilde{\beta}\frac{1}{4\pi}\left[\log(|\mathbf{x}|c)-\cos^2\left(\theta-\frac{2\pi}{3}\right)\right]\right\}\\
&-2\left(3-2\cos^2\left(\theta-\frac{4\pi}{3}\right)\right)\exp\left\{-4\pi^2 2\tilde{\beta}\frac{1}{4\pi}\left[\log(|\mathbf{x}|c)-\cos^2\left(\theta-\frac{4\pi}{3}\right)\right]\right\},
\end{aligned} \tag{14.62}$$

and Eq. (14.55) becomes

$$\tilde{\beta}^R = \beta\left[1 - 6\pi^2\tilde{\beta}z^2 e^{\pi\tilde{\beta}}(I_0(\pi\tilde{\beta}) - \frac{1}{2}I_1(\pi\tilde{\beta}))2\pi\int_1^\infty \frac{dR}{R}R^{4-2\pi\tilde{\beta}}\right], \tag{14.63}$$

i.e., the factor $4\pi^2$ of the square lattice is replaced by $6\pi^2$.

Were it only for this modificating, the critical behavior would have been the same for both lattices. On a triangular lattice, however, there is, an additional contribution to the defect sum. It consists of three dislocations pointing into the three different lattice directions (see Fig. 14.1). The relevance of such configurations derives from the fact that the special case when two of the partners coalesce reduces to the previous simple pairs. We may therefore view the additional triplet configurations

as a result of a break up of one partner in a dislocation pair into a further pair. As long as the "fragments" remain close to each other this produces only a small increase in the energy which, moreover, is partly compensated by an increase in configurational entropy. So what we have to do is supplement each of the three pair terms in (14.63),

$$2\pi^2 z^2 e^{\pi\tilde{\beta}}\left(I_0(\pi\tilde{\beta}) - \frac{1}{2}I_1(\pi\tilde{\beta})\right) 2\pi \int_1^\infty \frac{dR}{R} R^{4-2\pi\tilde{\beta}}$$

by a three-body term ($\Delta x^{(k)} \equiv x^{(\ell)} - x^{(n)}$, $k,\ell,n = 123, 231, 312$)

$$2z^3 \int d^2R \sum_{(k\ell n)} (3\Delta x^{(k)2}\delta_{ij} - 2\Delta x_i^{(k)}\Delta x_j^{(k)}) b_i^{(\ell)} b_j^{(m)} \int d^2x$$
$$\times \left(e^{8\pi^2\tilde{\beta} b_i^{(1)} b_j^{(2)} v_{ij}^T(\mathbf{R}+\mathbf{x}/2)} + e^{8\pi^2\tilde{\beta} b_i^{(1)} b_j^{(3)} v_{ij}^T(\mathbf{R}-\mathbf{x}/2)} + e^{8\pi^2\tilde{\beta} b_i^{(2)} b_j^{(3)} v_{ij}^T(\mathbf{x})}\right), \qquad (14.64)$$

where $\Delta\mathbf{x}^{(k)} \equiv \mathbf{x}^{(\ell)} - \mathbf{x}^{(m)} = (\mathbf{x},\ \mathbf{R} - \mathbf{x}/2,\ \mathbf{R} + \mathbf{x}/2)$ for $k\ell m = (123,\ 231,\ 312)$. We assume that the distance $r = |\mathbf{x}|$ between $\mathbf{x}_2$ and $\mathbf{x}_3$ is much smaller than the distance $R = |\mathbf{R}|$ between $\mathbf{x}_1$ and the center of mass of $\mathbf{x}_2$ and $\mathbf{x}_3$. Expanding the exponent in $\mathbf{x}$ up to quadratic terms gives

$$\exp\{8\pi^2\tilde{\beta}[b_i^{(1)}(b_j^{(2)} + b_j^{(3)}) v_{ij}^T(\mathbf{R}) + b_i^{(2)} b_j^{(3)} v_{ij}^T(\mathbf{x})]\}$$
$$\times [1 + \tfrac{1}{2} 8\pi^2\tilde{\beta}\, b_i^{(1)}(b^{(2)} - b^{(3)})_j\, \partial_k\, v_{ij}^T(\mathbf{R})\, x_k$$
$$+ \tfrac{1}{4}(8\pi^2\tilde{\beta})^2 b_i^{(1)}(b^{(2)} - b^{(3)})_j\, \partial_k v_{ij}(\mathbf{R})\, b_{i'}^{(1)}(b^{(2)} - b^{(3)})_{j'}\, \partial_{k'} v_{i'j'}(\mathbf{R})\, x_k x_{k'}$$
$$+ \tfrac{1}{4} 8\pi^2\tilde{\beta}\, b_i^{(1)}(b^{(2)} + b^{(3)})_j\, \partial_k \partial_{k'} v_{ij}(\mathbf{R})\, x_k x_{k'} + \ldots]. \qquad (14.65)$$

On integrating over $\mathbf{x}$, the linear terms vanish. The quadratic correction terms are of order $(r/R)^2$ and can be neglected as long as $r \ll R$. Thus the additional contribution reads

$$8\pi^3 z^3 e^{\pi\tilde{\beta}}\left(I_0(\pi\tilde{\beta}) - \frac{1}{2}I_1(\pi\tilde{\beta})\right)$$
$$\int_1^\infty \frac{dR}{R} R^{4-2\pi\tilde{\beta}} \int_1^{r_0} \frac{dr}{r} r^{2-\pi\tilde{\beta}} \int_0^{2\pi} d\varphi\, e^{2\pi\tilde{\beta}\hat{x}_i\hat{x}_j b_i^{(2)} b_j^{(3)}}, \qquad (14.66)$$

and $r_0 \ll R$ is the distance up to which the break up is included. It will be taken to be some fixed fraction of R, say

$$r_0 = \rho R. \tag{14.67}$$

Taking the Burgers vectors

$$b^{(2)} = \tfrac{1}{2}(-1, \sqrt{3}), \qquad b^{(3)} = \tfrac{1}{2}(-1, -\sqrt{3}) \tag{14.68}$$

and the relative direction

$$\hat{\mathbf{x}} = (\cos\varphi, \sin\varphi),$$

the integral over φ is seen to give

$$\int_0^{2\pi} d\varphi\, e^{2\pi\tilde{\beta}\cos(\varphi - \pi/3)\cos(\varphi + \pi/3)} = 2\pi e^{\pi\tilde{\beta}/2} I_0(\pi\tilde{\beta}). \tag{14.69}$$

Hence, the effect of the break up can be described as a change of the integral in (14.63) from $\int_1^\infty \frac{dR}{R} R^{4-2\pi\tilde{\beta}}$ to

$$\int_1^\infty \frac{dR}{R} R^{4-2\pi\tilde{\beta}} \left(1 + 2z\, e^{\pi\tilde{\beta}} I_0(\pi\tilde{\beta}) 2\pi \int_1^{r_0} \frac{dr}{r} r^{2-\pi\tilde{\beta}}\right) \tag{14.70}$$

and the renormalization equation becomes, at low fugacity,

$$\tilde{\beta}^R = \tilde{\beta}\Bigg[1 - 6\pi^2 z^2 e^{\pi\tilde{\beta}}(I_0(\pi\tilde{\beta}) - \frac{1}{2} I_1(\pi\tilde{\beta})) \times 2\pi \int_1^\infty \frac{dR}{R} R^{4-2\pi\tilde{\beta}} (1 + 2z e^{\pi\tilde{\beta}/2} I_0(\pi\tilde{\beta}) 2\pi \int_1^{\rho R} \frac{dr}{r} r^{2-\pi\tilde{\beta}})\Bigg]. \tag{14.71}$$

In order to extract from this equation reliable information on the critical regime we must again resort to a length-scale dependent self-consistent approach similar to that in the Villain model (see Section 11.7, Part II).

We first define a softened stiffness constant $\tilde{\beta}(\lambda)$ which contains all pairs of distances smaller than λ plus all possible split ups of each partner into two individual dislocations of radius smaller than $\rho\lambda$.

As a second step, we replace the potentials in the Boltzmann factors $R^{-2\pi\tilde{\beta}} = e^{-2\pi\tilde{\beta}\log R}$ by the integrals over the scale dependent force up

to the corresponding radius $\exp\left\{-2\pi\int_0^{\log R} d\log\lambda\tilde{\beta}(\lambda)\right\}$ [recall the treatment of (11.140) in Part II].

For the third step we introduce the auxiliary fugacity of a pair of dislocations separated by a distance R with the possibility of a break up of each partner [recall (11.144)]

$$z(R) = z\exp\left\{2\log R - \pi\int_{-\log c}^{\log R} d\log\lambda\tilde{\beta}(\lambda)\right\} \times\left(1 + ze^{\pi\tilde{\beta}/2} I_0(\pi\tilde{\beta})\, 2\pi\int_0^{\rho R}\frac{dr}{r} r^{2-\pi\tilde{\beta}}\right). \tag{14.72}$$

In the fourth step, we finally allow for the fact that the potential between the products of the break up is renormalized once more by pair fluctuations between them. Hence we push the factor $ze^{\pi\tilde{\beta}/2} I_0(\pi\tilde{\beta})$ *under* the integral and replace (14.72) by

$$z(R) = \exp\left\{2\log R - \pi\int_{-\log c}^{\log R} d\log\lambda\tilde{\beta}(\lambda)\right\} \times\left(1 + 2\pi\int_0^{\log(\rho R)} d\log r\, z(r)\, e^{\pi\tilde{\beta}(r)/2} I_0(\pi\tilde{\beta}(r))\right). \tag{14.73}$$

After these manipulations, the renormalization equation (14.71) turns into a pair of self-consistent integral equations, valid at low fugacity:

$$\tilde{\beta}(\lambda)^{-1} = \tilde{\beta}^{-1} + 6\pi^3\int_0^{\log\lambda} d\log R\, z^2(R)\,\alpha_0(\pi\tilde{\beta}(R)),$$

$$z(R) = z\exp\left\{2\log R - \pi\int_{-\log c}^{\log R} d\log\lambda\tilde{\beta}(\lambda)\right\} \times\left(1 + 2\pi\int_0^{\log(\rho R)} d\log r\, z(r)\,\alpha_1(\pi\tilde{\beta}(r))\right), \tag{14.74}$$

where we have abbreviated

$$\alpha_0(\xi) = 2e^{\xi}(I_0(\xi) - \tfrac{1}{2}I_1(\xi)), \qquad \alpha_1(\xi) = e^{\xi/2} I_0(\xi). \tag{14.75}$$

The corresponding equations for the square lattice are obtained by replacing [compare (14.60) and (14.61)]

$$6\alpha_0 \to 4\alpha_0, \qquad \alpha_1 \to 0. \tag{14.76}$$

We then differentiate both equations and find

$$\frac{d\tilde{\beta}^{-1}(\lambda)}{d\log\lambda} = 6\pi^3 z^2(\lambda)\ \alpha_0\ (\pi\tilde{\beta}(\lambda)),$$

$$\frac{dz(\lambda)}{d\log\lambda} = (2 - \pi\tilde{\beta}(\lambda))z(\lambda) + 2\pi z(\lambda)z(\rho\lambda)\alpha_1(\pi\tilde{\beta}(\rho\lambda)) + O(z^3). \tag{14.77}$$

This is a pair of ordinary differential equations which specifies the renormalization group trajectories in the $\tilde{\beta}^{-1}$, z plane as a function of λ.

As in (11.149), Part II, it is convenient to introduce the variable $\ell = \log\lambda$. We furthermore define $\ell_0 \equiv \log\lambda$. Then the equations read

$$\frac{d\tilde{\beta}^{-1}(\ell)}{d\ell} = 6\pi^3 z^2(\ell)\,\alpha_0(\pi\tilde{\beta}(\ell)),$$

$$\frac{dz(\ell)}{d\ell} = (2 - \pi\tilde{\beta}(\ell))z(\ell) + 2\pi z(\ell)z(\ell + \ell_0)\,\alpha_1(\pi\tilde{\beta}(\ell + \ell_0)) + O(z^3). \tag{14.78}$$

These can be solved numerically. The flow graphs are shown in Fig. 14.5.

For an approximate analytic solution we observe that $\alpha_0(\xi)$ and $\alpha_1(\xi)$ are smooth functions of ξ so that in the neighbourhood of the critical point $\xi = \pi\tilde{\beta} \approx 2$ they can be replaced by

$$\alpha_0 \equiv \alpha_0(2) = 2e^2(I_0(2) - \tfrac{1}{2}I_1(2)) \approx 21.9347,$$
$$\alpha_1 \equiv \alpha_1(2) = eI_0(2) \simeq 6.1966. \tag{14.79}$$

Expanding $z(\ell + \ell_0)$ in a power series in ℓ_0 and using repeatedly Eqs. (14.78) to express the derivatives of $z(\ell)$ in terms of $z(\ell)$ we realize that $z(\ell)z(\ell + \ell_0)$ on the right-hand side can be replaced by $z^2(\ell)$ with an error which is, at most, of the order $(2 - \pi\tilde{\beta})z^2(\ell)$ or $z^3(\ell)$. Close to the critical point, such terms can be neglected when compared with the two leading terms. We may therefore replace $z(\ell)z(\ell + \ell_0)$ by $z^2(\ell)$ with no

effect upon the critical behavior. With the same accuracy, we may replace $2 - \pi\tilde{\beta}$ by $2[(2/\pi)\tilde{\beta}^{-1} - 1]$.

14.4. CALCULATION OF CRITICAL TEMPERATURE

Let us use the renormalization group equations and calculate the critical temperature for both square and triangular lattices. The procedure becomes most similar to that of the Villain model by introducing the reduced variables [compare (11.148), Part II]

$$x = \frac{2}{\pi}\tilde{\beta}^{-1} - 1, \qquad y = \sqrt{6\alpha_0}\,\pi z, \tag{14.80}$$

which obey the reduced equations

$$\frac{dx}{d\ell} = 2y^2, \tag{14.81}$$

$$\frac{dy}{d\ell} = 2xy + 2ry^2, \tag{14.82}$$

where

$$r \equiv \frac{\alpha_1}{\sqrt{6\alpha_0}} \approx \begin{cases} 0 \\ 0.5401 \end{cases} \text{ on } \begin{cases} \text{square} \\ \text{triangular} \end{cases} \text{ lattices.} \tag{14.83}$$

We now determine the trivial straight-line solutions which separate the set of all trajectories into three classes (see Fig. 14.2). Inserting into (14.81), (14.82) the relation

$$y = mx, \tag{14.84}$$

we find the algebraic equation

$$m^2 - rm - 1 = 0 \tag{14.85}$$

or

$$m_{\pm} = \pm 1,$$

FIG. 14.2. The renormalization flow (schematic) in the $\bar{\beta}^{-1}$, z plane. Near $x = 0$, the two ν-like heavy lines are the separatrices $y = m_{\pm}x$ with $m_{\pm}$ given in (14.86). The solid line is the locus describing the melting model of the Villain type with no extra core energy and the purely elastic fugacity $z = Ac^{-\pi\bar{\beta}}$ ($A = \sqrt{6\alpha_0}\,\pi \approx 36$, $c \approx 10.17$). The dashed lines of the same thickness, with the core parameters $c \approx 6$ and $c \approx 20$ are drawn for *comparison*.

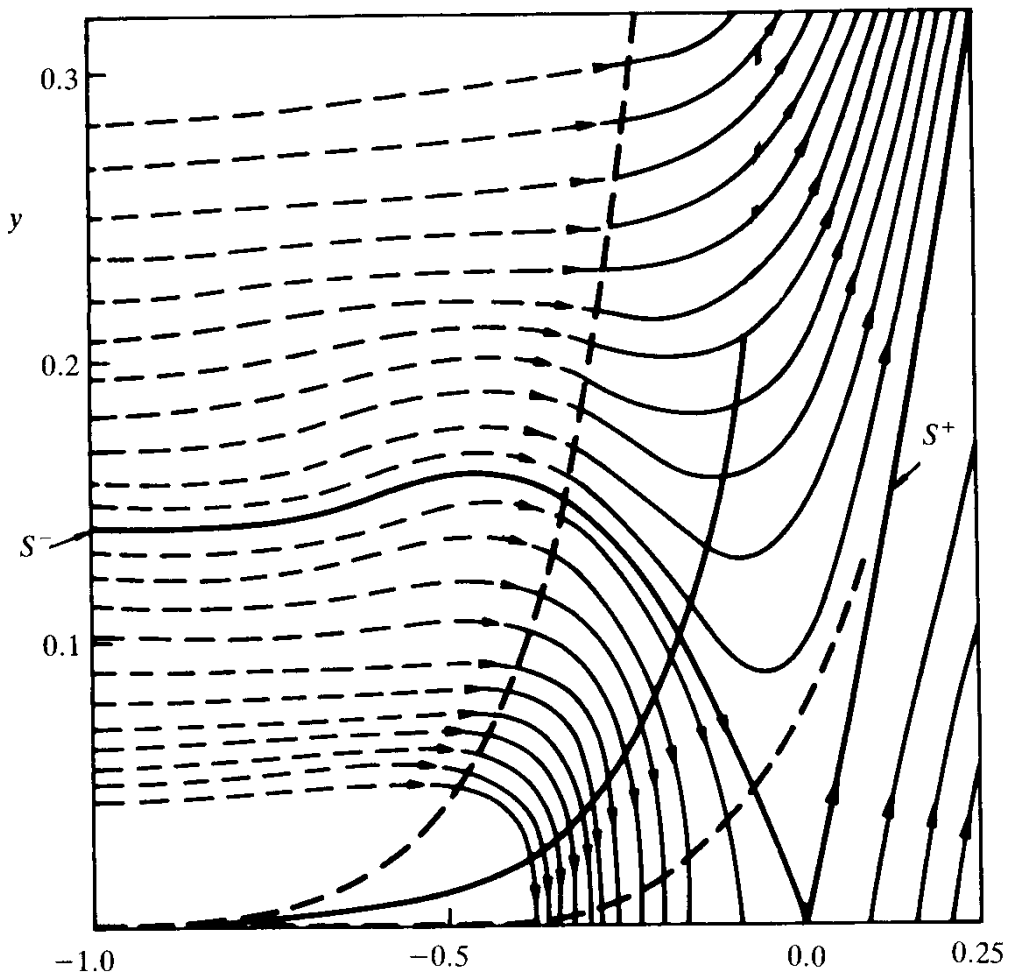

for square lattices and

$$m_{\pm} = \frac{r}{2} \pm \sqrt{\frac{r^2}{4} + 1} \approx \begin{cases} 1.3059, \\ -0.7658, \end{cases} \tag{14.86}$$

for triangular lattices. That r enters non-trivially into the solutions demonstrates that the y^2 term in Eq. (14.82) is relevant to the critical behavior. It can be easily verified that any higher term xy^2 or y^3 in either equation would change the separatrices only further away from the critical point and can therefore be ignored in the critical limit.

The critical temperature is found from the intersection of the separatrix S_- (i.e., $y = m_- x$) with the initial fugacity curve

$$z(\beta) = c^{-\pi\tilde{\beta}} = c^{-2/(1+x)}. \tag{14.87}$$

Recall that the number c was defined by the asymptotic behavior of the potential $v_{ij}^{'T}(\mathbf{x})$, i.e.,

$$v_{ij}^{'T}(\mathbf{x}) \to -\frac{1}{4\pi}\left(\log(|\mathbf{x}|\, c)\,\delta_{ij} - \frac{x_i x_j}{\mathbf{x}^2}\right) \tag{14.88}$$

and had the values

$$c_s = 2\sqrt{2}\, e^{\gamma}\sqrt{e} \approx 8.3057 \tag{14.89}$$

on a square lattice and

$$c_t \approx 2\sqrt{3}\, e^{\gamma}\sqrt{e} \approx 10.172 \tag{14.90}$$

on a triangular lattice [see (14.46), (14.48)].

In terms of the natural variables x, y, Eq. (14.87) amounts to

$$y = \begin{cases} A_s c_s^{-2/(1+x)} \\ A_t c_t^{-2/(1+x)} \end{cases} \quad \text{for} \quad \begin{cases} \text{square} \\ \text{triangular} \end{cases} \text{lattices}, \tag{14.91}$$

where the prefactor is $A_s = \sqrt{4\alpha_0}\,\pi \approx 29.427$ for square and $A_t = \sqrt{6\alpha_0}\,\pi \approx 36.0451$ for triangular lattices. The intersection of this curve with the separatrix S_- is given by the equation

$$x_c = \frac{A}{m_-} c^{-2/(1+x_c)}$$

or

$$x_c = -1 - 2\log c/\log\left(\frac{m_- x_c}{A}\right). \tag{14.92}$$

Solving for x by iteration we find

$$x_c = \begin{cases} -0.1744 \\ -0.1726 \end{cases} \text{ for } \begin{cases} \text{square} \\ \text{triangular} \end{cases} \text{ lattices,} \tag{14.93}$$

so that

$$\tilde{\beta}_c \equiv \frac{2}{\pi(1+x_c)} \approx \begin{cases} 0.7711 \\ 0.7694 \end{cases} \text{ for } \begin{cases} \text{square} \\ \text{triangular} \end{cases} \text{ lattices.} \tag{14.94}$$

It turns out that in both cases, x is somewhat too large to permit the use of the small fugacity approximation employed in the derivation of the critical stiffness. In going from (14.78) to (14.82) we replaced

$$\tilde{\beta}_c^{-1} \equiv \frac{\pi}{2}(1+x)$$

by

$$\tilde{\beta}_c \approx \frac{2}{\pi}(1-x).$$

The error involved is about 3% for the square lattice value of x_c as well as for the triangular lattice. We should therefore expect discrepancies of this order when comparing $\tilde{\beta}_c$ with the melting temperatures obtained previously for the Villain model, either by analytic calculations, or by Monte Carlo simulations. Indeed, for square lattices, we found at $\nu = 0$

$$\beta_m \approx 0.815 \tag{14.95}$$

which agrees to within 5% with (14.94). For triangular lattices, on the other hand, Strandburg *et al.* (1983) locate a transition between

$$\beta_{m_1}(1+\nu) \approx 0.9125, \quad \beta_{m_2}(1+\nu) \approx 0.9625.$$

A recent higher precision study by Janke and Toussaint (1986) finds a melting transition at

$$\beta_m(1+\nu) \approx 0.932. \tag{14.96}$$

Dividing this value by $2/\sqrt{3}$ [because of the normalization (14.88) as opposed to the one implied by (12.60)] gives

$$\tilde{\beta}_{m_1} \approx 0.79, \quad \tilde{\beta}_{m_2} \approx 0.834, \quad \tilde{\beta}_m \approx 0.807.$$

These numbers differ from the calculated value (14.94) by the expected amount.

14.5. THE CRITICAL BEHAVIOR OF THE COHERENCE LENGTH

Just as in the case of the ordinary Villain model, the renormalization group equations allows us to examine the manner in which the coherence length tends to zero as the crystal is heated beyond the critical temperature. For this purpose we have to study the solutions close to the separatrices. We shall proceed as in Chapter 11 of Part II: divide the two equations (14.81) and (14.82) by each other, and study the differential equation

$$\frac{dy}{dx} = \frac{x}{y} + r, \tag{14.97}$$

which for $r = 0$ was solved trivially by $y = \sqrt{x^2 + x_0^2}$.

On triangular lattices, for which $r \neq 0$, Eq. (14.97) is still a homogeneous differential equation so that it is possible to separate variables by introducing $u(x) = y/x$. This satisfies the differential equation

$$u + x\frac{du}{dx} = \frac{1}{u} + r, \tag{14.98}$$

which can be brought to the form

$$\begin{aligned} \frac{dx}{x} &= \frac{udu}{1 + ru - u^2} = -\frac{udu}{(u - m_+)(u - m_-)} \\ &= \frac{1}{m_+ - m_-}\left(\frac{1}{m_-}\frac{du}{u - m_+} - \frac{1}{m_+}\frac{du}{u - m_-}\right). \end{aligned} \tag{14.99}$$

The integration is now trivial and gives

$$x = \varkappa(u - m_+)^{1/(m_+ - m_-)m_-}(u - m_-)^{-1/(m_+ - m_-)m_+}, \tag{14.100}$$

where $\varkappa$ is a constant of integration. This can also be rewritten as

$$(y - m_+x)^{1-\nu}(y - m_-x)^{\nu} = \varkappa, \tag{14.101}$$

with

$$\nu \equiv \frac{1}{m_+ - m_-}\frac{1}{m_+} = \frac{m_-^2}{1 + m_-^2} = \frac{1_+^2}{1 + m_+^2}. \tag{14.102}$$

Using (14.86), we find

$$v = 0.36963. \tag{14.103}$$

For quadratic lattices, $r = 0$, $m_+ = 1$, ν becomes 1/2, and Eq. (14.101) reduces to

$$y^2 - x^2 = \varkappa^2 \equiv x_0^2 \tag{14.104}$$

as it should [compare (11.154), Part II].

The value of $\varkappa$ is determined by the initial condition which, close to the separatrix, i.e., close to the critical point, has the form [compare (11.134), Part II]

$$x = x_c + \tau, \qquad y \approx m_- x_c + \alpha\tau, \qquad \tau = \frac{2}{\pi}(T/T_c - 1). \tag{14.105}$$

Inserting this into (14.101) gives

$$[(m_- - m_+)x_c + (\alpha - m_+)\tau]^{1-\nu}(\alpha - m_-)^{\nu}\tau^{\nu} \approx \varkappa. \tag{14.106}$$

For small τ, this can be rewritten as

$$\varkappa \approx \mu^{1-\nu}(\alpha - m_-)^{\nu}\tau^{\nu} = \bar{\varkappa}\tau^{\nu}, \tag{14.107}$$

where

$$\mu = (m_+ - m_-)|x_c| = -\frac{m_-}{\nu}|x_c| \approx \begin{cases} 2|x_c| \approx 0.349 & \text{square,} \\ 2.0715|x_c| \approx 0.358 & \text{triangular.} \end{cases} \tag{14.108}$$

We can express the slope parameter α in terms of the critical value $|x_c|$ by taking the fugacity equation in terms of reduced variables,

$$y = A c^{-2/(1+x)}; \tag{14.109}$$

differentiating with respect to x, $\alpha = (\partial y/\partial x)|_{x^c} = 2 \log c \ (1/(1+x_c)^2) y_c$, and expressing $\log c$ once more in terms of x_c via Eq. (14.92),

$$x_c = \frac{A}{m_-} c^{-2/(1+x_c)}. \tag{14.110}$$

This gives

$$2 \log c = -(1 + x_c) \log \frac{m_- x_c}{A}, \tag{14.111}$$

and we have [compare (11.170b), Part II]

$$\alpha = -\frac{m_- x_c}{1 + x_c} \log \frac{m_- x_c}{A}. \tag{14.112}$$

For square and triangular lattices with $c = 8.3057$ and 10.172, $A = 29.427$ and 36.0451, respectively, this takes the values

$$\begin{array}{lll} -x_c \approx 0.1744: & \alpha \approx 1.083 & \text{square}, \\ -x_c \approx 0.1726: & \alpha \approx 0.896 & \text{triangular}. \end{array} \tag{14.113}$$

We are now ready to calculate the length scale from (14.81),

$$\ell = \frac{1}{2} \int_{x_0}^{x} \frac{dx}{y^2}. \tag{14.114}$$

The integral has to be carried from x_0, y_0 to $x_{\min}$, $y_{\min}$, where y reaches its minimal value [recall Part II, Eq. (11.136)], and further on to some place x_1, y_1, where the dependence $\ell(x)$ slows down. The minimum is given by the intercept of (14.101) with the line $dy/dx = 0 = x/y + r$, i.e., by

$$y_{\min} = \varkappa (1 + r m_+)^{\nu - 1} (1 + r m_-)^{-\nu} = \varkappa m_+^{2\nu - 2} m_-^{-2\nu}, \tag{14.115}$$

$$x_{\min} = -r y_{\min}. \tag{14.116}$$

For $\tau \to 0$, these quantities vanish like $\bar{x}_{\min}\tau^{\nu}$, $\bar{y}_{\min}\tau^{\nu}$ where[c]

$$\bar{y}_{\min} = \bar{\varkappa} m_+^{2\nu-2}|m_-|^{-2\nu} = \begin{Bmatrix} 1 \\ 0.8704 \end{Bmatrix} \bar{\varkappa} = \begin{Bmatrix} 0.852 \\ 0.550 \end{Bmatrix} \text{for} \begin{Bmatrix} \text{square}, \\ \text{triangular}, \end{Bmatrix}$$

$$\bar{x}_{\min} = -r\bar{y}_{\min} = \begin{Bmatrix} 0 \\ -0.296 \end{Bmatrix} \text{for} \begin{Bmatrix} \text{square}, \\ \text{triangular}, \end{Bmatrix} \tag{14.117}$$

in the three cases.

In the integral (14.115), the small τ dependence comes mostly from the region around the minimum of y with the dependence of x_0 on τ giving only higher order corrections. The leading behavior can best be exhibited by introducing further reduced variables $\bar{y} = y\tau^{-\nu}$, $\bar{x} = x\tau^{-\nu}$ and rewriting the integral as

$$\ell = \frac{1}{2}\int_{x_0}^{x_1} \frac{dx}{y^2} = \frac{\tau^{-\nu}}{2}\int_{x_0\tau^{-\nu}}^{x_1\tau^{-\nu}} \frac{d\bar{x}}{\bar{y}^2}. \tag{14.118}$$

Since the integral converges, the dependence on the limits of integration is very weak. We therefore separate the integral into three pieces

$$\ell = \frac{\tau^{-\nu}}{2}\left[\int_{-\infty}^{\infty} \frac{d\bar{x}}{\bar{y}^2} - \int_{-\infty}^{x_0\tau^{-\nu}} \frac{d\bar{x}}{\bar{y}^2} - \int_{x_1\tau^{-\nu}}^{\infty} \frac{d\bar{x}}{\bar{y}^2}\right]. \tag{14.119}$$

For small τ, the second and third integrals can be well approximated by

$$-\int_{-\infty}^{x_0\tau^{-\nu}} \frac{d\bar{x}}{m_-^2\bar{x}^2} - \int_{x_1\tau^{-\nu}}^{\infty} \frac{d\bar{x}}{m_+^2\bar{x}^2} = \left(\frac{1}{m_-^2 x_0} - \frac{1}{m_+^2 x_1}\right)\tau^{\nu} \tag{14.120}$$

and we find

$$\ell \approx h\tau^{-\nu} + \frac{1}{2m_-^2 x_0} - \frac{1}{2m_+^2 x_1}, \tag{14.121}$$

where h is the number

[c]For $m_+ = |m_-| = 1$, $\nu = 1/2$, $A = 2\pi$ this reduces correctly to the XY model formula (11.171) of Part II.

$$h = \frac{1}{2}\int_{-\infty}^{\infty} \frac{d\bar{x}}{\bar{y}^2} \tag{14.122}$$

and $x_0 = x_c + \tau$. For x_1 we may choose again [compare (11.166), Part II]

$$x_1 \approx 0.25, \tag{14.123}$$

which is large enough to put x_1, y_1 into the disordered phase and small enough to remain within the validity of the fugacity expansion. In order to estimate h we expand $\bar{y}$ around the minimum as

$$\bar{y} = \bar{y}_{\min} + \frac{1}{2\bar{y}_{\min}}(\bar{x} - \bar{x}_{\min})^2 + \ldots \tag{14.124}$$

The curvature $1/2\bar{y}_{\min}$ follows directly from the differential equation $dy/dx = x/y + r \approx x/y_{\min} + r = (x - x_{\min})/y_{\min}$ (now applied to $\bar{y}$, $\bar{x}$). Thus we find

$$h \approx \frac{1}{2}\int_{-\infty}^{\infty} \frac{d\bar{x}}{\bar{y}_{\min}^2 + (\bar{x} - \bar{x}_{\min})^2} = \frac{\pi}{2\bar{y}_{\min}} \tag{14.125}$$

and the coherence length becomes

$$\xi(\tau) \approx \xi(x_1, y_1)\exp\left\{\frac{\pi}{2y_{\min}}\tau^{-\nu} + \frac{1}{2m_-^2 x_0} - \frac{1}{2m_+^2 x_1}\right\} \tag{14.126}$$

[to be compared with the similar expression in Part II, Eq. (11.139) for the XY model].

For $\tau \to 0$, the coherence length diverges like

$$\xi(\tau) \propto e^{h\tau^{-\nu}} = e^{\tau^{-\nu}(\pi/2\bar{y}_{\min})}. \tag{14.127}$$

If we insert the numbers $-x_c \approx 0.1744$, 0.1726 and the corresponding values of A we find

$$h \approx \begin{cases} 1.84 \\ 2.86 \end{cases} \text{ for } \begin{cases} \text{square,} \\ \text{triangular.} \end{cases} \tag{14.128}$$

Given experimental or Monte Carlo data, the resolution of the critical behavior is just as difficult as it was previously in the XY model, due to the τ behavior of the second and third integrals in (14.119). In order to estimate the corrections we expand $\bar{y}(\bar{x})$ around the separatrices as follows

$$\bar{y} = m_{\pm}\bar{x} + p_{\pm}\begin{cases}\bar{x}^{1-1/(1-\nu)} \\ |\bar{x}|^{1-1/\nu}\end{cases} \text{ near } \begin{cases}S_+, \\ S_-,\end{cases} \tag{14.129}$$

where

$$p_+ = \frac{\bar{x}^{1/(1-\nu)}}{(m_+ - m_-)^{1/\nu(1-\nu)}}, \qquad p_- = \frac{\bar{x}^{1/\nu}}{(m_+ - m_-)^{1/\nu(1-\nu)}}. \tag{14.130}$$

This leads to the additional terms in (14.121)

$$\ell = \tau^{-\nu}\left[h + \frac{1}{2m_-^2\bar{x}_0}\left(1 - \frac{2}{1+\frac{1}{\nu}}\frac{p_-}{|m_-|}\frac{1}{|\bar{x}_0|^{1/\nu}}\right)\right.$$

$$\left. - \frac{1}{2m_+^2\bar{x}_1}\left(1 - \frac{2}{1+\frac{1}{1-\nu}}\frac{p_+}{m_+}\frac{1}{\bar{x}_1^{1/(1-\nu)}}\right) + \ldots\right], \tag{14.131}$$

with the small τ expansion,

$$\ell = h\tau^{-\nu} - \left(\frac{1}{2m_-^2|x_c|} + \frac{1}{2m_+^2 x_1}\right) - \frac{1}{2m_-^2}\frac{\tau}{|x_c|^2} + \frac{1}{1+\frac{1}{\nu}}\frac{p_-}{|m_-|^3}\frac{\tau}{|x_c|^{1+(1/\nu)}}$$

$$+ \frac{1}{1+\frac{1}{1-\nu}}\frac{p_+}{m_+^3}\frac{\tau^{\nu/(1-\nu)}}{x_1^{1+1/(1-\nu)}} + \ldots \tag{14.132}$$

As a cross check, we set $m_{\pm} = \pm 1$, $\nu = 1/2$, $\kappa = \bar{y}_{\min}$ and recover the correct XY model result (11.173b) of Part II.

Numerically, the expansions are, term by term,

$$\ell \approx 1.84\tau^{-1/2} - 2.86 - 2 - 16.44\tau + 2.85\tau + 2.85\tau + \ldots \text{ (square)}, \tag{14.133}$$

$$\ell \approx 2.86\tau^{-0.37} - 4.94 - 1.17 - 28.59\tau + 5.09\tau + 0.34\tau^{0.59} \text{ (triangular).} \tag{14.134}$$

On a triangular lattice, τ has to be considerably smaller than $\tau \approx 10^{-2}$ to see clearly the $\tau^{-\nu}$ dependence of the first term. This brings the coherence length to the order of a few hundred lattice units.

Experimentally, the coherence length has been measured up to several hundred Ångstroms by Heiney *et al.* (1982) (op. cit. in the Notes and References, see Fig. 14.4). Thus, under the assumption that the system has no extra core energy, this coherence length begins to barely invade into the scaling regime. Indeed, the data can be fitted quite well also by an ordinary scaling curve $\xi \approx a((T/T_c) - 1)^{\nu}$ [see also Eq. (14.142)–(14.143)].

14.6. TWO-STEP MELTING

In their work on the dissociation of dislocation pairs, Halperin, Nelson, and Young (HNY) realized that this dissociation alone could not readily be identified with a melting process. The high-temperature phase in which dislocation pairs are separated does not behave like a proper liquid. Even though the translational order is destroyed, there is still memory of the orientational order of the crystal. On triangular lattices, this phase with orientational order is referred to as the "hexatic phase." A further phase transition would be necessary to destroy this orientational order.

In order to describe it, HNY introduced an *independent* set of disclinations into the "hexatic phase". In that phase, these have once more the same interaction energy as vortices in a film of superfluid He. Therefore, when heating the "hexatic phase," they can undergo a further Kosterlitz-Thouless phase transition with a jump of the *orientational* elastic constant from a universal value to zero. This elastic constant is defined by the orientational energy of the bond angles $\omega(\mathbf{x})$. It can be parametrized by

$$E_{\bullet} = \frac{K_A}{2} \int d^2x (\partial_i \omega(\mathbf{x}))^2, \tag{14.135}$$

where the subscript A of the elastic constant K_A records the fact that K_A refers to the angular stiffness. In a hexatic phase, the fundamental disclinations have an angular defect [see (2.7), (2.118)]

$$\Omega = 60° = 2\pi/6, \tag{14.136}$$

and the disclination density $\Theta(\mathbf{x}) = \varepsilon_{ij}\partial_i\partial_j\omega(\mathbf{x})$ can be written as

$$\Theta(\mathbf{x}) = \Omega \sum_{\mathbf{x}^{(n)}} \delta^{(2)}(\mathbf{x} - \mathbf{x}^{(n)}), \tag{14.137}$$

where $\mathbf{x}^{(n)}$ are the positions of the disclinations. It is then possible to introduce[d] a "gauge field" of the "angular stress" and write

$$E = \frac{1}{2K_A}\int d^2x\,(\partial_i A)^2 + i\int d^2x\,\Theta(\mathbf{x})A(\mathbf{x}). \tag{14.138}$$

From this, the interaction energy between a disclination and an anti-disclination is, at long distances,

$$E_{\text{int}} = \Omega^2 K_A \frac{1}{2\pi}\log|\mathbf{x}|. \tag{14.139}$$

By the same argument as in (14.13), (14.14) it is now possible to conclude that a rare gas of such pairs undergoes a pair-unbinding transition whenever the angular stiffness drops to a point at which

$$\beta_A \equiv \frac{\Omega^2 K_A^R}{k_B T(2\pi)^2} = \frac{2}{\pi}, \tag{14.140}$$

corresponding to the universality relation ($\Omega = 2\pi/6$)

$$K_{Ac}^R = 72 k_B T_c/\pi. \tag{14.141}$$

14.7. EXPERIMENTAL EVIDENCES FOR AND AGAINST A HEXATIC PHASE

The work of Halperin, Nelson and Young catalyzed a large number of investigations on the two-dimensional melting process. Experiments were

[d]We write the angular stress as $\sigma_{Ai} \equiv \varepsilon_{ij}\partial_i A_j$. As was the case with χ in Eq. (14.26), $A(\mathbf{x})$ is not really a gauge field, due to the reduced space dimension $D = 2$. In higher dimensions it would be, though.

FIG. 14.3a.b. The ρ, T phase diagram of Xenon on graphite (ρ is the coverage of the adsorbed). The pioneering experiment is due to Thomy and Duval in 1970 (Fig. 14.3a) followed by Hammonds *et al.* in 1980 (Fig. 14.3b) (cited in the Notes and References). The dashed lines are paths traced in recent experiments of Heiney *et al.*, (Fig. 14.3b). There is a first-order melting transition at submonolayer density.

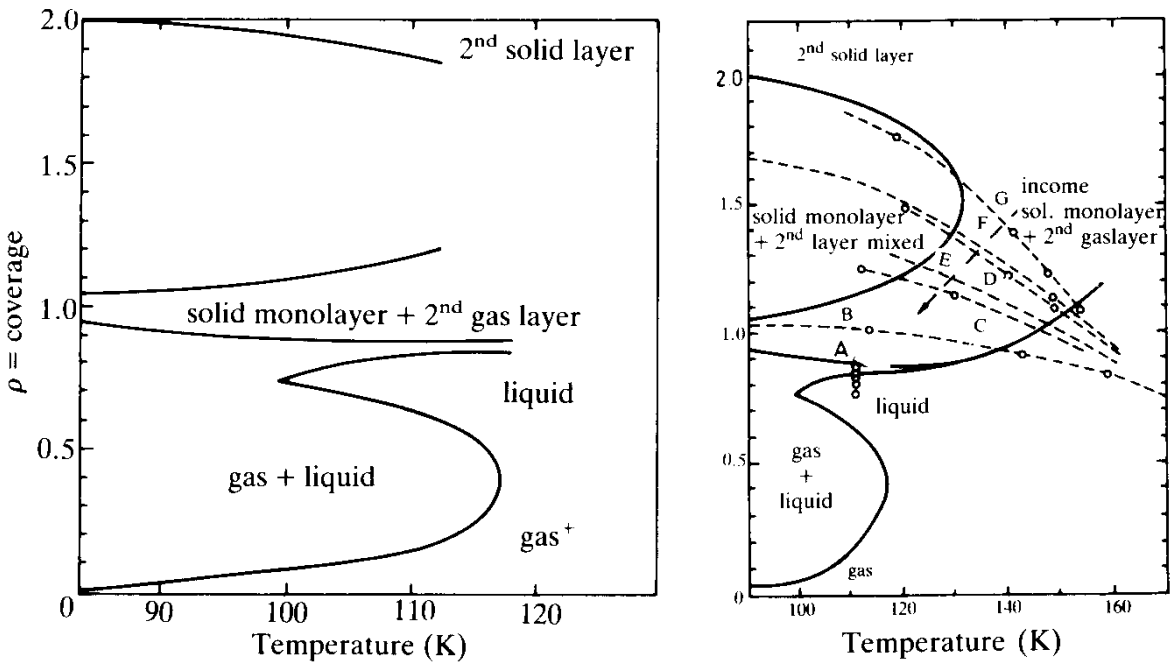

performed both in the laboratory and in model systems, via molecular dynamics or Monte Carlo simulations. In laboratory experiments there is now evidence for both continuous as well as first-order melting transitions. But none of the first type of experiments really separates the two transitions. Up to the end of 1988, evidence for the hexatic phase in atomic crystals has remained scarce and indirect. Only in crystals, which consist of rod-like molecules with an extra directional degree of freedom, and to which the above theory does not apply, the situation is different. Simulation studies with two-dimensional atomic crystals on the other hand, suggest that these melt in a single first-order phase transition as was obtained previously in our cosine model of defect melting. The only exception is the $2D$ Wigner crystal (electron lattice) which could undergo a continuous transition. This will be discussed later in detail. Let us first describe some of the important experimental data. The references can all be found in the notes at the end of this chapter.

In a pioneering vapor pressure isotherm experiment, Thomy and Duval showed in 1970 that Xenon adsorbed with less than a monolayer density on a (0, 0, 1) surface of graphite (see Fig. 7.9) exists in the three phases

FIG. 14.4. The coherence length of a layer of Xenon layers on graphite at a coverage $\rho = 1.1$ and a melting temperature of 152 K, as measured by Heiney *et al.* (1982). It is better fitted by the Kosterlitz-Thouless form $\xi^{-1} \sim e^{-1/(T-T_c)^{1/2}}$ than by the power law $\xi^{-1} \sim 0.24\,\text{Å}^{-1}(T/152.04\,\text{K} - 1)^{0.277}$.

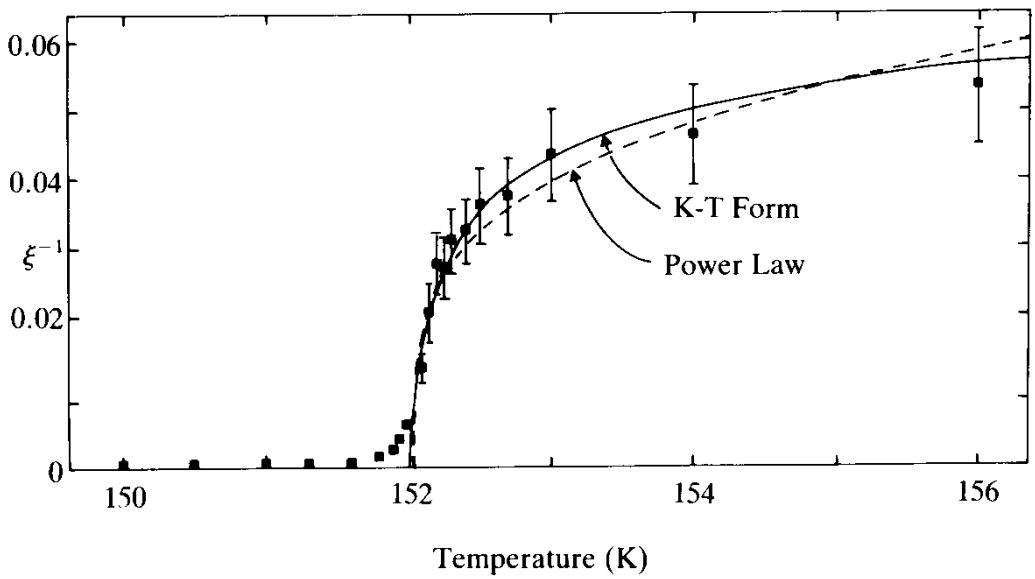

gas, liquid, (incommensurate) solid, with a phase diagram which is very similar to that of a three-dimensional system and with first-order transitions between the phases. The original phase diagram is shown in Fig. 14.3a. This behavior of Xenon is in contrast to Krypton or Nitrogen on graphite for which Butler *et al.* in 1979 found neither the triple point nor the critical point. The structure of the Xenon phase was investigated further by Hammonds *et al.* in 1980 (Fig. 14.3b) who found again a first-order transition up to 112K which was the highest temperature they studied.

In 1982 Heiney *et al.* reported that an increase of coverage to 1.1 monolayers softened the melting transition and made it continuous. This evidence was taken from a measurement of the coherence length which is shown in Fig. 14.4. It can be followed continuously to more than 100 Å (in their more recent 1983 paper to 200 Å) which would be impossible in a first-order transition unless it is extremely weak. A best fit to the Kosterlitz-Thouless form (14.127) gives

$$\xi^{-1} = 0.082\,\text{Å}^{-1}\exp\left[-0.0862\Big/\left(\frac{T}{152\,\text{K}} - 1\right)^{\nu}\right], \qquad (14.142)$$

where ν lies between 0.3690 and 0.4, in good agreement with the HNY number of 0.369. This fit reproduces the experimental points somewhat better than an optimally chosen power law formula[e]

$$\xi^{-1} = 0.24\,\text{Å}^{-1}\left(\frac{T}{152.04\,\text{K}} - 1\right)^{0.277}. \tag{14.143}$$

At the critical point, the cusp parameter η of the (1, 0) Bragg peak at the momentum transfer $q = 1.63\,\text{Å}^{-1} = (2\pi/a_0)(2/\sqrt{3})$ was found to be[d]

$$\eta \sim 0.28 \pm 0.05. \tag{14.144}$$

Using (14.52) and the lattice spacing $a_0 = (2/\sqrt{3})(2\pi/q) = 4.42\,\text{Å}$ this corresponds to a measurement of[f]

$$\beta_c^R \left.\frac{1 + \frac{1}{2}\frac{\lambda}{\mu}}{1 + \frac{1}{3}\frac{\lambda}{\mu}}\right|_R = \beta_c^R \frac{1}{1 - \nu^R/3} = \frac{3}{2}\frac{q^2 a_0^2}{\eta(2\pi)^2}\frac{1}{4\pi} = \frac{1}{\eta \cdot 2\pi} \sim 0.57, \tag{14.145}$$

a number which is compatible with what would be obtained from the universal pair unbinding value Eq. (14.15)

$$\beta_c^R(1 + \nu^R) = \frac{2}{\pi} \approx 0.64, \tag{14.146}$$

as long as ν^R is a small positive number (which is usually the case). Similar experimental results were reported by McTague *et al.* (1982) for monolayers of Argon.

At first sight, these results seem to give evidence that two-dimensional melting does proceed as described by the HNY theory. However, things are not as simple. First of all, one should remember that the two-dimen-

[e]It was argued by J.M. Greif *et al.* (1982) and by J.L. Cardy (1982) (see the Notes and References) that the scaling law (14.128) should not be applicable before ξ reaches $\sim 10^8$ lattice spacings. Experimentally, one never gets beyond 10^3 spacings so, if these authors are right, it would be futile to attempt fitting the anomalous behavior (14.142).

[f]Recall the definition of η in Eq. (7.199). Notice that we may use the inequality on ν, which follows from the positivity of $\kappa = \lambda + \mu$, $-1 < \nu \leq 1$ to derive, from (14.145) and the universality prediction (14.15), the inequality $\eta < 1/3$. Moreover, since ν is usually > 0, one also has a weak lower bound $\eta \gtrsim 1/4$ which is satified by (14.144).

FIG. 14.5. The phase diagrams of Xe, Kr and Ar, as given by McTague *et al.* (1982). The density is measured in units of the epitaxial density ρ_{ep} on the substrate.

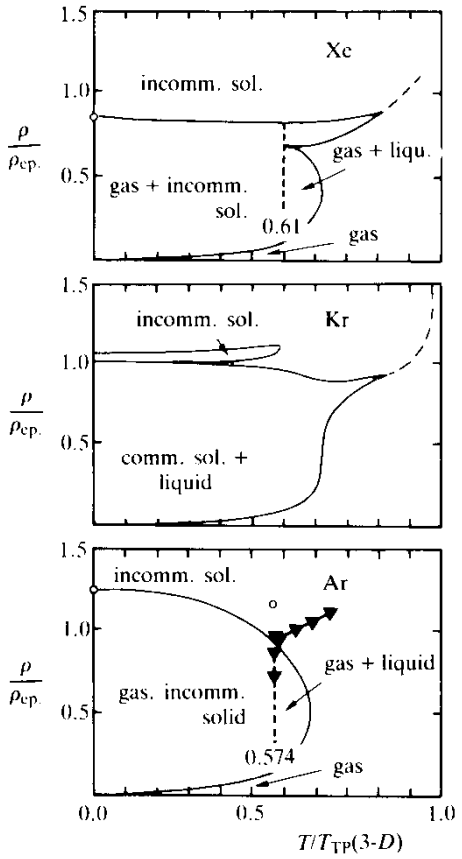

sional melting process in layers of ^{4}He exhibits a sharp peak in the specific heat [recall the data of M. Bretz *et al.* in Fig. 7.13]. Sharp peaks were also reported for Neon by G.B. Huff and J.G. Dash (1974). Such peaks are *incompatible* with the dislocation unbinding HNY mechanism which should not show up at all as a singularity in the specific heat, nor in any thermodynamic measurement.

Second, there are only two experiments which report orientational order in liquid layers of Argon, namely, one by Shaw *et al.* (1982), and another one by Rosenbaum *et al.* (1983), in Xenon. The evidence for the hexatic phase presented in these papers is, however, quite indirect and carries some theoretical bias (they apparently *wanted* to see the hexatic phase) so that it is hard to assess the systematic errors.

Third, none of the papers reporting a continuous transition has described the second transition from the hexatic phase to the proper liquid.

An additional difficulty is the following: when McTague *et al.* (see Fig. 14.5) compare the phase diagrams of Xenon, Argon and Krypton,

plotting them against a temperature T/T_{TP} $(D = 3)$, where T_{TP} $(D = 3)$ is the triple point of the three-dimensional system, the diagrams look quite different. They should, however, be very similar due to the law of corresponding states (which is clearly obeyed in $3D$). If substrate effects are as unimportant as often claimed, this is hard to understand.

A two-dimensional system which is free of substrate effects can be studied using smectic liquid crystals of Type B. When smearing such a material across a hole one can prepare well-defined few-layer systems of two-dimensional crystals lying on top of each other and coupled weakly to each other. In this system, D.E. Moncton *et al.* (1982) find a definite sharp first-order transition for two layers and, surprisingly, *two* successive *first-order* transitions for 3, 4, 5 layers. Unfortunately, it has been impossible to prepare thinner than two-layer systems so that the substrate problem is replaced by the disadvantage of not having a monolayer. Another disadvantage is that the system consists of rod-like molecules which can have additional directional fluctuations and these might easily change the order of the transition.[g]

14.8. COMPARISON WITH MOLECULAR DYNAMICS COMPUTER SIMULATIONS

Up to now, the only way of studying substrate free monoatomic two-dimensional systems is via Monte Carlo simulations. This road of approach has been followed by numerous authors and the outcome of their investigations conforms with the behavior of our cosine model of two-dimensional melting, which shows a first-order process. Early work by Hansen and Verlet on Lenard-Jones systems found a phase diagram of the usual type, with a first order transition and a density jump of the order of 5%. (See the phase diagram in Fig. 14.6 and 14.7.)

In 1979, *after* the theoretical work of HNY, McTague and Frenkel claimed to have seen two continuous transitions in a soft disc system with a potential $\Phi = \varepsilon(\sigma/r)^6$, just as is required by the theory, Working at a constant overall density $\rho\sigma^2 = 0.8$, they identified the following transition temperatures

$$T_{c_1} = 0.1525, \qquad T_{c_2} = 0.15625. \tag{14.147}$$

[g]Recall the discussion in Chapter 3, Part II. See also Section 18.7.

FIG. 14.6. The phase diagram of a 2-D Lennard-Jones system $[V(r) = 4\varepsilon((\sigma/r)^{12} - (\sigma/r)^6)]$ obtained via molecular dynamics calculations by Hansen and Verlet (1969).

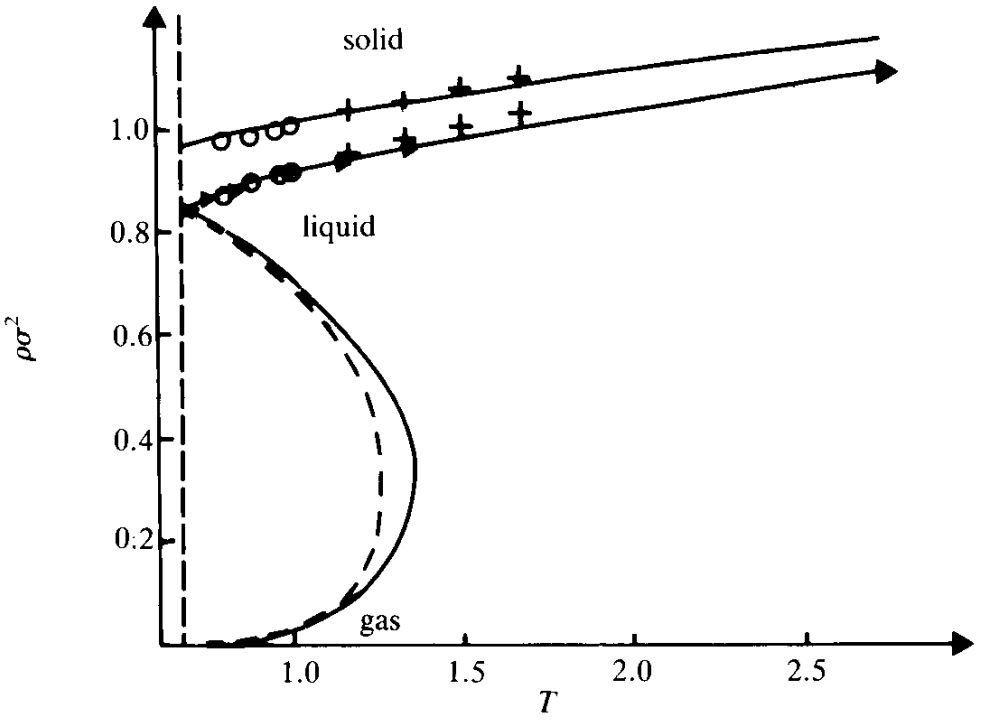

Moreover, in the small temperature interval between T_{c_1} and T_{c_2}, the correlation functions were reported to display a large-distance behavior as expected for the hexatic phase.

This appears to confirm the HNY theory. The picture is, however, not consistent. The internal energy (see Fig. 14.8) has a clear jump and this is in serious contradiction with the HNY theory. From what we have learned earlier in the Villain model, the pair-unbinding transition is practically undetectable in the internal energy. The specific heat should show only a smooth peak which lies considerably above the transition temperature. Thus the conclusions of McTague *et al.* are at variance with their own internal energy data. Incidentally, by counting the deviation from the coordination number q around each atom (see Fig. 14.9), the authors showed in which way the disclinations proliferate in the melting process and the result looks very similar to what we found in our cosine model (recall Figs. 13.20).

The contradictory situation was clarified by Toxvaerd in 1980 and by Abraham in 1980, who studied the same Lennard-Jones system once more at fixed pressure and various temperatures via Monte Carlo techniques. They observed discontinuities in the enthalpy and density

FIG. 14.7. The ρT diagram of the 2-D Lennard-Jones system as given by Abrahams (1980). The dashed line is extracted from simulation data of Toxvaerd (1978).

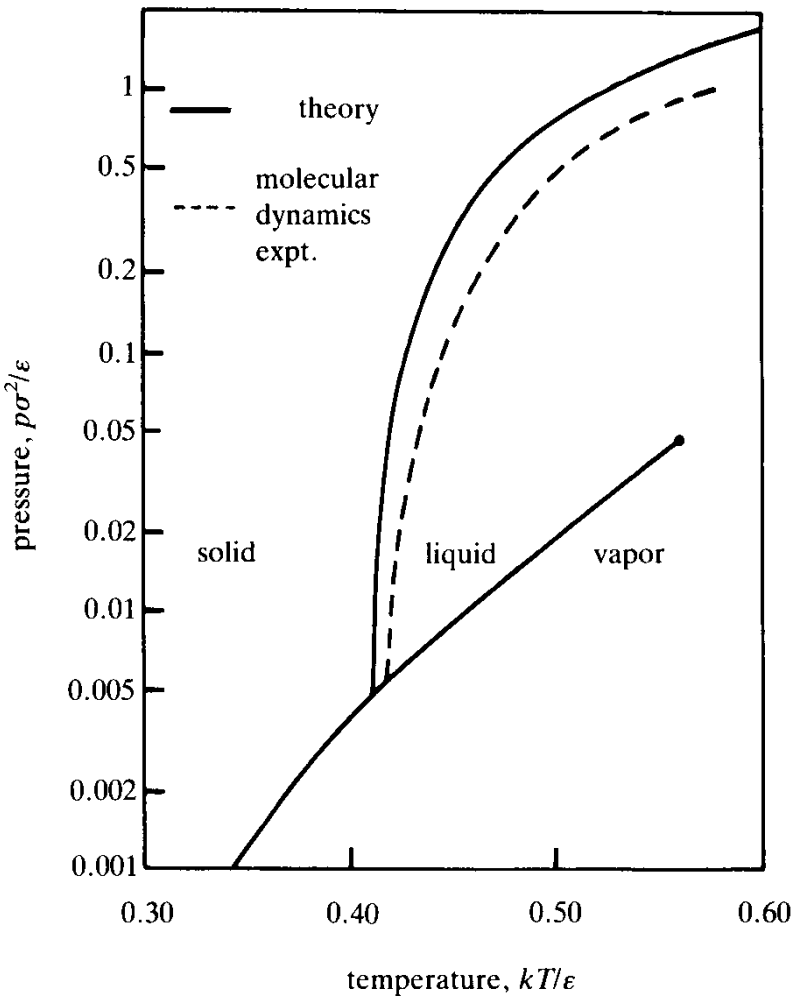

which are characteristic of a first-order transition (see Fig. 14.10). They also gave a simple reason why the previous authors had seen two transitions: if a first-order solid-liquid transition is studied at fixed overall density (i.e., along isochores) there exists a two-phase co-existence regime in which pieces of solid with lower density are in thermal equilibrium with surrounding regions of liquids of higher density (Figs. 14.11–14.12). Abraham also suggested an explanation for the observed stiffness K_A of the angular correlations in the two-phase regime: in the computer simulation, the solid pieces had not had enough time to change their crystalline orientation with respect to the initial solid. This is why some orientational memory is retained if one carelessly averages over the two-phase system. In fact, if extracted properly, the orientational order in the two-phase regime was shown to disappear by Zollweg (1982) in a simulation of a hard-disc system.

FIG. 14.8. Temperature dependence of internal energy as reported by McTague *et al.* (1980) in their simulation study of soft discs with an r^{-6} repulsive interaction potential. They claim to see two successive continuous transitions but the internal energy displays a clear first-order signal.

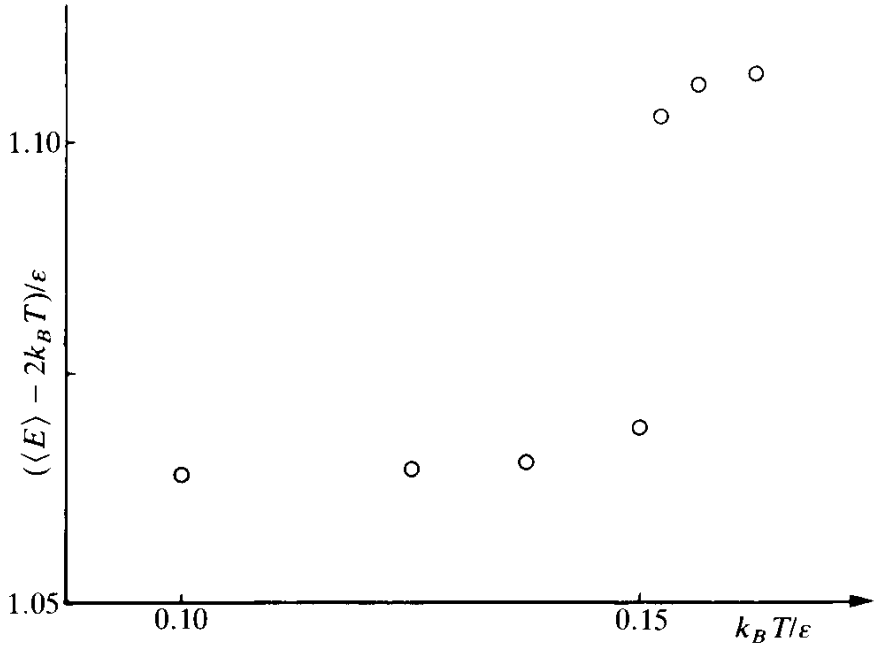

After these results, Abraham and Koch (1982) found it worthwhile to reinvestigate once more the importance of the subtrate by simulating Xenon atoms adsorbed on a graphite via Monte Carlo techniques subjected to the same conditions under which Heiney *et al.* (1982) had seen a continuous transition. Contrary to the laboratory experiments, they found a clear first-order transition. Since Heiney *et al.*'s coverage was 1.1 monolayers, Abraham and Koch also studied the effects of second-layer promotion. This did not affect the character of the transitions.

On the basis of these simulation results it thus appears that two-dimensional melting of Lennard-Jones soft-disc and hard-disc systems is a first-order process. The adsorption on a surface of graphits does not change this.

More work will be necessary to tell the difference between the laboratory and the simulated systems and to understand why one system can apparently undergo a continuous phase transition while the other cannot.

14.9. UNIVERSAL STIFFNESS

An important feature of the HNY theory is the prediction of a universal stiffness $\tilde{\beta}^R = [\beta(1+\nu)]^R = 2/\pi \approx 0.64$ at the transition, after which it

FIG. 14.9. The atomic positions as found by McTague *et al.* (1980) for soft discs of the potential $\varepsilon(\sigma/r)^6$ at $T^* = k_B T/\varepsilon = 0.150$. By counting the deviations from the regular coordination number $q = 6$ of the triangular solid they find pictures of the disclinations similar to those of the cosine melting model in Fig. 13.20. The pictures are taken at $T^* = 0.1$, $T^* = 0.15$, $T^* = 0.1525$. The melting temperature lies between $T^* = 0.15$ and 0.156.

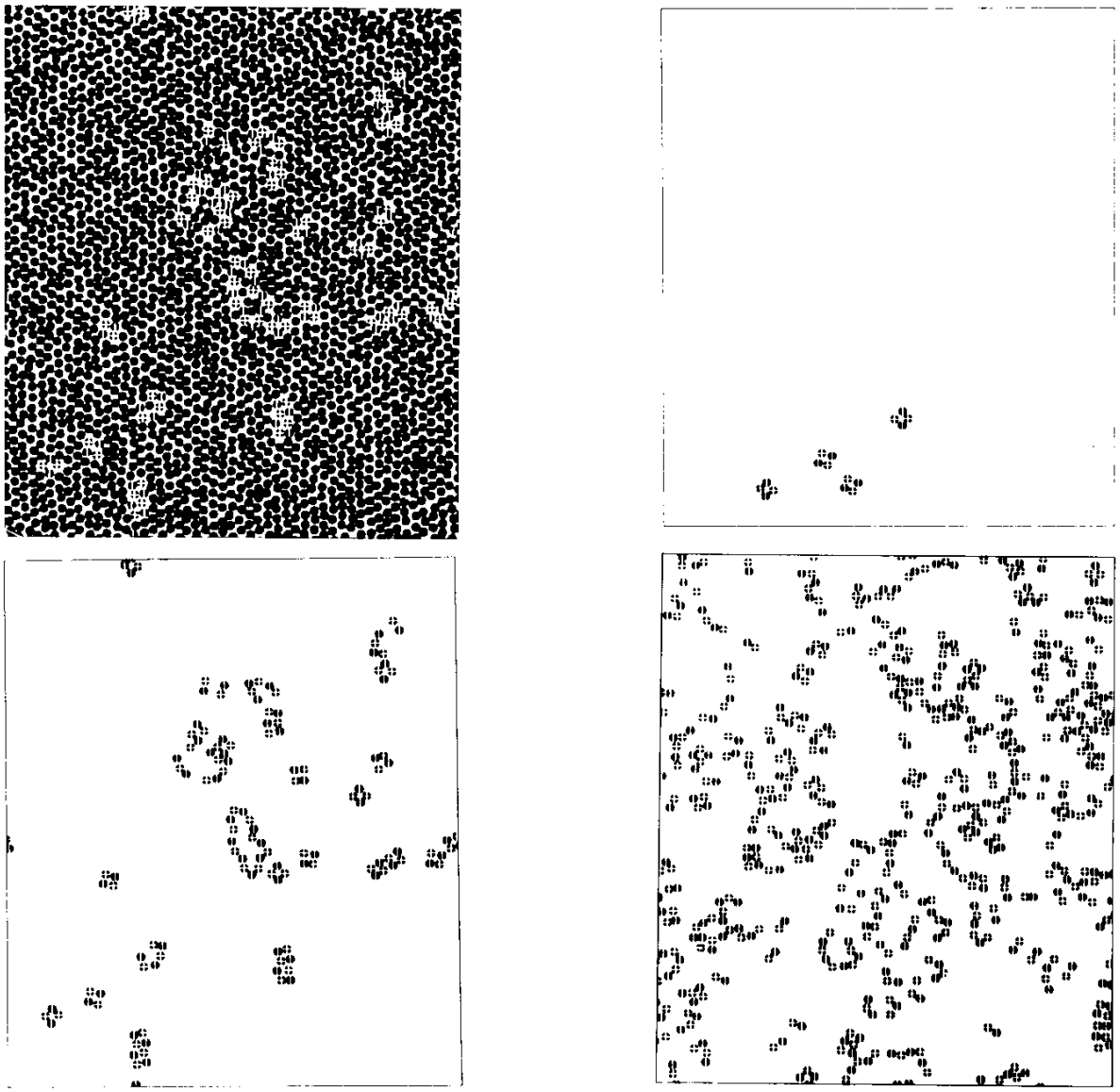

must fall rapidly to zero. This should happen significantly below the peak in the specific heat. Experimentally, Greif, Silva-Moreira and Goodstein (1980) noticed that the sharp peaks in the specific heats of solid helium lie considerably above the temperature T_m, calculated by using the zero-temperature elastic constants, i.e., they observed

$$\frac{a_0^2[\mu(1+\nu)]_{T=0}^R}{(2\pi)^2 k_B T_{\text{peak}}} < \frac{2}{\pi}. \tag{14.148}$$

FIG. 14.10. The discontinuities in density and enthalpy as observed by Abraham (1980) in a 16 × 16 Lennard-Jones system at two different pressures.

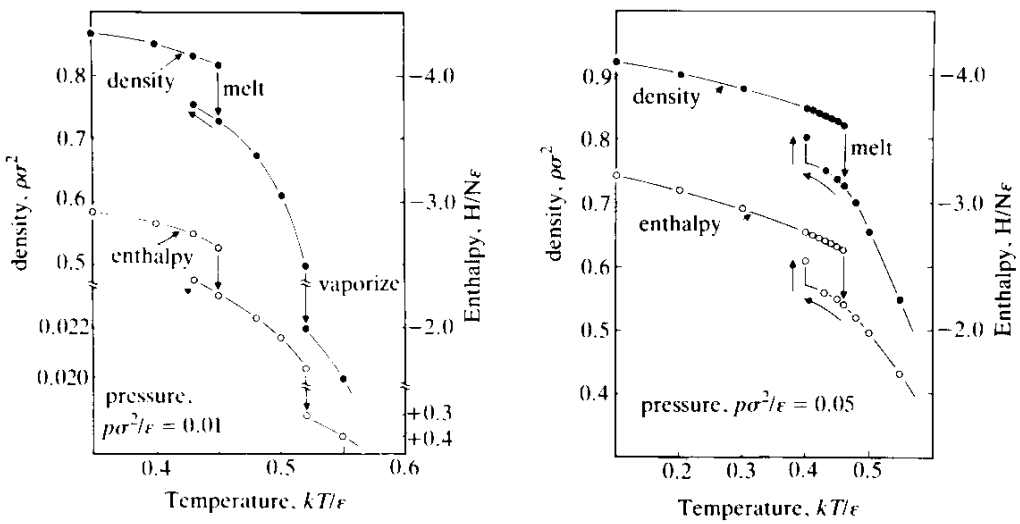

FIG. 14.11. The p = const. and ρ = const. cuts through the state diagram of a solid-liquid-gas system. While melting and evaporation are discontinuous processes at p = const. they appear as two successive continuous transitions at ρ = const., due to phase mixing.

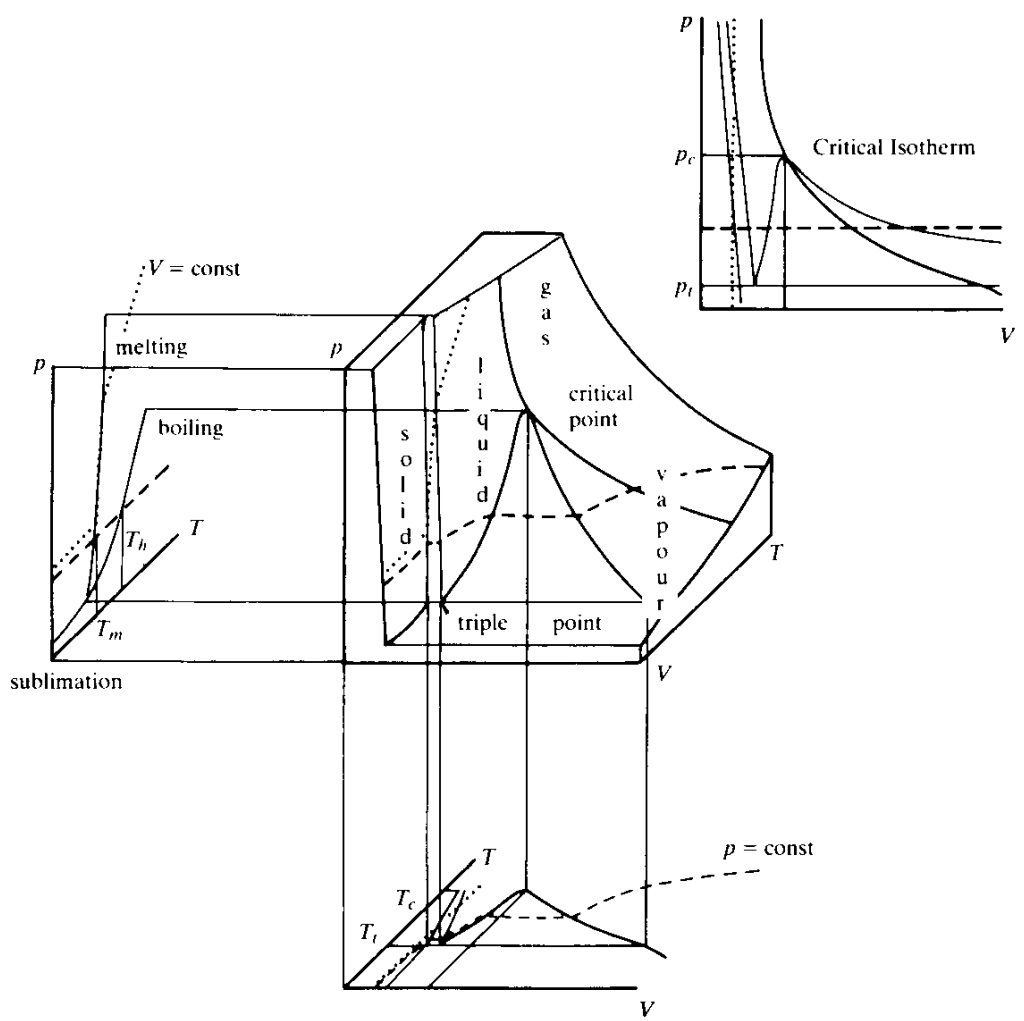

FIG. 14.12. Schematics of phase diagrams in a first order process at ρ-const. (after Abraham, 1980).

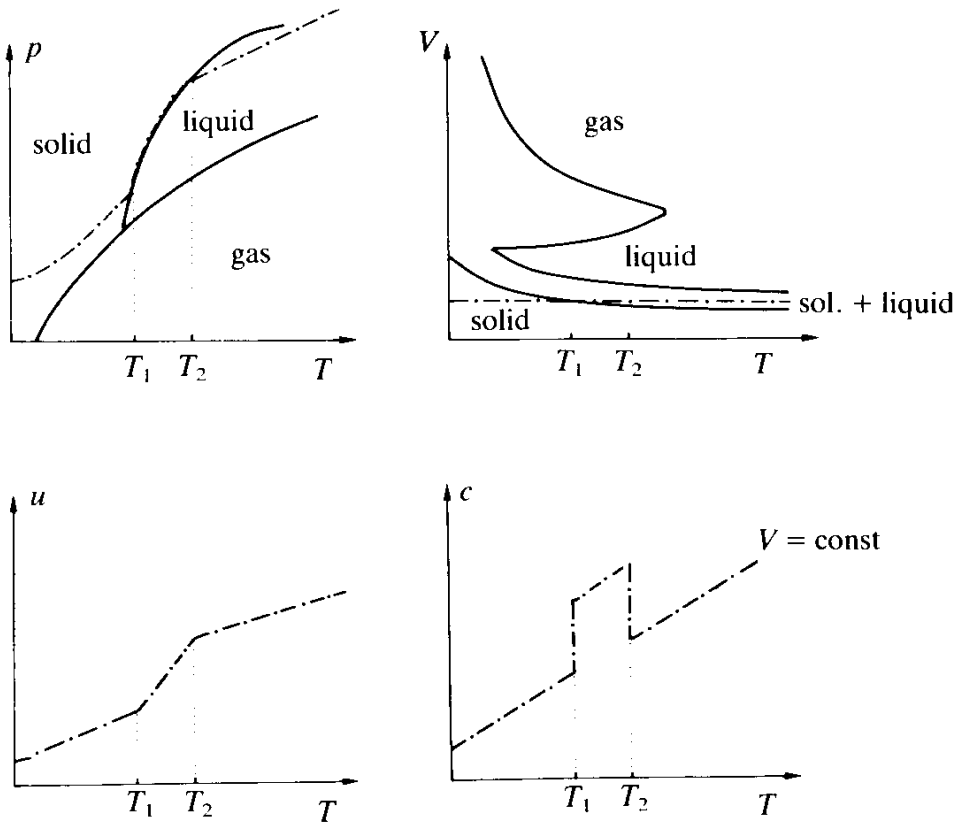

Since elastic constants usually soften with temperature, this is consistent with the HNY theory.

Tobochnik and Chester (1980), in a computer simulation of a Lennard-Jones system, found that at high densities[h] ($\rho\sigma^2 \sim 1.143$) the stiffness at the melting point is still higher than that predicted by theory (Fig. 14.13). At lower density ($\rho\sigma^2 \sim 0.86 - 0.89$), however, the universal value can be reached. These results indicate that at *higher*[i] density, melting is a first-order transition which takes place *before* the dislocation-unbinding mechanism can come into action. The coherence length does not have a chance to grow large enough so that the renormalization group procedure becomes applicable. The Monte Carlo data on the internal energy support this picture. For high densities they show a discontinuity, while for low densities they appear quite similar to the internal energy of the XY model for the superfluid phase transition for which pair unbinding is believed to be active.

[h]Remember that σ is the size parameter in the Lennard-Jones potential $V = 4\varepsilon[(\sigma/r)^{12} - (\sigma/r)^6]$.

[i]This is in contrast to the experimental finding that the transition softens with increasing density (see Figs. 14.3 and 14.5).

FIG. 14.13. The stiffness constant $K^R \equiv 8\pi^2\tilde{\beta}^R$ as a function of temperature in a 32×32 Lennard-Jones system as obtained by Tobochnik and Chester (1980) in a Monte Carlo simulation. Only at the lower densities (□, △) does the stiffness reach the universal value $16\pi \approx 50.27$. At higher densities, melting occurs slowly, indicating a first order transition.

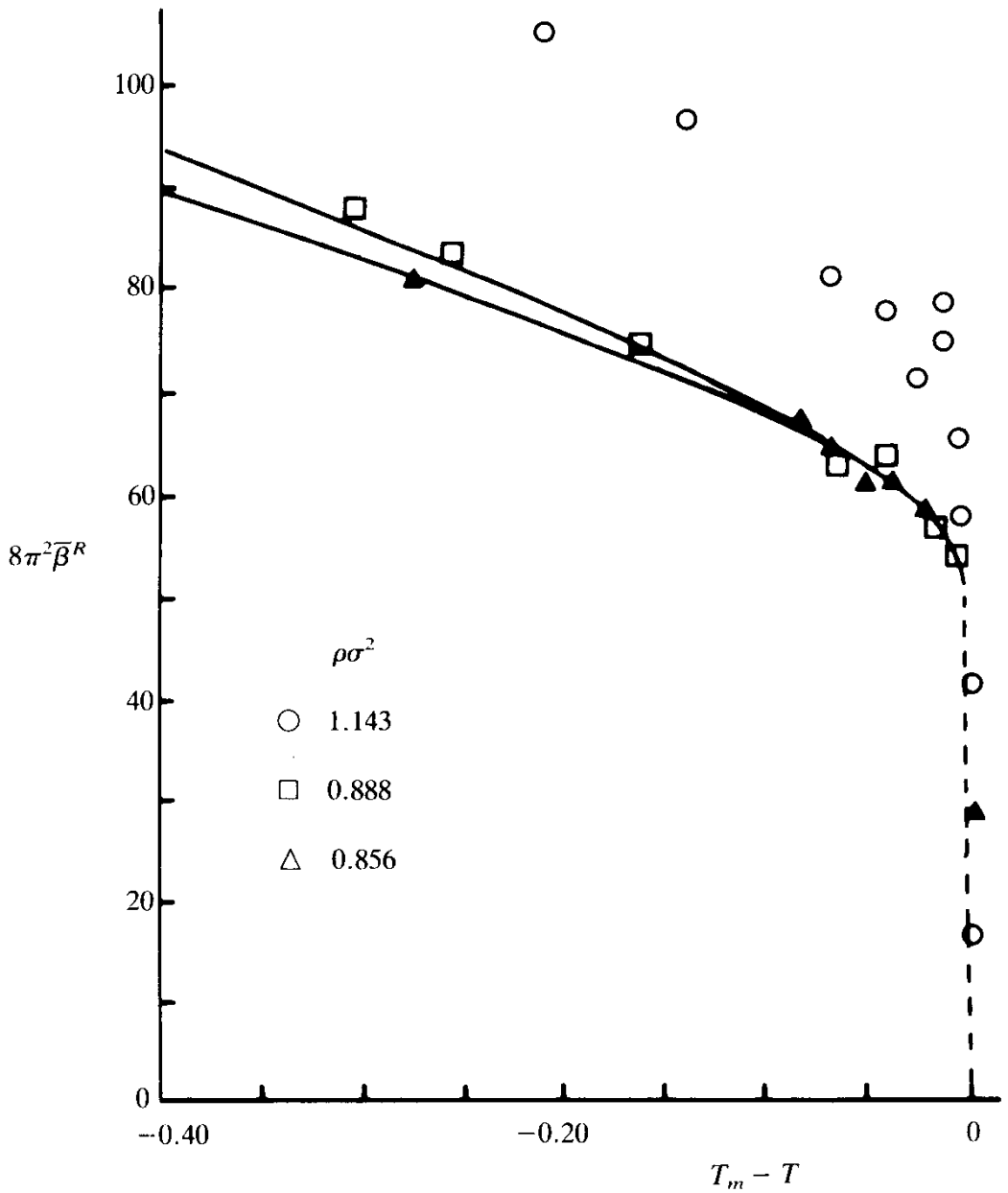

14.10. THE WIGNER ELECTRON LATTICE

Another two-dimensional crystal in which the melting transition has been studied in detail is the two-dimensional version of the electron lattice proposed by E.P. Wigner in 1934. It was pointed out in 1971 that by applying a strong electric field perpendicular to the surface of superfluid

helium it is possible to prepare an electron crystal in two dimensions. By calculating the ground state energy for all five possible two-dimensional Bravais lattices, i.e., square, triangular, centered-rectangular, primitive rectangular, and oblique,[j] Bonsall and Maradudin (1977) showed that the triangular lattice had the lowest energy. For this lattice they found the static ground state energy per electron [to be rederived latter in (18.224)]

$$E = -3.921034 \frac{e^2}{v^{1/2}} \tag{14.149}$$

and the eigenvalue equations for long wavelength phonons

$$m\omega^2 u_\alpha(\mathbf{q}) = \sum_\beta \Lambda_{\alpha\beta}(\mathbf{q})\, u_\beta(\mathbf{q}) \tag{14.150}$$

with [for a derivation see Eq. (18.343)]

$$\Lambda_{\alpha\beta} = \frac{e^2}{v^{1/2}}\left[\frac{2\pi q}{v^{1/2}}\frac{q_\alpha q_\beta}{\mathbf{q}^2} + \eta(\delta_{\alpha\beta}\mathbf{q}^2 - 6q_\alpha q_\beta)\right] + O(\mathbf{q}^4), \tag{14.151}$$

where η is a numeric constant

$$\eta = 0.245065. \tag{14.152}$$

The q factor in front of the longitudinal projection $q_\alpha q_\beta/\mathbf{q}^2$ implies that the Lamé constant λ is infinite, corresponding to an *incompressible* solid. The shear modulus μ is equal to

$$\mu = \eta \frac{e^2}{v^{3/2}}. \tag{14.153}$$

The quantum mechanical zero-point energy was calculated to be

$$E_{0\,\mathrm{pt.}} = \frac{1}{2}\sum_{\mathbf{q}} \omega(\mathbf{q}) = \frac{1}{2} N\hbar \left(\frac{e^2}{m a_0^3}\right)^{1/2}. \tag{14.154}$$

[j]The basic vectors and cell volumes v are $a_0(1, 0)$, $a_0(0, 1)$, a_0^2; $a_0(1, 0)$, $a_0(1/2, \sqrt{3}/2)$, $(\sqrt{3}/2)a_0^2$; $(a, 0)$, $(a/2, b/2)$, $ab/2$; $(a, 0)$, $(0, b)$, ab; $(a, 0)$, (c, b), ab, respectively.

In 1975, Hockney and Brown simulated a $2D$ Wigner crystal via molecular dynamics and found a melting transition at[k]

$$\Gamma_m \equiv \sqrt{\pi}\,\frac{e^2}{v^{1/2}}\,\frac{1}{k_B T_m} = 95 \pm 2, \tag{14.155}$$

with a transition entropy of

$$\Delta s = 0.3\, k_B/\text{particle} \tag{14.156}$$

distributed continuously over roughly 1 K. The specific heat they observed looked very much like that of a λ transition in bulk superfluid helium (see Fig. 14.14), and at the vicinity of the critical point could be fitted by a power behavior $c \sim \tau^{-0.08}$ on the low and $c \sim \tau^{-0.14}$ on the high τ side. This value of T_m was compared by Thouless with the universality prediction, using the zero-temperature elastic constants of Bonsall and Maradudin. We had seen in Eq. (14.151) that due to the $1/r^2$ forces, the $2D$ electron crystal is incompressible so that $\lambda = \infty$ and $\nu = \lambda/(2\mu + \lambda) = 1$, and hence the universality prediction (14.146) is

$$K^{\mathrm{R}} = \frac{a_0^2 \mu^R}{k_B T_m} 4\pi = 16\pi. \tag{14.157}$$

Using (14.155) and (14.153) this corresponds to

$$\frac{8}{\sqrt{3\pi}}\,\eta\,\Gamma_m^R = 16\pi \tag{14.158}$$

or

$$\Gamma_m^R \approx 78.71. \tag{14.159}$$

Since usually the elastic constants soften with increasing temperatures this could, in principle, be compatible with the value found by Hockney and Brown. However, in 1979 simulations were preformed by Gann, Chakravarty and Chester who could not reproduce the data of Hockney and Brown and found instead a much larger value of

[k]They used $v = 10^{-10}$ cm^2 so that $\Gamma_m = 296.12(1/T_m(\mathrm{K}))$.

FIG. 14.14. The specific heat of a 2-D electron lattice at a density of 10^{10} electrons/cm^2 as found in molecular dynamics simulations by Hockney and Brown (1975).

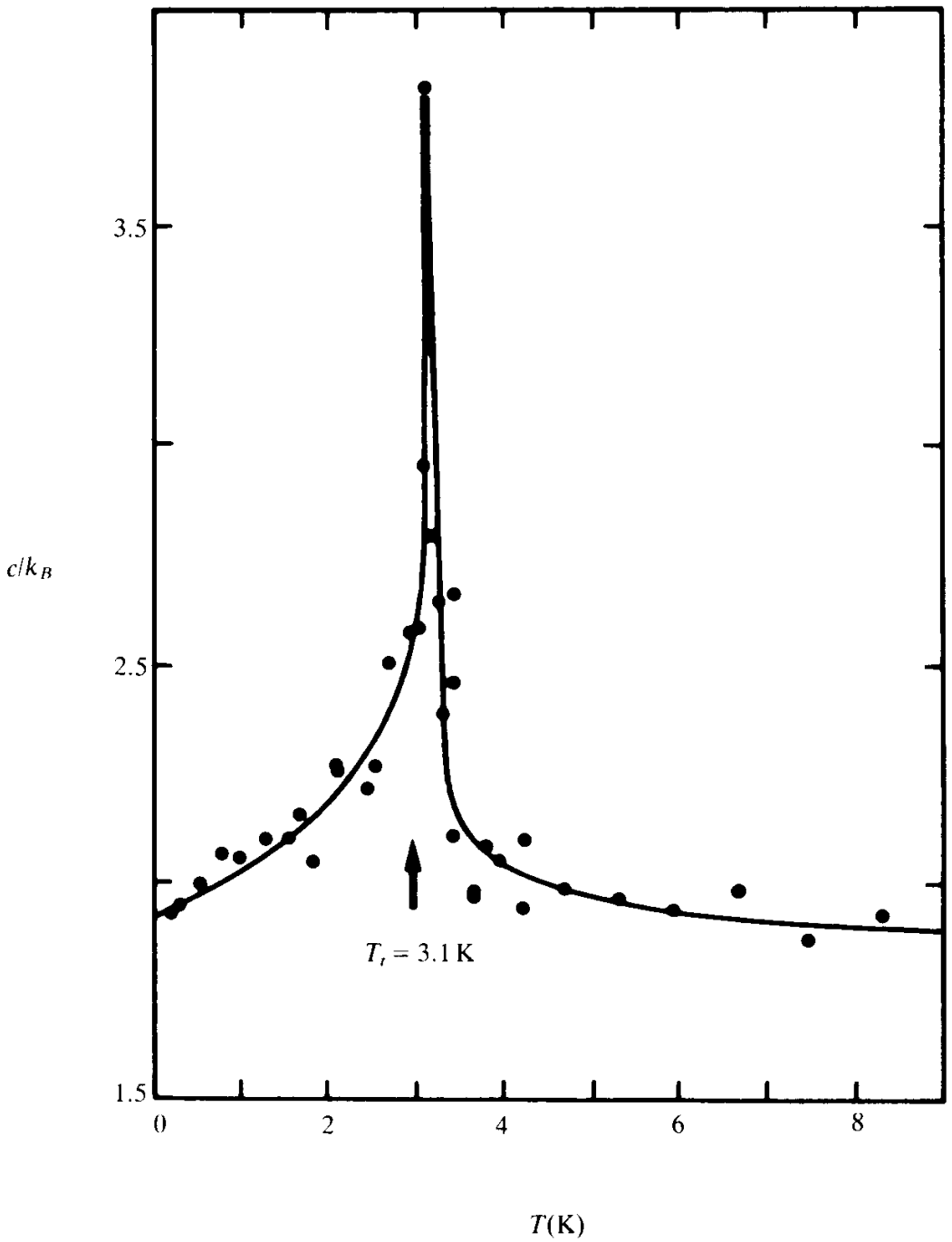

$$\Gamma_m \approx 125 \pm 15.$$

At the same time, Grimes and Adams (1979) performed a laboratory experiment observing a melting temperature consistent with this number. Such a large value for Γ_m would imply that the elastic constant μ could

soften by as much as 20%, from $T = 0$ to the melting temperature. Although this seems rather large, it could, in principle, be possible.

In 1979, however, Morf pointed out that according to the theory of Platzman and Fukuyama (1974) the elastic constant μ in a $2D$ electron gas should have an anomalous temperature behavior and *increase* with temperature. This would immediately destroy the possibility of a universal melting stiffness. Puzzled by this contradiction he performed a simulation in which he determined directly the shear modulus μ as a function of temperature. He found that the elastic constants soften linearly, at low temperature, behaving as

$$\mu(T) = \mu[1 - 30.8\Gamma^{-1} + O(\Gamma^{-2})] \tag{14.160}$$

and confirmed the value (see Fig. 14.15)

$$\Gamma_m \sim 130 \pm 10. \tag{14.161}$$

Thus he found a strong *decrease* of μ with a melting temperature only slightly below the universality prediction (see Fig. 14.15). In addition, he was able to fit his data with a curve obtained via a renormalization group calculation. For this he integrated Eqs. (14.81), (14.82), by assuming the initial stiffness $\tilde{\beta}(\ell_0)$ to soften linearly with temperature, with a slope obtained from the initial piece of his simulation data. He then took the estimated core energy of Fisher, Halperin, and Morf (1979) ($n_s \equiv r^{-1}$),

$$e_c \sim 0.1 \pm 0.02\, n_s^{1/2} e^2 = \mu \frac{a_0^2}{2\pi} \log \bar{c} \tag{14.162}$$

with $\bar{c} = 13 \pm 6$, estimated the natural core energy to be $\mu(a_0^2/2\pi)\log 2$, and worked with an initial fugacity of

$$z = (2\bar{c})^{-\pi\tilde{\beta}}. \tag{14.163}$$

While he claims to see agreement with the KTHNY theory, two problems arise. One is the sharpness of the peak in the specific heat, which a Kosterlitz-Thouless transition should not have. The second is the apparent absence of an intermediate hexatic phase. In fact, the data look very much like those of the melting model of the Villain type (recall the specific heat in Fig. 12.13). A further problem is prompted by the contra-

FIG. 14.15. The shear modulus of a 2-D electron lattice (26×26) obtained by Morf (1978) in a molecular dynamics simulation as a function of Γ^{-1} (labeling the abscissa directly with Γ values). The dashed-dotted line shows the locus where the stiffness should collaps according to the HNY theory [Eq. (14.158)] assuming linear softening of $\mu(T)$, $\lambda = \infty$. The triangle indicates Thouless' value $\Gamma \approx 78.71$ obtained from the use of the $T = 0$ elastic constants. The solid curve was obtained from renormalization group calculations by (a) assuming the bare elastic stiffness to soften linearly with temperature, as indicated by the dashed line, (b) including a core energy, $e_c \sim 0.1 \times \Lambda s^{1/2} e^2$ as calculated by Fisher, Halperin, and Morf (1979), and (c) adjusting one parameter, the size of the defect core. The value $\Gamma_m \approx 130 \pm 10$ is the presently accepted value.

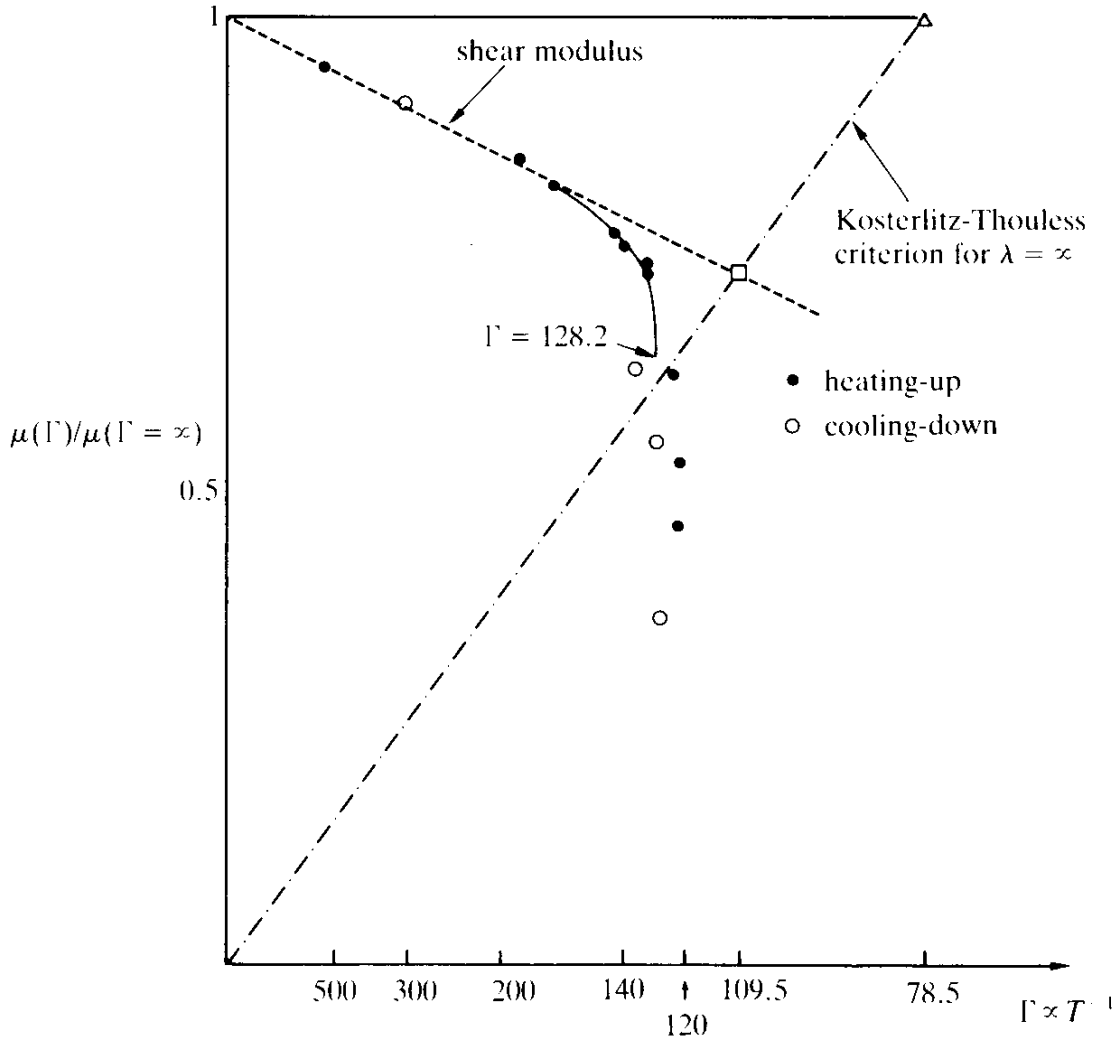

dictory simulation data of Kalia *et al.* (1981), who find a clear first-order transition.

Summarizing the status of experimental and simulation data one may say the following.

1. Experimentally $2D$ melting is mostly a first-order process, as in our models of defect melting, but may sometimes be continuous.
2. Molecular dynamics calculations have found a first-order transition

for Lennard-Jones systems and possibly a continuous transition for an electron lattice.

3. In many cases the specific heat has a clear single sharp peak which, if the transition is continuous, cannot be understood on the basis of the KTHNY theory.

4. The experiments which have measured the divergence of the coherence length à la Kosterlitz-Thouless, Eq. (14.134), have not simulaneously measured the peak in the specific heat to see whether it lies significantly above the transition as it should.

5. The experiments which, in atomic two-dimensional crystals, claim to have measured an angular stiffness as a signal for the hexatic phase have not seen the collapse of this stiffness and related this second point to the peak in the specific heat.

Thus, while first-order and continuous transitions both seem to occur in adsorbed atomic largers there is no convincing evidence as yet for the existence of *two* successive continuous transitions in the continuous case.

Some indirect evidence comes from NMR measurements of spin-spin and spin-lattice relaxation times which are claimed to show two successive anomalies in temperature, the first lying roughly at the universality point $\tilde{\beta}^R = 2/\pi$, the second at the peak of the specific heat [M.G. Richards (1982)]. Whether the first anomaly is really associated with the pair-unbinding transition is not clear and remains to be shown more convincingly.

Our models of defect melting have a first-order transition. Certain modifications will therefore be necessary in order to explain the experimental data, in which the transition is continuous. Preliminary steps in this direction have been undertaken in other models, such as the three-dimensional XY model and the four-dimensional Abelian lattice gauge model [see Janke, Kleinert (1986)]. We shall see in chap. 18, in particular Sec. 18.6, how we can generalize our models of defect melting so as to comprise both types of transitions.

14.11. FIRST ORDER VERSUS CONTINUOUS KTHNY TRANSITIONS

If $2D$ melting is of the first order, as in our models of defect melting, the question arises as to how the KTHNY formulation of defect melting has to be corrected in order to account for this. When deriving the partition

function of the dislocation gas KTHNY use the asymptotic form of the potential between two dislocations

$$v_{ij}^{\prime T}(\mathbf{x}) = \left(\frac{-\delta_{ij}\bar{\nabla}\cdot\nabla + \nabla_i\bar{\nabla}_j}{(\bar{\nabla}\cdot\nabla)^2}\right)' \xrightarrow[|\mathbf{x}|\to\infty]{} -\frac{1}{4\pi}\left[\log(|\mathbf{x}|2\sqrt{2}\,e^{\gamma+(1/2)})\,\delta_{ij} - \frac{x_i x_j}{\mathbf{x}^2}\right]. \tag{14.164}$$

They separate this into a term

$$-\frac{1}{4\pi}\left(\log|\mathbf{x}|\,\delta_{ij} - \frac{x_i x_j}{\mathbf{x}^2}\right) \tag{14.165}$$

and an x independent diagonal term[j]

$$-\frac{1}{4\pi}\log(2\sqrt{2}\,e^{\gamma+(1/2)})\,\delta_{ij}. \tag{14.166}$$

Contracting $v_{ij}^{\prime T}(\mathbf{x}-\mathbf{x}')$ with the Burgers vectors $b_i(\mathbf{x})$, $b_j(\mathbf{x}')$ and summing over $\mathbf{x}\neq\mathbf{x}'$, they use charge neutrality $[\Sigma_{\mathbf{x}} b_i(\mathbf{x}) = 0]$ to rewrite this latter term as a core energy,[1]

$$\frac{1}{4\pi}\log(2\sqrt{2}\,e^{\gamma+(1/2)})\sum_{\mathbf{x}} b_i^2(\mathbf{x}). \tag{14.167}$$

A core energy of this magnitude, if it exists, would indeed enforce a low density of dislocations, justify the fugacity expansion, and could lead to a pair-unbinding transition as envisaged by these authors. Unfortunately, this procedure violates an important fundamental property of the elastic energy between defects. We had seen in the general discussion of Chapter 5 that disclinations can be thought of as a string-like pile-up of dislocations. When such a pile-up takes place, the memory of the string disappears completely due to a perfect matching of the crystal faces along this string. A core energy of the type (14.167) would prevent this from happening. If it were present, the string would carry an infinite energy and no disclinations could form.

In the formalism, the disappearance of the string energy for dislocations with unit separation is a direct consequence of the fact that the

[1]Actually, their numerical constant is different since they work on a triangular lattice, but this is irrelevant to the discussion to follow. Also they did not know this term exactly on a triangular lattice; it is given by (14.43), (14.48).

FIG. 14.16. A nearest neighbor stack-up of dislocations which is equal to a disclination and a second-nearest neighbor stack-up which is equal to a large-angle grain boundary.

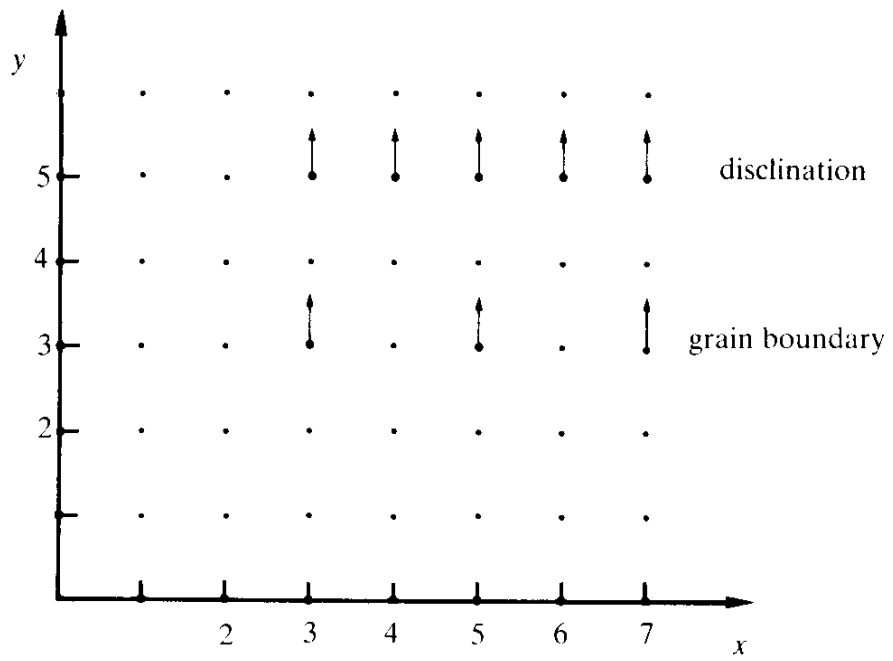

Boltzmann factor contains only the transverse projection of the dislocations density

$$\exp\left\{-4\pi^2\beta \sum_{\mathbf{x}\neq\mathbf{x}'} b_i(\mathbf{x})\left(\frac{-\delta_{ij}\nabla\cdot\bar{\nabla}+\nabla_i\bar{\nabla}_j}{(\bar{\nabla}\cdot\nabla)^2}\right)'(\mathbf{x},\,\mathbf{x}')\,b_j(\mathbf{x}')\right\}$$

$$=\exp\left\{-4\pi^2\beta \sum_{\mathbf{x}\neq\mathbf{x}'} \varepsilon_{ji}\bar{\nabla}_j b_i(\mathbf{x})\frac{1}{(\bar{\nabla}\cdot\nabla)^2}\varepsilon_{\ell k}\bar{\nabla}_\ell b_k(\mathbf{x}')\right\}. \qquad (14.168)$$

In order to see this let us form a string of Burgers vectors $b_i(\mathbf{x})$ which all point along the y-axis and are stacked up along the x-axis, starting from point X, Y (see Fig. 14.16):

$$b_i(\mathbf{x}) = \delta_{i2}\frac{1}{\bar{\nabla}_1}\delta_{x,X}\,\delta_{y,Y} = \delta_{i,1}\,\Theta_{x,X}\,\delta_{y,Y}. \qquad (14.169)$$

Here

$$\Theta_{x,X} = \frac{1}{\bar{\nabla}_1}\delta_{x,X} = \sum_{x'=-\infty}^{x}\delta_{x',X} \qquad (14.170)$$

is the lattice version of the Heaviside function which vanishes for $x < X$ and is equal to unity for $x \geq X$. Applying to this the operation $\varepsilon_{ji}\bar{\nabla}_j$ we find

$$\varepsilon_{ji}\bar{\nabla}_j b_i = \delta_{x,X}\delta_{y,X}. \tag{14.171}$$

This formula shows explicitly that the string has no elastic energy. The energy is focused roughly concentrically around the point (X, Y) which is the disclination generated by the string of dislocations.

Notice that if the long-distance limit (14.164) of the transverse potential $v_{ij}^T(\mathbf{x})'$ is employed too early (as Halperin, Nelson and Young have done) one is *incapable* of describing this phenomenon. The cancellation of the elastic energy makes *essential* use of the short-range properties of the potential $v_{ij}^T(\mathbf{x})$ on the lattice. As discussed in Section 2.5, a crystal may contain not only complete pile-ups of dislocations but also incomplete ones, where the Burgers vectors are stacked with a separation of 2, 3, or more lattice spacings. Such incomplete stack-ups are observed in the form of grain boundaries (see Fig. 14.16 and Fig. 2.6 in Section 2.1). The disappearance of the energy for nearest neighbour spacing has the consequence that strings with spacing 2 still have quite a moderate amount of energy. Since they carry, in addition (and in contrast to string of nearest neighbour dislocations), the configurational entropy of a random chain, this can outbalance their energy and we may expect the proliferation of grain boundaries at a certain temperature. It was suggested by Chiu (1982) that this proliferation would take place before pairs of individual dislocations could dissociate.

The results of simulations of our models of defect melting confirm this idea. In these models, the fundamental defects are carried by $\eta(\mathbf{x})$ and are disclinations. Pairs of these have the same interaction as a single dislocation with the Burgers vector pointing orthogonally to the dipole vector. If we look at the distribution of disclinations extracted from our simulation data (see Fig. 13.20) we see that for low temperature the disclinations always appear as quadruplets, corresponding to pairs of dislocations and antidislocations. As the system passes the melting transition, these quadruplets do not split up into pairs, as predicted by the KTHNY theory, with a subsequent unbinding transition of these pairs, but they blow up into larger and larger strings of alternating charge $\eta(\mathbf{x})$ with or without open ends, in a single transition. Interpreting each pair of neighboring disclinations as a dislocation, these strings may be viewed as string dislocations with spacing 2, i.e., they can be viewed as grain

boundaries. The reader is referred back to the end of Chapter 12 for a more detailed discussion of these features of the melting process.

It is not easy to reconcile the KTHNY theory with these findings. As long as the theory is formulated in the continuum and uses the long-distance form of the defect potential. The melting process requires stacks of defects at next-nearest neighbor positions and an additive core energy would prevent their formation.

14.12. DIRECT SIMULATION OF A GAS OF DISLOCATIONS

The importance of the pile-up of dislocations was confirmed in Monte Carlo simulations by Saito (1982). He considered directly the partition function of a gas of dislocations:

$$Z_{\text{disl}} = \sum_{\{b(\mathbf{x})\}} \exp\left\{-\beta \sum_{\mathbf{x},\mathbf{x}'} b_i(\mathbf{x}) \left(\frac{-\delta_{ij}\bar{\nabla}\cdot\nabla + \nabla_i\bar{\nabla}_j}{(\bar{\nabla}\cdot\nabla)^2} \right)(\mathbf{x},\mathbf{x}')\, b_j(\mathbf{x}')\right\}. \tag{14.172}$$

In order to enforce the validity of the dilute-gas limit, he followed Halperin, Nelson and Young and added on the core energy

$$e^{-\beta e_c \sum_{\mathbf{x}} b_i^2(\mathbf{x})}. \tag{14.173}$$

Working on a triangular lattice with lattice vector $a_0(1, 0)$, $a_0(-1/2, \sqrt{3}/2)$, he considered only the fundamental Burgers vectors

$$b^{(1)} = \pm a_0(1, 0), \quad b^{(2)} = \pm a_0\left(-\frac{1}{2}, \frac{\sqrt{3}}{2}\right), \quad b^{(3)} = \pm a_0\left(-\frac{1}{2}, -\frac{\sqrt{3}}{2}\right). \tag{14.174}$$

For the potential he took the long-distance approximation (14.43)

$$v_{ij}^{\prime T}(\mathbf{x}) = \left(\frac{-\delta_{ij}\bar{\nabla}\cdot\nabla + \nabla_i\bar{\nabla}_j}{(\bar{\nabla}\cdot\nabla)^2} \right)' \xrightarrow[|\mathbf{x}|\to\infty]{} -\frac{1}{4\pi}\left[\log(|\mathbf{x}|\, c)\,\delta_{ij} - \frac{x_i x_j}{|\mathbf{x}|^2} \right], \tag{14.175}$$

where, we recall, c is the constant (14.47) determined numerically by Saito. When he simulated the system using the above asymptotic form he

[m]His parameters are related ours by $\lambda a_0^2/k_B T = [\mu(\mu + \lambda)/(2\mu + \lambda)](a_0^2/\pi k_B T) = 2\pi\tilde{\beta}$.

found a continuous dislocation pair-unbinding transition as predicted by the HNY theory. He then reduced the natural core energy implied by (14.175) by an additional *negative* term, i.e., he used the core parameter

$$\bar{c} = c/\sqrt{e} \tag{14.176}$$

instead of c. This produced a first-order transition in which the dislocations piled up into strings of large-angle grain boundaries.

In view of the above discussion it is easy to interprete this result. While working with an unphysical model in which he had taken the long-distance limit of the lattice potential (thus destroying the proper pile-up behavior of the dislocations), the artificial reduction of the core energy partially corrected for the wrong starting point. It lowerest the energy of the nearest neighbor strings of dislocations so much that their configurational entropy led in the end to their proliferation before the pair-unbinding transition could set in. While Saito's result tells us how the parameters of the HNY theory can be modifed in order to generate a first order transition, his approach maintains the fundamental drawbacks of the HNY formulation. Saito's strings of dislocations are, by construction, nearest-neighbor strings on a triangular lattice which, as we have seen in Eq. (14.171), are really disclinations and thus should not carry any string energy at all (they are not even physical degrees of freedom). Only the next-nearest-neighbor strings are physical. It is the artificial core energy which gives rise to his model's nearest-neighbor strings. This must be kept in mind if we want to reinterprete Saito's result in terms of real crystals. Saito attempted to account for this short coming in *ad hoc* manner by taking, as a length scale over which the dislocations can be separated, twice the lattice spacing rather than the lattice spacing itself. This was certainly a step in the right direction although it introduced an error in the positional entropy of the single defect configurations.

NOTES AND REFERENCES

The KTHNY papers are listed at the end of Chapters 8 and 11 of Part II.
Papers on phases of adsorbed layers are legion:

A. Thomy and X. Duval, *J. Chem. Phys.* **67** (1970) 1101,
M. Bretz, J.G. Dash, D.C. Hickernell, F.O. McLean and O.E. Vilches, *Phys. Rev.* **A8** (1973) 1589, **A9** (1974) 2814 (on ^{4}He),
R.L. Elgin and D.C. Goodstein, *Phys. Rev.* **A9** (1974) 2671 (on ^{4}He),

S.V. Hering, S.W. Van Sciver and O.E. Vilches, *J. Low Temp. Phys.* **25** (1976) 793 (on ^{4}He),
E.M. Hammonds, P. Heiney, P.W. Stephens, R.J. Birgeneau and P. Horn, *J. Phys.* **C13** (1980) 1301,
J.M. Butler, J.A. Letzinger, G.A. Stewart and R.B. Griffiths, *Phys. Rev. Lett.* **42** (1979) 1289 (on Kr, N),
C. Tessier and Y. Larkers, in *Ordering in Two Dimensions*, ed. S.K. Sinha (North-Holland, Amsterdam, 1980) (on Ar, Kr, Xe, CH_4),
P.A. Heiney *et al.*, *Phys. Rev. Lett.* **48** (1982) 104 [For the other authors see Chapter 7. See also the more detailed paper in *Phys. Rev.* **28B** (1983) 6416 (on Xe).],
S.K. Sinha, P. Vora, P. Dutta and L. Passell, *J. Phys.* **C15** (1982) L275 (on CH_4).

The papers by Heiney *et al.*, and by Sinha *et al.*, found, at higher coverage, a single continuous melting transition with a coherence length of the Kosterlitz-Thouless type. This is found also by
J.P. McTague, J. Als-Nielsen, J. Bohr and M. Nielsen, *Phys. Rev.* **B25** (1982) 7765 (mainly on Ar).

Sharp peaks in the specific heat were found for Xenon on graphite by M. Bretz *et al.* (1973) (see Fig. 7.13),
for Neon on graphite by
G.B. Huff and J.G. Dash, in *13th Proc. Int Conf. Low Temp. Phys.*, (eds. R.H. Kropshot and K.O. Timmerhaus (Plenum Press, 1974),
for helium on graphite by
S.B. Hurlbut, J.G. Dash, *Phys. Rev. Lett.* **53** (1984) 1931, **55** (1985) 2227,
and for Argon on graphite
A.D. Migone, E.R. Li, M.H.W. Chan, *Phys. Rev. Lett.* **53** (1984) 810.

First as well as second order transitions in Xenon were found, depending on the coverage, by
P. Dimon, P.M. Horn, M. Sutton, R.J. Bigeneau and D.E. Moncton, *Phys. Rev.* **B31** (1985) 437.
At low densities, there seems to be a single rather sharp but continuous transition. The coherence length grows rapidly to very large values within 2 K. In Krypton, it grew up to 10,000 Å:
K.L. D'Amico, D.E. Moncton, D.E. Specht, E.D. Birgeneau, R.J. Nagler and P.M. Horn, *Phys. Rev. Lett.* **53** (1984) 2250;
and in Xenon up to 2000 Å, see
E.D. Specht, R.J. Birgeneau, K.L. D'Amico, D.E. Moncton, R.J. Nagler and P.M. Horn, *J. Physique Lett.* **46** (1985) L-561.
See also
R.S. Birgenau, G.S. Brown, P.M. Horn, D.G. Moncton, and P.W. Stephen, *J. Phys.* **C14** (1981) L49,
S.M. Coppersmith, D.S. Fisher, B.I. Halperin, P.A. Lee, and W.F. Brinkmann, *Phys. Rev. Lett.* **46** (1981) 549.
Orientational order in layers of liquid Argon was seen by
C.G. Shaw, S.C. Fain, Jr. and M.D. Chinn, *Phys. Rev. Lett.* **41** (1978) 955, C.G. Shaw and S.C. Fain, Jr., *Surf. Sci.* **83** (1979) 11
and in Xenon by
T.F. Rosenbaum, S.E. Nagler, P.M. Horn and R. Clarke, *Phys. Re . Lett.* **50** (1983) 1791.

Stacked hexatic liquid crystal phases were reported by R. Pindak, D.E. Moncton, S.C. Davey and J.W. Goodby, *Phys. Rev. Lett.* **46** (1981) 1135.
See also
S.B. Dierker, R. Pindak and R.B. Meyer, *Phys. Rev. Lett.* **56** (1986) 1819,

J.D. Brock, A. Aharony, R.J. Birgeneau K.W. Evans-Lufferodt, J.D. Litster, P.M. Horn, G.B. Stephenson and A.R. Tajbakhsh, *Phys. Rev. Lett.* **57** (1986) 98,
A. Aharony, R.J. Birgeneau , J.D. Brock and J.D. Litster, MIT preprint, 1986.
In a substrate-free double layer, a clear first order transition was observed
D.E. Moncton, R. Pindak and S.C. Davey, *Phys. Rev. Lett.* **49** (1982) 1865.
Two successive transitions are claimed to be seen in NMR experiments by
M.G. Richards, in *Phase Transitions in Interface Films*, eds. J.G. Dash and J. Ruwalds (Plenum Press, New York, 1980).

Evidence for a sequence of two melting transitions was found in films of liquid crystals by
J. Collett, P.S. Pershan, E.B. Sirota, and L.B. Sorensen, *Phys. Rev. Lett.* **52** (1984) 356,
E.B. Sirota, P.S. Pershan, L.B. Sorensen, and J. Collett, *Phys. Rev. Lett.* **55** (1985) 2039,
S.B. Dierker, R. Pindak, and R.B. Meyer, *Phys. Rev. Lett.* **56** (1986) 1819,
S.C. Davey, J. Budai, J.W. Goodby, R. Pindak, and D.E. Moncton, *Phys. Rev. Lett.* **53** (1984) 2129.
See also:
C.C. Huan, J.M. Viner, R. Pindak, and J.W. Goodby, *Phys. Rev. Lett.* **46** (1981) 1289,
J.M. Viner, D. Lamey, C.C. Auang, R. Pindak, and J.W. Goodby, *Phys. Rev.* **A28** (1983) 2433,
A. Aharony, R.J. Birgeneau, J.D. Brock, and J.D. Litster, *Phys. Rev. Lett.* **57** (1986) 1012,
R. Pindak, W.O. Sprenger, D.J. Bishop, D.D. Osheroff, and J.W. Goodby, *Phys. Rev. Lett.* **48** (1982), 173.

Simulation work on two-dimensional melting has been done by many workers, in particular for Lennard-Jones interactions, by
J.O. Hansen and L. Verlet, *Phys. Rev.* **184** (1969) 151,
see also
L. Verlet, *Phys. Rev.* **159** (1967) 98,
S. Toxvaerd, *J. Chem. Phys.* **69** (1978) 4750,
F.V. Swol, L.V. Woodcock and J.N. Cape, *J. Chem. Phys.* **73** (1980) 913.
A special purpose computer simulating 16,000 particles was built by
A.F. Bakker *et al.*, *Phys. Lett.* **93A** (1982) 67.
Further simulation work quoted in text was performed by
D. Frenkel and J.P. Mc Tague, *Phys. Rev. Lett.* **42** (1979) 1632
and
J.P. Mc Tague, D. Frenkel and M.P. Allen, in *Ordering in Two Dimensions*, ed. S.K. Sinha (North Holland, Amsterdam, 1980) p. 147.
F.F. Abraham, *ibid.*, p. 155,
J.M. Greif, A.F. Silva-Morera and D.L. Goodstein, *ibid.*, p. 297,
J. Tobochnik and G.V. Chester, *ibid.*, p. 339, and *Phys. Rev.* **25** (1982) 6778,
S. Toxvaerd, *Phys. Rev. Lett.* **44** (1980) 1002,
S.W. Koch and F.F. Abraham, *Phys. Rev.* **B27** (1983) 2964, *ibid.*, **B29** (1984) 2606,
F.F. Abraham, *Phys. Rev. Lett.* **50** (1983) 978.

The possible existence of an electron lattice was shown by
E.P. Wigner, *Phys. Rev.* **46** (1934) 1002.
The two-dimensional electron lattices were proposed by
A.A. Chaplick, *Zh. Eksp. Teor. Fiz.* **62** (1972) 746
for semiconductor surfaces and by
A.A. Crandall and R.W. Williams, *Phys. Lett.* **A34** (1971),
A.A. Crandall, *Phys. Rev.* **A8** (1973) 2136
for surfaces of liquid helium.

For calculations of ground state energy and elastic constants see
L. Bonsall and A.A. Maradudin, *Phys. Rev.* **B15** (1977) 1959.

Further theoretical work can be found in
P.H. Platzmann and H. Fukuyama, *Phys. Rev.* **B10** (1974) 3150.
D.J. Thouless, *J. Phys.* **C11** (1978) L189.
Experiments on $2D$ electron lattice were conducted by
C.C. Grimes and G. Adams, *Phys. Rev. Lett.* **42** (1979) 795,
R. Mehrota, B.M. Guenin, and A.J. Dahm, *Phys. Rev. Lett.* **48** (1982) 641,
C.J. Guo, D.B. Mast, Y.-E. Ruan, M.A. Slan, and A.J. Dahm, *Phys. Rev. Lett.* **51** (1983) 1461,
F. Gallet, G. Deville, A. Valdez, and F.I.B. William, *Phys. Rev. Lett.* **49** (1982) 212.
Computer experiments on a 2 D electron lattice were carried out by
R.W. Hockney and T.R. Brown, *J. Phys.* **C8** (1975) 1813,
R.H. Morf, *Phys. Rev. Lett.* **43** (1979) 931.
See also the review articles in *Helvetica Phys. Acta* **56** (1983) 743 and in *Lectures in Physics of Intercalating Compounds*, eds. L. Pietronero and E. Tossati, Springer Series in Solid State Sciences, Vol. 38 (Springer, Heidelberg, 1984),
R.C. Gann, S. Chakravarty, G.V. Chester, *Phys. Rev.* **B20** (1979) 326.

Defects in these lattices were first studied by
D.S. Fisher, B.I. Halperin and R. Morf, *Phys. Rev.* **B20** (1979) 4692.
See also the analysis by
D.S. Fisher, in *Ordering in Two Dimensions*, ed. S.K. Sinha (North Holland, Amsterdam, 1980) p. 189.

Grain boundaries as the driving mechanism for the melting transition were proposed by S.T. Chiu, *Phys. Rev. Lett.* **48** (1982) 933, *Phys. Rev.* **B28** (1983) 178.

The fact that the removal of the core energy leads to a first-order transition was found by Y. Saito, *Phys. Rev.* **B26** (1982) 6239, *Phys. Rev. Lett.* **48** (1982) 1114.
The fundamental problems associated with assuming a core energy of the HNY type was pointed out by
H. Kleinert, *Phys. Lett.* **95A** (1982) 38.

Further Monte Carlo evidence for the first-order nature of the model's melting transition was discussed in Section 12.4.
See, in particular, the papers by
W. Janke and H. Kleinert, *Phys. Lett.* **114A** (1986) 255,
W. Janke and D. Toussaint, *Phys. Lett.* **116A** (1986) 387,
which contrast with the earlier results of
K.J. Strandburg, S.A. Solla and G.V. Chester, *Phys. Rev.* **B28** (1983) 2717,
and the recent paper by
K.-J. Strandburg, *Phys. Rev.* **B34** (1986) 3536.
The author did not go to large enough lattices where she would have seen the finite size scaling typical for a first-order transition, as observed in the work of Janke and Toussaint. Similar criticism applies to
D.A. Bruce, *Materials Forum* **4** (1985) 5.
For other difficulties with the KTHNY mechanism, see
B. Joos and M.S. Duesburg, *Phys. Rev. Lett.* **55** (1985) 1997.
The scaling law for the coherence length is discussed in
J.M. Greif, D.L. Goodstein and A.F. Silva-Morera, *Phys. Rev.* **B25** (1982) 6838,
J.L. Cardy, *Phys. Rev.* **B26** (1982) 6311.

Modifications of lattice models involving the cosine of lattice gradients which allow one to choose the order of the transition are discussed in
W. Janke and H. Kleinert, *Phys. Rev. Lett.* **57** (1986) 279, *Nucl. Phys.* **B270** (1986) 399,
H. Kleinert, *Phys. Rev. Lett.* **56** (1986) 1441.
For recent experimental work, see

N. Greiser, G.A. Held, R. Frahm, R.L. Green, P.M. Horn, and R.M. Sutter, *Phys. Rev. Lett.* **59** (1987) 1625,
N.J. Collela and R.M. Suter, *Phys. Rev.* **B34** (1986) 2052.
For simulation of hard core liquids see,
C. Undink, and D. Frenkel, *Phys. Rev.* **B34** (1987) 6933,
C. Undink and J. van der Elsken, *Phys. Rev.* **B35** (1987) 279.

CHAPTER FIFTEEN

DISORDER FIELD THEORY OF DEFECT MELTING

Now that we possess a lattice model which respects all stack-up properties of the defects in a crystal it is possible to derive a consistent disorder field theory of crystalline defects. This field theory turns out to be rather different from the tentative construction presented in Chapter 8. In contrast to that theory for which a good deal of effort was spent in finding possible mechanisms for making the transition first-order, the proper disorder field theory to be proposed in this chapter will have a natural way of undergoing a first-order transition right at the mean field level. We shall see that as was the case with the field theory involving order fields [see Section 13.1] the disorder field theory will contain a temperature dependent *quartic* term which naturally causes a first-order transition (recall Fig. 13.1). The disorder field theory contains D complex disorder fields, one for every lattice direction. It describes all possible configurations of the defect tensor $\eta_{ij}(\mathbf{x})$ and consequently a grand canonical ensemble of dislocations as well as disclinations.

15.1. DISORDER LATTICE MODEL FOR THREE-DIMENSIONAL DEFECT CONFIGURATIONS

Our starting point is the defect representation (9.40) of the partition function of the melting model (omitting the bar on top of χ_{ij})

$$Z = \left[\frac{1}{8\xi^3}\left(1 - 3\frac{\xi}{\gamma}\right)\right]^{N/2} \frac{1}{(2\pi\beta)^{3N}}$$
$$\times \prod_{\mathbf{x}} \left[\int d\chi_{11}(\mathbf{x})\, d\chi_{22}(\mathbf{x})\, d\chi_{12}(\mathbf{x})\right] \sum_{\{\bar{\eta}_{ij}(\mathbf{x})\}} \delta_{\bar{\nabla}_i \bar{\eta}_{ij}(\mathbf{x}),0}$$
$$\times \exp\left\{-\frac{1}{2\beta}\sum_{\mathbf{x}}\left[\sum_{i<j}\sigma_{ij}^2 + \frac{1}{2\xi}\sum_i \sigma_{ii}^2 - \frac{1}{2\gamma}\left(\sum_i \sigma_{ii}(\mathbf{x}-\mathbf{i})\right)^2\right]\right.$$
$$\left. - 2\pi i \sum_{\mathbf{x},\ell,n} \chi_{\ell n}(\mathbf{x})\,\bar{\eta}_{\ell n}(\mathbf{x})\right\}. \tag{15.1}$$

A disorder-lattice model will now be introduced to replace the sum over the defect configuration $\bar{\eta}_{ij}(\mathbf{x})$. In order to achieve this, consider the following auxiliary sum over defects with an arbitrary core energy ε,

$$Z_{\text{def}} = \sum_{\{\bar{\eta}_{ij}(\mathbf{x})\}} \delta_{\bar{\nabla}_i \bar{\eta}_{ij}(\mathbf{x}),0} \exp\left\{-\varepsilon\left(\sum_{\mathbf{x},i<j}\bar{\eta}_{ij}^2 + \frac{1}{2}\sum_{\mathbf{x},i}\bar{\eta}_{ii}^2\right)\right\}, \tag{15.2}$$

where $\bar{\eta}_{ii}(\mathbf{x})$, $\bar{\eta}_{ij}(\mathbf{x})(i<j)$ run over all integer and half integer numbers, respectively. By comparison with (11.6) we see that the sum over $\bar{\eta}_{ij}(\mathbf{x})$ has exactly the same form as the sum over stress configurations, i.e.,

$$\sum_{\{\bar{\sigma}_{ij}(\mathbf{x})\}} \delta_{\bar{\nabla}_i \bar{\sigma}_{ij}(\mathbf{x}),0} \exp\left\{-\frac{1}{4\beta}\left(\sum_{\mathbf{x},i<j}\bar{\sigma}_{ij}^2 + \frac{1}{2}\sum_{\mathbf{x},i}\bar{\sigma}_{ii}^2\right)\right\}. \tag{15.3}$$

The only difference between the $\bar{\eta}_{ij}(\mathbf{x})$ and $\bar{\sigma}_{ij}(\mathbf{x})$ sums is that $\bar{\sigma}_{ij}$ are *all* integer numbers for $i=j$ and $i\neq j$ while $\bar{\eta}_{ij}(i<j)$ are half-integer. The sum (15.2) can be thought of as being the dual transform of a model

$$Z_{\text{def},V} = \sum_{\{n_{ij}(\mathbf{x})\}} \Phi[n_{ij}(\mathbf{x})] \prod_{\mathbf{x},i}\left[\int_{-\pi}^{\pi}\frac{d\gamma(\mathbf{x})}{2\pi}\right]$$
$$\times \exp\left\{-\frac{1}{\varepsilon}\left[\sum_{\mathbf{x},i<j}(\nabla_i\gamma_j + \nabla_j\gamma_i - 2\pi n_{ij})^2 + 2\sum_{\mathbf{x},i}(\nabla_i\gamma_i - \pi n_{ij})^2\right]\right\}, \tag{15.4}$$

where the symmetric jump numbers $n_{ij}(\mathbf{x})$ run over all integer values for $i=j$ and $i\neq j$. Indeed, if we introduce integrations over auxiliary variables $\eta_{ij}(\mathbf{x})$, we can write this, just as in (9.22), as

$$Z_{\text{def},V}=\frac{1}{2^{3N/2}}\prod_{\mathbf{x},i\le j}\left[\int\frac{d\eta_{ij}(\mathbf{x})}{\sqrt{2\pi^3}}\right]\sum_{\{n_{ij}(\mathbf{x})\}}\Phi[n_{ij}(\mathbf{x})]\exp\left\{-\varepsilon\sum_{\mathbf{x}}\left[\sum_{i<j}\eta_{ij}^2+\frac{1}{2}\sum_i\eta_{ii}^2\right]\right.$$
$$\left.+2i\left[\sum_{\mathbf{x},i<j}\eta_{ij}(\nabla_i\gamma_j+\nabla_j\gamma_i-2\pi n_{ij})+\sum_{\mathbf{x},i}\eta_{ii}(\nabla_i\gamma_i-\pi n_{ii})\right]\right\}. \tag{15.5}$$

This is the same as (15.2) since the integrations over γ_i, the conservation law $\bar{\nabla}_i\eta_{ij}(\mathbf{x})=0$, and the sums over η_{ij} force $\eta_{ii}(\mathbf{x})$ to be integer and $\eta_{ij}(\mathbf{x})(i<j)$ to be half-integer. The latter is the principal difference with respect to (9.22), where $\sigma_{ij}(\mathbf{x})$ had to be integer for $i=j$ *and* $i<j$.

In order to work toward the desired disorder field theory we now proceed in the same way as we did in the case of vortex lines in Chapter 12, Part II. We take the inverse Villain approximation to (15.4) and write

$$Z_{\text{def}}=\prod_{\mathbf{x},i}\left[\int\frac{d\gamma_i(\mathbf{x})}{2\pi}\right]\exp\left\{\frac{2}{\varepsilon}\left[\sum_{\mathbf{x},i<j}\cos(\nabla_i\gamma_j+\nabla_j\gamma_i)+\frac{1}{2}\sum_{\mathbf{x},i}\cos(2\nabla_i\gamma_i)\right]\right\}. \tag{15.6}$$

Notice the appearance of the double angle in the $i=j$ cosine [in contrast with the melting model in the cosine form (13.2)]. This partition function of all defect configurations can then be transformed into a disorder field theory just as the cosine form of the melting model in Sec. 13.2. Before doing this, however, let us see how the stress field enters into this partition function.

15.2. COUPLING THE STRESS GAUGE FIELD

Let us we add to the defect sum (15.6) the stress gauge field. According to (15.1), the coupling is

$$\exp\left\{2\pi i\sum_{\mathbf{x},\ell,n}\chi_{\ell n}(\mathbf{x})\bar{\eta}_{\ell n}(\mathbf{x})\right\}. \tag{15.7}$$

In the partition function (15.5), $\eta_{\ell n}$ appears in the last two terms, so (15.7) changes them to

$$2i\sum_{\mathbf{x}}\left[\sum_{i<j}\bar{\eta}_{ij}(\nabla_i\gamma_j+\nabla_j\gamma_i-2\pi\chi_{ij}-2\pi n_{ij})+\sum_i\bar{\eta}_{ii}(\nabla_i\gamma_i-\pi\chi_{ii}-\pi n_{ii})\right].$$

As a consequence, the disorder model (15.6) contains $\chi_{ij}(\mathbf{x})$ as follows,

$$Z_{\text{def}}[\chi] = \prod_{\mathbf{x},i}\left[\int \frac{d\gamma_i}{2\pi}\right] \times \exp\left\{\frac{2}{\varepsilon}\left[\sum_{\mathbf{x},i<j}\cos(\nabla_i\gamma_j+\nabla_j\gamma_i-2\pi\chi_{ij})+\frac{1}{2}\sum_{\mathbf{x},i}\cos(2\nabla_i\gamma_i-2\pi\chi_{ii})\right]\right\}. \tag{15.8}$$

Combining this with (15.1), the complete disorder lattice model becomes, in the presence of an extra core energy ε,

$$Z_{\text{disord}} = \left[\frac{1}{8\xi^3}\left(1-3\frac{\xi}{\gamma}\right)\right]^{N/2}\frac{1}{(2\pi\beta)^{3N}}\prod_{\mathbf{x}}\left[\int d\chi_{11}(\mathbf{x})\,d\chi_{22}(\mathbf{x})\,d\chi_{12}(\mathbf{x})\right] \times \exp\left\{-\frac{1}{2\beta}\left[\sum_{\mathbf{x},i<j}\sigma_{ij}^2+\frac{1}{2\xi}\sum_{\mathbf{x},i}\sigma_{ii}^2-\frac{1}{2\gamma}\sum_{\mathbf{x}}\left(\sum_i\sigma_{ii}(\mathbf{x}-\mathbf{i})\right)^2\right] + \frac{2}{\varepsilon}\left[\sum_{\mathbf{x},i<j}\cos(\nabla_i\gamma_j+\nabla_j\gamma_i-2\pi\chi_{ij})+\frac{1}{2}\sum_{\mathbf{x},i}\cos(2\nabla_i\gamma_i-2\pi\chi_{ii})\right]\right\}, \tag{15.9}$$

where

$$\sigma_{ij}(\mathbf{x}) = \varepsilon_{ik\ell}\,\varepsilon_{jmn}\,\bar{\nabla}_k\,\bar{\nabla}_m\,\chi_{\ell n}(\mathbf{x}-\boldsymbol{\ell}-\mathbf{n}). \tag{15.10}$$

Notice that the model is properly invariant under stress gauge transformations,

$$\chi_{ij}(\mathbf{x})\to\chi_{ij}(\mathbf{x})+\nabla_i\Lambda_j(\mathbf{x})+\nabla_j\Lambda_i(\mathbf{x}), \qquad \gamma_i(\mathbf{x})\to\gamma_i(\mathbf{x})+2\pi\Lambda_i(\mathbf{x}), \tag{15.11}$$

as it should.

The original melting model (15.1) corresponds to the limit $\varepsilon\to 0$, i.e., no extra core energy. In that case the model becomes the analogue of the "frozen lattice superconductor" treated in Part II [see the remark there before Eq. (12.8)].

For the case $\varepsilon\to 0$, the model (15.9) can be replaced by yet another one in which ε is nonzero and plays the role of the natural core energy associated with stress fluctuations [recall (9.116)],

$$\exp\left\{-4\pi^2\beta|c|\sum_{\mathbf{x}}\left[\bar{\eta}_{ij}^2(\mathbf{x})+\frac{\nu}{1-\nu}\left(\sum_{\ell}\bar{\eta}_{\ell\ell}(\mathbf{x}-\boldsymbol{\ell})\right)^2\right]\right\}, \tag{15.12}$$

where

$$|c| \approx 0.011 \tag{15.13}$$

is the constant by which the asymptotic behavior of the subtracted defect potential

$$v_4'(\mathbf{x}-\mathbf{x}') = \int \frac{d^3k}{(2\pi)^3} \frac{e^{i\mathbf{k}\cdot(\mathbf{x}-\mathbf{x}')}-1}{(\bar{\mathbf{K}}\cdot\mathbf{K})^2} \tag{15.14}$$

differs from the continuum form $-|\mathbf{x}-\mathbf{x}'|/8\pi$ [recall Eqs. (11.A65), (11.A71), $v_4'(\mathbf{x}-\mathbf{x}') \to -(|\mathbf{x}-\mathbf{x}'|)/8\pi + c$]. We may choose

$$\varepsilon = 8\pi^2\beta|c| \tag{15.15}$$

and modify the energy in (15.4) in such a way that the dual transform (15.2) involves the natural core energy

$$\exp\left\{-\frac{\varepsilon}{2}\left[\sum_{\mathbf{x}} \bar{\eta}_{ij}^2(\mathbf{x}) \frac{\nu}{1-\nu} \sum_{\mathbf{x}} \left(\sum_{\ell} \bar{\eta}_{\ell\ell}(\mathbf{x}-\boldsymbol{\ell})\right)^2\right]\right\}. \tag{15.16}$$

The removal of the natural core energy is to be accompanied by a change in the gradient terms of χ_{ij} in (15.9). Everything can be done in complete analogy with Sec. 12.4 of Part II.

15.3. DISORDER FIELD THEORY OF INTERACTING DEFECTS

After these preparatory steps, the derivation of the disorder field theory is straightforward. All we have to do is to transform the cosines into three sets pairs of complex fields u_i, α_i in the same way as we did in Chapter 13. The partition function (15.8) is rewritten as

$$\begin{aligned} Z_{\text{def}} \approx \prod_{\mathbf{x},i}\left[\int_{-\pi}^{\pi} \frac{d\gamma_i(\mathbf{x})}{2\pi}\right] \exp\left\{\frac{2}{\varepsilon}\operatorname{Re}\sum_{\mathbf{x},i<j} U_i^\dagger(\mathbf{x})\, U_j(\mathbf{x}+\mathbf{i})\right\} \\ \times \exp\left\{\frac{2}{\varepsilon}\operatorname{Re}\left[\sum_{\mathbf{x},i<j} U_i^\dagger(\mathbf{x})\, U_j(\mathbf{x}+\mathbf{i})\, U_i(\mathbf{x}+\mathbf{j})\, U_j^\dagger(\mathbf{x})\, e^{-2\pi i\chi_{ij}(\mathbf{x})}\right.\right. \\ \left.\left. + \sum_{\mathbf{x},i} U_i^\dagger(\mathbf{x})^2\, U^2(\mathbf{x}+\mathbf{i})\, e^{-2\pi i\chi_{ii}(\mathbf{x})}\right]\right\}, \end{aligned} \tag{15.17}$$

where

$$U_i(\mathbf{x}) \equiv e^{i\gamma_i(\mathbf{x})} \tag{15.18}$$

are pure phase variables. These are replaced by pairs of complex fields $u_i(\mathbf{x})$ and $\alpha_i(\mathbf{x})$ in the well-known way [see Eq. (13.25)].

Notice that the products

$$U_j(\mathbf{x}+\mathbf{i})\, U_i(\mathbf{x}+\mathbf{j})\, e^{-2\pi i \chi_{ij}(\mathbf{x})} \tag{15.19}$$

transform under stress gauge transformations (15.11) just as $U_j(\mathbf{x})$ themselves:

$$U_j(\mathbf{x})\, U_i(\mathbf{x}) \to e^{2\pi i(\Lambda_j(\mathbf{x})+\Lambda_i(\mathbf{x}))}\, U_j(\mathbf{x})\, U_i(\mathbf{x}). \tag{15.20}$$

Indeed

$$\begin{aligned} &U_j(\mathbf{x}+i)\, U_i(\mathbf{x}+\mathbf{j}) \exp\{-2\pi i \chi_{ij}(\mathbf{x})\} \to U_j(\mathbf{x}+\mathbf{i})\, U_i(\mathbf{x}+\mathbf{j}) \\ &\quad \times \exp\{2\pi i[\Lambda_j(\mathbf{x}+\mathbf{i}) + \Lambda_i(\mathbf{x}+\mathbf{j})] - 2\pi i[\chi_{ij}(\mathbf{x}) + \nabla_i \Lambda_j + \nabla_j \Lambda_i]\} \\ &\quad = U_j(\mathbf{x}+\mathbf{i})\, U_i(\mathbf{x}+\mathbf{j}) \exp\{-2\pi i \chi_{ij}(\mathbf{x})\} \exp\{2\pi i(\Lambda_j(\mathbf{x}) + \Lambda_i(\mathbf{x})\}\,. \end{aligned}$$

In contrast with the disorder theory of vortex lines in Part I, the symmetry of $\chi_{ij}(\mathbf{x})$ makes it impossible to rewrite (15.19) in terms of a covariant derivative of single $U_i(\mathbf{x})$'s [recall Eq. (12.10) of Part II].

The stress gauge invariant field theory involving $u_i(\mathbf{x})$, $\alpha_i(\mathbf{x})$, $\chi_{ij}(\mathbf{x})$ has a structure which is markedly different from the theory of dislocation lines studied in Chapter 8 in analogy with the theory of vortex lines. It does contain three pairs of complex fields u_i, α_i to describe the defects associated with the three spatial directions. In contrast to the vortex case, however, the β dependent terms appear with the *fourth* power in the disorder fields u_i. The quadratic powers in u and α remain stable at *all* temperatures. This is the crucial difference between defect and vortex disorder. The phase transition is caused by making β small, i.e., ε small. This produces a large negative *quartic* term in the energy. The u_i, α_i fields destabilize and acquire non-vanishing expectation values as a signal of the condensation of crystalline defects. Since these describe what happens to the total defect tensor, they comprise both dislocations and disclinations.

We observed previously in Chapter 13 that if a phase transition is

caused by the temperature variation of the quartic term at fixed stable quartic terms, the phase transition is always of first order. No subtle Coleman-Weinberg mechanism is required to generate a first order transition from stress fluctuations. The interplay of dislocations and disclinations is sufficient to generate a discontinuity in the phase transition. This is the lesson we can learn from the lattice model of defect melting and its disorder field theory.

CHAPTER SIXTEEN

GENERAL ANALYSIS OF DEFECTS ON THE LATTICE

In Chapter 15 we constructed a model of defect melting which, after a duality transformation, yielded a partition function with a sum over symmetric discrete defect tensors $\bar{\eta}_{ij}$ satisfying the conservation law $\bar{\nabla}_i \bar{\eta}_{ij} = 0$. The diagonal parts of $\bar{\eta}_{ij}$ were integer, the off-diagonal parts half-integer. Such a sum contained only three independent sets of integer numbers which were not able to distinguish the full variety of all possible defect lines. So the question arises as to how we have to modify the model so that all defect lines appear explicitly in the partition function. In order to work towards an answer to this question let us first try and reformulate the continuous decomposition of the defect tensor according to dislocations and disclinations in such a way that it can be used on a lattice.

16.1. DEFECT DENSITIES ON A LATTICE

In analogy with the differential definitions (2.42) we define dislocation and disclination densities on the lattice as follows:

$$\bar{\alpha}_{ij}(\mathbf{x}) \equiv \varepsilon_{ik\ell} \nabla_k \nabla_\ell u_j(\mathbf{x} + \mathbf{i}), \qquad \bar{\Theta}_{ij}(\mathbf{x}) \equiv \varepsilon_{ik\ell} \nabla_k \nabla_\ell \omega_j(\mathbf{x} + \mathbf{i}), \qquad (16.1)$$

where we have introduced the rotation field

$$\omega_i(\mathbf{x}) \equiv \tfrac{1}{2}\varepsilon_{ijk}\omega_{jk}(\mathbf{x}) \equiv \tfrac{1}{2}\varepsilon_{ijk}\nabla_j u_k(\mathbf{x}). \tag{16.2}$$

From the definition of $\bar{\Theta}_{ij}(\mathbf{x})$ we find directly the conservation law for disclinations on the lattice,

$$\bar{\nabla}_i \bar{\Theta}_{ij}(\mathbf{x}) = 0. \tag{16.3}$$

In order to derive the lattice analogue of the conservation law for dislocations we write

$$\begin{aligned}\bar{\alpha}_{in}(\mathbf{x}) &= \tfrac{1}{2}\varepsilon_{ik\ell}\nabla_k(\nabla_\ell u_n(\mathbf{x}+\mathbf{i}) + \nabla_n u_\ell(\mathbf{x}+\mathbf{i})) + \tfrac{1}{2}\varepsilon_{ik\ell}\nabla_k(\nabla_\ell u_n(\mathbf{x}+\mathbf{i}) \\ &\quad - \nabla_n u_\ell(\mathbf{x}+\mathbf{i})) \\ &= \varepsilon_{ik\ell}\nabla_k u_{\ell n}(\mathbf{x}+\mathbf{i}) + \varepsilon_{ik\ell}\nabla_k \omega_{\ell n}(\mathbf{x}+\mathbf{i}) \\ &= \varepsilon_{ik\ell}\nabla_k u_{\ell n}(\mathbf{x}+\mathbf{i}) + \delta_{in}\nabla_r \omega_r(\mathbf{x}+\mathbf{i}) - \nabla_n \omega_i(\mathbf{x}+\mathbf{i})\end{aligned} \tag{16.4}$$

and arrive at the conservation law

$$\begin{aligned}\bar{\nabla}_i \bar{\alpha}_{in}(\mathbf{x}) &= \nabla_i \bar{\alpha}_{in}(\mathbf{x}-\mathbf{i}) = \nabla_n \nabla_j \omega_j(\mathbf{x}) - \nabla_j \nabla_n \omega_j(\mathbf{x}) \\ &= -\varepsilon_{ijn}\varepsilon_{ik\ell}\nabla_k \nabla_\ell \omega_j(\mathbf{x}) = -\varepsilon_{ijn}\bar{\Theta}_{ij}(\mathbf{x}-\mathbf{i}).\end{aligned} \tag{16.5}$$

Furthermore, from (16.1) we see that

$$\alpha_{ii}(\mathbf{x}-\mathbf{i}) = \varepsilon_{ik\ell}\nabla_k \nabla_\ell u_i(\mathbf{x}) = 2\nabla_k \omega_k(\mathbf{x}), \tag{16.6}$$

implying that (16.3) can be rewritten as

$$\varepsilon_{ik\ell}\nabla_k u_{\ell n}(\mathbf{x}+\mathbf{i}) = \nabla_n \omega_i(\mathbf{x}+\mathbf{i}) + \alpha_{in}(\mathbf{x}) - \tfrac{1}{2}\delta_{in}\alpha_{rr}(\mathbf{x}-\mathbf{r}+\mathbf{i}).$$

Shifting the argument by $\mathbf{j}$ and applying the lattice curl $\varepsilon_{jmn}\nabla_m$ this becomes

$$\bar{\eta}_{ij}(\mathbf{x}) = \bar{\Theta}_{ji}(\mathbf{x}+\mathbf{j}) + \varepsilon_{jmn}\nabla_m[\bar{\alpha}_{in}(\mathbf{x}+\mathbf{j}) - \tfrac{1}{2}\delta_{in}\bar{\alpha}_{rr}(\mathbf{x}-\mathbf{r}+\mathbf{i}+\mathbf{j})], \tag{16.7}$$

where $\bar{\eta}_{ij}(\mathbf{x})$ is the defect tensor on the lattice,

$$\bar{\eta}_{ij}(\mathbf{x}) \equiv \varepsilon_{ik\ell}\varepsilon_{jmn}\nabla_k \nabla_m u_{\ell n}(\mathbf{x}+\mathbf{i}+\mathbf{j}). \tag{16.8}$$

Hence we may define Nye's contortion on the lattice by

$$\bar{K}_{in}(\mathbf{x}) \equiv -\bar{\alpha}_{in} + \tfrac{1}{2}\delta_{ij}\bar{\alpha}_{rr}(\mathbf{x} - \mathbf{r} + \mathbf{i}) \tag{16.9}$$

and write

$$\bar{\eta}_{ij}(\mathbf{x}) = \bar{\Theta}_{ji}(\mathbf{x} + \mathbf{j}) - \varepsilon_{jmn}\nabla_m \bar{K}_{in}(\mathbf{x} + \mathbf{j}), \tag{16.10}$$

which is the desired lattice analogue of the decomposition (2.80a).

It is also straightforward to derive the other form (2.80b) of this decomposition. For this we take the expression and apply the identity

$$\varepsilon_{jmn}\delta_{iq} - \tfrac{1}{2}\varepsilon_{ijm}\delta_{nq} = -\tfrac{1}{2}(\varepsilon_{min}\delta_{jq} + \varepsilon_{mjn}\delta_{iq}). \tag{16.11}$$

This gives

$$\begin{aligned}
&-\varepsilon_{jmn}\nabla_m \bar{K}_{in}(\mathbf{x} + \mathbf{j}) \\
&\quad = \varepsilon_{jmn}\nabla_m(\bar{\alpha}_{in}(\mathbf{x} + \mathbf{j}) - \tfrac{1}{2}\delta_{in}\bar{\alpha}_{rr}(\mathbf{x} - \mathbf{r} + \mathbf{i} + \mathbf{j})) \\
&\quad = -\tfrac{1}{2}\nabla_m(\varepsilon_{min}\bar{\alpha}_{jn}(\mathbf{x} + \mathbf{i}) + \varepsilon_{mjn}\bar{\alpha}_{in}(\mathbf{x} + \mathbf{i}) - \varepsilon_{jin}\bar{\alpha}_{mn}(\mathbf{x} - \mathbf{m} + \mathbf{i} + \mathbf{j}))
\end{aligned}$$

so that we obtain indeed the lattice version of (2.80b):

$$\begin{aligned}
\bar{\eta}_{ij}(\mathbf{x}) = \bar{\Theta}_{ji}(\mathbf{x} + \mathbf{i}) &- \tfrac{1}{2}\nabla_m(\varepsilon_{min}\bar{\alpha}_{jn}(\mathbf{x} + \mathbf{i}) + (ij)) \\
&+ \tfrac{1}{2}\varepsilon_{ijn}\nabla_m \bar{\alpha}_{mn}(\mathbf{x} - \mathbf{m} + \mathbf{i} + \mathbf{j}).
\end{aligned} \tag{16.12}$$

The conservation law (16.4) can be used to rewrite the last term as

$$\begin{aligned}
\varepsilon_{jin}\nabla_m \bar{\alpha}_{mn}(\mathbf{x} - \mathbf{m} + \mathbf{i} + \mathbf{j}) &= \varepsilon_{jin}\bar{\nabla}_m \alpha_{mk}(\mathbf{x} + \mathbf{i} + \mathbf{j}) \\
&= -\varepsilon_{jik}\varepsilon_{\ell nk}\nabla_k \bar{\Theta}_{\ell n}(\mathbf{x} - \boldsymbol{\ell} + \mathbf{i} + \mathbf{j}) \\
&= -\bar{\Theta}_{ji}(\mathbf{x} + \mathbf{i}) + \bar{\Theta}_{ij}(\mathbf{x} + \mathbf{j}).
\end{aligned}$$

Inserting this into (16.12) gives

$$\bar{\eta}_{ij}(\mathbf{x}) = \tfrac{1}{2}(\bar{\Theta}_{ji}(\mathbf{x} + \mathbf{i}) + (ij)) - \tfrac{1}{2}\nabla_m(\varepsilon_{min}\bar{\alpha}_{jn}(\mathbf{x} + \mathbf{i}) + (ij)), \tag{16.13}$$

which exhibits correctly the symmetry of the defect tensor.

Forming the lattice derivative $\bar{\nabla}_i \bar{\eta}_{ij}$ and using the conservation laws of dislocations and disclinations

$$\bar{\nabla}_i \bar{\alpha}_{in}(\mathbf{x}+\mathbf{j}) = -\varepsilon_{npq}\bar{\Theta}_{pq}(\mathbf{x}-\mathbf{p}+\mathbf{j}), \qquad \bar{\nabla}_i \bar{\Theta}_{ij}(\mathbf{x}+\mathbf{j}) = 0,$$

we can verify that the defect tensor is also properly conserved:

$$\begin{aligned}\bar{\nabla}_i \bar{\eta}_{ij}(\mathbf{x}) &= \tfrac{1}{2}\bar{\nabla}_i \bar{\Theta}_{ji}(\mathbf{x}+\mathbf{i}) + \tfrac{1}{2}\nabla_m \varepsilon_{mjn}\varepsilon_{npq}\bar{\Theta}_{pq}(\mathbf{x}-\mathbf{p}+\mathbf{j}) \\ &= \tfrac{1}{2}\nabla_i \bar{\Theta}_{ji}(\mathbf{x}) + \tfrac{1}{2}\nabla_p \bar{\Theta}_{pq}(\mathbf{x}-\mathbf{p}+\mathbf{j}) - \tfrac{1}{2}\nabla_q \bar{\Theta}_{jq}(\mathbf{x}) = 0.\end{aligned}$$

16.2. INTERDEPENDENCE OF DISLOCATIONS AND DISCLINATIONS

We now observe that for a given $\bar{\eta}_{ij}(\mathbf{x})$, the decomposition into dislocation and disclination densities is by no means unique. One possible trivial decomposition is

$$\bar{\alpha}_{ij}(\mathbf{x}) = 0, \qquad \bar{\Theta}_{ij}(\mathbf{x}) \equiv \bar{\eta}_{ij}(\mathbf{x}), \tag{16.14}$$

in which there are no dislocations but only a certain set of disclinations constrained so that $\bar{\Theta}_{ij}(\mathbf{x})$ is symmetric. Another possibility is

$$\begin{aligned}&\bar{\Theta}_{ij}(\mathbf{x}) = 0, \\ &\bar{\alpha}_{i\ell}(\mathbf{x}) = -\varepsilon_{\ell 3m}\sum_{x_3'=-\infty}^{x_3-1}\bar{\eta}_{mi}(\mathbf{x}'-\mathbf{m})\big|_{x_1'=x_1,\,x_2'=x_2}.\end{aligned} \tag{16.15}$$

The sum can also be written as

$$\bar{\alpha}_{i\ell}(\mathbf{x}) = -\varepsilon_{\ell 3m}\frac{1}{\nabla_3}\bar{\eta}_{mi}(\mathbf{x}-\mathbf{m}). \tag{16.16}$$

Instead of picking the z-direction for the sum we can use any direction $\mathbf{n} = \hat{\mathbf{x}}$, $\hat{\mathbf{y}}$, or $\hat{\mathbf{z}}$ and write

$$\bar{\alpha}_{i\ell}(\mathbf{x}) = -\varepsilon_{\ell km}\frac{1}{\mathbf{n}\cdot\nabla}n_k\bar{\eta}_{mi}(\mathbf{x}-\mathbf{m}). \tag{16.17}$$

By reinserting this expression into (16.13) we recover $\bar{\eta}_{ij}(\mathbf{x})$.

The operation (16.15) has a simple geometric meaning. Whenever there is a value $\bar{\eta}_{ni}(\mathbf{x}) \neq 0$ it may be viewed as a string of dislocations stretching from $\mathbf{x}$ along the positive z-axis to infinity.

The non-uniqueness of the decomposition of the defect-tensor is a manifestation of the interdependence of dislocations and disclinations which was discussed in general in Chapter 2 (and ignored in Chapter 8). It was also of importance in Section 14.11.

Whatever decomposition we choose, our model of defects and stresses involving only a sum over $\bar{\eta}_{ij}(\mathbf{x})$ contains only a *subset* of either dislocations or disclinations. In a real crystal, on the other hand, all configurations of dislocations and disclinations are possible and their elastic energies determine the probability of each configuration.

For a dislocation, each of the circuit integrals

$$\oint du_j(\mathbf{x}) = b_j \tag{16.18}$$

can be an arbitrary multiple of the basis vectors. This means that each of the displacement vectors $u_j(\mathbf{x})$ can have its own independent jumps across the links $\mathbf{j} = \hat{\mathbf{x}}$, $\hat{\mathbf{y}}$, and $\hat{\mathbf{z}}$. The energy must therefore contain jumping numbers $n_{ij}(\mathbf{x})$ corresponding to all lattice gradients $\nabla_i u_j(\mathbf{x})$. The model, up to now, was restricted to only symmetric matrices $n_{ij}(\mathbf{x})$. This restriction was a consequence of the fact that the elastic energy involves only the symmetric combination of gradients, i.e., the strain

$$u_{ij} = \tfrac{1}{2}(\nabla_i u_j + \nabla_j u_i). \tag{16.19}$$

In order to include the antisymmetric part of $n_{ij}(\mathbf{x})$, the elastic energy has to contain also the antisymmetric part of the gradients,

$$\omega_{ij} = \tfrac{1}{2}(\nabla_i u_j - \nabla_j u_i). \tag{16.20}$$

In the classical theory of elasticity this is not the case. The reason lies in the extreme long-wavelength approximation of that theory. Only first gradients of the displacement field $u_i(\mathbf{x})$ are considered. At that level the rotation field, which is itself a first-gradient field, is a constant and does not vary throughout the crystal. It corresponds to a global rotation of the entire crystal. It follows from rotational invariance that the energy is independent of $\omega_i(\mathbf{x})$.

When describing the situation in this way it becomes obvious that the absence of $\omega_i(\mathbf{x})$ is not an intrinsic property of the system but a consequence of the first-gradient approximation. This approximation is sufficiently accurate for most classical problems which involve only the long-range aspects of elasticity. Questions concerning disclinations,

however, are of a more microscopic nature and involve directly the rotation field $\omega_i(\mathbf{x})$. They cannot be answered within this approximation. This suggests a rather obvious way of extending the defect model of melting. The elastic energy must be made sensitive to variations of $\omega_i(\mathbf{x})$ in the crystal. Thus it must depend, at least, on $\partial_i \omega_j(\mathbf{x})$ which means that second gradients of the displacement field are present. Due to the absence of $\omega_i(\mathbf{x})$ in the classical theory of elasticity, the elastic energy depends entirely on the symmetric combination of gradients, the strain tensor $(\partial_i u_j + \partial_j u_i)/2$. This tensor can be calculated uniquely if the symmetric defect tensor $\eta_{ij}(\mathbf{x})$ vanishes. We had seen previously in Eqs. (2.105) that the distortion fields $\partial_i u_j(\mathbf{x})$ themselves cannot be determined knowing only that $\eta_{ij}(\mathbf{x}) = 0$ (besides boundary conditions). Their determination would require the additional knowledge of the vanishing of the rotational defects, $\Theta_{ij}(\mathbf{x}) = 0$. Only then can we reconstruct the field $\omega_{ij}(\mathbf{x}) = (1/2)(\partial_i u_j(\mathbf{x}) - \partial_j u_i(\mathbf{x}))$ which can be combined with $u_{ij}(\mathbf{x})$ to find $\partial_i u_j(\mathbf{x})$. The independence of $\omega_i(\mathbf{x})$ makes the classical elastic energy highly degenerate with respect to variations of the defect configurations. The degeneracy is described quantitatively via the decomposition (2.80) of the defect tensor. The tensor $\eta_{ij}(\mathbf{x})$ which uniquely determines the elastic energy consists only of three sets of independent integer of half-integer numbers. In contrast, the disclination tensor $\Theta_{ij}(\mathbf{x})$ has six independent elements and the dislocation tensor $\alpha_{ij}(\mathbf{x})$ another six. Of these twelve degrees of freedom, only three differ by their classical elastic energy. Our model of defect melting identifies all degenerate defect configurations and distinguishes only the three equivalence classes of defects which are characterized by different elastic energy densities. As far as the thermodynamic behavior of all defects is concerned, this identification is of no consequence since inclusion of the degenerate degrees of freedom in the partition function would merely result in a trivial, temperature independent, overall factor (albeit an infinite one). The situation is very similar to that encountered previously in gauge theories. Also there we were confronted with a degeneracy field configuration which were those differing by a gauge transformation. Had we performed the path integral naively, this would have resulted in an infinite overall factor. The overall factor was removed by a gauge-fixing condition. In the same sense we may view the present system as a model of dislocations and disclinations but with a "gauge-fixing condition" imposed so as to remove the energetically degenerate defect configurations, namely, those with different $\Theta_{ij}(\mathbf{x})$, $\alpha_{ij}(\mathbf{x})$ but equal $\eta_{ij}(\mathbf{x})$.

16.3. DEGENERATE DEFECT CONFIGURATIONS IN LINEAR ELASTICITY

Let us analyze the structure of these degenerate defect configurations in more detail. For simplicity, we shall work in the continuum limit. Then we can apply the helicity decomposition which simplifies the counting of the different components. First we rewrite the decomposition of the defect tensor,

$$\eta_{\ell n}(\mathbf{x}) = \Theta_{\ell n}(\mathbf{x}) + \tfrac{1}{2}(\partial_k \varepsilon_{\ell ki} \alpha_{ni}(\mathbf{x}) + (\ell n)) + \tfrac{1}{2}\varepsilon_{\ell ni}\partial_m \alpha_{mi}(\mathbf{x}), \tag{16.21}$$

in helicity form. Due to the conservation law $\partial_\ell \Theta_{\ell n}(\mathbf{x}) = 0$, the tensor $\Theta_{\ell n}(\mathbf{x})$ contains only the six components $\Theta^{(2,\pm 2)}$, Θ^{L}, $\Theta^{+\pm} \equiv (\Theta^{(2,\pm 1)} + \Theta^{(1,\pm 1)})/\sqrt{2}$ and $\Theta^{(1,0)}$ (as was the case with the divergenceless matrices $\alpha_{\ell n}(\mathbf{x})$ in Chapter 4). As for the eliminated 3 components $\Theta^{L'}$, $\Theta^{-\pm} \equiv (\Theta^{(2,\pm 1)} - \Theta^{(1,\pm 1)})/\sqrt{2}$, they correspond to the pure gauge components in Eq. (4.117).

The $\alpha_{\ell i}(\mathbf{x})$ tensor has 9 components. The last term in (16.21) is antisymmetric in ℓ, n and thus must be of unit spin (spins 2 and 0 have symmetric tensors). Since ∂_m is contracted with the first index of α_{mi}, it contains precisely those helicity components which are eliminated by a condition $\partial_m \alpha_{mi} = 0$, namely, $\alpha^{L'}$, $\alpha^{-\pm} \equiv (\alpha^{(2,\pm 1)} - \alpha^{(1,\pm 1)})/\sqrt{2}$. Hence we need to consider only these three components and we find in momentum space [recall Eqs. (4.62) and (4.57)–(4.62)]:

$$\frac{i}{2}\varepsilon_{\ell ni} p_m [e^{L'}_{mi}\alpha^{L'} + e^{-+}_{mi}\alpha^{-+} + e^{--}_{mi}\alpha^{--}] = \frac{i}{2} p\, \varepsilon_{\ell ni}[\hat{p}_i \alpha^{L'} + e_i \alpha^{-+} - e^*_i \alpha^{--}]$$

$$= \frac{1}{\sqrt{2}} p [e^{(1,0)}_{\ell n}\alpha^{L'} + e^{(1,1)}_{\ell m}\alpha^{-+} - e^{(1,-1)}_{\ell m}\alpha^{--}]. \tag{16.22}$$

The two other α terms are brought to helicity form by using the general formula (4.110), but taking care that the indices n and i appear in the opposite order so that $\alpha^{(1,\pm 1)}$ appears with the opposite sign. Symmetrizing in the indices ℓ and n removes the spin-1 polarization tensors and we have

$$\frac{1}{2}(\varepsilon_{\ell ki}\partial_k \alpha_{ni} + (\ell \leftrightarrow n)) = p\left\{ e^{(2,2)}_{\ell n}\alpha^{(2,2)} - e^{(2,-2)}_{\ell n}\alpha^{(2,-2)} - e^{L}_{\ell n}\alpha^{(1,0)} + \frac{1}{\sqrt{2}}e^{(2,1)}\alpha^{-+} - \frac{1}{\sqrt{2}}e^{(2,-1)}\alpha^{--}\right\}. \tag{16.23}$$

Inserting this and (16.22) into (16.21), the helicity components of the defect tensor decompose as follows:[a]

$$\eta^{(2,\pm 2)} = \Theta^{(2,\pm 2)} \pm p\,\alpha^{(2,\pm 2)}, \tag{16.24}$$

$$\eta^{L} = \Theta^{L} - p\,\alpha^{(1,0)}. \tag{16.25}$$

Remembering now that $\Theta^{-\pm} = 0$ (due to $\partial_i \Theta_{ij} = 0$) we see that the antisymmetric parts on the right-hand side cancel, i.e.,

$$\Theta^{+\pm} \pm p\,\alpha^{-\pm} = 0, \tag{16.26}$$

$$\Theta^{(1,0)} + p\,\alpha^{L'}/\sqrt{2} = 0. \tag{16.27}$$

These three relations are, of course, just the helicity version of the conservation law for dislocation densities, $\partial_m \alpha_{mi} = -\varepsilon_{ik\ell}\Theta_{k\ell}$. The components L, $((2, \pm 1) + (1, \pm 1))/\sqrt{2}$ of $\alpha_{\ell i}$ are absent, in agreement with their decoupling from the stress field observed in Eq. (4.127).

Equation (16.24)–(16.27) show clearly which changes can be made on the defect configuration without changing the stress field of linear elasticity:

$$\begin{aligned}
\alpha^{(2,\pm 2)} &\to \alpha^{(2,\pm 2)} + \Lambda^{(2,\pm 2)}, & \Theta^{(2,\pm 2)} &\to \Theta^{(2,\pm 2)} \mp |\mathbf{p}|\Lambda^{(2,\pm 2)},\\
\alpha^{(1,0)} &\to \alpha^{(1,0)} + \Lambda^{(1,0)}, & \Theta^{L} &\to \Theta^{L} + |\mathbf{p}|\Lambda^{(1,0)},\\
\alpha^{-\pm} &\to \alpha^{-\pm} + \Lambda^{\pm 1}, & \Theta^{+\pm} &\to \Theta^{+\pm} \mp |\mathbf{p}|\Lambda^{\pm 1},\\
\alpha^{L'} &\to \alpha^{L'} + \Lambda^{L'}, & \Theta^{(1,0)} &\to \Theta^{(1,0)} - |\mathbf{p}|\Lambda^{L'}/\sqrt{2}.
\end{aligned} \tag{16.28a}$$

In addition there are the changes of the three components α^{L}, $(\alpha^{(2,\pm 1)} + \alpha^{(1,\pm 1)})/\sqrt{2}$ of $\alpha_{\ell i}$ which do not appear in η_{ij} at all:

$$\alpha^{L} \to \alpha^{L} + \Lambda^{L}, \qquad \alpha^{+\pm} \to \alpha^{+\pm} + \Lambda^{\pm}. \tag{16.28b}$$

[a]The sign changes in the α parts are a reflection of the opposite parity of α and Θ.

These 9 transformations among degenerate defect configurations may be considered as a kind of gauge invariance associated with the linear long wavelength approximation of classical elasticity. Our model was based on this approximation. Thus, if we would have tried to include all defect configurations, we would have obtained a sixfold infinite temperature independent overall factor. By summing over only the three independent components of the defect tensor $\eta_{ij}(\mathbf{x})$, this factor did not appear.

In a physical crystal we expect the above described degeneracy to be removed by crystalline forces. If we want to find out how this happens we have to go beyond the classical theory of elasticity. There are two ways by which this theory may be extended.

1. If the length scale over which the displacement field varies is large compared with the atomic distances, but no longer extremely large, then higher derivative terms of the displacement field $u_i(\mathbf{x})$ have to be considered.

2. If any of the gradients of $\partial_i u_j$, $\partial_{i_1}\partial_{i_2}u_j$, ... becomes large, higher powers of the gradients, have to be considered, i.e., $(\partial u)^3$, $(\partial\partial u)^3$, ...

If we want to understand the elastic properties of realistic crystalline defects, then both extensions are necessary. In the neighbourhood of a defect, both the length scale over which the displacement varies as well as the size of the gradients become large. Thus we need terms of these two kinds in the elastic energy. The second kind is nonlinear and hard to handle. At best it can be treated perturbatively. The consequences of the first kind, on the other hand, are straightforward to evaluate, due to the linearity in the displacement field. They will be discussed in Chapter 17.

16.4. EXTENDING THE DEFECT SUM TO THE LATTICE

For the purpose of extending the defect sum, we have to find a proper lattice representation of all defect configurations. We recall the general continuum procedure of describing the plastic deformation associated with a general line-like defect as given in Section 2.10. There we began with the trivial Volterra operation of taking a volume piece of the crystal and shifting and rotating it by a lattice vector and a symmetry angle, respectively,

$$u_i(\mathbf{x}) = -\delta(V)(b_i + \varepsilon_{iqr}\Omega_q x_r). \tag{16.29}$$

By differentiation we found from this,

$$\tfrac{1}{2}(\partial_i u_\ell(\mathbf{x}) + \partial_\ell u_i(\mathbf{x})) = \tfrac{1}{2}[\delta_i(S)(b_\ell + \varepsilon_{\ell qr}\Omega_q x_r) + (i\ell)]$$
$$= \tfrac{1}{2}(\beta^p_{i\ell}(\mathbf{x}) + \beta^p_{\ell i}(\mathbf{x})), \tag{16.30}$$

$$\partial_n \omega_j(\mathbf{x}) = \tfrac{1}{2}\varepsilon_{jk\ell}\,\partial_n \beta^p_{k\ell}(\mathbf{x}) + \phi^p_{nj}(\mathbf{x}), \tag{16.31}$$

where

$$\beta^p_{i\ell}(\mathbf{x}) = \delta_i(S)(b_\ell + \varepsilon_{\ell qr}\Omega_q x_r), \qquad \phi^p_{i\ell}(\mathbf{x}) = \delta_i(S)\Omega_\ell \tag{16.32}$$

were the plastic distortions and rotations of the crystal. From these we obtained the defect densities [recall (2.68), (2.69)]

$$\bar{\alpha}_{i\ell}(\mathbf{x}) = \varepsilon_{ijk}\partial_j \beta^p_{k\ell} + \varepsilon_{i\ell}\phi^p_{kk} - \phi^p_{\ell i} = \varepsilon_{ijk}\partial_j \delta_k(S)(b_\ell + \varepsilon_{\ell qr}\Omega_q x_r)$$
$$= \delta_i(L)(b_\ell + \varepsilon_{\ell qr}\Omega_q x_r), \tag{16.33}$$

$$\bar{\Theta}_{ip}(\mathbf{x}) = \varepsilon_{ijk}\partial_j \phi^p_{k\ell} = \varepsilon_{ijk}\partial_j \delta_k(S)\Omega_\ell = \delta_i(L)\Omega_\ell, \tag{16.34}$$

exhibiting the physical boundary line L via Stokes' theorem on the δ-function [see (18.17), Part II]

$$\varepsilon_{ijk}\partial_j \delta_k(S) = \delta_i(L). \tag{16.35}$$

An ensemble of lines which can be either dislocations or disclinations (or both) was given by

$$\beta^p_{i\ell}(\mathbf{x}) = \sum_\alpha \delta_i(S_\alpha) b_{\alpha\ell} + \sum_\beta \delta_i(S_\beta)\varepsilon_{\ell qr}\Omega_{\beta q} x_r,$$

$$\phi^p_{nj}(\mathbf{x}) = \sum_\beta \delta_i(S_\beta)\Omega_{\beta j}, \tag{16.36}$$

where α runs through the Volterra surfaces with different possible Burgers vectors and β through those with different Frank vectors of the crystal. It has the defect densities

$$\alpha_{i\ell}(\mathbf{x}) = \sum_\alpha \delta_i(L_\alpha) b_{\alpha\ell} + \sum_\beta \delta_i(L_\beta)\varepsilon_{\ell qr}\Omega_q \delta_r,$$

$$\Theta_{i\ell}(\mathbf{x}) = \sum_\beta \delta_i(L_\beta)\Omega_{\beta\ell}. \tag{16.37}$$

Let us now see how this differential structure can be generalized to a discrete simple cubic lattice. Then δ-functions over a volume are given by lattice functions $N(\mathbf{x})$ which can take values 0 and 1 on the different sites $\mathbf{x}$. It is therefore suggestive to simply replace the continuous expression (16.29) by

$$u_\ell(\mathbf{x}) = -N(\mathbf{x})(b_\ell + \varepsilon_{\ell qr}\Omega_q x_r). \tag{16.38}$$

The alert reader will immediately realize that this Ansatz, while representing the most straightforward generalization of the trivial Volterra operation in the continuum to a discrete form, is physically not the proper analogue. The Volterra operation in the continuum is an *infinitesimal* translation plus rotation of a crystalline piece. In a real lattice, this should become a discrete translation plus a discrete rotation by an angle of the crystal symmetry. In simple cubic crystal, the minimal symmetry angle is $\Omega = \pm\pi/2$. But then the discontinuity across the surface can no longer be calculated using the infinitesimal formula of a vector product $\varepsilon_{\ell qr}\Omega_q x_r$.

The operation (16.38) is therefore not really a translation plus a rotation. It does, however, represent an allowed change of atomic rest positions from where to count the displacements vectors as long as b_ℓ and Ω_q are integer numbers. The translation by $\varepsilon_{\ell qr}\Omega_q x_r$ may be viewed as the straight-line continuation of an infinitesimal rotation along the tangent direction. In this way it accounts for the basic properties of crystal disclinations without introducing the non-Abelian complexities of the finite rotation group. We shall call this approach the *tangential approximation* to disclinations.

Within this approximation it is possible to carry out all the previous differential analysis on discrete crystals. Forming the lattice derivatives of (16.38) and respecting the product rule

$$\begin{aligned}
\nabla_i A(\mathbf{x})B(\mathbf{x}) &= A(\mathbf{x}+\mathbf{i})B(\mathbf{x}+\mathbf{i}) - A(\mathbf{x})B(\mathbf{x}) \\
&= (A(\mathbf{x}+\mathbf{i}) - A(\mathbf{x}))B(\mathbf{x}+\mathbf{i}) + A(\mathbf{x})(B(\mathbf{x}+\mathbf{i}) - B(\mathbf{x})) \\
&= (\nabla_i A(\mathbf{x}))B(\mathbf{x}+\mathbf{i})) + A(\mathbf{x})\nabla_i B(\mathbf{x}) \\
&= (\bar{\nabla}_i A(\mathbf{x}+\mathbf{i}))B(\mathbf{x}+\mathbf{i}) + A(\mathbf{x})\nabla_i B(\mathbf{x}),
\end{aligned} \tag{16.39}$$

we find

$$\nabla_i u_\ell(\mathbf{x}) = -\nabla_i N(\mathbf{x})(b_\ell + \varepsilon_{\ell qr}\Omega_q(x_r + \delta_{ir})) - N(\mathbf{x})\varepsilon_{\ell qi}\Omega_q \tag{16.40}$$

and

$$(\nabla_i u_\ell(\mathbf{x}) + \nabla_\ell u_i(\mathbf{x}))/2 = -\nabla_i N(\mathbf{x})(b_\ell + \varepsilon_{\ell qr}\Omega_q(x_r + \delta_{ir})) + (\ell i). \tag{16.41}$$

The derivatives $n_i(\mathbf{x}) \equiv -\nabla_i N(\mathbf{x})$ describe the boundary surface of the volume elements $N(\mathbf{x})$. They are the lattice version of the δ-functions $\delta_k(S) = -\partial_k \delta(V)$ [see (18.20), Part II]

A proper lattice defect is now obtained by taking the surface to be open. Then the components $n_i(\mathbf{x})$ become independent. We therefore introduce the plastic distortion on the lattice as follows:

$$\beta^p_{i\ell}(\mathbf{x}) \equiv n_i(\mathbf{x})(b_\ell + \varepsilon_{\ell qr}\Omega_q(x_r + \delta_{ir})). \tag{16.42}$$

A similar treatment can be given to the rotation field which we *defined* in (16.2) as the lattice gradient version of the usual rotation field

$$\omega_i(\mathbf{x}) = \tfrac{1}{2}\varepsilon_{ijk}\nabla_j u_k(\mathbf{x}). \tag{16.43}$$

Inserting here the Volterra operation (16.38), we find the lattice gradient of $\omega_j(\mathbf{x})$,

$$\nabla_n \omega_j(\mathbf{x}) = \tfrac{1}{2}\varepsilon_{jk\ell}\nabla_n \beta^p_{k\ell}(\mathbf{x}) + \phi^p_{nj}(\mathbf{x}), \tag{16.44}$$

where

$$\phi^p_{ij}(\mathbf{x}) \equiv n_i(\mathbf{x})\Omega_j \tag{16.45}$$

is the lattice version of the plastic rotation [recall Eqs. (2.62)–(2.68)].

We now use the lattice definitions (16.1), (16.2) and calculate the defect densities,

$$\begin{aligned}\bar{\alpha}_{i\ell}(\mathbf{x}) &= \varepsilon_{ik\ell}\nabla_k \nabla_\ell u_j(\mathbf{x} + \mathbf{i}) \\ &= \varepsilon_{ik\ell}\nabla_k n_\ell(\mathbf{x} + \mathbf{i})(b_j + \varepsilon_{jqr}\Omega_q(\mathbf{x} + \boldsymbol{\ell} + \mathbf{i})_r),\end{aligned} \tag{16.46}$$

$$\bar{\Theta}_{i\ell}(\mathbf{x}) = \varepsilon_{ik\ell}\nabla_k \nabla_\ell \omega_j(\mathbf{x} + \mathbf{i}) = \varepsilon_{ik\ell}\nabla_k n_\ell(\mathbf{x} + \mathbf{i})\Omega_\ell. \tag{16.47}$$

Defect lines are introduced by using Stokes' theorem on the lattice according to which the divergenceless vectors

$$\ell_i(\mathbf{x}) = \varepsilon_{ik\ell}\nabla_k n_\ell(\mathbf{x} + \mathbf{i}) \tag{16.48}$$

form the closed boundary lines of the surfaces described by $n_i(\mathbf{x})$. This was shown in Part II in connection with Eq. (8.3). Thus $\ell_i(\mathbf{x})$ represents the lattice analogue of the δ-function $\delta_i(L) = \varepsilon_{ik\ell}\partial_k \delta_\ell(S)$ and the defect densities become

$$\bar{\alpha}_{i\ell}(\mathbf{x}) = \ell_i(\mathbf{x})(b_j + \varepsilon_{jqr}\Omega_q(x_r + \delta_{\ell r} + \delta_{ir})), \tag{16.49}$$

$$\Theta_{i\ell}(\mathbf{x}) = \ell_i(\mathbf{x})\Omega_\ell. \tag{16.50}$$

For an ensemble of lines which can be either dislocations or disclinations, or both, the plastic fields are

$$\beta^p_{i\ell}(\mathbf{x}) = \sum_\alpha n_{\alpha i}(\mathbf{x}) b_{\alpha\ell} + \sum_\beta m_{\beta i}(\mathbf{x})\varepsilon_{\ell qr}\Omega_{\beta q}(x_r + \delta_{ir}), \tag{16.51}$$

$$\phi^p_{i\ell}(\mathbf{x}) = \sum_\beta m_{\beta i}(\mathbf{x})\Omega_{\beta\ell}, \tag{16.52}$$

where the sum over α and β covers all Burgers and Frank vectors, respectively, and $n_{\alpha i}(\mathbf{x})$, $m_{\beta i}(\mathbf{x}) = 0, 1$ describe the Volterra surfaces associated with these.

We now make use of the fact that the Burgers and Frank vectors occur in all integer multiples of three fundamental vectors. These integers can be absorbed into the numbers $n_{\alpha i}(\mathbf{x})$, $m_{\beta i}(\mathbf{x})$ which are then no longer restricted to 0, 1 but cover *all* integers $0, \pm 1, \pm 2, \ldots$

The defect densities associated with these plastic fields are

$$\bar{\alpha}_{i\ell}(\mathbf{x}) = \sum_\alpha \ell^\alpha_i(\mathbf{x}) b_{\alpha\ell} + \sum_\beta \ell^\beta_i(\mathbf{x})\varepsilon_{\ell qr}\Omega_{\beta q}(x_r + \delta_{\ell r} + \delta_{ir}),$$

$$\bar{\Theta}_{i\ell}(\mathbf{x}) = \sum_\beta \ell^\beta_i(\mathbf{x})\Omega_{\beta\ell}. \tag{16.53}$$

Since ℓ^α_i, ℓ^β_i are divergenceless, these densities satisfy the proper conservation laws on the lattice,

$$\bar{\nabla}_i\bar{\Theta}_{i\ell}(\mathbf{x}) = 0,$$

$$\bar{\nabla}_i\bar{\alpha}_{i\ell}(\mathbf{x}) = \nabla_i\bar{\alpha}_{i\ell}(\mathbf{x} - \mathbf{i}) = -\varepsilon_{\ell pq}\bar{\Theta}_{pq}(\mathbf{x} - \mathbf{p}), \tag{16.54}$$

as they should.

We shall use these results and construct an extended model, in which the full sum over all defect configurations appears explicitly with distinct contributions. Before we can do this we must first extend the classical theory of linear elasticity to higher gradients which will be the subject of Chapter 17.

16.5. TWO-DIMENSIONAL CONSIDERATIONS

It is useful to look at the same question in two dimensions where the situation is much simpler. There the total defect tensor as well as the disclination density reduce to one independent integer-valued component each, $\bar{\eta}_{33}(\mathbf{x}) = \bar{\eta}(\mathbf{x})$, $\bar{\Theta}_{33}(\mathbf{x}) = \bar{\Theta}(\mathbf{x})$. The dislocation density becomes an integer-valued vector field $\bar{\alpha}_i(\mathbf{x})$ (recall Section 2.13). For a single dislocation at $\mathbf{x}$, $\bar{\alpha}_i(\mathbf{x})$ has the form $b_i\delta^{(2)}(\mathbf{x})$ where b_i is the Burgers vector. Thus, a distribution of dislocations $\bar{\alpha}_i(\mathbf{x})$ may be pictured directly as a "gas of Burgers vectors" with integer components $b_i(\mathbf{x}) = \bar{\alpha}_i(\mathbf{x})$. The defect density can be written on the lattice as [compare (2.94)]

$$\bar{\eta}(\mathbf{x}) = \bar{\Theta}(\mathbf{x}) + \varepsilon_{ij}\bar{\nabla}_i b_j(\mathbf{x}). \tag{16.55}$$

The coupling to the stress "gauge" field is

$$\int d^2x\, \chi(\mathbf{x})\,\bar{\eta}(\mathbf{x}) = \int d^2x\,(\chi(\mathbf{x})\,\bar{\Theta}(\mathbf{x}) + \varepsilon_{ij}\nabla_i\chi(\mathbf{x})\,b_j(\mathbf{x})) \tag{16.56}$$

and we recognize the lattice version of the field used in Section 5.3, $A^i = \varepsilon_{ij}\partial_j\chi$ [recall (5.44)], which couples locally to dislocations.

Among the three sets of integer numbers $\bar{\Theta}(\mathbf{x})$, $b_i(\mathbf{x})$ only the single combination $\bar{\eta}(\mathbf{x})$ determines the stress energy of linear elasticity. Thus there are two "gauge transformations" which leave linear elasticity invariant. These are given by

$$b_i(\mathbf{x}) \to b_i(\mathbf{x}) + \delta_{i2}\frac{1}{\bar{\nabla}_1}B_1(\mathbf{x}) - \delta_{i1}\frac{1}{\bar{\nabla}_2}B_2(\mathbf{x}), \tag{16.57}$$

$$\bar{\Theta}(\mathbf{x}) \to \bar{\Theta}(x) - B_1(\mathbf{x}) - B_2(\mathbf{x}), \tag{16.58}$$

with integer-valued fields $B_1(\mathbf{x})$ and $B_2(\mathbf{x})$. This follows directly from $\varepsilon_{ij}\bar{\nabla}_i b_j \to \varepsilon_{ij}\bar{\nabla}_i b_j + B_1 + B_2$.

It is easy to understand these gauge transformations physically. If $B_1(\mathbf{x})$

vanishes everywhere but is equal to unity at the origin, say, then it contributes to $b_i(\mathbf{x})$ a string of Burgers vectors pointing along the 2-axis starting out at the origin and running along the 1-axis:

$$b_1(\mathbf{x}) = 0, \qquad b_2(\mathbf{x}) = \frac{1}{\bar{\nabla}_1}\delta_{\mathbf{x},\mathbf{0}} = \sum_{\mathbf{x}_1'=0}^{\infty} \delta_{x_1',x}\delta_{x_2,0} = \Theta_{x_1}\delta_{x_2,0}, \tag{16.59}$$

where Θ_x is the lattice version of the Heaviside function,

$$\Theta_x = \begin{cases} 0 & x = -1, -2, \ldots \\ 1 & x = 0, 1, 2, 3, \ldots \end{cases} \tag{16.60}$$

We have discussed this string of Burgers vectors before [see Eqs. (14.169)–(14.171)]. It can be compensated for by a disclination of negative charge at the origin [recall Fig. 14.16].

The same holds for a string of Burgers vectors pointing along the 1-axis and running up the positive 2-axis. This is the degeneracy at the level of linear elasticity if we include independent dislocations and disclinations. In order to lift this degeneracy we shall have to include more general terms into the elastic energy.

CHAPTER SEVENTEEN

EXTENDED THEORY OF ELASTICITY

17.1. TORQUE STRESSES

Let us recall here that according to the Newton-Euler axioms, a continuous body has to satisfy the following laws of motion:

1. momentum conservation,

$$\frac{d}{dt}P_j = \int_V d^3x f_j(\mathbf{x}) + \oint_S dS_i \sigma_{ij}(\mathbf{x}), \tag{17.1}$$

where P_j is the total momentum, $f_j(\mathbf{x})$ the external local force density, and σ_{ij} the stress tensor [i.e., each piece of a body exerts a force density $dS_i\sigma_{ij}$ upon its neighbor across the surface element dS_i].

2. angular momentum conservation,

$$\frac{d}{dt}J_i = \varepsilon_{ijk}\int_V d^3x\, x_j f_k(\mathbf{x}) + \varepsilon_{ijk}\int_S dS_\ell\, x_j \sigma_{\ell k}, \tag{17.2}$$

where $J_i \equiv \frac{1}{2}\varepsilon_{ijk}J_{jk}$ is the total angular momentum.

These laws hold for any finite part of the body with volume V and surface S. Using Gauss' formula, the surface integrals can be transformed into volume integrals so that (17.1) and (17.2) become

$$\frac{d}{dt}P_i = \int_V d^3x\,(f_i(\mathbf{x}) + \partial_i \sigma_{ij}(\mathbf{x})), \tag{17.3}$$

$$\frac{d}{dt}J_i = \varepsilon_{ijk}\int_V d^3x\,(x_j f_k(\mathbf{x}) + \partial_\ell x_j \sigma_{\ell k}(\mathbf{x})) = \varepsilon_{ijk}\int_V d^3x\, x_j(f_k(\mathbf{x}) + \partial_\ell \sigma_{\ell k}(\mathbf{x})). \tag{17.4}$$

Since this is valid for each volume element one deduces the equations

$$\partial_i \sigma_{ij}(\mathbf{x}) = -f_j(\mathbf{x}), \tag{17.5}$$

$$\varepsilon_{ijk}\sigma_{jk}(\mathbf{x}) = 0, \tag{17.6}$$

which were used extensively in Chapter 1.

Comparing Eqs. (17.1) and (17.2) one may wonder why the law of angular momentum conservation does not contain a direct term of the form

$$\int_S dS_k \tau_{ki}(\mathbf{x}) = \int_V d^3x\,\partial_k \tau_{ki}(\mathbf{x}), \tag{17.7}$$

by which a volume piece transfers torque to its neighbour via the common surface element. The tensor $\tau_{ki}(\mathbf{x})$ is called *torque stress* or *couple stress*. Its presence is natural in *orientable media* as was first discussed by E. and F. Cosserat in 1909.

If such a term is present, the law of angular momentum conservation leads to

$$\partial_k \tau_{ki}(\mathbf{x}) = -\varepsilon_{ijk}\sigma_{jk}(\mathbf{x}). \tag{17.8}$$

It is remarkable that in the absence of external body forces [i.e., $f_i(\mathbf{x}) = 0$], the two conservation laws (17.5) and (17.8) have precisely the same structure as the laws of defect conservation (2.45), (2.46),

$$\partial_i \Theta_{ij}(\mathbf{x}) = 0, \tag{17.9}$$

$$\partial_k \alpha_{ki}(\mathbf{x}) = -\varepsilon_{ijk}\Theta_{jk}(\mathbf{x}). \tag{17.10}$$

The reason is, of course, the essential role played by the space group in deriving both laws. It is curious, however, that the association with

translations and rotations is precisely the *opposite*. While $\partial_i \sigma_{ij}$ ensures *translational* equilibrium and $\partial_k \tau_{ki} = -\varepsilon_{ijk}\sigma_{jk}$ *rotational* equilibrium, the law $\partial_i \Theta_{ij} = 0$ conserves rotational defects (disclinations) and $\partial_k \alpha_{ki} = -\varepsilon_{ijk}\Theta_{jk}$ translational defects (dislocations). Formally, the reason is easy to see: Angular momentum is the cross product of position with linear momentum. In defect systems, on the other hand, the translational defects arise from the cross product of position $\mathbf{x}$ with rotational defects [recall Eq. (2.43)]. The cross products cause the inhomogeneous parts in the conservation laws (17.8) and (17.10).

The treatment of a crystal as an orientable medium becomes necessary if certain groups of atoms in a unit cell are tightly bound to each other so that they act like small composite objects. These require, in addition to their position, three Euler angles for their characterization,[a] and gradients of these Euler angles appear in the elastic energy. Such an extension of elasticity is of particular importance in the description of the phenomena of piezoelectricity.

Nevertheless, for simple monoatomic crystals which do not exhibit such phenomena, there exist physical circumstances under which torque stresses may become observable. This happens if higher gradients of stresses become so large that it is no longer admissible to omit them in the expression for the elastic energy. As soon as such higher gradients are present, the energy is no longer independent of the local rotation field $\omega_{ij} \equiv \frac{1}{2}(\partial_j u_k - \partial_k u_j)$. While ω_{ij} itself cannot occur in the energy (as a consequence of rotational symmetry), gradients of ω_{ij} can. This is why simple crystals with large higher gradients will display torque stresses. In fact, this is obvious on physical grounds since at the level of higher gradients the field equations must be able to account for restoring forces which arise if a small region of the crystal is rotated as a whole with respect to its neighborhood.

17.2. GENERAL FORM OF THE ELASTIC ENERGY

Let us briefly recall the standard symmetry arguments for the general form of the elastic energy. In the continuum limit, a distorted crystal is invariant under translations and rotations. If the positions of the atoms, initially situated at the coordinates $\mathbf{x}$, are described by

[a] It is sometimes necessary to allow also for distortions of these groups of atoms which require the inclusion of further fields, but these will not be discussed here.

$$\mathbf{x}'(\mathbf{x}) = \mathbf{x} + \mathbf{u}(\mathbf{x}), \tag{17.11}$$

the positions of the same atoms after a common translation

$$x_i^T = x_i + a_i \tag{17.12}$$

are given by

$$x'^T(\mathbf{x}) = x'(\mathbf{x} - \mathbf{a}). \tag{17.13}$$

After a common rotation

$$x_i^R = R_{ij}x_j, \tag{17.14}$$

they are given by

$$x_i'^R(\mathbf{x}) = R_{ij}x_j'(R^{-1}\mathbf{x}). \tag{17.15}$$

This shows that the distorted coordinates $x_i'(\mathbf{x})$ form a vector field as defined before [for example in Eqs. (4.9) and (4.10)].

The consequences of the transformation laws (17.13) and (17.15) are most easily found by considering infinitesimal transformations. For infinitesimal translations we have

$$\delta^T x_i'(\mathbf{x}) = x_i'^T(\mathbf{x}) - x_i'(\mathbf{x}) = -a_j\partial_j x_i'(\mathbf{x}) = -a_i - a_j\partial_j u_i(\mathbf{x}). \tag{17.16}$$

The displacement fields of the distorted and translated crystal are

$$u_i^T(\mathbf{x}) = x_i'^T - x_i. \tag{17.17}$$

Correspondingly we define the infinitesimal change of $u_i(\mathbf{x})$ under infinitesimal translations as

$$\delta^T u_i(\mathbf{x}) = u_i^T(\mathbf{x}) - u_i(\mathbf{x}) \tag{17.18}$$

and calculate

$$\begin{aligned}\delta^T u_i(\mathbf{x}) &= (x_i'^T(\mathbf{x}) - x_i) - (x_i'(\mathbf{x}) - x_i) = x_i'^T(\mathbf{x}) - x_i'(\mathbf{x}) \\ &= \delta^T x_i'(\mathbf{x}) = -a_j\partial_j u_i(\mathbf{x}) - a_i.\end{aligned} \tag{17.18'}$$

Thus, in addition to the normal translation law for vector fields, $\delta^T u_i(\mathbf{x})$ contains an extra piece $-a_i$. This is the reason why the elastic energy of a translationally invariant system cannot depend on the displacements. The derivatives $\partial_k u_\ell(\mathbf{x})$, however, do transform properly under translations

$$\delta^T \partial_k u_\ell(\mathbf{x}) = -a_j \partial_j \partial_k u_\ell(\mathbf{x}) \tag{17.18''}$$

and the energy can depend on them.

This dependence is not completely arbitrary since it is restricted by rotational symmetry. For infinitesimal rotations,

$$R_{ij} = -\alpha_k \varepsilon_{kij}, \tag{17.19}$$

and $\mathbf{x}$ and $\mathbf{x}'$ change as follows [see (4.14)]

$$\begin{aligned} \delta^R x_i &= x_i^R - x_i = \alpha_k \varepsilon_{kij} x_j, \\ \delta^R x_i'(\mathbf{x}) &= x_i'^R(\mathbf{x}) - x_i'(\mathbf{x}) = \alpha_k (\varepsilon_{kij} x_j'(\mathbf{x}) + \varepsilon_{k\ell j} x_\ell \partial_j x_i'(\mathbf{x})). \end{aligned} \tag{17.20}$$

For the displacement field $u_i(\mathbf{x}) = x_i'(\mathbf{x}) - x_i$ this implies

$$\begin{aligned} \delta^R u_i^R(\mathbf{x}) &= u_i^R(\mathbf{x}) - u_i(\mathbf{x}) = (x_i'^R(\mathbf{x}) - x_i) - (x_i'(\mathbf{x}) - x_i(\mathbf{x})) \\ &= x_i'^R(\mathbf{x}) - x_i'(\mathbf{x}) = \delta^R x_i'(\mathbf{x}) \\ &= \alpha_k (\varepsilon_{kij} u_j(\mathbf{x}) + \varepsilon_{k\ell j} x_\ell \partial_j u_i(\mathbf{x})) + \alpha_k \varepsilon_{kij} x_j. \end{aligned} \tag{17.21}$$

Thus, also with respect to rotations, displacements are no longer proper vector fields but transform with an additional rotation piece.

Since the additional piece depends on x_j, the gradient of the displacements is not a rotational tensor field. Rather, it transforms as follows,[b]

$$\delta^R \partial_\ell u_i(\mathbf{x}) = \alpha_k (\varepsilon_{kij} \partial_\ell u_j(\mathbf{x}) + \varepsilon_{k\ell m} \partial_m u_i(\mathbf{x})) + \alpha_k \varepsilon_{ki\ell}. \tag{17.22}$$

The additional piece disturbing the tensor transformation law is antisymmetric in ℓ and i. This is precisely what makes it convenient to introduce the strain tensor, which obviously is a proper tensor:

[b]Notice incidentally, that such additive transformations (17.18') and (17.22) are typical for gauge fields, as discussed in Chapter 4, Part I.

$$\delta^R u_{\ell i}(\mathbf{x}) = \alpha_k (\varepsilon_{kij} u_{\ell j}(\mathbf{x}) + \varepsilon_{k\ell m} u_{mi}(\mathbf{x})). \tag{17.23}$$

Hence the local rotation field $\omega_{\ell i}(\mathbf{x})$ carries all the non-tensorial properties of $\partial_\ell u_i(\mathbf{x}) = u_{\ell i}(\mathbf{x}) + \omega_{\ell i}(\mathbf{x})$,

$$\delta^R \omega_{\ell i}(\mathbf{x}) = \alpha_k (\varepsilon_{kij} \omega_{\ell j}(\mathbf{x}) + \varepsilon_{k\ell m} \omega_{mi}(\mathbf{x})) + \alpha_k \varepsilon_{ki\ell}\,. \tag{17.24}$$

This is what leads to the usual conclusion that the $\omega_{\ell i}(\mathbf{x})$ are absent in the classical theory of elasticity. If elastic distortions involve only small long wavelength displacements, the energy density must be quadratic in $u_{\ell i}(\mathbf{x})$, $\omega_{\ell i}(\mathbf{x})$. While terms like $u^2_{\ell i}(\mathbf{x})$ are rotationally invariant, $\omega^2_{\ell i}(\mathbf{x})$ is not and the energy density cannot depend on $\omega_{\ell i}(\mathbf{x})$.

As soon as higher gradients are allowed, however, the rotation field does in general appear in the energy. From (17.24) we see that $\partial_p \omega_{\ell i}(\mathbf{x})$ is a proper tensor field, since [compare (4.47)]

$$\delta^R \partial_p \omega_{\ell i}(\mathbf{x}) = \alpha_k (\varepsilon_{kij} \partial_p \omega_{\ell j}(\mathbf{x}) + \varepsilon_{k\ell m} \partial_p \omega_{mi}(\mathbf{x}) + \varepsilon_{kpq} \partial_q \omega_{\ell i}(\mathbf{x})). \tag{17.25}$$

As a matter of fact, from (17.22) it follows that starting from the second derivative, *all* $\nabla_{\ell_1} \ldots \partial_{\ell_n} u_i(\mathbf{x})$ are proper tensor fields. Thus, the most general form of the elastic energy density with higher gradients is obtained by directly contracting higher derivatives of $u_i(\mathbf{x})$ with each other and forming an invariant expression with the following variables

$$e(\mathbf{x}) = e(u_{\ell i}(\mathbf{x}),\ \partial_{\ell_1}\partial_{\ell_2} u_i(\mathbf{x}),\ \partial_{\ell_1}\partial_{\ell_2}\partial_{\ell_3} u_i(\mathbf{x}),\ \ldots). \tag{17.26}$$

17.3. CANONICAL FORMALISM FOR HIGHER GRADIENT THEORIES

Before developing the theory of elasticity for an energy expression such as (17.26) it will be useful to recall the canonical formalism for systems with more than one derivative. This formalism is best known for mechanical systems in which the "field variables" are the particle positions as functions of time rather than field variables as functions of space. For simplicity, let us consider only one such "field variable" $q(t)$. The dynamics of the mechanical system is governed by the action

$$A[q] - \int dt j(t) q(t) = \int dt\, L(q(t), \dot{q}(t), \ddot{q}(t), \ldots, q^{(N)}(t)), \tag{17.27}$$

where L is the Lagrangian. For future convenience, we have added an external source to the system. The physical field configurations are found by extremizing the action

$$\frac{\delta A[q]}{\delta q(t)} - j(t) = 0. \tag{17.28}$$

Using the general formula [recall Eq. (1.54), Part I]

$$\frac{\delta q(t')}{\delta q(t)} = \delta(t' - t), \tag{17.29}$$

we find

$$\frac{\delta A[q]}{\delta q(t)} = \int dt' \left(\frac{\partial L}{\partial q(t')} \delta(t' - t) + \frac{\partial L}{\partial \dot{q}(t)} \partial_{t'} \delta(t' - t) + \frac{\partial L}{\partial \ddot{q}(t)} \partial_{t'}^2 \delta(t' - t) + \ldots + \frac{\partial L}{\partial q^{(N)}(t)} \partial_{t'}^N \delta(t' - t) \right). \tag{17.30}$$

By performing partial integrations in all terms except the first this gives the Euler-Lagrange equation

$$\frac{\partial L}{\partial q(t)} - \frac{d}{dt} \frac{\partial L}{\partial \dot{q}(t)} + \frac{d^2}{dt^2} \frac{\partial^2 L}{\partial \ddot{q}(t)} + \ldots + (-)^N \frac{d^N}{dt^N} \frac{\partial L}{\partial q^{(N)}(t)} = j(t). \tag{17.31}$$

The N derivatives

$$p_n = \frac{\partial L}{\partial q^{(n)}} - \frac{d}{dt} \frac{\partial L}{\partial q^{(n+1)}} + \ldots + (-)^{N-n} \frac{d^{N-n}}{dt^{N-n}} \frac{\partial L}{\partial q^{(N)}}, \; n = 1, \ldots, N. \tag{17.32}$$

may be considered as higher analogues of the usual canonical momentum

$$p = \frac{\partial L}{\partial \dot{q}}. \tag{17.33}$$

These higher canonical momenta make it possible to reduce the single

higher order differential equation (17.31) to a sequence of first order equations. For this, let us define

$$q_1 \equiv q, \quad q_2 \equiv \dot{q}, \quad q_3 = \ddot{q}, \quad \ldots, \quad q_N = q^{(N-1)}, \tag{17.34}$$

as new independent variables of the system and rewrite the Lagrangian in the form

$$L(q, \dot{q}, \ddot{q}, \ldots, q^{(N)}) = L(q_1, \ldots, q_N, \dot{q}_N), \tag{17.35}$$

in which there is only one variable with a first derivative, namely q_N. The previously defined canonical momenta can be written recursively as

$$p_n = \frac{\partial L}{\partial q_{n+1}}(q_1, \ldots, q_N, \dot{q}_N) - \dot{p}_{n+1} \quad n = 1, 2, \ldots, N-1, \tag{17.36a}$$

$$p_N = \frac{\partial L}{\partial \dot{q}_N}(q_1, \ldots, q_N, \dot{q}_N). \tag{17.36b}$$

Note that with respect to the new variables $q_1, \ldots, q_{N-1}$, the Lagrangian has only one canonical momentum, namely, p_N.

We now consider the Legendre transform

$$\begin{aligned} -H(p_1, \ldots, p_N, q_1, \ldots, q_N) \\ &\equiv L(q, \dot{q}, \ldots, q^{(N-1)}, q^{(N)}) - p_1\dot{q}_1 - p_2\dot{q}_2 - \ldots - p_{N-1}\dot{q}_{N-1} - p_N\dot{q}_N \\ &= L(q_1, q_2, \ldots, q_N, \dot{q}_N(p_N, q_1, \ldots, q_N)) - p_1 q_2 - p_2 q_3 - \ldots \\ &\quad - p_{N-1} q_N - p_N \dot{q}_N(p_N, q_1, \ldots, q_N), \end{aligned} \tag{17.37}$$

where the derivatives $\dot{q}_1, \dot{q}_2, \ldots, \dot{q}_{N-1}$ have been eliminated in favor of $q_2, q_3, \ldots, q_N$ by (17.34) and $\dot{q}_N$ in favor of p_N by inverting equation (17.36b).

Obviously, H is constructed from L in complete analogy with the standard construction of a Hamiltonian from an ordinary first order derivative Lagrangian $L = L(q, \dot{q})$, for which the Hamiltonian is

$$-H(p, q) = L(q, \dot{q}) - \frac{\partial L}{\partial \dot{q}}\dot{q} = L(q, \dot{q}(p, q)) - p\dot{q}(p, q), \tag{17.38}$$

where $\dot{q} = \dot{q}(p, q)$ is determined by inverting $p = \partial L(q, \dot{q})/\partial \dot{q}$.

The Hamiltonian formalism permits reducing the second order Euler-Lagrange equation,

$$\frac{\partial L}{\partial q} - \frac{d}{dt}\frac{\partial L}{\partial \dot{q}} = j(t), \tag{17.39}$$

to two first order Hamiltonian equations: By extremizing the action

$$\begin{aligned} &A[q] - \int_{t_a}^{t_b} dt j(t) q(t) \\ &= \int_{t_a}^{t_b} dt (L(q(t), \dot{q}(t)) - j(t) q(t)) \\ &= \int_{t_a}^{t_b} dt (p(t)\dot{q}(t) - H(p(t), q(t)) - j(t) q(t)) = A[p, q] - \int_{t_a}^{t_b} dt j(t) q(t) \end{aligned} \tag{17.40}$$

in the new variables $p(t)$, $q(t)$ with fixed end points in $q(t)$ [i.e., $q_a = q(t_a)$, $q_b = q(t_b)$, fixed],

$$\begin{aligned} &\delta\left(A[p, q] - \int_{t_a}^{t_b} dt j(t) q(t)\right) \\ &\quad = \delta \int_{t_a}^{t_b} dt (p\dot{q} - H - jq) \\ &\quad = \int_{t_a}^{t_b} dt \left[\delta p \left(\dot{q} - \frac{\partial H}{\partial p}\right) + \left(-\dot{p} - \frac{\partial H}{\partial q} - j\right)\delta q\right] + \delta p q \Big|_{t_a}^{t_b}, \end{aligned} \tag{17.41}$$

we find the equation

$$\dot{q} = \frac{\partial H}{\partial p}(p, q), \qquad \dot{p} = -\frac{\partial H}{\partial q}(p, q) - j. \tag{17.41'}$$

In the present case we can go through the same procedure with (17.27) and minimize, at fixed $q_i(t_a)$, $q_i(t_b)$, the action,

$$\delta\left(A[p_n, q_n] - \int_{t_a}^{t_b} dt j(t) q_1(t)\right)$$

$$= \delta \int_{t_a}^{t_b} dt[p_1\dot{q}_1 + p_2\dot{q}_2 + \ldots + p_N\dot{q}_N - H(p_1, \ldots, p_N, q_1, \ldots, q_N) - jq_1]$$

$$= \int_{t_a}^{t_b} dt \sum_{n=1}^{N} \left[\delta p_n\left(\dot{q}_n - \frac{\partial H}{\partial p_n}\right) + \left(-\dot{p}_n - \frac{\partial H}{\partial q_n} - \delta_{n1} j\right)\delta q_n\right] + \sum_{n=1}^{N} \delta p_n q_n \Big|_{t_a}^{t_b}. \tag{17.42}$$

This yields the set of first order Hamilton equations

$$\dot{q}_r = \frac{\partial H(p_n, q_n)}{\partial p_r} \quad r = 1, \ldots, N, \tag{17.43a}$$

$$\begin{aligned} \dot{p}_1 &= -\frac{\partial H(p_n, q_n)}{\partial q_1} - j, \\ \dot{p}_r &= -\frac{\partial H(p_n, q_n)}{\partial q_r}, \quad r = 2, \ldots, N. \end{aligned} \tag{17.43b}$$

The equivalence to the single equation (17.31) can be seen by writing these equations down explicitly, using (17.37), i.e.,

$$\begin{aligned} &\dot{q}_n = \frac{\partial H}{\partial p_n} = q_{n+1} \quad n = 1, \ldots, N-1, \\ &\dot{q}_N = \frac{\partial H}{\partial p_N} = -\frac{\partial L}{\partial \dot{q}_N}\frac{\partial \dot{q}_N}{\partial p_N} + \dot{q}_N + p_N\frac{\partial \dot{q}_N}{\partial p_N} \\ &\dot{p}_1 = -\frac{\partial H}{\partial q_1} - j = \frac{\partial L}{\partial q_1} + \frac{\partial L}{\partial \dot{q}_N}\frac{\partial \dot{q}_N}{\partial q_1} - p_N\frac{\partial \dot{q}_N}{\partial q_1} - j = \frac{\partial L}{\partial q_1} - j, \\ &\dot{p}_r = -\frac{\partial H}{\partial q_r} = \frac{\partial L}{\partial q_r} + \frac{\partial L}{\partial \dot{q}_N}\frac{\partial \dot{q}_N}{\partial q_r} - p_{r-1} - p_N\frac{\partial \dot{q}_N}{\partial q_r} = \frac{\partial L}{\partial q_r} - p_{r-1} \quad r = 2, \ldots, N. \end{aligned} \tag{17.44}$$

The first line simply shows that the new variables q_r are to be identified with the time derivatives of q_1, as in (17.34). The second line gives (17.36b). The last line amounts to (17.32) and can be used, together with the previous line, to calculate

$$0 = \dot{p}_1 - (\dot{p}_2 + p_1)^{(1)} + (\dot{p}_3 + p_2)^{(2)} + \ldots + (-)^{N-1}(\dot{p}_N + p_{N-1})^{(N-1)} + (-)^N p_N$$

$$= \frac{\partial L}{\partial q} - j - \frac{d}{dt}\frac{\partial L}{\partial \dot{q}} + \frac{d^2}{dt^2}\frac{\partial L}{\partial \ddot{q}} + \ldots + (-)^N \frac{d^{(N-1)}}{dt^{N-1}}\frac{\partial L}{\partial q^{(N-1)}} + (-)^N \frac{d^N}{dt^N}\frac{\partial L}{\partial q^N}, \tag{17.45}$$

which is indeed the same as (17.31).

We shall be interested in linear elasticity with higher gradients. This implies that the energy is a quadratic form in the derivatives of the displacement fields. In the present analogous mechanical model, this corresponds to a Lagrangian of the type

$$L(q, \dot{q}, \ldots, q^{(N)}) = \frac{1}{2}\sum_{n,m=1}^{N} \ell_{nm} q^{(n)}(t) q^{(m)}(t), \tag{17.46}$$

with constant symmetric coefficients $\ell_{nm} = \ell_{mn}$. Then the momenta are

$$p_n = \sum_{n=1}^{N-1} \ell_{nm} q_{n+1} + \ell_{nN}\dot{q}_N - \dot{p}_{n+1}(1 - \delta_{nN}). \tag{17.47}$$

and the Hamiltonian can be written explicitly as

$$\begin{aligned} &H(p_n, q_n) \\ &= p_1 q_2 + p_2 q_3 + \ldots + p_N \frac{1}{\ell_{NN}}\left(p_N - \sum_{m=1}^{N-1} \ell_{Nm} q_{m+1}\right) \\ &\quad - \frac{1}{2}\sum_{n,m=1}^{N-1} \ell_{nm} q_{n+1} q_{m+1} - \sum_{n=1}^{N} \ell_{nN} q_{n+1} \frac{1}{\ell_{NN}}\left(p_N - \sum_{m=1}^{N-1} \ell_{Nm} q_{m+1}\right) \\ &\quad - \frac{1}{2}\frac{1}{\ell_{NN}}\left(p_N - \sum_{m=1}^{N-1} \ell_{Nm} q_{m+1}\right)^2. \end{aligned} \tag{17.48}$$

The action takes the canonical form

$$\begin{aligned} &A[p_n, q_n] - \int_{t_a}^{t_b} dt j(t) q_1(t) \\ &= \int_{t_a}^{t_b} dt \Bigg[p_1\dot{q}_1 + p_2\dot{q}_2 + \ldots + p_N\dot{q}_N - p_1 q_2 - p_2 q_3 - \ldots - p_{N-1} q_N \\ &\quad + \frac{1}{2}\sum_{n,m=1}^{N-1} \ell_{nm} q_{n+1} q_{m+1} - \frac{1}{2}\frac{1}{\ell_{NN}}\left(p_N - \sum_{m=1}^{N-1} \ell_{Nm} q_{m+1}\right)^2 - j(t) q_1(t) \Bigg]. \end{aligned} \tag{17.49}$$

This action governs the quantum fluctuations of the mechanical system. Arbitrary Green functions can be calculated from the generating functional

$$Z[j]=\prod_n \int \mathscr{D} q_n(t) \int \frac{\mathscr{D} p_n(t)}{2\pi} \exp\left\{ i\left(A[p_n, q_n] - \int dt j(t) q_1(t) \right)\right\}. \quad (17.50)$$

Notice that the source acts only on $q_1(t) = q(t)$ and the other coordinates $q_2, \ldots, q_N$ are just auxiliary variables.

The expression (17.50) can be simplified by observing that the first $N-1$ momenta $p_1, \ldots, p_{N-1}$ can be integrated out trivially resulting in a string of δ-functionals

$$2\pi\delta(\dot{q}_1 - q_2) \ldots 2\pi\delta(\dot{q}_{N-1} - q_N).$$

This allows one to integrate out all the $q_2, \ldots, q_N$ variables so that the integral reduces to

$$\int \mathscr{D} q \int \frac{\mathscr{D} p_N}{2\pi} \exp\left\{ i \int_{t_a}^{t_b} dt \left[p_N q^{(N)} + \frac{1}{2} \sum_{n,m=1}^{N-1} \ell_{nm} q^{(n)} q^{(m)} - \frac{1}{2} \frac{1}{\ell_{NN}} \left(p_N - \sum_{m=1}^{N-1} \ell_{Nm} q^{(m)} \right)^2 - j(t) q(t) \right] \right\}.$$

Finally, a quadratic completion of the p_N parts,

$$-\frac{1}{2} \frac{1}{\ell_{NN}} \left(p_N - \sum_{m=1}^{N-1} \ell_{Nm} q^{(m)} - \ell_{NN} q^{(N)} \right)^2 + \frac{1}{2} \ell_{NN} q^{(N)2} + \sum_{m=1}^{N} \ell_{Nm} q^{(N)} q^{(m)},$$

can be used to integrate p_N out and brings the generating functional to

$$Z[j] = \prod_t \left[\sqrt{\frac{\ell_{NN}}{2\pi i}} \right] \int \mathscr{D} q \exp\left\{ i \int_{t_a}^{t_b} dt \left[\frac{1}{2} \sum_{n,m=1}^{N} \ell_{nm} q^{(n)} q^{(m)} - j(t) q(t) \right] \right\}, \quad (17.51)$$

where the product in front covers all points on the grated time axis. The reader will have noticed that the canonical form of the partition function (17.50) is not a very aesthetic one, due to the special treatment of the last momentum variables p_N. This asymmetry can be removed by introducing a further independent variable q_{N+1} and generating the last term in the action (17.49) by an auxiliary Gaussian integral

$$\sqrt{\frac{\ell_{NN}}{2\pi i}}\int dq_{N+1}$$
$$\times\exp\left\{-i\int dt p_N q_{N+1}+\frac{i}{2}\int_{t_a}^{t_b}dt\left(\ell_{NN}q_{N+1}q_{N+1}+\sum_{m=1}^{N-1}\ell_{Nm}q_{N+1}q_{m+1}\right)\right\}. \tag{17.52}$$

Then the partition function reads

$$Z[j]=\prod_t\left[\sqrt{\frac{\ell_{NN}}{2\pi i}}\right]\prod_{n=1}^{N+1}\int\mathscr{D}q_n(t)\prod_{n=1}^{N}\int\frac{\mathscr{D}p_n(t)}{2\pi}$$
$$\times\exp\left\{i\int_{t_a}^{t_b}dt\left[p_1\dot{q}_1+p_2\dot{q}_2+\ldots+p_N\dot{q}_N-p_1q_2-p_2q_3-\ldots\right.\right.$$
$$\left.\left.-p_Nq_{N+1}+\frac{1}{2}\sum_{n,m=1}^{N}\ell_{nm}q_{n+1}q_{m+1}\right]\right\}. \tag{17.53}$$

Since the integrals over $p_1, \ldots, p_N$ ensure that $q_2, \ldots, q_{N+1}$ are identically equal to $\dot{q}_1\equiv\dot{q}$, $\dot{q}_2=\ddot{q}$, $\ldots$, $\dot{q}_N=q^{(N)}$, we can replace the exponent by

$$i\int_{t_a}^{t_b}dt\left[p_1\dot{q}+p_2\ddot{q}+\ldots+p_Nq^{(N)}-p_1q_2-p_2q_3-\ldots-p_Nq_{N+1}\right.$$
$$\left.+\frac{1}{2}\sum_{n,m=1}^{N}\ell_{nm}q_{n+1}q_{m+1}\right].$$

It is now possible to integrate out the variables $q_2, \ldots, q_{N+1}$ and we arrive at the partition function

$$Z[j]=\prod_t\left[\sqrt{\frac{\ell_{NN}}{2\pi i}}\det\left(\frac{\ell}{2\pi i}\right)^{-1/2}\right]\int\mathscr{D}q(t)\prod_{n=1}^{N}\int\frac{\mathscr{D}p_n(t)}{2\pi}$$
$$\times\exp\left\{i\int_{t_a}^{t_b}\left[p_1\dot{q}+p_2\ddot{q}+\ldots+p_Nq^{(N)}-\frac{1}{2}\sum_{n,m=1}^{N}(\ell^{-1})_{nm}p_np_m\right]\right\}. \tag{17.54}$$

This form will be much more convenient to work with and will be referred to as the *quasi-canonical representation* of the partition function. Performing the Gaussian integrals over the momentum variables brings us again to the pure $q^{(n)}$ representation (17.51).

As an example, consider the Lagrangian

$$L = \tfrac{1}{2}(a\dot{q}^2 + b\ddot{q}^2 + 2c\dot{q}\ddot{q}). \tag{17.55}$$

Defining $q_1 = q$, $q_2 = \dot{q}$ this becomes

$$L(q_1, q_2, \dot{q}_2) = \tfrac{1}{2}(aq_2^2 + b\dot{q}_2^2 + 2cq_2\dot{q}_2) \tag{17.56}$$

and the momenta are

$$p_1 = a\dot{q} + c\ddot{q} - \dot{p}_2 = aq_2 + c\dot{q}_2 - \dot{p}_2, \quad p_2 = b\ddot{q} + c\dot{q} = b\dot{q}_2 + cq_2. \tag{17.57}$$

This leads to the Hamiltonian

$$\begin{aligned} &H(p_1, p_2, q_1, q_2) \\ &\quad = p_1 q_2 + p_2 \dot{q}_2(p_2, q_1, q_2) - L(q_1, q_2, \dot{q}_2(p_2, q_1, q_2)) \\ &\quad = p_1 q_2 + p_2 \frac{1}{b}(p_2 - cq_2) - \frac{1}{2}\left(aq_2^2 + \frac{1}{b}(p_2 - cq_2)^2 + 2\frac{c}{b} q_2(p_2 - cq_2) \right). \end{aligned} \tag{17.58}$$

The path integral

$$\begin{aligned} Z[j] = \int \mathscr{D}q_1 \mathscr{D}q_2 \int \frac{\mathscr{D}p_1}{2\pi} \frac{\mathscr{D}p_2}{2\pi} \\ \times \exp\left\{ i \int_{t_a}^{t_b} dt (p_1\dot{q}_1 + p_2\dot{q}_2 - H(p_1, p_2, q_1, q_2) - jq_1) \right\} \end{aligned} \tag{17.59}$$

becomes

$$\begin{aligned} Z[j] &= \int \mathscr{D}q_1 \mathscr{D}q_2 \int \frac{\mathscr{D}p_1}{2\pi} \frac{\mathscr{D}p_2}{2\pi} \\ &\quad \times \exp\left\{ i \int_{t_a}^{t_b} dt \left[p_1(\dot{q}_1 - q_2) + p_2\dot{q}_2 + \frac{a}{2} q_2^2 - \frac{1}{2b}(p_2 - cq_2)^2 - jq_1 \right] \right\} \\ &= \int \mathscr{D}q_1 \int \frac{\mathscr{D}p_2}{2\pi} \exp\left\{ i \int_{t_a}^{t_b} dt \left[p_2\ddot{q}_1 + \frac{a}{2}\dot{q}_1^2 - \frac{1}{2b}(p_2 - c\dot{q}_1)^2 - jq_1 \right] \right\} \\ &= \prod_t \left[\sqrt{\frac{b}{2\pi i}} \right] \int \mathscr{D}q \exp\left\{ i \int_{t_a}^{t_b} \left[\frac{1}{2}(a\dot{q}^2 + b\ddot{q}^2 + 2c\dot{q}\ddot{q}) - jq \right] \right\}, \end{aligned} \tag{17.60}$$

just as in the general expression (17.51). Let us also write down the

quasi-canonical form (17.54) of the partition function which arises by integrating q_2 out in the first line of (17.60),

$$Z[j] = \prod_t \left[\sqrt{\frac{b}{2\pi i}} \frac{2\pi i}{\sqrt{(ab - c^2)}} \right] \int \mathscr{D}q \int \frac{\mathscr{D}p_1}{2\pi} \frac{\mathscr{D}p_2}{2\pi} \times \exp\left\{ i \int_{t_a}^{t_b} dt \left[p_1 \dot{q} + p_2 \ddot{q} - \frac{1}{2} \frac{1}{ab - c^2} (b p_1^2 + a p_2^2 + 2c p_1 p_2) \right] \right\}. \tag{17.61}$$

Upon performing the integral over p_1, p_2, this yields once more the last line of (17.60).

In order to apply this formula to higher derivative elasticity, only a few simple changes are necessary. We want to study fluctuations of the elastic energy as a function of derivatives of the displacement field, $\partial_\ell u_i(\mathbf{x})$, $\partial_{\ell_1} \partial_{\ell_2} u_i(\mathbf{x})$, ... instead of a Lagrangian as a function of $\dot{q}(t)$, $\ddot{q}(t)$, ... The transition to spatial variables is achieved by rotating the time t to the imaginary time $\tau = -it$ and identifying the Euclidean Langrangian $L(q, (1/i)(d/d\tau)q, ((1/i)(d/d\tau))^2 q, \ldots)$ with the energy density $e(u, \partial u, \partial\partial u, \ldots)$. It follows that the Euclidean path integral in the canonical formulation (17.50),

$$Z[j] = \prod_n \int \mathscr{D}q_n(\tau) \int \frac{\mathscr{D}p_n(\tau)}{2\pi T} \times \exp\left\{ \frac{1}{T} \int_{\tau_a}^{\tau_b} d\tau \left[i \sum_i p_n \frac{d}{d\tau} q_i - H(p_i, q_i) - j(\tau) q(\tau) \right] \right\}, \tag{17.62}$$

reduces in precisely the same way to the pure $q(\tau)$ form [with (17.46)],

$$Z[j] = \prod_\tau \left[\sqrt{\frac{\ell_{NN}}{2\pi\tau}} \right] \int \mathscr{D}q \exp\left\{ \frac{1}{T} \int_{\tau a}^{\tau b} d\tau \left[L\left(q, \frac{d}{di\tau} q, \frac{d^2}{d(i\tau)^2} q, \ldots \right) - j(\tau) q(\tau) \right] \right\}. \tag{17.63}$$

If there is time reversal invariance, the Euclidean Lagrangian has an even number of time derivatives so that it is real. We therefore define

$$L\left(q, \frac{d}{di\tau} q, \frac{d^2}{d(i\tau)^2} q, \ldots \right) \equiv -L_E(q, q', q'', \ldots, q^{(N)}) \tag{17.64}$$

where ′ denotes the derivative $d/d\tau$. The canonical momenta are given by

$$p_n = \frac{\partial L}{\partial\left(\frac{d}{dt}\right)^n q(t)} - \dot{p}_{n+1}(1-\delta_{nN}) = (-i)^n \frac{-\partial L_E}{\partial\left(\frac{d}{d\tau}\right)^n q(\tau)} - ip'_{n+1}(1-\delta_{nN}),$$

and the Legendre transform is

$$\begin{aligned} H &= p_1\dot{q} + p_2\ddot{q} + \ldots + p_N q^{(N)} - L(q, \dot{q}, \ldots, q^{(N)}) \\ &= p_1 q_2 + p_2 q_3 + \ldots ip_N q'_N + L_E(q, q', \ldots, q^{(N)}). \end{aligned}$$

In order to remove awkward powers of i it is preferable to define, in the Euclidean case,

$$q_n^E = \left(\frac{d}{d\tau}\right)^{n-1} q(\tau), \quad p_n^E = i\frac{\partial L_E}{\partial q^{(n)}(\tau)} - p_{n+1}^{E'}(1-\delta_{nN}), \quad n = 1, \ldots, N. \tag{17.65}$$

Then the Legendre transform becomes

$$\begin{aligned} H_E(p_n^E, q_n^E) &= i(p_1^E q' + p_2^E q'' + \ldots + p_N^E q^{(N)}) + L_E(q, q', \ldots, q^{(N)}) \\ &= i(p_1^E q_2^E + p_2^E q_3^E + \ldots + p_{N-1}^E q_N^E + p_N^E q'_N(p_N^E, q_1^E, \ldots q_N^E) \\ &\quad + L_E(q_1^E, q_2^E, \ldots, q_N^E, q'_N(p_N^E, q_1^E, \ldots, q_N^E)) \end{aligned} \tag{17.66}$$

and the path integral is

$$\begin{aligned} Z[j] = \prod_n \int \mathscr{D}q_n(\tau) \int \frac{\mathscr{D}p_n(\tau)}{2\pi T} \exp\Bigg\{\frac{1}{T}\int_{\tau_a}^{\tau_b} d\tau [i(p_1 q'_1 + p_2 q'_2 + \ldots \\ + p_N q'_N) - H_E(p_n, q_n) - j(\tau)q(\tau)]\Bigg\}, \end{aligned} \tag{17.67}$$

where we have dropped the superscript E of $q_n'^E$, q_n^E, since $q_2, \ldots, q_N$, $p_1, p_2, \ldots, p_N$ are dummy variables anyway and the only observable to which the external current is coupled, $q_1 = q_1^E$, is the same with or without subscript.

Obviously, all operations can be carried out in the Euclidean version just as before. A Euclidean Lagrangian

$$L_E(q, q', \ldots, q^{(N)}) = \frac{1}{2} \sum_{n,m=1}^{N} \ell_{nm} q^{(n)}(\tau) q^{(m)}(\tau) \tag{17.68}$$

can be treated as in (17.46)–(17.51) and we obtain, indeed, the partition function (17.63) in the form

$$Z[j] = \prod_t \left[\sqrt{\frac{\ell_{NN}}{2\pi}} \right] \int \mathscr{D}q \exp\left\{ -\frac{1}{T} \int d\tau \left[\frac{1}{2} \sum_{n,m=1}^{N} \ell_{nm} q^{(n)}(\tau) q^{(m)}(\tau) - j(\tau) q(\tau) \right] \right\}. \tag{17.69}$$

The Euclidean Lagrangian (17.68) is precisely of the generic type encountered in linear elasticity with higher gradients.

As a simple example let us study a one-dimensional system with a single displacement variable $u(x)$ and an energy density which is the Euclidean analogue of (17.56):

$$L_E(u', u'') \equiv e(u', u'') = \tfrac{1}{2}(au'^2 + bu''^2 + 2cu'u''). \tag{17.70}$$

Treating x like τ in (17.65)–(17.69), we define

$$q_1 = u, \quad q_2 = u' \tag{17.71}$$

and write the energy density as

$$e(q_2, q_2') = \tfrac{1}{2}(aq_2^2 + bq_2'^2 + 2cq_2q_2'). \tag{17.72}$$

We can now read off the momenta $p_1 = i(au' + cu'') - p_2' = i(aq_2 + cq_2') - p_2$, $p_2 = i(bu'' + cu') = i(bq_2' + cq_2)$ and construct the Legendre transform (17.67) [compare (17.58)]

$$\begin{aligned} h(p_1, p_2, q_1, q_2) &= i\left(p_1 q_2 + p_2 \frac{1}{b}(-ip_2 - cq_2) \right) \\ &\quad + \frac{1}{2}\left(aq_2^2 + \frac{1}{b}(-ip_2 - cq_2)^2 + 2\frac{c}{b} q_2(-ip_2 - cq_2) \right) \\ &= ip_1 q_2 + \frac{a}{2} q_2^2 + \frac{1}{2b}(-ip_2 - cq_2)^2, \end{aligned} \tag{17.73}$$

and the total energy reads, in p_n, q_n variables,

$$E[p_1, p_2, q_1, q_2] = \int dx\,[i(p_1 q_1' + p_2 q_2') - h(p_1, p_2, q_1, q_2)]$$
$$= \int dx \left[ip_1(q_1' - q_2) + ip_2 q_2' - \frac{a}{2} q_2^2 - \frac{1}{2b}(-ip_2 - cq_2)^2 \right]. \tag{17.74}$$

The canonical partition function becomes

$$Z[j] = \int \mathscr{D} q_1 \mathscr{D} q_2 \int \frac{\mathscr{D} p_1}{2\pi} \frac{\mathscr{D} p_2}{2\pi}$$
$$\times \exp\left\{ \frac{1}{T} \int dx \left[ip_1(q_1' - q_2) + ip_2 q_2' - \frac{a}{2} q_2^2 - \frac{1}{2b}(-ip_2 - cq_2) - jq_1 \right] \right\}$$
$$= \prod_x \left[\sqrt{\frac{b}{2\pi}} \right] \int \mathscr{D} u \exp\left\{ -\frac{1}{T} \int dx \left[\frac{1}{2}(au'^2 + bu''^2 + 2cu'u'') - ju \right] \right\}, \tag{17.75}$$

which is the Euclidean version of (17.60), as expected. The alternative form (17.61) now reads

$$Z[j] = \prod_x \left[\sqrt{\frac{b}{2\pi}} \frac{2\pi}{\sqrt{ab - c^2}} \right] \int \mathscr{D} u \int \frac{\mathscr{D} p_1}{2\pi} \frac{\mathscr{D} p_2}{2\pi}$$
$$\times \exp\left\{ \frac{1}{T} \int dx \left[ip_1 u' + ip_2 u'' - \frac{1}{2} \frac{1}{ab - c^2}(bp_1^2 + ap_2^2 - 2cp_1 p_2) \right] \right\}, \tag{17.76}$$

which will be of use in the next section.

We emphasize that the simplicity of the integration measure in (17.51), (17.54), (17.60), the last line of (17.75) and (17.76) is a consequence of the absence of the displacement fields u in the coefficients ℓ_{nm}, which, in turn, follows from translational invariance. If the ℓ_{nm} were functions of q the canonical formalism presented above would have led to q dependent measures,

$$\int \mathscr{D}q \sqrt{\frac{\ell_{NN}(q)}{2\pi i}} \left(\text{or} \int \mathscr{D}u \sqrt{\frac{\ell_{NN}(u)}{2\pi}} \right),$$

$$\int \mathscr{D}q \sqrt{\frac{\ell_{NN}(q)}{2\pi i}} \det(\ell/2\pi i)^{-1/2} \left(\text{or} \int \mathscr{D}u \sqrt{\frac{\ell_{NN}(u)}{2\pi}} \det(\ell/2\pi)^{-1/2} \right),$$

$$\int \mathscr{D}q \sqrt{\frac{b(q)}{2\pi i}} \left(\text{or} \int \mathscr{D}u \sqrt{\frac{b(u)}{2\pi}} \right),$$

$$\int \mathscr{D}q \sqrt{\frac{b(q)}{2\pi i}} \frac{2\pi i}{\sqrt{ab - c^2}} \left(\text{or} \int \mathscr{D}u \sqrt{\frac{b(u)}{2\pi}} \frac{2\pi}{\sqrt{ab - c^2}} \right).$$

17.4. SECOND-GRADIENT ELASTICITY

Let us now apply these techniques to linear elasticity with second gradients of the strain tensor. In an isotropic continuum, the invariance arguments given in Section 17.2 lead to the following most general energy involving second derivatives,

$$E = \int d^D x [b_1' \partial_i \partial_\ell u_\ell \partial_i \partial_\ell u_\ell + b_2' \partial_i^2 u_\ell \partial_k^2 u_\ell]. \tag{17.77}$$

By a partial integration, this can be cast in a form involving the strain $u_{k\ell}(\mathbf{x})$ and the rotation field $\omega_i(\mathbf{x}) = \frac{1}{2} \varepsilon_{ijk} \partial_j u_k(\mathbf{x})$,

$$E = \int d^D x (b_1 \partial_i u_{\ell\ell} \partial_i u_{\ell\ell} + b_2 \partial_i \omega_j \partial_i \omega_j), \tag{17.78}$$

with

$$b_1 = b_1' + b_2, \qquad b_2 = 4b_2'. \tag{17.79}$$

This follows from the equality of the first terms in (17.77) and (17.78), with the second term being equal to

$$\frac{1}{4} \int d^D x \, \partial_i \varepsilon_{jk\ell} \partial_k \partial_i \varepsilon_{jk'\ell'} \partial_{k'} u_{\ell'} = \frac{1}{4} \int d^D x (\partial_i \partial_k u_\ell \partial_i \partial_k u_\ell - \partial_i \partial_k u_\ell \partial_i \partial_\ell u_k)$$

$$= \frac{1}{4} \int d^D x (\partial_i^2 u_\ell \partial_k^2 u_\ell - \partial_i \partial_\ell u_\ell \partial_i \partial_\ell u_\ell). \tag{17.80}$$

The first term in (17.78) merely gives a higher gradient correction to the strain field. The second term is, on the other hand, qualitatively new since it contains the local rotation field and accounts for energies due to local twists in the material. We shall mainly be interested in the new features brought about by this term. For convenience, we shall write the new elastic constants as

$$b_1 = (2\mu + \lambda)\ell'^2/2, \qquad b_2 = 2\mu\ell^2, \tag{17.81}$$

where ℓ, ℓ' are two length scales characterizing the strength of b_1, b_2. We then arrive at the following elastic energy density,

$$\begin{aligned} E &= \int d^D x (e(\mathbf{x}) - f_i(\mathbf{x}) u_i(\mathbf{x})) \\ &= \int d^D x \left[\mu u_{ij}^2 + \frac{\lambda}{2} u_{\ell\ell}^2 + \frac{1}{2}(2\mu+\lambda)\ell'^2 (\partial_i u_{\ell\ell})^2 + 2\mu\ell^2 (\partial_i \omega_j)^2 - f_i(\mathbf{x}) u_i(\mathbf{x}) \right]. \end{aligned} \tag{17.82}$$

In terms of the displacement field, this takes the alternative form

$$\begin{aligned} E = \int d^D x \Bigg[& \frac{\mu}{2}(\partial_i u_j)^2 + \frac{\mu+\lambda}{2}(\partial_\ell u_\ell)^2 + \frac{2\mu+\lambda}{2}\ell'^2 \partial_i \partial_\ell u_\ell \partial_i \partial_\ell u_\ell \\ & + \frac{\mu\ell^2}{2}(\partial_\ell^2 u_i \partial_\ell^2 u_i - \partial_i \partial_\ell u_\ell \partial_i \partial_\ell u_\ell) - f_i u_i \Bigg]. \end{aligned} \tag{17.83}$$

From this it is easy to obtain the Euler-Lagrange equation

$$\begin{aligned} & -\mu \boldsymbol{\partial}^2 u_i - (\mu+\lambda)\partial_i \partial_\ell u_\ell + (2\mu+\lambda)\ell'^2 \boldsymbol{\partial}^2 \partial_i \partial_\ell u_\ell \\ & \quad + \mu\ell^2 (\boldsymbol{\partial}^4 u_i - \boldsymbol{\partial}^2 \partial_i \partial_\ell u_\ell) = f_i(\mathbf{x}). \end{aligned} \tag{17.84}$$

Going over to momentum space and regrouping the terms according to longitudinal and transversal projections, this becomes [compare (1.75)]

$$\mu\mathbf{q}^2(1+\ell^2\mathbf{q}^2)\left(\delta_{ij} - \frac{q_i q_j}{\mathbf{q}^2}\right) u_j(\mathbf{q}) + (2\mu+\lambda)\mathbf{q}^2(1+\ell'^2\mathbf{q}^2)\frac{q_i q_j}{\mathbf{q}^2} u_j(\mathbf{q}) = f_i(\mathbf{q}), \tag{17.85}$$

which is immediately inverted to give,

$$
\begin{aligned}
u_i(\mathbf{q}) &\equiv G_{ij}(\mathbf{q}) f_i(\mathbf{q}) \\
&= \left[\frac{1}{\mu \mathbf{q}^2 (1 + \ell^2 \mathbf{q}^2)} \left(\delta_{ij} - \frac{q_i q_j}{\mathbf{q}^2} \right) + \frac{1}{(2\mu + \lambda) \mathbf{q}^2 (1 + \ell'^2 \mathbf{q}^2)} \frac{q_i q_j}{\mathbf{q}^2} \right] f_j(\mathbf{q}) \\
&= \left[\frac{1}{\mu \mathbf{q}^2 (1+\ell^2 \mathbf{q}^2)} \delta_{ij} + \frac{1}{\mathbf{q}^4} \left(-\frac{1}{\mu(1+\ell^2 \mathbf{q}^2)} + \frac{1}{(2\mu+\lambda)(1+\ell'^2 \mathbf{q}^2)} \right) q_i q_j \right] f_j(\mathbf{q}).
\end{aligned}
\tag{17.86}
$$

In order to return to **x**-space we introduce the partial fractions

$$
\begin{aligned}
&\frac{1}{\mu \mathbf{q}^2 (1 + \ell^2 \mathbf{q}^2)} = \frac{1}{\mu} \left(\frac{1}{\mathbf{q}^2} - \frac{1}{\mathbf{q}^2 + 1/\ell^2} \right), \\
&\frac{1}{\mu \mathbf{q}^4 (1 + \ell^2 \mathbf{q}^2)} = \frac{1}{\mu \mathbf{q}^2} \left(\frac{1}{\mathbf{q}^2} - \frac{1}{\mathbf{q}^2 + 1/\ell^2} \right) = \frac{1}{\mu \mathbf{q}^4} - \frac{\ell^2}{\mu} \left(\frac{1}{\mathbf{q}^2} - \frac{1}{\mathbf{q}^2 + 1/\ell^2} \right), \\
&\frac{1}{(2\mu + \lambda) \mathbf{q}^4 (1 + \ell'^2 \mathbf{q}^2)} = \frac{1}{(2\mu + \lambda) \mathbf{q}^2} \left(\frac{1}{\mathbf{q}^2} - \frac{1}{\mathbf{q}^2 + 1/\ell'^2} \right) \\
&\qquad = \frac{1}{(2\mu + \lambda) \mathbf{q}^4} - \frac{\ell'^2}{2\mu + \lambda} \left(\frac{1}{\mathbf{q}^2} - \frac{1}{\mathbf{q}^2 + 1/\ell'^2} \right).
\end{aligned}
\tag{17.87}
$$

In three dimensions, the Fourier transform of $1/\mathbf{q}^2$ and $1/\mathbf{q}^4$ are $1/4\pi R$ and $-R/8\pi$, respectively. For $1/(\mathbf{q}^2 + 1/\ell^2)$ we calculate as in (1.81),

$$
\begin{aligned}
v_{1/\ell}(\mathbf{x} - \mathbf{x}') &= \int \frac{d^3 q}{(2\pi)^3} \frac{e^{i\mathbf{q} \cdot (\mathbf{x} - \mathbf{x}')}}{\mathbf{q}^2 + 1/\ell^2} = \frac{1}{4\pi^2} \int_0^\infty \frac{dq\, q^2}{q^2 + 1/\ell^2} \int_{-1}^{1} d\cos\theta\, e^{iqR\cos\theta} \\
&= \frac{1}{4\pi^2 R} \int_{-\infty}^{\infty} dq \frac{q}{q^2 + 1/\ell^2} \sin qR \\
&= \frac{1}{8\pi^2} \int_{-\infty}^{\infty} dq \left(\frac{1}{q - i/\ell} + \frac{1}{q + i/\ell} \right) \frac{e^{iqR} - e^{-iqR}}{2i}
\end{aligned}
\tag{17.88}
$$

Closing the contour of integration in the upper half plane for the first expansion and the lower one for the second, we find from the residues the Yukawa potential

$$v_{1/\ell}(\mathbf{x}-\mathbf{x}') = \frac{1}{4\pi R} e^{-R/\ell}. \tag{17.89}$$

Thus we can rewrite (1.87) in **x**-space as

$$\frac{1}{\mu \mathbf{q}^2(1+\ell^2\mathbf{q}^2)} \triangleq \frac{1}{\mu}\frac{1}{4\pi R}(1-e^{-R/\ell}), \tag{17.90}$$

$$\frac{1}{\mu \mathbf{q}^4(1+\ell^2\mathbf{q}^2)} \triangleq -\frac{1}{\mu}\frac{R}{8\pi} - \frac{\ell^2}{\mu}\frac{1}{4\pi R}(1-e^{-R/\ell}),$$

$$\frac{1}{(2\mu+\lambda)\mathbf{q}^4(1+\ell'^2\mathbf{q}^2)} \triangleq -\frac{1}{2\mu+\lambda}\frac{R}{8\pi} + \frac{\ell'^2}{2\mu+\lambda}\frac{1}{4\pi R}(1-e^{-R/\ell'}). \tag{17.91}$$

Hence (17.86) becomes, in **x**-space,

$$u_i(\mathbf{x}) = \frac{1}{4\pi}\int d'^3x' \left[\frac{1}{\mu R}(1-e^{-R/\ell})\,\delta_{ij} - \frac{1}{\mu}\partial_i\partial_j\left(\frac{R}{2} + \ell^2\frac{1}{R}(1-e^{-R/\ell})\right)\right.$$
$$\left. + \frac{1}{2\mu+\lambda}\partial_i\partial_j\left(\frac{R}{2} + \ell'^2\frac{1}{R}(1-e^{-R/\ell'})\right)\right] f(\mathbf{x}'). \tag{17.92}$$

In the special case $\ell = 0$, $\ell' = 0$ we recover the previous result (1.90).

Notice that the higher powers of **q** in the field equations regularize the Green function at the origin, $G_{ij}(\mathbf{0})$. The δ_{ij} part goes with $(1/R)$ $(1-e^{-R/\ell}) \sim (1/\ell) - (R/2\ell^2)$ which is regular at $R = 0$. In the derivative part we can expand

$$\partial_i\partial_j\left(\frac{R}{2} + \ell^2\frac{1-e^{-R/\ell}}{R}\right) \sim \partial_i\partial_j\left(\frac{R}{2} + \frac{\ell^2}{R}\left(\frac{R}{\ell} - \frac{R^2}{2\ell^2} + \frac{R^3}{6\ell^2}\right)\right)$$
$$= \partial_i\partial_j\left(\ell + \frac{R^2}{6\ell} - \dots\right) = \frac{1}{3\ell}\delta_{ij} + O(R), \tag{17.93}$$

which is also regular at $R = 0$. Hence we find

$$G_{ij}(\mathbf{0}) = \frac{1}{4\pi}\delta_{ij}\left(\frac{1}{\mu\ell} - \frac{1}{3\mu\ell} + \frac{1}{(2\mu+\lambda)\cdot 3\ell'}\right). \tag{17.94}$$

17.5. CANONICAL FORMALISM FOR SECOND-GRADIENT ELASTICITY

Let us now set up the canonical formalism for the elastic energy (17.82). According to (17.65) the "canonical momenta" are given by

$$\sigma_{ij}^{s} = \frac{\partial e}{\partial u_{ij}} = i(2\mu u_{ij} + \lambda \delta_{ij} u_{\ell\ell}),$$

$$\tau_i = \frac{\partial e}{\partial \partial_i u_{\ell\ell}} = i(2\mu + \lambda)\, \ell'^2\, \partial_i u_{\ell\ell},$$

$$\tau_{ij} = \frac{\partial e}{\partial \partial_i \omega_j} = i 4\mu \ell^2 \partial_i \omega_j. \tag{17.95}$$

Generalizing the expressions (17.75), (17.76) to several space dimensions we arrive at the two partition functions of second-gradient elasticity,

$$Z[f_i] = \int \mathscr{D} u_i(\mathbf{x}) \exp\left\{ -\frac{1}{T} \int d^D x \right.$$
$$\left. \times \left[\mu u_{ij}^2 + \frac{\lambda}{2} u_{\ell\ell}^2 + \frac{2\mu + \lambda}{2} \ell'^2 (\partial_i u_{\ell\ell})^2 + 2\mu \ell^2 (\partial_i \omega_j)^2 - f_i u_i \right] \right\} \tag{17.96a}$$

and its canonical form, the stress representation

$$Z[f_i] = \int \mathscr{D} u_i(\mathbf{x}) \int \mathscr{D} \sigma_{ij}^{s}(\mathbf{x}) \int \mathscr{D} \tau_i'(\mathbf{x}) \int \mathscr{D} \tau_{ij}(\mathbf{x})$$
$$\times \exp\left\{ -\frac{1}{T} \int d^D x \left[\frac{1}{4\mu} \left(\sigma_{ij}^{s2} - \frac{\nu}{1+\nu} \sigma_{\ell\ell}^{s2} \right) + \frac{1}{2(2\mu + \lambda)\, \ell'^2} \tau_i'^2 \right.\right.$$
$$\left.\left. + \frac{1}{8\mu\ell^2} \tau_{ij}^2 - i\sigma_{ij}^{s} (\partial_i u_j + \partial_j u_i)/2 - i\tau_i' \partial_i \partial_\ell u_\ell - i\tau_{ij} \partial_i \omega_j - f_i u_i \right] \right\}. \tag{17.96b}$$

The superscript s indicates that the "momentum variable" σ_{ij}^{s} is a symmetric tensor such that in $\int \mathscr{D} \sigma_{ij}$ only the components $i \geq j$ need be integrated.

Some trivial overall factors have been omitted in the measure. The equality of the two forms (17.96a) and (17.96b) is verified, as usual, by performing a quadratic completion in the momentum variables and

integrating them out. The complete squares arising in this process show that, in equilibrium, the fluctuating momenta σ_{ij}^s, τ_i', τ_{ij} are given by (17.95). In the limit $\ell = \ell' = 0$, the τ_i', τ_{ij} integrals are frozen out and we recover the usual path integral (1.44) or (1.45) of linear elasticity.

It is useful to introduce the ω_i variable as an independent field and to ensure the connection $\omega_i = \frac{1}{2}\varepsilon_{ijk}\,\partial_j u_k$ via an additional functional integration over an antisymmetric tensor field σ_{ij}^a. Then $Z[f_i]$ takes the form

$$\begin{aligned} Z[f_i] = \int \mathscr{D} u_i(\mathbf{x}) \int \mathscr{D} \sigma_{ij}(\mathbf{x}) \int \mathscr{D} \tau_i'(\mathbf{x}) \int \mathscr{D} \tau_{ij}(\mathbf{x}) \int \mathscr{D} \omega_i(\mathbf{x}) \\ \times \exp\left\{ -\frac{1}{T} \int d^D x \left[\frac{1}{4\mu} \left(\sigma_{ij}^{s2} - \frac{\nu}{1+\nu} \sigma_{\ell\ell}^{s2} \right) + \frac{1}{2(2\mu+\lambda)\ell'^2} \tau_i'^2 \right.\right. \\ \left.\left. + \frac{1}{8\mu\ell^2} \tau_{ij}^2 - i\sigma_{ij}(\partial_i u_j - \varepsilon_{ijk}\omega_k) - i\tau_i' \partial_i \partial_\ell u_\ell - i\tau_{ij}\partial_i \omega_i - f_i u_i \right] \right\}. \end{aligned} \tag{17.97}$$

We have joined the antisymmetric matrix σ_{ij}^a with σ_{ij}^s and formed the tensor $\sigma_{ij} = \sigma_{ij}^s + \sigma_{ij}^a$ which has no symmetry at all.

If we perform the integrals over the variable $u_i(\mathbf{x})$ and $\omega_i(\mathbf{x})$ we find the conservation laws

$$\partial_i(\sigma_{ij} - \delta_{ij}\partial_k \tau_k) = -f_j, \tag{17.98a}$$

$$\partial_i \tau_{ij} = -\varepsilon_{jk\ell}\,\sigma_{k\ell}\,. \tag{17.98b}$$

Identifying

$$\sigma_{ij}^{\text{phys}} = \sigma_{ij} + \delta_{ij}\partial_k \tau_k \tag{17.99}$$

as the physical stress tensor, the first relation reads

$$\partial_i \sigma_{ij}^{\text{phys}} = -f_i \tag{17.100}$$

and ensures the conservation of stress in the absence of external volume forces. Since the additional piece in $\sigma_{ij}^{\text{phys}}$ is symmetric in i and j, the second equation can also be written as

$$\partial_i \tau_{ij} = -\varepsilon_{jk\ell}\,\sigma_{k\ell}^{\text{phys}}. \tag{17.101}$$

This is just the Cosserat equation (16.8) relating the torque stress τ_{ij} to the antisymmetric part of the physical stress tensor.

As expected, the inclusion of higher gradients has led to the appearance of a field equation for the rotational degrees of freedom which describe the balance of torques and which is the stress analogue of the equation

$$\partial_i \alpha_{ij} = -\varepsilon_{jk\ell}\,\Theta_{k\ell}.$$

NOTES AND REFERENCES

The Cosserat medium is introduced by
E. and F. Cosserat, *Theories des Corps Deformables* (Herman, Paris).
It is further developed by
A.L. Aero and E.V. Kuvshinskii, *Fiz. Tverd. Tela* **2** (1960) 1399,
G. Grioli, *Ann. di Mat. Pura et Appl.* Secr. IV, **50** (1960) 389,
R.A. Toupin, *Arch. Rat. Mech. Anal.* **11** (1962) 385, **17** (1964) 113,
R.D. Mindlin and H.F. Tierstein, *ibid*, **11** (1962) 415,
R.D. Mindlin, *J. Elast.* **2** (1972) 217,
M. Sokolowski, *Theory of Couple-Stresses in Bodies with Constrained Rotations* (Springer, Wien, 1970).
[In some of the references, the gradient terms are, inconsistently, omitted and they find the singular behavior of the elastic Green function at the origin puzzling (see, for example, the remarks of M. Sokolowski, *op. cit.*, p. 46).]
See also the review of continuum mechanics by
C. Truesdell and R.A. Toupin, in *Handbuch der Physik*, III/1, ed. S. Flügge (Springer, Heidelberg, 1960).

CHAPTER EIGHTEEN

INTERACTION ENERGY OF DEFECTS IN SECOND-GRADIENT ELASTICITY

Our goal is to investigate how our model of defect melting must be modified if we are to account for the higher gradient terms in linear elasticity. For this it is first necessary to understand the elastic properties of a continuous material which has undergone a given set of plastic deformations.

18.1. ELASTIC ENERGY OF PLASTIC DEFORMATIONS

The elastic energy is given by

$$E_{\mathrm{el}} = \int d^3x \left\{ \mu u_{ij}^2 + \frac{\lambda}{2} u_{\ell\ell}^2 + \frac{2\mu + \lambda}{2} \ell'^2 (\partial_i u_{\ell\ell})^2 + 2\mu \ell^2 (\partial_i \omega_j)^2 \right\}. \tag{18.1}$$

In the presence of plastic deformations, the elastic energy is measured by the deviations of the total strain u_{ij} and the total gradient $\partial_i \omega_j$ from the plastic strain u_{ij}^p and the plastic gradient $\partial_i \omega_j^p$, respectively:

$$E = \int d^3x \left\{ \mu (u_{ij} - u_{ij}^p)^2 + \frac{\lambda}{2} (u_{\ell\ell} - u_{\ell\ell}^p)^2 + \frac{2\mu + \lambda}{2} \ell'^2 (\partial_i (u_{\ell\ell} - u_{\ell\ell}^p))^2 + 2\mu \ell^2 (\partial_i \omega_j - \partial_i \omega_j^p)^2 \right\}. \tag{18.2}$$

General plastic deformations were analyzed in Section 2.9. There we found that a defect line of Burgers vector b_ℓ and Frank vector Ω_ℓ is given by [see Eq. (2.61)]

$$u_{ij}^p = \tfrac{1}{2}(\beta_{ij}^p + \beta_{ji}^p) = \tfrac{1}{2}(\delta_i(S) B_j + (ij)), \tag{18.3}$$

and [see Eq. (2.65)]

$$\partial_i \omega_j^p = \varkappa_{ij}^p = \tfrac{1}{2}\varepsilon_{jk\ell}\partial_i[\delta_k(S) B_\ell - \delta(V)\varepsilon_{\ell qB}\Omega_q] = \tfrac{1}{2}\varepsilon_{jk\ell}\partial_i \beta_{k\ell}^p + \phi_{ij}^p, \tag{18.4}$$

where

$$B_\ell = b_\ell + \varepsilon_{\ell qr}\Omega_q x_r \tag{18.5}$$

is the total Burgers vector and

$$\beta_{k\ell}^p = \delta_k(S) B_\ell, \tag{18.6}$$

$$\phi_{k\ell}^p = \delta_k(S)\Omega_\ell \tag{18.7}$$

are the plastic distortions and rotations, respectively. Thus we can write

$$E = \int d^3x \Big\{ \mu(u_{ij} - (\beta_{ij}^p + \beta_{ji}^p)/2)^2 + \frac{\lambda}{2}(u_{\ell\ell} - \beta_{\ell\ell}^p)^2 + \frac{2\mu + \lambda}{2}\ell'^2(\partial_i(u_{\ell\ell} - \beta_{\ell\ell}^p))^2 + 2\mu\ell^2(\partial_i\omega_i - 1/2\,\varepsilon_{ik\ell}\partial_j\beta_{k\ell}^p - \phi_{ji}^p)^2 \Big\}. \tag{18.8}$$

Let us study the defect gauge invariance of this expression. The general trivial Volterra operation of translating and rotating a piece of material corresponds to a pure gauge transformation,

$$u_\ell(\mathbf{x}) \to u_\ell(\mathbf{x}) - \delta(V)(b_\ell + \varepsilon_{\ell qr}\Omega_q x_r). \tag{18.9}$$

Let us abbreviate this by

$$u_\ell(\mathbf{x}) \to u_\ell(\mathbf{x}) + N_\ell(\mathbf{x}) + \varepsilon_{iqr} M_q(\mathbf{x}) x_r \equiv u_\ell(\mathbf{x}) + \tilde{N}_\ell(\mathbf{x}), \tag{18.10}$$

with

$$N_\ell(\mathbf{x}) \equiv -\delta(V) b_\ell, \tag{18.11}$$

$$M_\ell(\mathbf{x}) \equiv -\delta(V) \Omega_\ell, \tag{18.12}$$

$$\widetilde{N}_\ell(\mathbf{x}) = -\delta(V) B_\ell. \tag{18.13}$$

From (18.10) we find directly the pure gauge transformations of the rotation angle,

$$\omega_i \to \omega_i + \tfrac{1}{2} \varepsilon_{ik\ell} \partial_k \widetilde{N}_\ell. \tag{18.14}$$

These transformations must accompany any shift of the Volterra cutting surface S to S' with V being the volume enclosed by $S' - S$.

From (18.6) and (18.7) we see that such a shift results in the following changes of the plastic distortions and rotations:

$$\begin{aligned} \beta^p_{k\ell} &\to \beta^p_{k\ell} + (\delta_k(S') - \delta_k(S)) B_\ell = \beta^p_{k\ell} - (\partial_k \delta(V)) B_\ell \\ &= \beta^p_{k\ell} - \partial_k(\delta(V) B_\ell) + \varepsilon_{\ell qk} \delta(V) \Omega_q = \beta^p_{k\ell} + \partial_k \widetilde{N}_\ell - \varepsilon_{\ell qk} M_q, \end{aligned} \tag{18.15}$$

$$\phi^p_{k\ell} \to \phi^p_{k\ell} + (\delta_k(S') - \delta_k(S)) \Omega_\ell = \phi^p_{k\ell} - \partial_k \delta(V) \Omega_\ell = \phi^p_{k\ell} + \partial_k M_\ell. \tag{18.16}$$

Inserting the transformation laws (18.10), (18.14), (18.15) and (18.16) into the energy (18.8) we see that it is invariant under defect gauge transformations, as it should.

There is yet one subtlety which must be noted in this construction. In the absence of plastic deformations, the rotation field ω_i satisfies $\partial_i \omega_i = 0$. For the plastic version, however, this is no longer true since in the presence of defects [recall (2.77)]

$$\varkappa^p_{ii} = \partial_i \omega_i = \tfrac{1}{2} \alpha_{ii}. \tag{18.17}$$

This leads us to introduce another energy expression,

$$\begin{aligned} &2\mu\ell^2\varepsilon \int d^3x (\partial_i \omega_j - \partial_i \omega^p_j)(\partial_j \omega_i - \partial_j \omega^p_i) \\ &= 2\mu\ell^2\varepsilon \int d^3x (\partial_i \omega_j - 1/2\, \varepsilon_{jk\ell} \partial_i \beta^p_{k\ell} - \phi^p_{ij})(\partial_j \omega_i - 1/2\, \varepsilon_{ik\ell} \partial_j \beta^p_{k\ell} - \phi^p_{ji}), \end{aligned} \tag{18.18}$$

which, in the absence of a plastic bend-twist, would be a pure surface term, and an energy

$$2\mu\ell^2\varepsilon' \int d^3x(\partial_i\omega_i - \partial_i\omega_i^p)^2, \tag{18.18'}$$

which can be directly expressed as an extra core energy of dislocations

$$8\mu\ell^2\varepsilon' \int d^3x\,\alpha_{ii}, \tag{18.18''}$$

and needs no further treatment; it will be ignored hence forth.

We shall thus study at the partition function of elastic fluctuations in the presence of plastic deformations,

$$\begin{aligned} Z = \int \mathscr{D}u_i(\mathbf{x}) \exp\Bigg\{ -\frac{1}{T}\int d^3x \Bigg\{ & \mu(u_{ij} - u_{ij}^p)^2 + \frac{\lambda}{2}(u_{\ell\ell} - u_{\ell\ell}^p)^2 \\ & + \frac{2\mu+\lambda}{2}\ell'^2(\partial_i(u_{\ell\ell} - u_{\ell\ell}^p))^2 \\ & + 2\mu\ell^2[(\partial_i\omega_j - \partial_i\omega_j^p)^2 + \varepsilon(\partial_i\omega_j - \partial_i\omega_j^p)(\partial_j\omega_i - \partial_j\omega_i^p)] \Bigg\}, \end{aligned} \tag{18.19}$$

with

$$u_{ij}^p = \tfrac{1}{2}(\beta_{ij}^p + \beta_{ji}^p), \qquad \partial_i\omega_j^p = \tfrac{1}{2}\varepsilon_{jk\ell}\,\partial_i\beta_{k\ell}^p + \phi_{ij}^p. \tag{18.20}$$

Invariance under defect-gauge transformations can be used to bring $\beta_{k\ell}^p$ into standard form. A convenient gauge is

$$\beta_{k\ell}^p = \beta_{\ell k}^p = u_{k\ell}^p, \qquad \beta_{3\ell}^p = u_{3\ell}^p = 0. \tag{18.21}$$

The symmetry of $\beta_{k\ell}^p$ is reached by an appropriate choice of M_p. After this, we can perform a further gauge transformation with arbitrary $\bar{N}_\ell$ and $M_p = \varepsilon_{pk\ell}\,\partial_k\bar{N}_\ell$ so that $\beta_{k\ell}^p$ remains symmetric while the strain changes like

$$u_{k\ell}^p \to u_{k\ell}^p + \tfrac{1}{2}(\partial_k\bar{N}_\ell + \partial_\ell\bar{N}_k). \tag{18.22}$$

In this manner $u_{k\ell}^p$ can be brought to the desired gauge $\beta_{3\ell}^p = u_{3\ell}^p = 0$.

18.2. CANONICAL FORM OF THE STRESS PARTITION FUNCTION

It is useful to rewrite (18.19) in canonical form, corresponding to (17.97), in which $u_i(\mathbf{x})$ and $\omega_i(\mathbf{x})$ are treated as *independent* variables and in which

the relation between them is enforced by an integration over an antisymmetric part of the stress tensor. We can easily verify that Z becomes

$$Z = \int \mathscr{D}u_i \int \mathscr{D}\sigma_{ij} \int \mathscr{D}\omega_i \int \mathscr{D}\tau'_i \int \mathscr{D}\tau_{ij}$$
$$\times \exp\left\{ -\frac{1}{T}\int d^3x \left[\frac{1}{4\mu}\left(\sigma^{s2}_{ij} - \frac{\nu}{1+\nu}\sigma^{s2}_{\ell\ell} \right) + \frac{1}{2(2\mu+\lambda)\ell'^2}\tau'^2_i \right.\right.$$
$$\left.\left. + \frac{1}{8\mu\ell^2}(\delta_1\tau^2_{ij} + \delta_2\tau^2_{\ell\ell}) \right] + i\int d^3x [\sigma_{ij}(\partial_i u_j - \varepsilon_{ijk}\omega_k - \beta^p_{ij}) \right.$$
$$\left. + \tau'_i(\partial_i\partial_\ell u_\ell - \partial_i\beta^p_{\ell\ell}) + \tau_{ij}(\partial_i\omega_j - \phi^p_{ij})] \right\}, \tag{18.23}$$

where

$$\delta_1 \equiv 1/(1-\varepsilon^2), \qquad \delta_2 \equiv -\varepsilon\delta_1. \tag{18.24}$$

To see the equality we perform a quadratic completion and integrate out σ^s_{ij}, τ'_i, τ_{ij}. The integral over σ^a_{ij} enforces the connection $\omega_i = \frac{1}{2}\varepsilon_{ijk}\partial_j u_k$. It is interesting to see the manner by which this generates the $\beta^p_{k\ell}$ parts of the $\partial_i\omega^p_j$ gradient terms of (18.19). Notice that in the canonical form (18.23), where $\omega_i(\mathbf{x})$ is an *independent* variable, the plastic rotation ϕ^p_{ji} plays a more fundamental role than the plastic bend-twists $\partial_j\omega^p_i$ which were the most natural plastic quantities in the original form (18.2).

Defect-gauge invariance of (18.23) holds now with respect to the transformation [compare (18.9)–(18.16)]

$$u_\ell(\mathbf{x}) \to u_\ell(\mathbf{x}) + \bar{N}_\ell(\mathbf{x}),$$
$$\beta^p_{k\ell}(\mathbf{x}) \to \beta^p_{k\ell}(\mathbf{x}) + \partial_k\bar{N}_\ell(\mathbf{x}) - \varepsilon_{k\ell p}M_p(\mathbf{x}), \tag{18.25}$$

$$\omega_i(\mathbf{x}) \to \omega_i(\mathbf{x}) + M_i(\mathbf{x}),$$
$$\phi^p_{ij}(\mathbf{x}) \to \phi^p_{ij}(\mathbf{x}) + \partial_i M_j(\mathbf{x}). \tag{18.26}$$

18.3. LATTICE MODEL OF DEFECT MELTING WITH SECOND-GRADIENT ELASTICITY

It is now straightforward to construct a suitable lattice model from the partition function (18.19). For the strain part, the procedure is clear. All

we have to do is to replace the continuous variable $\mathbf{x}$ by discrete lattice sites of a simple cubic lattice, the gradients ∂_i by lattice gradients ∇_i, and the plastic distortions $\beta^p_{k\ell}$ by integer numbers $n_{k\ell}$, multiplied by the lattice spacing a. When using rescaled variables $\gamma_i = (2\pi/a)u_i(\mathbf{x})$ we may simply take $\beta^p_{k\ell} = 2\pi n_{k\ell}$.

If we follow the same procedure for the rotation part we run into an immediate difficulty. In the continuum formulation, all quantities $u_i(\mathbf{x})$, $\omega_i(\mathbf{x})$ were infinitesimal. Only for this reason could we define the rotation field $\omega_i(\mathbf{x})$ by a simple differential operation,

$$\omega_i(\mathbf{x}) = \tfrac{1}{2}\varepsilon_{ijk}\partial_j u_k(\mathbf{x}).$$

On going over to a lattice, this relation has the trivial generalization

$$\omega_i(\mathbf{x}) = \tfrac{1}{2}(\nabla \times \mathbf{u})_i = \tfrac{1}{2}\varepsilon_{ijk}\nabla_j u_k(\mathbf{x}). \tag{18.27}$$

However, one should realize that this is a proper rotation field only for very smooth fields $u_k(\mathbf{x})$ and certainly cannot be maintained as soon as $u_k(\mathbf{x})$ has finite jumps across Volterra surfaces. We ran into a similar problem previously when we calculated the plastic quantities on a lattice. There, we resolved these difficulties by considering, instead of a finite translation plus rotation, a modified Volterra operation (16.45) which implied a "tangential approximation" to the rotation group.

In real crystals, the multivaluedness of the rotation angle is determined by the smallest finite discrete rotations around the symmetry axes. The derivation of the plastic distortions, however, was carried out in the continuum, where all quantities are infinitesimal. Thus it is obvious that in order to find a proper crystal version of the partition function (18.19) it is necessary to respect the full group structure of *finite rotations*. The result would be a non-Abelian gauge theory. This is somewhat discouraging since the defects in non-Abelian gauge theories pose complicated nonlinear problems which are far from being understood. Field theorists who have tried to explain the forces in elementary particle physics have studied such theories for several years now and progress has been rather limited. Faced with this difficulty, we have opted to proceed using the "tangential approximation." Within this approximation we consider (18.27) as the *definition* of an $\omega_i(\mathbf{x})$ field which plays the role of the rotation field $\omega_i(\mathbf{x})$ in the lattice model and which allows for integer-valued jumps in these quantities.

The model we are then led to has the following partition function

$$
\begin{aligned}
Z = \sum_{\{n_{ij},\, m_{ij}\}} \Phi[n_{ij},\, m_{ij}] \prod_{\mathbf{x},\, i} \left[\int_{-\infty}^{\infty} \frac{d\gamma_i(\mathbf{x})}{2\pi} \right] \\
\times \exp\left\{ -\beta \left[\frac{1}{4} \sum_{\mathbf{x},\, i,\, j} (\nabla_i \gamma_j + \nabla_j \gamma_i - 4\pi n_{ij}^s)^2 + \frac{\lambda}{2\mu} \sum_{\mathbf{x}} \left(\sum_i (\nabla_i \gamma_i - 2\pi n_{ii}^s) \right)^2 \right.\right. \\
+ \frac{2\mu + \lambda}{2} \frac{\ell'^2}{a^2} \sum_{\mathbf{x},\, i} (\nabla_i \nabla_\ell \gamma_\ell - 2\pi \nabla_i n_{\ell\ell}^s)^2 \\
+ \frac{\ell^2}{2a^2} \sum_{\mathbf{x}} [(\nabla_i \varepsilon_{jk\ell} \nabla_k \gamma_\ell - 2\pi(2m_{ij} + \nabla_i \varepsilon_{jk\ell} n_{k\ell}))^2 \\
+ \varepsilon (\nabla_i \varepsilon_{jk\ell} \nabla_k \gamma_\ell - 2\pi(2m_{ij} + \nabla_i \varepsilon_{jk\ell} n_{k\ell})) \\
\left.\left. \times (\nabla_j \varepsilon_{ik\ell} \nabla_k \gamma_\ell - 2\pi(2m_{ji} + \nabla_j \varepsilon_{ik\ell} n_{k\ell}))] \right] \right\},
\end{aligned}
\tag{18.28}
$$

where n_{ij}^s is the symmetric part of the jump numbers n_{ij} (which is half-integer for $i \neq j$). The canonical form of this partition functions is

$$
\begin{aligned}
Z = \left(\frac{1-\nu}{1+\nu} \right)^{N/2} (1+\varepsilon)^{-3N/2} (1-\varepsilon)^{-3N} \sum_{\{n_{ij},\, m_{ij}\}} \Phi[n_{ij},\, m_{ij}] \\
\times \prod_{\mathbf{x},\, i} \left[\int_{-\infty}^{\infty} \frac{d\gamma_i(\mathbf{x})}{2\pi} \right] \prod_{\mathbf{x},\, i} \left[\int_{-\infty}^{\infty} \frac{d\omega_i(\mathbf{x})}{2\pi} \right] \prod_{\mathbf{x},\, i<j} \left[\int_{-\infty}^{\infty} \frac{d\sigma_{ij}^s}{\sqrt{2\pi\beta}} \right] \prod_{\mathbf{x},\, i} \left[\frac{d\sigma_{ij}^s(\mathbf{x})}{\sqrt{4\pi\beta}} \right] \\
\times \prod_{\mathbf{x},\, i<j} \left[2 \int_{-\infty}^{\infty} d\sigma_{ij}^a(\mathbf{x}) \right] \prod_{\mathbf{x},\, i} \left[\frac{d\tau_i'(\mathbf{x})}{\sqrt{2\pi(2+\lambda/\mu)\beta\ell'^2/a^2}} \right] \prod_{\mathbf{x},\, i,\, j} \left[\int_{-\infty}^{\infty} \frac{d\tau_{ij}(\mathbf{x})}{\sqrt{8\pi\beta\ell^2/a^2}} \right] \\
\times \exp\left\{ -\frac{1}{\beta} \left[\sum_{\mathbf{x}} \frac{1}{4} \left(\sigma_{ij}^{s2} - \frac{\nu}{1+\nu} \sigma_{\ell\ell}^{s2} \right) + \frac{\mu a^2}{2(2\mu+\lambda)\ell'^2} \sum_{\mathbf{x}} \tau_i'^2 \right.\right. \\
+ \frac{a^2}{8\ell^2} \sum_{\mathbf{x}} (\delta_1 \tau_{ij}^2 + \delta_2 \tau_{\ell\ell}^2) + i \sum_{\mathbf{x}} \sigma_{ij} (\nabla_i \gamma_j - \varepsilon_{ijk} \omega_k - 2\pi n_{ij}) \\
\left.\left. + i \sum_{\mathbf{x}} \tau_i' (\nabla_i \nabla_\ell \gamma_\ell - 2\pi \nabla_i n_{\ell\ell}) + i \sum_{\mathbf{x}} \tau_{ij} (\nabla_i w_j - 2\pi m_{ij}) \right] \right\}.
\end{aligned}
\tag{18.29}
$$

The symbol $\Phi[n_{ij},\, m_{ij}]$ denotes a gauge-fixing functional which is necessary to remove in infinite overall factor due to gauge degeneracy. A simple choice is the quasi-symmetric gauge [recall Section 10.1] wherein

$$
\left.
\begin{aligned}
n_{ij} &= n_{ji} \\
n_{ij} &= n_{ji} + 1
\end{aligned}
\right\} \quad \text{if } n_{ij} + n_{ji} = \begin{cases} \text{even}, \\ \text{odd}, \end{cases}
\tag{18.30}
$$

and

$$n_{13} = 0, \qquad n_{22} = 0, \qquad n_{33} = 0. \tag{18.31}$$

$\Phi[n_{ij}, m_{ij}]$ contains the appropriate Kronecker δ's to enforce this gauge.

If n_{ij}, m_{ij} do not satisfy the conditions (18.30) and (18.31) we can always perform particular gauge transformations which achieve this goal. If we denote the antisymmetric part of n_{ij} by n^a_{ij}, these gauge transformations (18.10)–(18.16) are

$$n^s_{ij} \to n^{s0}_{ij} + \tfrac{1}{2}(\nabla_i \bar{N}_j + \nabla_j \bar{N}_i), \tag{18.32a}$$

$$n^a_{ij} \to n^{a0}_{ij} - \varepsilon_{ijk} M_k, \tag{18.32b}$$

$$m_{ij} \to m^0_{ij} + \nabla_i M_j, \tag{18.32c}$$

$$\gamma_\ell \to \gamma_\ell + 2\pi \bar{N}_\ell, \tag{18.33a}$$

$$\omega_\ell \to \omega_\ell + 2\pi M_\ell. \tag{18.33b}$$

We showed in Section 10.1 how to find integers N_i and M_i so that n_{ij} is quasi-symmetric and the three non-zero n^s_{ij} fields n^{s0}_{11}, n^{s0}_{12}, n^{s0}_{23} satisfy the further boundary conditions

$$\begin{aligned} &n^{s0}_{11}(x_1, x_2, 0) = 0, \quad n^{s0}_{12}(0, x_2, x_3) = 0, \quad n^{s0}_{23}(x_1, x_2, 0) = 0, \\ &\nabla_3 n^{s0}_{11}(x_1, 0, 0) = 0, \quad \nabla_2 n^{s0}_{12}(0, x_2, 0) = 0, \quad \nabla_3 n^{s0}_{23}(0, 0, x_3) = 0. \end{aligned} \tag{18.34}$$

Integrating out the γ_i and ω_i variables in (18.29) produces the proper conservation law of stresses and torque stresses, now with lattice derivatives:

$$\bar{\nabla}_i \sigma_{ij} = 0, \qquad \bar{\nabla}_i \tau_{ij} = -\varepsilon_{jk\ell} \sigma_{k\ell}. \tag{18.35}$$

For simplicity, we have ignored the τ'^2_i term since it produces only small quantitative corrections to linear elasticity[a].

The conservation laws are automatically satisfied by introducing the gauge fields $A_{\ell j}(\mathbf{x})$, $h_{\ell j}(\mathbf{x})$ and setting

[a]In the next sections this term will be included.

$$\sigma_{ij} = \varepsilon_{ik\ell}\bar{\nabla}_k A_{\ell j}(\mathbf{x}-\boldsymbol{\ell}),$$
$$\tau_{ij} = \varepsilon_{ik\ell}\bar{\nabla}_k h_{\ell j}(\mathbf{x}-\boldsymbol{\ell}) + \delta_{ij}A_{\ell\ell}(\mathbf{x}-\boldsymbol{\ell}) - A_{ji}(\mathbf{x}-\mathbf{j}). \tag{18.36}$$

The stresses are invariant under the following local gauge transformations

$$A_{\ell j}(\mathbf{x}) \to A_{\ell j}(\mathbf{x}) + \nabla_\ell \Lambda_j(\mathbf{x}), \tag{18.37}$$

$$h_{\ell j}(\mathbf{x}) \to h_{\ell j}(\mathbf{x}) + \nabla_\ell \xi_j(\mathbf{x}) - \varepsilon_{\ell jk}\Lambda_k(\mathbf{x}+\boldsymbol{\ell}). \tag{18.38}$$

Just as in our previous treatment of three-dimensional defects within classical elasticity, these have the same structure as the gauge transformations on the defect fields (18.15) and (18.16). The only difference is that the stress-gauge transformations are continuous while the defect-gauge transformations are integer.

In terms of $A_{i\ell}$, $h_{i\ell}$ the coupling to the defect-gauge fields becomes, after a partial integration in the last terms of the exponents (18.29),

$$-2\pi i \sum_{\mathbf{x}} A_{\ell j}(\mathbf{x})(\varepsilon_{\ell ki}\nabla_k n_{ij}(\mathbf{x}+\boldsymbol{\ell}) + \delta_{\ell j} m_{kk}(\mathbf{x}+\boldsymbol{\ell}) - m_{j\ell}(\mathbf{x}+\boldsymbol{\ell}))$$
$$- 2\pi i \sum_{\mathbf{x}} h_{\ell j}(\mathbf{x})\,\varepsilon_{\ell ki}\nabla_k m_{ij}(\mathbf{x}+\boldsymbol{\ell}). \tag{18.39}$$

Comparing the sources of $A_{\ell j}(\mathbf{x})$ and $h_{\ell j}(\mathbf{x})$ with (2.69) and (2.68) and recalling that n_{ij} and m_{ij} are the lattice versions of plastic distortions and rotations, we may identify these sources with the lattice versions of dislocation and disclination densities, $\bar{\alpha}_{\ell i}(\mathbf{x})$ and $\bar{\Theta}_{\ell i}(\mathbf{x})$, respectively, and write the interaction as

$$\frac{1}{T}E_{\text{int}} = -2\pi i \sum_{\mathbf{x}} (A_{\ell i}\bar{\alpha}_{\ell i} + h_{\ell i}\bar{\Theta}_{\ell i}). \tag{18.40}$$

In Section 16.1 we showed that the defect densities satisfy the conservation laws [see Eqs. (16.3), (16.5)]

$$\bar{\nabla}_\ell \bar{\alpha}_{\ell i}(\mathbf{x}) = -\varepsilon_{ik\ell}\bar{\Theta}_{k\ell}(\mathbf{x}-\mathbf{k}), \quad \bar{\nabla}_\ell \bar{\Theta}_{\ell i}(\mathbf{x}) = 0. \tag{18.41}$$

These guarantee the stress-gauge invariance of E_{int}, as can easily be verified by inserting the gauge transformations (18.37) and (18.38) and performing a couple of partial integrations.

18.4. CALCULATION OF THE INTERACTION ENERGY OF DEFECTS VIA STRESS-GAUGE FIELDS

Let us now see what the interaction energy of defects is in second-gradient elasticity. The problem is quite involved and it is preferable to study it in the continuum limit where we can use helicity amplitudes. We decompose A_{ij} and h_{ij} into $A^{(s,h)}$, $h^{(s,h)}$ according to the rules of Chapter 4. Then we can use formula (4.110) and find [compare Eqs. (16.23)]

$$\sigma^{(2,\pm 2)}(\mathbf{k}) = \pm kA^{(2,\pm 2)}(\mathbf{k}), \quad \sigma^{+\pm}(\mathbf{k}) = \pm kA^{+\pm}(\mathbf{k}), \quad \sigma^{-+}(\mathbf{k}) = 0,$$
$$\sigma^{(1,0)}(\mathbf{k}) = -kA^{L}(\mathbf{k}), \quad \sigma^{L}(\mathbf{k}) = -kA^{(1,0)}(\mathbf{k}), \quad \sigma^{L'}(\mathbf{k}) = 0. \tag{18.42}$$

The three components A^{-+}, A^{--} and $A^{L'}$ do not contribute to the stresses. Note that the momenta in these and the following formulas correspond to the continuum limit of the dimensionless lattice gradient ∇_i and therefore measure the physical momenta in units of $1/a$.

The stress energy contains only the symmetric parts of σ_{ij}, i.e., the spin-2 and spin-0 helicity components, so that it is equal to

$$\sum_{\mathbf{k}} \frac{k^2}{4\beta}\left\{|A^{(2,2)}|^2 + |A^{(2,-2)}|^2 + \frac{1-\nu}{1+\nu}|A^{(1,0)}|^2 + \frac{1}{2}|A^{++}|^2 + \frac{1}{2}|A^{+-}|^2\right\}. \tag{18.43}$$

Consider now the torque stresses τ_{ij}. From (18.36) we see that they have the same helicity content in terms of h_{ij} as σ_{ij} has in terms of A_{ij}. In addition, there is the term $\delta_{ij}A_{\ell\ell} - A_{ji}$. The $\delta_{ij}A_{\ell\ell}$ part can be written as

$$(\sqrt{2}\,e^{L} + e^{L'})_{ij}(\sqrt{2}\,A^{L} + A^{L'}). \tag{18.44}$$

Since A_{ji} is the transpose of A_{ij} we see that in the helicity decomposition of τ_{ij}, the sign of the spin-1 contribution of $A^{(1,h)}$ is reversed. Thus we have

$$\tau^{(2,\pm 2)} = \pm kh^{(2,\pm 2)} - A^{(2,\pm 2)}, \quad \tau^{+\pm} = \pm kh^{+\pm} - A^{-\pm}, \quad \tau^{-+} = -A^{+\pm},$$
$$\tau^{(1,0)} = -kh^{L} - A^{(1,0)}, \quad \tau^{L} = -kh^{(1,0)} + A^{L} + \sqrt{2}\,A^{L'}, \quad \tau^{L'} = \sqrt{2}\,A^{L}. \tag{18.45}$$

giving a torque stress energy of

$$\frac{a^2}{8\beta\ell^2}\sum_{\mathbf{k}}\Big\{(\delta_1+\delta_2)[|kh^{(2,2)}-A^{(2,2)}|^2+|kh^{(2,-2)}+A^{(2,-2)}|^2$$
$$+|-kh^{(1,0)}+A^L+\sqrt{2}A^{L'}|^2+2|A^L|^2]$$
$$+\delta_1[|kh^{++}-A^{-+}|^2+|kh^{+-}-A^{--}|^2+|A^{++}|^2+|A^{+-}|^2]$$
$$+\delta_2[-(kh^{++}-A^{-+})^*A^{++}-(-kh^{+-}-A^{--})^*A^{+-}+\text{c.c.}]$$
$$+(\delta_1-\delta_2)|kh^L+A^{(1,0)}|^2\Big\}. \tag{18.46}$$

The energy is invariant under the gauge transformations (18.37), (18.38), which read in the helicity basis,

$$A^{-\pm}\to A^{-\pm}+k\Lambda^{\pm},\quad A^{L'}\to A^{L'}+k\Lambda^0,$$
$$h^{(1,\pm1)}\to h^{(1,\pm1)}\pm\sqrt{2}k\Lambda^{\pm},\quad h^{(1,0)}\to h^{(1,0)}+\sqrt{2}k\Lambda^0, \tag{18.47}$$

and

$$h^{-\pm}\to h^{-\pm}+k\xi^{\pm},\quad h^{L'}\to h^{L'}+k\xi^0, \tag{18.48}$$

respectively, with all other components remaining unchanged.

These can be used to eliminate the anti-symmetric components $h^{(1,\pm1)}$, $h^{(1,0)}$ (as well as $h^{(2,\pm1)}$, $h^{L'}$ if they were present) so that only three components of h are dynamically relevant, namely, $h^{(2,2)}$, $h^{(2,-2)}$ and h^L. After gauge fixing, the elastic energy (18.23) reads

$$\frac{1}{T}E_{\text{el}}=\frac{1}{4\beta}\sum_{\mathbf{k}}k^2\Big\{|A^{(2,2)}|^2+|A^{(2,-2)}|^2+\frac{1-\nu}{1+\nu}|A^{(1,0)}|^2+\frac{1}{2}|A^{++}|^2+\frac{1}{2}|A^{+-}|^2\Big\}$$
$$+\frac{a^2}{8\beta\ell^2}\sum_{\mathbf{k}}\Big\{(\delta_1+\delta_2)[|kh^{(2,2)}-A^{(2,2)}|^2+|kh^{(2,-2)}+A^{(2,-2)}|^2$$
$$+|A^L+\sqrt{2}A^{L'}|^2+2|A^L|^2]+\delta_1[|A^{++}|^2+|A^{+-}|^2$$
$$+|A^{-+}|^2+|A^{--}|^2]+\delta_2[A^{-+*}A^{++}+A^{--*}A^{+-}+\text{c.c.}]$$
$$+(\delta_1-\delta_2)|kh^L+A^{(1,0)}|^2\Big\}, \tag{18.49}$$

where $\delta_1+\delta_2=1/(1+\varepsilon)$, $\delta_1-\delta_2=1/(1-\varepsilon)$, $\delta_1=1/(1-\varepsilon^2)$, $\delta_2=-\varepsilon/(1-\varepsilon^2)$. We now turn to the interaction energy (18.40).

In the continuum limit, the conservation laws (18.41) ensure that $\Theta_{k\ell}$ has

only the helicity components $\Theta^{(2,\pm 2)}$, $\Theta^{L'}$, Θ^{++}, $\Theta^{(1,0)}$, the latter three being identical to $\mp k\alpha^{--}$, $-k\alpha^{L'}/\sqrt{2}$, respectively. Hence the helicity decomposition of the interaction energy (18.40) reads

$$\begin{aligned}\frac{1}{T}E_{\text{int}} = -2\pi i \sum_{\mathbf{k}} \{&A^{(2,2)*}\alpha^{(2,2)} + A^{(2,-2)*}\alpha^{(2,-2)} + A^{(1,0)*}\alpha^{(1,0)} \\ &+ h^{(2,2)*}\Theta^{(2,2)} + h^{(2,-2)*}\Theta^{(2,-2)} + h^{L*}\Theta^{L} + A^{+++}\alpha^{++} \\ &+ A^{+-*}\alpha^{+-} + (A^{-+} - kh^{++})^*\alpha^{-+} + (A^{--} + kh^{+-})^*\alpha^{--} \\ &+ (A^{L'} - kh^{(1,0)}/\sqrt{2})^*\alpha^{L'} + A^{L*}\alpha^{L}\}. \end{aligned} \tag{18.50}$$

In the stress gauge for which $h^{(s,h)}$ has the three components $h^{(2,2)}$, $h^{(2,-2)}$, h^{L} only, this becomes

$$\begin{aligned}\frac{1}{T}E_{\text{int}} = -2\pi i \sum_{\mathbf{k}} \{&A^{(2,2)*}\alpha^{(2,2)} + A^{(2,-2)*}\alpha^{(2,-2)} + A^{(1,0)*}\alpha^{(1,0)} \\ &+ h^{(2,2)*}\Theta^{(2,2)} + h^{(2,-2)*}\Theta^{(2,-2)} + h^{L*}\Theta^{L} \\ &+ A^{-+*}\alpha^{-+} + A^{--*}\alpha^{--} + A^{+++}\alpha^{++} + A^{+-*}\alpha^{+-} + A^{L'*}\alpha^{L'} + A^{L*}\alpha^{L}\}. \end{aligned} \tag{18.51}$$

Noting that in the stress energy, the components $h^{(2,\pm 2)}$ and h^{L} always occur in conjunction with $A^{(2,\pm 2)}$ and $A^{(1,0)}$, it is useful to rewrite the second line in (18.51) as

$$\begin{aligned}&h^{(2,2)*}\Theta^{(2,2)} + h^{(2,-2)*}\Theta^{(2,-2)} + h^{L*}\Theta^{L} \\ &\quad= \left(h^{(2,2)} - \frac{1}{k}A^{(2,2)}\right)^*\Theta^{(2,2)} + \left(h^{(2,-2)} + \frac{1}{k}A^{(2,-2)}\right)^*\Theta^{(2,-2)} \\ &\qquad+ \left(h^{L} - \frac{1}{k}A^{(1,0)}\right)^*\Theta^{L} + \frac{1}{k}(A^{(2,2)*}\Theta^{(2,2)} - A^{(2,-2)*}\Theta^{(2,-2)} + A^{(1,0)*}\Theta^{L}). \end{aligned} \tag{18.52}$$

Recalling the composition of the total defect tensor in the helicity basis [i.e., (16.24) and (16.25)], we see that the second line can be combined with the first line in (18.51) to give the defect couplings,

$$-2\pi i \sum_{\mathbf{k}} \left\{ \frac{1}{k} [A^{(2,2)*} \eta^{(2,2)} - A^{(2,-2)*} \eta^{(2,-2)} + A^{(1,0)*} \eta^{L}] \right.$$
$$+ \left(h^{(2,2)} - \frac{1}{k} A^{(2,2)} \right)^{*} \Theta^{(2,2)} + \left(h^{(2,-2)} + \frac{1}{k} A^{(2,-2)} \right)^{*} \Theta^{(2,-2)}$$
$$\left. - \left(h^{L} + \frac{1}{k} A^{(1,0)} \right)^{*} \Theta^{L} \right\}. \tag{18.53}$$

We now change the variables from $A^{(2,\pm 2)}$, $A^{(1,0)}$, $h^{(2,\pm 2)}$, h^{L} to $A^{(2,\pm 2)}$, $A^{(1,0)}$, $h^{(2,\pm 2)} \mp (1/k) A^{(2,\pm 2)}$, $h^{L} + (1/k) A^{(1,0)}$. Then the integrals over these six fields can immediately be performed, giving the following Boltzmann factor:

$$\exp\left\{ -\beta 4\pi^2 \sum_{\mathbf{k}} \frac{1}{\mathbf{k}^4} \left(|\eta^{(2,2)}|^2 + |\eta^{(2,-2)}|^2 + \frac{1-\nu}{1+\nu} |\eta^{L}|^2 \right) \right.$$
$$\left. - 2\beta \frac{\ell^2}{a^2} 4\pi^2 \sum_{\mathbf{k}} \frac{1}{\mathbf{k}^2} [(1+\varepsilon)|\Theta^{(2,2)}|^2 + (1+\varepsilon)|\Theta^{(2,-2)}|^2 + (1-\varepsilon)|\Theta^{L}|^2] \right\}. \tag{18.54}$$

The first term contains the defect energy of classical linear elasticity. The second gives an additional Biot-Savart energy between disclination lines, which at long distances is negligible as compared with the linear forces implied by the first term. It modifies only the core of the disclinations.

As for the remaining fields, $A^{-\pm}$, $A^{+\pm}$, A^{L} and $A^{L'}$ these produce additional short-range effects for the remaining components of the defect densities. The fields $A^{\pm\pm}$ give

$$\exp\left\{ -2\beta \frac{\ell^2}{a^2} 4\pi^2 \sum_{\mathbf{k}} \left[\frac{1}{1+\ell^2 k^2/a} \left[|\alpha^{++}|^2 + |\alpha^{+-}|^2 \right.\right.\right.$$
$$\left. - \varepsilon^2 \left(\frac{k^2 \ell^2}{a^2} \right) (|\alpha^{-+}|^2 + |\alpha^{--}|^2) \right] + |\alpha^{-+}|^2 + |\alpha^{--}|^2$$
$$\left.\left. - \frac{\varepsilon}{1+\ell^2 k^2/a^2} (\alpha^{++*} \alpha^{-+} + \alpha^{+-*} \alpha^{--} + \text{c.c.}) \right] \right\}. \tag{18.55}$$

The fields A^{L}, $A^{L'}$ have a stress energy

$$\frac{1}{T}E_{\mathrm{el}} = \frac{a^2}{8\beta\ell^2}(\delta_1 + \delta_2)\sum_{\mathbf{k}} (A^L, A^{L'})^* \begin{pmatrix} 3 & \sqrt{2} \\ \sqrt{2} & 2 \end{pmatrix} \begin{pmatrix} A^L \\ A^{L'} \end{pmatrix}, \tag{18.56}$$

so that integration over them leads to

$$\exp\left\{ -\frac{\beta}{2}\frac{\ell^2}{a^2} 4\pi^2 (1+\varepsilon) \sum_{\mathbf{k}} (\alpha^L, \alpha^{L'})^* \begin{pmatrix} 2 & -\sqrt{2} \\ -\sqrt{2} & 3 \end{pmatrix} \begin{pmatrix} \alpha^L \\ \alpha^{L'} \end{pmatrix} \right.$$
$$\left. = \exp\left\{ -2\beta\frac{\ell^2}{a^2} 4\pi^2 (1+\varepsilon) \sum_{\mathbf{k}} \left[\frac{1}{2}|\alpha^L|^2 + \frac{1}{2}\left| \alpha^L - \frac{1}{\sqrt{2}}\alpha^{L'} \right|^2 \right] \right\}. \tag{18.57}$$

All these additional terms are of short range. They present obstacles to the formation of dislocations.

From the identity (16.26), we observe that the second term in (18.55) can also be written as

$$\exp\left\{ -2\beta\frac{\ell^2}{a^2} 4\pi^2 \sum_{\mathbf{k}} \frac{1}{\mathbf{k}^2} (|\Theta^{++}|^2 + |\Theta^{+-}|^2) \right\}, \tag{18.58}$$

and may be viewed as a Biot-Savart law for disclination lines. Similarly, using (16.27), the energy (18.57) may be written in terms of α^L, $(-\sqrt{2}/k)\,\Theta^{(1,0)}$, rather than α^L, $\alpha^{L'}$.

Then the total Boltzmann factor becomes[b]

$$\exp\left\{ -\beta 4\pi^2 \sum_{\mathbf{k}} \frac{1}{\mathbf{k}^4} \left(|\eta^{(2,2)}|^2 + |\eta^{(2,-2)}|^2 + \frac{1+\nu}{1-\nu}|\eta^L|^2 \right) \right.$$
$$- 2\beta\frac{\ell^2}{a^2} 4\pi^2 \sum_{\mathbf{k}} \frac{1}{\mathbf{k}^2} \left[[(1+\varepsilon)|\Theta^{(2,2)}|^2 + (1+\varepsilon)|\Theta^{(2,-2)}|^2 + (1-\varepsilon)|\Theta^L|^2] \right.$$
$$+ \left(1 - \frac{\varepsilon^2 k^2 \ell^2/a^2}{1 + k^2\ell^2/a^2} \right) (|\Theta^{++}|^2 + |\Theta^{+-}|^2) + (1+\varepsilon)|\Theta^{(1,0)}|^2 \Big]$$
$$+ \sum_{\mathbf{k}} \left[\frac{1}{1 + k^2\ell^2/a^2} (|\alpha^{++}|^2 + |\alpha^{+-}|^2) + \frac{1+\varepsilon}{2} \left| \alpha^L + \frac{1}{k}\Theta^{(1,0)} \right|^2 \right]$$
$$\left. + \sum_{\mathbf{k}} \left[\frac{-\varepsilon}{1 + k^2\ell^2/a^2} (\alpha^{++*}\alpha^{-+} + \alpha^{+-*}\alpha^{--} + \text{c.c.}) \right] \right\}. \tag{18.59}$$

[b] Recall that the defect densities in these formulas are the integer-valued lattice quantities. Thus they are related to the continuous ones by a factor $1/2\pi$ as well as an appropriate power of the lattice spacing. Similarly, the momenta are measured as multiples of $1/a$.

From this expression, it is straightforward to go back to tensor notation. Using the fact that η possesses only the three components $\eta^{(2,2)}$, $\eta^{(2,-2)}$, η^L we find that

$$|\eta_{ij}|^2 = |\eta^{(2,2)}|^2 + |\eta^{(2,-2)}|^2 + |\eta^L|^2, \qquad |\eta_{ii}|^2 = |\sqrt{2}\,\eta^L|^2, \tag{18.60}$$

and the first sum becomes

$$-\beta 4\pi^2 \sum_{\mathbf{k}} \frac{1}{\mathbf{k}^4}\left(|\eta_{ij}|^2 + \frac{\nu}{1-\nu}|\eta_{\ell\ell}|^2\right). \tag{18.61}$$

Similarly, Θ_{ij} has only the six components contained in the second sum so that this sum reads, for $\varepsilon = 0$,

$$-2\beta\frac{\ell^2}{a^2}4\pi^2 \sum_{\mathbf{k}} \frac{1}{\mathbf{k}^2}|\Theta_{ij}|^2. \tag{18.62}$$

Furthermore, using the polarization tensors $e^{+\pm}$ of Eq. (4.97), we obtain

$$\begin{aligned} |\alpha^{++}|^2 + |\alpha^{+-}|^2 &= \frac{1}{\mathbf{k}^2}|e_i k_j e^*_{i'} k_{j'} \alpha^*_{ij} \alpha_{i'j'} + \text{c.c.}|^2 \\ &= \frac{1}{k^6}|(\delta_{ii'}\partial^2 - \partial_i\partial_{i'})\,\partial_j \alpha_{i'j}|^2. \end{aligned} \tag{18.63}$$

It is useful to introduce the abbreviation

$$\alpha^T_{ij} \equiv \left(\delta_{ii'} - \frac{\partial_i \partial_{i'}}{\partial^2}\right)\alpha_{i'j} \tag{18.64}$$

for the transverse part of α_{ij} [i.e., that which contains only the $++$, $+-$, $-+$, $--$, $(1, 0)$, and L components]. Then

$$|\alpha^{++}|^2 + |\alpha^{+-}|^2 = \frac{1}{k^2}|\partial_j \alpha^T_{ij}|^2. \tag{18.65}$$

Similarly, using e^L of Eq. (4.97) and $e^{(1,0)}$ of Eq. (4.62) we find

$$\left|\alpha^L + \frac{1}{k}\Theta^{(1,0)}\right|^2 = \frac{1}{2k^4}|(\delta_{ij}\partial^2 - \partial_i\partial_j)\alpha_{ij} + \varepsilon_{i\ell k}\partial_k\Theta_{i\ell}|^2$$

$$= \frac{1}{2k^4}|\partial^2\alpha^T_{\ell\ell} + \varepsilon_{i\ell k}\partial_k\Theta_{i\ell}|^2. \tag{18.66}$$

With these formulas, we can collect the $\varepsilon = 0$ parts of (18.59) into the following tensor form,

$$\exp\left\{-\beta 4\pi^2 \sum_{\mathbf{k}} \frac{1}{k^4}\left(|\eta_{ij}|^2 + \frac{\nu}{1-\nu}|\eta_{\ell\ell}|^2\right)\right.$$
$$\left. - 2\beta\frac{\ell^2}{a^2}4\pi^2 \sum_{\mathbf{k}}\left[\frac{1}{k^2}|\Theta_{ij}|^2 + \frac{1}{k^2}\frac{1}{1+k^2\ell^2/a^2}|\partial_j\alpha^T_{ij}|^2 + \frac{1}{4k^4}|\partial^2\alpha^T + \varepsilon_{i\ell k}\partial_k\Theta_{i\ell}|^2\right]\right\}. \tag{18.67}$$

The ε terms require a little more work. Those in $\varepsilon|\Theta^{(\ell,h)}|^2$ can be grouped as follows:

$$\varepsilon(|\Theta^{(2,2)}|^2 + |\Theta^{(2,-2)}|^2 + |\Theta^L|^2 + |\Theta^{(1,0)}|^2) - 2\varepsilon|\Theta^L|^2. \tag{18.68}$$

Now, $2|\Theta^L|^2$ is just

$$2|\Theta^L|^2 = |\Theta_{\ell\ell}|^2. \tag{18.69}$$

The first sum may be rewritten as

$$\varepsilon(|\Theta_{ij}|^2 - |\Theta^{++}|^2 - |\Theta^{+-}|^2). \tag{18.70}$$

But from the same calculation as in Eq. (18.63) we have directly [recall that $\partial_i\Theta_{ij} = 0$]

$$|\Theta^{++}|^2 + |\Theta^{+-}|^2 = \frac{1}{k^2}|\partial_j\Theta_{ij}|^2, \tag{18.71}$$

so that (18.68) gives

$$\varepsilon\left(|\Theta_{ij}|^2 - \frac{1}{k^2}|\partial_j\Theta_{ij}|^2 - |\Theta_{\ell\ell}|^2\right). \tag{18.72}$$

The mixed terms in α^{++}, α^{-+}, etc. take the following tensor form,

$$\alpha^{++*}\alpha^{-+} + \alpha^{+-*}\alpha^{--} + \text{c.c.}$$

$$= \frac{1}{k^2}(e_i k_j k_{i'} e_{j'} \alpha^*_{ij}\alpha_{i'j'} + \text{c.c.}) + \frac{1}{k^2}(k_i e_j e_{i'} k_{j'} \alpha^*_{ij}\alpha_{i'j'} + \text{c.c.})$$

$$= \frac{1}{k^2}\left(\delta_{ij'} - \frac{k_i k_{j'}}{k^2}\right) k_j k_{i'} \alpha^*_{ij}\alpha_{i'j'} + \frac{1}{k^2}\left(\delta_{ji'} - \frac{k_j k_{i'}}{k^2}\right) k_i k_{j'} \alpha^*_{ij}\alpha_{i'j'}$$

$$= \frac{1}{k^2}(\partial_j \alpha^{T*}_{ij} \partial_\ell \alpha_{\ell i} + \text{c.c.}) = -\frac{1}{k^2}(\partial_j \alpha^{T*}_{ij} \varepsilon_{ipq}\Theta_{pq} + \text{c.c.}). \tag{18.73}$$

Using these formulas, the ε, ε^2 terms in (18.59) become

$$\exp\left\{-2\beta\frac{\ell^2}{a^2}4\pi^2 \sum_{\mathbf{k}} \varepsilon\left[\frac{1}{k^2}\left(|\Theta_{ij}|^2 - \frac{1}{k^2}|\partial_j\Theta_{ij}|^2 - |\Theta_{\ell\ell}|^2\right)\right.\right.$$
$$- \frac{\varepsilon\ell^2/a^2}{1 + k^2\ell^2/a^2}\frac{1}{k^2}|\partial_j\Theta_{ij}|^2 + \frac{1}{4k^4}|\partial^2\alpha^T_{\ell\ell} + \varepsilon_{i\ell k}\partial_k\Theta_{i\ell}|^2$$
$$\left.\left. + \frac{1}{1 + k^2\ell^2/a^2}\frac{1}{k^2}(\partial_j\alpha^{T*}_{ij}\varepsilon_{ipq}\Theta_{pq} + \text{c.c.})\right]\right\}. \tag{18.74}$$

At first sight it appears as though this expression is the best starting point for a disorder field theory of defect lines. Either defect systems, $\Theta_{\ell i}$ or $\alpha^T_{\ell i}$ could be turned separately into an XY model, one for each j. Unfortunately, this simplification is an illusion for two reasons. First, it is impossible to go from integers $\alpha_{\ell i}$ to integers $\alpha^T_{\ell i}$ since the lattice operator $(\nabla_\ell\bar{\nabla}_{\ell'}/\bar{\nabla}\cdot\nabla)\alpha_{\ell' i}$ produces non-integer numbers. Hence the sum over $\alpha^T_{\ell i}$ does not allow for an XY model representation. Second, the resulting field theory would not be local. The orthogonal part of $\alpha^T_{\ell i}$ still appears in the exponent which reads

$$\exp\left\{-2\pi i \sum_{\mathbf{x}}\left(A_{\ell i}\left(\alpha^T_{\ell i} + \frac{\partial_\ell\partial_{\ell'}}{\partial^2}\alpha_{\ell' i}\right) + h_{\ell i}\Theta_{\ell i}\right)\right\}$$
$$= \exp\left\{-2\pi i \sum_{\mathbf{x}}\left(A_{\ell i}\alpha^T_{\ell i} + \left(h_{\ell i} - A_{nk}\varepsilon_{\ell ik}\frac{\partial n}{\partial^2}\right)\Theta_{\ell i}\right)\right\}, \tag{18.75}$$

so that with $\alpha^T_{\ell i}$, $\Theta_{\ell i}$ as fundamental defect variables the field A_{nk} couples nonlocally to $\Theta_{\ell i}$, and such a nonlocal coupling cannot readily be incorporated into a covariant derivative of a disorder field for the disclination density $\Theta_{\ell i}$.

18.5. SECOND-GRADIENT INTERACTION ENERGY DERIVED FROM DEFECT GAUGE FIELDS

In linear elasticity we observed that it was simpler to calculate the interaction energy of defects by using defect gauge fields rather than stress gauge fields. Let us now see how this method works in higher gradient elasticity.

Our starting point is the partition function (17.19) with the energy expression

$$E = \int d^3x \Big\{ \mu(u_{ij} - u^p_{ij})^2 + \frac{\lambda}{2}(u_{\ell\ell} - u^p_{\ell\ell})^2 + \frac{2\mu+\lambda}{2}\ell'^2(\partial_i(u_{\ell\ell} - u^p_{\ell\ell}))^2 + 2\mu\ell^2[(\partial_i\omega_j - \partial_i\omega^p_j)^2 + \varepsilon(\partial_i\omega_j - \partial_j\omega^p_i)(\partial_j\omega_i - \partial_j\omega^p_i)] \Big\}, \tag{18.76}$$

where $u^p_{ij} \equiv (1/2)(\partial_i u^p_j + \partial_j u^p_i) = (1/2)(\beta^p_{ij} + \beta^p_{ji})$, $\partial_j\omega^p_i \equiv \varkappa^p_{ji} = (1/2)\,\varepsilon_{ik\ell}\partial_j \beta^p_{k\ell} + \phi^p_{ji}$ [recall (2.63), (2.64)]. In contrast to the discussion in the previous section we have now kept the ℓ'^2 term which corresponds to the stress energy τ'^2_i.

We now recall that the basic trick which simplified the calculation of the elastic energies in (10.6) was to impose improper transverse gauges. We had demonstrated in the XY model that this is admissible, as long as no knowledge is required on the correlation functions of the order parameter $e^{iu_i(\mathbf{x})}$, which is the case here. Then we can always choose noninteger gauge functions $\tilde{N}_i$, M_i to arrive at a gauge in which β^p_{ij} is properly symmetric but purely transverse, i.e.,

$$\beta^p_{ij} = \beta^p_{ji} = u^p_{ij}, \qquad \partial_i u^p_{ij} = 0. \tag{18.77}$$

Using this gauge and working out the different squares in (18.69) gives

$$E = \int d^3x \Big\{ \frac{1}{2}u_i(\mathbf{x}) \Big[-\mu\boldsymbol{\partial}^2(1 - \ell^2\boldsymbol{\partial}^2)\Big(\delta_{ij} - \frac{\partial_i\partial_j}{\boldsymbol{\partial}^2}\Big) - (2\mu+\lambda)\boldsymbol{\partial}^2(1 - \ell'^2\boldsymbol{\partial}^2)\frac{\partial_i\partial_j}{\boldsymbol{\partial}^2}\Big] u_j(\mathbf{x}) + \lambda u_i\partial_i u^p_{\ell\ell} - (2\mu+\lambda)\ell'^2 u_i\partial_i\boldsymbol{\partial}^2 u^p_{\ell\ell} - 2\mu\ell^2 u_i\varepsilon_{ik\ell}\partial_\ell\partial_j(\varkappa^p_{jk} + \varepsilon\varkappa^p_{kj}) + \mu u^{p2}_{ij} + \frac{\lambda}{2}u^{p2}_{\ell\ell} + \frac{2\mu+\lambda}{2}\ell'^2(\partial_j u^p_{\ell\ell})^2 + 2\mu\ell^2(\varkappa^{p2}_{ji} + \varepsilon\varkappa^p_{ji}\varkappa^p_{ij}) \Big\}. \tag{18.78}$$

A quadratic completion gives the defect energy

$$E_{\text{def}} = \int d^3x \left\{ \mu u_{ij}^{p2} + \frac{\lambda}{2} u_{\ell\ell}^{p2} + \frac{2\mu+\lambda}{2} \ell'^2 (\partial_j u_{\ell\ell}^p)^2 + 2\mu\ell^2 (\varkappa_{ji}^{p2} + \varepsilon \varkappa_{ji}^p \varkappa_{ij}^p) \right\}$$

$$- \frac{1}{2} \int d^3x\, d^3x'\, G_{ii'}(\mathbf{x}-\mathbf{x}')$$

$$\times [\lambda \partial_i u_{\ell\ell}^p - (2\mu+\lambda)\ell'^2 \partial_i \boldsymbol{\partial}^2 u_{\ell\ell}^p - 2\mu\ell^2 \varepsilon_{ik\ell} \partial_k \partial_j (\varkappa_{jk}^p + \varepsilon \varkappa_{kj}^p)](\mathbf{x})$$

$$\times [\lambda \partial_{i'} u_{\ell\ell}^p - (2\mu+\lambda)\ell'^2 \partial_{i'} \boldsymbol{\partial}^2 u_{\ell\ell}^p - 2\mu\ell^2 \varepsilon_{i'k\ell} \partial_\ell \partial_j (\varkappa_{jk}^p + \varepsilon \varkappa_{kj}^p)](\mathbf{x}'), \tag{18.79}$$

where $G_{ii'}(\mathbf{x}-\mathbf{x}')$ is the elastic Green function calculated in (17.106), (17.112) in momentum space

$$G_{ii'}(\mathbf{k}) = \frac{1}{\mu k^2 (1+\ell^2 k^2)} (\delta_{ii'} - k_i k_{i'}/k^2) + \frac{1}{(2\mu+\lambda) k^2 (1+\ell'^2 k^2)} \frac{k_i k_{i'}}{k^2}. \tag{18.80}$$

This satisfies

$$k_i G_{ii'}(\mathbf{k}) = k_j \frac{1}{(2\mu+\lambda)(1+\ell'^2 k^2)} \frac{1}{k^2}$$

$$k_i k_{i'} G_{ii'}(\mathbf{k}) = \frac{1}{(2\mu+\lambda)} \frac{1}{(1+\ell'^2 k^2)},$$

$$\varepsilon_{ik\ell} k_\ell \varepsilon_{i'k'\ell'} k_{\ell'} G_{ii'}(\mathbf{k}) = \frac{1}{\mu k^2 (1+\ell^2 k^2)} (\delta_{kk'} - k_k k_{k'}/k^2). \tag{18.81}$$

It follows that

$$G_{ii'}(\mathbf{k}) (k_i u_{\ell\ell}^p (\lambda + (2\mu+\lambda)\ell'^2 k^2) - 2\mu\ell^2 i \varepsilon_{ik\ell} k_\ell k_j (\varkappa_{jk}^p + \varepsilon \varkappa_{kj}^p))^*$$

$$\times (k_{i'} u_{\ell\ell}^p (\lambda + (2\mu+\lambda)\ell'^2 k^2) - 2\mu\ell^2 i \varepsilon_{i'k\ell} k_\ell k_j (\varkappa_{jk}^p + \varepsilon \varkappa_{kj}^p))$$

$$= \frac{1}{2\mu+\lambda} \frac{(\lambda + (2\mu+\lambda)\ell'^2 k^2)^2}{1+\ell'^2 k^2} |u_{\ell\ell}^p|^2 + \frac{1}{\mu} \frac{(2\mu\ell^2)^2}{1+\ell^2 k^2} k_j k_{j'} \left(\delta_{kk'} - \frac{k_k k_{k'}}{k^2} \right)$$

$$\times (\varkappa_{jk}^p + \varepsilon \varkappa_{kj}^p)^* (\varkappa_{j'k'} + \varepsilon \varkappa_{k'j'}^p). \tag{18.82}$$

Inserting this result into (18.79) we can collect the u_{ij}^p terms as follows,

$$\sum_{\mathbf{k}}\left[\mu|u_{ij}^{p}|^2+\frac{1}{2}\left(\lambda+(2\mu+\lambda)\ell'^2k^2-\frac{(\lambda+(2\mu+\lambda)\ell'^2k^2)^2}{(2\mu+\lambda)(1+\ell'^2k^2)}\right)|u_{\ell\ell}^{p}|^2\right]$$
$$=\sum_{\mathbf{k}}\left[\mu|u_{ij}^{p}|^2+\frac{\mu}{2\mu+\lambda}\frac{\lambda+(2\mu+\lambda)\ell'^2k^2}{1+\ell'^2k^2}|u_{\ell\ell}^{p}|^2\right]$$
$$=\mu\sum_{\mathbf{k}}\left[|u_{ij}^{p}|^2+\frac{\nu}{1-\nu}|u_{\ell\ell}^{p}|^2+\frac{1-2\nu}{1-\nu}\frac{\ell'^2k^2}{1+\ell'^2k^2}|u_{\ell\ell}^{p}|^2\right]. \tag{18.83}$$

Similarly, the $\varkappa_{ji}^{p}$ terms become

$$\sum_{\mathbf{k}}2\mu\ell^2\Bigg[|\varkappa_{ji}^{p}|^2+\varepsilon\varkappa_{ji}^{p*}\varkappa_{ij}^{p}$$
$$-\left(1-\frac{1}{1+\ell^2k^2}\right)\frac{k_jk_{j'}}{k^2}\left(\delta_{kk'}-\frac{k_kk_{k'}}{k^2}\right)(\varkappa_{jk}^{p}+\varepsilon\varkappa_{kj}^{p})^*(\varkappa_{j'k'}^{p}+\varepsilon\varkappa_{k'j'}^{p})\Bigg]$$
$$=2\mu\ell^2\sum_{\mathbf{k}}\Bigg\{|\varkappa_{ji}^{p}|^2-\frac{1}{k^2}|\partial_j\varkappa_{jk}^{p}|^2+\frac{1}{k^4}|\partial_j\partial_k\varkappa_{jk}^{p}|^2$$
$$+\frac{1}{1+\ell^2k^2}\left(\frac{1}{k^2}|\partial_j\varkappa_{jk}^{p}|^2-\frac{1}{k^4}|\partial_j\partial_k\varkappa_{jk}^{p}|^2\right)$$
$$+\varepsilon\left[\varkappa_{ji}^{p*}\varkappa_{ij}^{p}-\frac{1}{k^2}(\partial_j\varkappa_{jk}^{*}\partial_j\varkappa_{kj}^{p}+\text{c.c.})+\frac{2}{k^4}|\partial_j\partial_k\varkappa_{jk}^{p}|^2\right]$$
$$+\frac{\varepsilon}{1+\ell^2k^2}\left[\frac{1}{k^2}(\partial_j\varkappa_{jk}^{p*}\partial_j\varkappa_{kj}^{p}+\text{c.c.})-\frac{2}{k^4}|\partial_j\partial_k\varkappa_{jk}^{p}|^2\right]$$
$$-\frac{\ell^2\varepsilon^2}{1+\ell^2k^2}\left[|\partial_j\varkappa_{kj}^{p}|^2-\frac{1}{k^2}|\partial_k\partial_j\varkappa_{kj}^{p}|^2\right]\Bigg\}. \tag{18.84}$$

The plastic deformations in the energies (18.83), (18.84) must now be rewritten in terms of the defect tensors η_{ij}, Θ_{ij}, α_{ij}. For u_{ij}^{p} this was done in Section 10.6 [Eqs. (10.121), (10,122)] so that (18.83) becomes directly

$$E_{\text{def},u^p}=\mu\sum_{\mathbf{k}}\left[\frac{1}{k^4}\left(\eta_{ij}^2+\frac{\nu}{1-\nu}\eta_{\ell\ell}^2\right)+\frac{1-2\nu}{1-\nu}\frac{\ell'^2}{1+\ell'^2k^2}\frac{1}{k^2}\eta_{\ell\ell}^2\right]. \tag{18.85}$$

The first term is the usual defect energy of linear elasticity, the second term represents a modification of the short-range part of it.

A little more work is needed to translate the plastic rotations into defect tensors. For the first two terms in (18.84) this is simple enough since the disclination density $\Theta_{ij} = \varepsilon_{ik\ell}\,\partial_k\,\partial_\ell\,\omega_j^p = \varepsilon_{ik\ell}\,\partial_k\,\varkappa_{\ell j}^p$ gives directly

$$\sum_{\mathbf{k}} \frac{1}{k^2}|\Theta_{ij}|^2 = \sum_{\mathbf{k}} \left[|\varkappa_{ji}^p|^2 - \frac{1}{k^2}|\partial_j \varkappa_{ji}^p|^2 \right]. \tag{18.86}$$

The remaining terms have to be expressed in terms of Θ_{ij} and $\alpha_{k\ell}$. Since $\partial_i \alpha_{ij} = -\varepsilon_{jk\ell}\Theta_{k\ell}$, the divergence of α_{ij} is not an independent quantity and can be expressed in terms of $\Theta_{k\ell}$. Thus we choose the full $\Theta_{k\ell}$ plus the divergenceless part of α_{ij} for the parametrization of all defects. Recalling the relations

$$\alpha_{in} = \varepsilon_{ik\ell}\,\partial_k u_{\ell n}^p + \delta_{in}\varkappa_{kk}^p - \varkappa_{ni}^p, \tag{18.87}$$

we can calculate

$$\alpha_{in}^T \equiv \left(\delta_{ii'} - \frac{\partial_i \partial_{i'}}{\boldsymbol{\partial}^2}\right)\alpha_{i'n} = \varepsilon_{ik\ell}\,\partial_k u_{\ell n}^p + \left(\delta_{in} - \frac{\partial_i \partial_n}{\boldsymbol{\partial}^2}\right)\varkappa_{kk}^p - \varkappa_{ni}^p + \frac{\partial_i \partial_{i'}}{\boldsymbol{\partial}^2}\varkappa_{ni'}^p. \tag{18.88}$$

From this result we find

$$\alpha_{\ell\ell}^T = \varkappa_{kk}^p + \frac{\partial_i \partial_\ell}{\boldsymbol{\partial}^2}\varkappa_{\ell i}^p, \tag{18.89}$$

$$\boldsymbol{\partial}^2 \alpha_{\ell\ell}^T + \varepsilon_{ki\ell}\,\partial_k \Theta_{i\ell} = \boldsymbol{\partial}^2 \alpha_{\ell\ell}^T - \boldsymbol{\partial}^2 \varkappa_{ii}^p + \partial_n \partial_i \varkappa_{ni}^p = 2\partial_\ell\,\partial_i \varkappa_{\ell i}^p, \tag{18.90}$$

and due to the transverse gauge of $u_{\ell n}^p$,

$$\partial_j \alpha_{ij}^T = -\left(\delta_{i\ell} - \frac{\partial_i \partial_\ell}{\boldsymbol{\partial}^2}\right)\partial_j \varkappa_{j\ell}^p,$$

$$\sum_{\mathbf{k}} |\partial_j \alpha_{ij}^T|^2 = \sum_{\mathbf{k}} \left[|\partial_j \varkappa_{ji}|^2 - \frac{1}{k^2}|\partial_j \partial_i \varkappa_{ji}^p|^2 \right]. \tag{18.91}$$

Inserting (18.86), (18.90), (18.91) into the $\varepsilon = 0$ parts of (18.84) we see that they come to agree with the previous result (18.67) (with $a = 1$).

We now use once more $\Theta_{ij} = \varepsilon_{ik\ell}\,\partial_k \varkappa_{\ell j}^p$, to calculate

$$\sum_{\mathbf{k}} |\partial_j \Theta_{ij}|^2 = \sum_{\mathbf{k}} (|\partial_k \partial_j \varkappa_{ij}^p|^2 - |\partial_\ell \partial_j \varkappa_{ij}^p|^2) \tag{18.92}$$

and see that the ε^2 term agrees with that in (18.74).

Then we form

$$\sum_{\mathbf{k}} (\partial_j \alpha_{ij}^{T*} \varepsilon_{ipq} \Theta_{pq} + \text{c.c.}) = -\sum_{\mathbf{k}} \left[\left(\delta_{i\ell} - \frac{\partial_i \partial_\ell}{\partial^2} \right) \partial_j \varkappa_{j\ell}^{p*} \right] (\partial_i \varkappa_{qq} - \partial_g \varkappa_{ig}) + \text{c.c.}$$

$$= \sum_{\mathbf{k}} \left[(\partial_j \varkappa_{ji}^{p*} \partial_j \varkappa_{ij}^p + \text{c.c.}) - \frac{2}{k^2} |\partial_j \partial_k \varkappa_{jk}^p|^2 \right] \tag{18.93}$$

and see that the $\varepsilon/(1 + \ell^2 k^2)$ terms in (18.84) and (18.74) are the same.

Finally, we evaluate

$$\sum_{\mathbf{k}} |\Theta_{ij}|^2 = \sum_{\mathbf{k}} [|\partial_k \varkappa_{\ell j}^p|^2 - |\partial_j \varkappa_{ij}^p|^2], \tag{18.94}$$

$$\sum_{\mathbf{k}} |\Theta_{\ell\ell}|^2 = \sum_{\mathbf{k}} [|\partial_k \varkappa_{\ell j}^p|^2 + 2k_i \varkappa_{ij}^{p*} k_i \varkappa_{ji}^p - k^2 \varkappa_{ij}^* \varkappa_{ji} - |k_i \varkappa_{ij}^p|^2 - |k_j \varkappa_{ij}^p|^2], \tag{18.95}$$

$$\sum_{\mathbf{k}} \frac{1}{k^2} \left[|\Theta_{ij}|^2 - \frac{1}{k^2} |\partial_j \Theta_{ij}|^2 - |\Theta_{\ell\ell}|^2 + \frac{1}{4k^2} |\partial^2 \alpha_{\ell\ell}^T + \varepsilon_{i\ell k} \partial_k \Theta_{i\ell}|^2 \right]$$

$$= \sum_{\mathbf{k}} \left[\varkappa_{ij}^{p*} \varkappa_{ji}^p - \frac{1}{k^2} (\partial_i \varkappa_{ij}^{p*} \partial_i \varkappa_{ji}^p + \text{c.c.}) + \frac{2}{k^2} |\partial_i \partial_j \varkappa_{ij}^p|^2 \right], \tag{18.96}$$

so that the remaining ε terms also agree with (18.74).

18.6. SECOND-GRADIENT ELASTICITY AND THE PARTITION FUNCTION OF TWO-DIMENSIONAL DEFECTS

For completeness, let us perform a few of the manipulations of Section 18.4 in two dimensions. In this case there is only one rotational field and the jump numbers m_{ij} reduce to an integer-valued vector field m_i. The partition functions (18.28) and (18.29) have the exponents

$$\beta\Bigg\{\frac{1}{4}\sum_{\mathbf{x},i,j}(\nabla_i\gamma_j+\nabla_j\gamma_i-4\pi n^s_{ij})^2+\frac{\lambda}{2\mu}\sum_{\mathbf{x}}\Bigg(\sum_i(\nabla_i\gamma_i-2\pi n^s_{ii})\Bigg)^2$$
$$+\frac{2\mu+\lambda}{2}\frac{\ell'^2}{a^2}\sum_{\mathbf{x},i}(\nabla_i\nabla_\ell\gamma_\ell-2\pi\nabla_i n^s_{\ell\ell})^2$$
$$+\frac{\ell^2}{2a^2}\sum_{\mathbf{x},i}(\nabla_i\varepsilon_{k\ell}\nabla_k\gamma_\ell-2\pi(2m_i+\nabla_i\varepsilon_{k\ell}n_{k\ell}))^2\Bigg\} \tag{18.97}$$

and the canonical form

$$\frac{1}{\beta}\Bigg\{\sum_{\mathbf{x}}\frac{1}{4}(\sigma^{s2}_{ij}-\frac{\nu}{1+\nu}\sigma^{s2}_{\ell\ell})+\frac{\mu a^2}{2(2\mu+\lambda)\ell'^2}\sum_{\mathbf{x}}\tau_i'^2+\frac{a^2}{8\ell^2}\sum_{\mathbf{x}}\tau_i^2\Bigg\}$$
$$+i\sum_{\mathbf{x}}\sigma_{ij}(\nabla_i\gamma_j-\varepsilon_{ij}\omega-2\pi n_{ij})+i\sum_{\mathbf{x}}\tau_i'(\nabla_i\nabla_\ell\gamma_\ell-2\pi\nabla_i n_{\ell\ell})$$
$$+i\sum_{\mathbf{x}}\tau_i(\nabla_i\omega-2\pi m_i). \tag{18.98}$$

The measures of integration are

$$\sum_{\{n_{ij},m_i\}}\Phi[n_{ij},m_i]\prod_{\mathbf{x},i}\Bigg[\int_{-\infty}^{\infty}\frac{d\gamma_i(\mathbf{x})}{2\pi}\Bigg] \tag{18.99}$$

in the first and

$$\sum_{\{n_{ij},m_i\}}\Phi[n_{ij},m_i]\prod_{\mathbf{x},i}\Bigg[\int_{-\infty}^{\infty}\frac{d\gamma_i(\mathbf{x})}{2\pi}\Bigg]\prod_{\mathbf{x}}\Bigg[\int_{-\infty}^{\infty}\frac{d\omega(\mathbf{x})}{2\pi}\Bigg]$$
$$\times\Bigg(\frac{1-\nu}{1+\nu}\Bigg)^{N/2}\prod_{\mathbf{x}}\Bigg[\int_{-\infty}^{\infty}\frac{d\sigma^s_{12}(\mathbf{x})}{\sqrt{2\pi\beta}}\Bigg]\prod_{\mathbf{x},i}\Bigg[\int_{-\infty}^{\infty}\frac{d\sigma^s_{ii}(\mathbf{x})}{\sqrt{4\pi\beta}}\Bigg]\prod_{\mathbf{x}}\Bigg[\int_{-\infty}^{\infty}2d\sigma^a_{12}(\mathbf{x})\Bigg]$$
$$\times\prod_{\mathbf{x},i}\Bigg[\int_{-\infty}^{\infty}\frac{d\tau_i'(\mathbf{x})}{\sqrt{2\pi\beta(2+\lambda/\mu)\ell'^2/a^2}}\Bigg]\prod_{\mathbf{x},i}\Bigg[\int_{-\infty}^{\infty}\frac{d\tau_i(\mathbf{x})}{\sqrt{8\pi\beta\ell^2/a^2}}\Bigg] \tag{18.100}$$

in the second case.

In the following, we shall again ignore the coupling ℓ' since it causes no interesting qualitative changes. The physical observables of stresses and torque stresses at the minimum of the energy are given by

$$\sigma_{ij}^s = \beta\left[(\nabla_i\gamma_j + \nabla_j\gamma_i - 4\pi n_{ij}^s) + \frac{\lambda}{\mu}\delta_{ij}(\nabla_\ell\gamma_\ell - 2\pi n_{\ell\ell}^s)\right],$$

$$\tau_i = 4\beta\frac{\ell^2}{a}(\nabla_i\omega - 2\pi m_i) = 4\beta\frac{\ell^2}{a^2}\left[\nabla_i\frac{1}{2}\varepsilon_{k\ell}\nabla_k\gamma_\ell - \pi(2m_i + \nabla_i\varepsilon_{k\ell}n_{k\ell})\right]. \tag{18.101}$$

The stresses σ_{ij}^s are invariant under the simultaneous replacement

$$n_{ij}^s(\mathbf{x}) \to n_{ij}^s(\mathbf{x}) + \tfrac{1}{2}(\nabla_i\bar{N}_j(\mathbf{x}) + \nabla_j\bar{N}_i(\mathbf{x})), \qquad \gamma_i(\mathbf{x}) \to \gamma_i(\mathbf{x}) + 2\pi\bar{N}_i(\mathbf{x}), \tag{18.102}$$

the torque stresses under

$$m_i(\mathbf{x}) \to m_i(\mathbf{x}) + \nabla_i M(\mathbf{x}), \qquad \omega(\mathbf{x}) \to \omega(\mathbf{x}) + 2\pi M(\mathbf{x}),$$
$$n_{ij}^a(\mathbf{x}) \to n_{ij}^a(\mathbf{x}) - \varepsilon_{ij}M(\mathbf{x}), \qquad \gamma_i(\mathbf{x}) \to \gamma_i(\mathbf{x}). \tag{18.103}$$

In order to avoid an infinite overall factor in the partition function, we have to fix again the gauge. As in Section 18.3, we go to a gauge in which the antisymmetric part of $n_{ij}(\mathbf{x})$ vanishes if n_{ij}^s = integer or is equal to 1 of n_{ij}^s = half-integer. In two dimensions, this concerns only one component, namely n_{12}^s:

$$n_{12}^a(\mathbf{x}) = \tfrac{1}{2}(n_{12} - n_{21})(\mathbf{x}) = 0 \quad \text{for } n_{12}^s(\mathbf{x}) = \text{integer},$$
$$n_{12}^a(\mathbf{x}) = \tfrac{1}{2}(n_{12} - n_{21})(\mathbf{x}) = \tfrac{1}{2} \quad \text{for } n_{12}^s(\mathbf{x}) = \text{half-integer}. \tag{18.104}$$

After this, the symmetric part is taken to have the same gauge as in Section 10.3, i.e.,

$$n_{12}^s(\mathbf{x}) = 0, \qquad n_{22}^s(\mathbf{x}) = 0. \tag{18.105}$$

This choice was always possible. For, if n_{ij}, m_i do not satisfy these conditions, we can always go to new variables n_{ij}^{s0} which do, via the defect gauge transformation

$$n_{22}^s = n_{22}^{s0} + \nabla_2\bar{N}_2(\mathbf{x}), \qquad n_{12}^s = n_{12}^{s0} + \tfrac{1}{2}(\nabla_1\bar{N}_2(\mathbf{x}) + \nabla_2\bar{N}_1(\mathbf{x})), \tag{18.106}$$

with the fields $\bar{N}_1(\mathbf{x})$, $\bar{N}_2(\mathbf{x})$ of (10.5). These were shown to be unique solutions (up to a trivial translation plus rotation of the crystal as a whole), if the only nonzero component $n_{11}^s(\mathbf{x})$ satisfies the boundary conditions

$$n^s_{11}(x_1, 0) = 0, \tag{18.107}$$

$$\nabla_2 n^s_{11}(x_1, 0) = 0. \tag{18.108}$$

Let us now perform the integrals over $\gamma_i(\mathbf{x})$ and $\omega(\mathbf{x})$ in this gauge. This gives the conservation laws [corresponding to (18.35)]

$$\bar{\nabla}_i \sigma_{ij} = 0, \qquad \bar{\nabla}_i \tau_i = -\varepsilon_{k\ell}\sigma_{k\ell}. \tag{18.109}$$

These can be ensured by introducing "gauge fields" $A_j(\mathbf{x})$, $h(\mathbf{x})$ and $h(\mathbf{x})$ and writing

$$\sigma_{ij}(\mathbf{x}) = \varepsilon_{ik}\bar{\nabla}_k A_j(\mathbf{x}), \qquad \tau_i(\mathbf{x}) = \varepsilon_{ik}\bar{\nabla}_k h(\mathbf{x}) - A_i(\mathbf{x}). \tag{18.110}$$

Actually, in two dimensions there is really no gauge freedom in the decomposition. Still we have used the term "gauge fields" recalling that in three dimensions this name was appropriate. When going from the variables σ_{ij}, τ_i to A_j, h we have to watch out for the measure of integration. The δ-functions for the stress conservation laws $\delta(\nabla_i \bar{\sigma}_{ij})$, $\delta(\bar{\nabla}_i \tau_i + \varepsilon_{k\ell}\sigma_{k\ell})$ can be used to integrate out σ_{12}, σ_{22} and τ_2 (say). There is no Jacobian factor since $\det \nabla_2 = 1$. After this, the remaining integrals over σ_{11}, σ_{12} and τ_1 can be changed freely into integrals over $dA_1 dA_2 dh$ since

$$\sigma_{11} = \bar{\nabla}_2 A_1, \qquad \sigma_{12} = \bar{\nabla}_2 A_2, \qquad \tau_1 = \bar{\nabla}_2 h - A_1, \tag{18.111}$$

and there are again only trivial Jacobian factors $\det(\bar{\nabla}_2)$. In this way we ascend from (18.100) and (18.102) to a partition function

$$Z = \left(\frac{1}{4}\frac{1-\nu}{1+\nu}\right)^{N/2} \frac{1}{\sqrt{2\pi\beta}^{3N}} \frac{1}{\sqrt{8\pi\beta\ell^2/a^2}^{2N}} \prod_{\mathbf{x},i}\left[\int_{-\infty}^{\infty} dA_i(\mathbf{x})\right] \prod_{\mathbf{x}}\left[\int_{-\infty}^{\infty} dh(\mathbf{x})\right]$$

$$\sum_{\{m_i, n_{ij}\}} \Phi[m_i, n_{ij}] \exp\left\{-\frac{1}{4\beta}\sum_{\mathbf{x}}\left[\frac{1}{1+\nu}A_i(-\bar{\nabla}\cdot\nabla)A_i - \frac{1}{2}\frac{1-\nu}{1+\nu}A_i(-\nabla_i\bar{\nabla}_j)A_j\right]\right.$$

$$- \frac{a^2}{8\beta\ell^2}\sum_{\mathbf{x}}(\bar{\nabla}_k h - \varepsilon_{k\ell}A_\ell)^2 - 2\pi i\sum_{\mathbf{x}}\varepsilon_{ik}\bar{\nabla}_k A_j n_{ij}$$

$$\left. - 2\pi i\sum_{\mathbf{x}}(\varepsilon_{ik}\bar{\nabla}_k h - A_i)m_i\right\}. \tag{18.112}$$

The stress-energy terms arise as follows:

$$\sum_{\mathbf{x}} \sigma_{ij}^{s2}(\mathbf{x}) = \sum_{\mathbf{x}} \left[\frac{1}{2}(\varepsilon_{ik}\bar{\nabla}_k A_j + (ij)) \right]^2$$
$$= \frac{1}{4}\sum_{\mathbf{x}} \left[(\bar{\nabla}_i A_j)^2 + (ij) + 2\varepsilon_{ik}\bar{\nabla}_k A_j \varepsilon_{jk'}\bar{\nabla}_{k'} A_i \right]$$
$$= \sum_{\mathbf{x}} \left[A_i(-\bar{\nabla}\cdot\nabla)A_i - \frac{1}{2}A_i(-\nabla_i\bar{\nabla}_j)A_j \right], \qquad (18.113)$$

$$\sum_{\mathbf{x}} \sigma_{\ell\ell}^{s2}(\mathbf{x}-\boldsymbol{\ell}) = \sum_{\mathbf{x}} (\varepsilon_{\ell k}\nabla_k A_\ell(\mathbf{x}-\boldsymbol{\ell}))^2$$
$$= \sum_{\mathbf{x}} [A_i(-\bar{\nabla}\cdot\nabla)A_i - \nabla_\ell A_\ell(\mathbf{x}-\boldsymbol{\ell})\nabla_{\ell'}A_{\ell'}(\mathbf{x}-\boldsymbol{\ell}')]$$
$$= \sum_{\mathbf{x}} [A_i(-\bar{\nabla}\cdot\nabla)A_i - (\bar{\nabla}\cdot\mathbf{A}(\mathbf{x}))^2]. \qquad (18.114)$$

After a partial integration, the last two terms become [by (18.112)]

$$-2\pi i \sum_{\mathbf{x}} A_j(\varepsilon_{ki}\nabla_k n_{ij} - m_j) - 2\pi i \sum_{\mathbf{x}} h\varepsilon_{ki}\nabla_k m_i. \qquad (18.115)$$

We now compare the sources in parentheses with the continuum formulas (2.123) for the defect densities and see that we can identify

$$\bar{\alpha}_j(\mathbf{x}) = \varepsilon_{ki}\nabla_k n_{ij}(\mathbf{x}) - m_j(\mathbf{x}) \qquad (18.116)$$

as the integer-valued dislocation density on the lattice and

$$\bar{\Theta}(\mathbf{x}) = \varepsilon_{ki}\nabla_k m_i(\mathbf{x}) \qquad (18.117)$$

as the integer-valued disclination density.

Using the notation $\bar{\alpha}(\mathbf{x}) = b_i(\mathbf{x})$ on two dimensional lattices [recall (12.19)], the coupling (18.115) becomes simply

$$-2\pi i \sum_{\mathbf{x}} (A_i(\mathbf{x})\, b_i(\mathbf{x}) + h(\mathbf{x})\,\bar{\Theta}(\mathbf{x})). \qquad (18.118)$$

We now integrate out the fields $A_i(\mathbf{x})$ and $h(\mathbf{x})$. The stress energy σ_{ij}^{s2} is diagonal in the "transverse" and "longitudinal" parts of $A_i(\mathbf{x})$. Therefore it is useful to split $A_i(\mathbf{x})$ explicitly into these two parts[c]

$$A_i(\mathbf{x}) = \varepsilon_{ij}\bar{\nabla}_j\varphi_T + \nabla_i\varphi_L, \tag{18.119}$$

and cast the stress energy to the following form:

$$\frac{1}{4\beta}\sum_{\mathbf{x}}\left(\frac{1}{1+\nu}(\bar{\nabla}\cdot\nabla\varphi_T)^2 + \frac{1}{2}(\bar{\nabla}\cdot\nabla\varphi_L)^2\right)$$
$$+\frac{a^2}{8\beta\ell^2}\sum_{\mathbf{x}}[(\bar{\nabla}_k(h-\varphi_T))^2 + (\nabla_k\varphi_L)^2]. \tag{18.120}$$

By rewriting the coupling (18.120) as

$$-2\pi i\sum_{\mathbf{x}}[(\varepsilon_{ij}\bar{\nabla}_j\varphi_T + \nabla_i\varphi_L)b_i + h\bar{\Theta}]$$
$$= -2\pi i\sum_{\mathbf{x}}[\varphi_T(\varepsilon_{ij}\nabla_i b_j + \bar{\Theta}) - \varphi_L\bar{\nabla}_i b_i + (h-\varphi_T)\bar{\Theta}], \tag{18.121}$$

we see that we can integrate out independently the fields φ_T, φ_L, $h-\varphi_T$. The change of variables yields a Jacobian factor

$$\prod_{\mathbf{x}}\int dA_1\int dA_2\int dh = \det(-\bar{\nabla}\cdot\nabla)\prod_{\mathbf{x}}\int d\varphi_L\int d\varphi_T\int d(h-\varphi_T). \tag{18.122}$$

From the integrals $\int d\varphi_T$ and $\int d(h-\varphi_T)$ we then obtain a Boltzmann factor

$$\exp\left\{-\beta 4\pi^2(1+\nu)\sum_{\mathbf{k}}\bar{\eta}(\mathbf{k})^*\frac{1}{(\bar{\mathbf{K}}\cdot\mathbf{K})^2}\bar{\eta}(k) - 2\beta\frac{\ell^2}{a^2}4\pi^2\sum_{\mathbf{k}}\bar{\Theta}(\mathbf{k})^*\frac{1}{\bar{\mathbf{K}}\cdot\mathbf{K}}\bar{\Theta}(\mathbf{k})\right\}, \tag{18.123}$$

where the first term contains the lattice version of the total defect energy of classical elasticity,

[c]Explicitly, $\varphi_L = (1/\bar{\nabla}\cdot\nabla)\bar{\nabla}_i A_i$, $\varphi_T = (-1/\bar{\nabla}\cdot\nabla)\varepsilon_{ij}\nabla_i A_j$.

$$\bar{\eta}(\mathbf{x}) = \varepsilon_{ij}\nabla_i b_j(\mathbf{x}) + \bar{\Theta}(\mathbf{x}). \tag{18.124}$$

It is sensitive only to this combination of dislocations and disclinations [recall (12.19)] and not to the particular nature of the different defects. The second term removes part of the degeneracy discussed in (12.21), (12.22) by giving the disclinations an additional Coulomb energy. The integration over φ_L, finally, generates a Boltzmann factor involving the longitudinal part of the dislocation density,

$$\exp\left\{-2\beta\frac{\ell^2}{a^2}4\pi^2\sum_{\mathbf{x}}(\bar{K}_i b_i(\mathbf{k}))^*\frac{1}{\bar{\mathbf{K}}\cdot\mathbf{K}(1+(\ell^2/a^2)\bar{\mathbf{K}}\cdot\mathbf{K})}\bar{K}_i b_i(\mathbf{k})\right\}. \tag{18.125}$$

This fixes the remaining degeneracy. As a result, the partition function becomes

$$\begin{aligned} Z = {} & \left[\frac{1}{2}(1-\nu)\right]^{N/2}\frac{1}{\sqrt{2\pi\beta^{2N}}}\det(-\bar{\nabla}\cdot\nabla)^{-1}\sum_{\{b_i(\mathbf{x}),\,\bar{\Theta}(\mathbf{x})\}} \\ & \times\exp\left\{-\beta 4\pi^2(1+\nu)\sum_{\mathbf{x}}\bar{\eta}(\mathbf{x})\frac{1}{(\bar{\nabla}\cdot\nabla)^2}\bar{\eta}(\mathbf{x}) - 2\beta\frac{\ell^2}{a^2}4\pi^2\sum_{\mathbf{x}}\bar{\Theta}(\mathbf{x})\frac{1}{-\bar{\nabla}\cdot\nabla}\bar{\Theta}(\mathbf{x})\right. \\ & \left. - 2\beta\frac{\ell^2}{a^2}4\pi^2\sum_{\mathbf{x}}(\bar{\nabla}_i b_i(\mathbf{x}))[-\bar{\nabla}\cdot\nabla(1-(\ell^2/a^2)\bar{\nabla}\cdot\nabla)]^{-1}(\bar{\nabla}_i b_i(\mathbf{x}))\right\}. \end{aligned} \tag{18.126}$$

The sum runs over all three defect configurations $b_1(\mathbf{x})$, $b_2(\mathbf{x})$, $\bar{\Theta}(\mathbf{x})$, independently, and no infinite overall factor appears.

The new defect energies remove the degeneracy between strings of dislocations and single disclinations, in a way specified completely by the higher gradient elastic energy (18.97).

Consider a single dislocation

$$b_i = \delta_{i2}\delta_{\mathbf{x},\mathbf{X}}. \tag{18.127}$$

From (18.126) we see that it has an extra core energy,

$$E_{\text{core}} = -2\beta 4\pi^2 v_m(\mathbf{0}) \tag{18.128}$$

where $v_m(\mathbf{0})$ is the Yukawa potential on the lattice. A pair of disclinations, on the other hand, with

$$\bar{\Theta}(\mathbf{x}) = \delta_{\mathbf{x},\mathbf{X}+\mathbf{1}} - \delta_{\mathbf{x},\mathbf{X}} = \nabla_1 \delta_{\mathbf{x},\mathbf{X}} \tag{18.129}$$

[which gives the same contribution to $\bar{\eta} = \varepsilon_{ij}\nabla_i b_j + \bar{\Theta}$ as (18.127) and is indistinguishable from it in lowest gradient elasticity] has the extra core energy

$$E_{\text{core}} = -2\beta(\ell^2/a^2)4\pi 2v'_0(\mathbf{1}), \tag{18.130}$$

where $v'(\mathbf{x})$ is the subtracted Coulomb potential on the lattice. Conversely, a string of dislocations along the 1-axis from $\mathbf{X}$ to $\mathbf{Y} = \mathbf{X} + n \cdot \mathbf{1}$, say, has

$$b_i(\mathbf{x}) = \delta_{i2}\delta_{x_2,X_2}(\theta_{x_1,X_1} - \theta_{x_1,Y_1}), \tag{18.131}$$

where θ is the Heaviside function on the lattice defined in Eq. (14.170). Equivalently we can write

$$b_i(\mathbf{x}) = \delta_{i2}\bar{\nabla}_1^{-1}(\delta_{\mathbf{x},\mathbf{X}} - \delta_{\mathbf{x},\mathbf{Y}}). \tag{18.132}$$

For lowest gradient elasticity, the string would be equivalent to a pair of disclinations at the ends of the string,

$$\bar{\Theta}(\mathbf{x}) = \delta_{\mathbf{x},\mathbf{X}} - \delta_{\mathbf{x},\mathbf{Y}}. \tag{18.133}$$

The pair carries an extra energy depending on the distance,

$$E_{\text{extra}} = 2\beta(\ell^2/a^2)4\pi^2 2v'_0(\mathbf{X} - \mathbf{Y}). \tag{18.134}$$

On the other hand, the string has the much more involved extra energy,

$$E_{\text{extra}} = 2\beta 4\pi^2 \sum_{\mathbf{x},\mathbf{x}'} (\delta_{\mathbf{x},\mathbf{X}} - \delta_{\mathbf{X},\mathbf{Y}})(\bar{\nabla}_2/\bar{\nabla}_1)[-\bar{\nabla}\cdot\nabla)(-\bar{\nabla}\cdot\nabla + a^2/\ell^2)]^{-1}$$
$$\times (\bar{\nabla}_2/\bar{\nabla}_1)(\mathbf{x}, \mathbf{x}')(\delta_{\mathbf{x}',\mathbf{X}} - \delta_{\mathbf{x}',\mathbf{Y}}) = 2\beta 4\pi^2 2w(\mathbf{X} - \mathbf{Y}), \tag{18.135}$$

where

$$w(\mathbf{x}) = \bar{\nabla}_2\nabla_2(\bar{\nabla}_1\nabla_1)^{-1}[-\bar{\nabla}\cdot\nabla(-\bar{\nabla}\cdot\nabla + a^2/\ell^2)]^{-1}(\mathbf{x}, 0). \tag{18.136}$$

If one wants to study the full influence of the different extra energies upon the melting process, Monte Carlo simulations of the present model

will be necessary. Fortunately, the limiting situation of a large rotational stiffness, i.e., of a very large ℓ, can be dealt with analytically and we shall do this in the following section.

18.7 TWO SUCCESSIVE MELTING TRANSITIONS AT LARGE ROTATIONAL STIFFNESS

The present model with second gradient elasticity accommodates naturally the possibility of melting via two successive continuous transitions. This can be demonstrated most easily in the limit in which the length scale ℓ, which characterizes the rotational stiffness of the system, is sufficiently large. Our starting point is the partition function (18.112). We perform the sums over n_{ij} and m_i, thereby forcing the gauge fields of stresses and torque stresses to be integer-valued (to be denoted by $\bar{A}_i, \bar{h}$). Then Z becomes

$$Z = \left(\frac{1}{4}\frac{1-\nu}{1+\nu}\right)^{N/2} \frac{1}{\sqrt{2\pi\beta^3}^N} \frac{1}{\sqrt{8\pi\beta\ell^2/a^2}^{2N}} \sum_{\{\bar{A}_i,\bar{h}\}} \exp\left\{-(1/4\beta)\sum_{\mathbf{x}}\left[\frac{1}{1+\nu}(\nabla_i\bar{A}_j)^2 - \frac{1}{2}\frac{1-\nu}{1+\nu}(\bar{\nabla}_i\bar{A}_i)\right]\right.$$
$$\left. -(a^2/8\beta\ell^2)\sum_{\mathbf{x}}(\nabla_k\bar{h} - \varepsilon_{k\ell}\bar{A}_\ell)^2\right]. \tag{18.137}$$

Let us follow the behaviour of this model from small to large β.

For very small β, both $\bar{A}_i$ and $\bar{h}$ are squeezed to zero. If ℓ^2 is very large, however, the sqeezing of the $\bar{h}$ field in the second term is relaxed and follows an effective partition function (apart from a trivial shift of the $\bar{h}$ field),

$$Z \approx \sum_{\{\bar{h}\}} \exp\left\{(-a^2/8\beta\ell^2)\sum_{\mathbf{x}}(\nabla_k\bar{h})^2\right\}. \tag{18.138}$$

This is a discrete or Gaussian roughening model [see Eqs. (11.10), (11.254) of Part II] with $\beta_{DG} \equiv a^2/4\beta\ell^2$. It is known to have a continuous phase transition of the Kosterlitz-Thouless type at $\beta_{DG} \approx \pi/2$, (see Eqs. (11.11), (11.68a) of Part II) i.e., if $\beta = \beta_h$ is about equal to

$$4\beta_h \ell^2/a^2 \approx 2/\pi. \tag{18.139}$$

These approximate relation hold, of course, exactly for the renormalized quantities β_{DG}^R, β_h^R. The same will be true for similar approximate statements on transition points appearing later in this section, without being always stated explicitly. The subscript h records the fact that, in this transition, the fields $\bar{h}$ becomes rough.

For β of order unity, the prefactor $a^2/8\beta\ell^2$ is so small that the discreteness of $\bar{h}$ becomes irrelevant. It is then a good approximation to integrate out $\bar{h}$ as if it were a continous variable. By decomposing

$$\sum_{\mathbf{x}} (\bar{\nabla}_k \bar{h} - \varepsilon_{k\ell}\bar{A}_\ell)^2 = \sum_{\mathbf{x}} [\varepsilon_{k\ell}\bar{\nabla}_\ell(\bar{h} - (\nabla\cdot\bar{\nabla})^{-1}\varepsilon_{ij}\nabla_i\bar{A}_j) + (\bar{\nabla}\cdot\nabla)^{-1}\nabla_k\bar{\nabla}_i\bar{A}_i]^2, \tag{18.140}$$

we see that the energy separates into the squares of a longitudinal and a transverse part. Hence, after the $\bar{h}$ integration, the partition function becomes effectively

$$Z \approx \sum_{\{A_i\}} \exp\left\{-(1/4\beta)\sum_{\mathbf{x}}\left[\frac{1}{1+\nu}[(\nabla_i\bar{A}_j)^2 - \frac{1}{2}\frac{1-\nu}{1+\nu}(\bar{\nabla}_i A_i)^2] + (a^2/2\ell^2)\bar{A}_i(1/-\bar{\nabla}\cdot\nabla)(-\nabla_i\bar{\nabla}_j)\bar{A}_j\right]\right\}. \tag{18.141}$$

Under the assumption of a very large ℓ, the last term can be ignored and we remain with a discrete Gaussian vector model. For $\nu = 1$ (incompressible material), this takes a simple form, reducing to the product of two identical discrete Gaussian models with a phase transition of the Kosterlitz-Thouless type at $\beta = \beta_A$ with

$$4\beta_A \approx 2/\pi. \tag{18.142}$$

Below we shall find the same transition once more in the dual defect formulation of the partition function, (18.126), where it is easy to see that the same universality class prevails also for $\nu < 1$. The two continuous transitions and their characteristic properties are displayed graphically in Fig. 18.1.

In the opposite limit of small ℓ, the system has only a single first-order transition at $\beta = \beta_{h,A^T}$ with

FIG. 18.1. Schematic characterization of the three phases for large ℓ, with the two Kosterlitz-Thouless transitions (KT). The left-hand side indicates the field configurations in the roughening representations (18.137) (≈ 0 smooth, $\neq$ rough), the right-hand side indicates the defect excitations as deduced from the defect representation of the partition function (18.126) [from H. Kleinert (1988)].

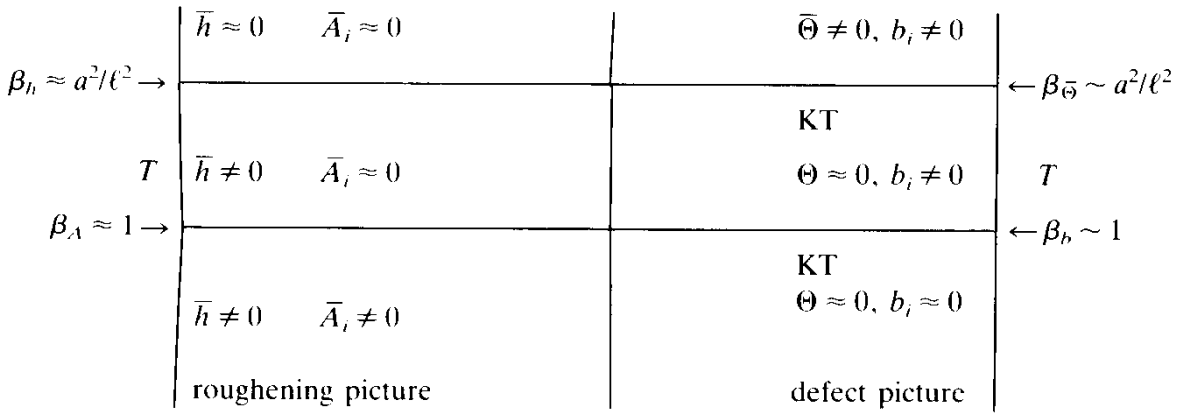

Large-ℓ transitions

$$\beta_{h,A^T}(1 + \nu) \approx 0.815. \tag{18.143}$$

This is the first-order melting transition discussed extensively in the Chapters 12–14 [see Eq. (12.35)]. Here it arises since, for small ℓ, the third term in (18.137) forces the vector field $\bar{A}_k$ to be equal to $\bar{A}_k^T \equiv -\varepsilon_{k\ell}\bar{\nabla}_\ell \bar{h}$, so that the first two terms combine to the Laplacian roughening model, with the associated known discontinuous transition [see Sec. 12.6]. In it, the fields $\bar{h}$ and $\bar{A}_i$ become simultaneously rough.

For β far above this transition, the effective partition function is

$$Z = \sum_{\{\bar{h},A_i\}} \exp\left\{-(a^2/8\beta\ell^2)\sum_{\mathbf{x}} (\bar{\nabla}_k \bar{h} - \varepsilon_{k\ell}\bar{A}_\ell)^2\right\}. \tag{18.144}$$

This looks like a Villain model [recall Part II, Chapter 7, Eq. (7.29)] in which $\bar{h}$ plays the role of the phase angle γ and $\varepsilon_{k\ell}\bar{A}_\ell$ that of the jump number n_i. There is, however, an important difference: The $\bar{h}$'s are integer numbers. A duality transformation following the steps (7.16)–(7.18) and Eq. (8.31) of Part II shows that Z is equivalent to a sum

$$Z = \sum_{\{b_i(x)\}} \exp\left\{-2\beta(\ell^2/a^2)4\pi^2 \sum_{\mathbf{x}} b_i^2(\mathbf{x})\right\}. \tag{18.145}$$

Since the $\bar{h}$'s are integers, there is no constraint $\bar{\nabla}_i b_i(\mathbf{x}) = 0$. But the unconstrained discrete Gaussian sum (18.145) is an analytic function of β

FIG. 18.2. For small ℓ, there is only a single first-order melting transition at $\beta \approx 1$, where $\bar{h}$ roughens or the defects $\bar{\Theta}$ proliferate in a background of random b_i fields.

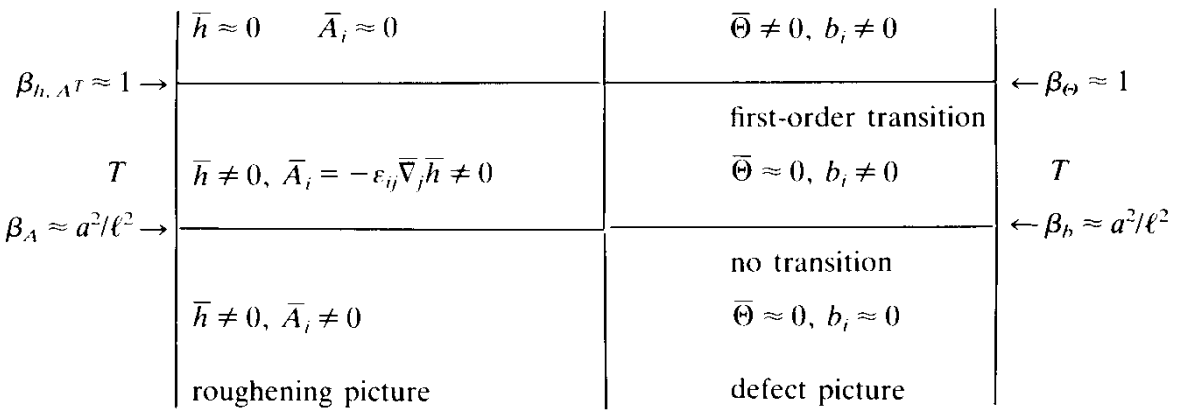

small-ℓ transitions

so that there is no phase transition. If $\bar{h}$ in (18.144) had been a continous variable, the ensuing constraint $\bar{\nabla}_i b_i(\mathbf{x}) = 0$ would have led to a Kosterlitz Thouless transition at

$$a^2/16\pi^2\beta_A\ell^2 \approx 2/\pi, \tag{18.146}$$

in which the $\bar{A}_i$ fields become rough. In Fig. 18.2 we have illustrated the properties of the two phases for small ℓ.

The sequence of transitions can also be studied in the defect representation of the partition function, Eq. (18.126). We follow the model from small to large temperature $T = \beta^{-1}$.

For large ℓ, the disclinations $\bar{\Theta}$ are frozen out and only the dislocations can be excited,

$$Z = \sum_{\{b_i(\mathbf{x})\}} \exp\left\{-2\beta 4\pi^2 \sum_{\mathbf{x}} b_i(\mathbf{x})(-\bar{\nabla} \cdot \nabla)^{-1} b_i(\mathbf{x})\right\}. \tag{18.147}$$

This is the partition function of two independent identical Coulomb gases with a Kosterlitz-Thouless transition at $\beta = \beta_b$ with

$$4\beta_b \approx 2/\pi. \tag{18.148}$$

The subscript b indicates the unbinding of dislocation pairs in this transition, which is to be identified with the roughening transition of the $\bar{h}$

field in (18.142). In the defect picture, it is easy to predict the position and character of the transition also for $\nu < 1$. Then the interaction (18.126) between dislocations can be written as

$$\beta E_{\text{int}} = \beta 4\pi^2(1+\nu)\sum_{\mathbf{x},\mathbf{x}'} b_i(\mathbf{x}) v_0^T(\mathbf{x}-\mathbf{x}')_{ij} b_j(\mathbf{x}') + 2\beta 4\pi^2 \sum_{\mathbf{x},\mathbf{x}'} b_i(\mathbf{x}) v_{a/\ell}^L(\mathbf{x}-\mathbf{x}')_{ij} b_j(\mathbf{x}'), \tag{18.149}$$

where $v_{0_{ij}}^T$ is the massless transverse Green function, $\bar{\nabla}_i\nabla_j/\bar{\nabla}\cdot\nabla$, and v_{mij}^L the massive longitudinal one, $-(\delta_{ij}\nabla\cdot\bar{\nabla} - \nabla_i\bar{\nabla}_j)/(m^2 - \nabla\cdot\bar{\nabla})$. The long-distance behaviour of $v_0(\mathbf{x})$ was calculated in Eqs. (1.123) and (1.124),

$$\begin{aligned} v_0^L(\mathbf{x}) &\underset{|\mathbf{x}|\to\infty}{\longrightarrow} -(1/4\pi)(\delta_{ij}\log|\mathbf{x}| + x_i x_j/|\mathbf{x}|^2), \\ v_0^T(\mathbf{x}) &\underset{|\mathbf{x}|\to\infty}{\longrightarrow} -(1/4\pi)(\delta_{ij}\log|\mathbf{x}| - x_i x_j/|\mathbf{x}|^2). \end{aligned} \tag{18.150}$$

Both together give the long-range Coulomb interaction energy of a pair of dislocations,

$$E_{\text{int}} = 2\pi\beta[(1+\nu)+2]\log|\mathbf{x}| \tag{18.151}$$

According to what we have learned in Chapter 14 [compare Eq. (14.13)], there is a pair-unbinding transition near

$$\beta_b \underset{\ell=\infty}{\approx} 4/2\pi[(1+\nu)+2]. \tag{18.152}$$

For a finite ℓ^2, the longitudinal part of the interaction (18.149) only has a finite range $\approx\ell$ and does not contribute in the critical limit. Then the 2 in the bracket of (18.152) is absent and the transition lies at

$$\beta_b \approx 2/\pi(1+\nu). \tag{18.153}$$

As stated above, these approximate relations hold exactly for the renormalized β [recall (14.19)].

For small $\beta \approx a^2/\ell^2$ the effective partition function is

$$Z \approx \sum_{\{\bar{\Theta}(\mathbf{x})\}} \exp\left\{-2\beta(\ell^2/a^2)4\pi^2 \sum_{\mathbf{x}} \bar{\Theta}(\mathbf{x})(-\bar{\nabla}\cdot\nabla)^{-1}\bar{\Theta}(\mathbf{x})\right\}. \tag{18.154}$$

It represents a Coulomb gas with a Kosterlitz-Thouless transition at

$$4\beta_\Theta \ell^2/a^2 \approx 2/\pi. \tag{18.155}$$

This is the defect version of the roughening transitions (18.139). See again Fig. 18.1 for a characterization of the phases.

For β of order unity, the $\bar{\Theta}$ and $\bar{\nabla}_i b_i$ terms in (18.126) can be dropped and the effective partition function is

$$Z \approx \sum_{\{\bar{\eta}(\mathbf{x})\}} \exp\left\{-\beta 4\pi^2(1+\nu)\sum_{\mathbf{x}} \bar{\eta}(\mathbf{x})(-\bar{\nabla}\cdot\nabla)^{-2}\bar{\eta}(\mathbf{x})\right\}. \tag{18.156}$$

This has a first-order phase transition at

$$\beta_\eta(1+\nu) \approx 0.815, \tag{18.157}$$

which is again the melting transition of the lowest gradient model. It corresponds to (18.143).

Consider now the defect picture for small ℓ. Then a phase transition might have been expected at large $\beta \sim 1/\ell$, in which $\bar{\eta}$ is frozen at zero so that $\bar{\Theta}$ is equal to $-\varepsilon_{k\ell}\nabla_k b_\ell$. The second and third terms in (18.126) can be added together and give an effective partition function,

$$Z \approx \sum_{\{b_i(\mathbf{x})\}} \exp\left\{-2\beta(\ell^2/a^2)4\pi^2\sum_{\mathbf{x}} b_i^2(\mathbf{x})\right\}. \tag{18.158}$$

Due to the absence of the constraint $\bar{\nabla}_i b_i(x) = 0$, this has no phase transition. With the constraint, there would have been a phase transition at

$$a^2/16\pi^2\beta_b\ell^2 \approx 2/\pi, \tag{18.159}$$

just as in (18.146). The characteristics of the two phases, as seen from the defect point of view, are illustrated in Fig. 18.2.

These considerations have led to the qualitative prediction of the phase diagram in the β, ℓ^2 plane sketched in Fig. 18.3 [Kleinert, 1988] A phase diagram of this kind was indeed found in recent Monte Carlo simulations of the model [Janke and Kleinert, 1988)], performed in the roughening version (18.137), with the trivial prefactors omitted, i.e., the partition function investigated was

FIG. 18.3. Phase diagram suggested by the three known transition points. It is not clear where the first-order transition line becomes that of the Kosterlitz-Thouless (KT) type. The dots indicate the would-be transition (18.146), (18.159) [compare with Fig. 18.5].

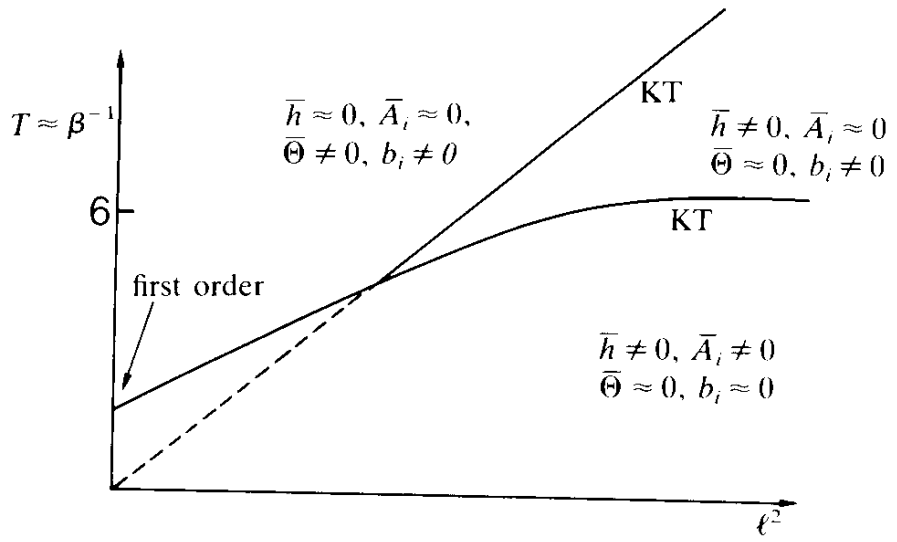

$$Z_r = \sum_{\{\bar{h},\bar{A}_i\}} \exp(-\beta E_r), \tag{18.160}$$

E_r being the $\bar{h}$, $\bar{A}_i$ energy in (18.137). Since the universality class does not depend on ν, its value was chosen to be 1, to have the simplest energy. The simulations were done with periodic boundary conditions using the the standard Metropolis algorithm, in which trial values for $\bar{h}(\mathbf{x})$ and $\bar{A}_i(\mathbf{x})$ were chosen randomly from one above or one below the current value at each site. The transition points were found by measuring at various fixed ℓ's, first the specific heats, for an estimate, and afterwards the correlation functions of $\bar{h}$ and $\bar{A}_i$, for a precise determination. Figure 18.4 shows the specific heat curves, with the definition $c \equiv T^2(\partial^2/\partial T^2) \ln Z_r/L^2$, where L^2 is the number of sites of the square lattice. It is advantageous to use T instead of β in this definition since in the roughening picture the temperature interpretation is usually inverted (cold $\triangleq$ smooth, hot $\triangleq$ rough). Then the curves allow for the easiest comparison with the curves of the known limiting cases of large ℓ^2, where we should see two rounded peaks of the discrete Gaussian model, and of small ℓ^2, where there is only a single first order transition of the Laplacian roughening model. The correlation functions which were studied are defined as follows,

$$\begin{aligned} c^h(x - x') &\equiv L \langle (\bar{h}(x) - \bar{h}(x'))^2 \rangle \\ c_i^A(x - x') &\equiv L \langle (\bar{A}_i(x) - \bar{A}_i(x'))^2 \rangle, \quad i = 1,2 \end{aligned} \tag{18.161}$$

where $\langle \ldots \rangle$ denotes a thermal average with respect to Z_r, and the wiggles on top are averages along columns in the y direction, $\bar{\bar{h}}(x) \equiv -\frac{1}{L}\sum_{y=1}^{L} \bar{h}(x,y)$. In momentum space, these averages are equivalent to a projection on the k_x-axis, leading to simple one-dimensional Fourier representations for $c^h(x)$ and $c^A(x)$, In the absence of defects, where $\bar{h}$ and $\bar{A}_i$ are continous free fields, these can be evaluated exactly (even on finite lattices).

Let us summarize the theoretically expected behaviour of these correlation functions, first in the limit of a large ℓ^2, where it is most obvious. In the low–temperature solid phase, there are very few defects and the discrete variables $\bar{h}, \bar{A}_i$ can be treated effectively as massless continuous fields. The dilute gas of bound defects manifests itself only in a renormalization of the temperature, i.e., $\beta \to \beta^R$. This is an exponentially small effect, due to the finite activation energies, i.e., to the low fugacities. The correlation functions of $\bar{h}$ and $\bar{A}_i$ can then be extracted from the energy in (18.137), or taken directly from the defect energy (18.126). After replacing β by the renormalized quantity β^R and projecting on to the k_x-axis in momentum space this gives (for $a = 1$)

$$c^h(x) = -2\beta^R \frac{1+\nu}{2}[v_4(x) + (2\ell^2/(1+\nu))v_2^{(0)}(x)],$$

$$c_1^A(x) = -4\beta^R v_2^{(1/\ell)}(x), \qquad c_2^A(x) = -2\beta^R \frac{1+\nu}{2} v_2^{(0)}(x), \tag{18.162}$$

where the $D = 1$ Green function are [see (I.6.184)]

$$v_2^{(m)}(x) = \frac{1}{L}\sum_{n=1}^{L-1} \frac{e^{ik_n x} - 1}{2(1-\cos k_n) + m^2}, \qquad k_n = \frac{2\pi}{L} n, \tag{18.163}$$

$$v_4(x) = \frac{1}{L}\sum_{n=1}^{L-1} \frac{e^{ik_n x} - 1}{[2(1-\cos k_n)]^2}.$$

With increasing temperature, we run into the first transition $\beta_c^{(1)}$ where dislocation pairs begin to unbind. There we expect the A_i-fields to become massive, as a two dimensional disorder version of the "Meissner" effect in superconductivity. In an ensemble of unbound dislocation pairs, a single pair has only a finite interaction range, due to the screening of the Coulomb forces by the ensemble. At the same time, the $\bar{h}$ correlations, which in the low temperature phase grow like $(1/8\pi)|\mathbf{x}|^2 \log|\mathbf{x}|$

[recall Eq. (11A.181)], are screened at long range to $\propto -(1/2\pi)\log|\mathbf{x}|$. The amplitude can be extracted from the effective discretize Gaussian model in Eq. (18.138). Hence, after a projection onto the k_x-axis, the $\bar{h}$ correlations are

$$c^{h}(x) = -4\beta^{R}\ell^{2}v_{2}^{(0)}(x). \tag{18.164}$$

From the defect version of the model (18.154) we see that, in this phase, the disclinations are bound together by a two-dimensional Coulomb potential. Upon a further increase in temperature, we run into the second phase transition where also the $\bar{h}$ correlations become massive and the pairs of disclinations unbind. The renormalized values of β at these transitions were given in Eqs. (18.139), (18.155).

In the low temperature phase, when we plot $c_2^A(x)$ as a function of $v_2^{(0)}(x)$ for many values of x, we expect the points to lie on a straight line for all $\beta > \beta_b$. Its slope decreases with temperature, but with a limiting minimal slope $\beta^R \cdot (1+\nu) = (\beta^R_{\mathrm{DG}c})^{-1} = 2/\pi$ at the critical point β_b [see Eq. (18.153)]. For $\beta < \beta_b$, the correlation length (= inverse mass) becomes finite. In the plot this is signaled by the straight line curving downward at large distances. If the lattice size is smaller than this finite correlation length, then the straight lines still appear straight, but now with a slope smaller than $4/\pi$. By a comparative finite-size scaling analysis of the correlation function near the transition in an ordinary discrete Gaussian model transition (to which it reduces for $\ell \to \infty$) it can be shown that using this "onset of curvature criterion" it is possible to determine the transition point β_c quite accurately, and with very little dependence on the finite lattice size, as long as $L^2 > 16 \times 16$. In this way one can reproduce the well known transition point of the discrete Gaussian model [compare Eq. (II.1.68b)]

$$\beta_{\mathrm{DG}c} \approx 1.354 \pm 0.02.$$

The correlation functions were measured on 32×32 lattices using 500 000 configurations for the thermal averages, after discarding 100 000 configurations for equilibration. The transition points (for $\nu = 1$) are shown in the $\ell^2 - T$ phase diagram of Fig. 18.5 as open circles. The solid lines are an interpolation of the data. The dotted tangential line has a slope 5.4. This agrees with what would have been expected from the approximate discrete Gaussian model (18.138), which would have a transition at $4\beta_c\ell^2 = (\beta_{\mathrm{DG}c})^{-1}$ or $T = 4\beta_{\mathrm{DG}c}\ell^2$, i.e., a slope of

FIG. 18.4. Specific heat versus temperature of the defect melting model on a 16×16 lattice with increasing length scale of rotational stiffness ℓ. The temperature scale is the same in all plots. Arrows indicate the transition points which, for $\ell^2 > 1$, lie clearly below the peaks. It is not necessary to plot the peaks for larger ℓ^2, since they follow quite well the appropriately rescaled specific heat curves of the ordinary discrete Gaussian model. The data are averages over 5000 configurations, after discarding 1000 configurations for thermalization [from Janke and Kleinert (1988)].

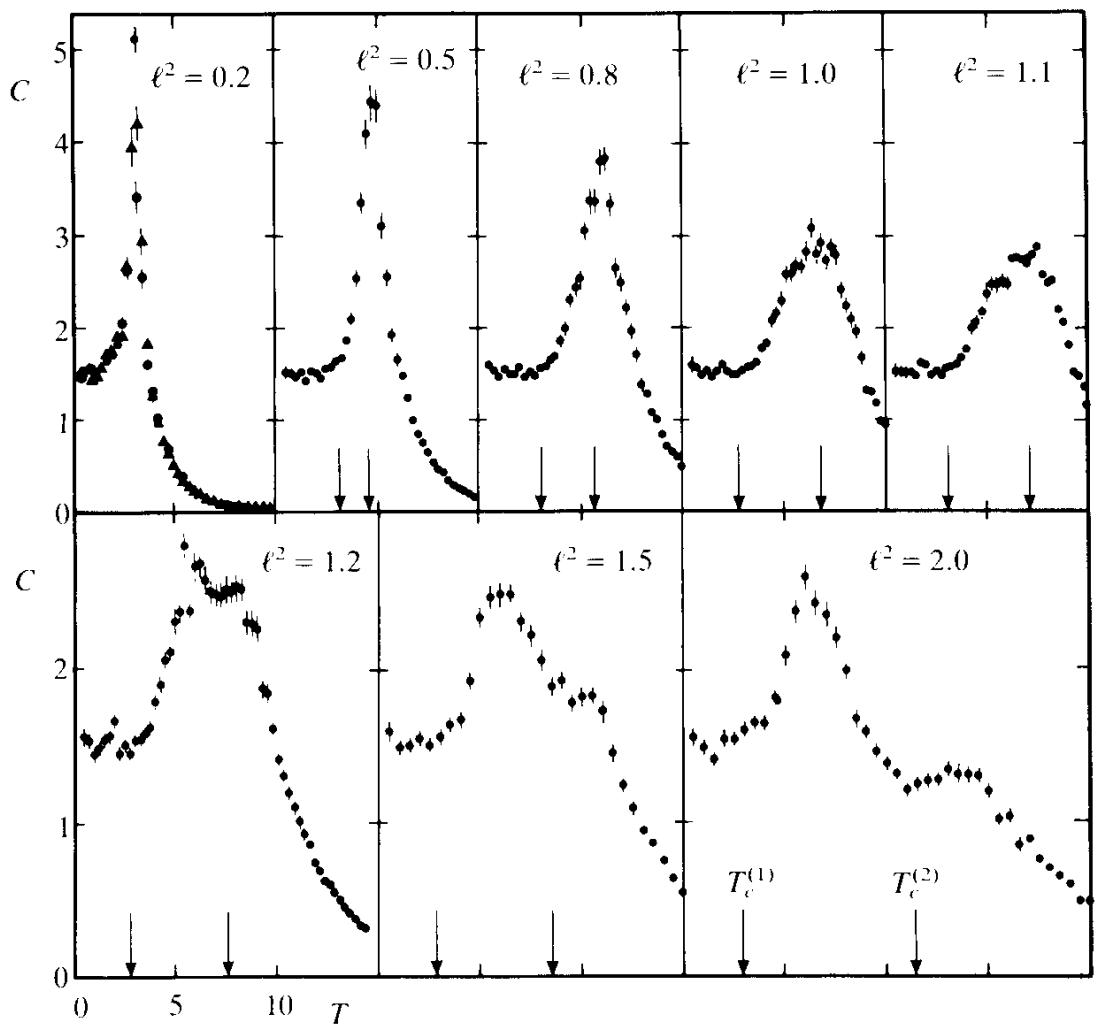

$4 \cdot 1.354 \approx 5.42$. The full circles show the location of the peaks of the specific heat, β_{peak}, as measured on 16×16 lattices and plotted in Fig, 18.4. Actually, to determine the precise location of the maxima, additional runs were performed near the tip of the peaks with much higher statistics. Furthermore, the finite-size scaling behavior for $\ell^2 = 0.2$, 0.5, 1.0, 3.0 was studied (using lattices up to 64×64) to make sure that there is no significant finite size dependence in β_{peak}. The dashed line with slope 6.9 agrees well with the peak position of the pure discrete Gaussian model (18.138), which has a peak position $\beta_{\text{peak}}^{\text{DG}} \approx 1.722 \pm 0.01$

FIG. 18.5. Phase diagram of the lattice-defect melting model for $\nu = 1$. The abcissa is the length scale of rotational stiffness, the ordinate the temperature. The transition points are determined from measurements of correlation functions on 32×32 lattices. In the upper phases we have indicated the roughness of the integer-field configurations and the defects as in Figs. 18.1, 18.2. The lower phase contains very few defects and is completely rough in $\bar{h}$, $\overline{A_i}$. The right-hand margin are marks for the position of lower peak and KT transition for $\ell = \infty$ [Eq. (18.152)]. For finite ℓ, the transition temperatures are lower than these, by a factor $(1 + \nu)/[1 + \nu + 2]$, since the longitudinal modes have only a finite range ℓ and do not contribute to the critical limit of the renormalization flow [compare (18.151)].

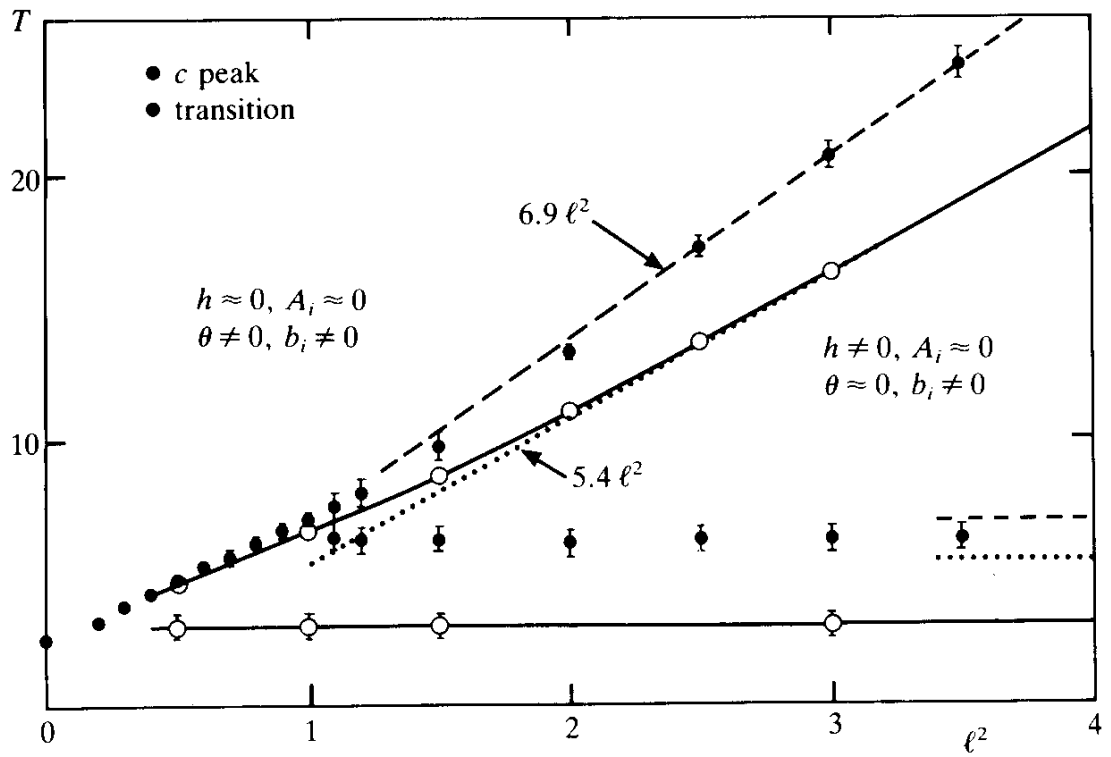

corresponding to a slope $4 \cdot 1.722 \approx 6.89$ for $\ell^2 > 2$. Not only the peak position, but also the peak height depends very little on L, as a reflection of the finite correlation length ξ under the peak ($\xi \approx 3a$). The transition temperatures, where the correlation length diverges, lie about 20%–25% below the peaks. Thus, for large ℓ, the Monte-Carlo data render clear evidence for two successive Kosterlitz-Thouless transitions.

At around $\ell^2 = 1$, the two peaks merge. The transition points, however, are still well separated. While the lower transition temperature remains almost independent of ℓ^2 near $T_c \approx 3$, the upper one moves closer and closer to the peak location until, at around $\ell^2 \approx 0.5$, a difference is hardly detectable. Simple extrapolations of the two transition lines suggest that they meet at around $\ell^2 \approx 0.1$–0.2. Since we know from earlier work that for $\ell^2 = 0$ there is a single first-order melting transition at $T_m \approx 2.45$ (with an entropy jump of $\Delta s \approx 0.2$ per site), we

expect the transition to continue to remain first-order up to the separation point around $\ell^2 \approx 0.1$–0.2. For larger ℓ^2, it is conceivable that the lower transition changes, at a tricritical point, to the Kosterlitz-Thouless type, while the upper one remains first-order up to some ℓ^2 between ≈ 0.2 and ≈ 0.5. This observation would explain the very small separation between peak locations and transition point. This picture is partly confirmed by simulations at $\ell^2 = 0.2$. Here, a clear hysteresis is observed in the internal energy, together with a pronounced finite-size scaling of the peak height of the specific heat with increasing L, indicating indeed a first order transition (with Δs per site remaining ≈ 0.2, as for $\ell = 0$). At $\ell^2 = 0.5$, on the other hand, no reliable hysteresis can be observed and the peak height depends only weakly on L (up to $L = 32$). However, at this ℓ it is very difficult to disentangle a possible weakly singular part of c from the large background contributions due to the lower Kosterlitz-Thouless-like transition (whose specific heat peak could be just be lying on top of the second transition).

In conclusion we see that the present lattice defect model with rotational stiffness resolves all open questions within the KTNHY approach of the two-dimensional melting process. It is apparently the simplest lattice model rich enough to describe the variety of different melting processes observed in recent experiments with liquid crystalline material.

18.8. APPLICATION OF ℓ^2 CRITERION TO LENNARD-JONES AND WIGNER LATTICES

With the results of the last section it is now easy to understand why the $D = 2$ Lennard-Jones crystal at low coverage has always been seen to undergo a clear first order transition, experimentally, (see Figs. 14.6–14.12) while the Wigner electron lattice has a sharp but continuous transition (see Fig. 14.15), with the stiffness constant K collapsing near the universal Kosterlitz-Thouless value (see Fig. 14.13). The reason lies, as we shall now demonstrate, in the different values of ℓ^2 in these systems.

According to Eq. (17.86), the ℓ^2 parameter occurs in the dispersion curve of the transverse sound waves as follows,

$$\omega^2(\mathbf{k}) = \mu k^2(1 + \ell^2 k^2 + \ldots). \tag{18.165}$$

For a lattice held together by a central potential $\Phi(\mathbf{x})$, the transverse frequencies $\omega^2_T(\mathbf{k})$ can be deduced from Eq. (7.140). They are given by the eigenvalues of the matrix

$$V_{ij}(\mathbf{k}) = \sum_{\mathbf{x}\neq\mathbf{0}} [1 - \cos(\mathbf{k}\cdot\mathbf{x})]\partial_i\partial_j\Phi(x), \tag{18.166a}$$

divided by the atomic mass M. Alternatively we can use the Fourier transform of the potential $\Phi(\mathbf{k})$, and have the formula [compare (7.161)]

$$V_{ij}(\mathbf{k}) = \frac{1}{M}\sum_{\mathbf{c}\neq\mathbf{0}} [(\mathbf{c}+\mathbf{k})_i(\mathbf{c}+\mathbf{k})_j\Phi(\mathbf{c}+\mathbf{k}) - c_ic_j\Phi(\mathbf{c})], \tag{18.166b}$$

where $\mathbf{c}$ is a reciprocal lattice vector. For an m, n Lennard-Jones lattice with a potential

$$\Phi(\mathbf{x}) = 4\varepsilon[(\sigma/r)^m - (\sigma/r)^n], \tag{18.167}$$

the $\mathbf{x}$-space representation (18.165a) converges so rapidly that in the sum over $\mathbf{x}$, the nearest neighbours almost give the entire contribution. We therefore calculate

$$\partial_i\partial_j\Phi(\mathbf{x}) = A\delta_{ij} + Bx_ix_j, \tag{18.168}$$

with

$$A = \Phi'/r, \quad B = \Phi''/r^2 - \Phi'/r^3, \tag{18.169}$$

and expand

$$V_{ij}(\mathbf{k}) = \sum_{\mathbf{x}\neq\mathbf{0}}\left[\frac{(\mathbf{x}\cdot\mathbf{k})^2}{2} - \frac{(\mathbf{x}\cdot\mathbf{k})^2}{24} + \ldots\right](A\delta_{ij} + Bx_ix_j). \tag{18.170}$$

The most stable lattice is of the triangular type, with lattice vectors

$$\mathbf{x} = a_0\left(\ell_1 - \frac{1}{2}\ell_2, \frac{\sqrt{3}}{2}\ell_2\right), \tag{18.171}$$

and cell "volume" $v = \frac{\sqrt{3}}{2}a_0^2$ (see Part I, Appendix 6A). The sum over

the nearest neighbours involves the six vectors $\mathbf{x} = a_0(\cos\varphi_n, \sin\varphi_n)$ with the azimuthal angles $\varphi_n = n\pi/3$. Over these we have to perform the angular averages

$$\langle(\mathbf{x}\cdot\mathbf{k})^2\rangle,\ \langle(\mathbf{x}\cdot\mathbf{k})^4\rangle,\ \langle(\mathbf{x}\cdot\mathbf{k})^6\rangle,\ \ldots \tag{18.172a}$$

If the rotation symmetry were perfect, this would give

$$\frac{1}{2}k^2,\ \frac{3}{8}k^4,\ \frac{5}{16}k^6,\ \ldots \tag{18.172b}$$

With only the sixfold symmetry, the first two averages are still correct, but the third (and the higher ones) depend on the azimuthal angle φ of the momentum $\mathbf{k} = |\mathbf{k}|(\cos\varphi, \sin\varphi)$. [Notice that in $(\mathbf{k}\cdot\mathbf{x})^6$ this dependence disappears again in the contribution of the higher lattice vectors $\mathbf{x}$ since there are more angles φ_n to be averaged over.] The φ dependence of $\langle(\mathbf{k}\cdot\mathbf{x})^6\rangle$ is

$$\langle(\mathbf{k}\cdot\mathbf{x})^6\rangle = \frac{10 + \cos(6\varphi)}{32}\cdot \tag{18.173}$$

Since the deviations from isotropy are at most 10% we shall ignore them in the following. We can then immediately calculate (using natural units with $\sigma = 1$, and $\hat{\mathbf{k}} \equiv \mathbf{k}/|\mathbf{k}|$).

$$V_{ij}(\mathbf{k}) = (V_T^{(2)}k^2 + V_T^{(4)}k^4)(\delta_{ij} - \hat{k}_i\hat{k}_j) + (V_L^{(2)}k^2 + V_L^{(4)})\hat{k}_i\hat{k}_j, \tag{18.174}$$

with

$$V_T^{(2)} = 6(Ar^2/4 + Br^4/16) = \frac{3\varepsilon}{2}[m(m-2)r^{-m} - (m \leftrightarrow n)],$$

$$V_T^{(4)} = -3Ar^4/32 - Br^6/64 = -\frac{\varepsilon r^2}{16}[m(m-4)r^{-m} - (m \leftrightarrow n)],$$

$$V_L^{(2)} = 6(Ar^2/4 + 3Br^4/16) = \frac{9\varepsilon}{2}[m(m+2/3)r^{-m} - (m \leftrightarrow n)],$$

$$V_L^{(4)} = -3Ar^4/32 = \frac{5\varepsilon r^2}{16}[m(m+4/5)r^{-m} - (m \leftrightarrow n)]. \tag{18.175}$$

FIG. 18.6. The length scale of rotational stiffness ℓ^2 (marked "transverse") as a function of the lattice spacing a_0 for a (12,6) Lennard-Jones crystal and for Wigner lattice. The place r_0 indicates the minimum of the Lennard-Jones potential. The effect of more distant neighbours places the equilibrium value of a_0 about 1% below r_0. The figure shows also the length scale ℓ'^2 of the longitudinal branch [recall (17.86)].

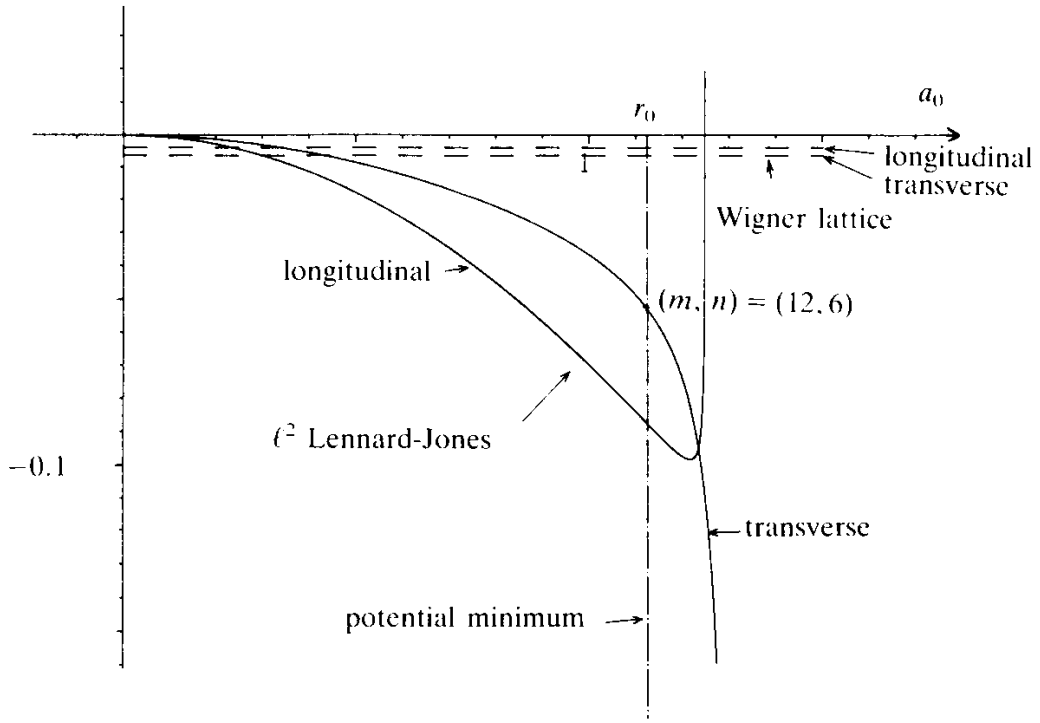

Each expression is to be evaluated at $r = a_0$.

For the most common set of parameters $(m, n) = (12, 6)$ we find from the transverse coefficients, the parameter ℓ^2:

$$\ell^2 = V_T^{(4)}/V_T^{(2)} = -\frac{a_0^2}{30}\frac{1 - a_0^6/8}{1 - a_0^6/5}. \tag{18.176a}$$

This is plotted in Fig. 18.6.

Although not of direct concern here, we also give the parameter ℓ'^2 for longitudinal modes (see again Fig. 18.6)

$$\ell'^2 = \frac{V_L^{(4)}}{V_L^{(2)}} = -\frac{4a_0^2}{57}\frac{1 - \frac{51}{192}a_0^6}{1 - \frac{5}{19}a_0^6}. \tag{18.176b}$$

In absence of an external pressure, the equilibrium value of r lies very close to the minimum of the potential, (18.167),

Table 18.1. Values of the lattice sums S_m for the triangular lattice for various m values. For large m one can use the lowest two neighbour correction to S_m, $S_m^{\text{app}} = 1 + 1/3^{m/2} + 1/2^m$ tabulated in the second column.

m	S_m	S_m^{app}	m	S_m	S_m^{app}
4	1.28510	1.17361	10	1.00524	1.00509
5	1.12697	1.09540	11	1.00292	1.00286
6	1.06264	1.05266	12	1.00164	1.00162
7	1.03254	1.02920	13	1.00092	1.00091
8	1.01741	1.01625	14	1.00052	1.00052
9	1.00949	1.00908	15	1.00030	1.00029

$$r_0 = (m/n)^{1/(m-n)}. \tag{18.177a}$$

i.e., for the (12,6) potential at (see Fig. 18.6)

$$r_0 = 2^{1/6}. \tag{18.177b}$$

If the sum over all neighbours is included in minimizing the energy, r_0 is decreased to

$$r_0 = (mS_m/nS_n)^{1/(m-n)}, \tag{18.177c}$$

where S_m is the sum

$$S_m = \frac{a_0}{6} \sum_{\mathbf{x} \neq \mathbf{0}} \frac{1}{|\mathbf{x}|^m} \tag{18.178}$$

The values are tabulated in Table 18.1.

For the (12.6) potential the correction is 0.9902. At $r_0 = 2^{1/6}$ we have

$$\ell_0^2 = -\frac{2^{1/6}}{24} \approx -0.0468. \tag{18.179}$$

Extrapolating our Monte Carlo data in Fig. 18.5 to negative values we conclude that a Lennard-Jones lattice must have a weakly first order melting transition. Monolayers of rare gases adsorbed on graphite under no external in-plane pressure are expected to have this property.

Equation (18.176a) has an interesting feature. At larger a_0, near $a_{\max} \sim 5^{1/6} \sim 1.3077 \sim 1.165 r_0$, i.e., at a density 36% lower than the density at zero external pressure, the size of $-\ell^2$ increases dramatically (see Fig. 18.6). The theory then predicts a strongly rising transition entropy. It is well known from Monte Carlo data and measurements on rare gases adsorbed on graphite that a lower coverage of the substrate is accompanied by an increasing discontinuity at the melting transition [see, for instance, Figs. (14.3), (14.5)]. Moreover, at $a_0 \sim a_{\max}$, ℓ^2 diverges. This may be interpreted as a signal, within this simple theory, for the onset of the gas phase.

Let us now turn to the Wigner lattice. Here $\Phi = e^2/r$ and the lattice sum (18.166a) converges very slowly. In the sequel, we shall use natural units with the charge e, the electron M, and the lattice spacing a_0 all equal to unity. The eigenvalues of $V_{ij}(\mathbf{k})$ will then be directly the squares of the eigenfrequencies ω^2 measured in frequency units $\omega_0^2 = e^2/Ma_0^3$. The convergency is improved by the following procedure, invented by P.P. Ewald in the 1920's. Consider the characteristic lattice sum $\sum_{\mathbf{x}} \frac{1}{|\mathbf{x}+\mathbf{u}|} e^{i\mathbf{k}\cdot\mathbf{x}}$ with an arbitrary displacement vector $\mathbf{u}$. Set $R = |\mathbf{x}+\mathbf{u}|$ and rewrite this sum by means of an auxiliary integral as follows

$$\sum_{\mathbf{x}} \frac{e^{i\mathbf{k}\cdot\mathbf{x}}}{R} = \frac{1}{\sqrt{\pi}} \int_0^\infty dt\, t^{-1/2} \sum_{\mathbf{x}} e^{-tR^2 + i\mathbf{k}\cdot\mathbf{x}}. \tag{18.180}$$

For finite t, this sum converges now very fast. The strongly convergent region of small t is treated using a generalization of Poisson's formula (6.37), Part II, valid for arbitrary periodic lattices in D dimensions with cell volume v,

$$\sum_{\mathbf{x}} e^{i\mathbf{x}\cdot\mathbf{k}} = \frac{(2\pi)^D}{v} \sum_{\mathbf{c}} \delta(\mathbf{k} - \mathbf{c}), \tag{18.181}$$

where the right-hand side runs over all reciprocal lattice vectors [recall the definition in Part I, Eq. (6.29)]. Multiplying this with the Fourier transform $\tilde{f}(\mathbf{k}) = \sum_{\mathbf{x}} f(\mathbf{x}) e^{-i\mathbf{k}\cdot\mathbf{x}}$ of an arbitrary function $f(\mathbf{x})$ and performing the sum $(1/N) \sum_{\mathbf{k}}'$, the formula (18.181) just reexpresses the well-known identity,

$$\sum_{\mathbf{x}} f(\mathbf{x}) = \sum_{\mathbf{c}} \tilde{f}(\mathbf{c}). \tag{18.182}$$

For the special case $f(\mathbf{x}) = e^{-tR^2 + i\mathbf{k}\cdot\mathbf{x}}$, this gives in two dimensions,

$$\sum_{\mathbf{x}} e^{-tR^2 + i\mathbf{k}\cdot\mathbf{x}} = \frac{\pi}{vt} \sum_{\mathbf{c}} e^{i\mathbf{c}\cdot\mathbf{u}} e^{-(\mathbf{k}+\mathbf{c})^2/4t}. \tag{18.183}$$

While the left-hand sum over lattice vectors converges fast for large t, the right-hand side over reciprocal lattice vectors does so for small t. We therefore choose an arbitrary separation parameter for the t integration, say ε, and decompose the lattice sum into two dual terms,

$$\sum_{\mathbf{x}} \frac{1}{R} e^{i\mathbf{k}\cdot\mathbf{x}} = \frac{1}{\sqrt{\pi}} \int_{\varepsilon}^{\infty} dt\, t^{1/2} \sum_{\mathbf{x}} e^{-tR^2 + i\mathbf{k}\cdot\mathbf{x}} + \frac{\sqrt{\pi}}{vt} \int_{0}^{\varepsilon} dt\, t^{-1/2} \sum_{\mathbf{c}} e^{-(\mathbf{k}+\mathbf{c})^2/4t + i\mathbf{c}\cdot\mathbf{u}}. \tag{18.184}$$

After a rescaling of t by ε, the sum on the right-hand side can be expressed in terms of the so-called *Misra functions*

$$\varphi_n(z) \equiv \int_1^{\infty} dt\, t^n e^{-zt}. \tag{18.186}$$

They are related to the incomplete Γ functions,

$$\Gamma(\alpha, z) = \int_z^{\infty} dt\, t^{\alpha-1} e^{-t}, \tag{18.187}$$

by

$$\varphi_n(z) = (z)^{-n-1}\Gamma(n+1, z). \tag{18.188}$$

They can be expanded as follows,

$$\varphi_n(z) = (z)^{-n-1}\left[\Gamma(n+1) - \sum_{k=0}^{\infty} (-)^k \frac{z^{k+n+1}}{k!(k+n+1)}\right]. \tag{18.189}$$

Then (18.184) becomes

$$\sum_{\mathbf{x}} \frac{1}{R} e^{i\mathbf{k}\cdot\mathbf{x}} = \sqrt{\varepsilon/\pi} \sum_{\mathbf{x}} \varphi_{-1/2}(\varepsilon R^2) e^{+i\mathbf{k}\cdot\mathbf{x}} + \frac{1}{v}\sqrt{\pi/\varepsilon} \sum_{\mathbf{c}} \varphi_{-1/2}\left(\frac{(\mathbf{k}+\mathbf{c})^2}{4\varepsilon}\right) e^{i\mathbf{k}\cdot\mathbf{u}}. \tag{18.190}$$

For a triangular lattice, the reciprocal lattice is also triangular and has the vectors

$$\mathbf{c} = \frac{2\pi}{a_0}\left(c_1, \frac{1}{\sqrt{3}}c_1 + \frac{2}{\sqrt{3}}c_2\right). \tag{18.191}$$

There exists then a particular convenient choice for the parameter ε with the property that it makes the two sums in (18.190) for $\mathbf{k} = 0$ and $\mathbf{u} = 0$ completely symmetric, namely,

$$\varepsilon = \pi/v. \tag{18.192}$$

Then the arguments εR^2 and $c^2/4\varepsilon$ of the Misra functions run through the same values,

$$s \equiv \varepsilon R^2 = \varepsilon a_0^2\left(\ell_1 - \frac{1}{2}\ell_2, \frac{\sqrt{3}}{2}\ell_2\right)^2 = (2\pi/\sqrt{3})(\ell_1^2 - \ell_1\ell_2 + \ell_2^2),$$

$$s \equiv \frac{c^2}{4\varepsilon} = \frac{(2\pi)^2}{a_0^2}\frac{v}{4\pi}\left(c_1, \frac{1}{\sqrt{3}}c_2 + \frac{2}{\sqrt{3}}c_2\right)^2 = (2\pi/\sqrt{3})(c_1^2 + c_1c_2 + c_2^2). \tag{18.193}$$

Hence we can write formally

$$\sum_{\mathbf{x}} \frac{1}{|\mathbf{x}|} = \frac{1}{\sqrt{v}}2 \cdot \sum_{s} \varphi_{-1/2}(s). \tag{18.194}$$

If this relation is to make sense, we have to remove the singular $\mathbf{x} = 0$ and $s = 0$ pieces on either side in (18.190). Both $\mathbf{x} = 0$ and $\mathbf{c} = 0$ are still admissible as long as $\mathbf{u} \neq 0$ and $\mathbf{k} \neq 0$, since then the Misra functions $\varphi_{-1/2}$ are finite. In order to treat the limit $\mathbf{u} \to \mathbf{0}$ we remove the $\mathbf{x} = \mathbf{0}$ and $\mathbf{c} = \mathbf{0}$ terms on both sides and write,

$$\sum_{\mathbf{x}\neq\mathbf{0}} \frac{1}{R}e^{i\mathbf{k}\cdot\mathbf{x}} = \left(-\frac{1}{|\mathbf{u}|} + \sqrt{\varepsilon/\pi}\,\varphi_{-1/2}(\varepsilon\mathbf{u}^2)\right) + \frac{1}{v}\sqrt{\pi/\varepsilon}\,\varphi_{-1/2}(\mathbf{k}^2/4\varepsilon)$$

$$+ \sqrt{\varepsilon/\pi}\sum_{\mathbf{x}\neq\mathbf{0}} \varphi_{-1/2}(\varepsilon R^2)e^{i\mathbf{k}\cdot\mathbf{x}} + \frac{1}{v}\sqrt{\pi/\varepsilon}\sum_{\mathbf{c}\neq\mathbf{0}} \varphi_{-1/2}\left(\frac{(\mathbf{k}+\mathbf{c})^2}{4\varepsilon}\right)e^{i\mathbf{c}\cdot\mathbf{u}}. \tag{18.195}$$

Then we use (18.189) and deduce the limit of the Misra function

$$\varphi_{-1/2}(z) \to \sqrt{\pi/z} - 2 + 2z/3 - z^2/5 + O(z^3). \tag{18.196}$$

This shows that for small $\mathbf{u} \to \mathbf{0}$, the quantity inside parentheses in (18.195) is regular and we have, for $\varepsilon = \pi/v$, $\mathbf{u} = \mathbf{0}$ and small $\mathbf{k}$

$$\sum_{\mathbf{x} \neq \mathbf{0}} \frac{1}{|\mathbf{x}|} e^{i\mathbf{k}\cdot\mathbf{x}} \underset{\mathbf{k} \approx \mathbf{0}}{=} \frac{1}{\sqrt{v}} 2\left(\sum_{s \neq 0} \varphi_{-1/2}(s) - 2\right) + \frac{4\pi}{v} \frac{1}{\mathbf{k}^2}, \tag{18.197}$$

where the sum over s is understood to comprise the correct multiplicity of each value (18.193).

As an example for the effectiveness of this resummation procedure, consider the energy of a single electron in the Wigner lattice (in units $e^2 = 1$)

$$E_e = \sum_{\mathbf{x} \neq \mathbf{0}} \frac{1}{|\mathbf{x}|}. \tag{18.198}$$

In order to obtain finite energy we have to add a neutralizing negative background charge which gives an additional energy

$$E_b = -\frac{1}{v} \lim_{\mathbf{k} \to \mathbf{0}} \int \frac{d^3x}{|\mathbf{x}|} e^{i\mathbf{k}\cdot\mathbf{x}} = -\frac{4\pi}{v} \lim_{\mathbf{k} \to \mathbf{0}} \frac{1}{\mathbf{k}^2}. \tag{18.199}$$

The total energy $E = E_e + E_b$ can then be directly evaluated using formula (18.197) since the background energy just removes the singular $1/\mathbf{k}^2$ piece. Hence

$$E = \frac{1}{\sqrt{v}} 2\left(\sum_{s \neq 0} \varphi_{-1/2}(s) - 2\right). \tag{18.200}$$

At the nearest neighborhood position,

$$s_1 = 2\pi/\sqrt{3}, \tag{18.201}$$

the Misra function has the value

$$\varphi_{-1/2}(s_1) = 0.065790. \tag{18.202}$$

Including the six neighbors, this gives the lowest approximation to the energy (to be multiplied by e^2, for proper physical units)

$$E = -3.921052\frac{1}{\sqrt{v}}\cdot \tag{18.203}$$

A full summation over all s in (18.200) changes this very little to [see (14.149)]

$$E \approx -3.921034\frac{1}{\sqrt{v}}\cdot \tag{18.204}$$

Thus, while the sum over Coulomb energies converges very slowly in x-space, the representation (18.190) with $\varepsilon = \pi/v$ is strongly dominated by the nearest neighbors in both, the direct and the reciprocal lattice.

After these preparations we are now ready to calculate the parameter ℓ^2 for the Wigner lattice with the help of formula (18.195). We rewrite the $\mathbf{x}$-sum in (18.165) as

$$v_{ij}(\mathbf{k}) \equiv V^x_{ij}(\mathbf{k}) + V^c_{ij}(\mathbf{k}) \equiv \sqrt{\varepsilon/\pi}\sum_{\mathbf{x}\neq\mathbf{0}}[1-\cos(\mathbf{k}\cdot\mathbf{x})]\partial_i\partial_j\varphi_{-1/2}(\varepsilon\mathbf{x}^2)$$
$$+\frac{1}{v}\sqrt{\pi/\varepsilon}\sum_{\mathbf{c}}[(\mathbf{k}+\mathbf{c})_i(\mathbf{k}+\mathbf{c})_j - c_ic_j]\varphi_{-1/2}\left(\frac{(\mathbf{k}+\mathbf{c})^2}{4\varepsilon}\right)\cdot \tag{18.205}$$

We expand the two sums in powers of $\mathbf{k}$ up to k_i^4, arriving at

$$V^x_{ij}(\mathbf{k}) = \sqrt{\varepsilon/\pi}\sum_{\mathbf{x}\neq\mathbf{0}}\left[\frac{1}{2}(\mathbf{k}\cdot\mathbf{x})^2 - \frac{1}{24}(\mathbf{k}\cdot\mathbf{x})^4\ldots\right][4\varepsilon^2x_ix_j\varphi_{3/2}(\varepsilon x^2)$$
$$-2\varepsilon\delta_{ij}\varphi_{1/2}(\varepsilon x^2)], \tag{18.206}$$

$$V^c_{ij}(\mathbf{k}) = \frac{1}{v}\sqrt{\pi/\varepsilon}\sum_{\mathbf{c}}\left\{(\mathbf{k}+\mathbf{c})_i(\mathbf{k}+\mathbf{c})_j\left[\varphi_{-1/2}\left(\frac{c^2}{4\varepsilon}\right) - \left(\frac{2\mathbf{c}\cdot\mathbf{k}+k^2}{4\varepsilon}\right)\varphi_{-1/2}\left(\frac{c^2}{4\varepsilon}\right)\right.\right.$$
$$\left.\left.+\ldots+\frac{1}{4!}\varphi_{7/2}\left(\frac{c^2}{4\varepsilon}\right)\left(\frac{2\mathbf{c}\cdot\mathbf{k}+k^2}{4\varepsilon}\right)^4\right] - c_ic_j\varphi_{-1/2}\left(\frac{c^2}{4\varepsilon}\right)\right\}, \tag{18.207}$$

where we have used the identity

$$-\varphi_n'(z) = \varphi_{n+1}(z). \tag{18.208}$$

Incidentally, all higher Misra functions in (18.207) can be reduced to the lowest one, $\varphi_{1/2}(z)$, via the iteration formula,

$$\varphi_{n+1}(z) = \frac{1}{z}[(n+1)\varphi_n(z) + e^{-z}]. \tag{18.209}$$

When summing over all $\mathbf{x}$, $\mathbf{c}$, the only (small) anisotropy arises from $(\mathbf{k}\cdot\mathbf{x})^4 x_i x_j$ and $(\mathbf{k}\cdot\mathbf{c})^4 c_i c_j$ for the nearest neighbor $\mathbf{x}$, $\mathbf{c}$ vectors. As before in the Lennard-Jones case, we shall again use the isotropic approximation. Expanding $V_{ij}(\mathbf{k})$ in powers of $\mathbf{k}$,

$$V_{ij}(\mathbf{k}) = V_{ij}^{(2)}k^2 + V_{ij}^{(4)}k^4 + \ldots, \tag{18.210}$$

we find for $\varepsilon = \pi/v$, keeping only the nearest neighbour contributions, from the $\mathbf{x}$ sum ($\hat{k}_i \equiv k_i/|\mathbf{k}|$),

$$V_{ij}^{(2)x} \to \frac{1}{\sqrt{v}} 6\left[\frac{1}{4}(\delta_{ij} + 2\hat{k}_i\hat{k}_j)s^2\varphi_{3/2}(s) - \frac{1}{2}\delta_{ij}s\varphi_{1/2}(s)\right] \tag{18.211}$$

$$V_{ij}^{(4)x} \to \frac{1}{\sqrt{v}}\frac{6}{4\varepsilon}\cdot\frac{1}{24}\left[(\delta_{ij} + 4\hat{k}_i\hat{k}_j)s^3\varphi_{3/2}(s) - 3\delta_{ij}s^2\varphi_{1/2}(s)\right]. \tag{18.212}$$

The $\mathbf{c}$ part of the sums (18.207) contributes first from $\mathbf{c} = \mathbf{0}$ a purely longitudinal term,

$$V_{ij}^{(\mathbf{c}=0)}(\mathbf{k}) = \frac{1}{\sqrt{v}}\left\{\frac{k_i k_j}{k^2}\sqrt{4\pi\varepsilon}\,k + \frac{k_i k_j}{k^2}\left(-2k^2 + \frac{k^4}{6\varepsilon} + \ldots\right)\right\}. \tag{18.213}$$

The first term is the origin of the incompressibility of the Wigner lattice, [recall Eq. (14.151)]. The sum over the nearest neighbor vectors on the reciprocal lattice gives

$$V_{ij}^{(2)c} = \frac{1}{\sqrt{v}}6\left\{\hat{k}_i\hat{k}_j\varphi_{-1/2}(s) - (\delta_{ij} + 4\hat{k}_i\hat{k}_j)\frac{s}{2}\varphi_{1/2} + (\delta_{ij} + 2\hat{k}_i\hat{k}_j)\frac{s^2}{4}\varphi_{3/2}\right.,$$

$$V_{ij}^{(4)c} = \frac{1}{\sqrt{v}}\frac{6}{4\varepsilon}\left\{-\hat{k}_i\hat{k}_j\varphi_{1/2}(s) + (\delta_{ij} + 12\hat{k}_i\hat{k}_j)\frac{s}{4}\varphi_{3/2}\right.$$

$$\left. - (\delta_{ij} + 6\hat{k}_i\hat{k}_j)\frac{s^2}{4}\varphi_{5/2}(s) + \frac{1}{24}(\delta_{ij} + 4\hat{k}_i\hat{k}_j)s^3\varphi_{7/2}(s)\right\}. \tag{18.214}$$

Projecting out the transverse parts gives

$$V_T^{(2)} = \frac{1}{\sqrt{v}} 6 \cdot 2 \left[-\frac{s}{2}\varphi_{1/2}(s) + \frac{s^2}{4}\varphi_{3/2}(s) \right],$$

$$V_T^{(4)} = \frac{1}{\sqrt{v}} \frac{6}{4\varepsilon} \left[\left(\frac{3s^2}{24}\varphi_{1/2}(s) - \frac{s^3}{24}\varphi_{3/2}(s) \right) + \left(\frac{s}{4}\varphi_{3/2}(s) - \frac{s^2}{4}\varphi_{5/2}(s) + \frac{s^3}{24}\varphi_{7/2}(s) \right) \right]. \tag{18.215}$$

Inserting $s = s_1$ we find, after factorizing out the standard frequency $\omega_p^2 = \dfrac{2\pi e^2}{Mva_0} = \dfrac{2\pi}{\sqrt{3}/2}\omega_0^2$ (listing **x** and **c** contributions separately),

$$V_T^{(2)} \approx 2 \cdot 0.0181 = 0.0362,$$

$$V_T^{(4)} \approx -0.000478 + 0.000252 = -0.000226, \tag{18.216}$$

Thus, the transverse frequency spectrum is, in proper physical units,

$$\omega_T^2 \approx \omega_p^2 [0.362(ka_0)^2 - 0.000225(ka_0)^4 + \ldots]. \tag{18.217}$$

This implies the following value for the angular stiffness parameter (in units of a_0^2)

$$\ell^2 \equiv V_T^{(4)}/V_T^{(2)} \approx -0.00622. \tag{18.218}$$

Since the dispersion curve of the square lattice in the simulations in Fig. 18.5 has a spectrum $2 - 2\cos k = k^2 - \dfrac{1}{12}k^4$, this value of ℓ^2 corresponds to a value of ℓ^2 in the lattice model of $\ell^2 + \dfrac{1}{12} \sim 0.1$. In this neighborhood the single first order melting transition is about to split into two Kosterlitz-Thouless transitions. The specific heat curve should therefore have about the same shape as that of the lattice defect model in the first of Figs. 18.4, i.e., it should look similar to a λ transition in superfluid helium. This is indeed what was observed by Hockney and Brown in 1976 (see Fig. 14.14). Near the splitting point, the elastic stiffness K^R at the melting transition is expected to have the universal Kosterlitz-Thouless

value (14.157). This is seen in the Monte Carlo simulations in Fig. 14.13.

For completeness, let us also state the longitudinal coefficients,

$$V_L(\mathbf{k}) = \sqrt{4\pi\varepsilon/v}\,k + V_L^{(2)}k^2 + V_L^{(4)}k^4 \ldots, \tag{18.219}$$

with

$$V_L^{(2)} = \frac{6}{\sqrt{v}}\left\{\left(\frac{s}{2}\varphi_{1/2} + \frac{3}{4}s^2\varphi_{3/2}\right) - \frac{1}{3} + \left(\varphi_{-1/2}(s) - \frac{5}{2}s\varphi_{1/2}(s) + \frac{3}{4}s^2\varphi_{3/2}(s)\right)\right\},$$

$$V_L^{(4)} = \frac{6}{\sqrt{v}}\frac{1}{4\varepsilon}\left\{\left(\frac{3}{24}s^2\varphi_{1/2} - \frac{5}{24}s^3\varphi_{3/2}\right) + \frac{1}{9}\right.$$

$$\left. - \left(\varphi_{1/2}(s) + \frac{13}{4}s\varphi_{3/2}(s) - \frac{7}{4}s^2\varphi_{5/2}(s) + \frac{5}{24}s^3\varphi_{7/2}(s)\right)\right\}, \tag{18.220}$$

where we have listed separately the contributions of the sum over $\mathbf{x}$, $\mathbf{c} = \mathbf{0}$, and the sum over $\mathbf{c} \neq 0$. The first term gives the well-known anomalous contribution to the longitudinal frequency,

$$\omega_a^2 = \frac{e^2}{M}\sqrt{4\pi\varepsilon/v}\,k = \frac{e^2}{M}\frac{2\pi}{v}k = \omega_p^2 k a_0, \tag{18.221}$$

which is responsible for the incompressibility of the Wigner lattice [recall Eq. (14.159)]. The term $V_L^{(2)}$ contributes to the longitudinal frequency

$$\omega_L^{(2)} \approx \omega_p^2(0.0809 - 0.2962 + 0.0336)(ka_0)^2 \approx -0.1818(ka_0)^2,$$

$$\omega_L^{(4)} \approx \omega_p^2(-0.0057 + 0.0068 - 0.0004)(ka_0)^4 \approx 0.0007(ka_0)^4. \tag{18.222}$$

Hence, the parameter ℓ'^2, defined in (17.86), has the value

$$\ell'^2 \approx -0.0038. \tag{18.223}$$

Notice that up to order k^2, the frequency spectrum is given by

$$\omega_T^2 \approx \omega_p^2 0.362(ka_0)^2, \qquad \omega_L^2 = \omega_p^2(ka_0) - 5\omega_T^2, \tag{18.224}$$

in agreement with Eq. (14.151).

NOTES AND REFERENCES

The references to the Kosterlitz-Thouless transitions are found in Chapter 11 of Part II and in Chapter 14 of Part III. For experimental data on the melting behaviour of crystals with large angular stiffness see
R. Pindak, D.E. Moncton, S.C. Davey and J.W. Goodby, *Phys. Rev. Lett.* **46** (1981) 1135;
D.E. Moncton, R. Pindak, S.C. Davey, G.S. Brown, *Phys. Rev. Lett.* **49** (1982) 1865;
T. Pitchford, C.C. Huang, R. Pindak, and J.W. Goodby, *Phys. Rev. Lett.* **57** (1986) 1239,
J.Z. Larese, L. Passell, A.D. Heidemann, D. Richter, J.P. Wicksted, *Phys. Rev. Lett.* **61** (1988) 432,
The lattice defect model with two successive melting transition was found by
H. Kleinert, *Phys. Lett.* **A130** (1988) 443.
The predicted phase properties were confirmed in Monte-Carlo simulations by
W. Janke and H. Kleinert, *Phys. Rev. Lett.* **61** (1988) 2344.
For dispersion relations of the Wigner lattice see the paper of Bonsall and Maradudin (1977), cited at the end of Chapter 14.
The calculation of ℓ^2 for Lennard-Jones and Wigner lattices was given in H. Kleinert, *Phys. Lett.* **A136** (1989) 468.

CHAPTER NINETEEN

DISORDER FIELD THEORY OF DISLOCATION AND DISCLINATION LINES IN THREE DIMENSIONS

19.1. THE PARTITION FUNCTION OF GENERAL DEFECT LINES IN THREE DIMENSIONS

The interaction energy given in (18.59) for defects in higher gradient elasticity puts us in a position of developing a disorder field theory which distinguishes the two types of defect lines. For this we extract some finite self-energy from the dislocations and disclinations in the Boltzmann factor,

$$e^{-(\beta/2)4\pi^2 \sum_{\mathbf{x}} (c_\alpha \bar{\alpha}_{ij}^2 + c_\Theta \bar{\Theta}_{ij}^2)}. \tag{19.1}$$

The remaining substracted energy can again be brought back to the gauge field formulation. In this way we arrive at the energy expression

$$\begin{aligned}\frac{1}{T}(E'_{\mathrm{el}} + iE_{\mathrm{int}} + E_{\mathrm{def}}) = \frac{1}{4\mu}\sum_{\mathbf{x}}\left(\sigma'^{s2}_{ij} - \frac{\nu}{1+\nu}\sigma'^{s2}_{\ell\ell}\right) + \frac{a^2}{8\ell^2}\sum_{\mathbf{x}}(\delta_1 \tau'^2_{ij} + \delta_2 \tau'^2_{\ell\ell}) \\ - 2\pi i \sum_{\mathbf{x}} (A_{\ell i}\bar{\alpha}_{\ell i} + h_{\ell i}\bar{\Theta}_{\ell i}) \\ + \frac{\beta}{2} 4\pi^2 \sum_{\mathbf{x}} (c_\alpha \bar{\alpha}_{ij}^2 + c_\Theta \bar{\Theta}_{ij}^2),\end{aligned} \tag{19.2}$$

where the primes indicate a modification of the elastic energy by higher gradients to compensate for the added last term in (19.2). As long as we are interested only in structural properties we do not have to write these terms out explicitly. (The procedure of Section 12.4, Part II is applicable.)

When brought to the above simple form, the construction of a disorder field theory becomes rather straightforward. Following the same steps as those of the XY model, we first observe that the sum over defects

$$Z_{\text{def}} = \sum_{\{\bar{\alpha}_{\ell i},\, \bar{\Theta}_{\ell i}\}} \delta_{\bar{\nabla}_\ell \alpha_{\ell i} + \varepsilon_{ik\ell} \bar{\Theta}_{k\ell},\, 0}\, \delta_{\bar{\nabla}_\ell \Theta_{\ell i},\, 0}$$
$$\exp\left\{ -\frac{\beta}{2} 4\pi^2 \sum_{\mathbf{x}} (c_\alpha \bar{\alpha}_{ij}^2 + c_\Theta \bar{\Theta}_{ij}^2) - 2\pi i \sum_{\mathbf{x}} (A_{\ell i} \bar{\alpha}_{\ell i} + h_{\ell i} \bar{\Theta}_{\ell i}) \right\}, \tag{19.3}$$

can be rewritten [up to the trivial overall factor $\mathcal{N} = (2\pi\beta c_\alpha)^{-9N/2} (2\pi\beta_{c_\Theta})^{-9N/2}$] as the partition function of a lattice model of the Villain type [compare Section 13.3, Part II]

$$Z_{\text{def}} = \mathcal{N} \sum_{\{\tilde{n}_{\ell i},\, \tilde{m}_{\ell i}\}} \sum_{\mathbf{x},\, i} \left[\int_{-\pi}^{\pi} \frac{d\gamma_i(\mathbf{x})}{2\pi} \int_{-\pi}^{\pi} \frac{d\delta_i(\mathbf{x})}{2\pi} \right]$$
$$\times \exp\left\{ -\frac{1}{2\beta} \frac{1}{4\pi^2} \left[\frac{1}{c_\alpha} \sum_{\mathbf{x}} (\nabla_\ell \gamma_i - A_{\ell i} - 2\pi \tilde{n}_{\ell i})^2 \right.\right.$$
$$\left.\left. + \frac{1}{c_\Theta} \sum_{\mathbf{x}} (\nabla_\ell \delta_i - \varepsilon_{\ell ik} \gamma_k - h_{\ell i} - 2\pi \tilde{n}_{\ell i})^2 \right] \right\}. \tag{19.4}$$

The proof proceeds as usual by introducing auxiliary fields $\alpha_{\ell i}$, $\Theta_{\ell i}$ to linearize the squares,

$$Z_{\text{def}} = \mathcal{N} \prod_{\mathbf{x},\, \ell,\, i} \left[\int_{-\infty}^{\infty} \frac{d\alpha_{\ell i}(\mathbf{x})}{\sqrt{2\pi/4\pi^2\beta c_\alpha}} \int_{-\infty}^{\infty} \frac{d\Theta_{\ell i}(\mathbf{x})}{\sqrt{2\pi/4\pi^2\beta c_\Theta}} \right]$$
$$\times \sum_{\{\tilde{n}_{\ell i},\, \tilde{m}_{\ell i}\}} \prod_{\mathbf{x},\, i} \left[\int_{-\pi}^{\pi} \frac{d\gamma_i(\mathbf{x})}{2\pi} \int_{-\pi}^{\pi} \frac{d\delta_i(\mathbf{x})}{2\pi} \right]$$
$$\times \exp\left\{ -\frac{\beta}{2} 4\pi^2 \sum_{\mathbf{x}} (c_\alpha \alpha_{ij}^2 + c_\Theta \Theta_{ij}^2) + 2\pi i \sum_{\mathbf{x}} \alpha_{\ell i} (\nabla_\ell \gamma_i - A_{\ell i} - 2\pi \tilde{n}_{\ell i}) \right.$$
$$\left. + 2\pi i \sum_{\mathbf{x}} \Theta_{\ell i} (\nabla_\ell \delta_i - \varepsilon_{\ell ik} \gamma_k - h_{\ell i} - 2\pi \tilde{m}_{\ell i}) \right\}. \tag{19.5}$$

Now we perform the sum over $\bar{n}_{ti}$, $\bar{m}_{ti}$ which makes α_{ti}, Θ_{ti} integer say $\bar{\alpha}_{ti}$, $\bar{\Theta}_{ti}$, and the integrals over γ_i, δ_i which enforce the conservation laws, $\bar{\nabla}_t \bar{\alpha}_{ti} + \varepsilon_{ikt} \bar{\Theta}_{kt} = 0$, $\bar{\nabla}_t \bar{\Theta}_{ti} = 0$. Thus (19.5) is indeed equal to (19.3).

19.2. COSINE FORM OF THE PARTITION FUNCTION

The next step consists in approximating the expression (19.4) à la Villain by a model of the XY type involving cosines rather than periodic Gaussians. Recall that the original Villain approximation went in the opposite direction,

$$e^{\beta \cos \nabla\Theta} \approx R(\beta) \sum_n e^{-(\beta_V/2)(\nabla\Theta - 2\pi n)^2}, \tag{19.6}$$

where

$$R(\beta) = I_0(\beta)\sqrt{2\pi\beta_V}, \qquad \beta_V = 1/(2\log(I_1(\beta)/I_0(\beta))). \tag{19.7}$$

In Section 9.3 we encountered the same problem and found it useful to define the inverse operation

$$\sum_n e^{-(\beta/2)(\nabla\Theta - 2\pi n)^2} \approx R_{V^{-1}}(\beta)\, e^{\beta_{V^{-1}} \cos \nabla\Theta}, \tag{19.8}$$

where $\beta_{V^{-1}}(\beta)$ is the solution of the equation

$$\beta = -1/(2\log(I_1(\beta_{V^{-1}})/I_0(\beta_{V^{-1}}))), \tag{19.9}$$

and

$$R_{V^{-1}}(\beta) = 1/(\log I_0(\beta_{V^{-1}}) \cdot \sqrt{2\pi\beta}). \tag{19.10}$$

With this notation we can approximate (19.4) by[a]

[a]Actually, we had seen in Section 13.4 that a much better approximation is given by replacing the second cosine by the mixed energy $\cos(\nabla_t \delta_i - \varepsilon_{tik}\gamma_k - h_{ti}) + \delta\cos(2(\nabla_t \delta_i - \varepsilon_{tik}\gamma_k - h_{ti}))$ where δ is determined by Eq. (13.101). We shall omit the second term, for brevity.

$$Z_{\text{def}} \approx \mathcal{N} R_{V^{-1}} \left(\frac{1}{4\pi^2 \beta c_\alpha}\right)^{3N} R_{V^{-1}} \left(\frac{1}{4\pi^2 \beta c_\Theta}\right)^{3N} \prod_{\mathbf{x},i} \left[\int_{-\pi}^{\pi} \frac{d\gamma_i(\mathbf{x})}{2\pi} \int_{-\pi}^{\pi} \frac{d\delta_i(\mathbf{x})}{2\pi}\right] \times \exp\left\{\tilde{\beta}_\alpha \sum_{\mathbf{x}} \cos(\nabla_\ell \gamma_i - A_{\ell i}) + \tilde{\beta}_\Theta \sum_{\mathbf{x}} \cos(\nabla_\ell \delta_i - \varepsilon_{\ell i k} \gamma_k - h_{\ell i})\right\}, \tag{19.11}$$

where

$$\tilde{\beta}_\alpha \equiv \left(\frac{1}{4\pi^2 \beta c_\alpha}\right)_{V^{-1}}, \qquad \tilde{\beta}_\Theta \equiv \left(\frac{1}{4\pi^2 \beta c_\Theta}\right)_{V^{-1}}. \tag{19.12}$$

As a third step we re-express the exponent in terms of the pure phase variables $U_i(\mathbf{x}) = e^{i\delta_i(\mathbf{x})}$, $V_i(\mathbf{x}) = e^{i\delta_i(\mathbf{x})}$ as follows

$$\begin{aligned} &\tilde{\beta}_\alpha \operatorname{Re} \sum_{\mathbf{x},i,\ell} U_i(\mathbf{x}) U_i^\dagger(\mathbf{x}+\boldsymbol{\ell}) e^{iA_{\ell i}(\mathbf{x})} + \tilde{\beta}_\Theta \operatorname{Re}\Bigg(\sum_{\mathbf{x},i} V_i(\mathbf{x}) V_i^\dagger(\mathbf{x}+\mathbf{i}) e^{ih_{ii}(\mathbf{x})} \\ &+ \sum_{\substack{\mathbf{x} \\ \ell ik = 123,231,312}} V_i(\mathbf{x}) V_i^\dagger(\mathbf{x}+\boldsymbol{\ell}) U_k^\dagger(\mathbf{x}) e^{ih_{\ell i}(\mathbf{x})} \\ &+ \sum_{\substack{\mathbf{x} \\ \ell ik = 213,321,132}} V_i(\mathbf{x}) V_i^\dagger(\mathbf{x}+\boldsymbol{\ell}) U_k(\mathbf{x}) e^{ih_{\ell i}(\mathbf{x})}\Bigg). \end{aligned} \tag{19.13}$$

19.3. DISORDER FIELDS FOR DISLOCATIONS AND DISCLINATIONS

The disorder field theory can now be obtained in the usual way by introducing a pair of complex fields u_i, α_i, v_i, λ_i via the identity

$$\int_{-\infty}^{\infty} du_i du_i^\dagger \int_{-i\infty}^{i\infty} \frac{d\alpha_i d\alpha_i^\dagger}{(2\pi i)^2} e^{-(1/2)(\alpha_i^\dagger u_i + \text{c.c}) + (1/2)(\alpha_i^\dagger u_i + \text{c.c.})} = 1, \tag{19.14}$$

and a similar one for v_i, λ_i. With these the integrations over the phases $\gamma_i(\mathbf{x})$, $\delta_i(\mathbf{x})$ can be done trivially, giving associated Bessel functions $I_0(|\alpha_i|)$, $I_0(|\lambda_i|)$. In this way we arrive at the partition function $Z' \equiv \mathcal{N}[R_{V^{-1}}(1/4\pi^2\beta c_\alpha)^{3N} R_{V^{-1}}(1/4\pi^2\beta c_\Theta)^{3N}]$

$$
\begin{aligned}
Z_{\mathrm{def}} \approx \mathcal{N}' \prod_{\mathbf{x},i} \left[\int_{-\infty}^{\infty} du_i du_i^{\dagger} \int_{-i\infty}^{i\infty} \frac{d\alpha_i d\alpha_i^{\dagger}}{(2\pi i)^2} \right] \prod_{\mathbf{x},i} \left[\int_{-\infty}^{\infty} dv_i dv_i^{\dagger} \int_{-i\infty}^{i\infty} \frac{d\lambda_i d\lambda_i^{\dagger}}{(2\pi i)^2} \right] \\
\times \exp \Bigg\{ \bar{\beta}_{\alpha} \operatorname{Re} \sum_{\mathbf{x},i,\ell} u_i(\mathbf{x})\, u_i^{\dagger}(\mathbf{x}+\boldsymbol{\ell})\, e^{iA_{\ell i}(\mathbf{x})} \\
+ \bar{\beta}_{\Theta} \operatorname{Re} \Bigg(\sum_{\mathbf{x},i} v_i(\mathbf{x})\, v_i^{\dagger}(\mathbf{x}+\mathbf{i})\, e^{ih_{ii}(\mathbf{x})} \\
+ \sum_{\substack{\mathbf{x} \\ \ell ik = 123,\,231,\,312}} v_i(\mathbf{x})\, v_i^{\dagger}(\mathbf{x}+\boldsymbol{\ell})\, u_k^{\dagger}(\mathbf{x})\, e^{ih_{\ell i}(\mathbf{x})} \\
+ \sum_{\substack{\mathbf{x} \\ \ell ik = 213,\,321,\,132}} v_i(\mathbf{x})\, v_i^{\dagger}(\mathbf{x}+\boldsymbol{\ell})\, u_k(\mathbf{x})\, e^{ih_{\ell i}(\mathbf{x})} \Bigg) \\
- \frac{1}{2} \sum_{\mathbf{x}} (\alpha_i^{\dagger} u_i + \text{c.c.}) - \frac{1}{2} \sum_{\mathbf{x}} (\lambda_i^{\dagger} v_i + \text{c.c.}) + \sum_{\mathbf{x},i} \log I_0(|\alpha_i|) \\
+ \sum_{\mathbf{x},i} \log I_0(|\lambda_i|) \Bigg\}. \qquad (19.15)
\end{aligned}
$$

It describes the fluctuations of dislocations and disclinations under the effect of *external* stresses and torque stresses carried by the gauge fields $A_{\ell i}(\mathbf{x})$, $h_{\ell i}(\mathbf{x})$.

The final total partition function for defects and stresses with higher gradient elasticity is then obtained by multiplying this expression by the Boltzmann factor of the stress energies and integrating over all stress gauge fields.

An important feature of the field energy is that, as a consequence of the defect conservation law $\bar{\nabla}_{\ell} \bar{\alpha}_{\ell i} + \varepsilon_{ik\ell} \bar{\Theta}_{k\ell} = 0$, there is now a coupling of the two types of disorder fields with each other, through the cubic terms $vv^{\dagger}u$. These terms have the capacity of making defect proliferation a first-order process even in the absence of screening effects. We recall that in our initial qualitative discussions in Section 8.5 we had identified a simple mechanism for driving the melting process to the first order. This mechanism was based on the Meissner screening of stress in the presence of dislocations which, in turn, liberated the disclinations and opened up a new reservoir of entropy. Here we find a further driving mechanism to achieve a this. It is the coupling of dislocations with the antisymmetric part of the disclination density.

In order to see this let us set the stress fields equal to zero and study

the mean fields alone. Giving all components an equal real mean value, the free energy of the defect system is

$$-\beta f_{\mathrm{def}} = \tilde{\beta}_\alpha 9u^2 + \tilde{\beta}_\Theta (3 + 6u)v^2 - 3\alpha u - 3\lambda v + 3\log I_0(\alpha) + 3\log I_0(\lambda). \tag{19.16}$$

In the absence of disclinations ($v = 0$), the dislocations by themselves would have an energy

$$-\beta f_{\mathrm{disloc}} = \tilde{\beta}_\alpha 9u^2 - 3\alpha u + 3\log I_0(\alpha). \tag{19.17}$$

This has the same form as the mean field energy of an ordinary XY model which has a second-order phase transition at [recall (5.28), (5.29) of Part II]

$$\tilde{\beta}_\alpha = 1/3. \tag{19.18}$$

Close to this, (19.17) has the Landau expansion [recall (5.31) of Part II]

$$-\beta f_{\mathrm{disloc}} \sim 3\left\{3\tilde{\beta}_\alpha u^2 - \alpha u + \frac{1}{4}\alpha^2 - \frac{1}{64}\alpha^4\right\} \triangleq 3\left\{-\frac{1}{4}\left(\frac{1}{3\tilde{\beta}_\alpha} - 1\right)\alpha^2 - \frac{1}{64}\alpha^4\right\}. \tag{19.19}$$

The second order character of the phase transition is physically understandable since, with $\bar{\Theta}_{\ell i} \equiv 0$, the dislocation density $\bar{\alpha}_{\ell i}$ forms three independent sets of closed dislocation lines, just as though there were three types of independent vortex lines in superfluid ^{4}He, each of them proliferating in a second-order phase transition. Consider now the disclination part and let us suppose, for a moment, that $\tilde{\beta}_\Theta$ is of the same magnitude as $\tilde{\beta}_\alpha$. Then we see that if $\tilde{\beta}_\alpha \approx \tilde{\beta}_\Theta$ is large enough to make the dislocations proliferate, it will be too small by a factor 3 to do the same thing for the disclinations. Only when u increases to order one, can v become nonzero. At fixed $\tilde{\beta}_\alpha$, $\tilde{\beta}_\Theta$, i.e., at fixed temperature, f_{def} of (19.16), when considered as a potential for disclination fields v at varying and fixed u has a second-order phase transition. We had observed before that this type of coupling between two second-order transitions can generate a first-order transition (see Figs 8.2–8.4).

19.4. TOWARDS A QUANTUM DEFECT DYNAMICS OF MOVING DEFECTS IN TWO DIMENSIONS

In two dimensions, there exists no comparable disorder field theory since the defects are pointlike. The situation changes, however, if quantum effects are included. Then, the points as a function of time describe orbits which are world lines in spacetime and these do allow again for a proper disorder field theory. In fact, in this way it is possible to solve an outstanding problem of second-gradient elasticity and defects, namely, the construction of a theoretically consistent dynamical quantum field theory of defects, which might be called *quantum defect dynamics*, in analogy with the quantum field theory of photons and electrons, called quantum electrodynamics, and with the quantum vortex dynamics discussed in Chapter 14, Part II.

The desired quantum field theory in $2+1$ dimensions is, of course, closely related to the three-dimensional theory developed in the last chapter. The main difference lies in a reinterpretation of one of the three spatial axes as a time axis, and in the anisotropies of the elastic and defect energies associated with space and time directions. After imposing the appropriate modifications upon Eq. (18.2), the elastic interactions between a given set of moving plastic distortions and rotations in motion are controlled by the action

$$\mathscr{A} = \int d^3x [(1/2)(\partial_0 u_i - \beta^p_{0i})^2 + \frac{1}{2}\iota(\partial_0\omega - \varkappa^p_0)^2 - \frac{1}{4}(\partial_i u_j + \partial_j u_i - \beta^p_{ij} - \beta^p_{ji})^2$$

$$- \frac{\lambda}{2}(\partial_i u^p_i - \beta^p_{ii})^2 - 2\ell^2(\partial_i\omega - \varkappa^p_i)^2], \tag{19.20}$$

where $x^i (i = 1, 2)$ are the space coordinates and x^0 is the time (the modified x^3). The quantum partition function of elastic fluctuations in the presence of an arbitrary given defect configuration is

$$Z_{\text{def}} = \int \mathscr{D}^2 u_i(x) \exp[(i/\hbar)\mathscr{A}]. \tag{19.21}$$

For simplicity, we have used natural units in which the transverse sound velocity $c_t = (\mu/\rho)^{1/2}$ and the shear modulus μ are both equal to unity. The constant ℓ is the length scale of rotational stiffness in second-gradient elasticity. The quantity ι is the density of inertia for the local rotations. As before, we have omitted possible gradients of the strain tensor since they produce no qualitatively new structure.

In the continuum, the plastic quantities $\beta^p_{\mu i}$, $\varkappa^p_\mu (\mu = 0, 1, 2)$ are given by

$$\begin{aligned}
\beta^p_{ij}(x) &= \delta_i(S)(b_j - \Omega \varepsilon_{jr}\chi_r) \\
\varkappa^p_i(x) &= \varepsilon_{k\ell}\partial_i \beta^p_{k\ell} + \phi^p_i, \qquad \phi^p_i = \delta_i(S)\Omega, \\
\beta^p_{0i}(x) &= -v_k \delta_k(S)(b_i - \Omega \varepsilon_{ir}\chi_r) \\
\varkappa^p_0(x) &= \varepsilon_{k\ell}\partial_0 \beta^p_{k\ell} + \phi^p_0, \qquad \varphi^p_0 = -v_k \delta_k(S)\Omega,
\end{aligned} \tag{19.22}$$

where b_i are the Burgers vectors, Ω the Frank scalars, and S the *time-dependent* Volterra cutting "surfaces" which, in two dimensions, are really lines. They move through space with the velocity v_k. The δ-function $\delta_i(S)$ is defined to be singular on S and to point along the normal vector. Since S is a line, we may also write $\delta_i(S)$ as $-\varepsilon_{ij}\bar{\delta}_j(S)$, where $\bar{\delta}_j(S))$ points in the tangential direction, $\bar{\delta}_j(S) = \int ds(d\bar{x}_j/ds)\delta^{(2)}(x - \bar{x}(s,t))$. We shall keep the first notation, however, because of its close analogy with the three-dimensional situation.

The stresses and torque stresses are introduced by taking (19.21) to the canonical form

$$Z = \int \mathscr{D}u_i(x) \int \mathscr{D}\sigma_{ij}(x) \int \mathscr{D}\omega(x) \int \mathscr{D}\tau_i(x) \int \mathscr{D}p_i \int \mathscr{D}\pi \exp\left[(i/\hbar)\mathscr{A}_{\text{canonical}}\right]$$

$$\begin{aligned}
\mathscr{A}_{\text{canonical}} = \int d^3x \Bigg\{ \Bigg[-\frac{1}{2}p_i^2 - \frac{1}{2}\iota\,\pi^2 - \frac{1}{4}[\overset{s}{\sigma}{}^2_{ij} - (\nu/(1+\nu))\overset{s}{\sigma}{}^2_{\ell\ell}] + (1/8\ell^2)\tau_i^2 \Bigg] \\
\times p_i(\partial_0 u_i - \beta^p_{0i}) + \pi(\partial_0 \omega - \phi^p_0) \\
- \sigma_{ij}(\partial_i u_j - \varepsilon_{ij}\omega - \beta^p_{ij}) - \tau_i(\partial_i \omega - \phi^p_i) \Bigg\} \\
\equiv \mathscr{A}_{e\ell} + \mathscr{A}_{\text{int}}
\end{aligned} \tag{19.23}$$

where the elastic energy contains only on the symmetric part $\overset{s}{\sigma}_{ij}$ of σ_{ij}. The integration over the antisymmetric part enforces the identity of ω and $(1/2)\varepsilon_{ij}\partial_i u_j$, modulo the plastic part $(1/2)\varepsilon_{ij}\beta^p_{ij}$. Integrating out $u_i(x)$ and $\omega(x)$ yields the dynamic defect conservation laws

$$\partial_i \sigma_{ij} = \partial_0 p_j, \qquad \partial_i \tau_j = \partial_0 \pi - \varepsilon_{k\ell}\sigma_{k\ell}. \tag{19.24}$$

They can be fulfilled by introducing the time-dependent stress gauge fields or *phonon gauge fields*, A_i, H, c_{ij}, d_{ij}:

$$\sigma_{ij} = \varepsilon_{ik}\partial_k A_j + \partial_0 c_{ij}, \qquad p_j = \partial_i c_{ij},$$
$$\tau_i = \varepsilon_{ik}\partial_k H - A_i + \partial_0 d_i, \qquad \pi = \partial_i d_i + \varepsilon_{ij} c_{ij}. \tag{19.25}$$

The gauge transformations which leave these decompositions invariant are somewhat degenerate, due to the reduced dimensionality of space:

$$A_i \to A_i + \partial_i \xi + \partial_0 \Lambda_i, \qquad H \to H + \partial_0 \xi, \tag{19.26}$$

$$c_{ij} \to c_{ij} - \varepsilon_{ik}\partial_k \Lambda_j, \qquad d_i \to d_i - \varepsilon_{ik}\partial_k \xi + \Lambda_i, \tag{19.27}$$

It is useful to introduce $A_{ij} \equiv \varepsilon_{i\ell} c_{\ell j}$, $H_i \equiv \varepsilon_{i\ell} d_\ell$, so that (19.27) becomes

$$A_{ij} \to A_{ij} + \partial_i \Lambda_\ell, \qquad H_i \to H_i + \partial_i \xi + \varepsilon_{i\ell}\Lambda_\ell. \tag{19.27'}$$

Inserting (19.25) into (19.23), the interaction with the defects can be brought to the form

$$\mathscr{A}_{\text{int}} = \int d^2x [A_i(\varepsilon_{kj}\partial_k \beta^p_{ji} - \phi^p_i) + H\varepsilon_{kj}\partial_k \phi^p_j$$
$$- A_{ij}\varepsilon_{i\ell}(\partial_0 \beta^p_{\ell j} - \partial_\ell \beta^p_{0j} + \varepsilon_{\ell j}\phi^p_0) - H_i \varepsilon_{i\ell}(\partial_0 \phi^p_\ell - \partial_\ell \phi^p_0)]$$
$$+ \int d^3x (A_i \alpha_i + H\theta - A_{ij}J_{ij} - H_j S_j). \tag{19.28}$$

The sources

$$\alpha_i \equiv \varepsilon_{kj}\partial_k \beta^p_{ji} - \phi^p{}_i, \qquad \Theta \equiv \varepsilon_{kj}\partial_k \phi^p_j,$$
$$J_{ij} = \varepsilon_{i\ell}(\partial_0 \beta^p_{\ell j} - \partial_\ell \beta^p_{0j} + \varepsilon_{\ell j}\phi^p_0), \qquad S_i = \varepsilon_{i\ell}(\partial_0 \phi^p_\ell - \partial_\ell \phi^p_0), \tag{19.29}$$

are identified with dislocation density, disclination density, and their respective currents. Inserting (19.22) we find explicitly

$$\alpha_j(x) = \delta(L(t))(b_j - \Omega\varepsilon_{jr}x_r), \qquad \Theta(x) = \delta(L(t))\Omega,$$
$$J_{ij}(x) = -v_i\delta(L(t))(b_{ij} - \Omega\varepsilon_{jr}x_r), \qquad S_i(x) = -v_i\delta(L(t))\Omega, \tag{19.30}$$

where L is the boundary "line" of the Volterra cutting "surface" S which, in two dimensions, consists of the two end points. The function $\delta(L)$ is positive on one end point and negative on the other. The densities and currents obviously satisfy the conservation laws,

$$\partial_i J_{ij} = \partial_0 \alpha_j - \varepsilon_{ji} S_i, \qquad \partial_i S_i = \partial_0 \Theta. \tag{19.31}$$

These are necessary to ensure stress gauge invariance under (19.26) and (19.27′).

The plastic quantities in (19.29) can be subjected to defect gauge transformations which correspond to changing the shape of the Volterra cutting "surface" at fixed boundary. Indeed, under $S \to S'$ we find that $\delta_j(S') = \delta_i(S) - \partial_i \delta(V)$ where V is the "volume" (here area) over which the surface S is swept. From (19.22) we see that under such a change

$$\begin{aligned} &\beta^p_{ij} \to \beta^p_{ij} + \partial_i N_j - \varepsilon_{ij} M, \qquad && \phi^p_i \to \phi^p_i + \partial_i M, \\ &\beta^p_{0j} \to \beta^p_{0j} + \partial_0 N_j, && \phi^p_0 \to \phi^p_0 + \partial_0 M, \end{aligned} \tag{19.32}$$

where $M = -\delta(V)\Omega$, $N_i = -\delta(V)(b_i - \Omega \varepsilon_{ir} x_r)$. These transformations obviously preserve the defect currents (19.29). Separating out some self-energies of the defects as in (19.2), we arrive at a partition function

$$\begin{aligned} Z = \int \mathscr{D}A_i \mathscr{D}H \mathscr{D}A_{ij} \mathscr{D}H_i \Phi^{\text{phon}}[A_i, H, A_{ij}, H_i] \exp\left(\frac{i}{\hbar}\mathscr{A}'_s\right) \\ \times \exp\left(\frac{i}{\hbar}\int d^3x (A_i \alpha_i + H\theta - A_{ij}J_{ij} - H_i S_i)\right) \\ \times \exp\left[-\frac{i}{\hbar}\int d^3x \left(\frac{1}{2\varepsilon_1}(\alpha_i^2 - J_{ij}^2) + \frac{1}{2\varepsilon_2}(\theta^2 - S_i^2)\right)\right], \end{aligned} \tag{19.33}$$

where $\mathscr{A}'_s$ is the quantity in large square brackets of the action (19.23), expressed in terms of the gauge fields, but modified at short distance, so as to separate out the core energies in the last line of (19.33). The symbol Φ^{phon} denotes a gauge-fixing functional for the phonon gauge fields.

The defect partition function (19.33) is the analogue of the Maxwell-Lorentz theory of the electromagnetic field around the world lines of an ensemble of electrons,

$$Z_{\ell m} = \int \mathscr{D}A_\mu \Phi^{\text{phon}}[A_\mu] \exp\left(\frac{1}{4\hbar}\int d^4x F_{\mu\nu}^2\right) \exp\left(\frac{i}{\hbar}\int dt(\varphi - A_i \dot{x}_i)\right)$$
$$\times \exp\left(-\frac{im}{\hbar}\int dt(1-\dot{x}^2)^{1/2}\right). \tag{19.34}$$

In order to turn (19.33) into the desired quantum field theory of defects and phonons we put the system on a square lattice with unit spacing $a = 1$. Then the plastic quantities become discrete. Rescaling u_i by $2\pi/a$ the plastic distortions $\beta_{ij}^p = 2\pi n_{ij}$ represent the jumps of the displacement variables u_j across the lines, thus parametrizing an ensemble of Volterra "surfaces" S_i while $\phi_j^p = 2\pi m_i$ are the jumping "surfaces" of the rotation angle. Taking a nonzero lattice spacing also for the time variable (which is sent to zero at the end) the surfaces perform hopping motion as a function of time.

The result is a theory of moving defects of the same form as in Eq. (19.15), with the only difference being the anisotropy of the space and time directions, the absence of $u_3(x)$, $v_\ell(x)$ and $A_{\ell 3}$, A_{33}, $h_{\ell i}$, $h_{3i}(\ell, i = 1,2)$, and the following replacements of the stress gauge fields

$$A_{3i} \to A_i, \qquad h_{33} \to H, \qquad h_{\ell 3} \to H_\ell.$$

The fields $A_{ij}(i, j = 1,2)$ are the same as before. After completing the modified partition function (19.15) by the stress partition function (19.23) we obtain a fully fledged quantum defect dynamics of moving dislocations and disclinations in $2 + 1$ dimensions. For more details, the reader is referred to the original papers quoted in the Notes and References. So far, this quantum field theory has not been studied in any detail.

NOTES AND REFERENCES

For the construction of a field theory of Quantum Defect Dynamics, see
H. Kleinert, *J. Phys.* A19 (1986) 1855, and *Int. J. Engng. Sci.* **23** (1985) 927.